imid.or.kr

Hybrid Event

iMiD 2021

The 21st International Meeting on Information Display

On Leap for Next 20: Breakthrough in Display Technology & Science

August 25-27, 2021 / COEX, Seoul, Korea

PROCEEDINGS (DIGEST)

Organized by

The Korean Information Display Society (KIDS)

The Society for Information Display (SID)

[Invited] **Seamless collaboration for Advancing Digital Living**

Dr. WooKyu Kim
Managing Director & Representative Director of Merck Korea

Merck as a leading technology company of display materials has been collaborating together with IMID through KIDS last 20 years. During these periods, KIDS has been contributing to connect between academia and industries for optimizing all our efforts and IMID has been a role of network platform successfully. With these contributions, we are experiencing the enormous development of Display industry worldwide and facing advancing digital living of our daily life. Previous 20 years will be a fuel of next 20 years forward data driving industries. Merck want to share how we are developing together and how we are collaborating across industries as like Healthcare, Life Science and Electronics within Merck.

Fluorinated Elevated-Metal Metal-Oxide Thin-Film Transistors for Flexible Electronics

Man Wong and Runxiao Shi
Department of Electronic and Computer Engineering, The Hong Kong University of Science and Technology, Clear Water Bay, Kowloon, Hong Kong
Tel.:+852 23587057, E-mail: eemwong@ust.hk

An enhanced elevated-metal metal-oxide (EMMO) thin-film transistor (TFT) technology (1) was developed for realizing electronic systems on flexible polyimide (PI) substrates. Indium-gallium-zinc oxide (IGZO) was used as the semiconducting active layer. The enchancement is realized by treating IGZO in a tetrafluoromethane plasma for 10 minutes to form IGZO:F. The fluorinated TFTs exhibit more positive threshold voltage (Fig. 1a), steeper pseudo-subthreshold swing (Fig. 1a), and reduced apparent short-channel effects (Fig. 1b). Based on the IGZO:F EMMO TFTs, a variety of digital circuit blocks, including a 4-stage gate driver were simulated, fabricated and characterized (Fig. 2).

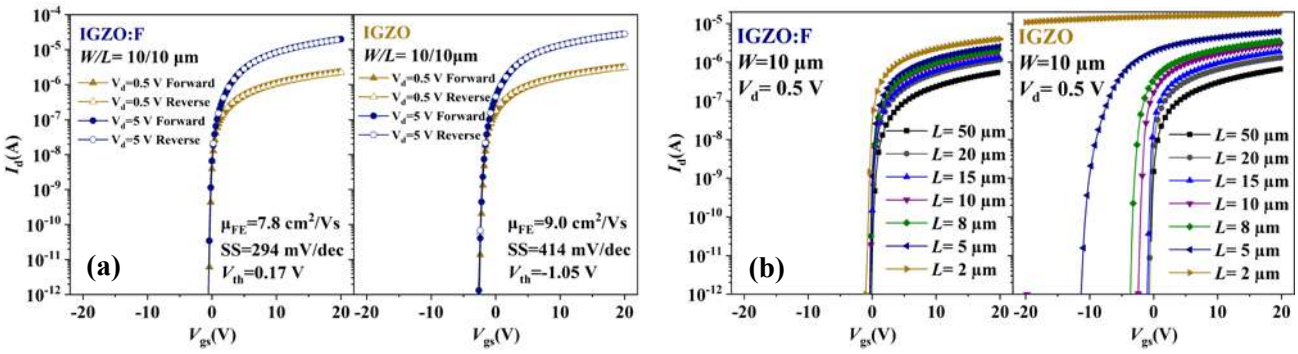

Figure 1. Comparison of (a) the transfer characteristics of the IGZO:F and IGZO TFTs and (b) the transfer characteristics of two sets of IGZO:F and IGZO TFTs.

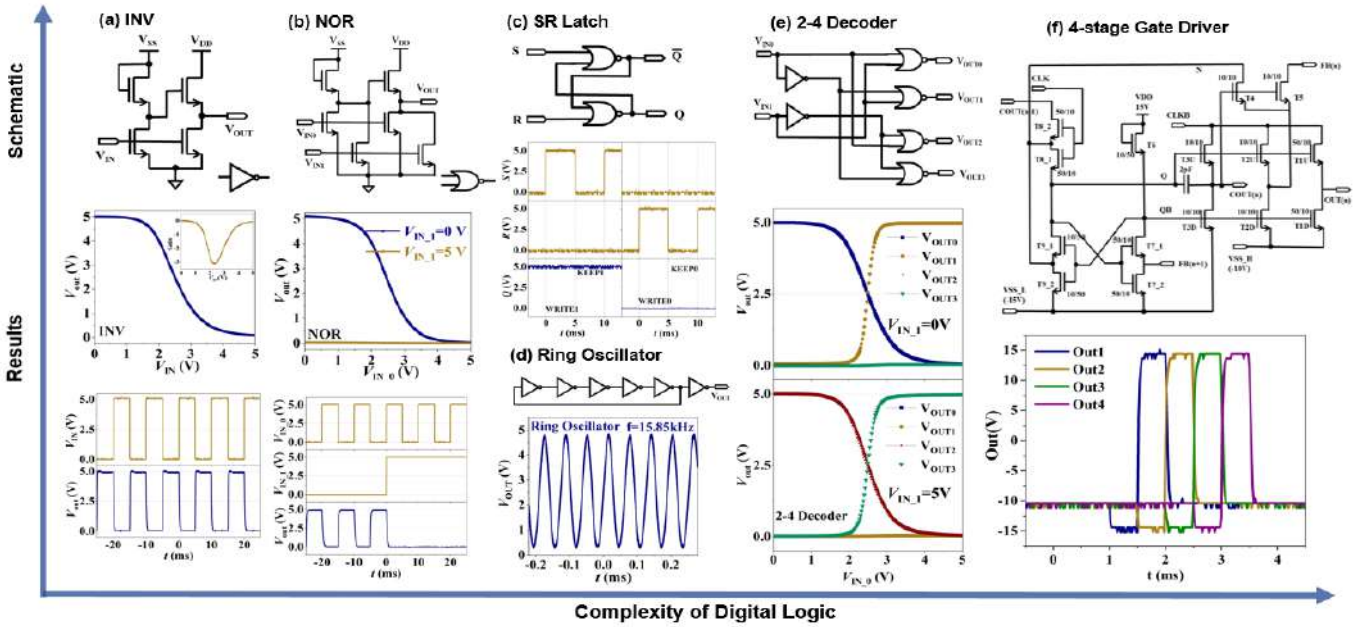

Figure 2. Digital circuit blocks based on IGZO:F EMMO TFTs on PI.

Reference

1. Lu L, Li J, Kwok HS, Wong M. High-performance and reliable elevated-metal metal-oxide thin-film transistor for high-resolution displays. Tech Dig - Int Electron Devices Meet IEDM. 2017;(December):32.2.1-32.2.4.

High Resolution OLED Display and AR/VR Application

Chiwoo Kim, Jae Hoon Jung, Kiro Jung
APS Research Corporation, Hwasung, Korea

Abstract

Recently, in the field of information and communications technologies (ICT), research on technologies that can lead the 4th industrial revolution is actively being conducted. Virtual Reality/Augmented Reality (VR/AR) technology plays the key role in this field.

We have developed the 3,000ppi FMM using UV laser patterning technology and the RGB side-by-side OLED micro-display using Si-wafer pixel driving circuits. These two key technologies enable us to realize AR devices with ultra-high pixel resolution, high brightness, long life time and high color purity.

The Invar slimming (TCP) and the state-of-the-art UV laser ablation process can realize the ultra-high-resolution (~3,00ppi) FMM fabrication. It is expected that with our ultra-high-resolution FMM sticks and RGB side-by-side OLED micro-display can be mass produced. In addition, AR applications adopting this RGB side-by-side OLED micro-display is expected to be realized in the near future.

Furthermore, by developing spot beam annealing (SBA) technology, Gen. 8 or larger size crystallization of s-Si film is available. Productivity of large size IT OLED display panels can be significantly improved. It was observed that the SBA technology works as expected. Experiment and simulation results show that the controls of residence time and heat spike engineering are possible. Polygon scanners can control both macro- and micro-scale uniformity with long scanning lengths. It is expected that this technology can be applied to the large area LTPO (Low Temperature Poly Oxide) backplane process.

Title: **Two decade of Revolutions in Korea Display Industry**

Author: Jun Souk

Abstract:
During the past 20 years, the display industry went through dynamic changes and rapid growth. We observed the rise of LCD and OLED and the fall of PDP and FED and other displays. At the same period of time, the competition among display technologies and display countries resulted in changing industry leadership. From the beginning of year 2000, Korea display industry has taken initiative in the large size TV panels, early construction of Gen 7 lines followed by volume production of large TV panels. From 2010 to 2020, the Korea display industry's major effort has been shifting to AMOLED and quantum dot technology. In this presentation, we focus on the Korea display industry's growth path that enabled maintaining the leadership position. Major landmark events and their significance in TFT-LCD and AMOLED are discussed.

Purely Organic Emitters for OLEDs: A Radical Proposition

Jean-Luc Brédas
Dept. of Chemistry and Biochemistry, The University of Arizona, Tucson, Arizona 85721-0088, U.S.A.
Tel.:1-520-626-7103, E-mail: jlbredas@arizona.edu

Since the seminal work of Tang and Vanslyke in 1987 on small-molecule emitters and that of Friend and co-workers in 1990 on conjugated-polymer emitters, organic light-emitting diodes (OLEDs) have attracted much attention from academia as well as industry, with the OLED market estimated to reach the $80B mark by the end of 2020. In these first-generation organic emitters, on the basis of simple spin statistics, electrical excitation resulted in the formation of ~25% singlet excitons and ~75% triplet excitons. Radiative decay of the singlet excitons to the singlet ground state leads to a prompt fluorescence emission, while the triplet excitons only lead to weak phosphorescence due to the very small spin-orbit couplings present in purely organic molecules. The consequence is a ca. 75% energy loss, which triggered wide-ranging efforts to try and harvest as many of the triplet excitons as possible. In 1998, Thompson, Forrest, and their co-workers reported second-generation OLED emitters based on coordination complexes with heavy transition metals (e.g., iridium or platinum). Here, the triplet excitons stimulate efficient and fast phosphorescence due to the strong spin-orbit couplings enabled by the heavy-metal atoms. Internal quantum efficiencies (IQE) up to 100% have been reported, which means that for every electron injected into the device, a photon is emitted. While these second-generation emitters are those mainly exploited in current OLED applications, there is strong impetus from both cost and environmental standpoints to find new ways of exploiting purely organic emitters, which in addition can offer greater flexibility to fine tune the electronic and optical properties by exploiting the synthetic organic chemistry toolbox.

Here, we focus on a recently applied strategy that was proposed by Feng Li and co-workers in 2015 and is based on the exploitation of stable organic radicals. In these materials, when the lowest excited state and the ground state both belong to the doublet manifold, high efficiencies can be obtained. see *e.g.* Ref. 1.

Molecular design principles to reach high efficiencies at high energy will also be discussed. In Ref. 2., we considered a series of emitters based on substituted triarylamine (TAA) donors and a radical-carrying perchlorotriphenylmethyl (PTM) acceptor. We evaluated, by means of quantum-chemical calculations and theoretical modeling, how chemical substitution affects the electronic structures and radiative and non-radiative decay rates. Our calculations show that the radiative decay rates are dominated in all instances by the electronic coupling between the lowest excited state, which has a charge-transfer (CT) character, and the ground state. On the other hand, the non-radiative decay rates in the case of TAA-PTM radicals that have high CT energies are defined by the electronic hybridization of the CT state with local excitations (LE) on the PTM moiety; also, these non-radiative rates deviate significantly from the gap-law dependence that is observed in the TAA-PTM radicals that have low CT energies. These findings underscore that hybridization of the emissive state with high-energy states can, in analogy with the intensity borrowing effect commonly invoked for radiative transitions, enhance the non-radiative decay rates as well. Our results highlight that, in order to understand the emissive properties of D–A• radicals, it is required that the electronic hybridization of the CT states with both the ground and LE states be properly considered, a finding confirmed in our very recent work on a series of tris(2,4,6-trichlorophenyl)methyl-pyridoindole radicals, see Ref. 3.

Acknowledgments

The author is grateful to Drs. V. Coropceanu, E.K. Cho, X.K. Chen. S. Pratik, and Y. Liu for their invaluable contributions to this work.

References

1. "High Stability and Luminescence Efficiency in Donor-Acceptor Neutral Radicals Not Following the Aufbau Principle", H.Q. Guo, R.H. Friend, J.L. Brédas, F. Li *et al*., *Nature Materials*, 18, 977-984 (2019).
2. "Organic Neutral Radical Emitters: Impact of Chemical Substitution and Electronic-State Hybridization on the Luminescence Properties", E.K. Cho, V. Coropceanu, J.L. Brédas, *J. Amer. Chem. Soc*., 142, 17782 (2020).
3. "Impact of Chemical Modifications on the Luminescence Properties of Organic Neutral Radical Emitters", E.K. Cho, V. Coropceanu, J.L. Brédas, *J. Mater. Chem. C*, in press (2021).

Multiscale calculation of carrier mobility in organic solids through the fine-tuned kinetic Monte Carlo Method

Gyubong Kim[1], Kyungchan Chae, Sunwoo Kang, Youngmi Cho, Hoilim Kim
[1]Display Research Center, Samsung Display Co., Yongin, Republic of Korea
Tel.:82-31-5181-6782, E-mail: kgb531@gmail.com

We calculated the carrier mobility in organic solids through a multiscale approach connecting the molecular-level simulations to the kinetic Monte Carlo (kMC) simulation [1,2]. The morphology of the amorphous organic bulk was constructed using molecular dynamic (MD) simulations, thereby the *ab initio* calculations of the electronic coupling can be conducted using the constituent molecule pairs in the organic bulk. The calculation results were used as input in the kMC simulation to calculate the carrier mobility. The kMC simulation in this work is based on the on-lattice scheme which is more advantageous in terms of scalability in comparison with the off-lattice scheme. We systematically tuned our kMC simulation to best mimic the morphological conditions of the carrier transport in the organic bulk (Fig. 1 and 2). The calculations with several well-known molecules demonstrated that our calculations agree well with the measurements from literature [3-5] regarding both the quantities and the molecule-wise order (Fig 3).

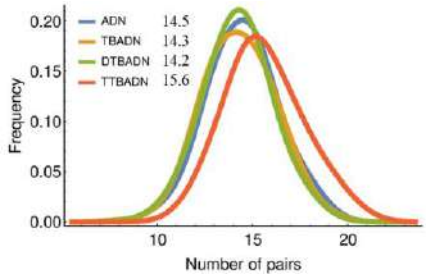

Fig. 1. Distribution of the close-contact numbers from MD calculations

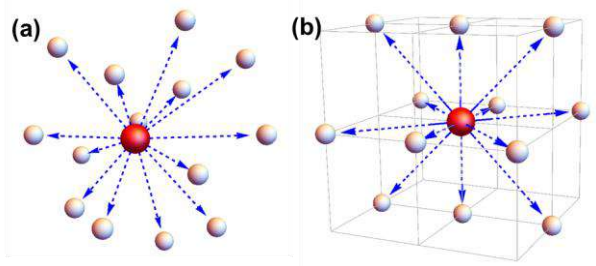

Fig. 2. (a) Example morphology of the close-contact in the organic bulk and (b) the modified geometry for the kMC simulation

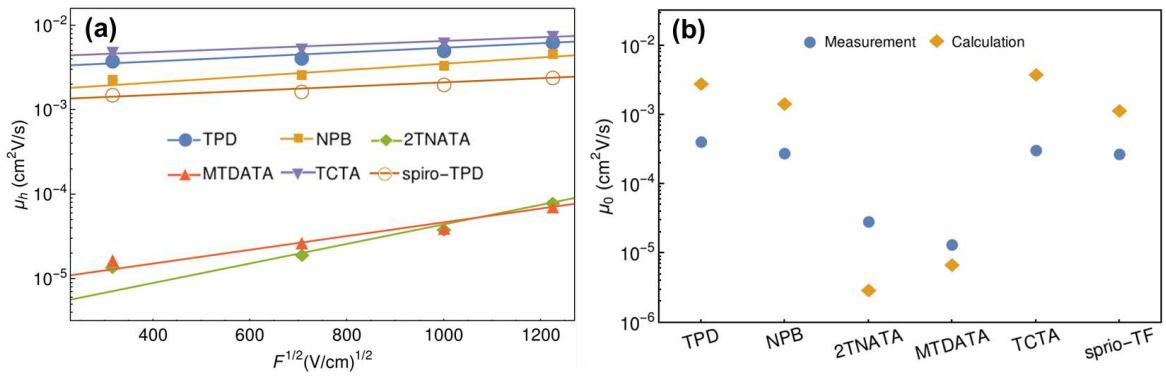

Fig. 3. (a) Calculated field-dependent hole mobilities of selected molecules and (b) the corresponding zero-field mobilities in comparison with the measurements

References

1. J. J. Kwiatkowski, J. Nelson, H. Li, J. L. Bredas, W. Wenzel and C. Lennartz, *Phys. Chem. Chem. Phys*., 10, 1852 (2008)
2. Veaceslav Coropceanu,Jéróme Cornil, Demetrio A. da Silva Filho, Yoann Olivier, Robert Silbey, and Jean-Luc Brédas, *Chem. Rev.*, 107, 926 (2007)
3. Cyrus Y.H. Chan, K.K. Tsung, W.H. Choi and S.K. So, *Organic Electronics*, 14, 1351 (2013)
4. Shu K. So, Shing C. Tse, and Ka L. Tong , *JDT*, 3, 225 (2007)
5. Sean W. Culligan, Andrew C.-A. Chen, Jason U. Wallace, Kevin P. Klubek, Ching W. Tang and Shaw H. Chen, *Adv. Funct. Mater.*, 16, 1481 (2006)

Autonomous Materials Design for More Efficient OLED Devices Using Machine Learning

Sohae Kim, Dongsun Yoo, Jihye Kim, Gyeongheon Kim, Jiyoo Park, Seran Kim, Dahye Cho, Hoilim Kim, Young Mi Cho and Yongjo Kim
CAE Team, Samsung Display, Gyeonggi-do, Republic of Korea
Tel.:82-31-5181-6893, E-mail: sohae.kim@samsung.com

Machine learning-based methods have been widely applied in recent years to aid the discovery of new chemical materials that can yield more efficient and durable OLED devices. For example, we previously developed internal tools to provide virtual high-throughput screening (*v*-HTS) of blue dopant materials based on machine learning (ML) prediction of key ab-initio properties that are relevant to the efficiency and stability of blue dopant materials. [1] In this manner, a large number of materials were analyzed at relatively low computational cost to identify candidate molecules for further examination using traditional ab-initio simulations and synthesis techniques. Although such tools may perform well for a group of materials similar to the trained data, the prediction accuracy of the material properties may decrease particularly for different groups of materials or materials that fall outside the range of the trained data. Because of such uncertainty, we previously devised a predictability scale to pre-screen materials before applying machine-learning to predict material properties. As a result, the target-in rate for both a triplet excited state and a triplet metal-ligand charge transfer state screening increased from 22% to 48% by implementing a *v*-HTS with ML prediction. The target in-rate further increased to 66% by employing a higher criterion for the ML-predictability scale during pre-screening. However, the coverage of ML prediction was limited to 52% coverage of the design space of 1.5 million molecules for a group of cyclometalated Pt (II) phosphor materials.

In the current work, we have further developed the *v*-HTS system by (a) expanding the design space of cyclometalated Pt (II) phosphor and thermally activated delayed fluorescence (TADF) materials; (b) curating data sampling, which minimizes the number of sampled molecules to reduce computational cost for ab-initio calculations while maintaining the predictability scale acceptably high enough for the whole design space; and (c) automatically building ML property prediction models with the expanded database. Therefore, once researchers examine a molecule, the autonomous materials design tool expands the ML prediction design space, updates ML models, and suggests other candidate molecules related to the input molecule based on the key ML-predicted properties and a synthetic accessibility score [2]. We believe that our autonomous materials design tool will enable researchers to continue expanding the materials design space automatically and to select candidate molecules more efficiently.

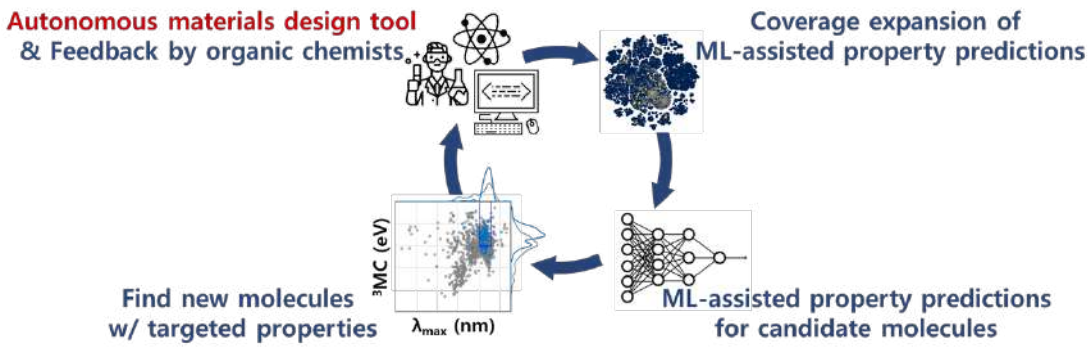

Fig. 1. A workflow schematic using the autonomous materials design and *v*-HTS

References

1. D. Cho, S. Kim, S. Kang, E. Koh, I. Kang, S.M. Choi, H. Kim, S.H. Jeon, Y.M. Cho and Y. Kim, *IMID 2020 Digest*, vol. 1, p. 2 (2020).
2. P. Ertl and A. Schuffenhauer, *J. Cheminfo.,* 1, 8 (2009).

Design Automation of Efficient Deep Neural Networks in Display Devices

Jae Hun Shim and Suk-Ju Kang
Dept. of Electronic Engineering, Sogang University, Seoul 04107, Korea
Tel.:82-2-705-8466, E-mail: sjkang@sogang.ac.kr

Recently, deep neural networks have been used in various applications for display devices. However, depending on the application, there may be restrictions on the size of the network or required hardware resources, and additional considerations such as inference time are sometimes required. Under such conditions, it is difficult to use an existing standardized neural network to improve performance.

In this paper, we present a neural architecture search, a design automation methodology for implementing an efficient deep neural network. This methodology is a technique that can optimize various variables such as the number of layers that can be changed in a neural network and kernel size. However, in general, when the search space is very wide, a very large hardware resource is required, and the time taken to search for an optimal value is very high. In this paper, we applied neural architecture search to multi-touch seperation as an application for display device and confirmed its performance. In the case of the proposed method, a deep neural network with higher accuracy was searched more efficiently than the existing neural architecture search.

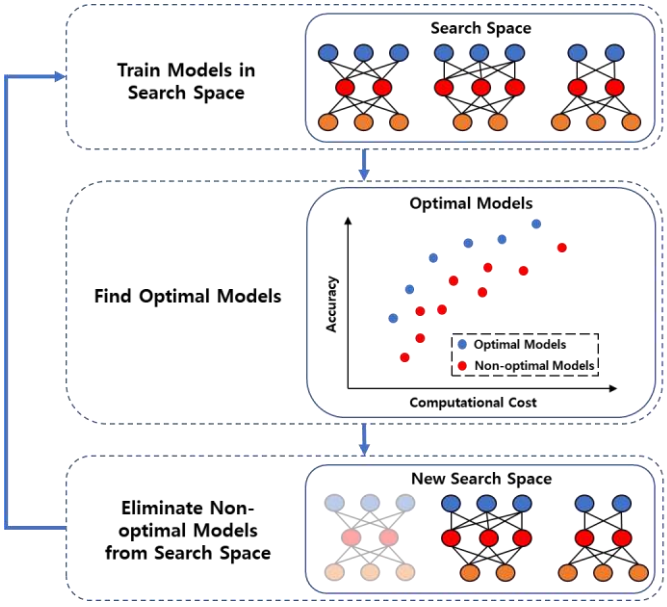

Fig. 1. Concept of neural architecture search

Acknowledgment

This research was supported by Samsung Display and the MSIT(Ministry of Science and ICT), Korea, under the ITRC(Information Technology Research Center) support program(IITP-2021-2018-0-01421) supervised by the IITP(Institute of Information & communications Technology Planning & Evaluation).

References

1. P. Hieu, et al. "Efficient neural architecture search via parameters sharing", *International Conference on Machine Learning. PMLR*, 2018.
2. M. Tan, B. Chen, R. Pang, V. Vasudevan, M. Sandler, A. Howard, and Q. V. Le, “Mnasnet: Platform-aware neural architecture search for mobile”, in *Computer Vision and Pattern Recognition*, 2019.
3. A. Howard, M. Sandler, G. Chu, L.-C. Chen, B. Chen, M. Tan, W. Wang, Y. Zhu, R. Pang, V. Vasudevan et al., “Searching for mobilenetv3”, in *Computer Vision and Pattern Recognition*, 2019.
4. H. Cai, C. Gan, and S. Han, “Once for all: Train one network and specialize it for efficient deployment”, in *International Conference on Learning Representations*, 2020.

Kinetic Monte Carlo modeling of organic light-emitting diodes containing molecules with large electric dipole moments

R. Coehoorn[1,2,3], X. Lin[3], C.H.L. Weijtens[1], S. Gottardi[4], and H. van Eersel[4]
[1]Department of Applied Physics, Eindhoven University of Technology,
P.O. Box 513, 5600 MB Eindhoven, The Netherlands
Tel.: +31 40 247 8321, E-mail: r.coehoorn@tue.nl
[2]Institute for Complex Molecular Systems, Eindhoven University of Technology,
P.O. Box 513, 5600 MB Eindhoven, The Netherlands
[3]Guangdong Provincial Key Laboratory of Optical Information
Materials and Technology and Institute of Electronic Paper Displays,
South China Academy of Advanced Optoelectronics,
South China Normal University, Guangzhou 510006, P. R. China,
[4]Simbeyond B.V., Het Eeuwsel 57, 5612 AS Eindhoven, The Netherlands

In principle, Kinetic Monte Carlo (KMC) modeling can provide an accurate three-dimensional (3D) molecular-scale view on the functioning of OLEDs and can in particular reveal where efficiency loss and degradation processes occur [1-4]. However, a necessary requirement for achieving a high reliability is that the 3D electrostatic potential distribution in the system is correctly included in the simulations. That distribution is often not only determined by the applied external field and by the space charge due to the injected charge carriers, but also by the stray fields from molecules with large static dipole moments. In disordered materials, this leads to a contribution to the width of the frontier orbital density of states, and hence to a reduced mobility. Furthermore, a small degree of dipole orientation, as is often observed experimentally ("giant surface potential" effect [5]) can already strongly affect the rate of injection from electrodes and the blocking of charges at internal interfaces.

In this talk, we show how the effect of molecular dipole moments can be added to 3D-KMC OLED device simulations, and we analyze how their presence can affect the device performance. We focus on efficient phosphorescent $Ir(ppy)_2(acac)$-based OLEDs in which the electron transport layer (ETL) is formed by TPBi (2,2',2''-(1,3,5-benzinetriyl)-tris(1-phenyl-1-H-benzimidazole) molecules, with a large (7 D) dipole moment, studied intensively in Ref. 6. After obtaining a fair agreement with the experimental current-voltage curve, the efficiency roll-off curve and the observed emission profile, utilizing experimental and theoretical information about the dipole orientation distribution function, we use the simulations to study the sensitivity to the size and the net orientation of the dipole moments, and to their detailed angular distribution function [7]. We also investigate under which conditions the injection of electrons from the cathode into the TPBi layer is influenced by a net dipole orientation.

The simulations show how the net orientation of the dipole moments in the TPBi electron transport layer affects the efficiency, due to an effect on the recombination efficiency (imperfect hole blocking) and due to an effect on the shape of the emission profile. The validation of the set of selected simulation parameters is partially based on a comparison with the experimental emission profile, that was obtained in Ref. 6 using the sense layer method. Even though this is an important method, its accuracy is not well known. We present the results of explicit 3D-KMC simulations of the sense layer experiments and show to what extent the method provides an accurate view on the shape of the emission profile.

References

1. M. Mesta, M. Carvelli, R.J. de Vries, H. van Eersel, J.J.M. van der Holst, M. Schober, M. Furno, B. Lüssem, K. Leo, P. Loebl, R. Coehoorn and P.A. Bobbert, *Nat. Mater.* 12, 652 (2013).
2. H. van Eersel, P. A. Bobbert, R. A. J. Janssen, and R. Coehoorn, *Appl. Phys. Lett.* 105, 143303 (2014).
3. R. Coehoorn, H. van Eersel, P. Bobbert, and R. Janssen, *Adv. Funct. Mater.* 25, 2024 (2015).
4. S. Gottardi , M. Barbry, R. Coehoorn, and H. van Eersel, Appl. Phys. Lett. 114, 073301 (2019).
5. Y. Noguchi, W. Brütting, and H. Ishii, *Jpn. J. Appl. Phys*. 58, SF0801 (2019).
6. B. Sim, C.-K. Moon, K.-H. Kim, and J.-J. Kim, *ACS Appl. Mater. Interf.* 8, 33010 (2016).
7. R. Coehoorn, X. Lin, C.H.L. Weijtens, S. Gottardi, and H. van Eersel (submitted).|

Refined models and machine learning for OLED display simulation

E. Knapp[2], M. Battaglia[2], S. Zeder[1], U. Aeberhard[1], E. Comi[2], C. Kirsch[2], S. Jenatsch[1], B. Blülle[1], B. Ruhstaller[1,2]
[1]Fluxim AG, Katharina-Sulzer-Platz 2, 8400 Winterthur, Switzerland
Tel.:41-44-500-4770, E-mail: beat.ruhstaller@fluxim.com
[2]Institute of Computational Physics, Zurich University of Applied Sciences (ZHAW), Winterthur, Switzerland

This contribution gives an update on recent progress in the implementation of refined physical models for organic and emerging perovskite LEDs as well as machine learning based analysis methods. As physical model refinements we first discuss advanced models for luminescence and for self-absorption and re-emission of light. The first, 3D excitonic modeling method is useful for studying exciton dynamics and energy transfer in OLED emitter films and devices [1]. The latter was recently introduced for studying photon recycling in perovskite solar cells [2], see Fig. 1, but can likewise be employed for analyzing self-absorption in perovskite LEDs.

In the second part of this contribution we introduce two machine learning (ML) approaches. Firstly, we combine the use of machine learning and a semiconductor device modelling tool (Setfos) to extract semiconductor material parameters from steady-state (JV) and frequency dependent (C-f and C-V) measurements whereby a gradient boosting method is employed for the refinement of the ML model [3] which in turn is trained with synthetic data originating from a semiconductor simulator. This provides an interesting alternative to traditional least-square fitting [4, 5] with the device simulator.

Finally, a novel electroluminescence (EL) imaging analysis method is presented wherein a convolutional neural network (CNN) is trained with synthetic data obtained from an electro-thermal FEM model (Laoss) [6]. The CNN is then applied to measured EL images whereby material parameters are extracted. This study is carried out with silicon solar cells to analyze defects (shunts) but EL and eventually lock-in IR images could likewise originate from OLED displays or lighting panels. Moreover, our electro-thermal FEM simulator Laoss was recently extended to the frequency domain in order to generate impedance spectra (IS) as well as lock-in IR images for up-scaled devices in the range of mili- and centimeters [7].

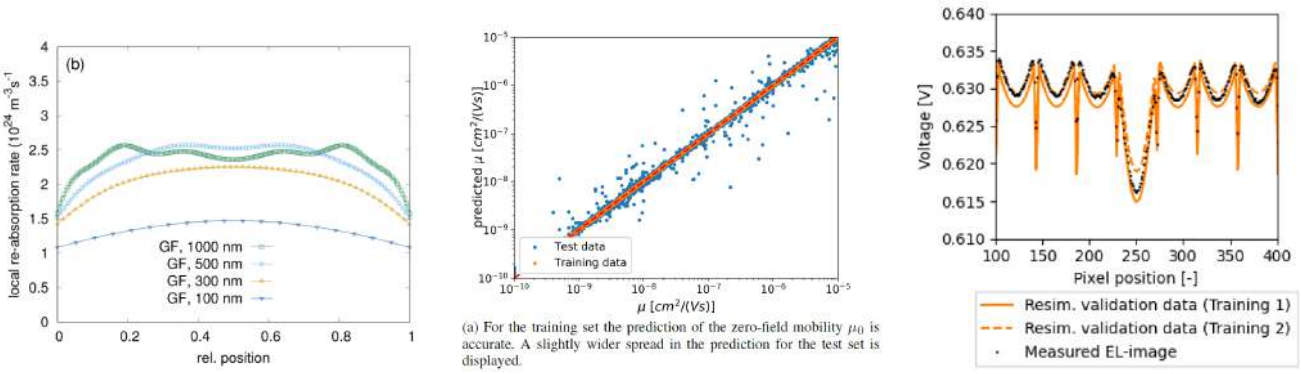

Fig. 1 a) layer thickness variation of photon self-absorption in a perovskite semiconductor device, plotted vs. relative position inside the luminescent perovskite layer [2] (left). b) performance evaluation of an ML approach to extract model parameters from JV, C-f and C-V data of an organic semiconductor device [4] (middle). c) ML based EL (cross-sectional) image analysis with a shunt defect in the center of the image as well as metal grid lines [7].

References

1. S. Zeder, C. Kirsch, U. Aeberhard, B. Blülle, S. Jenatsch, B. Ruhstaller, "Coupled 3D master equation and 1D drift-diffusion approach for advanced OLED modelling", J. of the Society for Information Display, 28 5, 440, https://doi.org/10.1002/jsid.903 (2020)
2. U. Aeberhard, S. Zeder, B. Ruhstaller, "Reconciliation of dipole emission with detailed balance rates for the simulation of luminescence and photon recycling in perovskite solar cells", Optics Express 29 10 14773, https://doi.org/10.1364/OE.424091 (2021)
3. E. Knapp, M. Battaglia, T. Stadelmann, B. Ruhstaller, "XGBoost Trained on Synthetic Data to Extract Material Parameters of Organic Semiconductors", 2021 8th Swiss Conf. on Data Science, https://doi.org/10.1109/SDS51136.2021.00015 (2021)
4. S. Jenatsch, S. Altazin, P.-A. Will, M.T. Neukom, E. Knapp, S. Züfle, S. Lenk, S. Reineke, B. Ruhstaller, "Quantitative analysis of charge transport in intrinsic and doped organic semiconductors combining steady-state and frequency-domain data", J. App. Phys. 124, 10, 105501, https://doi.org/10.1063/1.5044494 (2018)
5. S. Jenatsch, S. Züfle, B. Blülle, B. Ruhstaller, "Combining steady-state with frequency and time domain data to quantitatively analyze charge transport in organic light-emitting diodes", J. Appl. Phys. 127 (3), 031102, https://doi.org/10.1063/1.5132599 (2020)
6. M. Battaglia, E. Comi, E. Knapp, T. Stadelmann, B. Ruhstaller, "Silicon Solar Cell Parameter Estimation by Convolutional Neural Network Trained on Simulated Data", manuscript in preparation
7. E. Comi, E. Knapp, S. Weidmann, C. Kirsch, S. Jenatsch, R. Hiestand, B. Ruhstaller, "AC and DC Analysis of Large-Area Semiconductor Devices", manuscript submitted

First-Principles Modeling of Efficiency of Halide Perovskites

Chris G. Van de Walle
Materials Department, University of California, Santa Barbara, CA 93106-5050, USA
E-mail: vandewalle@mrl.ucsb.edu

Understanding recombination mechanisms in halide perovskites is of key importance to their applications in photovoltaics and light emission. We perform first-principles calculations to compute the radiative and nonradiative recombination coefficients in methylammonium lead iodide [$MAPbI_3$, MA=(CH_3NH_3)], as well as in other halide perovskites. To achieve accurate and reliable results, our first-principles calculations are based on hybrid density functional theory with spin-orbit coupling included [1]. The computed radiative recombination coefficient is as high as in typical direct-gap semiconductors used in optoelectronics [2]. The demonstrated high radiative recombination coefficient thus enables promising applications in light-emitting diodes. However, our first-principles calculations of nonradiative rates show that strong Auger recombination will suppress efficiency [3]. Fortunately, our insights into the origins of the strong Auger recombination indicate potential avenues for engineering the Auger coefficient [4].

I will also discuss defect-assisted recombination. The impact of point defects on device efficiency has not been properly assessed to date. Rigorous calculations of nonradiative recombination coefficients show the limitations of the widely adopted rule that only defects with charge-state transition levels deep in the band gap can be efficient nonradiative recombination centers [5]. We demonstrate that the position of the level does not directly determine the capture rates, due to exceptionally strong lattice coupling and anharmonicity in the halide perovskites [6]. Our results clearly show that (1) point defects can indeed be present in relevant concentrations in the halide perovskites and (2) some of these point defects lead to nonradiative recombination rates that are just as high as in conventional semiconductors. In addition to point defects on the inorganic lattice, hydrogen vacancies on the organic molecule can be major sources of nonradiative recombination [7]. We therefore conclude it is incorrect to call the halide perovskites “defect tolerant”. A more relevant distinction, compared to conventional semiconductors, is that halide perovskites with modest defect densities can be grown using low-cost deposition techniques; however, careful control of point defects is still essential to maximize the efficiency.

Acknowledgment

Work performed in collaboration with X. Zhang, J.-X. Shen, M. Turiansky, W. Wang, and E. Kioupakis, and supported by DOE.

References

1. X. Zhang, J.-X. Shen, and C. G. Van de Walle, *J. Phys. Chem. Lett.*, **9**, 2903 (2018).
2. X. Zhang, J.-X. Shen, W. Wang, and C. G. Van de Walle, *ACS Energy Lett.*, **3**, 2329 (2018).
3. J.-X. Shen, X. Zhang, S. Das, and E. Kioupakis, C. G. Van de Walle, *Adv. Energy Mater.*, **10**, 1801027 (2018).
4. X. Zhang, J.-X. Shen, and C. G. Van de Walle, *Adv. Energy Mater.*, **10**, 1902830 (2020).
5. X. Zhang, M. E. Turiansky, and C. G. Van de Walle, *J. Phys. Chem. C*, **124**, 6022 (2020).
6. X. Zhang, M. E. Turiansky, J.-X. Shen, and C. G. Van de Walle, *Phys. Rev. B*, **101**, 140101 (2020).
7. X. Zhang, J.-X. Shen, M. E. Turiansky and C. G. Van de Walle, *Nat. Mater.*, (2021) [doi: 10.1038/s41563-021-00986-5].

Quantum Computing Methods for OLED Materials Design

Scott N. Genin[1], Ilya G. Ryabinkin[1], and Michael G. Helander[1]
[1]OTI Lumionics Inc., Toronto, ON, Canada
Tel.:+1 (647) 479-4074, E-mail:michael.helander@otilumionics.com

Phosphorescent materials are some of the most widely commercialized emitters for Organic Light Emitting Diode (OLED) displays. Cylcometalated iridium (III) complexes remain some of the most widely studied systems [1], but simulating the phosphorescent emission remains difficult using conventional quantum chemistry simulations such as Density Functional Theory (DFT). High accuracy simulations have been shown to be a necessary input for AI driven materials design [2]. Quantum computers and quantum algorithms are hypothesized to improve simulation accuracy, but currently few simulations have been conducted at scale to sufficiently evaluate the accuracy of quantum computing methods on commercially relevant size problems. The iterative Qubit Coupled Cluster (iQCC) theory is a method for performing electronic structure calculations on quantum computers [3-4]. It was developed in response to issues with the Unitary Coupled Cluster (UCC) theory as iQCC requires fewer quantum gate operations and allows flexibility with entangling patterns on physical hardware [3].

Nine phosphorescent materials were simulated using common DFT functionals B3LYP and CAMB3LYP with the SBKJC effective core potential on Ir and 6-31G* basis set on the other atoms [5]. Qubit Hamiltonians were generated from these geometries using the same basis set using either RHF orbitals for singlet states (S_0) and ROHF orbitals for triplet states (T_1) with CAS(36,36), where orbitals outside are treated as frozen. The iQCC simulations were run on classical hardware via a simulator with PT corrections [4] for 75 iQCC iterations with eight entanglers per iterations selected from DIS space [3]. The S_0-T_1 gap is calculated from the delta of the two states and compared to experimental results reported by Sajoto et al. [1] presented in Fig. 1.

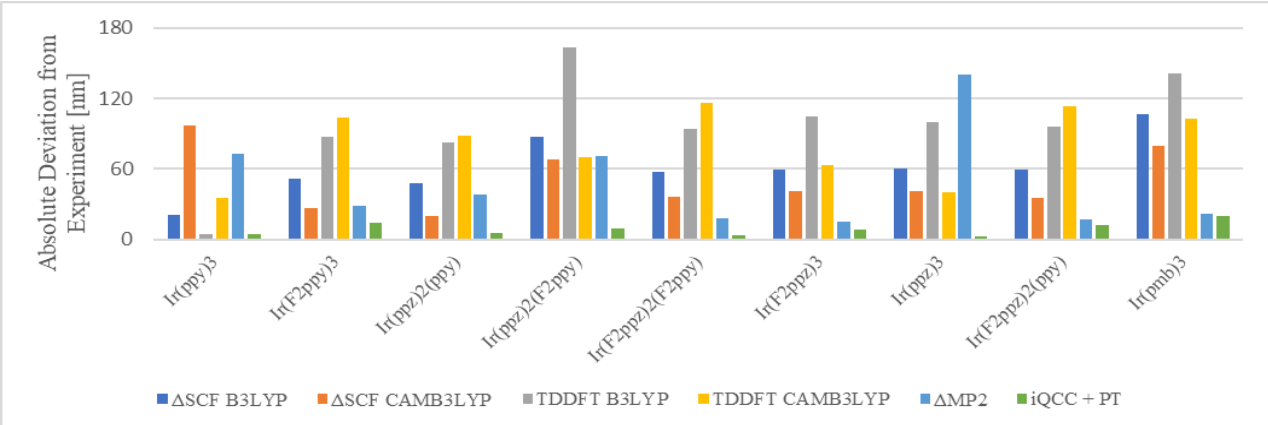

Fig. 1. Simulation comparison between selected DFT methods, MP2, and iQCC + PT vs experiment

The iQCC + PT correction provides a reliable estimate of the S_0-T_1 gap for the nine OLED phosphorecent materials and is more accurate and consistent than commonly used DFT methods. These results show that quantum computer methods, even when run on classical hardware via simulators, can improve the accuracy of materials simulations, and can potentially be a powerful new tool for enhancing the computational and AI driven design of display materials today.

References

1. Sajoto, T., Djurovich, P. I., Tamayo, A. B., Oxgaard, J., Goddard, W. A., Thompson, M. E. *J. AM. Chem. Soc.*, 131 p. 9813-9822 (2008).
2. Kim et al., SID 2021 Digest pp 314-316
3. Ryabinkin, I. G., Lang, R. A., Genin, S. N., Izmaylov, A. F. *J. Chem. Theo. Comp.*, 16(2) p.1055-1063 (2020)
4. Ryabinkin, I. G., Izmaylov, A. F., Genin, S. N., *Quantum Sci. Technol.* 6 (2021)
5. Ufimtsev, I.S., Martinez, T.J., *J. Chem. Theo. Comp.* 5, p.2619 (2009)

Digital twins in OLED development: A review on virtual characterization and improvement of OLED materials and devices

Tobias Neumann[1], Franz Symalla[1], Daniel Wehl[1], Timo Strunk[1], Simon Kaiser[2] and Wolfgang Wenzel[2]
[1]Nanomatch GmbH, Karlsruhe, Germany
Tel.:+49 721 95965454, E-mail: tobias.neumann@nanomatch.com
[2]Institute of Nanotechnology, Karlsruhe Institute of Technology, Karlsruhe, Germany

The vast chemical space of organic molecules promises the opportunity of designing materials and developing stack setups for perfect performance of organic electronic devices. As of now, experience and intuition of device designers and material scientists are the key drivers to optimized OLED materials and devices. This approach to R&D, however, is impeded by repeated trial&error and limited potential for automization. Computer simulations can support experimental efforts by (i) streamlining experimental efforts via efficient pre-screening of material performance and device setups (ii) enabling systematic, targeted design by allowing researchers to develop a fundamental understanding of how molecular properties trigger and balance microscopic processes and thereby impact device performance and (iii) applying AI-based approaches to enable a level of automization that is unmatched by purely experimental R&D. Key to achieve any of these goals are predictive models to compute performance of materials and stack setups with sufficient accuracy. Despite recent advances, fully predictive models connecting fundamental chemistry and device design still struggle due to the high level of complexity: a wide range of effects and processes need to be included, ranging from charge transport in pristine layers towards complex exticonic processes in mixed co-emission systems, and the complex interplay of processes renders the final outcome highly sensitive to the accuracy of each individual building block of comprehensive models.

In this work we present a review of recent improvements of our models for virtual material and device characterization based on first principles. Similar to prior work, we follow a seemless bottom-up multiscale simulation workflow to compute OLED material and device properties: We generate atomistic models of pristine or mixed thin films or interfaces with a simulation protocol mimicking physical vapor deposition using improved customized, molecule specific forcefields automatically derived from quantum chemistry. Subsequently we analyze the electronic structure of compounds in the thin film: We compute distributions of molecular properties such as transport energy levels, electronic couplings or excitation energies, taking into account the unique environment of molecules exclusively on a full-quantum-mechanical level to include local effects in mixed films or at interfaces. Using these distributions we construct digital twins of organic electronic (OE) devices on the 100nm-scale and conduct virtual measurements via simulations of charge and exciton dynamics to predict material and device properties such as mobility and I-V-characteristics. We conduct benchmarks of recent developments in various steps of the multiscale simulation workflow, leading to improved prediction accuracy especially regarding charge transport in layers and devices. We highlight how this approach can support experimental R&D with systematic identification of performance bottlenecks and targeted design of materials and devices.

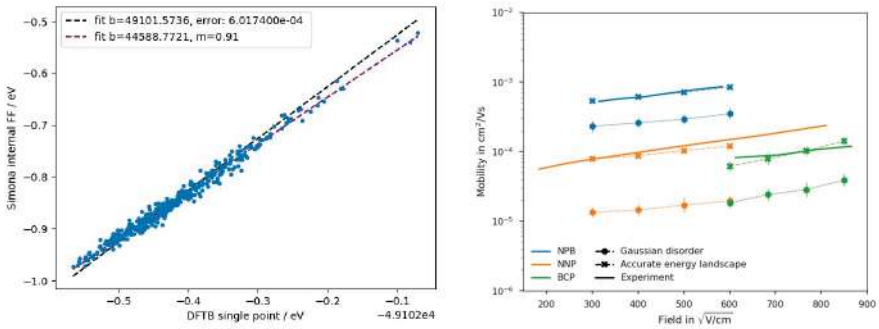

Fig 1: Left: Comparison of intramolecular energies of molecules in thin film morphologies computed with customized, molecule specific forcefields vs. DFT. Right: Using a more accurate model to compute site energies including local effects can impact prediction quality of charge carrier mobility positively (right panel from [4]).

References

[1] P. Friederich et al., *JCTC 10* (9), 3720-3725 (2014)
[2] F. Symalla et al., *SID Symp. Dig. of Tech. Pap.*, 50: 259-262, (2019)
[3] F. Symalla et al., *Materials. Adv. Theory Simul.*, 3 (2020)
[4] S. Kaiser et al., submitted (2021)

An Innovation Platform for Optoelectronics: Synergistic Acceleration of de novo Design Powered by Multiscale Simulations and Machine Learning

Mathew D. Halls[1], Yuling An[2], H. Shaun Kwak[3], Hadi Abroshan[2], Paul Winget[2], David J. Giesen[2], Anand Chandrasekaran[2], Mohammad Atif Faiz Afzal[3] and Christopher T. Brown[4]
[1]Schrödinger Inc., 10201 Wateridge Circle, San Diego, CA, 92121, United States.
Tel.: 01-858-822-9998, E-mail: mat.halls@schrodinger.com
[2]Schrödinger Inc., 120 West 45th Street, New York, NY, 10036, United States.
[3]Schrödinger Inc., 101 SW Main Street, Portland, OR, 97204, United States.
[4]Schrödinger Inc., 222 Third Street, Cambridge, MA, 02142, United States.

Future advancements in OLED displays depend on continued improvement and optimization of the constituent materials through rational design. Chemical innovation is needed to find solutions with superior efficiency, lifetime and processability. These required material performance improvements require both an efficient screen of large numbers of molecules and a conceptual understanding of the chemical properties leading to improved performance. The chemical design space for OLED materials is enormous, and complete enumeration to identify the most promising OLED material candidates for investigation remains impossible. Recent improvements in active learning lead to non-trivial improvements in the prediction of intrinsic chemical properties at significantly lower computational cost than brute force high-throughput approaches (Fig. 1a). However, these intrinsic properties do not necessarily lead to better OLED materials. Deleterious interactions between adjacent compounds can preclude the use of in real-world applications. The effect of processing conditions and the resulting solid-state effects alter the values and the distribution of controlling properties (Fig. 1b). It is through our combination of machine learning and physics-based approaches that material performance requirements can be met. Examples are presented in this work to demonstrate the effectiveness of these discovery techniques (Fig. 1c).

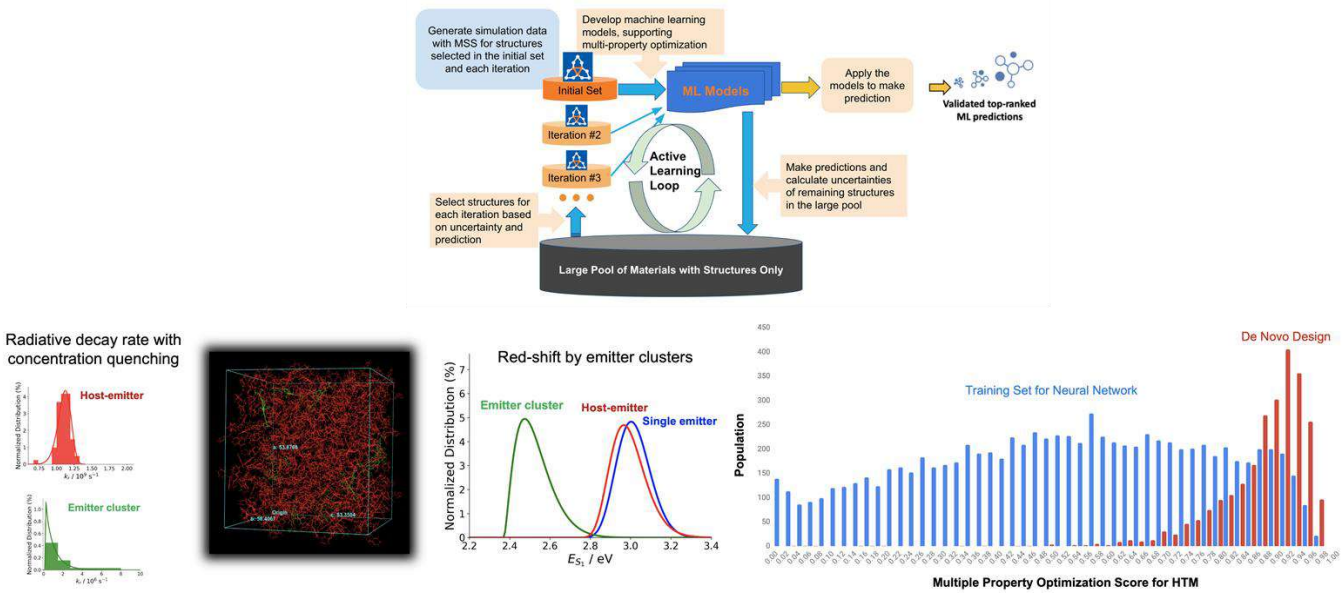

Fig. 1. (a, top) Active learning for optoelectronic property prediction workflow; (b, left bottom) Solid-state effect of a host-emitter film with concentration quenching and color shift by aggregation of emitters; (c, right bottom) Comparison of multiple property optimization (MPO) scores for HTM between training set and de novo designed structures.

Active Learning for the Accelerated Design and Optimization of Novel OLED Materials

Hadi Abroshan[1], Anand Chandrasekaran[1], Paul Winget[1], Yuling An[1], Shaun Kwak[1], Christopher Brown[1], and Mathew D. Halls[1]

[1]Schrödinger, Inc., New York, NY 10036, United States

Tel.:+1-503-299-1150, E-mail: hadi.abroshan@schrodinger.com

To date, the development of organic light-emitting diode (OLED) materials are primarily based on a combination of chemical intuition and trial-and-error experimentation. This Edisonian approach is often expensive and time-consuming, and in most instances fails to offer disruptive design directives for novel materials. Virtual high-throughput screening of molecular space assisted by machine learning (ML) has emerged as a powerful tool to accelerate the design and discovery of advanced OLED materials [1]. The key challenges for building predictive ML models for OLED materials are to acquire and manage a high volume of data, as well as to maintain high accuracy that properly assess the complexity of materials chemistry in OLED space.

Active learning (AL) machine learning is among several strategies developed to face the challenge in both materials science and life science applications [2,3], where the large-scale data management for the training set becomes a main bottleneck. In this work, we present a workflow that efficiently combines AL with atomic-scale simulations to reliably predict performance related optoelectronic properties of OLED materials. This study provides a robust and validated framework to account for multiple parameters that simultaneously influence OLEDs performance. Results of this work pave the way to better understand the activity of optoelectronic devices from a molecular perspective, and further screen candidate materials with superior efficiencies before laborious simulations, synthesis, and device fabrication.

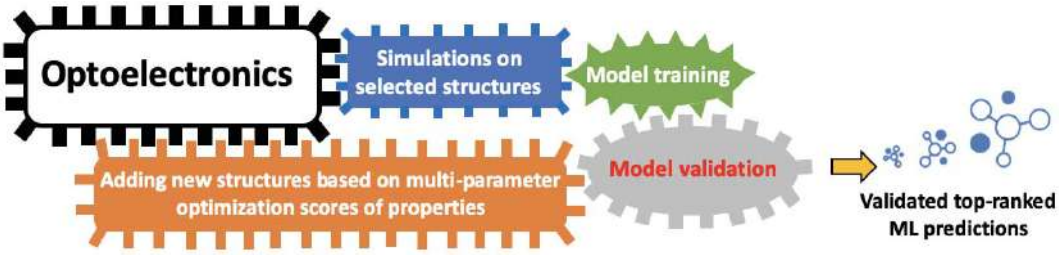

Fig. 1. Active Learning workflow for the design and discovery of novel optoelectronic molecules.

References

1. M.D. Halls, D. J. Giesen, T. F. Hughes, A. Goldberg, Y. Cao, H. S. Kwak, T. J. Mustard, and J. Gavartin, Proc. SPIE 9941, Organic Light Emitting Materials and Devices XX, 99411C (2016).
2. B. Rouet-Leduc, K. Barros, T. Lookman, and C. J. Humphreys, *Sci. Rep.*, 6, 24862 (2016).
3. K. D. Konze, P. H. Bos, M. K. Dahlgren, K. Leswing, I. Tubert-Brohman, A. Bortolato, B. Robbason, R. Abel, and S. Bhat, *J. Chem. Inf. Model.*, 59(9) 3782 (2019).

How to Make Fragile Bonds Less Fragile for Robust OLED Materials

Rui Wang[1], Qing-Yu Meng[1], and Juan Qiao[1]

[1]Department of Chemistry, Tsinghua University, Beijing, 100084, P. R. China

Tel.:82-2-563-7992, E-mail: qjuan@mail.tsinghua.edu.cn

The bond-dissociation energy of the most fragile bond (BDE_f) is a key parameter for the intrinsic stability of organic light-emitting diode (OLED) materials.[1-11] In particularity, many OLED molecules have the lowest BDE_f in anionic states ($BDE_f(-)$ ~1.6−2.5 eV),[3,8-10] which could be a fatal short-slab for device stability. We confirmed the close relationship between $BDE_f(-)$, intrinsic material stability, and device lifetime. Based on thermodynamic principles, we developed a general and effective strategy to greatly improve $BDE_f(-)$ by introducing negative charge manager within the molecule.[12] The manager must combine EWG with delocalizing structures to confine the negative charge. Consequently, it can substantially promote $BDE_f(-)$ by ~1 eV for various fragile bonds, which does outperform the effect of solely employing EWGs or delocalizing structures. This provides a new way to transform vulnerable building blocks for robust OLED materials and devices.

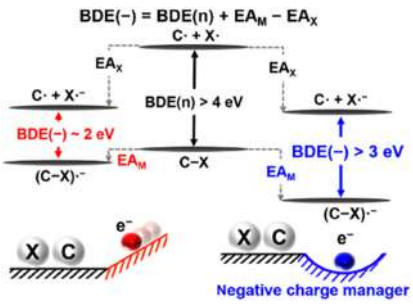

Fig. 1. Employing negative charge manager to make fragile bonds less fragile toward electrons.

Acknowledgment

This work was supported by the National Key R&D Program of China (grant nos. 2016YFB0401003 and 2016YFB0400702) and the National Science Fund of China (grant no. 51525304).

References

1. Scholz, S.; Kondakov, D.; Lüssem, B.; Leo, K. *Chem. Rev.*, *115*, 8449 (2015).
2. Zhao, C.; Duan, L. *J. Mater. Chem. C*, 8, 803 (2019).
3. Song, W.; Lee, J. Y. *Adv. Opt. Mater.* 5, 1600901 (2017).
4. Schmidbauer, S.; Hohenleutner, A.; König, B. *Adv. Mater.* 25, 2114 (2013).
5. Kondakov, D. Y.; Lenhart, W. C.; Nichols, W. F. *J. Appl. Phys.* 101, No. 024512 (2007).
6. Kondakov, D. Y. J. Appl. Phys. **2008**, 104, No. 084520 (2008).
7. Scholz, S.; Walzer, K.; Leo, K. *Adv. Funct. Mater. 18*, 2541 (2008).
8. Lin, N.; Qiao, J.; Duan, L.; Li, H.; Wang, L.; Qiu, Y. *J. Phys. Chem. C 116*, 19451 (2012).
9. Lin, N.; Qiao, J.; Duan, L.; Wang, L.; Qiu, Y. *J. Phys. Chem. C 118*, 7569 (2014).
10. Byeon, S. Y.; Han, S. H.; Lee, J. Y. *Adv. Optical Mater.* 5, 1700387 (2017).
11. Wang, R.; Wang, Y.-L.; Lin, N.; Zhang, R.; Duan, L.; Qiao, J. *Chem. Mater. 30*, 8771 (2018).
12. Wang, R.; Meng, Q.-Y.; Wang, Y.-L.; Qiao, J. *CCS. Chem.* doi.org/10.31635/ccschem.021.202100778 (2021).

Development of a New Blue Emitter Using Deep Learning Optical Spectroscopy

Joonyoung F. Joung[1], Minhi Han[1], Minseok Jeong[1], and Sungnam Park[1]
[1]Dept. of Chemistry, Korea University, Seoul 02841, Korea
Tel.:82-2-3602-3144, E-mail: spark8@korea.ac.kr

Over the decades, organic fluorescent and phosphorescent molecules used in organic light emitting diodes (OLEDs) have been extensively developed to meet several requirements including brightness and color purity. However, the full-width at half-maximum (FWHM) in the emission spectrum, which determines the color purity of organic emitters, is much broader than that of inorganic materials including quantum dots and perovskite materials. In addition, the FWHM in the emission spectrum of organic emitters is challenging to accurately estimate by any theoretical methods because it highly depends on several factors such as solute-solvent interactions and relaxation pathways. Bigdata-based deep learning method can be an alternative to overcome the limitation of theoretical methods and predict practically important properties including the FWHM and photoluminescence quantum yield (PLQY). In this work, we developed deep learning optical spectroscopy (DLOS) based on the experimental database. Our DLOS can accurately and quickly predict seven optical properties of organic molecules, namely, the absorption peak position and bandwidth, extinction coefficient, emission peak position and bandwidth, photoluminescence quantum yield (PLQY), and emission lifetime. Our deep learning model includes the solute-environment interactions so that the optical properties of organic molecules in solution, solid state, and gas phases can be distinctly predicted. Using our DLOS, we have successfully demonstrated the development of a blue emitter with desired optical properties as shown in Fig. 1. Our DLOS is an efficient and cost-effective tool to virtually screen pre-designed molecular structures for the optimal molecular structure with desired properties in the overall development process.

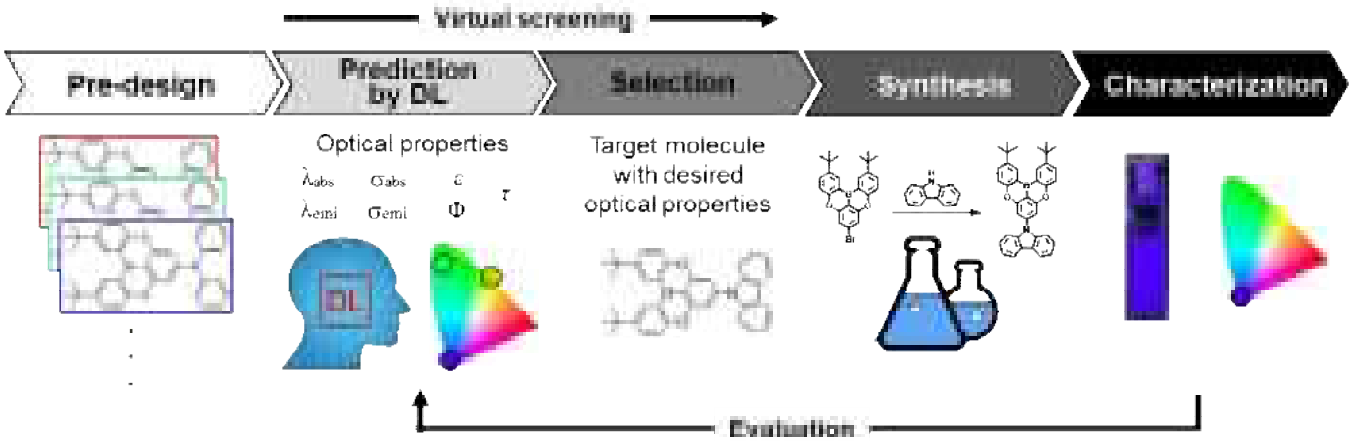

Fig. 1. Illustration of development of a new blue emitter using our deep learning optical spectroscopy.

In addition, we developed a web-based interface 'Deep4Chem' (http://deep4chem.korea.ac.kr/) that the general public can use to predict the optical properties, the electronic absorption and emission spectra, and the actual colors of organic molecules.

Acknowledgments

This study was supported by grants from the National Research Foundation of Korea (NRF) funded by the Korean government (No. 2019R1A6A1A11044070) and Korea University-Future Research Grant (KU-FRG).

References

1. J. F. Joung, M. Han, M. Jeong, and S. Park, *Sci. Data,* **7**, 295 (2020).
2. J. F. Joung, M. Han, J. Hwang, M. Jeong, D. H. Choi, and S. Park, *JACS Au*, online published, https://doi.org/10.1021/jacsau.1c00035 (2021).

Retrosynthesis Planning for Thermally Activated Delayed Fluorescence Molecules

Dongsun Yoo, Seran Kim, Sohae Kim, Jihye Kim, Saerom Park, Hoi-Lim Kim, Youngmi Cho, and Yongjo Kim
Display Research Center, Samsung Display Co., Ltd., Yongin-si, Gyeonggi-do 17113, Korea
Tel.:82-31-5181-6933, E-mail: dongsun.yoo@samsung.com

Designing novel molecules with the desired properties is a core problem in many fields of engineering, including display technology. However, it is extremely challenging because of the enormous design space. AI-assisted molecular design is attracting considerable interest as it can efficiently navigate through the huge design space, revealing novel molecular structures on its way. However, one of the biggest issue is that the proposed molecules are often not synthesizable or challenging to synthesize. To address this, there has been many efforts to assess synthetic accessibility (SA) of unseen molecules, from rather simple structural complexity score[1] to AI model trained on a huge reaction database[2]. Furthermore, there has been much study in the recent years on retrosynthesis planning, which suggests you the synthetic scheme leading to the target molecule.

In this work, we build a template-based retrosynthesis planning system specialized for thermally-activated delayed fluorescence (TADF) molecules, which is widely studied. Full retrosynthesis planning is performed by combining one-step retrosynthesis AI model with Monte Carlo tree search algorithm. We found that common reaction database extracted from United States Patent and Trademark Office (USPTO), which is widely used in retrosynthesis planning, cannot predict synthetic scheme well for TADF molecules. On the other hand, using the specialized reaction database, which contains synthetic scheme extracted from literatures for various TADF molecules, gives inferior prediction performance due to the small database volume. However, when we blend two databases together with appropriate weights on specialized database, we can achieve high prediction performance. With 3.6 million reactions of USPTO and a few hundreds of specialized reactions, we achieved about 67%/58% top-1 accuracy and 90%/89% top-5 accuracy on common/specialized database, respectively. In addition, we assess SA from the results of retrosynthesis planning. By extracting simple statistics from retrosynthesis results and using them as descriptors for simple machine learning model, we built a model which predicts total yield (which relates to SA).

References

1. P. Ertl and A. Schuffenhauer, *J. Cheminform*, 1, 8 (2009).
2. C. W. Coley, L. Rogers, W. H. Green, and K. F. Jensen, *J. Chem. Inf. Model*, 58(2), 252-261 (2018).

Core Technologies for High Resolution Stretchable AMOLED Display

H.W. Yoon[1], S.M. Shin[1], H.W. Kim[1], J.H. Kim[1], D.H. Kim[1], T.S. Park[1], T. Kim[11], B.S. Kim[1], K. Rhie[1], J. Kim[1], S.Y. Ryu[1], J. Song[1], B.-H. Cheong[1], T. Park[2], J.Y. Song[3], Y.-J. Kim[3], B.S. Bae[4], J.-H. Seo[5], H.K. Cho[6], J.K. Jeong[7], S.-M. Yoon[8], M.C. Suh[9], G. Domann[10], T.-W. Lee[11], W. Park[12], M.P. Hong[1]

[1]Department of Applied Physics, Korea University, Sejong, 33019, South Korea

Tel.:82-44-860-1321, E-mail: goodmoon@korea.ac.kr

[2]Department of Chemical Engineering, POSTECH, Pohang, Kyeongbuk, 37673, South Korea

[3]Advanced Manufacturing Systems Research Division, KIMM, Daejeon, 34013, South Korea

[4]School of Electronics & Display Engineering, Hoseo University, Asan, Chungnam, 31499, South Korea

[5]Department of Materials Engineering, Korea Aerospace University, Goyang, 10540, South Korea

[6]Research Center for Advanced Materials Technology, Sungkyunkwan University, Suwon, 16419, South Korea

[7]Department of Electronic Engineering, Hanyang University, Seoul, 04763, South Korea

[8]Department of Advanced Materials Engineering for Information and Electronics, Kyung Hee University, Yongin, Gyeonggi, 17104, South Korea

[9]Department of Information Display, Kyung Hee University, Seoul, 02447, South Korea

[10]Fraunhofer Institute for Silicate Research, Germany

[11]School of Chemical and Biological Engineering, Seoul National University, Seoul, 08826, South Korea

[12]LG Display R&D Center, Seoul, 07796, South Korea

Recent stretchable devices are focused on the high stretchability but clearly reveal poor resolution and productivity [1]. There have been a growing demand for the high image quality even if it is multi-folded or stretched. In order to create high-resolution stretchable displays beyond the limits, we have developed the proper solutions such as elastomeric substrate, stretching lamination, glassy metal, and pixelized encapsulation. Using these core technologies, we have fabricated a 3.4-inch stretchable active matrix OLED that provides 110 ppi full color, following the process flow shown in figure 1. The 0.6-um-thick ultra-thin polyimide film attached to the prestrain elastomer comprises a stretchable panel and operates under 20% strain using a combination of stress relieving glassy metel layers with conventional Al/Mo bus-line electrodes and wrinkles on the well-stretchable area that reduce the mechanical stress on sensitive devices. R-G-B OLED pixels were encapsulated individually by a photo-patterned bilayer consisted of advanced ORMOCER hybride polymer (2 um) and stoichiometric Si_3N_4 thin film (100 nm) which provides the WVTR of 6.2 x 10^{-6} g/(m^2day) [2]. We believe this approach could be most realistic strategy for high-resolution stretchable AMOLED displays enabling the cost-effective mass production.

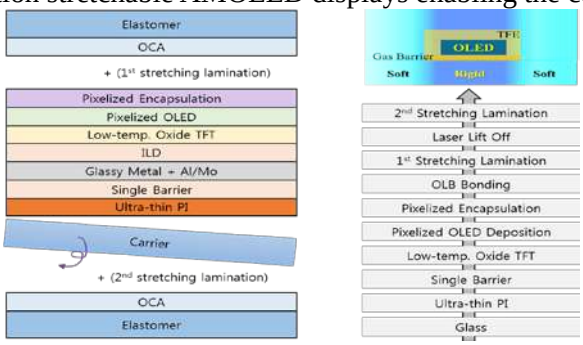

Fig. 1. A schematic of 3.4-inch stretchable active matrix OLED panel structure and process flow to fabricate on elastomers.

Acknowledgment

This work was supported by the Future Growth Engine Program (10079974, Development of core technologies on materials, devices, and processes for TFT backplane and light emitting front plane with enhanced stretchability above 20%, with application to stretchable display) funded by the Ministry of Trade, Industry and Energy (MOTIE, Korea).

References

1. Y. Lee, et al., Sci. Adv. 7, eabg9180 (2021).
2. S.M. Shin, et al., Appl. Phys. Lett. 118, 181901 (2021)

Highly Stretchable and Recoverable Rollable AMOLED Display

TaewoongiKim,iJinhwaniChoi,iDongwoniChoi,iSangjuniLee,iJonghwaiLee,iJaehoiAhn,iJiyeoniKim,iBeomjiniKim,iTaehoiKim,iSanghwaniCho,iSungchaniJo,iChangheeiLee,iandiJinohiKwagi
Display Research Center, Samsung Display, Youngin-si, Gyeinggi-do, 17113, Korea
Tel.:82-31-5181-5664, E-mail: taewoong68.kim@samsung.com

New backplane structure with flexible organic dielectric layer as ILD (Inter-Layer Deposition) layer has been proposed to effectively reduce mechanical stress in LTPS TFT under bending stress. With this new structure, the backplane and display panel are able to be bent to an ultimate bending radius of 1mm after 200,000 bending cycles without any TFT degradation, panel image degradation, and any mechanical damage observed.

For rollable displays undergoing extreme strain, new module structure using highly stretchable and elastic thermoplastic polyurethane layer has also been suggested to excellently distribute and minimize the accumulated stress exerted on module during rolling stress. With the new module structure, the rollable panel and module can be rolled up to an ultimate rolling radius of 5 mm after 100 hours (7.2 inch) or after up to rolling radius of 15 mm after 50,000 rolling cycles (14 inch) without any visible panel degradation and any noticeable physical damage observed and be returned to almost original flat state (deformation height of 14mm for 7.2 inch and 11mm for 14 inch) after static rolling of 100 hr and cyclic rolling of 50,000, respectively.

The new low stress panel and module structure enables the manufacture of rollable display with significant mechanical flexibility and robustness.

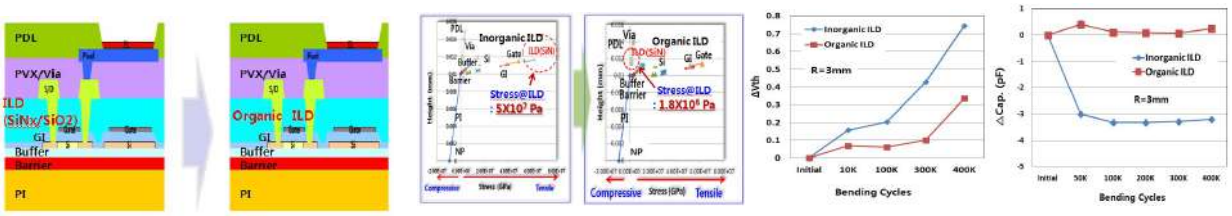

(a) (b)

Fig. 1. (a) Stress distribution inside LTPS TFT backplane for inorganic layer (SiNx) and organic layer, (b) electrical properties of LTPS TFT for inorganic layer (SiNx) and organic layer after bending cycles of 200,000 at bending radius of 3mm.

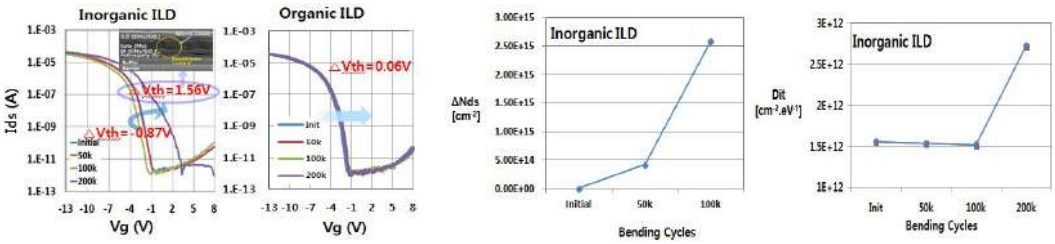

(a) (b)

Fig. 2. (a) Transfer curve of LTPS TFT for inorganic layer (SiNx) and organic layer, (b) Defect density and density of state at interfacial trap for LTPS TFT with inorganic ILD (SiNx) after bending cycles of 200,000 at bending radius of 1 mm.

References

1. Z. Suo, E. Y. Ma, H. Gleskova, and S. Wagner, *Appl. Phys. Lett.*, 74, 1177 (1999)
2. H. Gleskova, S. Wagner, W. Soboyejo and Z. Suo, *J. Appl. Phys.*, 92, 6224 (2002)
3. H. Gleskova, I. C. Cheng, S. Wagner, and Z. Suo, *Solar Energy*, 80, 687 (2006)

Highly Efficient, Heat Dissipating and Geometrically Stretchable Organic Light-Emitting Diodes Based on Thin Elastomer with Silicon Dioxide Nanoparticles

Dong Hyun Choi[1,2,3], Jun Su Yang[1], Dong Hyun Kim[1,2,3], Chang Min Lee[1,2,3], Hyung Ju Chae[1,2,3], Geon Woo Jeong[1,2,3], Tae Wook Kim[1,2,3], Subrata Sarker[1,2,3] and Seung Yoon Ryu[1,2,3,*]

[1]DivisioniofiDisplayiandiSemiconductoriPhysics,iDisplayiConvergence,iCollegeiofiScienceiandiTechnology,iKoreaiUniversityi SejongiCampus,i2511iSejong-ro,iSejongiCityi30019,iRepubliciofiKorea
[2]DepartmentiofiAppliediPhysics,iKoreaiUniversityiSejongiCampus,i2511iSejong-ro,iSejongiCityi30019,iRepubliciofiKorei
[3]E-ICT–Culture-SportsiConvergenceiTrack,iKoreaiUniversityiSejongiCampus,i2511iSejong-ro,iSejongiCityi30019,iRepublici ofiKoreaiE-maili:ijustie74@korea.ac.kr

We demonstrated highly efficient, and geometrically stretchable organic light-emitting diodes (GSOLEDs) with molybdenum trioxide (MoO_3)/gold (Au)/MoO_3 (MAM) as a transparent electrode[1]. The devices were fabricated on a mechanically pre-strained UV-curable elastomer (NOA63)/3M using the adjusted transfer printing method. The electroluminance (EL), color coordinates, and device performance of the remained unchanged during intense stretching (0%–100% strain). Also, the GSOLEDs did not show chromic shift in the color coordinates because of the highly transparent MAM electrode with an insignificant microcavity effect. For enhancing the geometrical stretchability and device performance, we reduced the substrate thickness dramatically. The reduced thickness improved heat dissipation owing to minimized triplet-triplet annihilation that resulted in a consistent performance at high exciton density. Additionally, enhanced out-coupling was achieved by inserting silicon dioxide nanoparticles (NPs) into NOA63 elastomer. Moreover, the porous scaffold design of NPs was helpful for heat dissipation as evidenced in the Time-resolved Electroluminescence (TREL) of the devices. Consequently, a remarkable device performance with a high current efficiency of 82.4 cd/A, and external quantum efficiency of 22.3% was achieved without critically significant efficiency roll-off. The device performance was verified with optical and mechanical simulations, which further confirmed that the proposed method has successfully developed efficient GSOLEDs for stretchable/flexible and wearable, optoelectronic, and biomedical applications. Moreover, the measurement of the lifetime of the encapsulated GSOLEDs with sandwich structure suggested that the stability of the GSOLEDS could be enhanced further with improved encapsulation.

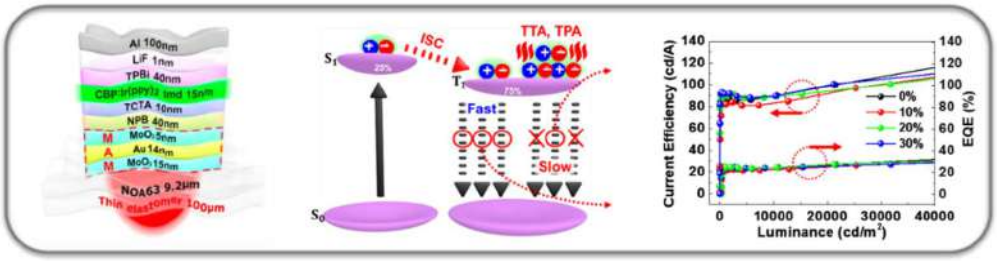

Fig 1. Schematic of the device, heat dissipation mechanism, and the performance of the GSOLEDs.

1. Choi et al., "Highly Efficient, Heat Dissipating, Stretchable Organic Light-Emitting Diodes Based on an MoO3/Au/MoO3 Electrode with Encapsulations", *Nature Communications*, 2021, In Press

Highly transparent OLED for Textile Displays utilizing Dielectric/Metal/Dielectric electrode

Junwoo Lee, Seungyeop Choi, Tae-Woo Lee, and Kyung Cheol Choi*
School of Electrical Engineering, KAIST, Daejeon 34141, Korea
**Tel.:82-42-350-3482, E-mail: kyungcc@kaist.ac.kr*

Recently, as state-of-the-arts displays, wearable electronic devices and free-form displays have begun to attract attention in the display market. With the growing demand for wearable devices, wearable displays are evolving to become thinner, softer, and more flexible. Thus, research on textile displays as ultimate platforms of wearable electronic devices has been active with many studies reported in the literature.

In our group's previous research, actual textile-based OLEDs were fabricated through an implanting process of an ultra-thin planarization layer[1,2]. Based on this outcome, textile-based transparent OLEDs utilizing dielectric/metal/dielectric transparent electrodes[3] were demonstrated. A thin silver layer with a thickness of 8 nanometers was used as metal layer on the anode and cathode. ZnS, MoO_3, Cs_2CO_3 serve as dielectric layers. Transmittance of the OLEDs is simulated by MATLAB code, which is formulated based on Fresnel's transfer equation. Measurements are taken using a UV-vis spectrometer. Figure 1 shows (a) a planarized textile substrate and a red textile trOLED which is turned on and off. Here, (b) shows the simulated (theoretical) and experimental transmittance results of red trOLEDs, and (c) compares the electrical performance outcomes of red trOLEDs formed on a textile substrate and on a glass substrate.

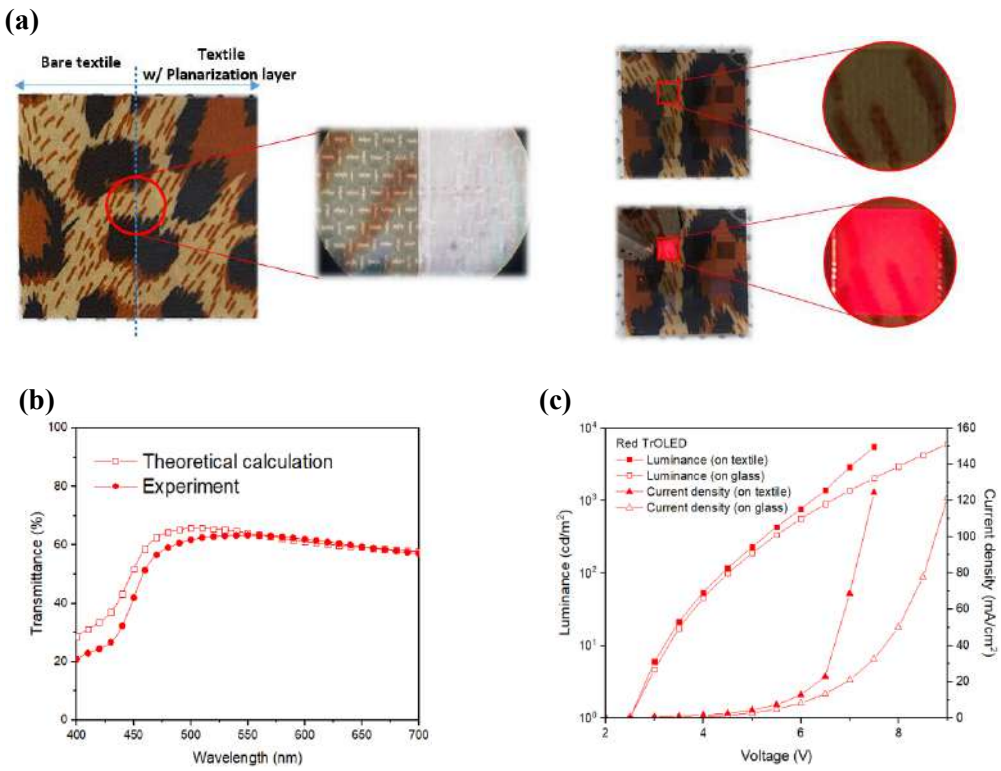

Fig. 1. Textile-based red trOLEDs: (a) planarized textile substrate and images of operating textile trOLEDs, (b) transmittance curve, and (c) current density-voltage-luminance curves of trOLEDs

Acknowledgment

This work was supported by the National Research Foundation of Korea(NRF) grant funded by the Korea government(MIST) (No.NRF-2019R1A2C3010012)

References

1. Choi, S., et al., *Scientific reports*, **7**(1), 1-8 (2017).
2. Choi, S., et al., *npj Flexible Electronics*, **4**(1), 1-9 (2020).
3. Kim, D., et al., *Advanced Functional Materials*, **25**(46), 7145-7153 (2015).

Water-resistant Stretchable Organic Light-emitting Diode via a Laser-cutting Process

Jaehyeock Chang, Minwoo Nam, and Kyung Cheol Choi
School of Electrical Engineering, KAIST, Yuseong-gu, Daejeon 34141, Korea
Tel.:82-42-350-3482, E-mail: kyungcc@kaist.ac.kr

Stretchable displays attract attention as an essential technology for the information interface between stretchable devices and users: They need to be expandable and deformable and have desired shapes. Numerous light sources have been introduced to realize the stretchable display, such as alternating current electroluminescent devices, quantum-dot devices, inorganic light-emitting diodes, and organic light-emitting diodes (OLEDs). Among them, OLEDs are considered a strong candidate for the realization of the stretchable light source due to their lightweight, harmless mechanism, and reasonably high efficiency compared to other light sources.

Three types of strategies have been presented for the realization of stretchable displays with organic-light emitting diodes. One is to employ intrinsically stretchable materials[1], another is to benefit from a wrinkled structure[2], and the other is to design a geometrically stretchable structure[3,4]. The geometrically stretchable design employs a thermally deposited OLED to achieve high efficiency and mechanically robust structure. Lim et al.[3] and Kim et al.[4] proposed hybrid stretchable platforms, which consist of a bi-substrate system: an OLED substrate and an elastomeric substrate. The OLED substrate has islands for OLED layers and serpentine-shaped electrode bridges supported by an elastomeric substrate with stress-relieving structures. However, their complicated fabrication process for patterning the OLED substrate (negative photoresist (SU-8)) results in long fabrication time and low throughput of devices.

This paper proposes a highly efficient and stretchable OLED with a simple laser-cutting process. With the laser-cutting process, it is fast and easy to accurately pattern the substrate with high throughput. The OLED structure shows little change in electro-optical performance until 60% elongation, as shown in Fig. 1(a), and has an operational lifetime of over 100 hours for a luminance loss of 50% in ambient air. The device is also water-resistant, as demonstrated in Fig. 1(b), so that it can be applied to bio-modulation or wearable display systems. To the best of our knowledge, it is the first stretchable OLED that can operate in water with high efficiency and mechanical robustness.

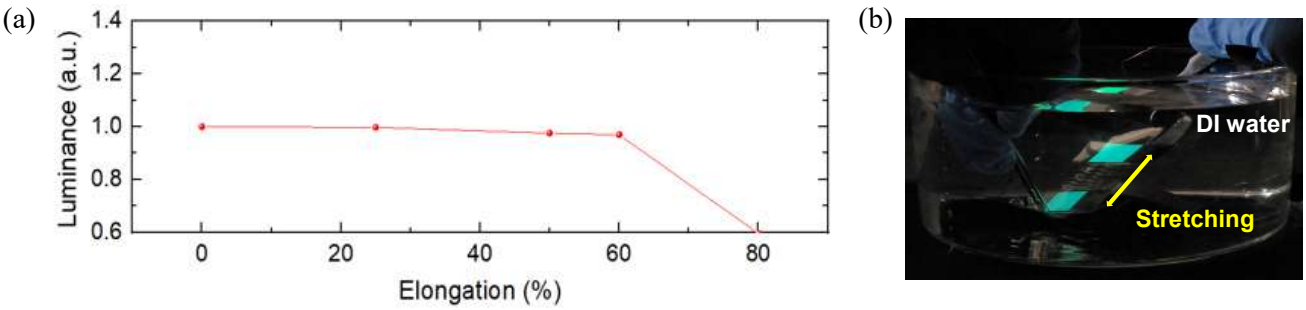

Fig. 1. (a) Luminance of the OLED under elongation, (b) the OLED device inside deionized water

Acknowledgment

This research was supported by the Nano·Material Technology Development Program through the National Research Foundation of Korea(NRF) funded by the Ministry of Science, ICT and Future Planning(NRF-2016M3A7B4910635)

References

1. H. Gao, S. Chen, J. Liang, and Q. Pei, *ACS Appl. Mater. Interfaces*, 8(47), 32504-32511 (2016)
2. S. Jeong, H. Yoon, B. Lee, S. Lee, and Y. Hong, *Adv. Mater. Technol.*, 5(9), 2000231, (2020)
3. M. S. Lim, M. Nam, S. Choi, Y. Jeon, Y. H. Son, S. M. Lee, and K. C. Choi, *Nano Lett.*, 20(3), 1526-1535 (2020).
4. T. Kim, H. Lee, W. Jo, T. S. Kim, and S. Yoo, *Adv. Mater. Technol.*, 5(11), 2000494, (2020)

Ghosts and Other Motion Artifacts that Haunt Displays

Dale Stolitzka
Samsung Display America Lab, San Jose, CA 95134, USA
Tel.:1-408-544-4499, E-mail: d.stolitzka@samsung.com

Motion artifacts are routinely identified through visual testing using scrolled or flickered motion patterns. New techniques to characterize the visual results will be part of upcoming certification procedures by VESA and others. Certifications that carry a logo are important because they can influence consumer buying decisions and help highlight awareness of a display's performance, thus justifying added market value. Users dislike blurry images, yet ghosts will appear when blur mitigation or sharpening is too aggressive.

Optimum panel technology renders an image and holds it perfectly during the frame time. OLED panels perform this task well by changing the luminance level from the old frame to the new one with remarkable speed, about 100 microseconds. Since the responsiveness to luminance change is sharp, blur occurs only due to frame persistence – the inverse of frame refresh rate. Displays may reduce frame persistence by faster refresh, say 240 Hz rather than 144 Hz or by strobing the backlight to flash images multiple times during the frame time – detectable by Flicker Modulation Amplitude tools. To characterize visible blur a high-speed camera can record the frame changes, with a moving bar pattern and then build a blur image based on the sharpness of the frame change and compensate for blur created when the human eye tracks motion across the screen, an analog effect. Excessive blur arises when the transition period is not fast. LCD monitor panels change luminance due to LCD transparency change in a few to ten milliseconds. In HDR TVs, a backlight ramp could last 100s of milliseconds. Sharpening and overdrive were invented to oppose slow ramping and clear up blur.

Excessive overdrive shown in Figure 1 led to visible artifacts that create ghosts. The test examined a 27-inch gaming monitor refreshing at 240 Hz. A high-speed camera recorded a moving gray bar from 0.7 m, a typical viewing distance. The top picture shows a visible line on either side of the bar caused by extremely overdriving the edge transitions. The overdrive causes more white than desirable as the white bar leads into a gray region and a black line on the trailing edge of the moving bar. The bottom picture shows the default performance out of the box where the moving bar appears blurry but without undershoot or overshoot. On the right, is the IDMS overdrive characterization figure and our equations for reporting overdrive as overshoot and undershoot.

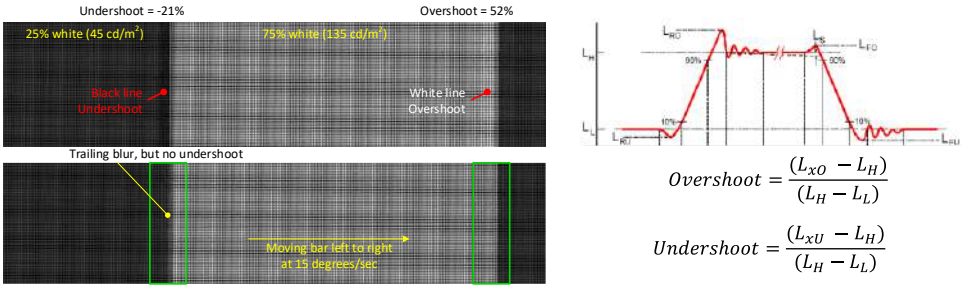

$$Overshoot = \frac{(L_{xO} - L_H)}{(L_H - L_L)}$$

$$Undershoot = \frac{(L_{xU} - L_H)}{(L_H - L_L)}$$

Fig. 1. Moving bar test shows artifacts from excessive overdrive (top); IDMS overdrive definitions (right).

This monitor as well as most monitors have overdrive controls. We used those controls to change the default response and found a visible threshold for ghosts just under 20% overdrive through a blind subjective test with eight participants and correlated their opinions to luminance recorded by the high-speed camera.

Identifying the threshold for ghost creation is critical in display compliance since it sets a metric by which excessive overdrive can be a disqualification for one display over another. In today's competitive landscape, fair testing is the only way a logo certification program will gain consumer and reviewer confidence. VESA has developed several programs in 2020 and the first half of 2021 that will aid consumer confidence toward great gaming displays with excellent market value.

References

1. VESA Motion Frequency Compliance Test Specification ver. 1.0, www.vesa.org (2020).
2. International Display Measurement Standard (IDMS) ver. 1.03b, www.sig.org (2012).

Deep Learning based Image Quality Restoration for Display Defects Detection using X-ray Inspection

Byungseok Min
XAVIS Co. Ltd, Pangyoyeok-ro 225-15 Seongnam-si ,Gyeonggi-do, Korea
Tel.:82-31-740-3811, E-mail:bmin@xavis.co.kr

Generally, most of display micro-defects such as pinholes, scratches and particles in TFT-LCD, OLED panels are automatically inspected by means of camera inspection system in presence of lighted condition, as known as Automated Optical Inspection(AOI). However, as the display paneles have additional layers on top of the panel by going through manufactoring processes, defects cannot be observed abserved and visually inspected. In that case, non-destructive testing method such as ultrasound or X-ray can be used, where Automated X-ray Inspection (AXI) are genrally used not only in display defects but also semiconductor and PCB defects inspection. However, the most critical shortcoming of the AXI systems is in the slow inspection speed compared to AOI, where most of times are spent on the X-ray image acquisition. From the fact that the better image quality is achieved with the higher amount of X-ray dose, there have been many research to improve X-ray image quality with smaller amount of X-ray dose to reduce the X-ray capturing time, and to minimize X-ray expose on human body.

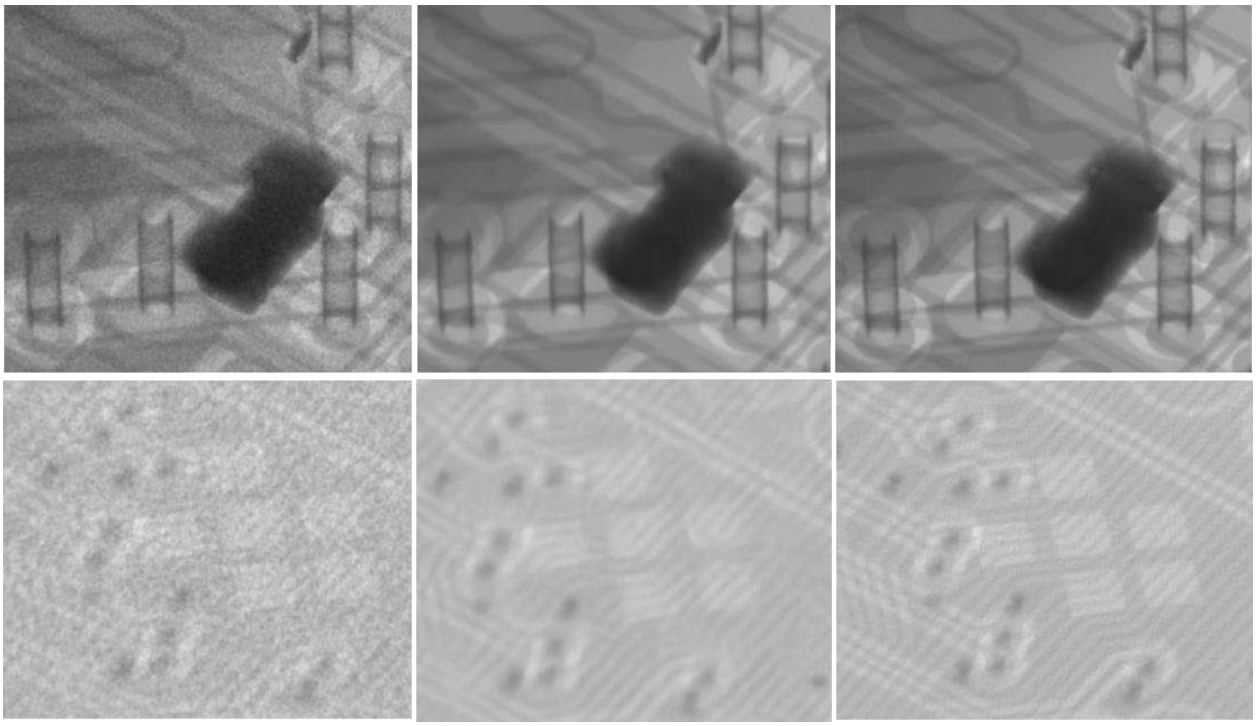

1) Low quality input (1/10 sec. Capture) | 2) Deep learning output (1/10 sec. Capture) | 3) Ground truth image (10 sec. Capture)

Figure 1. X-ray image comparison

In this paper, a CNN based deep learning model is introduced to inspect display defects, where a pairs of low quality and high quality X-ray images are given to the deep learning model for training. Five different data-set are acquired by changing capturing time for non-mocing objects, and fed to the deep learning model for training. Figure 1. shows a result for a semiconductor sample X-ray image that X-ray noise in the image is well reduced while showing slightly blurred edge, which needs to be improved by further experiments with various training set.

References

1. Y. Sun and X. Guo, *J. Xray Sci Technol.*, 25(6), p. 857 (2017).
2. Y. WangQ. Teng and T.Zhang, *Computer & Geosciences*, vol. 133, (2019).

Simulation of Image Quality using Optical Properties of Light-Emitting Device and Panel Structure

Gunshik Kim[1], and Jongbeom Hong[1]
[1]**Display Research Center, Samsung Display, Giheung-gu/Yongin-Si, Gyung-gi-Do 17113, Korea**
Tel.:82-31-5181-6761, E-mail: gunshik.kim@samsung.com

In recent years, OLED display has been used to premium models of smart-phones which give us a great image quality. But the exterior design of product leads the flexible OLED display manufacturing. So we consider that display images with the shape of product which means size, curvature and slope of display. With bended display, displayed pictures are slightly distorted in color, brightness, resolution and aspect ratio. So it is important to predict the displayed image quality in device design phase, or display shape concept-design phase.

For exterior design of product, bended or curved displays are used to new smart-phones in recent years. With this bended display, images are slightly distorted from color, brightness distribution because of pixel characteristic of viewing angle, viewer position, display bending shape and bending radius. For pre-design the product with edge shaped phone, we studied the Image Quality Prediction Method of Various Type of self-emissive display.

First, we need OLED thin-film optical device simulation and input digital signal of each pixel to optical characteristic internal the panel with angular distribution. Second, ray-tracing analysis of display pixel and viewer position to evaluate the luminance and the color of recognized. Last, display the predicted images to monitor, sub-pixel rendering to digamma the optical information to digital signal. This complex analysis method gives the predicted images from light-emitting materials, OLED device structure of R G B, input digital image, bended display shapes or bending radius and viewer position(Fig.1).

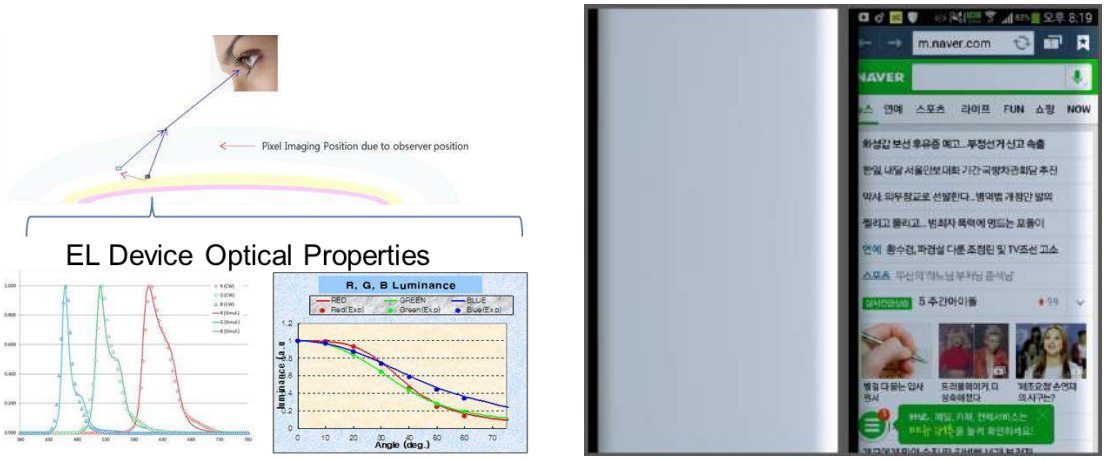

Fig. 1. Example of image quality prediction modeling and simulated images according to light-emitting devices and observation positions

We expect this simulation model will give helpful guide or results to design OLED light-emitting material, thin-film device structure development, the product designers and the GUI designers. In addition, by developing a technology for cognition and quantification of such predictive images, it has become possible to reflect and consider the product shape from the development stage of materials and devices.

Acknowledgment

References

1. Krlstiaan A. Neyts. Simulation of light emission from thin-film microcavities. *J. Opt. Soc. Am. A* 15, No. 4, 962–971 (1998)
2. Mukai N., Y.Makino and Y.Chang. Ray tracing based fast refraction method for an object seen through a cylindrical glass. *20th International Congress on Modelling and Simulation, Adelaide, Australia* (2013)

Visualization of Color Gamut Intersection Using Gamut Rings

Kenichiro Masaoka
NHK Science & Technology Research Laboratories, 1-10-11 Kinuta, Setagaya, Tokyo, Japan
Tel.:81-3-5494-3323, E-mail: masaoka.k-gm@nhk.or.jp

The color gamut of a display is a volume in a perceptually homogeneous color space, ranging from its black point at the bottom to white at the top, having cusps outward with its most saturated colors. To inspect at which points the range of hue, chroma, and lightness lie, a single-angle view in the cylindrical color space can frequently be misleading because parts of the gamut are almost always obscured from view. A solution to this problem is the use of a new diagram that displays "gamut rings."

The gamut ring framework unwraps the important volumetric information and lays it flat in a manner that provides the information required to describe the full-color capability. In the framework, a 3D color gamut is sliced at constant lightness intervals and the gamut volume is proportionally converted into 2D rings. Fig. 1 shows the 3D envelope of the Rec. 2020 color gamut in the CIELAB color space. The gamut is segmented into a 10-interval lightness scale. The areal dimension of the rings within a lightness and hue angle range corresponds to the volume within the same range. The outer gamut ring area corresponds to the gamut volume. The colored lines are constant-hue radial spokes of the RGBCMY primaries/secondaries. Note that the white point of the reference color space (originally CIE standard illuminant D65) is set to CIE illuminant D50 using the linear Bradford chromatic adaptation transform in the color gamut calculation.

A more useful technique is to visualize the gamut intersection between a display and a reference color gamut on the gamut rings of the reference gamut. Fig. 2 shows the envelope of the color gamut of a laser display and compares its gamut rings to the outer ring of Rec. 2020. The translucent orange regions shown in Fig. 3 indicate the gamut ring intersections between the display and Rec. 2020 on the Rec. 2020 rings. The total area of the regions corresponds to the volume of Rec. 2020 gamut covered by the display.

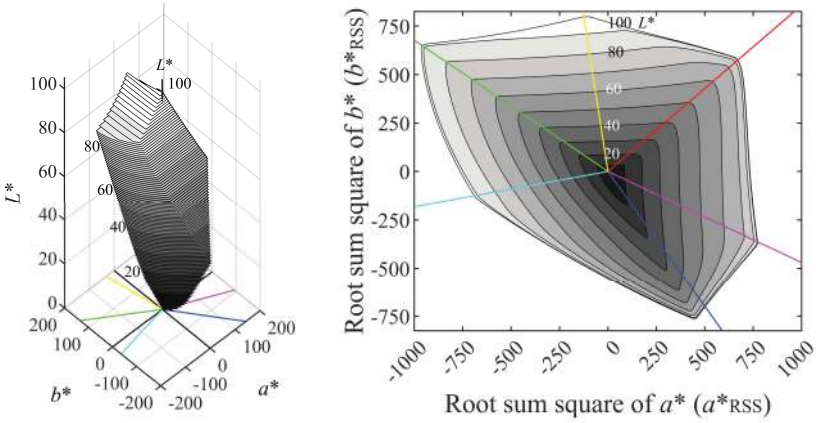

Fig. 1. Color gamut envelope and gamut rings of Rec. 2020.

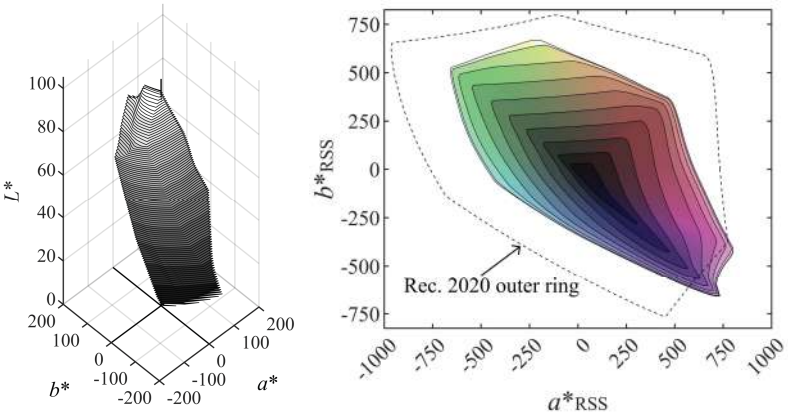

Fig. 2. Color gamut envelope and gamut rings of the laser display.

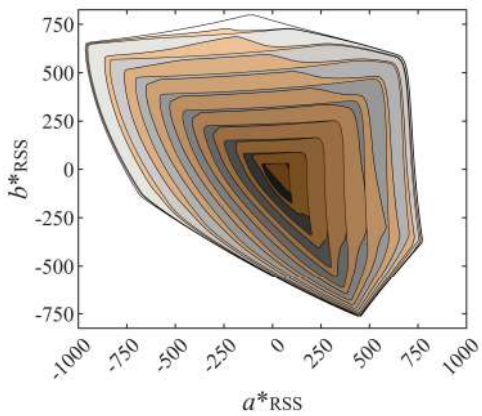

Fig. 3. Gamut ring intersections between the display and Rec. 2020.

References

K. Masaoka, F. Jiang, M. D. Fairchild, and R. L. Heckaman, *J. Soc. Info. Display*, 28, 273–286 (2020).

Tone Reproduction of Transparent Display Under Various Background-surround Conditions

Pei-Li Sun[1], and Yu-Ting Cheng[1] and Hung-Chung Li[2]
[1]National Taiwan Univ. of Science and Technology, Taipei, 10607, Taiwan
Tel.:82-2-563-7992, E-mail: plsun@mail. ntust.edu.tw
[2]Chang Gung University of Science and Technology, Taoyuan, 333, Taiwan

Transparent displays could be applied under different kinds of lighting environments, which would seriously affect its contrast of the on-screen image. Many studies have been contributed to finding the optimal tone curves for transparent displays with different viewing conditions[1,2,3]. TOLED performs color addition, which showed a clear image when the through-screen luminance was low; whereas TLCD performs color subtraction that needs a strong through-screen luminance to enhance its image contrast. The two types of transparent display must be studied individually.

In the study, psychophysical experiments were conducted to simulate various viewing conditions of both TOLEDs and TLCDs on a 400nit high dynamic range (HDR) LCD display. 12 young observers participated in this experiments. In order to find the best perceptual-match of the tone curve under each condition, the observer used a paired comparison method to select the image with a tone close to the reference sRGB condition. 4 gamma values (1.70, 1.95, 2.20, and 2.45) were tested. A GUI was used to simulate the virtual conditions. Observer viewed the GUI with a chin holder in 50 cm distance. The viewing field of the test image was in 20 degrees roughly. The background area was from 15 to 30 degrees. Surround area was within 25 to 50 visual degrees roughly. For TLCD simulation, the parameters included 3 levels of display luminance (denoted as Y_w), 4 levels of background luminance (Y_b), 2 levels of surround luminance (Y_s). In terms of TOLED simulation, the parameters included 4 levels of through screen luminance (denoted as Y_t), 2 levels of display luminance (Y_w), 4 levels of background luminance (Y_b), 2 levels of surround luminance (Y_s). The perceptual-matched gammas were summarized from the experimental data and predicted by surround-to-display luminance ratio (S_r). However, the S_r for TLCD and TOLED cannot predict the gamma well, the Pearson correlation coefficient (*r*) of the fitting were 0.388 and 0.028 respectively. We noticed that the background has much higher impact to the surround. After apply the ($0.9Y_b+0.1Y_s$) weighting for the surround luminance estimation, the *r* heightened to 0.836 for TLCD (referring $S_{r\,(TLCD)}$ in Table 1), however the TOLED were only 0.402 using the function. Modified functions there is needed for TOLED as shown in $S_{r\,(TOLED)}$ in Table 1. The X_2 is the Michelson contrast of TOLED where Y_w represents dynamic range and (Y_w+2Y_t) represents the sum of white and black luminances. The $S_{r(TOLED)}$ could enhance the *r* value to 0.677. Table 2 lists recommended gamma values under dim, average and bright conditions for TLCD and TOLED respectively.

Table 1. Input parameters

Symbol	Function	Corr.
$Sr_{(TLCD)}$	$(0.9Y_b+0.1Y_s)/Y_w$	0.836
$Sr_{(TOLED)}$	$X_1+0.9(1-X_2)$	0.677
X_1	$(0.9Y_b+0.1Y_s)/(Y_w+Y_t)$	
X_2	$Y_w/(Y_w+2Y_t)$	

Table 2. Recommended gamma values

Conditions	TLCD		TOLED	
	S_r range	Gamma	S_r range	Gamma
Bright	$S_r > 1.5$	1.89	$S_r > 1.8$	1.91
Average	$1.5>S_r>0.5$	2.23	$1.8>S_r>0.3$	2.01
Dim	$S_r < 0.5$	2.34	$S_r < 0.3$	2.32

Based on the psychophysical experiment mentioned above, we recommend gamma tables of transparent display (TLCD and TOLED) as Table 1 and Table 2 for image appreance match under various viewing condtions. More research is needed on image enhancement, quality assessemnt and measuring standards on the transparent displays under vairous environments.

References

1. Y. T. Cheng et al., *Proc. of IDW'20*, vol. 27, p. 592 (2020).
2. H. P. Chien and P. L. Sun., *Proc. of IDW'16*, vol. 21, p. 953 (2016).
3. Y. Kwak, et. al. *SID Digest*, vol. 45, p. 1123 (2014).

Subjective Quality Assessment of VESA Display Stream Compression Codecs

Robert S. Allison[1], and Laurie M. Wilcox[2]
[1]Centre for Vision Research, York University, Toronto, Ontario M3J 1P3, Canada
Tel.:1-416-736-2100 x20192, E-mail: allison@eecs.yorku.ca
[2]Centre for Vision Research, York University, Toronto, Ontario M3J 1P3, Canada
Tel.:1-416-736-2100 x20192, E-mail: lwilcox@yorku.ca

VESA DSC and VDC-M (https://vesa.org/vesa-display-compression-codecs/) are in widespread usage in millions of display systems. This rollout was preceded by extensive and targeted subjective quality assessment to validate predictions of codec quality and visually lossless behaviour. In this talk, we will overview the assessment activities to date and their extension to applications in immersive displays. Our focus will be on subjective testing at York University using the ISO 29170-2 Appendix A protocol (1).

In the ISO 29170-2 'flicker paradigm', the test and reference are presented side-by-side on the display (Figure 1). The test consists of the compressed image temporally interleaved (alternating) with the uncompressed version at a fixed frequency (typically 5 Hz). In the reference sequence, the uncompressed image alternates with itself. Participants view the test and reference sequences side by side and are asked to identify the compressed image (i.e., which image sequence contained flicker). We have also developed and implemented modified versions of the protocol to evaluate moving and stereoscopic displays. This testing has proceeded in discrete stages including:

- Validation of visually lossless performance in a wide range of representative image samples
- Confirmation of visually lossless performance in chroma subsampled images and moving content
- Assessment of compression performance with high-dynamic range content
- Assessment of compression performance with stereoscopic 3D content
- Assessment of the effects of chromatic aberration correction on codec performance

Testing has focused on challenging test cases to optimize the effort and benefit of time-consuming subjective assessment studies. Generally, both DSC and VDC-M have met expectations for visually lossless performance over a wide variety of content and use cases. Flicker testing is a highly conservative test procedure and codec performance in real world scenarios is expected to exceed that found under the harsher conditions of flicker testing.

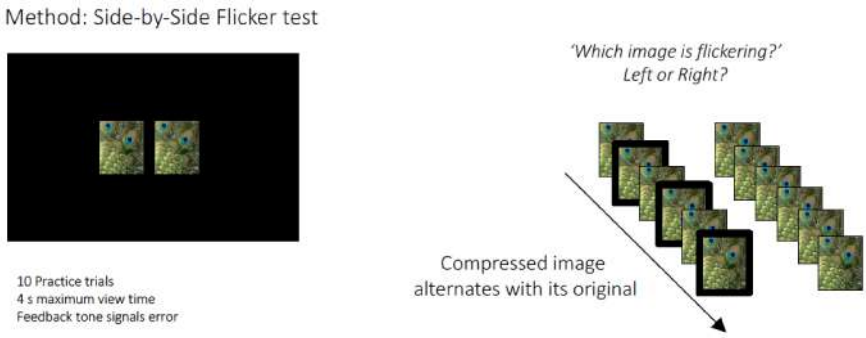

Fig. 1. ISO 29170 Flicker Test Paradigm

Acknowledgment

The authors would like to acknowledge support from VESA under several contracts to perform the subjective assessment experiments described here and for permission to summarize these findings in this presentation. We would also like to acknowledge the contributions of the VESA DSC task group (led by Dale Stolitzka, James Goel, and Jim Hunkins), Lesley Deas, Wei Wang, David M. Hoffman, Yuqian Hou, Aishwarya Sudhama, Matthew D. Cutone, Natan Jacobson, Mark Dalecki, Sanjida Sharmin Mohona, Domenic Au, Onoise Gerald Kio, Richard Robinson, Cyan Kuo, Saadia Riaz, Anna Danilova, Leesann Sutherland, Valeriya Tolstineva

References

1. International Standards Organization, Information technology — Advanced image coding and evaluation — Part 2: Evaluation procedure for nearly lossless coding, ISO/IEC 29170-2:2015 (2015).

Appearance transforms in video/HD/UHD/HDR consumer display

Charles Poynton, PhD
Toronto, Ontario, Canada
Tel.:+1 416 535 7187, E-mail: charles@poynton.ca

The acquisition, production, distribution, and presentation of commercially important images involves a complex imaging/colour pipeline [1]. The main elements of the pipeline are sketched below [from 2]:

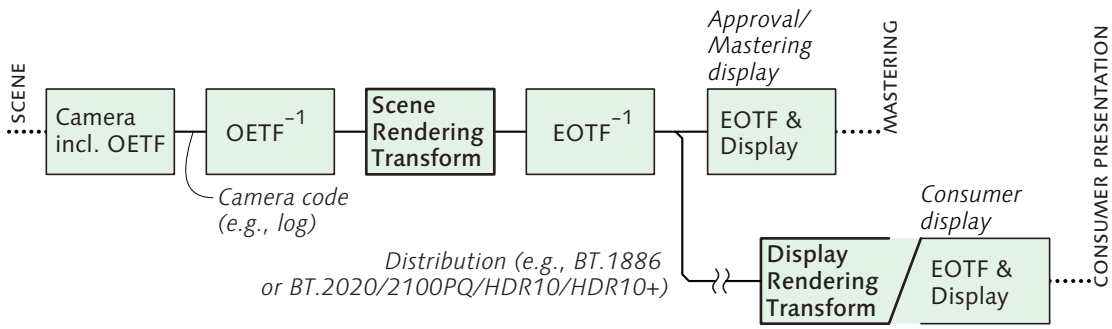

Image signal modification takes place in the *scene rendering transform,* which includes adjustments to compensate the visual response to the original scene (which is typically a bright environment), and also manipulation for æsthetic and creative purposes. The display developer is most interested in the *display* blocks – both the mastering display and the consumer display. Colour appearance effects are introduced when the mastered image is viewed at significantly lower luminance than the scene, as is usually the case; however, those effects are compensated when the mastered image is adjusted by the colourist. More problematic are the colour appearance effects that arise when consumer viewing involves different conditions than mastering – for example, when the average or peak absolute luminance differs from mastering luminance, or when surround conditions differ.

Historically, up to and including HD, a very crude treatment of appearance issues was effected by the mismatch in "gamma" values of the EOTFs: a 2.4-power EOTF is standard for mastering at 100 cd · m^{-2} [nt], and a 2.2-power was common practice for consumer display, typically at 320 nt. A 2.2-power EOTF is also a feature of the sRGB standard for computing. For HDR, there is no single, fixed reference/mastering display standard.

Colour appearance models (Fairchild [3], CIECAM02 [4]) seek to describe such effects, and have been used to impose compensation. However, most colour appearance models do not fully address the Helmholtz-Kohlrausch (H-K) effect. Stolitzka [5] recently proposed an algorithmic model to assess the H-K effect in HDR displays.

When colour appearance transforms increase chroma, care must be taken to avoid crossing the Evans [6] "zero-grayness" (G_0) boundary: Colour modification must be prevented from taking a surface (object) colour and increasing its chroma such that it appears fluorescent, more chromatic than a plausible surface reflectance.

Compensation for appearance effects at the consumer display is sensible when display and viewing conditions of presentation differ from mastering, and in particular, when the colour gamuts of the mastering display and the consumer display differ. With emergent display technology, we expect differences in mastering and consumer viewing; particularly, with commercialization of very wide gamut displays such as those using quantum dots.

References

1. POYNTON, Charles (2013), *Digital Video and HD Algorithms and Interfaces* (Elsevier/Morgan-Kaufmann).
2. POYNTON, Charles (2018), *Colour Appearance Issues in Digital Video, HD/UHD, and D-cinema*, PhD Dissertation, Simon Fraser University.
3. FAIRCHILD, Mark D. (2013), Color Appearance Models, 3rd edition (Wiley).
4. CIE 159:2004, *A colour appearance model for colour management systems: CIECAM02.*
5. STOLITZKA, Dale (2020), "A Model for Very Wide Gamut HDR Displays that Accounts for the H-K Effect," presented at SMPTE Annual Technical Conference, Nov. 10–12; in press, *SMPTE Motion Imaging Journal.*
6. EVANS, Ralph M. (1974), *The Perception of Color* (Wiley-Interscience).

Evaluating Display Ambient Contrast with Self Reflection

***John Penczek*[1]**
[1]NIST and University of Colorado, Boulder, CO 80305, U.S.A.
Tel.:+1-303-497-3159, E-mail: john.penczek@colorado.edu

Displays are used over a wide range of ambient illumination conditions. The readability of the display content is strongly impacted by the display brightness, the illumination conditions, and the screen reflection characteristics. Current standards evaluate the ambient contrast ratio using hemispherical illumination with specular included to (represent the diffuse background) together with a directional source (to simulate an indoor lamp or the sun outside).[1] However, the situation is typically more complex than that. The user's readability of the screen content is strongly dependent on the lighting in the specular direction. As suggested by the photo in Fig. 1, if the user is viewing content near the edges of the screen, the ambient contrast ratio will mainly be impacted by the background illumination. But for content near the center of the screen, the viewer often sees the reflection of their own face overlaid on the content. Therefore, the ambient contrast ratio can be different for the edge and center of the screen, caused by differences in color and illumination levels of the sources (background and face). This study addresses this complexity by introducing the analysis and corresponding measuring methods.

The ambient contrast ratio with the diffuse background in the specular direction is determined by using the standard methodology for hemispherical illumination with secular included.[1] For the case with face self reflection, the total luminance can be expressed as:

$$L_{tot} = L_{em} + L_{de} + L_{dir} + L_{spec} = L_{em} + \frac{\rho_{de}E_{hemi}}{\pi} + \frac{R_{dir}E_{dir}}{\pi} + \rho_{spec}L_{face}$$

where L_{em} is the luminance from the darkroom display emission, ρ_{de} is the hemispherical diffuse reflectance with specular excluded, R_{dir} is the non-specular reflectance factor of a directional light source, ρ_{spec} is the specular reflectance near normal incidence, L_{face} is the luminance from the face, and E_{hemi} and E_{dir} are the illuminance from the hemispherical diffuse background and directional light source, respectively. In this case, the scattered light outside the specular direction is accounted for, but the specular reflection is measured separately. An example of the spectral reflectance characteristics of an LCD laptop with a glossy surface is given Fig. 2 for the display set to its white state. In the example, the diffuse reflectance with specular included (di/8°) is similar to the specular reflectance (8°/8°), but the light source spectra will be different. The luminance from the face can be estimated using data from a recent study of face spectral reflectance for difference races.[2] Measured spectral reflectance data and ambient contrast ratio results will be presented to illustrate the method under different illumination environments.

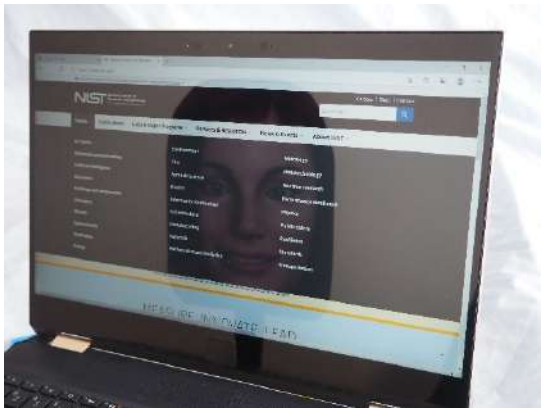

Fig. 1. Reflection of face from glossy screen

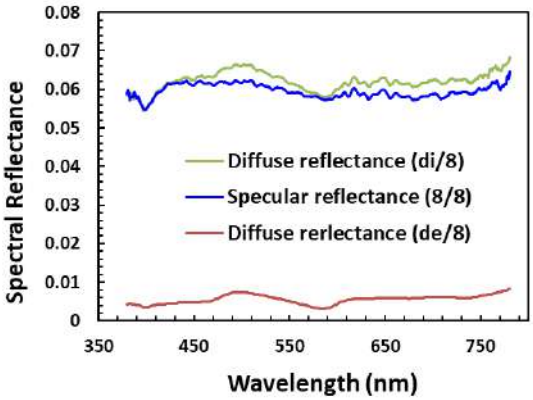

Fig. 2. Reflection spectra of screen

References

1. IEC 62977-2-2:2021 Electronic displays – Part 2-2: Measurement of optical characteristics – Ambient performance. (2021).
2. Y. Wang, *et al*, Spectrophotometric measurement of human skin colour, *Color Res.Appl.*, vol. 42, p. 764 (2017).

Sensitivity of VESA Display Stream Compression Codecs to Chromatic Aberration

DomeniciAu[1],iSanjidaiSharminiMohona[1],iYuqianiHou[1],iOnoiseiGeraldiKio[1],iJamesiGoel[2],iNataniJacobson[3],i RobertiS.iAllison[1],iandiLaurieiM.iWilcox[1]

[1]Centre for Vision Research, York University, Toronto, ON, M3J 1P3, Canada

Tel.:1 416-736-5659, E-mail: allison@eecs.yorku.ca, lwilcox@yorku.ca

[2]Qualcomm Canada Inc., Markham, ON, L3T 7W3, Canada

Tel.:1 (905) 482-5765, E-mail: jgoel@qti.qualcomm.com

[3]Qualcomm., San Diego, CA, 92121, U.S.A

Tel.:1 858-587-1121, E-mail: natanj@qti.qualcomm.com

Current virtual and augmented reality displays rely on image pre-processing or warping to correct for optical distortion and chromatic aberration introduced by magnifying lenses. This processing disrupts the spatial correlation between colour channels relied upon in state-of-the-art compression codecs. Using the ISO/IEC 29170-2 flicker protocol that has been adapted for 3D imagery, we evaluated the sensitivity of DSC 1.2a (Display Stream Compression) and VDC-M 1.2 (VESA Display Compression-M) [4] to characteristic distortions resulting from stereoscopic head-mounted display pre-processing [1, 2, 3]. Such pre-processing involves pre-warping source images with inverse pin-cushion (barrel) distortion to correct for the pin-cushion transform from the display optics. Also, the default compression operation involves a colour space conversion from RGB to YCoCg which normally improves compression performance by reducing the degree of correlation between components [5]. However, the typical lens correction pre-processing operates differentially on each of the colour channels to pre-correct chromatic aberration and thus disrupts their spatial correlation. The recommendation is to bypass the colour transform for images that have undergone chromatic aberration pre-correction. In many cases bypassing the colour transform slightly improves the PSNR for these compressed pre-distorted signals relative to the standard pipeline; it is unclear whether there is a corresponding improvement in subjective quality.

A set of 10 computer-generated stereoscopic high dynamic range images were tested. Images spanned a wide range of content and were designed to challenge the codecs. The pre-processing workflow involved pre-warping the images, compressing with each codec, and finally de-warping with pin-cushion distortion. De-warping was applied to simulate the distortion from magnifying lenses as all images were viewed on a mirror stereoscope without such lenses. The main image manipulations were the codec used, the compression levels and whether the colour transform was bypassed (bypass-on) or not (bypass-off). Images were compressed at the codec's respective nominal production level and at each image's estimated limit of visually lossless compression. 60 observers were tested in 3 groups of 10 for both VDC-M 1.2 and DSC 1.2a. Overall, we found little sensitivity to these distortions and confirmed that bypassing colour transforms in the codec can be beneficial for some images.

Acknowledgment

The authors wish to acknowledge funding in support of this work received from the Video Electronics Standards Association (VESA) and from Canada First Research to Innovation Funding to VISTA.

References

1. N. Jacobson, V. Thirumalai, R. Joshi, and J. Goel, "A new display stream compression standard under development in VESA," *Proceedings of SPIE*, 10396, 103960U1- 103960U12 (2017).
2. D. Au *et al.*, "3-4: Stereoscopic Image Quality Assessment," *SID Symposium Digest of Technical Papers*, 50(1), 13-16 (2019).
3. S.S. Mohona *et al.*, "Subjective Assessment of Stereoscopic Image Quality: The Impact of Visually Lossless Compression," *Twelfth International Conference on Quality of Multimedia Experience (QoMEX)*, 1-6 (2020).
4. Video Electronics Standards Association, "VESA Display Compression Codecs," https://vesa.org/vesa-display-compression-codecs/ (2021).
5. J. Limb, C. Rubinstein, and J. Thompson, "Digital Coding of Color Video Signals—A Review," *IEEE Transactions on Communications*, 25(11), 1349-1385 (1977).

Luminance and Color measurements at subpixel level using Microscopic and Macroscopic Lenses with Imaging Luminance Measurement Devices

Ingo Rotscholl[1], Shin Myung Choi[2], Tobias Porsch[1] and Udo Krüger[1]
[1]TechnoTeam Bildverarbeitung GmbH, Werner-von-Siemens-Str 5. 98693, Ilmenau, Germany
Tel.:+49 3677 4624 0, E-mail: ingo.rotscholl@technoteam.de
[2]IS-Soft co Ltd, M-Techno Center 140 Beon-gil, Gongdan-ro, 1003-1004, 15845 Gunpo-si, Gyeonggi-do South Korea

The variety of different measurement tasks that can be performed with Imaging Luminance and Color Measurement Devices (ILMD/ICMD), also called luminance cameras, is constantly increasing with the number of different specialized lenses. One examples is the one-shot quantification of luminance as a function of angle with conoscopic lenses. Other examples are special AR/VR lenses used to quantify near eye displays [1]. For spatial measurements, high magnification lenses can be used to quantify luminance characteristics at the subpixel level. This includes microscopic and macroscopic lenses.

In this contribution, we will show exemplary results on various spatial measurements obtained with microscopic and macroscopic lenses. The analyzed displays are an automotive LC display with a PPI of 224 and an OLED smartphone display with a PPI of 458. Figure 1 shows examples of a captured luminance image of both displays and both lenses in a deep grey state with the full field of view of the respective lenses.

We then use a method similar to [2] to analyze the crosstalk between different sub-pixels as a measure for image sharpness [3]. Here, we modify the crosstalk by applying different anti-glare layers (AGL), which are important components in both applications since both automotive displays and smartphones are used in direct sunlight. Figure 2 shows a zoomed-in microscopy-based luminance image of the OLED display with and without AGL on a logarithmic scale. Finally, we analyze the capabilities of both the macroscopic and microscopic lens to quantify the resolution and image quality parameters for both displays.

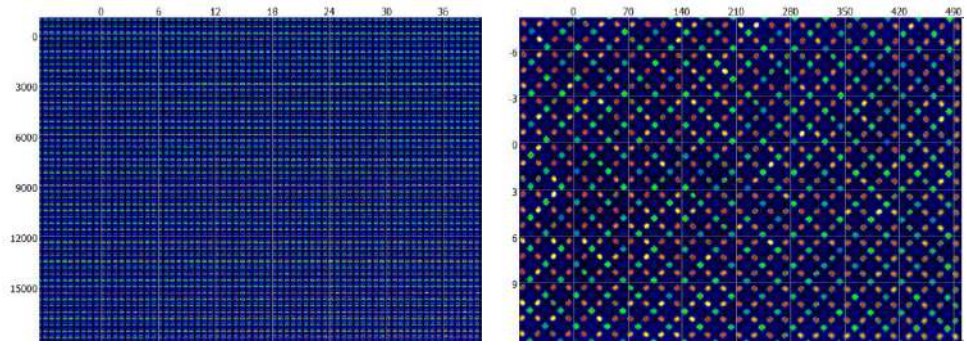

Fig. 1. Field of View: Left - Macroscopic measurement of automotive display and Right - Microscopic measurement of smartphone display

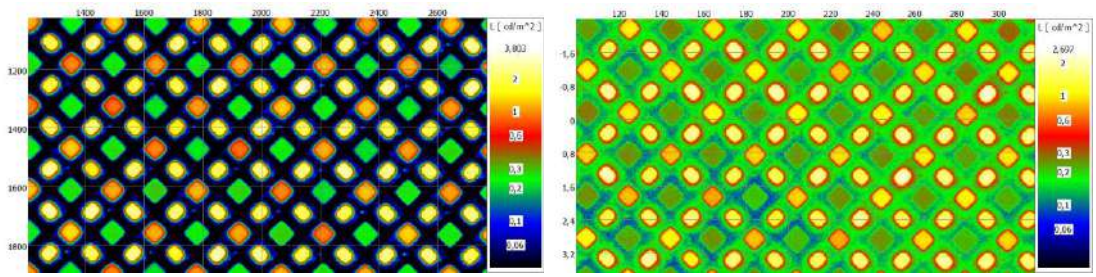

Fig. 2. Luminance distribution/crosstalk of smartphone display: Left - No AGL and Right - With AGL

References

1. N. Schuster, U. Krüger and T. Porsch, *Information Display.*, 35(3), 12 (2019)
2. T. Fink and U. Krüger, *SID'16 Technical Digest*, vol 47, p. 365 (2016)
3. M. E. Becker, T. Fink and U. Krüger, *SID'16 Technical Digest*, vol 47, p. 372 (2016)

Novel Image Quality Characteristics of microLED TV

Daeun Park[1], YoonJung Kim[1], and YungKyung Park[1]
[1]College of Art & Design, Ewha Womans University, Seoul 03760, Korea
Tel.:82-2-3277-2512, E-mail: yungkyung.park@ewha.ac.kr

MicroLED is well known as a point light source display with brilliant image quality due to high luminance and large color gamut. MicroLED is microscopic LED arrays, with each LED performing as the individual pixel elements, so that this becomes the display with better image quality impression. We conducted quality assessment experiments comparing microLED and QLED with the same white luminance to figure out the characteristic of image quality.

The subjects of experiments are general consumers, and they evaluated the images displayed at microLED 4K of 110 inches and QLED 8K of 85 inches in viewing distance 3m. The illuminance at eye-height is 1.8lx, and 7.2lx at the display surface. Whereas the luminace of QLED is fixed as 440 cd/m^2, we controlled the luminace of microLED to 3 levels, 592.7 cd/m^2, 734.6 cd/m^2, and 1283 cd/m^2. When the luminace of microLED is 592.7 cd/m^2, it is considered as the same perceptive brightness as QLED. The subjects performed the paired comparison and evaluated the image quality of microLED based on QLED display. The assessment items include questions about the Sensation factors Brightness, Contrast, Vividness, perception factors Sharpness, Texture, Clarity, and Image Quality. The evaluation items were presented in sentence form to be evaluated using Likert 7-point scale.

With the decrease in luminance, the preference of image quality of microLED was decreased, but still over score 4 in low luminance which means the image quality of microLED is better than QLED 8K in overall luminance. ‘Contrast’, ‘Brightness’, ‘Vividness’ of Sensation factors were decreased by the decline in luminance, and there was the biggest drop in ‘Brightness’. Because of the point light source display, microLED can express deeper black, even though similar levels of luminance allow for similar peak luminance and may have further amplified contrast perception. Contrast perception is the main factor affecting image Quality evaluation, and it was proved that image quality preference increases as contrast increases (Haun & Peli, 2013; Seetzen et al., 2006). Extended Contrast perceptions may have contributed to keeping microLED's image quality preferences higher. With ‘Sharpness’, ‘Texture’, ‘Clarity’ of perception, it turned out that there was an apparent connection with luminance change. Especially, ‘Sharpness’, ‘Clarity’ was strongly responded to decreasing luminance.

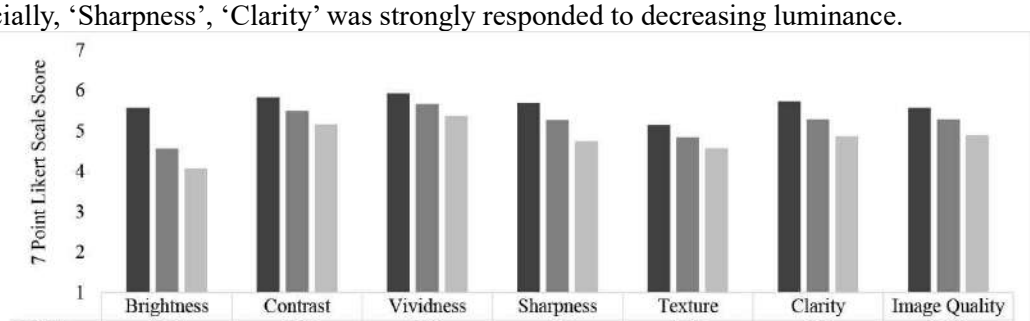

	Brightness	Contrast	Vividness	Sharpness	Texture	Clarity	Image Quality
High	5.57	5.83	5.93	5.7	5.15	5.73	5.57
Medium	4.57	5.5	5.67	5.28	4.85	5.3	5.3
Low	4.07	5.17	5.37	4.75	4.58	4.87	4.9

Fig. 1. Subjective evaluation results of microLED 4K quality compared to QLED 8K according to luminance level (high, medium, low)

We focused that there was a similar score in ‘Brightness’ in low luminance between microLED 4K and QLED 8K. However, the scores of ‘Contrast’ and ‘Vividness’ were superior in microLED 4K. It turns out that the black point is also attributed to amplification in contrast to microLED along with the white point.

References

1. Haun, A. M., & Peli, E. (2013, March). Is image quality a function of contrast perception?. In Human Vision and Electronic Imaging XVIII (Vol. 8651, p. 86510C). International Society for Optics and Photonics.
2. Seetzen, H., Li, H., Ye, L., Heidrich, W., Whitehead, L., & Ward, G. (2006, June). 25.3: Observations of luminance, contrast and amplitude resolution of displays. In SID Symposium Digest of Technical Papers (Vol. 37, No. 1, pp. 1229-1233). Oxford, UK: Blackwell Publishing Ltd.

A study of directivity characteristics for TV audio systems

Jang-Un Kwon[1], Jeong Man Lee[1] and Jang Jin Yoo[1]
[1]LG Display Co., Ltd.
LG Science Park, Gangseo-gu, Seoul, 07796, Korea
Tel.:82-2-6987-0488, E-mail: joyrabit@lgdisplay.com

When watching TVs or home theaters, 90% of TV viewers usually sit within ±35° horizontally in terms of viewing direction[1]. It is, therefore, desirable that the image and sound quality does not change depending on viewing direction. In ANSI/CEA[2] and IEC standard[3], there is *Directivity Index* to measure the sound characteristics in viewing directions. In addition, in case of TV audio systems, speakers are attached to top, bottom and sides of TVs. According to Kwon's paper[4], in case of TV audio systems, the direction of sound radiation of speakers has a great influence on its sound quality.

In this paper, the *Directivity Index* values were compared according to sound radiation direction of speakers in order to evaluate directivity characteristics of TV audio systems. Measurement condition and methods are shown in Fig. 1. For listening environment, referring to the the *listening window*[2], the frequency response was measured at 10 degree intervals within the ±30° horizontal angular range. The mean value of *Sound Pressure Level(SPL)* which is the average *SPL* from 200Hz to 20000Hz at each angle was calculated. The *Directivity Index* was calculated the difference of mean value of *SPL* between 0 degree and each degree. The smaller the *Directivity Index*, the less the change of *SPL* sound depending on the location of viewers. Front-firing type, down-firing type and side&up-firing type TV were prepared for evalution. Table 1 shows *Directivity Index* of each TV. Front-firing TV had the lowest maximum value of 1.0 dBSPL at -20degrees and the side & Up-firing type TV was the highest *Directivity Index* of 2.2 dBSPL at +30degrees.

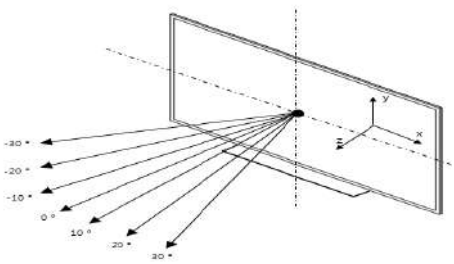

1) Mean value of SPL (*dBSPL*)
Average of SPL between 200Hz to 20,000Hz
2) Directivity Index (*dB*)
The difference of mean value of *SPL* between 0 degree and each degree

Fig.1. measurement configuration(left) and methods(right)

Sample	*Directivity Index* of each angle							Maximum value
	-30deg.	-20deg.	-10deg.	0deg.	+10deg.	+20deg.	+30deg.	
Front-firing type TV	0 dB	1.0 dB	0.5 dB	0 dB	0.1 dB	0.2 dB	0.4 dB	1.0 dB
Down-firing type TV	0.7 dB	0.7 dB	0.5 dB	0 dB	1.1 dB	1.1 dB	1.7 dB	1.7 dB
Side & Up-firing type	1.6 dB	1.1 dB	0.7 dB	0 dB	0.6 dB	1.6 dB	2.2 dB	2.2 dB

Table2. *Directive Index* for each TVs

References

1. Ergonomic design guidelines for flat panel display television, Japan Ergonomics Spciety (2012)
2. Standard Method of Measurement for In-Home Loudspeakers, ANSI/CTA-2034 (2015)
3. Sound system equipment-part21: Acoustical Measurements, IEC 60268-21(2018)
4. J-U Kwon and JM Lee, IMID'20, p.171 (2020)

Measurement methods for seam of tiled display

JaeHong Kim[1], HeeEun Lee, and Junwoo Jang[1]
[1]LG Display Co., Ltd.
LG Science Park, Gangseo-gu, Seoul, 07796, Korea
Tel.:82-2-6987-0382, E-mail: pro_jhkim@lgdisplay.com

In the case of a tiled display in which multiple displays are tiled to create a large screen, a difference in optical characteristics between each unit display and an alignment issue in the tiling process affects the overall display quality[1)]. Among various display characteristics, seam recognition that occurs only in tiled displays is a problem that does not exist in legacy displays, and many developments have been made to overcome this issue[2)].

As one of these efforts, this study attempts to quantify the seam area characteristics through the optical measurement method to overcome the limitations of the conventional method such as measuring the distance between the adjacent displays. Measurement configuration and pattern are shown in Fig. 1. In order to quantify the seam of a tiled display, an imaging colorimeter capable of acquiring the 2-D luminance distribution of the seam area was used. In the proposed evaluation methods, two test patterns are used: (1) 1x1 grilled pattern, (2) full gray pattern. The window width can be obtained through the grilled pattern, and the 1-D luminance profile of the seam area can be obtained in the full gray pattern. To remove noise, WMA was performed with the window width obtained through the first pattern. Depth was defined as the luminance difference from the area other than the seam, width was defined as the physical length at which the luminance difference occurred and detailed formula are shown in Fig. 2. Using the proposed measurement method, it is possible to analyze characteristics that have not been quantified by conventional methods, such as intentional luminance adjustment of the seam area and optical compensation through a diffusion lens.

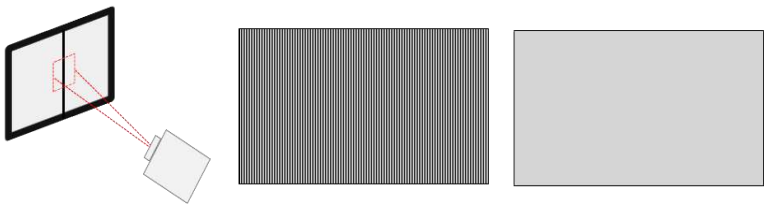

Fig.1. measurement configuration(left) and 1x1 grilled, full gray pattern pattern(right)

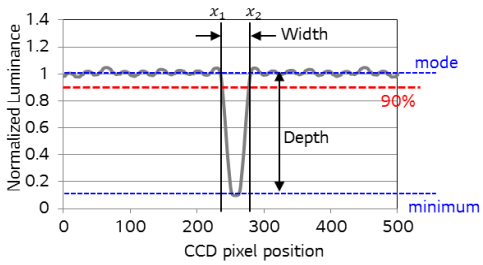

1) width (cpx)
$x_{1,90\%}-x_{2,90}$
2) depth (cd/m^2)
$y_{mode}-y_{minimum}$

Fig.2. 1-D luminance profile(left) and formula(right)of width and depth

References

1. R.G. Greene, Seamless Tiling Technology for Large Direct-View Color AMLCD's, SID-00 Digest,pp. 461-463, 2000.J-U Kwon and JM Lee, IMID'20, p.171 (2020)
2. Mark Aston, "Design of large-area OLED displays utilizing seamless tiled components", J.Soc. Inf. Display, pp.535-540, Vol. 15. (2007)

Optical Model of Organic Light-Emitting Diodes Based on the Generalized Poynting Vector Method

Jungho Kim
Dept. of Information Display, Kyung Hee University, Seoul 02447, Korea
Tel.:82-2-961-2165, E-mail: junghokim@khu.ac.kr

In the organic light-emitting diode (OLED), optical modeling and design is very important to maximize the quantum efficiency as well as to optimize output emission characteristics, where the micro-cavity effect should be taken into account. Dipole emission in the OLED has been optically modelled through several electromagnetic methods such as the Green's function method [1], the dipole radiation model [2], and the point dipole method (PDM) [3]. Output emission characteristics as well as the modal analysis have been successfully performed based on these three electromagnetic models. However, these methods have not yet completely investigated the optical power flow and absorption profiles inside the OLED cavity.

A so-called generalized Poynting vector method (GPVM) has been proposed to calculate the spatial and spectral characteristics of the electric field intensity, optical power flow, and optical absorption of all optical modes both inside and outside the OLED cavity [4]. The GPVM is based on the combination of the source term and transfer matrix methods with the use of the normalized in-plane wave vector u. The theoretical expressions of dipole excitation at the emitter position described by the GPVM are identical to those presented by the PDM, which verifies the validity of the GPVM.

In combination with the quantum-mechanical approach, the internal profile of the electric field intensity corresponds to the emission strength of a dipole emitter. Hence, the profile of the emission zone is well matched with the internal electric-field profile of the air mode within the emission zone, which can greatly reduces the number of calculations [5]. In addition, an improved formula to determine the optimal emitter position that maximize the two-beam interference effect can be derived, where the non-ideal phase shift at the metal electrode can be considered [5]. Furthermore, the spatial electric-field profiles of waveguide and surface plasmon modes calculated by the GPVM are in a good agreement with the numerical solution of the homogeneous wave equation such as the boundary modal analysis [4].

Regarding the internal optical power flow, the GPVM can provide the calculated optical power flow both inside and outside the OLED cavity. The physical origin and spatial distribution of absorption loss can be elucidated for the air mode [6]. Moreover, the internal optical power flows and absorption profiles of the trapped waveguide and surface plasmon modes are calculated so that the calculated ratio of the optical absorption distributed to each absorptive layer can be calculated as a function of the emitter position for three dipole orientations [4]. The calculated internal absorption profiles can be used as a detailed source of heat generation in the thermal analysis of the OLED.

In conclusion, the optical model of the GPVM has the merit that it can easily calculate all the spatial and spectral distributions of the electric field intensity, optical power flow, and optical absorption both inside and outside the OLED cavity compared with the currently-used methods. The GPVM can be used as a comprehensive optical modeling method to understand the internal emission process as well as to provide more efficient optical design of OLEDs.

Acknowledgment

This research was supported by the Basic Science Research Program (2018R1D1A1B07047249) through the National Research Foundation of Korea (NRF)

References

1. M. H. Lu and J. C. Sturm, *J. Appl. Phys.*, 91(2), 595 (2002).
2. J. A. E. Wasey and W. L. Barnes, *J. Mod. Opt.*, 47(4), 725 (2000).
3. K. A. Neyts, *J. Opt. Soc. Am. A*, 15(4), 962 (1998).
4. J. Kim, K.-Y. Kim, and J. Kim, *Opt. Express*, 27(16), A1261 (2019).
5. J. Kim, K.-Y. Kim, and J. Kim, *Appl. Opt.*, 57(28), 8394 (2018).
6. J. Kim, K.-Y. Kim, and J. Kim, *J. Korean Phys. Soc.*, 73(11), 1663 (2018).

Bidirectional-scattering-matrix-method based adjoint inverse design algorithm for diffractive display optic devices

Hwi Kim
Department of Electronics and Information Engineering, Korea University, Sejong 121-791, Korea
E-mail: hwikim@korea.ac.kr

This paper discusses the fundamental of the photonic inverse design theory [1] based on the discrete variational form and proposes an efficient bidirectional-scattering-matrix-method-based numerical inverse design algorithm. The inverse design theory aims to find the permittivity parameter $\bar{\bar{\varepsilon}}_r$ maximizing the figure of merit (FOM) function $\Phi\left(\bar{E},\bar{H},\rho\right)$, where ρ is a structural parameter. $\Phi\left(\bar{E},\bar{H},\rho\right)$ can be modeled for focal spot optimization and target diffraction mode efficiency maximization et cetera. In the inverse design framework, the gradient of the FOM w.r.t ρ $d\Phi/d\rho$ should be obtained, and its mathematical form is given by $d\Phi/d\rho = 2\,\mathrm{Re}\left\{j\omega\bar{P}_{ind}\cdot\bar{E}_{adj}\right\}$, where $\bar{P}_{ind} = \varepsilon_0\left(\varepsilon_r - 1\right)\bar{E}$, and $\bar{E}_{adj}$ are obtained by the forward and reverse electromagnetic analysis, respectively. ω, ε_0 and ε_r are the angular frequency, absolute vacuum permittivity and material relative permittivity.

The forward field $\bar{E}$ is analyzed by the forward Fourier modal method (FMM) analysis [2] of the Maxwell equations system

$$\nabla\times\bar{E} = j\omega\mu_0\bar{H} + j\omega\mu_0\bar{M}\,,\quad \nabla\times\bar{H} = -j\omega\varepsilon_0\bar{\bar{\varepsilon}}_r\bar{E} - j\omega\bar{P}\,, \tag{1}$$

where the permittivity profile is $\bar{\bar{\varepsilon}}_r = 1 + \left(\bar{\bar{\varepsilon}}_m - 1\right)\theta\left(\rho\right)$. $\theta\left(\rho\right)$ is the shape function s.t. $0 \le \theta\left(\rho\right) \le 1$. The adjoint field $\bar{E}_{adj}$ is obtained by the reverse FMM analysis of the adjoint Maxwell equations

$$\nabla\times\bar{E}_{adj} - j\omega\mu_0\bar{H}_{adj} = j\omega\mu_0\bar{M}_{adj}\,,\nabla\times\bar{H}_{adj} + j\omega\varepsilon_0\bar{\bar{\varepsilon}}_r\bar{E}_{adj} = -j\omega\bar{P}_{adj}\,, \tag{2}$$

where the polarization and magnetization sources are taken by the derivatives of the FOM function $j\omega\mu_0\bar{M}_{adj} = \left(\frac{\partial\Phi}{\partial H_{x,R}} - j\frac{\partial\Phi}{\partial H_{x,I}}, \frac{\partial\Phi}{\partial H_{y,R}} - j\frac{\partial\Phi}{\partial H_{y,I}}, \frac{\partial\Phi}{\partial H_{z,R}} - j\frac{\partial\Phi}{\partial H_{z,I}}\right)$ and $-j\omega\bar{P}_{adj} = \left(\frac{\partial\Phi}{\partial E_{x,R}} - j\frac{\partial\Phi}{\partial E_{x,I}}, \frac{\partial\Phi}{\partial E_{y,R}} - j\frac{\partial\Phi}{\partial E_{y,I}}, \frac{\partial\Phi}{\partial E_{z,R}} - j\frac{\partial\Phi}{\partial E_{z,I}}\right)$.

The key issue is the efficiency of the forward and adjoint solvers of Eqs. (1) and (2). We propose an efficient inverse design method exploiting the bidirectional-scattering-matrix-method (SMM) featured in the FMM. First, the bidirectional-SMM provides the forward and backward operators simultaneously, and second, the associative law of the SMM allows the efficient gradient update of the localized target structure. Let us assume that the total photonic structure is modeled by N layers, and the design task is finding the optimal structure of the *m*th layer surrounded by two compounds of fixed layers. The total S-matrix is represented by

$$\bar{\bar{S}}_{tot} = \bar{\bar{S}}_1 \otimes \cdots \bar{\bar{S}}_{m-1} \otimes \bar{\bar{S}}_m \otimes \bar{\bar{S}}_{m+1} \cdots \otimes \bar{\bar{S}}_N = \left[\bar{\bar{S}}_1 \otimes \bar{\bar{S}}_2 \otimes \cdots \bar{\bar{S}}_{m-1}\right] \otimes \bar{\bar{S}}_m \otimes \left[\bar{\bar{S}}_{m+1} \cdots \otimes \bar{\bar{S}}_N\right]. \tag{3}$$

The forward and adjoint simulation can be efficiently performed by updating the mth layer S-matrix analysis according to the associative law. The first compound $\left[\bar{\bar{S}}_1 \otimes \bar{\bar{S}}_2 \otimes \cdots \bar{\bar{S}}_{m-1}\right]$ and the second compound $\left[\bar{\bar{S}}_{m+1} \cdots \otimes \bar{\bar{S}}_N\right]$ are pre-calculated and kept, and the mth layer is iteratively updated in the inverse design process. This operator mathematical structure of the SMM is able to accelerate the iterative adjoint inverse design algorithm. We will present numerical examples of the diffractive display optic inverse design and evaluate the computational efficiency of the proposed method.

Acknowledgment
Samsung Research Funding & Incubation Center of Samsung Electronics (SRFC-TB1903-05)

References

1. J. S. Jensen and O. Sigmund, *Laser & Photon. Rev.* ***5***, 308 (2011).
2. H. Kim et al., *Fourier modal method and its applications in computational nanophotonics*, (CRC Press, 2017).

Anchor-free Fingerprint Core Detection Based on a Truncated GoogleNet Model

Shallon Stubbs[1], Soongyu Lee[2], Youngwook Yoo[3], and Pilho Kim[1]
[1]AI Team, Samsung Display Company Ltd, Yongin-si, Gyeonggi-do, 17113 Korea.
Tel.:82-31-8001-6869, E-mail: s.stubbs@samsung.com

Automatic fingerprint recognition systems (AFRS) are nowadays ubiquitous in biometric system used for various applications such as access control and forensics. AFRS implementation falls into two general categories, minutiae and correlation based designs [1]. Both designs typically require preprocessing operations comprising of ridge orientation modelling, filtering, normalization, etc. [1] [2]. For the correlation based detection system, fingerprint core point (region of interest ROI) extraction is used to enhance the correlation match accuracy.

This paper proposes a modification of the Inception v1 (GoogleNet) model to achieve a computationally efficient core location detection model. The base model (CovNet) shown in Fig. 1, is implemented using only the first auxiliary output of GoogleNet. Also, by applying a simple but strategic data augmentation and training technique, the model was trainable using a relative small image dataset and the implementation required no ROI proposal network (RPN) or additional preprocessing. The crop generator provides data augmentation by generating image crops randomly displaced relative to the core location of the fingerprint. The model is then trained to minimize the Euclidean distance between center of the crop and the core location. Fig. 2 compares the training performance of the partial and full GoogleNet base models. The results show that the smaller network requires half the training time without significant compromise to the model's accuracy. Furthermore, the 50% reduction in inference time facilitates repeated detections such that the final detection accuracy is improved over the full GoogleNet design.

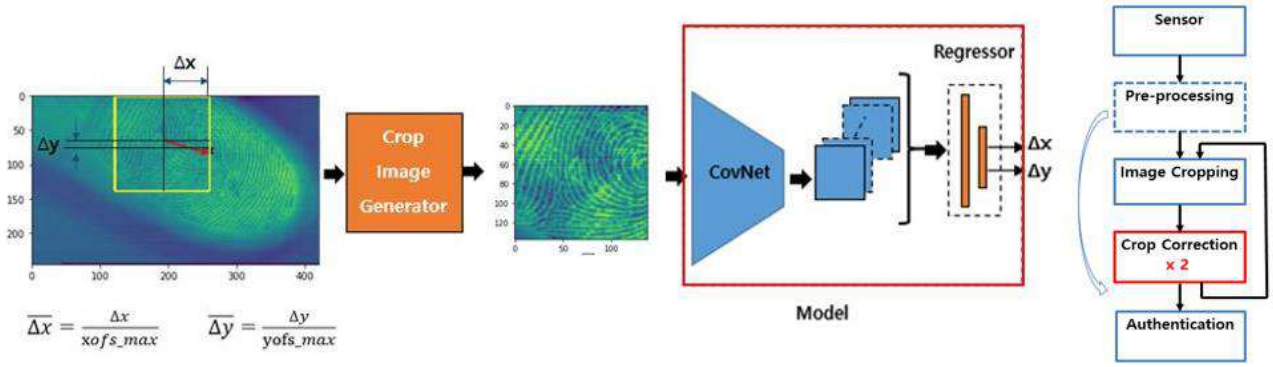

Fig. 1. Crop Generator and CNN Fingerprint Core Detection Model

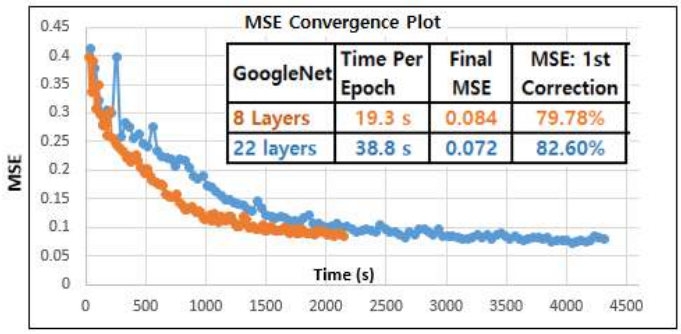

GoogleNet	Time Per Epoch	Final MSE	MSE: 1st Correction
8 Layers	19.3 s	0.084	79.78%
22 layers	38.8 s	0.072	82.60%

Fig. 2. MSE convergence time over 110 epochs

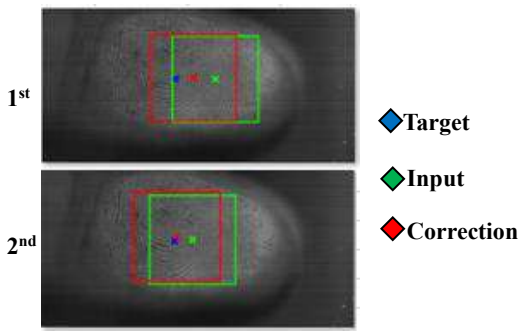

Fig. 3. 1st and 2nd Core Detection

References

1. Z. M. Win and M. M. Sein, Fingerprint Recognition System for Low Quality Images, *SICE Annual Conference*, p. 1133-1137 (2011).
2. B. Phandya and G. Cosma, Fingerprint Classification using a Deep Convolutional Neural Network, *IEEE International Conference on Information Management*, 4th, p. 86-91 (2018).

Optimization of Pixel Layout Generator for AMOLED Displays

Jungsuk Bang[3], Myunghun Lim [1], Min Kang[1], Yongwoo Lee[1] and Yongjo Kim[1]
[1]CAE Team, Display Research Center, Samsung Display, Giheung-Gu, Yongin-City, Gyeonggi-Do, Korea 121-791, Korea
Tel.:82-31-5181-5715, E-mail: eq.bang@samsung.com

An organic light emitting diode (OLED) display includes an array of OLEDs, each OLED is using low-temperature poly-silicon thin-film transistors(LTPS TFTs) But, the drawbacks of LTPS TFTs is in the obvious variations in the threshold voltage (VTH) and mobility. So OLED pixel circuit design, the method of detecting and compensating the non-uniformities in TFT characteristics is essential. These compensating make the circuit diagram more complicated.

This paper proposes a complete Pixel Layout Generator of using optimization. Pixel Layout Generator uses an algorithm that places transistors and connects nodes between transistors. The placement of transistors is most important to create various layouts and the placement of transistors is learned through actual product DBs to derive the optimal placement. Also, Routing can be optimized by learning through image GAN to add margin design for improving characteristics and yield.

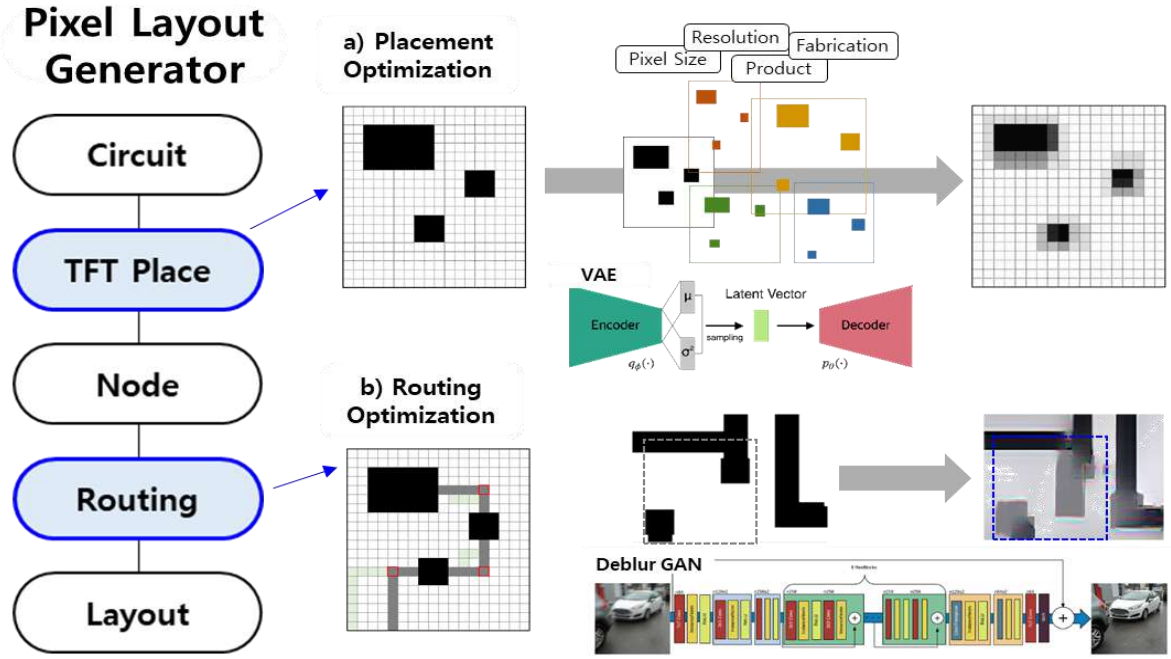

Fig. 1 Optimization of Pixel Layout Generator
(a) Placement Optimization using VAE (b) Placement Optimization using Deblur GAN

References

1. S. M. Choi, O. –K. Kwon, N. Komiya, H. K. Chung, “A self-compensated voltage programming pixel structure for active-matrix organic light emitting diodes,” International Display Workshop,535-538 (2003)
2. L. W. Liebmann, R. O. Topaloglu, "Design and technology co-optimization near single-digit nodes", Proc. IEEE/ACM Int. Conf. Comput.-Aided Design, pp. 582-585, Nov. 2014.
3. R. S. Ghaida, P. Gupta, "DRE: A framework for early co-evaluation of design rules technology choices and layout methodologies", IEEE Trans. Comput.-Aided Design Integr. Circuits Syst., vol. 31, no. 9, pp. 1379-1392, Sep. 2012.
4. Diederik P Kingma, Max Welling “Auto-Encoding Variational Bayes” ArXiv e-prints, May 2014
5. Orest Kupyn, Volodymyr Budzan “DeblurGAN: Blind Motion Deblurring Using Conditional Adversarial Networks”, ArXiv e-prints, Apr 2018

Artificial Neural Network Transistor Modelling and Display Compensation Method

Sang-ik Lee[1], Joonchul Goh[2], Minseok Bae[3], Junwoo Son[4] and Wonjun Choe
[1] Samsung Display Company, Yongin-si, Gyeonggi-do, Korea
Tel.: 82-31-5181-5647, E-mail: sangik85.lee@samsung.com
[2,3,4] Samsung Display Company, Yongin-si, Gyeonggi-do, Korea

Display productions are bigger and more brightness by development new TFT devices for high mobility annually. Many new display technologies are developed based on analysis of pixel driving transistors. To analysis action of transistors, modeling of transistor is very important. The precision of model affect the specification of display or driving algorithm for display. The most case of transistor modeling, mathematical equations are used by semiconductor physics. This approach is semi-empirical based on pre-existence equation and measured data. This modeling method is not suitable for every pixels in display, so it makes prediction error, not stable display production. We may make suitable model what has great performance by a lucky chance, but it is not easy for every cases. So TFT modeling method is important part for development of display devices.

Nowadays Artificial Neural Networks (ANNs) can be considered as method for empirical modelling. Training ANNs is efficient method for almost universal modelling. It takes short time to training compared with mathematical modelling. To modelling TFT characteristics, MLP (Multi-Layer Perceptions) networks can be used. It consist of simple structure, easy to implement. It has the number of hidden layers between input layer and out layer. Each layers in the network consists of neurons. Each neuron in layers made by simple equation which activation functions, summations, synaptic weights and bias.

We can use this model to compensate driving characteristic distribution of pixel transistor. The model can describes each pixels Vgs for drive specific current. The model can describe the transistors Ids characteristic by Vgs in the specific group in display. This means we can compensate transistors specification to target by some adequate data processing. Fitting test result shows test input data is equal to model prediction. This exact prediction model can used for display image quality compensation algorithm. The algorithm make driving TFT's Ids equal. Figure 5 is result to image quality compensation. When target Ids is 0.3nA, the model can make currents distribution's sigma 4.7nA to 0.15nA. It is same mean to improve current distribution 97%.

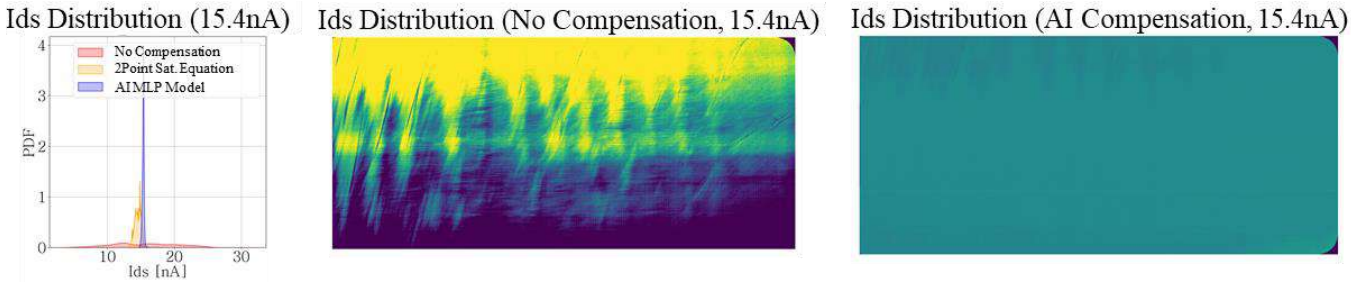

Fig. 1. Display TFT Compensation Result by AI Modelling

References

1. Hai-Jung In; Oh-Kyong Kwon. " External Compensation of Nonuniform Electrical Characteristics of Thin-Film Transistors and Degradation of OLED Devices in AMOLED Displays " International journal of information technology 4.2 (2008): 86-92.
2. Bahubalindruni PG, Tavares VG, Barquinha P, Duarte C, Cardoso N, de Oliveira PG, Martins R, Fortunato E " a-GIZO TFT neural modeling, circuit simulation and validation ".
3. Xiang Cheng, Sungsik Lee, Arokia Nathan, IEEE " TFT Small Signal Model and Analysis "
4. Lining Zhang, Mansun Chan "Artificial neural network design for compact modeling of generic transistors"

Inverse design of organic light-emitting diode structure based on deep neural network

Sanmun Kim[1], Jeong Min Shin[1], Jaeho Lee[2], Chan Hyung Park[1], Dongjin Seo[1,3], Sehong Park[2], and Min Seok Jang[1]

[1]Dept. of Electrical Engineering, KAIST, Daejeon, 34141, Korea

Tel.:82-42-350-7439, E-mail: jang.minseok@kaist.ac.kr

[2]OC Optical technology task, LG Display, Seoul, 07796, Korea

[3]KC Machine Learning Lab, Seoul, 06181, Korea

Organic light-emitting diodes (OLED) are widely used light-emitting diodes that utilize the light emission from an electron-hole annihilation inside an organic material. An optimization process is required for any OLED devices for maximization of light extraction efficiency (LEE) and color purity. Some classical approaches have been made to optimize the structure but the results are hardly global optima since the global optimization requires heavy computation [1, 2].

In this work, we present a neural network that receives the layer thicknesses and refractive indices as the inputs and predicts the LEE response of a given OLED structure. The network is trained with a dataset containing 260,000 structure parameter-LEE pairs which were obtained from the in-house Chance-Prock-Silbey (CPS) model [3]. The neural network trained in this work was implemented to solve non-trivial optimizations problems that are impossible to be performed with direct numerical calculations. The optimization tasks carried out in this work includes: reproduction of flat LEE in wide wavelength range, maximization of light extraction efficiency at a single wavelength, minimization angular color shift. These optimization tasks were based on the genetic algorithm, and was made possible through the parallelized neural network which provides a suitable platform for the calculation of 'Figure of Merit'. Furthermore, different aspects of the neural network including its one-to-many mapping behaviour, extrapolability, and comparison between the inverse design methods were investigated extensively.

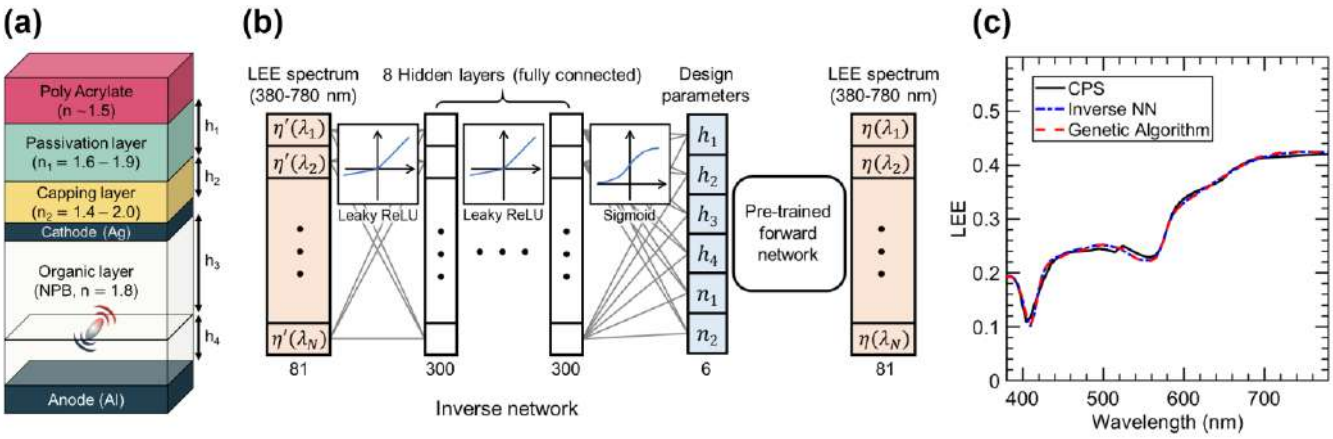

Fig. 1. (a) A schematic of the simplified OLED structure used in this work. (b) A schematic diagram of deep neural network for the inverse design of LEE. (c) An example of the inverse designed LEE.

Acknowledgment

This work was supported by LG Display.

References

1. Chan, J., et al., *Photonics: Design, Technology, and Packaging*, 5277: p. 311-319 (2004).
2. Quirino, W.G., et al., *Thin Solid Films*, 518(5): p. 1382-1385 (2009)
3. Chance, R.R., et al, *Advances in Chemical Physics*, p. 1-65 (1978)

Enhancing OLED Outcoupling Efficiency via Atomistic-scale Simulations

Paul Winget[1], H. Shaun Kwak[1], Hadi Abroshan[1], Christopher Brown[1], and Mathew D. Halls[1]
[1]Schrödinger, Inc., New York, NY 10036, United States
E-mail: paul.winget@schrodinger.com

Organic semiconductors have a wide range of electronic device applications, one of the most prominent being organic light-emitting diodes (OLEDs). Recent developments in phosphorescent and thermally activated delayed fluorescence (TADF) emitters have enabled high internal quantum efficiencies (IQEs) up to 100 %. Despite the extensive efforts to maximize IQEs by the design of novel materials, however, the amount of light extracted from the device remains relatively small in proportion. Conventional bottom-emitting OLEDs (Figure 1b), could often result in outcoupling efficiencies below 30% [1].

To overcome this challenge, a precise control of molecular orientations in the layers to induce horizontally-oriented transition dipole moments (Figure 1a) can be used to increase the efficiency by at least a factor of 1.5 compared with randomly oriented emitters [2]. Bottom-emitting OLEDs are generally designed with high reflective index layers (n_{ITO}≈1.8-2.0, $n_{organic}$≈1.8) sandwiched between a low refractive index substrate (n_{glass}≈1.5) and a reflective metal electrode. Such difference in index of refraction by the layers provides another opportunity to enhance outcoupling efficiency and to maintain color purity by tuning chemistry and morphology of the materials.

In this work, we describe an atomistic-scale modeling and simulation scheme to virtually screen both host materials and light emitters used in OLEDs while assessing molecular orientations in film. The work also demonstrates the ability to predict wavelength-dependent refractive indices from atomistic-scale up to achieve this goal. These findings would provide valuable guidelines for the development of new material architectures with superior optical loss properties as well as improved outcoupling efficiencies at the device level.

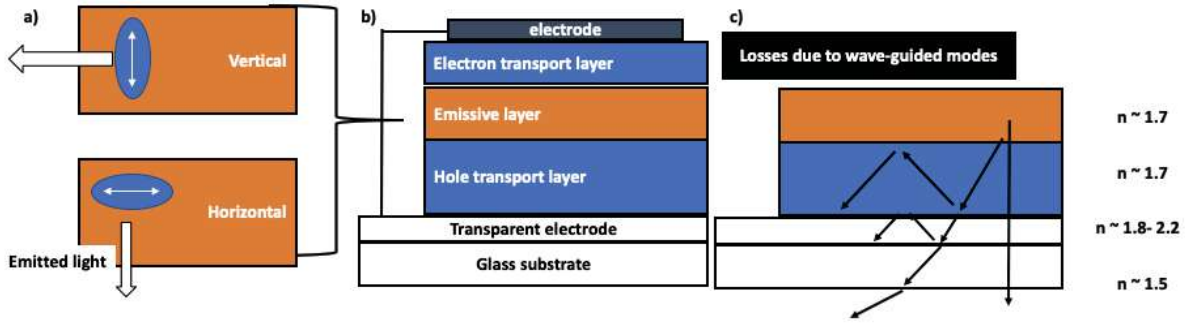

Fig. 1. a) horizontal and vertical orientation of emitters in OLEDs, b) design of a bottom-emitting OLED, and c) the effect of refractive index on emission modes

References

1. Salehi, A.; Fu, X.; Shin, D.; So, F. *Adv. Funct. Mater.* **2019**, *29* (15), 1808803.
2. Watanabe, Y.; Sasabe, H.; Kido, J. *BCSJ* **2019**, *92* (3), 716–728.

Development of Computational Optical Detection for Initial Uniformity Compensation and Defect Defection on AMOLED Displays

Shuenn-Jiun Tang, Tristan Le, Tong Liu, Tristan Doodnauth, and Junhu He
Ignis Innovation Inc. Waterloo, Ontario, Canada, N2V 2C5
Tel.: +1 519 772-1136, E-mail: sjtang@ignisinnovation.com

One of the most critical issues for AMOLED displays is non-uniformity of brightness induced by unsufficient uniform TFT characteristics in threshold voltage (Vth) and mobility [1]. Several methods using in-pixel compenation and external compensation for the issue were introduced [2]. Displays using LTPS or compenstable IGZO TFT backplanes are suitable for initial luminance correction and defect detection by optical compensation beacuse of less complexity on panel designs.

Higher luminance variation at lower Vgs was observed [3]. The luminance variation of displays driven at low data voltage is, therefore, anticipated to reflect closely the variance of TFT characteristics. However, the duration needed to grab exposure data in good quality at this range increases dramatically. In this work, we propose a computation method using optical detection with a 20MP FLIR camera for parameters prediction during detection which not only shorten the whole period but also enchance compenstion performance. Imaging at low gray-level (GL) takes typically 3 to 5 seconds. In addition, a method of camera calibration for accurately collecting luminance of every pixel on 15.6 inch 3840x2160 AMOLED display has been developed.

In Fig. 1, the proposed process flow mainly consists of the Display of input GL data per pixel and the Image by the camera, computations at the Global Parameter Calculation (GPC) for all measured GL and the Local Parameter Calculation (LPC) at a selected GL. Parameter prediction in GPC uses a equation given by

$$GL_{f,p} = A_p(GL_{i,p})+B_p\,, \qquad (1)$$

where $GL_{f,p}$, $GL_{i,p}$, A_p and B_p are the target gray level based on the most acceptable luminance, the initial/temporatay gray level, the slope and the interpretant obtained in linear regression. p represents the location of pixel on display. GL prediction in LPC performs with luminance input per pixel after imaging for one specific $GL_{t',p}$, presented by

$$GL_{t',p} = a_p(L_{t,p})+b_p\,, \qquad (2)$$

where $GL_{t',p}$, $L_{t,p}$, a_p and b_p are the targeted gray level, the luminance at $GL_{t,p}$, the slope and the interpretant obtained in linear regression.

In Fig. 2, targeted GL for every pixel was obtained by few iterations of Image assisted with LPC, that saved the period needed for a completed measuring at GL_i to around 5 to 10 seconds. Furthermore, the whole process with several different GL_i inputs was accelerated by GPC within 10 to 15 seconds while determining the final A_p and B_p. In Fig. 3(a), un-calibrated image of display at GL 90 was shown. Bright defect dots circled were also observed due to their wide TFT characteristics. Image of display reaching high uniform was shown in Fig. 3(b).

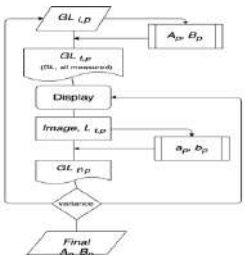

Fig. 1. The proposed Computional Optical Compensation

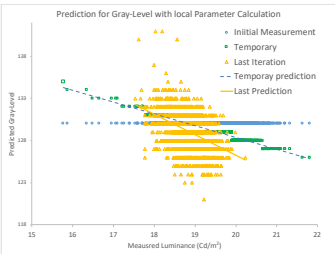

Fig. 2. Prediction for targeted GL in LPC

Fig. 3(a) Image of initial uncalibrated display driven at GL 90 with about 15% standard derivation in luminance.

Fig. 3(b) Image of the fully calibrated display driven at GL 90 with less than 2% standard derivation.

References

1. K. Oh, S. K. Hong and O. K. Kwon, J. Optical Soc. of Korea, vol. 20, p. 586 (2016)
2. S. J. Tang and J.H. He, Vehicle Display & Interfaces, Detroit 4.6 (2018).
3. Y. H. Sohn, G. J. Moon, K. H. Choi, Y. S. Kim and K. C. Park, J. Information. Display vol. 18, p. 25 (2017).

Perovskite light emitting diodes with good quantum efficiency at current densities of kA/cm^2

Paul Heremans[1,2], Iakov Goldberg[1,2], Karim Elkhouly[1,2], Weiming Qiu[1,2], Nirav Annavarapu[1,2], Robert Gehlhaar[1], Cedric Rolin[1], Tung-Huei Ke[1], Jan Genoe[1,2]

[1] imec, Kapeldreef 75, B3001 Leuven, Belgium
Tel.:32 16 281211, E-mail: Heremans@imec.be
[2] KULeuven, EE department (ESAT), Kasteelpark Arenberg, B3001 Leuven, Belgium

Metal-organic perovskite semiconductors are interesting contenders for thin-film light-emitting diodes. Their high carrier mobilities compared to organic semiconductors raises the expectation that high current densities could be reached, and hence possibly also high brightness. And, as many reports have shown low lasing thresholds by optical pumping, a further hope could be to reach injection lasing.

In the state of the art, high external quantum efficiency up to 20% has been shown in perovskite light-emitting diodes (PeLEDs). However, it is typically reached at very low current densities (typically only a few mA/cm^2), and EQE rolls off quickly for higher current densities. To reach high brightness, it is imperative to understand and combat the main root causes of EQE roll-off.

Several causes for EQE roll-off have been mentioned in literature. In particular, there is strong evidence that the EQE is sensitive to temperature, and that heating of the junction during device operation at increasing current density is a main cause for EQE to roll off with current density [1]. We have further investigated this hypothesis, and confirm that Joule heating is a main cause for EQE roll-off [2].

Our PeLED devices, fabricated on glass or sapphire with ITO transparent contact, are based on a $MAPbI_3$ perovskite active layer and polyTPD as hole injection layer. To reduce the operating voltage, we have replaced the conventional TPBi/LiF electron injection layer by PCBM/Mg:ZnO, which saves about 2V in operation voltage [2]. That in itself already considerably reduces Joule heating during operation. Furthermore, we employ photolithography to reduce the device size, and show scaled devices with diameters ranging from 1 mm down to 50 µm. Smaller diameter devices employ lower absolute current for equal current density, and therefore Joule heating in parasitic resistances is reduced. Furthermore, heat is dissipated faster from tiny structures, further reducing the junction temperature for given current density. Finally, we apply pulsed operation: curves are registered by applying sequences of pulses, whereby the device can cool down between the pulses. As shown in literature, a proper DC bias has to be applied op top of the pulses to prevent ion movement between pulses [1]. With these measures, we show in Fig. 1 successful PeLED operation from 100mA/cm^2 all the way to 5 kA/cm^2, with considerably reduced EQE roll-off (EQE is 6% peak and 0.14% at 5kA/cm^2).

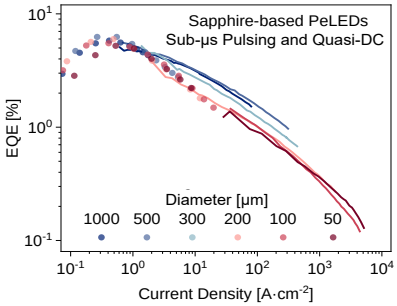

Fig. 1. External quantum efficiency versus current density for $MAPbI_3$ LEDs of different sizes

Acknowledgments

The authors acknowledge funding from the European Research Council under the European Horizon 2020 Programme/ERC grant agreement no. 835133 (ULTRA-LUX). W.Q. would like to thank the financial support of the postdoctoral fellowship grant (12Z4618N) from the Research Foundation Flanders (FWO).

References

1. See e.g. : K. Kim et al., *Nature Communications* **2018**, 4893
2. K. Elkhouly et al, *Adv. Optical Mater.* **2020**, 8, 2000941

Porous Conductive Textiles for Wearable Electronics

***Zijian Zheng*[1]**
[1]Research Center for Smart Wearable Technology, Institute of Textiles and Clothing, The Hong Kong Polytechnic University, Hong Kong SAR, China
Tel.:852-27666441, E-mail: tczzheng@polyu.edu.hk
[2]Research Institute for Smart Energy, The Hong Kong Polytechnic University, Hong Kong SAR, China

Wearable electronics plays an important role in the realization of health monitoring and rehabilitation, Internet of Things (IoTs), and soft robotics. These wearable devices and systems should be highly flexible, stretchable and even washable. In addition, they should be comfortable to wear in a long term. This talk will discuss the recent development of conductive textile materials and their applications in wearable electronics. In particular, we will discuss 1) the development of highly conductive, flexible and washable conductive fibers, yarns and fabrics through polymer-assisted metal deposition (PAMD), that can be used for a wide range of wearable sensory and energy-storage uses; and 2) the development of highly permeable stretchable conductors, namely liquid metal fiber mat (LMFM), which enables long-term wearable and 3D monolithic stretchable electronics.

References

1. Z. Ma, Q. Huang, Z. J. Zheng*, et al., *Nat. Mats.* 2021, *https://doi.org/10.1038/s41563-020-00902-3*.
2. Y. Yu, C. Yan, Z. J. Zheng*, *Adv. Mater.* 2014, *26*, 5508-5516.
3. P. Li, Y. Zhang, Z. J. Zheng*, *Adv. Mater.* 2019, *31*,*37*, 1902987.
4. R. Guo, Y. Yu, Z. Xie, X.,Y. Yang, Z. J. Zheng*, *Adv. Mater.* 2013, *25*, 3343-3350.
5. L. Liu, Y. Yu, C. Yan, K. Li, Z. J. Zheng*, *Nat. Commun*. 2015, 6, 7260.
6. Y. Yu, X. Xiao, Y. Zhang, K. Li, C. Yan, X. Wei, L. Chen, H. Zhen, H. Zhou, S. Zhang, Z. J. Zheng*, *Adv. Mater.* 2016, *28*, 4926-4934.
7. J. Chang, Z. J. Zheng*, et al., *Nat. Commun.* 2018, *9*, 4480.
8. J. Chang, Q. Huang, and Z. J. Zheng*, *Joule* 2020, *4*, *7*, 1346-1349.

Structural Engineering for Improving Flexibility and Stretchability of a-InGaZnO TFTs for Wearable Electronic Device Application

Ki-Lim Han, Won-Bum Lee, and Jin-Seong Park
Division of Materials Science and Engineering, Hanyang University, 222 Wangsimni-ro Seongdong-gu, Seoul, 04763, Republic of Korea
Tel.:82-2-2220-0401, E-mail: jsparklime@hanyang.ac.kr

Display products have been evolved in various forms such as foldable smartphone and rollable TV beyond the existing glass-based flat panel displays. Furthermore, the display industry is striving to develop free-form display. The stretchable display panel, one of the most representative of free-form display panels, is usually divided into soft areas and rigid islands[1-3]. In the basic concept of this panel, the interconnect electrodes in the soft area are stretched by elongation stress. On the other hand, the pixel circuits and the light emitting parts existing in the rigid islands (usually PI islands) do not stretched. Therefore, studies on the mechanical durability of stretchable panel tend to focus mainly on interconnect electrodes. In contrast, the mechanical durability of backplanes such as TFTs and pixel circuits in rigid islands tends to be overly optimistic. However, considering the wearable application of the stretchable panel, we must not overlook that devices are subjected to bending stresses as well as stretching stresses at three-dimensional body surface.

In this study, we fabricated a-IGZO TFT on the island PIs and thermoplastic polyurethane (TPU) hybrid structure to examine the effects of bending/stretching stresses on the TFT performance. In addition, we confirmed that the stress applied to the TFT layer can be effectively reduced by applying a polyacrylic (PA) organic passivation layer. A static structural module of ANSYS simulation was used to analyze the stress distribution at the bent/stretched state. Transmission line method (TLM) method and X-ray photoelectron spectroscopy (XPS) analysis were used to analyze the degradation mechanism of TFT. Finally, we confirmed that the logic circuits with optimize structure operate normally even under bending/stretching stress, showing the possibility of wearable device application.

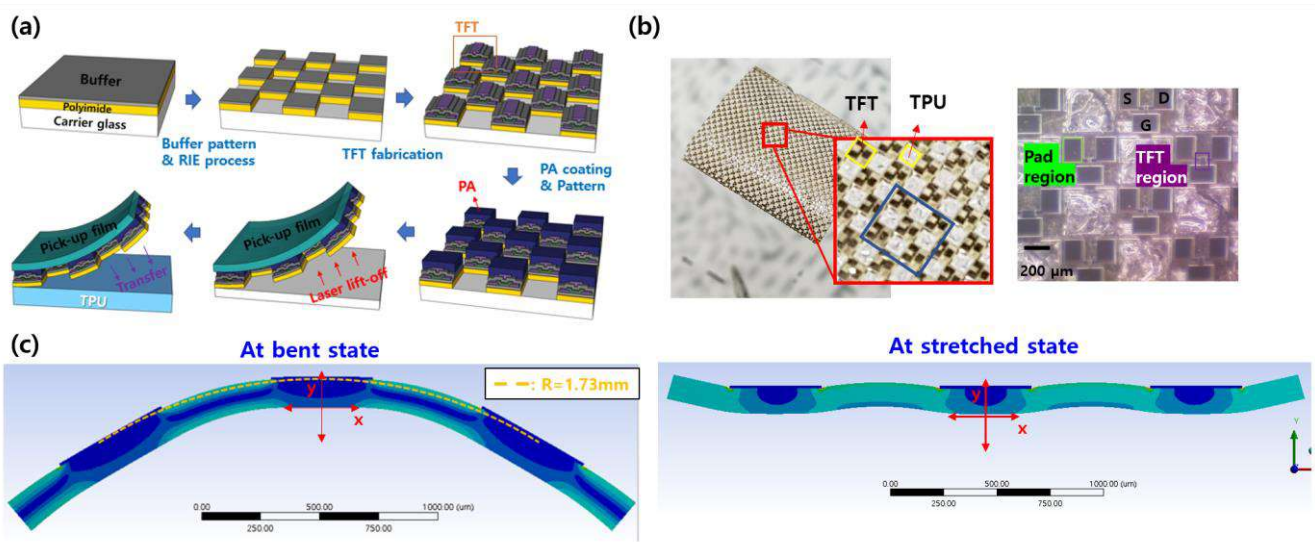

Fig. 1. (a) Fabrication process of the Flexible/Stretchable IGZO TFTs. (b) Photo and Optical image of fabricated Flexible/Stretchable IGZO TFTs. (c) Representative strain distribution at the bent (R = 1.73 mm) and stretched (Elongation : ~16 %) states obtained through 2D ANSYS simulation.

Acknowledgment
This research was supported by the MOTIE (Ministry of Trade, Industry & Energy), project number 20010690

References

1. Advanced Functional Materials 28.30 (2018): 1705132.
2. Nano letters 20.3 (2020): 1526-1535.
3. IEEE Journal of the Electron Devices Society 7 (2019): 801-807.

Highly-stable Stretchable Electrode for High Resolution Wearable Electronics

Ji Hun Choi[1,2], Chan Woo Park[1], Ji-Young Oh[1], Bock Soon Na[1], Jong-Heon Yang[1], Seunghyup Yoo[2], and Chi-Sun Hwang[1]

[1]Reality Device Research Division, Electronics and Telecommunications Research Institute (ETRI), Daejeon 34129, Korea

Tel.:82-42-860-1145, E-mail: hunbaksa@etri.re.kr

[2]School of Electrical Engineering, Korea Advanced Institute of Science and Technology (KAIST), Daejeon 34141, Korea

Stretchable electronic devices have been attracting a great deal of attention due to their potential for wearable and healthcare applications. To enable electronic devices or signal lines that are stretchable, numerous methods were proposed, such as nanowire-based percolation networks, wavy shape on a pre-stretched substrate, and deformable structure like kirigami/origami. Among them, 2-dimensional interconnection in a serpentine shape is considered as a good candidate for mass production due to its compatibility with conventional semiconductor fabrication process. However, the serpentine shape requires a relatively large footprint, so that the narrow line width is strongly desired. In this case, however, a critical problem can occur because of the high resistance associated with the narrow line width. Therefore, a low-resistivity metal should be adopted for those serpentine interconnects. Furthermore, the metal lines should have low Young's modulus to endure the mechanical stress when they are stretched.

In this study, two types of metal—molybdenum (Mo) and aluminum (Al)—were adopted for the serpentine-shape stretchable electrode. Mo-based electrode was easily fabricated, but showed low stretchability because of its high Young's modulus. On the other hand, there was a metal penetration problem in Al-based electrode fabrication process, and it often generated residues after polyimide (PI) dry etching process. The substrate and serpentine adhered to each other because of these residues, and detachment from each other was failed even after laser lift off process. It was able to be overcome by introduction of Mo/Al double-layered scheme. Fabricated Al-based electrode showed much stable stretchability than Mo-based one due to its malleable property. The resistance change of the serpentine line (ΔR) turned out to be only about 3 percent under 100% stretch test. For the cumulative stretch test with 30% elongation, ΔR remained less than 0.1% (Fig. 1), illustrating the feasibility of the proposed bilayer approach.

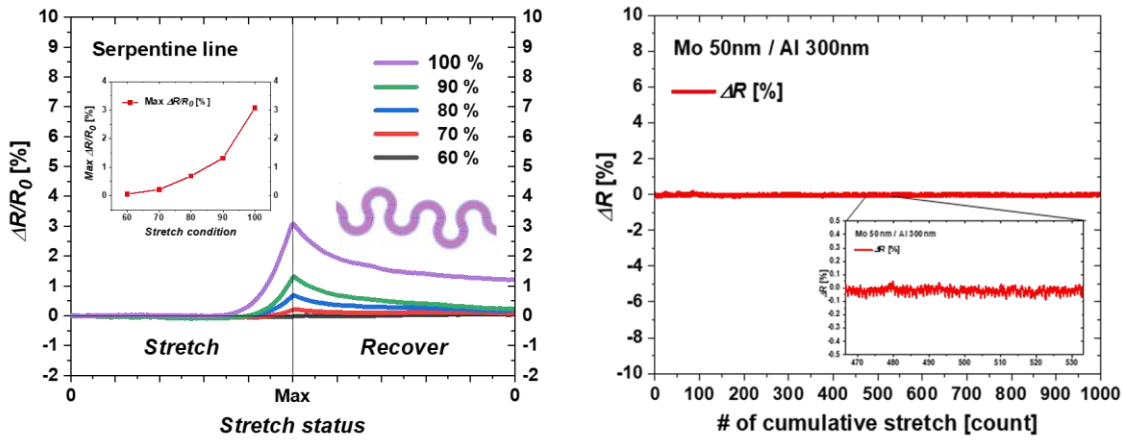

(a) (b)

Fig. 1. Elongation properties of Mo/Al double layered stretchable electrode. (a) Single stretch test result of various stretch conditions. (b) 30% cumulative stretch test result.

Acknowledgment

This work was supported by the National Research Foundation of Korea(NRF) grant funded by the Korea government(MSIT) (NRF-2020M3H4A3081897).

References

1. Y. Lie et al., *Chem. Rev.*, 117 (20), 12893-12941, 2017.

Recent Development of occlusion-capable optical see-through head-mounted displays for mixed reality

Hong Hua* and Austin Wilson

College of Optical Sciences, University of Arizona, 1630 East University Boulevard, Tucson 85721, Arizona, USA

**Corresponding Author: hhua@optics.arizona.edu*

Abstract:

Among the many challenges of developing optical see-through head-mounted displays (OST-HMD) for mixed reality applications, achieving a seamless blending the digital and physical objects is one of the key obstacles. Most of the state-of-the-art OST-HMDs lack the ability to dynamically and precisely control the opaqueness of the physical objects, thus fail to render correct occlusion relationships between virtual and real objects, which is a fundamentally important visual cue to depth perception. Furthermore, the rendered digital scene tends to be ghostly looking in bright-lit environments. In this paper, we will review the technical challenges and review the recent developments of occlusion-capable OST-HMD solutions.

Keywords: Head-mounted displays (HMD), occlusion, see-through, augmented reality

Thin Virtual Reality Display Using Fresnel Lenslet Array with Low Distortion

Kiseung Bang, Youngjin Jo, Minseok Chae, and Byoungho Lee
Dept. of Electrical and Computer Engineering, Seoul National University, Gwanak-gu, Seoul 08826, Korea
Tel.:82-2-880-9570, E-mail: byoungho@snu.ac.kr

Current commercialized virtual reality (VR) displays inevitably contain a large volume of empty space due to the primitive optical system using a single lens. In order to reduce the necessary empty space, various approches have been tried. A polarization-based optical path folding system, called pancake lens, has been widely studied for thin VR optics [1]. On the other hand, the use of a lenslet array was also applied to reduce the VR optics form factor using its short focal length [2]. Figure 1 shows the thin VR display structure using a lenslet array [3]. For the glasses-like thin form factor, it is advantageous to use Fresnel optical elements since they can be thin even with a high f-number.

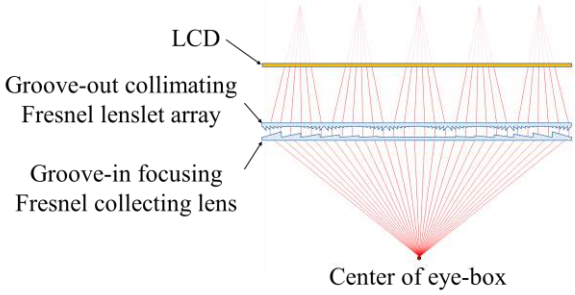

Fig. 1. The optical structure of the thin VR display using Fresnel lenslet array and Fresnel lens

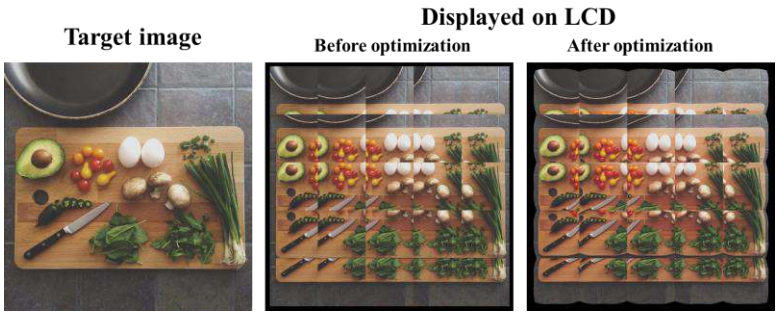

Fig. 2. Pre-compensation of displayed elemental images considering Fresnel lens distortion

With properly designed Fresnel lenses, the optical system can have no image distortion when the observer's pupil is at the center of the eye-box. Therefore, it is acceptable to display an elemental image made by simple crop and rearrangement. But we can further consider the distortion when the pupil deviates from the center by backtracing of the rays from the diviated pupil. With the optimization considering the pre-compensation, the discontinuous overlap between adjacent lenslets can be further alleviated.

Acknowledgment

This work was supported by Institute of Information & Communications Technology Planning & Evaluation (IITP) grant funded by the Korean government (MSIT) (No. 2017-0-00787)

References

1. A. Maimone and J. Wang, *ACM Trans. Graph.*, 39(4), 67, (2020).
2. J. Ratcliff, A. Supikov, S. Alfaro, and R. Azuma, *IEEE Trans Vis Comput Graph*, 26(5),1981–1990, (2020).
3. K. Bang, Y. Jo, M. Chae, and B. Lee, *IEEE Trans Vis Comput Graph*, 27(5), 2545-2554, (2021).

2D/3D image switching holographic waveguide-type HOE using the LC-MLA

Nyamsuren Darkhanbaatar[1], Munkh-Uchral Erdenebat[1], Anar Khuderchuluun[1], Byung-Chul Lee[2], Hak-Rin Kim[3], and Nam Kim[1,]*

[1]School of Inform. and Communications Engineering, Chungbuk National University, Cheongju, Chungbuk, Korea

**Tel.:043-267-8490, E-mail: namkim@chungbuk.ac.kr*

[2]Dept. of Industrial Artificial Intelligence, Chungbuk National University, Cheongju, Chungbuk, Korea.

[3]School of Electronics Engineering, Kyungpook National University, 80, Daehak-ro, Buk-gu, Daegu, Korea.

The improvement of holographic-type two-dimensional/three-dimensional (2D/3D) convertible augmented reality (AR) display system using the liquid-crystalline polymer microlens array (LC-MLA) with electro-switching polarizer is proposed. The LCP-MA has properties such as small focal ratio, high fill factor, low driving voltage and fast switching speed, which utilizes a well-aligned reactive mesogen on the imprinted reverse shape of the lens and a polarization switching layer. In case of holographic waveguide, two holographic optical element (HOE) films are located at the in-and-output parts of the waveguide. These two HOEs have functions like mirror and magnifier. Therefore, displayed elemental image set (EIS) is reconstructed by LC-MLA and reflects the transmitted light beams from the waveguide to the observer's eye as reconstructed images. The proposed system has some common features like holographic AR display's lightweight, thin size, and the observer can see the 2D/3D convertible images visualizations with the real-world scenes at the same time.

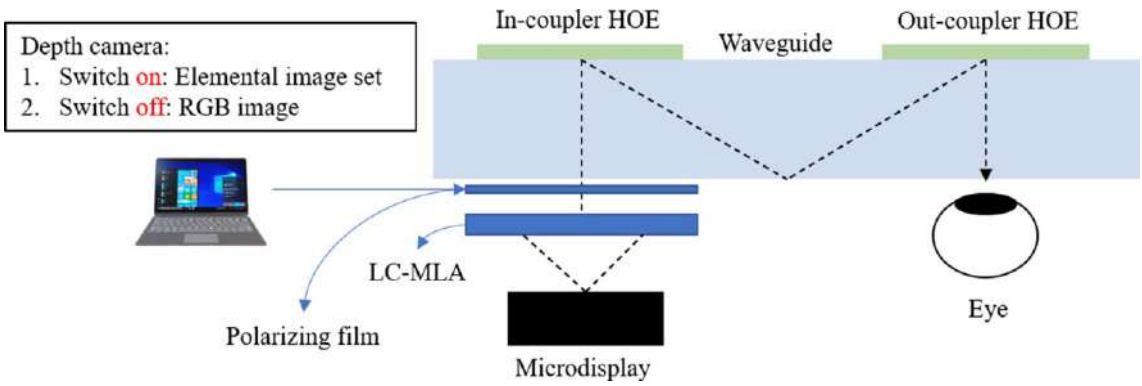

Fig. 1. Configuration diagram of the proposed method

Figure 1 is a schematic diagram of the proposed method, which is composed of a holographic waveguide type, microdisplay, lC-MLA, and switching polarizing film. The LC-MLA sits between the micro-display and the waveguide. When you turn on the mode of switching polarizer, the displayed image by the microdisplay is through the LC-MLA and polarizing film then the observer will see the 2D image. And the switch is off and the displayed EIS is reconstructed via LC-MLA and the observer sees the reconstructed 3D image. As a result of the experiment, it was confirmed that the real scene was observed at the same time as the reconstructed 2D/3D convertible image.

Acknowledgment

This work was supported by the National Research Foundation of Korea (NRF) (NRF-2020R1A2C1101258) and was supported under the ITRC (Information Technology Research Center) support program (IITP-2020-0-01846) supervised by the IITP (Institute of Information & Communications Technology Planning & Evaluation).

References

1. M. U. Erdenebat, Y. T. Lim, K. C. Kwon, N. Darkhanbaatar and N. Kim, State of the art virtual reality and augmented reality know-how, U.K, London, p. 41 (2018).
2. J.-A. Piao, G. Li, M.-L. Piao and N. Kim, J. Opt. Soc. Korea, vol. 17, p. 242 (2013).
3. K.-C. Kwon, Y.-T. Lim, C.-W. Shin, M.-U. Erdenebat, J.-M. Hwang, and N. Kim, Opt. Lett. Vol. 42, p. 3209 (2017).

See-through 360-degree high-speed light-field display using holographic asymmetric diffuser

Mun Seong Park, Myung jun Ko, Daerak Heo, Hosung Jeon, Minwoo Jung and Joonku Hahn*
School of Electronic and Electrical Engineering, Kyungpook National University, Buk-Gu Sankyuk-Dong, Daegu 41566, South Korea
Tel.:82-53-950-5514, E-mail: jhahn@knu.ac.kr

Three-dimensional (3D) displays allow observers to view a stereoscopic image by providing different viewpoints on each position. Among 3D displays, cylinder-shaped displays have benefits in 360-degree surround views. T. Yendo proposed a cylindrical 3D display with parallax barriers and 1D LED arrays where each LED array rotates in opposite directions to form multiple viewpoints along 360 degrees [1]. As another example, a cylindrical light-field display has been proposed by G. Choi, where this system displays two-dimensional(2D) image on the cylindrical screen and viewpoints are formed around the cylinder at rotating slits [2]. However, in previous systems, outside real scene is blocked by its structure. In the other word, it is impossible to present augemented reality by see-through. In this paper, we propose a see-through type light-field cylindrical system using a holographic diffuser. Figure 1 shows the schematic of the proposed system. A curved asymmetric holographic diffuser with different vertical and horizontal diffusing angles is attached to the cylinder surface. This holographic diffuser rotating at high speed forms multiple viewpoints in 360 degrees, and the high-speed DMD synchronized with the rotation of holographic diffuser displays different images according to the viewpoints. This allows the observer to watch floating 3D images from all directions.

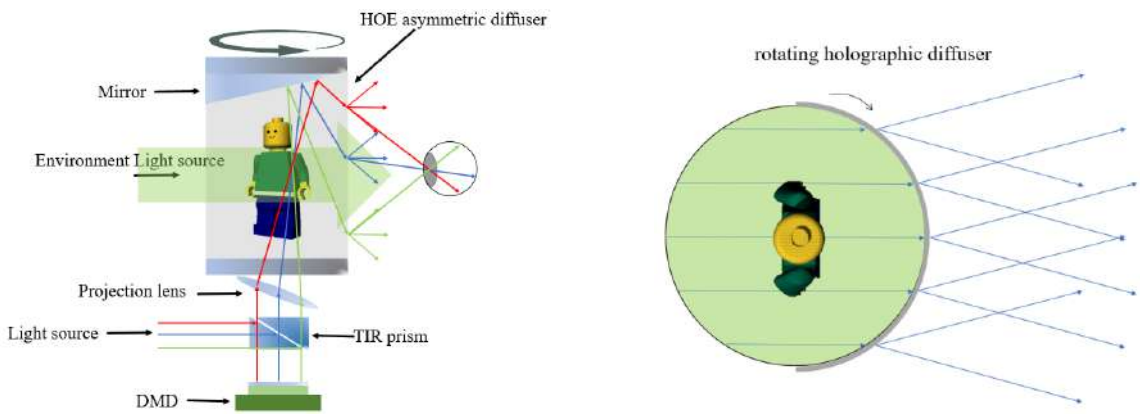

(a) **(b)**

Fig. 1.Schematic of the proposed system (a) Front view (b) Top view

Acknowledgment

This work was supported by Institute of Information & communications Technology Planning & Evaluation (IITP) grant funded by the Korea government(MSIT) (No. 2020-0-00929, Development of Authoring Tool for Digital HOE Hologram Generation Using Optical Simulation)

References

1. T. Yendo, T. Fujii, M. Tanimoto, and M. P. Tehrani, “The Seelinder: cylindrical 3D display viewable from 360 degrees,” J. Visual Commun. Image Represent 21(5-6), 586–594 (2010).
2. G. Choi, H. Jeon, D. Heo, H. Kim, and J. Hahn, “Horizontal-parallax-only light-field display with cylindrical symmetry,” Proc. SPIE **10556**, 1055605 (2018).

Light Field Display Modeling

*Ji Ho Lee, Hea In Jeong and Young Ju Jeong**
Dept. of Software, Sookmyung Women's University, Seoul, South Korea
E-mail: yjeong@sookmyung.ac.kr

Today, 3D displays are employed in various fields. As they have been utilized in various fields, the variety of 3D-display size and pixel structure has increased. Since 3D-displays have had an increase in variation, it becomes clear that a 3D quality prediction model is necessary to be applied to diverse pixel structures and sizes of 3D-displays. A preceding generalized measurement model for 3D-display design has a limitation that it can be used only to a single-pixel structure [1]. Accordingly, the goal of this paper is to simulate the 3D-image and develop a 3D-display design method that can measure the quality of the 3D-image regardless of the display size and the pixel structure.

With a way of using the 3D light field representation, we quantify the quality of the 3D images and do simulation [2] to predict the quality of 3D images no matter what the pixel structures are. First, one of the ways of prediction is the quality model. It is defined as a sum of the luminance and color uniformity because the display which shows the even light and color makes the 3D-images look real. Second, the other way of prediction is simulation. We define the light rays from the display using the 3D light field representation and estimate from which ray the viewer gets affected. The design model is developed to be implemented for various pixel structures. Figure 1 shows the simulation images of RGB horizontal stripe, Diamond PenTile, PenTile RGBG, and RGB S-Stripe. The pixels were divided into subpixels and the light field was used for the simulation.

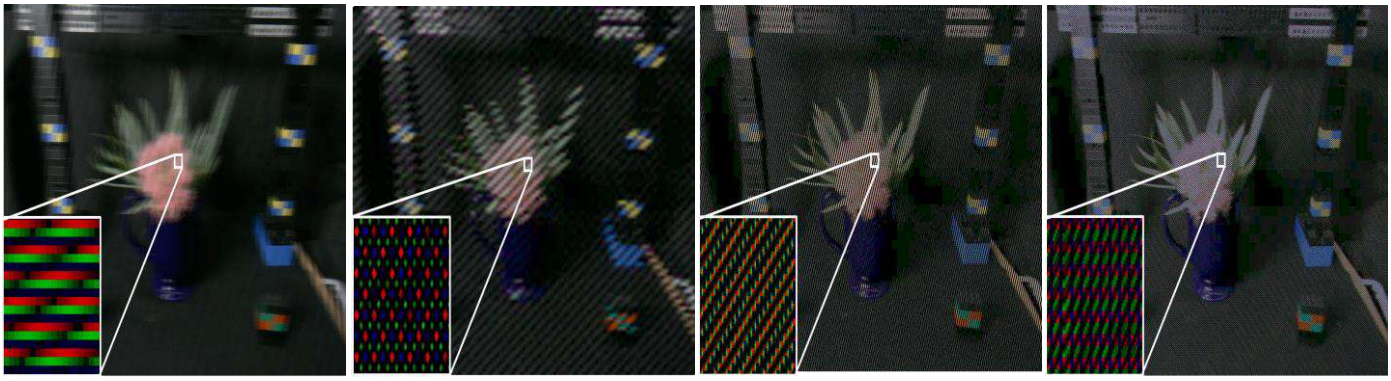

(a) RGB horizontal stripe (b) Diamond PenTile (c) PenTile RGBG (d) RGB S-Stripe

Fig. 1. Simulation images of (a) RGB horizontal stripe, (b) Diamond PenTile, (c) PenTile RGBG, and (d) RGB S-Stripe pixel structure 3D displays.

After the experiments, the results prove that the suggested 3D quality prediction model is valid. The manufactured displays were compared to the value of the quality model. The value was enough to be analyzed that it shows the high quality of 3D images on displays. Next, the 3D images of displays were contrasted to the simulated images using 3D light field representation. Additionally, the region which can not be shown on a 3D display was demonstrated using the light field simulation. Consequently, our proposed design method of 3D displays can perform a general design with diverse pixel structures.

Acknowledgment

This Research was supported by Ministry of Trade, Industry and Energy (MOTIE) (20001700).

References

1. Y.J. Jeong, K. Choi, Three-dimensional display optimization with measurable energy model, Opt. Express 25 (2017) 10500-10514.
2. H.I. Jeong, B.Kim, M.Ku, Y.J. Jeong, P-86: Light field simulation for 3d displays with various pixel structures, in: SID Symposium Digest of Technical Papers, volume 50, Wiley Online Library, 2019, pp. 1557-1560

Light-Field AR Glasses

Tomas Sluka
CREAL, Ecublens 1024, Switzerland
E-mail: tomas.sluka@creal.com

The state-of-the-art Virtual and Augmented Reality (VR/AR) 3D visualization systems fail to deliver a satisfying visual experience due to missing or conflicting depth cues. The absence of natural focal depth in digital 3D imagery causes the so-called vergence-accommodation conflict, focal rivalry, and possibly damage the eye-sight, especially during prolonged viewing of virtual objects within the arm's reach. It remains one of the most challenging and market-blocking problems in the VR/AR arena today. This talk introduces CREAL's unique near-to-eye light-field projection system [1,2] that provides high-resolution 3D imagery with fully natural monocular depth cues without any eye-tracking. Figure 1 illustrates the basic configuration of the sequential light-field projection system in Augmented Reality glasses. The light-field projectors are embedded in the temples of the glasses and project an array of perspective images to the eye-box via wavelength-selective reflection from a holographic combiner.

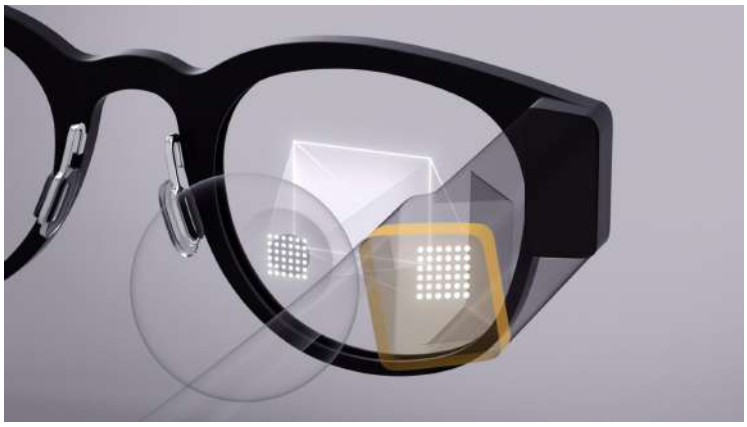

Fig. 1. Illustration of projection mechanism of light-field Augmented Reality glasses

The eye-box receives an array of nearly always-in-focus images, each entering the eye-box through a spatially disparate location. Since each viewpoint transmits to the eye pupil an image of the displayed digital scene as it is supposed to be seen from the perspective of the corresponding viewpoint, the composed 3D image is visually perceived in the correct focal distance providing correct focus cues and ocular parallax. The resulting light-field image can be blended with real-world objects without essential visual conflicts.

Acknowledgment

References

1. T. Sluka. Near-eye sequential light-field projector with correct monocular depth cues, EP2017783585 (2017).
2. T. Sluka, et al, Proc. SPIE 11765, Optical Architectures for Displays and Sensing in Augmented, Virtu al, and Mixed Reality (AR, VR, MR) II, 117650S (2021).

Recent Progresses in Time-Multiplexed Parallax Barrier Technologies

Faculty of Engineering, Information and Systems, University of Tsukuba, Tsukuba, Ibaraki 305-8573, Japan
Tel.:81-29-853-5255, E-mail: kake@iit.tsukuba.ac.jp

Parallax barrier and lenticular 3D displays are the easiest and the most common technologies to realize autostereosocpy (sterescopy without special goggles). The drawback of the parallax barrier display is the luminance loss caused by blockage of light by the barrier. Though the lenticular lens technology can maintain the luminance, the resolution of presented image is reduced because of spatial multiplexing. Both tehcnologies are used mainly for a single-viewer system, for the resolution loss becomes severer as the number of views increases.

Time-division multiplexing parallax barrier can avoid the problem of resolution loss by using time multiplexing in place of spatial multiplexing to deliver multiple views to the viewer [1-5]. With this technology, the spatial reslution of presented image can be as high as that of the display panel used in the system. The author has realized autostereoscopic displays with full HD or 4K resolutions [6].

In the conventioal parallax barrier systems, viewing zones in the depth direction are limited. Makiing use of the active barrier technology enables expansion of viewing zones in the depth direction by changing the width of barrier [5], by applying sub-subpixel phase shift of barrier [7], or by applying adaptive numbers of time division in accordance with the distance of the viewer from the screen [8].

The conventional 3D displays based on the time-division multiplexing parallax barrier have had a couple of drawbacks. One of them is the limited number of viewers. The conventional system basically allows only one viewer to see the sterescopic image, for the viewing zone for steresocopy follows the motion of a single viewer to maintain his or her stereoscopy.

In the parallax barrier system, the viewing zones for proper stereoscopy appear periodically in the horizontal direction. There is, however, no guarantee that two viewers are located in the proper viewing zones at the same time. It depends on the interval of two viewers. To keep the two viewers in proper steresoscopy regardless of the distance between them, we can change the number of time division adaptively in accordance with the interval of viewers to change the width of viewing zones [9]. In this way we can realize high resolution autostereoscopy for two viewers based on the time-division multiplexing parallax barrier technology.

Another problem of time-division multiplexing parallax barrier is high electric power consumption. Since this technology uses two LCD panels, one for the imaging and the other for the active barrier, the loss of luminance becomes servere. To overcome this problem, we can realize a time-division slit light by combining thick light bars with a lenticular lens [10]. Thin striped lights are generated as the real image of a thick light with a lenticular lens that has a fine pitch and a short focal distance. Since we use a single LCD panel and do not block light to realize a parallax barrier in this system, the power efficiency is drastically improved. This technology can also be applied to a traditional static parallax barrier to reduce its power loss.

Acknowledgment

This research is partially supported by JST CREST Grant Number: JPMJCR18A2.

References

1. Q. Zhang and H. Kakeya, Proc. SPIE 8648, 86481R.1-10 (2013).
2. Q. Zhang and H. Kakeya, Proc. SPIE 9011, 90111F (2014).
3. Q. Zhang and H. Kakeya, IEICE Transactions on Electronics, Vol. 97, No. 11, pp. 1074-1080 (2014).
4. Q. Zhang and H. Kakeya, Journal of Display Technology, Vol. 12, No. 6, pp. 626-631 (2016).
5. H. Kakeya, K. Okada, and H. Takahashi, ITE Transactions on Media Technology and Applications, Vol. 6, No. 3, pp. 237-246 (2018).
6. H. Kakeya, Proc. IMID, p.496 (2019).
7. H. Kakeya, A. Hayashishita, M. Ominami, Journal of the Society for Information Display, Vol. 26, No. 10, pp. 595-601 (2018).
8. A. Hayashishita, H. Kakeya, SID Symposium Digest of Technical Papers Vol. 49, No. 1, 1515-1518 (2018).
9. B. Yang, H. Kakeya, ITE Transactions on Media Technology and Applications, Vol. 9, No. 2, pp. 136-142 (2021).
10. H. Mitomi and H. Kakeya, Proc. IDW' 20, pp. 478-481 (2020).

Fast Tunable 8-Focus Ferroelectric Liquid Crystal Lenses for Virtual Reality

Zheng-Nan Yuan, Ming Cheng, Zhi-Bo Sun, An-Ran Li, Souptik Mukherjee, Hoi-Sing. Kwok and Abhishek. K. Srivastava*

State Key Laboratory of Advanced Displays and Optoelectronics Technologies, and Center for Display research, Hong Kong University of Science and Technology, Clear Water bay road, Kowloon, Hong Kong

In this paper, we propose a fast switchable lens system with multiple focal points. Specifically, the combination of the Electrically Suppressed Helix Ferroelectric Liquid Crystal (ESHFLC) based polarization rotator and a passive polarization-dependent LC lens can switch the focal points at high speed (50μs). Moreover, a cascaded assembly of 3 such lens units show 8-focal points, with a fast response time of 50μs. This device shows promising potential for VR and depth-mapping**.** As shown in Figure 1, the ESHFLCs have two switching positions. For N combination units, the lens has 2^N focal points that can switch at μs switching time. In this proposal, 3 lens stages can generate 8-focal points at high speed, which providing a possible solution to the vergence-accommodation conflict of VR system [1]. Furthermore, the small form factor of the lens offers it high flexibility in assembling for imaging and non-imaging systems [2-3].

In a nutshell a fast-switchable multi-focus lenses system is achieved, providing several accurate vergences in a compact size. It utilizes a combination of polarization rotation unit, based on the FLC, and a polarization-dependent passive LC lens. The proposed device shows five-fold advantages. First, the fast switching time is in the microsecond range. Second, the low driving voltages (~ 10V or less). Third, 8-tunable focus lengths switching at μs speed enable the ability to increase the depth of focus at a high frame rate. Furthermore, the aperture of the lens is 1cm, which is highly suitable for the AR/VR application. The focal length of the device is in the range of 1-5m. Last but not the least, the reduced light losses. These advantages over other existing devices are promising to meet the challenges for VR devices. Moreover, the existing limitations like the FOV, DOV can also be optimized.

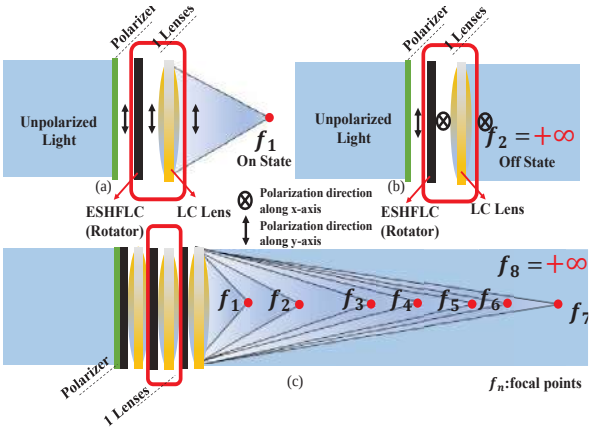

Fig. 1. (a). The schematic for focusing state at on state of the FLC rotator. (b). The schematic for focusing state at off state of the FLC rotator. (c). The schematic for assemble of 3 units with 8 switchable focal points.

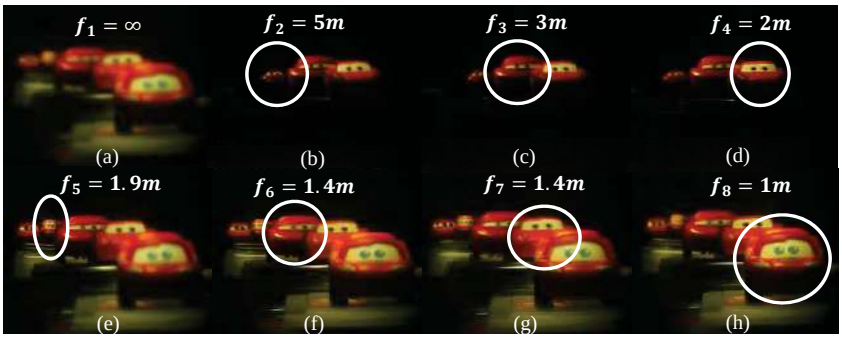

Fig. 2. (a)-(h). The defocusing and focusing effect of the FLC lenses.

Acknowledgement

We acknowledge the support of The State Key Laboratory of Advanced Displays and Optoelectronics through the Innovations and Technology Commission of Hong Kong and Hong Kong Gov. Innovations and Technology Commission of Hong Kong grant number PRP/049/19FX.

References

[1]. Lin Y-H, Wang Y-J, Reshetnyak V. Liquid crystal lenses with tunable focal length. Liq. Cryst. Rev. 2018;5(2):111-143.

[2]. Chen Z, Liu B, Liu E, et al. Adaptive polarization-modulated method for high-resolution 3D imaging. IEEE Photonics Technol. Lett. 2015;28(3):295-298.

[3]. Rahman MD, Mohd Said S, Balamurugan S. Blue phase liquid crystal: strategies for phase stabilization and device development. Sci Technol Adv Mater. 2015 Jun;16(3):033501.

Visual Discomfort Reduction in Head Mounted Display by Moving the Lens according to the Gaze-point Motion

Yuto Mori, Haruki Mizushina, Kenji Yamamoto and Shiro Suyama
Dept. of Optical Science and Technology, Faculty of Engineering, Tokushima Univ.,
2-1 Minamijyosanjima, Tokushima 770-8501 Japan
Tel.: +81 88-656-9427, E-mail: c612136025@tokushima-u.ac.jp

Recently, Head Mounted Display (HMD) has begun to spread rapidly, whereas the problem of visual discomfort such as VR sickness is left behind. Visual discomfort is considered to be caused by using lens with very short focal lengths in HMD, because short-focus lens has a tendency to bring large image distortion around the circumference of the lens. In this paper, we propose to move HMD lens according to gaze point movement for reducing the visual discomfort in HMD. The proposed HMD lens are moved synchronized with gaze-point movement where virtual objects can be observed through the center of moving lens to reduce the distortion around the circumference of the lens.

Our proposed HMD lens and experimental set-up are shown in Fig. 1. As shown in right figure, our proposed HMD lens are moved synchronized with gaze-point movement. For comparison, conventional HMD system with fixed lens in left figure were also estimated. The displayed image was a still image of the earth seen from space. Gaze points were given to both eyes of subject using phosphorescent tape so that they could be seen even in a dark room. Subject's visual discomfort was evaluated between left figure: the fixed lens and moving gaze point with the background, and right figure: fixing gaze point to the lens with phosphorescent tape and moving gaze point together with the lens. Gaze point moved for 3 minutes and Period of gaze point movement was 2 seconds. The Visual discomfort was evaluated using the Simulator Sickness Questionnaire (SSQ) questionnaire, which is used for simulator sickness [1].

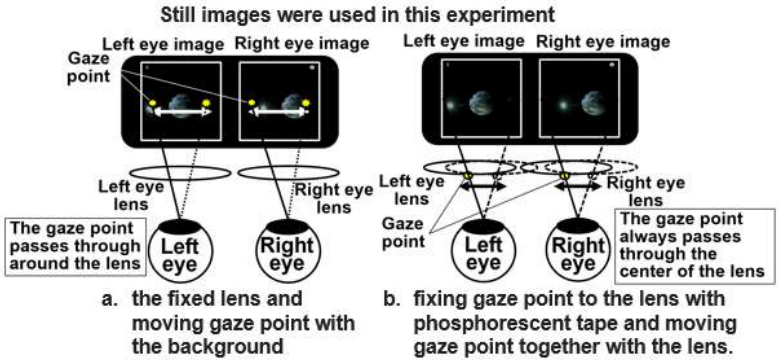

Fig. 1 Experimental diagram

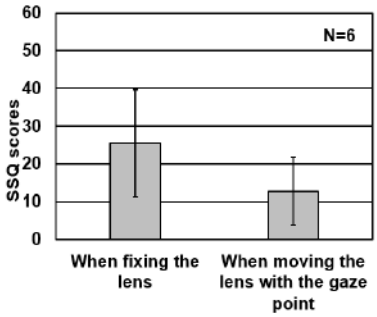

Fig. 2 Nausea SSQ scores

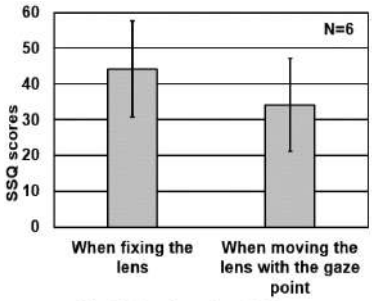

Fig. 3 Oculomotor SSQ scores

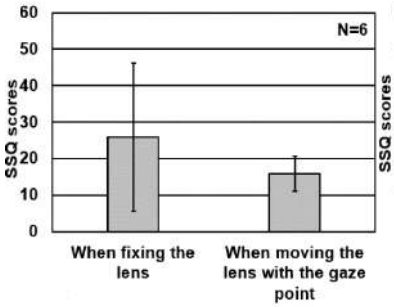

Fig. 4 Disorientation SSQ scores

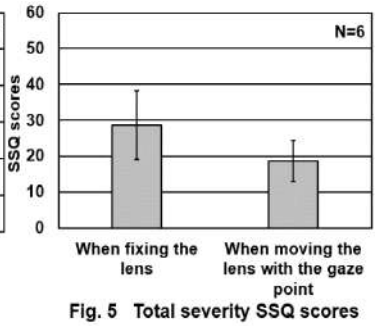

Fig. 5 Total severity SSQ scores

SSQ data are summarized for each score of nausea (Fig. 2), eyestrain (Fig. 3), disorientation (Fig. 4), and total score (Fig. 5). At all scores in Figs. 2-5. The scores of the moving lens with gaze point can be reduced from the scores of the conventional fixed lens. In particular, there is a large difference between the scores for nausea, and total score. These indicate that moving the lens with the gaze point can successfully reduce visual discomfort from conventional fixing lens.

Thus, moving HMD lens synchronize with the gaze point can reduce visual discomfort and is promising for various applications.

Acknowledgment

This work was supported by JSPS KAKENHI Grant Numbers JP19H04155, JP20K11919, JP20K21817, JP20H05702.

Reference

1. Robert S Kennedy and Norman E Lane "Simulator Sickness Questionnaire: An Enhanced Method for Quantifying Simulator Sickness." The International Journal of Aviation Psychology, 3, pp. 205-219 (1993).

Robust hazy film with high optical transmittance to reduce screen-door effect in virtual reality display

Won Seok Cho[1] and Jong-Lam Lee[1]
[1]Dept. of Material Science and Engineering, Pohang University of Science and Technology (POSTECH), Pohang 790-784, Korea
Tel.:82-54-279-2802, E-mail: jllee@postech.ac.kr

Virtual reality (VR) displays have great potential in a huge number of application fields such as a future display, industrial simulations, and medical treatment due to their inexpensive, simple, and effective systems to exhibit real-time three-dimensional (3D) images. In VR headset, lenses magnify the two-dimensional (2D) image to create an immersive 3D image[1]. However, the non-emissive region between the subpixels, which is called a black matrix, is visually recognized due to the enlargement of the images. This phenomenon is called the screen-door effect (SDE). The SDE decrease the clarity of the images and distort the images, so removing SDE is a great challenge in the VR displays. Flexible haze films have attracted much attention as one of the most promising candidates for reducing SDE with lightweight, low-cost, and enable roll-to-roll fabrication processes. When haze films are attached on display panel, the incident light is scattered and the scattered light covers the non-emissive region, resulting in the reduced SDE. The surface modulated film has been widely used for light scattering films such as micro-meshed surface, micro-lens array attached surface, nanostructured surface, and nanoimprinted surface. However, the modulated surface could be easily damaged and scratched[2]. The scratched surface produces non-uniform scattering such as sparkling and deteriorates their own optical properties. To overcome this problem, several authors have attempted to embed the light scattering center inside the flexible film rather than outside of that. The high refractive index materials such as TiO_2 nanoparticles, BaO_4SrTi nanoparticles, and Al_2O_3 nanoparticles were embedded as the light scattering centers[3,4]. However, the total transmittance of the film was degraded due to the Fresnel reflection induced by the high refractive index of the scattering center. One could solve such problem by embedding air-gaps with a low refractive index. The air-gaps can effectively scatter lights without sacrificing the optical transmittance.

Here, we report a simple way to control the size of the air-gaps embedding in the flexible hazy film by controlling the viscosity of protective layer. Nanopatterns were spontaneously produced at the surface of polyethylene terephthalate (PET) film by using oxygen (O_2) plasma treatment. Colorless curing material, poly(dimethylsiloxane) (PDMS), was coated on the surface to protect the nanopatterns. As the viscous liquid is coated on the nanoscopic patterned substrate, the liquid does not fully fill the valley of the patterns, resulting in the formation of the air-gap. The air-gap could act as a light scattering center due to the different refractive indices with the substrate. The size of the air-gaps is tuned by controlling the viscosity of the PDMS, leading to simultaneously increase in both haze and transmittance in visible wavelengths. Several simulations provide the evidence that air-gaps embedded in polymer film can effectively scatter the light due to the low refractive index of air-gaps. As a result, the hazy film significantly eliminates the SDE in the VR display about 84% compared to the planar PET film.

Acknowledgment

This research was financially supported by Brain Korea 21 PLUS project for Center for Creative Industrial Materials (F18SN25D1706). We also acknowledge Samsung Display Co., Ltd for financial support of this work.

References

1. Y. Wang, W. Liu, X. Meng, H. Fu, D. Zhang, Y. Kang, R. Feng, Z. Wei, X. Zhu and G. Jiang, *Appl. Opt.*, 55, 6969–6977 (2016).
2. N. E. Yeo, W. K. Cho, D.-I. Kim and M. Y. Jeong, *Appl. Surf. Sci.*, 458, 503–511 (2018).
3. K. Tong, X. Liu, F. Zhao, D. Chen and Q. Pei, *Adv. Opt. Mater.*, 5, 1700307 (2017).
4. D. W. Kim, J. W. Han, K. T. Lim and Y. H. Kim, *ACS Appl. Mater. Interfaces*, 10, 985–991 (2017).

Analysis of Zernike aberration in off-axis HOE for AR glasses

*Seongju Lee, Hosung Jeon, Daerak Heo, Woonchan Moon, Minwoo Jung, and Joonku Hahn**

School of Electronic and Electrical Engineering, Kyungpook National University, 80, Daehak-ro, Buk-gu, Daegu 41566, Korea

Tel.:82-53-950-5514, E-mail: jhahn@knu.ac.kr

Recently, augmented reality (AR) devices released in the market are attracting the attention of the world. These AR devices have complicated optical structure and it is hard to wear them for a long time. So it is important to reduce their size and weight for the convenience of the users. A holographic optical element (HOE) has an advantage in making complex optical components thin and light [1]. Some compact AR devices have been proposed by replacing the complex optical systems with a holographic optical element (HOE). Recently, A. Maimone has proposed a compact AR glasses using the HOE [2]. This device has wide field of view with a high numerical aperture (NA) HOE. However, the use of the high NA HOE results in aberration such as distortion of view information. In order to compensate the aberration, the aberration is measured experimentally and decomposed to Zernike polynomials [3]. It is hard to obtain enough number of data sets since elaborate skills such as Shack-Hartmann wavefront sensing are required.

In this paper, we propose a method of analyzing Zernike polynomial coefficients of the aberration with the Zemax. Then the results are used to generate a hologram for aberration compensation. Figure 1 shows a schematic of AR glasses and the change of Zernike polynomial coefficients according to the incident angle on the HOE.

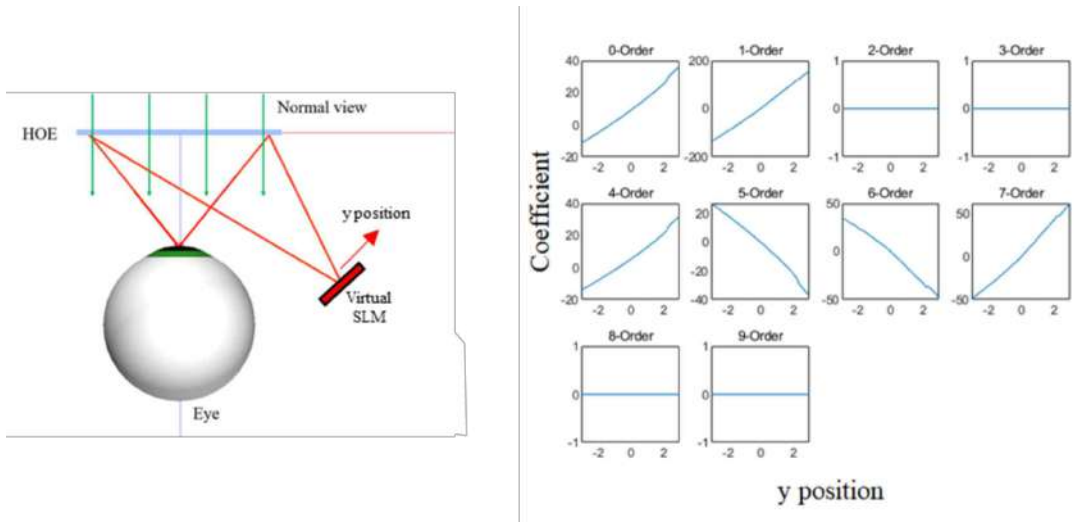

(a) (b)

Fig. 1. (a) Schematic of AR glasses and (b) Zernike coefficients according to the incident angle.

Acknowledgment

This work was supported by Institute of Information & communications Technology Planning & Evaluation (IITP) grant funded by the Korea government(MSIT) (No. 2020-0-00929, Development of Authoring Tool for Digital HOE Hologram Generation Using Optical Simulation)

References

1. D. H. Close, “Holographic optical elements,” Opt. Eng. **14**, 145402 (1975).
2. A. Maimone, A. Georgiou, and J. S. Kollin, “Holographic Near-Eye Displays for Virtual and Augmented Reality,” ACM Trans. Graph. **36**(1), 1–16 (2017).
3. Lakshminarayanan V and Fleck A, “Zernike polynomials: a guide,” J. Mod. Opt. **58**(7), 545–561 (2011).

Quality Control and Process Understanding in Display Manufacturing

Hyun-Ung Yu[1], DongHyeok Shin[1], Dongjun Kim[1], Il-Chul Moon[1], Kanghyun Choi[2], Eugene Kim[2], Daeyoun Cho[2]
[1]Dept. of Industrial and Systems Engineering, KAIST, Daejeon, 34141, Korea
Tel.:82-42-350-3118, E-mail: {chaos001, tlsehdgur0, dongjoun57, icmoon}@kaist.ac.kr
[2]Samsung Display
Tel.:82-42-350-3118, E-mail: icmoon@kaist.ac.kr

This presentation discusses a couple of case studies on quality analyses through machine learning approaches. Particularly, these analyses are interlinked to the understanding of the manufacturing process information, which means that the process information becomes the key factor in the quality prediction. In detail, our first case identifies defect-generating process step through the clustering analyses on the quality information. Second, we present the critical dimension prediction through neural networks and stochastic processes.

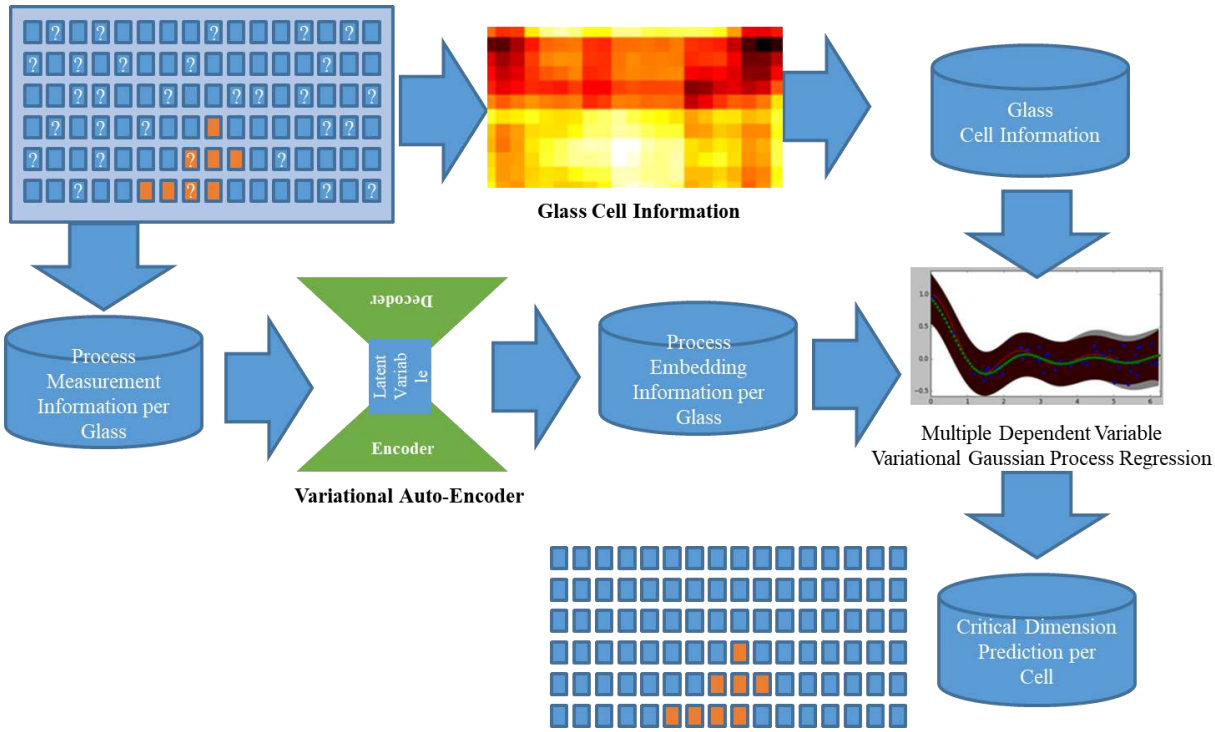

Fig. 1. An illustrative data flow for the critical dimension prediction

For instance, we consider a critical dimension prediction on multiple cells per a glass. This requries a complex interaction between the process information and the glass information. Moreover, the cell-based prediction assumes the locality of the critical dimension distribution. Here, we show the embedding space containing the process key information [1], and we demonstrate the locality modeling by the stochastic process [2]. This interaction can be further analyzed by the integration of the stochastic process and the neural network, and this presentation provides such examples.

Acknowledgment

This presentation is supported by the research grant from Samsung Display in 2020.

References

1. Kingma, D. P., and M. Welling. arXiv preprint arXiv:1312.6114 (2013).
2. Quinonero-Candela, J., and C. E. Rasmussen., Journal of Machine Learning Research 6 (2005): 1939-1959.

Targeted Machine Sound Separation by Deep Noise Verification

Jungwon Ryu[1], Hankyeol Lee[2], Euiyeol Oh[3], Changgone Kim[4], and Sooyoung Yoon[5]
LG Display Co., Ltd, LG Science Park, Seoul, 07796, Korea
Tel.:82-2-6987-0948, E-mail: jungwoncf@lgdisplay.com

In display manufacturing industry, enhancement of capability and consideration of maintenance costs are essential and important items. If a machine breakdown is detected in advance through analysis of various signals generated by machine and immediate actions are taken, it can reduce maintenance costs and greatly improve manageablility. This technique is called anomaly detection(AD), and in particular, mechanical sound-based research is being conducted. However, there are many difficulties when analyzing data from target machine(TM) for detecting an abnormality based on sound in an actual factory environment. For example, there are various noises such as background and peculiar noise, as well as interference signals from machine other than the TM. To solve these problems, a pre-processing technique for noise removal and target source separation must be applied.

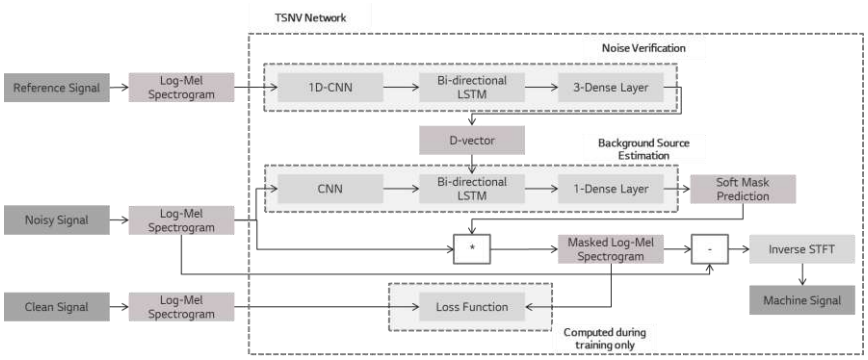

Fig. 1. TSNV Architecture.

In this paper, we present a deep learning system that separates the TM sound from background source(BS), by making use of a reference signals from other machines or noise data. Figure 1. shows the concept of our target source separation by deep noise verification network(TSNV) architecture. First, we evaluated TSNV by constructing a multi-microphone system each aiming the TM and BS near the TM. Through this environment configuration, a reference signal composed of a number of noises and other machine sounds is secured to perform noise verification(NV). In other words, the features of various machine and environmental noise can learn from our network. Second, BS estimation is performed to mask noises included in the data aimed at the TM. At this time, the input layer of Bi-LSTM is constructed by concatenating the d-vector, the last hidden layer of NV, and the output of CNN. Through the TSNV composed of two networks, soft mask prediction of noise features included in the TM can be performed. Therefore, it is obtained by calculating the mean squared error(MSE) loss between the masked log-mel spectrogram and the clean one. Finally, we can obtain an estimated clean signal of the TM by calculating the difference between the TM and the noise masked data.

We evaluated our algorithm using MIMII[1] dataset. Reference and clean signal consist of pump(id :0) and pump(id :2,4,6), which are disturbing target signals, respectively. And the Noisy signal consisted of random mixed signal of fan(id :0) and pump(id :0), which is the TM signal including BS. Lastly, the separation performance was evaluated by calculating the source-to-distortion ratio(SDR) between the clean and the masked signal according to the composition of the TSNV. As shown in Fig. 2, excellent result was obtained from CRNN based on Bi-LSTM.

TSNV Model	Mean SDR(dB)	Median SDR(dB)
No Model	7.2	2.5
1D CNN only+3 Dense Layer	7.8	8.1
1D CNN+LSTM+3 Dense Layer	11.9	9.2
1D CNN+Bi-LSTM+3 Dense Layer	**13.1**	**10.7**

Fig. 2. Experimental Results.

References

1. Purohit, Harsh, et al. MIMII Dataset: Sound dataset for malfunctioning industrial machine investigation and inspection. *arXiv preprint arXiv:1909.09347*, (2019).

Two-tier Ensemble Deep Learning Model for Anomaly Detection in OLED Encapsulation Process

Younggil Jin[1], Jongmyong Choi[1], and Pilho Kim[1]
[1]AI Team, Samsung Display, Yongin-si, Gyeonggi-Do, Korea
Tel.:82-31-5181-6860, E-mail: younggil.jin@samsung.com

This paper aims to address the improved methodology of rare event anomaly detection by hierarchical two-tier ensemble model. The rare event anomaly occurrence rate is extremly low while it induces non-negligible production loss when it causes the facility shutdown. The anomaly detection should be conducted with high recall, low false alarm rate (FAR), and class identification to prevent miss-leading of engineering action [1].

To solve the problem, this paper proposes a two-tier deep-learning ensemble model based on both classified probability of multi-class classificiation and a reconstruction error of manifold learning-based anomaly detection. Our model architecture consists of variational autoencoder(VAE) and 1-dimensional convolutional neural network(1DCNN) classifier as shown in Fig. 1. VAE enables to estimate a robust reconstruction error [2] assuming normal distribution while 1DCNN classfier provides a class probability. Predicted anomaly will be relabelled as normal class if it has low reconstruction error.

To validate effectiveness of our model, glass chucking fault of oranic light-emitting diode(OLED) encapsulation was selected with extremly low anomaly ratio(~0.01%) and multi-class(normal, anomaly1, anomaly2). As a result, developed ensemble model obtained high anomaly recall >90% and low FAR < 0.6%, while classify-only model shows relatively high FAR > 2%. This results implies that, by combining two architecture hierarchically, false alarm class of classifier can be suppressed by proper threshold of reconstruction error as a synergetic effect. To sustain the performance in practical use, the sensitivity for the ensemble model shoud be updated with transfer learning for every different anomaly. Based on that, this research can be applied to fabrication industry having diversified rare event anomaly.

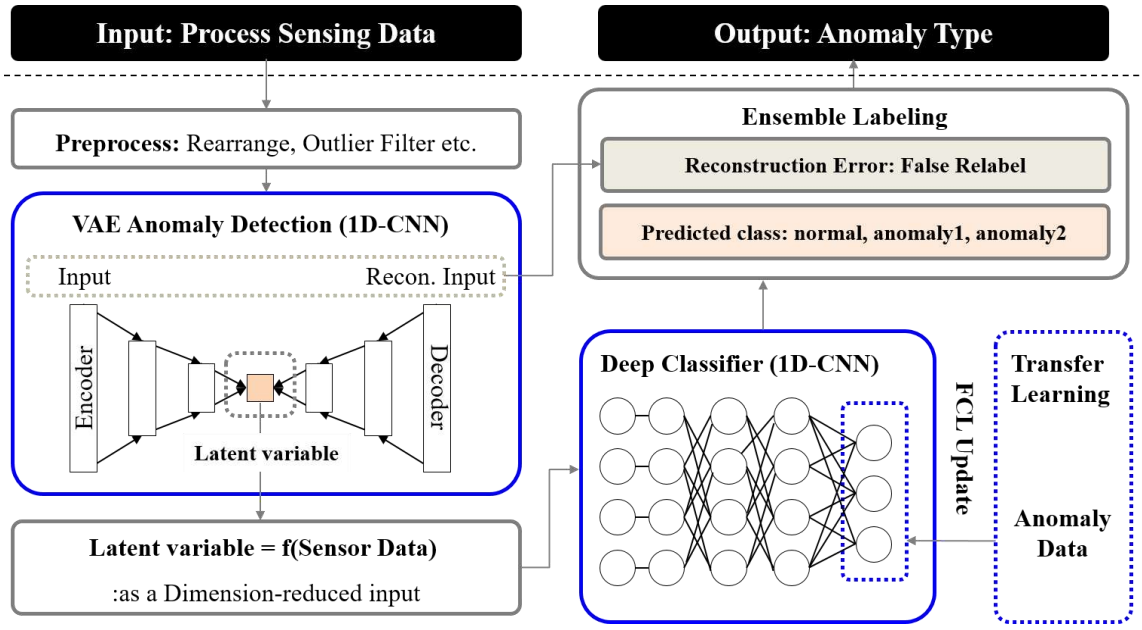

Fig. 1. Model flow chart of variational autoencoder-assisted ensemble classifier

References

1. Braei M et al., Anomaly detection in univariate time-series: a survey on the state-of-the-art. arXiv:200400433 (2020)
2. Longyuan Li et al., *IEEE Transactions on Neural Networks and Learning Systems*, Volume 32, Issue 3, (2021)

Edge-Aware Layer Segmentation for Scanning Electron Microscope Image

Jinwoo Seo*, Hyebin Lee*, Hyunji Pak*, Dongshin Choi, Minbeom Kim,
Ilho Kim, Seokwoo Lee and SooyoungYoon
LG Display Co., LTD., Gangseo-gu, Seoul, 07796, Korea
E-mail: jinwoo.seo@lgdisplay.com
**These authors contributed equally to the work*

In display industry, SEM(Scanning Electron Microscope) images are frequently used for analyzing the structure of thin-film layers. Classifying the stacked structure of layers is one of key factors in analysis. Although deep learning has achieved remarkable performance in image segmentation, its successful performance is guaranteed only in situations where well-labeled data and clear categories are defined. However, since characteritics of SEM images are diverse, it is time-consuming and requires many domain experts to label each image.

To tackle this issue, we propose Edge-Aware Layer Segmentation(EALS) method that enable segmentation from layer edges in SEM image. As identifying edge in image doesn't require much domain knowledge, annotating label information is relatively easy compared to segmentation task. Our proposed model incorporates deep learning based edge detection and segmentation module shown in Fig.1. Since we utilize modified Xception[1], of which blocks are densely interconnected, as a backbone network, the final edgemap fused by outputs from every block contains low enough level features to detect edges of SEM image. The segmentation module detects the regions of interest by distance transformation from the edge map, and then finalizes the segmented regions.

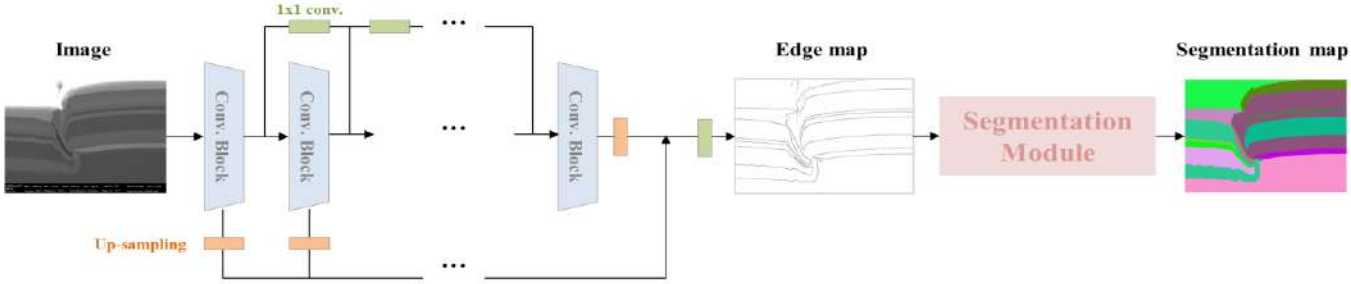

Fig. 1. Architecture of EALS

In order to experiment on SEM Image, we build datasets with carefully annotated edges of each image. We compare segmentation results with BDCN[2] and HED[3], well known deep learning based edge detection approaches, shown in Fig.2. We conclude that our method can predict more accurate segmentation maps. Furthermore, we conduct additional experiments on edge detection task of which accuracy is evaluated using 3 standard measures: average precision (AP), F-measure at the threshold from Optimal Dataset Scale (ODS) and Optimal Image Scale (OIS). Table 1 shows that our approach substantially outperforms other methods.

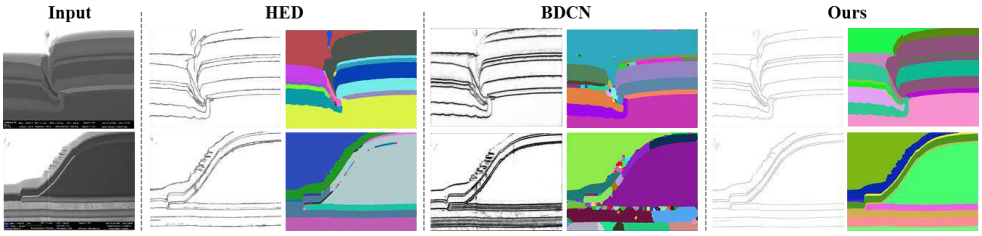

Fig. 2. Qualitative comparison on SEM image dataset

Method	OIS	ODS	AP
HED	0.841	0.838	0.771
BDCN	0.734	0.670	0.629
Ours	**0.886**	**0.877**	**0.876**

Table. 1. Quantitative result

References

1. X. Soria, E. Riba, A. Sappa. "Dense Extreme Inception Network: Towards a Robust CNN Model for Edge Detection", In *WACV*, 2020, pp.1923-1932.
2. J. He, S. Zhang, M. Yang, Y. Shan, T. Huang "Bi-Directional Cascade Network for Perceptual Edge Detection", In *CVPR*, 2019, pp.3828-3837.
3. S. Xie, Z. Tu. "Holistically-Nested Edge Detection", In *ICCV*, 2015, pp. 1395-1403.

eXplainable AI(XAI) for low gray failure analysis

KyongtaeiPark*,[i]ChangyuniMoon,iSungjuniKimiandiDonghooniJungi
Dept. of Product Engineering. Samsung Display, Gihung City, 121-791, Korea
Tel.:82-31-5181-3310, E-mail: ktman.park@samsung.com

AMOLED's low grayscale luminance and color deviation are critical quality that customers require continuous improvement.[1] Now, Process analysis and uniformity have been improved, and quality has been improved using optical compensation algorithms. [2] However, some products are poor in low quality and are not compensated well. The cause is influenced by various processes, and at the same time, it is difficult to investigate the cause of the non-linear operation of the optical compensation algorithm. (FIG.1)

In this paper, we applied eXplainable AI(XAI) has been used to analyze which FAB process dispersion caused low gray un-uniformity and why some cells could not be compensated for optical. [3] To do this, we developed an AI(Catboost etc) that predicts the final low gray color difference of a product by using numerous process data and low gray color difference information before and after compensation. [4] Then, we applied post-hoc explanation (model-agnostic) XAI (especially SHAP) to track the reasons for cases where optical compensation is working well and not, and at the same time, we were able to find out where the dispersion caused by a certain process is well compensated and the distribution of which process is not well compensated. [5] (Fig.2) By improving the newly discovered causal process using XAI, low gray color un-uniformity defects were improved by 0.52%. This result suggests that AI can be used to speed up and improve the analysis of complex influences through post-hoc analysis of AI, which was thought to be a black box, beyond the replacement of simple tasks using supervised learning.

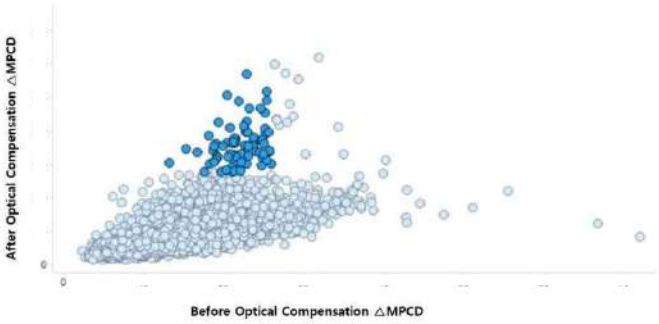

Fig. 1 Distribution of low gray color deviation(△MPCD) before and after optical compensation. Dark dots mean products that cannot be compensated. (Two axis are same scale)

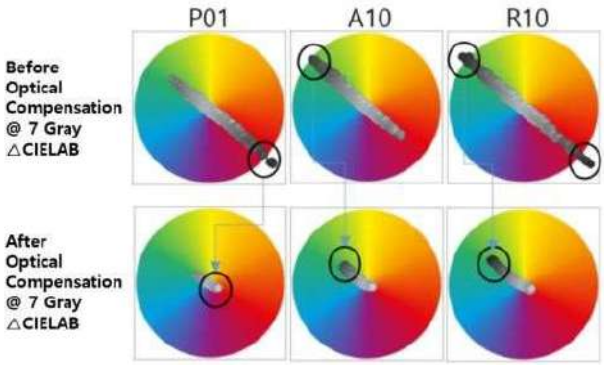

Fig. 2 As one of XAI analysis, optical compensation color distribution(△CIELAB) by location and its compensation capability limit.

Acknowledgment

References

1. "iPhone 12 OLED Screen Issue" (2020 nov) https://discussions.apple.com/thread/251997533
2. Park kyongtea "Color and Luminance Compensation for Large AMOLEDs" IMID 2009 pp.846~849
3. Shapley, Lloyd S. "A value for n-person games." Contributions to the Theory of Games 2.28 (1953): 307317.
4. Liudmila Prokhorenkova et al. "CatBoost: unbiased boosting with categorical features". In: Advances in Neural Information Processing Systems. 2018, pp. 6637–6647.
5. Lundberg, S.M., Erion, G., Chen, H. et al. From local explanations to global understanding with explainable AI for trees. Nature Mach Intell 2, 56–67 (2020). https://doi.org/10.1038/s42256-019-0138-9

Predictive Modeling of Thermal Reflow Process for Photosensitive Polyimide

Vitaly Domnenko[1], Eun-Soo Jeong[2], Sang Yil Chang[2],
Juergen Preuninger[3], Ulrich Klostermann[3], Mariya Braylovska[3]

[1]Synopsys SPb LLC, Prof. Popov str. 23D, St.Petersburg, Russia
E-mail: Vitaly.Domnenko@synopsys.com
[2]Synopsys Korea Inc, 235 Pangyoyeok-ro, Bundang-gu, Seongnam-si, Gyeonggi-do, Republic of Korea
[3]Synopsys GmbH, Karl-Hammerschmidt-Strasse 34, Aschheim/Dornach, Germany

High-volume production of dense pixel displays demands advanced and optimized manufacturing processes. Lithography simulations are actively used by industry leaders to predict and optimize process steps. One of the crucial process steps is photoresist or photosensitive polyimide curing by the post-development hardbake, when reflow leads to film thickness shrinkage and changes in the material profile shape. It can have a strong impact on mechanical and electrical properties of insulation and passivation layers [1], where polyimide materials are actively used, and optical properties in micro-lens arrays manufacturing. The predictive reflow modeling provides competitive advantage (TAT, QoR, costs) compared to an experimental "trial and error" approach.

Thermal reflow modeling solves the Navier-Stokes equations combined with free surface tracking [2]. For polyimide material the rigorous model must be able to handle thermal imidization reaction, when poly (amic acid) is imidized and the additional solvent is generated as byproduct [3]. The presence of solvent has a significant impact on material properties [4]. The increase of solvent concentration leads to viscosity reduction, while the increase of imidization degree leads to higher viscosity. The ratio between imidization and out-diffusion rates could lead to contradicting behavior for different patterns. Our new multicomponent (polymer-solvent) reflow model can successfully predict material profiles after bake including critical dimension and contact angle at substrate. Simulation results overlapped with profile measurements before and after reflowing are shown in Figure 1.

Pattern type	After development	After bake
Iso Space	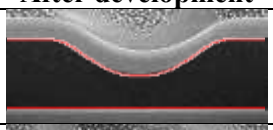	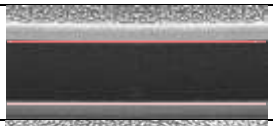
Periodic pattern 3.33:1	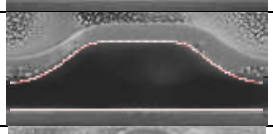	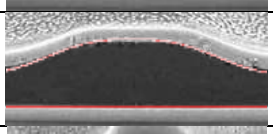
Periodic pattern 1:2	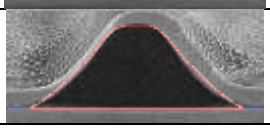	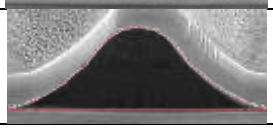

Fig. 1. Typical pattern profile measurements after development and after reflow with overlapped simulated profiles (red-white line).

The post-development hardbake model is integrated into Synopsys' rigorous lithography simulator S-Litho [5]. It allows to simulate and calibrate (based on measurements) a complete flow of manufacturing process steps including spin/slit coating, pre-bake, proximity/projection exposure, post-exposure bake, development (with developer loading), drying, and hardbake. Predictive modeling and sensitivity analysis of materials and process parameters allows to accurately optimize each process step and improve the overall manufacturing flow.

References

1. S. S. Mehta, et al. *Proc. SPIE* 10586, Advances in Patterning Materials and Processes XXXV, 1058612 (2018).
2. V. Domnenko, et al. *Proc. SPIE* 9051, Advances in Patterning Materials and Processes XXXI, 90511P (2014).
3. Fu M.-C., et al. *Polymer Journal* 50.1 pp. 57-76 (2018).
4. Chen X., et al. *Polymer* 143 pp. 46-51 (2018).
5. Synopsys S-Litho (https://www.synopsys.com/silicon/mask-synthesis/sentaurus-lithography.html).

High-resolution OLED microdisplays providing digital micro-photoemission and -detection for imaging and excitation

Uwe Vogel, Philipp Wartenberg, Judith Baumgarten, Bernd Richter
Div. Microdisplays & Sensors, Fraunhofer Institute for Organic Electronics, Electron Beam and Plasma Technology FEP, Dresden, D-01109, Germany
Tel.:+49-351-8823-282, E-mail: uwe.vogel@fep.fraunhofer.de

The prominent emissive microdisplay technology on the market is OLED-on-silicon. A single-crystalline silicon CMOS chip provides the active-matrix circuitry to address and drive millions of individual pixels (pixel cell circuitry also known as the backplane). Since the silicon substrate itself is intransparent in the visible spectrum, a top-emission OLED setup is required (emitting away from substrate). Those OLED microdisplay are regularly used in near-to-eye visualization (e.g., wearable virtual- or augmented-reality glasses).

Yet, OLED-on-Silicon microdisplay technology might is suited to bi-directional microdisplay techniques too, which combine both image display and image acquisition in a single chip. Image sensor elements, for example, pn-junction CMOS photodiodes are arranged in a fixed matrix/pixel pattern correlated to the image display pixel matrix/pattern. In a common case, both arrays have become intersected to each other, i.e., one photodetector pixel per display pixel. Other design arrangements are feasible and can be adapted to the application.

Certain applications can greatly benefit from an embedded light or even display source on an image sensor chip. That includes various approaches to surface sensing, e.g., optical finger-print sensing enabling 3rd level features detection, or surface topology scanning via inverse confocal imaging. Also non-imaging optical sensing based on the same technology is viable for chemical and physical parameter monitoring.

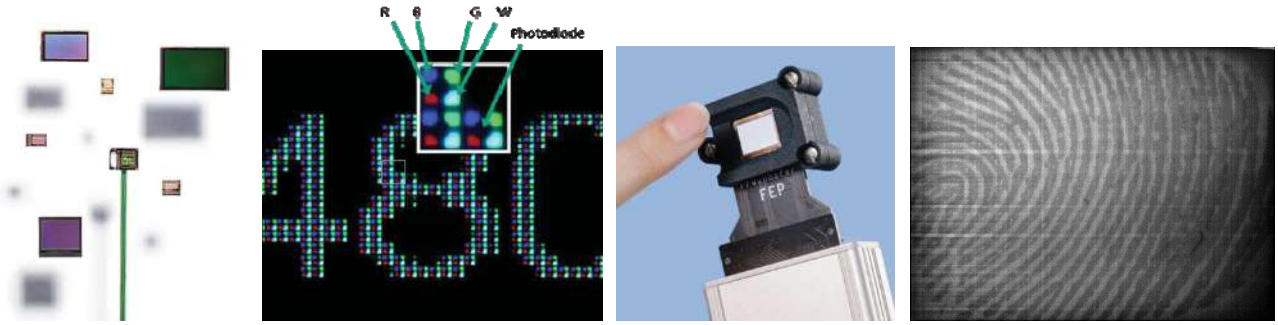

Fig. 1. High-resolution OLED microdisplay for illumination and imaging

Fig. 1 shows selection of high-resolution OLED microdisplays between 0.15” and 1” screen diagonal (left), exhibiting emitter dot pitches in the range of 4..10µm, even combining those with photodetectors at same resolution level (center), enabling use for various imaging applications, e.g., optical finger print recognition (right).

References

1. P. Wartenberg, B. Richter, S. Brenner, M. Rolle, G. Bunk, S. Ulbricht, ... & U. Vogel: A New 0.64” 720p OLED Microdisplay for Application in Industrial See-Through AR HMD. In SID Symposium Digest of Technical Papers (Vol. 50, No. 1, pp. 717-720), 2019
2. U. Vogel, P. Wartenberg, S. Brenner, G. Bunk, S. Ulbricht, M. Rolle, J. Baumgarten, P. König, B. Richter, K. Fehse, C. Schmidt, M. Schober: OLED Microdisplays for Smart Eyewear and Sensing, Workshop, The 19th Int’l Meeting on Information Display, August 27-30, 2019, Gyeongyu, Korea
3. K. Fehse, D. Schlebusch, P. Wartenberg, S. Ulbricht, G. Bunk, S. Brenner, M. Schober, B. Richter, U. Vogel: OLED/OPD-on-Silicon for Near-to-Eye Microdisplays and Sensing Applications, Proceedings of The International Display Workshops, Vol. 26, 2019, International Display Workshop IDW 2019, Sapporo, Japan, November 27-29, 2019

Development of RGB Direct Patterning OLED Micro-display

Jae Hoon Jung, Chiwoo Kim, Dong Young Sung, Jae Seok Park, Taekyung Kim*, Jong Kab Park, Doh Hoon Kim, Kiro Jung

APS Holdings Corporation, Hwasung, Korea

***Hongik University, Sejong, Korea**

Abstract

We have developed the 2,400ppi FMM using UV laser patterning technology and the RGB side-by-side OLED micro-display using Si-wafer pixel driving circuits. These two key technologies enable us to realize AR devices with ultra-high pixel resolution, high brightness, long lifetime and high color purity.

Author Keywords

FMM (fine metal mask); RGB SBS (side-by-side) OLED Micro-display; AR (augmented reality); UV (Ultra-Violet) Laser.

1. Introduction

Recently, in the field of information and communications technologies (ICT), research on technologies that can lead the 4th industrial revolution is actively being conducted. Virtual Reality/Augmented Reality (VR/AR) technology plays the key role in this field [1-3]. In particular, to increase the user's sense of immersion, a device capable of providing and interacting with multi-sensory stimulation experiences is required. Therefore, the performance of a display panel providing image information should be much better than that of a conventional television or mobile device. OLED micro-display is not a completely different technology from existing OLED mobile phone. However, there are differences in some structural and process respects. First, the pixel size is different. The pixel size of OLED panels used in televisions and mobile phones is between 40 to 200μm, while the pixel size of OLED micro-display is about 3 to 10μm, which is more than 15 times smaller. Therefore, the backplane also uses a glass-based Low Temperature Poly Silicon (LTPS) or oxide TFTs, whereas the OLED micro-display uses a Si-wafer-based CMOS process. OLED micro-display can only be manufactured by top-emission structure. In addition, for lower (anode) electrode, CMOS compatible process should be used, instead of the commonly used Indium-Tin-Oxide (ITO). For wide color gamut, RGB sub-pixels are required: red, green, and blue. Most OLED panels, widely used in smartphones, have a top light emission structure. Red, green, and blue light emitting organic layers of OLED are separately patterned by using FMM, so no color conversion layer (color filter) is required.

On the other hand, in the case of OLED micro-display, the pixel size is so small that it is difficult to elaborately patterning the red, green, and blue light emitting layers with the existing FMM technology. So, most full-color OLED micro-displays use color filters. For OLED TV, white OLED light is emitted toward the glass substrate so called bottom emission, the color filter process does not affect the OLED evaporation because the color filter is located beneath the OLED layers. On the other hand, since the OLED micro-display has a top emission structure, the color filter should be processed on top of the OLED layers.

It is well known that OLED materials are vulnerable to moisture and oxygen, and can be easily damaged by solutions, ultraviolet rays, and high temperatures under color filter patterning process.

Encapsulation and protective layers that can protect the OLED is required. In addition, low temperature special process is required for color filter formation. The color filter process should be carried out at a low temperature of 100 degrees or less. Figure 1 shows the general structure of a full color OLED micro-display.

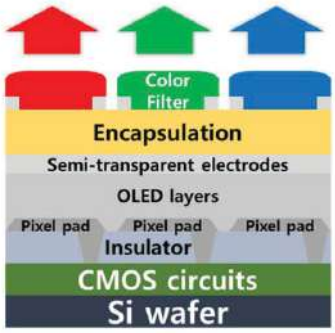

Figure 1. General Structure of White/CF Micro OLED

Some companies like eMagin [4] has recently implemented RGB SBS structure with no color filters by directly patterning the red, green, and blue OLED emitting layers. Since there are no color conversion layers, higher luminance is achieved, and the quantum efficiency is increased. This RGB SBS OLED micro-display can break-through the current bottle-neck low of brightness issue.

2. Laser patterned thin Invar FMM

FMM is conventionally manufactured by wet chemical etching process followed by well-established photo-lithography process. As the resolutions of OLED displays are soaring, the opening size of the FMM should be reduced accordingly. It is challenging to realize the fine pattern because the photo-resist masking pattern suffers under-cut after isotropic wet etching process. To circumvent this fine patterning issues, double-side wet etching process is normally used. But it causes shadow effect at the reverse-tapered region around the hole opening area. (Figure 2(a)) The reverse-tapered region and the non-linear round shaped hole formation affect the thickness uniformity under organic vapor deposition. With wet etching process, it looks like that the 600ppi QHD FMM is the resolution limit because it is very difficult to manufacture the good quality FMM sticks.

On the other hand, the laser patterned FMM can remove the reverse-tapered region because this process does not need double-side patterning. (Figure 2(b)) Spot size of the laser beam can be controlled well below the pixel size and the one side patterning is good enough to make openings of below 10um.

As shown in figure 2, to realize a high-resolution FMM stick, thickness of the FMM foil is another critical factor. To reduce the shadow distance, the Invar foil needs to be thinner. But the rolled invar made by the rolling process causes various problems when its thickness is decreased. This suggests that the current 20um is the thickness limit of the rolled Invar foil. Our approach for thin Invar sheet starts from the thick sheet. By using the TCP (Thickness Control Process), thick Invar foil is slimmed as targeted. TCP processed annealed Invar foil satisfies the thickness variation with less waviness, curling and surface roughness. [5-6]

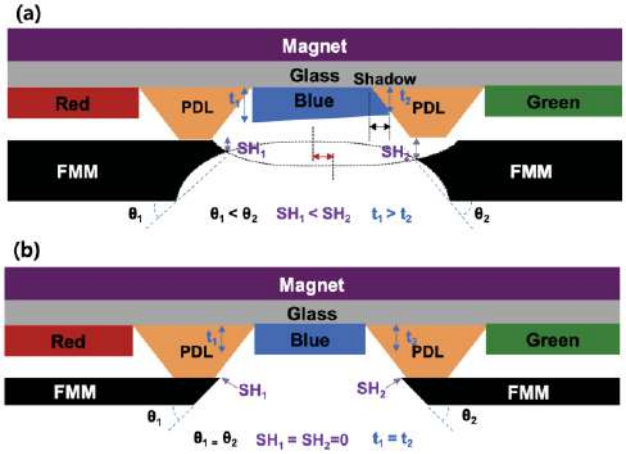

Figure 2. Schematic comparison of the (a) wet etched and (b) the laser patterned FMMs: Shadow distance is depending of the size of step height

3. Characteristics of 1,057ppi FMM

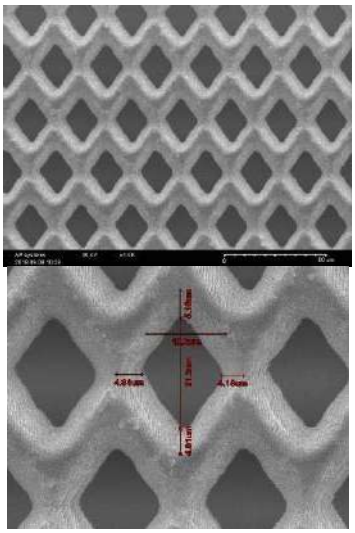

Figure 3. Top view of SEM picture of 1,057ppi FMM

In an intermediate stage to develop 2,400ppi FMM, we fabricated 1,057ppi FMM, first. 1,057ppi FMM has been fabricated for the first time by using thin TCP rolled Invar and laser patterning method as shown Figure 3. Well tapered and sharp rounding patterns can be obtained with the laser patterning process.

Figure 4 shows the optical image and shadow distance of the 100nm thick organic film deposited by using our 1,057ppi FMM. Thanks to very thin Invar thickness of active area and zero step height of Laser patterning process, FMM shows neglectable shadow distance of 0.29μm.

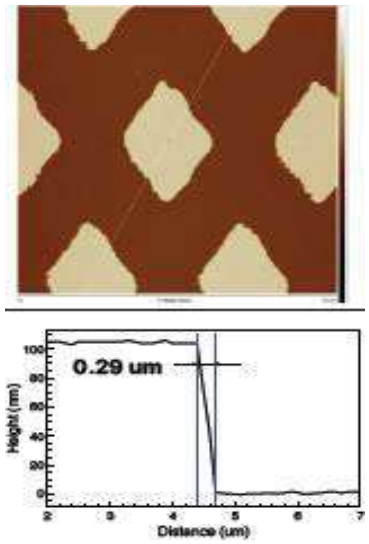

Figure 4. Optical image and shadow distance of deposited organic film using 1,057ppi FMM

With this result, we can expect that if the Invar thickness is thinner, it could be possible to develop ultra-high resolution FMM with 2,400ppi. Thanks to TCP process we can control the thickness of the FMM active area below 5um.

4. UV Laser System

In order to process an FMM with a resolution of 1,500ppi or higher, it is essential to reduce the laser beam spot size and the IR laser source does not fit our requirements. As shown Figure 5, we need shorter wavelength lasers.

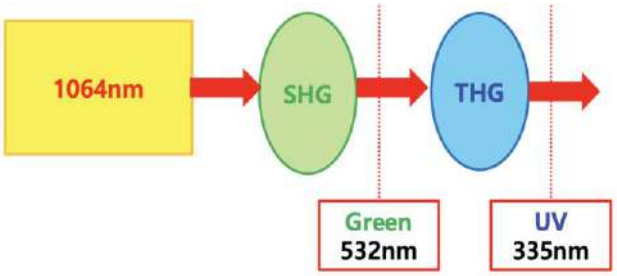

Figure 5. Schematic diagram of UV Laser System

UV Laser is made through optical coupling systems (SHG+THG). Instead of using a separate laser sources, IR laser with basic wavelength of 1064nm is used. SHG is the second harmonic generation and THG is the third harmonic generation. The conventional IR Laser's focused beam size is ~15μm, and the UV laser's is ~2μm. UV laser is our choice for producing 2,400ppi FMM with several um pixels.

5. Fabrication of 2,400ppi FMM

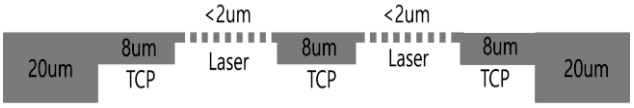

Figure 6. Schematic cross-sectional view of 2,400ppi FMM

In order to make 2,400ppi FMM, it is necessary to make thin Invar sheet. We make 8um thick Invar film using our TCP process. After that, the active area is process down to 2μm thick using the laser. Finally, ultra-thin active area is processed for pixel holes by UV laser as shown Figure 6.

Table 1. PDL (Pixel Defined Layer) margin by applying multiple factors

	Factor	2400ppi
FMM	Pixel Position Accuracy	0.3
	Pixel Shape Accuracy	0.3
	Shadow Distance	0.3
Equipment	Align accuracy	0.5
Si BP	Thermal expansion	0.05
	Pattern align accuracy	0.1
	PDL Margin	**2.03**

To design an RGB SBS pixel, PDL margin between each pixel must be applied. PDL margin is determined by the size of the individual parameters indicated in table1. This PDL margin plays a major role as preventing color mixing by depositing different color organic materials on each RGB pixel.

Furthermore, reducing the PDL margin increases the aperture ratio of the pixel, so the optical efficiency and lifetime of the OLED device can be improved. In particular, the shadow distance is a major factor that can reduce the PDL margin. Therefore, our laser patterned mask is optimum for producing RGB side-by-side OLED micro-display because the step height is negligible. The aperture ratio of the pixel can be increased, and the device lifetime can be increased accordingly.

6. Enhancing efficiency of Micro OLED device

In figure 7, pixel structures are compared in terms of the aperture ratio. The aperture ratio of S(Samsung)-Stripe is larger than RGB Stripe. The S-stripe is the OLED pixel structure applied to the early models of Galaxy series to increase the aperture ratio. If we compare these two pixels to our 2400ppi case, the aperture ratio of S-stripe is 45.5% and RGB stripe is 36.2%, respectively, for the case of 2μm PDL margin as described in Table 1. Pixel width of S-stripe is 5.4μm and RGB stripe is 3.6μm, respectively.

In terms of processing with a limited beam size (2~3μm), the processing margin of S-stripe pixel structure is larger, so it can be manufactured with higher yield. Furthermore, since the efficiency and lifetime of blue pixel are relatively low compared to red and green pixels, the efficiency and lifetime of the OLED device can be balanced by increasing the pixel size of blue.

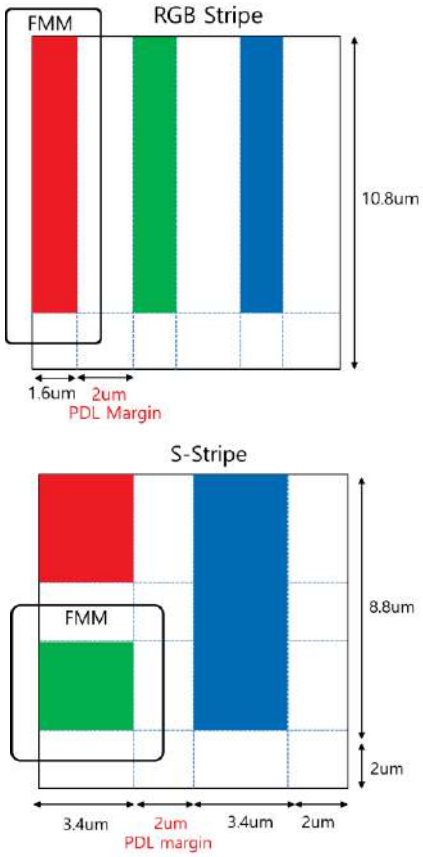

Figure 7. Pixel structure of RGB stripe and S-stripe

Recently, the efficiency of organic materials shows remarkable efficiency and lifetime by using phosphorescent materials for Red and Green. However, the case of Blue still depends on the fluorescent material, and the efficiency and lifetime are very low compared to Red and Green.

To overcome this, TADF (Thermally Activated Delayed Fluorescence) or Hyper-fluorescence materials are being developed to improve the efficiency of Blue device [7]. In this case, more than three co-deposition process are required, so it is necessary to develop the multiple deposition sources and process for multiple co-deposition.

However, increasing the size of Blue pixel size to improve the efficiency and lifetime of the OLED device is still limited until phosphorescent Blue material is developed and commercialized.

Figure 8(a) shows the conventional OLED device structure with top emission. As discussed above, this structure has fundamental limitations in improving the efficiency and lifetime of OLED devices. So to overcome this limitation, we propose a new OLED structure shown in Figure 8(b). This allows Red and Green to have a single stack, which is an existing structure, while Blue is fabricated as a dual stack to maximize the efficiency and lifetime of the OLED device.

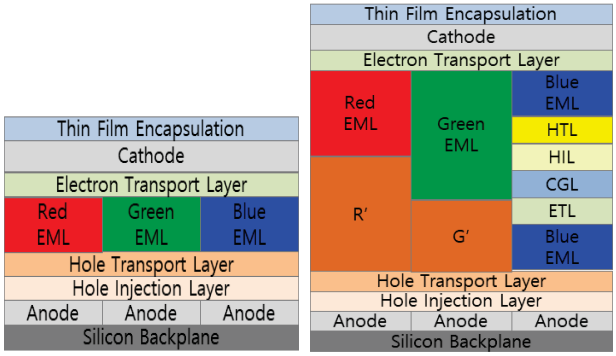

(a) Single OLED device (b) Single R/G and dual stack B

Figure 8. Schematic diagram of (a) conventional OLED device and (b) suggested OLED device

7. Impact

The Invar slimming (TCP) and the state-of-the-art UV laser ablation process can realize the ultra-high-resolution (~3,00ppi) FMM fabrication. It is expected that with our ultra-high-resolution FMM sticks, RGB side-by-side OLED micro-display can be mass produced. In addition, if the S-stripe structure, R/G single stack and B dual stack structure proposed by us are adopted, AR applications adopting this RGB side-by-side OLED micro-display is expected to be realized in the near future.

8. References

[1] G. Haas, "Microdisplays for Augmented and Virtual Reality," SID 2018 DIGEST, 2018, pp.506-509.

[2] P. Wartenberg, M. Buljan, B. Richter, G. Haas, S. Brenner, M. Thieme, U. Vogel, P. Benitez, "High Frame-Rate 1" WUXGA OLED Microdisplay and Advanced Free-Form Optics for Ultra-Compact VR Headsets," SID 2018 DIGEST, 2018, pp.514-517.

[3] T. Fujii, C. Kon, Y. Motoyama, K. Shimizu, T. Shimayama, T. Yamazaki, T. Kato, S. Sakai, K. Hashikaki, K. Tanaka, Y. Nakano, "4032ppi High-Resolution OLED Microdisplay", SID 2018 DIGEST, 2018, pp.613-616.

[4] A. Ghosh, E. P. Donoghue, I. Khayrullin, T. Ali, I. Wacyk, K. Tice, F. Vazan, O. Prache, Q.Wang, L. Sziklas, D. Fellowes, R. Draper, "Ultra-High-Brightness 2K×2K Full-Color OLED Microdisplay Using Direct Patterning of OLED Emitters", SID 2017 DIGEST, 2017, pp.226-229

[5] C. Kim, K. Kim. O, Kwon, J. Jung, J. Park, D. Kim, K. Jung, J. of SID, "Fine metal mask material and manufacturing process for high-resolution active-matrix organic light-emitting diode displays, 2020, pp.1-12

[6] K. Kim, C. Kim, J. Park, D. Kim, K. Jung "FMM Materials and Manufacturing Process: Review of the Technical Issues", SID Symposium Digest of Technical Papers, 75-4 (2018)

[7] G. W. Kim, H. W. Bae, R. Lampande, I. J. Ko, J. H. Park, C. Y. Lee, J. H. Kwon, "Highly efficient single-stack hybrid cool white OLED utilizing blue thermally activated delayed fluorescent and yellow phosphorescent emitters", Scientific Report, 2018, pp,1-11

Improving the Outcoupling of OLED Displays

Wan-Yu Lin[1], Chung-Chia Chen[1], Hyunsung Bang[1], Lisong Xu[1], Gang Yu[1], B. Leo Kwak[1], Robert Jan Visser[1], Yi-Ting Chen[2], Sheng-Wen Wen[2], Po-Hsiang Liao[2], Chang-Cheng Lee[2], Wei-Kai Lee[2], Chun-Wei Huang[2], Guo-Dong Su[2], Hoang Yan Lin[2], Chung-Chih Wu[2]

[1]Applied Materials, Inc., California 95052, United States of America

Tel: +1-408-748-5706, E-mail: Robert_Visser@amat.com

[2]Graduate Institute of Electronics Engineering, Graduate Institute of Photonics and Optoelectronics and Department of Electrical Engineering, National Taiwan University, Taipei 106, Taiwan

We prove successfully substantially greater EQE improvement, > 2.4x over the current baseline OLED as shown in, by combining it with the reflective mirror on PDL bank, the patterned, index-matched filler and the transparent IZO top electrode. The EQE improvement is enhanced further with smaller pixel for higher resolution applications as shown in **Fig. 2** and **Table 1. Fig. 3** demonstrates the top-view optical microscopical and cross-section SEM pictures of 300 ppi with aperture ratio 30 % device. Since filler thickness and horizontal profile are less relevant, the enhancement is kept with a concave filler as predicted in [1]. As this approach can be compatible to current panel fabrication process and is in principle wavelength insensitive, the approach is generally good for all colors, enabling our approach to be a practical breakthrough to OLED efficiency issue.

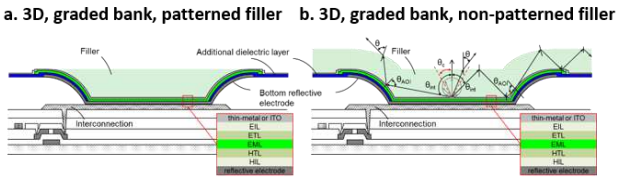

Fig. 1 Pixel and device configurations of 3D pixel configurations [1]

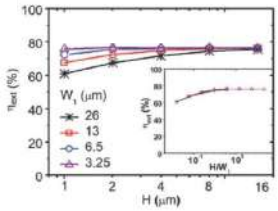

Fig. 2 EQE enhancement is more significant with smaller pixel (W_1) or higher bank thickness (H) [1]

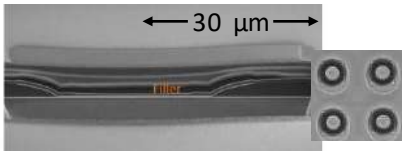

Fig. 3 Cross-section SEM of the 3D pixel configuration devices with IZO top electrode and five layers TFE encapsulation; insert: top view of the device

Table. 1 EQE enhancement of the 3D pixel configuration devices with IZO top electrode and five layers TFE encapsulation

Position		opening (um)	EQE ratio	EQE ratio_avg
Simulation		13	2.61	
100 ppi	AR30%	79	1.42	1.38
	AR50%	102	1.46	
	AR70%	120	1.25	
200 ppi	AR30%	39	2.12	1.94
	AR50%	51	1.92	
	AR70%	60	1.79	
300 ppi	AR30%	26	2.43	2.36
	AR50%	34	2.45	
	AR70%	40	2.21	

References

Chen YJ, Lee WK, Chen YT, Lin CY, Wen SW, Jian M, Adv. Sci.; 2018. Vol. 5, 1800467.
Chen CY, Lee WK, Chen YJ, Lu CY, Lin HY, Wu CC. Adv. Mater.; 2015, 27, 4883.
W. K. Lee, Y. T. Chen, S. W. Wen, P. H. Liao, M. C. Lee, Y. J. Chen, G. D. Su, H. Y. Lin, C. C. Wu, C. C. Chen, W. Y. L, L. Xu, G. Yu, B. L. Kwak and R. J. Visser, *SID'19 Technical Digest*, vol. 50, p. 1939 (2019).
C. C. Chen, W. Y. Lin, L. Xu, G. Yu, B. L. Kwak, R. J. Visser, Y.T. Chen, S. W. Wen, W. K. Lee, P. H. Liao, M. C. Lee, Y. J. Chen, G. D. Su, H. Y. Lin and C. C. Wu, *SID'19 Technical Digest*, vol. 50, p. 145 (2019).
SID2020
IMID2020

High-resolution patterning of OLEDs through solution and evaporation hybrid process

Kwan Hyun Cho[1], Jun Yeub Lee[1], Yong-Cheol Jeong, and Kyung-Tae Kang[1]
[1]Manfacturing process platform R&D Dept., Korea Institute of Industrial Technology, Ansan-si, Gyeonggi-do, 15588, Korea
Tel.:82-31-8040-6256, E-mail: khcho@kitech.re.kr

High-resolution patterning of display pixels is still on the one of important agendas in the display industry, and the requirements of high pixel-density are increasing for augmented reality (AR) and virtual reality (VR) devices. Conventional photolithography is not suitable for patterning of organic layer due to the problems of dissolving or contaminating the fragile organic materials. Although shadow mask technology has proven to be the method of mobile OLED displays, the fabrication of thin metal plate and tiny holes is still huge challenge for AR and VR devices. In our previous works, we presented a novel approach of a solution process followed by intense pulsed light (IPL) evaporation for the fabricating high-resolution line patterns of OLED [1-2]. Emitting layer (EML) inks prepared by using general organic solvents were easily deposited into only the micro-channels by using a conventional solution process, and then the patterned EML layers were transferred onto the device substrate by IPL evaporation process. Also, we demonstrated that the IPL-evaporated films have many advantages compared to those fabricated by the conventional solution process. We will be discussed the limitation factors to fabricate the high-pattern density from the intensive studies on the relation between IPL evaporated patterns and the dimensions of bank and micro-channel.

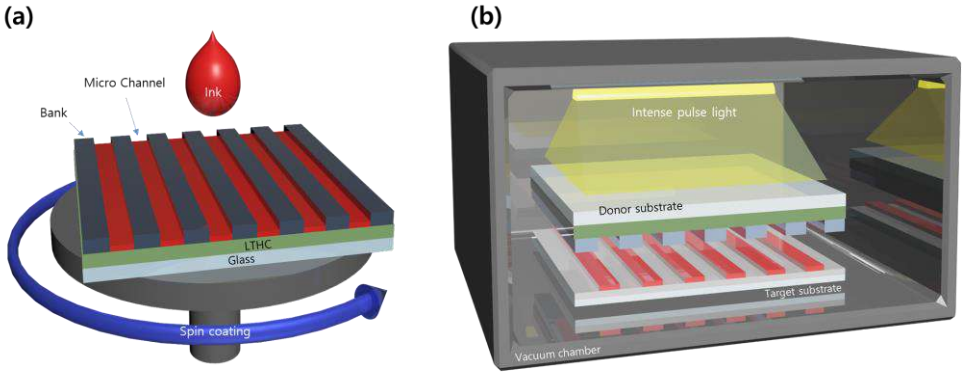

Fig. 1. Schematic diagrams of solution process for ink filling into the donor substrate (a), evaporation process by intense pulse light in the vacuum chamber (b)

Acknowledgment
This study was conducted with supported by Ministry of Trade, Industry & Energy (MOTIE, No. 20010459).

References

1. K.H. Cho, Y.C. Jeong, H.N. Lee, H.C. Cho, Y.M. Park, S.H. Lee, and K.T. Kang, SID Symposium Digest of Technical Papers, 50: 1507-1510 (2019).
2. H.C. Cho, H.N. Lee, Y.C. Jeong, Y.M. Park, K.T. Kang, and K.H. Cho, ACS Appl. Mater. Interfaces, 12, 40, 45064–45072 (2020).
3. Y. Lee, Y.J. Han, K. Y. Cho, K.H.Cho, Y.-C. Jeong, Macromolecular Research, 29 (2), 172-177 (2021).

Technology developments in FMM-free direct R-G-B smart OLED pixels

Tung-Huei Ke[1], Calvin Mona Sandeheng[1,2], Erwin Vandenplas[1], Pawel E. Malinowski[1], and Paul Heremans[1,2]
[1]imec, Kapeldreef 75, 3001 Leuven, Belgium
[2] KU Leuven, 3000 Leuven, Belgium
E-mail: tunghuei@imec.be
(2 line spacing)

Developments in OLED full-color fabrication processes are crucial for next-generation displays. Fine-Metal Mask (FMM) method is utilized to fabricate medium and small size OLED displays with high efficiency and high brightness for the direct RGB OLED pixels, even though the substrate size and pixel aperture ratio are limited due to the mask bending and mask clogging during OLED fabrications. Color-by-white (CBW) OLED is employed in OLED TVs and microdisplays fabrication for substrate size and pixel density, respectively. However, the light absorption in the color filter limits the maximum brightness and current efficiency in CBW OLED. High brightness and high pixel density are crucial for displays in VR/AR applications. Ultrahigh-resolution shadow masks have been realized with a pixel density of 2k ppi for OLED microdisplay [1]. Tandem white OLED has been introduced in the CBW OLED microdisplay to achieve high brightness with high OLED driving voltage [2]. It is essential to develop technology to achieve high brightness, high pixel density with low driving voltage simultaneously.

Photolithography has been employed in semiconductor development for decades to create high-resolution patterns. Although it was considered an extreme challenge to apply photolithography to pattern organic semiconductors for OLED applications for the incompatibility of chemistry and process environment, imec has been continuously working on patterning OLEDs by photolithography with a specialized photoresist system [3].

This presentation shows our OLED patterning technology development toward high-resolution FMM-free direct R-G-B OLED displays (Fig.1.). Because of the resolution of photoresist, high aperture ratio, and high-resolution multicolor OLED pixel arrays are demonstrated. We illustrate an integration route toward R-G-B side-by-side by photolithographic patterning. We investigate the possible extrinsic degradation mechanisms in photolithographic patterned OLEDs. Efforts have been made in OLED stacks, process steps, process environment, and photoresist to mitigate the potential OLED degradations to show the progress in patterned OLED lifetime (Fig. 2.).

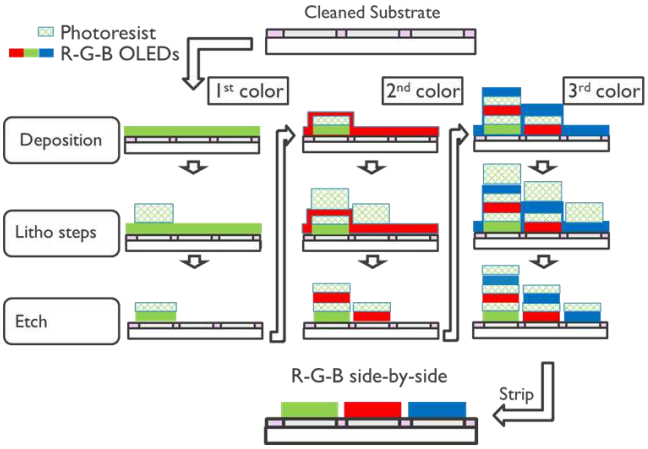

Fig. 1. Schematic fabrication flow of a photolithography-based RGB OLED

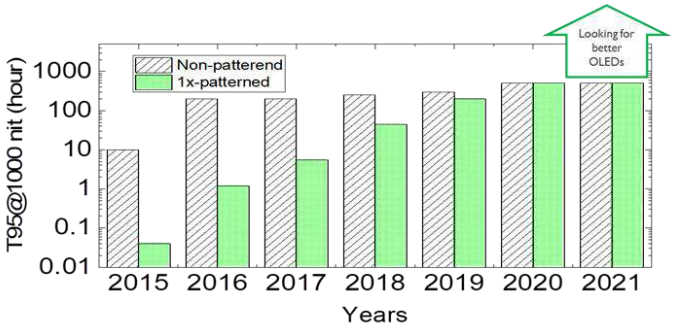

Fig. 2. Evolution of non-patterned and patterned OLED lifetime at 1000nit

References

1. Ghosh A, Donoghue EP, Khayrullin I, et al. *SID Symp Dig Tech Pap*. 2016;47(1):837-840.
2. Hamer J, Kondakova M, Spindler J, et al. *SID Symp Dig Tech Pap*. 2020;51(1):149-152.
3. Malinowski PE, Ke T, Nakamura A, et al. *SID Symp Dig Tech Pap*. 2015;46(1):215-218.

3,000 ppi Monochrome White Micro-Display Based on Organic Light Emitting Diodes on Silicon (OLEDoS) with Low Driving Voltage Characteristics

*Myungchan An, Yong Woo Kwon and Hyeong woo Bae**
Realistic Media Research Center, Innovative Technology Research Division, Gumi Electronics and Information Technology Research Institute (GERI), 350-27, Gumidaero, Gumi, Gyeongbuk 39253, Republic of Korea.
Tel.:82-54-460-9083, E-mail: hwbae@geri.re.kr

Virtual reality (VR) and augmented reality (AR) are attractive technologies to lead next-generation smart device platform which enables to provide realistic contents to users. In VR and AR devices, micro-display is most essential technology to present clear and realistic images [1-3]. Organic light emitting diodes on silicon (OLEDoS) is one of the powerful micro-display in VR and AR devices due to advantageous in reducing the volume and weight of optical systems and their self-luminous properties. In VR and AR devices, resolution of the micro-display is one of the important factors to obtain natural images. Moreover, in AR devices, low driving voltage property for high luminance is crucial for securing high outdoor visibilities under restricted driving voltage by back-plane.

Herein, we report a 0.7-inch size monochrome white OLEDoS micro-display panel of 3,000 ppi full high definition (FHD, 1920 × 1080) resolution with low driving voltage characteristics. To satisfy high luminance with low driving voltage, the blue-yellowish green tandem architecture which includes thin charge generation units for utilizing 1st order micro-cavity optical conditions was newly introduced. In order to compare with conventional tandem structure, device W1 and W2 were respectively fabricated as depicted in Fig.1(a). As can be seen in Fig.1(b) and (c), although electroluminescent (EL) spectra are almost identical each other, device W2 showed superior driving characteristics of 5.8 V driving voltage at 1,000 cd/m^2 and maximum luminance 50,015 cd/m^2 at 10.0 V while those of device W1 presented 9.4 V and 2,143 cd/m^2, respectively. By applying architecture of device W2 on back-plane, 3,000 ppi FHD resolution monochrome micro-display was fabricated as portrayed in Fig.1(d). Detailed experimental result will be presented in the presentation.

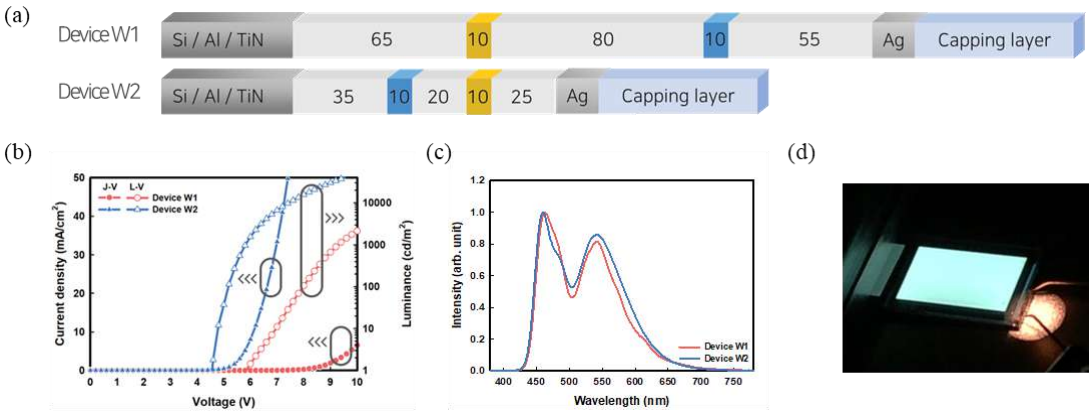

Fig. 1. Performances of the white OLEDoS devices: (a) Device architecture, (b) J-V-L characteristics, (c) normalized EL spectra, (d) fabricated 3,000 ppi monochrome white OLEDoS micro-display.

Acknowledgment

This work was supported by Institute of Information & communications Technology Planning & Evaluation (IITP) grant funded by the Korea government(MSIT) (No. 2020-0-00083, Development of Low MTP Latency Microdisplay and SoC technology for VR·AR devices).

References

1. P. K. Li, *Information Display*, Vol. 34, Issue. 2, pp. 12-15 (2014).
2. H. Cho *et al.*, *Journal of Information Display*, Vol. 20, Issue. 4, pp. 249-255 (2019).
3. A. Ghosh *et al.*, *Invited Paper*, Vol. 48, Issue. 1, pp. 226-229 (2017).

Key Devices for Slim Holographic Flat Panel Display

Hoon Song[1], Chil-Sung Choi[1], Jungkwuen An[1], Young Kim[1], Kanghee Won[1], Yunhee Kim[1], Hong Suk Kim[1], Jong-Young Hong[1], Hyeonseung Yu[1], Aleksander Morozov[2], German Dubinin[2], Andrey Manko[2], Hong-Seok Lee[1], and Sunghoon Hong[1]

[1]Multimedia Processing Lab, Samsung Advanced Institute of Technology, Suwon 443-803, Korea

Tel.:82- 31-8061-4672, E-mail: lhs1210@samsung.com

[2]Optics Lab, Samsung Research Russia, Moscow 127018, Russia

We introduce and integrate the holographic flat panel display (FPD) that satisfies human visual perception as shown in fig.1(a). The conventional holographic display has two key obstacles to commercialization. The first obstacle will be the requirement for the high computational power for real time hologram pattern generation. We presented the world first single chip field-programmable gate array holographic video processor.[1] The other obstacle will be requirements of enough viewing angle and large screen size using limited space-bandwidth product in a slim form factor.[2] In this paper, we will discuss the two issues and solutions on the key devices such as C-BLU and BD which are realizing the a steering BLU overcome the second obstacle.

The first issue is black stripe noise on the C-BLU. The C-BLU expands the aperture of the light steered by the BD. Even though the aperture of light is expanded, the collimation angle and the steered should be preserved. During the guiding, the light beam hits the out-coupling grating every guiding distance (d) which is defined by 2t tan(α') as shown in fig 1(b). However, the guiding distance (d) and beam width (bw) is the same length at the certain incident angle, the BD constantly changes the incident angle according to the detected eye position and the guiding angle varies over time. The larger guiding distance then the beam width induces the gap between the output beam and it will be perceived as a periodic black strip noise pattern on the image. To remove the stripe noise, the beam splitter coating is introduced at the interface between two substrates having different thickness. The number of beams is exponentially increased in the waveguide because the beam is split into two beams whenever the beam hits the coating. And the intensity fluctuation due to overlap will be decreased to 1/2n, where n is the number that hits the layer.

The second issue is independent control of two light beams for two eyes with the BD. The BD includes two BD cells for eyes configured to controllably deflect. The incident light having a first polarization state in a first horizontal direction is deflected by the first BD cell. A retarder (HWP) rotates a polarization of light transmitted by the first BD cell by 90°. And the second BD cell deflects light transmitted by the retarder as shown in fig 1(c).

The two devices are integrated to the slim holographic FPD and provide 12 degree viewing angle with 10.1" in a slim form factor.

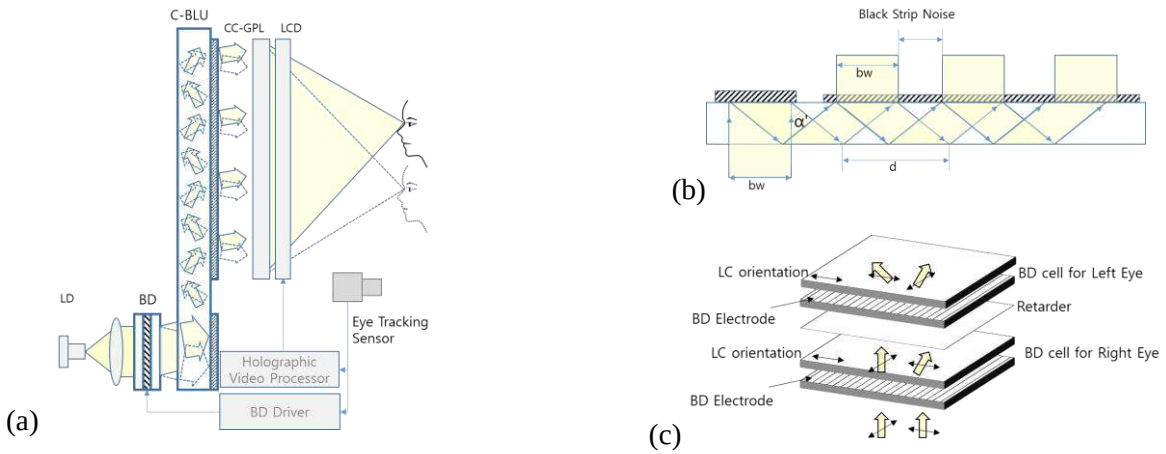

Fig. 1. (a) A concept drawing of proposed holographic FPD; (b) a C-BLU structure and black stripe; (c) BD that independently controls two light beams

References

1. H. Kim, et al. IEEE Trans. Ind. Electron. 66, 2066–2073 (2018).

2. J. An and K. Won, et al. Nature communications 11 (1), 1-7 (2020).

Standalone 360-degree digital holographic display

Daerak Heo[1], Hosung Jeon[1], Sunjin Lim[1], Hwi Kim[2], Youngju Kim[3], Kangbae Lee[3], and Joonku Hahn[1,*]
[1]School of Electronic and Electrical Engineering, Kyungpook National University, 80 Daehak-ro, Buk-gu, Daegu, South Korea
Tel.:82-53-951-5514, E-mail: jhahn@knu.ac.kr
[2]Dept. of Electronics and Information Engineering, Korea University, 2511 Sejong-ro, Sejong, South Korea
[3]Yunam Optics, 419-1 Bucheon-ro, Bucheon-si, Gyeonggi-do, South Korea

The shape of three-dimensional (3D) display is very important and tabletop-style has a strong advantage to show impressive 3D contents to plural people simultaneously[1]. Especially, a holographic tabletop display is proposed to provide accommodation effects[2]. Recently, we optimize the optomechanical structure of the digital holographic tabletop display which consists of three replacement modules. In this paper, we present the experimental results.

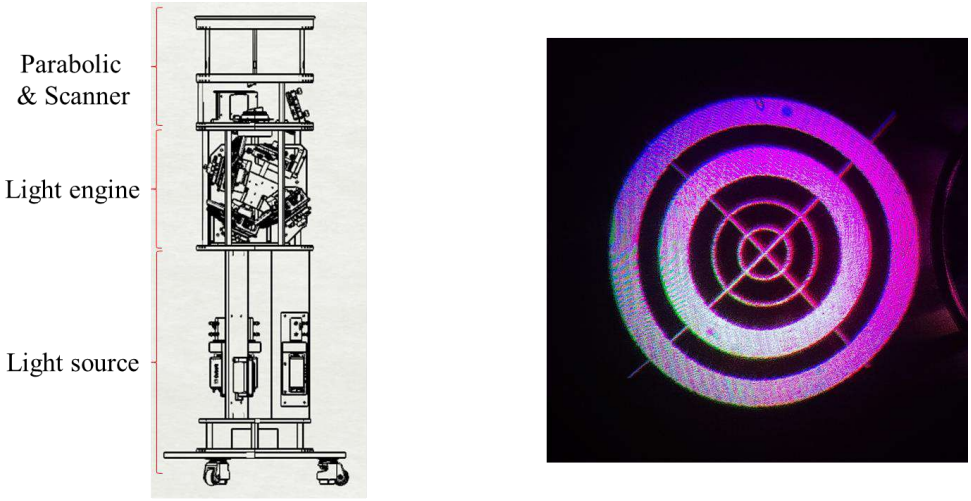

(a) (b)

Fig. 1. (a) Standalone holographic tabletop display, (b) Full-color target image combined with R, G, and B Colors.

Our system consists of three main parts: light source, light engine, and view-forming part. In this research, the light source part contains three laser sources with 473nm, 532nm, and 638 nm. In the light engine part, three digital micro-mirror devices(DMDs) reconstruct 3D contents time-sequentially. Then, a trichroic prism combines R, G, and B images. A Fourier-transform lens, and a spatial mask pass only a single-side band of the hologram. The view-forming part has five optical components; two folding mirrors, two parabolic mirrors, and a scanning mirror.

Acknowledgment

This work was supported by 'The Cross-Ministry Giga KOREA Project' grant funded by the Korea government(MSIT) (No.1711093796, Development of Telecommunications Terminal with Digital Holographic Tabletop Display).

References

1. Y. Lim, K. Hong, H. Kim, H.-E. Kim, E.-Y. Chang, S. Lee, T. Kim, J. Nam, H.-G. Choo, J. Kim, and J. Hahn, “360-degree tabletop electronic holographic display,” Opt. Express 24, 24999–25009 (2016).
2. S. Yoshida, “fVisiOn: 360-degree viewable glasses-free tabletop 3D display composed of conical screen and modular projector arrays,” Opt. Express 24, 13194–13203 (2016).

Binary-encoded full color hologram using error diffusion for a digital micro-mirror device

*Kyosik Min, and Jae-Hyeung Park**
Dept. of Electrical and Computer Engineering, Inha University, Michuhol-gu, Incheon 22211, Korea
*Tel.:82-32-860-7114, *E-mail: jh.park@inha.ac.kr*

Digital micro-mirror devices (DMDs), which have very fast refresh rate, are frequently used as a spatial light modulator. DMDs, however, can only modulate the light signal in binary amplitude fashion. For this reason, synthesized computer-generated hologram (CGH) should be encoded to binary signal before it is uploaded to the DMD. Encoding of complex-valued signal to binary signal with generally used normal thresholding technique gives rise to large errors between the original signal and binarized one.

Error diffusion (ED) technique has been applied to enhance the quality of the binary encoded CGH [1]. In this technique, the binarization is conducted pixel-wise while the difference between error-diffused original signal and its binarized signal is diffused to neighboring pixels with their own weights until whole pixels are binarized. The weights of the ED are designed to locate the low error region at the spectral area where the most signal of the CGH with a plane carrier wave is concentrated. However, this technique has only been applied to single color and the full-color applications have not been demonstrated.

In this presentation, we propose the method for binary-encoded full color hologram with a single DMD using ED. The proposed method consists of a few steps shown in Fig. 1. First, the angular frequency location of the RGB high order diffractions of the DMD is calculated by considering the DMD as a blazed reflection grating. Second, the holograms of each color are synthesized using the plane carrier waves which correspond to the same plane wave angle. Third, the synthesized holograms are shifted in the frequency region to locate the signal-concentrated region at the desired carrier wave location. In order to match between each hologram, steps 2 and 3 should be processed in sequence. In the optical reconstruction, the designed low error region where the most signal is concentrated is only filtered by 4-f system.

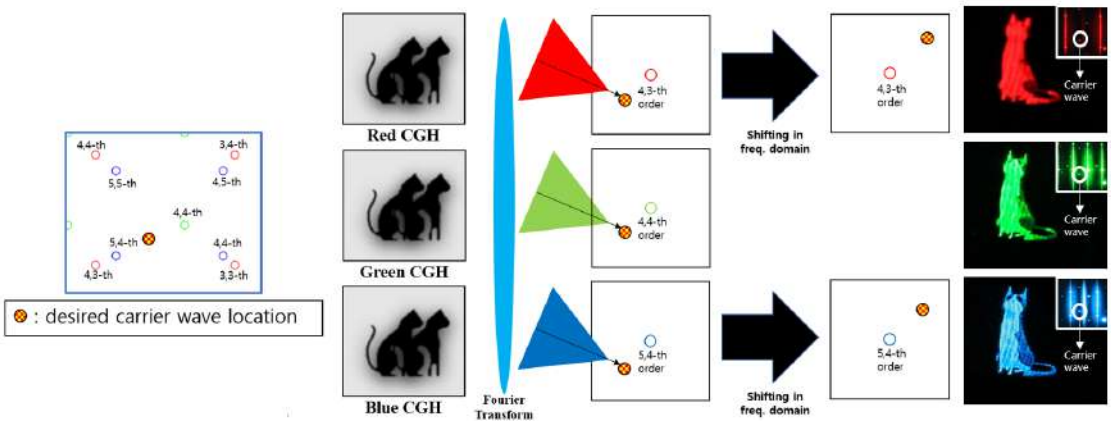

Fig. 1. Illustration of the proposed method and experimental results

In this presentation, we proposed the method for enhancement of binary-encoded full color hologram. The proposed method was successfully verified by the optical experiment, showing high quality speckle-less reconstruction of the holographic three-dimensional images. We expect this method can be applied to various three-dimensional CGH contents for holographic displays.

Acknowledgment
This work was supported by National Research Foundation of Korea (2017R1A2B2011084).

References

1. K. Min and J.-H. Park, *Opt. Express* 28(25), 38140 (2020).

Structured Light Depth Estimation System Using Geometric Phase Self-interference Incoherent Digital Holography

Youngrok Kim, Hogil Baek and Sung-Wook Min
Department of Information Display, Kyung Hee University, Dongdaimun-gu, Seoul 02447, Korea
Tel.:82-2-961-0801, E-mail:mins@khu.ac.kr

We propose a depth estimation method by means of geometric phase self-interference incoherent digital holography (GP-SIDH) and structured light. The structured light refers to the light distributed in a specific pattern, and the position/depth information can be extracted by geometrically analyzing the distortion of reflected patterns on object. The GP-SIDH means our compact digital holography system that can acquire holograms even under natural light conditions [1].

The proposed method estimates the depth by measuring the hologram and analyzing correspondence of the reflected pattern. In the testbed, we use the multiple binary patterns with a constant period as a structured light pattern. The depth information of the perpendicular direction of the structured light line can be obtained through the density of the pattern, while the depth information of the horizontal direction can be obtained through the focus of the hologram. To find the focus of the hologram, we apply the entropy minimization autofocus algorithm [2]. The larger entropy means the larger unpredictability of probability distribution, and it implies defocused. Therefore, the minimum entropy of the numerically reconstructed hologram can infer the depth of the structured pattern.

The proposed system can be applied to a compact and vibration-resistant system compared to the traditional interferometry, allowing the various applications such as precision surface measurement systems.

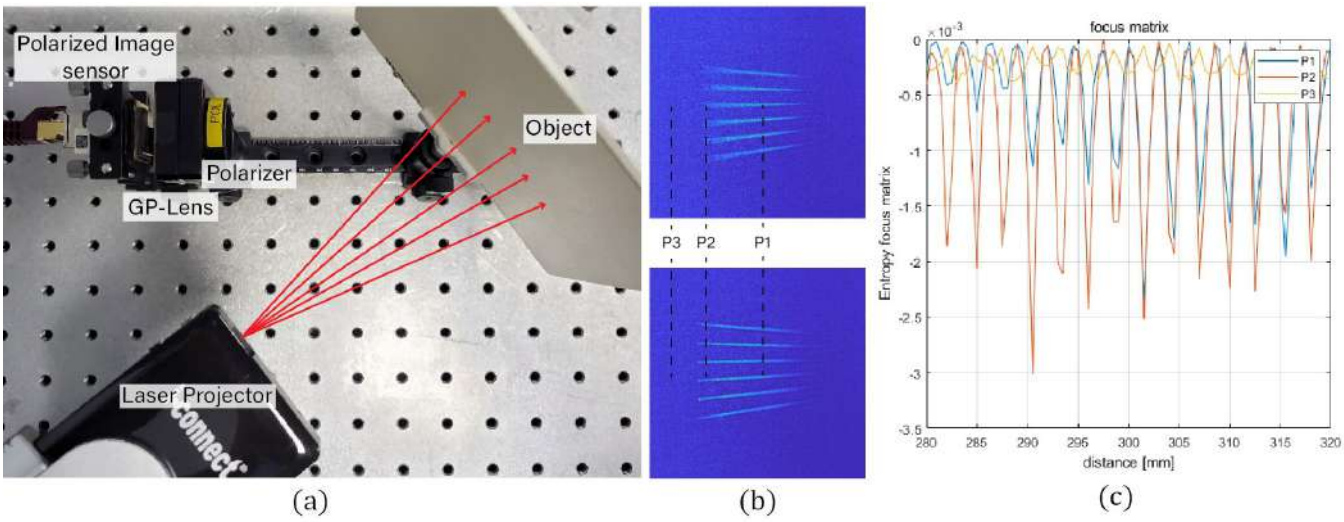

Fig. 1. Proposed depth estimate system using GP-SIDH and structured light pattern
(a) Implemented structured light GP-SIDH system (b) Numerically reconstructed pattern hologram (c) Focus matrix profile comparison between different location of point P1, P2, P3.

Acknowledgment

This work was supported by BK21 FOUR Program funded by the Ministry of Education (MOE, Korea) and National Research Foundation of Korea (NRF) (21A20130000018).

References

1. Choi, K., Joo, K.-I., Lee, T.-H., Kim, H.-R., Yim, J., Do, H., & Min, S.-W. *Compact self-interference incoherent digital holographic camera system with real-time operation*. Optics Express, 27(4), (2019).
2. Ren, Z., Chen, N., & Lam, E. Y. *Extended focused imaging and depth map reconstruction in optical scanning holography*. Applied Optics, 55(5), 1040. (2016).

Fabrication of holographic asymmetric diffuser for 360-degree light field display

*Myungjun Ko, Hosung Jeon, Daerak Heo, Minwoo Jung, and Joonku Hahn**

School of Electronic and Electrical Engineering, Kyungpook National University, 80, Daehak-ro, Buk-gu, Daegu 41566, Korea

Tel.:82-53-950-5514, E-mail: jhahn@knu.ac.kr

360-degree light-field displays form numerous viewpoints around 360 degrees, so the observer watches different views in each viewpoints [1]. In our group, a cylindrical 360-degree light field display was proposed and it consists of a cylindrical screen and three slits on the surface of the cylinder [2]. Two dimensional images on screens inside of the cylinder passes the slits in the specific direction. The slits and screens rotate together and make 288 viewpoints sequentially in 360 degrees. While the user moves around the display, motion parallax of 3D object is observed. However, this cylindrical display has some difficulties to be used as augmented reality (AR) display due to the opaqueness of the body. Recently, many studies on AR displays have been reported using holographic optical elements (HOEs).

In this paper, we propose a method for recording suitable holographic diffuser to implement a cylindrical light field display as an AR device. By using the HOE diffuser, observers watch both external real scenes and 3D virtual contents simultaneously. Figure 1(a) shows the layout of see-through light-field display. The image from the bottom is reflected in the mirror and imaged on the asymmetric holographic diffuser. Image projected on the HOE screen is diffused vertically by the holographic diffuser. Figure 1(b) shows the experimental setup for fabricating holographic asymmetric diffuser. The diffuser is located at the Fourier domain with respect to the HOE plane and the light after the diffuser is limited by the physical slit in order to restrict the bandwidth of diffusing angle of the HOE.

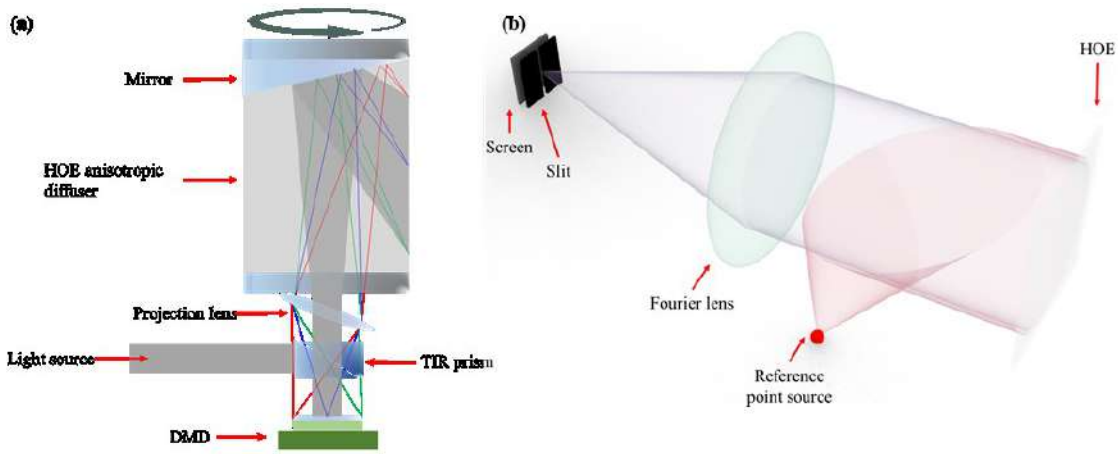

Fig. 1. (a) Layout of see-through light-field display and (b) experimental setup for fabricating holographic asymmetric diffuser.

Acknowledgment

This work was supported by Institute of Information & communications Technology Planning & Evaluation (IITP) grant funded by the Korea government(MSIT) (No. 2020-0-00929, Development of Authoring Tool for Digital HOE Hologram Generation Using Optical Simulation)

References

1. J. Hong, Y. Kim, H.-J. Choi, J. Hahn, J.-H. Park, H. Kim, S.-W. Min, N. Chen, and B. Lee, "Three-dimensional display technologies of recent interest: principles, status, and issues," Appl. Opt. **50**, H87 (2011).
2. G. Choi, H. Jeon, D. Heo, H. Kim, and J. Hahn, "Horizontal-parallax-only light-field display with cylindrical symmetry," Proc. SPIE **10556**, 1055605 (2018).

Generation of high view-reference-point density in time-sequential super multi-view display

Sungjin Lim, Hosung Jeon, Minwoo Jung, Daerak Heo, and Joonku Hahn*
School of Electronic and Electrical Engineering, Kyungpook National University, 80 Daehak-ro, Buk-gu, Daegu 41566, South Korea
Tel.:82-53-950-5514, E-mail: jhahn@knu.ac.kr

Super multiview displays (SMVs) has a potential to reduce 3D sickness such as the vergence-accommodation conflict since the displays provide more than two views within the pupil of the eye [1-4]. In the SMV displays, the number of views entering the pupil without a crosstalk is important related with accommodation effect and natural depth cognition of human [5]. In this paper, we present a time sequential SMV display which forms view reference points (VRPs) densely at the pupil plane. The proposed system consists of the projection part and the observation part. The projection part generates full color contents and contains three digital micro-mirror devices and a projection lens. The observation part defines VRPs densely and relay to the pupil of the eye by moving the slit between two telescopes. This part has the slit and two telescopes which are symmetric to each other based on the slit plane as shown in Fig. 1. Here, VRPs and the relayed VRPs are in the relation of optical conjugate. The projection of view images in the projection part are syncronized with the position of the slit in the observation part. In this paper, we demonstrate the expreimental results that 10 views enter the pupil of the eye, and the results show the accommodation effect obviously.

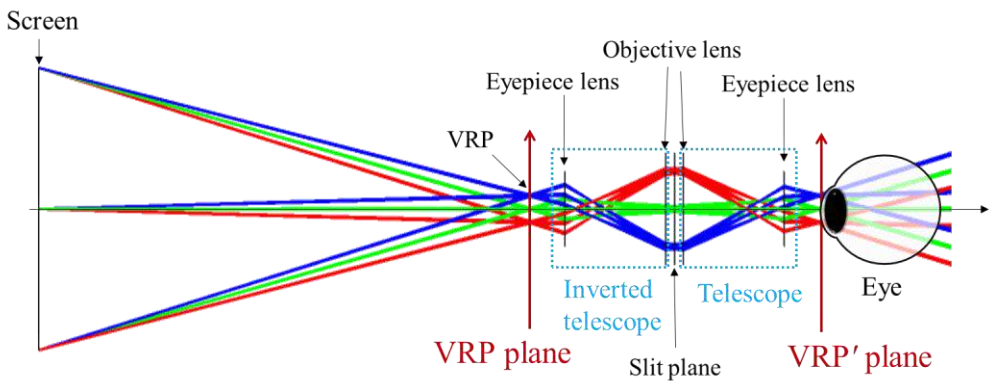

Fig. 1. Formation of VRPs in the proposed time-sequential SMV display

Acknowledgment

This work was supported by Samsung Research Funding Center of Samsung electronics under Project Number SRFC-IT1301052.

References

1. G. Kramida, "Resolving the vergence-accommodation conflict in head-mounted displays," Proc. IEEE **22**(7), 1912-1931 (2015).
2. T. Ueno, and Y. Takaki, "Super multi-view near-eye display to solve vergence-accommodation conflict," Opt. Express **26**(23), 30703-30715 (2018).
3. Y. Takaki, and N. Nago, "Multi-projection of lenticular displays to construct a 256-view super multi-view display." Opt. Express **18**(9), 8824-8835 (2010).
4. C. Lee, S. Lim, H. Jeon, and J. Hahn, "Super multi-view display for analyzing human cognition," Proc. SPIE **9770**, pp. 977006-1-997006-6 (2016).
5. K.-H. Lee, Y. Park, S. Yoon, and S. Kim, "Crosstalk reduction in auto-stereoscopic projection 3D display system," Opt. Express **20**(18), 19757-19768 (2012).

Fundamentals and Recent Developments on Aerial Display for Touchless Interface

Masaki Yasugi and Hirotsugu Yamamoto
Utsunomiya University, Utsunomiya City, Tochigi 321-0904, Japan
Tel.:81-28-689-7074, E-mail: hirotsugu@yamamotolab.science

In order to stop the pandemic of COVID-19, it is important to prevent infection through the control panel. Thus, touchless aerial interface is expected to be implemented in the public in this with-corona and after corona era. Typical examples of public terminals are buttons in an elevator and panels of ATM and vending machines. These terminals are used by the general public and require no special gesture. Aerial display technique enables us to change the conventional touch interfaces, such as buttons and touch panels, into touchless interface. Users can press a floating aerial button in an elevator. Aerial information screen is shown in mid air.

The purpose of this paper is to explain fundamentals of aerial display technique and to introduce recent developments for touchless interface. The definition of the aerial display is shown in the IEC technical report on aerial display.[1] The aerial display in the strict meaning is a display that forms a real image in the mid-air by use of a light-source display and a passive optical component to converge diverging light from the light-source display. Aerial imaging by retro-reflection (AIRR)[2] can form a real image by converging light from a wide angle and realizes an aerial display in the strict meaning. We have realized a wide variety of aerial display prototypes, including a secure aerial display that prevents peeping at the displayed information[3], an aerial depth-fused 3D (DFD) display[4], an omni-directional aerial display that surrounds a viewing space[5], a slim aerial display hardware by use of multiple reflections[6], and triple-views aerial display[7].

In combination of a sensor to detect finger position, touchless aerial interface has been realized. One of our developed prototypes for touchless aerial interface is shown in Fig. 1. A finger position is detected by a near-infrared sensor that is adjusted on the aerial screen position. The optical system is composed of a slanted beam splitter that is placed between a light-source display and a retro-reflector. Thus, the structure is transparent, that is, the user's face and gesture is visible from the opposite side.

A part of this work is supported by JSPS KAKENHI (19H04155, 20H05702).

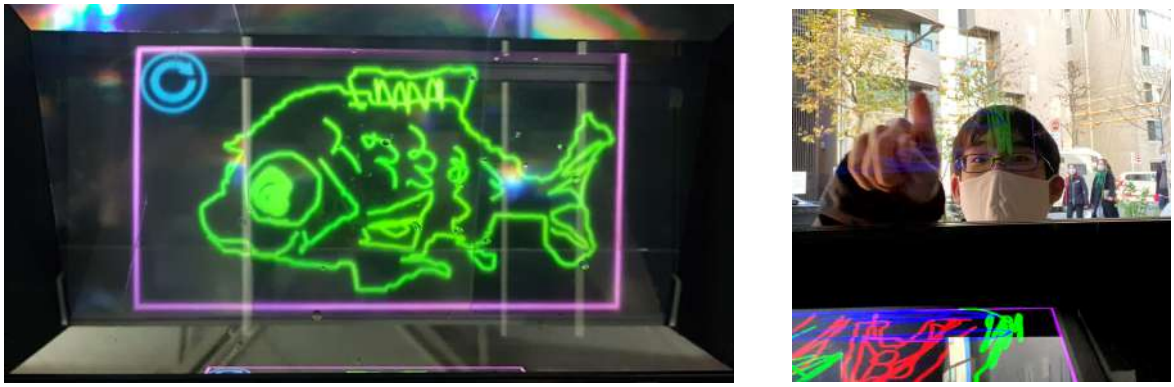

(a) (b)

Fig. 1 (a) Example of aerial drawing on a touchless aerial interface. (b) The user's gesture is visible through the aerial display hardware.

References

1. International Electrotechnical Commission, IEC TR 62629-51-1 (2020).
2. H. Yamamoto, Y. Tomiyama, and S. Suyama, *Opt. Express*, 22, 26919 (2014).
3. K. Uchida, S. Ito, and H. Yamamoto, *Opt. Review*, 24, 72 (2017).
4. Y. Terashima, S. Suyama, and H. Yamamoto, *Opt. Review*, 26, 179 (2019).
5. E. Abe, M. Yasugi, H. Takeuchi, E. Watanabe, Y. Kamei, and H. Yamamoto, *Opt. Review*, 26, 221 (2019).
6. K. Chiba, M. Yasugi, and H. Yamamoto, *Jpn. J. Appl. Phys.*, 59, SOOD08 (2020).
7. M. Yasugi and H. Yamamoto, *Opt. Express*, 28, 35540 (2020).

Enhanced resolution for computer generated holographic display using the phase-only SLMs

*Zehao He, Kexuan Liu, Xiaomeng Sui, Jiachen Wu, and Liangcai Cao**
Dept. of Precision Instruments, Tsinghua University, Beijing, 100084, P. R. China
Tel.:86-10-6279-5959, E-mail: clc@tsinghua.edu.cn

The computer-generated hologram (CGH), as a promising technology for three-dimensional display, has attracted broad attentions in the past two decades [1]. Since few display devices can modulate the amplitude and phase of the incident wavefront simultaneously, the complex amplitude holograms are converted or encoded to amplitude-only holograms or phase-only holograms (POH) for display [2]. The approaches to obtain POHs include the Gerchberg-Saxton algorithm, the one-step phase retrieval method, the error diffusion method, the double phase method, the deep learning method, and so on.

As is shown in Figure 1, for the error diffusion method, we proposed a pattern-adaptive bidirectional error diffusion algorithm for high-quality holographic reconstruction [3]. The optimized POH can be acquired for each object pattern and each propagation distance. We also proposed a band-limited double-phase method to improve the quality of reconstructions by POHs. Meanwhile, the spatiotemporal multiplexing method for the double-phase encoding could further suppress the spatial shifting noise [4]. To improve the generation speed, we proposed an autoencoder-based neural network for POHs [5]. Physical diffraction propagation was incorporated into the decoding part. The network can automatically learn the latent encodings of POHs in an unsupervised manner. The network was able to generate high-fidelity 4K resolution holograms in 0.15 s, with fewer speckles in the reconstructed images compared with the existing CGH algorithms.

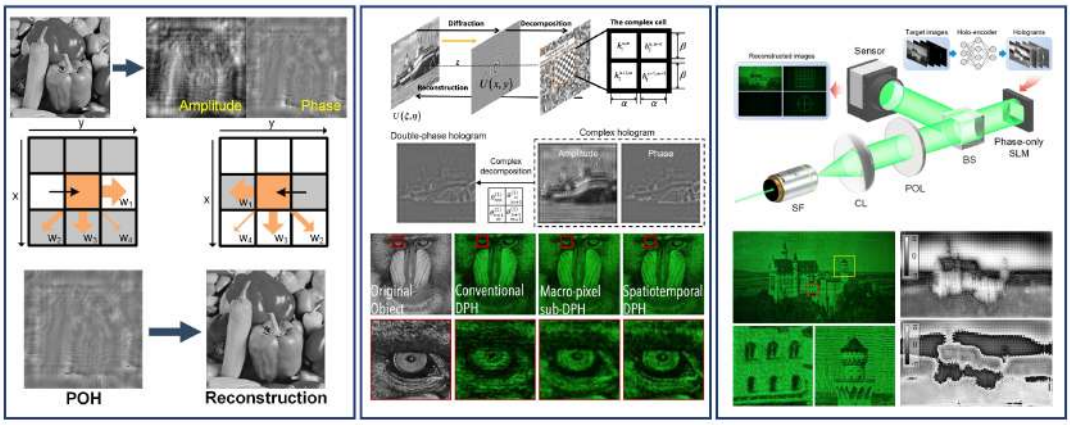

Fig. 1. Proposed method of error diffusion, double phase encoding and deep learning for POHs [3-5]

Acknowledgments

This work is partially supported by National Nature Science Foundation of China (61775117)

References

1. Yan Zhao, Liangcai Cao, Hao Zhang, Dezhao Kong, and Guofan Jin, "Accurate calculation of computer-generated holograms using angular-spectrum layer-oriented method," *Optics Express* 23, 25440-25449 (2015).
2. Zehao He, Xiaomeng Sui, Guofan Jin, Daping Chu, and Liangcai Cao, "Optimal quantization for amplitude and phase in computer-generated holography," *Optics Express* 29, 119-133 (2021).
3. Kexuan Liu, Zehao He, and Liangcai Cao, "Pattern-adaptive error diffusion algorithm for improved phase-only hologram generation," *Chinese Optics Letters* 19, 050501 (2021).
4. Xiaomeng Sui, Zehao He, et al, "Band-limited double-phase method for enhancing image sharpness in complex modulated computer-generated holograms," *Optics Express* 29, 2597-2612 (2021).
5. Jiachen Wu, Kexuan Liu, Xiaomeng Sui, and Liangcai Cao, "High-speed computer-generated holography using an autoencoder-based deep neural network," *Optics Letters* 46, 2908-2911 (2021).

Volumetric display with multicolor based on re-imaging of aerial graphics rendered by femtosecond laser excitation

Kota Kumagai, Shun Miura, and Yoshio Hayasaki
Center for Optical Research and Education (CORE), Utsunomiya University,
Yoto, 7-1-2, Utsunomiya, Tochigi 321-8585, Japan
Tel.:81-28-689-7121, E-mail: kumagai@cc.utsunomiya-u.ac.jp

Volumetric display creates a three-dimensional (3D) graphics that satisfy the depth perception of the human by rendering volume pixels (voxels) visualized by light emission or scattering in real space. In realization the volumetric display, we have presented display systems using a holographic laser drawing method based on computer-generated hologram and spatial scanning of focal points. In the search for screen medium, we have demonstrated solid-state fluorescent type [1, 4], liquid bubble type [3, 5], gas plasma type [2] which generate a voxel having different optical characteristics. Among them, the gas screen type using air as the screen medium realized touch interaction with the user, and augmented reality in real 3D space [2]. However, rendering multicolor graphics is still challenge because the color of voxels generated in the air is only bluish white. In this presentation, we describe a multicolor volumetric display that uses re-imaged voxel generated by focused femtosecond laser in the air. This display realizes multicolor graphics by selectively re-imaging white light from voxels using two parabolic mirrors including variable color filters implemented with a liquid crystal (LC) panel.

Fig. 1 shows an experimental setup. The femtosecond laser pulse was phase-modulated by the liquid-crystal on silicon-SLM (LCOS-SLM) on which a computer-generated hologram is displayed, and generates voxel by irradiating the drawing space after passing through the 3D beam scanner. The voxels are displayed with only desired color from the emission light using the re-imaging device composed of two parabolic mirrors and a LC color filter. The phase modulation of laser light by CGH contributes to the parallel generation of focal point for increasing the number of voxels that can be generated per unit time. The 3D beam scanner which was consisted with a 2D galvanometer scanner and a varifocal lens enables spatial generation of voxels for rendering volumetric graphics. Fig. 2(a) shows a vertex data of a target graphics. This graphics was constructed with 1889 points having seven different colors. Fig. 2(b) shows a volumetric graphics which was re-imaged in mid-air using this system. This image was taken with exposure time of 25 s. By synchronizing the color switching of LC panel and the voxel scanning, we achieved rendering a multicolor volumetric graphics as shown Fig. 2(b).

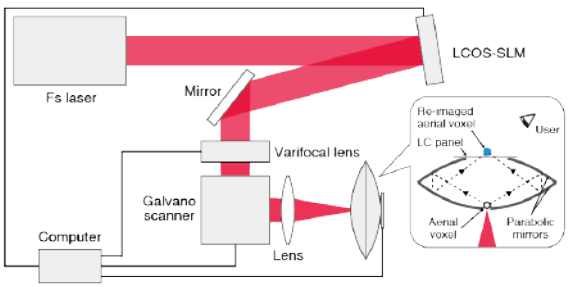

Fig.1. Experimental setup.

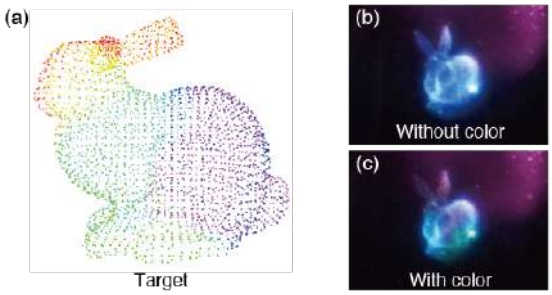

Fig. 2 (a) Vertex data of a target graphics. Re-imaged aerial graphics (a)with and (b)without color.

Acknowledgment
This work was supported by JSPS KAKENHI Grant Number JP20K23338.

References

1. K. Kumagai, D.Suzuki, S. Hasegawa and Y. Hayasaki, *Opt. Lett.*, 40(14), 3356 (2015).
2. Y. Ochiai, K. Kumagai, T. Hoshi, J. Rekimoto, S. Hasegawa and Y. Hayasaki, *Trans. Graph.*, 35(17), 1 (2016).
3. K. Kumagai, S. Hasegawa and Y. Hayasaki, *Optica*, 4(3), 298 (2017).
4. K. Kumagai, I. Yamaguchi and Y. Hayasaki, *Opt. Lett.*, 43(14), 3341 (2018).
5. K. Kumagai, T. Chiba and Y. Hayasaki, *Opt. Exp.*, 28(23), 33911 (2020).

A new rewriting method for Arc 3D display by utilizing Fresnel Arc structures and their vertical-shift arrangement

Haruto Taguchi, Haruki Mizushina, Kenji Yamamoto, and Shiro Suyama
Dept. of Science and Engineering, Faculty of Science and Engineering, Tokushima Univ,
2-1 Minamijyosanjima, Tokushima, 770-8506, Japan
Tel:+81 88 656 9427, E-mail:c612136009@tokushima-u.ac.jp

Long-viewing-distance large 3D display provide high impact to many viewers. Arc 3D display [1] with wide viewing angle and large image depth is useful for these long-viewing-distance large 3D display (Fig. 1). Although conventional arc 3D display has difficulty in rewriting or switching its 3D images, rewriting method has been proposed by using arranging grid-like array of arc-shaped scratch (one pixel in arc 3D display) and illumination angle change in previous study [2] (Fig. 2). However, this method has difficulty in selectively lighting desired arc-shaped scratch because crossing point of adjacent scratches have very narrow gaps.

In this paper, to solve this crossing-point problem in arc-shaped scratches, we have proposed to utilize Fresnel structure for packing Arc-shaped scratches into compact-vertical rectangle region without cross point in Arc 3D display (Fig. 3). Although our proposed Fresnel structure has a problem of a large horizontal pixel size because of large viewing angle, we propose the new pixel arrangement for the solution by shifting Fresnel arc pixel in horizontal direction and in vertical direction (Fig. 4). This arrangement provides high pixel density and makes horizontal pixel pitch almost the same as vertical pixel pitch. Fresnel arc 3D display constructed by this arrangement can provide a high resolution in horizontal and vertical direction in spite of horizontal large pixel (wide viewing angle).

We evaluated availability of rewriting arc 3D image by using proposed Fresnel structure (in case of 6×6 pixels). One pixel was 1 mm vertically by 53 mm horizontally. Two patterns of all of them (36 pixel) and square shape (12 pixel) were estimated. Figure 5 shows the availability of rewriting arc 3D image. Left and right side photographs shows illuminating patterns and perceived bright spot patterns. We can successfully select the desired arc-shaped scratches and obtain the desired bright spot patterns. These bright spot patterns make square image with 48 mm in depth, and their viewing angle is as wide as 75 degrees.

Thus, we can construct arc 3D display without cross point by using Fresnel structure and successfully rewrite arc 3D images easily. Moreover, new arrangement of Fresnel arc providing high pixel density is promising for various applications.

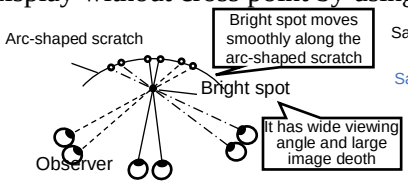

Fig. 1. Principle of Arc 3D

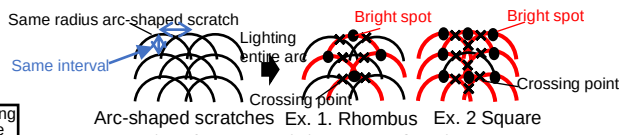

Fig. 2. Rewriting arc 3D image

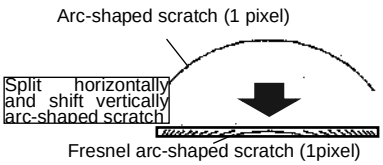

Fig. 3. Proposal of Fresnel arc-shaped scratch

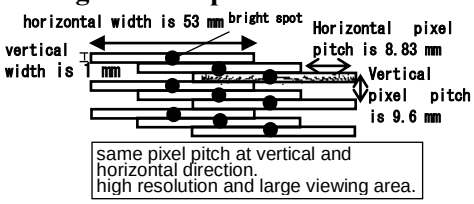

Fig. 4. New pixel arrangement in Fresnel arc

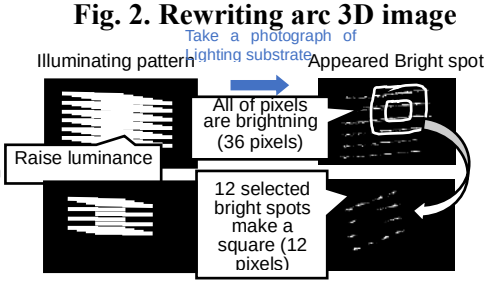

Fig. 5. Rewriting image by Fresnel arc-shaped scratch

Acknowledgment

This study was supported by JSPS KAKENHI JP19H04155, JP20K11919, JP20K21817, JP20H05702 Grant.

References

1. S. Suyama, H. Mizushina and H. Yamamoto, IEEE Industry Applications Magazine, 2019-IDLDC-0651(2020).
2. K. Seko, H. Mizushina, S. Suyama, IDW'19, FMCp4-1, (2019).

MTF measurement of aerial image formed by retro-reflection with polarization

Kazuaki Takiyama, Haotong Guo, Ryota Kakinuma, Masaki Yasugi, Hirotsugu Yamamoto

Utsunomiya University, Yoto 7-1-2, Utsunomiya City, Tochigi 321-0904, Japan

Tel.: +81-28-689-7074, E-mail: hirotsugu@yamamotolab.science

Aerial imaging by retro-reflection (AIRR) is a method of forming an aerial image that can be seen from a wide range.[1] Polarized AIRR (p-AIRR: polarized AIRR) has been proposed to improve the brightness of aerial images.[2] In order to evaluate the image quality of aerial images, it has been proposed that the modulation transfer function (MTF) is measured by the oblique knife edge method for AIRR.[3, 4] However, MTF measurements for p-AIRR have not yet been reported.

In this study, the MTFs of AIRR and p-AIRR are measured by the oblique knife edge method to clarify the differences due to the use of polarization.

The principle of p-AIRR is shown in Fig. 1(a). p-AIRR consists of a light source, a reflective polarizing plate, a quarter-wave retarder, and a retro-reflective element. The reflective polarizing plate reflects S-polarized light and transmits P-polarized light. The quarter-wave retarder gives a phase delay of $\pi / 2$ with respect to the electric field component in the slow phase axial direction. In Fig. 1(a), the display used as the light source emits linearly polarized light, and the polarization direction of the light source and the reflective polarizing plate are arranged in a cross Nicol. The quarter-wave retarder is arranged so that the slow axis is 45 degrees with respect to the polarization direction of the reflection direction of the reflective polarizing plate. Therefore, the polarization direction of the retroreflected light is rotated by 90 degrees, so that it passes through the reflective polarizing plate. The transmitted light is focused on the reflective polarizing plate at a position symmetrical to the light source to form an aerial image.

In this experiment, in AIRR's MTF measurement optical system[4], the beam splitter was replaced with a reflective polarizing plate, and a quarter-wave retarder covered the retro-reflector of prism type (Nippon Carbide Industries: RF-Ax). Then, p-AIRR's MTF has been measured. In order to compare the conventional AIRR, the MTF in the conventional AIRR has also been measured by use of the same retro-reflector. Fig. 1 (b) and (c) show the aerial image by AIRR and p-AIRR, respectively.

The results of MTF are shown in Fig. 1(d). The MTFs of AIRR and p-AIRR overlap. There is no significant difference between both MTF curves. Therefore, we conclude that the introduction of polarization modulation into AIRR improved the brightness of the aerial image and gives no significant change in MTF.

A part of this work was supported by JSPS KAKENHI (19H04155, 20H05702).

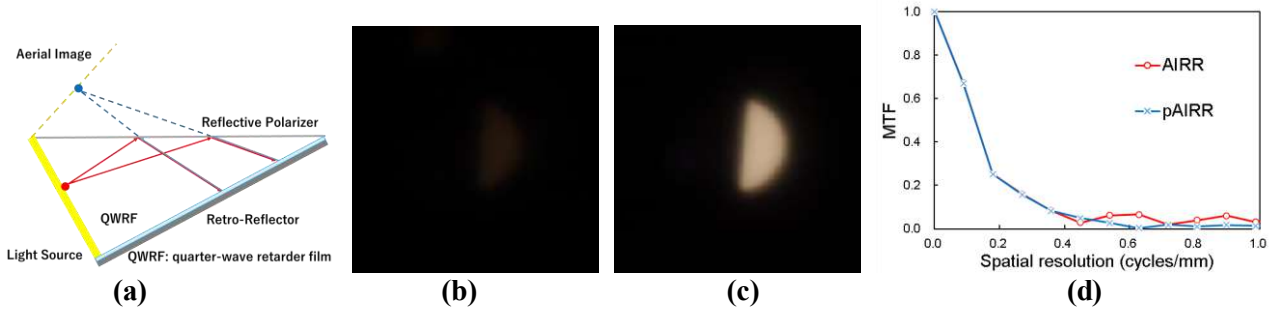

Fig. 1. (a) p-AIRR principle. (b) Aerial image using AIRR. (c) Aerial image using p-AIRR. (d) Changes in MTF at AIRR and p-AIRR.

References

1. H. Yamamoto, *et al.*, *Opt. Express*, 26, 26919 (2014).
2. H. Yamamoto, *The Journal of the Institute of Image Information and Television Engineers*, 75, 181 (2021).
3. N. Kawagishi, *et al.*, *Opt. Express*, 28, 35518 (2020).
4. R. Kakinuma, *et al.*, *OSA Continuum*, 4, 865 (2021).

Influence of Floating Distance on Imaging Resolution in Aerial Imaging by Retro-Reflection (AIRR)

Haotong Guo, Kazuaki Takiyama, Ryota Kakinuma, Masaki Yasugi, and Hirotsugu Yamamoto
Utsunomiya University, Yoto 7-1-2, Utsunomiya City, Tochigi 321-0904, Japan
Tel.: +81-28-689-7074, E-mail: hirotsugu@yamamotolab.science

Aerial imaging by retro-reflection (AIRR: aerial imaging by retro-reflection)[1] is a method for forming an aerial image. AIRR features a wide viewing angle and a large-size scalability. Thus, one of the prospective applications of AIRR is an aerial LED signage that is floating in mid-air. It was reported that the size of aerial image of an LED increases with the floating distance.[2] Recently, we have developed a method to evaluate the aerial imaging resolution by measuring the modulation transfer function (MTF) based on a slanted knife-edge method.[3] Furthermore, our measured MTF differed in two different floating distances.[4] However, the dependence of MTF on the floating distance is not clear.

The purpose of this research is to clarify the effect of floating distance on the image resolution of aerial images. In the experiments, we use a slanted knife edge on the aperture of an integral sphere as the light source. The real image of the knife edge is formed by changing the floating distance from 100 mm to 400 mm.

The retro-reflector has a characteristic that the light which emitted from the light source will be reflected in the same path as it was incident. The experimental setup is shown in Fig. 1(a). In this setup, the light from the light source enters the integrating sphere and scatters multiple times inside. Due to the knife edge, the light that emitted from the integrating sphere becomes a half-moon-shaped light source with the uniform light intensity distribution.[3] This light enters the beam splitter and reflected to the retro-reflector. Retro-reflected light transmits the beam splitter and converges to the position that is plane-symmetrical of the knife edge with respect to the beam splitter. We obtain the profile of the formed image and derive the MTF curve.[3]

The measured MTF curves are shown in Fig. 1 (b). These results are measured by use of a prism type retro-reflector for aerial display (Nippon Carbide Industries: RF-Ax). The results show that the MTF curve is greatly affected by the change in the floating distance, which was most remarkable at 0.2 to 0.4 lp / mm.

A part of this work was supported by JSPS KAKENHI (19H04155, 20H05702).

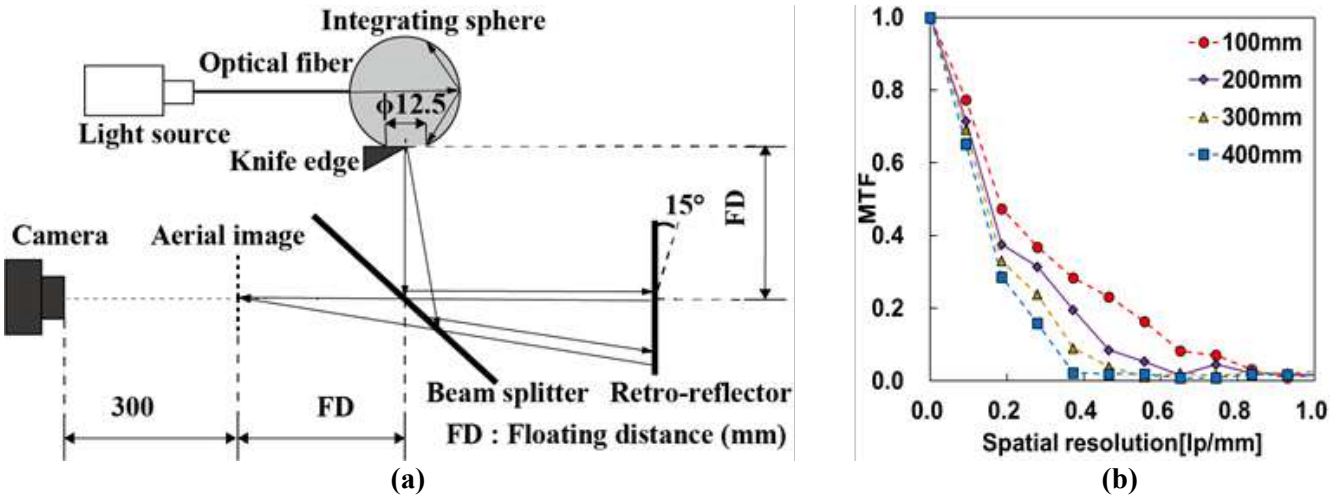

Fig. 1 (a) Experimental setup for MTF measurement with the slanted knife-edge method. (b) Obtained MTF curve in different floating distances.

References

1. H. Yamamoto, *et al.*, *Opt. Express*, 26, 26919 (2014).
2. Y. Tomiyama, *et al.*, *IMID 2014 DIGEST*, 67 (2014).
3. N. Kawagishi, *et al.*, *Opt. Express*, 28, 35518 (2020).
4. R. Kakinuma, *et al.*, *OSA Continuum*, 4, 865-876(2021).

Versatile Design of Oxide Semiconductor by Atomic Layer Deposition for High-Performance, Low-Power TFTs

Min Hoe Cho, Hyunjoo Seul, Jae Seok Hur, and Jae Kyeong Jeong
Department of Electronic Engineering, Hanyang University, Seoul, South Korea
Tel.:82-2-2220-2327, E-mail: jkjeong1@hanyang.ac.kr

Since the invention of amorphous IGZO (*a*-IGZO) channel material in 2004, the world-wide research and development has led to the commercialization of *a*-IGZO TFTs as a standard backplane technology for high-end mobile LCD and large-area OLED TV. However, the carrier mobility of IGZO TFTs should be enhanced to compete the LTPS TFTs, which are the primary choice in a high-end mobile OLED display. So far, the various approaches to improve the mobility of electron carriers in IGZO TFTs have been researched including the optimization of cation composition, stacked channel structure and the lattice ordering-induced crystallization. [1-3] In this presentation, we presented our recent efforts toward the high performance and good reliability, which is based on the atomic layer deposited IGZO system. First, the effect of cation composition on performance of IGZO TFTs was investigated. [4] Second, two types of IGZO TFTs using sputtering and ALD process were compared where both IGZO channel had the comparable cation composition and thermal budget. [5] Finally, the quantum confinement effect was realized in the bi-layered IGZO stacks through the design of appropriate thickness and cation composition to boost the mobility of IGZO TFTs with the low driving voltage operation. [6]

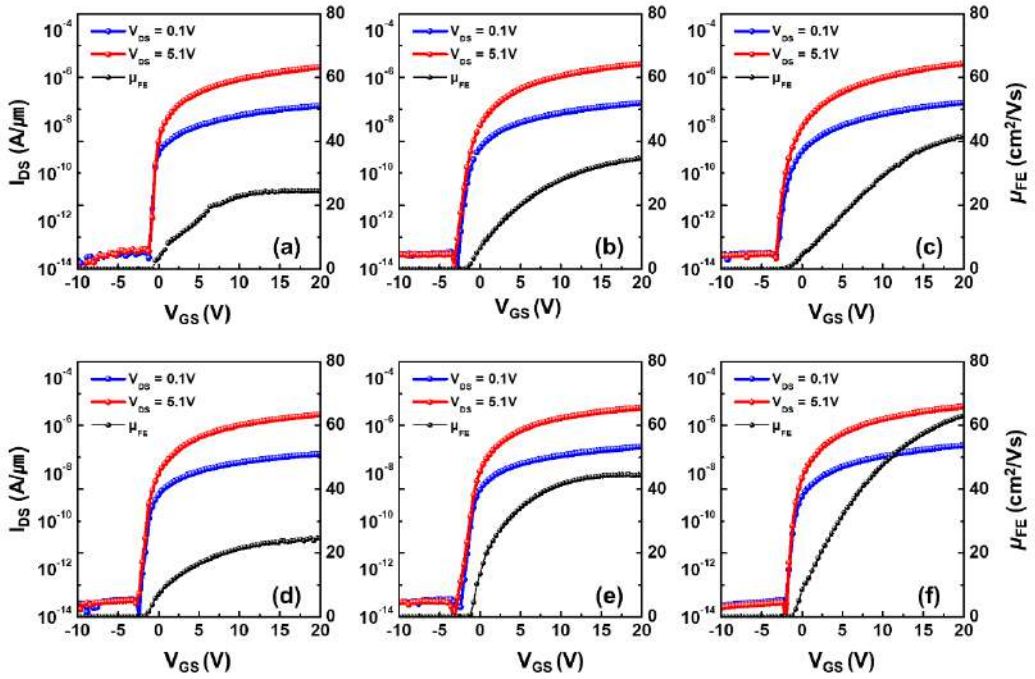

Figure 1. Transfer characteristics of the (a)-(c) IGO and (d)-(f) ZnO/IGO channel TFTs depending on the cation ratios: (a) $In_{0.65}Ga_{0.35}O_{1.5}$, (b) $In_{0.75}Ga_{0.25}O_{1.5}$, (c) $In_{0.83}Ga_{0.17}O_{1.5}$, (d) ZnO/$In_{0.65}Ga_{0.35}O_{1.5}$, (e) ZnO/$In_{0.75}Ga_{0.25}O_{1.5}$, and (f) ZnO/$In_{0.83}Ga_{0.17}O_{1.5}$. (adapted from reference [6])

References

1. K. Nomura *et al*., *Nature* **432**, 488 (2004).
2. J. Y. Kwon and J. K. Jeong, *Semicond. Sci. Technol*. **30**, 024002 (2015).
3. Y. Shin *et al*., *Sci. Rep*. **7**, 10885 (2017).
4. M. H. Cho *et al*., *J. Inf. Disp*. **20**, 73 (2019).
5. M. H. Cho *et al*., *IEEE Trans. Electron Devices* **66**, 1783 (2019).
6. H. J. Seul *et al*., *ACS Appl. Mater. Interfaces* **12**, 33887 (2020).

Highly Robust IGZO TFTs using Spreading Currents.

Suhui Lee* and Jin Jang
Department of Information Display and Advanced Display Research Center, Kyung Hee University, Seoul, 130-701, Korea
Tel.:82-2-961-0688, E-mail:shlee5@tft.khu.ac.kr

The active-matrix organic-light emitting diode (AMOLED) on plastic substrate are of increasing interest for mobile displays with high resolution and high flexibility. The thin-film transistors (TFTs) used for robust backplane should have high performance with high reliability under electrical and mechanical stresses. [1-6]

Amorphous indium-gallium-zinc oxide (a-IGZO) is the most popular AOS which is being studied intensively by many displays manufacturing companies and academic groups. In this study, the improvement of oxide TFT by modification of TFT structure is studied. The effects of spreading current in a-IGZO TFTs and its application to TFT and TFT circuit designs are investigated. To confirm the spreading currents in oxide TFTs, we made stripe-patterned S/D electrodes. It is confirmed that the drain currents are same with stripe patterns as the conventional TFTs without stripe pattern. It can significantly reduce the overlap capacitance between gate and source/drain electrodes. This spreading current concept can be widely used for the design of oxide TFT array with low RC (resistance capacitance product) delay for high-speed circuits. Additional benefit of stripe patterned S/D electrodes is excellent high current stability which is due to easier heat dissipation by reducing the S/D surface area. The mechanical stability of the flexible oxide TFT is also greatly improved and thus there is no crack generation after many times of mechanical bending. This leads to increase the speed of the TFT circuits and improve the high current stability and mechanical flexibility. The oxide TFTs could be applied to high yield and fast response integrated gate drivers for flexible displays.

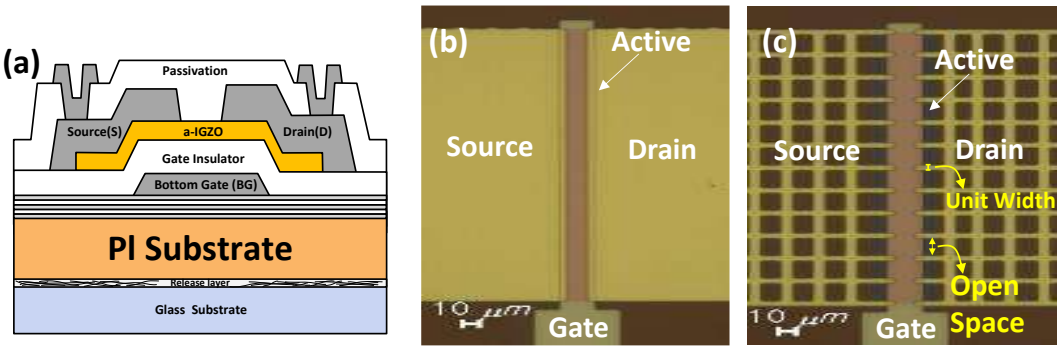

Fig1. Comparison of device structures between conventional BCE oxide TFT and low overlap capacitance TFT with stripe-patterned S/D electrodes. (a) Schematic cross-sectional views of BCE oxide TFT. Optical images of the fabricated TFTs with (b) standard and (c) stripe S/D electrodes

Acknowledgment

This work was supported by the Technology Innovation Program (20011317, Development of an adhesive material capable of morphing more than 50% for flexible devices with a radius of curvature of 1mm or less) funded By the Ministry of Trade, Industry & Energy(MOTIE, Korea)

References

1. M. Mativenga, S. An, J. Jang, *IEEE Electron Device Lett*., 34(12), 1533 (2013)
2. S. Lee, Y. Chen, J. Jeon, C. Park, and J. Jang, *Advanced electronic materials*., 4(4),1700550 (2018)
3. S. Lee, M. Mativenga, and J. Jang, *IEEE Electron Device Lett.*, 35(9), 930 (2014).
4. S. Lee, X. Li, M. Mativenga, and J. Jang, *IEEE Electron Device Lett.*, 36(9), 1329 (2015)
5. S. Lee, D. Jeong, M. Mativenga, and J. Jang, *Adv. Funct. Mater.*, 27(29),1700437 (2017).
6. S. Lee, J. Shin, and J. Jang, *Adv. Funct. Mater.*, 27(11), 1604921(2017).

Realization of High-Performance Oxide Thin-Film Transistors with Submicron Channel Length using Conventional Photolithography Process for High Resolution Active-Matrix Display Backplane

Chihun Sung[1, 2], Sooji Nam[1, 2], and Sung Haeng Cho[1]
[1]Flexible Electronics Research Section, Electronics and Telecommunications Research Institue, 218 Gajeong-ro, Yuseong-gu, Daejeon 34219, Korea
Tel.:82-42-860-6428, E-mail: helloshcho@etri.re.kr
[2]ICT (Advanced Device Technology), University of Science and Technology, 217 Gajeong-ro, Yuseong-gu, Daejeon 34113, Korea

Realistic display with versatile form factor is an eventual goal in the display world. Recently, the devices with functionality such as virtual reality (VR), augmented reality (AR), and holography have been one of the hot topics with advent of mobile devices and internet of thing. One of the key factors to realize these is the high-resolution display with extremely small pixel size. In order to drive the large size active-matrix display with high density pixel, the high-performance thin-film transistors (TFTs) are requisite[1,2]. Generally, there are two ways to enhance the performance of TFT; the mobility enhancement through the proper materials selection for semiconductor and the channel engineering and the scale down of the channel length.

In this study, we present the new fabrication process details and the electrical characteristics of metal oxide TFTs with 0.8 μm channel length fabricated employing the g, h, i-line lithographic tool which is conventional in the current display manufacturing facility and the lift-off process, where the field-effect mobility of > 50 cm^2/Vs, subthreshold swing of 90 mV/dec, I_{ON}/I_{OFF} ratio of > 10^7 and turn-on voltage (V_{ON}) of -0.24 V was obtained.

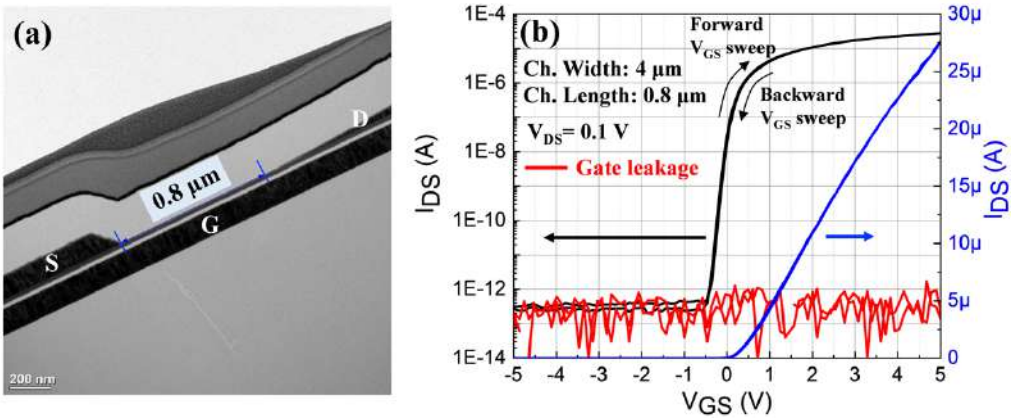

Fig. 1. TEM image and electrical characteristics of fabricated submicron channel length TFT. (a) channel length= 0.8 μm, (b) transfer curve at V_D= 0.1 V

Acknowledgment

This research was partly supported by the Technology Innovation Program (20012617, Core Technology Development of CMOS Device Fabricati on using Nonsilicon Semiconductor Thin Film Transistors for High Resolution Large Area Display) funded by the Ministry of Trade, Industry & Energy (MOTIE, Korea) and National R&D Program through the National Research Foundation of Korea (NRF) funded by Ministry of Scienc e and ICT (NRF-2020M3F3A2A01085791).

References

1. T. S. Kim, H. -S. Kim, J. S. Park, K. S. Son, E. S. Kim, J. -B. Seon, S. Lee, S. -J. Seo, S. -J. Kim, S. Jun, K. M. Lee, D. J. Shin, J. Lee, C. Jo, S. -J, Choi, D. M. Kim, D. H. Kim, M. Ryu, S. -H. Cho, and Y. Park, *Tech. Dig. Int. Electron Devices Meet,* P. 27-1 (2013)
2. T. Kamiya, K. Nomura, and H. Hosono, *Sci. Technol. adv. Mater.* Vol. 11, no. 4, p. 044305 (2010)

Stress Manipulated Metal-Oxide Thin-Film Transistors and Integrated Circuits for Highly Reliable Stretchable Electronics

Kyung-Tae Kim[1], Seung-Han Kang[1], Chan-Yong Park[1], Park Hunbum[1], and Sung Kyu Park[1]
[1]School of Electrical and Electronics Engineering, Chung-Ang University, Seoul 156-756, Korea
E-mail: skpark@cau.ac.kr

Recently, amorphous indium-gallium-zinc-oxide (*a*-IGZO) thin-film transistors (TFTs) have extended their applications to stretchable and wearable electronics, including sensor arrays and biosensors.[1)] These conformable electronics have required highly reliable mechanical stability. For the realization of stretchable electronics, *a*-IGZO materials have been considered as one of the most promising semiconductor candidates due to their high electron mobility, reliable stability, and good uniformity.[2)–4)] After completion of device fabrication on sacrificial polyimide (PI),[3)] polydimethylsiloxane (PDMS) substrates have been widely utilized to embed *a*-IGZO TFTs and integrated circuits by transferring process.[1)] However, the conventional plain-shaped structure for *a*-IGZO TFTs have major challenge by itself which induces highly deteriorative mechanical stress in the *a*-IGZO devices under strain deformation.

Here, we demonstrate highly reliable keystone-shaped PDMS substrate to obtain mechanically improved *a*-IGZO TFTs as shown in Fig. 1(a). In the COMSOL Multiphysics simulation, keystone structure reveals that the mechanical stress induced in device regions can be effectively reduced under 30% strain. We exploited conventional photolithography process to fabricate the keystone shape substrate using negative photoresist. This easily accessible process allowed the high-resolution patterning and the large-area scalability. The *a*-IGZO TFTs have saturation mobility of 6.06 $cm^2V^{-1}s^{-1}$ under drain bias of 10 V. Under tensile strain, *a*-IGZO TFTs show transfer characteristics with negative shift and increased on-current as depicted in Fig. 1(b). As a results, the keystone-structured *a*-IGZO TFTs show improved mechanical properties, exhibiting saturation mobility variation of 12.7% under 15% strain compared to conventional planar structure with the variation of > 10% even under 1% strain as shown in Fig. 1(c).

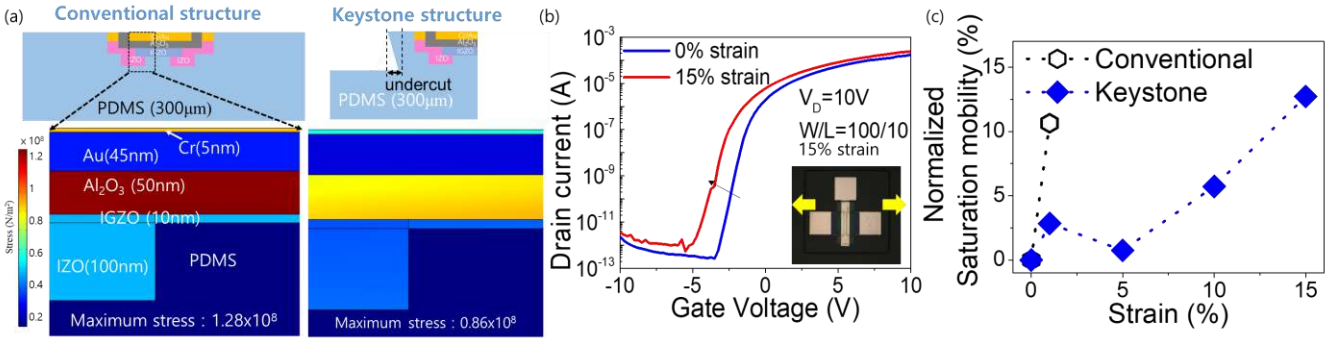

Fig. 1. Mechanically robust keystone structure for stretchable *a*-IGZO TFTs. (a) Illustrations for stress distribution in *a*-IGZO TFTs on conventional and keystone structures. (b) Transfer characteristics of *a*-IGZO TFTs on keystone structure. (c) Effect of mechanical strain on saturation mobility of *a*-IGZO TFTs on conventional and keystone structure.

Acknowledgment

This research was funded and conducted under 「the Competency Development Program for Industry Specialists」 of the Korean Ministry of Trade, Industry and Energy (MOTIE), operated by Korea Institute for Advancement of Technology (KIAT). (No. P0002397, HRD program for Industrial Convergence of Wearable Smart Devices)

References

1. N. Münzenrieder,G. Cantarella,C. Vogt,L. Petti,L. Büthe,G.A. Salvatore,Y. Fang,R. Andri,Y. Lam,R. Libanori,D. Widner,A.R. Studart,and G. Tröster:Adv. Electron. Mater. 1, 1 (2015).
2. Y.-H. Kim,J.-S. Heo,T.-H. Kim,S. Park,M.-H. Yoon,J. Kim,M.S. Oh,G.-R. Yi,Y.-Y. Noh,and S.K. Park:Nature 489, 128 (2012).
3. K. Kim,S. Moon,M. Kim,J. Jo,C. Park,S. Kang,Y. Kim,and S.K. Park:2003276, 1 (2020).
4. K.T. Kim,S.P. Jeon,W. Lee,J.W. Jo,J.S. Heo,I. Kim,Y.H. Kim,and S.K. Park:Adv. Funct. Mater. 29, 1 (2019).

Realization of Long-Term Visual Memory Enhanced Amorphous IGZO-based Optical Synaptic Transistor by Oxide Mesh and Insulator Insertion

Dongwoo Kim[1], Won Kyung Min[1], Hyung Tae Kim[1], Jusung Chung[1], Min Seong Kim[1], and Hyun Jae Kim[1]
[1]School of Electrical and Electronic Engineering, Yonsei University, Seodaemun-gu, Seoul 03722, Republic of Korea
Tel.:82-2-2123-5865, E-mail: hjk3@yonsei.ac.kr

Oxide semiconductor-based photodetectors are one of the widely researched areas since they are one of the most important sensors for interactive applications. These oxide-based photodetectors have a unique characteristic named persistent photoconductivity (PPC) that is caused by the trapped ionized oxygen vacancies that inhibit recombination after light illumination is removed [1]. This PPC effect has negative effect on photodetectors as this slows down the decay time of the photocurrent. Therefore, further studies have been conducted to utilize this slow decay of the photocurrent and have found that it could be used to mimic major synaptic functions such as short-term memory (STM) and long-term memory (LTM) [2]. However, due to lack of clear line between STM and LTM, the difference between STM and LTM is hard to discern [3].

Therefore, we have developed an optical synaptic transistor with enhanced LTM to widen the difference between STM and LTM by inserting mesh-structured oxide semiconductor and thin film-structured insulator inside the channel layer of the transistor. For this particular study, we used amorphous indium-gallium-zinc oxide (a-IGZO) as the channel layer, silicon dioxide (SiO_2) as the gate insulator, heavily boron doped silicon (p^+-Si) as the gate electrode, and aluminum (Al) as the source and drain electrodes. The channel layer is fabricated in this order: 1st a-IGZO, insulator, 1st oxide mesh, 2nd a-IGZO, 2nd oxide mesh, and 3rd a-IGZO, as shown in Fig. 1(a). After the device fabrication was completed, the STM and LTM functions were measured using red light pulse (wavelength: 635 nm, intensity: 1 (STM) or 10 (LTM) mW/mm^2, pulse frequency: 1 Hz), as shown in Fig. 1(b) and (c).

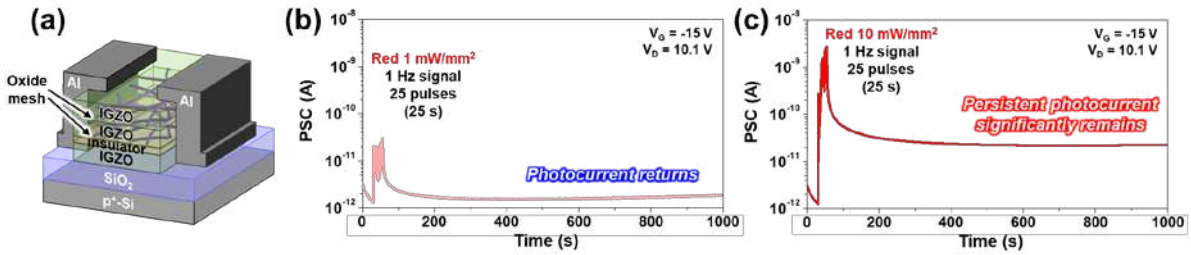

Fig. 1. (a) Structure of oxide-based optical synaptic transistor. (b) Short-term memory (STM) and (c) long-term memory (LTM) behaviors of the optical synaptic transistor using red light as the signal.

As can be seen in the Fig. 1, the difference between STM and LTM is clear. We believe that the mechanism of the optical synaptic transistor we developed is that, the low intensity light was absorbed by the back channel where the 2nd oxide mesh is, and the generated carriers could relatively easily recombine, achieving STM. On the other hand, the high intensity light could penetrate down to the front channel due it its high number of photons and was absorbed by the front channel where the insulator layer is. Then, the generated carriers at the front channel get trapped inside and at the interface of the insulator, realizing LTM due to high PPC.

Acknowledgment

This work was supported by the Technology Innovation Program (20010371, development of 4K level flexible display device and panel technology by inkjet pixel printing method) funded by the Ministry of Trade, Industry & Energy (MOTIE, Korea).

References

1. S.-E. Ahn, I. Song, S. Jeon, Y. W. Jeon, Y. Kim, C. Kim, B. Ryu, J.-H. Lee, A. Nathan, S. Lee, G. T. Kim and U.-I. Chung, *Adv. Mater.*, 24, 2631-2636 (2012).
2. M. Lee, W. Lee, S. Choi, J.-W. Jo, J. Kim, S. K. Park and Y.-H. Kim, *Adv. Mater.*, 29(28), 1700951 (2017).
3. N. Duan, Y. Li, H.-C. Chiang, J. Chen, W.-Q. Pan, Y.-X. Zhou, Y.-C. Chien, Y.-H. He, K.-H. Xue, G. Liu, T.-C. Chang and X.-S. Miao, *Nanoscale*, 11, 17590 (2019).

A technology for the monolithic integration of low-temperature polysilicon and elevated-metal metal-oxide thin-film transistors

Man Wong and Sisi Wang
Department of Electronic and Computer Engineering, The Hong Kong University of Science and Technology, Clear Water Bay, Kowloon, Hong Kong
Tel.:852-2358-7057, E-mail: eemwong@ust.hk

Offering the high driving capability of a low-temperature polysilicon (LTPS) thin-film transistor (TFT) and the low off-state current of a metal-oxide (MO) TFT, the monolithic integration of p-type LTPS and n-type MO TFTs has attracted much attention for implementing complementary circuits in displays and other applications. However, there are process and material incompatibility issues that need to be resolved while attempting such integration. Issues related to hydrogen cross-contamination has been reported previously (1), those presently being addressed are: i) the chemical conditioning process for the contacts to an LTPS TFT is detrimental to a MO TFT, and ii) the conductor materials required to realize the optimal source/drain (S/D) electrodes to LTPS and MO TFTs are different.

A technology for the monolithic integration of LTPS and elevated-metal metal-oxide (EMMO) (2) TFTs is presently described. Contacts to the MO TFT are first opened before the deposition of the contact Conductor #1 for the MO TFT. The contacts to the LTPS TFT are subsequently opened (Fig. 1a) and chemically conditioned before the deposition of a different contact Conductor #2 for the LTPS TFT. Finally, the stack of Conductor #2 on Conductor #1 is patterned to form the S/D electrodes to both types of TFTs (Fig. 1b). The nice transfer characteristics of the resulting TFTs are shown in Figs. 1c and 1d, exhibiting negligible parasitic S/D resistance. The voltage transfer characteristics of an inverter consisting of respective p-type LTPS pull-up and n-type MO pull-down TFTs are shown in Fig. 1e, exhibiting the expected rail-to-rail swing. A maximum gain of around 40 is obtained. This technology preserves the reduced mask-count, allows for unrestricted chemical conditioning of the S/D contacts to the two types of TFTs, and is applicable to all common top- and bottom-gated TFT structures.

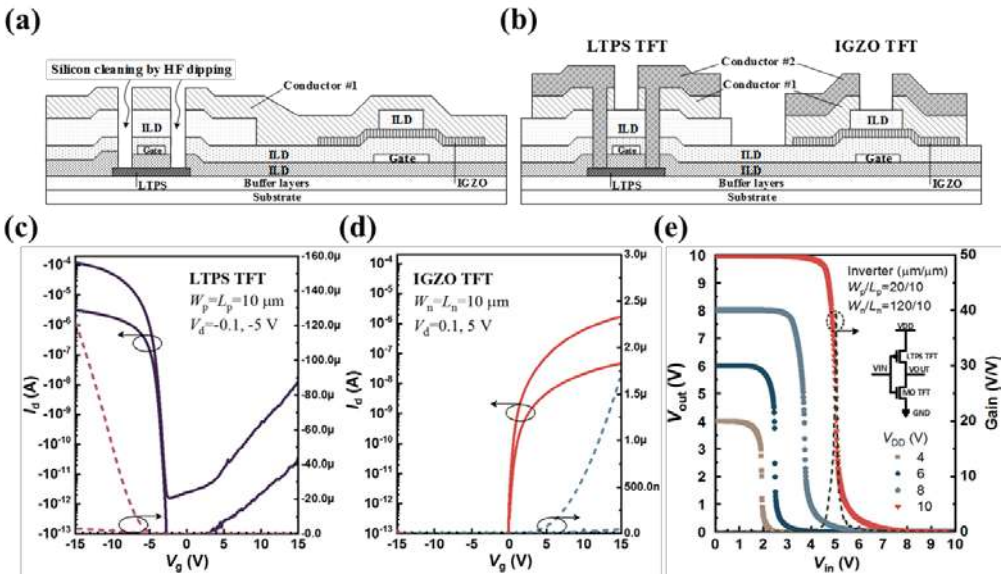

Fig. 1. (a) (b) Schematic cross-sections of the LTPO integration process. The transfer curves of the fabricated **(c)** p-type LTPS and **(d)** IGZO TFTs. **(e)** The voltage transfer characteristics of an LTPO inverter.

Reference

1. Wang S, Shi R, Li J, Lu L, Xia Z, Kwok HS, Wong M. Resilience of Fluorinated Indium-Gallium-Zinc Oxide Thin-Film Transistor Against Hydrogen-Induced Degradation. IEEE Electron Device Letters. 2020 Mar 27;41(5):729-32.
2. Lu L, Li J, Feng Z, Kwok HS, Wong M. Elevated-Metal Metal-Oxide Thin-Film Transistor: Technology and Characteristics. IEEE Electron Device Letters. 2016 Apr 11;37(6):728-30.

Scalable Atomic Layer Deposition for P-type and N-type Oxide Semiconductor TFTs

Rebecca L. Peterson[1,3], Chris Allemang[1], Tae Cho[2], Julia D. Lenef[3], Jaesung Jo[1], Neil P. Dasgupta[2]
[1]Dept. of Electrical Engineering and Computer Science, University of Michigan, Ann Arbor, MI, 48109, U.S.A.
Tel.:1-734-615-3105, E-mail: blpeters@umich.edu
[2]Dept. of Mechanical Engineering, University of Michigan, Ann Arbor, MI, 48109, U.S.A.
[3]Dept. of Materials Science and Engineering, University of Michigan, Ann Arbor, MI, 48109, U.S.A

Atomic layer deposition (ALD) is powerful process module for fabrication of thin films with precise control of chemical composition and thickness. ALD has been widely used in manufacturing for conformal deposition of dielectrics and electrodes for state-of-the-art CMOS transistors. However use of ALD for deposition of thin film semiconductors has been relatively rare, due to stringent requirements for purity, chemical co-ordination, and structural morphology. In this talk, I will describe our recent success and ongoing work developing ALD processes for deposition of *n*-type and *p*-type semiconductors for thin film transistors (TFTs), as shown in Fig. 1.

To achieve *n*-type amorphous zinc-tin oxide, we compared various oxidant approaches using thermal (H_2O-based) ALD, oxygen-plasma, and a hybrid method that combines thermal ALD of zinc precursors with oxygen-plasma ALD of tin precursors [1]. This hybrid process results in enhancement-mode TFTs with electron mobility as high as 22 $cm^2V^{-1}s^{-1}$ if the film is subjected to a post-deposition anneal at 400°C. The film electrical performance is found to directly correlate with the film density, which can be facilitated by increasing the ALD deposition temperature and/or using post-deposition anneals at 300°C or greater. By integrating high-*k* Al_2O_3 as a gate insulator and passivation layer, we can lower the switching voltage, reduce the sub-threshold slope to the Boltzmann limit, and increase the robustness of the devices to bias stress [2].

For *p*-type cuprous oxide (Cu_2O), we use a plasma-enhanced ALD process that sequentially applies O_2 and/or H_2 plasma with a non-fluorinated copper amidinate precursor [3]. The film phase (Cu, CuO, Cu_2O) can be controlled through PE-ALD process parameters and post-deposition anneals. Following a 600°C anneal in vacuum, the films have nanocrystalline Cu_2O morphology with a large Cu(I) fraction, as measured by x-ray absorption near-edge structure (XANES). TFTs made with these films exhibit on/off ratios of 10^5, and compare well with similar devices made by our group using RF sputtered Cu_2O [4].

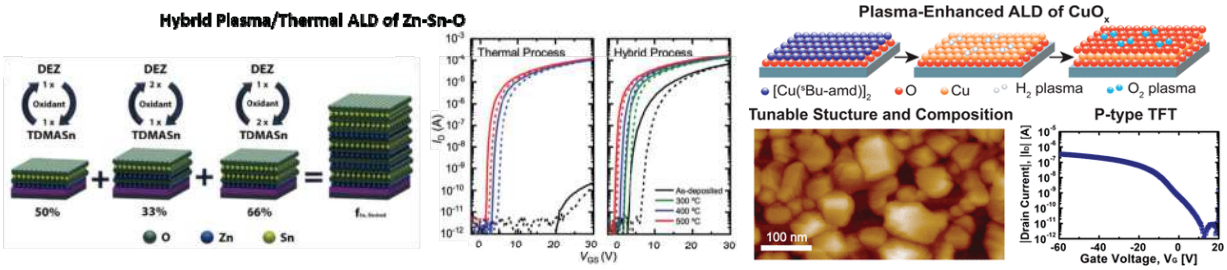

Fig. 1. Atomic Layer Deposition approaches and thin film transistor behavior for (left) n-type zinc tin oxide semiconductor, from [1] and (right) p-type cuprous oxide, from [3].

Acknowledgment

This work was supported by the National Science Foundation grant CMMI-1727918 and by the Intel Corporation through a PMOS Intel Strategic Research Alliance (ISRA).

References

1. C. R. Allemang, T. H. Cho, O. Trejo, S. Ravan, R. E. Rodríguez, N. P. Dasgupta, and R. L. Peterson, *Adv. Electron. Mater.*, 6(7), 2000195 (2020).
2. C. R. Allemang, T. Lu, S. Ravan, T. H. Cho, N. P. Dasgupta, and R. L. Peterson, *Device Research Conference*, 2021.
3. J. D. Lenef, J. Jo, O. Trejo, D. J. Mandia, R. L. Peterson, and N. P. Dasgupta, *J. Phys. Chem. C*, 125(17), 9383 (2021).
4. J. Jo, J. D. Lenef, K. Mashooq, O. Trejo, N. P. Dasgupta, and R. L. Peterson, *IEEE Trans. Electron Devices*, 67(12), 5557 (2020).

Novel Oxide TFTs that Show Immunity to Negative Bias Illumination Stress and Short Channel Effect

***Aimin Song*[1,2]**
[1]Department of Electrical and Electronic Engineering, The University of Manchester, Manchester M13 9PL, UK
E-mail: A.Song@manchester.ac.uk
[2]Center of Nanoelectronics and School of Microelectronics, Shandong University, Jinan 250100, China

Oxide semiconductors have opened a new era for large-area, flexible, and transparent applications. Despite the progresses, a bottleneck issue of oxide thin-film transistors (TFTs) is the instability either under bias stress or when used as a current source. Furthermore, the carrier mobility and current driving capability need to be improved for high-spec displays. It is still hugely challenging to overcome both issues using the conventional device structure and oxide material.

Here, we review our recent work on novel oxide TFTs that show intrinsic immunity to the negative bias illumination stress and short channel effect[1]. Rather than using an ohmic metal contact as the source electrode, a high work-function Schottky source contact enables depletion around the TFT source region, which results in several desirable properties including intrinsic immunity to the negative bias illumination stress, no obvious short channel effect, and superb current saturation over a wide range of drain voltage. The flat saturation current gives rise to an extremely high voltage gain reaching 23,000, which is, to the best of our knowledge, the highest gain ever achieved by a solid-state transistor to date. Furthermore, the depletion provided by the Schottky source electrode allows utilizing semi-metal ITO to replace IGZO as the TFT channel layer, which significantly enhances the carrier mobility and current driving capability. Other related work may also be introduced in the talk including oxide Schottky diodes operating beyond 10 GHz[2], oxide TFTs operating beyond 1 GHz[3], significantly enhanced carrier mobility by self-assembled monolayer treatment[4,5], and CMOS-like oxide-based logic circuits[6,7].

References

1. Extremely high-gain source-gated transistors, J Zhang, J Wilson, G Auton, Y Wang, M Xu, Q Xin, A Song, *Proceedings of the National Academy of Sciences* 116 (11), 4843-4848 (2019)
2. Flexible indium–gallium–zinc–oxide Schottky diode operating beyond 2.45 GHz, J Zhang, Y Li, B Zhang, H Wang, Q Xin, A Song, *Nature communications* 6 (1), 1-7 (2015).
3. Amorphous-InGaZnO thin-film transistors operating beyond 1 GHz achieved by optimizing the channel and gate dimensions, Y Wang, J Yang, H Wang, J Zhang, H Li, G Zhu, Y Shi, Y Li, Q Wang, Qian Xin, Zhongchao Fan, Fuhua Yang, Aimin Song, *IEEE Transactions on Electron Devices* 65 (4), 1377-1382 (2018).
4. Significant Performance Improvement of Oxide Thin-Film Transistors by a Self-Assembled Monolayer Treatment, W Cai, J Zhang, J Wilson, J Brownless, S Park, L Majewski, A Song, *Advanced Electronic Materials* 6 (5), 1901421 (2020).
5. Significant performance enhancement of very thin InGaZnO thin-film transistors by a self-assembled monolayer treatment, W Cai, J Wilson, J Zhang, J Brownless, X Zhang, LA Majewski, A Song, *ACS Applied Electronic Materials* 2 (1), 301-308 (2020).
6. Complementary integrated circuits based on p-type SnO and n-type IGZO thin-film transistors, Y Li, J Yang, Y Wang, P Ma, Y Yuan, J Zhang, Z Lin, L Zhou, Q Xin, Aimin Song, *IEEE Electron Device Letters* 39 (2), 208-211 (2017).
7. Thin Film Sequential Circuits: Flip-Flops and a Counter Based on p-SnO and n-InGaZnO, Y Yuan, J Yang, Y Wang, Z Hu, L Zhou, Q Xin, A Song, *IEEE Electron Device Letters* 42 (1), 62-65 (2020).

Low Cost Amorphous ZnSnO TFT Technology for Large Area Electronics

Shengdong Zhang*, Huan Yang, Gang Wang and Hongyang Zuo
School of Electrical and Computer Engineering, Peking University, Shenzhen, China
Tel.:85-0755-26035356, E-mail: zhangsd@pku.edu.cn

Amorphous oxide semiconductor (AOS) thin-film transistors (TFTs) have attracted huge attention due to their promising applications in larger area electronics [1]. In comparison to the most popular amorphous InGaZnO (a-IGZO) TFTs, amorphous ZnSnO (a-ZTO) TFTs are of low-cost and environment-friendly fabrication due to the abundant reserves and non-toxic of the Zn and Sn elements [2, 3]. Thus, a-ZTO TFT technology is also deserved to be developed for application in large area electronics with low cost. In this work, we developed the a-ZTO TFT technology including back channel etch (BCE) and self-aligned top-gate (SATG) processes.

Fig. 1(a) shows the XRD result of the sputter-deposited ZTO film, which keeps amorphous after annealing at 400 °C. Fig. 1(b) shows the transfer curves of the fabricated BCE a-ZTO TFT [2]. As shown, the fabricated TFT exhibits excellent performances, with a field-effect mobility of 15 cm^2/Vs, low off current of below 1 pA, and 0.5-V turn-on voltage. Fig. 1(c) shows the foreward and reverse transfer curves of the TFT, where no obvious hysteresis is seen, suggesting a low defects density in the a-ZTO and at the interface. Fig. 1(d) shows the transfer characteristic of the SATG a-ZTO TFT fabricated in this work [3]. Major performance paremeters include a mobility of 12 cm^2/Vs, low off current of below 1 pA, near-zero turn-on voltage, and low subthreshold swing of 0.3 V/Dec. Moreover, no current corwarding is observed as shown in Fig. 1(e), indicating a formation of low-resistance S/D and good Ohmic contact in the SATG TFTs.

The electrical stabilities of fabricated BCE and SATG a-ZTO TFTs under positive and negative bias stress (PBS and NBS) were also studied. As shown in Fig. 1(f), a threshold voltage shift of below 1 V under 3600-s stress is observed for both the BCE and SATG a-ZTO TFTs.

In conclusion, high performance and good stability are demonstrated for both bottom- and top-gate a-ZTO TFTs, confirming the feasibility for application in large area electronics.

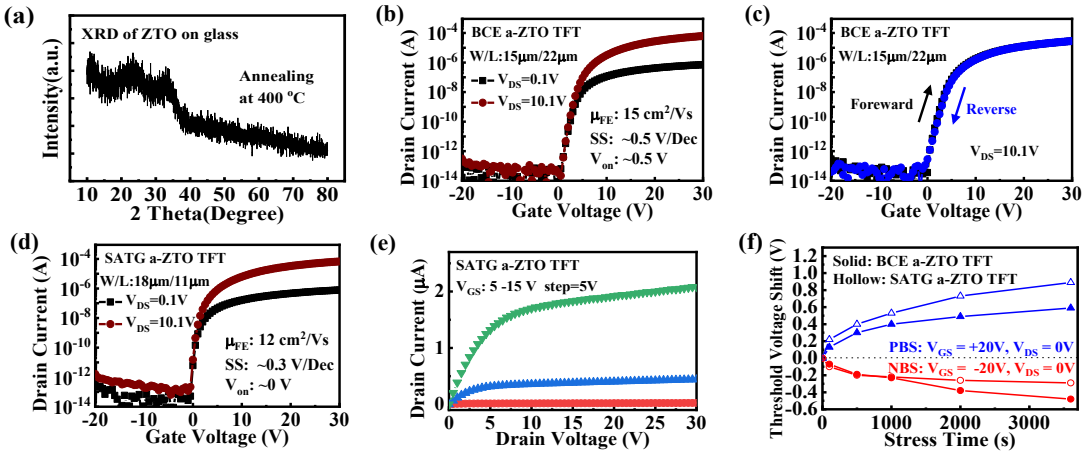

Fig. 1. (a) XRD image of ZTO film with annealing at 400 °C. (b) Transfer curves and (c) hysteresis characteristic of BCE a-ZTO TFT. (d) Transfer curves and (e) output curves of SATG a-ZTO TFT. (f) Threshold voltage shift for both BCE and SATG a-ZTO TFTs under positive and negative bias stress.

Acknowledgment

This work was supported financially by National Natural Science Foundation of China (NSFC) under projects 61774010, and by Shenzhen Municipal Scientific Program under Grants XMHT20190201013 and JCYJ20180504165449640.

References

1. E. Fortunato, P. Barquinha, and R. Martins, *Adv. Mater.*, 24(22), 2945 (2012).
2. H. Zuo, L. Zhang, Y. Yang, C. Fan and S. Zhang, *AM-FPD'19 Technical Digest*, vol. 4, (2019).
3. G. Wang, B. Chang, H. Yang, et al, *IEEE Electron Device Lett.*, 40(6), 901 (2019).

Incorporation of Small Radius Metallic Elements for Low Temperature-Processed Amorphous Oxide Thin-Film-Transistors

Jae Sang Heo[1,2], Seong-Pil Jeon[2], Chang-Yong Park[2], Hun Bum Park[2], Yong-Hoon Kim[1], Myung-Gil Kim[1], and Sung Kyu Park[2]

[1]School of Advanced Materials Science and Engineering, Sungkyunkwan University, Suwon 16419, Korea
[2]School of Electrical and Electronics Engineering, Chung-Ang University, Seoul 06974, Korea
Tel.:82-2-820-8547, E-mail: skpark@cau.ac.kr

Suppressing interfacial disorders between semiconductors and gate dielectrics has been revealed as one of the key issues to achieve high-performance amorphous oxide semiconductor (AOS) thin-film-transistors (TFTs) with the low-temperature process. Although various activation and doping processes have been suggested, a generation of efficient suppressors in both the semiconductor and dielectric layers under low-temperature conditions is remained as a challenge, requiring more in-depth studies for the passivation of disruptive interfaces. Here, we exploit a facile approach to suppress the residual impurities and dipole disorders in low-temperature AOS TFTs by providing elemental diffusive higher-order semiconductor alloys.[1,2]

Here, we exploit a facile route to improve the film quality and the interfacial property of low-temperature solution-processed oxide thin films via elemental diffusion process between metallic ion-doped InO_x ($M:InO_x$) ternary oxide semiconductor and aluminium oxide (AlO_x) gate dielectric layers. As a result, it was found that along with high Gibbs energy and bonding dissociation, large diffusivity of the metallic ions can also promote the formation of additional M-O-M bonding states in the InO_x film and increase the degree of reaction with residual hydroxyl or alkyl groups in the AlO_x gate dielectric film. Furthermore, metallic dopants with smaller ionic radii compared to the host metallic ions can have more effective diffusion behaviours into the AlO_x gate dielectric, providing high quality AlO_x film with lower defective interface[3], as shown in Fig 1(a) and (b). Finally, through a wide array of spectroscopic and electrical analysis for $M:InO_x/AlO_x$ TFTs, we provide direct evidences of elemental diffusion occurred between $M:InO_x$ and AlO_x layers as well as its contribution to the electrical performance and operational stability. Using the elemental diffusion process, we demonstrate solution-processed $Hf:InO_x$ TFTs using a low-temperature AlO_x gate dielectric having a field-effect mobility of 2.83 $cm^2 V^{-1}s^{-1}$ and improved bias stability, as shown in Fig 1(c) and (d).

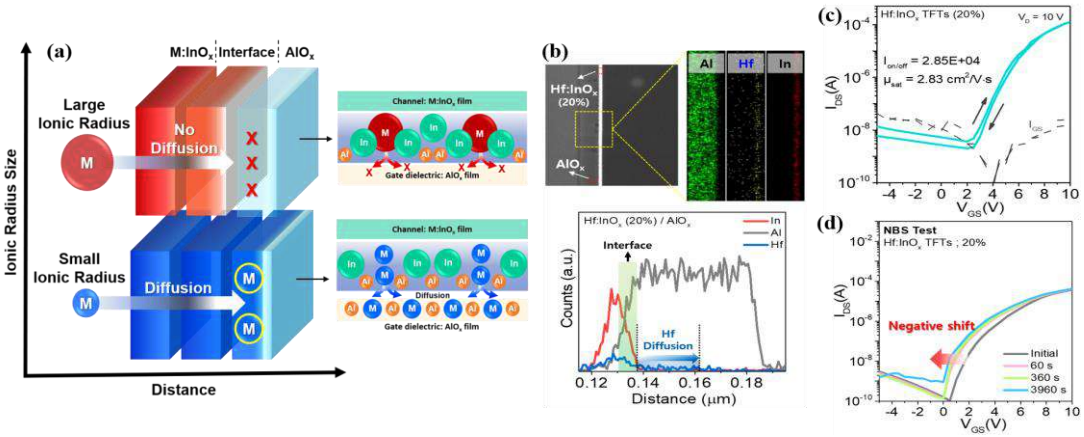

Fig. 1. (a) Schematic of metal ionic diffusion from $M:InO_x$ channel layer into the AlO_x gate dielectric layer depending on the ionic radius size of metallic dopants, (b) Cross sectional HADDF-STEM images with corresponding the line scans of EDS profile, (c) Transfer curve, and (d) Operational stability under the NBS for $Hf:InO_x/AlO_x$ with 20% of Hf.

Acknowledgment

This research was funded and conducted under [the Competency Development Program for Industry Specialists] of the Korean Ministry of Trade, Industry and Energy (MOTIE), operated by Korea Institute for Advancement of Technology (KIAT). (No. P0002397, HRD program for Industrial Convergence of Wearable Smart Devices).

References

1. X. Zhang, B. Wang, W. Huang, Y. Chen, G. Wang, L. Zeng, W. Zhu, M. J. Bedzyk, W. Zhang, J. E. Medvedeva, *J. Am. Chem. Soc.* 140, 12501–12510 (2018).
2. J. S. Heo, S. -P. Jeon, I. Kim, W. Lee, Y. -H. Kim, S. K. Park, *ACS Appl. Mater. Interfaces*. 11, 48054-48061 (2019).
3. S. Parthiban, J. -Y. Kwon, *J. Mater. Res.* 29, 1585–1596 (2014).

Direct Optical Patterning of Quantum Dot Light-Emitting Diodes

***Himchan Cho*[1]**
[1]***The Department of Materials Science and Engineering, Korea Advanced Institute of Science and Technology (KAIST), 291 Daehak-ro, Yuseong-gu, Daejeon,* Korea**
Tel.:82-42-350-3344, E-mail: himchan@kaist.ac.kr

Precision patterning of QDs is a critical step to fabricate displays incorporating QD color filters and QD light-emitting diode (QLED) subpixels in form of RGB matrix. However, high-resolution patterning of solution-processed QD layers is fundamentally challenging because conventional patterning methods cannot simultaneously meet the requirements of high resolution, pattern uniformity, high throughput, and high photoluminescence quantum yield. To overcome this challenge, we developed a direct, scalable, and nondestructive route for high-resolution patterning of QDs and QLEDs.[1] A specially designed nanocrystal ink, "photopatternable emissive nanocrystals (PEN)", consists of gradient core/shell QDs and photoacid generators which enable photochemically activated reactions leading to *in-situ* ligand exchange in the QD films. Uniform electroluminescence patterns of RGB QD LEDs with features size down to 1.5 μm were demonstrated while preserving the structural, electronic, and emissive properties of patterned QDs.

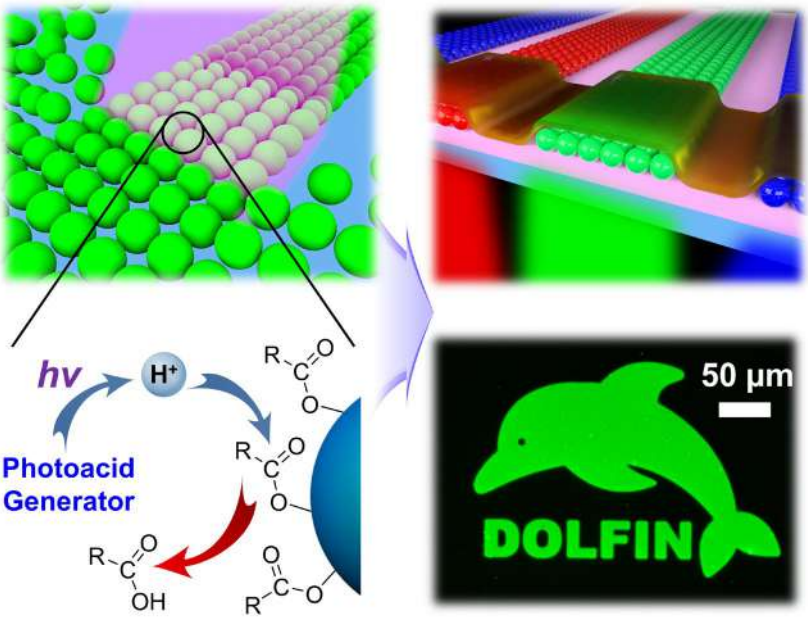

Fig. 1. Schematic illustrations and an optical microscope image showing the concept of direct optical lithography of functional inorganic nanomaterials (DOLFIN).

References

[1] H. Cho *et al., Adv. Mater.* **2020,** 32(46), 2003805

Timed Control of Tunable White LED for Creating a Supportive Learning Environment

Kyungah Choi
Dept. of Service Design Engineering, Sungshin Women's University, Seoul 02844, Korea
Tel.:82-2-920-7574, E-mail: kyungah.choi@sungshin.ac.kr

Short-wavelength light is a powerful agent that influences a large number of non-visual processes in the human body, including alertness, cognitive performance, work productivity, the sleep-wake cycle, and health and well-being. From the educational standpoint, current research has been focused primarily on its effects on the cognitive performance of students. However, prolonged exposure to blue-enriched white light in the evening suppresses melatonin secretion, which negatively affects sleep quality and circadian rhythm. The study therefore aims to deliver a lighting control scenario that helps to maintain circadian entrainment as much as possible while supporting the cognitive performance of students.

Two empirical studies were conducted. The first part of the study aims to provide a smooth reduction of the lighting CCT by taking into account the visual sensitivity of the human eye. A visual experiment was conducted to determine the optimal rate of change to avoid distraction and discomfort and the threshold at which the difference is detected. Within the experimental conditions, the detection threshold was a decrease of 25 percent from the initial CCT, regardless of the rate of change. Based on the results, a color temperature reduction from a 6500 K blue-enriched white light to a 5000 K neutral white light at a rate of 5 K/s was suggested. The second part of the study was conducted to investigate the influence of different lighting scenarios on physiological and subjective responses. Three lighting scenarios were tested: controlled (blue-enriched white to neutral white light), constant (neutral white light), and lights-off conditions. The level of concentration and arousal, as measured by brain and heart activity, respectively, was highest with the controlled lighting scenario. However, these effects were not reflected in the subjective assessments and the n-back task score.

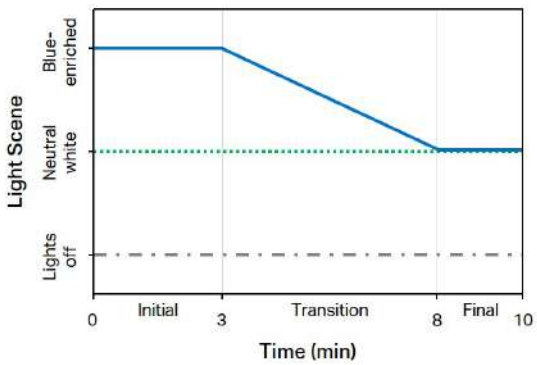

Fig. 1. The patterns of color temperature of three lighting scenarios: controlled (solid), constant (dotted), and lights-off (dash-dotted).

Taken together, the results demonstrated that a gradual lighting transition in which the blue-enriched white light changes into neutral white light could be beneficial in an educational context. Although further research is necessary, the results of this study may inspire and inform designers and engineers, thereby facilitating the creation of better learning environments.

Acknowledgment

This work was supported by the National Research Foundation of Korea (NRF-2019R1C1C1011411).

References

1. G. Vandewalle, P. Maquet, and D. J. Dijk, *Trends Cogn. Sci.*, 13(10), 429-438 (2009).
2. K. Choi and H. J. Suk, *Build. Environ.*, 180, 107046 (2020).
3. M. G. Figueiro, M. S. Rea, and J. D. Bullough, *Neurosci. Lett.*, 406(3), 293 (2006).

From Light Responsive Liquid Crystalline Polymers to Remote Controllable Smart Materials

Dae-Yoon Kim
Functional Composite Materials Research Center, Korea Institute of Science and Technology, Bongdong, Jeonbuk 55324, Korea
Tel.:+82-63-219-8184, E-mail: kdaeyoon@kist.re.kr

Molecular engineering of responsive materials has paved new ways to develop functional materials, such as tunable photonic crystals, versatile energy transducers, and shape memory devices.[1] Light is a common external stimulus that can be rapidly, remotely, and sequentially controlled.[2] Therefore, manipulating the hierarchical superstructure by incorporation of the photoresponsive moeities into the liquid crystalline molecules through chemical modification is one of the interesting approaches.

Various photoresponsive polymers have been developed for application in actuators that convert light to mechanical work or sometimes vice versa. However, studies on photomechanical behaviors with respect to molecular packing symmetry are quite limited.[3] From this perspective, dendronized polymers showing smectic liquid crystalline mesophase are designed and synthesized.[4] This study highlights how to estimate the directionality of the photodeformation process depending on the hierarchically self-assembled superstructures. Finally, fabrication of remote-controllable actuators are successfully demonstrated for photoresponsive logic devices.

Acknowledgment

D.-Y.K. acknowledges the support of the Open Research Program (2E31332) of the Korea Institute of Science and Technology and the National Research Foundation of Korea (2021R1R1R1004226).

References

1. D.-Y. Kim, J. Koo, S.-I. Lim and K.-U. Joeng, *Adv. Funct. Mater.*, 28, 1707075 (2018).
2. D.-Y. Kim, S.-A Lee, D. Jung, J. Koo, J. S. Kim, Y.-T. Yu, C.-R. Lee and K.-U. Jeong, *Soft Matter*, 13, 5759 (2017).
3. D.-Y. Kim, W.-J. Yoon, Y.-J. Choi, S.-I. Lim, J. Koo and K.-U. Jeong, *J. Mater. Chem. C*, 6, 12314 (2018).
4. D.-Y. Kim, S. Shin, W.-J. Yoon, Y.-J. Choi, J.-K. Hwang, J.-S. Kim, C.-R. Lee, T.-L. Choi and K.-U. Jeong, *Adv. Funct. Mater.*, 27, 1606294 (2017).

Liquid crystal smart glasses for higher color contrast and reduced glare

Seung-Won Oh[1], Jae-Won Huh[2], and Tae-Hoon Yoon[2]
[1] Department of Electronics Engineering, Kangwon National University, Gangwon, Korea
[2]Department of Electronics Engineering, Pusan National University, Busan, Korea
Tel.:82-51-510-1700, E-mail: thyoon@pusan.ac.kr

Switchable sunglasses or goggles allow users to control the throughput of sunlight into their eyes upon application of external stimuli while allowing them to see; thus, their view is not blocked even when the sunglasses are darkened [1]. Unlike the windows used in buildings, eyewear needs a color design to protect the users' eyes or to improve visibility [2]. Yellow-tinted sunglasses, which block blue light, are a popular choice for outdoor use because they can increase the contrast under low-light conditions. Additionally, special glasses that filter out yellow light can effectively reduce the eye glare and increase the contrast from strong sunlight or from high-beam headlights while driving during the night. Thus, products that can remove the yellow color at approximately 590 nm with a narrow bandwidth have been developed to minimize eye glare for eyewear or automotive applications without a severe decrease in brightness [2]. A dye-doped LC cell, which consists of host LCs and guest (rod-shaped) dichroic dyes, can be an excellent candidate for switchable glasses; however, it cannot filter out the yellow color [3].

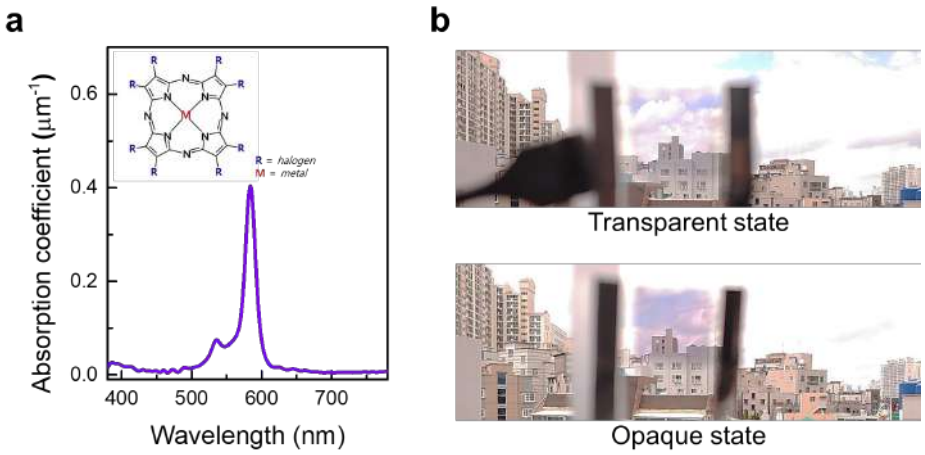

Fig. 1. a) Tetra-aza porphyrin: representative structure and absorption coefficient. b) photographs of the fabricated LC cell in the transparent and haze-free opaque states.

In this presentation, we propose a switchable glass that can control the transmittance of visible light while blocking yellow light. It is based on the switching of a dye-doped LC cell in which a yellow dye (Figure 1a) is used for filtering out the yellow color. In contrast to dichroic dyes having a rod-shaped molecular structure, which are switchable along the alignment direction of LCs, the yellow dye having a spherical molecular structure used in this study is not switched along the alignment direction of the LCs. Therefore, the yellow color, which can cause glare in both transparent and opaque states, can be removed (Figure 1b).

Acknowledgment
This work was supported by the National Research Foundation of Korea (NRF) grant funded by the Korea government (MSIP) (No. 2020R1A2C1006464).

References
1. C. G. Granqvist, *Solid State Ionics,* 53-56, 479 (1992).
2. Costa 580 lens *" https://www.costadelmar.com/us/en/performance-technology/lenses"*
3. G. H. Heilmeier, L A. Zanoni, L. A. Barton, IEEE Proc., 56, 1162 (1968).

Requirements for High-Resolution Stretchable Displays

Haeyoon Jung[1], Moon Bae Gee[1], Chanil Park[1] and Changdong Kim [1]
[1]LG Display R&D Center, E2 Block LG Science Park, 30 Magokjungang 10-ro, Gangseo-gu, Seoul, 07796, Korea
Tel.:82-2-6987-0458, E-mail: haeyoon.jung@lgdisplay.com

Stretchable is expected to be the next generation form factor of displays following flexible, foldable and rollable for free-form deformation. A lot of studies in stretchable electronics including stretchable interconnect materials, structures and substrates have been reported by many research groups, so that those enable us to realize stretchable displays, however more studies are still required considering high-resolution displays.

Generally display panels are mainly composed of 3 regions; pixel array, gate driver (side) region, data driver (top) region, and all areas are supposed to be stretchable in an ideal stretchable display, but that is difficult to achieve currently. The first step is making the pixel array where information is displayed stretchable and there are several approaches to make a pixel stretchable, one of the most practical ways is using 'hybrid-type devices' concept [1], which is dividing a pixel into stretchable area and non-stretchable area (rigid island) where stretchable interconnects are located and TFT and light emitting device are located, respectively. It allows us to make use of the conventional display backplane process [2], however, it also has a few technical issues as follows: The effective resolution for TFT and light emitting device is higher than the panel resolution and the stretchability that interconnects should take at a certain panel stretch ratio goes higher because the rigid island exist in the pixel. Moreover the number of interconnects at each side of rigid island should be more than 3 probably if we use conventional active matrix pixel driving circuits, that makes the design and fabrication of stretchable interconnects more difficult due to the limited space.

Besides the technologies about the patternable light emitting device which can be fabricated only on the rigid island and stretchable substrate are also required for stretchable displays [3]. For the highly stretchable display with high-resolution, the key technologies should be chosen and combined properly.

Acknowledgment

References

1. Y. Hong, B. Lee et al., Information Display 17.4 (2017):6-38.
2. A. K. Tripathi et al., IMID Digest (2015)
3. J. H. Koo, D. C. Kim, H. J. Shim, T. H. Kim, D. H. Kim, Adv. Funct. Mater. 2018, 28, 1801834.

Dynamic designer phase-change metafilm for versatile visible light modulation

***Sun-Je Kim*[1]**
[1]Dept. of Physics, Myongji University, Cheoingu/Yongin, 17058, South Korea
Tel.:82-31-330-6168, E-mail: sunjekim@mju.ac.kr

Strong and ultracompact modulation of visible light has been desired for next-generation display and sensing technologies. Recently, in particular, phase-change materials including vanadium dioxide (VO_2) [1-4] and chalcogenide compounds [5, 6] have attracted much attention as active material platforms owing to their tunability of optical dielectric functions induced by the temperature-dependent phase-changes. However, it is still limited to meet multi-objective high modulation performance owing to the limited quality factor and tunability in the visible regime. In this paper, a novel design of photonic pixel using phase-change metafilm absorber is proposed and verified by theoretical and experimental studies [4]. By engineering tunability of effective anisotropic permittivity of Ag-VO_2, strong active modulation of reflection and absorption spectrum is designed at certain desired wavelength regions without sacrificing bandwidth and efficiency. Based on effective medium theory of metamaterial and coupled mode theory, the intuitive design rules and theoretical analysis of resonances are proposed. It is experimentally proved that versatile applications of intensity modulation, coloring, and polarization rotation are enabled in a single device. By virtue of ultrathin flat configuration of a metafilm absorber, design extensibility of reflection spectrum is also verified.

It is expected that the proposed concept would be fruitful for improvement of various integrated optoelectronics technologies such as compact spatial light modulator, compact reflective display, and multiplexed image sensors that essentially require compact and dynamic visible range operation. Moreover, it seems to be promising that the proposed strategy based on noble metal-embedding could be a milestone research for sub-micron active modulator pixels, when pixel-by-pixel electro-thermal control is applied to the embedded silver nanobeams.

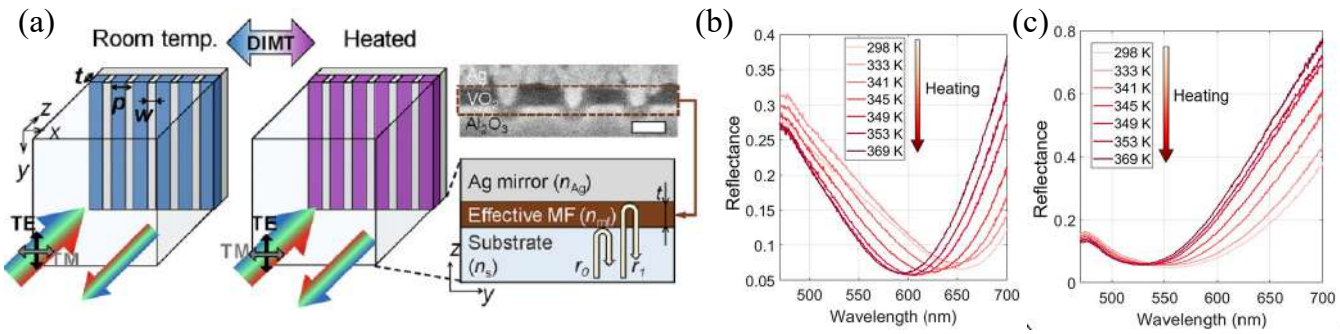

Fig. 1. Concept and experimental results of metafilm. (a) Conceptual schematic diagram and cross-sectional scanning electron beam micrograph of a fabricated Ag-VO_2 metafilm. (b, c) Measured temperature-dependent reflection spectra of the metafilm shown in (a) when heated. The spectra in (b) and (c) refer to dynamic reflections of the device for TM and TE polarized light, respectively.

Acknowledgment

This work was supported by the National Research Foundation of Korea(NRF) grant funded by the Korea government(MSIT) (NRF-2021R1F1A1062368).

References

1. N. R. Hosseini and J. Rho, *Materials*, 10(9), 1046 (2017).
2. M. J. Dicken *et al.*, *Opt. Express*, 17(20), 18330 (2009).
3. S. J. Kim *et al.*, *Sci. Rep.*, 7, 43723 (2017).
4. S. J. Kim *et al.*, *Nanophotonics*, 10(1), 713 (2020).
5. C. Choi *et al.*, *Adv. Func. Mater.*, 31(4), 2007210 (2021).
6. C.-Y. Hwang *et al.*, *Nanoscale*, 10(46), 21648 (2018).

Surface Modification of Graphene Quantum Dots for Optoelectronic Applications

Minsu Park
Dept. of Materials Science and Engineering, Northwestern University, Evanston, IL 60208, USA
Tel.:1-847-440-6437, E-mail: minsu.park@northwestern.edu

Graphene quantum dots (GQDs), a nanometer-sized graphene family are promising as the next-generation light-emitting materials owing to their advantages such as low-cost synthesis, unique photoluminescence (PL), and excellent biocompatibility. Many studies have been conducted over the years on tuning the emission wavelength and improving the PL quantum yields (PLQY) of GQDs, but efforts to enhance the applicability of GQDs as an active material of electroluminescent (EL) devices are insufficient. This paper presents two robust surface modification strategies that can both significantly improve the PL characteristics of GQDs, or explore new photophysics, thereby enabling various optoelectronics applications: i) Embedding GQDs into boron oxynitride matrix (GQD@BNO) provides excellent dispersion of GQDs in its solid-state, resulting in the high PLQY of up to 36.4 %, which is 8-fold higher than that of pristine GQDs in water. This makes the GQDs an ideal active material for use in alternating-current powder EL device, with the luminance exceeding 283 cd m^{-2}. Moreover, the BNO matrix stabilizes triplet excited states of GQDs to realize room-temperature phosphorescence emission for the first time with ultralong lifetime of 783 ms, which enables the first demonstration of anti-counterfeiting and multilevel information security using GQDs. ii) Surface functionalization of GQDs with polyhedral oligomeric silsesquioxane (POSS), poly(ethylene glycol) (PEG), and hexadecylamine (HDA) enables quenching-resistant PL in the solid-state due to the reduction of π−π stacking of GQDs by steric hindrance of functionalized molecules. Especially, the GQD-based white light-emitting diodes (GQD-WLEDs) fabricated by mounting HDA-GQDs on a UV-LED chip exhibits efficient down-conversion for white light-emission with a high color rendering index of 86.2 at Commission Internationale de l'Éclairage coordinates of (0.333, 0.359). These strategies will reduce the technical gap between GQDs and near-unity luminescent materials in the next-generation display fields.

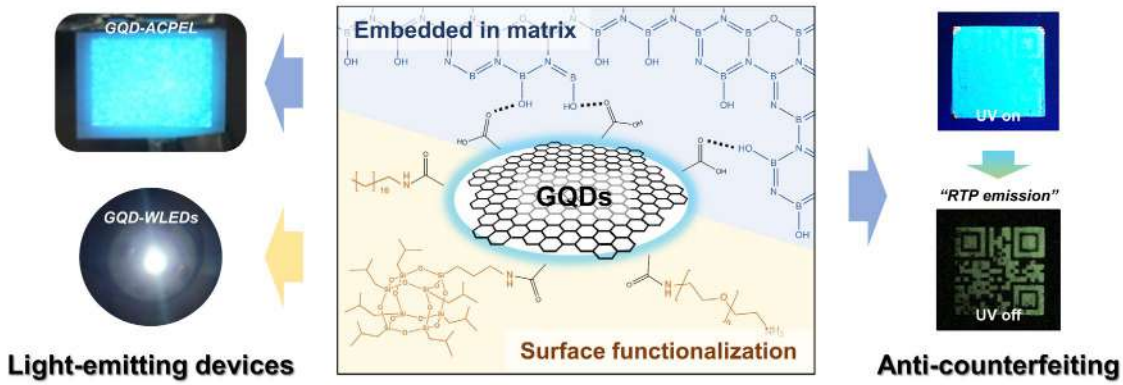

Fig. 1. Illustration for surface modification of graphene quantum dots and optoelectronic applications

Acknowledgment

This research was mainly supported by the Center for Advanced Soft-Electronics by the Ministry of Science, ICT and Future Planning as Global Frontier Project (CASE-2013M3A6A5073173).

References

1. M. Park, H. Yoon, J. Lee, J. Kim, J. Lee, S.-E. Lee, S. Yoo and S. Jeon*, *Adv. Mater.,* 30(38), 1802951 (2018).
2. M. Park†, H.S. Kim†, H. Yoon, J. Kim, S. Lee, S. Yoo* and S. Jeon*, *Adv. Mater.,* 32(31), 2000936 (2020).
3. M. Park†, Y. Jeong†, H.S. Kim†, W. Lee, S.-H. Nam, S. Lee, H. Yoon, J. Kim, S. Yoo* and S. Jeon*, *Adv. Funct. Mater.,* 31(29), 2102741 (2021).
4. H. Yoon†, M. Park†, J. Kim, T.G. Novak, S. Lee, S. Jeon*, *Chem. Phys. Rev.,* 2(3), 031303 (2021)

Contact-Electrification-Activated Artificial Afferents

Jinran Yu[1], and Qijun Sun[1]
[1] **Beijing Institute of Nanoenergy and Nanosystems, Chinese Academy of Sciences, Beijing 101400, P. R. China**
E-mail: yujinran@binn.cas.cn; sunqijun@binn.cas.cn

Low power electronics endowed with artificial intelligence and biological afferent characters are beneficial to neuromorphic sensory network. Highly distributed synaptic sensory neurons are more readily driven by portable, distributed, and ubiquitous power sources. Here, we report a contact-electrification-activated artificial afferent at femtojoule energy, as shown in Figure1. Upon the contact-electrification effect, the induced triboelectric signals activate the ion-gel-gated MoS_2 postsynaptic transistor, endowing the artificial afferent with the adaptive capacity to carry out spatiotemporal recognition/sensation on external stimuli (e.g., displacements, pressures and touch patterns). The decay time of the synaptic device is in the range of sensory memory stage. The energy dissipation of the artificial afferents is significantly reduced to 11.9 fJ per spike. Furthermore, the artificial afferents are demonstrated to be capable of recognizing the spatiotemporal information of touch patterns. This work is of great significance for the construction of next-generation neuromorphic sensory network, self-powered biomimetic electronics and intelligent interactive equipment.

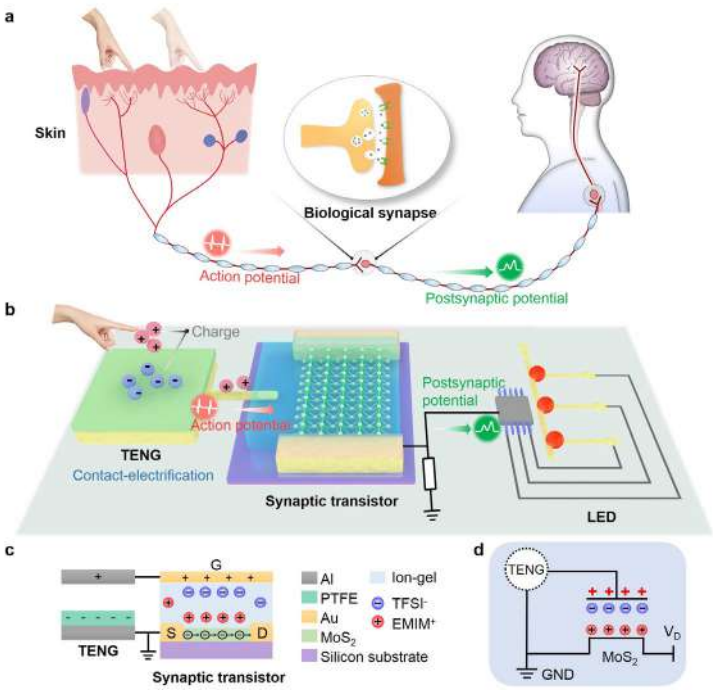

Fig. 1. Contact-electrification-activated artificial afferents.

References

1. Gao G, Yu J, Yang X, et al. *Adv. Mater.*, 31(7), 1806905(2019).
2. Yu J, Gao G, Huang J, et al. *Nat. Commun.*, 12(1), 1581(2021).

Group III-Nitride Semiconductor Micro and Nano Structures for Lighting and Display Applications

Yong-Hoon Cho
Department of Physics and KI for the NanoCentury
Korea Advanced Institute of Science and Technology (KAIST), Daejeon 34141, Korea
Tel.:82-42-350-2549, E-mail: yhc@kaist.ac.kr

Recently, on the basis of various advantages of nitride semiconductor materials and light emitting devices (LEDs), interest in applications to ultra-small high-efficiency light sources and high-resolution displays is dramatically increasing. In order to miniaturize the unit structure of nitride semiconductors for these applications, it can be grown by bottom-up growth methods or fabricated through top-down etching techniques. In this talk, we present the results on various micro- and nano-scale nitride semiconductor structures fabricated by bottom-up and top-down approaches and discuss structural, optical, and electrical characteristics of the fabricated structures. First, we demonstrated phosphor-less white LEDs using three-dimensional GaN micro-structures grown by selective area epitaxy using metal-organic chemical vapor deposition [1-3]. The annular and double concentric truncated pyramidal LEDs provide broad-band, white light generation from the QWs formed on various planes. Second, we fabricated an intriguing quantum wire structures spontaneously formed in a single microrod [4,5] or intentionally fabricated at the vertex of the triangular prism structures [6]. The quantum wire emitters, consisting of two sets of multiple quantum wires formed on the edges and the boundaries in a single microrod, exhibited efficient two different wavelength emissions with linear polarization parallel and perpendicular to the microrod axis, respectively, allowing mutually controllability of the wavelength and the polarization of light. Third, we fabricated micro-LED array samples with different sizes via top-down dry etching techniques and characterized optical and electrical properties depending on the size [7]. For all the above structures, we focused on various optical properties with high spatial resolution for single micro- and nano-structures. The optical properties of the micro-LED structures with different shapes and sizes were compared with their structural and electrical properties. Comparison and some critical issues on different types of micro-LED structures will be discussed.

References

[1] Y. C. Sim, S. H. Lim, Y. S. Yoo, M. H. Jang, S. H. Choi, H. S. Yeo, K. Y. Woo, S.W Lee, H. G. Song and Y. H. Cho*, Nanoscale 10, 4686 (2018).
[2] Y. S. Yoo, H. G. Song, M. H. Jang, S. W. Lee and Y. H. Cho*, Scientific Reports 7, 9663 (2017).
[3] S. H. Lim, Y. C. Sim, Y. S. Yoo, S. H. Choi, S. W. Lee and Y. H. Cho*, Scientific Reports 7, 9356 (2017).
[4] S. Choi, H. G. Song, S. Cho, Y. H. Cho*, Nano Letters 19, 8454 (2019).
[5] S. Choi, H. G. Song, Y. S. Yoo, C. Lee, K. Y. Woo, E. Lee, S. D. Roh, and Y. H. Cho*, ACS Photonics 5, 2825 (2018).
[6] H. S. Yeo, K. Lee, Y. C. Sim, S. H. Park, and Y. H. Cho*, Scientific Reports 10, 15371 (2020).
[7] K. Y. Woo and Y. H. Cho* (unpublished)

High Color Gamut OLED Material Sets for Reduced Power Consumption Laptop Applications

Mike Hack, Michael S. Weaver, and Julie J. Brown
Universal Display Corporation, 375 Phillips Blvd., Ewing, NJ 08618, USA
Tel.:001-609-964-5120, E-mail: mhack@oled.com

Kunjal Parikh, Kathy Bui, and Vishal Sinha
Intel Corporation, Santa Clara, CA 95054, USA

In this paper we discuss the benefits that can be realized by phosphorescent OLED technology for low power consumption high color gamut displays. We show that relative to LCD based displays, the higher the display color gamut, the more OLED displays have a power consumption advantage over LCDs, enabling high performance displays for laptops. Based on Intel's day in life PC usage model, our simulation shows that DCI-P3 and 97% BT2020 color profiles will deliver 13% and 18% improvement respectively in battery life for OLEDs versus equivalent LCDs.

We analyze the power consumption of OLED displays with increasing color gamut and show that the relative power consumption increase with increasing color gamut based on an OLED display is much less than for a LCD based display, and at a Digital Cinema Initiative P3 (DCIP3) color gamut and beyond, OLEDs become a lower power consumption and higher performance display. Moreover, when we consider the red to green to blue (RGB) color balance of an OLED display operating at an International Commission on Illumination (CIE) Standard Illuminant D65 white point, if we implement a higher color gamut using a green that is relatively more saturated than the red, we can further increase OLED display color gamut with only a very minimal increase in power consumption.

Our results have important implications at the system level. OLEDs offer unique form factor advantages on account of their thin and light weight profile, and the ability to produce a folding OLED display has enabled the production of laptops where the two main surfaces can be one continuous large area display which conveniently folds for storage. That OLEDs have both superior form factors and increased battery life than LCDs, through lower power consumption, should lead to their increased adoption in future laptops.

Graphene Interlayer for Metal/Semiconductor Junctions with Minimized Metal-induced Gap States

Jun-Ho Park[1,†], Seong-Jun Yang[1,†], Chang-Won Choi[2], Si-Young Choi[2,] and Cheol-Joo Kim[1,*]*

[1]Department of Chemical Engineering Pohang University of Science and Technology 77 Cheongam-Ro, Nam-Gu, Pohang 37673, Republic of Korea

[2]Department of Material Science & Engineering Pohang University of Science and Technology 77 Cheongam-Ro, Nam-Gu, Pohang 37673, Republic of Korea

†These authors contributed equally to this work.

ABSTRACT

Metal-induced gap states (MIGS) at Metal (M)/semiconductor (S) interface makes it difficult to engineer Schottky junctions. Graphene(Gr) interlayer has been expected to minimized MIGS at M/S interface. However, realization of the pristine M/Gr/S junctions without interfacial states has been challenging by unavoidable contaminants from wet-etching process. Here, atomically-clean M/Gr/*n*-type silicon (Si) junctions is successfully realized via all-dry transfer of M/Gr bilayers onto Si. Our designed M/Gr/Si junctions show significantly increased current density *J* at reverse bias (e.g., by 10^5 times for M = Au in Si(111)), compared with those of conventional M/Si junctions. Moreover, the reverse *J* by a Gr interlayer are more significantly increased in Si(111) than Si(100). We analyze the different transport data between M/Gr/Si(111) and M/Gr/Si(100) as Fermi-level pinning by different surface states of Si(111) and Si(100). Our results suggest that pristine Gr interlayer can minimize MIGS effectively to study intrinsic electrical properties of various semiconductor surfaces.

Aggregation-Induced Emission of Graphene Quantum Dot Modified with Molecular Rotors toward Efficient Solid-state Lighting

Sukki Lee[1], Jinho Lee[1], and Seokwoo Jeon[1]
[1]Dept. of Materials Science and Engineering, Korea Advanced Institute of Science and Engineering, 291, Daehak-ro, Yuseong-gu, Daejeon, Korea
Tel.:82-42-350-3382, E-mail: suki0487@kaist.ac.kr

Graphene quantum dot (GQD) is bandgap-opened graphene fabricated by reducing the physical size of graphene, which has no bandgap intrinsically. GQD exhibits excellent properties such as biocompatibility, photostability, water as well as thermal stability and most importantly, due to their stable blue light emission, GQD emerges as a potential candidates for next-generation optoelectronics. However, to use GQDs as the emission layer of light emitting diode, the low photoluminescence quantum yield (PLQY, Φ_{PL}) and low color purity resulting from uncontrollable charge transfer (CT) states must be overcome. Moreover, π-π interaction between large conjugation of sp^2 structures of GQDs provokes typical aggregation caused quenching (ACQ), exhibiting negligible PLQY and severely redshifted PL in their solid states. Aggregation-induced emission (AIE), an intriguing phenomenon that effectively restrict the intramolecular motion in solid state to hinder π-π interaction, was chosen as a strategy to convert GQDs from ACQ to AIE-active luminophores. Herein, efficient aggregated state emission of functionalized GQD was demonstrated, which could be realized by selective substitution of various functional group with freely-rotating molecular rotors, confirmed by various photophysical measurements.

Selective chemical substitutions of carboxyl and carbonyl functional group of GQDs into benzylamine (BZ), triphenylamine (TPA) and tetraphenylathane (TPE) rotors were conducted. Carbodiimide coupling chemistry and picoline-borane-mediated reductive amination were taken to convert each carboxyl group and carbonyl group into rotor groups selectively.

PL intensity of pristine GQD was quenched by increasing THF fraction (f_{THF}) in water, showing typical ACQ behavior. In contrast, carboxyl-to-BZ-substituted GQD (BZ-GQD 1) and carbonyl-to-BZ-substituted GQD (BZ-GQD 2) showed low PLQY at good solvent (f_{THF} = 0) enhanced PL intensity by increasing f_{THF} with maximum PLQY at f_{THF} = 90, implying that GQD was successfully converted into AIE-active luminophores. Pristine GQD showed Φ_{PL} of 4.5 % at f_{THF} = 0, and Φ_{PL} decreased to 1.0 % at f_{THF} = 90, whereas BZ-GQD 1 and BZ-GQD 2 showed Φ_{PL} of 3.2 % and 5.1 % each at f_{THF} = 0, increased to Φ_{PL} of 8.5 %, and 15.6 % each at f_{THF} = 90.

Excitation dependent behavior with non-characteristic emission was observed for pristine GQD, however, excitation independent behavior with vibrational peak was observed for BZ-GQDs at f_{THF} = 90. FWHM of BZ-GQDs were enhanced to ~70nm with deeper blue emission with coordinates of (0.015, 0.082) in CIE 1931 color space. These PL behaviors indicated that BZ substitutions to carboxyl and carbonyl group efficiently suppress the CT states and make transition occur mainly in locally excited (LE) states, which shows higher PLQY.

Powder and spin-coated thin film of BZ-GQDs also showed AIE behavior as seen on the aggregate states at f_{THF} = 90. With time-correlated single photon counting (TCSPC) measurement, reduced CT states and restriction of intermolecular vibration were revealed in BZ-GQDs, due to decreased tendency of non-radiative decay rates comparing to pristine GQDs in their solid states. Molecular rotor modification strategy exhibited successful suppression of π-π interaction as well as various CT states, which will seek future application on solid-state lighting devices.

References

1. Mei, J., Hong, Y., Lam, J. W., Qin, A., Tang, Y., & Tang, B. Z. (2014). Aggregation-induced emission: the whole is more brilliant than the parts. Advanced materials, 26(31), 5429-5479.
2. Park, M., Yoon, H., Lee, J., Kim, J., Lee, J., Lee, S. E., ... & Jeon, S. (2018). Efficient Solid-State Photoluminescence of Graphene Quantum Dots Embedded in Boron Oxynitride for AC-Electroluminescent Device. Advanced Materials, 30(38), 1802951.
3. Park, M., Kim, H. S., Yoon, H., Kim, J., Lee, S., Yoo, S., & Jeon, S. (2020). Controllable Singlet–Triplet Energy Splitting of Graphene Quantum Dots through Oxidation: From Phosphorescence to TADF. Advanced Materials, 32(31), 2000936. 4. D.L. Eaten, Porous Glass Support Material, US Patent no. 904, 422 (1975).

Graphene Nanoribbon Grid for Conducting Films with 1D Characteristics

Shinyoung Choi[1], Namjo Kim[1], Seong-Jun Yang[1], Jun-Ho Park[1], Nguyen Ngan Nguyen[1], Kwanghee Park[2], Sunmin Ryu[2], Kilwon Cho[1] and Cheol-Joo Kim[1]

[1]Department of Chemical Engineering, Pohang University of Science and Technology, Pohang, Gyeongbuk 37673, South Korea

Tel.:82-54-279-2335, E-mail: kimcj@postech.ac.kr

[21]Department of Chemistry, Pohang University of Science and Technology, Pohang, Gyeongbuk 37673, South Korea

Quasi-one-dimensional (1D) graphene nanoribbons (GrNRs) have finite band gaps and active edge states, and therefore can be useful for advanced optoelectric and electronic devices. However, the application of GrNR to an optpelectronic device has been a difficult task, requiring the manufacture of a GrNR film with high electrical conductivity over a large area. Here, we present the formation of a GrNR girds via seeded chemical vapor deposition (CVD) on Ge(100) substrates. The nucleation seeds, provided by unzipped C_{60}, initiated anisotropic growth of the GrNRs with uniform sub-10 nm widths toward two orthogonal directions, templated by the single crystalline substrate, and thereby formed grids that had seamless lateral stitching over centimeter scales. The spatially-uniform grid can be transferred and patterned for batch-fabrication of devices. The GrNR grids showed percolative conductivity with high electrical sheet conductivity of ~2 μS · □ and intrinsic field-effect mobility of ~50 $cm^2/(V\cdot s)$ in the percolation pathway, which confirm excellent lateral stitching between domains. From trans-conductance measurements, the intrinsic gap of GrNR with sub-10 nm width was estimated as ~80 meV, similar to theoretical expectation. Our method presents a scalable way to fabricate atomically-thin elements with 1D characteristics, for integration with various nano-devices.

Desolvation-Triggered Versatile Transfer-Printing of Pure BN Films with Thermal-Optical Dual Functionality

Yujin Han, Hyeuk Jin Han, Cheolkyu Kim, Moohyun Kim, Hunhee Lim, Hanhwi Jang, Taek-Soo Kim, Eugene N. Cho, and Yeon Sik Jung*

Department of Materials Science and Engineering, Korea Advanced Institute of Science and Technology (KAIST), 291 Daehak-ro, Yuseong-gu, Daejeon 34141, Republic of Korea

Tel.:82-42-350-3368, E-mail: huj0730@kaist.ac.kr

In this study, we developed a versatile method to transfer-print high-quality BN films composed of densely-stacked BN nanosheets based on a desolvation-induced adhesion switching (DIAS) mechanism. We show that edge functionalization of BN sheets and rational selection of membrane surface energy combined with systematic control of solvation and desolvation status enable extensive tunability of interfacial interactions at BN-BN, BN-membrane, and BN-substrate boundaries. Therefore, without incorporating any additives in the BN film and surface treatment on target substrates, DIAS achieves a near 100% transfer yield of pure BN films on diverse substrates, including substrates containing significant surface irregularities. The printed BNs demonstrate high optical transparency (> 90%) and excellent thermal conductivity (167> Wm-1K-1) for few-μm-thick films due to their dense and well-ordered microstructures. In addition to outstanding heat dissipation capability substantial optical enhancement effects were confirmed for light-emitting, photoluminescent, and photovoltaic devices, demonstrating their remarkable promise for next-generation optoelectronic device platforms.

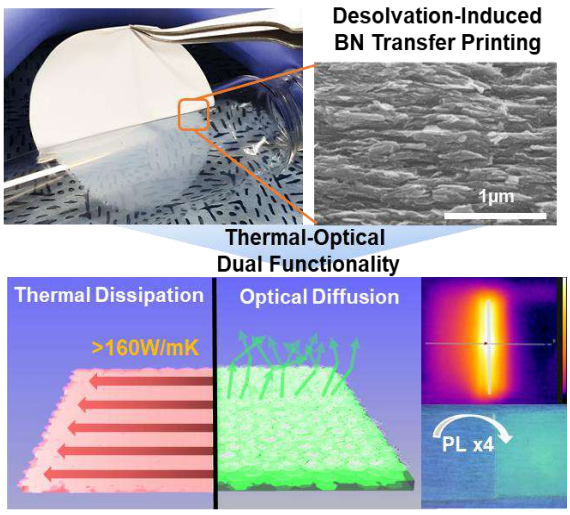

Fig.1 Overall Process of Boron Nitride Printing

Acknowledgment

This research was supported by Korea Evaluation Institute of Industrial Technology (KEIT) of the Ministry of Trade, Industry and Energy

References

[1] A. J. Cho, J. Y. Kwon, *ACS Appl. Mater. Interfaces* **2019**, *11*, 39765.

[2] G. Kim, M. Kim, C. Hyun, S. Hong, K. Y. Ma, H. S. Shin, H. Lim, *ACS Nano* **2016**, *10*, 11156.

[3] C. R. Dean, A. F. Young, I. Meric, C. Lee, L. Wang, S. Sorgenfrei, K. Watanabe, T. Taniguchi, P. Kim, K. L. Shepard, J. Hone, *Nat. Nanotechnol.* **2010**, *5*, 722.

[4] K. K. Kim, A. Hsu, X. Jia, S. M. Kim, Y. Shi, M. Dresselhaus, T. Palacios, J. Kong, *ACS Nano* **2012**, *6*, 8583.

[5] J. D. Caldwell, A. V. Kretinin, Y. Chen, V. Giannini, M. M. Fogler, Y. Francescato, C. T. Ellis, J. G. Tischler, C. R. Woods, A. J. Giles, M. Hong, K. Watanabe, T. Taniguchi, S. A. Maier, K. S. Novoselov, *Nat. Commun.* **2014**, *5*, 5221.

[6] A. J. Giles, S. Dai, O. J. Glembocki, A. V. Kretinin, Z. Sun, C. T. Ellis, J. G. Tischler, T. Taniguchi, K. Watanabe, M. M. Fogler, K. S. Novoselov, D. N. Basov, J. D. Caldwell, *Nano Lett.* **2016**, *16*, 3858.

[7] P. Li, M. Lewin, A. V. Kretinin, J. D. Caldwell, K. S. Novoselov, T. Taniguchi, K. Watanabe, F. Gaussmann, T. Taubner, *Nat. Commun.* **2015**, *6*, 7507.

[8] H. Y. Kim, D.-E. Yoon, J. Jang, D. Lee, G.-M. Choi, J. H. Chang, J. Y. Lee, D. C. Lee, B.-S. Bae, *J. Am. Chem. Soc* **2016**, *138*, 16478.

[9] K. Kwak, K. Cho, S. Kim, *Opt. Express* **2013**, *21*, 29558.
[10] H. Moon, C. Lee, W. Lee, J. Kim, H. Chae, *Adv. Mater.* **2019**, *31*, 1804294.
[11] C. Yuan, J. Li, L. Lindsay, D. Cherns, J. W. Pomeroy, S. Liu, J. H. Edgar, M. Kuball, *Commun. Phys.* **2019**, *2*, 8849.
[12] Q. Cai, D. Scullion, W. Gan, A. Falin, S. Zhang, K. Watanabe, T. Taniguchi, Y. Chen, E. J. G. Santos, L. H. Li, *Sci. Adv.* **2019**, *5*, eaav0129.

Rapid Photochemical Activation for High-Quality Sol-Gel Metal Oxide Dielectrics

***Sungjun Park*[1]**
[1]Dept. of Electrical and Computer Engineering, Ajou University, Suwon 16499, Republic of Korea
Tel.:82-31-219-2364, E-mail: sj0223park@ajou.ac.k

We report the rapid formation of high-quality sol-gel oxide dielectrics via deep-ultraviolet (DUV) photoactivation. The in-depth optical and physicochemical analysis with dielectric films prepared at various concentrations suggests the processable condition of DUV photoactivation, accelerating the efficient formation of highly dense aluminum oxide and aluminum silicate bilayer. As a result, the excellent dielectric properties in terms of low leakage current (～10^{-8} A/cm^2 at 1.0 MV/cm) and high areal capacitance (～0.4 μF/cm^2 at 100 kHz) with narrow statistical distributions of dielectrics processed at 150 ℃ within 5 min were achieved. To demonstrate their applications into thin-film-transistors, successive DUV photoactivation was additionally conducted for sol-gel indium–gallium–zinc oxide semiconductor on bilayer aluminum oxide dielectrics, resulting in prominent electrical characteristics with low operational voltage below 0.5 V. We expect that the photochemically activated sol-gel oxides are beneficial for various types of large-area silicon-compatible electronic devices, such as photoelectrochemical cell, memory, neuromorphic, and phase-transition devices.

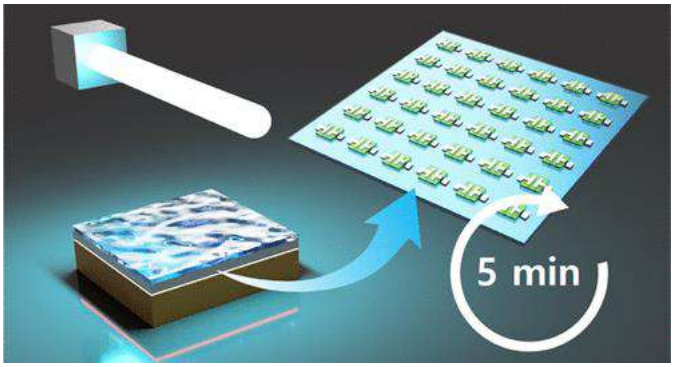

Fig. 1. Schematic image of rapid photochemical activation of sol-gel metal oxide film

Acknowledgment

This research was supported by the new faculty research fund of Ajou University and a research grant (NRF-2020R1F1A1073564) from the National Research Foundation (NRF) funded by the Ministry of Science and ICT, Korea and the Nano·Material Technology Development Program (2009-0082580) through the National Research Foundation of Korea (NRF) funded by the Ministry of Science, ICT and Future Planning.

References

1. Kim, Yong-Hoon, et al. "Flexible metal-oxide devices made by room-temperature photochemical activation of sol–gel films." Nature 489.7414 (2012): 128-132.
2. Park, Sungjun, et al. "In-Depth Studies on Rapid Photochemical Activation of Various Sol–Gel Metal Oxide Films for Flexible Transparent Electronics." Advanced Functional Materials 25.19 (2015): 2807-2815.
3. Lee, Won-June, et al. "Rapid and Reliable Formation of Highly Densified Bilayer Oxide Dielectrics on Silicon Substrates via DUV Photoactivation for Low-Voltage Solution-Processed Oxide Thin-Film Transistors." ACS Applied Materials & Interfaces 13.2 (2021): 2820-2828.

Enhanced Sensitivity Hybrid Channel Organic Phototransistor with Light-induced Contact Modulation for Under-display Applications

Dongho Choi[1], Haechang Lee[1], Jaehyeok Park[1], Hanul Moon[2,3] and Seunghyup Yoo[1]
[1]School of Electrical Engineering, KAIST, Daejeon, 34141, Korea
Tel.:82-42-350-3483, E-mail: syoo.ee@kaist.edu
[2]Department of Semiconductor, Dong-A University, Busan, 49315, Korea
[3]Department of Chemical Engineering (BK21 FOUR Graduate Program), Dong-A University, Busan, 49315, Korea

The organic phototransistor (OPT) is a device with multi-functions of light-sensing, signal amplification, and switching for addressing when it is used for matrix arrays. When light reaches the organic semiconducting layer and is within the absorption spectrum of the semiconductor, electron/hole pairs are generated and minority carriers are accumulated/trapped near the source electrode, and subsequently the injection barrier for majority carrier from the source to channel can be reduced. This light-induced Schottky contact modulation enables much more amount of carrier injection comparing to photo-generated carriers, and thus the photo-sensing signal can be amplified for sensitive detection of low-intensity light. This can be highly beneficial for applications like under-display imaging sensors where the amount of light reaching the sensors is limited.

In this study, we report on the device architecture of organic phototransistors fabricated with bottom-gate top-contact geometry. We study the underlying mechanism by comparing the change of contact and channel resistance with light irradiation, elucidating the nature of the photo-induced contact modulation. Based on the mechanism, we prove that the photo-sensing capability can be improved not only by enhancing light absorption in the channel layer but also by increasing the carrier mobility through the channel. We also suggest a systematic strategy to secure both the high light absorption and carrier mobility by employing multi-channel layer structures. Furthermore, the optical structure of the phototransistor is also optimized to maximize the photon absorption. The proposed devices showed four times enhanced responsivity when compared to that of an OPT with a single channel layer structure, illustrating the promising potential of the proposed approach.

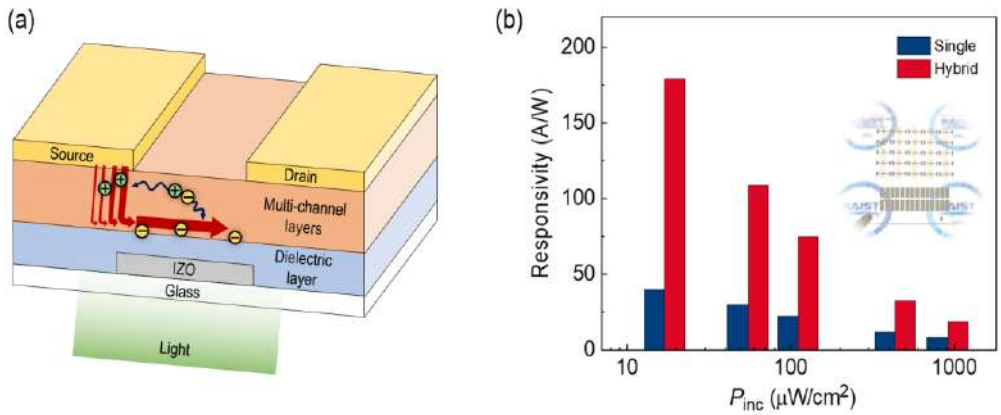

Fig. 1. (a) Schematic structure of the proposed multi-channel organic phototransistor and (b) Responsivity-incident light intensities graph with fabricated devices.

Acknowledgment

This work was supported by the Industry technology R&D program(20006476) funded By the Ministry of Trade, Industry & Energy(MOTIE, Korea)

References

1. Noh, Yong-Young, et al., *J. Appl. Phys.*, 100(9), 094501 (2006).
2. Richards, T. J. & Sirringhaus, H., *J. Appl. Phys.* 102(9), 094510 (2007).
3. Gao, Yuanhong, et al., *Adv. Mater.*, 31(16), 1900763 (2019).

Improved Charge Transport Behaviour and Trap-State Distribution in Donor-Acceptor Type Semiconducting Copolymer with Fluoropolymer Dielectric Layer

Doyeon Kim[1] and Jiyoul Lee[1,2]
[1] Dept of Smart Green Technology Engineering, Pukyong National University, Busan, 48547, Korea.
E-mail: jiyoul_lee@pknu.ac.kr (J. Lee)
[2]Dept of Nanotechnology Engineering, Pukyong National University, Busan, 48547, Korea.

In this presentation, we will report a p-doping method with fluoropolymer (Cytop) for Donor(D)-Acceptor(A) type conjugated semiconducting copolymer-based field-effect transistors (FETs). The polymeric FET (with staggered structure in figure 1a) initially shows ambipolar behaviour with a non-polar polymer dielectric layer (PMMA) because of well-balanced electron-accepting and -donating properties in the Cyclopentadithiophene(CDT)-based conjugated polymer backbone system.[1] However, as shown in figure 1b, the FET device with an amorphous fluoropolymer dielectric layer (Cytop) exhibits that their ambipolar behaviour remarkably changes to a high performance p-type FET[2]; the hole mobility is enhanced by a factor of ~3 and threshold voltage significantly shifts from -29 V to -12 V. The estimated density of state of our polymeric FETs becomes narrower and shallower,[3] implying the deep-trap states are filled with the additionally doped charges from the surface polarization induced by the fluorinated dielectrics (Cytop) at the interface between semiconductor and dielectrics.

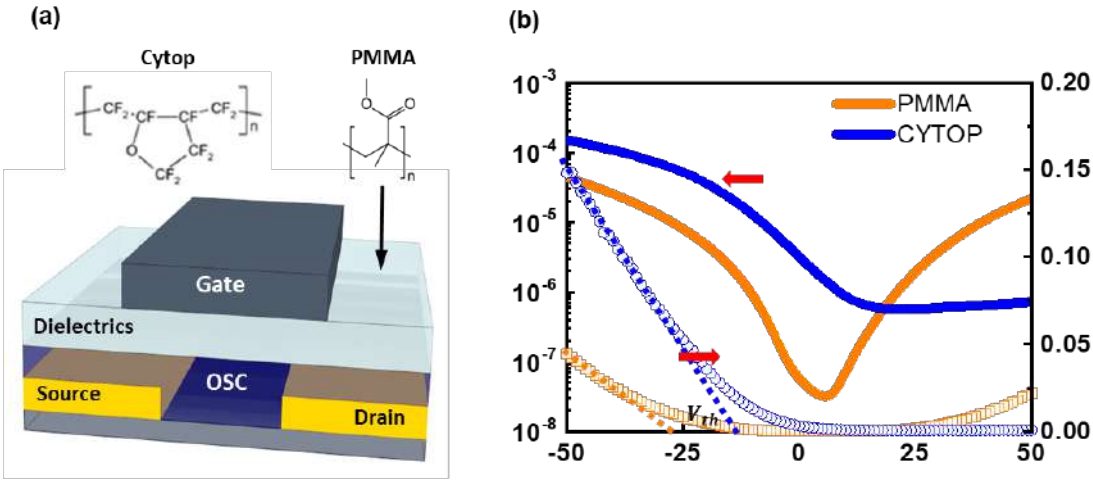

Figure 1. (a) Device configuration of the polymeric field-effect transistors (Staggered structure) used in this study with PMMA and Cytop dielectric. (b) Transfer curves of the CDT based polymeric FETs with PMMA and Cytop dielectric film in the linear regime (drain voltage, V_D = -20 V).

Acknowledgment

This work was supported by the National Research Foundation of Korea (NRF) grant funded by the Korea government. (2021R1A2C1007212).

References

1. W.-T. Park, G. Kim, C. Yang, C. Liu and Y.-Y. Noh, Advanced Functional Materials 26 (26), 4695-4703 (2016).
2. E.-S. Shin, W.-T. Park, Y.-W. Kwon, Y. Xu and Y.-Y. Noh, ACS Applied Materials & Interfaces 11 (13), 12709-12716 (2019).
3. J. Lee, J. W. Chung, G. B. Yoon, M. H. Lee, D. H. Kim, J. Park, J.-K. Lee and M. S. Kang, ACS Applied Materials & Interfaces 8 (44), 30344-30350 (2016).

Flexible and Printed Active-Matrix TFT Array for Sensor Applications

Sanghoon Baek[1], Sungju Kim[2] and Sungjune Jung[1,2,3]
[1]Dept. of Convergence IT Engineering, POSTECH, Pohang, Korea
[2]Dept. of Mechanical Engineering, POSTECH, Pohang, Korea
[3]Dept. of Materials Science and Engineering, POSTECH, Pohang, Korea

Tel.:82-54-279-8868, E-mail: sjjung@postech.ac.kr

Here, we report the design and fabrication of an organic printed active-matrix TFT array on an ultrathin substrate. We fabricated a 10 × 10 array of organic transistors by inkjet-printing Ag source and drain electrodes and dispensing p-type semiconductor Poly(N-alkyl diketopyrrolo-pyrrole dithienylthieno-[3,2-b]thiophene) in a Teflon bank. Interconnections were made by inkjet-printing of Ag ink through via-holes formed by a nanosecond pulsed laser. The Parylene C was used as a substrate and as a gate dielectric. We carefully established the design rules for inkjet printing to determine drop spacing, line width, and channel geometry. This approach enabled us to achieve TFT devices with 100% yield and high uniformity. Finally, we demonstrated that the flexible and printed active-matrix array could be used as a wearable multisensor platform.

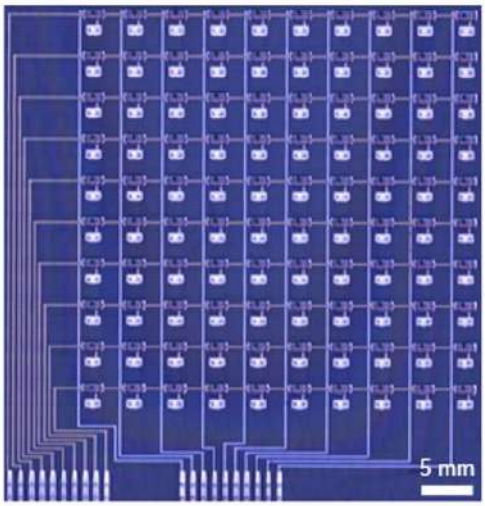

Fig. 1. An image of an organic printed TFT array on flexible substrate

References

1. Kwon, et.al., Nature Commun. 10, 54 (2019)
2. Baek, et.al., ACS Appl. Mater. Interfaces. 11(34), 31111 (2019)

A Novel Fabrication Method of a High Sensitivity and Low Leakage Current Phototransistors Based on a Homojunction Porous IGZO Thin-Film Transistors

*I Sak Lee[1], Sujin Jung[1], Jong Bin An[1], and Hyun Jae Kim[*1]*
[1]School of Electrical and Electronic Engineering, Yonsei University, 50 Yonsei-ro, Seodaemun-gu, Seoul 03722, Republic of Korea
*Tel.:82-2-2123-5865, *E-mail: hjk3@yonsei.ac.kr*

As the field of internet of things (IoT) grows, various sensors become increasingly important due to their applications in consumer electronics. As such, there has been a growing interest in improving the electrical and optical characteristics of photonic devices. In recent times, oxide-based thin film transistors (oxide TFTs) have exhibited optimal electrical and optical characteristics such as high uniformity over large areas, low off current, and high transparency in the visible light region. [1] Therefore, these characteristics imply that oxide TFTs are suitable for superior photonic devices. [2] However, oxide TFTs are not able to absorb visible light due to wide bandgap (> 3 eV) of the channel layer, hence their applicability has been limited to ultraviolet and blue light absorption applications. As such, many researches have been conducted to enable oxide TFTs to absorb visible light using absorption layers such as organic polymers, carbon composites, metal nanoparticles, and quantum dots. [3] Although the use of these materials allowed oxide TFT to absorb visible light, these materials can be costly and complex to fabricate in thin film structures. In this paper, we represent a novel homojunction-porous IGZO (HPI) phototransistor which is mechanochemically treated to enlarge photosensitivity and photoresponsivity under visible light (as shown in **Fig 1**). Moreover, we evaluated reliable sensing ability and endurance using the sputtering and solution based IGZO (SSI) and HPI phototransistors. Compared with conventional IGZO phototransistors, our HPI phototransistor displayed outstanding optoelectronic characteristics and responsivity: we measured a threshold voltage (V_{th}) shift from 3.64 V to –6.27 V and an on/off current ratio shift from 4.21×10^{10} to 4.92×10^{2} under illumination with 532 nm green light of 10 mW/mm^2 intensity, and calculated a photoresponsivity of 1.63×10^{10}. Based on these results, we hastened the realization of the photo-sensing system which can be adopted in conventional applications furthering its sensitivity and stability.

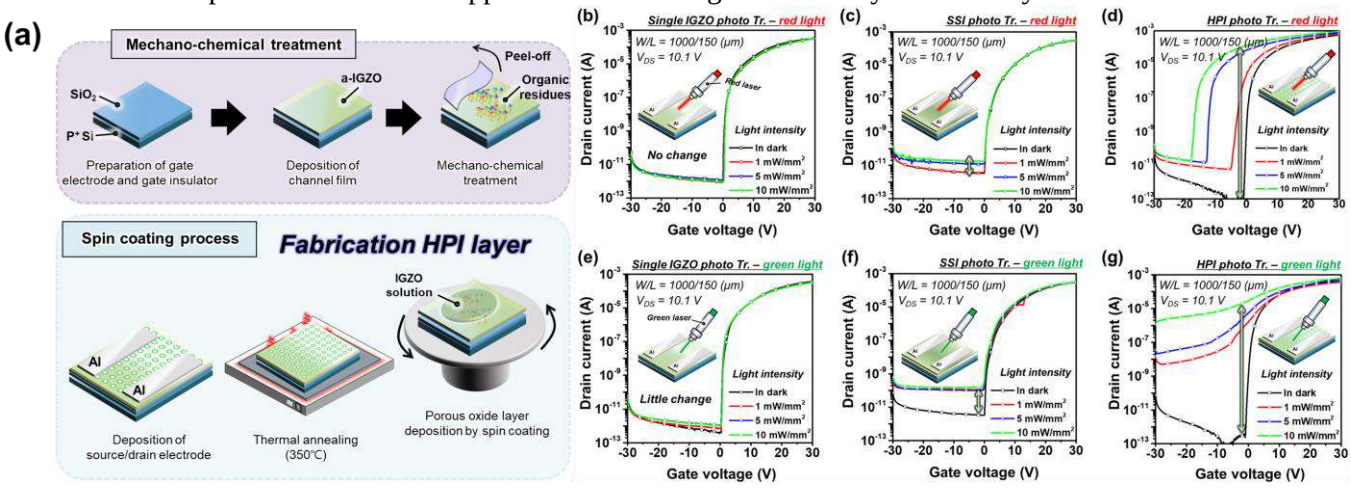

Fig. 1. (a) Fabrication process of HPI phototransistors. Transfer characteristics of IGZO based phototransistors under red light illumination at different intensities; (b) single IGZO, (c) SSI, and (d) HPI phototransistors. Transfer characteristics of IGZO based phototransistors under green light illumination at different intensities; (e) single IGZO, (f) SSI, and (g) HPI phototransistors

Acknowledgment

This work was supported by the National Research Foundation of Korea (NRF) grant funded by the Korea government (MSIT) (No. NRF-2018M3A7B4071521).

References

[1] K. Nomura, H. Ohta, A. Takagi, T. Kamiya, M. Hirano, and H. Hosono, *Nature*, 432, 488 (2004)
[2] J. -S. Park, J. K. Jeong, H. -J. Chung, Y. -G. Mo, and H. D. Kim, *Applied Physics Letters*, 92, 072104 (2008)
[3] X. Yu, T. J. Marks, and A. Facchetti, *Nature materials*,15, 383 (2016)

Organic Permeable Base Light-Emitting Transistors - An Innovative Device for Active-Matrix Displays

Hans Kleemann, Zhongbin Wu, Erjuan Guo, and Karl Leo
[1]Dresden Center for Applied Photophysics and Photonic Materials, TU Dresden, Germany
Tel.:4935146343379, E-mail: hans.kleemann1@tu-dresden.de
(2 line spacing)

Organic light-emitting transistors, three-terminal devices combining a thin-film transistor with a light-emitting diode, have generated increasing interest in organic electronics. However, increasing their efficiency while keeping the operating voltage low still remains a key challenge.
Here, we demonstrate organic permeable base light-emitting transistors; these three-terminal vertical optoelectronic devices operate at driving voltages below 5.0 V; emit in the red, green and blue ranges; and reach, respectively, peak external quantum efficiencies of 19.6%, 24.6% and 11.8%, current efficiencies of 20.6 cd A^{-1}, 90.1 cd A^{-1} and 27.1 cd A^{-1} and maximum luminance values of 9,833 cd m^{-2}, 12,513 cd m^{-2} and 4,753 cd m^{-2}. Our simulations demonstrate that the nano-pore permeable base electrode located at the centre of the device, which forms a distinctive optical microcavity and regulates charge carrier injection and transport, is the key to the good performance obtained. We highlight the benefits of this vertical light-emitting transistor architecture over conventional OLED display driving and discuss strategies how such a vertical light-emitting transistor could be integrated into AMOLED displays. Furthermore, we discuss the requirements for pixel driving and limitations of the technology.

Insulator-to-Semiconductor Conversion of Solution-processed Amorphous Gallium Oxide Thin Film Transistor through Hydrogen Annealing

Diki Purnawati[1], Juan Paolo Bermundo[1], and Yukiharu Uraoka[1]*
[1]Division of Materials Science, Graduate School of Science and Technology,
Nara Institute of Science and Technology, 8916-5 Takayama, Ikoma, Nara, 630-0192, Japan
*Tel.:+81-743-72-6064, *E-mail: b-soria@ms.naist.jp*

Amorphous oxide semiconductors (AOSs) have become promising channel materials for thin-film transistor (TFT) because of valuable features such as high mobility, excellent uniformity, low threshold voltage, low subthreshold swing, low-temperature processability and compatible with solution process [1]. In order to widen its application, solution process is proposed to substitute vacuum process due to some advantages such as large-area fabrication, equipment simplicity, atmospheric processing, and low cost [2]. However, AOS TFTs, especially when fabricated through solution-process, exhibit instability which is a major drawback to its device performance and hinder its wide adoption. To overcome this issue, ultrawide bandgap amorphous oxide semiconductor materials, such as amorphous Gallium Oxide (a-GaO_x), have been proposed since a-GaO_x evidently improves device stability [3]. Nevertheless, GaO_x-based TFT shows poor mobility due to its low carrier concentration. For instance, a-Ga_2O_x is an electrical insulator because the combination of an ultra-wide bandgap and an amorphous structure has serious difficulties in attaining electronic conduction. Hence, semiconducting behavior has been difficult to attain. With relatively few-research on solution-processed ultra-wide bandgap amorphous GaO_x TFTs and with most studies employing GaO_x with crystalline structure processed at high temperatures, this work on solution processed amorphous GaOx TFT becomes promising and interesting to report.

Hydrogen annealing has been successfully shown to enhance the electrical properties of amorphous oxide semiconductor [4]. This promising method can also be employed on ultrawide bandgap oxide materials. In this work, solution-processed a-GaO_x (bandgap ~4.8 eV) was converted to their semiconducting state through hydrogenation as the comparison of as-deposited and H_2 annealed TFTs shown in Figure 1. The H, which is incorporated into the a-GaO_x channel through H_2 gas continuously flowed during hydrogenation treatment, act as donor which likely increased carrier concentration of the a-GaO_x channel. This carrier concentration increase correlated well to the Fermi level energy (E_f) of each condition estimated through XPS and UV-Vis Spectroscopy. Figure 2 shows that the E_f of hydrogenated sample shifted closer to the CBM (1.18 eV) implying higher carrier (electron) concentration. Thus, insulator-to-semiconductor conversion of the a-GaO_x channel has been successfully shown through the observed switching obtained after hydrogenation. Moreover, we expect that this remarkable effect will remain robust [4].

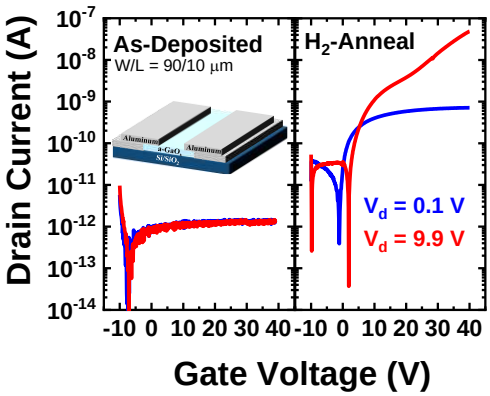

Fig. 1. Transfer curves of a-GaO_x TFT

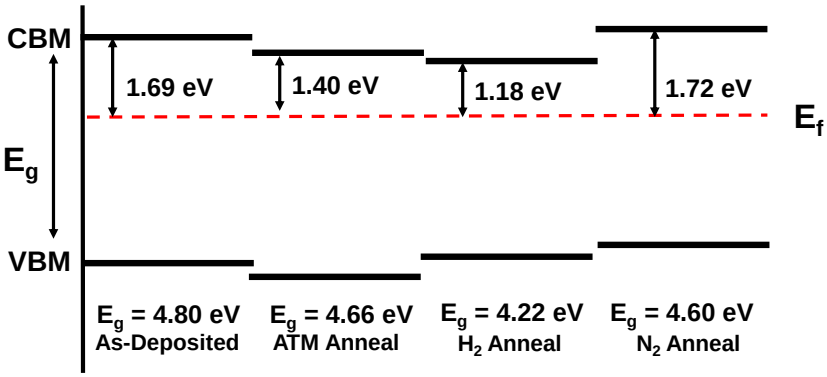

Fig. 2. Band diagram of a-GaO_x annealed at various atmosphere

References

1. T. Kamiya, et al., Sci. Technol. Adv. Mater. 11, 044305 (2010)
2. W. Xu, et al., ACS Appl. Mater. Interfaces 10, 25878 (2018)
3. J. Kim, et al., APL Mater. 7, 022501 (2019)
4. S. Oh, et al., IEEE Trans. Elec. Dev. 60 (8), 2537-2541 (2013)

Field-Effect Transistors Based on Solution Processed sp-Hybridized Organic Semiconducting Molecules

Steafano Pecorario,[1,2], Carlo Casari[2], and Mario Caironi[1]
[1]Center for Nano Science and Technology@PoliMi, Istituto Italiano di Tecnologia, Milan 20133, Italy
E-mail: mario.caironi@iit.it
[2]Department of Energy, Politecnico di Milano, 20133 Milano, Italy

Sp-hybridized carbon atomic wires are intensively investigated as they offer very appealing one-dimensional electronic features [1]. To date, most of the experimental efforts aimed at assessing and exploiting their electronic properties in solid-state devices are focused on molecular junctions or monolayers. Sp-carbon wires have instead not been investigated towards solution-processed thin-film electronics. Here, we discuss the use of cumulenic sp-carbon atomic wires in solution-processable field-effect transistors (FETs). First, we report on the possibility to observe clear field-effect behavior in simple devices, based on short cumulenic molecules casted from solution, namely tetraphenylbutatriene [3]Ph. The latter is the first example of a FET based on cumulenic sp-carbon atomic wires [2]. On the basis of this evidence, we report our recent results in the direction of understanding and optimizing charge-transport properties in thin films based on such molecules. In particular, we show how it is possible to achieve field-effect mobilities up to 0.1 cm^2/Vs, mainly through the control of the deposition process. Strictly related, we show how the micro-structure of the thin films is directly connected to the electronic properties, towards an establishment of structure-property relationship. Finally, evidence of ambient stability of cumulenic FETs in dark conditions directly addresses one of most obvious concerns related to the use of sp-carbon atomic wires in electronics, and holds great promises for the concrete development of a new paradigm for organic electronics.

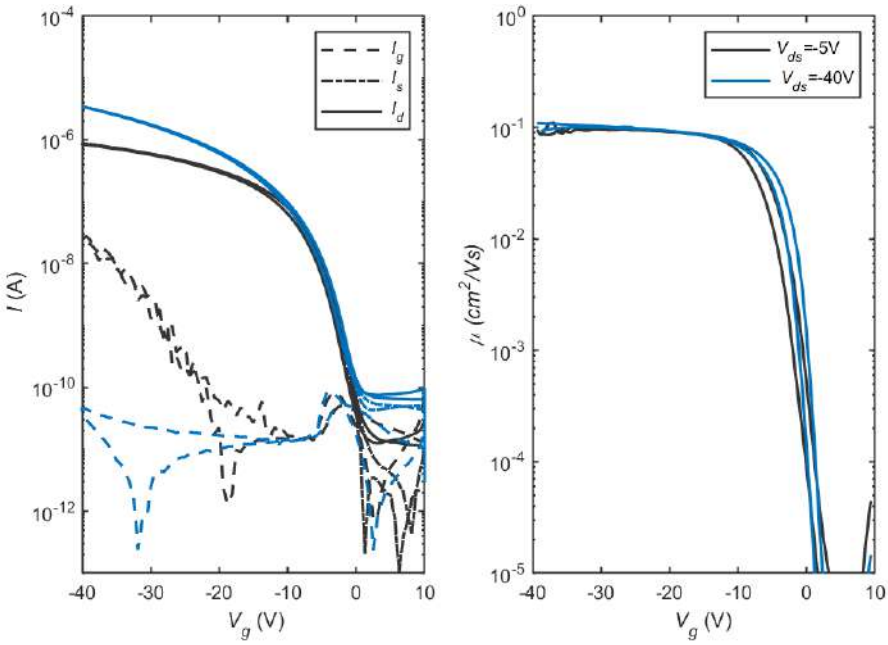

Fig. 1. Representative transfer characteristic curves of a FET based on [3]Ph, with a channel length of 20 μm and a channel width of 200 μm (I_d: drain current; I_s: source current; I_g: gate current; V_{ds}: drain-source voltage).

References

1. C. S. Casari, M. Tommasini, R. R. Tykwinski and A. Milani, *Nanoscale* 8 (8), 4414−4435, (2016).
2. A. D. Scaccabarozzi, A. Milani, S. Peggiani, S. Pecorario, B. Sun, R. R. Tykwinski, M. Caironi, and C. S. Casari, *J. Phys. Chem. Lett.* 11, 1970−1974, (2020).

High performance organic field effect transistors developed by solution processing

Paddy K. L. Chan
Mechanical Engineering, The University of Hong Kong, Hong Kong

The development of organic filed effect transistors has come to a critical moment. A number of reported devices have demonstrated carrier mobility higher than ten which, in principle, has outperformed the amorphous silicon counter parts, such carrier mobility values are still incompatible with the applications in the advanced processors or chips. However, other application directions such as wearable sensors, health monitoring system or memory devices have been proposed based on the OFETs, which are believed to be the most suitable application directions for these low cost devices. In the current talk, I will present some of the recent achievement in both solution processing and thermal evaporated devices and their novel applications in varies engineering aspects.

Deep-Subthreshold Ambipolar TFTs for Self-Powered Electronics

***Vincenzo Pecunia*[1]**
[1] Institute of Functional Nano & Soft Materials, Soochow University, Suzhou, Jiangsu 215123, China
Tel.: 86-512-65882657, E-mail: vp293@suda.edu.cn

Thin-film transistors (TFTs) based on printed semiconductors have formidable potential for the realization of low-cost smart sensor nodes of the Internet of Things (IoT) ecosystem.[1,2] Crucially, ultra-low-power operation is key to fulfilling this potential.[3] Indeed, ultralow-power electronics would enable IoT nodes to function using ambient energy, thereby overcoming the sustainability and feasibility limitations of battery-powered operation.[3]

Despite the recent progress, an outstanding challenge in printed electronics has been to develop a robust and simple approach to ultra-low-voltage (< 0.5 V) and ultra-low-power (< 1 nW per gate) circuit operation, as required for its use with compact ambient energy harvesters. On the one hand, unipolar solutions are problematic in terms of noise immunity and robust large-scale circuit integration.[4] On the other hand, while ensuring low static power dissipation, complementary solutions developed to date require manifold materials and process steps,[5] which counters the overarching aim of realizing easy-to-fabricate and low-cost TFT electronics.

Herein, we present our breakthrough in ultra-low-power printed electronics, demonstrating easy-to-fabricate TFT circuits capable of operating with the lowest power consumption and supply voltage to date.[6] Our platform relies on the newly-established paradigm of *deep-subthreshold, balanced, ambipolar* TFT electronics, which involves TFTs with balanced ambipolar characteristics in the deep-subthreshold region. We implemented this paradigm using printed semiconducting carbon nanotubes and hybrid nanodielectrics. We engineered the characteristics of the resultant TFTs by fine-tuning their flatband voltage in the 0.1 V range through the application of self-assembled monolayers at the active interface, achieving state-of-the-art mobilities and symmetric subthreshold slopes.

To demonstrate the viability of the deep-subthreshold ambipolar route to printed TFT electronics, we then discuss the integration of *deep-subthreshold, balanced, ambipolar* TFTs into digital logic gates in CMOS fashion. These circuits exhibited complementary-like characteristics with large gains and ample noise margins while operating at record-low levels of supply voltage—down to 0.2 V—and power consumption—down to the femtowatt range per micrometer of channel width.[6] Crucially, these circuits were realized with only one semiconductor and one single source-drain metal, thereby illustrating the strength of the *deep-subthreshold, balanced, ambipolar* paradigm to deliver electronics that is also easy to fabricate.

Building on the aforementioned ultra-low-power capability, we finally provide the first-ever demonstration of printed TFT electronics powered by indoor light. Specifically, by connecting our deep-subthreshold circuits to millimeter-scale, solution-processed, lead-free-perovskite photovoltaic cells, we showed that our digital gates can function using the energy harvested from standard indoor light.[7] By allowing the facile realization of complementary-like and ultra-low-power circuits that can function using ambient energy, our deep-subthreshold ambipolar platform thus paves the way for batteryless smart devices for a sustainable IoT.

References

1. V. Pecunia, M. Fattori, S. Abdinia, H. Sirringhaus, and E. Cantatore, Organic and Amorphous-Metal-Oxide Flexible Analogue Electronics, Cambridge University Press, Cambridge, UK (2018).
2. M. Caironi and Y.-Y. Noh (eds.), Large Area and Flexible Electronics, Wiley-VCH Verlag GmbH & Co. KGaA, Weinheim, Germany (2015).
3. A. Keshavarzi and W. van den Hoek, *IEEE Des. Test*, 36(2), 41 (2019).
4. C. Jiang, H. W. Choi, X. Cheng, H. Ma, D. Hasko, and A. Nathan, *Science*, 363(6428), 719 (2019).
5. H. Zhang, L. Xiang, Y. Yang, M. Xiao, J. Han, L. Ding, Z. Zhang, Y. Hu, and L. M. Peng, *ACS Nano*, 12(3), 2773 (2018).
6. L. Portilla, J. Zhao, Y. Wang, L. Sun, F. Li, M. Robin, M. Wei, Z. Cui, L. G. Occhipinti, T. D. Anthopoulos, and V. Pecunia, *ACS Nano*, 14(10), 14036 (2020).
7. Y. Peng, T. N. Huq, J. Mei, L. Portilla, R. A. Jagt, L. G. Occhipinti, J. L. MacManus-Driscoll, R. L. Z. Hoye, and V. Pecunia, *Adv. Energy Mater.*, 11(1), 2002761 (2021).

Polymer Transistors With Sub-Domain-Size Channels

Huabin Sun[1], Dakuang Zhang[2], and Yong Xu[1]
[1]Nanjing University of Posts and Telecommunications, Nanjing, China
E-mail: hbsun@njupt.edu.cn
[2] Nanjing University, Nanjing, China

An overview extending from the macroscopic electrical characteristics of a solid-state device to the microscopic charge transport in the corresponding polymer film remains unexplored [1]. For example, structural disorder, domain aggregation, and mobility anisotropy would strongly influence charge transport and thus device performance. However, such fundamental studies have been complicated by the complex polymer microstructures in practical devices . A simple system that enables a close look at the intrinsic charge transport inside polymer domains and therefore profound understanding of charge transport in conjugated polymers is strongly desired, and will contribute to further polymer optimization to improve the performance of polymer devices.

In our work[2,3], we fabricated polymer transistors with sub-domain-size channels. Experimental results (Fig.1) and a velocity calculation suggested that the bottleneck of charge transport in electronic devices is domain boundaries. The results highlight the importance of high-efficiency intra-domain charge transport and also the inter-domain limitation.

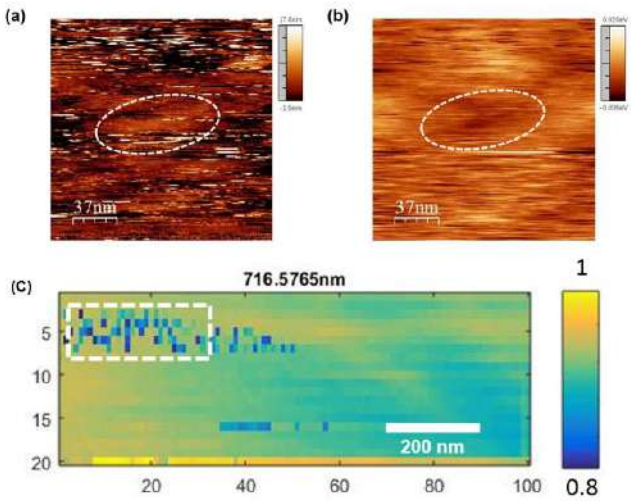

Fig. 1. KPFM of aligned DPPT-TT film (a) height and (b) surface potential, (c) Near-field scanning optical microscopy (NSOM) mapping of aligned DPPT-TT film

Acknowledgment

This work was supported in part by the National Natural Science Foundation of China under Grant 61804078 and Grant 61705197, in part by the Natural Science Foundation of Jiangsu Province under Grant BK20180759 and Grant BK20161008, and in part by the Start-Up Fund from the Nanjing University of Posts and Telecommunications under Grant NY218149 and Grant NY219003.

References

1. M. Li, C. An, T. Marszalek, M. Baumgarten, K. Müllen, and W. Pisula, *Adv. Mater.*, 11(28), 2245, (2016).
2. Zhang, D. et al. *IEEE Electron Device Lett.*, 41, 589–592, (2020).
3. Zhang, D. et al. *Organic Electronics*, 105742, (2020).

n-Type Polymer Semiconductors Based on Bithiophene Imide

Xugang Guo
Department of Materials Science and Engineering, Southern University of Science and Technology of China (SUSTech), Shenzhen, Guangdong, 518055, China
Tel.:86-755-8801-8307, E-mail: guoxg@sustech.edu.cn

Imide-functionalized π-conjugated polymers are the most promising n-type semiconductors in the field of organic electronics. Semiconducting polymers derived from naphthalene diimide (NDI) and perylene diimide (PDI) are the "benchmark materials" in organic thin-film transistors (OTFTs). We report here a series of novel imide-functionalized ladder-type bithiophene imide derivatives (BTIn, n = 1-5; Fig. 1) with up to 5 imide groups and 15 rings in a row. The homopolymers show tunable frontier molecular orbital (FMO) energy levels and film morphologies and exhibit unipolar n-type transport in OTFTs with the highest electron mobilities (μ_es) > 3 cm^2 V^{-1} s^{-1}. Novel imide-functionalized thiazoles are also synthesized, enabling the access of acceptor-acceptor (or all-acceptor) homopolymers. Notably, these polymers do not show undesirable kink in transistor curves, thus avoiding mobility overestimation. The deep-lying polymer FMO energy levels lead to suppressed I_{off}s of 10^{-10}-10^{-11} A, thus remarkable I_{on}/I_{off}s of 10^7-10^8 achieved while maintaining a large μ_e of 1.6 cm^2 V^{-1} s^{-1}. Besides all-acceptor homopolymers, these novel bithiophene imide derivatives were incorporated to donor-acceptor and donor-acceptor-acceptor copolymers, which also showed unipolar n-type transport with substantial μ_es > 1 cm^2 V^{-1} s^{-1}. We further developed a series of highly electron-deficient BTI derivatives (Fig. 1) which combine both strong electron-withdrawing imide functionality and cyano group, the resulting polymers showed very low-lying lowest unoccupied molecular orbitals (LUMO) levels (~ -4.1 eV) and stable performance in OTFT devices.

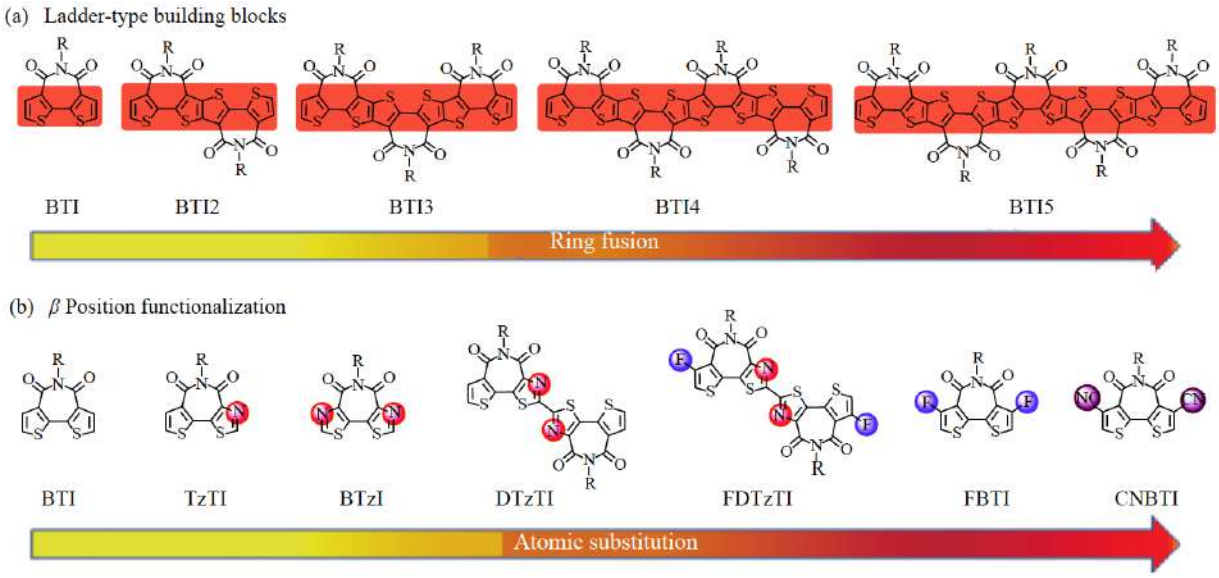

Fig. 1. Two strategies for developing bithiophene imide (BTI) derivatives for constructing high-performance n-type polymer semiconductors: (1) ring fusion and (b) atomic substitution at *β*-positions.

References

1. Y. Wang, H. Guo, S. Ling, I. Arrechea-Marcos, Y. Wang, J. T. L. Navarrete, R. P. Ortiz, X. Guo, *Angew. Chem. Int. Ed.* 56, 9924-9929 (2017).
2. Y. Shi, H. Guo, M. Qin, J. Zhao, Y. Wang, H. Wang, Y. Wang, A. Facchetti, X. Lu, X. Guo, *Adv. Mater.* 30, 1705745 (2018).
3. Y. Wang, H. Guo, A. Harbuzaru, M. A. Uddin, I, Arrechea-Macos, S. Ling, J. Yu, Y. Tang, H, Sun, J. T. L. Navarrete, R. P. Ortiz, H. Y. Woo, X. Guo, *J. Am. Chem. Soc.* 140, 6095 (2018).
4. H. Sun, X. Guo, A. Facchetti, *Chem* 6, 1310-1326 (2020).
5. K. Feng, H. Guo, J. Wang, Y. Shi, Z. Wu, M. Su, X. Zhang, J. H. Son, H. Y. Woo, X. Guo, *J. Am. Chem. Soc.* 143, 1539-1552 (2021).

Foundry-Compatible High-Resolution Patterning of Organic Thin-film Transistors

Binghao Wang[1,2,3], Wei Huang[2], Sunghoon Lee[3], Tomoyuki, Yokota[3], Takao Someya[3], Tobin J. Marks[2], Antonio Facchetti[2]*

[1]School of Electronic Science and Engineering, Southeast University, 2 Sipailou, Nanjing, Jiangsu 210096, China

Tel.:86-158-6291-7623, E-mail: suzhoudaxue2006@gmail.com

[2]Department of Chemistry and the Materials Research Center, Northwestern University, 2145 Sheridan Road, Evanston, IL 60208, USA

[3]Department of Electrical Engineering and Information Systems, School of Engineering, The University of Tokyo, 7-3-1 Hongo, Bunkyo-ku, Tokyo 113-8656, Japan

Foundry-compatible patterning of functional layers is essential for minimizing electronic device feature sizes, eliminating crosstalk in circuitry and systems integration.[1-3] Polymer semiconductors play important roles in organic electronics, which features low-cost solution processability, materials diversity, good flexibility. However, patterning of polymer semiconductors is very complicated and lack of versatility as the underlying layer would be vulnerable to subsequent solution processing. In this talk, I would present a foundry-compatible patterning process for patterning of known p- and n-type polymer semiconductors, which meet the requirements of high-throughput and high-resolution patternability, broad generality, ambient processability, benign solvent, and, minimal device performance degradation. As shown in Figure 1a, through introduction of UV-crosslinkable additives (like SU8) into the precursors, vertically phase separation is achieved during film coating and crystalline polymer semiconductors nanofibers are formed at the bottom. In this way, the above additives can protect the underlying polymer semiconductors during photolithography, which involves UV irradiation and solvents exposure. Therefore, we achieve high pattern submicrometer resolution within three steps. The patterned semiconducting films can be integrated into thin-film transistors having excellent transport characteristics and low off-currents.

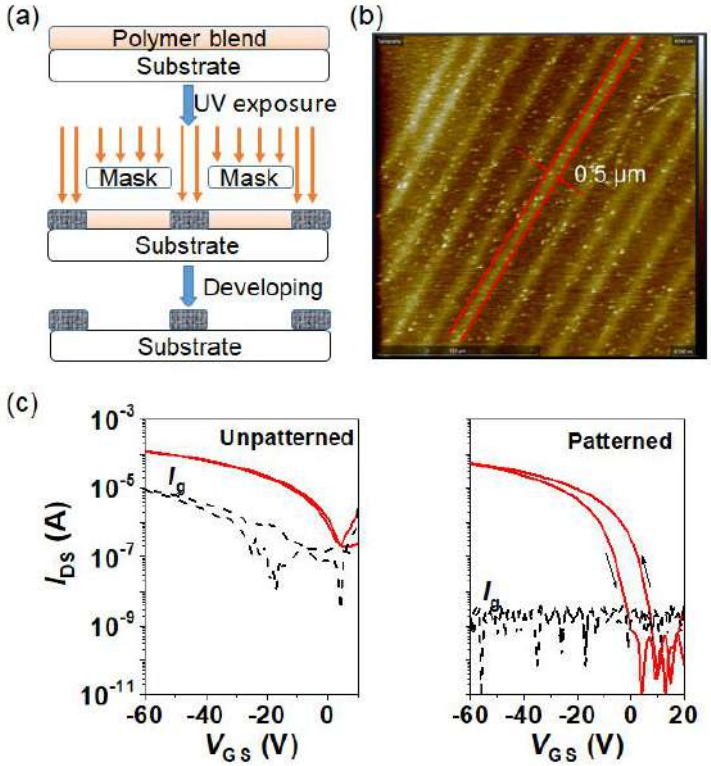

Fig. 1. (a) Schematic of the three-step photolithographic process. (b) An AFM image of patterned lines. (c) Transfer curves for unpatterned and patterned organic thin-film transistors.

Acknowledgment

We thank AFOSR (FA9550-18-1-0331), the Northwestern U. MRSEC (NSF DMR-1720139), the US Department of Commerce, National Institute of Standards and Technology as part of the Center for Hierarchical Materials Design Award 70NANB10H005, the Department of Energy under contract no. DE-AC02-05CH11231, at beamline 8-ID-E of the Advanced Photon Source, a U.S. Department of Energy (DOE) Office of Science User Facility operated for the DOE Office of Science by Argonne National Laboratory under Contract No. DE-AC02-06CH11357, the Japan Science and Technology Agency Exploratory Research for Advanced Technology Someya Bio-Harmonized Electronics Project, Japan Society for the Promotion of Science KAKENHI (Grant 17H06149), and Flexterra Corp. for support of this research.

References

1. Park, H. W. *et al*. *Adv Mater* **31**, e1901400, (2019).
2. Noh, Y. Y., Zhao, N., Caironi, M. & Sirringhaus, H. *Nat Nanotechnol* **2**, 784-789, (2007).
3. Park, S. *et al. Proc Natl Acad Sci U S A* **112**, 5561-5566, (2015).

Solution-Processable Stretchable Polymer Semiconductor for Field-Effect Transistors

Wen-Ya Lee*

Dept. of Chem. Eng. & Biotech., National Taipei University of Technology, Taipei, 10608, Taiwan

E-mail: wenyalee@mail.ntut.edu.tw

Solution-processable stretchable field-effect transistors based on the high-mobility donor-acceptor conjugated copolymers are demonstrated. To improve mechanical compliance and stretchability of the polymer semiconductors. We have employed two approaches. One is to engineer the chemical structures of the polymer backbone and side chain structures. Another one is to incorporate with a insulating polymer for improving elasticity. Additionally, the parameters of solution processing also act as a critical role for the stretchability of the polymer semiconductors. We have found that the the parameter of solution shearing can manipulate the phase separation and charge transport properties of the conjugated polyme blends. Compared with the spin-coated counterpart, the solution-sheared polymer-blend films maintain high mobility (>1 $cm^2 V^{-1} s^{-1}$). The polymer blend films can even achieve a high mobility with great stretchability. Furthermore, the alignment of the solution-sheared blends show the influence of the stretchability of the conjugated polymer chains. The polymer blends exhibit great stretchability and high charge mobilities even under a strain of 100%. Moreover, solution shearing not only improves polymer alignment but also controls surface morphology to enhance stretchability. This presentation reveals the influence of solution shearing in high-mobility stretchable polymer semiconductor devices.

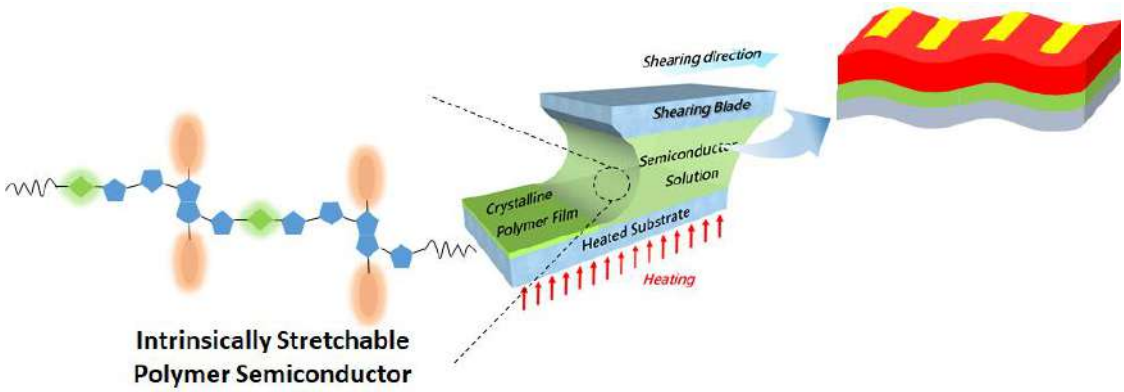

Fig. 1. Schematic strategy of stretchable polymer semiconductor for field-effect transistors.

References

(1) Lu, C.; Lee, W.-Y.; Gu, X.; Xu, J.; Chou, H.-H.; Yan, H.; Chiu, Y.-C.; He, M.; Matthews, J. R.; Niu, W.; Tok, J. B.-H.; Toney, M. F.; Chen, W.-C.; Bao, Z. Effects of Molecular Structure and Packing Order on the Stretchability of Semicrystalline Conjugated Poly(Tetrathienoacene-diketopyrrolopyrrole) Polymers. *Adv. Electron. Mater.* **2017,** *3* (2), 1600311.

(2) Tien, H.-C.; Huang, Y.-W.; Chiu, Y.-C.; Cheng, Y.-H.; Chueh, C.-C.; Lee, W.-Y. Intrinsic Stretchable Polymer Semiconductors: Molecular design, process and Device applications *J. Mater. Chem. C* **2020**, under review.

(3) Yan, Q.-Y.; Shia, Y.-W.; Guo, D.-Y.; Lee, W.-Y. Shear-Enhanced Stretchable Polymer Semiconducting Blends for Polymer-based Field-Effect Transistors. *Macromolecular Research* **2020,** *28* (7), 660-669.

(4) Zhu, W.-C.; He, P.-Q.; Tien, H.-C.; Liu, H.-L.; Chen, W.-C.; Lv, W.; Lee, W.-Y. Solvent-Enhanced Transparent Stretchable Polymer Nanocomposite Electrode for Supercapacitors. *ACS Applied Energy Materials* **2021**.

(5) Lu, C.; Lee, W.-Y.; Shih, C.-C.; Wen, M.-Y.; Chen, W.-C. Stretchable Polymer Dielectrics for Low-Voltage-Driven Field-Effect Transistors. *ACS Appl. Mater. interfaces* **2017,** *9* (30), 25522-25532.

Efficient Doping of Organic Semiconductors for High-Performance Devices

***Yuanyuan Hu*[1]**
[1]School of Physics and Electronics, Changsha 411082, China
Tel.:86-731-88822332, E-mail: yhu@hnu.edu.cn

Organic semiconductor (OSC) doping is a powerful technique for tuning the electrical properties of organic semiconductors and has been intensively studied for achieving high-performance devices. However, in contrast to doping in silicon, where a small amount of substitutional dopants can efficiently generate electrons (n-doping) or holes (p-doping), efficient and controllable doping in organic semiconductors is an intensively studied topic yet remains a challenge.

In this presentation, we shall introduce our recent studies on developing novel dopants for OSCs and the application of these dopants in organic thin-film transistors (OTFTs). Specifically, we have developed some dopants including both p- and n-dopants that have higher doping efficiency than the commonly used molecular dopants. Moreover, these dopants may not be limited by the energy level matching rule followed by conventional molecular dopants, indicating new doping mechanisms. Such efficient and universally applicable dopants enable the fabrication of high-performance OTFTs.

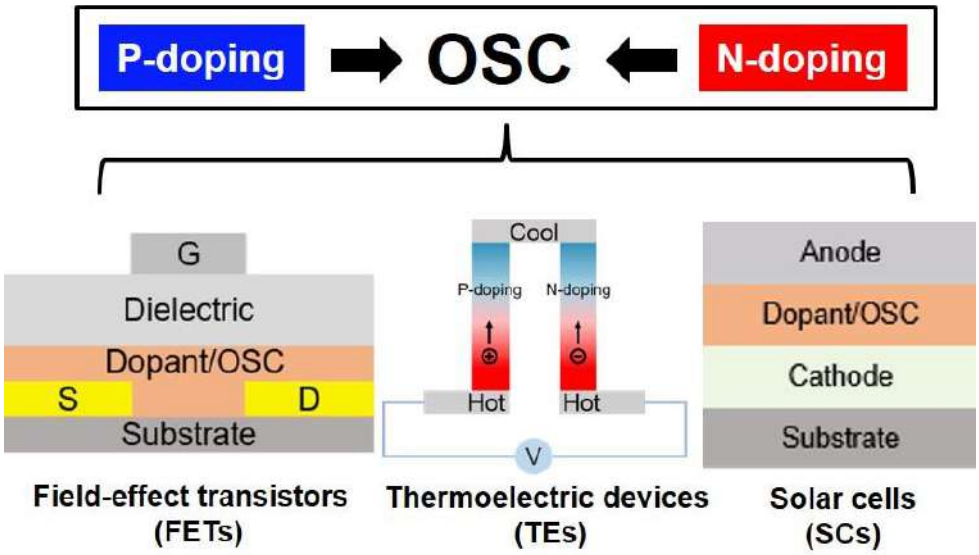

Fig. 1. Investigation and application of organic semiconductor doping.

Acknowledgment

Y. Hu thanks the National Natural Science Foundation of China (61804051; 62074054) and Natural Science Foundation of Hunan Province (2018RS053; 2019GK2245; 2020JJ1002), and Shenzhen Science and Technology Innovation Commission (RCYX20200714114537036) for financial support.

References

1. H. Sirringhaus, *Adv. Mater.* **2009**, 21, 3859-3873.
2. S. Park, S. H. Kim, H. H. Choi, B. Kang, K. Cho, *Adv. Funct. Mater.* **2020**, 30, 21.
3. J. Liu, K. Zhou, J. Liu, J. Zhu, Y. Zhen, H. Dong, W. Hu, *Adv. Mater.* **2018**, 30, 1803655.
4. H. Gao, J. Liu, Z. Qin, T. Wang, C. Gao, H. Dong, W. Hu, *Nanoscale* **2020**, 12, 18371-18378.
5. Z. Wu, Y. Liu, E. Guo, G. Darbandy, S.-J. Wang, R. Hübner, A. Kloes, H. Kleemann, K. Leo, *Nat. Mater.* **2021**, 1-8.

Merits of Narrow FWHM Blue Emitter in Top Emission OLED

Hye In Yang, Sang Min Cho, Seung Hyun Lee, and Jang Hyuk Kwon
Dept. of Information Display, Kyung Hee University, Dongdaemun-gu, Seoul 02447, Korea
Tel.:82-2-961-9147, E-mail: jhkwon@khu.ac.kr

One of the recent organic light emitting diodes (OLEDs) display development goals is the 8K display with high resolution. The 8 K display may require better color reproducibility like the BT. 2020 standards. To achieve BT. 2020 color, light-emitting materials should have narrow full width at half maximum (FWHM) and proper wavelength of each primay color. In current display application, strong micro-cavity top emission OLED (TEOLED) is using due to various advantages such as excellent color purity and higher efficiency in a normal direction. Such strong micro-cavity generates the narrow FWHM and higher luminescence intensity compared to the non-cavity device due to slective wavelength amplication [1]. Recently, a new di-boron multi-resonance (MR) type blue thermally activated delayed fluorescence (TADF) material, ν-DABNA, was reported [2]. Unlike other fluorescent blue materials, DABNA type emitter exhibits narrow FWHM of 15 nm.

In this study, we investigate the merits of DABNA type emitter compared with wide FWHM pyrene type emitter in the micro-cavity TEOLEDs. Optical simulation was performed using pyrene emitter, BD-1, with a short-wavelength peak (453 nm) and a wide FWHM (30 nm) and DABNA type emitter, BD-2, with a long-wavelength peak (466 nm) and narrow FWHM (15 nm). Firstly, the overlapping of the out-coupling curves and PL spectrum according to the optimal cavity length of each emitter was confirmed under 2-order optical condition. In the case of BD-1, there are some unoverlapped areas between the out-coupling curve and the PL spectrum (Fig. 1 (a)), whereas in BD-2, is all overlap (Fig. 1 (b)) due to the influence of the narrow FWHM. The simulated values of blue index of TEOLED devices with BD-1 and BD-2 were 96.78 and 126.01, respectively. It indicates that the smaller FWHM result in a large enhancement factor in TEOLED efficiency. Secondly, color changes with respect to viewing angle were investigated for both devices. The BD-2 TEOLED device shows a color change of less than 0.02 in any viewing angle than the BD-1 as shown in Fig 1 (c). Since the viewing angle is observed with the side peak, the narrower FWHM has the more advantageous. In summary, we found that BD-2 with a narrow FWHM could have about 30% improvement in efficiency in a normal direction and smaller color change with viewing angle. In the conference, we will present the comparision of simulation and experimental results.

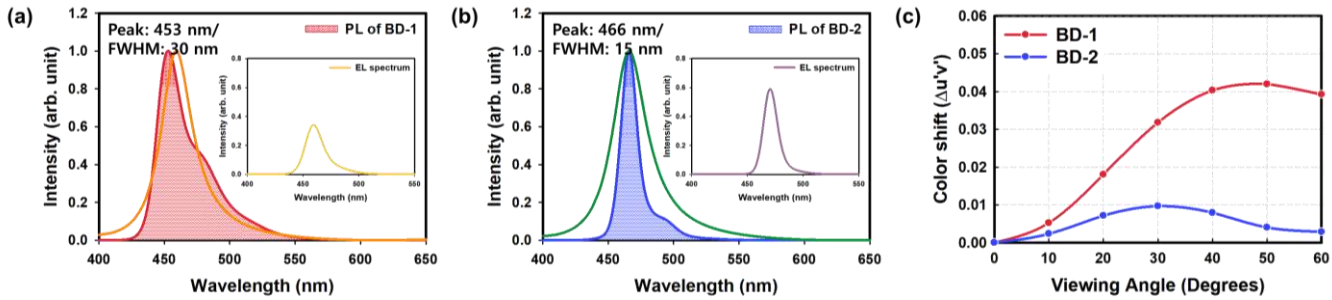

Fig. 1. Overlap of PL spectrum and out-coupling curve of (a) BD-1 (b) BD-2 according to the optimal cavity length (inset) The EL intensity of BD-1 and BD-2 (c) Color variation with respect to viewing angle of BD-1 and ν-DABNA devices.

Acknowledgment

This work was supported by BK21 FOUR Program (Department of Information Display, Kyung Hee University) funded by Ministry of Education (MOE, Korea).

References

1. S. K. Kim, M. J. Park, R. Pode, and J. H. Kwon, *Adv. Photonics Res.*, 2000122 (2021).
2. Y. Konde, K. Yoshiura, S. Kitera, H. Nishi, S. Oda, H. Gotoh, Y. Sasada, M. Yanai, and T. Hatakeyama, *Nat. Photonics*, 13, 678-682 (2019).

Quantum-Dot and Organic Hybrid Light-Emitting Diodes with Reduced Process Steps for Full-Color Displays

SuhyeoniLeeiandiJeonghuniKwaki
Dept. of Electrical and Computer Engineering, Inter-University Semiconductor Research Center, Seoul National University, Seoul 08826, Korea
Tel.:82-2-880-1781, E-mail: jkwak@snu.ac.kr

Quantum dot (QD) light-emitting diodes (QLEDs) have been in the forefront of the up-to-date display devices with their outstanding performances and excellent color purity, following the progress of organic light-emitting diodes. With these devices, it is highly demanded for display industry to develop technologies requiring high resolution such as AR, VR, and UHD. However, indispensable solution process using colloidal QDs has not only been to be the advantageous properties for simplicity and low-cost manufacturing but the obstacle to pattern each color of sub-pixels. Although several studies proposed various kinds of techniques to pattern the QDs,[1,2] it is still difficult to achieve full-color display with sufficiently simple and low-cost fabrication process. Thus, to guarantee the realization of full-color display based on QLEDs, patterning techniques by the solution process have to be ensured.

Here we report a novel concept to reduce one patterning step for blue sub-pixel by sharing the blue common layer (BCL) as an emitting layer (EML) in the blue-emitting device and charge transport layer in the red/green-emitting devices. Using this skill, only two colors of QD need to be patterned with solution process since the blue EML is formed by thermally evaporated BCL with an open-mask. Furthermore, by the energy transfer process as well as balanced carrier injection, the external quantum efficiency was enhanced by 11.7% and 38.4% in red and green-emitting QLEDs, respectively. We also demonstrated a full-color light-emitting device employing the BCL in a single substrate which exhibited the exclusive color-emission at each sub-pixel. We believe that this new approach to patterning technique will provide the way for QLEDs to be employed in the practical applications demanding high resolution.

Acknowledgment

This work was supported by the Technology Innovation Program (Grant No. 20010371) funded by the Ministry of Trade, Industry & Energy (MOTIE, Korea).

References

1. L. Xie, X. Xiong, Q. Chang, X. Chen, C. Wei, X. Li, M. Zhang, W. Su, and Z. Cui, *Small,* 15, 1900111 (2019).
2. H. Cho, J. Kwak, J. Lim, M. Park, D. Lee, W.K. Bae, Y.S. Kim, K. Char, S. Lee, and C. Lee, *ACS Appl. Mater. Interfaces*, 7(20), 10828 (2015).

Transparent Flexible Nanoline Field-Effect Transistor (NL-FET) Array with High-Integration in Large-Area

Dong Wook Kim[1], and Unyong Jeong[1]
[1]Department of Materials Science and Engineering, Pohang University of Science and Technology (POSTECH), 77 Cheongam-Ro, Nam-Gu, Pohang, Gyeongbuk 37673, Republic of Korea
Tel.:82-10-5830-6979, E-mail: dongwkim@postech.ac.kr

Transparent flexible transistor array requests large-area fabrication, high integration, high manufacturing throughput, inexpensive process, uniformity in transistor performance, and reproducibility. This study suggests a novel reliable approach to meet the requirements. We use the Al-coated polymer nanofiber patterns obtained by the electrohydrodynamic (EHD) printing as a photomask. We use the lithography and deposition to produce highly-aligned nanolines (NLs) of metals, insulators, and semiconductors on large substrates. With these NLs, we demonstrate a highly integrated NL field effect transistor (NL-FET) array ($10^5/(4 \times 4\ in^2)$, 254 pixel-per-inch) made of pentacene and indium zinc oxide semiconductor NLs. In addition, we demonstrate a NL complementary inverter (NL-CI) circuit consisting of pentacene and fullerene NLs. The NL-FET array shows high transparency (~90 %), flexibility (stable at 2.5 mm bending radius), uniformity (~90 %), and high performances (mobility = 0.52 cm^2/Vs, on-off ratio = 7.0×10^6). The NL-CI circuit also shows high transparency, flexibility, and typical switching characteristic with a gain of 21. The reliable large-scale fabrication of the various NLs proposed in this study is expected to be applied for manufacturing transparent flexible nanoelectronic devices.

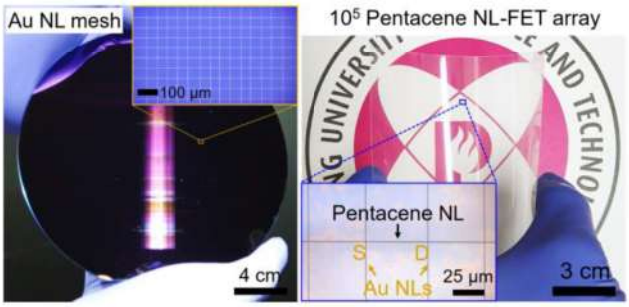

Fig. 1. Flexible, transparent, large-area metal nanolines (NLs) array and NL-Field Effect Transistor (NL-FET) array with high integration

References

1. D. W. Kim, S.-Y. Min, Y. Lee, and U. Jeong, *ACS Nano,* 14(1), 907 (2020).

Dynamic vectorial holographic color prints by liquid crystal-integrated metasurface for anti-counterfeiting

Gyeongtae Kim [1], Inki Kim [1], Jaehyuck Jang [2], and Junsuk Rho [1, 2]
[1]Dept. of Mechanical Engineering, Pohang University of Science and Technology (POSTECH), Pohang 37673, Republic of Korea
Tel.:82-54-279-2834, E-mail: gyeongtaekim@postech.ac.kr
[2]Dept. of Chemical Engineering, Pohang University of Science and Technology (POSTECH), Pohang 37673, Republic of Korea

We propose bi-functional metasurface which contains structural color prints and vectorial holograms with eight polarization channels towards advanced encryption applications (Fig. 1). The encoded structural color prints can be observed under white light and the fully polarized holograms can be reconstructed using coherent laser source with combination of output polarizer/retarder [1]. To encode multiple hologram images having different polarization states, a pixelated metasurface is adopted thereby digitalizing sets of phase distribution retrieved from the images into single metasurface [2]. Such superpixel consists of four phase-gradient meta-atom groups: meta-atom group rotated either clockwise or counterclockwise. Depending on the combination of clockwise and counterclockwise rotating meta-atom group, the polarization states of the reconstructed images are determined. The meta-atom contains specifically designed geometric and propagation phase, and reflection spectrum at each spatial location. As a proof-of-concept, we devise electrically tunable optical security platform using our multifunctional metasurface incorporated with liquid crystal. The optical security platform is double encrypted: Color printing image that can be decrypted by camera scanning provides first key and corresponding information will be used to fully unlock the double-encrypted information via projected vectorial hologram images. Such an electrically tunable optical security platform will provide a new route towards internet-of-things sensors for security and anticounterfeiting applications.

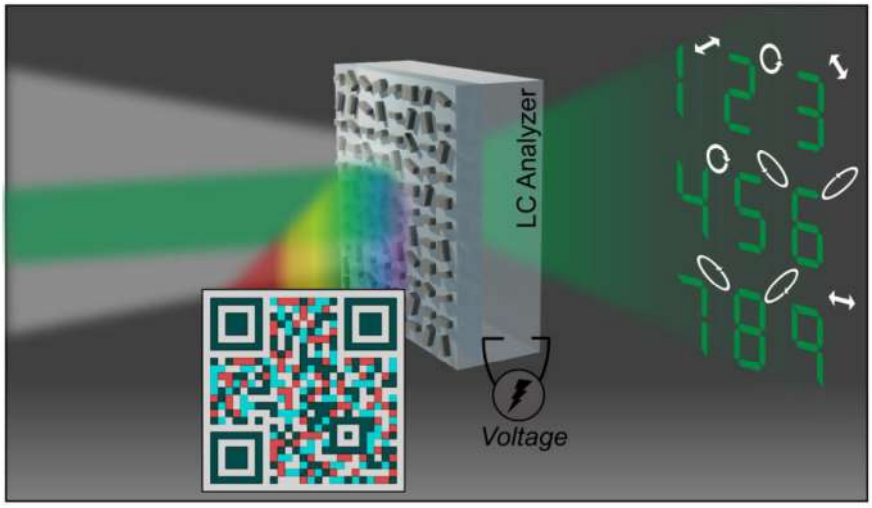

Fig. 1. Schematic of dynamic vectorial holographic color prints using a pixelated metasurface and liquid crystal (LC) analyzer. Under ambient white light, the device displays a two-colored QR code image. On the other hand, with laser illumination the vectorial hologram images can be rendered. With an aid of LC analyzer, electrically tunable vectorial holographic color prints can be realized.

References

1. Yoon, G., Lee, D., Nam, K. T. & Rho, J. "Crypto-Display" in Dual-Mode Metasurfaces by Simultaneous Control of Phase and Spectral Responses. ACS Nano 12, 6421–6428 (2018).
2. Song, Q. *et al.* Ptychography retrieval of fully polarized holograms from geometric-phase metasurfaces. *Nature Communications* 11, 2651 (2020).

Near-Infrared Phosphorescence Enhancement by Intermolecular Metal-to-Ligand-to-Ligand Charge Transfer

Hae Un Kim[1], Taehyun Kim[1], and Taiho Park[1]*
[1]Dept. of Chemical Engineering, Pohang University of Science and Technology (POSTECH), Pohang, Gyeongbuk 37673, Korea
Tel.:82-54-279-5295, E-mail: hukim@postech.ac.kr

Aggregation-induced phosphorescent enhancement (AIPE)-active deep-red and near-infrared (NIR) emissive iridium(III) complexes are designed to overcome the triplet–triplet annihilation and vibrational deactivation shown by low bandgap emitters, by anchoring various electron-withdrawing substituents such as -phenyl (**Ir2**), -ethyl ester (**Ir3**), and -trifluoromethyl (**Ir4**) groups on the N-coordinating quinoline moiety of a (benzo[*b*]thiophen-2-yl)quinoline cyclometalated ligand. The origin of AIPE on **Ir2** and **Ir4** and its associated excited-state properties are studied with the help of density functional theory (DFT) and single-crystal X-ray diffraction (XRD) analysis. AIPE-active **Ir2** is employed for the fabrication of PhOLEDs by hybrid solution-process, in which the AIPE effect of **Ir2** achieves a maximum external quantum efficiency (EQE) of 7.29%. The efficient NIR emission could be achieved by the metal-to-ligand-to-ligand charge transfer (MLLCT) process of the light-emitting materials, controlling the level of triplet-triplet interaction.

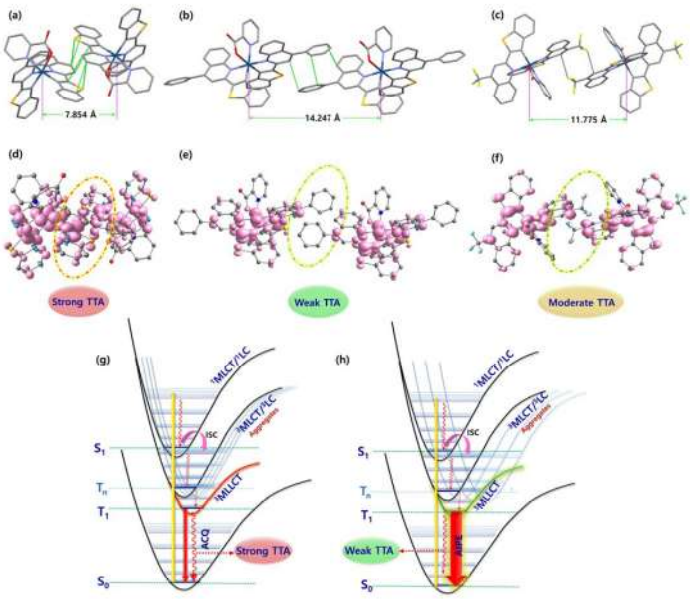

Fig. 1. (a-c) Various interactions observed between the neighbouring units from the crystal packing structure. (d-f) Mapping of triplet spin density states identical to their respective crystal packing structure. A schematic drawing of the ground and excited-state potential energy surfaces and their aggregation explains (g) quenching of emission in Ir1 and (h) AIPE effect in Ir2 and Ir4.

Acknowledgment

This work was supported by grants from the Center for Advanced Soft Electronics under the Global Frontier Research Program (2012M3A6A5055225), and the Technology Development Program to Solve Climate Changes of the National Research Foundation (NRF) of Korea (2015M1A2A2056216). This research was also partially supported by the Samsung Display Corporation.

References

1. A. Bondi, *J. Phys. Chem.*, 68, 441 (1964).
2. N. J. Turro, V. Ramamurthy and J. C. Scaiano, Modern Molecular Photochemistry of Organic Molecules, University Science Books, Sausalito, California (2010).

Ink-jet Printing Perovskite Emissive Color Filter for Liquid Crystal Display

Yiyang Gao[1], Maksym F. Prodanov [1], Chengbin Kang[1],Valerii V. Vashchenko[1] and Abhishek K. Srivastava[1]
[1]Dept. of Electronics and Computer Engineering, Hong Kong University of Science and Technology
Hong Kong S.A.R, China
Tel.:852-5674328, E-mail: ygaobg@connect.ust.hk

Abstract

Advanced color converting materials such as quantum dots (QD), quantum rods (QR) and perovskite nanoparticles (PNP) are predicted to lead the next generation of display with the concept of emissive color filters (CF). It brings about many benifits such as larger color gamut and higher efficiency. We successfully fabricate full color emissive CF arrays using green PNP and red QR. The usage of a porousf polymer film enable a bank-free printing. The printed patterns have good uniformity, high resolution and is quite stable for as long as 4 months.

1. Introduction

Future display await wider color gamut, higher contrast ratio, luminance, resolution and effieincy. The introduction of BT.2020 color range, which is the newest recommeded standard for Ultra HD video broadcasting, puts extremely high requirement on the color gumut of display. Perovskite nanoparticles and semiconductor Quantum dots are believed to be the most promising luminescent material to realize BT.2020. And in recent decades, emissive color filter comprised of patterned photoluminescent matrixs have received great research concerns from academics[1,2] and industries. Many giant display and material companies are devoting to developing QD color filters (QDCF) or under the name QD color converter (QDCC). For example, Samsung are working on QD-OLED and QNED,[3] Avantama and Nanosys are trying to improve PNP and QD material property and using Ink Jet Printing (IJP) and Photolithography to pattern CF structures.[4–7] The QDCF is functional in various displays, including LCD, OLED, mini-LED and μLED.By replacing conventional broadband absorptive color filter, problem of spectrum crosstalk is elimintated. QD-OLED induces better color saturation than white OLED (WOLED). And for LCD, it further improves color performance in comparison to LCD with PNP or QD composite color enehancement film at the bottom with passive color filter on top.[1,2,8] In regard of efficiency, color downconversion could solve efficiency problems for full color μLED display, where "green-gap" and turn-on voltage discrepency exsits which makes integrating individual RGB μLED on one chip quite complicated and inefficient. It plays even more important role in LCD and WOLED, since the traditional color filter waste up to 66.7% light due to absorptive nature.With high photoluminescence quantum yield (PLQY) and tunable wavelength, from photometry point of view, PNP and QD are ideal materials which can gurantee high power conversion efficiency and luminous efficacy. Therefore, pixellated QD and PNP color down converisoin layers are expected to renovate the next generation display with better colors and higher efficiency.

However, it's not easy task to truelly fullfill this conception. Several obstacles are on the way concerning about pixel patterning techniques and optics design. Micro-contact printing, nanoimprint, IJP, and photolithography are three of the most popular fabrication methods of patterned arrays. They are generally speaking prospective techniques for mass production beacause of the scalability and low cost. But none of them is proved to be good enough to complete this task. Micro-contact printing or transfer are good technical method to fabricate thin layers, so they are normally applied in μLED.[9–11] Whereas color down conversion color filters require thicker film. Researches find concensual estimation of a film thickness larger than 5 μm is needed to acquire adequate blue light absorption.[12] Photolithography is a matual technology for fine pattern production processing. By blending or combining PNP or QD with photoresist, pixel size down to several micron or sub-micron can be fabricated well.[13,14] Nevertheless, PNP and QD sometimes need to be modified to have better adhesion to the photoresists matrixs. What's more, development process is needed to remove unwanted part, where the solvents are usually harmful and could leads to quantum material decompsition or aggregation. These procedures therefore lower down the PLQY of the and impair device performance. And it's pretty hard to have high concentration of QDs in photoresists with good dispersion.[14] Compared to semiconductor QDs, photolithography will be even harder for PNPs material because of their poor stability. Another alternative method for PNP patterning is IJP. It allows more material flexibility for ink. To solve material stability issues, PNP can be mixed with polymer or monomers in ink or printed to polymer substrate.[15,16] But to insure a jettable ink, the monomer load is limited which

reduce the effectiveness of stabilization. And reported works that prove good stability are faced with coffee-ring problems.[15,17] And the minimal printed PNP pattern size are above 90 μm, limiting the display resolution. Besides, most IJP works require banks to confine the ink spreading on the substrate to make fine patterns. But bank means additional processing and it will increase the cost. Up to now, a multi-color ink jet printing using perovskite with good pattern uniformitiy, good stability and acceptable resolution has not been reported yet.

In this article, we use green $CsPbBr_3$ nanoparticles and red CdSe quantum rod (QR) to make full color emissive color filter. The patterned PNP and QR matrix was fabricated by ink-jet printing to a porous polyethylene terephthalate (PET) film. Due to the strong capilary force of the sub-micron pores in the template, the printing pattern was free of coffee-ring effect. And the minimal printing dot size is as small as 40μm (printing nozzle diameter ~ 21.5μm) without using any bank structure.

2. Experiment Section

IJP ink preperation: $CsPbBr_3$ perovskite nanoparticles were synthesized following the method of reference 18.[18] Red emitting $CdSe/Zn_xCd_{1-x}S$ quantum rods were perepared by the method described in reference 19.[19] The final materials were separately dispersed in toluene. Then, the required amont of 2-Ethylhexyl acrylate (EHA) was added to each solution and the solvent was evaporated by N_2 flow for 2 hours resulting in EHA dispersions of PNPs and QRs in EHA with concentration of 8.9 g/L and 10 g/L respectively. Photo-initiator 2,2-Dimethoxy-2-phenylacetophenone (DMPAP) was added to both solutions with concentraiton of 3 wt.%.

The porous polyethylene terephthalate (PET) film is 23 μm thick. The film has thorough pores developed by nuclear etching. The pores have diameters of 0.45 μm and are randomly distributed with pore densitiy of around 0.6. The film was clapps by holders and use as substrate for ink jet printing.

Luminescent material characterization : the absorption spectrum of PNP and QR are measured by Perkin Elmer Lambda 20 UV VIS Spectrometer. The photoluminescence spectrum was detected by Ocean Optics USB4000 spectrometer.

PLQY of the solution and film was measured using Spectrofluorometer FS5 (Edinburgh Instruments).

Ink jet printing was performed using Dimatix Materials Printer DMP-2850 (Fujifilm). We use 10pl cartridges with nozzles of 21.5 μm diameter.

3. Results and Discussions

The normalized emission spectrum and absorption spectrum of the green $CsPbBr_3$ PNP and red QR ink are illustrated in Figure 1. The ink was diluted when measured absorption spectrum to improve accuracy and fit in the instrument measurment range. The full width half maximum (FWHM) of synthesized PNP and QR emission is as narrow as 20nm and nm which gives good color saturation. The photoluminesence quantum yield (PLQY) of the green and red ink are % and % . The PLQY of continous green and red porous film are % and %. The green film was illuminated by UV light for polymerization, due to poor UV stability of perovskite, QY dropped from the solution. The PLQY difference may leads to intensity difference of green and red pixel in devices, but this can be overcomed by arranging larger green pixel area or by modify the transmittance of liquide crystal of correspoding subpixels to balance the brightness.

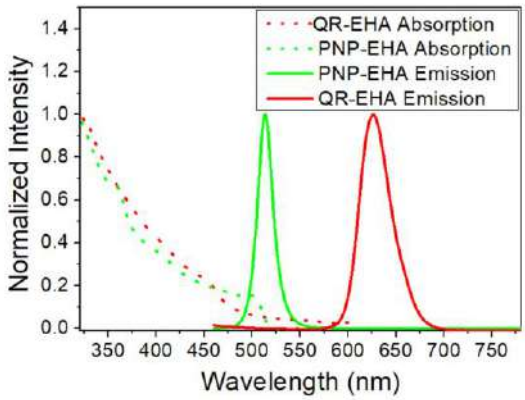

Fig. 1. Emission and absorption spectrum of $CsPbBr_3$ nanoparticles and CdSe quantum rod ink

The green and red ink composition are descirbed in the experiment section. The organic monomer EHA has low boiling point and is liquid at room temperature. It's used as polymerizable solvent. And its nonpolar nature makes EHA compatible with perovskite which is pretty sensitive to polar chemicals. Ink jet printing process are governed by the physical property of ink and jetting waveform applied on to the piezoelectric bimorph.[20] Inverse Ohnesorge number (Z number) is a parameter that summarize the requirement of all essential properties for a stable and high quaility jetting. It is defiend as

$$Z = \frac{\eta}{\rho \sigma d}$$

where η is the viscosity in $\mathrm{mPa \cdot s}$, σ is the surface tension in mN/m, ρ is the density in $\mathrm{g/cm^3}$. d is the nozzle diamter in μm. It's recognized that printable and stable ink has Z number in range of 1 to 14. The parameters of EHA are listed in the table in Figure 2.

	Viscosity (cp @20C mPa * s)	Surface tension (mN/m = dyen/cm)	Boiling point (C)	Density (g/cm3)
EHA	1.7	26	214	0.885

Fig. 2. Physical property of EHA

With pirnter 21.5 μm diamter nozzle, the Z number of solvent EHA are caculated to be 13.05. The solutes, PNP and QR will influence all paramter discussed above for the ink. But since the concentration are quite small for the solutes (8.9mg/mL for PNP and 10mg/mL for QR), the variation of the Z number should be small. And our success of printing verify that the Z number of the overall solution is in resonable range. The droplet was plump without any satellite drops. The merit of using EHA as solvent is not only limited to the good printing ability, but also in its function to stablitze color converting material, especially PNPs. Unlike methods using PNP-monomer-solvent system, here PNP is totally disssolved in EHA. In the previous case, needless solvents needs moderate heating, vacuum or relative long time for evaporation. During this period, PNPs are prone to degrade and thus PLQY is dropping. And usually there is limitation of the polymer contents because of their solubitliy in solvents and their influence on the prinitability of ink. With inadequate quantity, the stabilization effect of polymer on PNP is always far from expectation. But in our case, solvent evaporation is not needed and the system has high content of monomers. So it's more benificial for maintaining high PLQY of PNP.

The other innovation of this work is the use of porous PET film as printing substrate. With the porous film, no bank structures are required. This is benifited from the small pore size and the resultant capilary effect. After the ink drop onto the surface of the film, the cylindral pores will quickly absorb the ink once contacted to the solution. So the liquid will not undergo wide spread as what is happened to normal rigid nonporous substrate. The single drop size is thus samller. To demonstrate the ability of high printing resolution. We use green PNP-EHA ink to print on the porous film substrate and get 40μm dot size. The printing of the red single dots array result is shown in Figure 3. The single dot pattern is

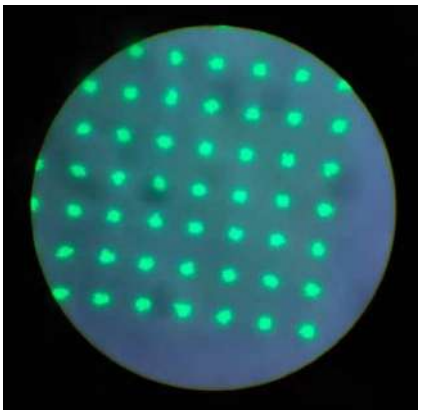

Fig. 3. Single dot arrays printed on the porous film

uniform. The size regularity depends on the random position of the pores. With increased pore density and more homogeneous position distribution, the single dot pattern will be more inerratic. Full color CF arrays are realized by printing green and red color converters and leave blank for blue pixels. We use square pixels of 320 μm length and 360 μm pitch for CF demonstration. The CF pattern prototype is illustrated in Figure 4. Two red, one green and one blue subpixels compose one square pixel. Pixel pitch is thereby 720 μm.

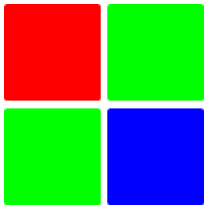

Fig. 4. Physical property of EHA

Following this idea, we print red and green pixels in sequence on to the porous film. After printing each two layers, the film is polymerized under UV light for 5 minutes. Total layers of the prepared sample is 6 layers. Brightness can be further improved by printing more layers and will be limited by the porous film thickness. Figure 5 shows the printed patterns using a 10X microscopy. We manually make the pixel alignment and it can be easily improved with better equipment. Dot spacing can be adjust to make the patterns more intact. Generally speaking, the printed patterns have clear borders and regular arrangement.

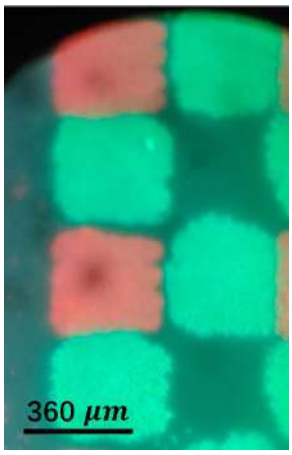

Fig. 5. Printed red and green patterns

Ambient stability is always a big issue prohibiting the wide application of organic and inorganic perovskite nanoparticles. The method we use take into account of this problem and is proved to improve improve the stability of PNP. In our previous work, we use the same kind of porous film to encapsulate PNPs.[21] The PNP in polymerized polymer film has improved stability against high temperature, various humidity condition and strong and high energy UV illumination. The good encapsulation is the collective effect of the polymer and the porous film template. Here, a printed full color porous CF film sample was stored in ambient environment for 4 months. The film still shows quite bright emission. Figure 6. shows the same sample film excitated by UV light when the film is freshly prepared (Figure 6. (a)) and when the film is stored for 4 months (Figure 6 (b)). The overall size of the enclosed region in Figure 6(b) is about 100 mm ×120 mm. Figure 6(a) is basically the enclosed region of Figure 6(b) but is taken with different magnitude. The blue and purple color inside the photos comes from the fluorosence of the tapes we use to fix the samples.

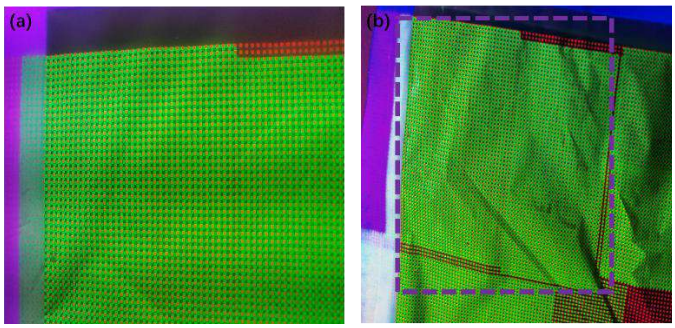

Fig. 6. Photos of a full color printed film under UV excitation at different time (a) freshly printed. (b) after stored in ambient envronment for 4 months.

Though photos are taken at different positions. The excitation source is the same, and from the photos it's clear that the brightness almost didn't decreased. This justify the stabilization ability of the porous film, especially for the perovskite.

4. Conclusions

We propose a bank-free method to fabricate green perovsktie nanoparticle and red quantum rod color converting color filter arrays through ink jet printing. Based on our investagation, this is the first demonstration of full color pattern arrays printing involving perovskite nanoparticles. With special porous film templates, the printing is endowed with uniform morphology and small dot size. The printed patterns thus have clear borders, which is hard to achieve without using bank structures. The polymer matrix and porous film encapsulation stablize PNPs inside. The printed fine patterns still shows stable emission for 4 months. The porous film is flexible making it compatible to all kinds of displays. Applying this emissive color filter with narrow band and high PLQY perovskite and quantum materials to the LCD, OLED or μLED display, we can expect larger color gamut and higher deice effiency.

Acknowledgment

This work was supported by the RGC of Hong Kong SAR (Grant Nos. 26202019, AoE/P-02/12), and the funding's for The State Key Laboratory of Advanced Displays and Optoelectronics Technologies.

References

1 H. Chen, J. He and S. Wu, IEEE Journal of Selected Topics in Quantum Electronics, vol. 23, no. 5, pp. 1-11, Sept.-Oct. 2017.
2 H.-J. Kim, M.-H. Shin, J.-Y. Lee, J.-H. Kim and Y.-J. Kim, *Opt. Express*, 2017, **25**, 10724–10734.
3 B. Raikes, *Inf. Disp. (1975).*, 2020, **36**, 34–38.
4 N. A. Luechinger, M. Oszajca and S. Loher, *SID Symp. Dig. Tech. Pap.*, 2018, **49**, 522–524.
5 E. Lee, R. Tangirala, A. Smith, A. Carpenter, C. Hotz, H. Kim, J. Yurek, T. Miki, S. Yoshihara, T. Kizaki, A. Ishizuka and I. Kiyoto, *SID Symp. Dig. Tech. Pap.*, 2018, **49**, 525–527.
6 E. Lee, S. Kan, C. Hotz, J. Yurek, Z. Luo, H. Kim, J. Yamanaga and A. Carpenter, *SID Symp. Dig. Tech. Pap.*, 2017, **48**, 984–987.
7 N. A. Luechinger, *SID Symp. Dig. Tech. Pap.*, 2020, **51**, 1178–1181.
8 J. H. Lee, *Inf. Disp. (1975).*, 2020, **36**, 9–13.
9 M. K. Choi, J. Yang, K. Kang, D. C. Kim, C. Choi, C. Park, S. J. Kim, S. I. Chae, T.-H.

Kim, J. H. Kim, T. Hyeon and D.-H. Kim, *Nat. Commun.*, 2015, **6**, 7149.

10 T.-H. Kim, K.-S. Cho, E. K. Lee, S. J. Lee, J. Chae, J. W. Kim, D. H. Kim, J.-Y. Kwon, G. Amaratunga, S. Y. Lee, B. L. Choi, Y. Kuk, J. M. Kim and K. Kim, *Nat. Photonics*, 2011, **5**, 176–182.

11 Z. Liu, C.-H. Lin, B.-R. Hyun, C.-W. Sher, Z. Lv, B. Luo, F. Jiang, T. Wu, C.-H. Ho, H.-C. Kuo and J.-H. He, *Light Sci. Appl.*, 2020, **9**, 83.

12 J. Osinski and P. Palomaki, *SID Symp. Dig. Tech. Pap.*, 2019, **50**, 34–37.

13 Y. Nakanishi, T. Takeshita, Y. Qu, H. Imabayashi, S. Okamoto, H. Utsumi, M. Kanehiro, E. Angioni, E. A. Boardman, I. Hamilton, A. Zampetti, V. Berryman-Bousquet, T. M. Smeeton and T. Ishida, *J. Soc. Inf. Disp.*, 2020, **28**, 499–508.

14 H.-M. Kim, M. Ryu, J. H. J. Cha, H. S. Kim, T. Jeong and J. Jang, *J. Soc. Inf. Disp.*, 2019, **27**, 347–353.

15 L. Shi, L. Meng, F. Jiang, Y. Ge, F. Li, X. Wu and H. Zhong, *Adv. Funct. Mater.*, 2019, **29**, 1903648.

16 M. Duan, Z. Feng, Y. Wu, Y. Yin, Z. Hu, W. Peng, D. Li, S. Chen, C.-Y. Lee and A. Lien, *Adv. Mater. Technol.*, 2019, **4**, 1900779.

17 S. Shi, W. Bai, T. Xuan, T. Zhou, G. Dong and R.-J. Xie, *Small Methods*, 2021, **5**, 2000889.

18 L. Protesescu, S. Yakunin, M. I. Bodnarchuk, F. Krieg, R. Caputo, C. H. Hendon, R. X. Yang, A. Walsh and M. V Kovalenko, *Nano Lett.*, 2015, **15**, 3692.

19 X. Li, F. Cao, D. Yu, J. Chen, Z. Sun, Y. Shen, Y. Zhu, L. Wang, Y. Wei and Y. Wu, *Small*, 2017, **13**, 1603996.

20 S. K. Gupta, M. F. Prodanov, W. Zhang, V. V Vashchenko, T. Dudka, A. L. Rogach and A. K. Srivastava, *Nanoscale*, 2019, **11**, 20837–20846.

21 Y. Gao, M. F. Prodanov, C. Kang, V. V Vashchenko, S. K. Gupta, C. C. S. Chan, K. S. Wong and A. K. Srivastava, *Nanoscale*, 2021, **13**, 6400–6409.

Overcoming Fundamental Limitations of Perovskite Light-Emitting Diodes

***Himchan Cho*[1]**
[1]***The Department of Materials Science and Engineering, Korea Advanced Institute of Science and Technology (KAIST), 291 Daehak-ro, Yuseong-gu, Daejeon,*** **Korea**
Tel.:82-42-350-3344, E-mail: himchan@kaist.ac.kr

In this talk, I will present my research to overcome fundamental limitations of metal halide perovskites for their light-emitting diode (LED) applications. I have identified efficiency-limiting factors of metal halide perovskites as emission layers in light-emitting diodes and solved the problems by developing novel strategies: (1) *In-situ* fabrication of perovskite nanocrystals based on crystallization control,[1] (2) removal of impurities and defects,[1] (3) A-site cation engineering,[2,3] and (4) introduction of quasi-2D structures with ligand-like A-site cations (Ruddlesden-Popper phase).[4,5] Those strategies led to a world-first breakthrough in brightness and efficiency of perovskite LEDs at room temperature. These works greatly stimulated perovskite LED research and totally changed the paradigm of display industry that focused only on organic emitters or inorganic quantum dot emitters.

References

[1] H. Cho *et al., Science*, 350(6265), 1222-1225 (2015)
[2] H. Cho *et al., Advanced Materials*, 29(31), 1700579 (2017)
[3] H. Cho *et al., ACS Nano*, 12(3), 2883-2892 (2018)
[4] J. Byun *et al., Adv. Mater.* 28(34), 7515–7520 (2016)
[5] H.-D. Lee et al., *Adv. Funct. Mater.* 29, 1901225 (2019)

High-Performance Perovskite LEDs and Their Applications

Feng Gao

Department of Physics, Chemistry and Biology, Linköping University, Sweden

feng.gao@liu.se

Metal halide perovskites have shown promising optoelectronic properties suitable for light-emitting applications. The development of perovskite light-emitting diodes (PeLEDs) has progressed rapidly over the past several years, and molecular additives have played an important role in these advances. By rational design of these molecular additives, we can significantly enhance the interaction with defects sites and minimize non-radiative recombination losses. In addition, we also demonstrate that the molecular additives can manipulate the perovskite crystallization and help to enhance the radiative recombination. As such, we have been able to demonstrate perovskite LEDs with high external quantum efficiencies over 20%. We find that our devices can also work efficiently in an emitting/detector switchable mode, with tens-megahertz speed for both functions. We further demonstrate the potential of the dual-functional diode for biomedicine diagnosis applications (as a monolithic heart pulse sensor) and for inter- and intra-chip bidirectional optical communications.

Effect of Monovalent Metal Iodide in Organic-Inorganic Tin-based Perovskite Transistor

Youjin Reo[1], Huihui Zhu[1], Ao Liu[1], Ji-Young Go[1], and Yong-Young Noh[1]
[1]Dept. Chemical Engineering, Pohang University of Science and Technology (POSTECH), Pohang, Gyeongbuk, 37673, Republic of Korea
Tel.:82-54-279-2265, E-mail: yynoh@postech.ac.kr

The application of organic–inorganic perovskites has recently attracted increasing interest due to their excellent optoelectronic properties. As an emerging semiconductor, the doping capability and efficiency of these materials require further clarification, but have rarely been studied previously. In this study, diverse monovalent cations, Cu^+, Na^+, and Ag^+, are incorporated into phenethylammonium tin iodide ($(PEA)_2SnI_4$) perovskite, and the resultant lattice structural variation, film properties, and thin-film transistor (TFT) performance are systematically investigated by combining theoretical and experimental methods. Theoretical studies claim that the hypothetical monovalent cation substitution on the Sn^{2+} B-site creates undesired vacancies and destabilizes the perovskite lattice structure. The experimental results show that the incorporated foreign aliovalent cations are not doped inside the perovskite lattice but segregated along the grain boundaries. Benefiting from the excellent hole transport property and passivation effect of copper iodide (CuI), the CuI-$(PEA)_2SnI_4$ heterostructure composite channel layers exhibit most improved film properties and device performance.

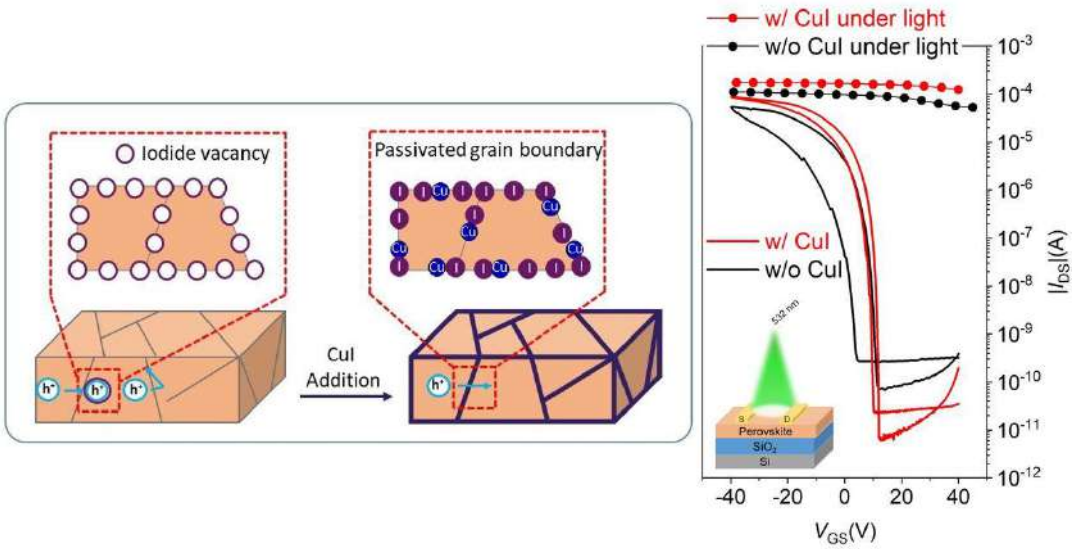

Fig. 1. Grain boundary passivation (left) and enhancement of TFT and phototransistor performance (right) by CuI incorporation

Acknowledgment

This study was supported by Ministry of Science and ICT through the National Research Foundation, funded by the Korean government (2017R1E1A1A01075360, 2020R1A2C4001617, 2020R1A4A1019455). This research was supported by National R&D Program through the National Research Foundation of Korea (NRF) funded by Ministry of Science and ICT (2020M3F3A2A01085792). This research was also supported by the Samsung Display Corporation.

References

1. T. Matsushima et al. *Adv. Mater.* 28, 10275 (2016).
2. S. P. Senanayak et al. *Sci. Adv.* 6, eaaz4948 (2020).
3. H. Zhu et al. Adv. Mater. 32, 2002717 (2020).

High-Efficiency Perovskite Nanocrystal Light-Emitting Diodes via Defect Suppression

Young-Hoon Kim(+)[1,2] Sungjin Kim(+)[1,2], Arvin Kakekhani(+)[3], Jinwoo Park[1,2], Jaehyeok Park[4], Yong-Hee Lee[1], Hengxing Xu[5], Satyawan Nagane[6], Robert B. Wexler[3], Dong-Hyeok Kim[1,2], Seung Hyeon Jo[1,2],iLauraiMartínez-Sarti[7], Peng Tan[3,8], Aditya Sadhanala[6,9], Gyeong-Su Park[1], Young-Woon Kim[1], Bin Hu[5], Henk J. Bolink[7], Seunghyup Yoo[4], Richard H. Friend[6], Andrew M. Rappe[3,] and Tae-Woo Lee[1,2,*]*

[1]Department of Materials Science and Engineering, Seoul National University, Seoul, Republic of Korea.

Tel.:82-2-880-8021, E-mail: twlees@snu.ac.kr

[2]School of Chemical and Biological Engineering, Institute of Engineering Research, Research Institute of Advanced Materials, Nano Systems Institute, Seoul National University, Seoul, Republic of Korea. [3]Department of Chemistry, University of Pennsylvania, Philadelphia, PA, USA. [4]School of Electrical Engineering, Korea Advanced Institute of Science and Technology, Daejeon, Republic of Korea. [5]Department of Materials Science and Engineering, University of Tennessee, Knoxville, TN, USA. [6]Cavendish Laboratory, University of Cambridge, Cambridge, UK. [7]Instituto de Ciencia Molecular, Universidad de Valencia, Paterna, Spain. [8]Department of Physics, Harbin Institute of Technology, Harbin, China. [9]Clarendon Laboratory, Department of Physics, University of Oxford, Oxford, UK.

Perovskite nanocrystals (PNCs) are regarded as promising emitters due to their outstanding properties. Such properties have led to perovskite light-emitting diodes (PeLEDs), which have exhibited a rapid increase in electroluminescence efficiency. To further improve electroluminescence efficiency, (1) increasing the radiative recombination and (2) lowering the non-radiative recombination should be considered. Here, we report a one-dopant alloying strategy that confines more carriers and reduces non-radiative recombination. Doping of guanidinium into $FAPbBr_3$ PNCs yields limited bulk solubility while creating an entropy- stabilized phase in the PNCs and leading to smaller PNCs with more carrier confinement. The increased surface stability is driven by the extra amino group in the GA^+ due to its extra hydrogen bonds and more uniformly distributed positive charges. To reduce extra defects, 1,3,5-tris(bromomethyl)-2,4,6-triethylbenzene is applied as a vacancy healing agent. Through these defect suppression strategies, high-efficiency PeLEDs that have current efficiency of 108 cd A^{-1} (EQE of 23.4%) are achieved.

Zinc Doped Copper Iodide (CuI) as Hole Transport Layer for Light-emitting Diodes

Taesu Choi, Gi-Seong Ryu, and Yong-Young Noh
Department of Chemical Engineering, Pohang University of Science and Technology (POSTECH), Pohang 37673, Republic of Korea
Tel.:82-54-279-8265, E-mail: yynoh@postech.ac.kr

Organic light-emitting diodes (OLEDs) are currently increasing the market size due to its excellent efficiency, flexibility and simple fabrication. In case of bottom-emitting structure of OLED, high transmittance is required for the hole transport layer (HTL). Copper iodide (CuI) has received great attention for HTL due to its large bandgap, high conductivity, optical transparency, proper energy level alignment with other layers and low cost. It also has much higher hole mobility than other organic HTL. Thus, a thick CuI film can be applied as HTL to improve the yield of large-area OLEDs. To optimize the properties of HTL in OLEDs, a method to control charge carrier density of CuI film should be required. In this study, we suggested Zn doped-CuI as HTL. The Zn-doping can effectively control the carrier density of CuI film and thus, OLED with CuI HTL showed better external quantum efficiency with much longer device life time.

Acknowledgment

This research was supported by the Basic Research Program through the National Research Foundation of Korea(NRF) funded by the MSIT(2020R1A4A1019455)

References

1. A. Liu, H. Zhu, W.T. Park, S.J. Kim, H. Kim, M.G. Kim, Y.Y. Noh, *Nat. Commun*. *11* (2020).
2. W.Y. Chen, L.L. Deng, S.M. Dai, X. Wang, C.B. Tian, X.X. Zhan, S.Y. Xie, R. Bin Huang, L.S. Zheng, *J. Mater. Chem. A. 3* (2015).
3. M. Shan, H. Jiang, Y. Guan, D. Sun, Y. Wang, J. Hua, J. Wang, *RSC Adv. 7* (2017).

Photothermally Cross-linked Hexanuclear Oxozirconium Cluster as an Organic-Inorganic Hybrid Dielectric Material

Ga Hye Kim[1], Do Jeon Kim[2], and Myung-Gil Kim[1]
[1]School of Advanced Materials Science and Engineering, Sungkyunkwan University, Suwon 16419, Republic of Korea.
Tel.:82-31-299-7392, E-mail: myunggil@skku.edu
[2]Department of Chemistry, Chung-Ang University, Seoul, 06974, Republic of Korea.

A hybrid structure of organic and inorganic building blocks enables us to design and tailor new materials with desired features and functions. Metal-oxo cluster molecules is one of the organic-inorganic hybrid materials. Metal-oxo cluster molecules having functional capping ligands offer remarkable promise in terms of thin film applications. Although there are a lot of metal-oxo cluster molecules reported so far, harnessing their potential is largely limited by lack of material processing strategy. We adopt a photothermally activated, cross-linked, and stable metal-oxo cluster molecular assembly based on hexanuclear zirconium-oxo cluster (Zr6O4OH4(OMc)12) (OMc: methacrylate) which can be a suitable for a new dielectric material in terms of electronic device applications since the zirconium-oxo core enhances the dielectric functionality and together the organic ligand (methacrylate) imparts a polymerizable functionality. Overall study not only proves that zirconium-oxo cluster activated by soft photothermal processing can be a new dielectric material candidate, but also other metal-oxo cluster thin film system may be further investigated by similar approach.

The hexanuclear zirconium-oxo cluster is synthesized, and its thin film is prepared by a solution process and then photothermally treated with various conditions. The effect of DUV irradiation on zirconium-oxo cluster thin film is characterized by a leakage current profile and dielectric constant measurements. Very interestingly, the photothermal activation strategy used in this work enables a direct patterning of the thin film like photolithography. We find that both a cluster spacing and degree of polymerization in the zirconium-oxo cluster molecular assembly can be well modulated by photothermal processing conditions. We demonstrate that the photothermally activated zirconium-oxo cluster thin film can be successfully applied to a gate dielectric material for thin-film field-effect transistors with different active layers. We believe that the photothermal activation strategy in this work allows a variety of metal-oxo cluster materials to be a promising dielectric material system for soft electronic applications, which could be generalized to other material systems.

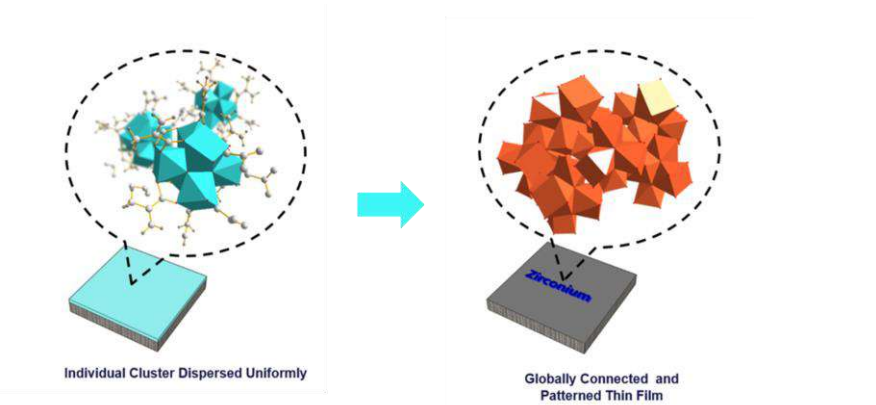

Fig. 1. Schematic description of zirconium-oxo cluster thin film fabrication

References

1. Liu, J.X., et al., Bandgap Engineering of Titanium-Oxo Clusters: Labile Surface Sites Used for Ligand Substitution and Metal Incorporation. Angewandte Chemie-International Edition, 2016. 55(17): p. 5160-+.
2. Rozes, L. and C. Sanchez, Titanium oxo-clusters: precursors for a Lego-like construction of nanostructured hybrid materials. Chemical Society Reviews, 2011. 40(2): p. 1006-1030.
3. Schubert, U., Cluster-based inorganic-organic hybrid materials. Chemical Society Reviews, 2011. 40(2): p. 575-582.

Large-Area Micro and Nanoelectronics Manufactured at a Flash

Thomas D. Anthopoulos
King Abdullah University of Science and Technology (KAUST), KAUST Solar Centre, Thuwal 23955-6900, Kingdom of Saudi Arabia
Tel.: +966-12-808-7283, E-mail: thomas.anthopoulos@kaust.edu.sa

In traditional electronics the ability to downscale critical dimensions of its building block, the transistor, has proven extremely successful in advancing the computational power of modern-day microelectronics. However, adopting established techniques for the manufacturing of emerging technologies, such as large-area printed electronics, has proven challenging both in terms of technology and economics. Despite the difficulties, however, these new forms of electronics have been gaining ground, transforming both the research & development landscape as well as the broader marketplace of electronics and the manufacturing infrastructure behind them. In this talk I will focus on progress being made downscaling emerging forms of large-area electronics through new materials and fabrication paradigms and their application in the ever expanding device ecosystem of the future.

High-Mobility TFTs Based on Zinc Oxynitride: Beyond Backplane for Display

Hyun-Suk Kim
Dept. of Materials Science and Engineering, Chungnam National University,
99 Daehak-ro, Yuseong-gu, Daejeon 34134, Korea
Tel.:82-42-821-6634, E-mail: khs3297@cnu.ac.kr

Increasing demands for high-performance switching or driving transistors in the display industry have led to the development of amorphous oxide semiconductors (AOSs) such as In-Ga-Zn-O (IGZO)[1]. Thin-film transistors (TFTs) based on a-IGZO semiconductor exhibit relatively high field-effect mobility (> 10 cm^2/Vs) compared to the a-Si based TFTs, and IGZO TFTs are suitable for the large size and high-resolution active matrix light-emitting diode (AMOLED) panels. However, for the next-generation display applications, the performance of TFT devices should be further improved. In particular, the higher field-effect mobility characteristics comparable to the low-temperature polycrystalline silicon (LTPS) TFTs (> 50 cm^2/Vs)[2] is strongly required.

In this regard, Zinc oxynitride (ZnON) is a prospective semiconductor that fulfills the demands for next-generation display applications. ZnON has unique characteristics, such as high mobility (> 50 cm^2/Vs), and superior stability under bias/illumination stress, compared with the conventional AOSs[3]. Therefore, TFTs with ZnON semiconductors were intensively researched by controlling the annealing conditions[4], anion/cation doping[5,6], and changing oxygen/nitrogen composition ratio[7], etc. Based on these advantages, ZnON could be utilized to not only switching/driving TFTs for display backplane but also high-speed electronic applications which require high mobility and reliability.

In this study, various ZnON-based electronic devices were investigated with the optimization of ZnON TFTs. First, the electrical characteristics of ZnON TFTs were optimized through the heterojunction active layer formation using a thin ZnF_2 layer (ZnF_2/ZnON active layer). As a result of the interaction between ZnF_2 and ZnON, the TFTs with ZnF_2/ZnON active layer exhibited improved transfer characteristics and stability compared to ZnON TFTs without ZnF_2 thin layer. Next, the high-frequency operation of ZnON TFTs was studied using a pulsed-gate signal (> 100 kHz) for potential high-speed switching applications such as ultrasonic detectors. Finally, the complementary metal oxide semiconductor (CMOS) inverter devices was demonstrated by combining n-type ZnON and p-type tellurium (Te) devices. Te is a promising material as high mobility p-type semiconductors that could overcome the limitations of p-type oxide semiconductors (e.g., low field-effect mobility, high off-state current, etc.). Furthermore, The electrical characteristics of ZnON/Te CMOS inverter was evaluated by changing the device configuration.

Acknowledgment

This work was mainly supported by the National Research Foundation of Korea (NRF) through the Ministry of Education (Grant no: NRF-2019R1I1A2A01064153, NRF-2021M3F3A2A03017873).

References

1. K. Nomura et al, *Nature*, vol. 432, p. 488 (2004).
2. T. Arai, *J. Soc. Inf. Display*, vol. 20, p. 156 (2012).
3. H.-S. Kim et al, *Sci. Rep.*, vol. 3, p. 1459 (2013).
4. J. Park et al, *J. Alloys Compd.*, vol. 688, p. 666 (2016).
5. H.-D. Kim et al, *ACS Appl. Mater. Interfaces*, vol 9. p. 24688 (2017).
6. A. Song et al, *Sci. Rep.*, vol. 10, p. 719 (2020).
7. J. Park et al, *Sci. Rep.*, vol. 6, p. 24787 (2016).

The oxide and oxynitride semiconductor and its TFTs for display application

Hyun-Jun Jeong[1] and Jin-Seong Park[1]
[1]**Division of Materials Science and Engineering, Hanyang University, Seoul 04763, Korea**
Tel.:82-2-2220-0401, E-mail: mse_hyunjun@naver.com

In the modern electronic devices need extremely high-performance such as high-reolution (> 8K), high frame rate (>120 Hz) operation, and form-factor free to satisfy the diverse need and experience of customers. The list of future display is anticipated such as virtual/augmented display (VR/AR), fully-flexible display that possible to stretching user's need, automobile display and multi-function device that allows users to explore health information in real time.

Despite of its myriad application, various technical issues are solved first. **Figure 1** illustrates the requirement of technologies for future display. Especially, TFT backplane has many problems such as fabrication temperature, TFT mobility and instability, defects control and device intgration. Amorphous silicon (a-Si), low-temperature polycrystalline silicon (LTPS), oxide semiconductor and oxynitride semiconductor are candidated for future-display backplane active materials. Among these candidates, oxide and oxynitride semiconductor has strong advantages, for example, moderate field effect mobility (> 10 ~ 50 cm^2/Vs), extremely low off-current (especially oxide semiconductor, it is not detected dut to detect limit of device), large-area uniformity for mass-production.

In this talk, we introduce the oxide and oxynitride semiconductor and its TFTs for display application. Our presentation is divided in 3 parts 1) ALD-based oxide semiconductor and its TFTs, 2) flexible oxide TFTs and 3) oxynitride semiconductor and its TFTs. These technologies are expected to be key technologies that can solve the problems facing future displays.

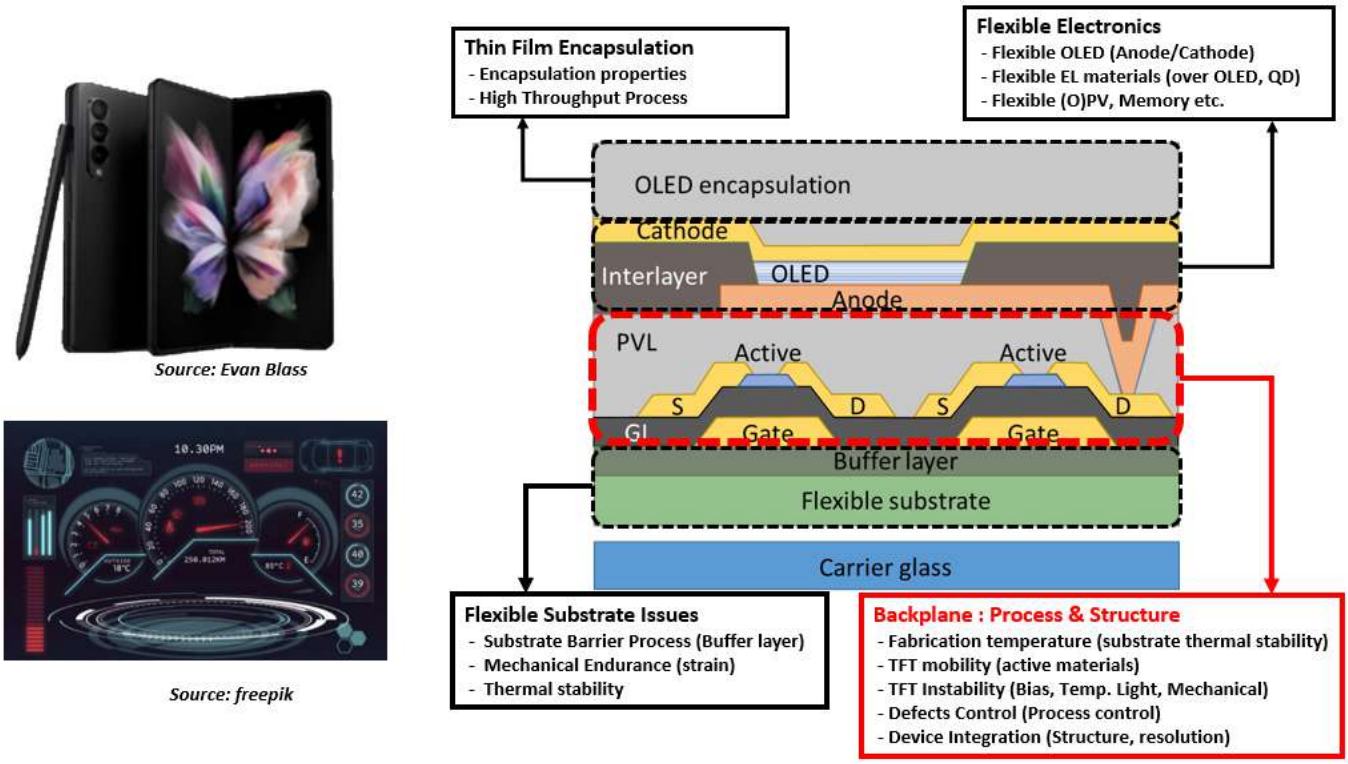

Fig. 1. Requirement of techniques for future display

Acknowledgment

This research was supported by the MOTIE (Ministry of Trade, Industry & Energy), project number #20006400. This research was also supported by the National Research Foundation of Korea (NRF) funded by the Ministry of Science and ICT (NRF-2020M3H4A3081867)

Substrate Biasing Approach to Generate Artificial Oxygen Vacancy for Stable Nitrogen-Doped IGZO Thin-Film Transistors

Jueun Kim, Seongmin Park, Gilsu Jeon, Suwon Seong and Yoonyoung Chung
Department of Electrical Engineering, POSTECH, Pohang, Gyeongbuk 37673, Korea
Tel.:82-54-279-2225, E-mail: ychung@postech.ac.kr

Amorphous indium gallium zinc oxide (a-IGZO) thin-film transistors (TFTs) have been widely used as switching and driving elements for flat-panel displays due to its large-area uniformity, low-temperature process, and high field-effect mobility. However, instability under bias and temperature stresses are still problematic, requiring complex compensation circuitry.

Recently, nitrogen-doped a-IGZO has been suggested to improve the stability of TFTs by filling oxygen vacancies (V_O) with stable metal-nitrogen (M-N) bonding [2]. However, the insufficient N doping concentration is known to limit the effects on the TFT stability.

In this study, we propose a novel approach to improve the stability of a-IGZO TFTs by increasing the density of M-N bonding. We increased the V_O density by applying a substrate bias during a-IGZO sputtering, followed by N_2 plasma treatment to fill the V_O with nitrogen. Generation of V_O was confirmed by negative V_{TH} shift and persistent photoconductivity. As shown in Fig. 1b, a-IGZO:N TFT with substrate bias exhibited a much smaller V_{TH} shift under positive bias stress condition, compared to conventional IGZO TFT. This result demonstrates that the increased M-N bonding by substrate bias significantly improves the stability of a-IGZO TFTs.

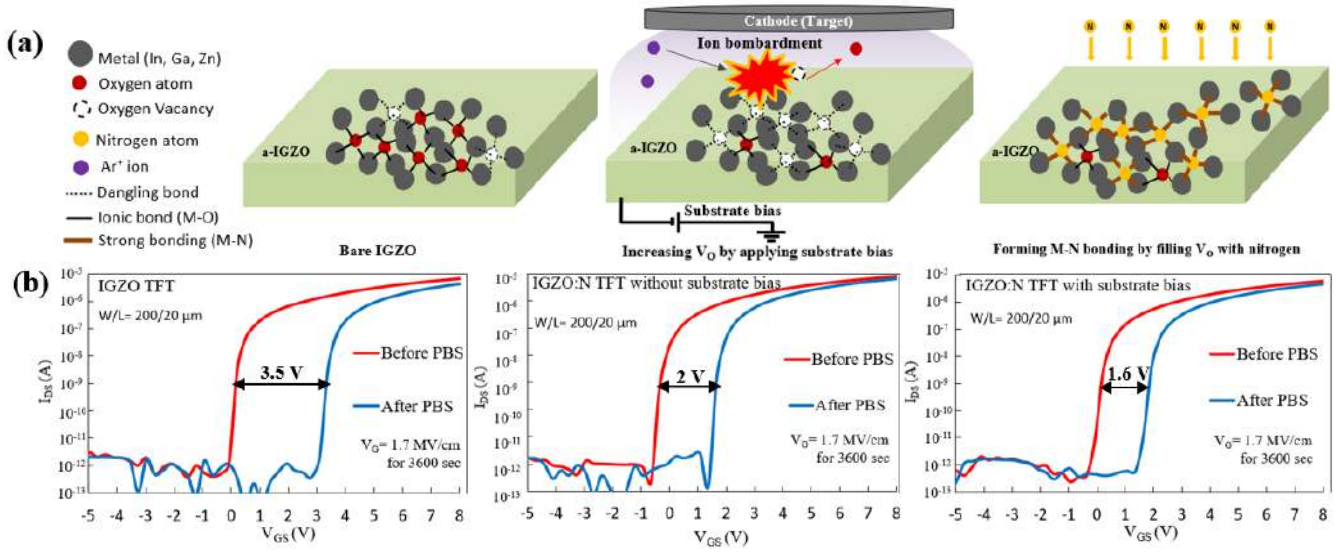

Fig. 1. (a) Schematic diagrams of α -IGZO thin film. (b) V_{TH} shift under PBS.

We significantly improved the stability of a-IGZO TFT by generating oxygen vacancies with substrate bias during sputter deposition and filling them with nitrogen with post plasma treatment. With this approach, a-IGZO:N TFTs with improved stability can be achieved to guarantee an improved product lifetime.

Acknowledgment

This research was supported by the national R&D program through National Research Foundation funded by Ministry of Science and ICT (2020M3F3A2A02082437) and Basic Science Research Program through the National Research Foundation of Korea funded by the Ministry of Education (2018R1D1A1A02086266).

References

1. Seyeoul Kwon et al., *Electrochem. Solid-State Lett.*, **12**, H278 (2009).
2. Haiting Xie et al., *Results. Phys.*, **11**, 1080 (2018).
3. K. Park et al., *IEEE Trans. Electron Devices*, **66**, 1, 457 (2019).

$MASnI_3$-based perovskite transistors and inverters

*Huihui Zhu, Ao Liu, Taoyu Zou, Youjin Reo, and Yong-Young Noh**

Department of Chemical Engineering, Pohang University of Science and Technology, 77 Cheongam-Ro, Nam-Gu, Pohang 37673, Republic of Korea

*Corresponding author: Y. Y. Noh (yynoh@postech.ac.kr)

The fields of solar cells, light detection and emission have experienced tremendous activities in recent years with the advent of organic-inorganic metal halide perovskite (MHP) semiconductors.[1] Yet, there have been far fewer reports of perovskite-based thin-film transistors (TFTs), mainly two kinds up to now: 3D Pb- and 2D Sn-based perovskites TFTs.[2] The former kind suffers from Pb toxicity and high off-state originating from balanced ambipolar character; in the latter, the bulky/insulating organic layers can limit carrier transport. Combining the isotropic 3D structure with stronger p-channel transport of Sn halide perovskites, we develop a 3D Sn-based perovskite platform of $MASnI_3$ that can realize demanding high-performance p-channel TFTs via halide anion engineering. Chloride additives increase film quality and decrease defect density by regulating crystallization kinetics. The optimized TFTs based on $MASn(I_xCl_{1-x})_3$ exhibit high hole mobilities of ~10 $cm^2 V^{-1} s^{-1}$ and on/off current ratio over 10^7 at room temperature with high operational stability and reproducibility, and when combined with n-channel metal oxide TFTs, yield complementary inverters with remarkable gain over 100. This work shines a light on the use of MHPs in low-cost solution-processable electronic circuits beyond solar cells and LEDs. Although the role perovskites, which have lingering concerns over ambient stability, can play commercially remains to be seen,[3] it will be intriguing to see how close perovskite TFTs may reach to their intrinsic performance limits.[4]

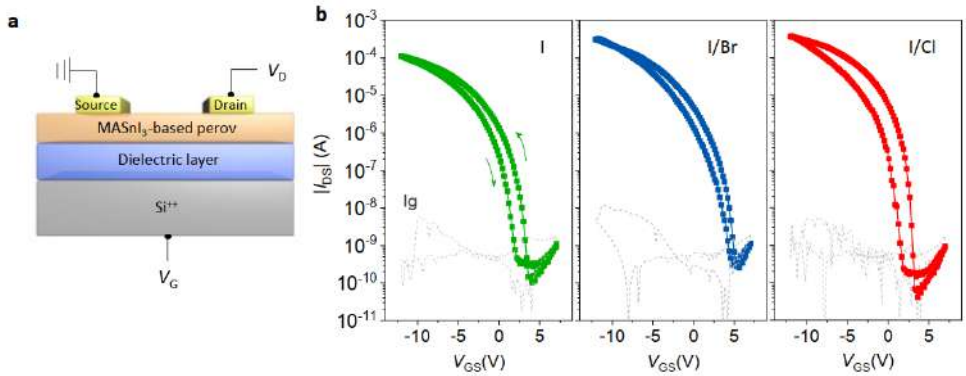

Fig. 1. (a) $MASnI_3$-based perovskite TFT configuration. (b) Transfer characteristics of $MASnI_3$, $MASn(I_xBr_{1-x})_3$, and $MASn(I_xCl_{1-x})_3$ TFTs.

Acknowledgment

This study was supported by Ministry of Science and ICT through the National Research Foundation, funded by the Korean government (2017R1E1A1A01075360, 2020R1A2C4001617, 2020R1A4A1019455, 2020M3F3A2A01085792). This research was also supported by the Samsung Display Corporation.

References

1. Sum, T.-C.; Mathews, N., *Halide Perovskites: Photovoltaics, Light Emitting Devices, and Beyond*. Wiley-VCH: 2019.
2. Zhu, H.; Shin, E. S.; Liu, A.; Ji, D.; Xu, Y.; Noh, Y. Y., Printable Semiconductors for Backplane TFTs of Flexible OLED Displays. *Adv. Funct. Mater.,* Vol.n/a, pp. 1904588 (2019).
3. Shining a light on perovskite devices. *Nat. Electron.,* Vol.3, pp. 657 (2020).
4. Zhu, H.; Liu, A.; Noh, Y.-Y., Perovskite transistors clean up their act. *Nat. Electron.,* Vol.3, pp. 662 (2020).

Tunable Light-Matter Interactions in Excitonic Semiconductors

Deep Jariwala[1]

[1]Department of Electrical and Systems Engineering, University of Pennsylvania

Abstract:

The isolation of stable atomically thin two-dimensional (2D) materials on arbitrary substrates has led to a revolution in solid state physics and semiconductor device research over the past decade. A variety of other 2D materials (including semiconductors) with varying properties have been isolated raising the prospects for devices assembled by van der Waals forces.[1] Particularly, these van der Waals bonded semiconductors exhibit strong excitonic resonances and large optical dielectric constants as compared to bulk 3D semiconductors. .

First, I will focus on the subject of strong light-matter coupling in excitonic 2D semiconductors, namely chalcogenides of Mo and W. Visible spectrum band-gaps with strong excitonic absorption makes transition metal dichalcogenides (TMDCs) of molybdenum and tungsten as attractive candidates for investigating light matter interaction and applications as absorbing media in opto-electronics.[2, 3] We will present our recent work on the fundamental physics of light trapping in multi-layer TMDCs when coupled to plasmonic substrates. We systematically demonstrate via calculations and matching experiments that the presence of strong excitonic resonances in multilayers (< 20 nm thickness) combined with surface plasmon excitations of the nearby metals can achieve strongly coupled modes with apparent voided crossings in reflectance spectra.[4]

Next, we will show the extension of these results to multilayers and superlattices of excitonic chalcogenides with alternating layers of boron nitride and aluminum oxide. These hybrid multilayers offer a unique opportunity to confine light in < 3 nm thick direct band gap absorbers over cm^2 scale areas.[5] We will discuss the physics of strong light-matter coupling and applications of these multilayers. Finally, we will also present our recent and on-going works on tunable light-matter interactions in hybrid organic-inorganic perovskites[6] where we observe exciton-polariton hybrid state emission at room temperatures in an external cavity-less geometry. Finally, I will also present our recent work on giant gate-tunability of optical constants in the telecom band in thin-films of high purity, semiconducting, carbon nanotubes.[7] Our results highlight the vast opportunities available to tailor light-matter interactions in quantum confined materials in simple and practical designs enabling study of novel photonic phenomena and presenting avenues for practical technologies.

References:

1. Jariwala, D. et al. *ACS Nano* **2014,** 8, (2), 1102–1120.
2. Jariwala, D. et al. *ACS Photonics* **2017,** 4, 2692-2970.
3. Brar, V. W.; Sherrott, M. C.; Jariwala, D. *Chemical Society Reviews* **2018,** 47, (17), 6824-6844.
4. Zhang, H. et al. Jariwala, D. *Nature Communications* **2020,** 11, (1), 3552.
5. Kumar, P. et al.Jariwala, D. *arXiv:2103.14028* **2021,** arxiv.
6. Song, B. et al. Jariwala, D. *ACS Materials Letters* **2021,** 3, (1), 148-159.
7. Song, B. et al. Jariwala, D. *ACS Photonics* **2020,** 7, (10), 2896-2905.

Two-Dimensional Organic-Inorganic Hybrid Perovskite Field-Effect Transistors

Letian Dou
Davidson School of Chemical Engineering, Purdue University, USA

Abstract
Two-dimensional halide perovskites are exciting new semiconductors that show great promising in low cost and high-performance optoelectronics devices including solar cells, LEDs, photodetectors, transistors, *etc*. In the first part of this talk, I will present a molecular approach to the synthesis of high-quality organic-inorganic hybrid perovskite quantum wells through incorporating widely tunable organic semiconducting building blocks as the surface capping ligands. By introducing sterically tailored groups into the molecular motif, the strong self-aggregation of the conjugated organic molecules can be suppressed, and single crystalline organic-perovskite hybrid quantum wells and superlattices can be easily obtained via one-step solution-processing. This conjugated ligand design greatly enhances materials chemical stability and suppresses halide anion migration. Based on this, we demonstrate for the first time an epitaxial halide perovskite heterostructure with near atomically-sharp interface. Finally, we demonstrate stable FETs with hole mobilities ~ 10 cm^2/Vs and on/off ratio over 10^6 using the novel 2D hybrid materials.

Patterning of Photosensitive Perovskite Materials on IGZO TFT Arrays for Imaging Applications

***Hang Zhou*[1]**
[1]School of Electronic and Computer Engineering, Peking University Shenzhen Graduate School, Peking University, Shenzhen, 518055, China
Tel.:86-755-26036997, E-mail: zhouh81@pkusz.edu.cn

Low cost organolead halide perovskite materials, with their outstanding optoelectronic properties, provide new opportunities for developing highly sensitive photodetectors for various sensing scenarios, ranging from UV, Infrared to X-ray imaging. To realize high-resolution imaging, pixel separation is necessary for reducing crosstalk between neighboring pixels. Here, the development of perovskite patterning techniques is reviewed. In particular, the development of patterned hybrid perovskite/IGZO phototransistor is discussed. Heterogenous integration of oxide TFT with an organolead halide perovskite photoabsorbing layer is an attractive approach for developing low noise sensors. In theory, a wide spectral response and an ultralow low dark current can be achieved in one single phototransistor device at the same time. Nonetheless, the performance of oxide TFT is usually affected by the perovskite deposition process, leading to a high off current. By inserting an interlayer between the patterned MAPbI3 and IGZO, or by adoption of quasi-two-dimensional perovskites, the negative impact on the IGZO TFT performance can be suppressed. Assisted by a low temperature oxide encapsulation layer, the perovskite photoabsorbing layer can also be patterned by conventional photolithography techniques. Via optimisation, perovskite-IGZO phototransistors with channel length of less than 10 μm can be fabricated. The patterned phototransistor achieves a suppressed off-state drain current of ~10 pA, a high responsivity of larger than 10^3 A/W, and a detectivity of greater than 1×10^{14} Jones.

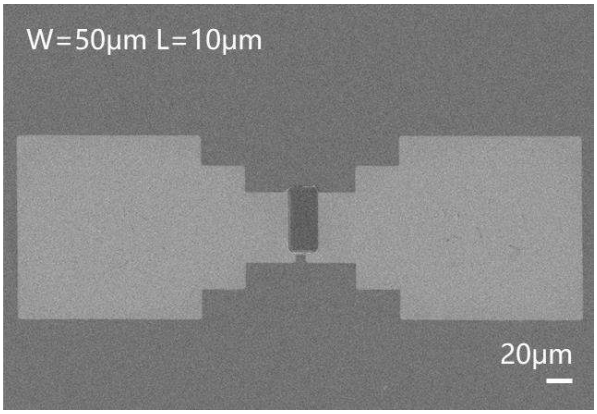

Fig. 1. A perovskite/IGZO phototransistor with channel length of 10 μm and a perovskite photosensitive capping layer with length of 20 μm

Acknowledgment

This work is financially supported by the National Natural Science Foundation of China(61974006), Guangdong Natural Science Foundation (2018A030313332) and the The Shenzhen Municipal Scientific Program (JCYJ20200109140610435,ZDSYS201802061805105).

References

1 . X.Xu, L.Yan, et al., ACS Applied Materials & Interfaces, 2019, vol.10, pp.44144-44151
2 . Y . Tan,B.Xiang,T.Zou,C.Liu, K.Wang,J.Chen,H. Zhou,2020,4th IEEE Electron Devices Technology & Manufacturing Conference (EDTM), 2020, pp. 1-3
3. T. Zou et al., IEEE Journal of the Electron Devices Society, 2021, vol. 9, pp. 96-101

2D Organic Crystals and Their Applications

Yun Li
School of Electronic Science and Engineering, Nanjing University, Nanjing, Jiangsu 210093, China
Tel.:86-25-83686164, E-mail: yli@nju.edu.cn

Recently, we are interested in 2D organic crystals with in-plane vdW forces among molecules that possess unique characteristics for electronic applications. We successfully developed methods for fabricating 2D organic semiconducting crystals with precise layer definition. Field-effect transistors (FETs) yielded excellent performance with high carrier mobility. And their applications have been well extended to ferroelectric memories, ultrafast UV phototransistors, and optically modulated artificial synapses. Moreover, since 2D organic semiconducting crystals possess highly ordered molecular packing and disorder-free structures, they exhibit novel interfacial effects, also serving as platforms for studying interesting device physics.

References

1. Advanced Materials Technologies, 2019, 4, 1800182.
2. Advances in Physics: X, 2020, 5, 1747945.
3. Advanced Electronic Materials, 2020, 2000136.
4. ACS Applied Materials & Interfaces, 2020, 12, 26267.
5. Physical Review Materials, 2020, 4, 044604.

Film Cinematic Sound OLED

Chiwan Kim[1], SeungRyull Park[1], Sungwook Ko[1], YongWoo Lee[1] and JounHo Lee[1], JeomJae Kim[1], SooYoung Yoon[1]
[1]Dept. of Material Research, LG Display, LG Science Park, Gangseo-gu, Seoul 07796, Korea
Tel.:82-2-3773-1114, E-mail:ailsherazard@lgdisplay.com

Piezoelectric materials have special properties that convert mechanical energy into electrical energy and vice versa. They have long history on research and commercial applications such as medical, military, industrial appliance and so on. (actuating devices, sensors and energy harvesters) Despite many researches, It can not be studied for speaker application a lot.

LG Display has shown Cinematic Sound OLED(CSO) technology for TV in many different tech shows. The OLED TV has a thin and light panel suitable for an actuating panel. CSO TVs offer great value to customers compared to normal speaker. The CSO TV generates directly sound on Panel. In the Figure1. CSO TV makes customers to feel actual sound that matches display image, but normal speakers can not match the image&sound because of reflected sound. In samll size TV, People may not be aware of it in common situation watching TV. however, The larger the panel, the more severe the mismatch between image and sound. We can give customer a better user-experience by a more natural sound system.

The 1st generation CSO TV product was made of the voice coil motor. It can be called coil-type CSO. It would be achieve higher speaker performance than normal speaker (sound pressure level, frequency range). However, voice coil is limited by their mass and thickness on OLED or POLED form factor TV.

The 2nd generation CSO TV product was made of film type actuator, which is Film CSO. It's very thin and light feature. In the figure 2. Large size Wallpaper TV is very large and thin, conventional speaker and coil type CSO is hard to apply to panel. In order to develop film type CSO, We focus on a piezoelectric material research. Typical piezoelectric module is small size and thicker. So, It was impossible to commercialize before. Our state of the art film CSO has the highest piezoelectricity, large dimension size and thin thickness. We do make the new and excellent panel speaker system in the display industry.

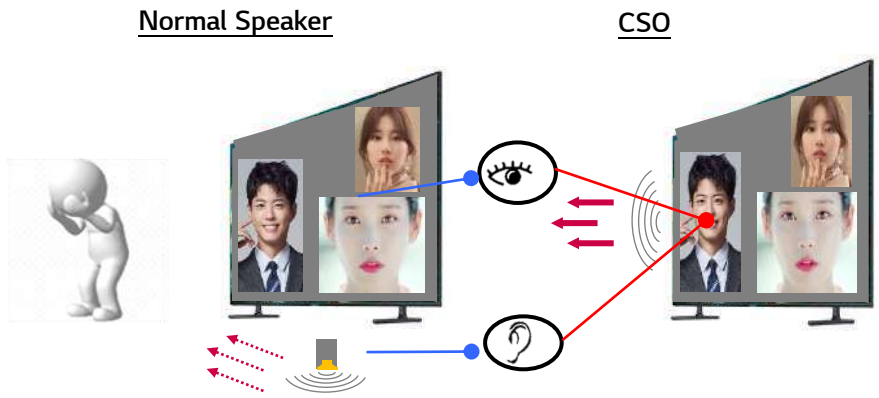

Fig. 1. Comparison of Normal speaker vs CSO

Fig. 2. OLED Wall Paper

Acknowledgment

References

Highly Sensitive Pyramid-Plug Shaped Tactile Sensor for Detecting External Mechanical Stresses

Daehwan Choi[1], Taehoon Sung[1], and Jang-Yeon Kwon[1]
[1]**School of Integrated Technology, Yonsei University, Incheon, Republic of Korea**
Tel.:82-32-749-5916, E-mail: jangyeon@yonsei.ac.kr

Biological skin is an ideal electronic sensory system, and it contains a variety of neural mechanoreceptors for the ionic mechanotransduction that sense to various external stimuli such as pressure, shear, torsion vibration, and temperature. One of the most important capability of sensors that try to mimic the multifunctional properties of the biological skin is detecting and discriminating different types of external mechanical stimuli such as normal, shear and torsional stress. Here, we demonstrate a pyramid-plug structure for highly sensitive tactile sensor that enables to detect and discriminate the above-mentioned external mechanical stimuli.

The device is composed of pyramid-patterned ionic gel inspired by neural mechanoreceptor and engraved electrodes. Due to the pyramid-plug shape, the deformation mechanism is different for each type of external mechanical stimuli. As shown in **Figure 1**, The sensor provided high sensitivities of 1.93 kPa^{-1}, 29.88 N^{-1}, and 3.39 $N{\cdot}cm^{-1}$ and large detection range that is capable to cover wide range of tactile stresses that is induced during daily activity. Moreover, it is noted that this tactile sensor can function with two different transduction modes (capacitive and piezoresistive). We show that the tactile sensor can be used to monitor the change in electrical signals ranging from human breathing to an arbitrary multiplex human touching.

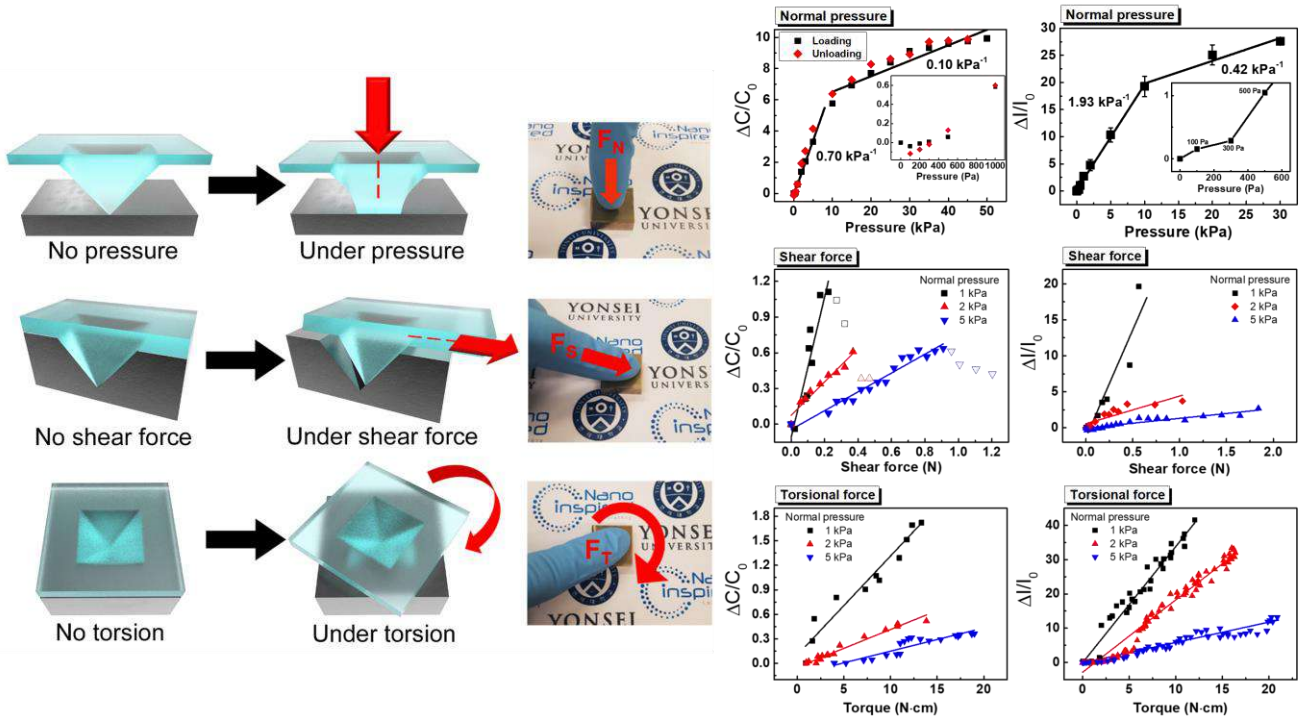

Fig. 1. Type of external forces and according sensitivity graphs

References

1. P. Delmas, et al. Molecular mechanisms of mechanotransduction in mammalian sensory neurons. Nature Reviews Neuroscience 12, 139-153 (2011).
2. S. S. Ranade et al. A. Mechanically Activated Ion Channels. Neuron 87, 1162-1179 (2015).
3. J. Park et al. Tactile-Direction-Sensitive and Stretchable Electronic Skins Based on Human-Skin-Inspired Interlocked Microstructures. Acs Nano 8, 12020-12029 (2014).
4. M. L. Jin et al. An Ultrasensitive, Visco-Poroelastic Artificial Mechanotransducer Skin Inspired by Piezo2 Protein in Mammalian Merkel Cells. Advanced Materials 29, 9 (2017).

Antenna-on-Display (AoD): Latest Developments and Future

Wonbin Hong
[1]Dept. of Electrical Engineering, POSTECH (Pohang University of Science and Technology), Pohang, 37673 Korea
Tel.:82-54-279-2366, E-mail: whong@postech.ac.kr

Electronic devices equipted with high-resoluations display panels with the capability of high-speed, low-latency wireless communication are becoming increasingly popular. State-of-the-art wireless generations such as 5G, ultra-wideband (UWB), Wi-Fi 6 will rely on the implementation of efficient and intelligent radio antennas. However, the evolution of display panels such as foldabble, stretchable, bezeless and large-screen displays have triggered the need to reevaluate antenna design strategies and methodologies. Classical antenna theory professes the radiation efficiency of an antenna to be proportional to the effective antenna volume. Given the fact that conventional antennas have been designed and implemented as indepement components, antenna radiation and peformance suffers as the antenna real esate is further decreased amid the increased portion of display panels within a device. This eventually leads to performance degradation of wireless devices which use the latest display panel technologies.

This paper introduces the original concept of incorporating a transparent, optically invisible antenna circuitry within the display panel. Denoted as an Antenna-on-Display (AoD), this approach demonstrates that electromagnetic fields can be generated and controlled within the view area of the display. Similar to a touch sensor layer, the newly devices antenna layer can be integrated indepdently or combined with conventional touch sensor layers without any additional thickness or fabrication process. The AoD allows the effective volume of the antenna to be maximized leading to enhanced wirelss performance. This concept is applied and demonstrated across a variety of different wireless standards such as GPS, Wi-Fi and millimeter-wave 5G for real-life smartwatch and smartphone devices [1-3] as it can be observed in Fig. 1. This demonstration serves as a starting point for a new class of multifunctional display panels for future devices.

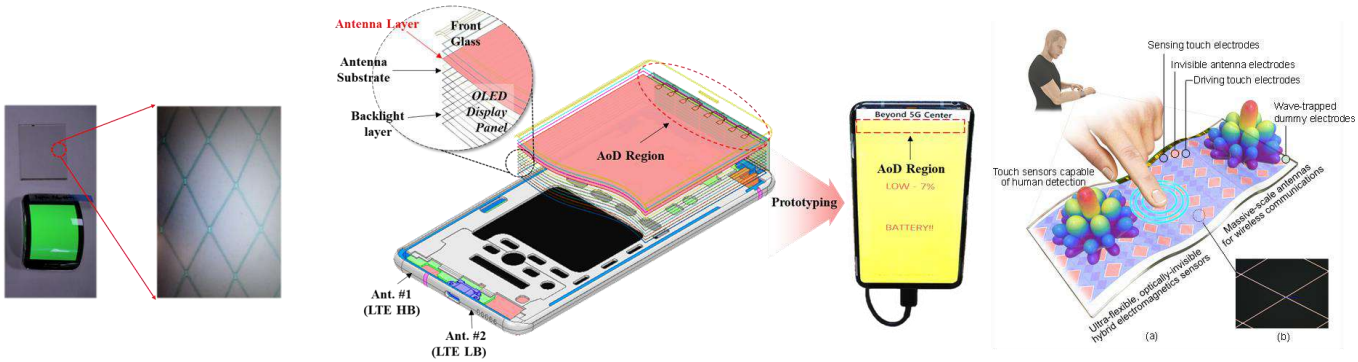

Fig. 1. Demonstration examples of Antenna-on-Display [1-3]

Acknowledgment

This work was supported in part by the Institute of Information and Communications Technology Promotion (IITP) grant funded by the Korean Government (MIST) under Grant 2020-0-00858

References

1. W. Hong, S. Lim, S. Ko and Y. G. Kim, "Optically Invisible Antenna Integrated Within an OLED Touch Display Panel for IoT Applications," in *IEEE Transactions on Antennas and Propagation*, vol. 65, no. 7, pp. 3750-3755, July 2017, doi: 10.1109/TAP.2017.2705127.
2. W. Hong, J. Choi, D. Park, M. Kim, C. You, D. Jung and J. Park, "mmWave 5G NR Cellular Handset Prototype Featuring Optically Invisible Beamforming Antenna-on-Display," in *IEEE Communications Magazine*, vol. 58, no. 8, pp. 54-60, August 2020, doi: 10.1109/MCOM.001.2000115.
3. J. Park, D. Park, M. Kim, D. Jung, C. You, J. Lee and W. Hong, "Circuit-on-Display: A Flexible, Invisible Hybrid Electromagnetic Sensor Concept," in IEEE Journal of Microwaves, vol. 1, no. 2, pp. 550-559, Spring 2021, doi: 10.1109/JMW.2021.3063510.

Ultra-flexible Bimodal Sensor-based High-resolution Tactile Interfaces for Immersive Interactive Display

Hanbit Jin[1], Yunjeong Kim[1], Wooseup Youm[1], Yulim Min[3], Bocksoon Na[1], Seyoung Kwon[2], Gyeongseok Park[2], Chan-Hwa Hong[1], Chanwoo Park[1], Steve Park[2], Hye Jin Kim[1,3]
[1]Electronics and Telecommunications Research Institute (ETRI), Daejeon, Korea
Tel.:82-42-860-6152, E-mail: nolawara@etri.re.kr
[2]Korea Advanced Institute of Science and Technology (KAIST), Daejeon, Korea
[3]University of Science and Technology (UST), Daejeon, Korea

Interactive tactile displays are drawing tremendous attentions due to the growing demand for an immersive user experience (UX) that can provide virtual tactile interactions beyond the conventional visual and auditory media. Tactile sensor is a basic element for the interactive tactile display, especially, flexible tactile sensors are expected to open up an emerging field of applications such as wearable tactile displays for extended reality (XR), robotic prosthetics and haptic communications. Previous studies have demonstrated flexible pressure sensors to record spatiotemporal tactile stimuli as similar as possible to human mechanoreceptors[1,2,3]. However, major challenges still remain in simultaneous sensing of static/dynamic pressures with high spatial resolution. In addition, thick multi-layered structures for bimodal pressure sensing are restricting their mechanical flexibility. Here, we report ultra-flexible bimodal tactile sensor array which can discriminate static and dynamic pressure with 1 mm-pitch spatial resolution. The sensor array is thin and flexible enough to conformably laminate on curvilinear surface (Fig.1. a-d). To realize human-like tactile sensing, 64-channel static and dynamic pressure sensors in total are densely packed on a 2 um-thick polyimide substrate. PVDF-TrFE film are dry-etched in a chess board pattern for piezoelectric dynamic pressure sensing which has a fast response time of 0.25 ms. And polypyrrole grafted micropyramid structure PDMS sheet is stacked on interdigit electrode array for piezoresistive static pressure sensing which has a sensitivity of 0.6 kPa^{-1} (<30kPa) and 0.27 kPa^{-1} (<50kPa) covering a wide pressure range. The static and dynamic pressures are successfully measured at the same time by the ultra-flexible bimodal tactile sensor array (Fig.1 e-g). Finally, tactile signals recorded from the bimodal sensor array were transferred to the actuator array in real time, and successfully demonstrated the 'record and playback' of tactile information for interactive display (Fig.1 h-k).

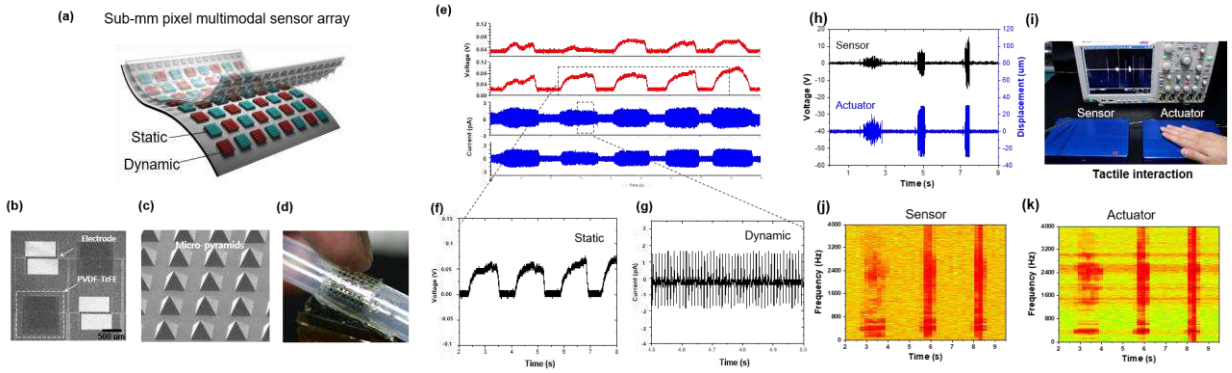

Fig. 1. Ultra-flexible bimodal pressure sensor array and static/dynamic sensing-based tactile interface, (a) schematic of ultra-flexible bimodal sensor array, (b) SEM image of dry-etched PVDF-TrFE and (c) micropyramid structure, (d) ultra-flexible bimodal sensor laminated on a disposable pipette, (e) output voltage of bimodal sensor while static/ dynamic pressures (hand push /100 Hz vibration) are applied, (f) schematic of static/dynamic pressure measurement setup, (g) magnified plot of dynamic pressure, (h) record and playback of tactile information by sensor/actuator, (i) output voltage of sensor and displacement of actuator, (j) STFT results of sensor and (k) actuator.

Acknowledgement

This work was supported by Institute for Information & communications Technology Promotion (IITP) grant funded by the Korea government (MSIT) (Grant No. 2017-0-00048, Development of Core Technologies for Tactile Input/Output Panels in Skintronics and Grant No. 2020-0-00003, Development of High Piezoelectric Coefficient Composite and Ultra-low Power Multilayered Piezoelectric Sensor/Actuator Multi-functional Module).

References

1. J. Park, H. Ko et al, Sci. Adv., 1, e1500661 (2015).
2. S. Chun, C. Choi et al, Nano Lett., 19, 3305-3312 (2019).
3. W. Navaraj and R. Dahiya, Adv. Intell. Syst., 1, 1900051 (2019).

Intrinsically Stretchable, Multimodal Tactile Sensor System based on Ion Relaxation Dynamics

Insang You[1], and Unyong Jeong[2]
[1]Dept. of Chemical Engineering, POSTECH, Pohang 37673, Korea
E-mail: sang4413@postech.ac.kr
[2]Dept. of Materials Science and Engineering, POSTECH, Pohang 37673, Korea

Skin-like, deformable tactile sensor system has been studied for an interactive intelligent system.[1,2] Measuring deformation and temperature profiles at the same time has been rarely achievable.[3] In this work, we propose and demonstrate a new concept of artificial multimodal ionic receptor (AMI-receptor) which can detect the thermal and mechanical stimulation simultaneously, from a single sensing unit.[4] The signal decoupling of intrinsically stretchable sensor is achieved for the first time, using the concept of ion relaxation dynamics (**Fig. 1A**). Two variables are derived; the charge relaxation time as a strain-insensitive intrinsic variable to measure absolute temperature (<0.29℃ of temperature error at 50% strain), and the normalized capacitance as a temperature-insensitive extrinsic variable to measure the strain. We propose to acquire ion resistance (*R*) and geometric capacitance (*C*) at only two fixed frequencies, which allows the real-time monitoring of the two variables. Temperature measurement does not request any calibration process and the temperature error at the stretched state is the smallest among the reported values so far.

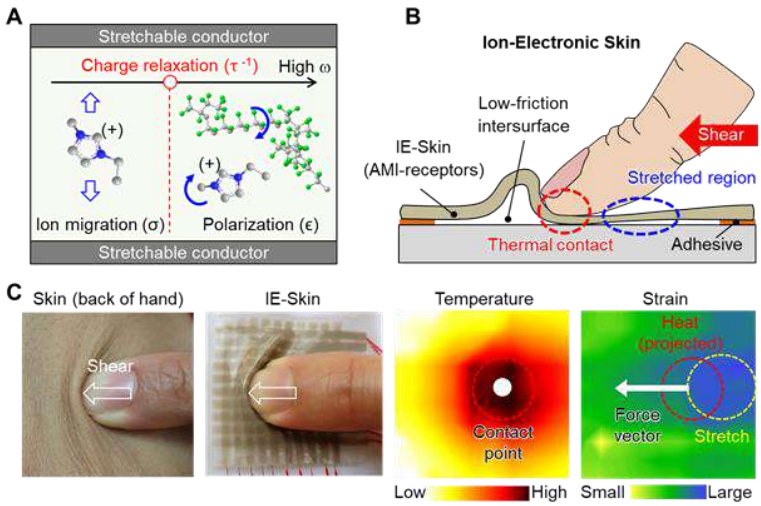

Fig. 1. AMI-receptor and IE-skin. (A) Observable behavior of solid state ionic conductor (AMI-receptor). **(B)** Response of IE-skin to a shear force. **(C)** Camera image, temperature and strain profiles of IE-skin presenting force vector.

We fabricated ion-electronic skin (IE-skin) with the 10×10 matrix of the AMI-receptors. The IE-skin presents 3-dimensional deformation forming wrinkles with the help of a low-friction interface (**Fig. 1B**). Similar with the behavior of the real skin, a single layer of the IE-skin can provide the temperature profile and the strain profile in real-time. The force vector can be estimated by the relative position of contact region and stretched region (**Fig. 1C**). Thus, it is possible to recognize the directions of various tactile motions (pinch, spread, tweak, torsion, etc.) through the derived force vectors. The ability to detect the detailed tactile motions is realized for the first time using the stretchable sensor system and it is expected to help us understand the real tactile sensing mechanisms in human skin.

References

1. T. Someya, and M. Amagai, *Nat. Biotechnol.* 37, 382-388 (2019).
2. G. Cheng *et al.*, *Proc. IEEE* 107, 2034-2051 (2019).
3. F. Zhang, Y. Zang, D. Huang, C.-a. Di, D. Zhu, *Nat. Commun.* 6, 8356 (2015).
4. I. You *et al.*, *Science* 370, 961 (2020).

User interactive display system for integral imaging microscopy using a head tracking camera

Shariar Md Imtiaz[1], Ki-Chul Kwon[1], Oh-Seung Nam[1], Jong-Rae Jeong[2], Seok-Hee Jeon[3], Sang-Keun Gil[4], and Nam Kim[1]

[1]Dept. of Computer and Communication Engineering, Chungbuk National University, Cheongju, Chungbuk 28644, South Korea.

Tel.:82-043-267-8490, E-mail: namkim@chungbuk.ac.kr

[2]Dept. of Information and Communication, Suwon Science College, 288 Seja-ro, Jeongnam-myun, Hwaseong, Gyeonggi 18516, South Korea.

[3]Department of Electronics Engineering, Incheon National University, 119 Academy-ro, Yeonsu-gu, Incheon 22012, South Korea.

[4]Department of Electronics Engineering, Suwon University, 567 17 Wauan-gil, Bongdam-eup, Hwaseong, Gyeonggi 18323, South Korea.

Integral imaging microscopy IIM system with microlens arrays can capture both angular and spatial information from light. Using this capturing process multi-view display is one of the method delivering 3D images. In this case, there are some limitations such as a low resolution, lack of motion parallax, and a narrow viewing angle [1]. We suggest a method for implementing a multi-view display system that provides a real 3D image for IIM system.

Fig. 1 depicts the proposed multi-view display system based on head tracking in this work there are four main parts such as IIM capturing system, stereo image generation, head tracking, and visualize those images in a 3D display. The head position was measured using a depth camera, and the stereo image was projected according to that viewing position. A conceptual capturing system is shown in Fig. 1.

Fig. 1. The proposed head tracking based multi-view display system for an IIM system.

There are 53×53 views in the multi-view pictures that were captured [2]. Converting a single multi-view image to a stereo image is needed to visualize such images in a 3D stereo display screen. It was accomplished by combining two images side by side. A head tracking sensor is attached in front of the viewer, as shown in Fig. 1. The real sense 3D camera application programming interface (API) tracks the position of the head. According to the head position, the processed stereo-view images were projected in a stereo 3D display panel.

Acknowledgment

This work was supported by the National Research Foundation of Korea (NRF) grant funded by the Korea government (NRF 2018R1D1A3B07044041 & NRF 2020R1A2C1101258).

References

1. M. S. Alam, K. C. Kwon, S. M. Imtiaz, J. K. Pan, J. R. Jeong, and N. Kim, In Advances in Display Technologies XI, SPIE, Vol. 11708, p. 117080E (2021).
2. K. C. Kwon, K. H. Kwon, M. U. Erdenebat, Y. L. Piao, Y. T. Lim, Y. Zhao and N. Kim, IEEE Photonics Journal, Vol. 12(4), p. 1-14 (2020).

Electro-Photoluminescence Color Changing System for Interactive Display and Deformable Visual Encryption

Gilwoon Lee[1], Salma Faiz[1], Yebin Park[1], Hyeongseok Choi[1] and Unyong Jeong[1]
[1]Dept. of Materials Science and Engineering, Pohang University of Science and Technology (POSTECH), Pohang, 37673, Korea
Tel.:82-54-279-5431, E-mail: ujeong@postech.ac.kr

We propose a new strategy for radiation-responsive color changes in interactive display. Radiation-responsive color change is often observed in nature. Several studies have attempted to mimic it through photochromic behavior and structural coloring, however, such non-luminous color change works only in bright light condition. If one can create luminous color change it enables long-distance visibility in dark. Surprisingly, the radiation-responsive electroluminous color change has not been investigated so far because most of electroluminescence (EL) materials shows similar colors in photoluminescence (PL).

For the first time, we present a UV-responsive electroluminous color changing system, named electro-photoluminescence (EPL) color change. As a model system, we used the stretchable alternating-current electroluminescence (ACEL). The phosphors in ACEL act simultaneously as the luminophores for EL and PL. We proved that the EL and PL could be controlled independently so that the resulting color change of EPL is predictably tunable. We systematically investigated the EPL chromaticity depending on the ACEL frequency and UV intensity, and revealed that the EPL chromaticity can be controlled by a linear combination of colors by EL and PL. The color changing device is used for deformable dynamic responsive displays, such as visual encryption and decryption of electronic-skin system and UV colorimetric sensor for soft robotic rover. Fig. 1 shows the concept of the UV-responsive EPL color changing system

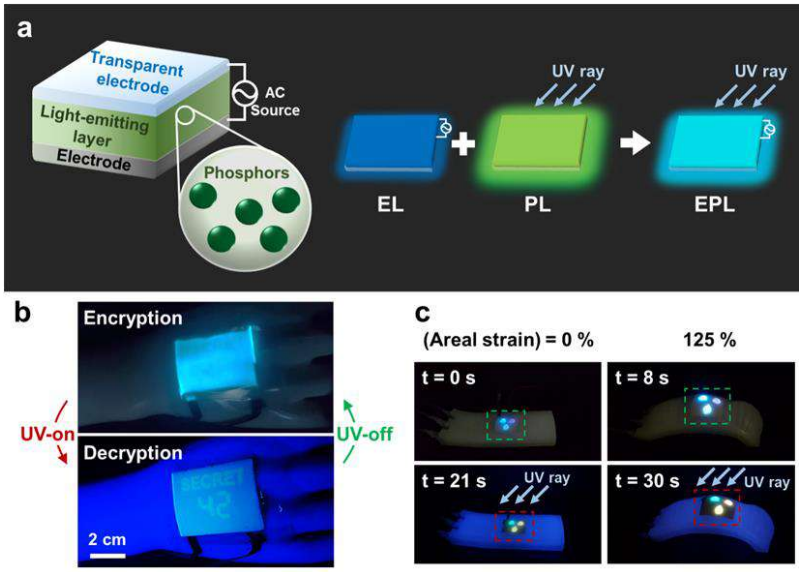

Fig. 1. Radiation-responsive color changes in electro-photoluminescence (EPL). a) Structure and concept of electro-photoluminescence color changing devices, b) Flexible EPL electronic-skin with the encryption and decryption function, c) Soft robotic rover integrated with the deformable EPL color changing device.

References

1. G. Lee, M. Kong, D. Park, J. Park and U. Jeong, *Adv. Mater.*, 32(22), 1907477 (2020).
2. H. Roh, S. Cho, G. Lee, S. Moon, M. Kong, I. You and U. Jeong, *ACS Appl. Mater. Interfaces*, 11(29), 26204-26212 (2019).

Dispersion-engineered Metasurface Components

Wei Ting Chen
[1]AMS sensors, Trenton, NJ 08619, USA
[2]Harvard University, Cambridge, MA 02138, USA
E-mail: weiting.chen@ams.com

Optical dispersion results from the index of refraction of a material varying with the frequency of incident light. Accurate control over this property is crucial in numerous industrial and research applications. For example, it mitigates pulse spreading in optical fibers, which are the backbone of modern telecommunications, enables pulse compression in ultrafast laser optics (2018 Nobel Prize in Physics), and ensures faithful image reproduction in imaging systems by reducing chromatic aberrations. By customizing the geometric parameters of the constituent nanostructures, metasurfaces provide a disruptive way to control dispersion [1]. Specifically, metasurface provides a unique way to control phase, group delay and group delay dispersion. This spurs widespread applications and, in this talk, I will show dispersion-engieered metasurface components for achromatic imaging[2, 3], broadband aberration correction [4] and aberration-corrected spectrometer [5].

References

1. W. T. Chen, A. Y. Zhu, and F. Capasso, "Flat optics with dispersion-engineered metasurfaces," *Nat. Rev. Mater* **5**, 604-620 (2020).
2. W. T. Chen, A. Y. Zhu, J. Sisler, Z. Bharwani, and F. Capasso, "A broadband achromatic polarization-insensitive metalens consisting of anisotropic nanostructures," *Nat. Commun.* **10**, 355 (2019).
3. W. T. Chen, A. Y. Zhu, V. Sanjeev, M. Khorasaninejad, Z. Shi, E. Lee, and F. Capasso, "A broadband achromatic metalens for focusing and imaging in the visible," *Nat. Nanotechnol.* **13**, 220-226 (2018).
4. W. T. Chen, A. Y. Zhu, J. Sisler, Y.-W. Huang, K. M. A. Yousef, E. Lee, C.-W. Qiu, and F. Capasso, "Broadband Achromatic Metasurface-Refractive Optics," *Nano Lett.* **18**, 7801-7808 (2018).
5. A. Y. Zhu, W. T. Chen, J. Sisler, K. M. A. Yousef, E. Lee, Y.-W. Huang, C.-W. Qiu, and F. Capasso, "Compact Aberration-Corrected Spectrometers in the Visible Using Dispersion-Tailored Metasurfaces," *Adv. Opt. Mater* **7**, 1801144 (2019).

Low-Cost Scalable Manufacturing of Dielectric Metasurfaces

***Gwanho Yoon*[1]**
[1]Department of Manufacturing Systems and Design Engineering, Seoul National University of Science and Technology, Seoul 01811, Korea
Tel.:82-2-970-7213, E-mail: gwanho@seoultech.ac.kr

Metasurfaces that consist of subwavelength antenna array have demonstrated many promising applications such as achromatic lenses, high-resolution holograms and subwavelength color printing. Plasmonic metasurfaces suffer from low efficiency in the visible whereas dielectric materials such as titanium dioxide drastically increase efficiency in the whole visible range. However, practical use of metasurfaces is still hindered by limitations of conventional nanofabrication. Since optical metasurfaces require tiny nanostructures which are smaller than the diffraction limit of typical photolithography, most of reported metasurfaces have been demonstrated by electron beam lithography which is not suitable for commercial use due to the extremely low throughput and high cost either. Moreover, dielectric metasurfaces for high efficiency in the visible require highly challenging processes such as atomic layer deposition of over 500-nm-thick titanium dioxide films. These are bottlenecks for practical applications of metasurfaces, and large-scale manufacturing methods are required for commercialization of metasurfaces.

Here, we demonstrate a highly-productive scalable nanoprinting method to manufacture dielectric metasurfaces at low cost. A main idea is that transferred patterns of UV-curable resin from a printing mold directly work as metasurfaces without any secondary operations such as thin film deposition and etching, but the problem is that the refractive index of the typical resin is not high enough for metasurfaces. Therefore, we develop the effective medium of nanoparticle composite (NPC) that consists of high-index dielectric nanoparticle (NP) inclusion in the matrix of UV-curable resin. This hierarchy enables to achieve the sufficiently-high refractive index for metasurfaces. The effective refractive index of the NPC is calculated using an effective medium approximation, and the theoretical prediction agrees well with experimental measurements which confirm that the effective refractive index of the NPC can be increased and controlled by the content of NPs. Experimental demonstration of high-efficiency dielectric metasurfaces including metaholograms [1] and metalenses [2,3] confirms the feasibility of our method that overcomes the bottlenecks in practical use of metasurfaces.

References

1. K. Kim, G. Yoon, S. Baek, J. Rho and H. Lee, *ACS Appl. Mater. Interfaces*, 11, 26109-26115 (2019).
2. G. Yoon, K. Kim, D. Huh, H. Lee and J. Rho, *Nat. Commun*., 11, 2268 (2020).
3. G. Yoon, K. Kim, H. Lee and J. Rho, *ACS Nano*, 15, 698-706 (2021).

High-capacity Optical Data Storage using Orbital Angular Momentum Holography

Jaehyuck Jang[1†], Haoran Ren[2†], Xinyuan Fang[3†], Johannes Bürger[2], Stefan A. Maier[2], and Junsuk Rho[1]*

[1] Department of Chemical Engineering, Pohang University of Science and Technology (POSTECH), 77 Cheongam-Ro, Pohang 37673, Korea

[2]Chair in Hybrid Nanosystems, Nanoinstitute Munich, Koeniginstr. 10, Ludwig Maximilian University of Munich, 80539 Munich, Germany

[3]School of Optical-Electrical and Computer Engineering, University of Shanghai for Science and Technology, Shanghai, 200093, China

([†] Equally contributed) *E-mail:* jsrho@postech.ac.kr

Recent advances in nanophotonics enable to manipulate light at the interface using an array of nanostructures, *i.e.* metasurface. In particular, a metasurface holographic device, consisting of nanoscale structures on a flat surface to manipulate wavefront of light, has great potential toward high-capacity optical data storage due to its small pixel size down to a few hundred nanometers and large field of view. Furthermore, the number of the information channel in metasurface holography has been increased by multiplexing with several optical properties such as polarization [1], wavelength [2], and angle of incidence [2]. However, these properties have a fundamental limitation as information channel, for instance, only two possible spin states of photon and limited bandwidth. Recently, it is reported that orbital angular momentum (OAM), accompanied by the helical phase-front of a vortex beam, can be used as an information carrier [3]. Unlike spin of the photon, helical mode number is theoretically unlimited, thus showing great potential to increase the number of encoded information in optical devices [4]. In this study, we introduce the design principle of OAM-multiplexing holography, and experimentally demonstrate OAM-multiplexing holographic device using three-dimensional metasurface fabricated by laser-based lithography. The fabricated device successfully reconstructs two sets of 101 hologram images in two different focal planes.

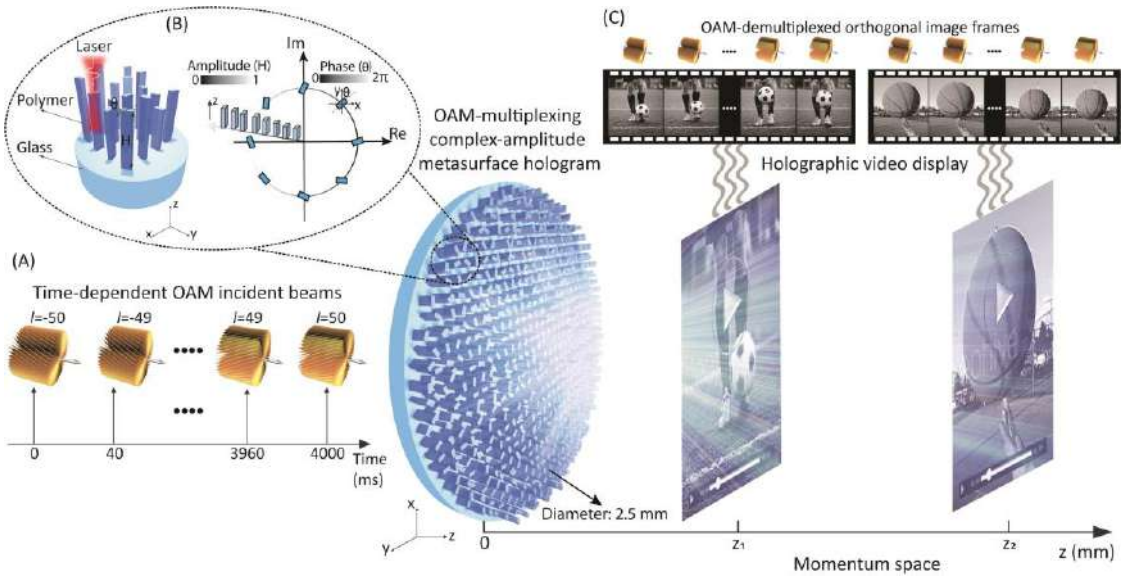

Figure 1. Schematics of OAM-multiplexing holographic device using metasurface

References

1. J. P. Balthasar Mueller, N. A. Rubin, R. C. Devlin, B. Groever, F. Capasso, *Phys. Rev. Lett. 118*, 113901. (2017)
2. X. Li, L. Chen, Y. Li, X. Zhang, M. Pu, Z. Zhao, X. Ma, Y. Wang, M. Hong, X. Luo, *Sci. Adv. 2*, e1601102. (2016)
3. X. Fang, H. Ren, M. Gu, *Nat. Photonics*, *14*, 102. (2020)
4. H. Ren[†], X. Fang[†], J. Jang[†], J. Buerger, J. Rho, and S.A. Maier, *Nat. Nanotechnol.*, 15, 948-955 (2020)

Dynamic meta-holograms with designer liquid crystals for interactive displays and unconventional photonic sensors

Inki Kim[1], Won-Sik Kim[2], Young-Ki Kim[2] and Junsuk Rho[1,2*]

[1] *Department of Mechanical Engineering, Pohang University of Science and Technology (POSTECH), Pohang 37673, Republic of Korea*
[2] *Department of Chemical Engineering, Pohang University of Science and Technology (POSTECH), Pohang 37673, Republic of Korea*
**E-mail address: jsrho@postech.ac.kr*

Computer-generated holography (CHG) involves iterative numerical algorithms to obtain the phase and/or amplitude profiles needed to physically realize holograms. Metasurfaces consist of arrays of subwavelength nanoresonators that can control the wavefront of light in a desired way. They recently proved themselves to be an effective platform for CGH by surpassing the quality of traditional holograms in terms of image resolution and field-of-view. Those metasurface holograms showed prospects not only in imaging and display but also in security applications [1]. In particular, applying metaholograms to anticounterfeiting applications requires not only the technology of encoding multiple pieces of information, but also the manufacturability of highly efficient devices. To meet these complex needs, we have implemented high-efficiency metaholograms based on hydrogenated amorphous silicon (a-Si:H), which realize pragmatic images holograms working under unpolarized light (*e.g.* sunlight or flashlight of cellphone) and spin/direction-multiplexed metaholograms [2-4]. However, 'real-time' active operations of those flat optical devices have remained unresolved yet.

In this abstract, I will discuss our efforts in realizing dynamic metaholograms by leveraging specifically-designed ('designer') liquid crystals that can respond to target external stimuli. First, I will present high-efficiency interactive holographic displays, which can switch holographic images according to external stimuli like voltage, heat and touch sensing [5]. For examples, the voltage-responsive metahologram is able to switch the holographic images within few milliseconds promising for real-time video holographic displays demanding 60 ~ 120 frames/s. Also, the heat or touch-responsive metaholograms can monitor external temperature and impact by visualizing different hologram images according to the pre-programmed external stimuli standard. Such demonstrated systems may permit a diverse range of smart sensing and display applications such as smart hologram labels monitoring temperature/pressure/touch changes and interactive holographic displays recognizing haptic motions. Secondly, I will propose a compact gas sensor platform to autonomously sense the existence of a toxic volatile gas and provide an immediate visual holographic alarm [6]. By combining the advantage of the rapid responses to gases realized by liquid crystals with the compactness of holographic metasurfaces, we develop ultra-compact gas sensors without the requirement of additional complex instruments or machinery to report the visual information of gas detection. It is expected that such a holographic metasurface gas sensor platform will provide a path to ubiquitous, compact, and smart unconventional photonic sensing applications that quickly alert users about harmful gases or biochemical leaks.

[1] I. Kim *et al.*, *ACS Photonics* 5, 3876-3895 (2018)
[2] I. Kim* *et al.*, *ACS Nano* 11, 9382-9389 (2017)
[3] I. Kim* *et al.*, *Laser and Photonics Reviews* 13, 1900065 (2019)
[4] I. Kim* *et al.*, *Nanoscale Horizons* 5, 57-64 (2020)
[5] I. Kim *et al.*, *Advanced Materials* 32, 2004664 (2020)
[6] I. Kim *et al.*, *Science Advances* 7, eabe9943 (2021)

Negative Differential Resistance and Negative Differential Transconductance: New Switching Behaviors from Heterojunction Devices

***Hocheon Yoo*[1]**
[1]Dept. of Electronic Engineering, Gachon University, Seongnam 13120, Republic of Korea
Tel.:82-31-750-8802, E-mail: hyoo@gachon.ac.kr

Negative differential resistance (NDR) and negative differential transconductance (NDT) are emerging and gaining attentions as it can be applied to various devices such as relaxation oscillators, multi-valued logics, negative-impedance converters, and Hodgkin-Huxley neuromorphic circuits. In devices with either NDR or NDT, the current does not monotonically increase with the increased voltage bias, which possibly offers unprecedented new switching characteristics. Here, we introduce our recent efforts implementing and further controlling NDR and NDT. We also present our strategies to make NDR and NDT devices operate with excellent endurance. Furthermore, by means of these controllable and robust NDR and NDT characteristics, applications to optical and electrical devices are introduced in this talk.

Novel Pixel Circuit for Micro LED Display Suppressing Color Shift

Hwarim Im[1], Eun Kyo Jung[1], Sara Hong[1], Eunho Kim[1], and Yong-Sang Kim[1]
[1]Dept. of Electrical and Computer Engineering, Sungkyunkwan University, Suwon, 16419, Korea
Tel.:82-31-299-4640, E-mail: yongsang@skku.edu

Micro light-emitting diode (μLED) displays have attracted much attention as next-generation displays because of many advantages of a long lifetime, excellent efficiency, and high brightness without the burn-in phenomenon [1]. Although μLEDs have many benefits, the color shift issue should be solved to realize a high-quality μLED display. Color shift issue is attributed to the wavelength shift of μLED depending on the current density [2]. Therefore, it is required to develop a new pixel circuit and driving method for μLED displays.

We have proposed a novel low-temperature polycrystalline silicon (LTPS) thin-film transistor (TFT) pixel circuit for μLED display using pulse width modulation (PWM). The proposed circuit modulates the grayscale by controlling the emission time of μLEDs. As a result, it can exhibit a 10-bit grayscale without the wavelength shift of μLED. Furthermore, an internal compensation scheme is implemented in the proposed circuit for compensating for the threshold voltage (V_{TH}) variation. When the V_{TH} changes as ±1 V, the simulated error rate of μLED emission time was under 1%. Consequently, the proposed pixel circuit can exhibit excellent grayscale-expression capability and reliable operation with the V_{TH} variation.

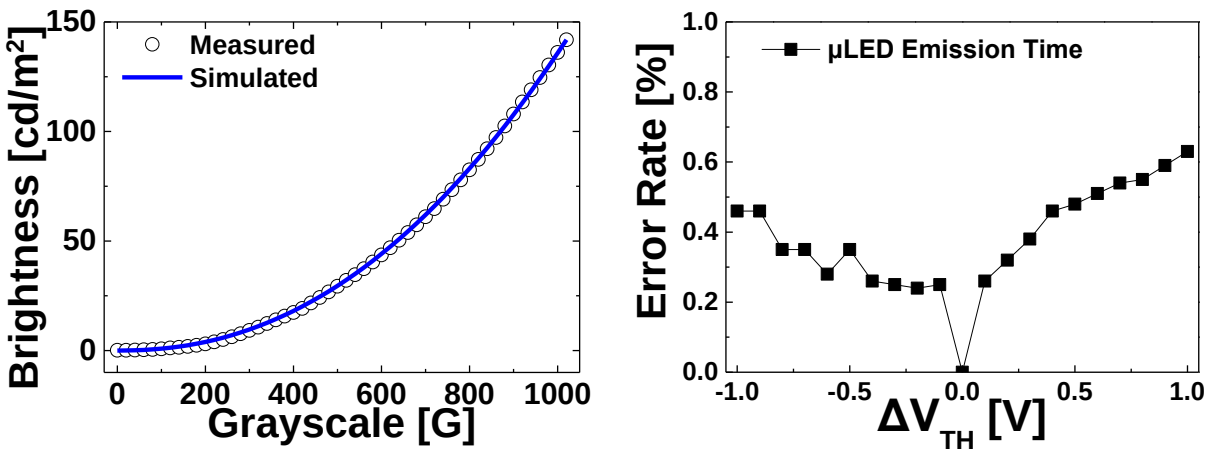

(a) **(b)**

Fig. 1. (a) The measured and simulated brightness of the μLED, (b) the error rate of μLED emission time for the threshold voltage shift (ΔV_{TH}=±1 V)

References

1. H.-A. Ahn, S.-K. Hong, and O.-K. Kwon, *IEEE Trans. Circuits Syst. II-Express Briefs*, vol. 65, no. 6, pp. 724-728, (2018).
2. Z. Gong, S. Jin, Y. Chen, J. McKendry, D. Massoubre, I. M. Watson, E. Gu, and M. D. Dawson, *J. Appl. Phys.*, vol. 107, no. 1, pp. 013103, (2010).

A New Pixel Circuit for Externally Compensated OLED Display

Kook Chul Moon, KeeChan Park

School of Electrical Engineering. KonKuk University, Seoul, Seoul 05029, Korea

Tel.:82-10-3507-7040, E-mail: gairgear@konkuk.ac.kr

AMOLED (Active-Matrix Organic Light Emitting Diode) display has been expanding its application from mobile phone to large area TV [1]. The pixel circuit for internal compensation has been used for mobile applications while the external compensation scheme has been implemented for AMOLED TV [2][3]. The external compensation requires additional fan-out lines and pads from the driver IC to read out the pixel characteristics. Generally, the cost of IC is determined by chip area, which is affected by the number of pads, so-called 'Pad limit'[4]. Therefore, the cost of IC is cut down if the number of I/O pads is reduced by combining the sensing line and the data line. In addition, the area of pixel circuit can be also reduced as the number of vertical lines decreases. Fig.1 shows the OLED pixel circuit for conventional external compensation which requires two vertical signal I/O lines for each pixel. [2] One is for video data input and the other is used to read out the characteristics of TFT (Thin film transistor) and OLED in each pixel. As for Fig. 1, several pixels may share the sensing line to reduce the pixel circuit area and the number of I/O pads of the driver IC. However, we still cannot eliminate the additional sensing line.

We propose a new pixel circuit in order to further reduce the I/O pads for the external compensation. Fig. 2 is the schematic diagram of our new pixel circuit. In the conventional pixel circuit of Fig. 1, the Vgs of M3 TFT is the difference between Vdata and Vini of the sensing line, while in our pixel circuit of Fig. 2, that is the difference between Vref and Vdata. Vdata is determined based on the characteristics of M3 and the OLED while Vref is a constant bias voltage. As shown in Fig.2, the data line is also used to read-out the characteristics of M3 and the OLED. We will report the process of V_T and mobility extraction of M3 as well as OLED charactrization in detail based on Spice simulation. Although the Vref line is still required in Fig. 2 instead of the sensing line in Fig. 1, it can be drawn as a horizontal line through a couple of sub-pixels in the pixel area and converged into a single pad of the driver IC because it is a DC bias voltage. As a result, the area of the pixel circuit is reduced and the number of IC pads is minimized.

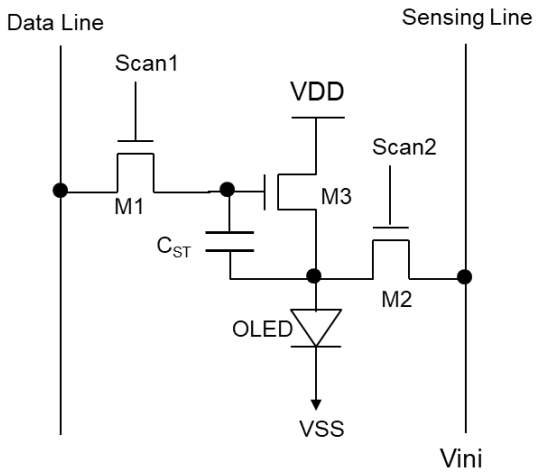

Fig. 1 Conventional pixel circuit for external compensation

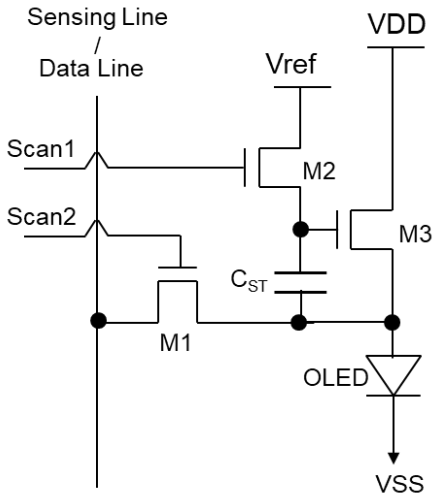

Fig. 2 New pixel circuit for external compensation

References

1. Takatoshi Tsujimura, "OLED Display Fundamentals and Applications" 2nd Ed., Wiley, ISBN: 978-1-119-18748-6, pp. 2-4 (2017)
2. Ryosuke Tani, Jet al, " Panel and Circuit Designs for the World's First 65-inch UHD OLED TV" SID2015 Digest, 64-2, pp950-953 (2015)
3. U-J Chung, et al, "Manufacturing Technology of LTPO TFT" SID 2020 Digest, 15-1, pp. 192-195 (2020)
4. https://www.edaboard.com/threads/pad-limited-vs-core-limited.47542/

Bottom gate-controlled LTPS TFT technologies for improving device reliability in AMOLED displays

Keunwoo Kim[1], Jaehwan Chu, Hanbit Kim, Sangun Choi, Jaeseob Lee, Dokyeong Lee, Joonwoo Bae, Tiennguyen Thanh, Taewook Kang, Hyeyong Chu, Changhee Lee, and Jinoh Kwag
[1]Display Research Center, Samsung Display Co., LTD., Giheung-Gu, Youngin-Si, Gyeonggi-Do, Korea
Tel.:82-31-5181-6762, E-mail: keunwoo7.kim@samsung.com

In first-principle physics, double-gate field effect transistors appear more electrostatic than single-gate counterparts due to the electrical coupling of two gates [1]. This fundamental benefit can be applied to low-temperature polysilicon (LTPS) thin-film transistor (TFT) structures in display applications using optimal bottom gate-controlled device structures. This paper presents a new LTPS TFT technology having a bottom-gate device/pixel structure to improve device characteristics and reliability. Since the TFTs in pixels and peripherals are biased/suffered by external DC and AC signals, the device characteristics are degraded as stress time increases. To improve device characteristics and reliability, we fabricate a mesh-contact bottom-gate device structure in the flexible LTPS TFT process, utilizing a global (positive) bottom-gate voltage (e.g., GH or ELVDD) for all pixels in the entire columns and lows, thereby reducing the area penalty. This innovative TFT architecture and technology-design integration methods can facilitate further decrease of electric fields in the depletion region of polysilicon, thereby yielding significantly-lesser charge injection and defect creation [2].

Fig. 1(a) shows measured data of stress time-dependent V_{th} degradation for the bottom-gate controlled LTPS TFTs (case 2, 3) in different device architectures vis-à-vis a nominal LTPS technology (case 1). In this experiment, compatible stress is induced to Test Element Group (TEG) devices to consider device reliability for V_{th}-compensation/DATA-writing functional devices in the panel operation. Thus, analyzed results are representative and demonstrate that the proposed technology will be more reliable and robust in AMOED displays. Fig. 1(b) shows drain-induced barrier lowering (DIBL) vs. (positive) bottom-gate voltage (V_{bottom}) with varying V_{bottom}. In the bottom-gate LTPS device, the longitudinal electric field generated by the drain is better screened from the source end of the channel due to the electrical (transverse) coupling of channel-to-bottom gates, resulting in over x2-reduced DIBL due to the improved gate controllability [3]. Fig. 1(c) depicts the fabricated device schematic and its energy band diagram based on numerical device simulations calibrated against measured data.

In displays, we achieve noticeable improvement (over 2x) of device reliability (e.g., NBTI and AC stress) due to the bottom-gate control effect through fully-depleted thin film. For the brevity of abstract, details of physical analysis of reliability for LTPS TFTs in the bottom-gate configuration will be described later. Other unique features of bottom-gate LTPS TFTs including on-bias/off-bias stress effects will be physically analyzed and linked to panel characteristics.

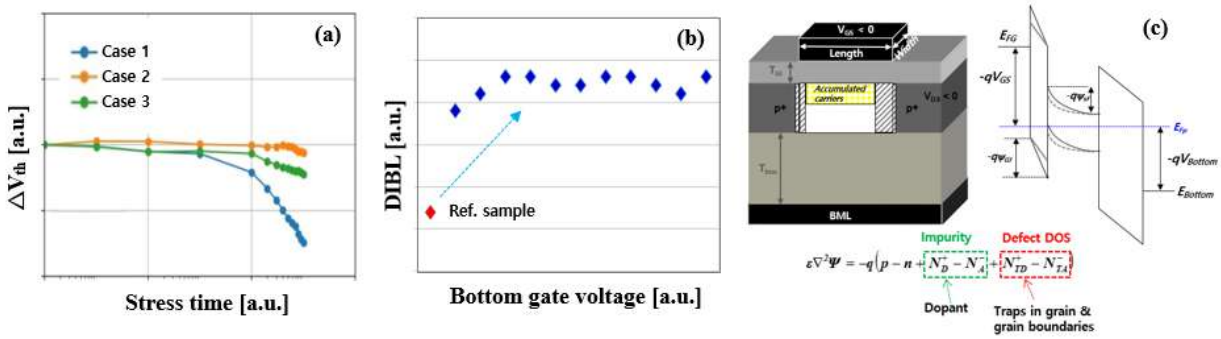

Fig.1. (a) Experimental data of stress time vs. V_{th} variation and (b) bottom-gate voltage vs. DIBL, and (c) Energy band diagram for gate-to-bottom gate across the poly-Si based on physics-based simulations [4].

References

1. K. Kim et al., *IEEE Trans. Electron Devices*, vol. 54, no. 9, p. 2263 (2007).
2. J. Kuang et al., *IEEE Trans, VLSI Sys*, vol. 16, no. 12, p. 1657 (2008).
3. K. Kim et al., *IEEE Trans. Electron Devices*, vol. 54, no. 9, p. 3033 (2009).
4. SILVACO, Inc., Santa Clara, CA, USA, *Atlas Device Simulation Framework* (2015).

Alleviation of hot-carrier stress degradation in transversely tensile-strained *p*-channel poly-Si TFTs fabricated on plastic substrate

***Jaeseob Lee*, Sanggun Choi, Taewook Kang, Hyeyong Chu, Changhee Lee, Jinoh Kwag**
Display Research Center, Samsung Display Co., LTD., Giheung-gu, Yongin-si, Gyeonggi-do, Korea
Tel.:82-31-5181-6047, E-mail: jaeseob.lee@samsung.com

In this work, non-uniform hot-carrier degradation of flexible *p*-channel low-temperature polycrystalline-silicon thin-film transistors is investigated with mechanical bending status. Experimental results reveal that with width-axis tensile strain, hot carrier degradation (HCD) is alleviated with the reduction of increments in interface state density (N_{it}) and grain boundary trap density (N_{trap}). With width-axis compressive strain, HCD is elevated with the enhanced increments in N_{it} and N_{trap}. Effective density-of-states (DOS) distributions extracted using field-effect conductance method demonstrate the reduced increase in DOS during HCD with tensile strain and the accelerated increase with compressive strain, especially DOS located at 0.05-0.3eV above the valence band maximum. We propose that strain-induced hydrogen passivation of defects is effective with tensile strain, but strain-induced additional generation of defects is dominant with compressive strain. These understandings will be helpful in designing the peripheral circuits on plastic substrate for the system-on-panel display.

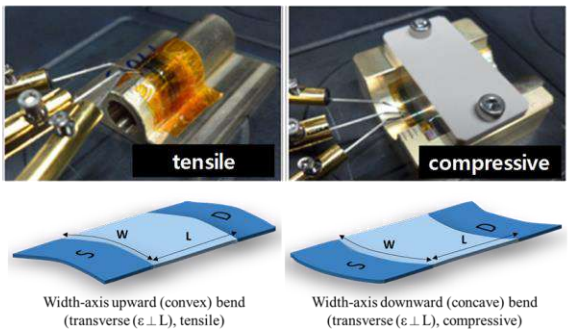

Figure 1

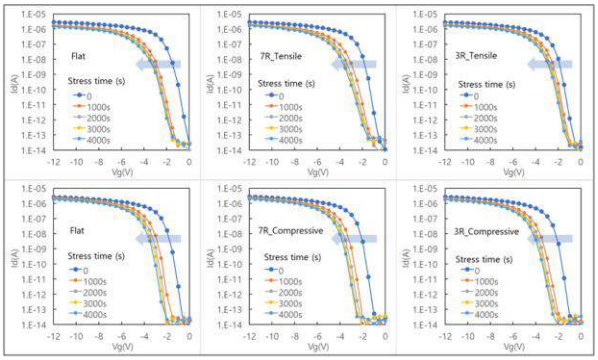

Figure 2

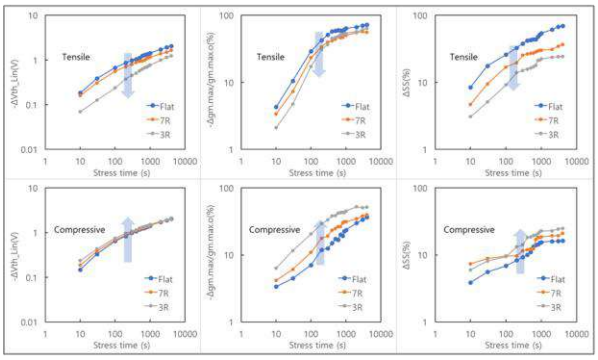

Figure 3

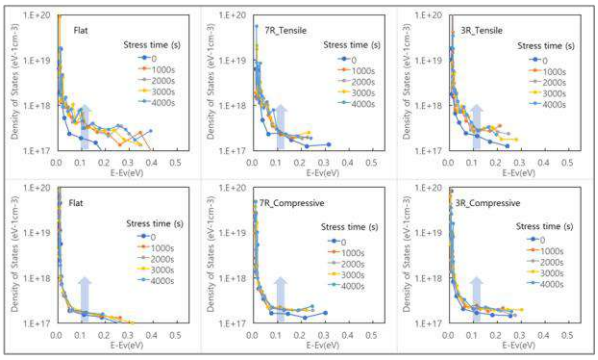

Figure 4

Figure 1. Photograph of customized cylindrical metal tube and illustration of width-axis, upward (convex) and downward (concave) bending. **Figure 2.** Evolution of transfer characteristics of *p*-ch. LTPS TFTs on PI during hot-carrier stressing under V_G=-12V, V_D=-22V and mechanical bending with flat, transverse tensile- and compressive-strain at bending radius R=7 and 3mm. **Figure 3.** Variation of threshold voltage, normalized maximum transconductance, and subthreshold swing during hot-carrier stressing for flat, transverse tensile- and compressive-strained LTPS TFTs. **Figure 4.** Increase of effective density-of-states distributions during hot-carrier stressing for flat, transverse tensile- and compressive-strained LTPS TFTs

References

1. J. Lee, Y. Lee, T. Kang, H. Chu, and J. Kwag, "Alleviation of abnormal NBTI phenomenon in LTPS TFTs on polyimide substrate for flexible AMOLED," J. Soc. Inf. Disp., vol.28, pp. 333-341, (2020).
2. G. P. Kontogiannopoulos, F. V. Farmakis, D. N. Kouvatsos, G. J. Papaioannou, and A. T. Voutsas, "Hot-carrier stress induced degradation of SLS ELA poly Si TFTs," Solid-State Electronics, vol.52, pp. 388-393, (2008).
3. M.-H. Lee, K.-H. Chang, and H.-C. Lin, "Effective density-of-states distribution of polycrystalline silicon thin-film transistors under hot-carrier degradation," J. Appl, Phys., vol.102, pp. 054508, (2007).

Viable Approach to Convert LCD Lines for AMOLED Production: A Proof-of-concept WOLED Plus Color Filter Display Panel

Xiao Chen[1], Hiromitsu Katsui[2], Keisuke Kuriyama[2], Wooram Youn[1], Gyungmin Kim[1], In Sik Cho[1], David Cheney[1], Ramesh Jayaraman[1], Chris Samouce[1], Svetlana Vasilyeva[1], Andrew Rinzler[1,3], Max Lemaitre[1], and Bo Liu[1]
[1]Mattrix Technologies, Gainesville, Florida 32601, U.S.A.
Tel.:1-352-641-0557, E-mail: bo.liu@mattrixtech.com
[2]JSR Corporation, Yokkaichi, Mie 510-8552, Japan
[3]University of Florida, Gainesville, Florida 32601, USA

The Vertical Organic Light Emitting Transistor (VOLET) combines three key components of an AMOLED display pixel: the drive transistor, the storage capacitor, and the OLED stack into a single, bias-stress stable, bottom-emission device. The resulting two-component (sw-TFT + VOLET) pixel circuit maximizes aperture ratio, increases brightness, and improves the lifetime of display panels, while enabling fully depreciated, large Gen, LCD manufacturing lines to be repurposed for AMOLED mass production.

Here we demonstrate a 4.7" full-color AMOLED display panel with a white light VOLET plus color-filter (CF) frontplane on an a-Si switching-TFT backplane. In this bottom-emission prototype panel, the RGB color-filter layer was formed directly on the a-Si switching backplane, sandwiched between the TFT passivation layer and the ITO pixel electrode, which serves as the Gate electrode for the VOLET in each sub-pixel. Standard photolithographic patterning and subtractive etch processes were used to define each thin-film layer of the VOLET up to the Pixel Definition Layer (PDL). The organic semiconducting channel layer, tandem white-OLED (Blue + Yellow-Green emitters), and Al cathode were then subsequently deposited by open-mask, vacuum thermal evaporation. Fig. 1. shows a schematic cross-section of the panel. The bottom-emission, white-VOLET plus CF architecture lends itself well to large-area displays for which Mura, IR-drop, and definition of the RGB sub-pixels pose significant challenges for traditional AMOLED manufacturing.

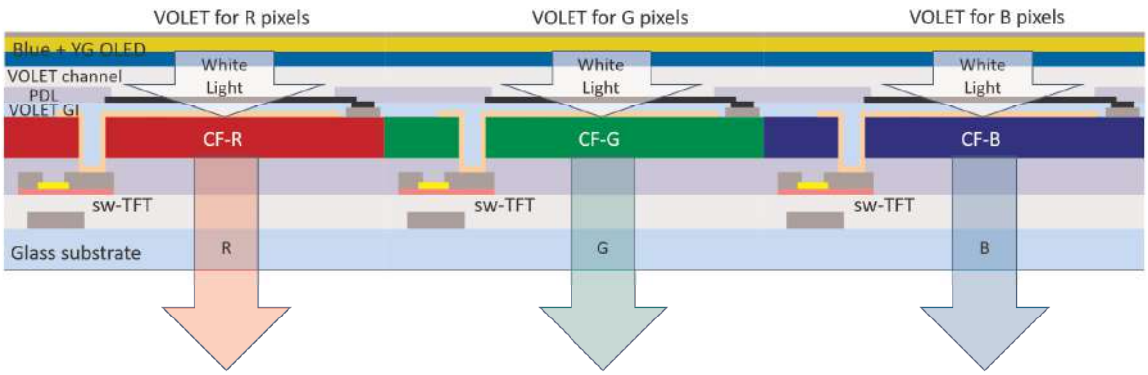

Fig. 1. Cross-section Schematic of the Active-Matrix White Light VOLET + CF Display Pixel

By combining a bottom-emission VOLET frontplane with standard LCD display components (including the a-Si sw-TFT backplane and RGB CF), we have demonstrated a proof-of-concept for profitable, large-area AMOLED display production on converted LCD manufacturing lines.

References

1. M. A. McCarthy, B. Liu et. al. and A. G. Rinzler, *Science*, 332, p. 570 (2011).
2. M. A. McCarthy, B. Liu et. al. and A. G. Rinzler, *SID 2016 Digest*, p. 1796 (2016).
3. B. Liu, M. A. McCarthy et. al. and A. G. Rinzler, *Proceedings of the International Display Workshops*, IDW '17, AMD6-1 (2017).
4. A. G. Rinzler, M. A. McCarthy and B. Liu, Active Matrix Dilute Source Enabled Vertical Organic Light Emitting Transistor, US Patent no. 9214644.

Temperature-compensated pulse-width modulation using multimodal transistors

Eva Bestelink[1], Olivier de Sagazan[2], and Radu A. Sporea[1]
[1] Advanced Technology Institute, University of Surrey, GU2 7XH, United Kingdom
E-mail: e.bestelink@surrey.ac.uk
[2] IETR-DMM-UMR6164, University of Rennes, Rennes, France

We present a circuit which exploits the operation of the multimodal thin-film transistor (MMT) [1] to produce temperature-compensated pulse-width modulation (PWM) of an output signal using an input current (Fig. 1a). PWM is becoming important for displays in which constant-current driving of the emissive device is critical [2].

The MMT can be realized with a linear dependence of drain current on source control gate voltage [1]. Together with the many benefits granted by contact-controlled architectures, such as low saturation voltage, flat saturated characteristics (see Fig. 1b for measured microcrystalline silicon MMT output curves) and reduced susceptibility to manufacturing variations [3], [4], the MMT is well suited to a variety of analog and mixed signal applications [5]. However, in common with similar contact-controlled transistors [6], the MMT has a non-negligible variation of drain current with temperature. This limitation can be overcome by using a current mirror configuration.

Circuit (Fig. 1a) operation: an external reference current is passed to transistor M_1, which, together with M_2, forms a current mirror. M_1 and M_2 only differ in their widths. The channel control gate (CG) of M_1 is connected to the positive power supply, ensuring that its current is exclusively controlled by its source control gate (SG) potential. M_2's CG is connected to the negated RESET signal, so that the transistor conducts when RESET is not asserted. M_4 forms an amplifier/inverter together with R_L (an active load in practice, but here realized as a resistor to speed up TCAD simulations). In normal operation, M_2 charges capacitor C_L with a constant current. This lowers the gate voltage of M_4 at a constant rate, eventually switching node OUT to VDD. This event depends on I_{IN} but not on temperature, as shown in the results of simulations performed with Silvaco Atlas (Fig. 1c). When the RESET signal is asserted, M_3 discharges C_L to VDD while M_2 is on, switching node OUT to ground. As such, the circuit has a programmable delay or PWM function. The present standalone realization can be adapted for applications as part of an active matrix of pixels for the control of display or detector arrays. For low current (1 µA), the circuit performance with temperature reduces, as M_1 starts operating in the linear region.

The MMT's unique operation [1], device geometry, tolerance to variability, low saturation voltage and flat output characteristics allow a robust and compact implementation.

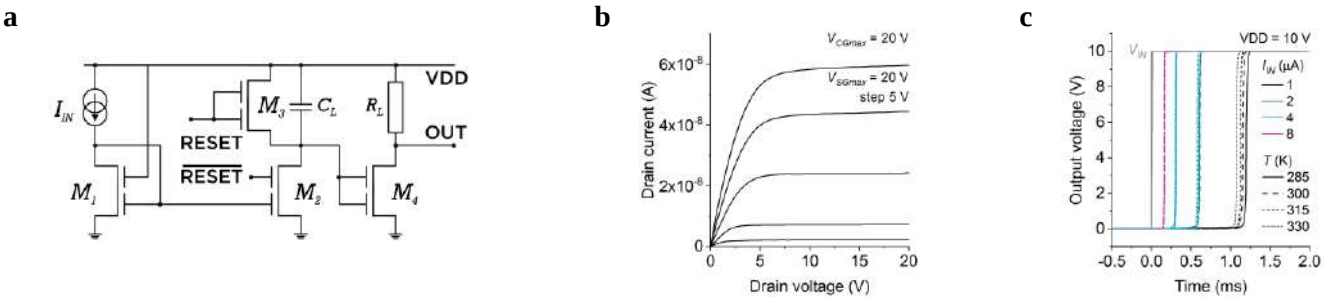

Fig. 1. a) Proposed circuit diagram; b) Measured microcrystalline multimodal transistor output characteristics; c) Circuit output waveform for a variety of input currents and temperatures.

Acknowledgment

EPSRC grants EP/R511791/1, EP/R028559/1, EP/V002759/1 partially supported the project. Fabrication was performed on the NanoRennes platform. We thank B. H. Le Borgne and J. M. Shannon for advice and discussions.

References

[1] E. Bestelink *et al.*, *Adv. Intell. Syst.*, vol. 3, no. 1, p. 2000199, 2020.
[2] Y. Huang *et al.*, *Light Sci. Appl.*, vol. 9, no. 1, 2020.
[3] J. M. Shannon and E. G. Gerstner, *IEEE Electron Device Lett.*, vol. 24, no. 6, pp. 405–407, 2003.
[4] R. A. Sporea et al., *Sci. Rep.*, vol. 4, pp. 1–7, 2014.
[5] E. Bestelink, O. de Sagazan, and R. A. Sporea, *SID Symp. Dig. Tech. Pap.*, 51, 1, pp. 1375–1378, 2020.
[6] R. A. Sporea, M. Overy, J. M. Shannon, and S. R. P. Silva, *J. Appl. Phys.*, vol. 117, no. 18, 2015.

OFET Memory for Selective Light Monitoring

Xu Gao, Zhong-Da Zhang, Jing-Jing Lv, Lin-Xi Zhang, Jian-Long Xu, Sui-Dong Wang

Institute of Functional Nano & Soft Materials (FUNSOM), Soochow University, Suzhou, China

Email:gaoxu@suda.edu.cn

OFET Memory for Selective Light Monitoring

With the increasing demand for flexible and wearable electronic devices, functional organic field-effect transistor (OFET) memories have attracted more and more attentions in a wide range of applications, such as pressure sensor, sterilization monitor, biosensor, artificial synapse and so on. In particular, the integration of photodetection and signal storage in an OFET memory well meets the demand for light monitoring in the fields of environment monitoring and skin healthcare, where the recording of light exposure could be realized by nonvolatile cumulative charge trapping. Furthermore, the photo-energy-dependent charge trapping process provides a new approach to distinguish the lights of different wavelength.[1] In comparison, either a semiconductor with suitable bandgap or an additional expensive and bulky optical filter is required for traditional implementation of wavelength identification. In our work, several kinds of charge trapping layer (CTL) were employed in an OFET memory to demonstrate the potential applications for selective light monitoring.[2-4] The simple device configuration with an easy way to modulate light selectivity provides a novel and feasible route to meet various requirements of future wearable electronics.

Keywords: Organic Field-Effect Transistor; OFET Memory; Charge Trapping; Light Monitoring

References

1 Xu Gao, Chang-Hai Liu, Xiao-Jian She, Qin-Liang Li, Jie Liu, Sui-Dong Wang*, *Org. Electron.*, **2014**, 15, 2486.

2 Zhong-Da Zhang, Xu Gao*, Ya-Nan Zhong, Jie Liu, Lin-Xi Zhang, Shun Wang, Jian-Long Xu, Sui-Dong Wang*, *Adv. Electron. Mater.*, **2017**, 3, 1700052.

3 Jing-Jing Lv, Xu Gao*, Lin-Xi Zhang, Yang Feng, Jian-Long Xu, Jing Xiao, Bin Dong, Sui-Dong Wang*, *Appl. Phys. Lett.*, **2019**, 115, 113302.

4 Lin-Xi Zhang, Xu Gao*, Jing-Jing Lv, Ya-Nan Zhong, Chao Xu, Jian-Long Xu, Sui-Dong Wang*, **2019**, 11, 40366.

Design Considerations for µLED Displays.

Lynn Verschueren[1,2], Jan Genoe[1,2], Mauricio Velazquez Lopez[1], Firat Tankut[1], Wim Van Eessen[3], Patrick Willem[3], Wim Dehaene[2,1], and Kris Myny[1,2]
[1] imec, Kapeldreef 75, 3001 Leuven, Belgium
E-mail: Kris.Myny@imec.be
[2] ESAT, KU Leuven, Kasteelpark Arenberg 10, 3001 Leuven, Belgium
[3] Barco, Beneluxpark 21, 8500 Kortrijk, Belgium

Lately, µLED displays have gained a lot of interest. However, designs for µLED displays still encounter many challenges. Different approaches exist to tackle these challenges, one starting from LED wall PCB designs, and one starting from AMOLED designs. We propose a new hybrid approach, by combining the best of these approaches. LED wall-based designs usually use passive matrix driving, whereas AMOLED designs use active matrix driving. Since active matrix designs are beneficial for power, cost and visual image quality, they are preferred over passive matrix.

AMOLED displays mostly use analog driving, i.e., the gray level is determined by an analog voltage. Nevertheless, µLEDs, like LEDs, are suffering from wavelength shifts when the drive current is varied [1]. Since this color point shift is undesirable, we propose a digital driven implementation, like typical LED wall designs. To implement the digital driving with active matrix, different coding schemes for PWM exist [2]. We propose a 12-bit coding table with minimal dark time and optimized optical appearance. Fig. 1a shows the amplitude of the first harmonic in its Fourier spectrum of the proposed coding table and a standard single pulse PWM implementation. This figure clearly shows the amplitude of the first harmonic is reduced for all gray levels by implementing the proposed coding table, resulting in reduced flickering in the display. Moreover, the brightness measurements of green LEDs driven with this coding table, presented in Fig.1b, show very good linearity.

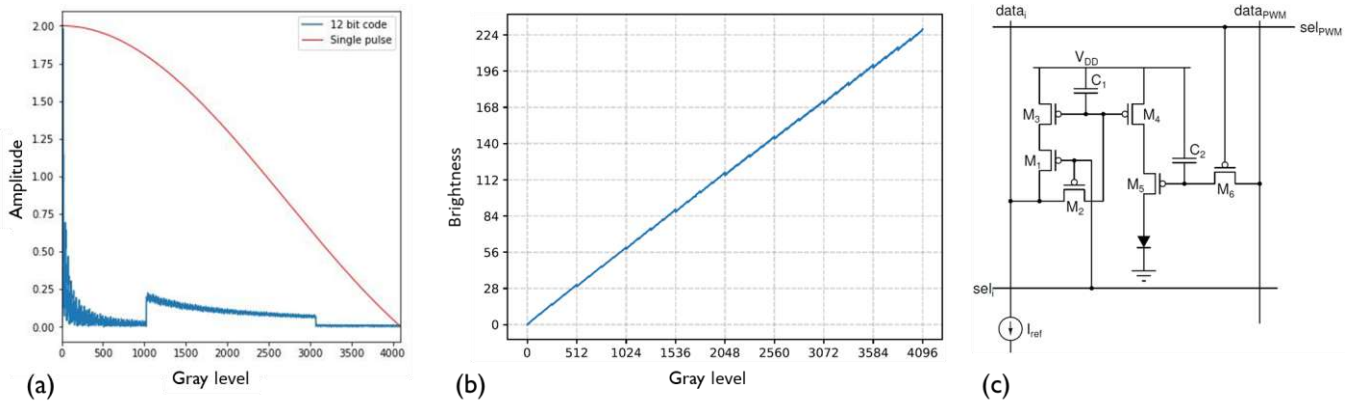

Fig. 1. Proposed implementation for µLED designs. (a) First harmonic amplitude for the selected coding scheme compared to the single pulse PWM for all grey levels. (b) Measured brightness for all gray levels. (c) Proposed pixel circuit.

Since µLEDs are current driven devices, and experience wavelength shifts when the current is varied, setting an accurate current through the µLED is vital. Therefore, we propose a novel 6T2C pixel circuit, shown in Fig.1c, using a current mirror to accurately set a fixed current level, and switching transistors to apply the PWM signal for setting the gray level. By using this pixel circuit, we can implement the proposed hybrid design approach to drive µLED displays with the best performances.

References

1. Yawale PR, Wagh VG, and Shaligram AD. Impact of current controlled dimming on spectral characteristics of high power LEDs. Optics and Laser Technology. 2019. pp. 289-291.
2. Genoe J. Digital driving of active matrix displays. US9905159B2
3. Verschueren L, Myny K, Genoe J, Dehaene W, Van Eessen W, and Willem P. Pixel circuit. EP 20215452.2

Transferable and deformable light-emitting diodes fabricated by remote epitaxy of microrod heterostructures

Young Joon Hong[1]
[1]**Dept. of Nanotechnology and Advanced Materials Engineering, Sejong University, Seoul 05006, Korea**
Tel.:82-2-3408-4382, E-mail: yjhong@sejong.ac.kr

Flexible electronics are emerging, and the use of polymeric substrate enabled fabrication of the flexible inorganic devices via transfer of the inorganic devices onto the soft substrates. For fabricating the flexible devices, however, the epitaxy of the inorganic devices must be carried out on the other thermally tolerant crystalline substrate, typically via covalent epitaxy. Because of the strong bonding between the epi-layer and the crystalline substrate, it needs high energy or chemically reactive process (e.g., laser lift-off, chemical etching, mechanical dicing, etc.) to separate them from the substrate. This causes the chemical and physical damages onto the epi-structures of devices. To minimize the damage, gentler delamination is necessary, and the so-called 'remote epitaxy' is an ideal way for ease of delamination as well as obtaining high quality overlayer.[1] In this talk, we introduce the remote epitaxy of spatially separate GaN microrod p–n junction arrays with InGaN/GaN heterostructures on graphene-coated Al_2O_3 wafer for fabricating transferable and deformable short wavelength light-emitting diodes (LEDs) (Figure 1a).[2] The method of growing the microrod LEDs that are easily transferred onto other foreign substrate is demonstrated, and the flexibility of the LEDs is also presented. Our density-functional theory simulation result shows how graphene insertion enabled the remote epitaxy despite the far distance between GaN and Al_2O_3. We additionally demonstrate the strategy of site-selective remote epitaxy using patterned graphene layer based on hydrothermal synthesis of ZnO microrods (Figure 1b).[3,4] The principles of selective remote epitaxy are discussed in terms of lattice transparency attenuation across ultrathin intaglio graphene and thick-embossed patterned areas.

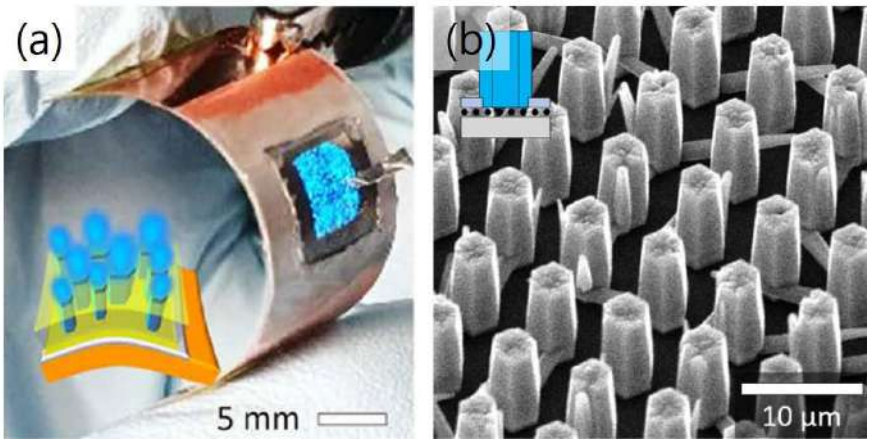

Fig. 1. (a) Blue InGaN/GaN microrod LEDs fabricated by remote epitaxy. (b) Site-selective remote epitaxy of ZnO microrod arrays.

References

1. Y. Kim et al., *Nature*, 544, 340 (2017).
2. J. Jeong et al., *Sci. Adv.*, 6, eaaz5180 (2020).
3. J. Jeong et al., *ACS Appl. Nano Mater.*, 3, 8920 (2020).
4. D. K. Jin et al., *APL Mater.*, (in press).

Improvement of the Electrical and Optical Performance of LED Array for Vehicle Headlight Application by optimizing processes

Sang-Youl Lee[1,2], Ho-Young Kim,[2,3], Hiroshi Amano[4], and Tae-Yeon Seong[1,3]*
[1]Dept. of Nanophotonics, Korea University, Seoul 02841, Korea
Tel.:82-2-3290-3288, E-mail: tyseong@korea.ac.kr
[2]LED Division, LG Innotek Co., Ltd., Paju, Gyeonggi 10842, Korea
[3]Department of Materials Science and Engineering, Korea University, Seoul 02841, Korea
[4]Center for Integrated Research of Future Electronics, and Institute of Materials and Systems for Sustainability, Nagoya University, Nagoya 464-8603, Japan

GaN-based LEDs have been extensively applied to a wide variety of areas, including displays, visible light communication, vehicle exterior and interior lamps, neuron stimulation, optogenetics, etc. For the realization of these applications, the fabrication of high-performance LED array is essentially required by solving many technological issues. in particular, for vehicle lamp application, an important issue is known to be crosstalk between LEDs, degrading the performance of LED array. Further, LED packages are directly affected by the heat from the engine, heater, and a cooling system. Thus, heat dissipation structure for preventing the degradation of LED reliability, efficient heat-dissipation design of PCB/heat sink/reflector to handle the self-heating of LEDs, and reduction of the weight of heat-dissipation materials and system are particularly important factors. In addition, as the emission area of LEDs increases, leakage current increases owing to the presence of defects. For GaN epilayer wafers, a high density of epitaxial defects (~10^6 cm^{-2}), e.g., nano-pipes, is generated because of large lattice-mismatch, resulting in poor performance of LEDs.

Thus, in this study, to solve these issues, first we investigated the leakage characteristics of LEDs as a function of chip sizes. Wet etching was found to drastically increase the reverse leakage current. The plasma-etching process using Ag particles as micro-masks for *n*-GaN surfaces was found to be suitable to increase the light-extraction abilities of vertical geometry GaN-based LEDs for use in vehicle headlamp applications. Moreover, we examined the luminance and thermo-mechanical properties of vertical-geometry (V) LED and flip-chip (FC) LED packages with different types of white silicones. Regardless of white silicones, the FC-LED package showed higher luminous flux drop-rate than the V-LED package when the temperature increased to 85 ℃. The use of V-LED and soft white silicone (WR-3001) was suggested to be an efficient package process for realizing high-performance white LED packages for vehicle adaptive driving beam (ADB) headlamp applications. Then, we investigated the effects of pixel distance and LED thickness on the luminance distribution and contrast ratio of a 16 × 16 blue and white LED array for vehicle headlamp application. It was observed that LED array with the self-aligned Si barrier presented smaller dark space than that with the ultrathin-GaN. A headlamp unit using 16 × 16 LED array was demonstrated with LEDs with the Si self-aligned barrier. The self-aligned Si barrier was shown to serve as a promising process tool for the fabrication of high-performance LED array for vehicle headlamp application.

Acknowledgment

TYS and HA gratefully acknowledge financial support from the Global Research Laboratory (GRL) program through the National Research Foundation (NRF) of Korea (NRF-2017K1A1A2013160). The authors are greatly grateful to Kiman Kang, Min-Su Kim, Eunduk Lee, Kwang-Hee Lee, Yoomin Jo, Kyoung-Mo Kang, Doyub Kim, Doyub Kim, Se-Yeon Jung, Jeong Tak Oh, Hwan-Hee Jeong (LG Innotek Co.) for their technical help and discussion.

Extremely Stable Luminescent Siloxane-Encapsulated Perovskite Resin as Color Converting Materials in Display

Junho Jang[1], Young-Hoon Kim[3], Yongmin Shin[1], Tae-Woo Lee[2], Byeong-Soo Bae[1]
[1]Wearable Platform Materials Technology Center, Dept. of Mater. Sci. Engineering, Korea Advanced Institute of Science and Technology, Daejeon 34141, Korea
Tel.:82-42-350-5119, E-mail: jhjang0427@kaist.ac.kr
[2]Dept. of Mater. Sci. Engineering, Seoul National University, Seoul 08826, Korea.
[3]Chemistry and Nanoscience Center, National Renewable Energy Laboratory, Golden, CO 80401, U.S.A.

Herein, we report a simple but effective material-design approach to achieve extraordinary-long stability of crosslinked methylammonium (MA) lead bromide ($MAPbBr_3$) nanoparticle (NP) composite (CPN) film in various harsh environments (air, water, chemicals, and high temperature (85 °C) with high relative humidity (85%RH) ((85 °C/85%RH)) by employing methacrylate-functionalized siloxane matrix. The methacrylate groups in the siloxane matrix induce a crosslinking with unsaturated hydrocarbon in acid and base ligands (oleic acid and oleylamine) in perovskite NPs at a molecular scale, which prevents the decomposition of MA from the perovskites. As a result, CPN films exhibited exceptional stability with high photoluminescence quantum yield in water, acid, or base solutions, various polar solvents, and under 85 °C/85%RH. The resulting CPNs films also showed a wide color gamut compared to Cd-based quantum-dots. Moreover, water- and chemical-persistent CPNs were successfully applied to cell proliferation which has been impossible with water-sensitive materials with toxic elements.

Fig. 1. Photographs of CPN films in (a) water, (b) on mobile phone and (c) with large-area (10 cm x 10 cm)

Acknowledgment

This work was supported by the Wearable Platform Materials Technology Center (WMC) funded by the National Research Foundation of Korea (NRF) Grant of the Korean Government (MSIT) (Grant No.: NRF-2016R1A5A1009926).

References

1. J. Jang, Y.-H. Kim, S. Park, D. Yoo, H. Cho, J. Jang, H. B. Jeong, J. M. Yuk, C. B. Park, D. Y. Jeon, Y.-H. Kim, B.-S. Bae, and T.-W. Lee, *Adv. Mater.* 33(3), 2005255 (2021)
2. H. Y. Kim, D.-E. Yoon, J. Jang, D. Lee, G.-M. Choi, J. H. Chang, J. Y. Lee, D. C. Lee, B.-S. Bae, *J. Am. Chem. Soc*., 138(50), 16478-16485 (2016)

Efficient Red Hyperfluorescence Device with Novel Design of Multi-Resonance Boron-based Fluorescent Dopant

Soon Jae Hwang[1], Kenkera Rayappa Naveen[1], Jang Hyuk Kwon[1]*
[1]Department of Information Display, Kyung Hee University, 26, Kyungheedae-ro, Dongdaemun-gu, Seoul, 02447, Republic of Korea.
Tel.:82-2-961-9147, E-mail: jhkwon@khu.ac.kr

Thermally activated delayed fluorescence (TADF) attracts large attention as a next-generation light emitting material as it can achieve 100% of internal quantum effficiency (IQE) without heavy metal. However, due to the intra charge transfer (ICT) characteristic, TADFs exhibit wide full width at half maximum (FWHM) and bad color purity. To overcome such limitation and achieve a BT 2020 color coordinate of red (0.70, 0.30), hyperfluorescence (HF) system is hlghly desired. In HF system, TADF acts as assistant host and the fluorescent dopant (FD) exhibits the final emission. So, HF system benefits high effieicney of TADF and high color purity of FD. Thus, it is important to develop narrow FWHM of FD with bright deep red color. Nowadays, multi-resonance (MR) type of boron-based dopants are widely researched.[1] MR-type material has the alternating molecular orbital strucure between highest occupied molecular orbital (HOMO) and lowest unoccupied molecular orbital (LUMO), so it shows high photoluminescence quantum yield (PLQY) and narrow FWHM. To design the red MR-type of FD, conjugation length was increased by adding polyaromatic structure in a MR-core and fabricated the HF device with novel FD materials.

In this study, we designed two red MR-type FDs, RD1 and RD2. By adding polyaromatic structure to basic MR-core, RD1 shows the red emission wavelength of 599 nm. However, it has an intensive second vibronic peak as shown in **Fig 1(b)**. Therefore, we modified RD1 by attaching a bulky electron donor group on polyaromatic structure, and synthesized RD2. This RD2 could have lowered second vibronic peak and increased PLQY by avoiding pi-pi stacking of polyaromatic structure without changing emission wavelength. Additional photophysical properties of RD1 and FD2 is summarized in **Table 1**.

To evaluate the device performance of these two materials in the HF system, highly efficient yellow to orange TADF material was selected to consider the large spectral overlapping between its emission spectrum and absorption spectra of red MR-type FDs. In addition, deeper LUMO energy level of TADF material was considered in order to prevent the electron trap in red MR-type FD. As an appropriateTADF assistant host material, KHU-TADF is selected and fabricated the red HF device consisted of 20 wt% of KHU-TADF and 0.7 wt% of RD1 or RD2. The detailed device performances will be discussed in presentation.

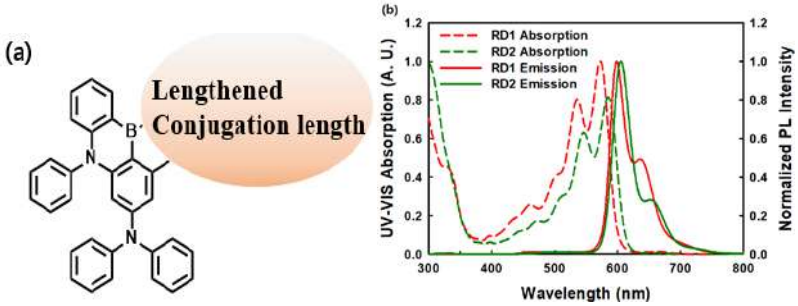

	PL peak (nm)	FWHM (nm)	Stokes Shift (nm)	HOMO/ LUMO (eV)	PLQY
RD1	599	34	26	5.50/3.45	0.95
RD2	605	34	20	5.42/3.40	0.97

Fig. 1 (a) Molecular structures of Red MR-type FDs, (b) Absorption and Emission spectra of Red MR-type FDs.
Table 1. Photophysical properties of RD1 and RD2.

Acknowledgment

This work was supported by the Technology Innovation Program (20006464, Development of TADF sensitized fluorescence RGB emitting layer materials with high color purity and high efficiency for BT 2020) funded by the Ministry of Trade, Industry & Energy (MOTIE, Korea).

References

1. T. Hatakeyama, et al., Adv Mater, 28, p 2777 (14) (2016).

Dual Thermally Activated Delayed Fluorescence for High Efficiency Fluorescent Organic Light Emitting Diodes

*Kyung Hyung Lee, Jun Yeob Lee**

School of Chemical Engineering, Sungkyunkwan University, 2066 Seobu-ro, Jangan-gu, Suwon, Gyeonggi 440-746, Korea

Email: leej17@skku.edu

Abstract

Dual Thermally Activated Delayed Fluorescence (TADF) mechanism utilizing DMAC-DPS TADF material and the exciplex of the DMAC-DPS:POT2T, is developed to increase external quantum efficiency (EQE) in fluorescent organic light emitting diodes by controlling the Dexter energy transfer to the fluorescent emitter (6tBPA, green fluorophore). The DMAC-DPS simultaneously plays role of the main TADF matrix and forming excitons, while the DMAC-DPS:POT2T exciplex plays a role of assisting TADF which harvests the singlet excitons of the fluorescent emitter. Here, three systems of the conventional TADF (DMAC-DPS only), conventional TADF exciplex (DMAC-DPS:POT2T, 50 wt%) and dual TADF (DMAC-DPS:POT2T, 10wt%) are demonstrated by managing the POT2T content, which reduced triplet-triplet annihilation of the exciplex while preventing Dexter energy transfer to the fluorescent emitter. The emission mechanism of the dual TADF is presented in **Figure 1**. As a result, the EQE of the dual TADF device is enhanced from 10.3% to 15.0% compared with the conventional systems.

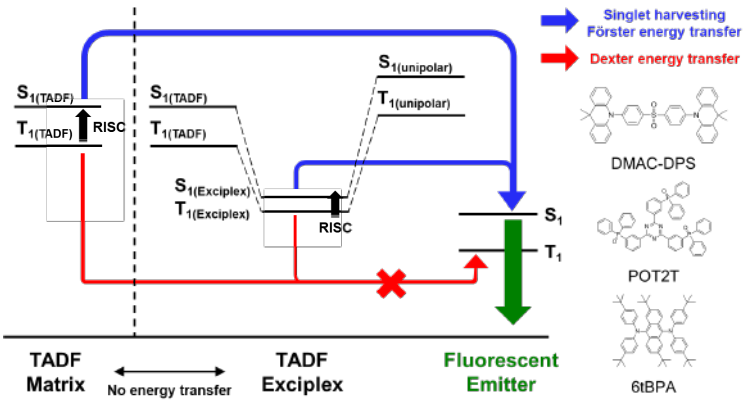

Figure 1. Emission mechanism of the dual TADF mechanism in detail.

Keywords: fluorescent organic light-emitting diodes·thermally activated delayed fluorescence·exciplex·external quantum effieciency

Strong light-matter coupling allows efficient micro-cavity OLEDs with high angular stability

Andreas Mischok[1,2], Sabina Hillebrandt[1,2], Seonil Kwon[1], Malte C. Gather[1,2]
[1] Organic Semiconductor Centre, SUPA, School of Physics and Astronomy, University of St Andrews, St Andrews, KY16 9SS, United Kingdom
E-mail: mcg6@st-andrews.ac.uk
[2] Humboldt Centre for Nano- and Biophotonics, Department of Chemistry, University of Cologne, 50939 Köln, Germany

Organic materials are good emitters and allow the creation of efficient LEDs, largely due to the high oscillator strength of these materials. However, this comes at the cost of broad spectral linewidths, which restricts colour purity in displays. Interference-based structures, such as optical microcavities, offer narrow spectra but show an intrinsic and often substantial angle dependence [1].

Here, we overcome these limitations by combining the concepts of absorption and interference, through strong-light matter coupling and the formation of polariton states [2-4]. Introducing absorbers into a microcavity leads to a coupled polariton state that inherits the low dispersion of the material exciton and the narrow linewidth of the cavity mode and thus enables efficient OLEDs with angle-independent, narrowband emission (EQE >10%, FWHM <20nm, angle shift <10nm @60° tilt).

Acknowledgment

The authors acknowledge funding by the Volkswagen Foundation (No. 93404) and the Leverhulme trust (RPG-2017-213). A.M. acknowledges funding through an individual fellowship of the Deutsche Forschungsgemeinschaft (404587082). M.C.G. acknowledges funding by the Alexander von Humboldt Foundation (Humboldt Professorship).

References

[1] Murawski, C. et al. Narrowband Organic Light-Emitting Diodes for Fluorescence Microscopy and Calcium Imaging. Adv. Mater. 31, 1–8 (2019).
[2] Deveaud-Pledran, B. Polaritronics in view. Nature 453, 297 (2008).
[3] Nikolis, V. C. et al. Strong light-matter coupling for reduced photon energy losses in organic photovoltaics. Nat. Commun. 10, 3706 (2019).
[4] Dietrich, C. P. et al. An exciton-polariton laser based on biologically produced fluorescent protein. Science Advances 2, e1600666 (2016).

Soft, Resorbable Bioelectronics

Suk-Won Hwang
KU-KIST Graduate School of Converging Science and Technology, Korea University, Seoul 02841, Korea
Tel.:82-2-3290-5970, E-mail: dupong76@korea.ac.kr

An ultimate goal of a conventional silicon-based integrated system is its capability to last forever without any malfunction and physical deformation, in almost any practical uses. Recent works demonstrate a new class of electronics that has the opposite behavior -- it physically dissolves or disappears in water, environment or biofluids, in a controlled fashion, at predefined times or on demand and with programmed rates. This type of 'transient' technology opens up completely new application opportunities for electronic devices in areas, such as implantable medical devices that exist for medically useful timeframes but then dissolve and disappear completely by resorption into the body. This talk summarizes recent works on bioresorbable electronic systems with mechanically soft, deformable platforms, ranging from fundamental chemistry of the key materials, to development of various components and systems for biosensors, to in vivo evaluations for biocompatibility and potential applications [1-3].

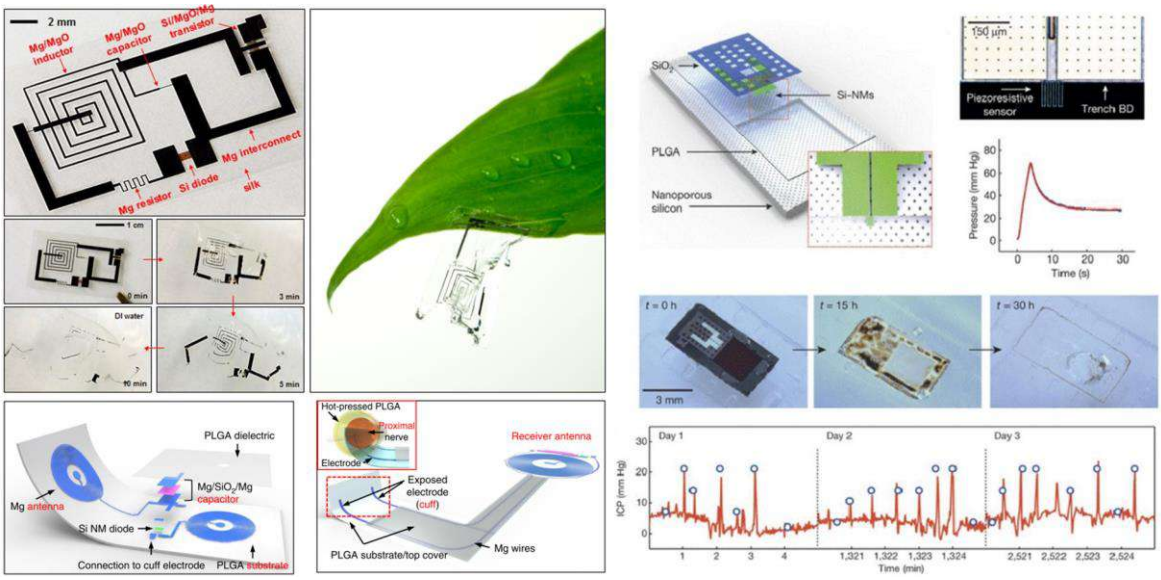

Fig. 1. Exampled demonstrations in soft, resorbable electronics

References

1. S.-W. Hwang et al., *Science* 337, 1640 (2012)
2. S.-K. Kang et al., *Nature* 530, 71 (2016)
3. J. Koo et al., *Nature Medicine* 24, 1830 (2018).

Flexible, infrared covert displays with hybrid planar-plasmonic cavities

***Young Min Song*[1,*]**
[1]School of Electrical Engineering and Computer Science, Gwangju Institute of Science and Technology, Gwangju 61005, Korea
Tel.:82-62-715-2655, E-mail: ymsong@gist.ac.kr

Artificial covert infrared (IR) displays have recently emerged as an anti-counterfeiting method for spontaneous thermal emissive surfaces and optically encoded information. However, the unnatural appearance of a conventional thermal emissive label in the visible region limits the widespread application of an artificial covert IR display [1-3]. This presentation shows a colored, covert IR display exhibiting visible color patterns and thermally encoded data simultaneously based on a hybrid planar-plasmonic cavity (HPPC). The HPPC is composed of two spectrally distinguished resonant structures: 1) an ultrathin planar cavity with an amorphous silicon (a-Si) layer on gold (Au) for visible coloration and 2) an IR plasmonic cavity with hole-patterned Au on a polymer substrate with a back mirror for thermal data encoding. Such hybridization of multi-band resonance can not only enhance the vivid coloration but also enhance the data storage capacity per unit. Camouflage labels with encrypted thermal data are successfully demonstrated for practical applications using a flexible HPPC. Collectively, the proposed HPPC enables a new type of anticounterfeiting method that achieves both esthetic, visibly encoded data, and covert, thermally encoded data [4].

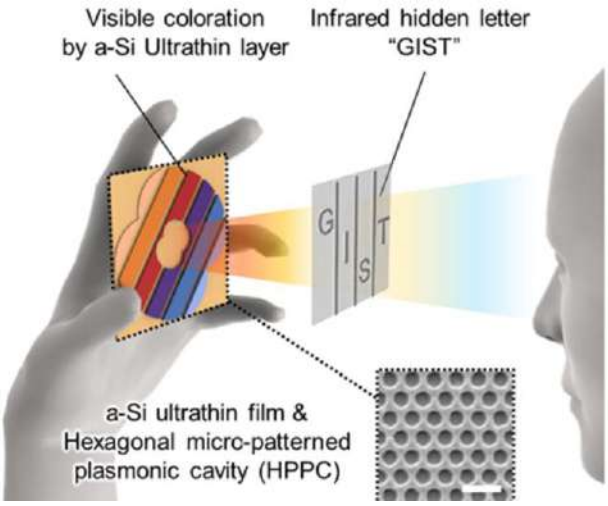

Fig. 1. Schematic illustration of flexible, infrared covert displays with hybrid planar-plasmonic cavities

Acknowledgment

This research was supported by the National Research Foundation of Korea (NRF), funded by the Korean government (NRF-2018R1A4A1025623 and NRF-2020R1A2C2004983), the Korean Institute of Energy Technology Evaluation and Planning (KETEP) and the Ministry of Trade, Industry & Energy (MOTIE) of the Republic of Korea (No. 20183010014310), and by the GIST Research Institute (GRI) through a grant funded by the GIST in 2020. This work was also supported by the Institute of Information & Communications Technology Planning & Evaluation (IITP) through a grant funded by the Korean government (MSIT) (No. 2020-0-01000, light field and LiDAR sensor fusion systems for full self-driving).

References

1. Ko, J. H. et al., *Adv. Funct. Mater.* 1908592 (2020).
2. Lee, G. J. et al., *Advanced Optical Materials* 6, 1870085 (2018).
3. Yoo, Y. J. et al., *Adv. Sci.* 2000978 (2020).
4. Lee, J. H. et al., Adv. Opt. Mater. 2100429 (2021).

Psoriasis Treatment Using a High Power Deformable OLED Patch

Young Cheol Seo[1], Ilkoo Noh[2], Yongmin Jeon[1], Hyeongseop Keum[2], Changjin Seo[2], Sangyong Jon[2] and Kyung Cheol Choi[1]

[1]School of Electrical Engineering, Korea Advanced Institute of Science and Technology (KAIST), 291 Daehak-ro, Yuseong-gu, Daejeon 34141, Republic of Korea

Tel.:82-42-350-3482, E-mail : kyungcc@kaist.ac.kr

[2]Dept. of Biological Sciences, Korea Advanced Institute of Science and Technology (KAIST), 291 Daehak-ro, Yuseong-gu, Daejeon 34141, Republic of Korea

Organic light-emitting diodes (OLEDs) have considerable potential in wearable healthcare applications ranging from optical sensors for real-time medical diagnostics to phototherapeutics for direct treatment. Among these applications, phototherapeutics, which can be divided into photobiomodulation (PBM) and photodynamic therapy (PDT), offers the advantages of being non-invasive, effective, and free from side effects and drug resistance. Unlike PBM [1][2], which requires relatively weak power (> 5 mW/cm^2), PDT requires a strong light of more than 30 mW/cm^2. PDT approaches with conventional OLEDs thus require high voltage, and still have the problem of requiring long-term treatment due to low power intensity [3][4]. To solve this problem, a parallel-stacked organic light-emitting diode with 100 mW/cm^2 output at low voltage (< 8V) was developed in our previous study [5].

In the present study, in order to verify the effectiveness of this device beyond cell-level in an animal model, a more flexible device that can withstand skin flexion and folding with an attached flexible battery on a band-aid platform was implemented. Red light of 630 nm wavelength was irradiated once a day to mice with psoriasis at 35 mW/cm^2 for 35min (73.5 J/cm^2). With only three treatments, a therapeutic effect was confirmed: the thickness of the diseased area was significantly reduced by more than 66% after three 35 min irradiations.

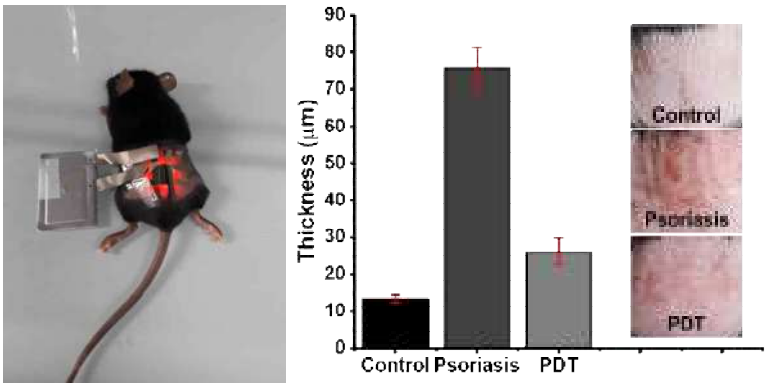

Fig. 1. Schematic of attachable OLED patch and changes in skin thickness after PDT treatment

Acknowledgment

This work was supported by the Engineering Research Center of Excellence (ERC) Program supported by National Research Foundation (NRF), Korean Ministry of Science & ICT (MSIT) (Grant No. NRF-20 17R1A5A1014708) and Basic Science Research Program through the National Research Foundation of K orea (NRF) funded by the Ministry of Science and ICT (NRF-2018R1A3B1052661).

References

1. JEON, Yongmin, et al. Advanced Materials Technologies, 3.5, 1700391 (2018).
2. JEON, Yongmin, et al. Light: Science & Applications, 8.1, 1-15 (2019).
3. ATTILI, S. K., et al. British Journal of Dermatology, 161.1, 170-173 (2009).
4. GUO, Han-Wen, et al. Photodiagnosis and photodynamic therapy, 12.3, 504-510 (2015).
5. JEON, Yongmin, et al. ACS nano, 14.11, 15688-15699 (2020).

2D Interlayer Enabled Electrical Ductility for Flexible Electronics and Display

Pilgyu Kang[1], Chullhee Cho[2], Amir Taqieddin[2], Yuhang Jing[3], Keong Yong[2], Jin Myung Kim[2], Md Farhadul Haque[2], Narayana R. Aluru[2,3], and SungWoo Nam[2,4]

[1]Department of Mechanical Engineering, George Mason University, Fairfax, VA, USA.

Tel.:1-703-993-5973, E-mail: pkang7@gmu.edu

[2]Department of Mechanical Science and Engineering, University of Illinois at Urbana-Champaign, Urbana, IL, USA.

[3]Beckman Institute for Advanced Science and Technology, University of Illinois at Urbana-Champaign, Urbana, IL, USA.

[4]Department of Materials Science and Engineering, University of Illinois at Urbana-Champaign, Urbana, IL, USA.

Flexible electrodes allow sustainable electrical conductance against various mechanical deformation. However, flexible electrodes suffer unexpected electrical disconnection resulting from inevitable mechanical fracture across metal thin-films during their uses, severely reducing the functional lifespan of flexible/wearable electronics. We present a 2D-interlayer approach that enhances strain-resilient electrical performance, dubbed as 'electrical ductility', of metal thin-film electrodes under a high degree of multimodal deformation. Atomically thin 2D-interlayers, such as graphene, induce continuous in-plane crack perturbation of metal thin-film electrodes and enable unique electrical characteristics of 'electrical ductility', where electrical resistance gradually increases with strain allowing orders-of-magnitude ($>10^4$~10^5) lower electrical resistance beyond a strain where conventional metal electrodes would be completely disconnected. We show that our 2D-interlayer approach is not limited to a certain combination of metals and 2D materials. Finally, flexible electroluminescent light emitting device integrated with metal-2D interlayers showcases augmented strain resilient electrical functionality with early damage diagnosis capability via electrical ductility.

Polymeric Devices for Infrared Upconversion Imagers and Haptic Interfaces

Ning Li, Yichen Zhai, and Tse Nga Ng
Dept. of Electrical and Computer Engineering, University of California San Diego, USA
E-mail:tnn046@ucsd.edu

The shortwave infrared spectral region is particularly powerful for a variety of applications including environmental monitoring and medical diagnosis, enabling greater penetration depth and improved resolution in comparison to visible light. Upconversion imagers that combine photo-sensing and display in a compact structure are attractive since they avoid the costly and complex process of pixilation. Here, we have implemented polymeric upconversion imagers that combine photo-sensing and display in a compact structure, to extend the capability of human and machine vision to 1400 nm. The photoresponse is comparable to state-of-the-art organic infrared photodiodes exhibiting a high external quantum efficiency of 35% at a low bias of ≤3 V and -3 dB bandwidth of 10 kHz. The large active area of 2 cm^2 enables demonstrations such as object inspection, imaging through smog, and concurrent recording of blood vessel location and blood flow pulses in Fig. 1a (*1*).

In addition to visualisation of infrared radiation, we are also developing polymeric actuators that generate touch sensations in human-machine interactions. We demonstrated the printing integration of multi-material actuators and achieved a compact tactile display by using liquid-crystal elastomers patterned by extrusion in Fig. 1b (*2*). Printing with organic materials is a versatile approach that can lead to devices that are ergonomic, readily customizable, and economical for everyone to explore potential benefits and create new haptic applications.

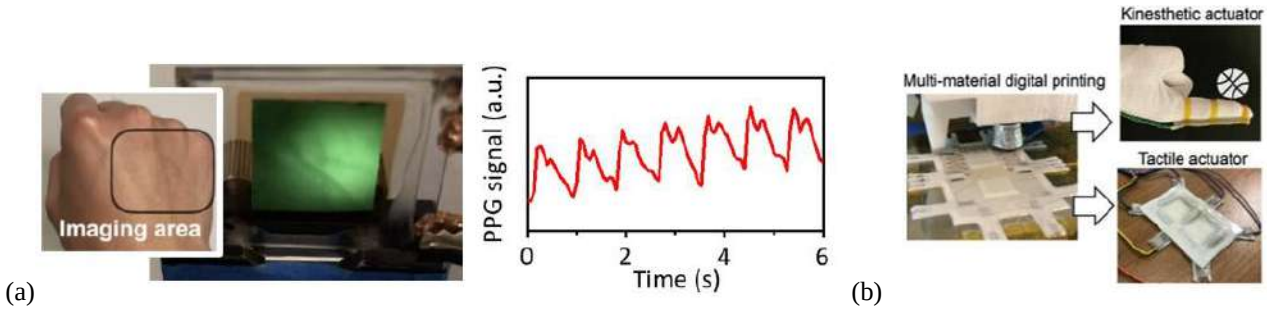

(a) (b)

Fig. 1. (a) Upconversion imager displaying vasculature and blood flow.

Acknowledgment

The research was supported by National Science Foundation (ECCS-1839361) and the UCSD Center for Wearable Sensors.

References

1. N. Li, N. Eedugurala, D. S. Leem, J. D. Azoulay, T. N. Ng, Organic Upconversion Imager with Dual Electronic and Optical Readouts for Shortwave Infrared Light Detection. *Advanced Functional Materials*, 2100565 (2021).
2. Y. Zhai, Z. Wang, K. S. Kwon, S. Cai, D. Lipomi, T. N. Ng, Printing Multi-Material Organic Haptic Actuators. *Advanced Materials*, 2002541 (2020).

Organic LEDs as Bio-Integrated Stimulation Platform

Caroline Murawski,[1,2] Ilenia Meloni,[1] Changmin Keum,[2] Yali Deng,[2] Andrew Morton,[2] Stefan R. Pulver,[3] Malte C. Gather[2,4]

[1] Kurt-Schwabe-Institut für Mess- und Sensortechnik Meinsberg e.V., Kurt-Schwabe-Str. 4, 04736 Waldheim, Germany

E-mail: caroline.murawski@ksi-meinsberg.de

[2] Organic Semiconductor Centre, SUPA, School of Physics and Astronomy, University of St Andrews, St Andrews, KY16 9SS, United Kingdom

[3] School of Psychology and Neuroscience and Centre of Biophotonics, University of St Andrews, St Mary's Quad, South Street, St Andrews KY16 9JP, United Kingdom

[4] Humboldt Centre for Nano- and Biophotonics, Department of Chemistry, University of Cologne, 50939 Köln, Germany

Organic light-emitting diodes (OLEDs) are attractive light sources for biomedical applications due to their high mechanical flexibility and their possibility to form high-resolution displays. This makes them ideal light sources for optogenetics, a neuroscience method that enables light-gated manipulation of neural activity in culture and in living organisms. Challenges of using OLEDs in this context include the need for stacks that reach high light output at low drive voltages,[1] the development of mechanically flexible devices with water-proof thin-film encapsulation,[2] and the requirement of patterning devices to small areas.[3]

This presentation will present ways to address these challenges and will give examples how OLEDs can be applied in optogenetics.[3–5]

Acknowledgment

Diese Arbeit wurde mitfinanziert durch Steuermittel auf der Grundlage des vom Sächsischen Landtag beschlossenen Haushaltes.

References

[1] Y. Deng, C. Murawski, C. Keum, K. Yoshida, I. D. W. Samuel, M. C. Gather, *Adv. Opt. Mater.* **2020**, *8*, 1901721.

[2] C. Keum, C. Murawski, E. Archer, S. Kwon, A. Mischok, M. C. Gather, *Nat. Commun.* **2020**, *11*, 6250.

[3] C. Murawski, S. R. Pulver, M. C. Gather, *Nat. Commun.* **2020**, *11*, 6248.

[4] A. Morton, C. Murawski, Y. Deng, C. Keum, G. B. Miles, J. A. Tello, M. C. Gather, *Adv. Biosyst.* **2019**, *3*, 1800290.

[5] I. Meloni, D. Sachidanandan, A. S. Thum, R. J. Kittel, C. Murawski, *Sci. Rep.* **2020**, *10*, 17614.

LEDs and MicroLEDs for Biophotonics Applications

Ioannis Kymissis[1], Keith Behrman[1], and Christopher Choi[1]
[1]Department of Electrical Engineering, Columbia University, New York, NY 10027, USA
Tel.:347-850-0235, E-mail: joee.columbia.edu

LEDs and microLEDs offer extraordinary luminance and efficiency; as a consequence, these devices offer a number of new opportunities for light source integration in biomedical systems. This presentation will review three applications for LED and microLED integration into bioelectronics (diffuse scattering, as a light source for miniature suprresolution microscopes, and for contact mapping of blood flow in the brain) and some results showing the advantages of these systems. Many of the same advantages that LEDs offer for displays also provide significant promise for non-display applications of the future.

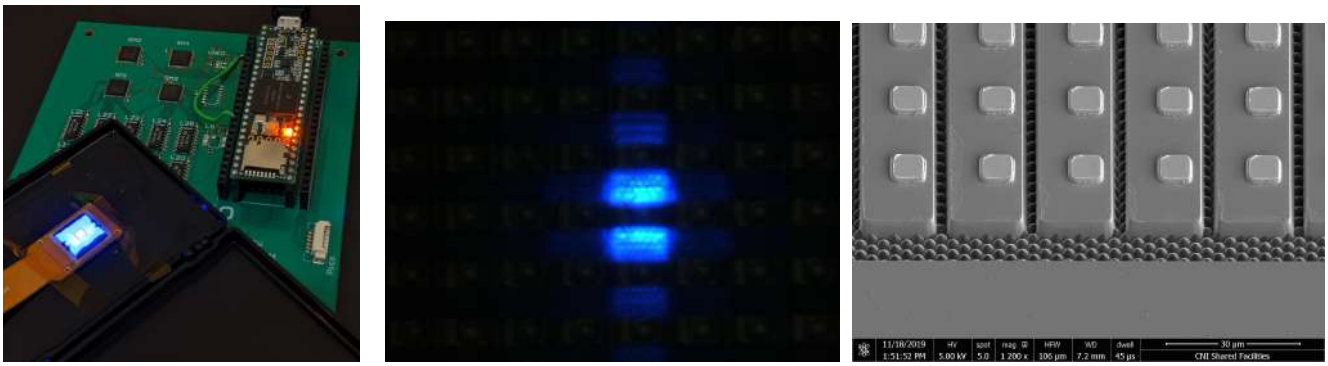

Fig 1. MicroLED-based light sources developed for superresolution microscopy; one of the applications reviewed in this presentation

Acknowledgment

The authors appreciate the support of the National Science Foundation of the United States under program BCS:1926747, and the National Institute of Health under grant 1UF1NS116241-01.

References

1. Choi C, Colón-Berríos AR, Hamachi LS, Owen JS, Schwartz TH, Ma H, Kymissis I. Localizing Seizure Activity in the Brain Using Implantable Micro-LEDs with Quantum Dot Downconversion. Advanced Materials Technologies. 2018 Jun;3(6):1700366.
2. Cox MP, Ma H, Bahlke ME, Beck JH, Schwartz TH, Kymissis I. LED-based optical device for chronic in vivo cerebral blood volume measurement. IEEE transactions on electron devices. 2009 Nov 10;57(1):174-7.
3. Kim Y, Choi C, Chen EC, Daniel AG, Masurkar A, Schwartz TH, Ma H, Kymissis I. An ultra thin implantable system for cerebral blood volume monitoring using flexible OLED and OPD. In2015 IEEE International Electron Devices Meeting (IEDM) 2015 Dec 7 (pp. 29-6). IEEE.
4. Diffuse reflectance
5. Kim Y, Marone A, Tang W, Gartshteyn Y, Kim HK, Askanase AD, Kymissis I, Hielscher AH. Flexible optical imaging band system for the assessment of arthritis in patients with systemic lupus erythematosus. Biomedical Optics Express. 2021 Mar 1;12(3):1651-65.
6. Kim Y, Marone A, Danias G, Neville KE, Frantz AT, Kapoor T, Geraldino-Pardilla L, Kim HK, Askanase AD, Kymissis I, Hielscher AH. Flexible electronic bands for the dynamic optical spectroscopic assessment of systemic lupus erythematosus in finger joints. InOptical Diagnostics and Sensing XIX: Toward Point-of-Care Diagnostics 2019 Feb 20 (Vol. 10
7. Wang F, Kim Y, Altoe M, Marone A, Trippeer B, Edwards A, Sperber A, Goetz S, Schiros T, Kymissis I, Hielscher AH. Development of a Prototype of a Wearable Flexible Electro-Optical Imaging System for the Breast. InClinical and Translational Biophotonics 2020 Apr 20 (pp. TM4B-4). Optical Society of America.885, p. 108850Z). International Society for Optics and Photonics.
8. Kim Y, Marone A, Thompson SM, Sowah JN, Shulevitz HJ, Kim HK, Kymissis I, Hielscher AH. Conformable, Wearable and Scalable Imaging Bands for Assessing Joints Diseases. InClinical and Translational Biophotonics 2018 Apr 3 (pp. JTh3A-34). Optical Society of America.

Strain-engineered Van der Waals Materials for Deformable Electronics

SungWoo Nam[1]
[1]Mechanical Science and Engineering, University of Illinois at Urbana-Champaign, Urbana, IL 61801, USA
Tel.:1-217-300-0267, E-mail: swnam@illinois.edu

Many mechanical deformations, such as buckling, wrinkling, collapsing, and delamination, are usually considered as threats to mechanical integrity and are avoided or reduced in the traditional design of materials and structures. My work goes against these conventions by tailoring such mechanical instabilities to create strain-engineered functional morphologies. We use ultralow bending stiffness and semiconducting properties of atomically-thin van der Waals (vdW) materials to enable strain-engineered properties and device-level multi-functionalities that extend beyond those of bulk material systems. I will present our research on strain engineering of two-dimensional (2D) vdW materials, and the new and reconfigurable materials properties exhibited in such deformed and strain-engineered materials. First, I will introduce controlled mechanical deformation of 2D materials, and the wide range of strain-engineered properties engendered by these deformed materials, such as strain-engineered exciton transport.[1] Furthermore, I will present our work on interfacial control using vdW materials to modulate fracture modes of thinfilms to enable a new phenomenon of strain resilient electrical functionality for flexible electronics.[2] These mechanical instability-induced modulations of materials at the atomic level will open the door to unconventional and reconfigurable properties for applications in next generation deformable electronics and quantum devices.

Acknowledgment

We acknowledge support from NSF (MRSEC DMR-1720633, ECCS-1935775, DMR-1708852 and CMMI-1554019), AFOSR (FA2386-17-1-4071), NASA ECF (NNX16AR56G), ONR YIP (N00014-17-1-2830) and LLNL (B622092).

References

1. J.-P. So, K.-Y. Jeong, J. M. Lee, K.-H. Kim, S.-J. Lee, W. Huh, H.-R. Kim, J.-H. Choi, J. M. Kim, Y. S. Kim, C.-H. Lee, S. Nam, and H.-G. Park, *Nano Letters* 21, 1546 (2021).
2. C. Cho, P. Kang, A. Taqieddin, Y. Jing, K. Yong, J. M. Kim, M. F. Haque, N. R. Aluru, and S. Nam, *Nature Electronics* 4, 126 (2021).

Integrated Retinal Prosthesis with Three-Dimensional Soft Bioelectrodes for Murine Vision Restoration

Won Gi Chung [1], Jiuk Jang [1], Hyobeom Kim [1] and Jang-Ung Park [1]
[1] Department of Materials Science and Engineering, Yonsei University, Seoul 03722, Republic of Korea.
Tel.:82-2-2123-2851, E-mail: jang-ung@yonsei.ac.kr

Retinal degenerative diseases, such as retinitis pigmentosa (RP) and age-related macular degeneration (AMD), can cause permanent damage or even loss of those photoreceptors, which leads to disability of vision and blindness. (1) Recently, electronic retinal prosthesis, which stimulates inner retinal neurons electrically based on photo-responsive components within the device, has emerged as a promising way to restore vision. A three-dimensional (3D) neural microelectrode has been developed to record neural signals or stimulate the nervous system, providing greater spatial resolution, efficient charge injections, and excellent selectivity compared to the two-dimensional (2D) planar electrode by focusing the electric fields. This enhanced proximity to sensory neurons can be effective for the degenerative surfaces because penetrated 3D electrodes are surrounded conformally by the neighboring retinal tissues. However, conventional penetrating neural electrodes, utilizing materials with high modulus, induces undesired space between the surface of the target tissue and the electrode array causing inflammation and hemorrhage. (2)

Herein, we demonstrate a high-resolution, flexible retinal prosthetic device, which consists of Si phototransistor array and 3D soft stimulation electrodes as shown in figure 1. First, we fabricated stimulation electrodes in a 3D pillar structure to reduce their impedances. This 3D stimulation electrode can induce larger neural responses in the retina by reducing threshold current density originated from the increased surface area of the electrode, suggesting effective charge injections. Second, we utilized eutectic gallium-indium alloy (EGaIn) as a soft material for 3D stimulation electrodes in the phototransistor array. Because 3D structure interfacing with biological tissues can cause damages, this liquid metal-based 3D stimulation electrode which has the comparable modulus with that of the retina can minimize the undesired tissue damages. Lastly, based on the in vitro animal tests, we implanted the retinal prosthetic device into the innermost retinal surfaces of the rd1 mouse in vivo for the vision restoration. In this experiment, we confirmed that the signal amplification within the pillar-shaped 3D EGaIn electrodes due to the incident light induces the increment in neural activity (i.e., firing rate of the evoked potentials) in the retinal neurons in real time for a live rd1 mouse, which has totally degenerated photoreceptor layers. Also, the object recognition by illuminating patterned laser was demonstrated, suggesting the restoration of vision of live rd1 mouse.

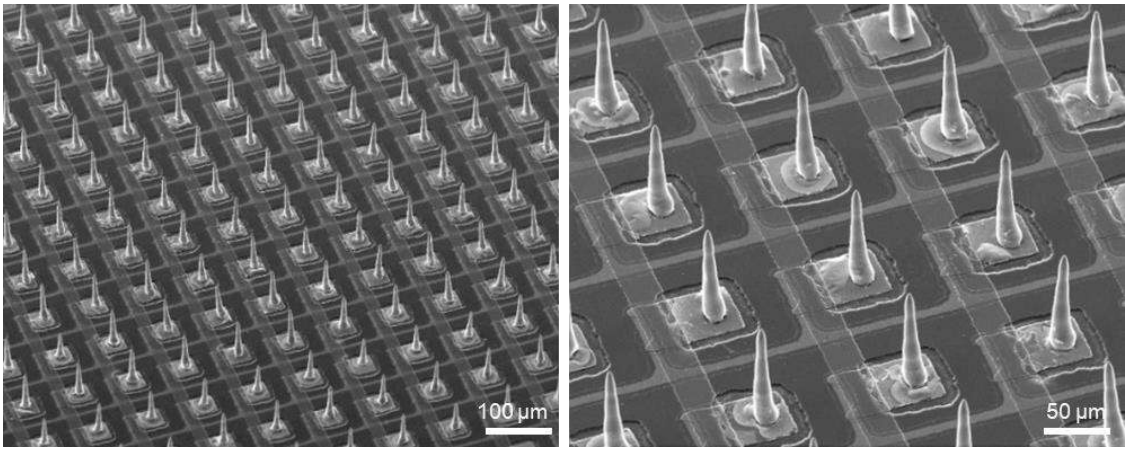

Fig. 1. SEM images of the flexible phototransistor array with three-dimensional stimulation electrodes

References

1. C. Choi, M.K. Choi, S. Liu, M.S. Kim, O.K. Park, C. Im, J. Kim, X. Qin, G.J. Lee, K.W. Cho, M. Kim, E. Joh, J. Lee, D. Son, S-H. Kwon, N.L. Jeon, Y.M. Song, N. Lu & D.H. Kim, *Nat Commun.*, 8, 1664 (2017).
2. J. Jang, H. Kim, Y.M. Song, J.-U. Park, *Opt. Mater. Express.*, 9, 3878-3894 (2019).

Multimodal Cardiac Organoid Sensing for Biomedical Modelling

Moohyun Kim [1], Jae Chul Hwang[1], and Jang-Ung Park [1]
[1] Department of Materials Science and Engineering, Yonsei University, Seoul 03722, Republic of Korea.
Tel.:82-2-2123-2851, E-mail: jang-ung@yonsei.ac.kr

Human stem cell derived organoids provide cellular models of human diseases without the need for in vivo trials, removing non-genetic pathological factors in disease modelling. (1) Current physical modelling of myocardial infarction and drug cardiotoxicity in cardiac organoid is limited to optical image analysis. This method of analysis ranges from spatial proteomics to fluorescent imaging. However, diagnostic modelling of cardiac organoids requires a higher degree of precision and sensitivity in order to accurately measure beating frequency and intensity. In mechanically energetic cardiac organoids, actual collection and interpretation of raw physical data of organoid beating are important to better understand the contractility implication after drug screening. Herein, we introduce an innovative technology that analyze the activity of cardiac organoid using a highly sensitive pressure sensor, which is fabricated from Si transistor with air dielectric component. Previous work has shown sensing capability that was able to capture motion of even up to cellular beating. (2) This device is integrated with electrical stimulating capability that can detect and modulate cardiac organoid beating simultaneously. This sophisticated active-matrix pressure array has a high spatial resolution, providing 2D tactile pressure mapping of cardiac organoid beating. Our novel device is capable of detecting real-time cardiac organoid physical functions, such as beating frequency and intensity, to model various cardiac conditions based directly on the organoids' mechanical parameter. The periodic beatings of cardiac organoids are converted from physical parameters into electrical signals within the pressure sensor. Our device innovatively replaces the conventional method of image analysis, where the organoid beating measurement is derived by dissecting video frames, for myocardial infarction and drug cardiotoxicity modelling. As seen in figure 1, we have successfully mapped beating of cardiac organoid using our pressure sensor. Our device was able to capture the changes in drain current through the active-matrix pressure sensing array.

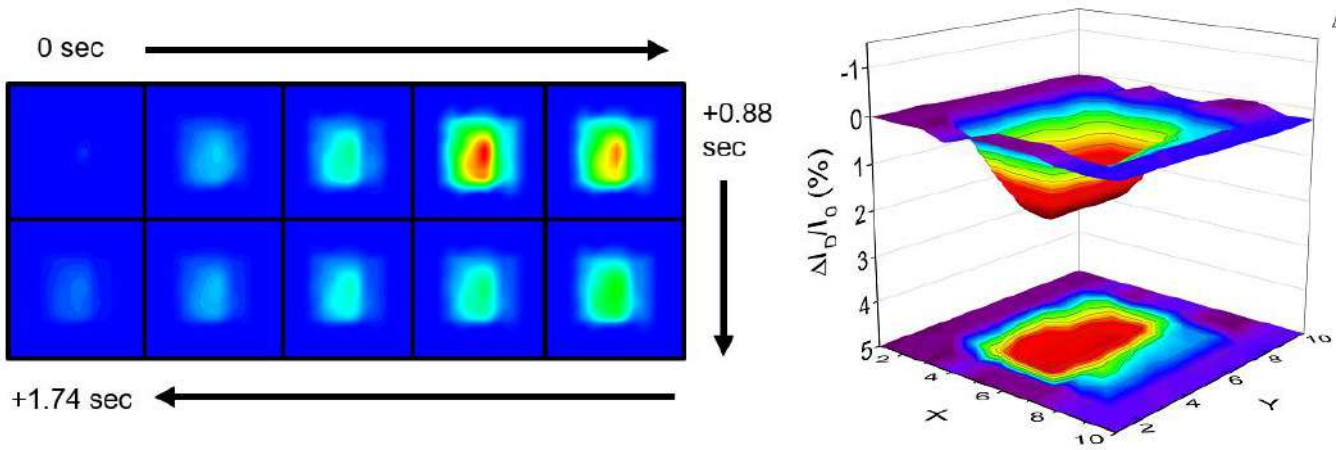

Fig. 1. 2D beating mapping with corresponding drain current

References

1. E. Garreta, R. D. Kamm, S. M. C. de Sousa Lopes, M. A. Lancaster, R. Weiss, X. Trepat, I. Hyun and N. Montserrat, Nature Materials, 1-11 (2020).
2. J. Jang, H. Kim, S. Ji, H. J. Kim, M. S. Kang, T. S. Kim, J.-E. Won, J.-H. Lee, J. Cheon, K. Kang, W. B. Im and J.-U. Park, Nano letters, 20(1), 66-74 (2019).

OLEDs: Pushing Towards Their Limits and Finding New Opportunities

Seunghyup Yoo[1], Jinouk Song[1], Hyeonwoo Lee[1], Seunghee Lee[1], and Taehyun Kim[1]
[1]School of Electrical Engineering, KAIST, Daejeon 34141, Korea
Tel.:82-2-563-7992, E-mail: syoo@ee.kaist.ac.kr

This talk intriduces our efforts to push the organic light-emitting diode (OLED) technoligies to their limits – whether in terms of efficiency or form factors - and find new opportunities beyond their conventional applications. OLEDs being established as a key light source for displays in smart phones and TVs, their applications are being expanded more and more to new types of consumer electronic devices. Regardless of their end applications, one cannot overemphasize the importance of achieving high efficiency and taking full advantages of their potential in form factors. In this respect, the first half of the talk will be dedicated to presenting our engineering efforts to enhance the external quantum efficiency (EQE) of OLEDs to their ultimate limits [1,2] as well as to realize OLEDs with unique form factors [3]. The second half talk will present recent efforts being made to find new opportunities in OLEDs beyond conventional display applications [2,4]. In particular, wearable pulse oximetry based on OLEDs and organic photodiodes will be introduced with emphasis on their potential to become wearable sensors with power consumption that is sufficiently low enough for continuous health-monitoring [5].

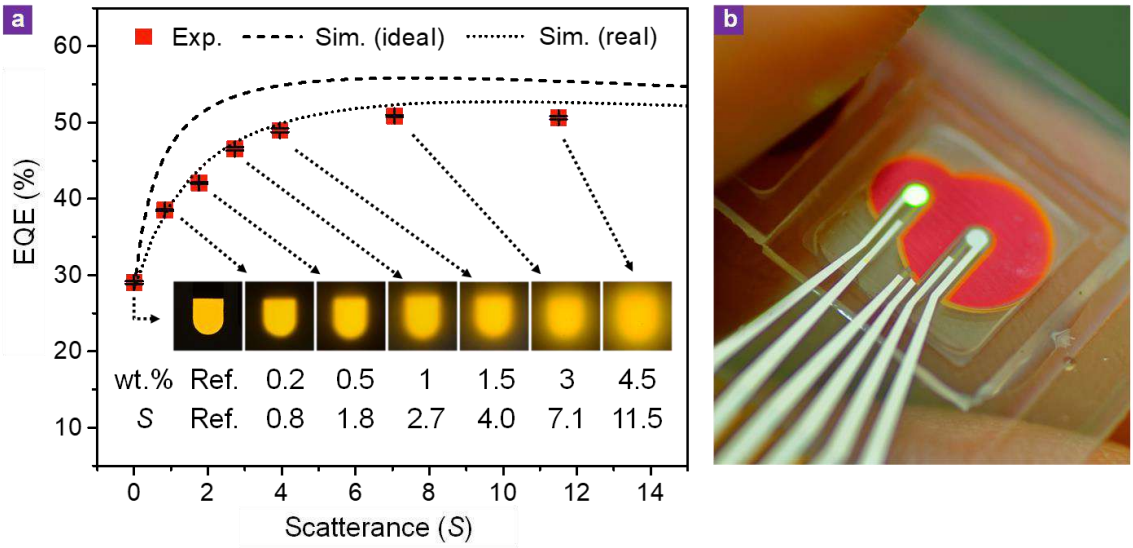

Fig. 1. (a) Highly efficient OLEDs with outcoupling based on scattering layers (SLs) consisting of SiO_2 nanoparticles embedded in optical resin. Their external quantum efficiency (EQE) vs. the scatterance of the SLs. (b) A photograph of an organic pulse oximeter based on OLEDs and an organic photodiode.

Acknowledgment

This research was supported in part by the Nano·Material Technology Development Program through the National Research Foundation of Korea (NRF) funded by the Ministry of Science and ICT(NRF-2016M3A7B4910631), and by the Engineering Research Center of Excellence Program supported by the same (NRF-2017R1A5A1014708).

References

1. J. Song, K.-H. Kim, E. Kim, C.-K. Moon, Y.-H. Kim, J.-J. Kim, S. Yoo, *Nat. Commun.* 9, 3207 (2018).
2. J. Song, H. Lee, E. Jeong, K.-C. Choi, S. Yoo, *Adv. Mater.* 32 (35), 2070266 (2020).
3. T. Kim, H. Lee, W. Jo, T.-S. Kim, S. Yoo, *Adv. Mater. Tech.* 2000494 (2020).
4. G.-H. Lee, H. Moon et al., *Nat. Rev. Mater.* 5, 149-165 (2020).
5. H. Lee, et al. *Sci. Adv.* 4(11), eaas9530 (2018).

Circularly Polarized Luminescence from Chiral Superstructures

Jae-Jin Lee and Suk-Won Choi*
Department of Advance Materials Engineering for Information and Electronics (BK21 Four), Kyung Hee University, Youngin-shi, Gyeonggi-do, 17104, Korea

Tel.: +82-(0)31-201-2256, E-mail: schoi@khu.ac.kr

Recently, several attempts have been made to construct chiroptical soft materials using mixed systems of achiral bent-core and rod-like mesogenic molecules. Bent-core (BC) liquid crystal (LC) molecules are chemically achiral, but turn out to be chiral when they form Helical Nanofilament (HNF) structures. Circularly Polarized Luminescence (CPL) materials were successfully obtained by mixing with fluorescent molecules (guest dyes). This was attributed to the helix of the HNF affecting the structure of the embedded nematic (N) phase doped with the guest dye, there by forming self-assembled chiral aggregates associated with the helix of the HNF phase, despite having a mixed system consisting of only chemically achiral molecules.

First, a chiral nanoporous film with excellent functionality was fabricated based on spontaneous nanoscale segregation in an achiral binary system of BC and rod-like NLC molecules. We successfully demonstrated that this chiral nanoporous film could work as a three-dimensional nano-mold to bring about interesting chiroptical properties, that is, stimuli-responsive circular dichroism (CD). By refilling the chiral nanoporous film with a NLC doped with fluorescent dye, it exhibits stimuli-responsive circularly polarized luminescence.

In addition, we observed an enhancement in the g_{lum} value in a nano-segregated phase system, generated by the phase separation between HNFs (originating from an achiral BC molecule) and a LC SmA phase (originating from an achiral rod-like mesogen). The g_{lum} value observed in the nano-segregated phase <HNF/SmA> was larger than that in the nano-segregated <HNF/N> phase.

Finally, a polymerized twisted nematic (TN) network was used as an extrinsic chiral platform to overcome the heterogeneity during spontaneous symmetry breaking in a mixed system comprising an achiral BC molecule and rod-like mesogen. When the achiral mixture doped with a luminescent guest molecule was refilled into this extrinsic chiral platform, preferential deracemization of the achiral mixture occurred with one-handedness, corresponding to the handedness of the TN platform, resulting in CPL with a preferential handedness.

References

1. J.-J. Lee, B.-C. Kim, H.-J. Choi, S.-W. Bae, F. Araoka, and S.-W. Choi, ACS Nano 2020, 14, 5243−5250.
2. J.-J. Lee and S.-W. Choi, Crystals 2020, 10, 952.
3. J.-J. Lee and S.-W. Choi, Polymers 2020, 12, 2529.
4. B.-C. Kim, H.-J. Choi, J.-J. Lee, F. Araoka, and S.-W. Choi, Advanced Functional Materials, 2019, 29, 1903246.

Improved Efficiency of Organic Light-Emitting Diodes Utilizing Visible Parylene Films

Akpeko Gasonoo[1], Ye-Seul Lee[2], Ji-Hyeon Yoon[2], Baeksang Sung[2], Seung-Yo Baek[2], Yoonseuk Choi[3], Jae-Hyun Lee[2,], and Jonghee Lee[2,*]*

[1]Research Institute of Printed Electronics & 3D Printing, Industry University Cooperation Foundation, Hanbat National University, Daejeon, 34158, South Korea

[2]Department of Creative Convergence Engineering, Hanbat National University, Daejeon, 34158, South Korea

[3]Department of Electronic Engineering, Hanbat National University, Daejeon 34158, South Korea

Tel.: +82-42-828-8802, E-mail: jhyunlee@hanbat.ac.kr, jonghee.lee@hanbat.ac.kr

We applied visible poly-dichloro-para-xylylene (parylene C) films as conformal light extraction enhancement layers in organic light-emitting diodes (OLEDs) [1]. A single-step chemical vapor deposition technique was deployed to deposit the layers directly on the OLEDs at room temperature. The visible parylene C films were fabricated by pyrolyzing sublimed parylene C dimers between 400 °C and 500 °C. We report that the films exhibit unique light scattering properties due to the formation of uniformly distributed dimer crystals. A novel visible parylene film with total transmittance and high haze of 79.5% and 93.6, respectively, is achieved. It is investigated that the OLEDs equipped with the visible films exhibit improved light extraction characteristics. A bottom-emitting OLED equipped with the visible parylene film achieved 45.8% of light intensity enhancement. Additionally, the OLED with the visible parylene film shows limited angle-dependency of emission spectrum over viewing angles. The single-step room-temperature fabrication process of the visible parylene film as a high-performance light extraction layer, using commercially available parylene C, without any combination with other materials and techniques, makes it adaptable to highly efficient commercial OLEDs and other optoelectronic devices.

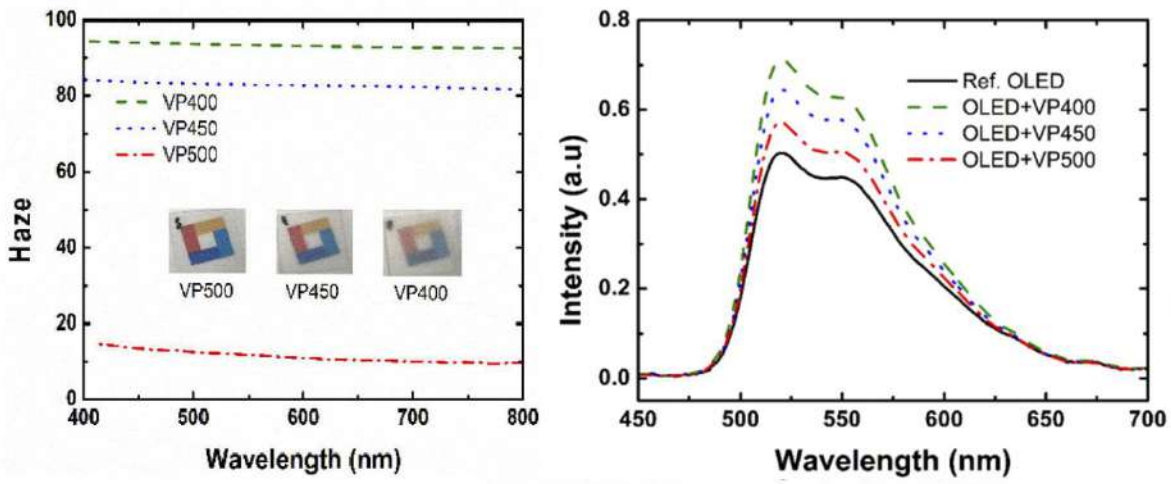

Figure. (a) Measured haze of VP400, VP450 and VP500 films (inset: photograph of glass samples with films placed on a background image) and (b) Electroluminescence spectra of reference OLED (Black solid line) and OLEDs with VP400, VP450 and VP500 films.

References

1. A. Gasonoo, Y.-S. Lee, J.-H. Yoon, B.-S. Sung, Y. Choi, J. Lee and J.-H. Lee, *Optics Express*, 28, 26725 (2020).

Recent Development in Soluble Blue-OLED Materials with High Efficiency and Long Lifetime

Jaechol Lee, and Byungjae Kim
Future Technology R&D Center, LG Chem, Seoul 07796, Korea
Tel.:82-2-6987-5163, E-mail: jcleeb@lgchem.com

Inkjet printing has been widely considered as a potential technology for manufacturing high resolution and large size organic light emitting diodes (OLEDs). Especially, recent progress of soluble OLED materials and inkjet printing equipments have contributed to extend the range of applicable targets from large size TVs to IT/monitor display.[1-3] In this paper, recent progress in soluble OLED materials will be reviewed to achieve high efficiency and long lifetime.

Our soluble OLED materials have been mainly demonstrated by top emission blue devices. The printed layer sequence is hole injection layer (HIL), hole transport layer (HTL) and emission layer (EML). Electron transport layer (ETL), cathode and capping layer (CPL) are thermally evaporated. HTL is composed of polymers, while HIL and EML are based on small molecules. Small molecules in emissive layer are highly preferred to achieve high resolution over 200ppi due to their good processability and low effect on ink viscosity. In addition, narrow full width half maximum (FWHM) and molecular engineering for EML contributed to achieve high efficiency and long lifetime of soluble blue OLED devices. Common layers as HIL and HTL also showed excellent device performance on soluble blue OLED devices.

Ink formulation has been developed in view of film uniformity and intermixing between inkjet printed layers. As shown in Fig. 1, HIL/HTL/EML inkjet pinted layers showed flat and uniform profile. Pixel-to-pixel profile uniformity has been also demonstrated. Intermixing issue has been successfully solved by crosslinking of the preceding layer and solvent orthogonality. In addition, ink formulation for high resolution printing is recently being developed in consideration of various factors such as film uniformity, intermixing, processability, vacuum drying and device performance. Details in our recent progress including device performance will be presented in conference.

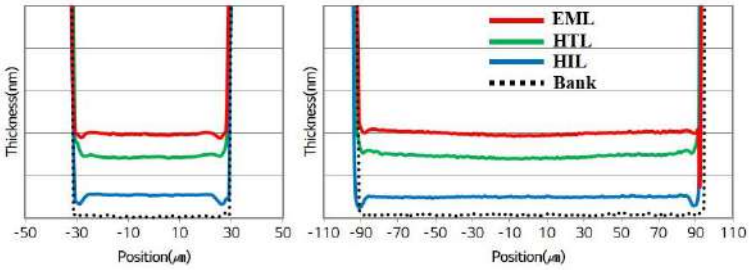

Fig. 1. Film profile of inkjet printed HIL/HTL/EML

References

1. J.-G. Kang, Y. Koo, J. Ha and C. Lee, *SID'20 Technical Digest*, vol. 51, p. 591 (2020).
2. S. Meyer, S. Stolz, M. Hamburger, H.-R. Tseng, M. Engel, A. Hayer, R. Linge, S. Tierney, G. Bernatz and R. Anemian, *SID'20 Technical Digest*, vol. 51, p. 391 (2020).
3. Z. Wu, L. Yan, Y. Li, H. Shih, X. Feng, T. Kim, Y. Peng, J. Yu and X. Dong, *SID'20 Technical Digest*, vol. 51, p. 481 (2020).

Solvent formulation and annealing of high-boiling-point OLED inks for improved jetting behavior and dried surface morphology

Hyun Jun Kim, Min Young Kim*, Robert Bail*, Chil WoniLee**,iByungiDooiChin*†*
***Dept. of Polymer Science and Engineering, Dankook University, Yongin-si, Gyeonggi-do, 16890, Korea**
**** Dept. of Chemistry, Dankook University, Dongnam-gu/Cheonan-si, Chungcheongnam-do, 31116, Korea**
†Tel.:82-31-8005-3587, E-mail: bdchin@dankook.ac.kr

Inkjet printing technology for microscale patterning of pixels in organic light emitting diode (OLED) is significantly attracting the industry due to its large-area process capability without facing the drawback of vacuum-deposited patterning of organic pixel. While the supply of good soluble light-emitting materials (inks) is very important, more attention is drawn for the solvents with a stability during the printing process, ideal in-pixel surface film morphology characteristics after drying process [1], and an orthogonality for a freedom of multilayer-stack of the organic films at the device [2]. In this work, we have prepared green-emitting phosphorescent emitter inks with mixtures of methyl benzoate as primary solvent and other high-boiling solvent additives. The secondary additive solvent is chosen with different boiling point and surface tension compared to methyl benzoate, which become important control parameters toward an improvement of dried film surface morphology. Inks with 4,4',4"-Tris(carbazol-9-yl)triphenylamine (TCTA) : bis[3,5-di(9H-carbazol-9-yl)phenyl] diphenylsilane (SiMCP2) : tris[2-(p-tolyl)pyridine] iridium (III) (Irmppy3) 0.45:0.45:0.10 (wt% ratio) dissolved in solvent mixture with methyl benzoate primary solvent showed superior solubility up to 2.0 wt% (persistent with more than 2 week) and stable jetting behavior with proper piezoelectric waveform using Fuji-Dimatix printheads (DMC11610 and Sapphire QS-256-10 AAA nozzle). Fig. 1 shows the flight of droplet in a jetting cycle during the time interval of 10μs and resultant dot/lines formed by inkjet printing on the substrate coated with poly(9-vinylcarbazole; PVK (Mw 1100K)/PEDOT:PSS/polyimide bank/ITO. Using the optimized conditions of drying (moderate hot-plate thermal annealing followed by solvent-vapor-filled post processing), printed lines in 80μm×240μm scale pixels yield smooth and uniform patterns with less than 10% line-edge-uniformity. More than 80% of efficiency of a reference spin-device obtained with an inkjet-printed device at a 120μm sub-pixel pitch. These results will provide a blueprint for an enhanced uniformity as well as excellence in jetting process via the approach of high-boiling-point novel solution mixture design.

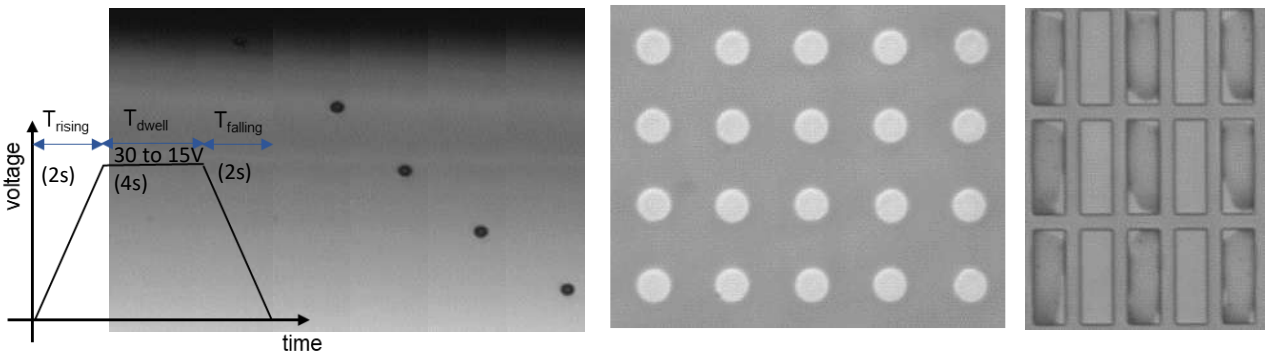

Fig. 1. Flight of droplets in a jetting cycle with 10μs time interval, applied waveform, and inkjet printed dot/line patterns with green phosphoprescent emitter/methyl benzoate : benzyl benzoate 0.9:0.1 inks

References

[1] G. Bernatz, G, Béalle, M. Hamburger, H. Tseng, S. Stolz, A. Hayer, N. Koenen, R. Linge, M. Engel, S. Meyer, R. Anemian, and E. Boehm, *SID'19 Technical Digest*, May 2019, 10.1002/sdtp.13134
[2] S. Ho, S. Liu, Y. Chen, F. So, J. of Photonics for Energy, 5(1), 057611 (2015)

Study on Matrix Perovskite Light-Emitting Devices

Junjie Wang, Danyang Li, Junbiao Peng*

*** Institute of Polymer Optoelectronic Materials & Devices, State Key Laboratory of Luminescent Materials & Devices, South China University of Technology, Guangzhou, China**

***psjbpeng@scut.edu.cn**

Full-color matrix devices based on perovskite light-emitting diodes (PeLEDs) formed via inkjet printing are increasingly attractive, due to their tunable emission, high color purity and possible low cost.[1,2] A key challenge for realizing PeLED matrix devices is achieving uniform and smooth perovskite films with high PLQY via inkjet printing techniques. Here we proposed a full-color PeLED by using an inkjet printing technique.

For perovskite quantum dot ink systems, a smooth perovskite film with high PLQY was achieved through inks optimization and perovskite quantum dot optimization. For perovskite precursor ink systems, a high-quality perovskite film with a favorable emission structure was obtained by drying process control and interface wetting modification. Furthermore, a full-color matrix perovskite device with a color gamut of 102% (NTSC 1931) was realized. To the best of our knowledge, this is the first report on a full-color matrix perovskite device through inkjet printing technology.

References

[1] Jiang. C, *ACS applied materials & interfaces*, **2016**, *8*, 26162-26168.

[2] Cho. H, *Science* **2015**, *350*, 1222-1225.

Self-regulation of infrared with a liquid crystal smart window for energy-saving

Seung-Won Oh[1], Sang-Hyeok Kim[2], Wook-Sung Kim[3], Tae-Hoon Yoon[2]
[1]Division of Electronics Engineering, Kangwon National University, Samcheok, Korea
[2]Department of Electronics Engineering, Pusan National University, Busan, Korea
Tel.:82-2-563-7992, E-mail: kids@k-ids.or.kr
[3]Department of Electrical Engineering, POSTECH, Pohang, Korea

Almost 40% of the total energy is used by buildings in developed countries, and nearly half of the energy is used to drive heating, cooling, and ventilation [1,2]. Windows whose opacity changes in response to external stimuli can reduce the energy cost of heating, cooling, and lighting, while also providing a comfortable environment for occupants. The NIR region contains wavelengths ranging from 800 to 2500 nm; it accounts for 49% of the total energy from direct sunlight and reaches the surface of the earth (Figure 1). This light produces internal heating of the building, although it is not detectable to the naked eye.

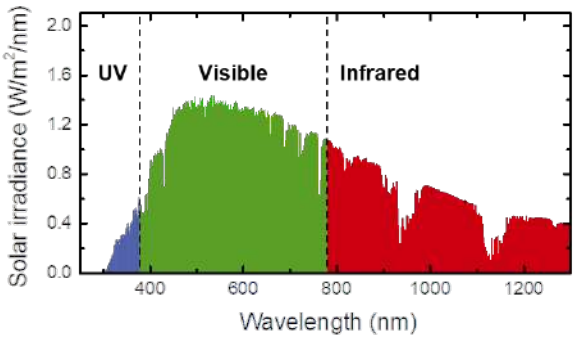

Fig. 1. Solar spectrum offered by the National Renewable Energy Laboratory

Photoresponsive liquid crystals (LCs) can switch among the smectic A (SmA), nematic (N), and isotropic (I) phases in response to the incident light [3−5]. As a smart window, their transmittance can be changed by ultraviolet (UV) and visible lights. Moreover, the transmittance of LCs doped with push–pull azobenzene materials can be controlled with only UV light. These smart windows can reduce heating or cooling cost, while remaining sufficiently transparent to see through even when they are darkened. However, because they cannot be controlled with near-infrared (NIR) light, which is around 50% of the total energy from the direct sunlight, their ability to reduce these costs is limited.

In this presentation, we would like to introduce a self-regulating liquid crystal (LC) smart window whose NIR reflectance changes with environmental conditions such as the sunlight intensity or the outside temperature. Self-regulation between the initial transparent state and the thermally or optically induced NIR-reflective state can be used for energy-saving windows. NIR reflection excludes NIR light while remaining transparent for visible light. Therefore, the proposed window can reduce the energy cost of cooling and heating. The window is transparent in the chiral SmA (SmA*) phase because LCs are self-aligned initially, whereas it reflects NIR light in the chiral nematic (N*) phase.

Acknowledgment

This work was supported by the National Research Foundation of Korea (NRF) grant funded by the Korea government (MSIP) (No. 2020R1A2C1006464).

References

1. M. Isaac and D. P. Van Vuuren, *Energy Policy*, 37, 507 (2009).
2. N. DeForest, A. Shehabi, J. O'Donnell, G. Garcia, J. Greenblatt, E. S. Lee, S. Selkowitz, and D. J. Milliron, *Build. Environ.*, 89, 107 (2015).
3. S.-W. Oh, J.-M. Baek, S.-H. Kim, T.-H. Yoon, RSC Adv., 7, 19497 (2017).
4. S.-W. Oh, S.-H. Kim, T.-H. Yoon, Sol. Energy Mater. Sol. Cells, 183, 146 (2018).
5. S.-W. Oh, S.-M. Nam, S.-H. Kim, T.-H. Yoon, and W. S. Kim ACS Appl. Mater. Interfaces, 13, 5028 (2021).

Traveling Waves of Molecular Reorientation in Homeotropic Cells

Vitaly Petrovich Panov[1], Jiseon Yang[1], Karunarathne L. Migara[1,2], Hyun-JinYoon[1,3] and Jang-Kun Song[1]

[1]**Department of Electrical and Computer Engineering, Sungkyunkwan University, Suwon, Republic of Korea**

Tel.: 82-31-299-4599, E-mail: jk.song@g.skku.edu

[2]**School of Engineering, Sri Lanka Technology Campus, Padukka 10500, Sri Lanka**

[3]**Merck Performance Materials Ltd., Pyeongtaek 17956, Republic of Korea**

Recently reported spontaneous, nematodynamic standing waves [1] in a liquid crystal medium has become intriguing research topic. The standing waves hold unique features such as diagonal nodal lines, self-adaption to broad resonance frequencies and a step-like change of the wavelength with the frequency. Furthermore, the standing wave causes unexpected phenomena that can be used in various applications; for example, it can manipulate the molecular orientation to form tunable, periodic defect arrays with concentric director profiles, which can serve as an optical vortex array inducer or tunable micro-liquid crystal lens array [2,3]. The results lead to new approaches in director manipulation, colloidal assembly and singular optics.

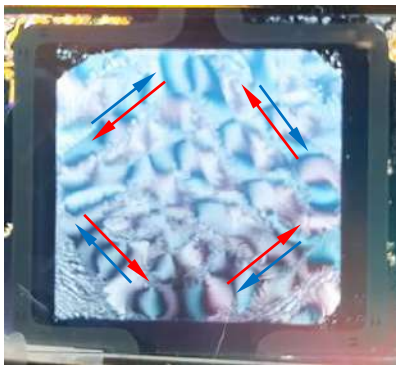

Fig. 1. Traveling wave changing direction with relative phase of the waveform. Crossed polarizers view. Cell size is 20 mm.

Here we report that not only standing waves, but also traveling waves can be produced by applying specifically designed waveforms (Fig. 1.). The time-dependent patterns are caused by change of cell plane projection of the nematic director with every next cycle of the applied voltage. Rotation frequency of the director projection can be as fast as 1Hz, i.e. up to 12° per input waveform cycle. Travel direction and other parameters can easily be controlled by changing the waveforms of the applied electric field.

However, the mutual relation of standing waves reported by Migara et. al. [1,2] and travelling waves presented in this work is totally different from the case of classical waves. Usually, a standing wave is a special case of travelling waves happening at a point of exact match between the wavelength and the boundary conditions. By contrast, in our case these are rather two separate phase states, each existing within own range of input parameters.

We have investigated the existence of this intriguing phase state in multi-dimensional space of the input waveform parameters. Both experimental results (including video) and theoretical analysis will be presented.

Acknowledgment

This work was supported by the National Research Foundation of Korea (NRF) funded by the Ministry of Science and ICT (NRF-2018R1D1A1B07048166) and by ICT Creative Consilience program (IITP-2020-0-01821). V. P. was supported through the Brain Pool Program (NRF−2019H1D3A2A02060963) and Creative Challenge project (NRF-2020R1I1A1A01072707).

References

1. L. K. Migara, J.-K. Song, *NPG Asia Materials*, **10**, e459 (2018).
2. L. K. Migara, *et al.*, *Current Applied Physics*, **18**, 7, 819-823 (2018).
3. R. You, *et al.*, *Advanced Materials Technologies*, **4**, 11, 1900454 (2019).

Analysis about Novel Design of Liquid Crystal Based Floating Electrode Free Coplanar Waveguide Phase Shifter for Performance Improvement

Junseok Ma[1], Hyunji Shin[1], and Wooksung Kim[1]
[1]**Dept. of Electrical Engineering, POSTECH, Pohang, Gyeongbuk, 37673, Korea**
Tel.:82-54-279-8097, E-mail: majun97@postech.ac.kr

Liquid crystals (LCs) have been widely used in the display industry thanks to its unique anisotropic characteristics. Recently, the LC is also one of the materials attracting biggest interests in the antenna technology field. A dielectric constant is an important variable for EM wave applications, and it can be easily controlled by changing the alignment of LCs. Considering the low-lossy characteristics of LCs in the high frequency region, higher price competitiveness compared to other high-freqeucny band devices, and implementability of a low profile structure with a small volume, there is no doubt that the LC is a noteworthy material for the future telecommunication technologies over 5G [1].

Regarding the LC as a phase shifting material, there have been many precedent study subjects including a microstrip line LC phase shifter, a coplanar waveguide (CPW) LC phase shifter [2]. In the CPW phase shifter case, there are also a number of studies about the sturctures such as a floating electorde (FE) CPW, an FE-free CPW, and an enclosed phase shifter (ECPW) [3], [4]. When it comes to the FE-free CPW, it can be simply fabricated with a low cost, however it has very low tuning range (TR). And about the ECPW, although it has improved TR and figure-of-merit (FoM) than the FE-free CPW, it is too bulky and hence the advantanges of the coplanar structure are vanished becuase of the upper ground electrode. For achieving wider TR, lower losses, and higher FoM, many studies in a viewpoint of the phase shifter have been caried out.

In this paper, we devised a new structure for the FE-free CPW phase shifter to compensate for the shortcomings of the conventional structures and improve the performance with ANSYS HFSS and Techwiz at 28GHz. In the structure, we improved the performance while maintaining the advantages of the coplanar structure. With this novel design, we could enhance the FoM and TR of the FE-free CPW more than five times. We also analyzed the tendency of the performance change of the new FE-free CPW design with the various signal width, electrode thickness, and LC thickness. From the analysis, we finally proposed ideas of the optimized design for a new FE-free CPW.

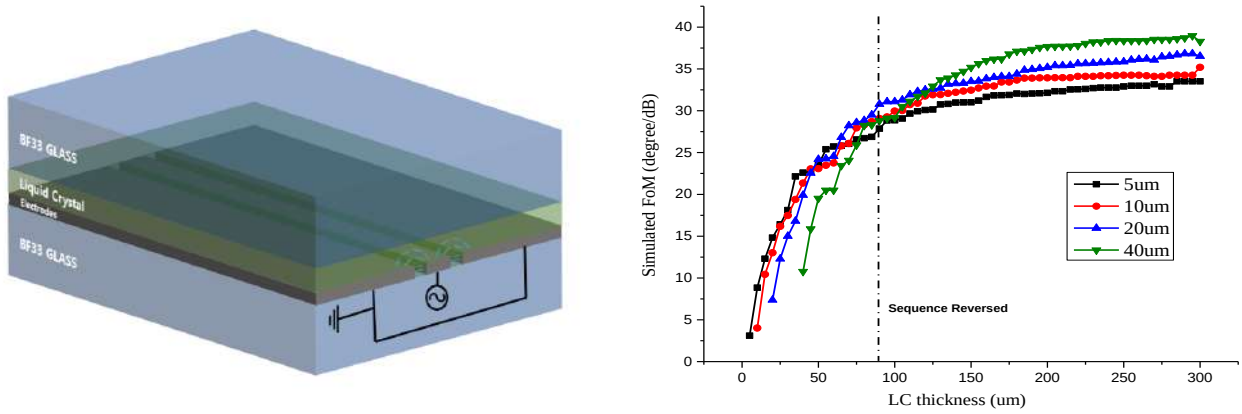

Fig. 1. (a) A novel design of FE-free CPW. (b) Figure-of-merit dependence on LC thickness (simulation)

Acknowledgment

Authors appreciate the kind support of the company Nepes in Korea and JNC Corporation in Japan for this study.

References

1. T.-L. Ting, *Opt. Express.*, **27(12)**, 4(2019).
2. M. Golio (2nd)., "RF and Microwave Passive and Active Technologies", *CRC Press*, (2008).
3. T. Kamei, H. Moritake, Y. Utsumi, Erratum, *Japanese Journal of Applied Physics*. 49(2010).
4. J. Li, D. Chu, *Crystals*, **9**, 650(2019).

Form Birefringence Based +*c*-plate Made by ZnO Nanorods

Jongyoon Kim, Van Chuc Nguyen, and Ji-Hoon Lee*
Division of Electric Engineering, Jeonbuck National University, Jeonju, Jeonbuck 54896, Korea
*Tel.:82-63-270-2476, E-mail: *jihoonlee@jbnu.ac.kr*

The +*c*-plate is a uniaxial birefringent optical retarder with positive birefringence (Δn), and the optical axis is at the out-of-plane. The birefringence ($\Delta n \equiv n_e - n_o$) is defined by the difference between extraordinary refractive index (n_e) and ordinary refractive index (n_o). The +*c*-plate is usually used to improve the viewing angle of the displays by adding additional retardation in oblique angle [1]. This function can be applied not only to liquid crystal displays (LCDs) but also to -anti-reflective films for organic light-emitting diodes (OLEDs). The +*c*-plate can be made by vertically aligned reactive mesogens (RMs) or stretched amorphous polymer in the out-of-plane direction. These conventional methods are based on the intrinsic birefringence of materials. Another method is using form birefringence which origin from the geometrical structure of at least two different materials [2]. One of the benefits of form birefringence-based retarder is is that can be embedded in displays during the display manufacturing process. Nevertheless, the +c-plate based on orbirefringence was not well studied.

In this study, a +*c*-plate based on form birefringence using zinc oxide (ZnO) nanorods were investigated. The ZnO has been actively studied semiconductor due to its high mobility and small reverse current [3]. In contrast, the optical application of ZnO has not yet been studied well. The ZnO nanorod in the +*c*-plate was developed in the out-of-plane direction of quartz substrate using a chemical batch. The fabricated ZnO nanorods retarder has zero in-plane retardation and negative out-of-plane retardation (R_{th}). Thus, the ZnO nanorods retarder is +c-plate. The birefringence of ZnO +c-plate was 0.3 and 0.36 when using zinc nitrate and zinc acetate precursor, respectively [4]. The chemical bath deposition is the proper technique for mass production. Therefore, these results are can be useful in sense of practical application.

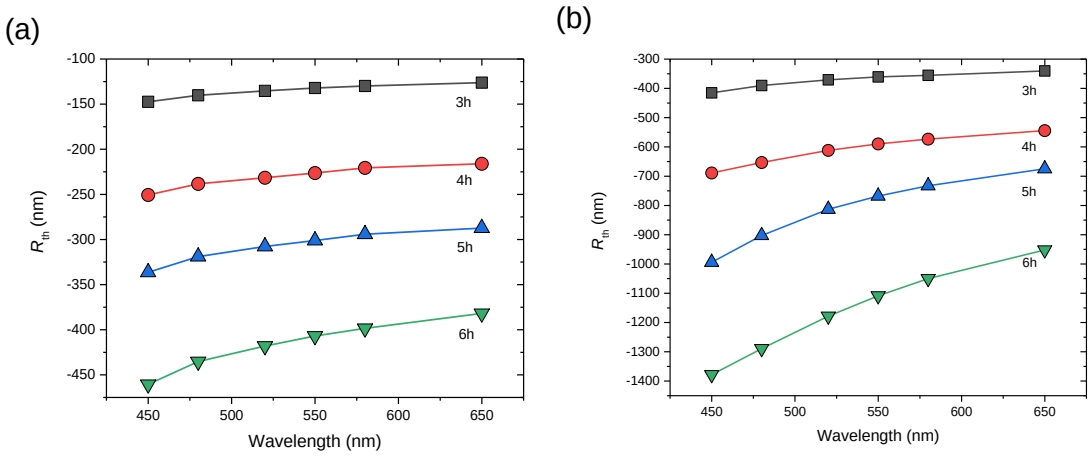

Fig. 1. Out-of-plane retardation (R_{th}) of ZnO +*c*-plate with various chemical bath deposition time using (a) zinc nitrate and (b) zinc acetate precursor.

Acknowledgment

This study was supported by the National Research Foundation (NRF, 2019R1A2B5B01069580, 2019R1A6A1A09031717, 2019H1A2A1074764), and Ministry of Trade, Industry, and Energy (20011031).

References

1. P. Yeh and C. Gu, Optics of Liquid Crystal Display, 2nd edition, John Wiley & Sons, Inc., NJ, chap. 9 (2010).
2. C. Gu and P. Yeh, Opt. Lett. 21(7), 504–506 (1996).
3. C. Klingshirn, ChemPhysChem, 8(6), 782–803 (2007).
4. V.C. Nguyen, J. Kim, P.T. Dang, M. Zumuukhorol, T.V. Cuong, C.-H. Hong, and J.-H Lee, Opt. Mater. Express, 10(12), 3315-3327 (2020).

High-Definition pixelated wrinkles of liquid crystalline polymer for electro-optics applications

***Jun-Hee Na*[1,2*]**

[1]Convergence System Engineering, Chungnam National University, Daejeon 34134, Republic of Korea
[2]Department of Electrical, Electronics and Communication Engineering Education, Chungnam National University, Daejeon 34134, Republic of Korea

Tel.:82-2-821-7978, E-mail: junhee.na@cnu.ac.kr

We propose a novel approach to generate pixelated wrinkles that freely change their orientation at a small area via controlling the alignment of mechanically anisotropic, reactive mesogens (RMs)[1]. An optical setup employing a spatial light modulator illuminates polarized ultraviolet light on a particular area of photoalignment layers, such that RMs, when in contact with these photoalignment layers, can reorient to the respective direction of the incident polarization. Wrinkles that are produced during the plasma-assisted polymerization of RMs can accordingly be aligned. Using a 1280 × 800 array of pixelated wrinkles, our approach assembles complex topographies on various formats of any significant curvatures. We highlight that these topographies show optical patterns based on the birefringence and, as such, permit high-definition image construction and electro-optics applications. Especially, the surface wrinkles can yield obtain excellent light extraction characteristics, and it is expected to be utilized for the development of high-efficiency opto-electronics[2].

Acknowledgment

This work was supported by the National Research Foundation of Korea (NRF) grant funded by the Korean government (MSIT) (no. NRF-2017R1D1A1B03029573 and NRF-2020R1C1C1012757).

References

1. K. Kim, S.-U. Kim, S. Choi, S.-k. Ahn, and J.-H. Na, *Adv. Sci.* 7(24), 2002134 (2020).
2. S. Yeom, H. Kim, K. Kim, C. W. Joo, H. Cho, H. Cho, S. Choi, W. J. Lee, Y. S. Jung, B.-H. Kwon , and J.-H. Na, *Opt. Express* 28(18) 26519 (2020).

Liquid crystal lens array based on polymer protrusion

Fan Chu, Qiong-Hua Wang*
School of Instrumentation and Optoelectronic Engineering, Beihang University, Beijing 100191, China
Tel.: 010-62066854, E-mail: qionghua@buaa.edu.cn

Adaptive liquid crystal (LC) lens offers a tunable focal length, which has widely used in auto-focusing, 2D/3D switchable displays, tunable photonic devices and so on. Many approaches using nematic LC have been demonstrated, and the basic operation principle is to generate electric-field-induced gradient refractive index profile across the LC layer. An LC lens array based on polymer protrusion is proposed. The indium tin oxide (ITO) electrodes are coated on the periodic polymer protrusion, a dielectric layer is used for flattening phase profile, and the vertical electric field across the LC layer varies linearly over the lens aperture, which is obtained in the voltage-on state. As a result, a centrosymmetric gradient refractive index profile within the LC layer is generated, which causes the focusing behavior. As a result of the optimization, a thin cell gap which greatly reduces the switching time of the LC lens array can be achieved in our design. The main advantages of the proposed LC lens array are the comparatively low operating voltage, the flat substrate surface, the simple electrodes, and the uniform LC cell gap. The simulation results show that the focal length of the LC lens array can be tuned continuously from infinity to 1.28 mm by changing the applied voltage.

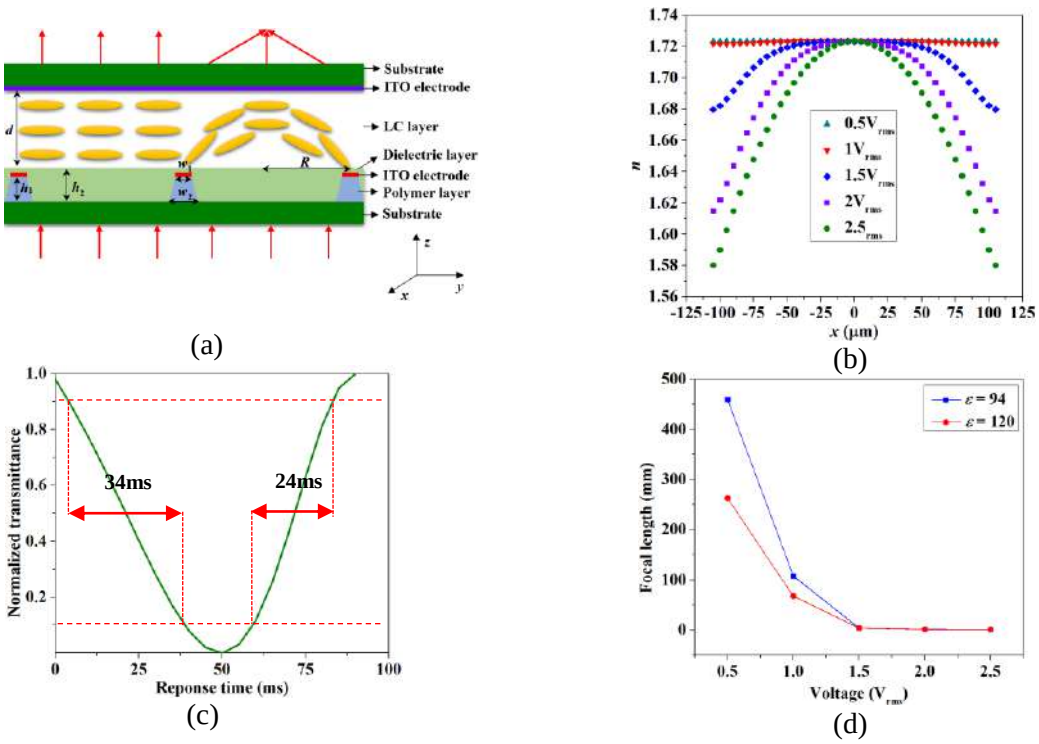

Fig. 1. (a) Structure of the liquid crystal lens array based on polymer protrusion (b) refractive index distribution of a single liquid crystal lens with different operating voltages (c) response time of the liquid crystal lens array (d) voltage-dependent focal length of the liquid crystal lens array under different dielectric constants.

Acknowledgment

This work was supported by the National Natural Science Foundation of China under Grant No. 61927809.

References

1. F. Chu, L. L. Tian, R. Li, X. Q. Gu, X. Y. Zhou, D. Wang, and Q. H. Wang, *Liq. Cryst.*, 47(4), 563-571 (2020).
2. L. L. Tian, F. Chu, H. Dou, L. Li, and Q. H. Wang, *Liq. Cryst.*, 47(1), 72-82 (2020).
2. H. Dou, F. Chu, Y. Q. Guo, L. L. Tian, and Q. H. Wang, *Opt. Express.*, 26(7), 9254-9262 (2018).

Electrically Active and Thermally Responsive Liquid-Crystal Smart Window

Guan-Fu Sung, Po-Chang Wu, and Wei Lee*
College of Photonics, National Yang Ming Chiao Tung University, Tainan 711010, Taiwan
Tel.:886-6-303-2121, E-mail: wlee@nctu.edu.tw

Cholesteric liquid crystals (CLCs) are important in display and sensing applications due to their optical and dielectric anisotropy that is susceptible to stimuli such as the electric field and temperature [1]. A CLC in its intrinsically and periodically helical structure is characterized by the selective reflection following Bragg's law. Although CLCs are promising in window applications, virtually all suggested mechanisms to date can allow only either active or passive operation [2–4]. In the suggested thermo- or photo-sensitive CLCs for the employment of smart windows, there exists a serious weakness of lacking human-based consideration for a human inhabitant living in a specific climate zone. In this work, an intriguing dual-mode CLC device was manifested, enabling the transparency of a laminated CLC film to be automatically adjustable in response to the temperature while simultaneously allowing a user to take the control in the fully on-demand function. The principle originates in the voltage-controllable extent of the electrohydrodynamic (EHD) effect in CLC [5], causing temperature-dependent dynamic scattering and, in turn, the transmission switchable and tunable by the frequency and amplitude of applied voltage. The characteristic Bragg reflection band designated to occur in the near-infrared region offers a value-added benefit to partially reject the undesired thermal radiation in the transparent state.

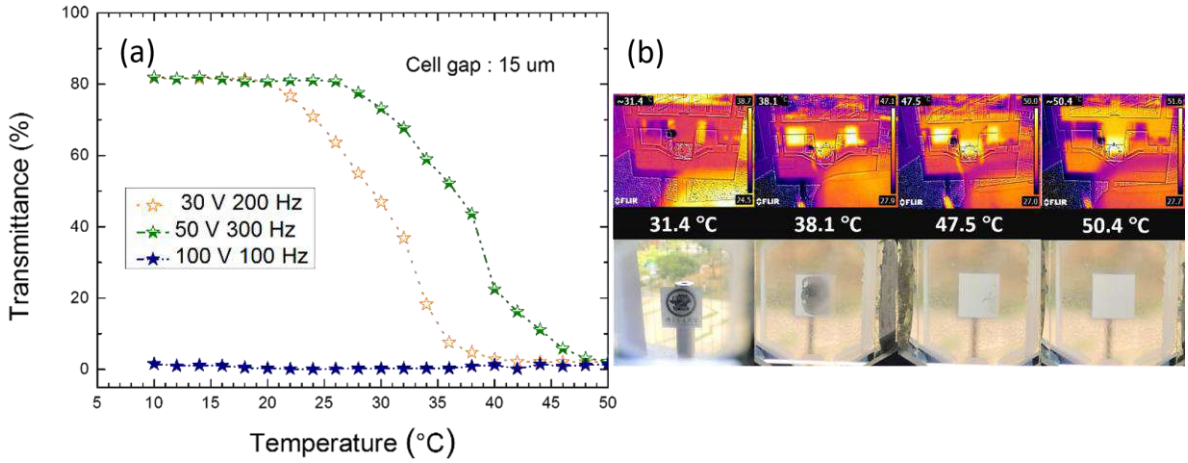

Fig. 1. (a) Temperature-dependent transmission curves in various AC voltage conditions and (b) actual operation demonstrating the varying cell transparency in response to a given ambient temperature.

Figure 1(a) reveals that the transmission is strongly dependent on the extent of light scattering controlled by the EHD effect, which is, in turn, regulated by the external voltage. This enables the CLC cell to be an active device for transparency or privacy control. Based on the data, the highest contrast ratio beyond 820 is deduced. To present a more realistic test, Fig. 2(b) depicts its application for a windowpane based on the (50 V, 300 Hz) curve.

Acknowledgment

This work was financially supported by the Ministry of Science and Technology, Taiwan, under Grant No. 107-2112-M-009-012-MY3.

References

1. Y.-L. Nian, P.-C. Wu, and W. Lee, *Photonics Res.* **4**(6), 227 (2016).
2. D. Cupelli et al., *Sol. Energy Mater. Sol. Cells* **93**(11), 2008 (2009).
3. E. W. Aslaksen and B. Ineichen, *J. Appl. Phys.* **42**(2), 882 (1971).
4. P.M. Alt and P. Pleshko, *IEEE Trans Electron Devices.* **21**(2), 146 (1974).
5. Orsay Liquid Crystal Group, *Mol. Cryst. Liq. Cryst.* **12**(3), 251 (1971).

Photo-Induced Liquid Crystal Alignment for Light Conversion

Wanlong Zhang[1,2], Juncheng Fang[1], Abhishek Srivastava[2], Ting Lei[1], Hoi-Sing Kwok[2] and Xiaocong Yuan[1]
[1]Nanophotonics Research Center, Shenzhen Key Laboratory of Microscale Optical Information Technology & Institute of Microscale Optoelectronics, Shenzhen University, Shenzhen, China
[2]State Key Laboratory of Advanced Displays and Optoelectronics Technologies, Hong Kong University of Science and Technology, Hong Kong S.A.R., China
E-mail: zwl@szu.edu.cn

Photo-induced alignment technology offer the flexibility to orient liquid crystal molecules to desired alignment by exposure to polarized light [1]. Based on this technique, this paper presents the conversion of light in terms of colors and modes.

The colors conversion is facilitated by the alignment of highly luminescent CdSe/CdS core/shell quantum rods (QRs) in the photo-induce aligned liquid crystal monomer, obtaining solid QRs in liquid crystal polymer matrix after UV polymerization. Optical and structural characterization reveals QRs alignment with highly polarized emission, indicating the potential applications in liquid crystal display area. By utilizing reorientation property of photoalignment material SD1, the pattern-alignment of QRs is also achieved. Fig. 1(a) presents the positive and negative QR emission pattern "SKL", with the polarizer parallel and perpendicular to QRs alignment direction, respectively. Fig. 1(b) presents the emissive QR display with controlling polarization azimuth of excitation light by twist nematic liquid crystal cell [2, 3].

The modes conversion of light for LC mode multiplexer/demultiplexer application is realized by reverse-designed liquid crystal holographic phase retarders. As shown in Fig. 1(c), the LP mode multiplexer generated LP01, LP11a, LP11b, LP21 and couples to the few-mode fiber with low insertion loss and mode crosstalk, indicating the promising application in optical communication system with high robust as well as low cost.

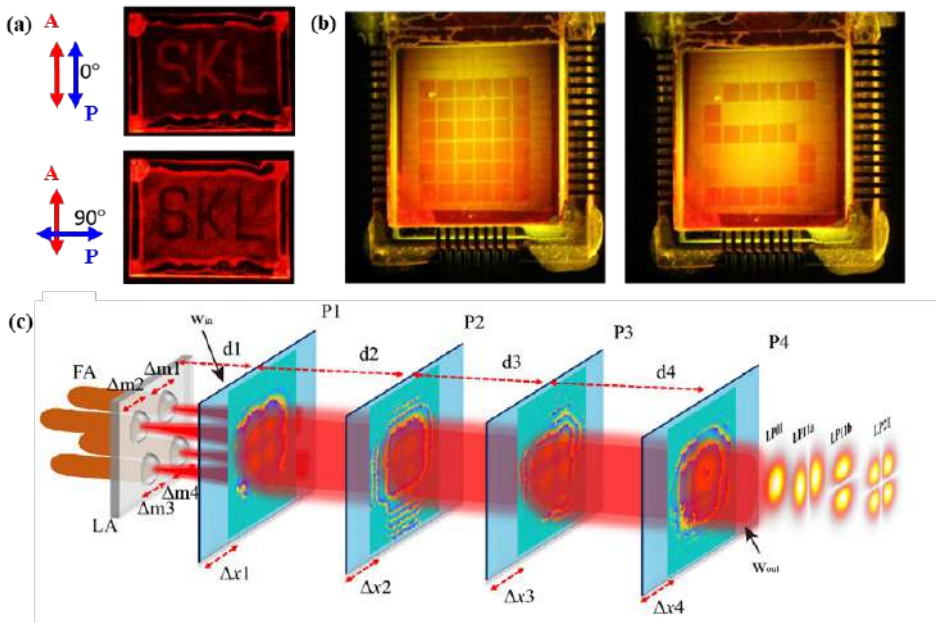

Fig. 1. (a) Emission from QR pattern-alignment with polarizer, (b) an emissive QR display, (c) Schematic of LP mode multiplexer based on reverse-designed liquid crystal holographic phase retarders.

Acknowledgment

The financial support from the National Natural Science Foundation of China(NSFC) 62005180 is gratefully acknowledged.

References

1. M. Schadt, *et al., Jpn. J. Appl. Phys.,* 31(7), p. 2155 (1992).
2. J. Schneider, *et al., Nano Lett.,* 17(5), p. 3133 (2017).
3. W. Zhang, *et al., Adv. Opt. Mater.,* 6(16), 1800250 (2018).

Novel structure for 2-dimensional liquid crystal phase grating with a vertically aligned fringe-field switching mode

Hyeon-seok Eo[1], Seung-won Oh[2], and Wook-sung Kim[1]
[1]Dept. of Electrical Engineering, POSTECH, Pohang, Gyeongbuk, 37673, Korea
Tel.:82-54-279-2363, E-mail: ehs209@postech.ac.kr
[2]Division of Electronics Information & Communication Engineering, Kangwon National University, Samcheok, Kangwon, 25913, Korea
E-mail: ohseungwon@kangwon.ac.kr

The liquid crystal (LC) phase gratings induce electrically switchable diffraction through the spatial phase modulation by the LC director profile under the carefully designed electric field distribution. The convenient diffraction control makes those LC gratings attractive for the laser beam steering and fiber-optic communication [1]. Recent studies about smart windows also used LC grating to solve the conventional LC/polymer mixture's disadvantages for practical applications. When dealing with smart windows using the mixture, the operating voltage, response time, and transparent-to-translucent transition characteristics are considered altogether. However, the conventional LC mixtures can be optimized for one performance parameter, while the LC gratings can be designed to obtain the optimum condition for all the significant parameters by changing structure, LC driving mode, and properties of the compound materials. Recently, T.-H. Choi reported the interdigitated electrode structure for LC gratings in the vertically-aligned fringe-field switching (VA-FFS) mode. The LC grating had a 95.4% translucent state, 1.62/3.37ms turn-on/off response time, and 16V operating voltage [2]. Although most values are higher than conventional electrically switchable LC gratings, the response time is relatively slower than the existing cases. Moreover, the structure needs a complicated driving circuit and process that causes the electrode alignment's low stability.

This paper investigates an LC phase grating in a VA-FFS mode with a lattice-structure electrode. Due to the initial LC state in the homeotropic alignment, LCs on the central parts of the electrode act as virtual walls when electric fields are applied, reinforcing the anchoring of the LCs along to the initial direction. Those walls of LCs in the initial director profile make LCs around those walls return to the initial state more quickly, and hence a fast response time can be observed. The lattice-structure has four virtual walls at all sides as shown in Fig. 1(a) and enhances the anchoring effect further. The two-dimensional phase grating can be constructed with only one electrode pattern so that the fabrication process and driving circuit become more straightforward. We simulated the lattice-structure LC grating with the commercial LC simulation software, TechWiz 3D (SANAYI, Korea), and analyzed the LC director distribution, phase retardation, diffraction phenomena, and response time. The results show that the new LC grating can have a sub-millisecond response time while maintaining the other performance characteristics of the conventional LC gratings.

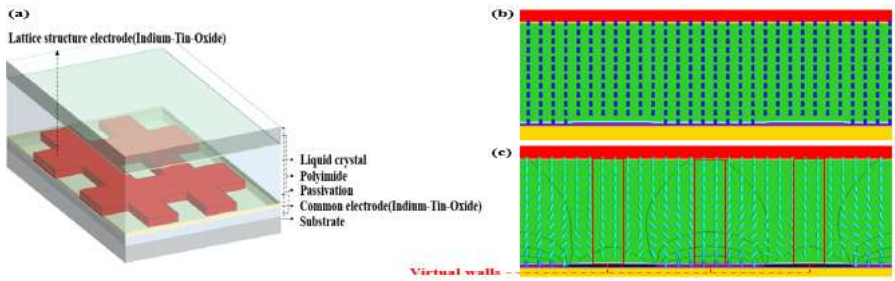

Fig. 1. (a) Scheme of the proposed lattice structure. LC director profiles with an applying voltage of (b) 0V and (c) 8V.

References

1. H. Chen, G. Tan, Y. Huang, Y. Weng, T.-H. Choi, T.-H. Yoon, S.-T. Wu, *Scientific reports*, 7(1), 1-8 (2017)
2. T.-H. Choi, J.-H. Woo, B.-G. Jeon, J. Kim, M.S. Cha, T.-H. Yoon, *Liquid Crystals*, 45:10, 1419-1427 (2018)

Low Complexity Foveation-based Driving Pipeline for High Resolution Head Mounted Displays

Hyoungsik Nam, Seungjun Park, Young In Kim, Jina Bae, and Junhee Lee
Dept. of Inform. Display, Kyung Hee University, Seoul 02447, Korea
Tel.:82-2-961-0925, E-mail: hyoungsiknam@khu.ac.kr

Despite many advanced technologies regarding display panels, rendering algorithms, eye tracking solutions, and image data interfaces, there remains a critical issue to implement the human visual system (HVS) matched virtual reality (VR) system. Because the moving eyes require very high visual acuity everywhere on a display, VR display panels should be able to provide the full-resolution image even for lower acuity areas processed by foveated-rendering, which leads to the insufficient charging time problem.

This paper proposes a foveation-based driving scheme that enables the substantially extended charging time. In the proposed method, a panel reconstructs the full-resolution foveated-rendering image directly from the reduced vertical resolution image, making the high acuity of the foveation area possible everywhere. Therefore, the proposed scheme achieves the reduction on the data bandwidth and the extension of the charging time by the increased line time as shown in Figure 1. The vertical resolutions of 4,800 and 9,600 can be reduced to 30.3 % and 21.0 % that are equivalent to the line times extended to 330.0 % and 476.2 %, respectively. We introduce the overall architecture of resolution reduction, foveation-based panel driving, multi-output shift register, clock generation, as well as foveated super resolution algorithm.

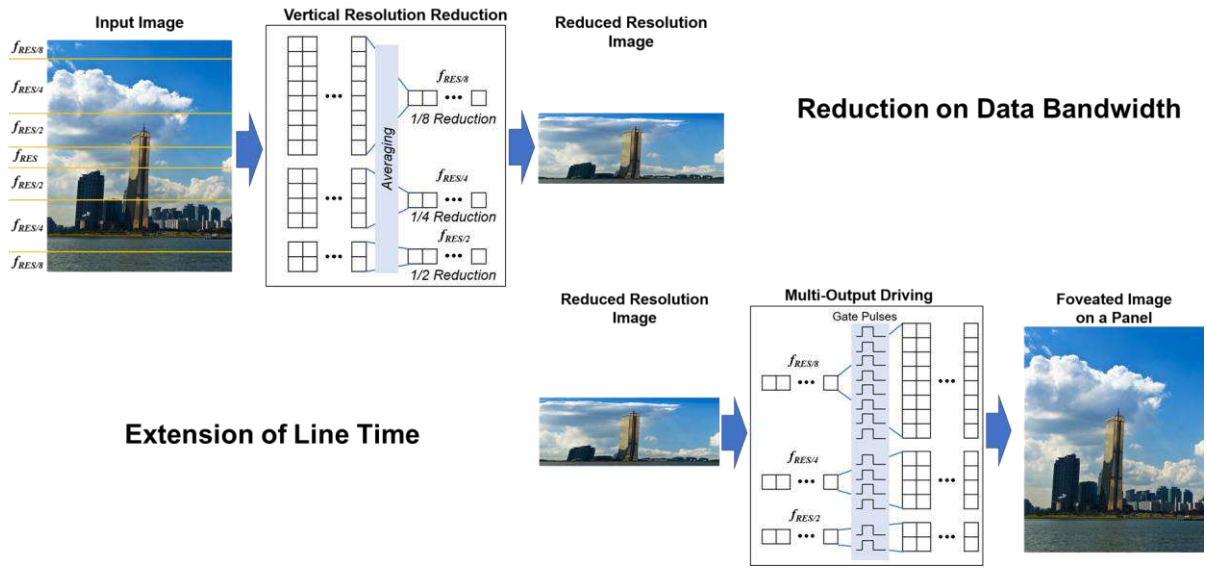

Fig. 1. Foveated-based driving scheme

Acknowledgment

This research was supported by Samsung Display.

References

1. Y. Kim et al., *Electron. Lett.*, 54(20), pp. 1162-1164 (2018).
2. S. Park et al., *Opt. Express*, 27(21), 29594 (2019).
3. J. Bae, J. Lee, and H. Nam, *Electronics*, 10, 538 (2001).

A Fast Bootstrapping Oxide TFT Gate Driver for High-Resolution and High-Frame-Rate Displays

Jun-Hyeok Kim[1], Yong-Duck Kim[1], and Byong-Deok Choi[1]
[1]Dept. of Electronic Engineering, Hanyang University, Seoul 04763, Korea
Tel.:82-2-2220-4344, E-mail: bdchoi@hanyang.ac.kr

Gate driver circuits integrated on display substrate mostly use the bootstrapping technique to address the problems that happen when only either n-type or p-type transistors are available. However, it is quite challenging to apply the bootstrapping technique to very high resolution displays, especially driven at a high frame rate, because the precharging phase that is essential in the bootstrapping takes too long a time. To solve this problem, there have been previous studies [1-2], but need more number of signals[1] or suffer from the slow precharging speed[2]. We propose a circuit technique to boost up the precharging speed that is simple and efficient.

As shown fig.1(a), in a conventional gate driver, the gate node of the output driving transistor, Q[N], is precharged through a diode-connected transistor M1. In this structure, as Q[N] rises, the V_{GS} of M1 decreases, slowing down the precharging operation. On the contrary, in the proposed gate driver, the precharging operation is performed by using two stacked transistors as shown in fig.1(b). Since the V_{GS} of M1 does not decrease, but is kept constant by holding charges in the parasitic capacitance(C_{GS1}), there is no slowing down in the precharging C_B. Therefore, the proposed bootstrapping technique is applicable to even high resolution and high-frame-rate displays where the 1H time is very short. The proposed gate driver with amorphous Indium-Gallium-Zinc-Oxide(a-IGZO) Thin Film Transistor(TFT) fabricated on a polyimid substrate in fig.1(c) can support the 1H time of about 3.85us in fig.1(d) that corresponds to the UHD format display driven at 120Hz.

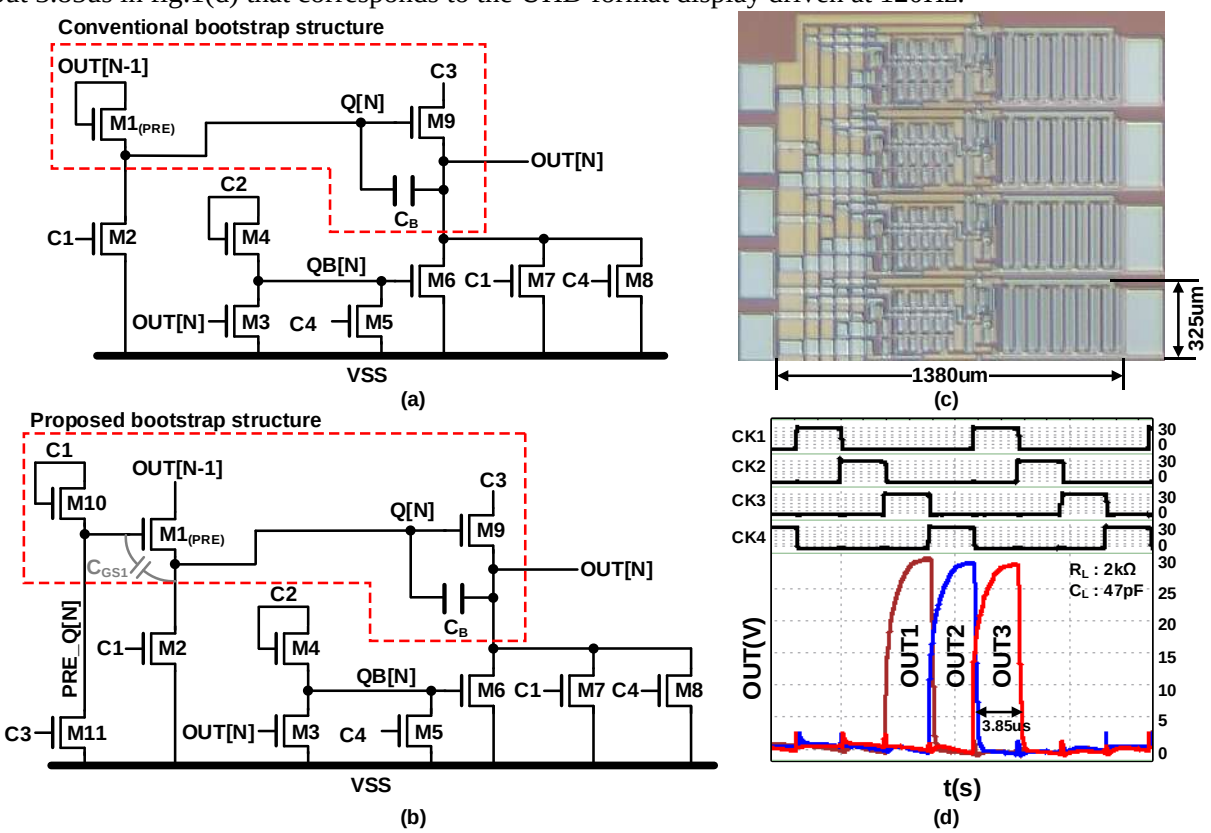

Fig. 1. Schematic of gate driver with (a) conventional bootstrap structure and (b) proposed bootstrap structure. (b) Microphotograph and (c) measurement results of proposed gate driver.

References

1. J.-S. Kim et al., IEEE Trans. Electron Devices, vol. 65, no. 8, pp. 3269–3276 (2018)
2. C.-L. Lin et al, SID Symposium Digest of Technical Papers, vol. 46, no. 1, pp. 1304–1307 (2015)

Double-gate AM-OLED Pixel Circuit Independent on TFT and OLED V_{th} Variation

Ji-Min Kang[1], Kyeong-Soo Kang[1], Ji-Hwan Park[1] and Soo-Yeon Lee[1]*
[1]**Dept. of Electrical and Computer Engineering, Inter-university Semiconductor Research Center (ISRC), Seoul National University, Seoul 08826, Korea**
**Tel.:82-2-880-7273, E-mail: sooyeon.lee@snu.ac.kr*

For the past decade, active-matrix organic light emitting diode display (AM-OLED) has been in the spotlight due to its high contrast ratio, and low power consumption [1]. Since the OLED is a current-driven device, thin flim transistors (TFTs) are connected to each OLED to control the luminance. As for TFTs, oxide TFTs have been widely investigated due to their high mobility and good uniformity [1]. However, the threshold voltage (V_{th}) of TFT and OLED changes under electrical bias or temperature stress, varying the luminance of OLED in each pixel. Thus, compensating for the V_{th} variation of TFT is essential to improve display image quality.

Recently, several compensation methods using the double-gate (DG) structure TFT have been introduced [2-4]. V_{th} variation can be effectively compensated using the fact that the V_{th} of the DG TFT changes linearly depending on the top-gate (TG) voltage. However, previously proposed circuits did not consider the effect of OLED V_{th} variation or negative V_{th} of TFT.

Fig. 1 shows the schematic and control signals of the proposed pixel circuit. We use a DG TFT as a driving TFT (T1). C1 is connected to the bottom-gate (BG), and C2 is connected to TG. The circuit operation stage is divided into four parts; (1) reset, (2) V_{th} detection, (3) data input, and (4) emiss ⊨ on. After initializing the BG, TG, and anode at (a), C1 stores V_{th} of T1 at (2). Then, C2 stores data voltage at (3).

Simulation results shows that the current error after compensation is less than 3%, which is an acceptable error considering the just noticeable difference (JND) based on the human visual system (HVS) [5].

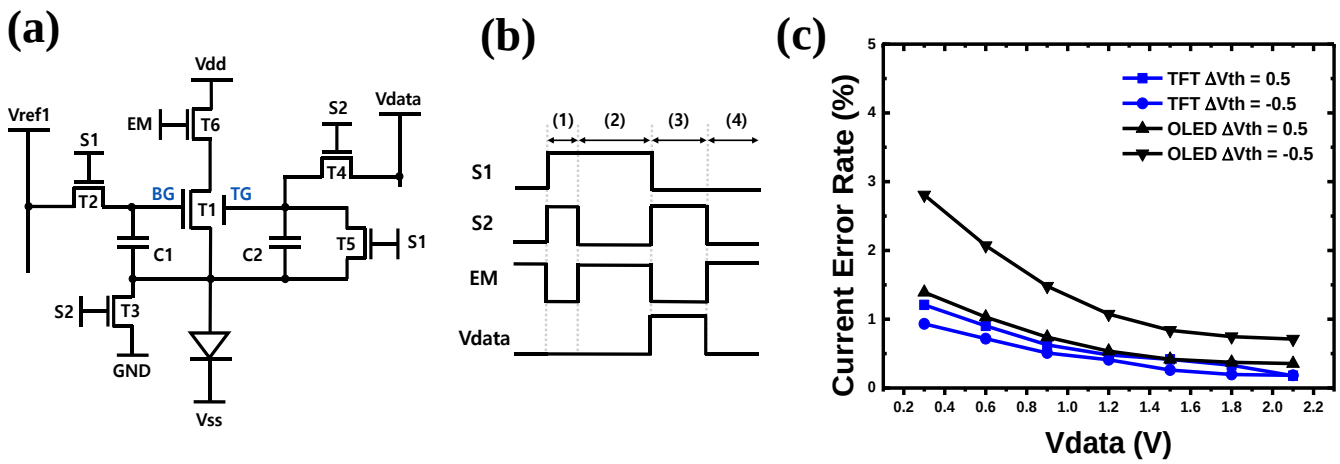

Fig. 1. (a) Schematic of proposed pixel circuit, (b) controlling signals, and (c) current error rate of circuit

Acknowledgment

This work was supported by Samsug Display Co., LTD.

References

1. I. J. Kim, S. Noh, M. H. Ban, K, Son, I. Han, H. K. Shin, K. Oh, B. Kim, I. B. Kang, *J. Soc. Info. Disp.*, 27(5), p.313 (2019).
2. Y. H. Tai, L. S. Chou, H. L. Chiu, B. C. Chen, *IEEE electron device letters.*, 33(3), p.393-395, (2012).
3. C. H. Jeon, M. Mativenga, D. Geng, J. Jang, *SID Symposium Digest of Technical Papers.,* 47(1), p.65-68 (2016).
4. C. H. Jeon, J. G Um, M. Mativenga, J. Jang, *IEEE electron device letters.*, 37(11), p.1450-1453 (2016).
5. K. S. Kang, J. K. Lee, J. M. Kang, S. Y. Lee, *IEEE Journal of the Electron Devices Society*, (2021).

Contents-based Low Power Driving Technology using Variable Potential for Large Panel Display

Seokha Hong, Dongjoon Kwag, Jaesung Bae, Joonchul Goh, and Wonjun Choe
Display Electronics Research Team, Samsung Display, Yongin-si, Gyeonggi-do, Republic of Korea
Tel.:82-31-5181-4890, E-mail: seokha.hong@samsung.com

Recently, Conditions for regulating power consumption of all products are becoming stricter. Large panel displays are no exception. In Europe, energy efficiency grades are designated and managed based on EEI(Energy Efficiency Index). For that reason, research and development to reduce power consumption are becoming important.[1,2] in this paper, contents-based low power driving technology using variable potential and loading-effect compensation is proposed. So, contents-adaptive and real-time processing algorithm can reduce more 15% power consumption in IEC Standard Video Contents without degradation of image quality.

Generally, most display systems consist of constant voltage. This voltage is designed with a margin for the worst image patterns. For low power consumption, variable voltage potential driving technology is proposed. To get the optimum(minmum) voltage level, it requires a few information. First of all, IR-drop of active area in panel should be calculated using power line resistance data. Second, input image data should be anlayzed for determining minimum potential(voltage). Third, driving TFT I-V curve is required for loading-effect data compensation.

To calculate IR-drop Map, panel resistance shoud be transformed mesh-type circuit model, as shown in Fig1. And Block (16x9) current of input image data should be calculated using red/green/blue current ratio. Using both information, 2-Dimensional IR-drop value can be computed and utilized for real-time data processing.

Next, effective input data(gray or voltage) should be recalculted from cognitive picture quality's viewpoint. Using effective input data and as aforementioned 2-Dimensional IR-Drop map, minmum voltage in every frame can be computed with zero-latency. To the following step, display luminance and color characteristic shold be constant and stable in spite of variable potential condition. Using TFT I-V Curve of several gray level, compensation parameter can be caculated compared to target value, as shown in Fig2 .

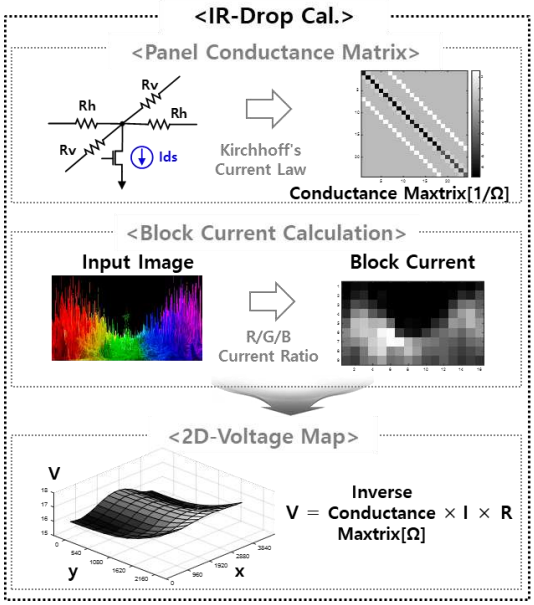

Fig. 1. 2-Dimensioal IR-Drop Simulator

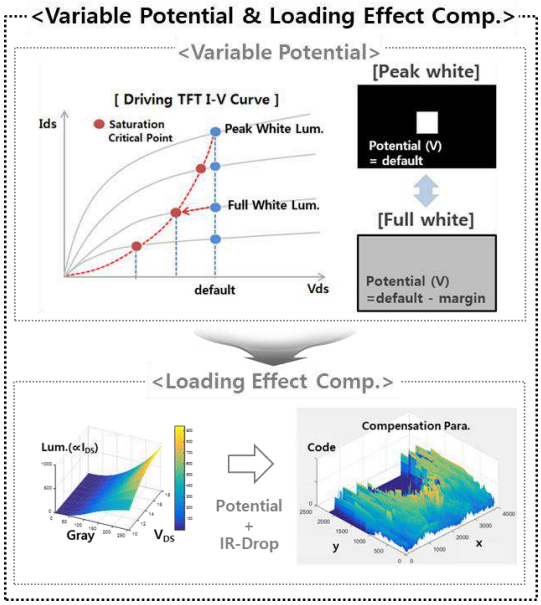

Fig. 2. Variable Potential & Data Compensation

Acknowledgment

References

1. En-Lin Hsiang, *SID'20 Technical Digest*, vol. 51, p. 528 (2020).
2. YongDuck Ahn, *SID'15 Technical Digest*, vol. 46, p. 254 (2015).

Intrinsic Stability of Thermally Activated Delayed Electroluminescence Materials

***Youngmin You*[1]**
[1]Department of Chemical Engineering and Materials Science, Ewha Womans University, Seoul 03760, Korea
Tel.:82-2-3277-4275, E-mail: odds2@ewha.ac.kr

Organic electroluminescence technologies have benefited from the development of luminescent materials capable of exciton harvest. Recent demonstrations of high-efficiency electroluminescence with thermally activated delayed fluorescence (TADF) molecules have spurred enormous research. One challenge that retards commercial applications of TADF devices is their insufficient operational lifetime. Actually, exciton harvest by TADF dopants is slower than that of conventional dopants based on late transition metal complexes, such as Ir(III) and Pt(II). This slow process evokes a growing concern of the instability of TADF devices due to destructive exciton annihilation processes, particularly under high current density regimes. My group initiated mechanistic studies of understanding chemical mechanisms of the intrinsic degradation of TADF materials. Chemical techniques are employed to identify and to directly monitor the key intermediate of the degradation. Our investigations reveal a loose tie between the intrinsic stability and the excited-state lifetime. Spectroscopic and device results collectively point to polarons (radical ions) of TADF dopants being the most vulnerable species. This conclusion is consistent with our previous results of phosphorescence devices,[1] and is further corroborated by the coincidence between the operational device lifetime and the longevity predicted based on our numerical model that involves polarons as the key degradation intermediate.[2] In addition to polarons, our studies also reveal the key role of the conformer on the intrinsic stability of TADF dopants bearing cyclic amino donors.[3] I hope that these understandings will provide useful guidance toward the development of high-stability TADF materials.

Acknowledgment

The author acknowledges the support of the Ministry of Science, Information, and Communication Technology and Future Planning of Korea through the Midcareer Research Program (NRF-2019R1A2C2003969).

References

1. S. Kim, H. J. Bae, S. Park, W. Kim, J. Kim, J. S. Kim, Y. Jung, S. Sul, S.-G. Ihn, C. Noh, S. Kim, and Y. You, *Nat. Commun.,* 9, 1211 (2018).
2. Y. K. Moon, H. J. Jang, S. Hwang, S. Kang, S. Kim, J. Oh, S. Lee, D. Kim, J. Y. Lee, and Y. You, *Adv. Mater.,* 33 2003832 (2021).
3. S. Hwang, Y. K. Moon, H. J. Jang, S. Kim, H. Jeong, J. Y. Lee, and Y. You, *Commun. Chem*., 3, 53 (2020).

The Relation between Spin-circulation and Roll-off Behavior of TADF-based OLEDs with Fast Reverse Intersystem Crossing

Hyung Suk Kim[1], Ja Yeon Lee[2], Seongjun Shin[3], Wonkyo Jeong[3], Sang Hoon Lee[2], Seonghyeon Kim[3], Jihoon Lee[3,*], Min Chul Suh[2,*], and Seunghyup Yoo[1,*]

[1]School of Electrical Engineering, Korea Advanced Institute of Science and Technology, Daejeon 34141, Republic of Korea

Tel.:82-42-350-3483, E-mail: syoo.ee@kaist.edu

[2]Department of Information Display, Kyung Hee University, Seoul 02447, Republic of Korea

E-mail: mcsuh@khu.ac.kr

[3]Department of Polymer Science and Engineering & Department of IT·Energy Convergence (BK21 FOUR), Korea National University of Transportation, Chungju 27469, Republic of Korea

E-mail: jihoonli@ut.ac.kr

Abstract

Reverse intersystem crossing (RISC), if efficient in the ambient temperature, is an effective route to harvest triplet excitons with high internal quantum efficiency in TADF-based organic light-emitting diodes (OLEDs). However, the relatively long time-scale of the RISC in typical TADF emitters is regarded as a big hurdle in suppressing or at least mitigating the device efficiency roll-off at high brightness level. To cope with such issues, we explore a system that shows a very fast RISC on the order of ca. 10^8 s^{-1} by introducing internal heavy atom effect. The study based on the proposed system unravels the relation between the spin-circulation and roll-off behavior with a strong dependence on the positive charge of the nucleus, providing a potential means to mitigate the roll-off behavior at TADF based OLEDs.

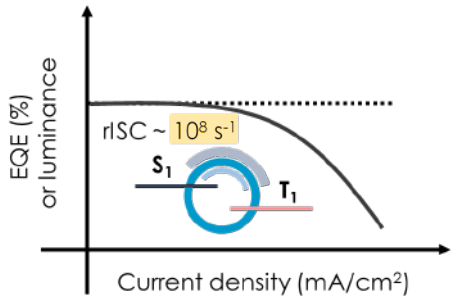

Fig. 1. Fast spin-flip process and its implication on OLED device performance.

Acknowledgment

This research was supported by the Engineering Research Center of Excellence (ERC) Program supported by National Research Foundation (NRF), Korean Ministry of Science & ICT (MSIT) (Grant No. NRF-2017R1A5A1014708). We also acknowledged the support from the National Research Foundation of Korea (NRF) funded by the Korea government (MSIP) (NRF2021R1A2C1008725) and the support from Basic Science Research Program through the National Research Foundation of Korea (NRF) funded by the Ministry of Education (2018R1A6A1A03023788).

References

[1] H. Uoyama, K. Goushi, K. Shizu, H. Nomura, C. Adachi, *Nature* **2012**, *492*, 234
[2] C. Murawski, K. Leo, M. C. Gather, *Adv. Mater.* **2013**, *25*, 6801
[3] A. Kretzschmar, C. Patze, S. T. Schwaebel, U. H. F. Bunz, *J. Org. Chem*. **2015**, 80, 9126.

A New Exciplex host for Solution-Processed Green Phosphorescent Organic Light-Emitting Diodes

Bonju Koo[1,2], Hyejin Na[1], Sangwook Lee[2] and Jaemin Lee[1]
[1]Advanced Materials Division, Korea Research Institute of Chemical Technology, Daejeon 34114, Korea
Tel.:82-42-860-7212, E-mail: jminlee@krict.re.kr
[2]School of Materials Science and Engineering, Kyungpook National University, Daegu 41566, Korea

In recent years, solution-processing for organic light-emitting diodes is gaining much attention in display industry due to its merits such as low material consumption, direct patterning, and low production cost. However, solution-processing still has a problem of lower device performance compared with vacuum evaporation. Especially, the efficiency roll-off at higher luminance is usual in common solution-processed OLEDs. To solve this problem, use of the exciplex system as a host in the emitting layer was one of the way to improve the device efficiency and to reduce the roll-off phenomena. The excipelx system is formed by mixing *p*-type materials and *n*-type materials in one layer, and the the choice of each of the *p*-/*n*-type materials determines the reusultant exciplex characteristics. While thare have been reported many kinds of *p*-/*n*-type materials for OLEDs, only limited materials have been applied to the solution-processed explex system, and therefore it is necessary to develop new materials that are suitable such solution-processed exciplex formation.

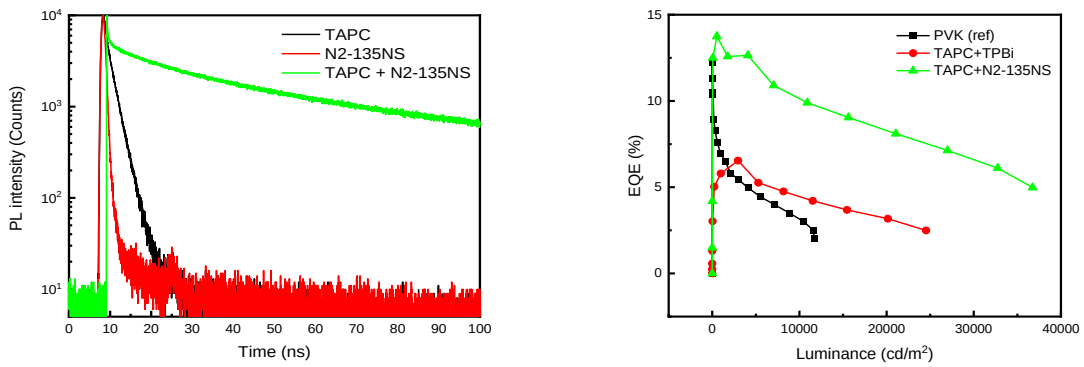

Fig. 1. Comparison of time-resolved PL of single and mixed materials (left) and EQEs of OLEDs containing single host and two mixed host of different n-type materials (right).

In this work, a new *n*-type material, N2-135NS, has been synthesized and the optical properties of the material have also been carefully analyzed. When N2-135NS was mixed with TAPC, a typical *p*-type material, a new PL emission peak was evolved. And the formatin of the exciplex was confirmed by comparing the TRPL decay curves. The exciplex system was then used as a host of green phosphorescent emission layer. The OLED device configuration was [ITO / PEDOT:PSS / **HOST**:Ir(mppy)$_3$ / TPBi / LiF / Al]. The exciplex host resulted in a high EQE of 13.75%. Furthermore, the explex host also showed a 0.75 times lower driving voltage than the single host. Details of the material and device characterizations will be discussed in the presenation.

Acknowledgment

This work was supported by the Materials Innovation Project (2020M3H4A3081790) funded by National Research Foundation of Korea.

References

1. M. Sarma and K. –T. Wong, *ACS Appl. Mater. Interfaces*, 10(23), 19279 (2018).
2. Q. Wang, Q. –S. Tian, Y. –L. Zhang, X. Tang and L. –S. Liao, *J. Mater. Chem. C*, 7, 11329 (2019).

A Soluble Host Material with Indenocarbazole Moiety for Green Phosphorescent Organic Light Emitting Diodes by Solution Process

Eun Young Park[1], Da Hwan Lee[1], Thi Na Le[1], Jihoon Lee[2] and Min Chul Suh[1,]*
[1]Organic Electronic Materials Laboratory, Department of Information Display, Kyung Hee University, Seoul 02447, Republic of Korea
[2]Dept. of Polymer Science and Engineering and Dept. of IT Convergence (BK21 PLUS), Korea National University of Transportation, Chungju, 27469, Republic of Korea

Previously, organic light-emitting diodes (OLEDs) were fluorescent-based devices, but now devices are manufactured using phosphorescent materials. In addition, in order to construct a solution processed phosphorescent device using phosphorescent materials, a lot of research has also been done for solution materials. However, there are still lots of problems such as efficiency and lifetime to be commercialized. The reason for this problem is that the annealing process is always essential after the coating step. We reported that red dopants can be liberated from the host matrix when we anneal the materials at about 150 °C. To make matters worse, under high current density driving conditions, phosphorescent devices are affected by triplet-triplet annhilation or exciton-polaron quenching processes from dopant agglomeration. And, this could be a main cause of reduced efficiency and lifetime.[1,2]

Another problem is an interface mixing of hole transport layer (HTL) and emitting layer (EML), which also cause a serious problem on lifetime. Specially, in this mixed region (HTL/EML), the formation of excitons can lead to material degradation due to severe exciton-polaron quenching. To solve this problem, the material must be designed so that electrons do not pass through the EML and approach to this interface. In other words, it can be much more advantageous when the material in EML has strong hole transport properties.

On the other hand, even if the blue light-emitting material is formed into a thin film by thermal evaporation technology, the lifetime is still short. So the solution process cannot guarantee a long lifetime. Therefore, we tried to prepare a green PHOLED with a structure in which a blue common layer is inserted in the final form of the green OLED device. From this approach, we could realize a operational lifetime (LT_{50}) longer than 1,000 hours.

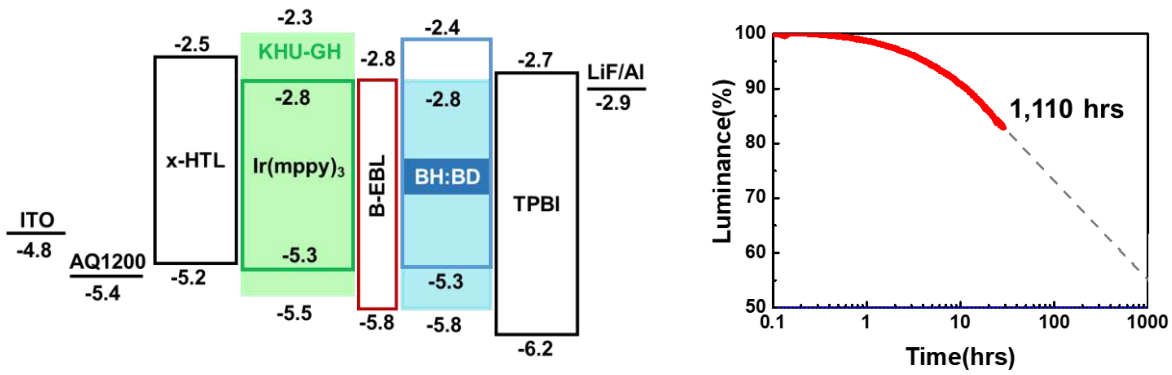

Fig. 1. Energy band diagram of solution processed OLEDs (left), Lifetime data according to BCL thickness

Acknowledgment

This work was supported by the Industrial Strategic Technology Development Program (20011059) funded By MOTIE, Korea. This work was also supported by NRF,Korea (NRF 2021R1A2C1008725) and funded by the MOTIE, Korea (20011059).

References

1. S. Lamansky, R. C. Kwong, M. Negent, P. I. Djurovich, M. E. Thompson, Organic Electronics. 2001, 2, 53.
2. L. Duan, L. Hou, T.-W. Lee, J. Qiao, D. Zhang, G. Dong, L. Wang, Y. Qiu, J. Mater. Chem. 2010, 20, 6392.

Solution Processed Organic Light Emitting Diodes with Single Component Emitters Crosslinkable below 150°C for Solution Process

Da Hwan Lee[1], Jae-Min Yoo[1], Kanghyuck Lee[2], Jihoon Lee[2] and Min Chul Suh[1,]*
[1]Organic Electronic Materials Laboratory, Department of Information Display, Kyung Hee University, Seoul 02447, Republic of Korea
Tel.:82-2-961-0694, E-mail: mcsuh@khu.ac.kr
[2]Dept. of Polymer Science and Engineering and Dept. of IT Convergence (BK21 PLUS), Korea National University of Transportation, Chungju, 27469, Republic of Korea

Recently, due to the problem of process cost, many studies are being conducted to replace organic light emitting diode (OLED) devices with solution process technology as a method to replace the thermal vacuum deposition method.[1] However, since the solution processed OLEDs are fabricated of multi-layer thin films, a problem of interfacial mixing occurs.[2] In order to solve this problem, a method for designing a substance exhibiting orthogonal solubility and/or a method for complete crosslinking of the substance is very important. However, in most cases, a temperature higher than 200°C is required for complete crosslinking of a certain organic materials. Unfortunately, when the crosslinking temperature is raised so much, the dopant melts in the light emitting layer (EML) and separates.[3] This can lead to very serious deterioration of the device due to various self-quenching processes. This is contrary to the results that annealing above 200°C improves device stability, as reported by the Adachi group.

So, we abandoned the system of mixing the small-molecular host material with the small-molecular dopant and developed a crosslinked polymer light emitting layer that can minimize the diffusion of the dopant. In order to confirm the possibility of these materials as host materials, the luminescence characteristics were confirmed by coating and crosslinking the materials. In particular, the two polymers reported in this study are unique polymers that exhibit high solvent resistance due to crosslinking at 135°C, and this method has also been applied to hole transport layer (HTL). In this presentation, we would like to report the results of using these materials as a single component and the luminescence properties obtained by adding several dopants.

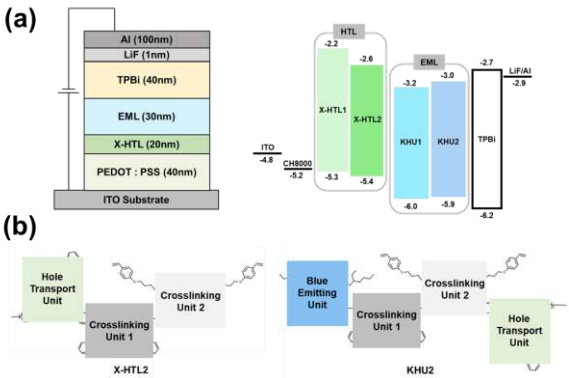

Fig. 1. (a) Energy band diagram of solution processed OLEDs (b) utilized materials structure

Acknowledgment

This work was supported by the Industrial Strategic Technology Development Program (20011059) funded By the MOTIE, Korea. This work was also supported by NRF, Korea (2021R1A2C1008725).

References

1. S. H. Cho, J. S. Park, J. H. Kwon and M. C. Suh, J. Nanosci. Nanotechnol., 2012, 12, 1271.
2. H. Sasabe, J. Kido, "Multifunctional Materials in HighPerformance OLEDs: Challenges for Solid-State Lighting", Chemistry of Materials, 23 621 (2011)
3. Lee, J. Y., Kim, J., Kim, H., Suh. M. C. Molecular Stacking Effect on Small-Molecular Organic Light Emitting Diodes Prepared with Solution Process. Appl, mater. Interfaces. 2020, 12, 23244-23251.

Pushing the colour of multi-resonance thermally activated delayed fluorescence materials towards the red for organic light-emitting diodes

***Eli Zysman-Colman*[1]**
[1] Organic Semiconductor Centre, EaStCHEM School of Chemistry, University of St Andrews, St Andrews, KY16 9ST, United Kingdom
Tel.: +44 1334 463826, E-mail: eli.zysman-colman@st-amdrews.ac.uk

Multi-resonance thermally activated delayed fluorescence (MR-TADF) materials are an exciting subclass of TADF emitters for us in organic light-emitting diodes (OLEDs) as they are very bright and show narrow-band emission providing a solution for organic materials that can meet the industry display standards.[1]

We present our recent efforts for the design of MR-TADF compounds that emit beyond the green, where there are currently a paucity of examples. We show how computations guide molecular design, to expand the chemical space for this class of emitter.

References

1. S. M. Suresh, D. Hall, D. Beljonne, Y. Olivier, E. Zysman-Colman, *Adv. Funct. Mater.,* 1908677, (2020).

Merck OLED: Beyond Materials Towards The Next Generation Display

Rémi Anémian et al.
Merck KGaA, Frankfurter Str. 250, 64293 Darmstadt, Germany
Tel.:49-6151-72-3720, E-mail: remi.anemian@merckgroup.com

In the recent years, OLED has created a world of new opportunities, which are now all becoming reality. Whether thin, flexible, foldable, or even rollable, OLED displays are breathtaking and the possibilities seem almost unlimited. With brilliant colors and sharp picture quality, OLED displays are also environment friendly. They can show, for example, in the dark mode functionality a dramatic battery life increase, contributing to significant energy savings. Being energy-efficient and long lasting, they are perfectly adapted to a more caring and sustainable society.

As an innovation pioneer in the display industry, Merck OLED materials can be found in all cutting-edge displays, for mobile and TV applications.

In this talk, we will discuss how our large and complete material portfolio combined with our original approach based on simulation from atom level towards full device understanding could bring OLED displays to their next level of performances, transforming electronics day by day.

Foldable Nano-Phase-Separated LCDs with 2.5 mm Radius of Curvature using Polymerization Inhibitor

Takahiro Ishinabe, Akane Arakawa, Yosei Shibata and Hideo Fujikake
Dept. of Electronic Eng., Grad. School of Eng., Tohoku University, Sendai, Miyagi 980-8579, Japan
Tel.:81-22-795-7119, E-mail: takahiro.ishinabe.c4@tohoku.ac.jp

Sheet-type liquid crystal displays (LCDs) [1-2] using plastic substrates have many advantages such as ultra-thin, light-weight and unbreakable. These features enable layered displays that improve an optical performance and functionality of display devices such as the high-contrast dual-layered LCDs and the viewing angle controllable LCDs. In addition, sheet-type LCDs can achieve an extremely narrow borders less than 0.3 mm by folding the edge of display panel. For these reasons, sheet-type LCDs are attracting significant interest for new applications, including curved automotive displays, large digital signages, high contrast rollable screen televisions, foldable and wearable devices.

We have developed the foldable LCDs using nano-phase-separated (NPS) LCs [3-4]. By introducing the nano-size polymer network into the LCs and controlling the viscoelasticity of LC materials, we successfully suppressed the flow of LCs and improved the luminance uniformity in the bending state.

In addition, we established the control method of the structure of polymer spacers by using the polymerization inhibitors [5]. By controlling the polymerization stopping period with the inhibitor concentration and the UV irradiation time, the polymerization in the vicinity of the polymer spacer was suppressed and the low driving voltage was realized. The foldable nano-phase-separated LCD has high contrast ratio over 1300:1 and 2.5 mm radius of curvature with 80 μm polycarbonate substrate, therefore, it is promising for future flexible LCD applications.

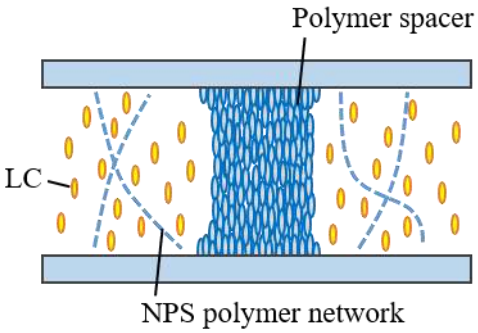

Fig. 1. Flexible NPS-LCD with polymer spacers.

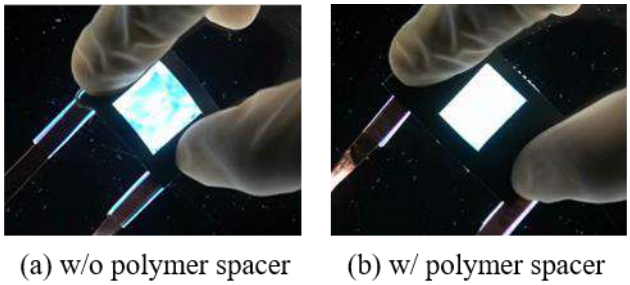

Fig. 2. Comparison of LC cells in the bending state.

References

1. Yuusuke Obonai, Yosei Sshibata, Takahiro Ishinabe, Hideo Fujikake, Foldable Liquid Crystal Devices Using Ultra-Thin Polyimide Substrates and Bonding Polymer Spacers, IEICE TRANSACTIONS on Electronics, Vol.E100-C, No.11, pp.1039-1042 (2017).
2. T. Ishinabe, S. Takahashi, Y. Shibata, H. Fujikake, "Evaluation of Capability to Maintain Thickness of LC layer of Flexible LCDs with Bonding Polymer Spacers," ITE Transactions on Media Technology and Applications, 7(4), pp. 183-189 (2019).
3. T. Fujisawa, K. Jang, H. Hasebe, H. Takatsu, “Novel E-O Properties in Nano-Phase-Separated LCs”, SID 2017 DIGEST, pp.188-191(2017).
4. T. Ishinabe, S. Takahashi, N. Kosaka, S. Honda, Y. Shibata, H. Fujikake, “Flexible Nano-Phase-Separated LCDs for Future Sheet-Type Display Applications”, SID 2019 DIGEST, pp.589-592(2019).
5. Francoise Lartigue-Peyrou, "The use of phenolic compounds as free-radical polymerization inhibitors," Industrial Chemistry Library, 8, pp.489-505 (1996).

Transfer Molecular Functions to Anisotropic Liquid Crystal Material Properties

***Kwang-Un Jeong*[1]**
[1]Dept. of Polymer Nano Science and Technology, Jeonbuk National University, Jeonju, Jeonbuk 54896, Korea
Tel.:82-8917-0905, E-mail: kujeong@jbnu.ac.kr

Liquid crystal (LC) materials are widely used in a variety of optoelectronic devices due to their inherent properties. The alignment of LC molecules is one of the important points in both fundamental and technical levels of LC device applications. Because of the anisotropy of LC molecule, the anisotropic properties can be adjusted by the director of LC molecules, which means that the alignment of LC molecules in monodomain can tranfer and control the anisotropic properties over a large area. Thus, the physical and chemical properties of organic devices are greatly influenced by the orientation of anisotropic materials.

Anisotropic LC network prepared with reactive mesogens (RM) is useful for stabilizing chemical and physical properties. Polymer-stabilized LC network can fix an ordered phase, indicating that molecular orientation can be maintained. To fabricate the robust LC thin films with excellent thermal, chemical, and mechanical stabilities, the photo-polymerization of anisotropically pre-oriented RMs should be conducted on the optimized conditions. Since the final physical properties of anisotropic LC networks depend on chemical functions and physical intermolecular interactions, the hierarchical superstructures of the programmed RMs with specific chemical functions should be controlled on the different length and time scales before polymerization. The characteristic properties of anisotropic LC networks, elastomers and gels fabricated using various programmed RMs have numerous advantages that can be commercially applied to a variety of LC displays and device applications.

Acknowledgment

This work was supported by Basic Research Laboratory Program (2020R1A4A1018259) and BK21 FOUR program.

References

1. W. J. Yoon, K. M. Lee, D. R. Evans, M. E. McConney, D. Y. Kim and K. U. Jeong, *J. Mater. Chem. C*, 7(28), 8500-8514 (2019).
2. M. Schadt, K. Schmitt, V. Kozinkov and V. Chigrinov, *Jpn. J. Appl. Phys.*, 31, 2155-2164 (1992).
3. B. H. Hwang, H. J. Ahn, S. J. Rho, S. S. Chae and H. K. Baik, *Langmuir*, 25(14), 8306–8312 (2009).
4. R. S. Kularatne, H. Kim, J. M. Boothby and T. H. Ware, *J. Polym. Sci., Part B: Polym. Phys.*, 55, 395–411 (2017).

Design of Holographic Gas Sensor Using Liquid Crystallinity

Won-Sik Kim[1], Inki Kim[2], Jin-Kang Choi[1], Junsuk Rho[1,2], and Young-Ki Kim[1]*
[1]Dept. of Chemical Engineering, Pohang University of Science and Technology (POSTECH), Pohang 37673, Korea
[2]Dept. of Mechanical Engineering, Pohang University of Science and Technology (POSTECH), Pohang 37673, Korea
*Tel.:82-54-279-2267, *E-mail: ykkim@postech.ac.kr

The quick and precise detection of hazardous compounds is important in a variety of fields. If the visual reporting is integrated with the detection, there could be a profound impact on practical applications.

In this work, we present a new class of compact sensor platform by combining a stimuli-responsive liquid crystals (LCs) and holographic metasurface (MS) as shown in Figure 1 [1]. Specifically, the metasurface composed of nano structures with sub-wavelength scale is programmed to display two holographic images (smile face for safety signal and exclamation mark for alarm signal) upon the transmission of left- (LCP) and right-circularly polarized light (RCP), respectively. The metasurface is integrated with the LC layer that was designed to transform LCP to RCP in the presence of a target gas by leveraging stimuli-responsiveness and optically anisotropic nature of LCs. Consequently, we demonstrate that the LC-MS system to autonomously sense a target gas (e.g., IPA, methanol, chloroform) and instantaneously report it via the holographic alarm. For instance, the proposed LC-MS gas sensor could detect the ultra-low concentration of IPA gas from a marker pen.

Moreover, for their wide applicability, we demonstrate the LC-MS sensors to be selectively responsive to various stimulus (e.g., electrical field, heat, pressure) and to be attachable to flat, curved, and flexible surfaces (e.g., safety goggles) via a one-step nanocasting process [1, 2].

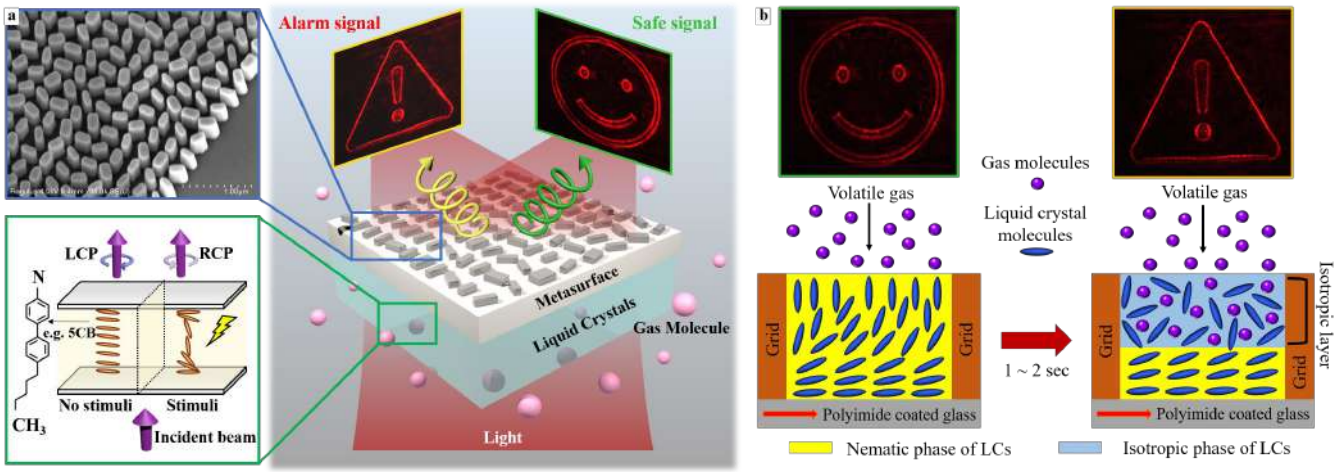

Fig. 1. a) Schematic illustration of LC-MS gas sensor. b) Changes in molecular ordering of LCs upon the exposure of volatile gas.

Acknowledgment

This work was supported by the Korea National Research Foundation (NRF-2020R1F1A1066377).

References

1. I. Kim, W.-S. Kim, K. Kim, M. A. Ansari, M. Q. Mehmood, T. Badloe, Y. Kim, J. Gwak, H. Lee, Y.-K. Kim, J. Rho, *Sci. Adv.* 7, eabe9943 (2021).
2. I. Kim, M. A. Ansari, M. Q. Mehmood, W.-S. Kim, J. Jang, M. Zubair, Y.-K. Kim, J. Rho, *Adv. Mater.* 32, 2004664 (2020).

Fabrication of chiral M13 bacteriophage film by evaporation-induced coating method

Soon Mo Park[1], Won-Geun Kim[2], Junkyu Kim[3], Eun-Jung Choi[4], Hyoungsoo Kim[3], Jin-woo Oh[2,4,5], and Dong Ki Yoon[1,6]*

[1]Graduate School of Nanoscience and Technology, KAIST, Daejeon, 34141, South Korea

Tel.:82-42-350-2888, E-mail: nandk@kaist.ac.kr

[2]Dept. of Nano Fusion Technology, Pusan National University, Busan, 46241, South Korea

[3]Dept. of Mechanical Engineering, KAIST, Daejeon, 34141, South Korea

[4]BIT Fusion Technology Center, Pusan National University, Busan, 46241, South Korea

[5]Dept. of Nano Energy Engineering, Pusan National University, Busan, 46241, South Korea

[6]Dept. of Chemistry and KINC, KAIST, Daejeon, 34141, South Korea

Biomacromolecules are likely to undergo self-assembly and show specific collective behavior concentrated in the medium. Although the assembly procedures have been studied for unraveling their mysteries, there are few cases to directly demonstrate the collective behavior and phase transition process in dynamic systems.

We try to directly investigate the evaporation-induced self-assembly of M13 bacteriophages following Figure 1 to understand the forming mechanism of chiral M13 film. For this, we observe the drying process of the M13 droplet. Then the evaporation-induced self-assembly of M13 bacteriophages is carried out by varying the dewetting speed of the solution at a contact line. The thoroughly dried film morphologies are measured by atomic force microscopy (AFM), similar to those with the droplet's case. Besides, we directly observe the LC phase generation in real-time using a polarized optical microscope (POM) during the coating process and characterize the shape of the meniscus curve using a side-view optical microscope, rheological properties of the phage solution, and the particle moving velocity a function of the shear rate. Last, our resultant M13 film provides the hierarchically structured template to guide other anisotropic materials, here gold nanorods.

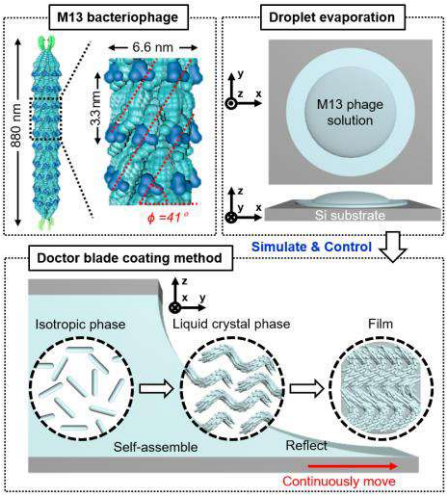

Fig. 1. Schematic illustration of molecular structure of single M13 bacteriophage and evaporation-induced self-assembly in drying process. The molecular structure of M13 phage are expressed as cylindrical rods for simplifying assembled structure in illustration.

Acknowledgment

This work was supported by a grant from the National Research Foundation (NRF) and was funded by the Korean Government (MSIT) (2017R1E1A1A01072798, 2018R1A5A1025208, 2019K1A3A1A14065772, and 2017M3D1A1039287).

References

1. W.-J. Chung, J.-W. Oh, K. Kwak, B. Y. Lee, J. Meyer, E. Wang, A. Hexemer, S.-W. Lee, *Nature* 478, 364 (2011).
2. Z. Dogic, S. Fraden, *Phys. Rev. Lett.* 78, 2417 (1997).

Fabrication of Liquid Crystal Solitonic Structures for Physical Unclonable Function

Geonhyeong Park[1], and Dong Ki Yoon [1]
[1]Dept. of Chemistry, Korea Institute of Advanced Science and Technology (KAIST), Yuseong-gu, Dajeon 34141, Korea
Tel.:82-31-350-2848, E-mail: nandk@kaist.ac.kr
[2] Graduate School of Nanoscience and Technology, KAIST, Yuseong-gu, Dajeon 34141, Korea
[3] KAIST Institute for the NanoCentury, KAIST, Yuseong-gu, Dajeon 34141, Korea

Most defects are regarded as entities that have to be eliminated to improve properties and efficiency in most of materials science. However, in recent years, interests in controlling the defect structure itself of liquid crystals on a regular basis are increasing. This defect engineering with liquid crystals is drawing attention because it can be applied to various scaffold for lithography, soft actuators, controlling living matter, and scaffold for self-assembly. The defects of the liquid crystals have various structures such as point, ring, and line according to the molecular arrangement around the defect cores. Here, we fabricated the more complex defects arrays by using the appropriate confinement effect and the intrinsic elasticity of the liquid crystal [1]. We showed that these defect arrays can be applied on a physical unclonable function (PUF) such as random number generation. In addition, it is expected that they are able to use as a template to induce the self-assembly of molecules or colloids [2] or to be applied to the wave front engineering of various light [3].

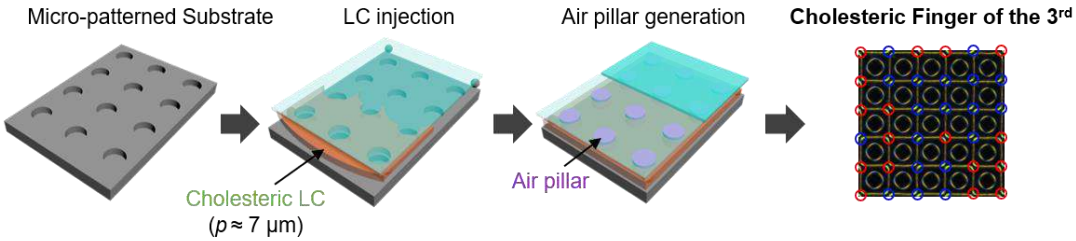

Fig. 1. Schematic illustration for the fabrication methods of periodic solitonic structures, and polarized optical microscope image of the structures.

Acknowledgment
This work was supported by National Research Foundation of Korea.

References

1. D. S. Kim, S. Čopar, U. Tkalec, and D. K. Yoon, *Sci. Adv.*, 4(11), eaau8064 (2018).
2. D. K. Yoon *et al.*, *Nat. Mat.*, 6, 866 (2007).
3. R. You *et al.*, *Adv. Mater. Technol.*, 4, 1900454 (2019)

Chiral Volume Holograms obtained by Alignment Control of Blue Phase Liquid Crystals

Hiroyuki Yoshida[1], SeongYong Cho[1], Jun-ichi Fukuda[2], and Masanori Ozaki[1]
[1]Div. of Electrical, Electronic and Information Engineering, Osaka University, Osaka 565-0871, Japan
Tel.:81-6-6879-7702, E-mail: yoshida@eei.eng.osaka-u.ac.jp
[2]Dept. of Physics, Faculty of Science, Kyushu University, Fukuoka 819-0395, Japan.

Blue phases are liquid crystals in which the constituent rod-like molecules self-assemble into three-dimensional crystallograpic structures [1]. They are potentially useful as fast optical switches and tunable reflective filters owing to their chiral cubic structure [2]. One of the challenges of blue phase technology, however, is their alignment control: preparation of monocrystalline blue phases is extremely difficult, typically resulting in polycrystalline samples with a spatially non-uniform response. Here, we report a method to control the three-dimensional crystallographic orientation of blue phase liquid crystals via exploiting field-induced phase transitions. By varying the applied field on a blue phase material to pass through the homeotropic, chiral nematic, and tetragonal blue phases, macroscopic alignment of BP I with the (110) plane parallel to the substrate and [001] axis parallel to the alignment easy axis is obtained. Patterning of the alignment easy axis on the substrate then allows the crystal orientation of the blue phase crystal to be patterned, resulting in a Bragg-Berry type volume hologram (VH) [3].

The Bragg-Berry effect is an effect in which the phase of light that is reflected from an anisotropic perodic structure is varied due to the modulation in the orientation of the anisotropic optical axis [4]. The distribution of molecular orientation on the substrate thus defines their diffraction behavior, resulting in various thin-film reflective VHs. Bragg-Berry VHs have mainly been studied using cholesteric liquid crystals which possess one-dimensional helical structures. Blue phases operate in a similar manner, but owing to their cubic strucutre, the circular polarization selectivity is maintained over much wider light incident angles, i.e., effectively for all incident angles accesible from air. The presentation will discuss our present understanding of alignment control in blue phases and their photonic properties.

Acknowledgment

This work was partly supported by JSPS Kaknehi (JP17H02947, JP19H02581, JP20H00391, JP20H04672, JP20K2115, JP21H01049), and MEXT LEADER program. The authors acknowledge BASF, DIC, and JNC Corporation for providing materials.

References

1. D. C. Wright, and N. D. Mermin, *Rev. Mod. Phys.* 61, 385-432 (1989).
2. Y. Hisakado, H. Kikuchi, T. Nagamura, and T. Kajiyama, *Adv. Mater.* 17, 96-98 (2005).
3. S. Cho, M. Takahashi, J. Fukuda, H. Yoshida, and M. Ozaki, *Commun. Mater.* 2, 39 (2021).
4. J. Kobashi, H. Yoshida*, and M. Ozaki, *Nat. Photonics* 10, 389-392 (2016).

Polar Cholesteric Liquid Crystal Phase - Its Appearance and Electro-Optic Properties

Fumito Araoka and Hiroya Nishikawa
RIKEN Center for Emergent Matter Science, Wako, Saitama 351-0198, Japan
Tel.:81-48-462-1111, E-mail: fumito.araoka@riken.jp

We have successfully realized a novel thermotropic chiral nematic liquid crystal phase with a polar helical order by introducing helical twisting power into the recently-found polar nematogen.[1,2] Physical properties of the induced polar chiral nematic (polar cholesteric: Np*) phase were unique and distinct from those of the conventional cholesteric (N*) phases. The behavior of the Np* phase is characterized by the non-degeneracy of the nematic director, $\mathbf{n} \neq -\mathbf{n}$, because both the nematic director and spontaneous polarization are synchronously twisting along the cholesteric helix. Although the transmission spectrum of the Np* phase in the non-perturbed state showed just a trivial Bragg reflection corresponding to the half pitch of the cholesteric helix, the Grandjean-Cano lines in a wedge cell appear with the period of the full helical pitch. This discrepancy is a typical representation of the non-degeneracy of the local nematic director in the present Np* system, in which the neighboring half-pitches are no longer equivalent. The existence of the local polar order was confirmed also by dielectric and second harmonic generation experiments. Furthermore, the above-mentioned transmission spectra altered by electric-field perturbation – in addition to the half-pitch Bragg reflection, unprecedented full-pitch band Bragg reflection and its overtones appeared upon electric-field application. Since the local spontaneous polarization can couple with the electric field, the coupled region is elongated with keeping the full pitch as proven by optical simulation. We also confirmed ultra-fast electro-optic switching ($\tau_{OFF} < 20$ μs) based on this polar helix deformation. Such unique features may further propose new potential applications, such as for deformed-helix mode cholesteric liquid crystal displays or electrically interchangeable photonic band gaps.

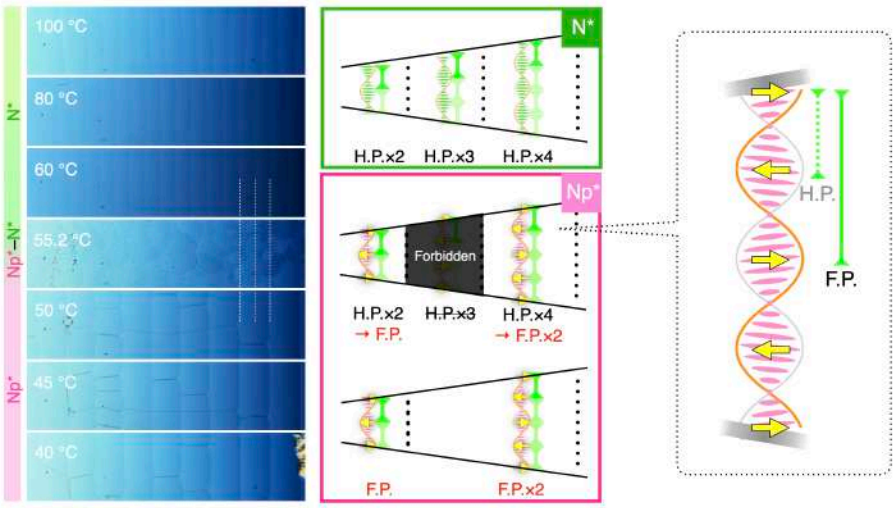

Fig. 1. Polar Cholesteric Liquid Crystal in a Wedge Cell

Acknowledgment

This work was financially supported partially by JST CREST, Grant Number JPMJCR17N1, Japan, and KAKENHI Grant Number JP50835519 and 21H01801 from the Japan Society for the Promotion of Science.

References

1. H. Nishikawa, K. Shiroshita, H. Higuchi, Y. Okumura, Y. Haseba, S-I. Yamamoto, K. Sago, and H. Kikuchi, *Adv. Mater.,* 29(43), 1702354 (2017).
2. H. Nishikawa and F. Araoka, *Adv. Mater.,* doi: 10.1002/adma.202101305.

Simple Methods for Measuring Flexoelectric Coefficients: $e_{11}+e_{33}$ with Capacitance Characteristics and e_{11}-e_{33} with Disclination Lines

Yukihiro Kudoh, Noriki Shirai, Hiroki Shimoda, and Taiju Takahashi
Dept. of Information and Communications Engineering, Kogakuin University, Hachioji, Tokyo, Japan
Tel.:81-42-628-4604, E-mail: kudoh@cc.kogakuin.ac.jp

The flexoelectric effect[1] is one of the most important topics for the future development of liquid crystal displays (LCDs). This effect has been applied to low-voltage IPS-LCDs[2] and DC switching in bistable LCDs[3]. On the other hand, it has been pointed out that this effect is a cause of the unstable electro-optic response at the electrode edge.[4] However, it is very difficult to measure the flexoelectric coefficients (e_{11}, e_{33}), which are physical properties of liquid crystal (LC) materials that indicates the flexoelectric effect. The main reasons for this are that it is necessary to measure minute changes in the orientation of LCs and that it is difficult to separate the response from that caused by impurity ions. In general, the fitting method with numerical calculated results and measurement results is used to determine the coefficients as an additional value $e_p=e_{11}+e_{33}$ or a difference $e_n=e_{11}-e_{33}$. Because it is difficult to independently evaluate e_{11} and e_{33} due to the continuity of the director distribution. We proposed each method to measure e_p and e_n, respectively. The first one is to determine e_p by using the capacitance characteristics with HAN cell under DC bias voltage along with the cell thickness direction. This method can measure the change in the LC orientation sensitively without using precise optical axis alignment. In addition, by using an adsorption chromatography phenomenon during the LC injection process, we were able to successfully estimate the e_p when the effect of the impurity ion is zero. [5] The other one is to measure e_n by applying an in-plane electric field with HAN cell that rubbed in a concentric direction. [6] In this method, the coefficient is evaluated with in-plane electrodes, taking advantage of the fact that under certain conditions the LC director is driven by the flexoelectric effect in the direction opposite to the dielectric response. The feature of this cell is that the direction of the electric field applied to the hybrid orientation changes every other electrode within a rotating rubbing method or concentric in-plane electrodes. If LC materials have the flexoelectric effect, a reverse twist defect appears that is observed as a disclination line (DL), schematic diagrams of the sample cells are shown in Fig. 1. The larger the flexoelectric coefficient, the more it can overcome the dielectric response, and thus the larger the angle of the electric field, the more reversal will occur. The coefficient e_n is calculated from the angle of the pseudo DLs formed by the two regions of the director with different rotation directions.

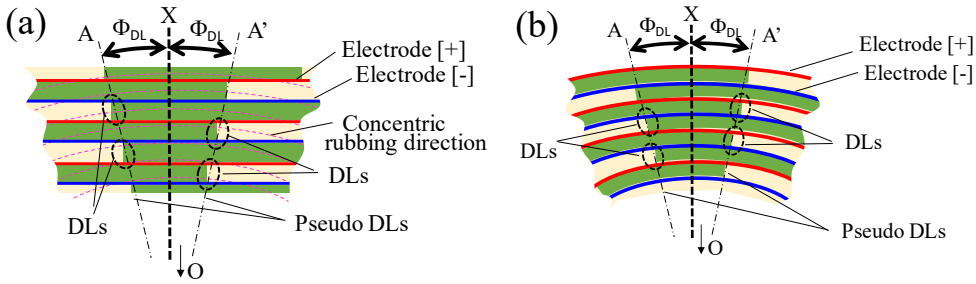

Fig. 1 Schematic models of sample HAN cells for e_n measurement with (a) concentric rubbing treatment and with (b) concentric in-plane comb electrodes. (front view)

Acknowledgment

We would like to thank Merck Performance Materials Limited and Toyo Corporation for their cooperation and useful advice on the measurements. We also t hank to Nissan Chem Corporation for supplying the polyimide materials.

References

1. R. B. Meyer: Phys. Rev. Lett., 22, 918 (1969).
2. S. Oka, *et al.*: The institute of Image Information and Television Engineers, IDY2010-22, 87 (2010). [in Japanese]
3. K. Imina, *et al.*: Mol. Cryst. Liq. Cryst., 646, 142 (2017).
4. T. Suzuki, *et al.*: Proc. of Japanese Liquid Crystal Society Meeting 3D06, 514 (1999). [in Japanese]
5. K. Imina, *et al.*: Proc. of International Display Workshops, 23, 83 (2016)
6. T. Takahashi, *et al.*: Proc. of International Display Workshops, 26, 303 (2019)

Programmable Crack Patterning with Liquid Crystal Polymer Substrates

***Hyun Kim*[1]**
[1]Sensors and Electron Devices Directorate, US Army Research Laboratory, Adelphi, MD, 20783, United States
E-mail: hyun0225@gmail.com

Cracks are normally classified as uncontrollable material or process failures to be prevented. This research describes a process that enables unprecedented control of crack formation on polymer substrates. By using photoalignment methods to orient liquid crystal polymer networks, the molecular orientation, and therefore the cracking direction, can be freely programmed spatially within the substrate. Without using any conventional lithography or other labor-intensive processes, we present control over crack orientation, density, and size. This programmable cracking enables high-resolution patterning in a high-throughput manner and may serve as an alternative fabrication strategy for various applications including sensors, optics, electronics, fluidics, and other devices with micro- and nanoscale features.

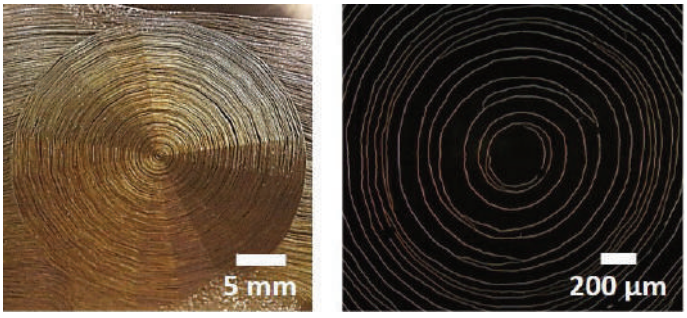

Fig. 1. Azimuthal patterning of cracks with photopatterned liquid crystal polymer networks.

Acknowledgment
Research was partially sponsored by the Army Research Laboratory and was accomplished under Cooperative Agreement Number W911NF-19-2-0317.

References

1. H. Kim, M. K. Abdelrahman, J. Choi, H. Kim, J. Maeng, S. Wang, M. Javed, L. K. Rivera-Tarazona, H. Lee, S. H. Ko, T. H. Ware, From Chaos to Control: Programmable Crack Patterning with Molecular Order in Polymer Substrates, *Adv. Mater.*, 2008434, (2021).

Thin-Film Photodetectors Enabling Infrared Vision in Future Consumer Devices

PawełiE.iMalinowski[1], Jiwon Lee[1], Epimitheas Georgitzikis[1], Vladimir Pejovic[1,2], Itai Lieberman[1], Joo-Hyoung Kim[1], Myung-Jin Lim[1], Griet Uytterhoeven[1], Luis Moreno Hagelsieb[1], TungHuei Ke[1], Yunlong Li[1], Renaud Puybaret[1], Gauri Karve[1], Tom Verschooten[1], Steven Thijs[1], Paul Heremans[1,2], and David Cheyns[1]

[1]imec, Kapeldreef 75, 3001 Leuven, Belgium
[2]ESAT, KU Leuven, Kasteelpark Arenberg 10, 3001 Leuven, Belgium
Tel.:+32-1628-1938, E-mail: Pawel.Malinowski@imec.be

Image sensors innovations have been propelling adoption of billions of cameras in consumer devices. Silicon-based imagers are perfect for the visible range (to reproduce human vision) and are constantly improving also in the near-infrared range (especially at 940 nm used in sensors with active illumination). Imaging further in the spectrum, in the short-wave infrared (SWIR) range, promises several benefits: lower background (better contrast), augmented vision (seeing through fog/smoke/clouds), material identification (e.g. water content) and low-light visibility (e.g. night vision). The fundamental limit of the Si bandgap forces the search for alternative absorber materials. Thin-film photodetectors (TFPD) are proposed as an affordable and better scalable alternative to III-V materials such as InGaAs. Monolithic integration enables small pixel size, high resolution and industrial throughput, while providing sufficient sensitivity for many applications [1-3].

In this talk, we will describe the challenges of realizing infrared image sensors based on organic and quantum dot pixel stacks. We will present our manufacturability-aware development leading to a foundry-friendly fabrication flow. Proof-of-concept imagers have state-of-the-art pixel pitch below 2 µm [4], enabling high resolution in a compact form factor. This leads to high image quality and enables miniaturization of infrared cameras to fit seamlessly in consumer systems. External quantum efficiency above 40% and video frame rates make this approach already very attractive, with an outlook for implementation in cameras modules such as under-display cameras, eye-safe eye-tracking in AR/VR, biometric identification or enhanced visibility.

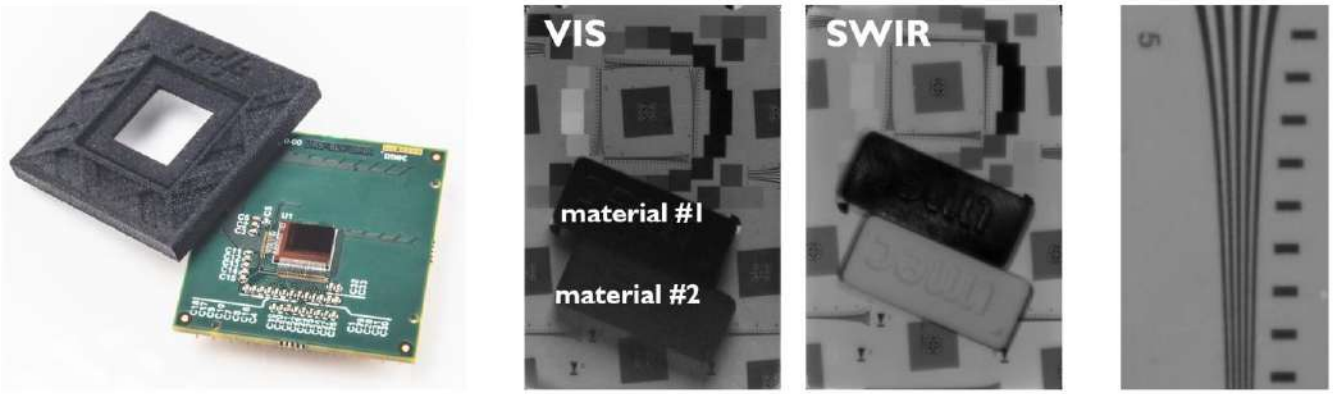

(a) packaged image sensor (b) 768x512 px / 5 µm pitch / PbS QD1450 (c) 2.5 µm pitch

Fig. 1. A packaged QD image sensor (a) and images acquired with different prototypes (b,c)

Acknowledgment

The Authors would like to acknowledge all teams across imec that make these innovations possible.

References

1. E. Georgitzikis et al., *IEEE Sensors Journal* 20/13 (2020), DOI: 10.1109/JSEN.2019.2933741
2. E. Klem et al., *SID Display Week 2021*, paper 66.3 (2021)
3. T. Ryhanen et al., *SID Display Week 2021*, paper 66.4 (2021)
4. J. Lee et al., *IEDM 2020 Technical Digest*, paper 16.5 (2020), DOI: 10.1109/IEDM13553.2020.9372018

Facile Fabrication Process of a-IGZO Thin-Film Transistor Array using Multi-level Self-Aligned Imprint Lithography

Changyun Na and Sung Min Cho
School of Chemical Engineering, Sungkyunkwan University, Suwon 16419, Korea
Tel.:82-31-290-7251, E-mail: sungmcho@skku.edu

Amorphous indium gallium zinc oxide (a-IGZO) has been extensively studied for use as a semiconductor material for thin-film transistors (TFTs) in active matrix displays. The IGZO semiconductor is important for realizing a large area display because it has higher carrier mobility compared to conventional amorphous silicon semiconductor. In the case of current-driven organic light-emitting diode (OLED) displays, a semiconductor with high mobility is even more essential for representing the higher number of gray levels. For this reason, a-IGZO semiconductor is mainly used as TFTs for driving large-area active-matrix OLED displays.

In this study, a self-aligned imprint lithography (SAIL) fabrication process of a-IGZO TFT arrays without using a photolithography process was studied. The SAIL process reported here provides a very simple method of fabricating an a-IGZO array using a single imprint process and a series of plasma etching processes without the need for pattern alignment in photolithography processes. A master template for a 3D TFT array on a silicon wafer was designed and fabricated. After imprinting on an UV-curable resin coated on a substrate using an imprint mold that replicated the template, the imprinted resin and the underlying TFT layers were plasma-etched to finally form the designed TFT array structure. In addition, it was confirmed that OLED pixels can be driven by the fabricated TFT array. These step-by-step SAIL processes were reported in detail in this study, and finally showed that they can be applied to TFT array fabrication for active-matrix OLED displays.

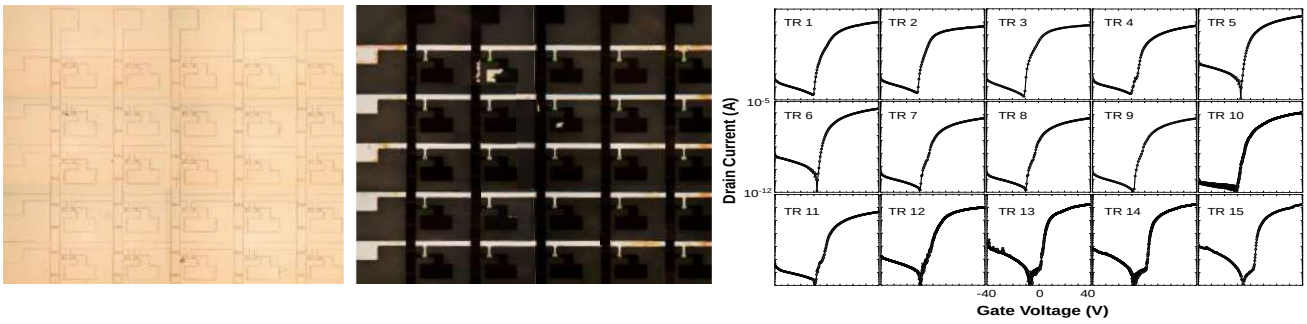

Fig. 1. Optical microscopy images of imprinted and fabricated TFT array, and the transfer curves of the TFTs.

References

1. S. Li and D. Chu, *Flex. Print. Electron.*, 2, 013002 (2017).
2. S. J. Kim, H. T. Kim, J. H. Choi, H. K. Chung, and S. M. Cho, *Appl. Phys. Lett. 112*, 152104 (2018).
3. M. S. Ram, L. Kort, J. Riet, R. Verbeek, T. Bel, G. Gelinck, and A. J. Kronemeijer, *IEEE Trans. Electron Dev.*, 66, 1778 (2019).
4. T. Dogan, J. Riet, T. Bel, I. Katsouras, L. Witczak, A. J. Kronemeijer, R. A. J. Janssen, and G. H. Gelinck, *IEEE Electron Dev. Lett.*, 41, 1217 (2020).

A Thin Polymer Layer via initiated Chemical Vapor Deposition for the Encapsulation of High Resolution OLEDs

Byeong Gyu Roh[1], Seung Chul Park[1], Yong Cheon Park[2], Sung Gap Im[2], and Ji Ho Baek[1]
[1]LG Display, 245, LG-ro, Wollong-myeon, Paju-si, Gyeonggi-do, 10845, Korea
Tel.:82-2-3773-1114, E-mail: bgroh@lgdisplay.com
[2]Dept. of Chemical & Biomolecular Engineering, KAIST, 291, Daehak-ro, Yuseong-gu, Daejeon, 34141, Korea

With the increasing demand for the OLED application to high resolution display requiring the resolution larger than 3,500ppi, the pixel size and pixel pitch (< 3um) must be reduced substantially. However, the down-scaling of the pixel size is inevitably accompanied by color mix, and thus blurring of the image, as shown in Fig. 1(a). To address this issue, the encapsulation layer must also be modified accordingly. Especially, it is necessary to decrease the thickness of the polymer layer in the triple thin film encapsulation (TFE). Here, a TFE structure was newly developed by using initiated chemical vapor deposition (iCVD) process, for high-resolution OLEDs with minimized color mix. Fig. 1(b) shows the schematic illustration of the iCVD equipment, and the vapor-phase deposition process enabled a conformal thin polymer layer with the substrate temperature less than 40 ℃.

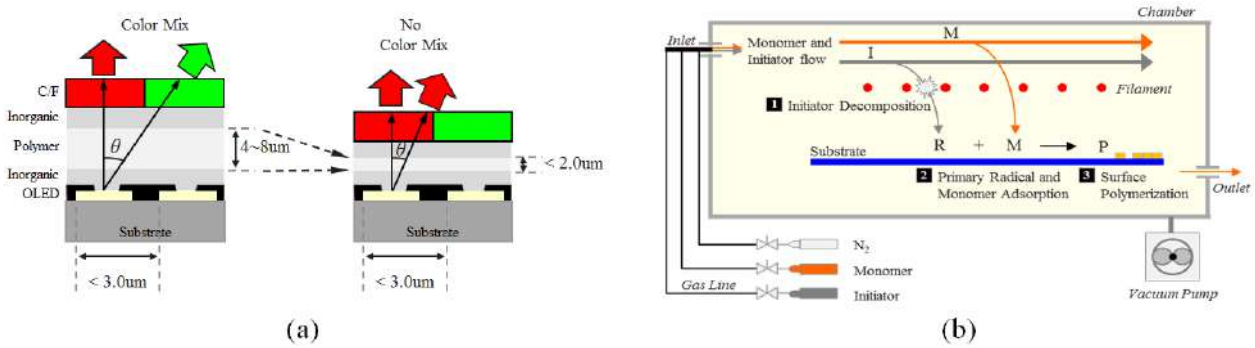

Fig. 1. (a) reducing the encapsulation thickness, (b) schematic diagram of the iCVD for the polymer layer

In the iCVD process, a thin polymer layer was deposited by using an initiator, *tert*-Butyl peroxide (TBPO) and acrylate monomers. The transmittance of the polymer layer was larger than 99.7%. The outgassing level of the polymer layer was extremely low – less than 20 ppm. Most of all, a foreign particle covering mechanism by the iCVD polymer layer was established and proposed. The side step coverage of the 0.5 μm-thick polymer layer was 53.5% and the bottom step coverage was 90.9% in the 5:1 trench wafer. The 0.5 μm-thick iCVD polymer layer could cover irregular particles with the size of 3.0 μm without forming any seam. Thus, the subsequent SiN_x passivation layer via PECVD could be deposited successfully on the polymer layer without any apparent plasma damage such as haze. A 1.1" OLED was manufactured as shown in Fig. 2 to confirm its potential to OLED encapsulation, where the thickness of iCVD polymer and the inorganic layers (SiNx) were 0.5 μm and 1.0 μm, respectively.

Fig. 2. 1.1" OLED encapsulated with the 0.5 μm-thick polymer layer deposited by iCVD

References

1.W. E. Tenhaeff, K. K. Gleason, *J. Adv. Funct. Mater., vol.18*, 984 (2008).
2. B. J. Kim, H. J. Seong, H. J. Shim, Y. I. Lee, S. G. Im, *Adv. Eng. Mater., vol. 19, No. 7,(2017).*

A Study on Crucible Inner Pressure Change during Degradation of Liq

Sungmoon Kim[1], Taekgi Lee[1], Daejoon Chi[1], Gyoung O Ko[1], Yeonjin Yi[2], Junho Kim[2]
[1]R&D Center of Depolab inc., Paju-si, Gyeonggi-do, Korea
Tel.:82-10-2364-9943, E-mail: smkim@depolab.co.kr
[2]Institution of Physics and Applied Physics, Yonsei University, Seoul, Korea

The inner pressure of a linear source in large size AMOLED mass production line is getting higher to achieve high productivity and uniform film thickness. On the other hand, high inner pressure can cause organic material degradation. The material should have higher vapor pressure than inner pressure at the evaporation surface to be emitted from nozzle of source. And the vapor pressure depends on temperature of material. So, when evaporation temperature of material become higher than degradation temperature due to high inner pressure, the material degradation can occur.

We developed the inner pressure sensor (Figure 1) that can be installed at crucible directly and measure the inner pressure of crucible. The inner pressure sensor we developed have similar principle to capacitance diaphragm gauge that is used conventionally for vacuum gauge. We placed metal diaphragm and electrodes in crucible. The capacitance between diaphragm and electrode will change as the diaphragm deformation according to the pressure difference between chamber pressure and crucible inner pressure. It will be heated up to same temperature with crucible itself by evaporation source heater. So, it cannot be contaminated by evaporation material because it can re-evaporate the material due to its temperature.

We tested the inner pressure change during degradation of Lithium Quinolate (Liq). Liq has been commonly used in AMOLED pixel patterning process as electron transfer layer (ETL). It is a kind of thermally unstable organic material and sometimes can cause material degradation issue.

We measured inner pressure as deposition rate increased gradually, 0.4A/s, 0.6A/s, 0.8A/s, 1A/s, 1.2A/s. Figure 2 shows the graph of that. As you can see in Figure 2, the inner pressure increases proportional to the deposition rate change because the amount of vapor emission is relevant to inner pressure of source.

However, the behavior of inner pressure is slightly different with deposition rate. While deposition rate approximately keep constant at each deposition rate step, the inner plate increases slightly especially at higher rate. At rate 0.4A/s and 0.6A/s, the inner pressure is stable. But it increases at 0.8A/s, 1A/s, 1.2A/s. We assumed that inner pressure increase at constant rate condition is caused by degradation of Liq. So, we check the purity of residues with differential scanning calorimetry (DSC). The picture of remains and the result of purity test at each rate are displayed in Figure 2. As we expected, the purity is getting lower as deposition rate become higher.

Fig. 1. Inner Pressure Sensor

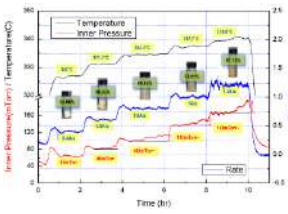

Fig. 2. Inner Pressure Graph

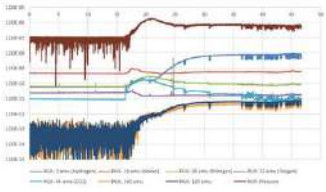

Fig. 3. RGA data during degradation

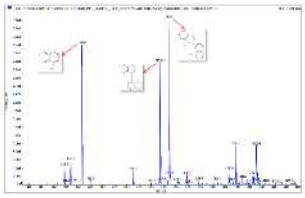

Fig. 4. LC/MS data of degradant

We measured partial pressure of residual gas in chamber with RGA during degradation of Liq, as shown in Figure 3. Three kinds of gases are increase as Liq is heated. The most increased gas is hydrogen (2 amu) that can be made during decomposition of Liq. And the other gases are supposed to be quinoline (129 amu) and phenylacetylene (102 amu). Both also can be degradation product of Liq but is negligibly small amount. And we analyzed degradant of Liq with APCI LC/MS(Atmospheric Pressure Chemical Ionization Liquid Chromatography Mass Spectrometry). We can find highest spectrum peak at 289.3m/z that is expected as degradation product that is compounded from two hydrogen omitted Liq as shown in Figure 4.

We can assume that hydrogen gas is degradation product of Liq and it make the inner pressure increase at constant rate condition. It can be used as alarm signal of degradation in mass production and can prevent the loss which can happen without notice.

References

1. S. Kim et al, *Display Week 2021 Technical Digest*, 23-2(2021)

Fundamentals of semidried ink patterning for high-resolution printed electronics

KUSAKA Yasuyuki[1] and FUKUDA Nobuko[1]
[1]**Sensing System Research Center, AIST, Tsukuba, 305-8565, Japan**
Tel.:81-29-860-5707, E-mail: y-kusaka@aist.go.jp

Printing methods are expected to provide facile, high-mix and cost-effective manufacturing tools for electronic devices such as displays, packaging, passive components, batteries, sensors, etc. While various printing methods including inkjet, flexographic and gravure printing offer a high-throughput or on-demand patterning of functional inks, such techniques suffer from wetting/dewetting and thus unavoidable restrictions in cross-sectional morphology and resolution still remain. On the other hand, in gravure offset printing and reverse offset printing (ROP), ink patterns formed on silicone surfaces are semidried before transfer so that structural changes driven by Laplace pressure can be negligible and thus well-defined patterns at single-micrometer level can be achieved [1].

In the presentation, a fundamental concept for semidried ink formulation is presented. Here, it will be shown that not only nanoparticle-based but also metal complex-based inks can be printed by the ROP process [2-3]. The direct observation of the ROP process using a see-through glass cliché enabled to visualize the generation of rate-dependent transfer failures uniquely found in the semidried ink patterning (Fig. 1a) [4]. As the miscibility and inter-contamination between two adjacent semidried layers are considerably supressed due to a low liquid content inside the layers, wet-on-wet process where thermal sintering of intermediate layers is skipped can be applied to the fabrication of organic thin-film transistors (Fig. 1b) [5]. With a similar concept, buried electrodes can be formed by transferring a patterned conductive layer overcoated by a dielectric ink (Fig. 1c) [6].

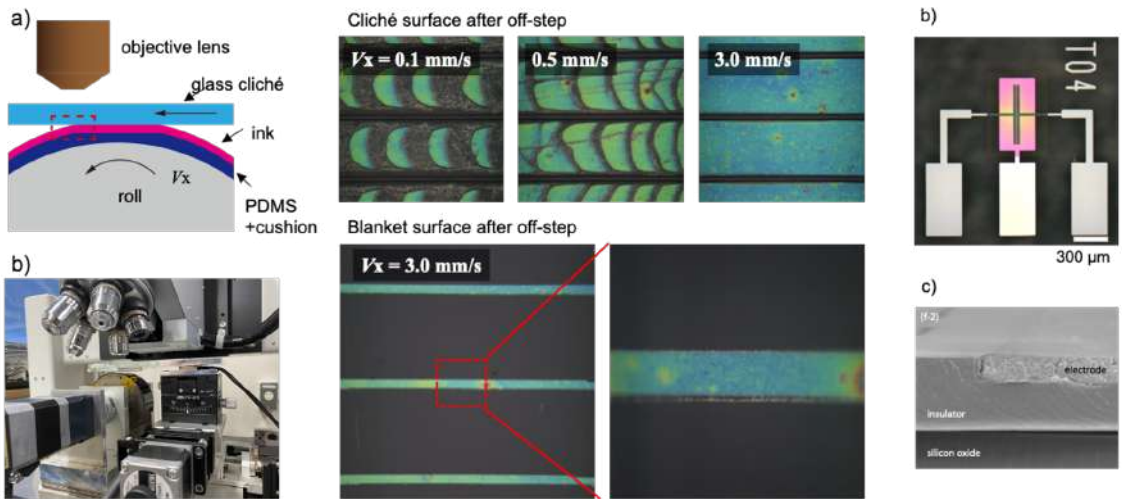

Fig. 1. a) A direct observation of ROP patterning process: rate-dependent transfer failures. b) Wet-on-wet fabrication of organic transistors and c) printed buried electrodes.

Acknowledgment

The authors gratefully acknowledge the technical assistance of Mariko Fujita. Y K express thanks for the JSPS KAKENHI Grant-in-Aid for Scientific Research C 19K05134.

References

1. Y. Kusaka, N. Fukuda, H. Ushijima, Jpn. J. Appl. Phys. 59 SG0802 (2020)
2. J. Leppäniemi, A. Sneck, Y. Kusaka, N. Fukuda, A. Alastalo, Adv. Elec. Mat. 5 1900272 (2019)
3. Y. Kusaka, N. Shirakawa, S. Ogura, J. Leppäniemi, A. Sneck, A. Alastalo, H. Ushijima, N. Fukuda, ACS Appl. Mater. Inter. 10 24339-24343 (2018)
4. Y. Kusaka, A. Takei, M. Koutake, T. Fukasawa, T. Ishigami, N. Fukuda, Soft Matter 16 3276-3284 (2020)
5. Y. Kusaka, K. Sugihara, M. Koutake, H. Ushijima, J. Micromech. and Microeng. 24 035020 (2015)
6. Y. Kusaka, M. Koutake, H. Ushijima, J. Micromech. and Microeng. 25 045017 (2014)

Highly Flexible TFT Arrays for Sensor Applications

M. Ito, N. Ikeda, C. Miyazaki, Y. Tanaka K. Hatta and M. Ishizaki
Technical Research Institute, Toppan Printing Co., Ltd. Sugito, Saitama, 345-8508, Japan
Tel.:81-480-33-9576, E-mail: manabu.ito@toppan.co.jp

Flexible thin film transistors (TFT) have been attracting a lot of attention due to the applicability to foldable smarphone, IoT sensors, and photodetectors [1-3]. Transparent amorphous oxide semiconductor (TAOS) TFT is regarded as one of the most promising candidates for flexible device due to its high performance at relatively low processsing tempearature [4]. However, conventional oxide TFT sufferes from relatively poor flexibility because inorganic dielectric, such as SiO_2 or Si_3N_4 are vulnerable to bending [5-6]. Therefore, hybridization of inorganic and organic dielectric have been proposed for bottom gate oxide TFT [7-9]. In this structure, very thin inorganic layer serves as a plasma resistant layer for beneath organic dielectric layer during sputtering process of TAOS. While rather thick organic dielectric layer gurantee the insulation resitance and flexibility. However, reported results were not flexible enough to be used for werable sensor applications. We attribute this inadequate flexibility as the fragility of the thin inorganic dielectric.

Here, we adopt inorganic / organic bilayer dielectric, whose inorganic layer is patterned to isolate each device. Moreover, less than 10 nm - thick inorganic layer are employed. IGZO channel layer were sputtered onto bilayer dielectric. After fabrication, flexible TFT were bent 1,000,000 times at a curvature radius of 1 mm using Yuasa system's clamshell-type enduring test machines. Before and after bending test, we do not observe any noticeable change in device characteristics. It should be noted that our TFT does not employ neutral plane concept, which places the channel layer at a mechanical neutral position [10]. As far as we know, this is the first results which can withstand million times bending test at r = 1 mm. We see a big potential for the application of wearable sensors.

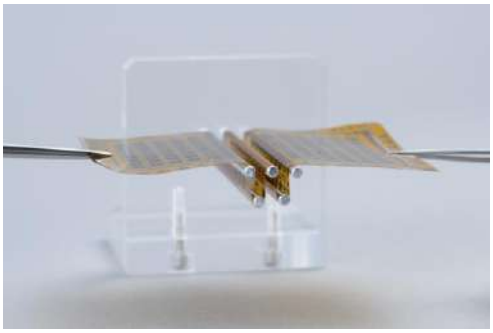

Fig. 1. Photograph of flexible TFT, which can withstand a million times bending cycles at r = 1 mm

References

1. J.-S. Park, T. -W. Kim, D. Stryakhilev, J.-S. Lee, S.-G. An, Y. -S. Pyo, D. -B. Lee, Y. G. Mo, D. -U. Jin, and H. K. Chung, Appl. Phys. Lett. 95, 013503 (2009).
2. H. Oh, G. -C. Yi, M. Yip, S. A. Dayeh, Sci. Adv. 5 eabd7795 (2020).
3. A. T. Yokota, Y. Inoue, Y. Terakawa, J. Reeder, M. Kaltenbrunner, T. Ware, K. Yang, K. Mabuchi, T. Murakawag M. Sekino, W. Voitc, T. Sekitani and T. Someya, Proc. Natl. Acad. Sci.112, 14533 (2015).
4. K. Nomura, H. Ohta, A. Takagi, T. Kamiya, M. Hirano and H. Hosono, Nature 432, 488 (2004).
5. M. Ito, C. Miyazaki, M. Ishizaki, M. Kon, N. Ikeda, T. Okubo, R. Matsubara, K. Hatta, Y. Ugajin, and N. Sekine, J. Non-Cryst. Solids. 354, 2777 (2008).
6. M. Ito, M. Kon, C. Miyazaki, N. Ikeda, M. Ishizaki, R. Matsubara, Y. Ugajin, and N. Sekine, phys. stat. sol.(a) 205, 1885 (2008).
7. B. -U. Hwang, D. -I Kim, S. -W. Cho, M. -G. Yun, H. J. Kim, Y. J. Kim, H. –K. Cho, N. –E. Lee, Org. Electron, 15, 1458 (2014).
8. Y. Kumaresan, Y. Pak, N. Lim, Y. Kim, M. -J. Park, S. -M. Yoon, H. -M. Youn, H. Lee, B. H. Lee and G. Y. Jung Sci. Rep. 6, 37764 (2016).
9. J. Y. Choi, S. Kim, B. –U. Hwang, N. –E. Lee, and S. Y. Lee, Semicond. Sci. Technol. 31, 125007 (2006).
10. T. Sekitani, U. Zschieschang, H. Klauk and T. Someya, Nature Mater. 9, 1015 (2010).

Recent progress of ultraflexible organic solar cells and photodetectors

Kenjiro Fukuda[1], Takao Someya[12]
[1]Thin-Film Laboratory and Center for Emergent Matter Science, RIKEN, 2-1 Hirosawa, Wako, Saitama, 351-0198, Japan
Tel.:81-48-467-9174, E-mail: kenjiro.fukuda@riken.jp
[2]Electrical and Electronic Engineering and Information Systems, The University of Tokyo, 7-3-1 Hongo, Bunkyo-ku, Tokyo 113-8656, Japan

Flexible or stretchable electronics has being much attention because the new type of electronic devices can open new avenue for soft applications. Especially, the combination of flexible/stretchable electronics and other components such as flexible sensors and soft actuators will make synergetic effects on wearable and soft-robot applications. Such applications require "self-powered" electronic device system. Therefore electronic components such as energy harvesters, energy storages, sensors, circuits, and antennas must be integrated on or in such systems. Flexible and stretchable electronic devices do not disturb the softness of the soft actuators.

In this talk, we will introduce the recent progress of flexible/stretchable electronic devices using organic materials as semiconducting layers. The main achievement by us is "ultraflexible" organic solar cells [1-3], photodetectors [4,5], and integrated devices [6,7]. We established fabrication methodology of organic devices onto 1-micron-thick polymer substrates, which enables unprecedented flexibility or even "stretchability". I will discuss the possibility and remaining issues of such ultraflexible electronic devices.

Acknowledgment
This work was financially supported by JSPS KAKENHI, Grant No. JP18H05469.

References

[1] X. Xu *et al.*, *Proc. Natl. Acad. Sci.* **115**, 4589 (2018).
[2] W. Huang *et al.*, *Joule*, **4**, 128 (2020).
[3] Z. Jiang et al., *Proc. Natl. Acad. Sci.* **117,** 6391 (2020).
[4] S. Park *et al.*, *Adv. Mater.* **30**, 1802359 (2018).
[5] Y. L. Wu *et al.*, *Adv. Mater.* **31**, 1903587 (2019).
[6] S. Park *et al.*, *Nature*, **551**, 516 (2018).
[7] H. Jinno *et al.*, *Nat. Commun.* **12**, 2234 (2021).

Fully-Printed Electronics Using Metal Nanoparticle Inks

Takeo Minari [1], Lingying Li [1], Qingqing Sun [2], Wanli Li [3], and Xuying Liu [2]*
[1]National Institute for Materials Science (NIMS), Tsukuba, Ibaraki 305-0044, Japan
Tel.:81-29-860-4918, E-mail: MINARI.Takeo@nims.go.jp
[2]Zhengzhou University, Zhengzhou 450001, P. R. China
[3] School of Mechanical Engineering, Jiangnan University, Wuxi City, Jiangsu 214122, P. R. China

Printed electronics - electronic circuits printed using metallic and semiconducting inks - have been developed for a wide range of applications. In particular, a metal nanoparticle ink is one of the best candidates for direct printing of electronic circuits. We have developed the π-junction metal nanoparticles having π-conjugated planer molecules as the ligands, which exhibits high conductivity by room-temperature printing process [1]. We have also developed high-resolution printing technique based on the patterned chemical polarity on the surface, enabling the printing with 0.6-μm line width on flexible substrates (Figure 1) [2]. We also report high-performance fully-printed thin-film transistors (TFTs) with high mobility of 70 $cm^2 V^{-1} s^{-1}$ at the operation voltage of 1 V, which are the indispensable building blocks for practical electronic circuits [3].

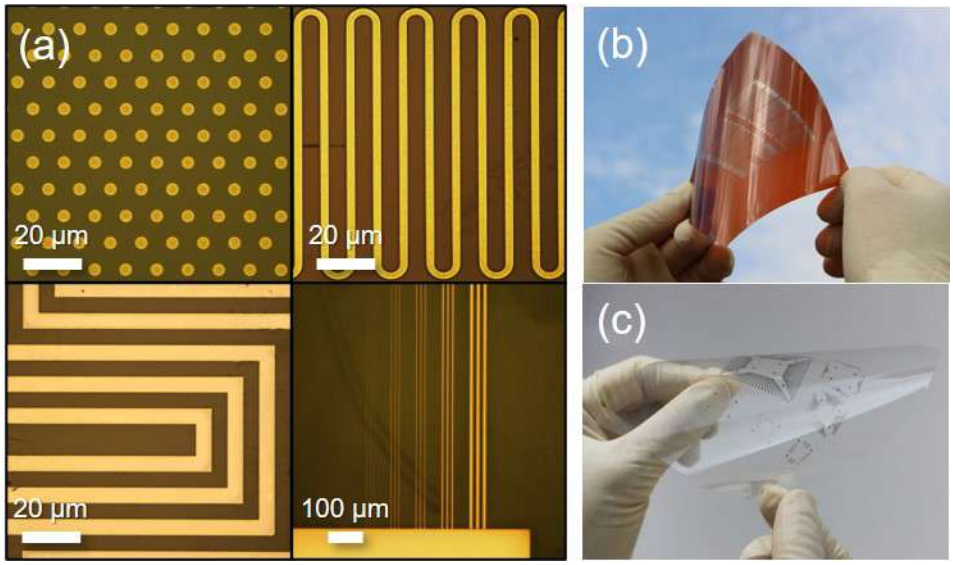

Fig. 1. Printed circuits using a metal nanoparticle ink on flexible substrates.

References

1. X. Liu, T. Minari, et. al., *Advanced Materials,* 28, 6568 (2016).
2. L. Li, T. Minari, et. al., *Small,* 17, 2101754 (2021).
3. Q. Sun, T. Minari, et. al., *Small Methods,* published online (2021).

Tunability of PIB-CVD Organosilicon Thin Films on Flexible Substrates

Ravindranath Viswan, and David Douglass
Denton Vacuum, LLC, 1259 North Church Street, Building 3, Moorestown, NJ 08057, USA
Tel.:1-856-380-5221, E-mail: rviswan@dentonvacuum.com

Organosilicon thin films have been deposited by a variety of methods using precursors that are volatile at room temperature, nonflammable, relatively non-toxic, and inexpensive [1]. Due to their organic-inorganic character organosilicon precursors can be used for deposition of polymers as well as inorganic coatings. As a result, these thin films have a broad range of applications ranging from diffusion barrier thin films for flexible OLED encapsulation to hard abrasion resistant coatings for automotive glazing [2,3]. However, most deposition methods have limited capability to exploit the full range of their properties due to limitations in the available range of ion energy and ion current density. Here we demonstrate tunability of properties such as hydrophobicity and nano indentation hardness on a variety of substrates using our proprietary linear radio frequency (RF) ion source. This ion source, by design, has independent control of both ion current density and ion energy over a wide range. It is capable of producing high deposition rate multilayer coatings with a single low maintenance source, making it well suited for high volume manufacturing.

Multilayer organosilicon films were deposited by plasma ion beam CVD (PIB-CVD) using Denton's patented linear RF ion source on polycarbonate (PC), polymethyl methacrylate (PMMA) and glass substrates. All the films were deposited using Hexamethyldisiloxane (HMDSO), oxygen and argon gases. Flow ratios were adjusted to deposit multilayer films that have low stress and good adhesion to the plastic substrates. Fig. 1 shows the static water contact angle (WCA) and nanoindentation hardness of the organosilicon films plotted as a function of a pulsed DC bias voltage applied to the source body. It is observed that as the bias voltage increases from 0 to 300V, WCA decreases from 102º to 16º, and nanoindentation hardness increases from 0.2 GPa to 13 GPa indicating a wide range of tunability of these properties.

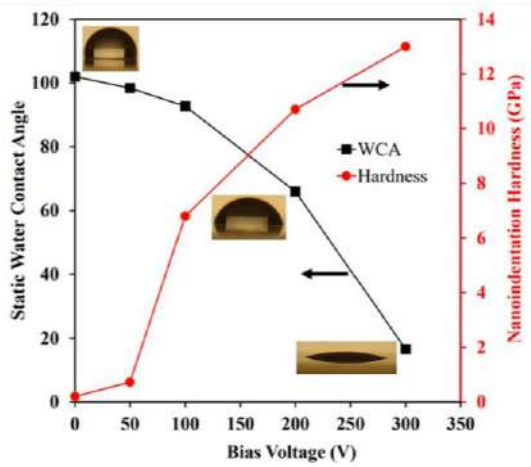

Fig. 1. Tunability of WCA and nanoindentation hardness of organosilicon films

Further work is in progress to study the diffusion barrier properties of these films for OLED encapsulation applications.

References

1. R. d'Agostino (ed.), Plasma Deposition, Treatment, and Etching of Polymers, Academic Press, San Diego, CA, p. 163 (1990).
2. Seung-Woo Jang, Hyung-Rang Moon, Chang-Su Woo, Woo-Jin Lee, Hwan-Seung Jeong, and Dong-il Han, Composition for encapsulation of OLED device and OLED display prepared using the same, Korea Patent no. KR101676520B1(2013).
3. Fred M. Kimock, Bradley J. Knapp, and Steven J. Finke, Kutztown, Process of making abrasion wear resistant coated substrate product, US Patent no. 5,635,245 (1997).

Cu Process Development 50UD 120Hz LCD TVs Integrated Gate Driver GOA Circuit using Four-Mask a-Si TFT

Hao Dong, An-thung Cho, Wen-Bing Wu, Yao-Feng Tsai, Yong Zhang, James Hsu, Wade Chen

ChuZhou HKC Optoelectronics technology Co., Ltd., China

Abstract

A mechanism of high doped N+ film was used to lower the contact resistance between metal and semiconductor to achieve ohmic contact in 4-mask process. In this article, the improvement mechanism to reduce contact resistance by using high doped N+ layer will be investigated in conjunction with energy level diagram.

The copper process mainly uses copper wires to replace existing aluminum wires as scan lines and data lines, as shown in Fig.1. When using copper wires, it can reduce the resistivity of the signal line, introduce high-frequency drive technology, design large-tolerance circuits, reduce the number of ICs, and reduce costs; it is conducive to narrow bezels, increasing aperture ratio, improving image quality, energy saving and environmental protection, and meeting Large size, high resolution and high refresh rate, high functionality. Now, enhancing the production yield rate are critical for the mass production. A-Si:H TFT manufactured by using four-mask process instead of normal five-mask process to improve the low manufacturing cost and high yield rate is a good solution, the four-mask technology is used to reduce a photolithography steps, the two-Wet and two-Dry(2W2D) technology is adopted.

Because copper has the characteristics of corrosion and oxidation, it is very challenging in production. At present, most panel factories use copper acid with fluoride and high H2O2 to etch Cu. But this method will be harmful to human body and machine. After repeated trials and optimization of the process, we use fluorine-free and low H2O2 cupric acid and successfully imported it into Mo/Cu structure TFT-LCD, as show in Fig.2.

The Cu process has many advantages compared to the Al process, but in the Cu process TFT, the contact resistance between the metal and the semiconductor is larger, which will lead to insufficient charging rate of the TFT. We discuss its mechanism in detail and give improvement measures.

Fig.3 (a) shows the IdVd diagram of Cu process and Al process when Vg=10V, it can be seen that under the same Vd voltage, the current I of Al process is much larger than that of Cu process. K=(Id-I0)/(Vd-V0), the slope K is expressed as the reciprocal of resistance, which is the conductivity σ. The electrical conductivity of Al process TFT is much greater than that of Cu process as shown in Fig.3 (b). Table 1 is obtained by calculation. When Vd=5V, the conductivity of Al process is 100%, Cu process is only 60%. When Vd=30V, the conductivity of Al process is 50.3%. Cu process is only 14.6%. In order to more clearly analyze the reason why the conductivity of Cu process is much lower than that of Al process, a detailed explanation is given below through the band diagram.

In order to solve the problem of G picture difference caused by insufficient Ion in Cu process TFT-LCD. Comparative of the electrical characteristics of the Cu process and the Al process, the conductivity of Cu process is less than that of Al process. And analyze this reason in detail through the metal-semiconductor contact energy level diagram. Provide feasible measures to solve the problem of Cu process TFT-LCD.

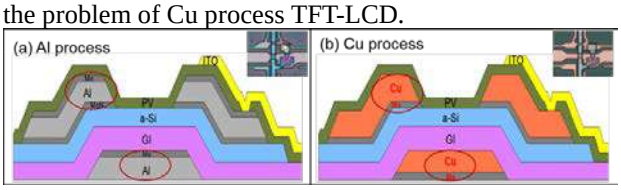

Fig. 1 (a) Cu-Cu 4 Mask structure diagram (b) AL-Al 4 Mask structure diagram

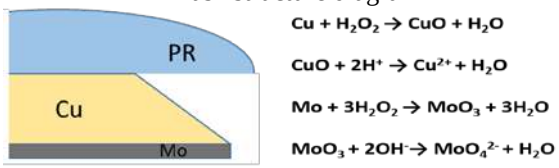

Fig.2 Acid etching Cu principle

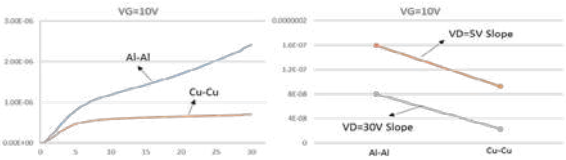

Fig. 3 (a) the IdVd diagram of Cu process and Al process (b) the slope diagram of Cu process and Al process at Vd=5V and Vd=30V

Fig.4 50 inch UHD 120Hz TFT-LCD panel with the Cu process using 4-mask a-Si TFT

References

[1] Kim, Da Eun, et al. "Corrosion Behavior and Metallization of Cu-Based Electrodes Using MoNi Alloy and Multilayer Structure for Back-Channel-Etched Oxide Thin-Film Transistor Circuit Integration." IEEE Transactions on Electron Devices 64.2(2017):447-454.

[2] Yeon, Han Wool, et al. "Cu Diffusion – Driven Dynamic Modulation of the Electrical Properties of Amorphous Oxide Semiconductors." Advanced Functional Materials 27.25(2017):1700336.

Ultra-Precise Deposition for Display Manufacturing: from Rapid Prototyping to Mass Production

Aneta Wiatrowska, Piotr Kowalczewski, Karolina Fiączyk, Łukasz Witczak, Jolanta Gadzalińska, Mateusz Łysień, Ludovic Schneider, Filip Granek

XTPL SA, Stabłowicka 147, 54-066 Wrocław, Poland

Tel.: 0048 662 291 617, E-mail: piotr.kowalczewski@xtpl.com

We will demonstrate a novel ultra-precise deposition (UPD) technology for display manufacturing. UPD allows a direct deposition of silver and copper inks with metal content as high as 82% wt. Due to careful process and hardware optimization, such highly-concentrated inks can be extruded using a 1 to 10 µm diameter printing nozzle. This results in printed feature size as small as 1 µm with up to 45% bulk value electrical conductivity.

We will present how UPD technology can be used for different display technologies and at different stages of the manufacturing process. This includes open-defect repair in high-resolution organic light-emitting diode (OLED) displays; making micrometer size, mechanically robust, and high-conductivity interconnectors in micro-LED (µLED) displays; as well as printing segments for thin-film transistor arrays.

In Fig. 1a) we show a render of the XTPL's printing module based on the UPD technology. During the deposition process, high-viscosity silver or copper ink (from 10,000 to 2,500,000 cP) is directly extruded using a nozzle with the diameter in the range from 0.5 to 10 µm, which gives the printed feature size in the range from 1 to 10 µm. The combination of high-viscosity inks and fine printed features defines a unique operating range for the UPD technology and allows to make arbitrarily-shaped conductive structures on challenging substrates. An example of such a complex substrate is shown in Fig. 1b), where we demonstrate a silver line with a width of 1.7 µm and length of 20 µm, printed on an OLED substrate. Finally, in Fig. 1c) we present part of the sample of 7500 automatically printed segments for a thin-film transistor array. The linewidth is 4 µm and the interline distance is reduced to single micrometers. This sample demonstrates the capability of the UPD technology to achieve high throughput, one of the key parameters in the fabrication of modern displays.

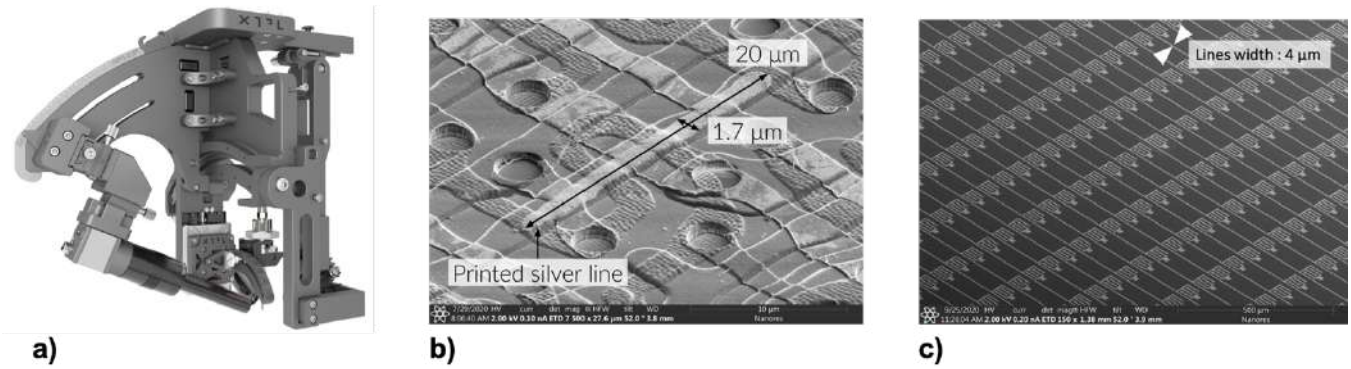

Fig. 1. a) Render of the XTPL's printing module based on the UPD technology; b) Silver line with a width of 1.7 µm and length of 20 µm printed on an OLED substrate; c) Segments for a thin-film transistor array printed using the UPD approach. The line width is 4 µm

UPD allows to print arbitrarily-shaped interconnectors on vertical steps much higher than the width of the printed structure. Moreover, the electrical conductivity of printed structures is up to 45% of the bulk metal. Finally, the process is governed by pressure and no external electric field is required, which makes it safe to print close to fragile electrical components. Thanks to all these features, we will argue that the UPD technology answers major challenges in display manufacturing, offering high throughput, precision, and low cost at the same time. This technology can be used both for rapid prototyping at the R&D stage, as well as it can become a part of a production line of modern displays.

Extremely precise laser glass cutting technology for future display

Woohyun Jung[1], Hyungsik Kim[1], Sunggyu Park[1], Joongsung Lee[1], SeungHoon Jang[1], Junghwa You[1], Kyunghan Yoo[1], Jekil Ryu[1], SeongHo Jeong[1] and Cheol Lae Roh[1]*

[1]Samsung Display, 1 Samaung-ro, Giheung-gu, Yongin-si, Gyeonggi-do, 17113, Republic of Korea
**Tel.:82-31-5181-5709, E-mail: hsnix.kim@samsung.com*

As one of the various attempts to reduce the size of display bezel, high-precision glass cutting process is required to be developed for future displays [1]. Laser-based Bessel-beam cutting (LBC) technology has been attractive for its chipping-less cutting edge of glasses compared with the conventional laser processes using ablation and thermal shock mechanism. Nonetheless, heat damages caused by high-order Bessel beam in the LBC have been imperative on a display panel [2-4]. Here, the LBC process has been studied, which is capable of minimizing the thermal deformation of the black matrix (BM) material on glass. As well as laser pulse energy, burst mode condition and pulse pitch in laser significantly impact on the heat propagation on materials. In an experimental setup composed of IR-ps laser and Bessel optics, the smallest thermal degradation of BM and the highest glass cutting precision are achieved as 40µm and 10µm, respectively. When reducing thermal effects caused by high-order beams without sacrificing glass breaking strength, effective heat-affected zone (HAZ) could be reduced under 33um width from the cutting line. This high precision cutting technology will contribute to realize extremely narrow bezel display near future.

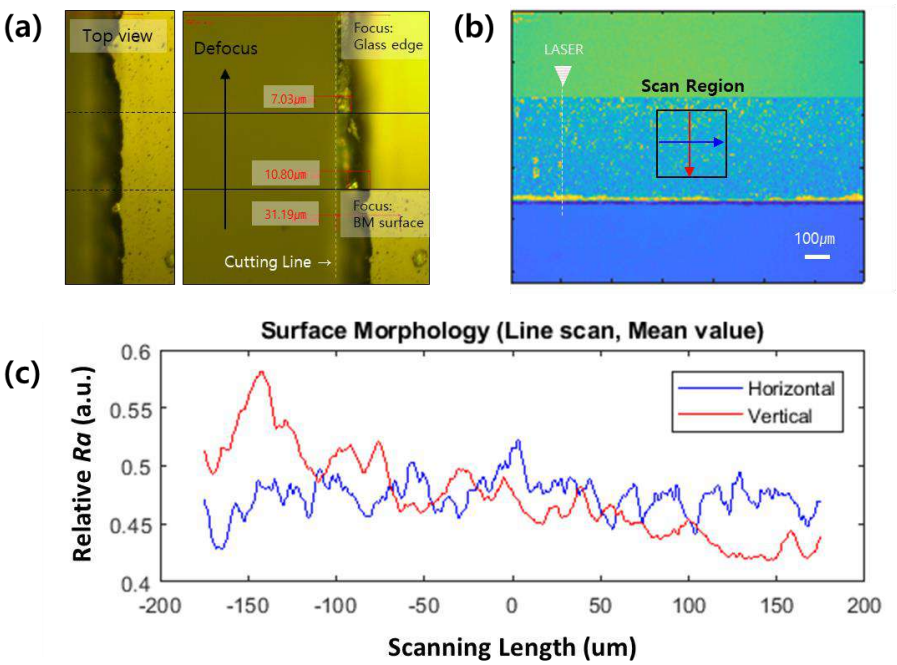

Figure 1. (a) Microscope image according to the laser cutting process through 0.5T BM/Glass (Top View). Heat-affected zone around the laser cutting line is measured about 33um. (b) The fractured plane is shown at the side-walls. White arrows indicate the origin of the input laser beam. In the bottom of the sample, Bessel-beam trajection is observed. The black box area is scanned to measure the surface roughness, and its relative values are indicated in (c).

References

1. J. Dudutis, J. Pipiras, R. Stonys, E. Daknys, A. Kilikevičius, A. Kasparaitis, G. Račiukaitis, P. Gečys, *Opt. Express*, 28(21), 32133-32151 (2020).
2. O. Brzobohatý, T. Čižmár, P. ZemánekJ, *Opt. Express*, 16(17), 12688-12700 (2008).
3. S. Rajesh, Y. Bellouard, *Opt. Express*, 18(20), 21490-21497 (2010).
4. R. Meyer, L. Froehly, R. Giust, J. Del Hoyo, *Appl. Phys. Lett.*, 114(20), 201105, (2019).

Breakthrough Technology; First Plane Source Evaporator for 10,000ppi AMOLED.

[1]Changhun Hwang, [2]Sung Su Kim, [3]In Ho Jeong, [3]Byung Doo Chin

[1]Link Plus, Dankook University, Korea
[2]OLEDON, Dankook University, Korea
[*] Tel: 82-10-7114-9523, E-mail: chriss.hwang@oledon.co.kr
[3]Dept of Polymer Science & Engineering, Dankook University, Korea

The linear source evaporation technique is being currently used in AMOLED industry. However, in the FMM process, it has large shadow distance so AMOLED is limited to be very high ppi resolution for AR application.[1] The plane source evaporator has been recently developed as a new way of high-resolution evaporation technology using the rotatable plane source for the first time, as shown in Fig. 1. [2]

Fig.1 Rotatable Plane Source and Plane source FMM evaporator

The shadow distance measurements are appeared as sub-micron scale covering from 0.2um to 0.7um. This proves an improvement of 3 times better than linear source FMM evaporation in shadowing effect.[3~5] For the 10,000ppi AMOLED as the AR display application, the current FMM evaporation deposition technique should modified by plane source evaporation.

References

[1] CH Hwang, BD Chin et al, “Plane source evaporation techniques for super ultra-high resolution flexible AMOLED”, 37-2, SID2017

[2] C.H.Hwang et al, “Novel plane source FMM evaporation techniques for manufacturing of 2250ppi flexible AMOLEDs”, 75-2, SID2018

[3]C.H.Hwang, S.S.Kim, B.D.Chin, Ultimate Solution: The Belt Plane Source Evaporators for Future AMOLED and QD OLED TV, SID2020,1530-1533, P49. (2020)

[4]C.H.Hwang, S.S.Kim, H.K.Ko, B.D.Chin, Unique Belt Plane Source Evaporation Techniques for the mass production of 2,250ppi AMOLED and 77” QD-OLED TV, SID2019, 67.3 (2019)

[5]C.Hwang, SS Kim, SW Bang, BD Chin et, Seho Choi, et. al., Review of vacuum thermal evaporation for future AMOLED, Physics & High Technology, 04, p29(2018)

Highly Efficient and Stable Blue Organic Light-Emitting Diodes

Jun Yeob Lee
Department of Semiconductor and Display Engineering, Sungkyunkwan University, Suwon, Gyeonggi-do 16419, South Korea
Tel.:82-31-299-4716, E-mail: leej17@skku.edu

The commercialization of highly efficient and stable blue organic light-emitting diodes is one of the most challenging issues in the organic light-emitting diode industry. Although a lot of high efficiency blue devices have been developed, they suffered from poor stability shortening the device operational lifetime. In recent years, material and device approaches avoiding the degradation process of the high efficiency blue devices opened a pathway enhancing the device lifetime. New blue materials including host and dopant materials were effective to extend the device lifetime from material side, while a hybrid device approach combining thermally activated delayed fluorescence emitter or phosphor with a fluorescent emitter also enabled stable blue organic light-emitting diodes. In this work, I present our research work extending the device lifetime of the blue organic light-emitting diode by both material and device engineering.

Fig. 1. Highly efficient blue organic light-emitting diodes

References

1. S. O. Jeon, K. H. Lee, J. S. Kim, S. -G. Ihn, Y. S. Chung, J. W. Kim, H. Lee, S. Kim, H. Choi, J. Y. Lee, Nat. Photonics, 15, 208 (2021).
2. S. K. Jeon, H. L. Lee, K. S. Yook and J. Y. Lee, *Adv. Mater.*, 31, 1803524 (2019).

Blue Emitting Square Planar Metal Complexes for Displays and Lighting Applications

Jian Li
Materials Science and Engineering, Arizona State University, Tempe, Arizona, USA
Tel.:1-480-727-8938 E-mail: jian.li.1@asu.edu

The successful development of efficient and stable molecular blue emissive materials will have a significant impact on the continued deployment of organic light emitting diodes (OLEDs) technology for display and lighting applications. Moreover, the successful development of alternate low cost technology for current solid state lighting devices will have a significant impact on the U. S. economy and national security. In this presentation, we will discuss our continuing efforts on the design, synthesis and characterization of novel platinum and palladium complexes for displays and lighting applications. The photo-physics, electrochemistry, electroluminescent properties and operational stability of these novel metal complexes, including deep blue narrowband emitters and amber emitting phosphorescent molecular aggregates, will be discussed. The rational molecular design enables us to develop cyclometalated metal complexes with both photon-to-photon (in thin film) and electron-to-photon (in device settings) conversion efficiency close to 100% for OLED applications. Our approaches to achieve high efficiency white OLED will be also included.

Fluorescence materials with core and side concepts remain to be areas to be further explored: Highly efficient dual-core derivatives with EQEs of 8.38%

Seokwoo Kang, Hayoon Lee, Sunwoo Park and Jongwook Park*
[1]*Integrated Engineering, Department of Chemical Engineering, Kyung Hee University, 1732, Deogyeong-daero, Giheung-gu, Yongin-si, Gyeonggi-do,17104,Republic of Korea*
Tel:82-31-201-3675, Email: jongpark@khu.ac.kr

For industrial application of OLED displays, there is a need to develop a stable blue-light-emitting dopant that is highly efficient at high brightness without roll-off. In our previous work, we studied the use of dual-core and fused-core-type emitters combining two chromophores as emitting materials.[1] In the current work, we designed a new blue-light-emitting material including a dopant to enhance the color purity of the light emitted and to realize stable efficiency without roll-off at high brightness. We used the following strategy to design the new emitter. (1) We used a dual core combining anthracene and pyrene, which are chromophores with high luminous efficiency levels. In a previous study, we observed that using this dual core rather than a single core outstanding EL efficiency and long lifetime were obtained, and these advantages were attributed to both anthracene and pyrene contributing to the absorption and emission processes.[1-2] (2) We used a triphenylamine (TPA) group as a side group because it contains a nitrogen atom capable of improving the charge transfer. Also, the use of bulky TPA as a side group yielded a twisted molecular structure, preventing intermolecular interactions. (3) We attached the TPA substituent at its ortho, meta, and para positions to the dual core to provide a series of isomers with varying conjugation lengths and bulkiness levels, and in this way developed a means of controlling the emission of light in the blue region.[2]

In this work, three blue fluorescent materials were newly synthesized by attaching triphenylamine side groups at their ortho, meta, and para positions to a dual core moiety of anthracene and pyrene, two chromophores with good luminous efficiency; these three materials were 2-(6-(10-(2-(diphenylamino)phenyl)anthracen-9-yl)pyren-1-yl)-N,N-diphenylaniline (o-TPA-AP-TPA), 3-(6-(10-(3-(diphenylamino)phenyl)anthracen-9-yl)pyren-1-yl)-N,N-diphenylaniline (m-TPA-AP-TPA), and 4-(6-(10-(4-(diphenylamino)phenyl)anthracen-9-yl)pyren-1-yl)-N,N-diphenylaniline (p-TPA-AP-TPA), respectively. The optical, thermal, and electroluminescence (EL) properties of the synthesized materials were measured. All three materials were found to be real blue emitters in the solution state and display high PLQY values. A device doped with p-TPA-AP-TPA displayed a very high efficiency of 9.14 cd A^{-1} and an EQE of 8.38% at a high luminance of 5000 cd m^{-2} as shown in Figure 1.

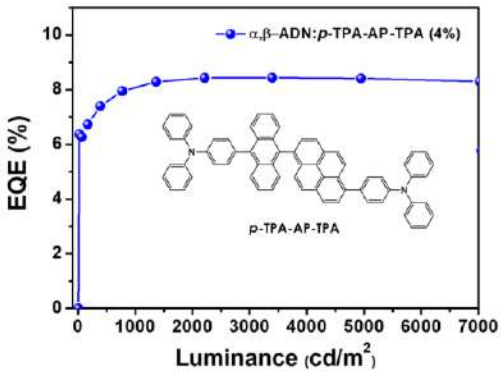

Fig. 1. EQE–luminance curves of the OLED doped devices based on *p*-TPA-AP-TPA.

Acknowledgment

References

1 H. Shin, B. Kim, H. Jung, J. Lee, H. Lee, S. Kang, J. Moon, J. Kim and J. Park, RSC Adv., 20(7), 55582–55593 (2017).
2 S. Kang, H. Lee, H. Jung, M. Jo, M. Jung and J. Park, Dyes Pigm.,156, 299–306 (2018).

Blue Organic light-emitting diodes by TADF emitters

Soon Ok Jeon
Samsung Advanced Institute of Technology, Samsung Electronics Co., Ltd., Suwon 16678, Korea
Tel.:82-10-6821-0406, E-mail: so.jeon@samsung.com

Thermally activated delayed fluorescence (TADF) organic light-emitting diodes (OLEDs) have demonstrated potential as the leading technology for highly efficient OLEDs by achieving a high external quantum efficiency (EQE) comparable to that of state-of-the-art phosphorescent OLEDs. The most popular material design platform of the TADF emitters is the donor-π linker-acceptor structure. The donor and acceptor parts in the TADF structure mainly govern the charge transfer (CT) characteristics related with the singlet and triplet energies, and the π-linker part dominates the orbital overlap for efficient light emission. The donor and acceptor engineering were the main approach to manage the TADF performances of the TADF emitters because the key process of RISC was mostly determined by the donor and acceptor. Recently, TADF molecular design concept has been developed to narrow-banded spectrum with FWHM < 30 nm to realize deep blue color. It was based on multiple-resonance (MR) effect that the distributions of the frontier orbitals alternate within a rigid π-conjugation scaffold to realize a short-range charge transfer (CT). In here, I would like to introduce the characteristics of basic materials, molecular design methods, and application technologies by TADF emitters for blue OLEDs.

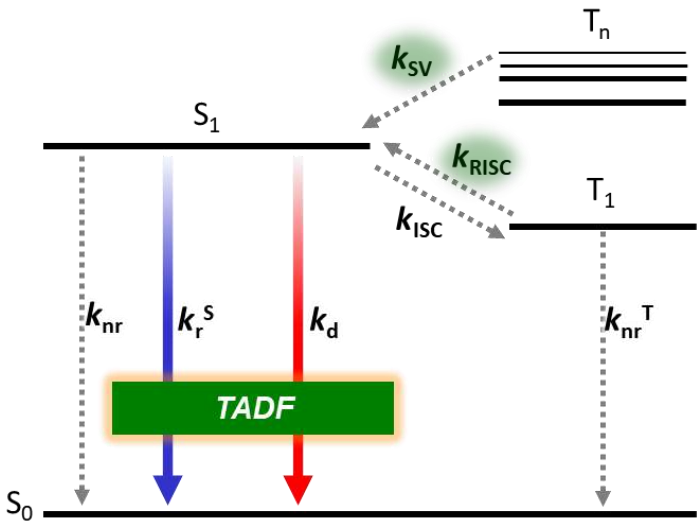

Fig. 1. TADF OLEDs mechanism.

Acknowledgment

This work was supported by Samsung Advanced Institute of Technology (SAIT).

References

1. S. O. Jeon and J. Y. Lee *J. Mater. Chem. C*, 8, 1736 (2020).
2. Hatakeyama et al, *Angew. Chem. Int. Ed.*, 60, 1 (2021).
3. S. O. Jeon, K. H. Lee, J. S. Kim, S-G. Ihn, Y. S. Chung, J. W. Kim, H. Lee, S. Kim, H. Choi and J. Y. Lee, *Nat. Photonics*, 15, 208 (2021).
4. I. Kim, S. O. Jeon, D. Jeong, H. Choi, W-J., Son, D. Kim, Y. M. Rhee and H. S. Lee, *J. Chem. Theory Comput.*, 16, 621. (2020)
5. I. Kim, K. H. Cho, S. O. Jeon, W-J., Son, D. Kin, Y. M. Rhee, I. Jang, H. Choi and D. S. Kim, *JACS Au*, in press (2021)

Indolo[3,2,1-jk]carbazole Based Multi-Resonance Materials for Blue Fluorescent Organic Light Emitting Diodes

Eui Gun Lee[1], Won Jae Chung[2], and Jun Yeob Lee[*]
School of Chemical Engineering, Sungkyunkwan University, 2066, Seobu-ro, Jangan-gu, Suwon-si, Gyeonggi-do, 16419, Republic of Korea
Tel.: +82-31-299-4807, E-mail : leej17@skku.edu

The indolo[3,2,1-jk]carbazole were derived to construct core structure.

Fig. 1, shows the molecular structure of p-pDIDCz. The emitter was embodied with multi-resonance character by alternating molecular orbital distribution through the polycyclic structure bridged by a nitrogen atom.

Fig. 2, shows the PL spectra of emitters. A narrow emission spectrum with a full width at half maximum of 16 nm in solution and 22 nm in the device was achieved by the multi-resonance effect and rigid molecular structure of the p-pDIDCz emitter. Main emission came from the core structure and the peripheral phenyl units surrounding the core suppressed intermolecular aggregation in solid state for narrow emission.

The optimized p-pDIDCz device achieved high external quantum efficiency of 23.5%, pure blue color coordinate of (0.144, 0.057), and small full width at half maximum of 22 nm. This shows that compared to other blue organic light emitting diodes that have been studied recently, the materials in this study have excellent color purity and, at the vi same time, high external quantum efficiency and full width at half maximum, resulting in superior results. Table 1 summarizes the device performance.

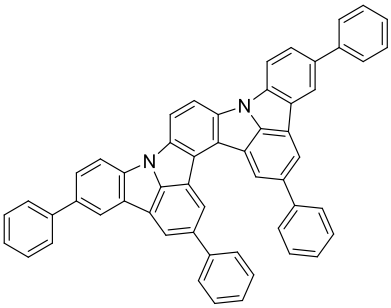

p-pDIDCz

Fig. 1. Molecular structure of material

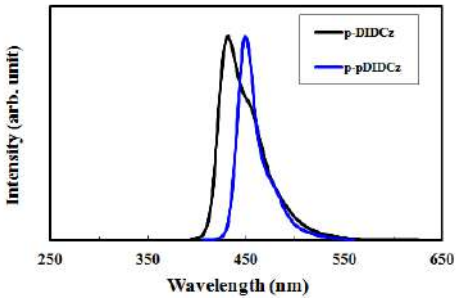

Fig. 2. PL spectra of emitters

Table 1. Device performance of blue emitters measured at 100 cd/m^2

	p-pDIDCz
Maximum Quantum efficiency(%)	23.5
Color coordinate (1wt%)	(0.144, 0.057)
FWHM(nm)	22
Driving Voltage(V)	5.1
Power efficiency(lm/W)	34.2

References

1. M. A. Baldo, D. F. O' Brien, Y. You, A. Shoustikov, S. Sibley, M. E. Thompson, S. R. Forrest, *Nature* **1998**, *395*, 151.
2. C. Adachi, M. A. Baldo, S. R. Forrest, *Appl. Phys. Lett* **2001**, 78, 1622-24.
3. C. Adachi, M. A. Baldo, M. E. Thompson, S. R. Forrest, *J. Appl. Phys.***2001**, *90*, 5048.
4. H. Uoyama, K. Goushi, K. Shizu, H. Nomura, C. Adachi, *Nature* **2012**, *492*, 234.
5. Q. S. Zhang, J. Li, K. Shizu, S. P. Huang, S. Hirata, H. Miyazaki, C. Adachi, *J. Am. Chem. Soc.* **2012**, *134*, 14706.
6. K. S. Yook, J. Y. Lee, *Adv. Mater* **2012**, 24, 3169
7. H. Hirai, K. Nakajima, S. Nakatsuka, K. Shiren, J. Ni, S. Nomura, T. Ikuta, T. Hatakeyama, *Angew. Chem., Int. Ed.* **2015**, *54*, 13581.
8. T. Hatakeyama, K. Shiren, K. Nakajima, S. Nomura, S. Nakatsuka, K. Kinoshita, J. Ni, Y. Ono, T. Ikuta, *Adv. Mater.* **2016**, *28*, 2777
9. Y. Kondo, K. Yoshiura, S. Kitera, H. Nishi, S. Oda, H. Gotoh, Y. Sasada, M. Yanai, T. Hatakeyama, *Nature Photonics*, **2019**, 13, 678–682.
10. V. V. Patil, K. H. Lee, J. Y. Lee, *Dyes and Pigments*, **2020**, 174, 108070.
11. H. L. Lee, W. J. Chung, J. Y. Lee, small,2020, 16, 14, 1907569.

Relationship of device lifetime and bond dissociation energy of the organic materials in OLEDs

*Thangaraji Vasudevan, Young Jae Shim, Ji Hun Kim, Seungjun Lee, Yongsup Park and Min Chul Suh**
Dept. of Information Display, Kyung Hee University, Dongdaemun-Gu, Seoul 02447, Korea
Tel.:82-2-961-0694, E-mail: mcsuh@khu.ac.kr

In the past decades, research on the causes of deterioration of organic light-emitting diodes (OLEDs) has been actively conducted, and various causes of deterioration have been proposed. We calculated the bond dissociation energy (BDE) of the organic material and studied the intrinsic decomposition of organic matter, which generates fragmentation when holes or electrons become trapped at a certain interface. Especially, there has been lots of reports that the hole transport material could be damaged when an anionic excited state can be formed inside HTL by inflow of electron carriers.

To clearly understand such possibility, we calculated the BDE and measured mass spectroscopy (MS) of 11-(4,6-diphenyl-[1,3,5]triazin-2-yl)-12-phenyl-11,12-dihydro-11,12-diazaindenofluorene (DIC-TRZ), a negative host to investigate which carrier is the most harmful source for such molecular degradation as shown in Fig 1. To confirm such weakest bond dissociation, we made a hole only device (HOD) and an electron only device (EOD) to check how much an anion state or the cation state formation accelerates deterioration. Finally, we confirmed a bond dissociation by MS and assign the possible fragmentation trend. As we expected, an anionic state formation of aryl-amine moiety is critical for molecular degradation. Thus, we designed a full device which can suppress such bond dissociation by using hole-dominant host with a large electron-trapping level to improve a device operation lifetime as shown in Fig 2.

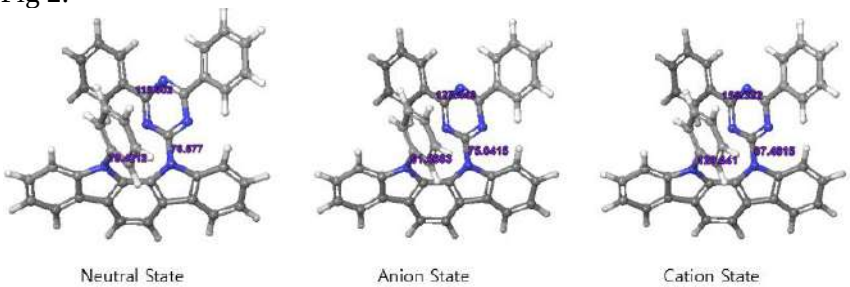

Fig. 1 Molecular simulation BDE

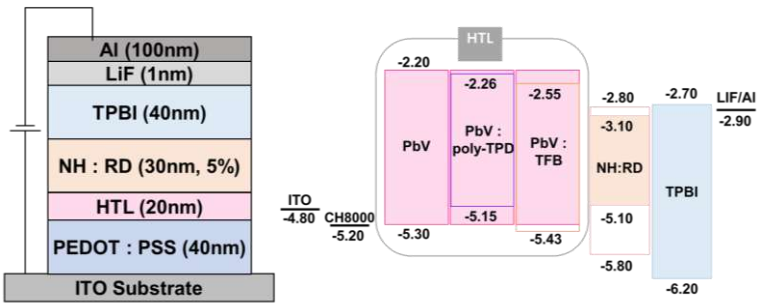

Fig. 2 Negative host DIC-TRZ device strucutre

Acknowledgment

This work was supported by the Technology Innovation Program (20010443, Development of mass spectrometry for OLED structure and stability analysis) funded by the Ministry of Trade, Industry & Energy (MOTIE, Korea). Also, this research was also supported by Basic Science Research Program through the National Research Foundation of Korea (NRF) funded by the Ministry of Education (2021R1A2C1008725).

References

1. Scholz, S., Kondakov, D., Lussem, B., & Leo, K. ACS Publications 115. 16, p8449-8503 (2015)

High Efficiency (23%), Narrow-Emitting (21 nm) and Ultrapure Deep Blue (CIEy~0.05) Organic Light-Emitting Diodes Based on a New Mechanism of Purely Spin-Vibronic Coupling Assisted Thermally Activated Delayed Fluorescence

*Ha Lim Lee[1], Vilas Venunath Patil[1], Inkoo Kim[2], Kyung Hyung Lee[1], Won Jae Chung[1], Joonghyuk Kim[3], Sangho Park[3], Hyeonho Choi[3], Won-Joon Son[2], Soon Ok Jeon[3], and Jun Yeob Lee[1]**

[1]School of Chemical Engineering, Sungkyunkwan University, Suwon 16419, Korea

E-mail: leej17@skku.edu

[2]Data and Information Technology Center, Samsung Electronics, Hwaseong 18448, Korea

[3]Samsung Advanced Institute of Technology, Samsung Electronics, Suwon 16678, Korea

In this work, we developed highly efficient and ultrapure deep blue emitters based on purely carbon and nitrogen type polycyclic system without boron atom and donor-acceptor structure through a new emission mechanism of pure spin vibronic coupling (SVC) assisted thermally activated delayed fluorescence (TADF). The designed emitters did not harvest triplet excitons by direct spin-orbit coupling from the lowest triplet excited state (T_1) but harvested them via high-lying triplet excited state (T_2) by second-order reverse intersystem crossing called SVC. The new purely SVC type TADF emitter can fully utilize both singlet and triplet excitons. The synthesized emitters realized narrow emission spectrum with a full width at half maximum (FWHM) of 21 nm, small Stokes shift (<20 nm) and high photoluminescence quantum yield (>90%). The fabricated OLEDs showed pure blue emission spectrum with FWHM of 21 nm, maximum external quantum efficiency (EQE) of 23.1% and ultrapure deep blue color coordinate of (0.15, 0.05) satisfying BT2020 color specification. This is the first work reporting high EQE over 20%, FWHM of 21 nm and color coordinate of (0.15, 0.05), overcoming the challenging hurdle of the blue OLEDs.

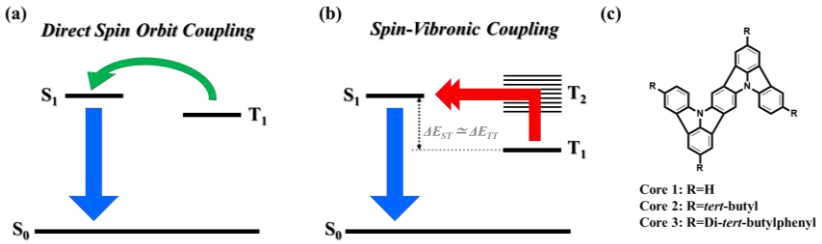

Fig. 1. The RISC mechanism of (a) direct spin orbit coupling and (b) spin-vibronic coupling, and (c) chemical structures of SVC-TADF emitters

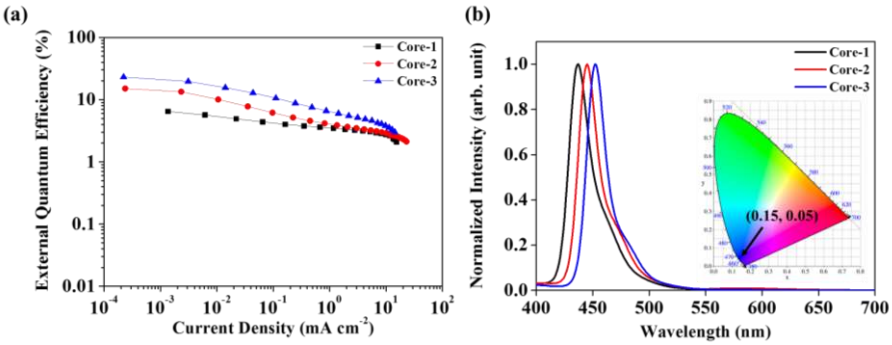

Fig. 2. (a) EQE-current density curves and (b) electroluminescence spectra, CIE coordination of ultrapure deep blue SVC-TADF OLEDs

References

1. H. Uoyama, K. Goushi, H. Nomura and C. Adachi, *Nature* 492, 234-238 (2012).
2. I. Kim, S. O. Jeon, D. Jeong, H. Choi, W.-J. Son, D. Kim, Y. M. Rhee and H. S. Lee, *J. Chem. Theory Comput.*,16, 621-632 (2020).
3. M. K. Etherington, J. Gibson, H. F. Higginbotham, T. J. Penfold and A. P. Monkman, *Nat. Commun.*, 7, 13680 (2016).

Phenol and diverse Aromatic Amines Based Asymmetric Blue Multi-Resonance TADF Emitters with Narrow Emission Band

Jinho Park[1], Jun Seop Lim[1], Junyoung Moon[2], Jeongkyu Woo[2], Seung Soo Yoon[2]*, Jun Yeob Lee[1]*

[1]School of Chemical Engineering, Sungkyunkwan University, 2066 Seobu-ro, Jangan-gu, Suwon, Gyeonggi-do, 16419, Korea

Tel.:82-31-290-4716, E-mail: leej17@skku.edu

[2]Department of Chemistry, Sungkyunkwan University, 2066 Seobu-ro, Jangan-gu, Suwon, Gyeonggi-do, 16419, Korea

Unlike previously well-known boron-based MR TADF emitters, the compounds synthesized in this study have an asymmetric molecular structure consisting of one boron, one oxygen and one nitrogen. The light emission properties of the emitters are controlled by changing the aromatic units connected to the nitrogen into diphenyl amine, carbazole, and acridine derivatives. Because of the weak electron-donating oxygen atom, the TADF emitters showed blue emission, and emission color is controlled by the aromatic group attached to the nitrogen. One of the emitters, **'A'** exhibited the real deep-blue color coordinate of (0.15, 0.05), a small full width at half-maximum of 32 nm, and a maximum external quantum efficiency of 16.3%. The data of the EL spectra is presented in **Figure 1.**

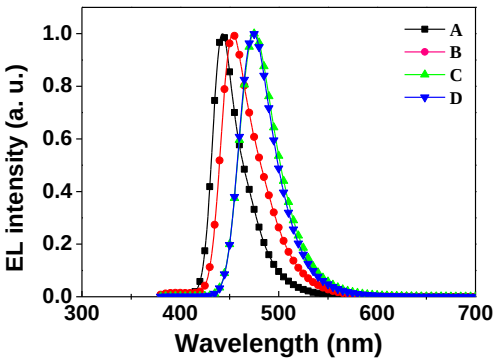

Fig. 1. EL spectra

References

1. H. Hirai, K. Nakajima, S. Nakatsuka, K. Shiren, J. Ni, S. Nomura, T. Ikuta, T. Hatakeyama, *Angew. Chem. Int. Ed.*, 54, 13581 (2015).
2. K. Shiren, K. Nakajima, S. Nomura, S. Nakatuka, K. Kinoshita , J. Ni , Y. Ono, T. Ikuta, T. Hatakeyama, *Adv. Mater.*, 28, 2777 (2016).

A novel electroplex host with dual triplet exciton up-converting channels for long lifetime blue phosphorescent organic light-emitting diodes

Ju Hui Yun[1], Jae Min Kim[1], Won Jae Chung[1], Junseop Lim[1], and JunYeob Lee[1], Yoonkyoo Lee[2], Changwoong Chu[2]

[1]Dept. of Chemical Engineering, Sungkyunkwan University, Suwon-si, Gyeonggi-do, 16419, Korea

[2]Display Research Center, Samsung Display Co., Giheung-gu, Yongin-si, Gyeonggi-do, Korea

Tel.:82-31-299-4807, E-mail: leej17@skku.edu

A novel electroplex host with dual triplet exciton up-converting channels using a thermally activated delayed fluorescence (TADF) type n-host was developed to improve the device lifetime of deep blue phosphorescent organic light-emitting diodes (PhOLEDs). The TADF type n-host (SiTCNCz) was derived from triazine with benzonitrile and carbazole units to induce the TADF characteristics and it generated TADF type electroplex by mixing with a common mCBP. The singlet and triplet energies of SiTCNCz host were 3.08 and 2.95 eV, respectively, with a small difference of 0.13 eV, which induced TADF emission with a short delayed fluorescence lifetime of 2.16 μs. Moreover, the electroplex of mCBP : SiTCNCz exhibited TADF bahavior up-converting triplet excitons into singlet excitons. As a result, the electroplex host of mCBP :SiTCNCz doubly up-onverted triplet excitons into singlet excitons to minimize the triplet exciton density in excited state for long device lifetime and more than doubled the device lifetime of the deep blue PhOLEDs compared to the state of the art electroplex host while maintaining high exteranl quantum efficiency over 20% and deep blue color coordinate of (0.14,0.18). This work is the first demonstration of the TADF type n-host for deep blue phosphors and realization of the electroplex host with TADF behaviors. The dual up-conversion mechanism based electroplex ideally minimized the triplet exciton density in the emitting layer by TADF process, which dramatically extended the device lifetime of the deep blue PhOLEDs. This work opened a new pathway maximizing the device lifetime of the deep blue PhOLEDs by host engineering and achieved state of the art device liftime by ideal host design fully suppressing triplet excitons in the emitting layer by ideal triplet up-converting mechanism.

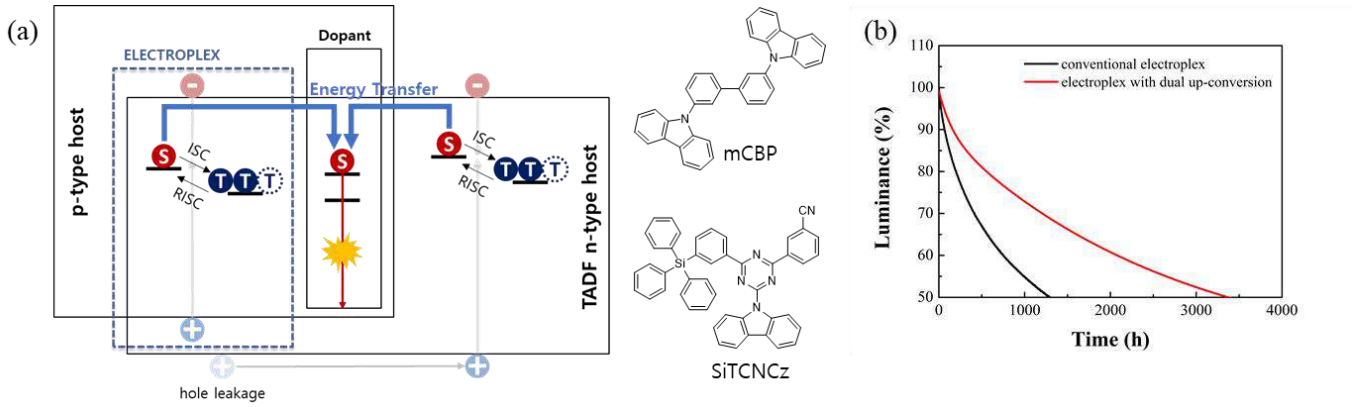

Fig. 1. (a)Schematic mechanism of the electroplex device with dual triplet exciton up-conversion mechanism and molecular structure of mCBP and SiTCNCz (b)device lifetime curves of electroplex based mCBP:SiTrz (single up-conversion) and mCBP:SiTCNCz (dual up-conversion) devices

References

1. H. Lim, H. Shin, K. H. Kim, S. J. Yoo, J. S. Huh, J. J. Kim, *ACS Appl. Mater. Interfaces*, 9, 37883 (2017).
2. W. Song, J. Y. Lee, Y. J. Cho, H. Yu, H. Aziz, K. M. Lee, *Adv. Sci.*, 5, 1700608 (2018).
3. M. Jung, K. H. Lee, J. Y. Lee, T. Kim, *Mater. Horizons*, 7, 559 (2020).

Improving the stability of blue OLEDs with TADF sensitized fluorescence

Lian Duan
Department of Chemistry, Tsinghua University, Beijing 100084, China.
Email: duanl@mail.txinghua.edu.cn

Prof. Lian Duan was born in 1975. He received his Ph. D from Department of Chemistry, Tsinghua University, in 2003. He is now with the Department of Chemistry, Tsinghua University. His research interests focus on new organic materials for flexible optoelectronics.

Improving the stability of blue OLEDs with TADF sensitized fluorescence

Blue TADF emitters with both linear donor-π-donor and acceptor-π-acceptor structures are constructed to facilitate delocalized excited states for enhanced mixing between charge-transfer and locally excited states. Consequently, high k_{RISC}s over 10^6 s^{-1} can be achieved. When utilizing these materials to sensitize a blue multiple-resonance TADF emitter, a TADF sensitized fluorescence (TSF) OLED realized maximum external quantum efficiency up to 35% and high stability.

Keywords: thermally activated delayed fluorescence, delocalized excited states, multiple donors and acceptors, sensitized emission, stable deep blue device

Introduction

To achieve efficient and stable organic light-emitting diodes (OLEDs) based on materials with thermally activated delayed fluorescence (TADF)[1], a key parameter is a high reverse intersystem crossing (RISC) rate (kRISC) for efficient triplet (T1)-to-singlet (S1) up-conversion. It has been recognized that kRISC is proportional to A ×exp(-ΔEST/kBT), where A is the pre-exponential factor, ΔEST is the energy gap between singlet (S1) and triplet (T1), kB is the Boltzmann constant and T is the temperature. A common strategy to promote kRISC is to decrease the ΔEST by enhancing the charge-transfer (CT) character of the compounds with spatially separated donor (D) and acceptor (A) subunits. However, for blue TADF emitters, a weakened CT character is usually required to guarantee wide energy gap, conversely leading to a relatively large ΔEST and thus a small kRISC. The inefficient RISC process consequently results in the slow exciton emission dynamics, to the detriment of device efficiency and stability in organic light-emitting diodes, especially for deep blue emitters.

Given that a spin-flip transition from CT triplet (3CT) to CT singlet (1CT) is generally forbidden because of their different spin multiplicities and similar orbital characters, the exact mechanism of RISC currently has been subject to debate, with one popular theory involving a second-order process mediated by vibrionic coupling between a local triplet (3LE) and 1CT/ 3CT. In that scenario, materials with relatively large ΔESTs may also possess the potential for high kRISCs with accessible 3LE states. In our previous work, we have explored blue emitters based on multiple Ds-A-type carbazole-ben (CzBN) derivatives, exhibiting good kRISCs with relatively high ΔESTs of ~0.2 eV. Further studies revealed that such multiple donors motifs naturally facilitate efficient triplet up-conversion due to two key factors: linearly aligned Ds in the structure of D-π-D motif facilitates the formation of delocalized excited states; intermediate T1 states that corresponds to a partial molecular structure of the systems have been observed. Both are critical for the mixing of CT and LE states, benefiting for the efficient T1-to-S1 up-conversion process and thus high kRISCs. Efficient and stable sky-blue OLEDs have been demonstrated based on these CZBN derivatives, making them a good starting point for further investigation. Moreover, the broad CT emissions of the CZBNs render them good sensitizers for TADF sensitized fluorescence (TSF) OLEDs[2], as they show perfect match with the absorption of narrowband final fluorescent emitters such as DABNAs[3,4].

CzPhBN sensitizers

Here, we report a sterically crowded structure with multiple D and A-type carbazole-benzonitrile (CzPhBN) derivative. This motif is made possible by adopting a weak acceptor-cyanophenyl unit to replace the CN group. The adoption of multiple weak As not only finely tunes the CT energy levels so that they approach the 3LE states, but also allows both linear D-π-D and A-π-A structures for enhanced delocalization of excited states. Under this circumstance, the mixing of the wave function between CT and LE excited states is greatly enhanced, leading to a high kRISC with blue-shifted emission.

The newly developed CzPhBNs are shown in Figure 1, with the relative positions and numbers of A-units manipulated to observe their influence on the photophysical properties. 3,6-di-tert-butyl-9H-carbazole was chosen as the D unit, since the electronically inert tert-butyl moiety as peripheral unit has been proven to improve the stability of the devices. All single-crystal structures of CzPhBNs feature highly twisted structures with Ds and As forced out of plane on average by 66° and 55° to the phenyl ring core, respectively. The spatial distributions of the frontier molecular orbitals (FMOs) of the optimized ground states (S0) were predicted by the density functional theory (DFT) using the widely-employed Lee-Yang-Parr functional (B3LYP) with the 6-31G* basis set, also illustrated in Figure 1.

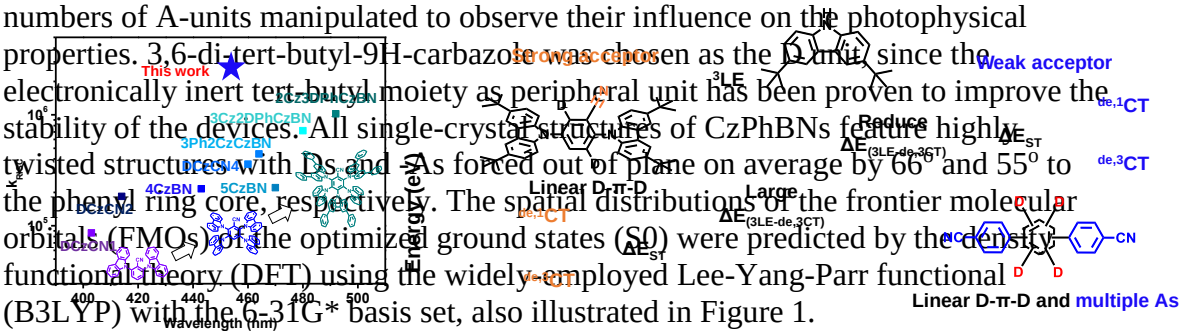

Molecule	Crystal structure	HOMO	LUMO	State levels	
4TCBN	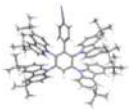	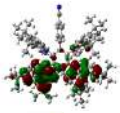	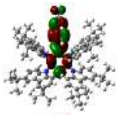	S_1=3.09 eV ΔE_{ST}=0.17 eV	T_3=3.08 eV T_2=3.02 eV T_1=2.92 eV
o4TCDBN	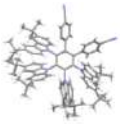	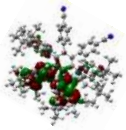	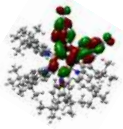	S_1=2.87 eV ΔE_{ST}=0.14 eV	T_1=2.73 eV
m4TCDBN	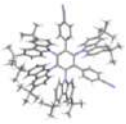	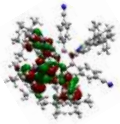	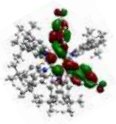	S_1=2.88 eV ΔE_{ST}=0.05 eV	T_2=2.84 eV T_1=2.83 eV
p4TCDBN	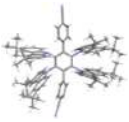	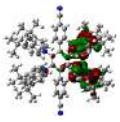	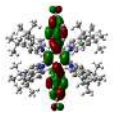	S_1=2.91 eV ΔE_{ST}=0.07 eV	T_3=2.87 eV T_2=2.86 eV T_1=2.84 eV

Figure 1. Structure and the distribution of the frontier orbitals of the CzPhBNs.

For all CzPhBNs, the highest occupied molecular orbitals (HOMOs) are mainly distributed over the Czs, while their lowest unoccupied molecular orbitals (LUMOs) are primarily located on the PhBNs. Notably, not all Czs participate in the HOMO distributions. They are however still necessary to alleviate the rotation of the subunits that may lead to non-radiative decay. Also, it is important to note that both the distribution of the FMOs and the spin-densities of the T1 states of all CBNs do not extend to the tert-butyl units attached on the 3- and 6-positions of carbazole units, indicating that they are electronically inert terminal substituents. Moderate oscillator strengths in the range of 0.0095-0.0312 were observed, originating from the slight HOMO-LUMO overlap on the center phenyl ring. Compared with 4TCBN, the other three CzPhBNs show relatively smaller ΔESTs, explained by the enhanced electron-withdrawing ability of multi-acceptors, but larger oscillate transition strength (f) values, derived from the more delocalized LUMO distributions.

The electroluminance of CzPhBNs were evaluated in the device structure of ITO/ TAPC (30 nm)/ TCTA (10 nm)/ mCP (10 nm)/ DPEPO: 15% (30 nm)/ DPEPO (10 nm)/ Bphen (30 nm)/ LiF (0.5 nm)/ Al (150 nm). EL spectra with the peaks at 468 nm, 457 nm, 468 nm and 448 nm were recorded. Remarkably, an EQE_{max} of 22.8% was obtained for p-4TCDBN while only 8.1%, 13.5% and 7.5% were observed for o-, m-4TCzPhBN and 4TCzPhBN, respectively. The enhanced performance of the p-4TCzPhBN based device can be attributed to the most efficient RISC. Given the superior performance for a blue emitter, the stability of p4TCzPhBN was further tested with a more stable host, 9-(3-(9H-carbazol-9-yl)phenyl)-9H-3,9'-bicarbazole (mCPCz), exhibiting a T80 of 40.4 h for p4TCzPhBN at an initial luminance of 500 cd/m^2, with CIE coordinates of (0.17, 0.21).

With the aim of realizing stable deep blue OLEDs, p4TCzPhBN was further utilized as the sensitizer for a TADF emitter, 12-di-tert-butyl-5,9-bis(4-(tert-butyl)phenyl)-5,9-dihydro-5,9-diaza-13b-boranaphtho[3,2,1-*de*]anthracene (t-DABNA). The energy transfer process of such TADF-sensitizing-TADF system is shown in **Figure 2**, illustrating that after the charge recombination on TADF sensitizer, the formed T_1 can be upconverted into the S_1, from where energy will be transferred to the S_1 of the other TADF emitter. Consequently, the initial ratio of S_1 of TADF emitter can be greatly enhanced while that of T_1 is reduced, which reduces the ratio and lifetimes of the delayed component, allowing for suppressed exciton annihilation and extended device lifetimes. Although one can not totally rule out the Dexter energy transfer in this sensitizing system, such process can be suppressed by manipulating the dopant concentration. Also, the formed triplet can also be, at least, partly recycled due to the TADF character of the emitter.

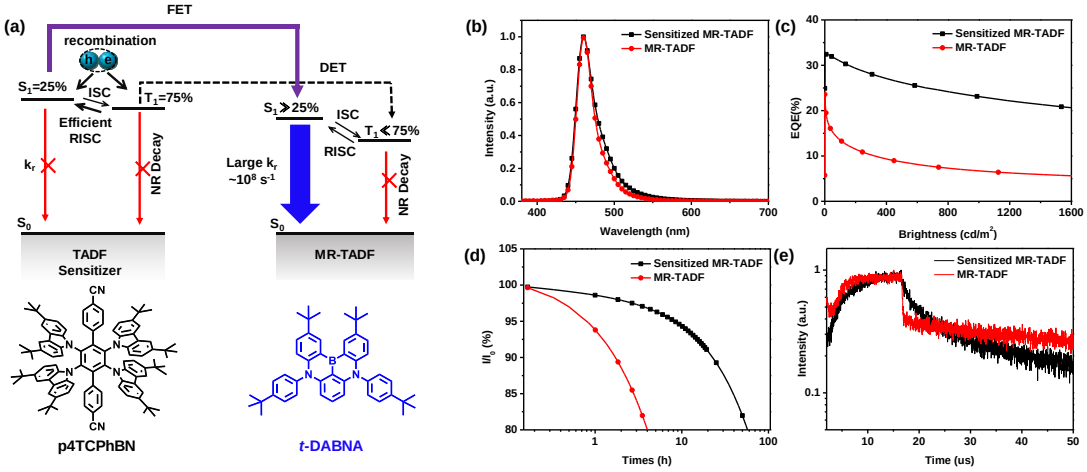

Figure 2. (a) The energy transfer process in the sensitizing system. (b) The EL spectra, (c) the EQE-brightness curves, (c) The lifetimes measured under 1000 cd/m2 and (e) the EL transient decay curves of the devices with or without sensitizer.

In such a system, the high k_{RISC} of p4TCzPhBN naturally serves to accelerate the triplet exciton dynamics. However, for the final emitter, a high k_r is prioritized over a fast k_{RISC}. Featuring a multiple resonance effect from the oppositely positioned boron and nitrogen (B-N) atoms in the framework, *t*-DABNA may be seen as an ideal deep blue dopant in the sensitizing system. On one hand, a high k_r in the order of 10^8 s^{-1} was recorded; on the other hand, fluorescent emission with extremely narrow linewidth was observed, not only leading to high color purity but also reducing the singlet energy under the same CIE coordinates compared with the conventional TADF emitter, which should greatly benefit the device stability.

We fabricated devices with structures of ITO/ HATCN (5 nm)/ NPB (30 nm)/ TCTA (10 nm)/ mCPCz: 40 wt% p4TCzPhBN: 2wt% *t*-DABNA (30 nm)/ CzPhPy (10 nm)/ DPPyA: Liq (1:1, 30 nm)/ LiF (0.5 nm)/ Al (150 nm). Also, for comparison, the device with an emitting layer of mCPCz: 10 wt% *t*-DABNA was fabricated to study the influence of the TADF sensitizer on performance. The EL spectra of the devices were shown in **Figure 3b**, both showing an extremely small FWMH of <30 nm. It is noted that device with p4TCzPhBN as sensitizer showed a slightly larger FWMH of 29 nm than the one without sensitizer (25 nm). One plausible reason may be attributed to the increased polarity of the EML introduced by the D-A type sensitizer, which has also been observed in previous reports. The Commission Internationale de L'Eclairage (CIE) coordinates of (0.13, 0.12) and (0.13, 0.11) were recorded for devices with and without sensitizer, respectively, confirming that deep blue emissions were realized.

Figure 3c showed the EQE-brightness characteristics, revealing an EQE_{max} of 32.5% for the sensitized device, which indicates unity exciton utilization efficiency, assuming a light out-coupling efficiency of 30%. Additionally, a significantly suppressed efficiency roll-off was recorded, with EQE of 26.4% and 23.2% at practical brightness's of 500 cd/m^2 and 1000 cd/m^2, respectively. As a reference, the device without sensitizer only showed an EQE_{max} of only 18.0%, which further fell to 6.6% and 5.2% under the same brightness's of 500 cd/m^2 and 1000 cd/m^2, respectively. Furthermore, the device lifetimes were evaluated at an initial luminance of 1000 cd/m^2. Interestingly, compared to the device without the sensitizer, which possesses a T80 of only 10 hours, the sensitizing device demonstrates an improved lifetime of over 60 h.

To reveal the origin of the significantly improved device efficiency and stability, the EL transient decay curves of the two kind devices were recorded. As illustrated in **Figure 3d,** for the device without sensitizer, the prompt and delayed components were clearly observed, arising from the TADF process of *t*-DABNA. Theoretically, the ratio of prompt and delayed part should be in consistence the ratios of singlet and triplet, which is 25% and 75%, respectively. However, the delayed part only accounts for less than 50% of the decay curve with a long exction lifetime, which means that significant exciton loss through non-radiative decay of triplet states owing to the inefficient RISC process of t-DABNA itself, reflected by the inferior efficiency of the corresponding device. Additionally, under high current density, significant exciton annihilation effects can be anticipated due to the long lifetime of the excited states, which not only leads to the efficiency roll-off but also accounts for the short device lifetimes. Contrarily, after a sensitizer was introduced, the ratio of the delayed component was significantly increased up to 85%, while the exciton lifetime was reduced. Those changes originate from the sensitizing process between p4TCDBN and t-DABNA, not only promoting the exciton utilization efficiency, but also suppressing the exciton annihilation. Consequently, state-of-the-art efficiency and stability were recorded simultaneously for the sensitized device. Recently, how to overcome the drawbacks of low k_{RISC} of MR-TADF emitters has been a hot topic given the strikingly narrow band emission of such emitter, which is usually accomplished by difficult molecule design and synthesis. our work provides an alternation strategy by adopting a TADF material to sensitizer MR-TADF emitter, which can combine the advantages of both kind materials.

High PLQY sensitizers

The linear D-π-D and A-π-A structure has been proved viable to attain efficient and stable blue emitters. We modified the acceptor and donors in the well-known blue TADF emitter 4tCzBN, and synthesized two new TADF emitters, namely 4mt and 4tph.

As shown in **Figure. 3**, 4mt and 4tph have faster decay rates than 4tCzBN and both emitters show PLQYs close to unity when doped into the host of DPEPO. The k_{RISC} of them are calculated to be 0.61×10^6 s^{-1}, 3.14×10^6 s^{-1} and 3.05×10^6 s^{-1}, for 4tCzBN, 4mt and 4tph, respectively.

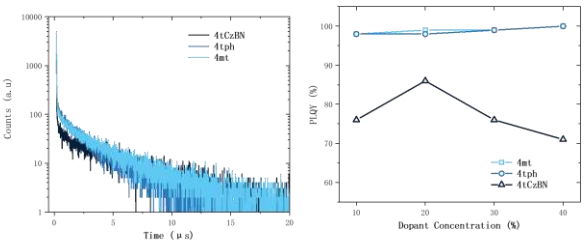

Figure 3. Transient PL curves and PLQYs of the blue 3 emitters (4tCzBN, 4tph and 4mt).

To test the EL properties of these emitters, we fabricated devices with structures of: ITO/HAT(5 nm)/NPB(30 nm)/TCTA(5 nm)/PH204(5 nm)/PH204:dopants (24 nm)/DCZPPy(10 nm)/ET396(30 nm)/LiF(0.5 nm)/Al. As depicted **Figure 4**, all devices gave blue to sky-blue emissions between 468 and 480 nm. 4mt based device showed the highest EQE of over 33%, which is much higher than those of 4tCzBN (~22%) and 4tph (~26%) based OLEDs. 4mt and 4tph based OLEDs exhibited slower efficiency roll-offs compared to 4tCzBN one, owing to their much faster k_{RISC}. Even at a high brightness of 10000 cd/m^2, an EQE over 24% is maintained for 4mt. The driving voltage of the 4mt based OLED is also the lowest. For a practical brightness of 1000 cd/ m^2, only a driving voltage as low as 3.4V is required. More importantly, 4mt based OLED achieved the longest operating lifetime, which is more than an order of magnitude longer than those of the 4tCZBN based one.

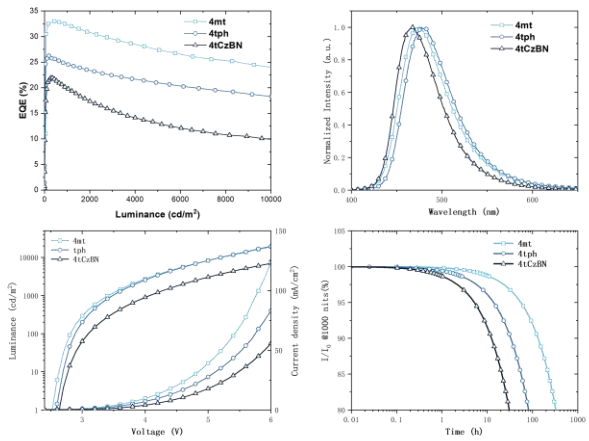

Figure 4. Performances of 4tCzBN, 4tph and 4mt based devices.

To attain pure blue emission, 4mt was used as a TADF sensitizer for a homemade BN type dopant. The FWHM is largely reduced after doping the BN dopant. The EQE of the TSF OLED is as high as 31%, rendering it one of the best results ever reported.

Conclusions

In conclusion, sterically crowded molecules with multiple Ds and linearly positioned As have been developed. The enhanced delocalization allowed by linearly positioned Ds and As promoted the mixing between LE and CT states, resulting in high k_{RISC}s. When these material was utilized as the sensitizer in TSF OLEDs with BN type MR-TADF emitters, high performance and stable deep blue OLEDs can be obtained. Our work may shed light on the development of TSF OLEDs for commercial displays.

References

1. H. Uoyama, K. Goushi, K. Shizu, H. Nomura, C. Adachi, *Nature*. **2012**, 492, 234;
2. Zhang, D.; Duan, L.; Li, C.; Li, Y.; Li, H.; Zhang, D.; Qiu, Y. Adv. Mater. 2014, 26, 5050-5055.
3. Y. Kondo, K. Yoshiura, S. Kitera, H. Nishi, S. Oda, H. Gotoh, Y. Sasada, M. Yanai, T. Hatakeyama, *Nat. Photon.* **2019**, 13, 678.
4. S. H. Han, J. H. Jeong, J. W. Yoo, J. Y. Lee, J. Mater. Chem. C, 2019, 7, 3082.

Deep-blue OLED material discovery by machine learning models with high predictive power

Matthias Budzynski[1], Patrick Ruoff[1], and Thomas Baumann[1]
[1]cynora GmbH, 76646 Bruchsal, Germany
Tel.:+49-7251-919670, E-mail: info@cynora.com

In recent years, fueled by the progress in machine learning (ML) and virtual high-throughput methods, data-driven approaches have become important tools in the field of materials discovery[1]. Two of the main challenges for such approaches are finding suitable representations of chemical structure data and acquiring sufficient amounts of high-quality training data. For material design problems like high-efficiency organic light-emitting diode (OLED) emitters, the physical processes determining material performance are complex. In this case, defining a scoring function that can quickly be evaluated and at the same time correlates well with real-world performance is another challenge. That is one reason why early efforts[2], while representing major conceptual steps forward, have thus far not led to a breakthrough in this area.

Here, we report on the implementation of an evolutionary algorithm to solve the inverse design problem for deep-blue OLED emitter materials based on innovative ML models with high predictive power. Utilizing our large databases of both in-depth quantum chemical characterizations and well-curated experimental data of emitter materials, we have trained ML models that accurately predict material properties correlated with all major OLED figures of merit (color point, efficiency and lifetime). As Fig. 1 shows, using a novel architecture employing transformer-based networks[3] operating on a molecular graph representation, we were able to significantly increase predictive power. The predictions of these models form the basis of the scoring function for the evolutionary algorithm, which also uses chemical knowledge to ensure a high degree of synthetic accessibility for all output structures.

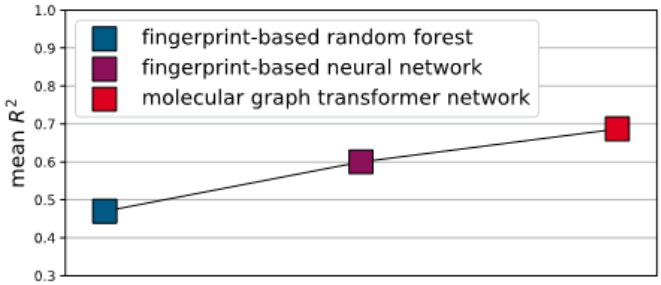

Fig. 1. Performance improvement in prediction of key experimental OLED emitter properties using state-of-the-art machine learning models

Named "generative exploration model" (GEM), this inverse design approach allows fast exploration of chemical space for discovery of novel high-performance materials. Applied to our deep-blue emitter development, the algorithm has been able to independently re-discover many of the current top-performing material structures and has become a core tool in our material design toolbox, generating many novel, promising candidate structures. Efforts are currently ongoing to expand the approach to other material classes and to increase its reliability in areas far away from the parts of chemical space that have been mapped experimentally. An active learning approach using Bayesian optimization for targeted generation of the most valuable training data holds promise to achieve the latter.

References

1. L. Himanen et. al., *Advanced Science*, 6(21), 1900808 (2019)
2. R. Gómez-Bombarelli et. al., *Nature Materials*, 15(10), 1120 (2016)
3. P. Veličković et. al., *ICLR 2018*, arXiv:1710.10903 (2018)

Key optical properties of hyperfluorescent TADF OLEDs based on the v-DABNA fluorescent emitter.

Andy Monkman[1], Kleitos Stavrou[1], Andrew Danos[1], Toshiki Hama[2] and Takuji Hatakeyama[2]
[1]OEM Research Group, Dept of Physics, Durham University, Durham, DH1 3LE, UK
Tel.:+441913343616, E-mail: a.p.monkman@durham.ac.uk
[2] Department of Chemistry, School of Science and Technology, Kwansei Gakuin University, Sanda, Japan

The photophysics of the multiple resonance TADF molecule v-DABNA will be described. We show coupling of a 285 cm^{-1} stretching/scissoring vibrational mode of the peripheral phenyl rings to the S_1 state. This leads to hot vibrational states emitting at room temperature that dictates the ultimate emission linewidth. However, a separate high amplitude mode, 945 cm^{-1} of the N-biphenyl units mediates the rISC mechanism. A monotonic increase of the exciton emission linewidth with temperature indicates the role of hot transitions from vibrational excited states at RT, and combined with an observed temperature dependency of ΔE_{ST} we deduce that the rISC mechanism is thermally activated rIC of T_1 to T_N ($n \geq 2$) followed by rapid rISC of T_N to S_1, i.e. upper state triplet crossing mediates rISC not second order vibrational coupling as in D-A TADF systems. Thus, the rISC rate, between 3-6x10^5 s^{-1} measured in both different solvents and solid hosts, is independent of environment, relatively slow leading to triplet polaron quenching at moderate drive currents and strongly temperature dependent even though the measured ΔE_{ST} is effectively zero at RT.

Concentration dependence studies in solution and solid state reveals a second emission band that increases non-linearly with concentration, independent of environment assigned to excimer emission. Even at concentrations well below those used in devices, the excimer contribution affects performance. At 20K over the first 10 ns, we observe a broad Gaussian excimer emission band with energy on-set above the S_1 exciton band. An optical singlet triplet gap (ΔE_{ST}) of 70 meV is measured, agreeing with previous thermal estimates, however the triplet energy is also found to be temperature dependent. We discuss the trade-off between narrowing the emission linewidth through further molecular rigidification and removal of free periphery against the need for vibrionic coupling to mediate the rIC mechanism and prevent excimer formation.

TADF sensitised OLEDs with v-DABNA as a hyperfluorescent emitter (0.5 wt% and 1 wt%) exhibit an increase of maximum EQE, reaching 27.5% for the lower v-DABNA concentration. On the contrary, a Förster radius analysis indicated that the energy transfer ratio is smaller due to higher donor-acceptor separation (>2.4 nm) with weak sensitizer emission observed in the electroluminescence. This indicates excimer quenching in the 1 wt% devices. Last, we will highlight how it is not possible via optical measurements to show that Dexter transfer occurs between the TADF sensitiser and the hyperfluorescence emitter.

Acknowledgment

The authors acknowledge the EU's Horizon 2020 for funding, TADFlife project under grant agreement No 812872 and Grant-in-Aid for Scientific Research (JP18H02051), Japan Society for the Promotion of Science.

References

1. Kondo, Y.; Yoshiura, K.; Kitera, S.; Nishi, H.; Oda, S.; Gotoh, H.; Sasada, Y.; Yanai, M.; Hatakeyama, T. Narrowband Deep-Blue Organic Light-Emitting Diode Featuring an Organoboron-Based Emitter. *Nat. Photonics* **2019**, 13, 678-682. https://doi.org/10.1038/s41566-019-0476-5.
2. Etherington, M. K.; Gibson, J.; Higginbotham, H. F.; Penfold, T. J.; Monkman, A. P. Revealing the Spin–Vibronic Coupling Mechanism of Thermally Activated Delayed Fluorescence. *Nat. Commun.* **2016**, *7* (1), 13680. https://doi.org/10.1038/ncomms13680.
3. Stavrou, K.; Danos, A.; Hama, T.; Hatakeyama, T.; Monkman, A. Hot Vibrational States in a High-Performance Multiple Resonance Emitter and the Effect of Excimer Quenching on Organic Light-Emitting Diodes. *ACS Appl. Mater. Interfaces* **2021**, *13*, 8643–8655. https://doi.org/10.1021/acsami.0c20619
4. Haase, N.; Danos, A.; Pflumm, C.; Stachelek, P.; Brütting W.; Monkman, A.P. Are the Rates of Dexter Transfer in TADF Hyperfluorescence Systems Optically Accessible? Materials Horizons **2021**. https://doi.org/10.1039/d0mh01666g.

Tuning the Excited State of Tetradentate Pt(II) and Pd(II) Complexes Through Intramolecular Hydrogen Bond

*Guijie Li**
State Key Laboratory Breeding Base of Green Chemistry-Synthesis Technology,
College of Chemical Engineering, Zhejiang University of Technology, Hangzhou, 310014, P. R. China
Tel.:86-13357130360, E-mail: guijieli@zjut.edu.cn

Organic light-emitting diodes (OLEDs) is a key technology for full-color display and solid-state lighting applications and have attracted great attention in both academic and industrial fields. Although pure organic thermally activated delayed fluorescence (TADF) is also a new kind of promising candidate as emitters for OLED fabrications, and great progress have been made in the past decade, phosphorescent heavy metal complexes are still critical emitters because of their high quantum efficiency, short excited-state lifetime and large radiative decay rate.

The structure-property relationship, especially the effect of molecular structure on the excited-state property, is an essential research topic. In our study, it was found that both the central metal inos and the cyclometalating ligands had a profound influence on the photophysical properties of the Pt(II) and Pd(II) complexes. Using the same 1-phenyl-1,2,3-trazole-based ligand, tetradentate Pt(1-*ptz*) and its analogues could realized concentration-dependent excimer emissions both in the solution and solid states enabled by intramolecular hydrogen bond between the pyridine and triazole rings and strong intermolecular Pt–Pt interaction, and all of the Pt(II) emitters have high photoluminescent quantum efficiency of up to 100% and luminescent lifetime as short as 1.4 μs at room temperature, achieving a radiative rate of 7.14×10^{5} s^{-1}. However, no excimer emission was observed for the Pd(1-*ptz*) and its analogues, which exhibited deep-blue emissions with CIEy < 0.1. The narrowing of the emission spectra for the Pd(1-*ptz*) complexes was attributed to weak intermolecular Pd–Pd interaction and the existence of an intramolecular hydrogen bond, resulting in more rigid molecular geometries and weaker v_{0-1} vibrational bands, making them good candidates for F-free deep-blue emitters.

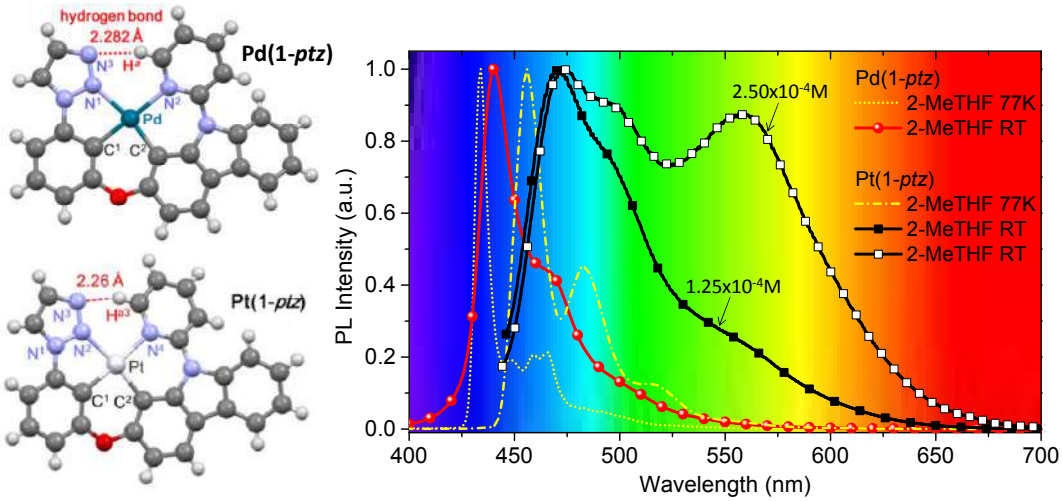

Fig. 1. X-ray molecular structures and ORTEP drawing of the crystal packing of Pd(1-*ptz*) (CDCC 2003072) and Pt(1-*ptz*) (CCDC 1935692), and their emission spectra in various conditions.

Acknowledgment

We thank the National Natural Science Foundation of China (grant no. 21878276) and the Fundamental Research Funds for the Provincial Universities of Zhejiang (RF-A2019013) for financial supports.

References

1. G. Li, X. Zhao, T. Fleetham, Q. Chen, F. Zhan, J. Zheng, Y.-F. Yang, W. Lou, Y. Yang, Kun Fang, Z. Shao, Q. Zhang, Y. She. *Chem. Mater.*, 2020, 537 (2020).
2. G. Li, J. Zheng, X. Zhao, T. Fleetham, Y.-F. Yang, Q. Wang, F. Zhan, W. Zhang, K. Fang, Q. Zhang, Y. She. *Inorg. Chem.*, 13502 (2020).

Highly Efficient, Long Lasting, and Color Pure Green and Blue devices utilizing Shared Exciton Energy Transfer

Dr. Georgios Liaptsis[1], Dr. Hamed Sharifidehsari, Dr. Henning Marciniak [1]
[1]cynora GmbH, Bruchsal, Germany
Tel.:+49-7251-919-670, E-mail: info@cynora.com

In today's OLED display applications high efficiency, high color purity, as well as long lasting materials are key success parameters to release valuable products. The missing high-efficiency blue pixels within RGB side-by-side and WRGB displays are still the bottleneck for panel makers. In addition, with respect to power consumption, this efficiency lack becomes even more crucial for portable devices. The OLED device efficiency is mainly determined by the light emitting material. The current emitter technology for the red and green pixels is based on phosphorescent materials with internal quantum efficiencies (IQE) of ~100% approaching the theoretical limit. Despite years of research, blue phosphorescent emitters have not reached the commercial specifications due to their very short device lifetime and lack of color purity.[1] Consequently, the OLED panel makers still refer to narrow spectrum fluorescent emitters (NSE) in their applications, which are limited to an IQE of ~25% under direct electrical excitation. Hence, one of the industry's biggest challenges is the further development of the blue pixel based on innovative emitter technologies to overcome this efficiency limitation without sacrificing stability of the established systems.

One of the most promising approaches to solve the issue of the inefficient blue pixel has emerged in the last few years: thermally activated delayed fluorescence technology (TADF), which was introduced 2011.[2] TADF is equally as efficient as phosphorescence: it can deliver 100% IQE. TADF materials can be used in two different approaches: either as emitter in the self-emitting TADF approach, or together with a co-emitter in the so-called hyper-approach yielding improved color purity. This co-emitting approach utilizes the TADF material as exciton energy transfer (EET) agent which is capable of harvesting electrically generated triplet excitons and pass over their energy via Förster Resonant Energy Transfer (FRET) or Dexter Energy Transfer (DET) to the emissive narrow spectrum fluorescent emitter.

We report high efficiency, high color purity, as well as long lasting green and blue devices utilizing at least two EETs in a shared EET approach, advanced charge carrier management for recombination zone fine tuning, and accelerated exciton dynamics yielding outstanding results.

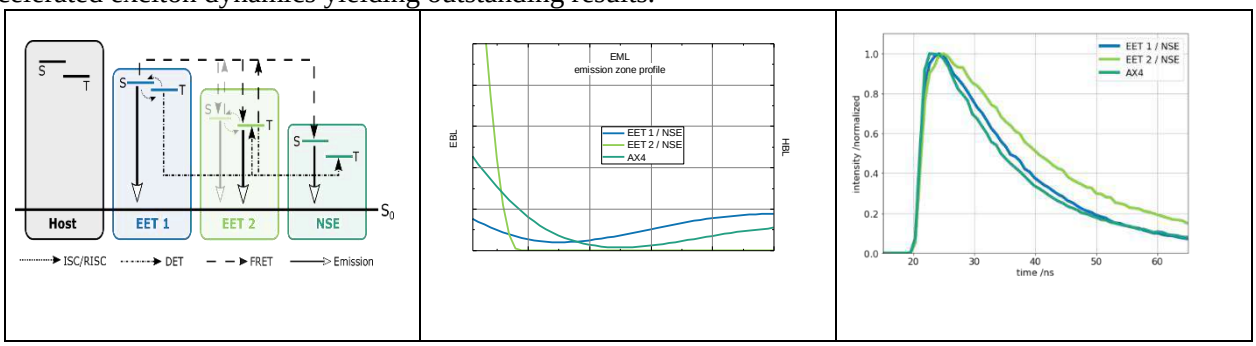

Fig. 1. Left showing excitation energy transfer between EETs and NSE; middle showing recombination zone profile improvements; right showing accelerated decay dynamics.

Establishing a suitable energy cascade among all utilized materials within the EML, each EET is capable of transferring its excitation energy to the NSE with immediate effect of distributing the excitation energy among the individual EETs. Further this cascade accelerates the exciton dynamics according to photoluminescence measurements. Alignment of the energy levels of frontier molecular orbitals, such as highest occupied molecular orbital (HOMO) and lowest unoccupied molecular orbital (LUMO) further allows fine tuning the recombination zone profile. These three factors establish highly efficient, long lasting and color pure OLEDs.

References

1. J. S. Kim, Adv. Optical Mater., 2001103 (2020).
2. A. Endo, et al., *Appl. Phys. Lett*., 98, 083302 (2011).

Increasing OLED Stability: Plasmonic PHOLED

Nicholas J. Thompson, Michael A. Fusella, Renata Saramak, Rezlind Bushati, Haridas Mundoor, Vinod M. Menon, Michael S. Weaver, Julia J. Brown
Universal Display Corporation, 375 Philips Blvd., Ewing, NJ 08618, USA
E-mail: nthompson@oled.com

We demonstrate a new organic light emitting device utilizing the surface plasmon mode of a metallic film to give rise to a broadband decay rate enhancement of the phosphorescent emitter $Ir(ppy)_3$ (1). The use of the surface plasmon mode as a fast energy sink breaks the conventional organic light emitting device (OLED) operational paradigm and increases stability by decreasing the steady state exciton density within the device. We then recover the energy coupled into the surface plasmon mode using a nanoparticle-based plasmon outcoupling scheme. This architecture realizes both increased stability and efficiency compared to conventional OLED architectures.

The operating principle of the phosphorescent plasmonic OLED is as follows: charges are injected and subsequently transported through the device under an electric field; charges are converted to excitons; the excitons decay non-radiatively via coupling to the surface plasmon mode; and the energy within the surface plasmon mode is released to free space by a nanoparticle-based outcoupling scheme. In Fig. 1(a), we demonstrate that the plasmonic PHOLED is stabilized compared to the reference conventional PHOLED, which has an emissive layer (EML) thickness of 40 nm when driven at a constant current density of 80 mA/cm^2. The plasmonic PHOLED is stabilized by more than two-fold compared to a reference thin EML which matches the EML thickness of the plasmonic PHOLED but has a thickened electron transport layer to minimize any plasmonic coupling. In Fig. 1(b) we demonstrate that energy intentionally coupled to the surface plasmon mode can be recovered as light outside of the device. We plot the external quantum efficiency (EQE) vs. current density of the reference devices as squares and triangles. These devices achieve 13% EQE at 10 mA/cm^2. In filled circles, we plot the top emission EQE of the green plasmonic device, which emits light only from the surface plasmon mode of the top Ag contact, achieving an EQE of 11% at 10 mA/cm^2. Finally, in diamonds we plot the BE EQE of the plasmon OLED which represents energy that is not coupled into the surface plasmon mode of the Ag cathode. The total EQE from the top and bottom of the plasmonic PHOLED is 17% which exceeds that of the reference devices. Thus, the plasmonic PHOLED can simultaneously increase OLED device efficiency and stability. Future work will extra light only out one of side of the device while also increasing efficiency and stability of the plasmonic PHOLED.

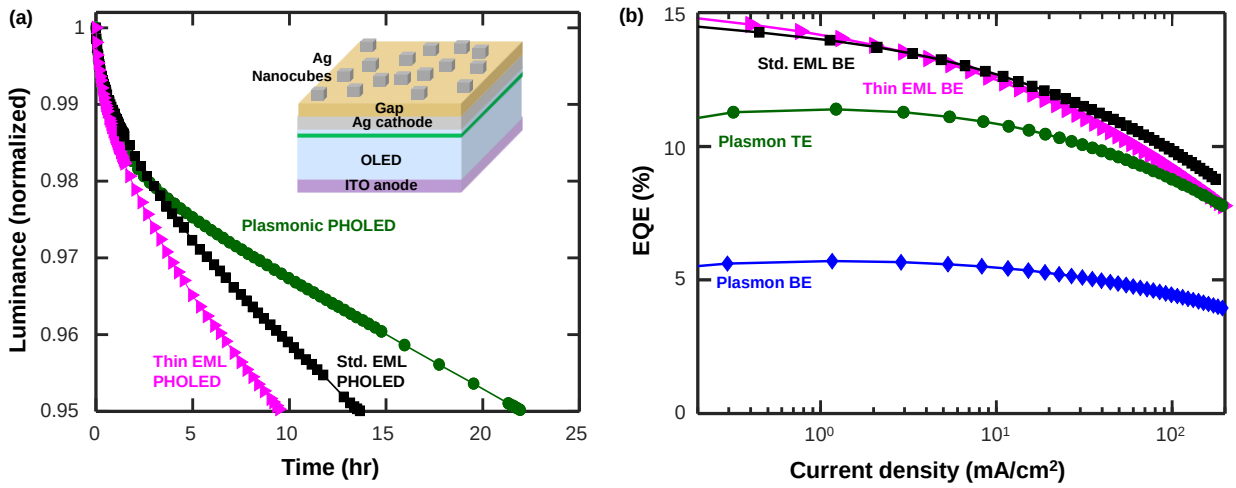

Fig. 1: (a) Lifetime curves of the plasmonic PHOLED and reference thin and standard EML devices aged at 80 mA/cm^2. Inset is a schematic depiction of the plasmonic PHOLED device where the EML is depicted as the thin green region. (a) EQE vs. current density for the plasmonic PHOLED and the reference devices. For the plasmonic PHOLED, the TE (filled circles) and BE (filled diamonds) are plotted.

References

1. M. A. Fusella, R. Saramak, R. Bushati, V. M. Menon, M. S. Weaver, N. J. Thompson, J. J. Brown, *Nature*, 585(7825):379–82.

A Sensitized Way towards Stable Blue OLEDs

*Dongdong Zhang**
***Dept. of Chemistry, Tsinghua University, Beijing, China.**
Tel.:82-62782197, E-mail: ddzhang@mail.tsinghua.edu.cn

Deep-blue organic light-emitting diodes (OLEDs) with high efficiencies and long lifetimes remain the "Holy Grail" for the organic electronics research community. Materials with thermally activated delayed fluorescence (TADF) offer an alternation to circumvent the above issues. In 2016, our group developed a series of cyano/carbazole (CzBN) derivatives as blue TADF emitters, realizing high efficiency and improved stability by wise designing of molecular structures using tert-butyl units. However, such a motif still suffers from low reverse intersystem crossing rates (k_{RISC}) with emission peaks <470 nm. Recently, a weak acceptor of cyanophenyl was adopted to replace the stronger cyano one to construct blue emitters with multiple donors and acceptors. Both linear donor-π-donor and acceptor-π-acceptor structures are observed to facilitate delocalized excited states for enhanced mixing between charge- transfer and locally excited states. Consequently, a high k_{RISC} of 2.36 × 106 s^{-1} with an emission peak of 456 nm and a maximum external quantum efficiency of 22.8% is achieved. When utilizing this material to sensitize a blue multiple- resonance TADF emitter, the corresponding device simultaneously realizes a maximum external quantum efficiency of 32.5%, CIEy~0.12, a full width at half maximum of 29 nm, and a T80 (time to 80% of the initial luminance) of >60 h at an initial luminance of 1000 cd m^{-2}. Those findings not only shed new light on developing blue TADF materials with high k_{RISC} but also demonstrate highly efficient, stable and high color-purity deep blue OLEDs utilizing TADF-sensitizing-MR-TADF strategy, which should pave the way toward practical applications.

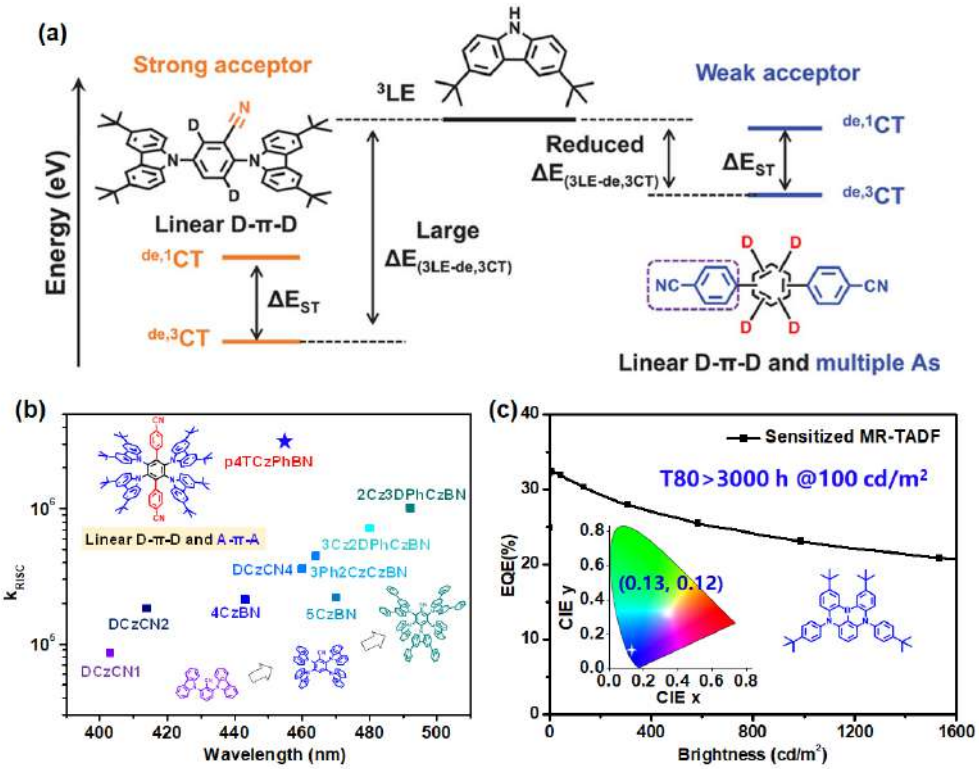

Fig. 1. (a) The molecular design strategy. (b) The k_{RISC}-wavelength character of CzBNs. (c) The device performances.

References

1. D. Zhang, M. Cai, Y. Zhang, D. Zhang, L. Duan, Mater. Horizon., 3, 145 (2016).
2. D. Zhang, L. Duan, C. Li, Y. Li, H. Li, D. Zhang, Y. Qiu, Adv. Mater. 26 (29), 5050 (2014).
3. D. Zhang, X. Song, A. Gillett, B. Drummond, S. Jones, G. Li, H. He, M. Cai, D. Credgington, L. Duan, Adv. Mater. 32 (19), 1908355 (2020).

Quantum Dots: Photo-luminance and Electro-luminance Materials for Display Manufacturing

Joon-Hyung Kim
Display Research Center, Samsung Display, Giheung-gu, Yongin-si, Gyeonggi-do, 17113, Korea
Tel.:82-31-5181-5040, E-mail: joon.kim.phd@samsung.com

Quantum Dot (QD) has been used for display manufacturing, and its applications will be expanded further in the future. LCD panels with photoluminescence QD color conversion layer have the advantage of high color gamut. On the other hand, WOLED TVs have excellent contrast ration and viewing angles due to their self-emitting properties. Currently, both QD-LCD and WOLED are sold as high-end TV products.

Samsung is preparing to mass-produce QD-OLED display. This display has QD color filter with blue OLED backlight. The QDs emit red and green light by down-converting the blue backlight. QD-OLED combines the advantages of QD and OLED to provide a contrast ration of 1,000,000 :1, a color gamut of over 90% of BT2020 or full coverage of DCI-P3 and a wider viewing angle than LCD[1]. The QD color filter is created by filling individual pixels with solvent-less InP QD inks through the inkjet process.

We are developing electroluminescence (EL) QD devices as future displays. Both EL-QD and OLED are self-emissive devices and have similar basic structures. However, QD emits light with a narrower FWHM compared to that of OLED, so color purity is higher, IQD 100% and more precise wavelength tuning is possible (including deep blue). The efficiency of eco-friendly Cd-free QDs has improved dramatically over the past few years. As a result, the quantum efficiency of current Cd-free EL-QD devices is comparable to that of competing technologies. However, several challenges must be overcome, including the lifetime of blue and green quantum dots.

In order to improve the performance of QD, many advances have been made in the design and synthesis of QD cores and shells. Studies have been conducted to use alloy cores or to form multilayer shells of appropriate composition and thickness. Recently, through more sophisticated synthesis methods, QD performance is more improved, for example, by selectively growing the specific crystal plane of QDs[2], gradually changing the shell composition[3], or removing the oxide layer[4] that occurs during the crystal growth. After synthesizing QDs, it is possible to further improve the performance by treating the QD surface with metal halides[5] or replacing their ligand with more appropriate other ligand[4].

Inkjet printing was used to generate RGB pixels for EL-QD displays. The mixed solvent formulation is designed to prevent QD ink from drying out at inkjet nozzles, increasing inkjet processability to ensure high landing accuracy and create uniform layers within pixels. In addition, the panel's drying conditions should be well controlled to further improve the internal pixel and inter-pixel layer uniformity when the panel was built.

The EL-QD device is composed of multiple layers, and all layers except for the electrode are manufactured by an inkjet process. Because device is multi-layered, it is important to ensure that the underlying layers are not damaged when building a layer. Orthogonal solvents or crosslinking agents may be used.

We made full-color RGB EL-QD panels with Cd-free QDs. Except for QD emitting layer, charge transport layers (CTLs) were made of either organic or inorganic materials. For better display performance, it is necessary to replace the CTLs' organic materials with inorganic materials, and it is also necessary to increase the lifetime of the device. Further research on these topic is needed.

References

1. Jong Hyuk Lee, *Information Display*, 36(6), 9-13 (2020).
2. Y. Xia *et al.*, *Adv. Funct. Mater.*, 30, 2000594 (2020).
3. D.A. Taylor *et al.*, *Chem. Mater.*, 33, 4399-4407 (2021).
4. Y.-H. Won *et al.*, *Nature*, 575, 634-638 (2019).
5. T.G. Kim *et al.*, *ACS Nano*, 12(11), 11529-11540 (2018).

Environmentally Friendly Quantum Dot Light-Emitting Diodes

Hyosook Jang and Eunjoo Jang
Samsung Advanced Institute of Technology, Samsung Electronics, Suwon 16678, Korea
Tel.:82-31-8061-1101, E-mail: hs07.jang@samsung.com

Quantum dot (QD) is excellent light-emitting platform material due to color tunability, high efficiency and narrow spectral width. Its solution processability expands the compatibility of QDs with current and next-generation displays having various form factors. Also, the importance of environmentally friendly QD material is growing up on much attention and various studies. Herein, I present our strategies and results to develop nontoxic InP- and ZnSe-based QDs with high efficiency and long lifetime.

It is necessary to control the emission wavelength and narrow down the spectral width for getting high color purity. InP-based QDs are good candidates for red and green emission but they are sensitive to the change of size and oxidation. To optimize the reaction temperature and purify the precursors leads to the increase of core uniformity. Also, the removal of oxidative phase on the core by HF etching is effective for both narrow width and high photoluminescence (PL) quantum yield (QY).

Unpassivated core has many surface defects/traps and well-passivated ZnSe/ZnS multi-shell with optimal shell thickness results in high PL QY. However, ZnSe structure easily generates stacking faults because of low energy barrier, which lowers PL QY, especially in thick ZnSe shell. Stacking faults in ZnSe shell were confimed by TEM analyses and eliminated using the addition of HF and $ZnCl_2$ and high temperature reaction at 340°C. The kinetically fast growth also has effects on more uniform shape and size distribution of QDs.

In addition, both qualitative and quantitative analyses for surface ligands provide better understanding of device applications. Native oleic acid (OA) ligand with long alkyl chain is unfavorable for charge injection/transport in quantum dot light-emitting diode (QD-LED). Small inorganic ligand like $ZnCl_2$ was introduced via two steps of ligand exchange: a liquid-phase treatment and a film-washing treatment. $ZnCl_2$ improves passivation of surface defects and increased PL QY and thermal stability. Our efficient and stable QD-LEDs using well-controlled QDs will be presented.

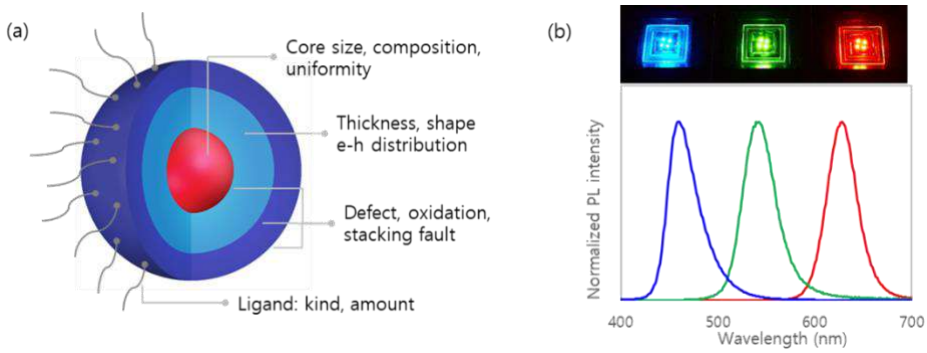

Fig. 1. (a) The critical parameters for highly efficient QDs, (b) The representative PL spectra of red, green and blue QDs and photograph of their QD-LEDs

References

1. E. Jang, Y. Kim, Y.-H. Won, H. Jang and S.-M. Choi, *ACS Energy Lett,* 5, 1316 (2020).
2. T. Kim, K.-H. Kim, S. Kim, S.-M. Choi, H. Jang, H.-K. Seo, H. Lee, D.-Y. Chung and E. Jang, *Nature*, 586, 385 (2020).
3. Y.-H. Won, O. Cho, T. Kim, D.-Y. Chung, H. Jang, J. Lee, D. Kim and E. Jang, *Nature*, 575, 634 (2019).

Large Size Colloidal InAs QD Synthesis: Unraveling the Origin of Growth Limitation of Nanoparticles

Taewan Kim[1], Seongmin Park[1], and Sohee Jeong[1]
[1] Department of Energy Science (DOES) and Center for Artificial Atoms, Sungkyunkwan University (SKKU), Suwon, Gyeonggi-do 16419, Korea
E-mail: twkim0807@gmail.com

Colloidal quantum dots (QDs) are free-standing optoelectronic materials showing tunable band gap and energy alignment with controllable electrical properties. Especially, their wide spectral coverage produced by the particle size control enables various applications for optoelectronic devices. In other words, extending particle size in colloidal synthesis is key issue for further implication in both academic and industrial fields.

Herein, we discussed the origin of growth limitaion in colloidal particle synthesis by observing the growth of InAs QDs, which is emerging materials for Pb-free infrared devices but classical synthetic approaches are not effective. In our work, we provided new synthetic approach produced by modeling of nanoparticle growth in diffusion-controlled mode. By validation of model, we confirmed that the growth limitation occurred by inversion of precursor injectionrate and monomer diffusion rate. Our method which is not limited the underlying chemistry suggests rational design to extend the nanoparticle growth including InP and other QDs.

Colloidal Quantum Well Heterostructures with Widely Tunable Emission for Application in Light-Emitting Diodes

Da-Eun Yoon and Doh C. Lee*
Dept. of Chemical and Biomolecular Engineering, Korea Advanced Institute of Science and Technology (KAIST), Daejeon 34141, Korea
Tel.:82-42-350-3977, E-mail: dclee@kaist.edu

Colloidal quantum wells, commonly called as semiconductor nanoplatelets (NPLs), with a thickness of only a few atomic layers have unique properties such as extremely narrow emission bandwidth, supressed Auger combination and polarized emission.[1,2] Superior optical and electronic properties of NPLs make them promising candidates for light-emitting devices. In particular, inorganic shell passivated core/shell NPLs such as CdSe/ZnS and CdSe/CdZnS, which have significantly improved PL quanutm yield and stability, have attracted much attention.[3] However, the emission range of CdSe based core/shell NPL is limited from yellowish green-to-red because of thickness-dependent band gap of core NPL and charge delocalization into the shell. In this study, we precisely control the emission wavelength of core/shell NPLs from red-to-blue by tuning the composition of core NPL via Cd-to-Zn cation exchange (Fig. 1). We anlayzed the structural and optical properties of novel CdZnSe/ZnS core/shell NPL heterostructures. In addition, we studied optoelectronic properties of heterostructured NPL based light-emitting diodes.

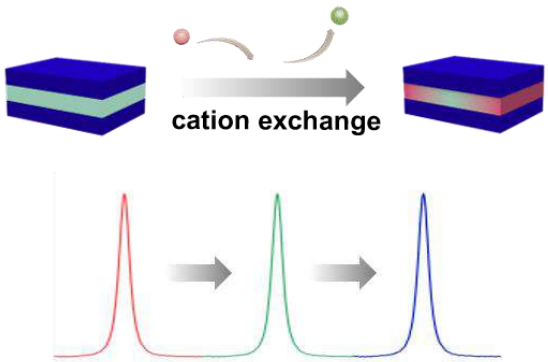

Fig. 1. Tailoring the emission wavelength of $Cd_{1-x}Zn_xSe/ZnS$ NPLs via Cd-to-Zn cation exchange.

Acknowledgment
This work was supported by the National Research Foundation (NRF) grants funded by the Korean government.

References

1. S. Ithurria, M. D. Tessier, B. Mahler, R. P. S. M. Lobo, B. Dubertret and A. Efros, *Nat. Mater.*, 10(12), 936 (2011).
2. D. E. Yoon, W. D. Kim, D. Kim, D. Lee, S. Koh, W. K. Bae and D. C. Lee, *J. Phys. Chem. C*, 121(44), 24837 (2017).
3. B. Liu, Y. Altintas, L. Wang, S. Shendre, M. Sharma, H. Sun, E. Mutlugun and H. V. Demir, *Adv. Mater.*, 32(8), 1905824 (2020).

InP QDs with enhanced blue light absorption for color filter

Armin Wedel[1], Yohan Kim[1], André Gessner[1], Hyung Seok Choi[1], Jiyong Kim[1], Chul Jong Han[2], Min Suk Oh[2], Byungwook Yoo[2]

[1]Fraunhofer Institute for Applied Polymer Research, QD Display Group, Geiselbergstrasse 69, 14476 Potsdam, Germany

Tel.:49-331-568-1910, E-mail: armin.wedel@iap.fraunhofer.de

[2]Display Research Center, Korea Electronics Technology Institute, Seongnam-si, Gyeonggi-do, 463-816, Korea

Introduction

Recently, InP quantum dots (QDs) materials have received a lot of attention in the display field because of their bandgap engineering properties, theoretically obtainable narrow Full Width at Half Maximum (FWHM), and relatively eco-friendly character as compared to CdSe type QDs. (Chemistry of Materials 28(8): 2491-2506.)

Technologically important, environmentally friendly InP QDs typically used as green and red emitters in display devices can have outstanding photoluminescence (PL) quantum yields (QYs) of near-unity (95-100%) when the state-of-the-art core/shell heterostructure of ZnSe inner/ZnS outer shell is elaborately applied (ACS. Appl. Nano. Mater. 2019, 2, 1496-1504, Nature 575 (7784): 634-638).

Indiumphosphid (InP) based quantum dots

In the QD-display, the degree of blue absorption is extremely important factor to decide whether the efficiency in photoluminescence devices is high or not (Figure 1). The absorption property of InP/ZnSe/ZnS QD applied in the display industry has originally down-converted emission character, in which InP Green QD inherently has weak absorption properties in 450 nm blue regime relative to CdSe QD because of their energy separation in bandgap structure.

There have been efforts to increase the blue absorption of InP green QD layer in the QD-CF display, such as the increase of (1) film thickness, (2) the number of InP green particles, and (3) ZnSe shell thickness. Despite diverse trials to improve blue absorption, all scenarios including above mentioned three kinds of methods have a negative trade-off in their efficiency.

(1) the increase of InP green film thickness accompanies by higher manufacturing prices. And when it considers the whole structure of QD-CF, a thicker layer over 10 μm is hard to apply because of their total panel thickness.

(2) a large number of InP green particle applied in QD-CF film induces self-absorption between QDs and backward emission, by which max EQE can be dropped even in high concentrated QD-CF film.

(3) thicker ZnSe shell onto InP core is not effective on 450 nm blue regime because band gap of ZnSe is matched to near 400nm area.

In the previous report, (Figure 4) thicker ZnSe shell is only attributable to absorption of the 400 nm wavelength regardless of whether ZnSe is alloyed with ZnS or not.

As a result, the proper solution has not been established to date, which is one of a huge hence to the commercialization in QD-CF display. There are other efforts to find the post-InP, such as Perovskite, ZnTeSe, and AgInS, which has different composition relative to InP, but their optical properties and stability in the device do not reach to the grade of commercialization. And then, we strongly suggest our new structural InP QD having InZnPSe alloyed multi-shell layer, by which the higher blue absorption near 450 nm wavelength is implemented than general InP/ZnSe/ZnS QD.

The alloyed InZnPSe multi-shell layer between InP and ZnSe absorbs 450 nm blue wavelength better than InP/ZnSe QD because the position of band gap of InZnPSe muti-shell layer is located between InP and ZnSe. We could show Gamma value (γ) of about 1.9.

Acknowledgment

The authors would like to thank the Korea government Ministry of Trade, Industry and Energy (MOTIE) for financial support via “2016 Consulting business through utilization of excellent technical manpower in Germany” (CoCoMe: **Co**lor **Co**nverting **M**icro-L**E**Ds) for financial support.

Advances In The Photostability Of RoHS-Compliant QDs For On-Chip Down-Conversion: A Path Forward For QD-MicroLED Displays

Igor Nakonechnyi[1], Valeriia Grigel[1], Rafael Prato[1], Adelaide Araujo[1], Bruno Janssens[1], Kim De Nolf[1] and Willem Walravens[1],
[1]QustomDot BV, Zwijnaarde, 9052, Belgium
E-mail: info@qustomdot.com

Quantum Dots (QDs), semiconductor nanocrystals that can down-convert light with high efficiency, are on their way to revolutionize display and lighting applications. MicroLEDs, another emerging technology that will change the way the displays are produced is coming alive. While potentially having a lot of benefits such as high brightness, great dynamic range, etc. microLEDs are still to be proven to be produced efficiently. QDs can become an enabler material to RGB microLED displays that don't require waveguiding and that avoid pick and place and further repair process.

There are challenges ahead of QDs in this new application as well. One of the most critical being the photothermal stability of QDs. When exposed to blue light flux, especially in close distance to the chip, the efficiency of the QDs drops instantly. Cadmium based QDs are more resistant to photothermal degradation and a lot of research has been done to control and eliminate the degr ation processes [1]. However, the use of cadmium is restricted through the EU's RoHS directives and a lot of countries worldwide are following these guidelines. The main replacement material, InP has already demonstrated great optical properties [2,3] yet is still not near the stability characteristics of Cd-based QDs[4].

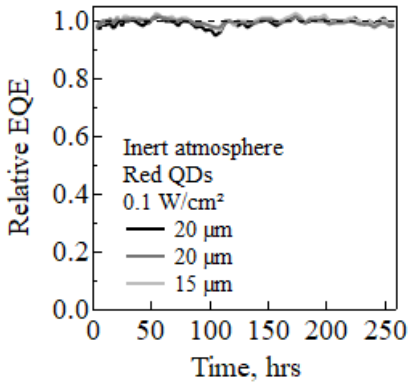

Fig. 1. Photostability of thin film QD samples under blue light flux of 0.1 W/cm^2

At Ghent University we have developed an InP-based technology that can withstand these harsh conditions and can be used directly on the LED chip. This technology is being further developed to reach the performance requirements of microLED displays by QustomDot, a spin-off company. Here we want to demonstrate our recent developments related to the photostability of InP-based QDs in an on-chip configuration relevant for microLED applications. As illustrated in Fig. 1, our technology results in a stability of >250 hrs in densely packed 15-20 um QD films that are continuously exposed to ~0.1 W/cm^2 blue light flux in inert atmosphere. Further developments will allow QustomDot to make single-color, µm-resolution QD patterns with excellent stability at flux intensities and temperatures that are directly relevant for microLED displays.

Acknowledgment

QustomDot acknowledges support by Flanders Innovation & Entrepreneurship (Vlaio) via the project ReQLED2020 (HBC.2020.2383).

References

1. K. T. Shimizu et al., *Photonics Res.*, vol. 5, no. 2, p. A1, (2017).
2. Y.-H. Won et al., *Nature,* vol. 575, no. 7784, pp. 634–638, (2019).
3. D. Hahm et al., *Chem. Mater.*, vol. 31, no. 9, pp. 3476–3484, (2019).
4. E. Jang et al., *RCS Adv.*, pp. 10057–10063, (2018).

Quantum Nanorods Embedded into Hole Transport Material for Solution Processed Light-Emitting Diodes with Low Turn-on Voltage

Mikita M. Marus, Maksym F. Prodanov, Kumar Mallem, Valerii V. Vashchenko, and Abhishek K. Srivastava
State Key Laboratory of Advanced Displays and Optoelectronics Technologies, Department of Electronics and Computer Engineering, Hong Kong University of Science and Technology, Hong Kong
Tel.: (852) 3469 2485, E-mail: eeabhishek@ust.hk

Quantum dots (QDs) emerged as attractive materials for light and display applications owing to size-tunable emission, narrow spectral bandwidth, high photoluminescence efficiency (PLQY), and full compatibility with the solution process. These qualities are highly valued for QD-based light-emitting diodes (QLEDs), which have recently achieved a pinnacle of their maximum theoretical internal quantum efficiency (IQE) [1]. Further improvement in external quantum efficiency would require either a major rehaul of QLED architecture or switching to alternative light-emitting nanocrystals. The 1D quantum rods (QRs) offer an alternative, where shape-related advantage can theoretically double the outcoupling efficiency while retaining all other advantages of nanocrystals [2, 3]. However, due to much deeper highest occupied molecular orbital (HOMO) compared to CdS/CdSe-based QDs, QR-LEDs require much higher energy for hole injection compared to electron injection, which results in the charge imbalance of carrier injection and compromised radiative recombination efficiency [3]. Adding an electron blocking layer (EBL) between the electron transport layer (ETL) and QRs helps to balance the charge injection, but at the cost of an additional insulative interface in the device. Here, we propose a composite emitting layer (EML) based on a poly-N-vinylcarbazole (PVK) hole-transporting layer (HTL) inter-mixed with QR EML at a ratio of 1:1 to form HTM:EML (Figure 1).

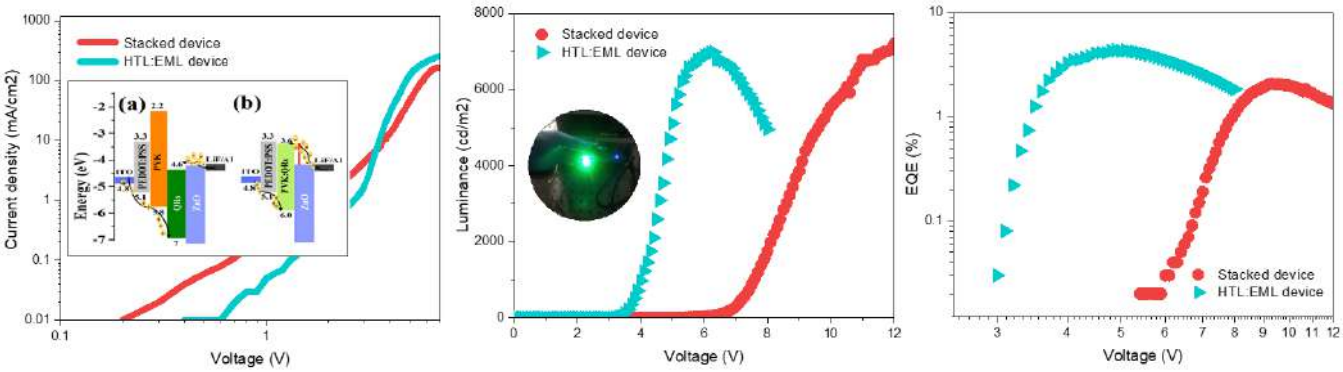

Fig. 1. Stacked vs HTL:EML QR-LEDs: (a) Current density vs voltage characteristics; the inset shows the energy level diagram of stacked vs HTL:EML QR-LEDs; (b) luminance vs voltage; (c) EQE vs voltage.

Through this approach, we not only reduced the barrier for hole injection, but simultaneously balanced the electron injection, reduced the number of interfaces, and allowed additional control over inter-QR separation, promoting radiative recombination. We have effectively slashed the turn-on voltage of green QR-LED by two times – from 5.8V (stacked device) to 2.9V (HTL: EML device), while the EQE had been increased from 2.1 to 4.4%. Such low turn-on voltage and improved hole injection make HTL: EML viable for future display applications.

Acknowledgment

This work was supported by the RGC of Hong Kong SAR (Grant No. 26202019), 18191050 from Microlite Display Technology Ltd. Hong Kong, and the funding's for The State Key Laboratory of Advanced Displays and Optoelectronics Technologies.

References

1. Shirasaki, Y., Supran, G., Bawendi, M. et al. Nature Photon 7, 13–23 (2013).
2. Nam, S., Oh, N., Zhai, Y., Shim, M. ACS Nano 9, 1, 878–885 (2015).
3. Prodanov, M.F., Gupta, S.K., Kang, C., et al. Small 17, 2004487 (2021).
4. Mallem, K., Prodanov, M. F., Chen, et al. SID Symposium Digest of Technical Papers, accepted (2021).

Optical Anisotropy in Cadmium-Free Colloidal Branched Nano-Heterostructures

Sungjun Koh[1] and Doh C. Lee[1]
[1]Dept. of Chemical and Biomolecular Engineering, KAIST Institute for the Nanocentury, Korea Advanced Institute of Science and Technology (KAIST), Daejeon 34141, Korea
Tel.:82-42-350-3937, E-mail: dclee@kaist.edu

Geometric anisotropy in colloidal semiconductor nanocrystals (NCs) results in polarized light absorption and emission.[1,2] Studies of shape and optical anisotropy have been mostly limited to Cd chalcogenide and Pb-containing perovskite NCs, because of the difficulty with which to synthetize anisotropic NCs of other materials, particularly nonionic crystals. Obviously, the use of toxic elements, *e.g.*, Cd or Pb, would hamper the application of NCs in display devices. We report the linearly polarized photon absorption and emission from core/shell nanotetrapods (NTPs) comprising relatively nontoxic elements, *e,g.*, ZnSe/ZnS, InP/ZnS and InAs/ZnS. The synthesis of NTPs involves the high-temperature growth of ZnS on seed NCs in the presence of primary amine to induce zincblende/wurtzite core/shell structure. With the change in size and composition, the linearly polarized absorption and emission by NTPs range from ultraviolet to near-infrared. Small-angle X-ray scattering analysis reveals that InP/ZnS NTPs show broken geometric symmetry which results in asymmetric delocalization of electron wavefunction. In addition, the permanent dipole moment of NTPs gives rise to uniaxial alignment of NTPs under external electric field. This work sheds light on the utilization of optically anisotropic NCs in practical applications which essentially demand the low toxicity of materials.

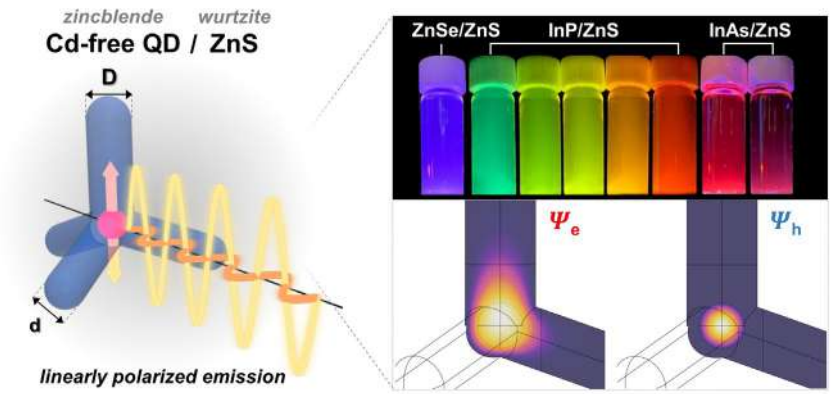

Fig. 1. A schematic description of Cd-free branched nanocrystals emitting linearly polarized photons

Acknowledgment

This work was supported by the National Research Foundation (NRF) grants funded by the Korean Government (NRF-2016M3A7B4910618, NRF-2020M3D1A2101310, and NRF-2020M3H4A1A01086888) and by the Industrial Strategic Technology Development Program No. 10077471 "Development of core technology for highly efficient and stable, non-cadmium QLED materials" funded by the Ministry of Trade, Industry & Energy (MOTIE, Korea).

References

1. Peng, X.; Manna, L.; Yang, W.; Wickham, J.; Scher, E.; Kadavanich, A.; Alivisatos, A. P., *Nature,* 404, 59 (2000).
2. Ithurria, S.; Tessier, M.; Mahler, B.; Lobo, R.; Dubertret, B.; Efros, A. L., *Nat. Mater.* 10, 936 (2011).

Laser-driven Transfer Printing Techniques for Mico-LED Displays

Chengjun Wang, Hongyu Luo, Jizhou Song*

Department of Engineering Mechanics, Soft Matter Research Center, and Key Laboratory of Soft Machines and Smart Devices of Zhejiang Province, Zhejiang University, Hangzhou 310027, China

* Corresponding author. Email address: jzsong@zju.edu.cn

Abstract

Micro-LED display, which is regarded as the next-generation display technology, has obtained immense attention and great development during the past two decades. Mass transfer is the key step for the assembly of Micro-LED displays, which require the integration of Micro-LED chips from the fabrication wafers onto the display panel. Transfer printing is an emerging deterministic assembly technique and provides a versatile solution with great promise for mass transfer. Here, we will present our recently developed laser-driven transfer printing techniques with massive and selective capabilities, which are essential in applications of micro-LED displays.

Keywords: transfer printing; laser-driven; Micro-LED display

GaN-based micro-LEDs for Technological Convergence between Displays and Optical Wireless Communications Systems

M.D. Dawson[1], J. Herrnsdorf[1], J. McKendry[1], E. Xie[1], E. Gu[1], and M.J. Strain[1]
[1]Institute of Photonics, Department of Physics, University of Strathclyde, Glasgow G1 1RD, UK
Tel.:44-141-548-4663, E-mail: m.dawson@strath.ac.uk

Micro-LEDs are currently the subject of intense worldwide interest as the basis of a new form of electronic visual display technology.[1,2] These light-emitting diode arrays, comprising a high-density of pixels each of a few microns to few 10's of microns in size, are based on inorganic semiconductors, in particular gallium nitride. They show attractive characteristics including very fast (ns) response, high resolution (down to a few microns) and high brightness $>10^6$ cd/m^2). Moreover they are applicable in a diverse range of display formats including micro-displays, wearables, and large area displays.

Micro-LEDs' fast response, sophisticated spatio-temporal control mediated by compatibility with electronics including CMOS, together with compatibility of their output with solid-state photodetectors and cameras, offers the possibility of these displays being used for advanced projection applications.[2] This includes optical wireless communications (OWC) in a range of environments. The individual micro-LED pixels can be modulated at GHz rates producing per-pixel data rates of up to ~10Gb/s, and a variety of data encoding, spatial modulation and multiplexing protocols can readily be implemented.[2,3] Here we will review the pertinent characteristics and performance of micro-LEDs for OWC applications as diverse as visible light communications and light fidelity (LiFi), underwater optical communications and inter-satellite communications.

Acknowledgement
We acknowledge funding for this work through the UK EPSRC, in particular in programmes UP-VLC (EP/K00042X/1) and Quantic (EP/M01326X/1 and EP/T00097X/1).

References

1. J.Y. Lin and H.X. Jiang, *Appl. Phys. Lett.*, 116, 100502 (2020).
2. A.D. Griffiths, J. Herrnsdorf, J.J.D. McKendry, M.J. Strain, and M.D. Dawson, Phil. Trans. R. Soc. A 378: 20190185 (2020).
3. S. Rajbhandari, J.J.D. McKendry, J. Herrnsdorf, E. Xie, H. Chun, G. Faulkner, E. Gu, S. Collins, A.V.N. Jalajakumari, K. Cameron, R. Henderson, D. Tsonev, H. Haas, D. O'Brien, and M.D. Dawson, *Semicond. Sci. Technol.*, **32**, 023001 (2017).

Direct Red-emitting InGaN microLEDs Based on Relaxed InGaN Templates

Lars Samuelson[1,2]
[1]Dept. of Physics/NanoLund, Lund University, Lund, Sweden
[2]Dept. of Electronics and Electrical Engineering, SUSTech, Shenzhen, China

Tel.:+46-70 317 7679, E-mail: lars.samuelson@ftf.lth.se

One big challenge for realization of high-performing micro-LED displays is the need to create ultra-small devices in the size range 1-5µm, still emitting efficiently [1,2]. We have pioneered a method based on the formation of relaxed and dislocation-free, c-oriented, InGaN platelets serving as ideal templates for long-wavelength emission. These nano-LED devices are effectively passivated via the way they are self-formed in the size range 0.3-1.5µm and may function as ideal building blocks for assembly into different pixel sizes for micro-LED applications.

III-Nitride based light-emitting diodes [2] based on InGaN active layers formed on GaN can produce efficient blue and green emitting LEDs. However, the large lattice mis-match between red-emitting active layers, with at least 35% indium in the active layers, and the GaN substrate still limits the efficiencies obtained to very low values, typically <5%. The approach to use GaAs based (AlInGaP) devices for the red, leads to issues of mixing technologies and to severely reduced efficiencies for LEDs much smaller than 50µm, while some of the key applications (such as Augmented Reality displays) require sized down to, or below, 2µm. We propose to use seeding techniques originally developed for nanowire growth, to seed the formation of ternary InGaN pyramids [3] which later are converted to thin c-facet platelets of InGaN [4,5]. The top-facet of each such template is on the scale of 300nm to 1.5µm, thus better described as template for nanoLEDs. These can either be used as single nanoLED for a pixel or as an array of such nanoLEDs, constituting a complete microLED pixel. I will in this presentation show that with such relaxed, and dislocation-free, InGaN platelets with In-composition about 20%, have the potential as ideal templates for red-emitting microLEDs, with device design and performance mimicking that of blue-emitting devices formed on GaN substrates.

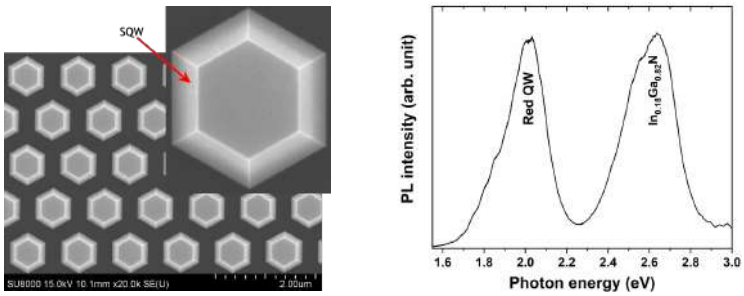

Fig. 1. Red-emitting QW on a planar, relaxed InGaN template

Acknowledgment

This research effort is based on several people's contributions, primarily MOVPE-growth headed by Dr. Zhaoxia Bi, cathodoluminescence by Prof. Anders Gustafsson, and TEM-investigations by Prof. Reine Wallenberg. We have also benefited from support and stimulating collaboration with the companies Glo AB and Hexagem AB.

References

1. Z. Bi, Z. Chen, F. Danesh and L. Samuelson, *Semiconductors and Semimetals, MicroLEDs, Elsevier Inc.,* Vol 106, Chapter 7, in press (2021)
2. *MicroLED Displays – Market, Industry and Technology Trends 2020, Yole Developpement,* (2020).
3. Z. Bi, A. Gustafsson, F. Lenrick, D. Lindgren, O. Hultin, L R. Wallenberg, B.J. Ohlsson, B. Monemar and L. Samuelson, *J. Appl. Phys.* 123, 025102 (2018).
4. Z. Bi, F. Lenrick, J. Colvin, A. Gustafsson, O. Hultin, A. Nowzari, T. Lu, R. Wallenberg, R. Timm, A. Mikkelsen, B.J. Ohlsson, K. Storm, B. Monemar and L. Samuelson, *Nano. Lett.* 19, 2832 (2019)
5. Z. Bi, T. Lu, J. Colvin, E. Sjögren, N. Vainorius, A. Gustafsson, J. Johansson, R. Timm, F. Lenrick, R. Wallenberg, B. Monemar and L. Samuelson, *ACS Appl. Mater. Interfaces* 12, 17845 (2020)

Directional GaN micro-LED for VR/AR applications

Xuelun Wang
[1]GaN Advanced Device Open Innovation Laboratory, National Institute of Advanced Industrial Science and Technology (AIST), Furo-cho, Chikusa-ku, Nagoya 464-8601, Japan
Tel.:81-29-861-5299, E-mail: xl.wang@aist.go.jp
[2]Institute of Materials and Systems for Sustainability, Nagoya University, Nagoya 464-8601, Japan

A novel directional GaN micro-LED is proposed as a promising device to realize the high-resolution (>4,000 ppi) and high-brightness (>100,000 cd/m^2) micro-LED displays required for VR/AR head-mount displays (HMD).[1] In this device (Fig. 1), an active region with a lateral dimension on the order of 100 nm is embedded at the center of a micron-sized truncated cone. Light generated inside the truncated cone is emitted into air through the top surface with a high directionality (directionality angle ~30°) and high efficiency resulted from a novel evanescent wave coupling effect occurring on the truncated cone surface. By using this directional micro-LED, optical crosstalk between adjacent display pixels which is a fundamental problem of the conventional planar-type micro-LEDs can be avoided, making the realization of 4,000 ppi resolution possible.

It is also very difficult for the conventional micro-LED to realize the 100,000 cd/m^2 luminance under the condition that heat generation during display operation is suppressed to a reasonable level (~20°C) due to its low light-extraction efficiency (~10%, light extracted from the top surface) and low coupling efficiency (~10%) of LED light into the optics of a VR/AR HMD. The directional micro-LED shown in Fig. 1 can provide a 5-times higher light-extraction efficiency compared to the conventional micro-LED and a near complete coupling of LED emission into the VR/AR optics. Assuming an internal quantum efficiency of 80%, 50%, and 30% for blue, green and red LEDs, a simple simulation shows that luminance higher than 100,000 cd/m^2 can be realized for all the three primary colors for a 4,000-ppi-resolution display by using the directional micro-LED while keeping a low heat generation (~20°C).

We are developing a top-down process to realize the proposed directional micro-LED.[2] The 100-nm InGaN/GaN active region is first fabricated by damage-free neutral beam etching technique.[3] The above active region is then buried in GaN by MOCVD regrowth, followed by fabrication of the truncated cone. Fig. 2 shows a typical TEM image of a GaN truncated cone with buried InGaN/GaN nanodisk active region.

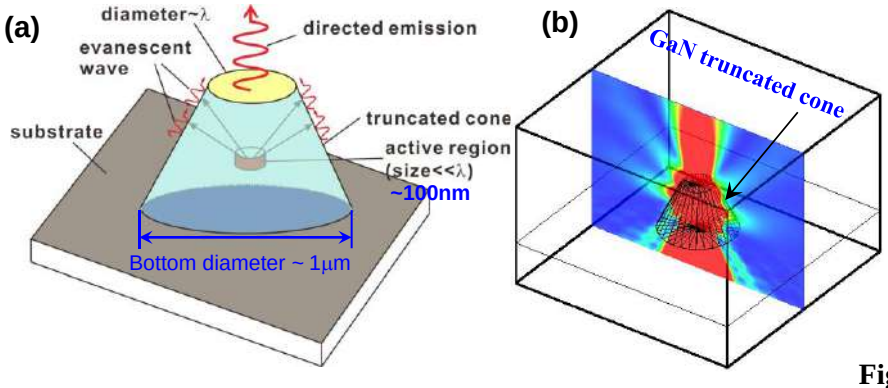

Fig. 1. (a) Schematic and (b) an FDTD simulation image of the directional GaN micro-LED proposed in this work

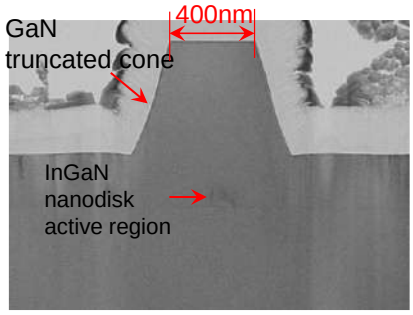

Fig. 2. Cross-sectional TEM image of a GaN truncated cone with buried InGaN nanodisk active region

Acknowledgment

Part of this work is performed in cooperation with Prof. Seiji. Samukawa at Tohoku University, Japan

References

1. X. L. Wang, G. D. Hao, and N. Toda, *Appl. Phys. Lett.*, 107, 131112 (2015).
2. K. X. Zhang et al., *Semicond. Sci. Technol.*, 35, 075001 (2020).
3. J. Zhu et al., *Phys. Status Solidi A*, 216, 1900380 (2019).

Emerging Field of Quasi-2D Flat Nanocrystal Optoelectronics

Hilmi Volkan Demir

NTU Singapore – Nanyang Technological University School of Electrical and Electronic Engineering, School of Physical and Mathematical Sciences, School of Materials Science and Engineering, Singapore

Bilkent University Department of Electrical and Electronics Engineering, Department of Physics, UNAM--Institute of Materials Science and Nanotechnology, Ankara, Turkey

hvdemir@ntu.edu.sg, volkan@bilkent.edu.tr, volkan@stanfordalumni.org

Semiconductor nanocrystals have attracted great interest for color conversion and enrichment in quality lighting and displays. These colloids span different types and heterostructures of semiconductors in the forms of quantum dots to the latest family of atomically-flat nanocrystals, the colloidal quantum wells (CQWs). In this talk, we will introduce the emerging field of semiconductor nanocrystal optoelectronics employing tightly-confined, quasi-2-dimensional CQWs, also popularly nick-named 'nanoplatelets' with a variety of recent examples of their photonic structures and optoelectronic devices. Different demonstrations, which will be presented in this talk, using these CQWs include record high optical gain coefficients, gain thresholds at the level of sub-single exciton population per CQW on the average, ultrathin optical gain media and lasers, record high-efficiency colloidal LEDs utilizing the CQWs as the electrically-driven active emitter layer, and record low-threshold solution lasers using the same CQWs employed as the optically-pumped fluidic gain medium.

Fluidic self-assembly of micro-LED chips with shaped magnetic heads and InGaP/InAlGaP red LED with plasmonic nanohole structures: Toward micro-LED displays

***In-Hwan Lee*[1]**
[1]Dept. of Materials Science and Engineering, Korea University, Seoul 02841, Korea
Tel.:82-2-3290-3814, E-mail: korea.ac.kr

Micro-LED display, arrays of sub-100um inorganic LED which individually operates as a pixel, has been considered as a next generation display. For that, transferring millions of chips with low cost and high-throughput is necessary. Another important issue to be solved is a decreased quantum efficiency of micro InGaP/InAlGaP red LED. Here, we demonstrate a high yield fluidic self-assembly technology to transfer GaN LED microchips with shaped magnetic head and an improved quantum efficiency of InGaP/InAlGaP red LED with plasmonic nanohole structures.

References

1. R. J. Knuesel et al, PNAS, 107(3), p. 993–998, (2010).
2. P. J. Schuele et al, Patent No. 9,825,202 (2017).
3. M. S. Wong et al, Opt. Express 28, 5787 (2020).
4. J.-T. Oh et al, Opt. Express 26, 11194 (2018).

Simultaneous Transfer and Bonding (SITRAB) Process for Mini- and Micro-LEDs

Kwang-Seong Choi[1], Jiho Joo[1], Gwang-Mun Choi[1], Ki-seok Jang[1], Chanmi Lee[1], Seok Hwan Moon[1], Ho-Gyeong Yun[1], Ji-Hoon Choi[2], Ji-Woong Choi[2], and, Yong-Sung Eom[1]
[1]ICT Creative Laboratory, ETRI, Daejeon 34129, Korea
Tel.:82-42-860-6033, E-mail: kschoi@etri.re.kr
[2]AQLASER Co., Ltd, Daejeon 34025, Korea

We have successfully developed a novel process for mini- and micro-LEDs, in which transfer and bonding occur at the same time, as shown in Fig. (1). This process was named SITRAB, standing for SImultaneous TRAnsfer and Bonding. The SITRAB process was developed by applying our proprietary material called SITRAB adhesive to the LABC (Laser-Assisted Bonding with Compression) process, which we proposed several years ago [1]. The total process time of SITRAB was less than 10 s. Its working area could be easily enlarged, according to the homogenized area of the LABC equipment. Because the LABC process uses an IR laser, it is much cheaper than processes that require UV laser equipment. The major features of the SITRAB adhesive are that it is fume free, and it is compatible with the LABC and repair process [2]. The SITRAB adhesives are used as a paste or a film depending on the application. The adhesive used during the SITRAB process is not cured, so additional transfer and bonding is possible with the applied adhesive on the substrate. Figure 2 shows a interposer with a 35 × 35 micro-LED array, a display substrate with SnAg solder, an optical photograph of the micro-LED array lighting, and a cross-sectional SEM image of a micro-LED on the substrate. The size of the micro LED-chip was about 80 μm × 130 μm, for which the conventional pick-and-place process could not be applied. Two types of solder materials were adopted and proven to be applicable: SnAg and In solder. The repair process was confirmed based on SITRAB technology. With such a very short process time and scalability to a large area, SITRAB can be considered a strong enabling technology to accelerate the commercialization of mini- and micro-LED displays.

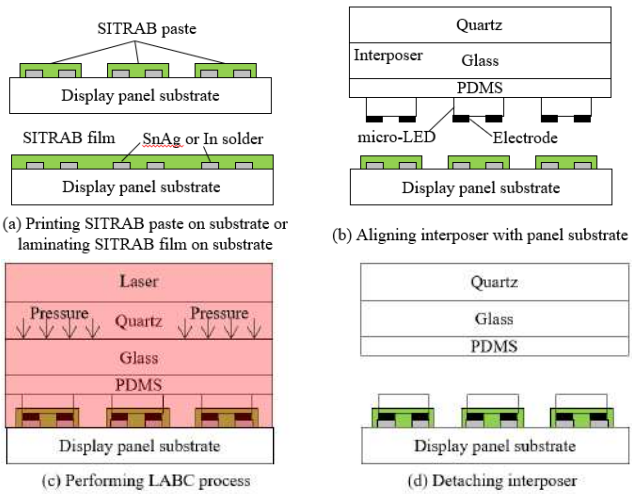

Fig. 1. Process flow of SITRAB

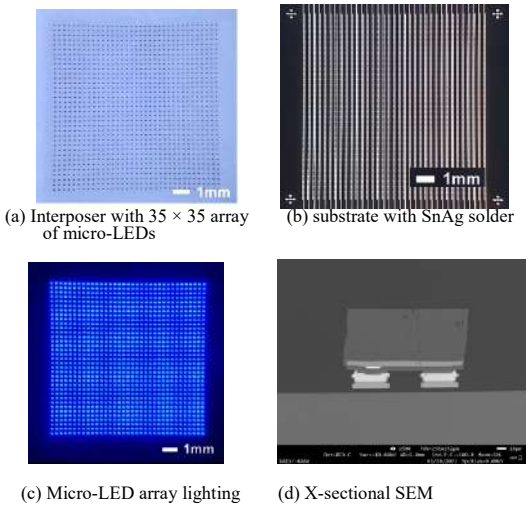

(a) Interposer with 35 × 35 array of micro-LEDs
(b) substrate with SnAg solder
(c) Micro-LED array lighting
(d) X-sectional SEM

Fig. 2. Process flow of SITRAB

Acknowledgment

This research was supported by the National R&D Program through the National Research Foundation of Korea (NRF) funded by the Ministry of Science and ICT (NRF-2020M3H4A3106383, NRF-2020M3H4A3081764).

References

1. K. -S. Choi, et al, ECTC'19 Proceeding, p. 197 (2019)
2. Y. S. Eom, et al, ETRI J. Vol. 35, no. 3. P. 343 (2014)

Wave Energy Assisted Fluidic Self-Assembly of LED Chips for Display Application

J. J. Ryu[1], S. H. Noh[1], C. W. Park[1], S.J. Lee[2], Y. R. Do[2] and J. S. Yoo[1]
[1]Dept. of Chemical Engineering, Chung-Ang University, Seoul 06974, Korea
Tel.:010-7277-5274, E-mail: jsyoo@cau.ac.kr, yrdo@kookmin.ac.kr ,
[2]Dept. of Applied Chemistry, Kook-Min University, Seoul 02707, Korea

The micro-LED displays are available in commercial market. Their image characteristics are excellent particularly in contrast ratio, response to electric field, and color expression. But the street price is too high to be acceptable for general consumers. The main reason may be the LED chip price. It can be overcome by reducing the size even in considering the efficiency decrease with chip size. However, the rapid and accurate arrangement of a few million chips with a size of ~ 50μm for forming the pixels on the substrate is challenging work.

As of now, pick and place technique is popular one for chip arrangement. In this work, fluidic self-assembly process was introduced. Design and implementation of self-assembly are limited to construction of micro-scale system. The external forces and geometric constrains can control the outcome of a self-assembled product. In this work, wave energy as the external force was used to well manipulate the LED chips on the substrate. The motion of LED chips was controlled by using target-generated waveforms in fluid. The Arrays of LED Chips on the fine metal mask (FMM), i.e., transfer cartridge as shown in Fig. 1. The chips were transferred to the circuit-printed glass plate by face to face pressing. Here, anisotropic conductive film was inserted between the FMM and the circuit-printed glass, as shown in Fig.2. Two plates were pressed at the temperature of 200℃ with 3N. Figure 3 shows the image of light-on. For self-assembly, the LED chips of C_2 symmetry are fabricated and should be used.

Wave energy assisted fluidic self-assembly was successfully demonstrated for mass transfer of LED chips in this work. It was found to be straight forward and decisive process for LED display application. In addition, repairing work can be minimized by using the FMM, which is very important for efficient manufacturing process.

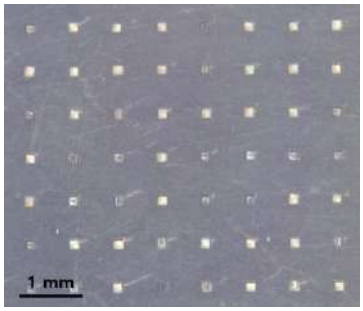

Fig. 1. Chips Array on FMM

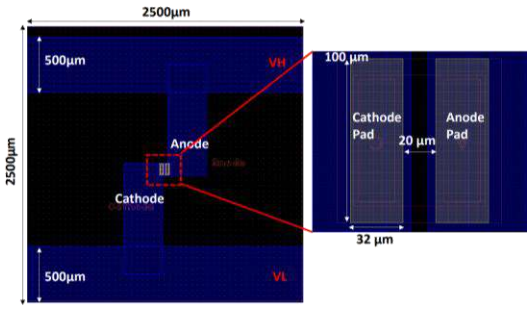

Fig. 2. Pixel Electrode

Fig. 3. Image of light-on

Acknowledgment

This research was supported by the Basic-science research program through the national Research Foundation of Korea(NRF) funded by the Ministry of Education (No. 2018R1D1A1A02086231). Circuit board was designed and fabricated by Wongyeong Yoon under Prof. J. Jang's guide in ADRC, Kyung Hee University.

References

1. H.E. Lee, J.H. Shin, J.H. Park, S.K. Hong, S.H. Park, S.H. Lee, J.H. Lee, I.S. Kang and K.J. Lee, *Adv. Funct. Mater.* 29, 1808075 (2019).
2. Q. Zhou, V. Sariola, K. Latifi and V. Liimatainen, *Nat. Commun.* 7, 12764 (2016)
3. Y. Song, B.S. Yim, J.S. Joung and J.M. Kim, *Journal of KWJS* 29, 25 (2011)

An Integrated Scan Driver Circuit based on LTPS TFTs for AM µLED Displays

Eun Kyo Jung, Yong-Hoo Hong, Sung-Hyuck Ahn, Sara Hong, Eunho Kim, Hwarim Im, and Yong-Sang Kim
Dept. of Electrical and Computer Engineering, Sungkyunkwan University, Suwon, 16419, Korea
Tel.:82-31-299-4640, E-mail: yongsang@skku.edu

Micro light-emitting diode (µLED) refers to an ultra-miniature LED of less than 100 µm and has the advantage of realizing low power consumption, miniaturization, and lightweight of the display. Besides, unlike organic light-emitting diodes (OLEDs), which show weaknesses in luminous efficiency and lifespan, it has excellent efficiency and lifespan and can operate in extreme conditions below -20°C and over 100°C [1]. Meanwhile, low-temperature polycrystalline silicon (LTPS) thin-film transistors (TFTs) have been widely used as backplane technology in display panels because of their high mobility, stability, and fast response speed compared to a-Si:H TFT and oxide TFT [2]. In general, the pixel circuit structure based on the LTPS-TFT for the µLED display consists of pulse width modulation (PWM) unit and constant current generation (CCG) unit [3]. Since the two data voltages (PWM data, CCG data) are required to apply to the driving TFTs of each part, the two scan signals are needed.

In this paper, we propose a novel integrated scan driver circuit based on LTPS TFTs for two scan outputs in µLED displays. Fig. 1, (a) exhibits the proposed circuit schematic which is composed of 12 LTPS-TFTs and 2 capacitors for the two scan outputs. The proposed circuit applies a bootstrapping technique for the Q[n] node of the pull-down TFT (T7). Therefore, the SPWM[n] and SCCG[n] are outputted using CLK signals through T9 and T11, respectively. In addition, we simulated the Q[n], SPWM[n], and SCCG[n] of the proposed scan driver circuit as shown in Fig. 1, (b).

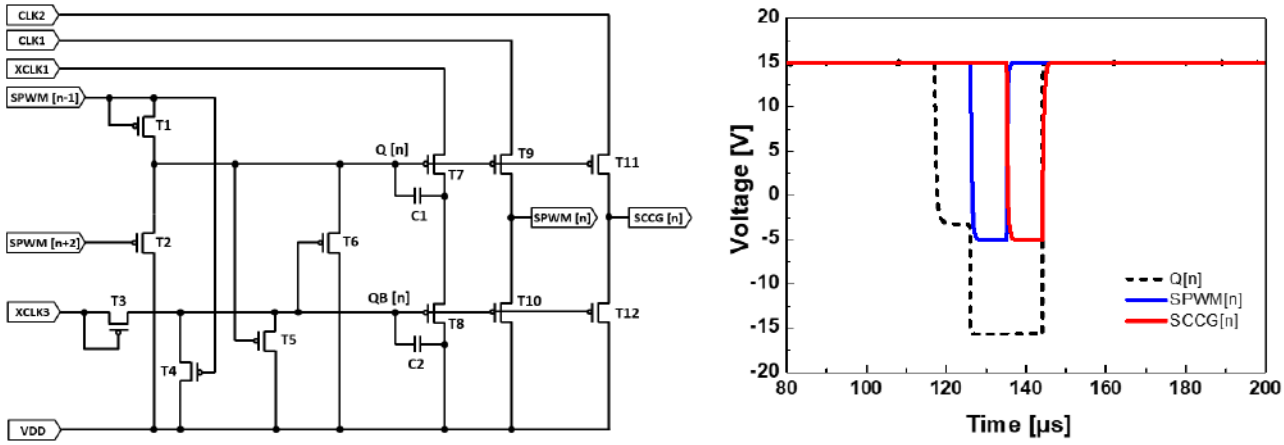

(a) **(b)**

Fig. 1. (a) Proposed circuit schematic and (b) Voltage waveforms of the Q[n], SPWM[n] and SCCG[n]

The 1H time is 9 µs based on the µLED display panel (480 (horizontal) × RGB × 270 (vertical)) of a modular type and the frame rate of 120 Hz. It was confirmed that the SPWM[n] and SCCG[n] are stably output during the bootstrapping period of the Q[n] node, respectively.

References

1. J. Kim, J. Ko, J. Park, G. Jeong, H. Maeng, S. Park, and W. Choe, *SID Symp. Dig. Tech. Papers*, vol. 49, no. 1, pp. 445-448 (2018).
2. C. L. Lin, P. C. Lai, L. W. Shin, C. C. Hung, P. C. Lai, T. Y. Lin, K. H. Liu, and T. H. Wang, *IEEE J. Solid-State Circuit*, vol. 54, no 2, pp. 489-500 (2019).
3. J.-H. Kim, S. Shin, K. Kang, C. Jung, Y. Jung, T. Shigeta, S.-Y. Park, J. Min, J. Oh, and Y.-S. Kim, *SID Symp. Dig. Tech. Papers*, vol. 50, no. 1, pp. 192-195 (2019).

A Light-Induced Cu Conductor on Glass Substrates for Thin Film µLED Application

Jung Ho Shin[1], Seung Hyung Lee[1], Jae Hee Lee[1], Sang Hyun Park[1], Jungwon Oh[1], and Keon Jae Lee[1]
[1]Dept. of Materials Science and Engineering, Korea Advanced Institute of Science and Technology (KAIST), 291 Daehak-ro, Yuseong-gu, Daejeon 34141, Republic of Korea
Tel.:82-42-350-3343, E-mail: keonlee@kaist.ac.kr

In this work, we report Cu electrode for thin-film µLEDs fabricated by the flash-induced interlocking between Cu and glass. During light illumination, CuO nanoparticles on the glass substrate were transformed into Cu by reduction and sintering. Simultaneously, focused heat at the boundary of nanoparticles and glass caused the Cu_2O interlayer within Cu/glass interface. Cu nano-interlocking was generated via glass softening and interface fluctuation to improve contact area. Due to these interactions, the light-activated Cu showed the adhesion energy of 10 J m^{-2}, 500 % higher than that of vacuum deposited Cu. An AlGaInP thin-film µLED formed a interconnection with the Cu electrode via thermo-compressive bonding, and exhibited a optical power of 41 mW mm^{-2}. The conductor enabled stable µLED operation in spite of strong thermal stress and moisture infiltration. 50 × 50 array of VLEDs on the light-induced Cu exhibited high illumination yield and uniform distribution of µLED properties.

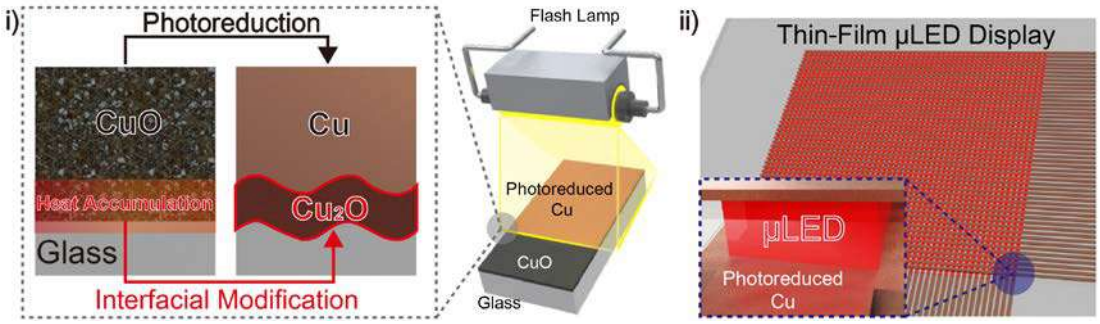

Fig. 1. Schematic showing the Cu electrode induced by flash light on a glass substrate and its application for thin-film µLED fabrication.

Surface Passivation of AlGaInP/GaInP Red Micro-LED

Juhyuk Park[1], Dae-Myeong Geum[2], Woo Jin Baek[1], and SangHyeon Kim[1]
[1]School of Electrical Engineering, Korea Advanced Institute of Science and Technology (KAIST), Daejeon 34141, Republic of Korea
Tel.:82-42-350-7552, E-mail: shkim.ee@kaist.ac.kr
[2]Infromation and Electronics Research Institute, Korea Advanced Institute of Science and Technology (KAIST), Daejeon 34141, Republic of Korea

Inorganic micro-LED is in the spotlight for ultra-high resolution display devices due to its high performance such as high brightness, scalability and contrast ratio, etc. In order to make energy-efficient micro-LED display, high external quantum efficiency(EQE) should be achieved under 100×100μm^2 pixel size. However, as the device size is reduced, the degradation of external quantum efficiency becomes severe and current density showing the peak EQE shifts to higher current density due to the carrier recombinations at side wall [1,2]. Especially in the case of the AlGaInP/GaInP MQW system, which has been widely used for commercial red LED device, has a large surface recombination velocity(SRV), therefore the degradation of scaling is more vulnerable than GaN-based blue and green LED devices[3]. Therefore, to minimize the degradation, we introduced the sidewall passivation strategy by using ammonium sulfide treatment and Al_2O_3 deposition. In figure 1(c), we compared the EQE of the commercial AlGaInP/GaInP LEDs with a size of 20×20μm^2 before and after passivation. Here the EQE was normalized by maximum EQE of passivated LED. After passivation, almost 20% normalized EQE was enhanced and current density showing the peak EQE was reduced.

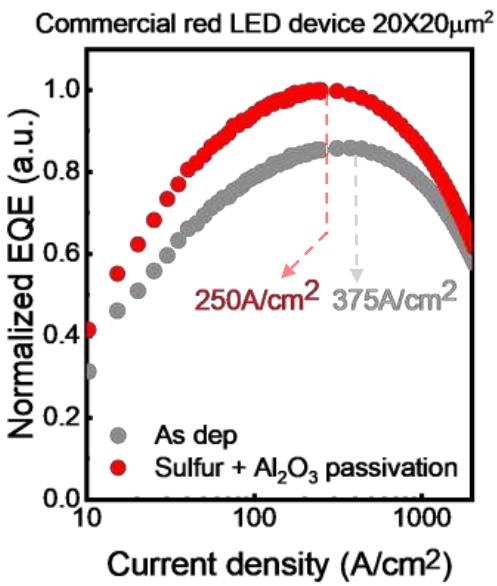

Figure 1. Normalized external quantum efficiency of AlGaInP/GaInP MQW LED with or without passivation.

In this work, we effectively removed the surface recombination sites by passivation process and analyzed the peak shift tendency of red LED devices by extracting surface recombination velocity.

Acknowledgment

This work was supported by Samsung Research Funding & Incubation Center of Samsung Electronics under Project number SRFC-TB2003-02.

References

1. J. T. Oh, *Optics Express,* **26**(9), 11194-11200 (2018)
2. D. -M. Geum et al., *Nanoscale* **11**, 23139 (2019)
3. Bulashevich.K.A and Karpov.S.Y. *Phys. Status Solidi RRL* **10**(6), 480-484 (2016)

Critical Challenges in microLED Testing and Inspection

David Lewis[1], Rimma Dechter[2], Ryan Ley[3], Matthew Wong[4], Michel Khoury[5]

[1,2]InZiv Ltd., Jerusalem, Israel

Tel.:+972-2-591-3400, E-mail: david@inziv.com

[3]Dept. of Chemical Engineering, UCSB, Santa Barbara, CA [4]Materials Dept., UCSB, Santa Barbara, CA

[5]Applied Materials, Santa Clara, CA

In the ever-evolving industry of display manufacturing, microLED is emerging as the most promising technology. With the potential for single-micron sized active emissive pixels, microLEDs offer a number of advantages over the current leading display technologies, including higher resolution, brighter colors, true blacks, reduced power consumption, and flexible form capabilities. However, as a result of microLEDS being produced with dimensions under 10 microns, testing and inspection is increasingly challenging, with single wafers containing millions of pixels and sub-pixels. Methodologies for fast yet high resolution metrology are needed in order to enable the manufacture of these devices. This paper presents a brief overview/introduction of some of the unique challenges facing leading microLED companies, and the most critical testing and inspection criteria for effectively progressing to achieve economically viable manufacturing.

1. Optical resolution is a first requirement for any inspection methodology hoping to characterize microLEDs. The inspection technique must achieve deep submicron resolution in order to effectively be applied to emerging microLED dimensions. This is based on the need to image with light at resolutions that are well below the diffraction limit which is generally in the range of 0.5 microns.

2. Any microLED metrology application must profile the emission of light with resolutions as high as 100nm. These small dimensions require sensitive detectors so that even at the lowest power levels, imaging can be effectively and rapidly accomplished. Furthermore, the inspection system must allow for effective probing of electroluminescence even when structures for the pads of the microLEDs are complex in geometry and resolution. This results in significant difficulties in contacting the microLEDS - both due to the pad dimensions and their position vis a vis the microLED.

3. Electrical probing must be extended to understanding the angular divergence of the light being emitted by the microLED, and the correlation of this emission with structural defects. The scope of such measurements encompasses intricate locations such as the emission from the sidewalls of the microLED.

4. All the light from the microLED and its surroundings has to be effectively collected in order to understand critical parameters such as EQE – External Quantum Efficiency, which is a metric for fundamental understandings of microLEDs and their defects.

All of the above measurement capabilities must be performed with considerable attention to the need for speed.

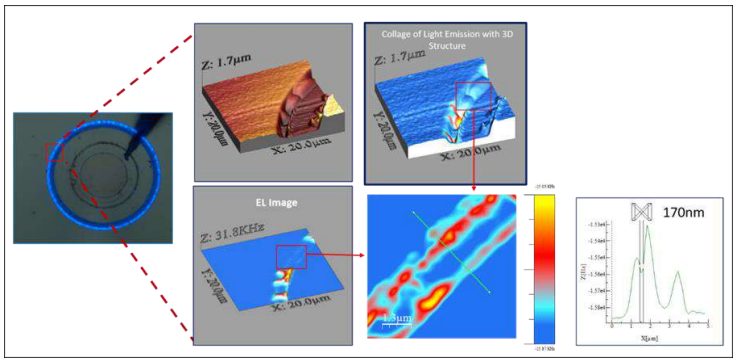

Figure 1. EL measurements of an ultrasmall 2µm die showing correlated structure and light emission from the side walls at sub-diffraction resolutions.

Acknowledgment

InZiv wishes to acknowledge and thank Ryan Ley and Matthew Wong from University of California Santa Barbara and Michel Khoury from Applied Materials for providing samples presented in images in this paper.

The role of emitters and host molecules in Organic LEDs

Jeong-Hwan Lee[1,2]
[1]Dept. of Materials Science and Engineering, Inha University, Incheon 22212, Korea
[2]3D Convergence Center, Inha University, Incheon 22212, Korea
Tel.:82-32-860-7525, E-mail: jeong-hwan.lee@inha.ac.kr

The External quantum efficiency (EQE) of organic light-emitting diodes (OLEDs) are intimately linked to the dipole orientation of emissive dopants and the use of a proper host system. Horizontally aligned phosphors or thermally assisted delayed fluorescent (TADF) molecules in a complementary host matrix lead to harvest both singlet and triplet energy and induce extraction of the generated light in a certain direction. Therefore, it gives rise to accomplish 100% internal quantum efficiency (IQE) as well as to enhance the outcoupling efficiency of OLEDs significantly, potentially opening a way to achieve the EQE of OLEDs over 45% without any outcoupling-enhancement structures. In this talk, we will discuss the charge recombination and emission mechanisms of OLEDs depending on different types of oriented emitters and hosts with various trap depths and dipole moments, and how they influence the EQE and efficiency roll-offs in OLEDs.

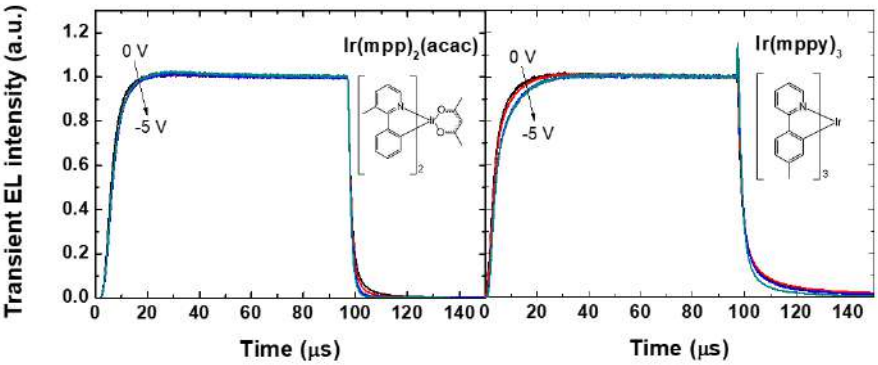

Fig. 1. Influence of dopants and hosts on the recombination and emission mechanism in OLEDs

Acknowledgment

This work was supported by to the Technology Innovation Program (20010484) funded by the Ministry of Trade, Industry & Energy (MOTIE, Korea) and by the Basic Research Program through the National Research Foundation of Korea(NRF) funded by the MSIT(2020R1A4A1019455)

References

1. J.-H. Lee, S. Lee, S.-J. Yoo, K.-H. Kim, J.-J. Kim, *Adv. Funct. Mater.*, 24, 4681 (2014).
2. K.-H. Kim, J.-J. Kim, *Adv. Mater.*, 30, 1705600 (2018).
3. C.-H. Lee, J.-H. Lee, K.-H. Kim, J.-J. Kim, *Adv. Funct. Mater.*, 28, 1800001 (2018).

Efficiency Enhancement of Top-Emitting Organic Light Emitting Diode by Multiple Capping Layer

Jin Young Kim, Han-un park, Seong Keun Kim and Jang Hyuk Kwon*
Dept. of Inform. Display, Kyung Hee University, Dongdaemoon-gu, Seoul 130-701, Republic of Korea
Tel.:82-2-961-0948, E-mail: jhkwon@khu.ac.kr .

Top-emitting organic light emitting diode (TEOLED) is used for small-sized displays like smart mobile phone due to their high aperture ratio, great color purity, and high light efficiency in a normal direction compared to bottom-emitting OLED (BEOLED). The TEOLED structure is composed of semi-transparent cathode with thin Mg:Ag or Ag electrode and reflective anode such as thick Ag. Both reflective electrodes make internal constructive interference in cavity structure, which it called micro-cavity effect. Due to this effect, TEOLED has high color purity and high efficiency in normal direction. As the cathode metal, Mg has high extinction coefficient which decrease device efficiency. To enhance the device efficiency, it is important to minimize the absorption effect of the metal with keeping good reflection. Thus, we applied Mg doped Ag (1:10) to provide low absorbance and high electron injection property. In order to enhance device efficiency in TEOLED, thin thickness of cathode with high reflection dielectric capping layer will be one of good approach to enhance device efficiency.

In this paper, we report high efficiency and good color purity multiple capping layer (MCL) blue TEOLEDs. This structure is composed of high refractive index material of MoO_3 (n=2.1) and low refractive index material of HATCN (n=1.5) for improving reflectivity as like Bragg reflector. Fig. 1(a) shows the Single CL (SCL) and MCL of device structure. As the control device, Ag:Mg (22 nm)/SCL (60 nm) device was fabricated. Fabricated TEOLEDs having one pair and two pair MCL structures with thin cathode metal thickness were as follows: Ag:Mg (12 nm)/HATCN (75 nm)/MoO3 (55 nm)_(1P), Ag:Mg (12 nm)/HATCN (75 nm)/MoO3 (55 nm)/HATCN (75 nm)/MoO3 (55 nm)_(2P). Fig. 1(b) shows summarized performance results of our fabricated and simulated devices. Our calculated results show 2P device exhibited 17% higher efficiency than SCL device, despite their spectrum shapes are almost same. It is due to the difference in absorbance of metal at similar micro-cavity condition. Fabricated 2P has similar color coordinates and FWHM with fabricated SCL, and efficiency enhancement factor is well coincidence with calculated results. Detailed optical analysis and device characteristic will be discussed in the presentation.

(a)

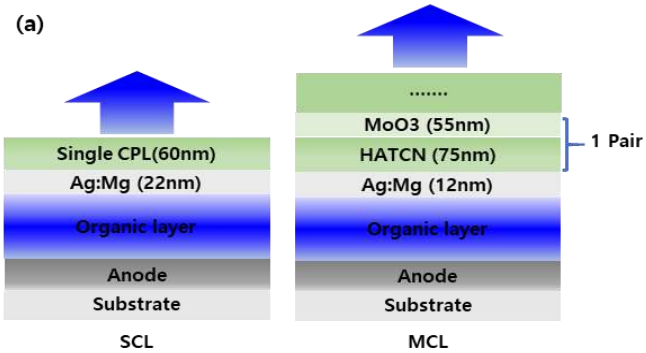

(b)

Device	Simulation (Measured)		
	SCL	1P	2P
Radiance (W*m-2*sr-1)	1.00 (1.00)	1.18 (1.17)	1.17 (1.22)
CIE (x,y)	0.137,0.049 (0.141,0.041)	0.138,0.053 (0.139,0.049)	0.140,0.047 (0.141,0.045)
Peak (nm)	459 (459)	460 (460)	459 (460)
FWHM (nm)	17 (16)	20 (20)	16 (16)

Fig.1 (a) is device structure of SCL and MCL (b) Simulation and measured device performances of Multi capping layered TOLEDs.

Acknowledgment

This work was supported by the Technology R&D Program (20006511, Development of electrode materials for OLED pixels and core technology for printing processes to apply on a nonvacuum process) funded by the Ministry of Trade, Industry and Energy (MOTIE, South Korea), and Korea Evaluation Institute of Industrial Technology (KEIT).

References

1. Wu, C.; Chen, C.; Lin, C.; Yang, C. Advanced organic light emitting devices for enhancing display performances. J. Disp. Technol. vol. 1, p. 248 (2005).

Accurate Optical Simulation Method for Tandem Organic Light-Emitting Diodes

Seong Keun Kim, Han-un Park, and Jang Hyuk Kwon
Dept. of Information Display, Kyung Hee University, Kyungheedae-ro/Dongdaemoon-gu, Seoul 02447, Korea
Tel.:82-2-961-0971, E-mail: jhkwon@khu.ac.kr

As the development of display technology, the structure of organic light-emitting diode (OLED) is gradually becoming complicated. Thereby, prediction of device performance by using optical simulation became important before fabricating device for reducing process error. To calculate complex condition, transfer matrix method and Fresnel equation is commonly used for multilayer calculation and it corresponds to wave and electro-magnetic optics region. However, there was almost no consideration about influence of emitter dipole in aspect of quantum-electrodynamic optics. When the emitter dipole is spontaneous emission state near electric field, its radiative decay rate is affected by Fermi's golden rule. In free space, we can set the radiative decay rate and non-radiative decay rate, Γ_r and Γ_{nr}, respectively. As the change of medium, dipole radiative decay rate is changed to effective radiative decay rate Γ_r^* [1]. We can express Γ_r^* using Purcell factor F(λ) as $\Gamma_r^* = F(\lambda)\Gamma_r$. As the consideration of Purcell effect, more accurate calculation is possible in performing optical simulation.

In this paper, we introduce the calculation method for achieving tandem OLED efficiency more accurately. We set the common calculation method as 'normal method' and the calculation with Purcell effect as 'Purcell method'. Using the normal method, we can attain the optimal emissive layer (EML) position and thickness condition of each organic layer at radiance distribution. To compare both optical simulation method, we designed 2-stacked tandem BEOLED (2T) which has thick thickness of 2nd order cavity and complex optical design (Fig.1(a)). Based on the 1st order BEOLED, we calculated efficiency of 2nd and 3rd order BEOLEDs (2SH, 2SE, and 3C) as shown in Fig.1(a). Calculated results exhibited almost similar results between both methods, however there is large difference condition when the EML is far from the cathode (Fig.1(b)). This experimental tendency is matched with Purcell method calculation. To identify the influence of Purcell effect OLED, we measured effective lifetime τ^* which has relationship with Purcell factor, $\tau_0/\tau^* \propto F(\lambda)$ (if non-radiative decay Γ_{nr} is almost 0). Measured lifetime tendency is almost matched with calculation by Purcell effect, and it indicates this method is reliable in complex OLED calculation. Detailed results of our optical simulation method will be discussed in the presentation.

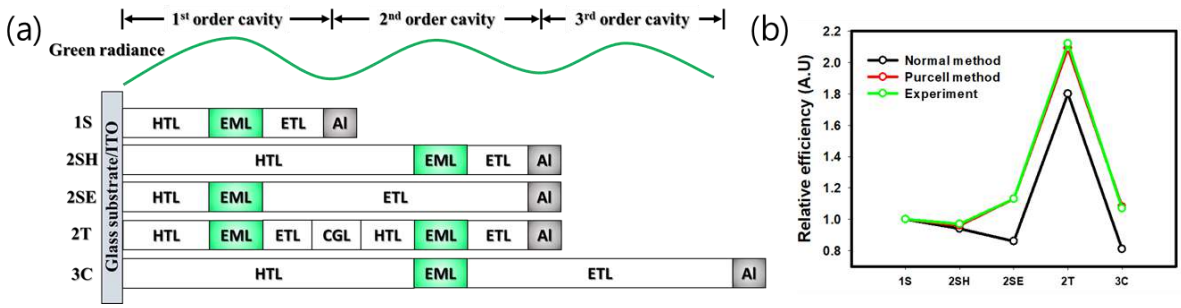

Fig. 1. (a) Diagram of fabricated device structures, and (b) relative efficiency of each device with different calculation method.

Acknowledgment

This work was supported by the Technology R&D Program (20006511, Development of electrode materials for OLED pixels and core technology for printing processes to apply on a nonvacuum process) funded by the Ministry of Trade, Industry and Energy (MOTIE, South Korea), and Korea Evaluation Institute of Industrial Technology (KEIT).

References

1. K. A. Neyts, J. Opt. Soc. Am. A, 15(4), 962-971 (1998).

A Study on the Stability Improvement of Solution processed Organic Light Emitting Diodes (OLEDs) Device through Control of Electron Mobility

Eun Young Park[1], Jae-Ho Jang[2], Do-Hoon Hwang[2], and Min Chul Suh[1,]*
[1]Organic Electronic Materials Laboratory, Department of Information Display, Kyung Hee University, Seoul 02447, Republic of Korea
Tel.:82-2-961-0694, E-mail: mcsuh@khu.ac.kr
[2]Dept. of Chemistry and Chemistry Institute, Pusan National University, Busan 609-735, Korea

Organic light-emitting diodes (OLEDs) are rapidly increasing interest in next-generation construction methods through inkjet printing due to the advantage of enabling a large-area, high-resolution process. [1] Mostly, multi-layered thin-film OLEDs are processed by thermal vacuum evaporation, but due to the problem of material consumption, OLEDs for solution processing are being studied a lot. However, in the OLED for solution process, interfacial mixing occurs between HTL and ETL. This is a major obstacle to replacing it for solution processing. Therefore, we have previously analyzed the effects of interfacial mixing in continuous solution processes and annealing processes. [2,3] And it was confirmed that the device stability deteriorated when the recombination region was generated in the interfacial mixing region. So, in order to move to the EML or EML/ETL interface, the recombination region must be separated from the HTL/EML interface. In this study, the change of recombination region according to the mobility of ETL was analyzed. Also, in order to increase the efficiency of these solution devices, it was necessary to change the mobility value of the HTL. So we applied a new crosslinked hole transport layer x-HTL crosslinked at a fairly low temperature of 135°C, and as a result, the efficiency of the OLED for solution treatment can be improved by up to 300%.

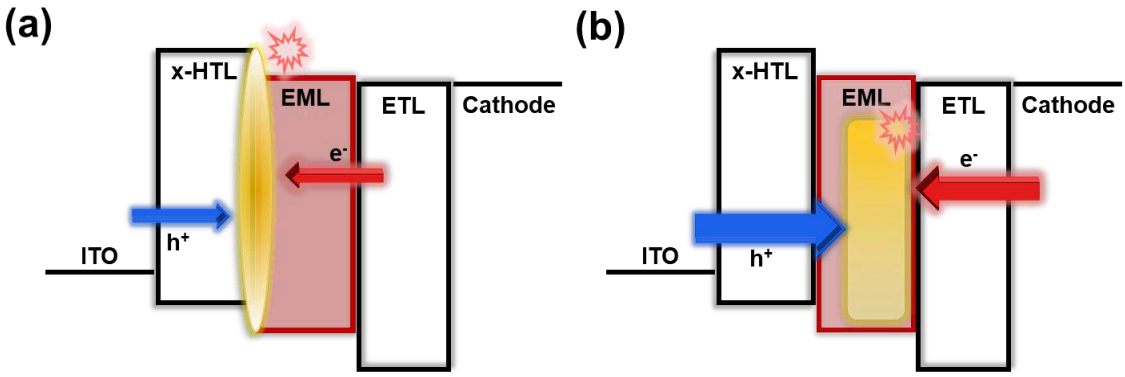

Fig. 1. (a) Recombination region formed between HTL and EML (b) EML and ETL

Acknowledgment

This work was supported by the Industrial Strategic Technology Development Program (20011059) funded By MOTIE, Korea. This work was also supported by NRF,Korea (NRF 2021R1A2C1008725) and funded by the MOTIE, Korea (20011059).

References

[1] Tang, C. W.; Vanslyke, S. A. Organic Electroluminescent Diodes. Appl. Phys. Lett. **1987**, 51, 913−915.
[2] Ahn, D. A.; Lee, S. J.; Chung, J. W.; Park, Y. S.; Suh, M. C.; ACS Appl. Mater. Interfaces **2017**, 9, 22748−22756
[3] Park, S. -R.; Kang, J. H.; Ahn, D. A.; Suh, M. C.; J. Mater. Chem. C, **2018**, 6, 7750-7758.

Predicting the Effects of Degradation on the Efficiency and Lifetime of OLEDs

Siebe van Mensfoort[1], Stefano Gottardi[1], Arthur Vauzelle[1], Christoph Hauenstein[1,2], Engin Torun[1], Ruud Gijsen[1], Peter Bobbert[2], Reinder Coehoorn[2], Harm van Eersel[1]
[1]Simbeyond B.V., Het Eeuwsel 57, 5612AS Eindhoven, The Netherlands
Tel.:+31-6-3346-1600, E-mail: contact@simbeyond.com
[2]Department of Applied Physics and Institute for Complex Molecular Systems, Eindhoven University of Technology, Eindhoven, The Netherlands

At present, the development of organic electronic devices largely occurs by following empirical recipes and by trial-and-error. This is a cumbersome process that often does not lead to the expected results and unpredictably delays the release of a new product or a new device technology. Rational design, based on predictive device simulations, is currently gaining more and more interest due to the large acceleration it can bring to research and development cycles, thus reducing time-to-market.

Among the top priorities in the OLED industry is to understand, predict and optimize the lifetime of devices. This is a hard challenge due to the multiple pathways in which the device can degrade, especially at the material level. In fact, degradation of few key molecular sites can result in a large and unexpected performance drop. Although experimental characterization of the degradation products is possible, it is usually insufficient to allow for developing a strategy towards devices with improved lifetime. To make this transition, the support of simulations becomes critical and allows to account for the large impact the three-dimensional carrier and exciton dynamics within the device have on degradation.

In this talk we show how 3D kinetic Monte Carlo (KMC) simulations can be used to study and predict the lifetime of OLED devices and how the insights gained from simulations can quickly lead to the design of devices with improved lifetime. The results are obtained using the advanced simulation software **Bumblebee**, provided by Simbeyond B.V. [1]. The mechanistic character of KMC gives Bumblebee the ability to easily simulate degradation of OLED stacks resulting from complex optoelectronic processes by performing virtual experiments.

Chemical decomposition of molecular sites is likely triggered by exciton-exciton annihilation and exciton-polaron quenching events [2-4]. The energy released by these processes is high enough to cause a molecular site to degrade into one or more products. As a result, molecular sites may become inaccessible to carriers and excitons or, alternatively, electron, hole and exciton traps may form. The properties of the degradation products and their location will determine how the device operation is affected. Moreover, they can affect the speed at which further degradation develops.

In our study, we explore various stacks and degradation scenarios and investigate the impact that different degradation products can have on the device efficiency and lifetime. The effect of electron and hole traps, gradients in the emitter concentration and formation of charge transfer (CT) states are discussed. Simulations were performed under constant current driving, so that the shift in the operating voltage during degradation is obtained. Moreover, Bumblebee gives a molecular-scale and nanosecond-resolved view of the optoelectronic processes occurring in OLEDs, including the actual 3D spatial non-uniformity of the current density and emission [5], a decomposition of the efficiency loss in terms of fundamental loss processes [6]. We will show how Bumblebee makes it easy to simulate OLED degradation scenarios and detect the key bottlenecks that limit device lifetime. Addressing these bottlenecks is then possible by material and stack design improvements.

References

1. Bumblebee software - Simbeyond B.V, https://simbeyond.com/bumblebee/.
2. D.Y. Kondakov, W.C. Lenhart, and W.F. Nichols, Operational degradation of organic light-emitting diodes: Mechanism and identification of chemical products. *J. Appl. Phys.*, 101(2), 024512 (2007).
3. N.C. Giebink, B.W. D'Andrade, M.S. Weaver, J.J. Brown, and S.R. Forrest, Direct evidence for degradation of polaron excited states in organic light emitting diodes. *J. Appl. Phys.*, 105(12), 124514 (2009).

4. R. Coehoorn, H. van Eersel, P.A. Bobbert, and R.A.J. Janssen, Kinetic Monte Carlo study of the sensitivity of OLED efficiency and lifetime to materials parameters, *Adv. Funct. Mater.*, 25(13), 2024 (2015).
5. M. Mesta, M. Carvelli, R.J. de Vries, H. van Eersel, J.J.M. van der Holst, M. Schober, M. Furno, B. Lüssem, K. Leo, P. Loebl, R. Coehoorn, and P.A. Bobbert, Molecular-scale simulation of electroluminescence in a multilayer white organic light-emitting diode, *Nat. Mater.*, 12(7), 652 (2013).
6. S. Gottardi, M. Barbry, R. Coehoorn, and H. van Eersel, Efficiency loss processes in hyperfluorescent OLEDs: A kinetic Monte Carlo study, *Appl. Phys. Lett.*, 114(7), 073301 (2019).

Advanced Characterization and Device Simulation towards better Understanding of OLED Degradation Mechanisms

M. Regnat[1,2], S. Jenatsch[2], S. Züfle[1,2], K. P. Pernstich[1], B. Ruhstaller[1,2]
1 Institute of Computational Physics, Zurich University of Applied Sciences, Winterthur, Switzerland
E-Mail: markus.regnat@zhaw.ch, beat.ruhstaller@zhaw.ch
2 Fluxim AG, Winterthur, Switzerland
E-mail: sandra.jenatsch@fluxim.com

Despite the successful commercialization of organic light-emitting diodes (OLEDs) in displays, there are still challenges with regard to the lifetime of these devices. It is therefore of great importance to better understand the device physics in general and the origins of degradation in these devices. State-of-the-art OLEDs usually consist of various layers in which several different physical processes occur at the same time. The three examples presented here show that the combination of advanced characterization tools and device simulations [1] can be the key towards a better understanding of OLED degradation mechanisms and thus improved future OLED devices.

In a first study a thermally activated delayed fluorescent (TADF) OLED stack with different layer thicknesses is extensively characterized and a quantitative device model is set up. Based on constant current stressing of individual pixels, intermediate steady-state, impedance and transient measurements (see Fig.1a), and qualitative model parameter screening, the observed degradation can be explained by hole transport deterioration and local formation of non-radiative recombination centers in the emitting layer [2].

In a second study with a more complex, highly-efficient, multilayer TADF OLED stack, we quantitatively analyze the electrical degradation via advanced characterization and device simulations and can pinpoint the driving voltage increase during prolonged operation at constant current to the degradation of mainly the hole transporting layer wherein traps are formed (see Fig. 1b) [manuscript in preparation].

In a third study, the degradation of a phosphorescent OLED stack is investigated via accelerated lifetime testing [3], where 16 similar pixels were individually stressed at the same time with various constant currents and temperatures, to analyze and reliably extrapolate the lifetime for different OLED operation conditions (see Fig.1c). Additional intermediate measurements consistently show the acceleration effects of increased current and temperature conditions on the degradation behavior.

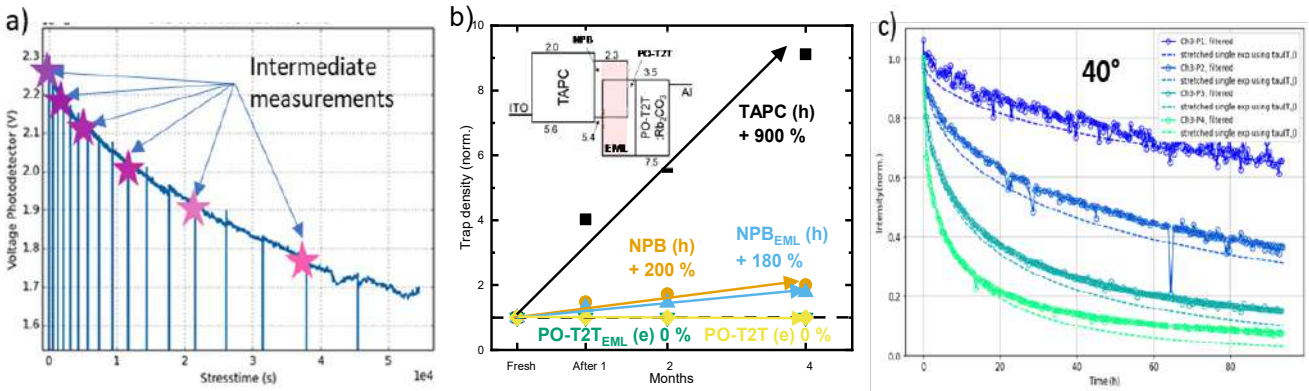

Fig. 1. (a) Measured light reduction over stress time and analyzed intermediate measurement points from the first TADF OLED study. (b) Evolution of the trap density over stress time of the individual layers from the second TADF OLED study, showing strong increase of traps in the hole transport material/layer. (c) Measured light intensity over stress time for varied constant currents at 40°C and calculated lifetime behavior (broken line) from the third phosphorescent OLED study.

References

1. Paios and Litos measurement systems and Setfos simulation software, Fluxim AG, www.fluxim.com
2. S. Jenatsch, S. Züfle, B. Blülle and B. Ruhstaller, *Journal of Applied Physics 127, Nr. 3*, 031102 (2020).
3. T. Yoshioka, S. Kazunori, O. Hiroshi, M. Satoshi and T. Tsutsui. SID Symposium Digest of Technical Papers 46, Nr. 1 (2015): 1650–53.

Controlling spontaneous orientational polarization in OLEDs and its impact on their efficiency and lifetime

Noel Giebink
[2]**Dept. of Electric Engineering, Penn State University, University Park, PA 16802, U.S.A.**
Tel.:01-814-865-2229, E-mail: ncg2@psu.edu

We show that diluting the TPBi electron transport layer of blue fluorescent OLEDs with medium density polyethylene (MDPE) increases their external quantum efficiency by ~25% and boosts operational lifetime by a factor of three. Both effects result from a significant decrease in spontaneous orientational polarization of the MDPE-diluted TPBi layer, which in turn reduces the density of accumulated holes in the recombination zone and thus the degree of exciton-polaron annihilation during device operation. We show that the improvements in quantum efficiency and lifetime are directly linked by a reduction of exciton-polaron annihilation, confirming the important role of this process in limiting blue OLED reliability.

Acknowledgment

References

Designed Synthesis of Nanocrystal Quantum Dots for Efficient and Stable Emitters

Lei Wang, Ruili Wu, Huaibin Shen, and Lin Song Li,
Key Laboratory for Special Functional Materials of Ministry of Education,
Henan University, Kaifeng 475004, China
Tel.: 86-371-23881358, E-mail: lsli@henu.edu.cn

Here we report how to design and synthesize of high luminescence ZnCdSe-based core/shell QDs by precisely controlled shell growth. We utilized high-temperature injection for the synthesis of QD cores and an even higher temperature for shell growth to obtain core/shell QDs that showed high QYs near to 100% as well as high photostability. Due to higher temperature shell growth procedure, the as-synthesized QDs can have higher chemical/photochemical stability than QDs prepared by low temperature shell growth method. Alloyed ZnCdSe core with certain ratio of Cd and Zn have been pre-synthesized first. Following by accurate ZnS shell growth, the as-synthesized core/shell QDs are nonblinking with the nonblinking threshold volume of > 100 nm^3. Förster resonance energy transfer can be effectively suppressed after growing ZnS shell. All these superb characteristics including nonblinking, single exponential PL decay dynamics, and supressed Förster resonance energy transfer can be beneficial to high quality QD-based LEDs.

Acknowledgment

The authors gratefully acknowledge the financial support from the National Natural Science Foundation of China (grant numbers 51972098).

References

1. Huaibin Shen, Qiang Gao, Yanbin Zhang, Yue Lin, Qingli Lin, Zhaohan Li, Ling Chen, Zaiping Zeng, Xiaoguang Li, Yu Jia, Shujie Wang, Zuliang Du, Lin Song Li and Zhenyu Zhang, *Nature Photonics* 13, 192–197 (2019).
2. Jiaojiao Song, Ouyang Wang, Huaibin Shen, Qingli Lin, Zhaohan Li, Lei Wang, Xintong Zhang, and Lin Song Li, *Adv. Funct. Mat.* 1801602 (2019).
3. Zhaohan Li, Fei Chen, Lei Wang, Huaibin Shen, Lijun Guo, Yanmin Kuang, Hongzhe Wang, Ning Li, and Lin Song Li, *Chem. Mater.* 30, 3668 (2018)
4. Qingli Lin, Lei Wang, Zhaohan Li, Huaibin Shen, Lijun Guo, Hongzhe Wang, and Lin Song Li, *ACS Photonics* 5, 939 (2018).
5. Ruili Wu, Tianyue Wang, Min Wu, Yanbing Lv, Xueping Liu, Jinjie Li, Huaibin Shen, and Lin Song Li, *Chem. Eng. J* 348, 447 (2018).

Surface engineering in colloidal quantum dots for infrared optoelectronic devices

***Min-Jae Choi*[1]**
[1]Dept. of Chemical & Biochemical Engineering, Dongguk University, Seoul 04620, Korea
Tel.:82-2-2660-8660, E-mail: minjae.choi@dongguk.edu

Colloidal quantum dots (CQDs) are compelling semiconductor materials for optoelectronic applications owing to their tunable bandgap, solution-processibility, and ambient stability. Of chief importance is the ability to tune their absorption and emission into the infrared, a region of interest in optical communications, night vision, biological imaging, and infrared photovoltaics [1, 2].

Solution-processed infrared CQDs enable to fabricate unique devices that can be combined with other devices. Here we show infrared CQD solar cells that can harvest light beyond 1100 nm. We further combine infrared CQD solar cells with c-Si and perovskite, in four-terminal tandem configuration, which results in complementary light harvesting system beyond bandgap of c-Si and perovskite. This enables to add extra power conversion efficiency to c-Si and perovskite solar cells [3,4].

In addition, we studied changes on CQD surface for infrared CQD applications. The CQD surface has different dominant surface facet depending on their size. This makes random alignment of CQD facet, leading to reduced CQD coupling in CQD solids. We perform colloidal atomic layer deposition (CALD) on CQD surface to tune CQD facet and this leads to (100) dominant CQDs, whereas as-synthesized CQDs show 1:1 ratio of (100) and (111) facets. The (100)-coupled CQD solids exhibit enhanced hole mobility compared to control CQDs, resulting in improvement on external quantum efficiency and photodetector performance at ~1500 nm range.

References

1. Chuang, C. H. M., Brown, P. R., Bulovic, V. & Bawendi, M. G. Improved performance and stability in quantum dot solar cells through band alignment engineering. *Nat. Mater.* 13, 796 (2014).
2. Liu, M. X. et al. Hybrid organic-inorganic inks flatten the energy landscape in colloidal quantum dot solids. *Nat. Mater.* 16, 258 (2017).
3. Choi, M.-J. et al. Colloidal Quantum Dot Bulk Heterojunction Solids with Near-Unity Charge Extraction Efficiency. *Adv. Sci.* 7, 15 (2020).
4. Lee. Seungjin et al. Orthogonal colloidal quantum dot inks enable efficient multilayer optoelectronic devices. *Nat. Commun.* 11, 4814 (2020).

Restructuring Surface of All Inorganic Cesium Lead Halide Perovskite Nanocrystal Quantum Dots for High Stability

Jusun Park[2], Seongwoo Cho[1], Youngsik Kim[2], Sung Nam Lim[1], Shin Ae Song[1], Kiyoung Kim[1], Sohee Jeong[2,*] and Ju Young Woo[1,*]

[1]Manufacturing Process Platform R&D Department, Korea Institute of Industrial Technology, Ansan 15588, Korea

Tel.:82-31-8040-6823, E-mail: jywoo@kitech.re.kr

[2]Dept. of Energy Science, Sungkyunkwan University, Suwon 16419, Korea

Recently all inorganic cesium lead halide (CsPbX3, X=Cl, Br, I) perovskite nanocrystal quantum dots (pNQDs) have emerged as an attractive emitter at room temperature. However, instability of CsPbX3 pNQDs, for example drastic drop of photoluminescence (PL), has been considered as a serious drawback for realization of pNQDs in various device forms operating under ambient conditions.

In this talk, I present effective post-synthetic strategy to significantly stabilize the CsPbX3 pNQDs. Post-synthetically modified CsPbX3 pNQDs with restructured surfaces exhibit extreme stability under ambient conditions. Based on diverse microscopic and spectroscopic analyses, for the first time, we propose the model for surface-restructured and stable CsPbX3 pNQDs.

High-Resolution, High-Yield Patterning of Quantum Dots via Controlling Solvent-Surface Interactions

Tae Won Nam[1], Moohyun Kim[1], Kyeong Min Song[1] and Yeon Sik Jung[1]
[1]Department of Materials and Science and Engineering, KAIST, 291 Daehak-ro, Yuseong-gu, Daejeon, 34141, Republic of Korea
Tel.:82-42-350-3328, E-mail: ysjung@kaist.ac.kr

The next-generation wearable near-eye displays inevitably require extremely high pixel density due to significant decrease in the viewing distance. For such denser and smaller pixel arrays, the emissive material must exhibit wider colour gamut so that each of the vast pixels maintains the colour accuracy. Electroluminescent quantum dot light-emitting diodes are promising candidates for such application owing to their highly saturated colour gamuts and other excellent optoelectronic properties. However, previously reported quantum dot patterning technologies have limitations in demonstrating full-colour pixel arrays with sub-micron feature size, high fidelity, and high post-patterning device performance. Here, we show thermodynamic-driven immersion transfer-printing, which enables patterning and printing of quantum dot arrays in omni-resolution scale; quantum dot arrays from single-particle resolution to the entire film can be fabricated on diverse surfaces. Red-green-blue quantum dot arrays with unprecedented resolutions up to 368 pixels per degree is demonstrated.[1]

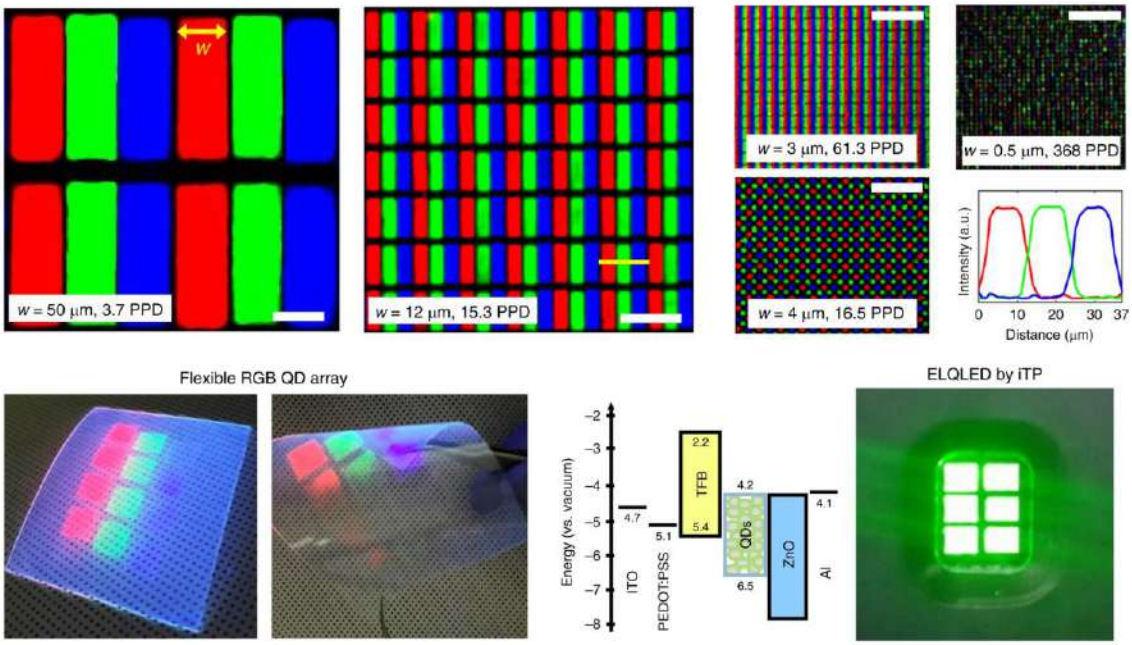

Fig. 1. Examples of quantum dot patterns obtained via iTP technology

Acknowledgment

This research was supported by Creative Materials Discovery Program (NRF-2016M3D1A1900035) and the Global Frontier Program through the Global Frontier Hybrid Interface Materials (GFHIM) (2013M3A6B1078874) of the National Research Foundation of Korea (NRF) funded by the Ministry of Science and ICT.

References

1. Tae Won Nam, Moohyun Kim, Yanming Wang, Geon Yeong Kim, Wonseok Choi, Hunhee Lim, Kyeong Min Song, Min-Jae Choi, Duk Young Jeon, Jeffrey C. Grossman & Yeon Sik Jung, *Nature Communications* 11, Article number: 3040 (2020)

Analysis on the degradation of Cd-free InP based quantum dot light-emitting diode

Kyunghwan Kim [1] and Jeonghun Kwak [1]
[1] **Department of Electrical and Computer Engineering Inter-University Semiconductor Research Center, Seoul National University, Seoul 08826, Republic of Korea**
Tel.:82-2-880-9559, E-mail: jkwak@snu.ac.kr

As the growth of the demand for next generation optoelectronics material which has outstanding optical characteristics, quantum dots (QDs) attract attention for the one of the candidates. Although the cadmium based QDs have distinguished stability and optical efficiency[1,2], use of the substance is reconsidered because of the harmful elements and therefore InP/ZnSeS/ZnS QDs can be used for the substitute as the eco-friendly material. InP based QDs has distinct electrical characteristics compared to Cd based QDs due to the difference in material, and the novel degradation analysis is required when applied to a light-emitting devices[3,4]. Here, we present the luminescence degradation of quantum dot light-emitting diode (QD-LED) is mainly caused by leakage electron and hole accumulation between QDs layer and hole transport layer (HTL). Because of the low electron confinement of QDs, electron injected into QDs layer can be easily pass through and induce the modification of hole injection characteristics. In addition, hole accumulation between QDs layer and HTL provokes the formation of trap which acts as quenching site. Confining electron in QDs layer can be alleviates the rapid degradation of early period.

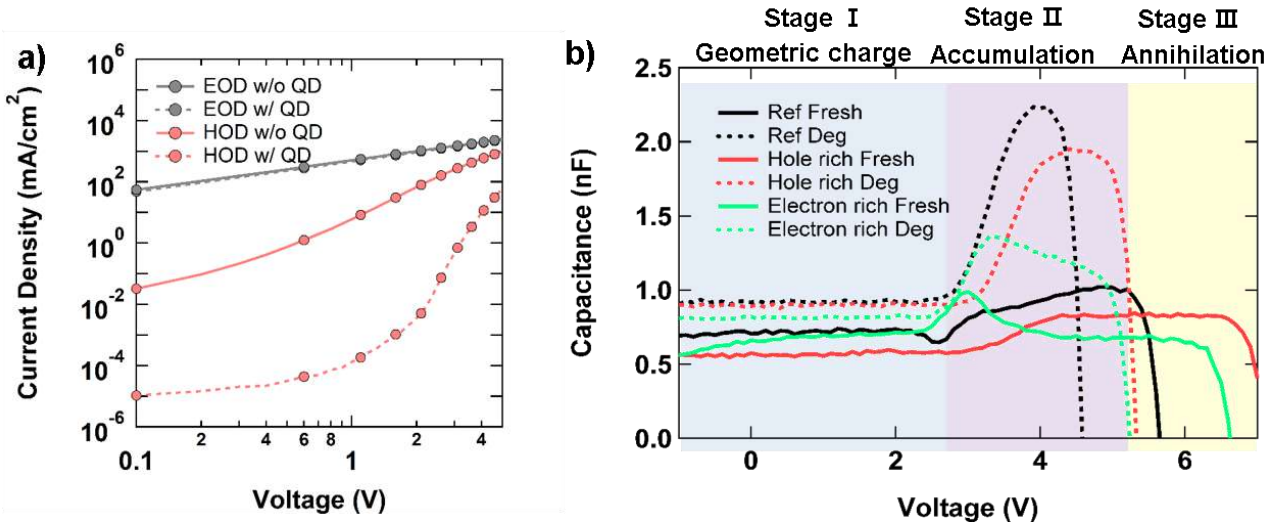

Fig. 1. a) Current density – voltage characteristics of EOD, HOD w/, w/o QDs, b) capacitance – voltage curve of the QLED device before and after degradation

Acknowledgment

This work was supported by Samsung Display Co.,Ltd and Technology Innovation Program (20010737) funded by the Ministry of Trade, Industry & Energy (MOTIE, Korea).

References

1. Dai, Xingliang, et al., *Nature* 515.7525, 96-99 (2014).
2. Pu, Chaodan, et al., *Nature communications* 11.1 1-10 (2020).
3. Chang, Jun Hyuk, et al., *ACS nano* 12.10, 10231-10239 (2018).
4. Han, Moon Gyu, et al., *ACS Energy Letters* 6, 1577-1585 (2021).

Considerations in Advanced Inkjet Printed Layers for Current and Future Display Processes

Mr. Christopher R. Hauf[1], Dr. Valerie Gassend[2], and Dr. Noa Cohen[3]
[1]Vice President, Technology, Kateeva, Inc., Newark, CA, USA 94560, U.S.A.
Tel.:+1-650-350-2351, E-mail: chauf@kateeva.com
[2]Sr. Manager & Co-Founder, Technology, Kateeva, Inc., Newark, CA, USA 94560, U.S.A.
Tel.:+1-650-319-5342, E-mail: valerie@kateeva.com
[3]Sr. Print Engineer, Technology, Kateeva, Inc., Newark, CA, USA 94560, U.S.A.
Tel.:+1-781-707-8406, E-mail: ncohen@kateeva.com

Inkjet printing has proven itself to be a viable manufacturing technology for a variety of processes within the manufacturing of displays including the Thin Film Encapsulation (TFE) layer[1] used in various types of OLED displays. One of the benefits of inkjet is the ability to flexibly pattern the ink layer and print a highly uniform layer at a calibrated thickness. These were the initial critical parameters for the adoption of inkjet printing in TFE, however, new device designs, e.g. in panel cameras or under the display cameras are now pushing the technology to do more for both TFE layers and beyond. A user may now need to be able to leave holes in the main film to allow for a camera to look through, produce a small isolated feature within a hole or holes needed for a follow on process or a multithickness layer that allows the filling of a differing topology below the level of the base TFE film allowing for the use of under the panel cameras. The printing of these features for TFE process and beyond need to concern themselves with both the capabilities of the printer and with the physics of the interaction of the chosen ink and the substrate.

In some processes, it is critical to be able to print small isolated circular features. It is important to understand how small printed features can differ from their target shapes, thicknesses and width. Understanding these behaviors can guide the development of design rules for small features in an inkjet printed thin film.

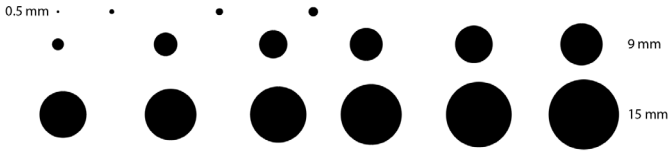

Figure 1. Example of circular print features.

As the diameter of a printed circle gets smaller, edge effects predominate, and the resulting structure will be shaped like a dome instead of having a flat central region. Minimizing the surface energy of the ink will cause the ink pattern to take the shape of a spherical cap. At small dimensions, the effects of viscosity do not slow down the redistribution of ink significantly, and a rounded shape is obtained before the ink is cured.

In Figure 2, we show the profiles of printed circles of target diameters 0.5 mm to 15 mm and 8 µm target thickness printed on PECVD coated bare glass using a UV curable TFE ink.

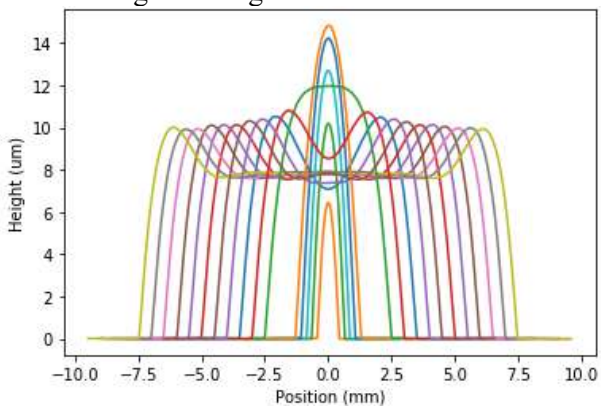

Figure 2. Cross-section height across 8 µm thick circular features of varying target diameters: 0.5 to 15 mm.

The larger circular features have flat regions in the center with "dog-ear" non-uniformities near the edges. However, the features of diameter smaller than 5 mm are shaped like domes. The 6 mm and 7 mm diameter profiles are composed of two distinct "dog-ears" but without a flat region in the center.

For thinner films, smaller features can generally be achieved with better results. For example, Figure 3 shows that for a 4 µm target print thickness, smaller diameter circular features can be printed with a flat center region than for the 8 µm print (down to 5 mm diameter vs. 8 mm).

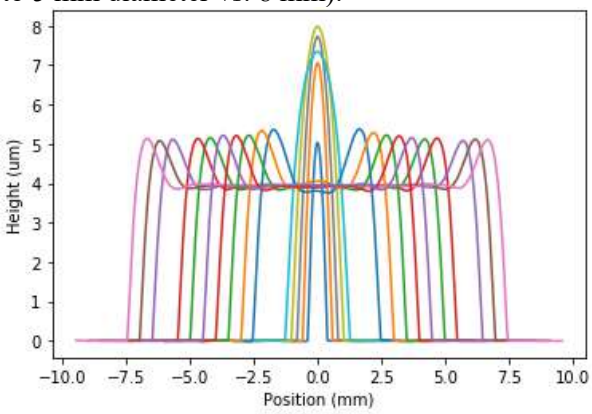

Figure 3. Cross-section height across 4 µm thick circular features of varying target diameters from 0.5 to 15 mm.

In Figures 2 and 3, the thickness at the center of the small diameter circles differs from the expected thickness. When the dog-ears begin to merge, the resulting thickness of the feature is affected by the non-ideal shape.

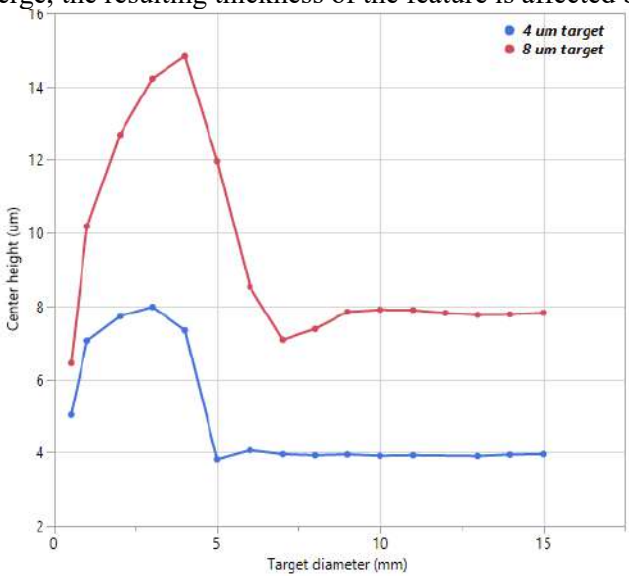

Figure 4. Thickness at the center of circular printed features of 0.5 to 15 mm target diameter, for 4 and 8 µm target thicknesses.

In Figure 4, we show the center thickness of the circular features as a function of target diameter. For the thinner (4 µm) film, the center thickness is close to target down to 5 mm diameter. As the shape becomes rounded below 5 mm diameter, the thickness at the center increases up to 8 µm (double the target) at a 3 mm diameter then decreases for smaller diameters towards the target thickness, reaching about 5 µm at 0.5 mm diameter. For the thicker (8 µm) film, the trend is similar, but the thickness is close to target only above 9 mm diameter. The center thickness also dips below target at 0.5 mm and at 7 and 8 mm.

This is just one of many different scenarios that need to be considered to make successful inkjet printed layers for more complex TFE processes and beyond, including multi-thickness TFE layers, microlens planarization layers and liquid optical clear adhesive (LOCA) layers.

Acknowledgment

The authors would like to acknowledge the contributions of the Kateeva Technology Team for their contributions in both printing and metrology needed to make this paper and talk possible.

References

1. Moro, L. and Hauf, C.R. (2021), Large-Scale Manufacturing of Polymer Planarization Layers. Information Display, 37: 10-15. https://doi.org/10.1002/msid.1194

Study on Dynamic Folding Reliability of Amorphous Metal Foil for Foldable Display Applications

*TaeWoo Kim[1], JungKyu Park[1], SangJun Lee[1], SeungJun Han[1], Nadine Wolf[2], Thomas Strache[2], Julia Hahn[2], Christian Polak[2], and JiGeun Nam[1]**

[1]Convergence Technology Research Division, LG Display, Seoul 07796, Republic of Korea

[2]VACUUMSCHMELZE GmbH & Co. KG, Grüner Weg 37, D-63450 Hanau, Germany

Tel.:82-2-8037-0229, E-mail:ramji74@lgdisplay.com

The mechanical reliability issues have emerged as key factors in designing display-integrated products with rapidly increasing needs and application scenes for flexible display panels.[1] Among them, folding reliability is relatively new yet crucial topic of study as a number of products are being introduced to adopt outer, inner, or even multi-foldable panels.[2] Stainless steel metal foils have widely been used for the backbone structure of foldable display panel modules, whose main role is to assure the mechanical reliability of display panels in terms of warpage, shock resistance, *etc*. However, as the folding radius is continuously becoming smaller (~1.5R for commercial smartphone models), the need for alternative materials that can endure extreme bending stress (folding reliability) has been emerged.[3] One possible substitute is amorphous metal foil, whose elastic limit is larger than crystalline metal composites, making them suitable for extreme folding conditions without the initiation of any crack or crease.[4,5]

The prepared amorphous metal foils for fodable display applications had shear band at the cutting edges (Fig.1(a)) and plenty of dimple structures on the whole surfaces (Fig. 1(b)), which can act as seed sites for crack initiation under folding conditions.[5,6] Thus, additional surface treatment procedures such as surface etching and polishing were adopted to eliminate the shear bands and dimples. The resulting microscope images of the surfaces after treatment procedures are shown in Fig. 1(c) and (d). Remarkable progresses in reducing shear band and dimple sites on the amorphous metal surfaces could be achieved through these additional surface treatments. This improvement in surface quality also affected the dynamic folding reliability of amorphous metal foils as shown in Fig. 1(e). Before surface treatment, only 50 % of amourphous metal foils survied 180° dynamic folding test for 200,000 cycles under 1.5R condition. After eliminating shear bands and dimples, however, 100 % of amorphous metal foils endured the same condition, showing no sign of any crack and crease initiation. As a result, it could be concluded that amorphous metal foils could serve as a substitute for stainless steel foils for foldable display applications with higher elastic limit and excellent folding reliability.

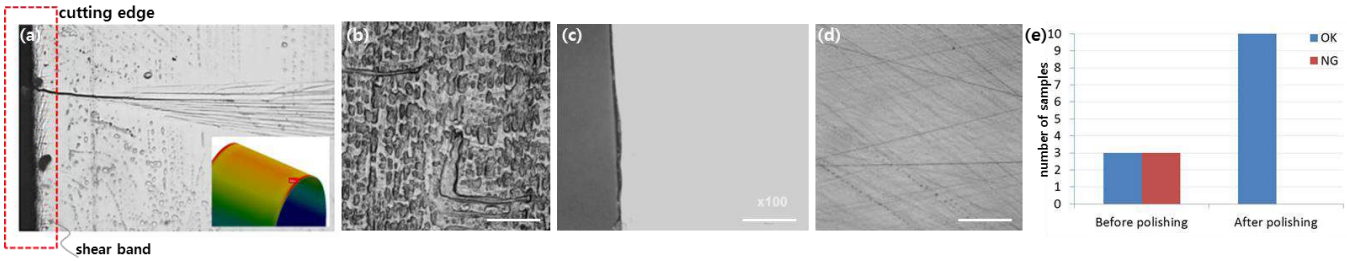

Fig. 1. (a) shear bands at the amorphous metal foil edge **(b)** dimples at the amorphous metal surface **(c)** clean edge and **(d)** surface after surface treatment **(e)** dynamic folding test results before/after surface treatment

References

1. E. Huitema, *Information Display*, 28, 6 (2012).
2. L. Chen, *et. al.*, *Adv. Mater. Interfaces*, 7, 2000928 (2020).
3. C. Lee, *et. al.*, *SID Symposium Digest of Technical Papers*, 46, 238 (2015)
4. J. Kruzic, *Adv. Eng. Mater.*, 18(8), 1308 (2016)
5. E. Park, *Applied Microscopy*, 45(2), 63 (2015)
6. S. Huang, *et. al.*, *Metall. Trans. A*, 12A, 1107 (1981)

A Thin, High-Resolution Touch/Stylus Digitizer for under-OLED Force-Sensing Applications

Sarah Dempsey[1], Tolis Voutsas[1]
[1]Peratech Holdco Ltd., Old Repeater Station, Brompton-on-Swale, North Yorkshire, UK
Tel.:44(0)1748 813670 , E-mail: info@peratech.com

Consumer electronic devices such as phones, tablets and laptops are undergoing a revolution in form-factor as there is increasing consumer interest and market demand for flexible, foldable, rollable and stretchable devices, and the display technologies which enable them. These new form factors enable new ways for users to interact with their devices - for example, a phone-sized device may open up to a larger tablet, which allows stylus or pen input. The addition of force-sensing to these devices is incredibly advantageous, as this provides depth-of-touch or pressure information which can vastly improve user experience for either finger or stylus input. It also permits more elegant ways for false-touch elimination, simplified or augmented HMI's, and even back-side sensing on larger displays, which has real value for improving gaming experience.

Peratech have developed a novel, thin (35um) flexible force sensor that can be integrated behind a flexible/foldable OLED display. In preliminary tests, the sensor is laminated under 300um stack-up, replicating a flexible OLED integration. The sensor has an active area of 147 mm x 104 mm, with 150 x 106 sensing elements at 0.98mm pitch. This provides a high-resolution sensing array capable of capturing stylus input with high fidelity, as shown in Fig.1A for a test script at 30pt font size at 50g input force.

The sensor can capture force information from 10g – 600g, demonstrating good force uniformity across the entire sensing area with 10.7% variation % at 100g and 5.8% at 600g force for a finger press, for the 'standard' build configuration. In addition, the dynamic range of the force input can be further tailored by changing either the electrical properties of the constituent sensing materials, or the design of each force sensing element (i.e. the number and order of sensing layers). Two designs (1 and 2) with two material options (A and B) are presented here, alongside the 'standard' design. Fig.1B shows the change in ADC signal (as a percentage of the maximum change detected at 600g) for stylus input for each matrix variant, showing demonstrable signal change over the full force range.

In addition, the force sensing technology also displays excellent mechanical reliability after folding, where after 100k bend cycles to 4mm bend radius (from flat to folded) there is no significant degradation or change in sensor performance, as demonstrated in Fig.1C.

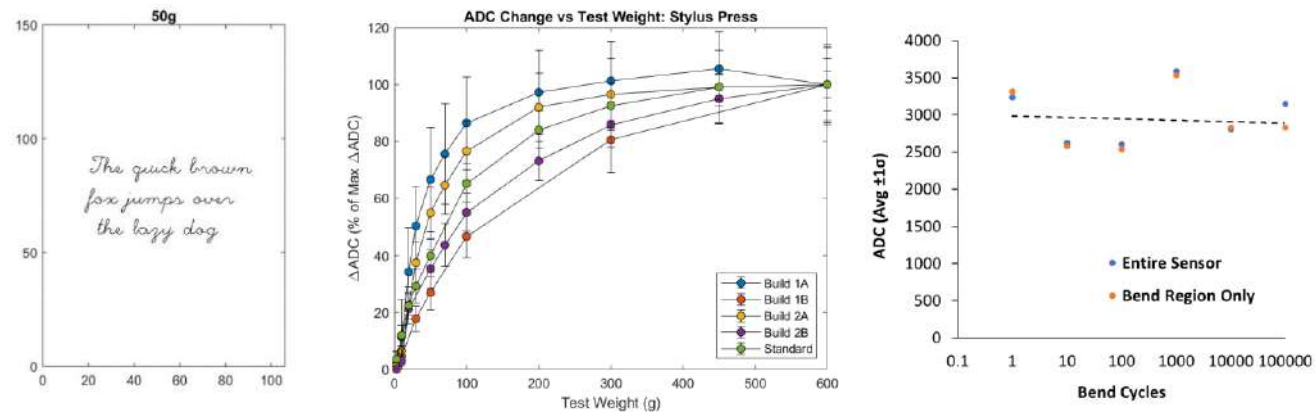

Fig. 1A (left). Stylus capture fidelity for 30pt cursive handwriting input, at 50g force.
Fig. 1B (middle) Change in ADC signal for stylus touch as a function of input force.
Fig. 1C (right) ADC signal stability at 50g after 100k fold cycles to Ø4mm.

Design of stable blue phosphorescent OLEDs using state interaction between exciplex and component host

Joonghyuk Kim[1], Yeon Sook Chung[1], Soo-Ghang Ihn[1], Soon Ok Jeon[1], Jongsoo Kim[1], Yongsik Jung[1], Sungho Nam[1], Hosuk Kang[1], and Hyeonho Choi[1]**

E-mail: hosuk7.kang@samsung.com, hono.choi@samsung.com

[1]Samsung Advanced Institute of Technology, Samsung Electronics, Suwon 16678, Korea

Blue phosphorescent organic light-emitting diodes (OLEDs) have difficulty to use commercially in displays because of their insufficient operational lifetime. In several studies, it mainly results from the degradation of OLED materials by high-lying triplet excited state (hot exciton). Here we introduce mixed hosts with a small gap (< 0.1 eV) between the triplet energy state of electron-transporting type (ET) host and the triplet energy state of exciplex formed from mixed hosts. Small gap makes hot energy to transfer readily between the triplet energy state of host and the triplet energy state of exciplex, leading to the suppression of molecular bond dissociation of host material by hot energy. As a result, the operational lifetime of blue OLED device employing adjusted triplet energy states of ET host and exciplex has threefold increase compared to conventional devices employing mixed hosts. We investigate the long decay time of mixed hosts to complement this mechanism.

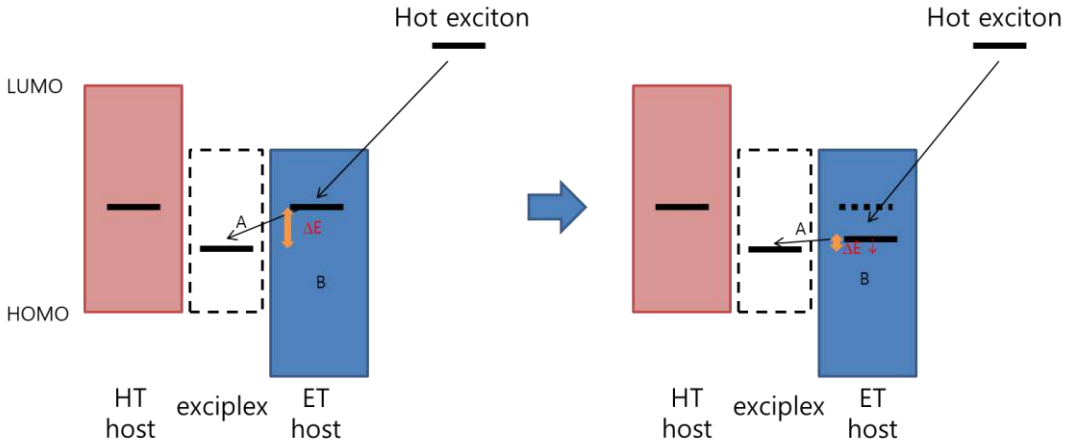

Fig. 1. HOMO/LUMO levels and T1 states of mixed hosts and hot exciton transfer.
(a) Typical mixed hosts (b) Mixed hosts having the small gap between ET host T1 and exciplex T1

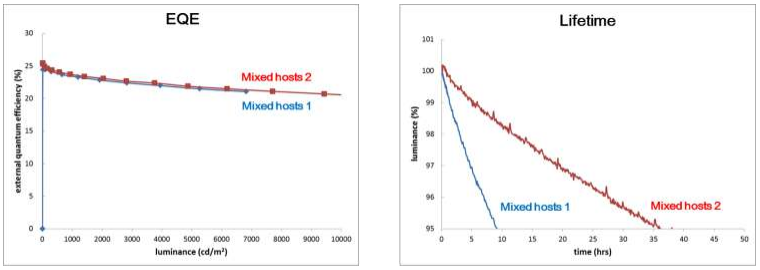

(a) External quantum efficiencies (b) Device lifetimes

Fig. 2. EQE and lifetime of mixed hosts 1 and mixed hosts 2

References

1. Tang, C. W. and Vanslyke, S. A. Organic electroluminescent diodes. Appl. Phys. Lett. 51, 913. (1987)
2. Park, Y. et al. Exciplex-forming co-host for organic light-emitting diodes with ultimate efficiency. Adv. Funct. Mater. 23, 4914 (2013)
3. Lee, J. et al. Hot excited state management for long-lived blue phosphorescent organic light-emitting diodes. Nature comm.8, 15566 (2017)

Integration of Colloidal Quantum Dots with Micro LEDs

Kai-Ling Liang[1], Wei-Hung Kuo[1], Hui-Tang Shen[1], Chun-I Wu[1], Yen-Hsiang Fang[1], and Chien-chung Lin [1,2]
[1]Industrial Technology Research Institute, Hsinchu 310401, Taiwan
Tel.:886-3-591-5747, E-mail: chienchunglin@faculty.nctu.edu.tw
[2]Institute of Photonic System, National Chiao Tung University, Tainan 71150, Taiwan

The emerging demands on the micro-display products have prompted the development of fine-pitched micro LED arrays[1-3]. While most of the researches focused on the formation of individual red/green/blue chips, there are concerns on the limitation of such method. One of them is the degradation of the quantum efficiency as the chip size shrinks which rises from the increased non-radiative recombination centers in the devices. Another one is the difficulty in transferring the tiny chips from one substrate to the destination. To overcome these difficulties, we need to resort to the heterogeneous integration of light-emitting nanoparticles with micro LEDs[3].

To incorporate these nanoparticles (or colloidal quantum dots, CQDs), many methods can be applied. The most popular methods are: direct deposition, photolithography method, and nano-imprint method. The direct deposition can be achieved by pulsed spray or inkjet printing, and the CQD patches are directly placed on the surface of micro LEDs. The photolithography method involves the mixture of CQD and photo-sensitive resin, which can bring us great advantages of semiconductor fabrication and it can raise the throughput greatly. The third method of nano imprint can be done by pre-patterned substrate and uniform CQD layers. The finest pixel size in nano-imprint can be demonstrated is around 6 μm[4]. In this talk, we will demonstrate our latest progress in direct deposition and photolithography method. The subpixel size of direct deposition can be as small as 5 microns, while the photolithography method can show a wide range of arrays with various sizes like 30 microns or 6.4 microns of subpixels, as we can see in Fig. 1.

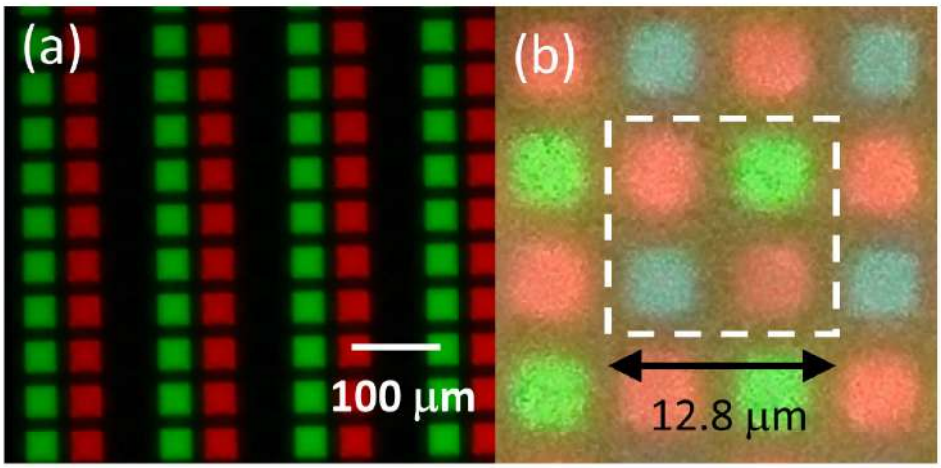

Fig. 1. (a) A 30 μm sub-pixel of quantum dot array (b) a 6.4 μm sub-pixel quantum dot array.

Acknowledgment

The authors would like to thank the financial support of Ministry of Economic Affairs of Taiwan (MOEA) under the contract number: MOEA 110-EC-17-A-24-1579

References

1. H.-H. Huang, et al., Optics Express **28** (25), p. 38184-38195 (2020).
2. Y. L. Tsai, et al., IEEE Photonics Journal **12** (6), p. 1-9 (2020).
3. K.-L. Liang, et al., Japanese Journal of Applied Physics **60** (SA), SA0802 (2020).
4. M. K. Choi, et al., Nat Commun **6**, 7149 (2015).

Development of InGaN-based red LEDs and fabrication of their micro-LEDs

Kazuhiro Ohkawa, Daisuke Iida, Zhe Zhuang*

Computer, Electrical and Mathematical Sciences and Engineering (CEMSE) Division, King Abdullah University of Science and Technology (KAUST), Thuwal, 23955-6900, Saudi Arabia

Tel: +966-12-808-00701, E-mail: kazuhiro.ohkawa@kaust.edu.sa

Micro-LED displays are promising tools for the coming AR and VR usages and others. InGaN-based red micro-LEDs will be one of the keys to solving the cost issue in the production of the micro-LED displays. We are developing InGaN-based red LEDs and their micro-LEDs based on our original technologies [1-8]. Our target wavelength of the red LEDs is over 630 nm to meet the recommendation 2020 standard for 4K-televisions (TVs) and ultra-high-definition TVs.

Metalorganic vapor-phase epitaxial (MOVPE) growth of high-quality and high-In-content (In > 30%) InGaN is a key for the abovementioned red LEDs. We adopt four kinds of methods for the MOVPE growth of red LED structures: (i) our original micro-flow channel MOVPE method for the growth of high-quality InGaN [1, 2]; (ii) the pseudomorphic LED structures to compensate the strain in InGaN active region [3]; (iii) the hybrid structure to enhance red emission [4]; and (iv) the thick GaN under-layer to control strain [5].

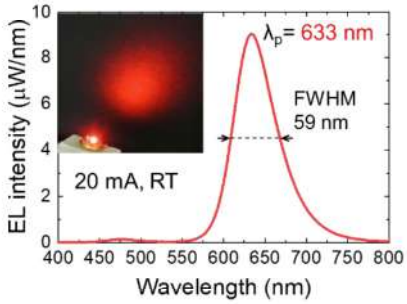

Fig. 1 An InGaN-based red LED.

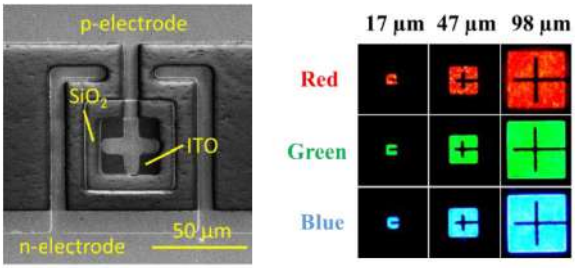

Fig. 2 SEM and optical microscope photos of RGB micro-LEDs.

Based on those technologies, we have realized InGaN-based red LEDs with peak wavelengths over 630 nm [5, 6]. Its temperature dependence of light output is stable. The characteristics temperatures of our InGaN- and InGaP-based red LEDs were 399 K and 304 K, respectively [7]. The peak wavelength shift of our red LED was as good as 0.066 nm/K that is less than half of that of the InGaP-based one [7]. Figure 2 shows the demonstration of RGB micro-LEDs at KAUST [8]. More details will be presented at IMID.

References

[1] K. Ohkawa, T. Watanabe, M. Sakamoto, A. Hirako, et al., J. Cryst. Growth **343**, 13 (2012).
[2] K. Ohkawa, F.Ichinohe, T.Watanabe, K.Nakamura, D. Iida, J. Cryst. Growth **512**, 69 (2019).
[3] D.Iida, S.Lu,S.Hirahara,K.Niwa,S.Kamiyama,K.Ohkawa, J.Cryst. Growth **448**, 105 (2016).
[4] D. Iida, K. Niwa, S. Kamiyama, and K. Ohkawa, Appl. Phys. Express **9**, 111003 (2016).
[5] D. Iida, Z. Zhuang, P. Kirilenko, M. Velazquez-Rizo, M. Najmi, K. Ohkawa, Appl. Phys. Lett. **116**, 162101 (2020).
[6] D. Iida, Z. Zhuang, P. Kirilenko, M.Velazquez-Rizo, K. Ohkawa, Appl. Phys. Express **13**, 031001 (2020).
[7] Z. Zhuang, D. Iida, and K. Ohkawa, Appl. Phys. Lett. **116**, 173501 (2020).
[8] Z. Zhuang, D. Iida, and K. Ohkawa, Opt. Lett. **46**, 1912 (2021).

Role of Intrinsic Surface States in Efficiency Attenuation of GaN-Based Micro-LEDs

Byung-Ryool Hyun, Fulong Jiang, Mengyuan Zhanghu and Zhaojun Liu
[1] **Department of Electrical and Electronic Engineering, Southern University of Science and Technology, Shenzhen, 518055, China**
Tel.:0086-0755-88018506, E-mail: Liuzj@sustech.edu.cn

The intrinsic surface effect on internal quantum efficiency (IQE) of gallium nitride (GaN) based micro-light emitting diodes (μ-LEDs) are numerically investigated in the wide size range of 1 - 300 μm. Due to the energy difference between the bulk Fermi level and surface states, electrons could diffuse to the surface and occupy the Ga-dangling bonds, leading to the surface depletion region and making the surface band upward bending. Valence band holes are naturally pushed toward the surface and are accumulated at the surface, resulting in a significant non-radiative recombination. Consequently, the intrinsic surface states affect remarkably the IQE of μ-LEDs with size of less than 30 μm due to the large surface-to-volume ratio, while the IQE of devices with size of more than 30 μm are relatively insensitive to the intrinsic surface states. In particular, the holes accumulation is more significant for μ-LEDs with size of less than 10 μm, resulting in a significant efficiency loss and the peak current density shifts to a higher value.

Fig. 1 shows the proposed mechanism of the effect of the intrinsic surface property on the efficiency of μ-LEDs. The dangling bond of the Ga and N atoms form two surface bands with the energy close to the CBM and VBM, respectively. As the carrier is injected into the QW, holes are driven by the surface depletion field and drift to the surface region, causing nonradiative recombination with the electrons occupied on the N-deprived states. Therefore, holes accumulation and nonradiative recombination at surface further deteriorates the device performance and results in a significant efficiency loss on the μ-LEDs with size of less than 10 μm. Our results strongly indicate that hole accumulation due to the upward bending of the surface energy band is the main physical mechanism for nonradiative recombination between the electrons occupied at N atoms of the surface and holes at the surface. Thus, we propose the passivation with purposive surface energy band engineering in the μ-LED fabrication process to improve the device performance of small-sized GaN-based μ-LEDs.

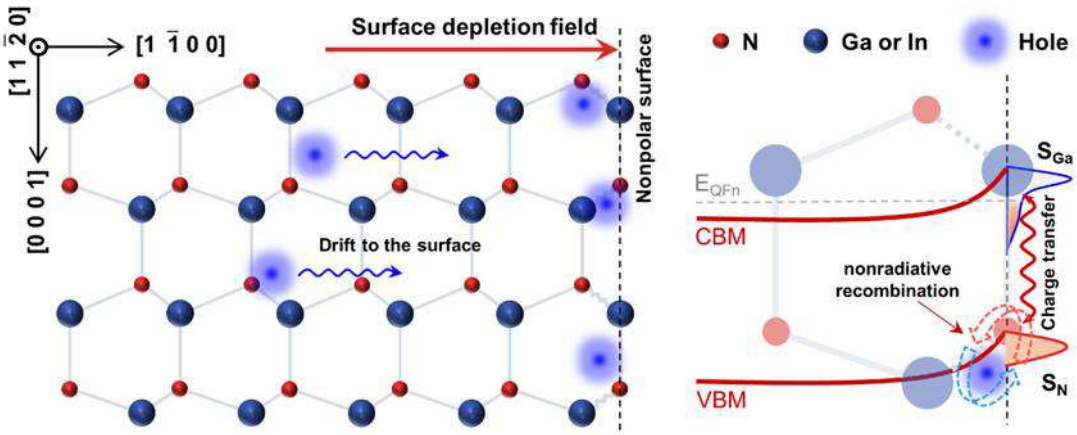

Fig. 1. The schematic diagram of surface recombination model

Acknowledgment

This work was supported by the Shenzhen Science and Technology Program (Grant No. KQTD20170810110313773) and the Guangdong Provincial Science and Technology Program (Grant No. 2018A050506002).

References

1. F. Jiang, B. R. Hyun, Y. Zhang and Z. Liu *Phys. Status Solidi RRL.*, 15(2), 2000487 (2021).

Efficient III-nitride LEDs for displays

J. J. Wierer, Jr., S. A. A. Muyeed, X. Wei, H. Xue, and R. Song,
Center for Photonics and Nanoelectronics, Dept. of Electric and Computer Engineering, Lehigh University, Bethlehem, PA 18015, U.S.A.
E-mail: jwierer@lehigh.edu

Light-emitting diode (LED) based emissive displays with high pixel density, luminance, efficiency, and large color gamut are of great interest for existing and emerging applications such as watches, phones, and virtual/alternative reality viewers. The pixel density and luminance requirements of emissive displays require a particular class of LEDs that are sub-20-micron in length called micro-LEDs[1]. State-of-the-art emissive displays use organic LEDs (OLEDs). Here an alternative is investigated using III-nitride LEDs with potential reliability and efficiency benefits.

In the first part of this presentation, we explore the performance, challenges, and prospective outcomes for III-nitride micro-LEDs targeted for efficient emissive displays[2]. Calculations merge models for colorimetry, displays, and III-nitride LEDs[3]. In the calculations, the display is formed from blue-, green-, and red-emitting III-nitride micro-LEDs using state-of-the-art performance. The display calculations allow us to determine the operating points for the micro-LEDs and the efficiency of the overall emissive display. We show that III-nitride micro-LEDs suffer from some of the same problems as their larger-sized solid-state lighting LED counterparts; however, the operating conditions of micro-LEDs can result in different challenges and research efforts. These challenges include — operating points tend to be at lower current densities and necessitates improvements in defect recombination; improving the efficiency of longer wavelength (green and red) LEDs; and creating device designs that can overcome low coupling efficiency, high surface recombination, and display assembly difficulties.

Next, we discuss recent advances in green- and red-emitting III-nitride LEDs, including work from our group on light-emitting active layers consisting of AlGaN/InGaN/GaN multiple quantum wells (MQW). Including the AlGaN interlayers on top of the InGaN quantum well results in higher efficiencies[4]. The AlGaN interlayer helps retain Indium, enables annealing of the quantum well, and provides strain balancing to prevent defect formation. We will show recent red-emitting LED results from our lab that exploit this design. Higher efficiencies are achieved by reducing non-radiative defect recombination. However, further improvements will require increasing spontaneous recombination rates, which are low due to inhomogeneities in the InGaN quantum well.

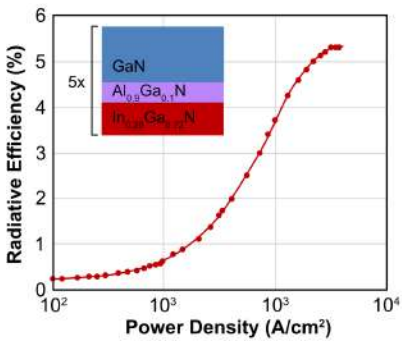

Fig. 1. Radiative efficiency versus power density of a red-emitting AlGaN/InGaN/GaN MQW.

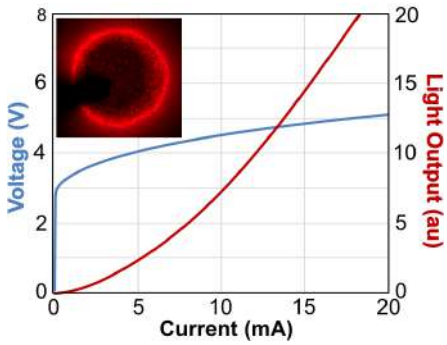

Fig. 2. Light and voltage versus current of a red LED. Inset: Top view through an opaque contact.

References

1. H. X. Jiang, S. X. Jin, J. Li, J. Shakya, and J. Y. Lin, "III-nitride blue microdisplays," Applied Physics Letters, 78, p. 1303 (2001).
2. J. Wierer and N. Tansu, "III-Nitride Micro-LEDs for Efficient Emissive Displays," Laser & Photonics Reviews, 13, p. 1900141 (2019).
3. J. J. Wierer, J. Y. Tsao, and D. S. Sizov, "Comparison between blue lasers and light-emitting diodes for future solid-state lighting," Laser & Photonics Reviews, 7, p. 963 (2013).
4. S. A. Al Muyeed et al., "Recombination rates in green-yellow InGaN-based multiple quantum wells with AlGaN interlayers," Journal of Applied Physics, 12, p. 213106 (2019).

Environmentally Robust Narrow-band Quantum Rods for Next Generation Solid -State Lighting

*C. Kang, M.F. Prodanov, P. Chaudhari, V.V. Vashchenko, A.K. Srivastava**

1. State Key Laboratory on Advanced Displays and Optoelectronics Technologies, Department of Electronics and Computer Engineering, The Hong Kong University of Science and Technology, Clear Water Bay, Hong Kong, China.

2. Centre for Display Research, The Hong Kong University of Science and Technology, Clear Water Bay, Hong Kong, China.

E-mail: eeabhishek.ust.hk

Power efficiency, color performance, and reliability are the three fundamental factors determining the performance of a light source. 20% of the generated electricity on the earth is consumed by domestic and industrial lighting applications [1]. In past years, people achieved great progress in replacing CFL and incandescent lamps with more energy-efficient LED lamps. The luminous efficacy (LE), which is defined by lumen flux divided by electric power, is used to evaluate the performance of a light source. A higher LE means more energy-savings over the long term of a lighting device by using less energy to deliver higher lumens. Use of the combination of different emitting wavelength, efficient luminous down-converters are necessary [2 3]. The commonly used phosphor-based white LEDs usually have LE ~100 lm/W and low CRI Ra=85 and R9=60, which is not suitable for modern applications. In this study, gradient alloyed CdSe/$Cd_XZn_{1-X}S$/ZnS quantum rods (QRs) with narrow emitting bandwidth are applied as a color conversion material on the blue LED for the solid-state lighting application. The Cd amount has been significantly reduced by replacing the CdS with ZnS in the core-shell quantum rods. The fabricated LEDs provide Ra=95 with high R9 up to 90 for CCT at 2700K with LE=84lm/W. Furthermore, these LEDs show the least temperature dependence, and therefore, these LEDs can be used for high-power lighting and display backlights.

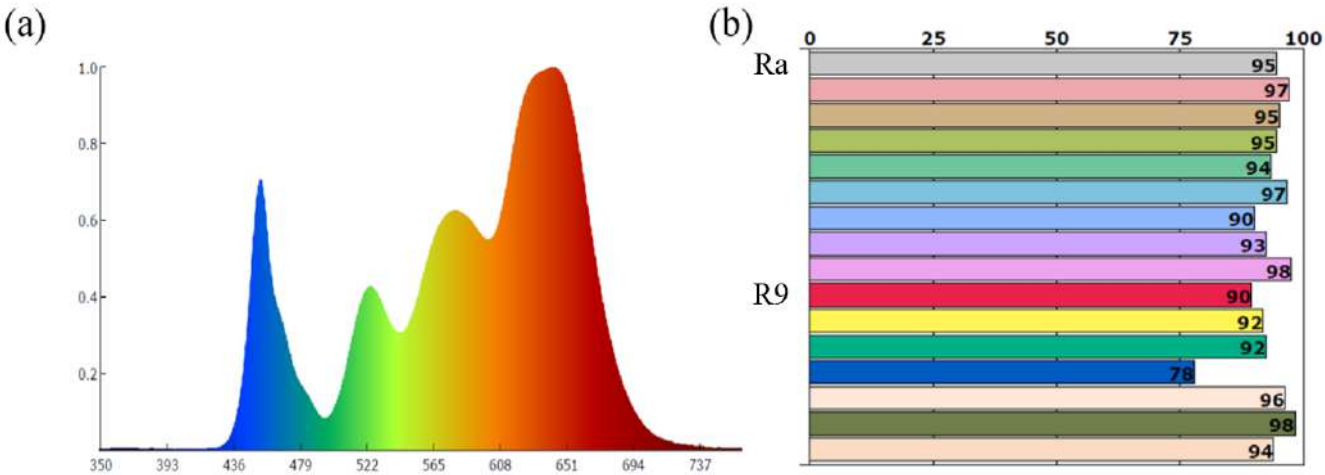

Fig. a) Spectra and b) CRI value of QR lighting

Acknowledgment

This work was supported by the RGC of Hong Kong SAR (Grant No. 26202019), 18191050 from Microlite Display Technology Ltd. Hong Kong, and the funding's for The State Key Laboratory of AdvancedDisplays and Optoelectronics Technologies.

References

1. Pattison, P. M., Hansen, M. & Tsao, J. Y. Comptes Rendus Physique 19, 134-145 (2018).

2. Prodanov, M. F. et al. Application. Small 17, 2004487 (2021)

3. Srivastava, A. K, Zhang, W., Schneider, J., Halpert, J. E. & Rogach, A. L. Advanced science 6, 1901345-n/a (2019).

A Study on the Enhancement of Blue Index through Spectrum Modulation for Top-emission Blue OLEDs

Liang Gao, Huiqing Pang, Xin Bi, Zheng Wang, Xiao Chen, Ray Kwong, Sean Xia*
Beijing Summer Sprout Technology Co., Ltd. Beijing, China
*Tel.:86-010-60860068, *E-mail: pang@summersprout.com*

The improvement of blue organic light-emitting devices (OLEDs) performance still remains as one of most significant challenges. The blue index (BI), defined as CE/ CIE y is commonly used as a figure of merit to characterize the efficiency of the blue devices. The efficiency of a top-emission OLED is found to be closely dependent on the electroluminescent (EL) spectrum shape of the emissive layer (EML) [1] [2]. We designed a series of artificial EL spectra of bottom emission blue OLEDs and simulated the BI values with them input in the top emission devices accordingly. The external quantum efficiency (EQE) of the bottom emission device is kept the same for all devices. Figure 1a shows that the maximum BI values of top emission devices increase significantly with the reduction of the shoulder peak at the long-wavelength side of the EL spectra. On the contrary, while keeping the shoulder on the long-wavelength side unchanged, shrinking of the short-wavelength side of the spectra has hardly any impact on BI, as seen in Figure 1b. This holds true even when the shoulder peak is eliminated (see Figure 1c). We believe suppressing the intensity of shoulder peak on the long-wavelength side of the spectra reduces resonant energy loss when transferred to top emission devices. Finally, we selected two synthesized fluorescent blue dopants BD1 and BD2 and built both top and bottom emission devices. Figure 2 shows the BI values as a function of CIE y from both experimental (open circular symbols) and simulation results (solid lines). Inset is the normalized bottom emission EL spectra of BD1 and BD2, where BD1 has a shoulder peak at 490 nm and BD2 has none. The BI of top emission devices using BD2 is 195 at CIE y=0.045, while that of BD1 is 176 at CIE y=0.051. Detailed device performances are summarized in Table 1. The experimental results agree very well with the simulation, which proves it is most essential to reduce the shoulder peak of the emitter spectrum on the long-wavelength side in order to achieve higher BI for blue OLEDs.

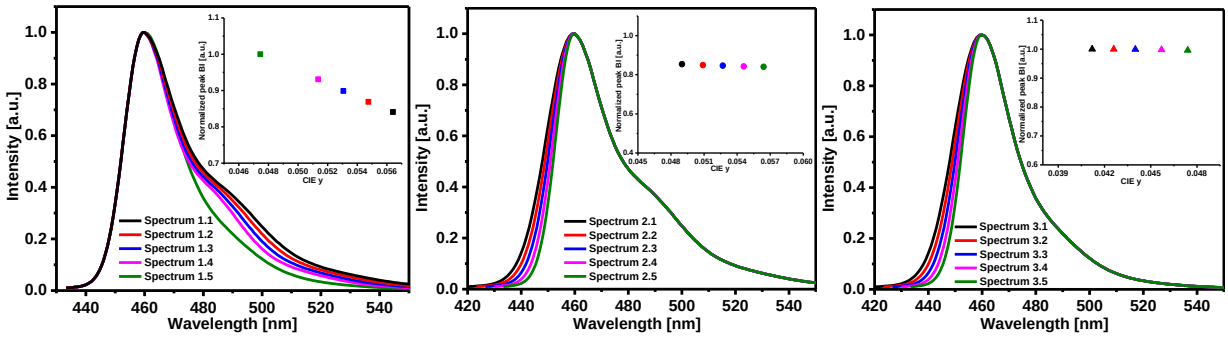

(a) (b) (c)

Fig. 1. A series of artificial EL spectra of bottom emission blue OLEDs (a) with reduction of the shoulder peak on the long-wavelength side, and with narrowing on the short-wavelength side with shoulder peak on the long-wavelength side (b) unchanged, and (c) eliminated. Insets are the simulated maximum BI values of top emission OLEDs as a function of CIE y associated with the spectra.

Table 1. Device performances of bottom and top emission blue OLEDs using BD1 and BD2 at a current density of 10 mA/cm^2.

	Bottom emission			Top emission		
BD	FWHM [nm]	EQE [Norm.]	λ_{max} [nm]	CIE y	CE [cd/A]	BI
BD1	28.4	1.00	461	0.051	8.72	176
BD2	23.9	0.99	461	0.045	9.04	195

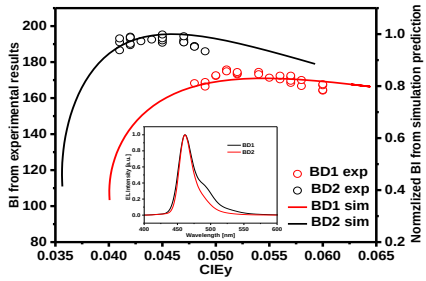

Fig. 2. BI from experimental (open circular symbols) and normalized BI from simulation (solid lines). Inset is the normalized bottom emission EL spectra of BD1 and BD2.

Reference

1. Takahashi, R., et al., SID Symposium Digest of Technical Papers, 51: 703-706.
2. Margulies, E.A., et al., SID Symposium Digest of Technical Papers, 50: 911-913.

Deep Input Normalization for Machine Sound Anomaly Detection with Convolutional Recurrent Neural Network

Hankyeol Lee, Jungwon Ryu, Euiyeol Oh, Changgone Kim, and Sooyoung Yoon
LG Display Co., Ltd, LG Science Park, Seoul, Korea
Tel.:82-2-8037-0978, E-mail: hankyeol.lee@lgidisplay.com

Machine maintenance is crucial in the display manufacturing factory to improve production capability and yield management. Since unexpected breakdowns or failures of machines cause huge costs, machine anomaly detection which detects anomalous before it breaks is an essential part of machine maintenance. In recent years, deep learning has been proven to be a powerful method in various tasks. However, there is a problem to apply deep learning to machine anomaly detection. There is little or even no abnormal data to train the deep learning network because most operations of the machines are in normal action.

To address this problem, we propose Deep Input Normalization with Convolutional Recurrent Neural Network. Our model is based on Autoencoder, which learns to produce the same output as a given input, training only with normal data. It is assumed that reconstruction error is low for normal data since the autoencoder is trained only with normal data while a high reconstruction error considers as an anomaly.

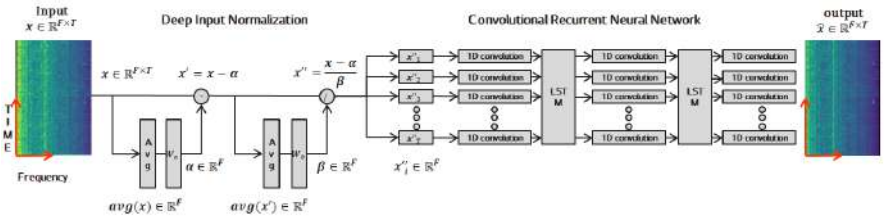

Fig. 1. Deep Input Normalization with Convolutional Recurrent Neural Network

As shown in Fig. 1, our model consists of Deep Input Normalization (DIN) and Convolutional Recurrent Neural Network (CRNN). First, the sound data is converted to Mel-spectrogram (Mel), which is a time-frequency representation of the sound. In DIN, given Mel $x \in \mathbb{R}^{F\times T}$, we estimate $\alpha \in \mathbb{R}^F$ and $\beta \in \mathbb{R}^F$ to perform input normalization. To obtain α, we calculate the average of the input through the time axis and multiply it by a learnable matrix $W_a \in \mathbb{R}^{F\times F}$. Then, we can get $\alpha = W_a \cdot ave(x)$. After that, we can get $x' = x - \alpha$ and obtain $\beta = W_b \cdot ave(x')$ with matrix W_b. Finally, normalized input is obatained by $x'' = (x - \alpha)/\beta$.

CRNN consists of 1-dimensional convolution layers (1D-conv) and Long Short-term Memory (LSTM). 1D-conv is applied for each time frame to extract features independent of time information. To incorporate temporal information of extracted features, LSTM is used. Mean Absolute Error (MAE) between input Mel and reconstructed Mel is employed for loss function to train the network. In the testing phase, the anomaly score of a test Mel data x is calculated by $\|x - \hat{x}\|$, where $\hat{x}$ denotes reconstructed Mel.

	Fan	Pump	Slider	Valve	Average
Baseline	65.83	72.80	84.71	66.24	72.39
Ours	**81.16**	**84.74**	**91.10**	**77.66**	**83.66**

Table. 1. AUC result of on the MIMII dataset

We evaluated our network on the MIMII [1] dataset given by DCASE 2020 task2 challenge. MIMII dataset consists of four types of machine sound. As shown in Table 1, our network achieved better performance than the baseline which is provided by DCASE 2020 task2. This result demonstrates that our network is effective to detect anomalies in the sound of machines.

References

1. Purohit, Harsh, et al. "MIMII dataset: Sound dataset for malfunctioning industrial machine investigation and inspection." arXiv preprint arXiv:1909.09347 (2019).

Pruning for an Image Restoration Network

Hyun-joo Hwang, Jaebum Cho, Daewook Kim, Jewon Yoo, Sujin Choi, Hyunjin Son, Sang-Gu Lee, Hyunguk Cho, Seungin Baek, Won-Hyouk Jang, Yongjo Kim, and Eunkyung Koh
Display R&D Center, Samsung Display, Gyeonggi-do, Republic of Korea
Tel.:82-31-5181-6776, E-mail: eunkyung.koh@samsung.com

Image restoration techniques based on deep learning have been intensively studied in display industry recently, for instance in [1][2] to restore degraded images captured by under panel cameras. However, the image processing rates had been measured on GPU or evaluated as less than 2.5 Hz on CPU for a FHD resolution image. The rate is inadequate to be applied to a real-time video system that is one of the most interesting applications.

We here aim to reduce the computation complexity of image restoration networks, measured by the number of MAC(multiplier-accumulator)s while sustaining the quality of image restoration. The inference time is generally proportional to the computation complexity, albeit not strictly proportional. We used PSNR (Peak Signal-to-Noise Ratio) as the metric for the quality of image restoration. Data is obtained both by experiments and computations based on ASM (angular spectrum method)[3] that simulates diffraction due to an optical element of a under panel camera. 29k image pairs are utilized to train networks where the size of images is 640 x 480 in pixels. For the evaluation, we take the average of PSNR over 1k image pairs in the test set.

Our baseline model is a modified UNet. The width and height of feature maps are halved/doubled in the 3 encoding/decoding blocks, and each block consists of multiple convolutional/normalization/activation layers and skip connections. The baseline model showed 28.8 BMACs, and PSNR 39.1dB. We implemented a random search on the number of channels to result in 19.0 BMACs and PSNR 39.7 dB. In turn, we prun a channel with the smallest sum of kernel weights in one iteration, retrain the network for 30 epochs, then iterate the pruning/retraining process. Pruning indeed improved the image restoration quality for the first few iterations. After 19 iterations, the network showed 12.3 BMACs and PSNR 39.5 dB that corresponds to 57.3% of reduction of computatin complexity without decrement in the image restoration quality from the baseline.

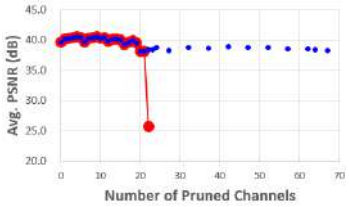

Model	BMACs	PSNR (dB)	Latency (%)
Baseline	28.8	39.1	100
Random Search	19.0	39.7	86.3
Pruning	12.3	39.5	56.7
Restricted Pruning	3.2	38.3	24.2

Fig 1. (Left) A graph that shows the average PSNR of the test set versus the number of pruned channels. (Middle) Image examples (Right) Summary of the results

Let us discuss a few observations and conclude. At the 21st pruning, the PSNR drops from 38.2 to 25.7 when one of the numbers of the channels becomes less than 3 (see the red line of the left graph, Fig.1). Suspecting that this is due to information loss, we imposed a restriction on the prunning process to leave more than 3 channels in every layer. With the restriction, pruning could proceed to 66 iterations, resulting in a 3.2 BMACs network with PSNR 38.3 dB (blue dots in the graph, Fig.1). Image samples are shown in Fig. 1. Note that the network not only restores degradation due to diffration but also removes a glare due to the saturation of the image sensor. The table in the right side of Fig.1 summarizes our results. The latency was measured 5 times for 100 images on Intel CPU i5-6500, then averaged. Although our pruning method could reduce the computation complexity and latency considerably, future works are required for further accelerations.

References

1. Y. Zhou et al., Image Restoration for Under-Display Camera, arXiv:2003.04857 (2020)
2. Y. Zhou et al., UDC 2020 Challenge on ImageRestoration of Under-Display Camera: Methods and Results, arXiv:2008.07742 (2020)
3. Goodman J.W, Introduction to Fourier Optics, Roberts and Company Publishers (2005)
4. H. Li et al., Pruning Filters for Efficient ConvNets, arXiv:1608.08710, ICLR (2016)

Development of 3D Crosstalk Classification Model Using Deep Learning

Young-Sang Ha, Je-Hong Ryu, Beom-shik Kim and Young-Chan Kim
Advanced Research Team, Samsung Display, Yongin-si, Gyeonggi-do 17113, Korea
Tel.:82-31-5181-6667, E-mail: y.ha@samsung.com

Among the methods for implementing a glassless 3D display, light field display (LFD) is one of the methods that combines a panel and a lenticular lens array (LLA) to produce three-dimensional images. The LFD uses a 3D crosstalk(X-Talk) evaluation method to evaluate image quality of 3D images. The 3D X-Talk evaluation method is a method for determining the quality of 3D image after measuring the LFD spatial luminance distribution to calculate the X-Talk value of the binocular image. In order to acquire LFD spatial luminance distribution, the camera acquires images for each viewpoint projected on the reflective screen surface. As the number of viewpoints increases, the number of images to be acquired increases. In addition, if you need to obtain image data for the entire reflection screen, the number of image data to process increases exponentially. This requires a faster and more accurate classification model to classify X-Talk levels in the quality inspection process for commercial LFD product production (Fig. 1). Therefore this paper proposes the development of a 3D X-Talk classification model using deep learning. Secures the X-Talk image data of various LFD products and classifies classes for each image feature. After image labeling and feasibility evaluation to utilize the deep learning model as a learning image, the performance of the model was improved and the platform was developed (Fig. 2). In summary this paper proposes the development of a deep learning classification model to shorten 3D X-Talk evaluation time and improve evaluation accuracy.

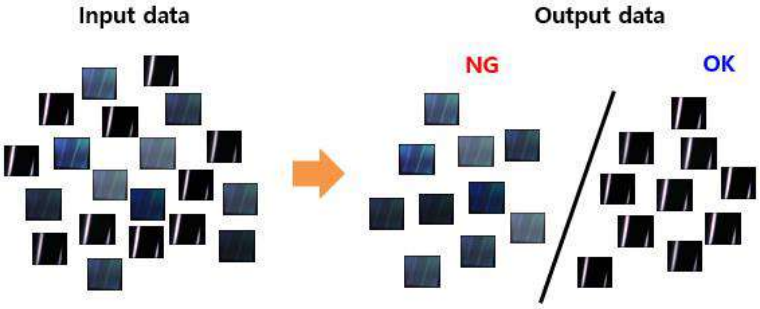

Fig. 1. 3D X-Talk images classification.

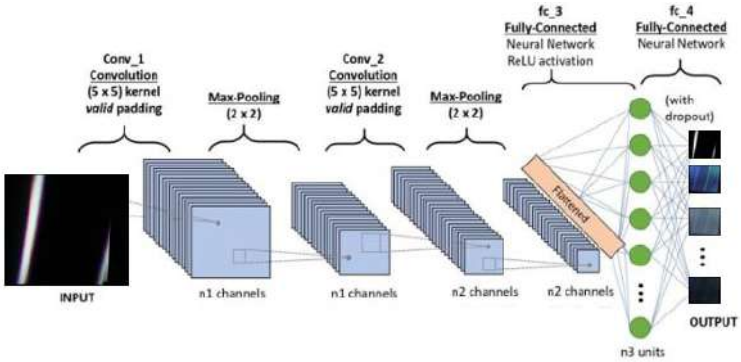

Fig. 2. Images classification process using deep learning.

References

1. S. PalaR. StevensP. Surman, *SPIE Optical crosstalk and visual comfort of a stereoscopic display used in a real-time application*, 6490 649011 (2007)
2. M Manoj krishna, M Neelima, M Harshali, M Venu Gopala Rao, *SPC Image classification using Deep learning*, p. 614-617 (2018).

Beyond Human Inspection: Focusing Networks for Review System

Eui-Young Jeong[1], Jong-Myong Choi[1], Hanaul Noh[2], and Pilho Kim[1]
[1]AI Team, [2]Inspection Equipment Development Team
Samsung Display, 1 Samsung-ro, Giheung-gu, Yongin-si, Gyeonggi-do, South Korea
E-mail: imate.jeong@samsung.com

This paper proposes an AI-based Review System (RS) algorithms for general purposes in the product inspection. RS takes and inspects images in high-resoultion multi-channel to find product defects and its physical layer location aiming to replace the human assistance in the inspection stage.

The proposed Focusing Networks is an ensemble model composed of cascaded convolutional autoencoder models to find the best focused images. Using the spatial information of focused images, our algorithm identifies if the defect exists on the surface or in the internal of product. When classified as an internal, RS determines whether the size of the defect is in and out of required specification. If classified as a surface defect, the contamination and the type of defect are estimated. The overwhole inspection process of RS is shown in Figure 1.

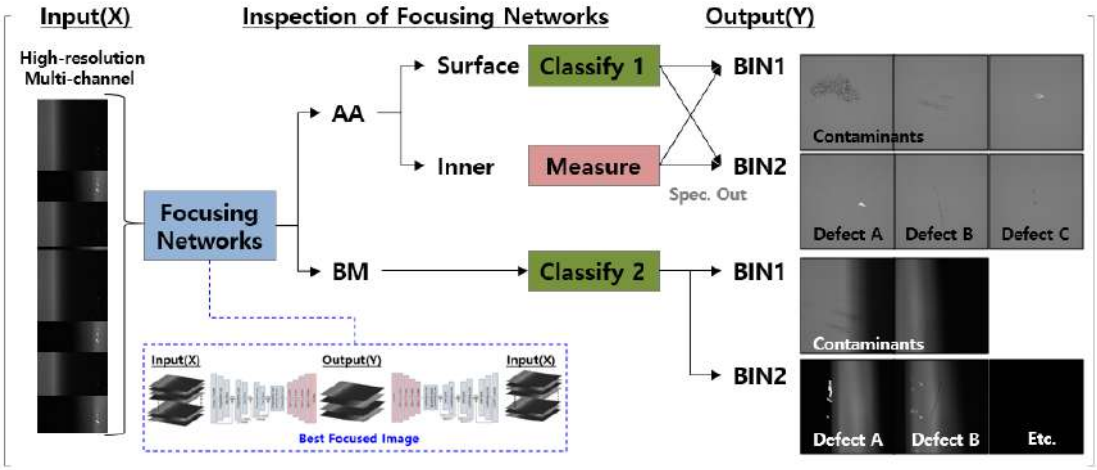

Fig. 1. AI-based Inspection Model for Review System

We built up a pilot application to test two different products and two RS lines. The ratio of BIN1 determination by RS re-inspection achieves 54.1% and 56.5%, respectively, which exceeds the current human inspection peformance. Our proposed model also achieves similar BIN1 conversion rate for different products. This convinced us that the AI-based RS inspection model with one recipe can be applied to various products.

Moreover, the proposed inspection model shortens the time to reach the optimal performance comapred to the existing computer vision-based inspection algorithm when inspecting product types are changed. Typically computer vision-based algorithms take a long time to develop algorithms for new defect types and set criteria, whereas our AI-based RS inspection model can learn defects in real time. So that RS can achieve the optimal inspection performance in a short period of time comparable to human's adaptation time for an new product. Also unlike human assistance, RS can qucikly extend its coverage by simply adding more computing power. In conclusion, the proposed AI-based inspection model and Review System is expected to overcome the limitations of the existing automatic visual inspection.

References

1. SZEGEDY, Christian, et al. Going deeper with convolutions. In: Proceedings of the IEEE conference on computer vision and pattern recognition, p. 1-9. (2015).
2. CHOLLET, François. Xception: Deep learning with depthwise separable convolutions. In: Proceedings of the IEEE conference on computer vision and pattern recognition, p. 1251-1258. (2017).
3. LONG, J. et al. Fully convolutional networks for semantic segmentation. Proceedings of the IEEE conference on computer vision and pattern recognition, p.3431-3440. (2015).
4. GUNNING, David. Explainable artificial intelligence (xai). Defense Advanced Research Projects Agency (DARPA), nd Web, 2: 2. (2017).

Efficiently Generate Train Data with Uncertainty of Prediction Values

Daewoo Myoung[1], Won-Hyouk Jang[1], Yoonjung Chai,[1] Wonjun LEE[1] and Chol Ho Kim[1]
[1]Samsung Display, Korea
Tel.:82-10-6799-4781, E-mail: dw0916.myoung@samsung.com

This paper proposed a methodology to effectively create a machine learning model to replace simulation. In the display and semiconductor manufacturing industry, a lot of simulation work is required during the product development process. In the past, engineers simulated for verification after product development, but nowadays, products are developed by optimizing various factors through many simulations from the early stages of development. Therefore, the number of iterations of the simulation required has increased dramatically. We need to reduce simulation time due to the large number of simulation iterations. That's why we want to replace simulation with machine learning and deep learning models. We need to generate training data through simulation. However, if the tact time to simulate is taking a long time, we have to put a lot of effort into generating the data the model needs. We propose a method of generating additional data that can improve the metric of the model with less data by using the uncertainty of the predicted value of the model. In addition, we propose a method to replace the simulation with only predicted values with low uncertainty.

The uncertainty of the machine learning model is calculated as Fig. 1 (a) by learning the K-fold emsemble model and using the predicted values of each single model [1]. Simulation data generation is generated by sampling the values with high uncertainty among the predicted values of the previous model, as shown in Fig. 1 (b) This will gradually improve the model's metric score. As a result, as shown in Fig. 1 (c), this method increases R^2 faster than adding it by random sampling.

Also, as shown in Fig. 1 (d), we can divide a section with a high metric and a section with a low metric according to the uncertainty threshold value. Using this, we can selectively replace only values with low uncertainty among model predicted values. We use simulation values for the model predicted values with high uncertainty. This way, we can use it even if the metric score of the initial model is insufficient.

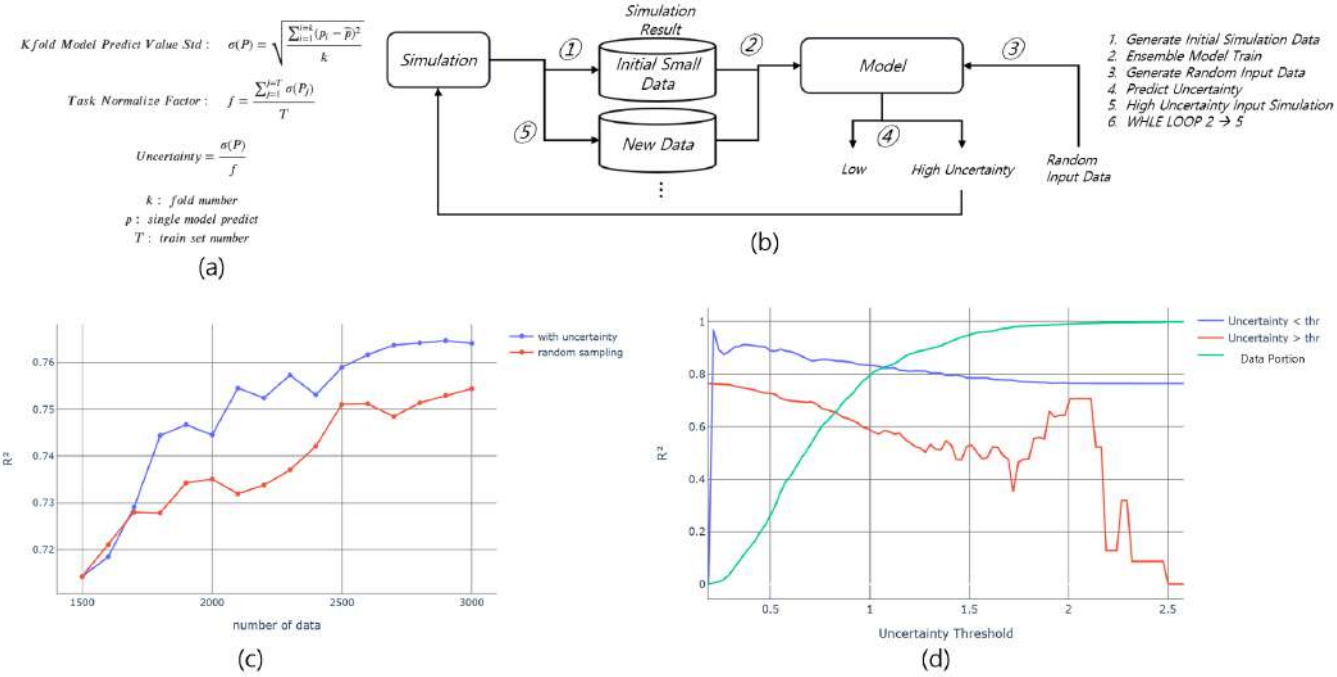

Fig. 1.(a) Uncertainty of Prediction Values, (b) Efficiently Generate Train Data with Uncertainty, (c) Sampling with Uncertainty vs Random Sampling, (b) Data Portion and R^2 with Uncertainty

References

1. Balaji Lakshminarayanan, Alexander Pritzel, Charles Blundell (2017, Nov). Simple and Scalable Predictive Uncertainty Estimation using Deep Ensembles

A Study on the Simulation Automation and Design Improvement of PCB for Display

Jiwon Kim, Jungsoo Youn, Hyochul Lee, Insoo Wang and Yongjo Kim
CAE Team, Samsung Display, Gyeonggi-do, Korea
Tel.:82-31-5181-6797, E-mail:jiwons.kim@samsung.com

The resolution and frequency of displays are increasing, so the PCB design is also becoming more complex and important. In this paper, we describe a technology that can quickly perform automatic simulation using 2.5D-based software. And by using the technology, the design of PCB for high frequency display was improved.

First, the technology that improves the simulation accuracy of 2.5D-based software to the level of 3D-based software will be described. The mobile display is thin, so a flexible pcb is used. In general, it is designed with meshed ground for impedance matching in thin thickness. However, since the 2.5D-based software calculates the impedance only with the ground in the vertical direction, it is inaccurate when the ground is a mesh type. It was improved by including virtual ground modeling in the simulation. It is optimization of the design of the virtual ground by using the metal thickness, dielectric thickness, mesh line width and void size. As a result, the simulation time was reduced from 24hours to less than 1hour with R^2=0.92 of s-parameter compared to mesurement.

We developed a PCB simulation automation platform that includes accuracy improvement technique. PCB designers spent a lot of time setting up the simulation environment and analyzing the results. So we standardized the simulation process and automated it using the tool command language. In addition, we decided the SI and PI Spec, and made the result analysis automatically reported.

Finally, we improved the design of PCB for display using this platform. The insertion loss of the signal nets was improved by optimizing the ground design and dielectric thickness, and the coupling defects between the signal nets were improved by optimizing the spacing. Designers can automatically analyze simulation results and get quick feedback on design optimization. In addition, it is possible to shorten the schedule of product development by obtaining an accuracy similar to that of 3D-based software with fast simulation time.

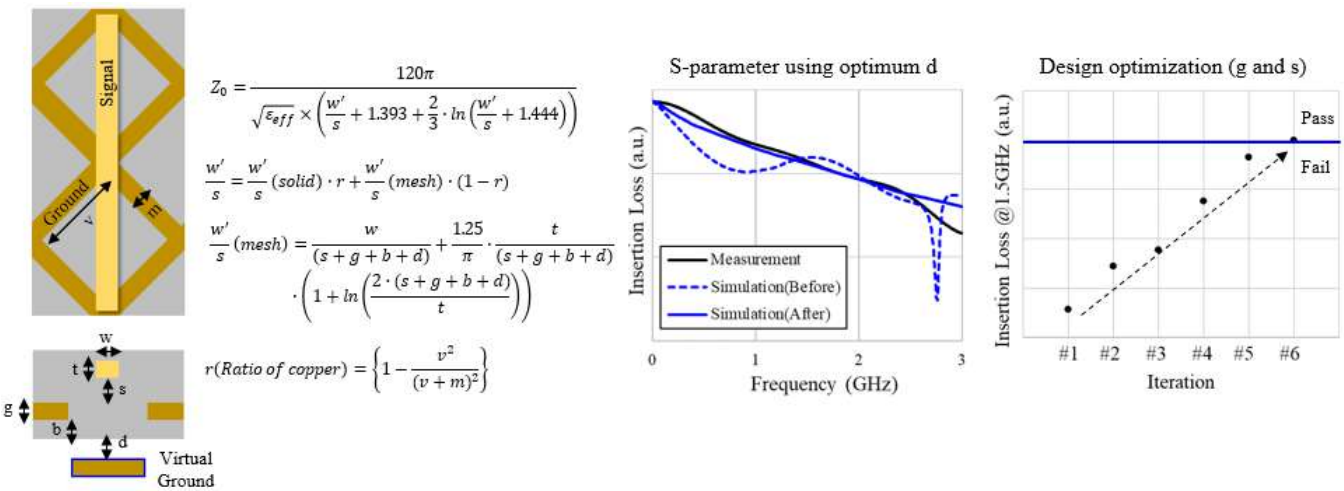

Fig. 1. Improved equation and design optimization

References

1. Silva, Zachary J., Christopher R. Valenta, and Gregory D. Durgin. "Design and characterization of meshed microstrip transmission lines." *2019 IEEE MTT-S International Microwave Symposium (IMS)*. IEEE, 2019.
2. Yu, Tiejun, Jian Chen, and Chiawen Shih. "Efficient methodology for modeling structure of high-speed long transmission lines." *2015 IEEE 24th Electrical Performance of Electronic Packaging and Systems (EPEPS)*. IEEE, 2015.

Automatic Measurement with TEM/FIB Images by Convolution Neural Network

Seokkwon Kim, Taesoek Jeong, Kyunghun Shin, Junghoon Jo, Seungin Baek and Yongjo Kim
CAE Team, Samsung Display, Gyeonggi-do, Republic of Korea
Tel.:82-31-5181-7992, E-mail: seokkwon.kim@samsung.com

There are many successful deep neural networks for semantic segmentation. Especially, a number of FCNs [1] based on feature fusion networks are proposed to improve the segmentation performance like U-Net [2], RESUNet [3] etc. We show experimental results on semantic segmentation models(U-Net, RESUNet, USE-Net [4]) for measurement with transmission electro microscope (TEM) and focused ion beam (FIB) images. Among them, we selected the best effective model, that was further improved with inception blocks [5].

We considered three segmentation models, U-Net, RESUNet, USE-Net. These models have been developed as various medical segmentation tasks. Because most features between medical and TEM/FIB images are very similar, such as color composition of data set, unclear boundries and the points that networks focus on a specific part of the image for tumors in medical images, or target layers in FIB/TEM images. Therefore, we applied them for TEM/FIB measurement tasks. Additionally, we used weighted loss function from groud truth for detecting precise edges, and apply inception blocks into USENet backbone architecture for improving network's capability. The comparison of each model is illustrated in Fig.1.

The networks based on U-Net detect each area effectively, and all models achieve above 92% of accuracy. The result of USENet has better performence than U-Net and RESUNet. In USENet, soft self-attention SE(Squeeze-And-Excitation) blocks [4] make the network more effective in classifying similar contextures of electron microscopy. Our USENet model achieved 98.05% of accuracy with test images, and USENet(+inception block) has been improved the accuracy up to 98.06%.

In this paper, we developed segmentation network to segment TEM/FIB images, which was effective for detecting their structures. Also the USENet(+ inception) model show high performance in finding edge on the TEM/FIB images.

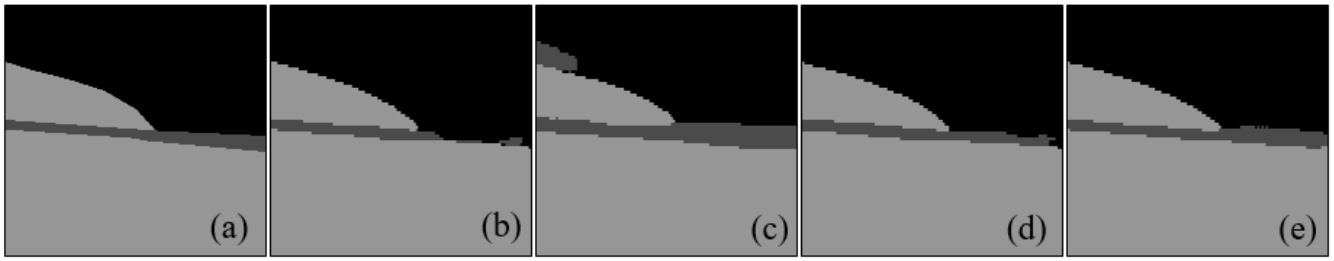

Fig. 1. Comparison of each model. (a) Ground Truth, (b) U-Net(accuracy 98.02%), (c) RESUNet(92.32%), (d) USE-Net(98.03%), (e) USE-Net(+inception block)(98.06%)

References

1. J.Long, E.Shelhamer, and T.Darrell. "Fully Convolutional Networks for Semantic Segmentation", in *CVPR, 2015* (2015).
2. O.Ronneberger, P.Fischer, and T.Brox, "U-Net: Convolutional Networks for Biomedical Image Segmentation", in *MICCAI*, pp. 234-241, Springer (2015).
3. X. Xiao, S. Lian, Z. Luo and S. Li, "Weighted Res-UNet for High-Quality Retina Vessel Segmentation," in *9th International Conference on Information Technology in Medicine and Education (ITME)*, pp. 327-331, (2018)
4. L. Rundo, C. Han et al., "USE-Net: Incorporating Squeeze-and-Excitation blocks into U-Net for prostate zonal segmentation of multi-institutional MRI datasets", in *Neurocomputing(vol. 365),* pp.31-43, (2019)
5. C. Szegedy, et al., "Going deeper with convolutions," in *CVPR 2015*(2015)

Full IR-drop Simulation with Display Adapted Solve Methods for High Resolution OLED Display Panel

Chol Ho Kim[1], Won Jun Lee[1], Hae Ryeong Park[1], Yongwoo Lee[1], and Yongjo Kim[1]
[1]**Display Research Center, Samsung Display Co., Ltd , Samsung-ro 1, Gihrung, Yongin, Korea**
Tel.:82-31-5181-6798, E-mail: railroads.kim@samsung.com

OLED display has been widely used recently for the high definition and large-sized display [1]. High resolution OLED panels have more than 1-billion-pixel elements, and complexity of the wiring connection. As the complexity of the wiring increases, the problem of power wiring and influence analysis becomes serious when analyzing the panel. This makes it more important to accurately and efficiently predict the voltage analysis of the pixel power in the panel, that is, the IR-drop deviation. In the panel analysis, IR-drop refers to the voltage difference in both sides of the load when the current is applied to the power and load connection circuit [2].

The IR-drop analysis in the full panel must solve the entire circuit node and uses numerical parsing-based distributed computing technology. As shown in Fig. 1 (a), one matrix (M) is divided into certain regions and connection matrix (C_M) is generated for connection analysis between the divided matrices. After analyzing individual matrix, iteration is calculated until the boundary value between each matrix becomes saturation through connection matrix (C_{MN}). However, in the high-resolution panel, the number of connection matrix increases exponentially, there are limitations such as analysis speed and memory [3]. To overcome the analysis speed, the number of solving iterations must be reduced.

This paper shows a Mini batch DB that configures the entire panel into a certain area as shown in fig. 1 (b). It gradually increases the analysis area density of the DB to obtain the initial initialization value of the circuit analysis quickly. This method predicts the initial value of each node in advance without analyzing the full panel through the change slope of the value interpreted in the DB. The initialization value obtained by prior prediction can be used to reduce the number of iterations during matrix operation to shorten the full panel analysis TAT. Fig. 1. (c) shows the flowchart of matrix solving methods for full panel IR-drop circuit analysis. Each step of analysis consists of a circuit matrix composition step, a matrix calculation step, and an initial condition-based matrix solve. The proposed method reduces the number of iterations up to 1 / 10 times according to the mini-batch DB analysis. To demonstrate the performance of proposed methods, a full pixel array circuit of QUHD (8K) OLED panel was formed, and simulation time show that 80% of reduction was confirmed as shown in Fig. 1 (d).

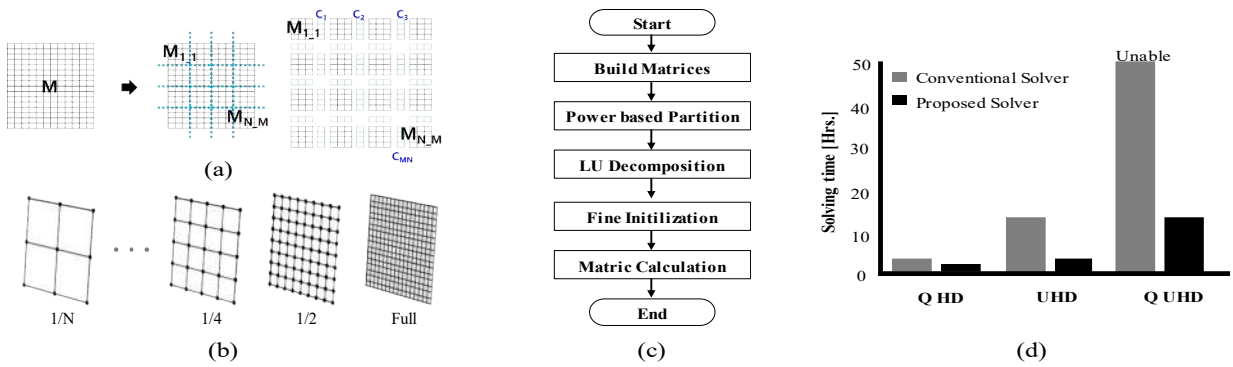

Fig. 1. (a) Numerical matrix partition, (b) Fine initial condition using mini-batch DB, (c) Flowchart of proposed matrix solver, (d) Experimental results of IR-drop analysis

References

1. C.-J. Lee, et al., A Study on a Lattice Resistance Mesh Model of Display Cathode Electrodes for Capacitive Touch Screen Panel Sensors. *Procedia Engineering,* 168, 884–887 (2016)
2. Y Rius, J. Dept., IR-Drop in On-Chip Power Distribution Networks of ICs With Nonuniform Power Consumption, IEEE Trans. Very Large Scale Integration (VLSI) Systems, 21, 3 (2013)
3. Pi Sheng Chang, Analysis of Conjugate Gradient Algorithms for Adaptive Filtering. IEEE Transactions on Signal Processing (Volume: 48, Issue: 2 , Feb 2000)

A Study on the Dimensional Accuracy of Super-Resolution SEM Images Upscaled by Deep Learning

Hyunjoo Hwang, Daewook Kim, Sujin Choi, Jewon Yoo, Eunkyung Koh, Hyunsang Seo, Hyunguk Cho, Seungin Baek, Yongjo Kim, and Jaebum Cho
Display R&D Center, Samsung Display, Gyeonggi-do, Republic of Korea
Tel.:82-31-5181-6949, E-mail: jaebum.cho83@samsung.com

High-resolution was usually performed using linear interpolation or polynomial-based interpolation techniques. These techniques can generate high-resolution images with relatively little complexity and computational amount, but it is difficult to implement high-resolution image from a complex and nonlinear low-resolution image. High resolution scanning electron microscope (SEM) images are required to obtain high accuracy for failure analysis or length measurement. Unfortunately high-resolution SEM images are time-consuming and expensive. In this paper, we attempt to upscale a low-resolution SEM image to a high-resolution image using a deep learning-based super-resolution algorithm, and verify whether it is possible to achieve higher dimensional accuracy.

SRGAN[1] was used to restore the low-resolution SEM image. For training, we obtain the low-resolution images (100 × 100) by down-sampling the 6,000 high-resolution SEM images (1200 × 1200), and random noise is added to make it look similar to an actual low-resolution SEM image. Each network was trained with 4x/6x upscaling factor. Fig.1 shows the results of improving noise and sharpness of the real low-resolution SEM image with SRGAN. However, some details already lost in the low-resolution image could not be restored. These distortion affect to length measurement as shown in Fig. 1.

The accuracy of measurement of length has been advanced up to 0.35% with generation of high-resolution image by SRGAN(with 4x upscaling factor) compare to the low-resolution SEM image. Since network is trained only with SEM images of the same region in samples, it was expected that the network can estimate the ground truth. However, as a result so far, single-shot super-resolution technique was not enough to enhance the measurement precision. Further study is required to overcome this limit.

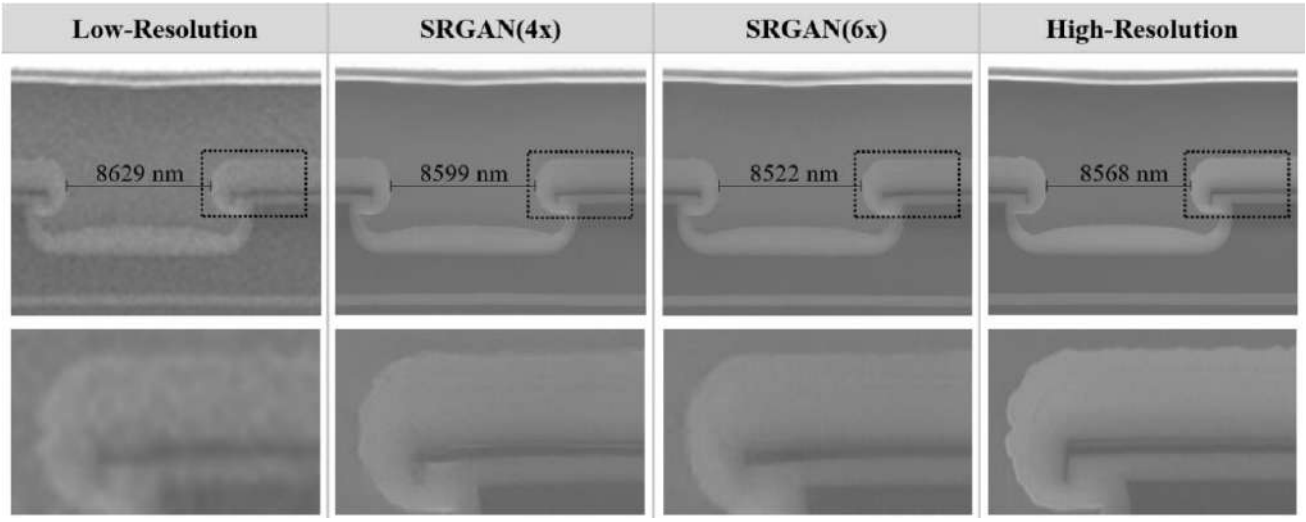

Fig 1. In the real low-resolution SEM image, noise is severe and sharpeness is remarkably low due to short exposure. Noise and sharpness of the image are enhanced by SRGAN. However, the details that were already lost in the low-resolution image is not restored. It makes the difference in the length measurement.

References

1. C. Ledig, L. Theis, F. Huszar, J. Caballero, A. Cunningham, A. Acosta, A. Aitken, A. Tejani, J. Totz, Z. Wang, W. Shi, Proceedings of the IEEE Conference on Computer Vision and Pattern Recognition (CVPR), pp. 4681-4690 (2017)
2. W. Shi, J. Caballero, F. Huszár, J. Totz, A.P. Aitken, R. Bishop, and Z. Wang, Proceedings of the IEEE conference on computer vision and pattern recognition (CVPR), pp. 1874-1883, (2016).

A Study on the Evaluation Index of Glare Restoration Performance based on Deep Learning

Jewon Yoo, Sujin Choi, Hyunjoo Hwang, Daewook Kim, Hyunguk Cho,
Seungin Baek, Yongjo Kim, and Jaebum Cho
Display R&D Center, Samsung Display, Gyeonggi-do, Republic of Korea

Under-panel camera(UPC) is a new technology that enables full screen display by installing a camera under the panel. However, in the UPC structure, image quality degrades due to diffraction of incident light caused by the panel in front of the camera. In particular, when strong light is incident, the phenomenon of glare appears. Glare appears as a star-shape when strong light is diffracted. Information is lost in the glare area due to the limitation of acceptance capability of camera sensors. For this reason, while the diffracted blurry image can be reconstructed with the traditional deconvolution method, the glare cannot be reconstructed. Therefore, a deep learning-based image restoration technology is being actively researched to restore glare. Quantification is very important in the study of glare restoration technology to evaluate restoration performance.

In this paper, various image quality assessment (IQA) were compared and analyzed to quantify the glare restoration level. For the analysis, the reconstructed image according to the number of channels of U-Net implemented for glare restoration was used. In general, the glare restoration quality is improved as the number of channels increases. In our experiment, mean deviation similarity index (MDSI) shows most reliable results to rate quality of the restoration. Since MDSI is composed of the sum of two elements, gradient and chromaticity, it is easy to compare RGB images.

$$\text{MDSI} = \alpha \cdot \underline{\text{Gradient Similarity}} + (1-\alpha) \cdot \underline{\text{Chromaticity Similarity}}$$

Fig. 1. Mean Deviation Similarity Index Equation

The analysis was based on 19 sets of restored glare images. As a result, MDSI has an almost linear relationship for their computational load, as shown in Fig 1. When applied as a loss function of deep learning for glare restoration, it is expected to improve restoration performance.

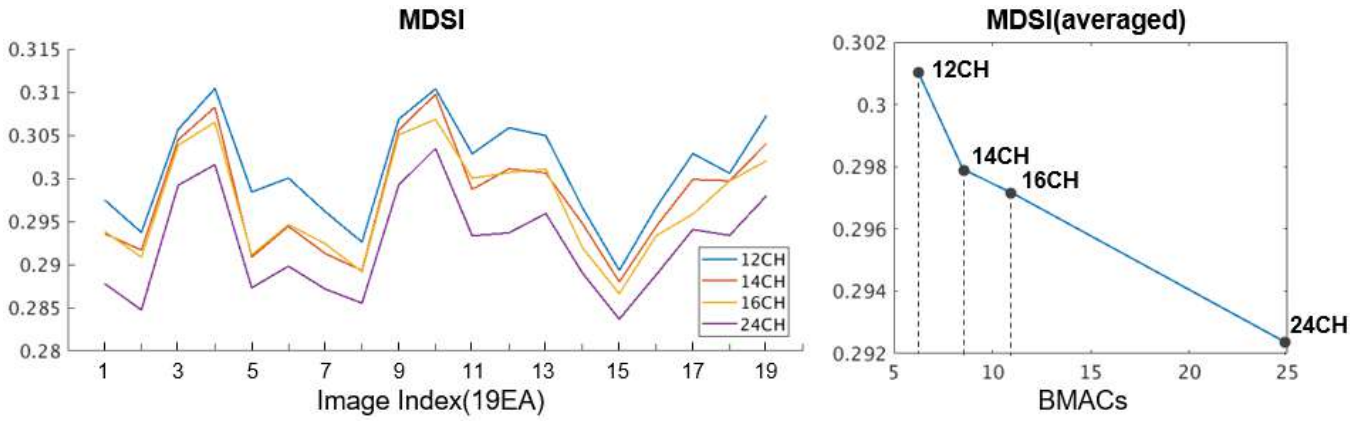

Fig. 2. MDSI comparison graph according to the number of U-net channels

References

1. Nafchi, Hossein Ziaei, et al, Mean deviation similarity index: Efficient and reliable full-reference image quality evaluator. *Ieee Access*, 4, p. 5579-5590(2016).
2. Belthangady, Chinmay, and Loic A, Applications, promises, and pitfalls of deep learning for fluorescence image reconstruction, *Nature methods*, 16.12, p. 1215-1225(2019).
3. Ronneberger O, Fischer P, Brox T. U-net: Convolutional networks for biomedical image segmentation. *International Conference on Medical image computing and computer-assisted intervention*. Springer, Cham, p. 234-241(2015).

Design Automation and Verification Platform of PCB for Display

Younyee Kang, Sungkwon Kim, Yongsang Cho, Jiwon Kim, Insoo Wang and Yongjo Kim
CAE Team, Samsung Display, Gyeonggi-do, Republic of Korea
Tel.:82-31-5181-6752, E-mail: younyee.kang@samsung.com

As the customer's needs are gradually diversified and the product is rapidly becoming high-performance, it is important to complete the development within a short period of time and to ensure stable quality without problems in mass production.

In order to secure stable quality within a short period of time considering the high performance of the product and the gradually shortening product life cycle, human errors should be eliminated from the initial design drawings through various DRC reflections, design Utility should be developed, and the function of frequently used should be automated and pre-simulation should be possible automatically.

Since the display module is delivered to customers in a non-completed state and is evaluated after assembling the set, it is necessary to establish a platform structure that can be confirmed in a place that is standardized, automatic design, design rule check, and pre-simulation to secure stable module quality in a short period of time.

In order to verify the characteristics of the PCB before the PCB design is made in the library with CAD Tool, a platform structure is created using the Skill Language, which can control the information of the design drawing, and the items are automatically designed and automatically verified according to the product.

It very efficiently can check in the quality inspection as well as the structural inspection it is heteromorphic at the PCB manufacture former design step the advance and the potential routing problem can be rapidly distinguished.

To secure reliable PCB quality, it is possible to perform the items that the designer manually verified for a long time automatically and automatically for a short time by constructing a PCB design verification automation platform to expand the design automation rate (△51%), reduce the design TAT (▽29%).

As the product is aiming for high performance, it is necessary to have complex specifications and a heterogeneous structure, but it is expected that the limitations of display module production will be overcome by constructing an automatic verification platform that predicts design constraints.

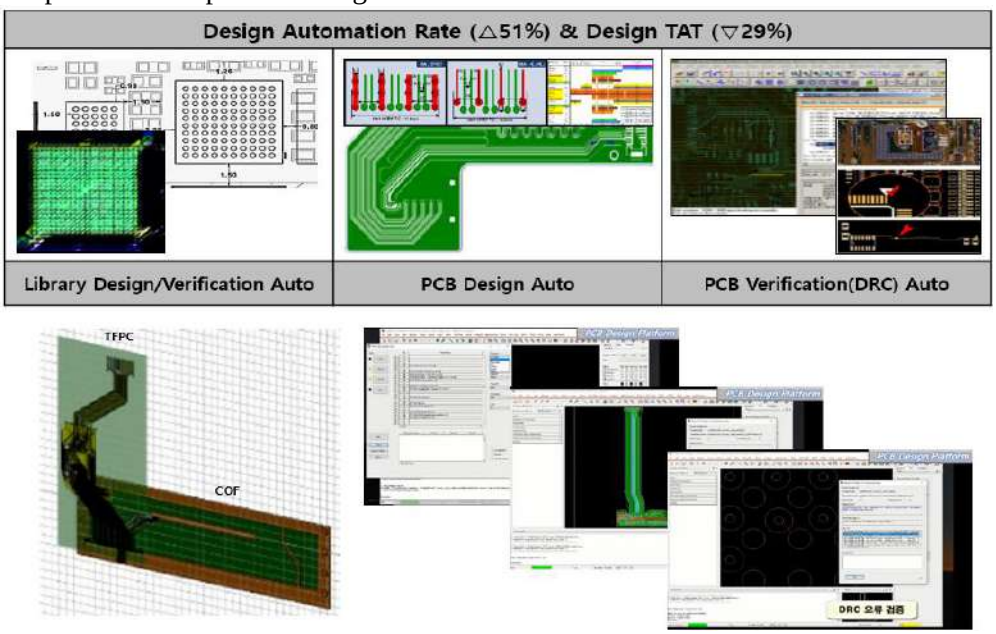

Fig. 1. Design Automation and Verification Platform

References

[1] Jimmy Hsu Fast Signal Integrity Methodology for PCB pre-layout analysis and layout quality check 2013 IEEE 63rd Electronic Components and Technology Conference

[2] Kang, Y. Y. Prediction of the Characteristics and Effect of Grounding Signal Intervals through Antenna Simulation. 2009 Spring Conference Korean Semiconductor and Display Equipment Society

Fast Image Restoration for Under-Panel Camera

Daewook Kim, Sujin Choi, Jewon Yoo, Hyunjoo hwang, Hyunguk Cho,
Seungin Baek, Yongjo Kim, and Jaebum Cho
Display R&D Center, Samsung Display, Gyeonggi-do, Republic of Korea
Tel.:82-31-5181-6949, E-mail: jaebum.cho83@samsung.com

Under-panel camera (UPC) is an emerging technology to realize full-screen displays without any camera hole or notches. Since it can hide a camera under a panel, the screen to body ratio (STBR) can be maximized.

However, there are several problems for UPC to be used in practice. The display panel diffracts and absorbs incident light before a camera. It causes severe degradation on the image quality. Specifically, the star-shaped glare with long tails due to strong light is one of the serious noises. While deconvolution methods can reconstruct the blurry images [1], they cannot remove the glare. For these reasons, UPC glare images cannot be reconstructed by traditional image processing.

A neural network is required to reconstruct the irreversible loss of the UPC images. The main application of UPC will be a video conference requiring a real-time processing, but the neural networks are often required heavy computation load. Bilateral filter [2] and guided filter [3] are proposed to reduce the computation load. These methods apply a desired processing on the downscaled images, and deduce filters between the input and output images.

In this paper, the method to restore UPC images degraded by glares is proposed. We show that the U-Net [4] trained by synthetic dataset using Fourier optics can restore real UPC images. The guided filter is also used for reducing calculation load. With the guided filter, the network size can be reduced 5 times lighter. While the guided filter is based on simple local linear operation, it shows decent reconstruction ability.

Figure 1 shows the experimental results. The network without the guided filter can restore blurry images and remove glare successfully. Although the network with guided filter cannot perfectly recover around of the light source, it still shows descent image quality for their computation size. Since the guided filter has an assumption that the difference between the input and the output is consist of low frequency components, the defects can be remained in details.

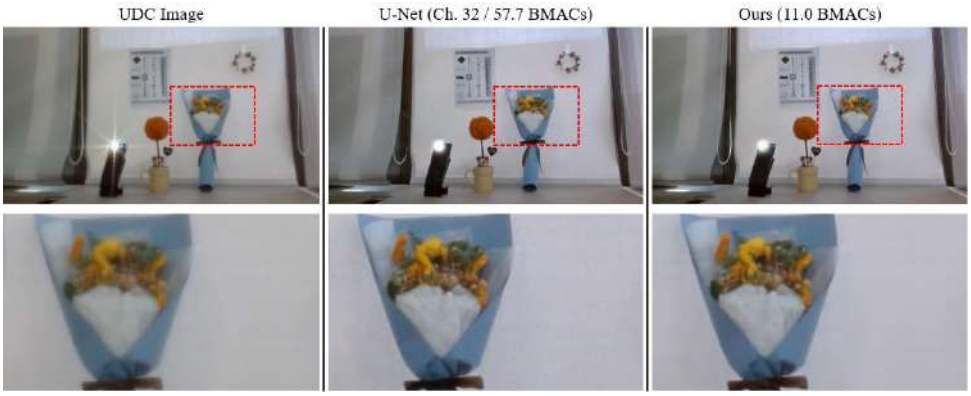

Figure 1. The UPC image shows star-shaped glare and severe blurring effect. In this experiment, U-Net with and without the guided filters is compared.

References

1. Goodman J. W. Introduction to Fourier optics. Roberts and Company Publishers. 2005.
2. Gharbi M, Chen J, Barron J. T, Hasinoff S. W, Durand F. Deep bilateral learning for real-time image enhancement. ACM Transactions on Graphics (TOG). 2017;36(4):1-12.
3. Wu H, Zheng S, Zhang J, Huang K. Fast end-to-end trainable guided filter. In Proceedings of the IEEE Conference on Computer Vision and Pattern Recognition. 2018;1838-1847.
4. Ronneberger O, Fischer P, Brox T. U-net: Convolutional networks for biomedical image segmentation. International Conference on Medical image computing and computer-assisted intervention. Springer, Cham. 2015;234-241.

Implementation of Template Based Web Simulation System

Jiyoo Park, Jihoon Shin, Eunji Kim, Junghoon Jo, Seungin Baek, and Yongjo Kim
1, Samsung-ro, Giheung-gu, Yongin-si, Gyeonggi-Do, Korea
Tel.:82- 31-5181-6886, E-mail: jiyou.park@samsung.com

There are many simulation softwares in the world, but most of them are very difficult to use or learn.
So normally, only specially trained people can use the simulation softwares. But what if anyone could easily use it? Many people will be able to save their time and money by simulations before actually taking action.
Therefore, We want to provide a simulation platform that anyone can easily use without specialized training. A simulation platform should satisfy all of the following points :

1. Easy to access and use.
2. It should be applicable to various types of inputs/outputs and simulation softwares.
3. Simple maintenance and management.

We chose a web-based system for convenient access and use. The system architecture is modularized so that each part can operate independently. This allows any type of solver (simulation software) to operate within a standardized platform. Figure 1 is a simulation framework that is composed of three parts: Web user interface (UI), Job controller, and Solving.

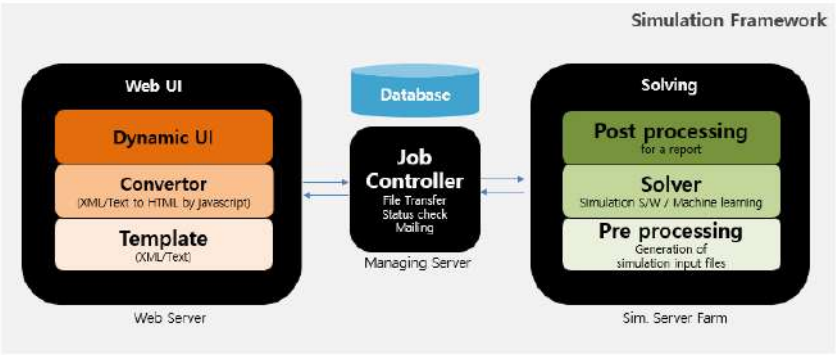

Fig. 1. Simulation Framework Design

Fig. 2. Web UI

Particularly, Web UI as shown in Fig. 2is a dynamic UI based on standardized templates (XML/Text), which is visualized through Convertor.
The converter reads the template and creates the UI according to the pre-set rules. There are rules for drawing various UIs such as tree, grid, input box, select box, file box, and chart. And we can create various UIs by combining them with each other. As a result, by editing this template, it is possible to respond to various input/outputs that change frequently without adding or modifying codes.

In conclusion, the biggest advantage of this framework is that it can be applied to any simulation softwares through modularization and the development/maintenance period is shortened.
We have confirmed that the development man-month (M/M) is reduced by 90% on average. (2→0.2M/M)

References

1. Zach Heath, Automated user interface generation for dynamically integrated simulations in the SUMMIT framework, MODSIM World 2014 (2014).

Pixel Layout Generation algorithm for AMOLED Displays

Myunghun Lim[3], Jungsuk Bang [1], Min Kang[1], Yongwoo Lee[1] and Yongjo Kim[1]
[1]CAE Team, Display Research Center, Samsung Display, Giheung-Gu, Yongin-City, Gyeonggi-Do, Korea 121-791, Korea
Tel.:82-70-0111-6912, E-mail: myunghun.lim@samsung.com

AMOLED displays are using low-temperature poly-silicon thin-film transistors (LTPS TFTs) show better performance. But, the drawbacks of LTPS TFTs is in the obvious variations in the threshold voltage (VTH) and mobility. So OLED pixel circuit design, the method of detecting and compensating the non-uniformities in TFT characteristics is essential. for Compensating the non-uniformities need more Transistors. So state of the art OLED pixel circuit is getting more complicated.

In this paper, we recommend Pixel Layout Generator for AMOLED Display. For Pixel Layout Generation we focus on Transistors's Placement and their connections. First, it places the transistors based on the circuit diagram and creates nodes between the transistors. And then we connect those nodes to the shortest distance. During this process, the DesignRule is considered, and if the nodes are not connected, relocate the transistor or find a the avoidance path. So we can get the layout automatically and it can reduce the development period or get a new Pixel layout.

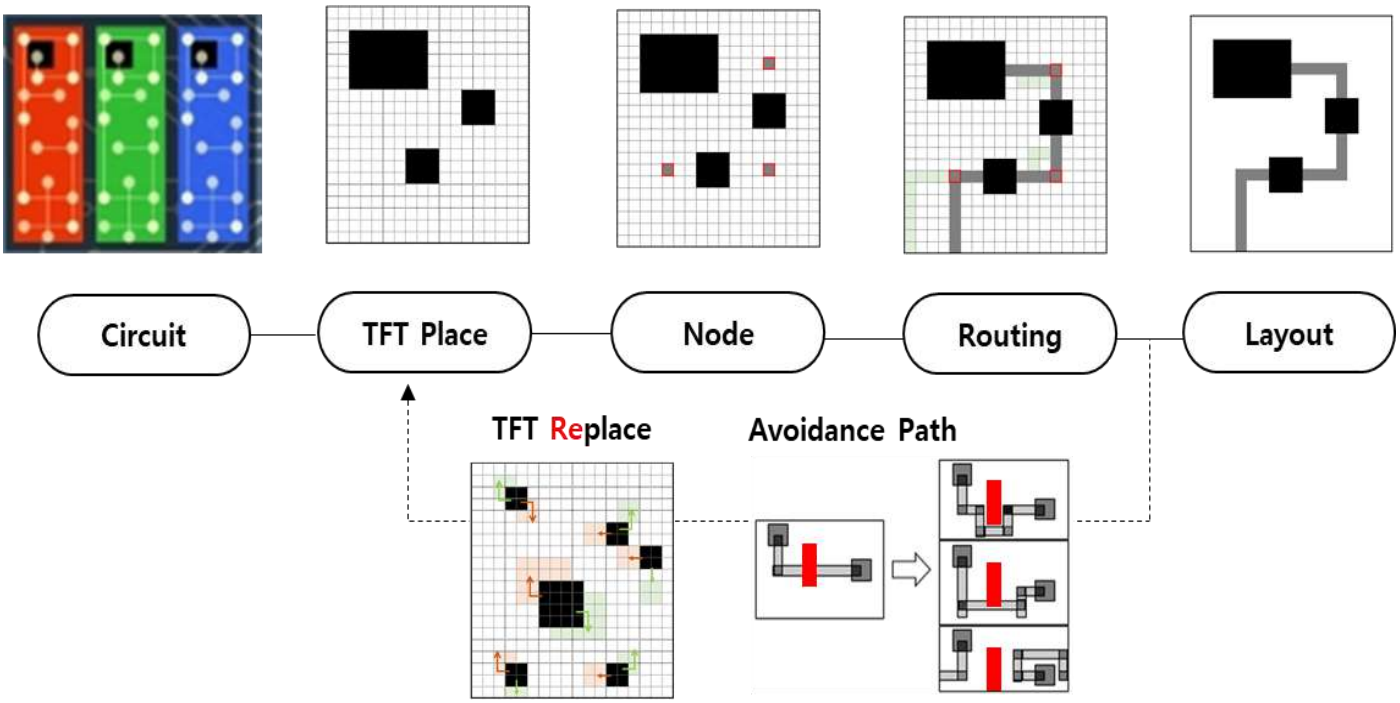

Fig. 1 Pixel Layout Generator Flow chart and Algorithm

References

1. N. –H. Keum, and O. –K. Kwon, "High Resolution AMOLED Pixel Using Negative Feedback Structure for Improving Image Quality," SID Symposium Digest, pp.461-464 (2013)
2. Warren, CW; "Fast path planning using modified A* method". IEEE. Robotics and Automation, Atlanta, USA. 1993.
3. L. W. Liebmann, R. O. Topaloglu, "Design and technology co-optimization near single-digit nodes", Proc. IEEE/ACM Int. Conf. Comput.-Aided Design, pp. 582-585, Nov. 2014.
4. W. Wolf, "Modern VLSI Design System On Chip Design", 3 rd ed., Prentice Hall, 2002.
5. Naveed A. Sherwani, "Algorithms for VLSI Physical Design Automation", 3rd Edition, Kluwer Academic Publishers. Dordrecht1999.

Multi-output convolutional neural network model for RC extraction

Keuk Jin Jeong[1], Myunghun Lim[1], Min Kang[1], Yongwoo Lee[1] and Yongjo Kim[1]
[1]Display Research Center, Samsung Display Co., Ltd., Yongin-si, Gyeonggi-do, 17113, Korea
Tel.:82-31-5181-6847, E-mail: keukjin.jeong@samsung.com

Fast and accurate multiple RC extractions is critical to optimizing the pixel design. The AI-based capacitance extraction model ascertains the correlation between 3D design information and the capacitance. AI model is much faster than a finite element method (FEM), which takes minutes to hours to calculate a physics equation.

In order to predict the relationship between 3D design information and 1D physical properties(R, C), you need an algorithm that data-driven image. Geometric design information is converted into a layer image and a convolutional layer is used to extract features. Compressed feature is used as a training data for a neural network model that predicts capacitance. During layout design, the AI model provides high speed evaluation of the capacitance.

Reshape the CNN network to predict multiple outputs and optimize the modeling to avoid performance degradation due to cost functions.

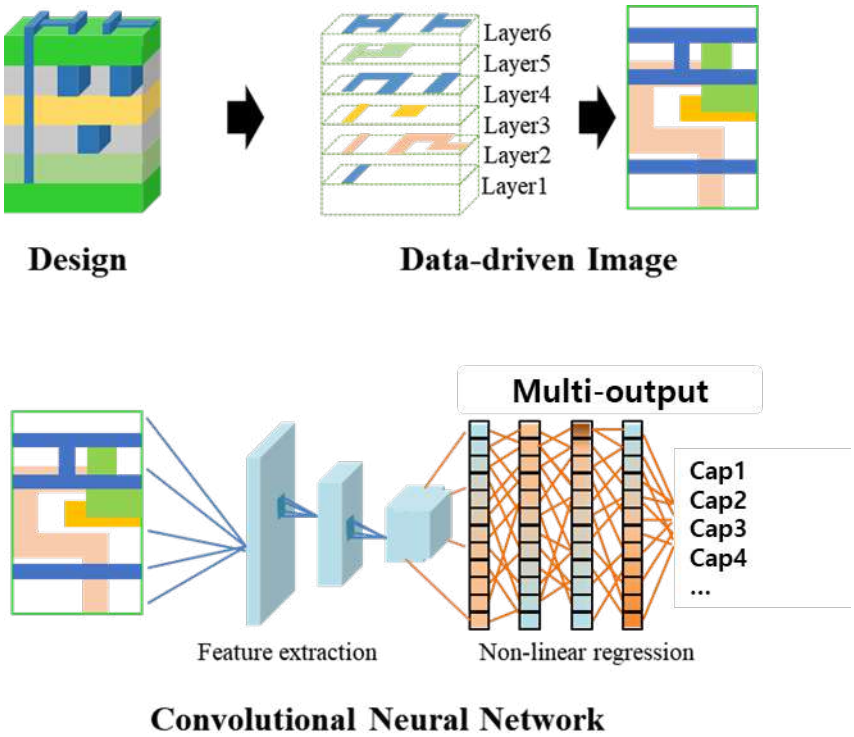

Fig. 1. Multi-output CNN model using data-driven Image for RC extraction

As a result of building a DB through a large amount of FEM simulation and inferring with an AI model trained through it, it shows very good prediction performance.

References

1. Park, Hyun Sung, et al. "P-143: TSP Pattern Design and Sensitivity Characterization via Convolutional Neural Networks." SID Symposium Digest of Technical Papers. Vol. 50. No. 1. (2019)
2. Sanders, David A., and Giles E. Tewkesbury. "A pointer device for TFT display screens that determines position by detecting colours on the display using a colour sensor and an artificial neural network." Displays 30.2 (2009): 84-96.

In-fab monitoring method based on artificially intelligent optical property prediction technology

Youngjun Yoo[1], Jongbeom Hong[1], Eunkyung Koh[1], Changhun Lee[1], Younho Han[1], Gunshik Kim[1], Won-Hyouk Jang[1] and Yongjo Kim[1]

[1]CAE, Samsung Display Research Center, 95 Samsung 2-ro, Giheung-gu, Yongin-si, Gyeonggi-do, Korea

Tel.:82-31-5181-6897, E-mail: youngjun1.yoo@saumsung.com

As the design of the display is diversified, demand for Flexible OLED is increasing. Conventional rigid OLED encapsulated with the glass window while the flexible display encapsulated with various films, so the optical characteristics change at each stage. In addition, the production time is increased in proportion to the complicated process. It is expected that it will become more difficult to monitor the characteristics of the process, and it will become increasingly difficult to predict the optical characteristics of the product state from the initial measurements. We have developed a technology that can predict the optical characteristics of the product state from the initial monitoring data through machine learning of the Fab data.

Figure 1(a) shows the result of predicting the initial measurement data of mass production and the optical characteristics of the product by simple polynomial empirical equation. This prediction equation needs to be updated whenever process change point is occurred. Fab data is vast and contains all events in the process. We have created a prediction model using machine learning algorithm because there are limits to how engineers deal with large amounts of data, and the results are shown in Figure 1(b). 51% accuracy was obtained using a single regression algorithm. To improve the accuracy of prediction models, we introduced ensemble methods which is a way to improve generalization performance by harmoniously combining various models learned by individual. The calculation time before and after applying ensemble mode is similar, it is enough to take into account the improved the accuracy of prediction models. As a result, the accuracy of the prediction model was improved from 51% to 67%.

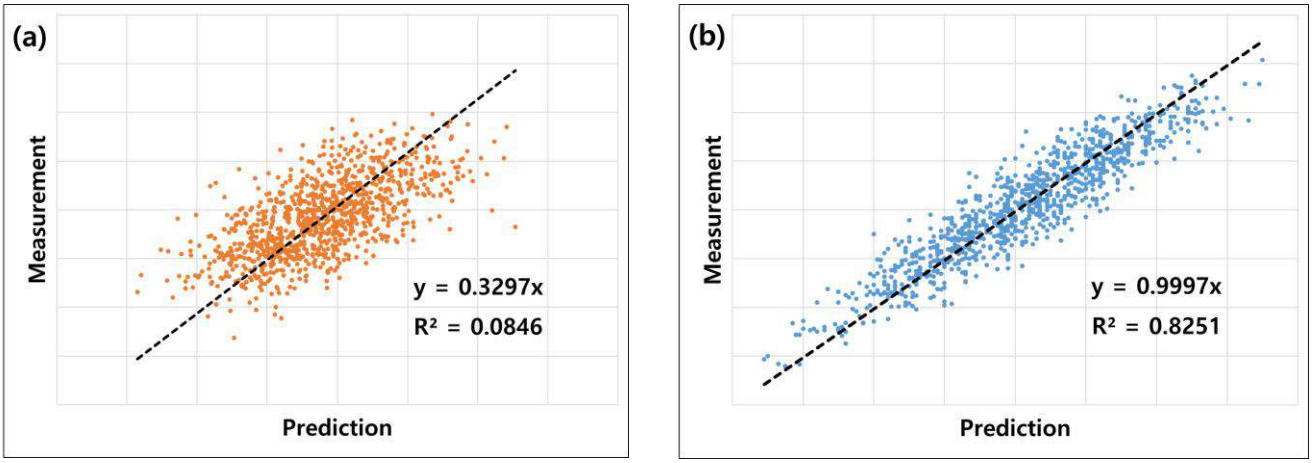

Fig. 1. (a) Optical characteristics predicted with empirical equations. (b) Optical characteristics predicted with A.I prediction technology.

References

1. Franky So. *Organic electronics: Materials, Processing, Devices and applications* (CRC Press, New York, 2010).
2. Chun-Liang Lin et al., Examining microcavity organic light-emitting devices having two metal mirrors, *Appl. Phys. Lett.* 87, 021101 (2005).
3. Zheng Yuan et al., Combining Linear Regression Models, *JASA.* 472, 12021214 (2005).

Target-oriented material design based on a key parameter: new blue thermally activated delayed fluorescent emitters with long lifetime

Seran Kim[1], Dongsun Yoo[1], Hoilim Kim[1], Junha Park[2], Hyosup Shin[2], Hyunyoung Kim[2], Jiyoung Lee[2], Youngmi Cho[1] and Yongjo Kim[1]

[1]CAE Team, Samsung Display, Gyeonggi-do, Republic of Korea

Tel.:82-31-5181-6794, E-mail: seran.kim@samsung.com

[2]Materials Research Team, Samsung Display, Gyeonggi-do, Republic of Korea

In organic light emitting diode (OLED) industry, there have been many research on improving lifetime of high-efficiency blue thermally activated delayed fluorescent (TADF) materials. Research on target-oriented molecular design to discover materials that satisfy multi-objective properties have also grown rapidly with the recent development of artificial intelligence (AI) technology [1]. We report on following results; design a new blue TADF emitting material with long lifetime based on a key parameter, and discover more robust emitters based on an enhanced AI model.

Multiple resonance TADF emitters with high color-purity have been recently proposed [2]. We discover a critical bond that representing a transition stability of MR emitters. It was confirmed that the longer lifetime of device using the emitter with the more robust bond of a substituent which injects electrons to exhibit multiple resonances (R^2 = 0.98 ~ 0.99) by DFT simulation (B3LYP/6-311G(d,p)). We define an A_BDE, a dissociation energy of the bond as a key parameter of the material that correlates with the lifetime of TADF device. A novel material with improved A_BDE was designed by introducing the substituent that enhances conjugation of the bond. As a result of the device evaluation of the synthesized material, the correlation of the key parameter was experimentally verified as the device lifetime was improved by 40 %.

We built an AI model that can quickly predict the A_BDE and discover more improved materials. In order to prevent the A_BDE property error from acting as a noise due to various conformations of the input material structure, a constraint code was added to an input generator so that a global minimum structure was created. This model with 3D feature applied shows improved performance by test accuracy 10 % and property deviation 22 % compared to 2D model [3]. We discovered materials with 32 ~ 328 % improvement in target property compared to the previous one by applying the model.

We present a new paradigm of OLED material design through this research; discover key parameters based on simulation results of target characteristics and screen target materials by building an AI model for predicting physical properties through learning of accumulated databases. Using this method, high-performance materials can be developed within a dramatically shortened turnaround time in an infinite design space that transcends the engineer's intuition.

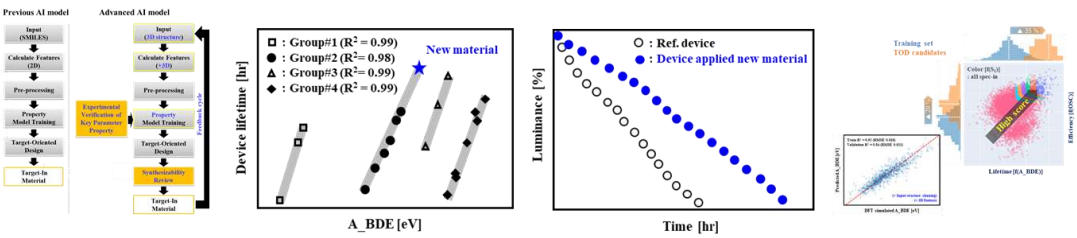

Fig. 1. Workflow (left), results of the key parameter correlated with target property (middle) and the TOD model (right).

References

1. M.D. Halls et al, *Virtual Screening for OLED materials*, Proceedings Vol. **9183**, Organic Light Emitting Materials and Devices XVIII (2014)

2. T. Hatakeyama et al. *Ultrapure Blue Thermally Activated Delayed Fluorescence Molecules: Efficient HOMO–LUMO Separation by the Multiple Resonance Effect*, Adv. Mater. **28**, 2777–2781 (2016)

3. E. Koh, *Deep Learning Based Inverse Design Model for Blue OLED Materials*, **06_02_1163**, International Meeting on Information Display (2020)

Novel Verification Operation Design Methodology using Timing Assertion for Display Product

MinJoo Lee[1], Insoo Wang and Yongjo Kim
[1] **CAE Team, Samsung Display, Gyeonggi-do, Korea**
Tel.:82-31-5181-4262, E-mail: mansemin.lee@samsuing.com

Register Transfer Level or RTL represents digital functionality using programming statements and moperators. These models are functional models that do not contain the details on how that functionality will be implemented in silicon. The typical flow for ASIC design is shown Figure1.

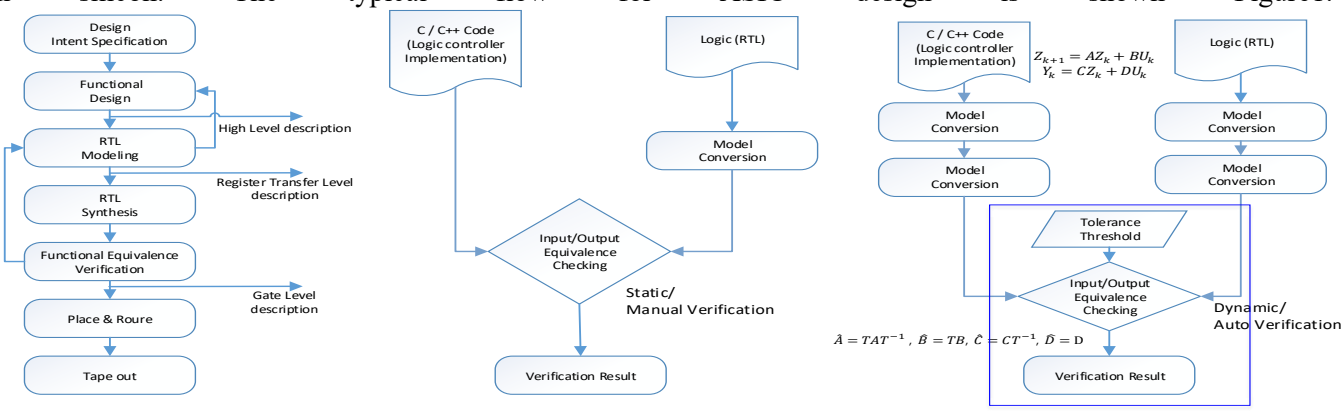

(A) ASIC flow (B). Conventional Verification flow (C). Proposed Verification Flow

Fig. 1. ASIC FLOW, Traditional Verification flow and Proposed Verification Flow

RTL verification in modeling stage provides the confidence that a digital circuit is functionally correct. Moreover the bugs in RTL description can be easily modified and save plenty of development time and cost. Therefore RTL modeling is the key of ASIC design. To design better RTL modeling, conventional verification methods first made functional model in high level description's implementation then RTL modeling. And they aim is to detect different results between them. However, Software developing is sequential mentality whereas RTL parallel mentality, which should be might district operating schema.

We proposed that adaption time notion in functional design like RTL behavior's to the high level languages. With High Level synthesis (HLS) tools, we can be obtained timing operation map automatically. Desperate of optimum problems in HLS tools, this is the way to express algorithm as clock timing operation with at least effort. We need another concept of tolerance threshold for comparing result of algorithms and hardware for standalone IP verification or verifications at multiple IPs linked. First, in standalone IP verification case such as fixed point calculation or floating point calculation can generate unwanted differential which can be ignored in display area according to Drive-IC resolution is 8 bit or 10bit. Second, undefined error from previous IP or unwanted error from current IP to concurrent IP can be happened in system level. Therefore we need to verify circumstances error between multiple IP connections for robustness. Another advantage of tolerance threshold concept is reducing simulation time and auto verification environment even if low level degree. In display panel use 8 bit or 10 bit driver IC for express grey level. One logic value is too small in voltage level at panel, it comes to unconsciousness to human eyes. As a result, static and manual verification system in Figure 1 (B) can be dynamic and automatic verification system in shown Figure 1 (C).

To consider spontaneous display characteristics which is sensitive to clock timing and human eyes awareness, we proposed timing and tolerance control based verification in logic design. As a result, we can reduce developing time and verification cost for ASIC chip in display area

References

1. Y. C. Nam and M. J. Kim. "Study and Analysis of RTL Verification Tool" IEEE Students' Conference on Engineering & Systems (SCES) (2020)
2. Vanessa R. Cooper. "Getting Started with UVM: A Beginners' Guide", Verilab Publishing (2013)
3. Anmol Mathur, "Functional EquivalenceVerification Tools inHigh-Level Synthesis Flows", EEE Design and Test of Computers, P. 88 -95 (2009)

Automated Interconnection Method for Freeform Displays

Jeongcheol Noh[1], Jiyoung Lee[1], Deawoo Myoung[1], Hyunyoung Choi[1], Hearyeong Park[1], Yongwoo Lee[1] and Yongjo Kim[1]
[1]CAE Team, Samsung Display, Gyeonggi-do, Republic of Korea
Tel.:82-31-5181-6783, E-mail: jc.noh@samsung.com

In freeform displays, the various shape of displays complicates the wiring of the connection between the pixel and the gate driver. Due to the bezel-less design trend, it takes a lot of time and effort to design regular wiring connections while ensuring enough space between the lines in a confined space. This is because the wiring thickness and conductivity must be considered for stable current supply, and process distribution must be considered at the same time. [1] In this paper, we use the simple logic and equations of the mass spring system, a classic system with several degrees of freedom, to propose a wiring connection design method in a narrow and high density area.(Fig. 1.) In the simplest case of the mass spring system, we can ignore the forces of friction and air resistance and consider only the elastic force that obeys Hooke's law. [2] Despite the diverse nature of the movement, the system is linear and, therefore, can be solved exactly. The mass spring system consists of the same masses and the same springs with the same stiffness coefficient, as shown in Figure 1. The initial positions of the masses are determined by dividing the straight line connecting the starting and ending points at regular intervals. The next position of each mass is determined by the sum of the attractive force and the repulsive force as shown in the following equation..

$$f_{Attractive} = K_{coeff.A} \times r_{distance} \text{ (Attractive Force)}, \quad f_{Replusive} = -\frac{K_{coeff.R}}{(r_{distance})^2} \text{ (Repulsive Force)}$$

The next position is updated repeatedly until the moving sum of all masses is below a certain criterion. In order to achieve a design that meets our purpose, the logic of the boundary line and the connecting line, the logic between the same segment points for each connecting line, and the logic for the starting point and the destination point are added. In addition, logic has been added to reflect the differential movement between points with large movable space and points with small movable space. An evaluation index is calculated to evaluate how well the spacings between connecting lines are widened. The points for calculating the evaluation index were extracted by three criteria: the vertical line from the pixel to the gate driver , the point with the highest density of the connecting line, and the narrow point between the gate driver boundary and the pixel boundary.

As shown in Figure 2, it can be seen that the evaluation index value of the final result is greatly improved by comparing it with the evaluation index value extracted at the time of initial connection. In a typical personal computer environment(Intel(R) i5-6500 CPU@3.20GHz), it only takes a few minutes to connect 254 points from Gate Driver to Pixel in 1/4 area of the actual smartphone panel. This suggested wiring connection method can select the connect shape by purpose do mixing the maximize spacings and minize line lengths by adjusting the parameters of attractive force and repulsive force. It is the reason that this method can be used in various fields to solve the wiring connection problem regularly and quickly in a confined space.

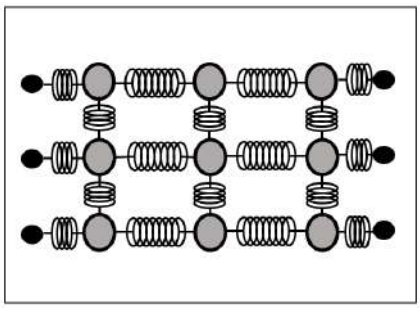

Fig. 1. The structure of mass spring system

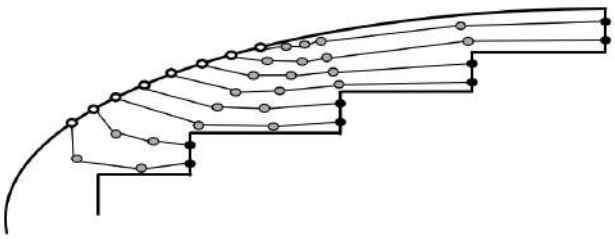

	Avg(d_{min})	Min(d_{min})	Max(d_{min})
Initial vs Final	42.5% ↑	32.2% ↑	128.8% ↑

Fig. 2. An actual example of wiring connection design method

1. Thickness and conductivity of metallic layers from eddy current measurements Review of Scientific Instruments 63, 3455 (1992);
2. Rychlewski, J. Journal of Applied Mathematics and Mechanics (0021-8928), 48 (3), p. 303 (1984).

Implentation of Convolution Neural Network in display IC maintaining accuracy

Jun-gyu Lee[1], Kuk-hwan Ahn[2], Hyun-jun Kim[3], Hyeon-min Kim[4]
[1] Samsung Display Company, Yongin-si, Gyeonggi-do, Korea
Tel.: 82-31-5181-5647, E-mail: jungyu.lee@samsung.com
[2,3,4] Samsung Display Company, Yongin-si, Gyeonggi-do, Korea

Neural network technology among deep learning technologies is being used in more and more fields recently. In the image processing area, the neural network usually requires multiplication and addition operation count of Giga Floating-Point Operation (GFLOPS). If you do not use a chip dedicated to neuromorphic, it will occupy a very large IC area and it is difficult to apply in reality. In addition, the result of each neural network layer uses several Mega Bytes memory, which is also a significant IC cost increase.

Therefore, this paper introduces pre-CNN and post-CNN technologies for maintaining the performance of the neural network, and applies techniques for reducing the neural network and reducing the memory to reduce gate count, so that tens of Mega Gate Counts are applied to 2 Mega or less Gate Counts.

In this paper, 7 layers of neural network technology were applied to Object Detection. What is remarkable about TV images is that there is continuity of images within the same Scene. Using this feature, the accuracy was improved by accumulating the image in the same scene and putting it into the input of CNN. In addition, since the position of the object detected in the image does not change rapidly, an appropriate filter is applied to the object position in the post-processing to improve the detection position stability.

In order to reduce gate count, Node pruning and statistical weight quantization are applied to reduce the number of operations of the network itself, and the number of multiplier is minimized by reusing the operator. By separating the memory that stores the output values for each neural network layer into odd layers and even layers, the memory usage is halved. Fig. 1.

As a result, the memory could be reduced to 1 / 2 and the gate count to 1 / 20 while maintaining detection performance and operation latency.

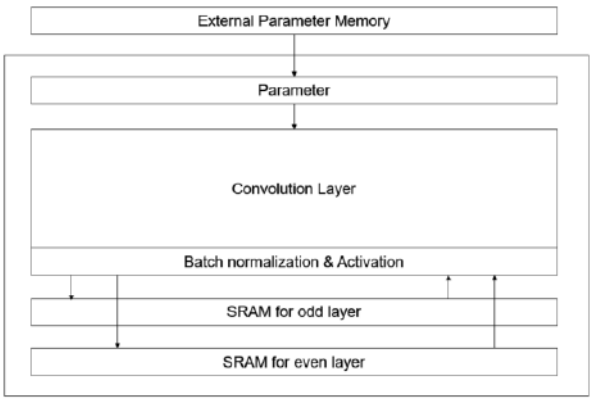

Fig. 1. Memory reduction scheme

Acknowledgment

References

1. Muthuramalingam, A., S. Himavathi, and E. Srinivasan. "Neural network implementation using FPGA: issues and application." International journal of information technology 4.2 (2008): 86-92.
2. Qiu, Jiantao, et al. "Going deeper with embedded fpga platform for convolutional neural network." Proceedings of the 2016 ACM/SIGDA International Symposium on Field-Programmable Gate Arrays. 2016.
3. Sahin, Suhap, Yasar Becerikli, and Suleyman Yazici. "Neural network implementation in hardware using FPGAs." International Conference on Neural Information Processing. Springer, Berlin, Heidelberg, 2006.

Novel Optical Simulation Method for flexible OLED with Optically Thick Incoherent Layers

Yong Sub Shim[1*], Younho Han[1]
[1]CAE, Samsung Display Research Center, 95 Samsung 2-ro, Giheung-gu, Yongin-si, Gyeonggi-do, Korea
Tel.:82-31-5181-6882, E-mail: yongsub.shim@samsung.com

When calculating optical propertis of OLEDs including thick incoherent layer via Trasnfer Matrix Method(TMM), temporal incoherence must be considered to remove the coherent properties of light. Random phase method**[1]** or Equi-distant phase method**[2]** are well known for solving optical incoherent multilayer system, but they need high computational cost because of taking multiple times depending on the number of phase splits.

In this study, we present a novel approach for modeling OLEDs with thick incoherent layer at much lower computational cost. Generally, a thick protective layer is deposited on top of flexible OLED as in a **Fig.1(a)**, thus optical coherence should be considered from light source to the protective layer and ignored after the protective layer. We designate the protective layer as an intermediate point of calculation. In this way, the radiant intensity(I_{bot}) & the reflectance(R_{bot}) of the bottom layers, and the transmittnace(T_{upp}) & Reflectance(R_{upp}) of upper layers all can be solved by fast coherent TMM calculations. The final radiant intensity(I_{OLED}) with thick incohent layer can be expressed in the following simplifed equations:

$$T_{total} = T_{upp} + (T_{upp}*R_{upp}*R_{bot}) + (T_{upp}*R_{top}^2*R_{bot}^2) + (T_{upp}*R_{upp}^3*R_{bot}^3) \ldots = T_{upp} / (1-R_{upp}*R_{bot})$$

$$I_{OLED} = (n_{air}/n_i) * T_{total} * I_{bot}$$

Fig.2(b), (c) shows comparison of the radiant intensity obtained by the conventional and new method. The accuracy(R^2) is greater than 99.5% and TAT is less than 1/5. Futher, it has been verified that this methodology can be applied to more complex OLED structures with multiple incoherent layers. We hope this novel method will greatly reduce computational resources in the cases that require many parameter controls in mass production.

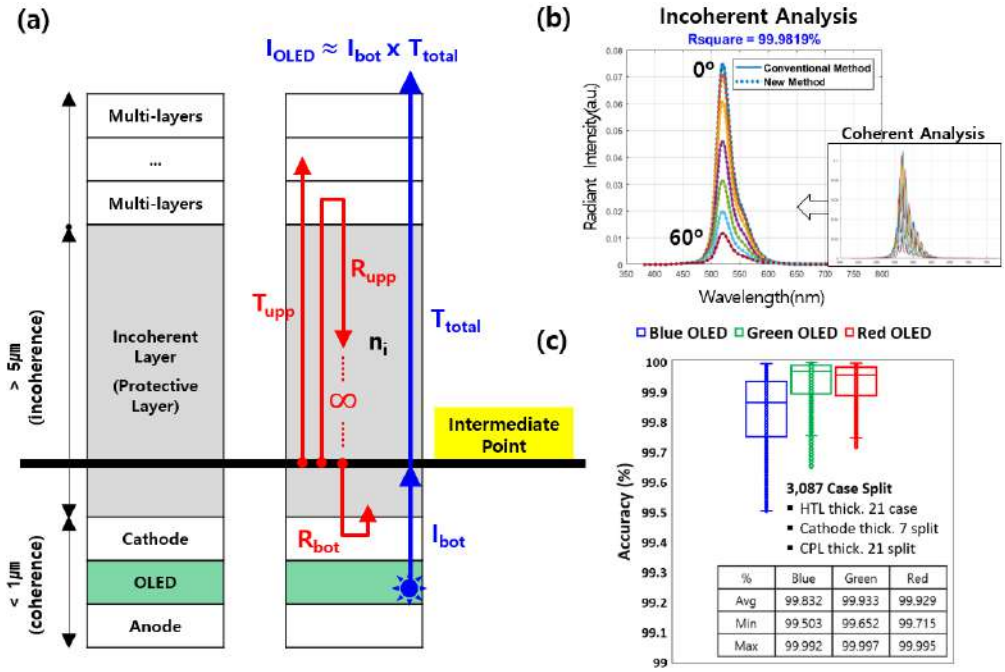

%	Blue	Green	Red
Avg	99.832	99.933	99.929
Min	99.503	99.652	99.715
Max	99.992	99.997	99.995

Fig. 2. (a) Shematic diagram and analysis logic of OLEDs with thick incohernt layer
(b), (c) Comparison of the radiant intensity obtained by the conventional and the new method

References

[1] M. Claudia Troparevsky et al, "Transfer-matrix formalism for the calculation of optical response in multilayer systems: from coherent to incoherent interference," Optics Express 2010 18, 24715
[2] Rudi Santbergen et al, "Optical model for multiplayer structures with coherent, partly coherent and incoherent layers." Optics Express 2013 21, A262

Numerical study on the behavior of conductive particles in the bonding process

Daeyong Kim[1], JinSung Hwang[2]
[1]Samsung Display, Gi-heung/Yong-in, Gyeonggi-do, Korea
Tel.:82-31-5181-6784, E-mail: dy0408.kim@samsung.com

Anisotropic conductive film (ACF) has been used as interconnect material for flat-panel display module packages, such as chip-on-film (COF). Two-layer ACF film is recently required to use for fine pitch interconnection. Two layers consist of anisotropic conductive film (ACF) and non-conductive film (NCF) which have different viscosities. In general, ACF has lower viscosity than that of NCF, and the conductive particles are placed in ACF. The number of conductive particles between two electrodes can be controlled by the properties of two-layer ACF film. Especially, the viscosity and thickness of each film and particle number density are main parameters to affect the number of conductive particles captured between electrodes. In this paper, the effect of two-layer ACF features on the conductive particles in motion was investigated through the simulation of resin flow and conductive particles. Simulation was carried out with various different types of two-layer ACF film, which was shown in Figure 1. It was assumed that the bonding process was completed after 0.3 second, and the electrodes gas was reduced from 18 ㎛ to 2 ㎛. The conductive particle was located in ACF. Conductive particles in the case3 and case4 of two-layer ACF film were placed in the diamond array.

ACF Film	Particle denstiy [#/㎟]	NCF/ACF Viscosity [cP]	NCF/ACF thickness[㎛]	Particle array
case1(ref.)	A	B/C	D/E	random
case2	0.86A	6.55B/3.75C	0.90D/1.25E	random
case3	0.86A	10B/1.25C	0.60D/E	regular
case4	1.14A	10B/1.25C	0.60D/E	regular
case5	0.86A	B/C	D/E	random
case6	1.14A	B/C	D/E	random
case7	A	B/C	0.60D/E	random
case8	1.14A	B/C	0.60D/E	random

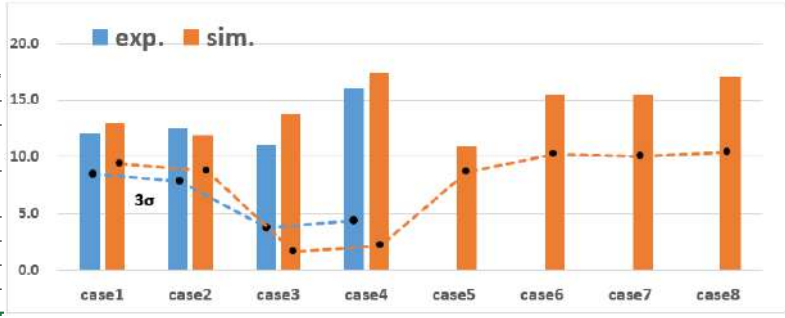

Fig. 1. Number of conductive particles between electrodes

Because conductive particles in the case 1 and case 2 two-layer ACF filme were arranged at random, three standard deviation(3σ) of condutive particle between two electrode was greater than that of case 3 and case 4 two-layer ACF film with particles in regular array. In the cases of ACF film with particles in random array, viscosities of ACF/NCF had little effect on the number of particle between two elecetrodes. The result of case 3 and case 4 AFC films represents that the main parameter to affect the number of particles captured between two electrodes is the particle number density rather than particle array or viscosities of ACF/NCF. This phenomenon is also shown in the case 5 and case 6 ACF film. The numer of particles between two elecetrodes was increased by the particle number density. Compared with case 1 and case 7 or with case 6 and case 8, the decrease in NCF film thickness caused to reduce the amount of resin flow in the bonding process, which was able to capture more conductive particles between two electrodes.

As result, two-layer ACF film with higher particle number density and particle array in regular array is able to capture more conductive particles with less standard deviation between two electrodes. Also, thinner NCF film has adventage in remaining conductive particles in the initial position.

References

1. Myung-Jin Yim, Kyung-Wook Paik, *IEEE Transactions on Components Packaging and Manufacturing Technology*, Part A, 21(2), p. 226 (1998)
2. Yoo-Sun Kim, Kiwon Lee and Kyung-Wook Paik, *IEEE Transactions on Components, Packaging and Manufacturing Technology*, vol. 3, (2013)

SPICE TFT Modeling using Reinforcement Learning

Wonwoo Choi, Sooyoung Lee, Younyeol Yu, Kiseok Chang,
Ilho Kim, Seokwoo Lee and Sooyoung Yoon
LG Display Co., LTD., Gangseo-gu, Seoul, 07796, Korea
E-mail: wonwooddo@lgdisplay.com

To ensure the reliability of SPICE simulation, accurate physical parameters of TFT are required with an integrated circuit design. The TFT parameters can be obtained by iteratively fitting SPICE model to measured transfer and output characteristics of TFTs. This process, known as SPICE TFT modeling, is not only laborious and time consuming, but also requires extensive engineering expertise to arrive at meaningful parameter sets. Machine learning is shown as a promising tool to automate this process based on previous studies [1,2,3]. In this paper, we propose reinforcement learning (RL) method for efficient optimization of SPICE TFT modeling with following two reasons: 1) Targeted TFTs are a novel structure, making them expensive to collect large-scale datasets; 2) RL learns from the agent-generated simulated data.

RL is a type of machine learning technique that forces an agent to learn in an interactive environment by trial and error using feedback from its own actions and experiences. We frame SPICE TFT modeling task as a sequential decision making problem, as shown in Fig. 1. In each iteration, the RL produces an action (a set of model parameters) to make SPICE TFT model library, and then receives next observation (simulated result) with calculated reward (negative normalized root mean squared error). Given history of parameter configurations and corresponding rewards, agent adjusts its policy using Soft Actor Critic algorithm in a way that increases the future reward and is able to optimize the model parameters. This methodology can save tremendous time and engineering resources compared to manual adjustment as the agent learns to efficiently generate optimized parameter configuration. To demonstrate that the proposed approach is beneficial in production, we applied it to Oxide TFT modeling. SmartSpice simulator with the Rensselaer Polytechnic Institute (RPI) poly-Si TFT model (level 36) were used and search space is determined based on parameters that are empirically tuned. Fig. 2 shows the TFT modeling result of 4 hours of hand tuning and agent tuning. We trained our agent from scratch without giving it any rules about modeling for same amount of time and scored similar performance. Compared to traditional optimization algorithms, RL automation has the advantage of being able to make engineer more productive and learn to optimize faster by using distributed agent or pre-train the agent as used. In addition, this methodology has the potential to be applied to other tasks and outperform.

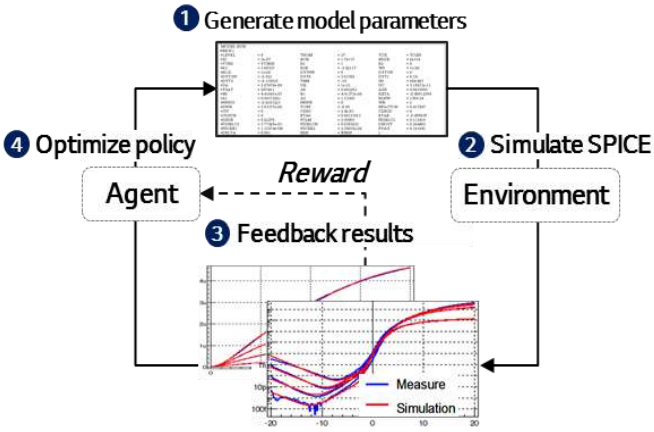

Fig. 1. Reinforcement Learning Framework in SPICE TFT Modeling

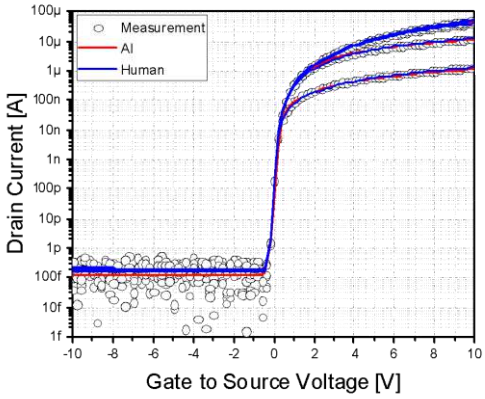

Fig. 2. Transfer Characteristics (AI error = 3.71%, Human error = 3.79%)

References

[1] Wang, Hanrui, et al. "Learning to design circuits." arXiv preprint arXiv:1812.02734 (2018).
[2] Wu, Jia, SenPeng Chen, and XiYuan Liu. "Efficient hyperparameter optimization through model-based reinforcement learning." Neurocomputing 409 (2020): 381-393.
[3] Estrada, M., et al. "Accurate modeling and parameter extraction method for organic TFTs." Solid-state electronics 49.6 (2005): 1009-1016.

Fast and rigorous electromagnetic simulation of dipole emission in a periodically corrugated light-emitting diode structure based on diffraction tracking

Chanhyung Park[1], Jeong Min Shin[1], Sanmun Kim[1], Juho Park[1] and Min Seok Jang[1]
[1]Dept. of Electric Engineering, Korea Advanced Institute of Science and Technology, Daejeon 34141, Korea
Tel.:82-42-350-7439, E-mail: jang.minseok@kaist.ac.kr

Organic light-emitting diodes (OLED) have become one of the major light sources for display use due to high color accuracy and luminosity. The external light efficiency of conventional OLEDs ranges around 20% while the internal quantum efficiency approaches ~100%. The discrepancy arises from the total internal reflection and a relatively large refraction index of emission layers. It has been reported that the external light efficiency of an OLED can be improved by introducing a periodically corrugated layer boundary [1, 2], but the effect has not been analyzed quantitatively. Electromagnetic analysis of a dipole layer in a periodically corrugated LED has been done previously [3], but the approach used in that work cannot deal with the emission from a single dipole, which is crucial for analyzing a periodically corrugated dipole layer. In this work, we demonstrate how the emission from a single dipole in a periodically corrugated LED structure can be calculated by diffraction tracking. Diffraction efficiency was calculated by rigorous coupled-wave analysis method (RCWA) [4]. We have confirmed that the results from our calculation model agree well with the simulation values from finite-difference time-domain method (FDTD) in terms of far-field image and light extraction efficiency (LEE) while alleviating the computational load by a significant amount.

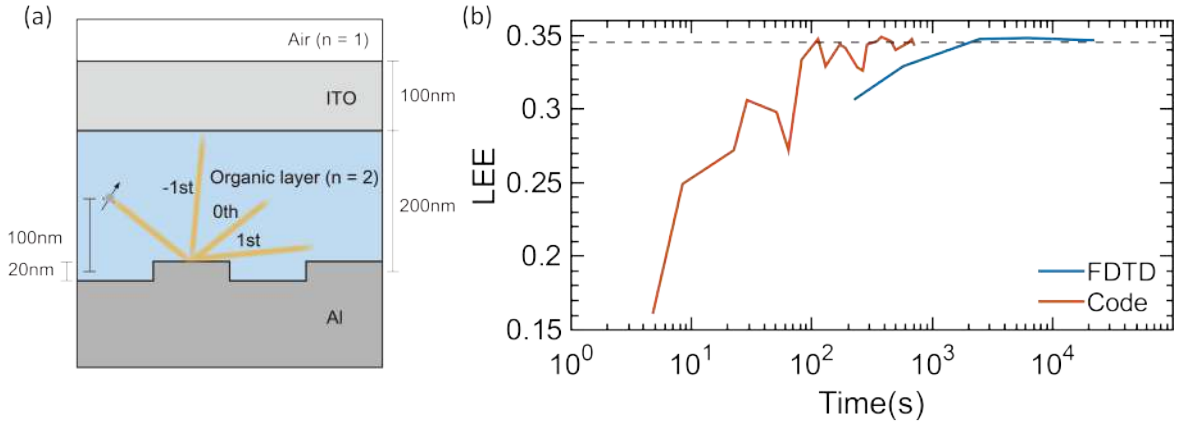

Fig. 1. (a) An example schematic of the simplified OLED structure (b) Calculated LEE value as a function of time. FDTD and our calculation converges to the same LEE value but our calculation is much faster.

The advantages of our method become clear during the OLED structure optimization process. The diffraction coefficients obtained from the RCWA calculation depends only on the shape of the corrugation, hence the calculation for different dipole position, dipole orientation and different emission layer thicknesses can be completed with minimal computation. Also, the analysis involving multiple dipoles can be calculated in parallel, facilitating the optimization task even more.

Acknowledgment

This work was supported by LG Display.

References

1. Zhang, Xu-Lin, et al, *Optics Letters*, Vol. 36, Issue 19, pp. 3915-3917 (2011)
2. Jeon, Sohee, et al, *Nanoscale* 6.5 (2014): 2642-2648.
3. Delbeke, Danaë, et al, *Journal of the Optical Society of America A* Vol. 19, Issue 5, pp. 871-880 (2002)
4. J.P.Hugonin, et al, *arXiv*:2101.00901

Holistic Optimization of Periodically Corrugated Organic Light-Emitting Diodes for Extraordinary Front Emission

Jeongmin Shin[1], Chanhyung Park[1], Sanmun Kim[1], and Min Seok Jang[1]
[1]**Dept. of Electrical Engineering, KAIST, Daejeon, 34141, Korea**
Tel.:82-2-350-7439, E-mail: jang.minseok@kaist.ac.kr

Light extraction efficiency (LEE) is the most important limiting factor in determining the efficiency of organic light-emitting diodes (OLEDs) and many approaches have been made to increase the value [1]. Here, we focus on the front LEE value, which is defined as the proportion of light escaping the device at an angle perpendicular to the device surface. In this work, we optimized the front LEE of a 1D grating corrugated OLED that only consists of two electrodes and an emissive layer. The front LEE is obtained from a calculation model based on rigorous coupled-wave analysis (RCWA) [2,3] and transfer matrix method (TMM). The model finishes the calculation within an order of minutes that would have taken more than a few days with finite-domain time-domain method (FDTD). This computation tool is joined with a genetic algorithm and a particle swarm optimization method to optimize the front LEE within a reasonable time. The optimization led to a 413.8% increase in front LEE value compared to the planar structure when the corrugation was applied to the anode-emissive layer boundary. Also, the relationship between the corrugation parameters (corrugation period, amplitude, duty cycle) and front LEE was analyzed by using Bragg's Law and mode analysis. Finally, we demonstrate a different method of optimization, where we first optimize the planar structure thickness and then add an adequate corrugation to maximize the front LEE. The outcomes from the aforementioned method and the latter method are compared

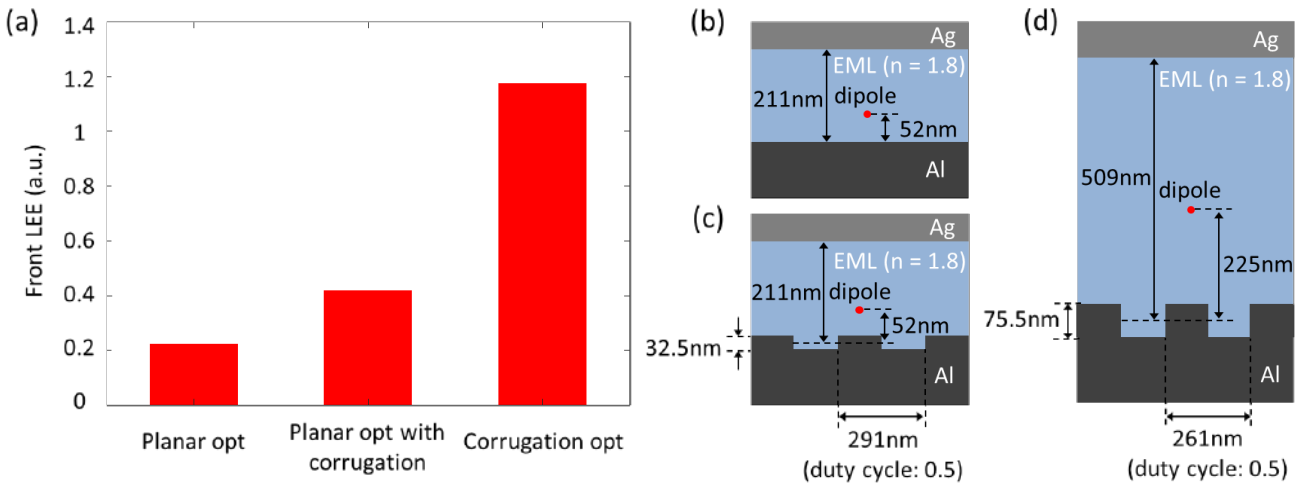

Fig. 1. (a) Front LEE of optimized planar structure, optimized planar structure with corrugation, and optimized corrugation structure. (b), (c), (d) Schematic figure of optimized planar structure, optimized planar structure with corrugation, optimized corrugation structure, respectively.

Acknowledgment

This work was supported by LG Display.

References

1. Salehi, A., Fu, X., Shin, D.-H., So, F., *Adv. Funct. Mater*. 2019, 29, 1808803.
2. Moharam, et al. *Optical Society of America,* vol. 12, no. 5, p. 1077-1086 (1995)
3. Hugonin. J.P., et al. arXiv:2101.00901

Effect of Resistive Switching by inserting Al_2O_3 thin layer in Peptide Memristor

Hae Chan Choi [1], Jeong Hyun Yoon [1], Min-Kyu Song [1], and Jang-Yeon Kwon [1]
[1]**School of Integrated Technology, Yonsei University, Incheon 21983, South Korea**
Tel.:82-032-749-5916, E-mail: jangyeon@yonsei.ac.kr

Because of its electrical advantage that can be controlled with both voltage and humidity, Y7C(YYACAYY) peptide material was proposed for switching layer of memristor[1]. Bimodal memory which can modulate synaptic weight in neuromorphic system can be also realized. Linearity and symmetry of conductance change are important factors to implement neuromorphic device based on deep neural network (DNN), in aspect of its controllability.

For these requirements, Al_2O_3 thin layer is inserted in Ag/Y7C/Pt memristor (Fig. 1). Its electrical performance is analyzed, compared with original Ag/Y7C/Pt memristor. I-V curve, cycle endurance, stability, potentiation & depression of conductance were tested for each device, with variations in thickness of Al_2O_3 (5nm, 10nm, 20nm) and Relative Humidity (50%, 70%, 90%). Ag top electrode and Pt bottom electrode were deposited with thermal evaporator, Y7C layer was spin coated, and Al_2O_3 was deposited with PEALD. The interfaces between Y7C/Al_2O_3, Al_2O_3/Pt will be observed by SEM (Scanning Electron Microscope).

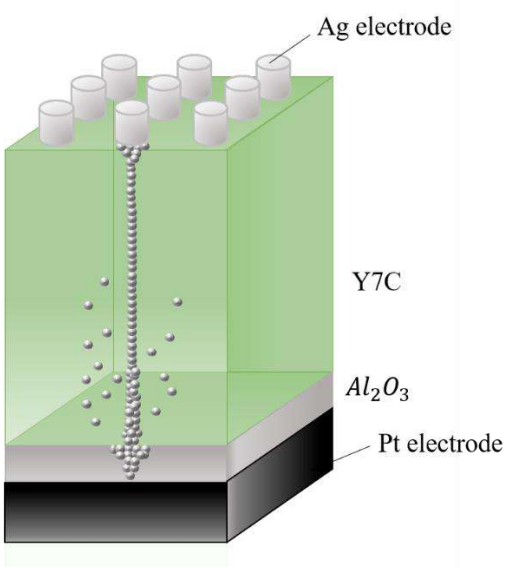

Fig. 1. Diagram of Ag/Y7C/Al_2O_3/Pt Memristor

Acknowledgment
This work was supported by the National Research Foundation of Korea (NRF) grant funded by the Korea government (MSIT) (No. 2020R1A2C2004864).

References

1. Song, Min-Kyu, et al. "Proton-enabled activation of peptide materials for biological bimodal memory." *Nature Communications* 11.1 (2020): 1-8.

Multi-Resistive State IGZO-Based Memristor by Controlled Set Voltage Region

Jeong-Min Park[1], Young-Woong Song[1], and Jang-Yeon Kwon[1,]*
[1]**School of Integrated Technology, Yonsei University, Yeonsu-gu, Incheon 21983, Republic of Korea**
Tel.:82-32-749-5837 , E-mail: jangyeon@yonsei.ac.kr

Recently, the amount of computation required for devices for more complex artificial intelligence has continued to increase. Neuromorphic structure can fasten the computation speed by implementing memristors as artificial, in-memory computing synapses as a single device capable of both memory and learning, just like a human brain.

Amongst various emerging neuromorphic technologies, oxide based resistive random access memory(ReRAM) has advantages including high density, stability, high operation speed, and low cost.[1] IGZO-based memristor is driven by ion filament formed by migration of oxygen ions.[2] Therefore, precise analysis of the correlation between oxygen concentration in IGZO and device performance is the key link for IGZO ReRAM with multiple resistive states as shown in Fig1.a.

The oxygen partial pressure is controlled in IGZO RF-sputtering process, thus finding where set/reset process is observed as shown in Fig1.b. Then, the multi-resistive-state memristor by reconstructed bi-layered ReRAM which enables deeper neural networks with faster computation speed.

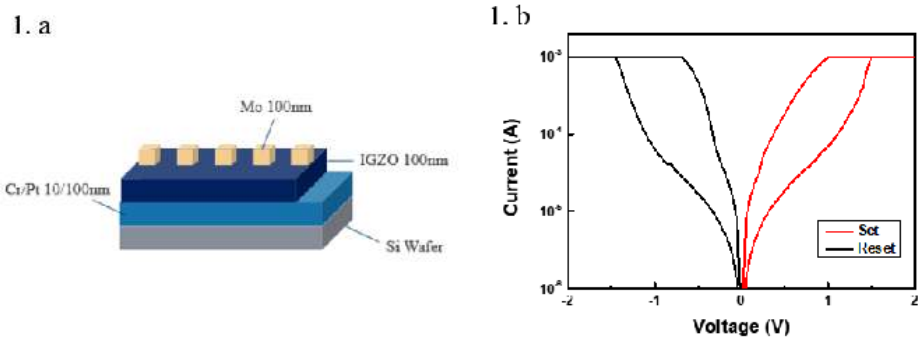

Fig. 1. IGZO-based RRAM (a) Schematic Image (b) I-V Characteristic of PO_2:30 Hysteresis Case

Acknowledgment

This work was supported by the National Research Foundation of Korea (NRF) grant funded by the Korea government (MSIT) (No. 2020R1A2C2004864).

References

1. P. Ma *et al.*, "High-Performance InGaZnO-Based ReRAMs," IEEE Transactions on Electron Devices, vol. 66, no. 6, pp. 2600-2605, 2019
2. Wang, Z.Q. *et al.*, "Synaptic Learning and Memory Functions Achieved Using Oxygen Ion Migration/Diffusion in an Amorphous InGaZnO Memristor" Adv. Funct. Mater., 22: 2759-2765. 2012

Image Classification : 3D Display Lens Alignment Inspection

Je-Hong Ryu[1], Young-Sang Ha[2], and Ki-Don Joo[1]
[1]AI team, [2]Advanced Research team, Samsung Display Company, Ltd.
Samsung Display, 1 Samsung-ro, Giheung-gu, Yongin-si, Gyeonggi-do, South Korea
E-mail: jh79.yoo@samsung.com

This paper proposes a deep learning-based image classification model. It's for inspection of the three-dimensional luminance quality of the 3D display panel. That inspection checks panel's luminance quality of various points of view using reflected luminance images. The bad quality sample is due to alignment accuracy between the 3D lens and panel. Abnormal patterns are shown through those images. Inspection has been executed manually by checking a small part of the panel after the area is converted to a digit value. It takes too much time to analyze the whole data of the panel. So inspection is limited to coverage and time for the entire panel analysis. The proposed model could improve such limitations and applies to an automatic inspection.

Training data of classification model is several viewpoint images for panel's reflected luminance. As mentioned above, these images could show alignment accuracy. The class was defined as visually distinguishable. Total five classes dataset was used for training. This classification was focused on the overall trends and characteristics of the images. Original data was preprocessed by downsizing. Based on the Xception model, while maintaining the target accuracy level, we optimized the lightweight model through layer size, hyperparameter, and image size. The structure of the panel and 3D lens alignment and classification flow is shown in Figure 1.

The base model was selected of VGG, Xception, and the Efficientnet as their classification performance. The Xception model was the best for train and test results. Classification accuracy was not affected by input image downsizing to 1/10. The best model showed 99% accuracy for five classes. Almost all classes were perfectly distinguished except for one class. Classification results showed the possibility of applying the model to automatic 3D display luminance inspection. If the bad sample is further classified in detail, it is possible to quantification alignment. Furthermore accurate and detailed feedback for the reflected luminance images could improve 3D lens and panel alignment.

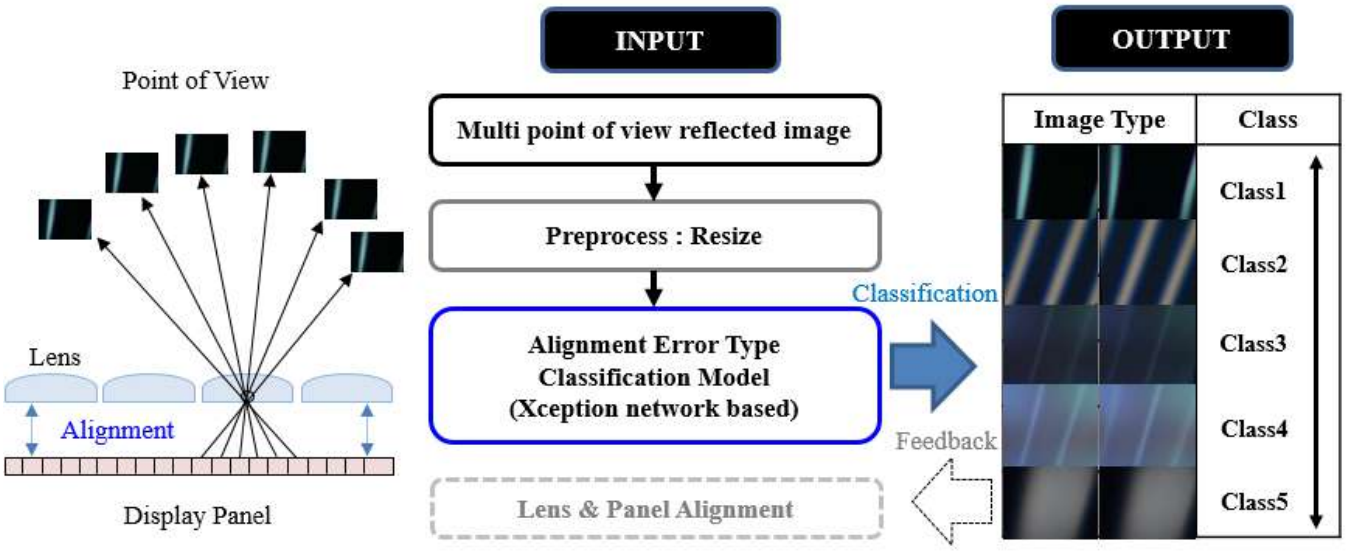

Fig. 1. Panel-Lens alignment structure and error type classification flow

References

1. Chollet, F. Xception : Deep learning with depthwise separable convolutions. *Google, Inc.* (2017).
2. Clevert, D. A. et al. Fast and accurate deep network learning by exponential linear units (elus). arXiv preprint arXiv:1511.07289 (2015).

Hinges in Foldable and Rollable Devices, Technical Review

Insun Hwang[a,b], Hyun Min Park[a] and Yeoung Jin Chang[c]*

[a]AUFLEX, Gyeonggi-Do, Korea

[b]AUHUA 奥华精密, Dongguan, China

[c]Department of Computer Engineering, Gachon University, Korea

Abstract

The form factor of a mobile phone device becomes diversely. After a foldable mobile phone's success, a rollable device has received a great attention in the market. In this paper we reviewed the hinge technology for foldable and rollable devices and their issues. A rollable device is seemed to be suffered by the rigidity issue of its cover window like an out-foldable device. We have compared these devices in the viewpoint of product and technology. The folding trace, one of the weakest points for foldable device will be lessen in a rollable device, but it also have lots of technical huddles. We hope we can find various form factor products in the market such a multi-foldable, foldable-rollable hybrid product in near future.

Author Keywords

Flexible display; Foldable device, Rollable device; Folding hinge; Rolling hinge; In-foldable; Out-foldable

1. Introduction

Considering the change of display device in mobile phone products in the past, there are three trends we can find. One is the performance improvement of display device such as size of display device, pixel density, color gamut, refreshing frame rate, dynamic range, and so on. Another one is the function integration of other components such as on-cell touch sensor, on-cell polarizer, hole in active area, under display camera, and so on. Performance improvement of a mobile device is almost saturated recently. So some players in the market focus to find new thing in the last trend which is the change of its form factor such as foldable and rollable devices. After success of the foldable phone of Galaxy Z Fold in 2019, many panel makers and mobile phone makers are trying to resolve some unsatisfactory issues such as folding trace, rigidity of cover window, thickness and weight problem.[1]

Figure 1. In-folding and out-folding hinges which are set in their mock-ups.

So far, the display area of a mobile device increases continuously. But there is a limitation by a grip size and inconvenience of portability. In contrast, the needs for multi-tasking work and enjoying game and video clips still prefers to a larger screen size. In this situation, some companies demonstrate prototypes of a rollable display recently.[2.3] It has slimmer design and lighter weight comparing to a foldable device. So, it has taken a great attention in the market for resolving folding trace and thickness problems of a foldable device. But it also has its own technical issues.[4] In this paper we'd like to compare these foldable and rollable technologies in the viewpoint of hinge and summary their developing status.

2. Foldable and Rollable Devices and their Hinges

Figure 1 shows in-folding and out-folding type hinges which are built in their mock-ups. Many companies are trying to commercialize an out-folding type foldable device because it can use its screen at both folded and unfolded situations. But it does not reach to customer's expectation in durability of its cover window, and some of them turned direction to develop in-foldable device preferentially.

There are two kinds of hinge in in-folding device according to its folding shapes, U-type and water-drop (WD) type as shown in figure 2. For an U-type device its folding radius influences on device thickness directly, so it should be minimized as possible and resulted in increase of difficulty on OLED panel. While, for a WD-type device, it has afford in folding radius, but it has to occupy some space in its device. At the hinge's viewpoint, a hinge controls two plates which OLED panel laminated on for an U-type device. Folding movement can apply stress on OLED panel, so hinge has to control the folding trajectory precisely. For WD type device it has more plates to control precisely.

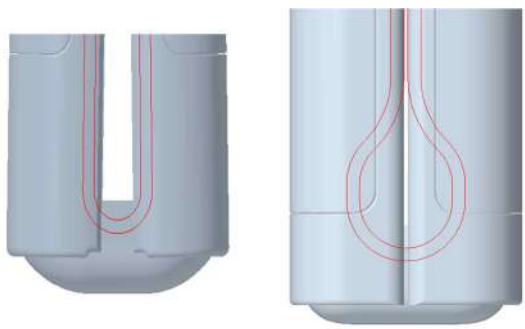

Figure 2. Folding shapes of in-folding devices, U-type(left) and WD-type(right).

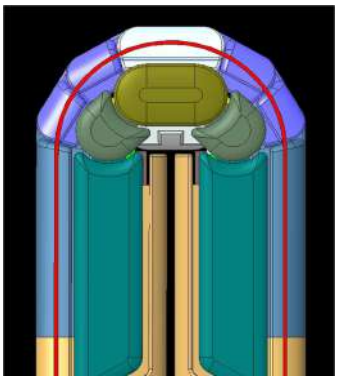

Figure 3. An example of out-folding hinge.

In the case of out-folding device, it has much more afford in its folding radius because other components of mobile phone located under the display panel, so display screen can secure a certain reliable folding radius. Its hinge has to have multi-joint structure (MJS) for folding movement as shown in figure 3. It is hard to control a movement of every links in multi-joint structure, and thus other hinge parts control its folding trajectory and MJS is folded passively. MJS has not to change its length for OLED panel and jointing axes plane is as close to OLED panel plane as possible in order to minimize additional stress during folding movement. On the other hand, we have explained how to make stress-free folding trajectory for an in-folding device.[1,5]

Figure 4 shows the concept of a rollable device. It can be driven by manual, semi-auto and auto ways. Many companies prefer to auto driving method since there is some possibility for an OLED panel to be damaged by manual driving. For auto-type rolling hinge small size motor, gearing unit and moving rail are needed, and these occupy some space in the device.[4] Besides, it also need a specially designed back-plate in order to protect an OLED panel and spread the stress by rolling movement. A rollable device is an out-folding one basically, so it also has the surface hardness issue of the cover window.

3. Technical Comparison and Issues

Figure 5 shows a WD-type foldable device mock-up comparing to Galaxy Z Fold2 which has an U-type folding hinge. In the case of an U-type hinge, the thickness of hinge side is thicker than that of

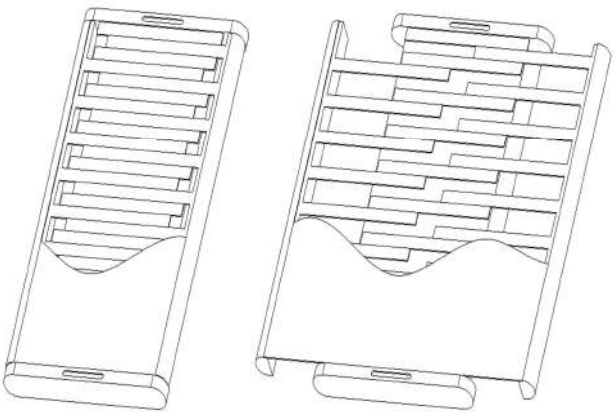

Figure 4. Concept of a rollable mobile phone.

Figure 5. Picture of a WD-type foldable device (right) comparing with Galaxy Z Fold2 which has a U-type hinge (left).

the opposite side, so the device thickness is not even but a wedge shape, while a WD-type device has a plat shape.

As mentioned in section 2, a WD-type hinge has more plates to be controlled than an U-type one. A recent foldable device has a free-stop function that the device can be maintained its folding angle at an arbitrary value as shown in figure 5(bottom). For this function the half screen should be kept almost flat up to 90 degree folding angle. Figure 6 shows the folding sequences of a WD type hinge plates, (a)~(c) in figure 6 sustain almost flat half-screen state, and then be transformed to WD shape ((d)~(g)). A foldable hinge needs an appropriate torque value for free-stop function. It can be designed by controlling its rotational friction.

In the case of a rollable device it doesn't need to apply MJS for whole rolling area which is wider than a foldable device. We have developed a novel patterned back-plate which is very flexible along its rolling direction. This back-plate gives a mechanical support for an OLED panel, but has not to apply any additional

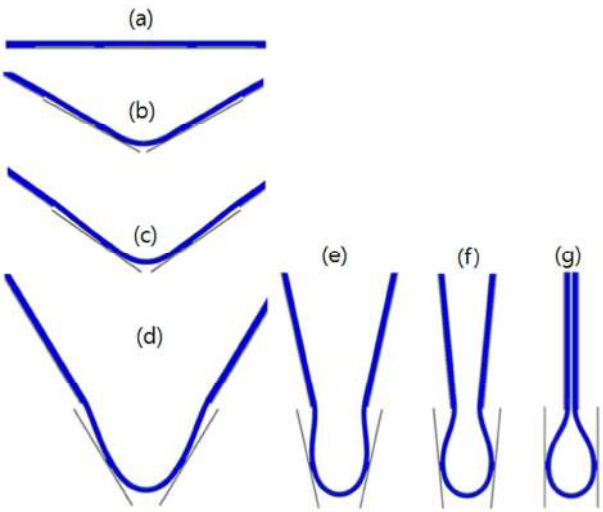

Figure 6. Movement of hinge plates and the shape change of OLED panel in WD-type foldable device when it folds.

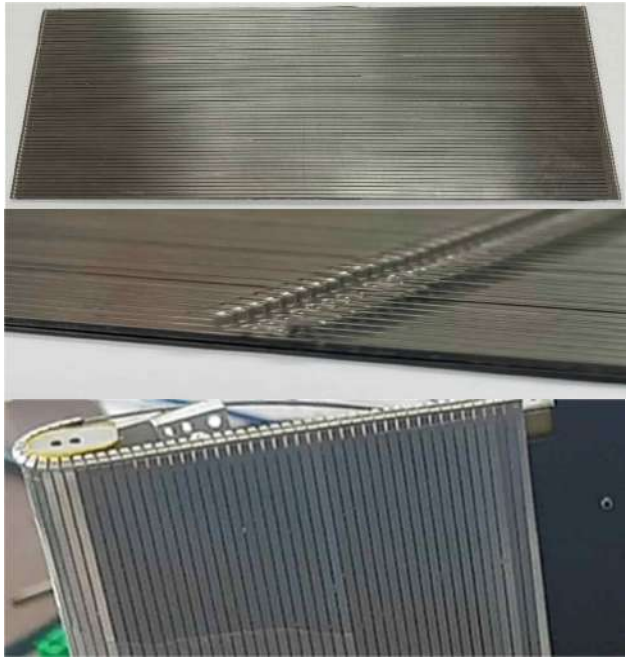

Figure 7. Novel concept of a back-plate for a rollable device. Top, bottom sides and rolled shape of a back-plate,

stress on an OLED panel when it drives as shown in figure 7. It has multi-layer structure having different pattern size. Of course, a foldable device also has a back-plate under an OLED panel which is single layer, patterned by etch process in the folding region.

We have compared these hinge technologies in product viewpoints in table 1. The estimation is subjective and relative in a certain degree. For screen extension, foldable devices is almost twice as possible, while rollable device can be 1.3~1.6 times range. For device design, U-type has a wedge shape, but the others have a flat one and rollable is slimmer than foldable.

As a hinge structure is more complex, its number of parts and its space in device are increased. In the case of a rollable device these depend on its driving way, of course an auto way needs more space and parts than a manual way. Folding trace is one of the

Table 1. Comparison of foldable and rollable devices in the viewpoint of product and hinge technology.

Comparison Items	Foldable Device			Rollable Device
	In-Foldable		Out-Foldable	
	U-type	WD-type		
Screen Extension	◎	◎	◎	△
Device Design	x	○	○	◎
Hinge Space in Device	◎	○	○	△/x
# of Hinge Parts	◎	○	△	x
Folding/ Rolling Trace	△/x	△	△	△
Folding/ Rolling Durability	○	○	△	(△)

◎ better, ○ good, △ so so, x worse, ( ) estimated

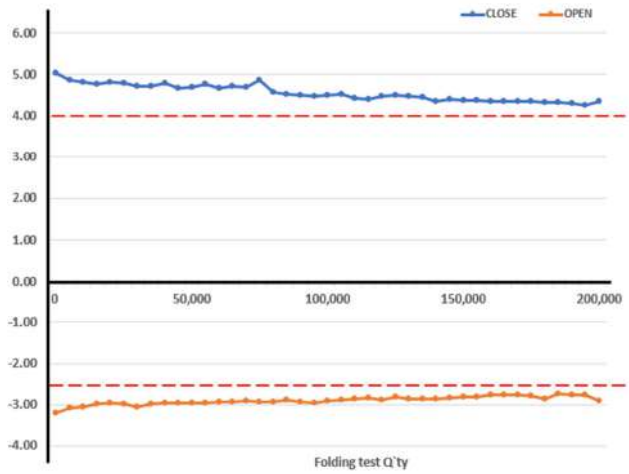

Figure 8. Torque reduction of SFF hinge in the 200k lifetime folding test.

weakest points for a foldable device. It is narrow and deep for an U-type, and be shallower and wider for a WD-type in-foldable and an out-foldable. If one optimizes its folding trajectory to minimize the stress on an OLED panel, then it can be lessen in a certain range. Perception of human eye on the folding trace is different from physical quantities of depth and width. Wider trace can be more offensive to the eye than deeper trace. Anyways, we consider these traces are unavoidable for foldable and rollable devices in a certain degree.

4. Folding and Rolling Lifetime Test

It is not determined yet in industry how many times folding durability should be guaranteed, but many makers have testing in

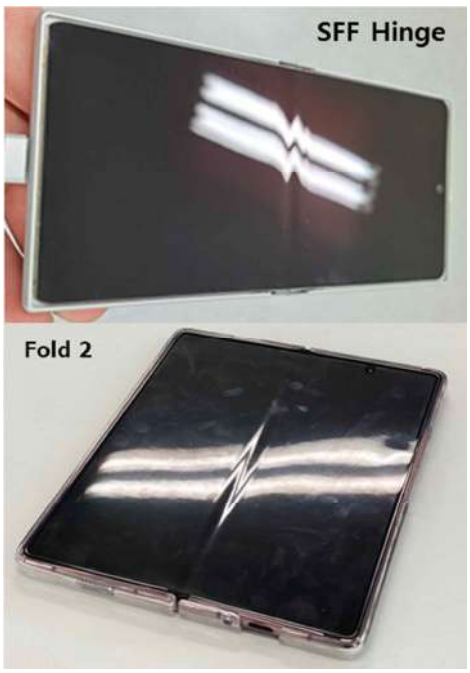

Figure 9. Folding trace comparison of the mobile phone mock-up with SFF hinge to the Galaxy Z Fold2.

the range of 100k to 200k. We measured the change of torque value with our mock-up. In general the torque is reduced 20~40% by abrasion after 200k folding. But we optimized surface properties and component shapes of our hinge in order to lessen this reduction under 20%. Figure 8 shows the testing result. Sometimes, the torque value is increased as a folding test goes on because its folding motion is disturbed by wear dust. Thus a monotonous reduction like the graph in figure 8 is the best result.

Figure 9 shows the folding trace of our mock-up after 200k lifetime test. It is much weaker than Galaxy Z Fold2 which was bought last year and used in daily routine. But for a rollable device we don't have any result of rolling lifetime test yet. It is needed to decide a driving method and mechanical structure and so on before the rolling lifetime test.

5. Conclusion

So far, we have lots of experience on foldable and rollable devices and its hinges. Foldable device has two types, in-foldable and out-foldable, and there are also two-types, U-type and WD-type in in-foldable device. Each technology has its own merits and demerits. We have explained these at this point in time. Technical hurdles will be overcome in near future and various foldable and rollable products such as multi-foldable, foldable-rollable hybrid device will be showed in the market.

Out-foldable and rollable devices are good for an OLED panel, but they have window hardness issue. Folding/rolling trace will be shallower and wider, but it does not correspond to the perception of human eye. As hinge structure becomes complex, its parts number and the hinge space in device are increased. In the case of rollable device there is no data of lifetime rolling test yet.

6. References

1. H.J. Han, W.J. Cho, S.J. Lee, H.M. Park and I. Hwang; 'Stress-Free Folding Hinge for Foldable OLED Display Device', accepted for SID conference 2021.
2. Roger Cheng, 'The LG Rollable phone with expandable display is real, and coming in 2021', cnet news; Available from: https://www.cnet.com/news/the-lg-rollable-phone-with-expandable-display-is-real-and-coming-in-2021/
3. Sean, 'Oppo X 2021 unveiled as the world's first smartphone concept with an extending display', Gizmochina news; Available from: https://www.gizmochina.com/2020/11/17/oppo-x-2021-worlds-first-extending-concept-smartphone/
4. H.J. Han, H.M. Park and I. Hwang; 'Novel Rolling Hinge for Rollable Mobile Device', submitted to ICDT conference 2021.
5. H.J. Han, S.J. Lee, H.M., Park and I. Hwang; 'Stress-Free Folding Hinge for In-Foldable Device'; J. of Information Display, submitted, 2021

Fabrication of stretchable and transparent nanonetwork electrode using electrospinning and sacrificial layer

Kyungmin Kim[1], and Jung-Yong Lee[1]
[1]School of Electrical Engineering (EE), Korea Advanced Institute of Science and Technology (KAIST), Daejeon 34141, Korea
Tel.:82-42-350-7528, E-mail: jungyong.lee@kaist.ac.kr

Stretchable electronics are essential for the next generation electronic devices such as wearable devices, stretchable displays, and skin attachable bio-sensors[1]. Also, transparency of electronic devices is important especially for optoelectronics[2]. Therefore, researches of electrode that have both stretchability and transparency are currently being reported. Here, we introduce the facile fabrication method for stretchable and transparent electrode. We adapted electrospinning and physical vapor deposition of sacrificial layer to configure it. The electrospun nanofibers can be used as a template for conductive nano-networks and sacrificial layer is to remove conductive material for void region. The final structure of conductive nanonetwork is follows the electrospun polymer nanofiber template, so we can handle the transparency and conductivity by adjusting nanofiber density. This fabrication method can use various conductive materials that can be deposited by any deposition method. For example, liquid metal can be used for stretchable and conductive material. Also by choosing proper solvent, various materials for stretchable substrate can be used. The candidate material of sacrificial layer is monomer C_{60}, which can be deposited by physical vapor deposition to maintain the structure of electrospun naofibers and removed by organic solvents which do not damage the conductive material.

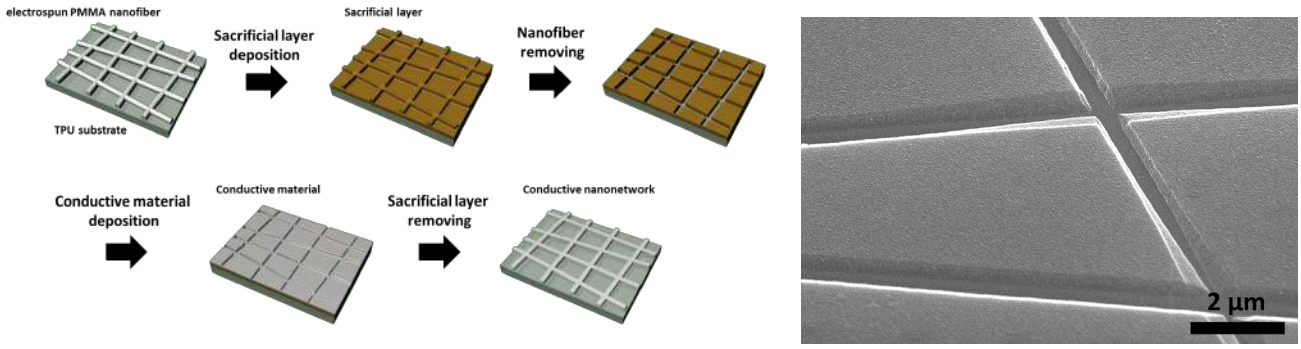

Fig. 1. Fabrication method for conductive nanonetwork electrode, and SEM image after removing electrospun nanofibers

Acknowledgment

References

1. J.-W. Seo, *Adv. Funct. Mater.*, 30(34), 2000896 (2020).
2. K.-W. Seo, *Adv. Mater.*, 31(36), 1902447 (2019).

Electrically Controlled Bendable Actuator for Deformable Display

Jun Hyuk Shin[1,3], Ji Yoon Park[2,3], Sang Hyun Han[1,3] and Su Seok Choi[1,3]*
[1]Dept. of Electrical Engineering, POSTECH, Pohang, Gyeongbuk 37673, Korea
[2]Dept. of Physics, Kyung Hee University, 26 KyungHeeDae-Ro ,DongDaeMun-Gu, Seoul, Korea
[3]CSS Research LAB @ Dept. of Electrical Engineering, POSTECH, Pohang, Gyeongbuk 37673, Korea

Tel.:82-54-279-2228, E-mail: choiss@postech.ac.kr

Soft Actuator can result in responsive mechanical shape deformations by various stimulating stress such as thermal, magnetic, photonic and electroactive methods. Technical benefits of soft actuator can be used for soft robots, sensors and also for shaping deformable display as well.[1] In particular, electrically controlled actuator, in other words electroactive polymer acutator (EAP actuator), is highly desired for electronic device application including deformable bendable display. For large bending deformation, it is desired to obtain a high powered EAP by higher voltage or higher properties material synthesis. Also, much stronger bending deformating displacement or lower triggered electrical field can be approached by multilayered actautor stucture. [2-3]

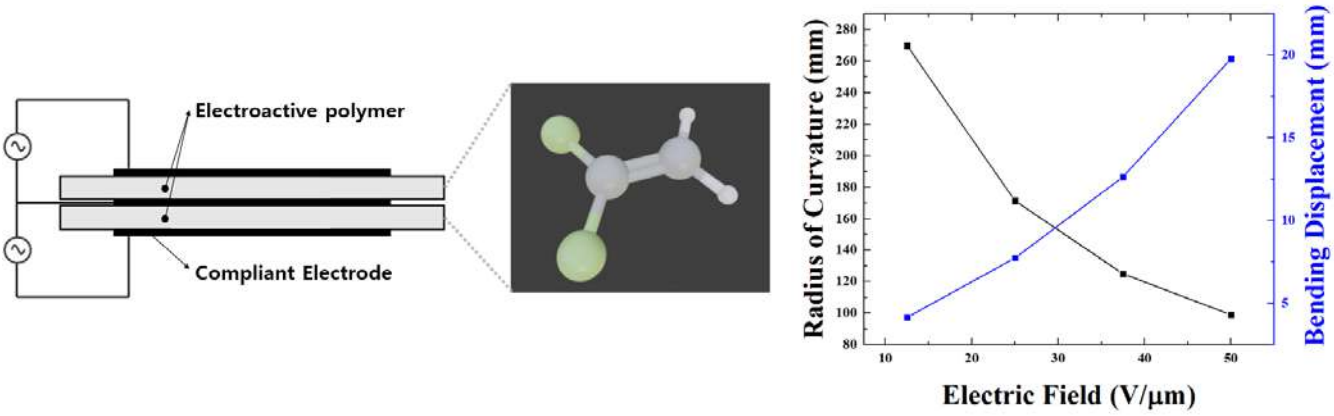

Fig. 1. Radius of curvature and bending displacement properties of multilayered EAP actuator

In this study, we studied detailed evaluation of radius of curvature and bending displacement behaviors by multilayered EAP soft actuator system. For the molecular polarization properties of EAP such as ferroelectric polymer, applying an electric field triggered strain and actuating properties generated with bending actuation was studied. From this experimental observation, we report higher powered stacked layered actuation with positive strain and compressing negative strain together and high bending displacement. (Fig. 1)

Acknowledgment

This research was supported by the Technology Innovation Program (20010690, Development of 12inch panel (20% stretch) and module process technology for massproduction of stretchable display) funded By the Ministry of Trade, Industry & Energy(MOTIE, Korea) and Nano Material Technology Development Program through the National Research Foundation of Korea(NRF) funded by Ministry of Science and ICT (NRF2018M3A7B4089670).

References

1. Clarisse Ribeiro, Carlos M Costa, Daniela M Correia, João Nunes-Pereira, Juliana Oliveira, Pedro Martins, Renato Gonçalves, Vanessa F Cardoso and Senentxu Lanceros-Méndez, Nature protocols 13.4 (2018)
2. MyungJin Lim, Su Seok Choi,Yong-Su Ham, Taeheon Kim, YongWoo Lee, Seulgi Choi, US 9748469 B2 (2017)
3. Choi, Seung Tae, Jong Oh Kwon, and François Bauer., Sensors and Actuators A: Physical 203 (2013)

Analytical Study of Multilayered Rollable OLED Display Structure using Finite Element Method

Sang Hyun Han[1], Jun Hyuk Shin[1], and Su Seok Choi[1]*
[1]**Dept. of Electrical Engineering, POSTECH, Pohang, Gyeongbuk 37673, Korea**
Tel.:82-54-279-2228, E-mail: choiss@postech.ac.kr

Recently flexible display evolves in terms of shape deformable display with various form factor merits. More recently, technical interest in Rollable OLED Displays which can be rolled up screen is rapidly increasing beyond curved, bendable and foldable displays toward expandable and on-demand screen variable display. Based on this expanded shape deformation, Rollable OLED Display is expected to bring innovations in various IT devices such as smartphones and TVs. However, from the technical point of view, it is highly challengeable due to the multi-layer stacked structures of Rollable OLED, which has not uniform and large sized deformation characteristic behaviors. In order to overcome this problematic deformation, multi-layered Rollable OLED structure studies are highly required [1-3].

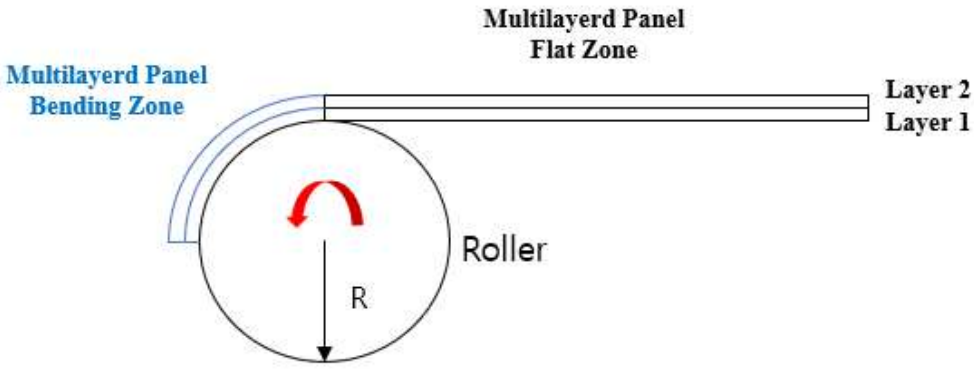

Fig. 1. Rollable simulation model with two-layer structure

In order to obtain mechanical reliability, we studied the delamination behaviors in multi-layered Rollable OLED Display. This problematic large deformation of multi-layered structures under rolling deformation stress condition was observed by analytic study using Finite Element Method (FEM). The Rollable multi-layered structures were studied based on the rolling multi-layered model with radius R, such as Fig 1. In this study, with additional complex boundary conditions study, we will present visual and mechanical stress-strain studies how to improve the delamination problem in multi-layered structures.

Acknowledgment

This research was supported by the Technology Innovation Program (20010690, Development of 12inch panel (20% stretch) and module process technology for mass production of stretchable display) funded By the Ministry of Trade, Industry & Energy(MOTIE, Korea), Nano Material Technology Development Program through the National Research Foundation of Korea (NRF) (NRF2018M3A7B4089670) and Next Generation Engineering Research Program of National Research Foundation of Korea (NRF) funded by the Ministry of Science, ICT (No. 2019H1D8A2106519).

References

1. A. Cheng., et al., The Society for Information Display (2020).
2. Nam, J., Lee, S., Han, M. et al., Int. J. Precis. Eng. Manuf (2021).
3. Ma, B. S., Jo, W., Kim, W., Kim, T.-S., Journal of the Microelectronics and Packaging Society, 27(2), 19–26 (2020)

Parametric Study of Serpentine Electrode Shape for Stretchable Display

Suan Lee, Jiyoon Lee and Su Seok Choi*
[1]Dept. of Electronic Engineering, POSTECH,
77 Cheongam-Ro. Nam-Gu. Pohang. Gyeongbuk. Korea 37673
Tel.:82-054-279-2228, E-mail: choiss@postech.ac.kr

The importance of display form factor is rapidly increasing in various display applications. As a result, shape deformable display evolves in terms of bendable, rollable and stretchable display. In particular, stretchable display is highly desirable and ideal due to its free and random shape transformability on various user and application demands. However, in order to fabricate realistic stretchable electronic device, technical challenge regarding how stable the electode under strain stress condition while maintaining high conductivity is crucial[1]. There are wo ways to fabricate stress-strain stavle electrode. One is to use intrinsically stretchable material such as conductive polymer.[2] Another appoach is to use conventional electrode material such as copper or aluminum and adjust eletrode shape structure. Considering that conventional electode materials in display lack stretchability, the materials provide good condcutivity in unstressed condition. Introdution of serpentine shape structure to conventional electrode material can effectivly allow good stretchable electric circuit connection. Since the effective extended stretchability is achieved by combining multiple shape parameters of sepentine electrode, shape paramatic analysis study of this sepentine electrode is highly demanding.

In this study, we approached this analtical method to study serpentine electrode shape parameters and tried to figure out stable serpentine electode under stretching stress condition. From the four paramters analysed desing of sepentine electrode, computer based anlaytical study of strain-stress vulnerability is computed and anlaysed. In this study we report the parameterized alaytical stretchable sepentine electrode properties and suggest the better contioned serpentine shape design study in detail (Figure 1).

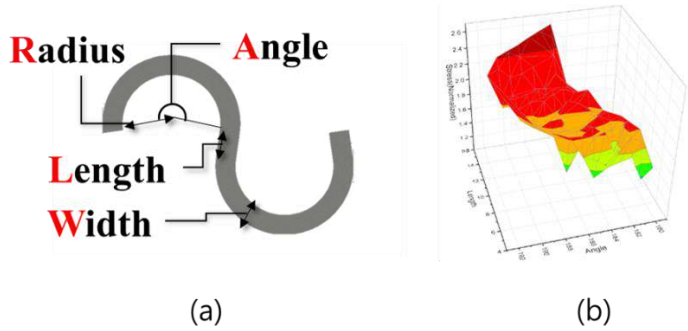

Figura 1. Parametric Study of Serpentine Stretchable Electrode

Acknowledgment

This research was supported by the Technology Innovation Program (20010690, Development of 12inch panel (20% stretch) and module process technology for massproduction of stretchable display) funded By the Ministry of Trade, Industry & Energy(MOTIE, Korea) and and Next Generation Engineering Research Program of National Research Foundation of Korea (NRF) funded by the Ministry of Science, ICT (No.2019H1D8A2106519).

References

[1] L. Xu, S. R. Gutbrod, Y. Ma, A. Petrossians, Y. Liu, R. C. Webb, J. A. Fan, Z. Yang, R. Xu, J. J. Whalen, J. D. Weiland, Y. Huang, I. R. Efimov, J. A. Rogers, Advanced Materials 2015, 27, 1731.
[2] D. Zhang, S. Xu, X. Zhao, W. Qian, C. R. Bowen, Y. Yang, Advanced Functional Materials 2020, 30, 1910809.

Optimization of Free-form Electrode Based on Inkjet Printing Method

Seyoung Choi[1], Soyul Kwak[1], Jihyeon Kang[1], Seohyeon Jang[1], Hojong Eom[1], Ohhyun Kwon[1], Inho Nam[1]*
School of Chemical Engineering and Materials Science, Department of Intelligent Energy and Industry, Chung-Ang University, Seoul 06974, Republic of Korea
Tel: 82-2-820-5936, E-mail: chy5376@cau.ac.kr

Over the past decade, highly deformable electronics have attracted considerable attention as promising alternatives to conventional rigid electronics. In particular, the electronic components of soft and stretchable devices have remarkably advanced for the next generation. However, mechanical compliance is critical in the manufacture of stretchable electronic devices, and devices should not incur physical damage or change their performance under the bending or stretching states. Several important discoveries and breakthroughs in the fundamentals of this technology and fabrication strategies to face these challenges and achieve the above-mentioned targets. Among these enormous efforts, inkjet printing is a very promising technology with great commercialization potential for fabricating flexible electronics. Herein, we demonstrate a set of materials and design concepts for a flexible device that exploits thin, low modulus silicone elastomers as top and bottom substrates, and wavy interconnects between them. By adjusting the ideal setting parameters, we obtained the finest metal lining resulting in reversible levels of flexibility, while maintaining its structure and intensity of LED light emission.

Acknowledgment

The work was supported by the Competency Development Program for Industry Specialists of the Korean MOTIE operated by KIAT (No. P0012453, Next-generation Display Expert Training Project for Innovation Process and Equipment, Materials Engineers).

Curable hard coating additive for anti-scratch, transparent, hydrophobic flexible cover window

Kang-Han Kim[1,2] and Yong-Cheol Jeong[1]
[1]Process Platform R&D Department, KITECH, Ansan, 426-910, Korea
Tel.:82-31-8040-6197, E-mail: ycjeong@kitech.re.kr
[2]Department of Materials Science and Chemical Engineering, Hanyang University ERICA Campus, Ansan, 426-791, Korea

In this study, we present curable additive materials for anti-scratch and hydrophobic foldable hard coating materials. general hard coating materials present high durability and transparency while also show poor surface functionality such as hydrophobic-based anti-fingerprint property and anti-reflective property. To impart these functional characteristics, usually, fluorine-based additives are added to the coating solution. However, these additives are generally incurable materials, causing a decrease in surface hardness and increasing haze issue, although low content is used. We have developed a durable hard coating additive material that can be applied to a foldable cover window through a single coating process by synthesizing a fluorinated core nano-sol material having one-component water-repellent properties, high hardness, and high flexibility at the same time.

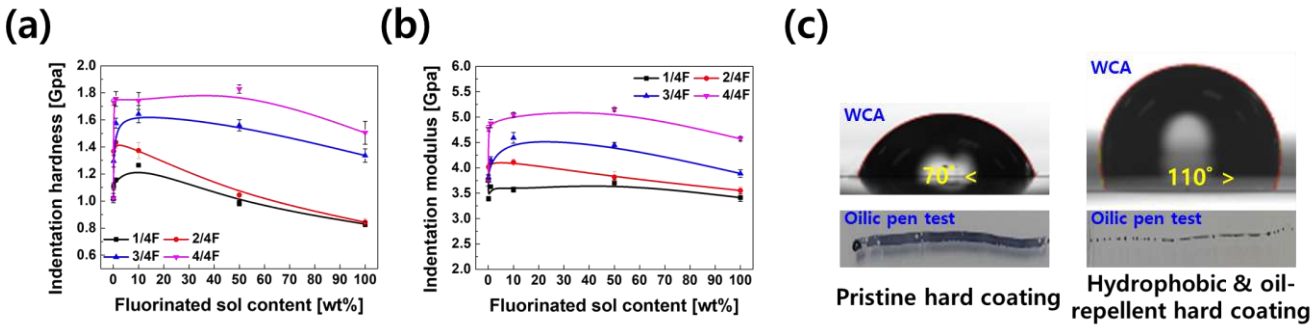

Figure 1. (a) Nanoindentation hardness and (b) nanoindentation modulus of fluorinated hard coating with different fluorine content (c) water contact angle and oil pen test of pristine coating and fluorinated coating

Acknowledgment

This research was supported by the MOTIE (Ministry of Trade, Industry & Energy (10077471)) support program for the development of future devices technology for display industry.

References

1. Kim, K. H., Jung, B., Jeong, Y. C, *Progress in Organic Coatings.*, 143, 105639, (2020).

On demand flammable yet stable OLED device based on paper for security device

Do-Gwan Kim [1,2] and Yong-Cheol Jeong[1]
[1]Process Plat form R&D Department, KITECH, Ansan, 426-910, Korea
Tel.:82-31-8040-6197, E-mail: ycjeong@kitech.re.kr
[2]Department of Materials Science and Chemical Engineering, Hanyang University ERICA Campus, Ansan, 426-791, Korea

In this study, we fabricated flammable OLED device with multi-layered substrate structure based paper OLED device for security device. In the case of the multi-layered structure described above, it was also improved the surface properties of inherent issues of paper. Through these structure, a stable OLED device was produced in a daily environment and even in a harsh condition like floating on water. But when the security is required, the security device can destroy the device partly and and complete destruction of OLED device. It is designed to flammable the device locally at a desired point that has multi-layered structure of a material with voltage reaction. Especially, The difference of thickness of multistructure can manage the turn off voltage that we intended to disposable the divice.

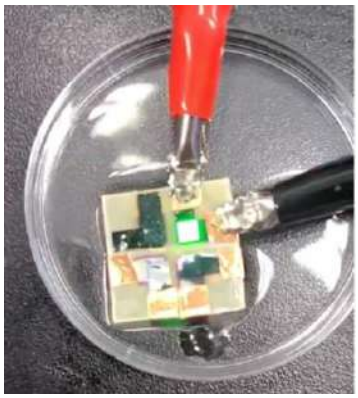

Fig. 1. a) image of the on-demand flammable multi-structured paper for OLED security device in harsh conditon.

Acknowledgment

This research was supported by the MOTIE (Ministry of Trade, Industry & Energy (10077471)) support program for the development of future devices technology for display industry.

References

1. Kim, D.; Jung, B.; Kim, K.; Cho, K. Y.; Jeong, Y. C. Highly Robust and Transparent Flexible Cover Window Films Based on UV-curable Polysilsesquioxane Nano Sol. J. Appl. Polym. Sci. 2020, No. November 2019, 1–13. https://doi.org/10.1002/app.49012..
2. Kim, K.; Jung, B.; Jeong, Y. C. Foldable hard coating materials based on reaction-controlled polysilsesquioxane resion for flexible electronics. Prog. Org. Coat. 2020, 143. https://doi.org/10.1016/j.porgcoat.2020.105639.
3. D.-G. Kim, D. Ahn, K.-H. Kim, Y.-C. J. Mater. A flexible yet wear-resistant co-citrate elastomer for on-demand disposable patch sensors. Chem. C, 2020,8, 10047-10059, https://doi.org/10.1039/D0TC02058C.

Hydrogel of ion side chain polymer for ionic conductor with versatile properties

*Sungryong Kim, Jungsu Kim, Junwoo Lee and Taiho Park**
Dept. of Chemical Engineering, Pohang University of Science and Technology (POSTECH), Pohang, Gyeongbuk 37673, Korea
Tel.:82-54-279-5295, E-mail: srkim96@postech.ac.kr

Recently, as intrinsically stretchable wearable devices have attracted a lot of interest, additional properties have been required as well as the stretchable properties. Here, we synthesized hydrogel with intrinsically stretchable (2636%) self-healable (98.3% in 3hr) and solution processable properties using the ion side chain. The ion side chains form the ionic bond between the polymers, and ionic bond acts as dynamic crosslinking in the polymers. Thus, it is possible that these polymers are self-healing. And salt in the ion side chains also give hydrophilic properties to polymers. These hydrophilic polymers are soluble in water. Therefore, using these polymers, solution processes could be applied. These polymers could be applied to ionic conductor area. We fabricated actuators and thermal sensors with the polymers. These thermal sensors operated in extreme environment and also showed the constant performance in spite of damage by external stress, repeated bending, and stretchable strain.

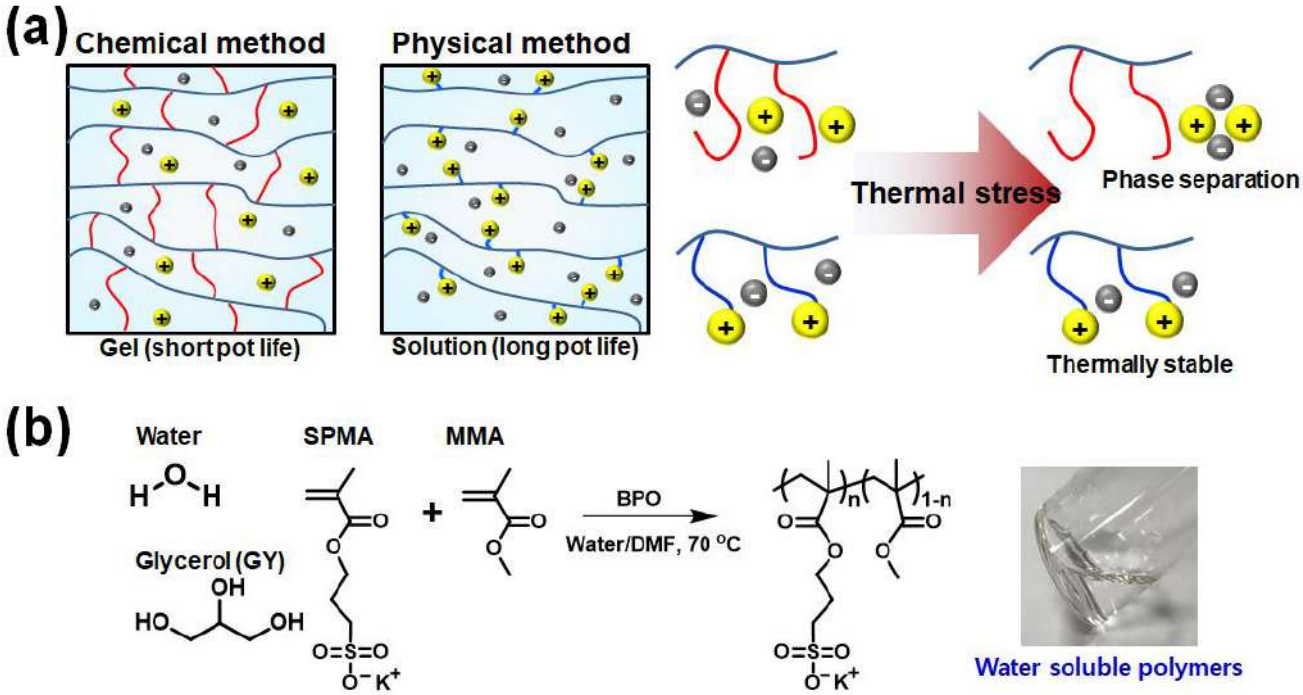

Fig. 1. The effects of ionic side chain. a) Schematics indicating difference regarding pot life and thermal stability according to chemical and physical methods. b) Scheme for P(SPMA-r-MMA)s and water solubility.

Transparent and Stretchable Interconnects with Ag-nanomesh/ITO Double Layer Structure

Young Ho Kim[1,2], Hyuk-Jun Kang[3], Dae-Geun Choi[3] and Chan Woo Park[1,2]
[1]Department of Advanced Device Technology, Korea University of Science and Technology (UST), Daejeon 34113, Republic of Korea
Tel.:82-42-860-5249, E-mail: chanwoo@etri.re.kr
[2]Flexible Electronics Research Section, Electronics and Telecommunications Research Institute (ETRI), Daejeon 34129, Republic of Korea
[3]Department of Nano Manufacturing Technology, Korea Institute of Machinery & Materials (KIMM), Daejeon 34103, Republic of Korea

As the form of displays is evolving into three-dimensionally curved shapes, freely deformable and transparent touch or pressure sensing panels are also required. Currently, indium tin oxide (ITO) and oxide-metal-oxide thin films are mainly used as transparent electrodes, but they are highly brittle with no stretchability. [1] Mixtures of carbon nanotubes or metallic nanowires with an elastomer are also employed [2], but they are hardly compatible the current display technology due to high resistivity and low pattern resolution. In the present work, we propose a new stretchable interconnect structure with Ag-nanomesh on an ITO serpentine body, which provides high transparency, low resistivity, and high mechanical stability as well as high compatibility with the current flexible circuit processes. In this structure, an ITO thin film is patterned into a serpentine shape, on which a top Ag nanomesh layer is formed by the nano-imprint technique. With the mesh structure, the resistance can be lowered by increasing the thickness of Ag layer with little loss of transmittance, and the crack propagation is suppressed during repetitive stretching. The Ag-nanomesh/ITO double layer shows the transmittance of 70~80%, and sheet resistance of 17.4 ohm per square. After being transferred onto an elastomeric substrate, the hybrid interconnect exhibits resistance change of less than 2%, during 10,000 cycles of 20% stretching. We also confirmed that the stretching behavior can be controlled by the shape and size of mesh or nano-imprinting conditions. Based on conventional thin film deposition and photolithography techniques, the new structure is readily applicable to various fields such as stretchable and transparent touch panels, artificial skins, or other wearable devices.

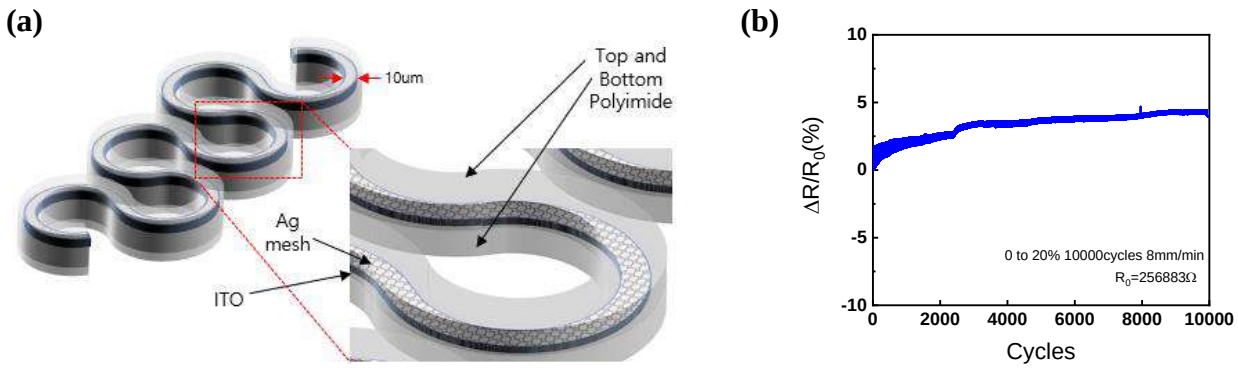

Fig. 1. (a) Structure of Ag-nanomesh/ITO double layer interconnect, and (b) the variation of electrical resistance under cyclic stretching of 20% for 10,000 cycles.

Acknowledgment

This work was supported by the Industry technology R&D program (20006467) funded by the Ministry of Trade, Industry & Energy (MOTIE, Korea).

References

1. Weiran Cao, Ying Zheng, Zhifeng Li, Edward Wrzesniewski, William T. Hammond, Jiangeng Xue, *Organic Electronics* 13 2221-2228 (2012).
2. Ying Zhou, Reiko Azumi, Satoru Shimada, *Nanoscale*, 11, 3804 (2019).

Supramolecular Movable Cross-linker in Pressure Sensitive Adhesives: Movable Cross-linking Effects on Adhesion Properties

Mo-Beom Yi, Tae-Hyng Lee, and Hyun-Joong Kim
Program in Environmental Materials Science, Seoul National University, Seoul, Korea

Cross-linking is an essential element to enhancing mechanical properties of polymers in elastomers, hydrogels, and adhesives. However, covalency in pressure sensitive adhesives introduces a trade-off between cohesive interactions and chain mobility, thus restricting the efficient use of cross-linker. We prepared a supramolecular movable cross-linker by attaching 2-isocyanatoethyl acrylate to β-cyclodextrin. The modified supramolecule formed a threaded compound with poly(butyl acrylate) via its cavity. The supramolecular cross-linker exhibited a sliding effect through the polymer chains like a poly-rotaxane. With the movable cross-linker, we could obtain outstanding mechanical properties in pressure sensitive adhesives, surpassing the limitation of the covalent cross-linker. This new supramolecular cross-linker could potentially broaden the application of adhesives lifting a restriction of cross-linker.

Acknowledgment

This work was financially supported by Samsung Display Co., Ltd.

A Fiber-Based White Organic Light-Emitting Diode for Truly Wearable Display Applications

*Yong Ha Hwang, Kyung Cheol Choi**
School of Electrical Engineering, KAIST, Daejeon 34141, Republic of Korea
**Tel.:82-42-350-5482, E-mail: kyungcc@kaist.ac.kr*

Advances in textile displays, one of the most notable free-form devices, stem from various studies on fiber-based organic light emitting diodes (fiber OLEDs) for providing visualization-interactivity between humans and machines based on the inherent deformability of the fiber and the high optoelectronic performance including a low operation voltage, brightness and current efficiency.[1-3] However, although notable studies have served as milestones, challenges remain for achieving a white OLED (WOLED), essential for solid-state lighting applications and full-color displays, on a cylindrical-shaped fiber due to limitations including the geometry and device configuration that are suitable for the fiber. Here, the first fiber WOLED is reported enabled by a single emission layer using the dip-coating method to overcome the aforementioned limitations. Based on the carefully designed configuration of the WOLED, the resulting fiber WOLED demonstrated a high optoelectronic performance and flexibility comparable to previously reported fiber OLEDs. Furthermore, the fiber WOLED was encapsulated by Al_2O_3/elastomer bilayers to obtain durability such as oxygen and sweat-resistance, pressure-resistance, and biocompatibility from external stimulus. The fiber WOLED could be easily integrated into daily clothes. Additionally, the fiber WOLEDs have been found to operate reliably in a saline solution which is similar to human body fluids and under repeated pressure tests, suggesting the promising potential of the fiber WOLED for truly wearable display applications.

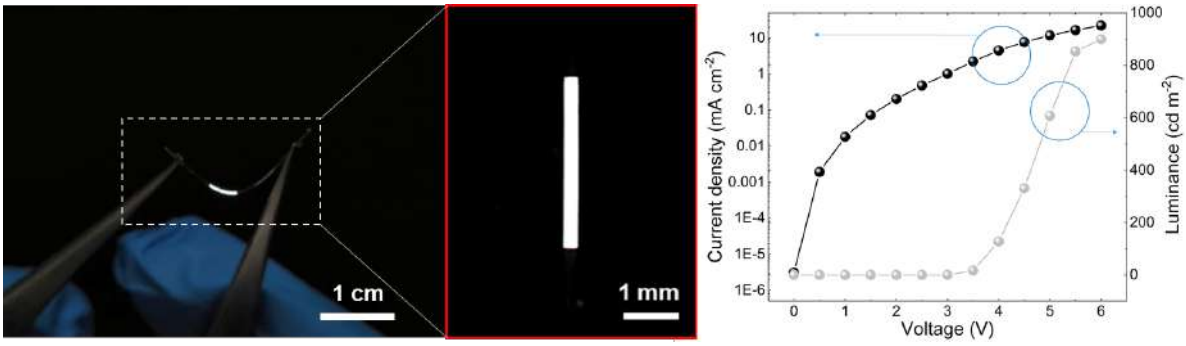

Fig. 1. A photographic image and a microscope image of the fiber WOLED (red box) and current density-voltage-luminance (J-V-L) curves

Acknowledgment

This work was supported by the Technology Innovation Program (20000489, Interactive fiber-based wearable display platforms for clothing displays) funded by the Ministry of Trade, Industry & Energy (MOTIE, Korea) and National Research Foundation of Korea (NRF) grant funded by the Korea government (MSIT) (No.2019R1A2C3010012). This work was also supported by the LG Display under LGD-KAIST Incubation Program.

References

1. S. Kwon et al, *Nano Lett.* **2018**, *18*, 347.
2. S. Kwon et al, *Adv. Mater.* **2019**, *1903488*, 1903488.
3. Y. H. Hwang et al, *Adv. Funct. Mater.* **2021**, *2009336*, 1.

Monolithic Integration of Stretchable and Transparent Indium-Tin-Oxide Interconnects with Oxide Thin-Film Transistors

Sohee Kim[1,2], Ilgeum Lee[1], Jae Bon Koo[1], Chan Woo Park[1], Sooji Nam[1]
[1]Electronics and Telecommunications Research Institute (ETRI), 218, Gajeong-ro, Yuseong-gu, Daejeon, Republic of Korea
Tel.:82-42-860-1479, E-mail: sjnam15@etri.re.kr
[2]Dept of Electrical Engineering, Korea University, 145, Anam-ro, Seongbuk-gu, Seoul, Republic of Korea

Recently, there has been increasing demands for not only flexible but also both stretchable and transparent electronic circuits, targeting wearable devices, displays, and electronic skins. In particular, fabrication of transparent and stretchable thin-film transistor (TFT) arrays is a key technology for realizing stretchable active matrix display or sensor panels. For oxide TFTs, many previous studies have demonstrated successfully that highly transparent circuits can be achieved by employing transparent conducting oxide (TCO) interconnects, but the realization of both transparent and stretchable properties is still considered as quite difficult due to high brittleness of TCOs. For achieving high integration density and process reliability, it is also required that TFTs should be integrated with stretchable interconnects monolithically by conventional TFT processes. In this present work, stretchable 4 × 4 and 8 × 8 arrays of oxide TFTs are produced, and fully transparent amorphous oxide semiconductor (AOS)-based TFTs have been fabricated on a transparent polyimide (PI) substrate, and then patterned into highly stretchable configuration. In this structure, oxide TFT layers are formed within stiff island regions, and connected to external pads through serpentine indium-tin-oxide (ITO) interconnects. Then, after producing TFTs and serpentine interconnects on polyimide layers, those arrays are transferred onto a stretchable elastomeric substrate. As most strain is accommodated by the soft elastomeric substrate, oxide TFTs on stiff islands can show stable performance irrespective of the amount of tensile strain as large as 40-50%, with little variation in the on-off or transfer characteristics. Such results show that, with proper serpentine shapes, even a highly brittle thin ITO film can provide high stability under stretched condition. The mechanical stability of serpentine interconnects can be enhanced by locating the ITO layer within the neutral mechanical plane between two identical polyimide layers. As the oxide TFTs and serpentine ITO interconnects are fabricated by a photolithography-based techniques compatible with conventional flexible circuit technology, the proposed device structure and process scheme could be widely used in producing transparent and stretchable TFT circuits for various applications.

Acknowledgment

This work was supported by Electronics and Telecommunications Research Institute (ETRI) grant funded by the Korea government (21PB3110).

References

1. C. W. Park, J. B. Koo, C. S. Hwang, H. K. Park, S. G. Im and S. Y. Lee, *Appl. Phys. Express* vol. 11 p. 126501 (2018).

Encapsulated Stretchable OLEDs on LASER patterned polyimides

Taehyun Kim[1], Subon Kim[1], Donggyun Lee[1], and Seunghyup Yoo[1]
[1]School of Electrical Engineering, KAIST, Daejeon, 34141, Korea
Tel.:82-42-350-3483, E-mail: syoo.ee@kaist.edu

Optoelectronic devices are the main components for information display devices as well as for emerging applications like phototherapeutics [1]. In particular, phototherapetic healthcare devices could be attached directly to the human body for operation, and thus it is preferred for them to have a high degree of stretchability. Furthermore, wearable devices often rely on the limited on-board power source, demanding high efficiency of their light sources. While organic materials are regarded well fitted for flexible and/or stretchable devices for their low process temperature and soft nature [2-3], but there are still challenges due to the low stretchability of conventional electrodes and other key ingredients (e.g. encapsulation layers). Furthermore, those engineered for extreme level of deformability are subject to performance degradation [1].

In this work, stretchable organic light-emitting diodes (OLEDs) are realized in a way that is stratightforward yet still performs relatively well. In the proposed approach, LASER-patterned polyimide (PI) substrates are proposed for the stretchable platform that includes biaxially stretchable interconnectors and rigid islands. For the stable operation under ambient environment, an encapsulation film is formed with a 2-dyad multilayer barrier structure. Additionally, stretchable OLEDs are laminated onto a low modulus layer for stress relief. The proposed OLEDs are shown to be stretchable up to ε_{system} = 30% without difference in performance (Fig. 1). Through a cyclic test, it is confirmed that the device characteristics remain constant even when the proposed OLEDs are stretched 1000 times.

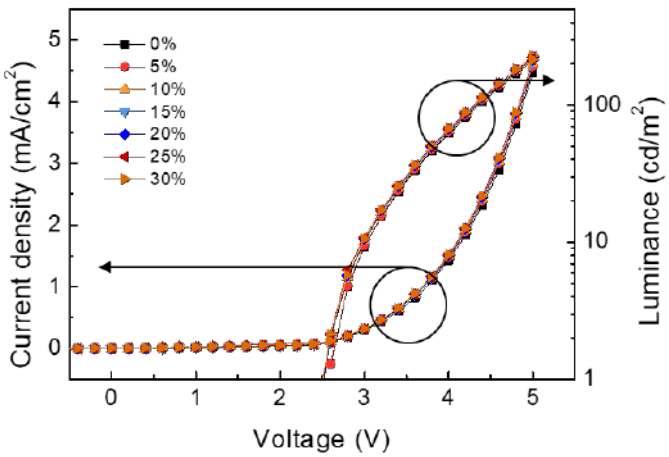

Fig. 1. Characteristics of the OLEDs on the proposed strethchable platform measured at ε_{system} = 0 ~ 30%

Acknowledgment

This work was supported by the Nano-Material Technology Development Program (Grant No. NRF-2016 M3A7B4910631) supported by the National Research Foundation (NRF), Korean Ministry of Science & I CT (MSIT) and by the Engineering Research Center of Excellence (ERC) Program (Grant No. NRF-2017 R1A5A1014708) supported by the NRF, MSIT.

References

1. J. K. Song, M. S. Kim, S. Yoo, J. H. Koo, & D. H. Kim, *Nano Research*, 1-20, (2021).
2. J. Song, H. Lee, E. G. Jeong, K. C. Choi, and S. Yoo, *Advnaced materials*, 32(35), (2020)
3. Y. Jeon, H. Choi, M. Lim, S. Choi, H. Kim, J. H. Kwon, K. Park, K. C. Choi, *Advanced materials technologies*, 3(5), 2018

Highly Stretchable and Transparent Adhesive Films Using Hierarchically Structured Rigid-Flexible Dual-Stiffness Nanoparticles

Jongil An[1], Seung-Rak Son[1], Jin-Wook Choi[1], Soyern Kim[1], Jisung Park[1], Chan Beom Park[1], Hoyun Byun[2], and Jun Hyup Lee[1,*]

[1]Department of Chemical Engineering, Soongsil University, Seoul 06978, Republic of Korea

Tel.:82-2-829-8329, E-mail: junhyuplee@ssu.ac.kr

[2]Module Research Team, Samsung Display, Yongin 17113, Republic of Korea

Innovation in the form factor of the display has resulted in evolution from the rigid, square shape to a more flexible form that can be freely transformed. In response to these changes, many different studies on the various elements of display devices, such as cover windows, touch sensors, substrates, transistors, and light-emitting layers, among others, have been conducted to ensure flexibility, leading to commercialization [1−3].

Herein, we present the unprecedented fabrication strategy for highly stretchable and transparent optical adhesive films for flexible displays using hierarchically structured rigid-flexible dual-stiffness nanoparticles (DSNs) composed of a rigid inorganic core and an elastic reactive coil shell (Fig. 1). The hierarchically structured nanoparticles were prepared from SiO_2 nanoparticles via the sequential surface modification with photoreactive flexible chains. The fabricated elastic adhesive film containing DSNs with an average diameter of 20 nm showed high optical transmittance of 92% and adhesion strength of 19.9 N/25 mm. Increasing the content of the tailored nanoparticles in the adhesive film improved the elastic properties of the film such as elastic modulus (7.0 kPa), stress relaxation ratio (18.4%), and strain recovery rate (73.6%) due to the efficient elastic motion of the embedded DSNs. Thus, the utilization of novel dual-stiffness nanoparticles produces optical adhesive films with high elasticity and optical transparency that are capable of withstanding external forces such as folding and stretching, which is essential for flexible electronic devices.

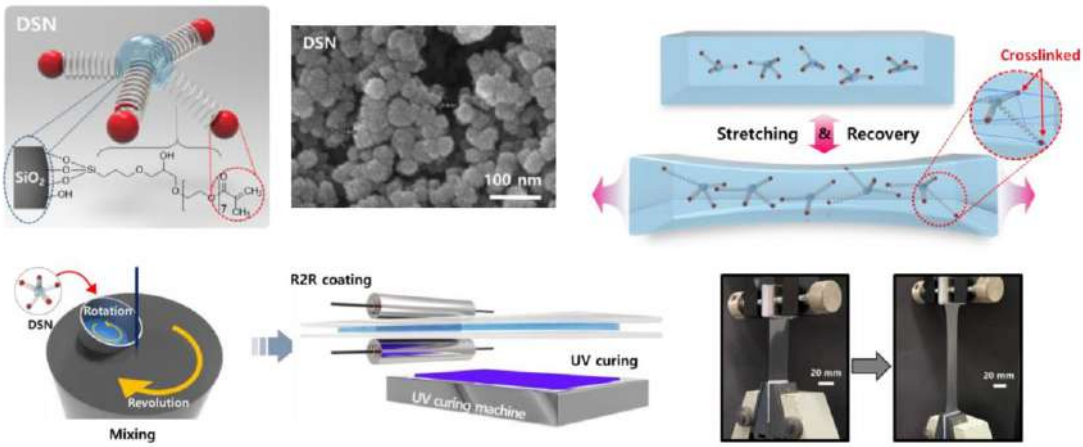

Fig. 1. Schematic diagram of the fabrication process for the stretchable optical adhesive film with DSNs

Acknowledgment

This work was supported by Samsung Display Co. Ltd. and by the National Research Foundation of Korea (NRF) grant funded by the Korea government (MSIT) (No. NRF-2018R1A5A1024127). This work was also supported by Korea Institute for Advancement of Technology (KIAT) grant funded by the Korea Government (MOTIE) (P0012770).

References

1. Y. T. Lai and N. H. Tai, *ACS Appl. Mater. Interfaces*, 7, 18553 (2015).
2. Y. Guo, X. Zhou, Q. Tang, H. Bao, G. Wang, P. Saha, *J. Mater. Chem. A*, 4, 8769 (2016).
3. J. Miao, S. Chen, H. Liu, X. Zhang, *Chem. Eng. J.*, 345, 260 (2018).

Dynamic Stretchable OLED Display having Individually Encapsulated Pixels

Gyujeong Lee[1], Sangwoo Kim, Jangyeol Yoon, Jeong-Tae Park, Jong-Ho Hong and Sung-Chan Jo

[1]Display Research Center, Samsung Display Co., LTD., Giheung-Gu, Yongin-Si, Gyeonggi-Do, Korea

Tel.:82-31-5181-6620, E-mail: gyujeong.lee@samsung.com

Recently, the stretchable OLED display has attracted great attention for the near future display such as healthcare, IoT, and wearable electronics. A lot of studies have been conducted in terms of new materials[1] and/or novel structures[2], but most of them show low resolution that cannot present high quality images or video. Moreover, OLEDs require high quality encapsultion layer to block moisture/oxygen in atmosphere conditions[3]. The most well-known encapsulation method is deposition of inoraginc layers on the display panel. However, in case of the stretchable display, the inorganic layer can be easily cracked by induced stress during stretching process, which limits OLED adopted in strechable electronics.

Here, we present the stretchable OLED display consists of individually encapsulated rigid unit pixels and stretchable interconnect area between pixels. We introduced the mirco-patterned encapsulation layer which exists only on the unit pixels. When the display is stretched, most of strain will be distributed to stretchable interconnect region where consists of organic materials and metal electrode. The metal electrode is sandwiched between organic layers to minimize the stress applied to the electrode. Therefore, the interconnect area can sustain high degree of strain while the unit pixels and encapsulation layers experience little strain. With the micro-encapsulation and stretchable interconnection area, our strechable OLED can be dynamically transformed without degradation of display panel.

In this paper, we demonstrated a novel dynamically stretchable OLED based on LTPS process. By micro-encapsulating each unit pixel, the effective aperture ratio of stretchable OLED was greatly increased. Our stretchable display with high resolution can be dynamically transformed in real-time. We believe our micro-encapsulation of stretchable OLED with high resolution will offer new potential for future wearable display applications.

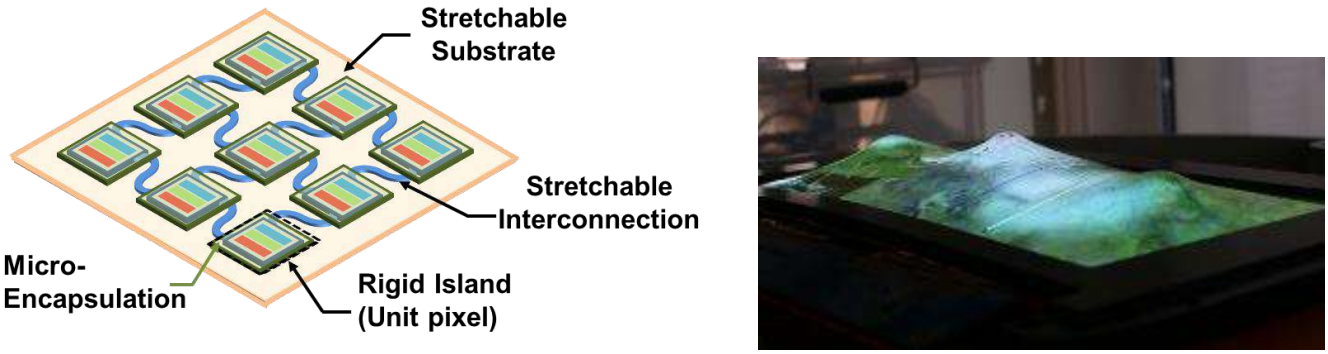

Fig. 1. Simplified structure of stretchable display and 13" dynamic stretchable AMOLED

References

1. K. Cherenack, C. Zysset, T. Kinkeldei, N. Münzenrieder, and G. Tröster, Adv. Mater. 2010, 22, 5178
2. M. K. Choi, J. Yang, K. Kang, D. C. Kim, C. Choi, C. Park, S. J. Kim, S. I. Chae, T.-H. Kim, J. H.; Kim, T. Hyeon, and D.-H. Kim, Nat. Commun. 2015, 6, 7149
3. J-H. Hong J. M. Shin, G. M. kim, H. Joo, G. S. Park, I. B. Hwang, M. W. Kim, W.-S. Park, H. Y. Chu and S. Kim, J. Soc. Info. Display, 2017, 25, 194

Precise Subtractive Patterning Method of AgNWs on Deformable Platform

Geonhee Kim[1], Jinsu Yoon[1], and Yongtaek Hong[1]*
[1]Department of Electrical and Computer Engineering, Inter-university Semiconductor Research Center (ISRC), Seoul National University, Seoul 08826, Republic of Korea
Tel.:82-2-880-9567, E-mail: yongtaek@snu.ac.kr

We suggested a facile fabrication method of silver nanowires (AgNWs) on various substrates including stretchable platforms through subtractive patterning. For applying AgNWs to free-form electronics, patterning process should be proceded. Several patterning methods including spray coating[1] and photo-induced patterning[2] have been investigated, but requirement of patterning masks according to the different shapes of electrode patterns and device cost of lithographic process hinder the commercialization. Meanwhile, a simple patterning process of AgNWs achieved by selective transfer of AgNWs on inkjet-printed polymer template was reported recently[3], but the applications of the electrodes were limited to flexible electronics. In this work, a subtractive patterning method of the AgNWs were demonstrated and fabricated conductive electrodes were successfully transferred on deformable platform. Inkjet-printing of poly(3,4-ethylenedioxythiophene):poly(styrenesulfonate) (PEDOT:PSS) mixed with D-sorbitol ink enables formation of desired patterns. Spray-coating of AgNWs was followed both on the surface of PEDOT:PSS patterns and substrate without a patterning mask. After annealing of spray-coated AgNWs, samples were dipped in dionized (DI) water. Through the dipping process in the DI water, the modified PEDOT:PSS pattern was partially dissolved due to the high solubility of D-sorbitol in DI water. Subtractive pattern of the AgNWs can be easily achieved through bath sonication, which removes both weakened PEDOT:PSS pattern and the AgNWs placed on the PEDOT:PSS (Fig. 1). Various patterns of the AgNWs were obtained including mesh electrodes with width of 80 µm and pitch of 600 µm (Fig. 2). In addition, patterned AgNWs can be easily embedded onto the polyimide varnish, and flexible applications such as flexible polymer light-emitting diodes (PLEDs) were successfully demonstrated (Fig. 3). This fabrication process can be extended to stretchable platform, through the lamination of plastic substrates onto the pre-stretched elastomers and fabrication of wrinkled structure after releasing.

Fig. 1. Subtractive patterns on glass substrate.

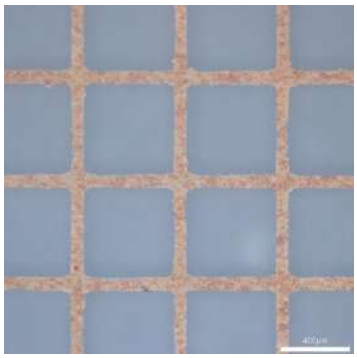

Fig. 2. AgNW mesh pattern with width of 80 µm and pitch of 600 µm

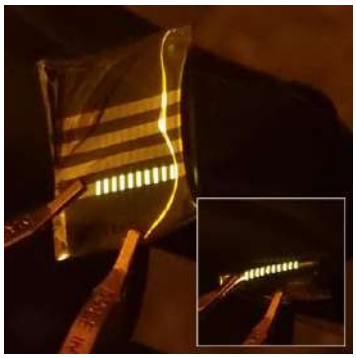

Fig. 3. Flat and bending states of PLED arrays with patterned AgNWs

Acknowledgment

This research was supported by National R&D Program through the National Research Foundation of Korea(NRF) funded by Ministry of Science and ICT(2020M3D1A2101801) and the Display Center of Samsung Display and Seoul National University.

References

1. S.-E. Park, S. Kim, D.-Y. Lee, E. Kim and J. Hwang, *J. Mater. Chem. A*, 1, 14286 (2013).
2. D. Kim, Y. Ko, W. Kim, D. Kim and J. You, *Opt. Mater. Express*, 7(7), 2272 (2017).
3. J. Park, G. Kim, B. Lee, S. Lee, P. Won, H. Yoon, H. Cho, S. Ko and Y. Hong, *Adv. Mater. Technol.*, 5, 2000042 (2020).

Enhancement of Adhesion and Reflectance of Silver Thin-film via Thiol-terminated Self-assembled Monolayer for Reliable Stretchable Electronics

Sujin Jeong[1,2], Hyungsoo Yoon[1,2], Dahyun Kim[1,2], and Yongtaek Hong[1,2]
[1]Department of Electrical and Computer Engineering, Seoul National University, Seoul 08826, Korea
[2]Inter-University Semiconductor Research Center (ISRC), Seoul National University, Seoul 08826, Korea
Tel.:82-2-880-9567, E-mail: yongtaek@snu.ac.kr

Stretchable electronics have been investigated to enable various applications of 3D, wearable, or bio-integrated electronics. To realize stretchable electronics, stretchable electrodes are fundamental elements. And thin-film-based metallic electrodes with wrinkled structure are one of the representative approaches. Metallic thin-film deposited on a prestretched elastomer forms out-of-plane wavy structure when prestrain is released and achieves stretchability by changing from wavy to planar geometry during stretching. Thin-film-based metallic electrodes have advantages of uniform surface morphology and high reflectance, which is worth considering to integrate with electro-optical devices directly (e.g., organic light-emitting diodes (OLEDs)). Meanwhile, strong adhesion between electrodes and substrate determines the mechanical stability, leading to electrical failure due to formation of delamination or crack if it is not ensured.[1] Therefore, employing adequate surface modification to stretchable substrate is necessary. In this work, we report a highly reflective and mechanical durable silver (Ag) electrode on polydimethylsiloxane (PDMS) by following surface modification of (3-Mercaptopropyl)trimethoxysilane (MPTMS) self-assembled monolayer (SAM) treatment. After UV/O_3 treatment on PDMS, a thiol-terminated MPTMS SAM was sequentially treated through the vapor-phase deposition method (Fig. 1 (a)). Then, Ag electrodes are vacuum-evaporated on the PDMS using a shadow mask. As shown in Fig. 1 (b), the Ag electrode showed excellent adhesion on MPTMS-treated PDMS due to the formation of a covalent bond between Ag and MPTMS,[2] exhibiting high endurance to the tape test (3M 810D tape). Furthermore, while the relative reflectance of evaporated Ag is usually degraded on PDMS,[3] relative reflectance was improved by about 6% in MPTMS-treated sample, which became comparable to Ag on glass substrate(Inset in Fig. 1 (b)). Our fabrication method has the potential to be developed for stretchable applications by adopting an additional wrinkled structure, realizing a demonstration of reliable stretchable electrodes and facile integration with stretchable OLED applications.

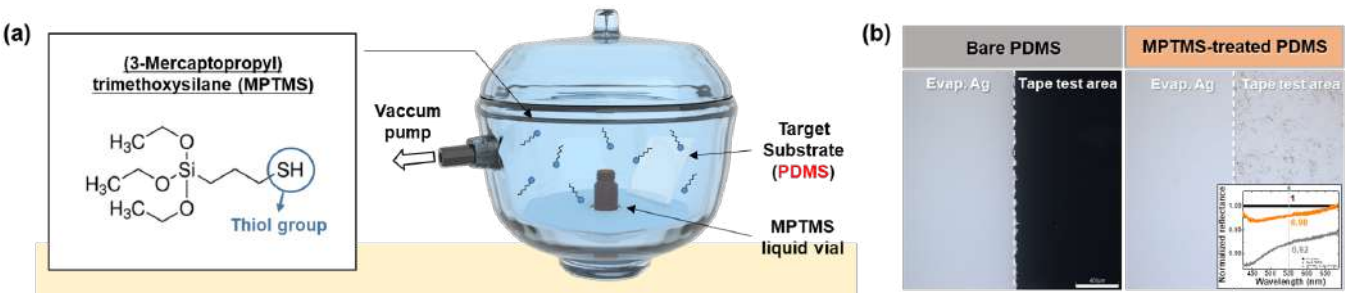

Fig. 1. (a) Schematic illustraion of vapor-phase deposition of MPTMS SAM, (b) Optical images of vacuum-evaporated Ag on bare PDMS (left) and MPTMS-treated PDMS (right) before & after tape test. (Inset : relative reflectance for glass (black line), bare PDMS (gray line) and MPTMS-treated PDMS (orange line))

Acknowledgment

This research was supported by National R&D Program through the National Research Foundation of Korea(NRF) funded by Ministry of Science and ICT(2020M3D1A2101801).

References

1. T. Cheng, Y. Zhang, W.-Y. Lai and W. Huang, *Adv. Mater.,* 27(22), 3349 (2015).
2. M. N. Kirikova, E. V. Agina, A. A. Bessonov, A. S. Sizov, O. V. Borshchev, A. A. Trul, A. M. Muzafarov and S. A. Ponomarenko, *J. Mater. Chem. C*, 4, 2211 (2016).
3. J.-P. Déry, D. Brousseau, M. Rochette, E. F. Borra, and A. M. Ritcey, J. Appl. Polym. Sci. 134(9), 44542 (2017).

Study on structure and process optimization of color modulation hole-only quantum dot light emitting diode

Young-Min Park[1], Jae-In You[2], Suk-Ho Song[2], and Jang-Kun Song[2]
[1]Department of Semiconductor and Display Engineering, Sungkyunkwan University, Suwon, Gyeonggi-do 16419, South Korea
Tel.:82-31-299-4631, E-mail: 5416park@g.skku.edu
[2]Department of Electrical and Computer Engineering, Sungkyunkwan University, Suwon, Gyeounggi-do 16419, South Korea

In order to increase the resolution of the display and increase the aperture ratio of the high-resolution display, the development of color modulation displays is actively progressing. In this paper, we studied a structure that can modulate color according to the voltage application direction and duty by applying the HOD (Hole Only Device) structure.

As shown in Figure 1a, both electrodes were applied with ITO and Al, and PEDOT:PSS and PVK were applied equally to both electrodes, and QDs with different colors of red and green were used. Mainly, research was conducted on the efficient structure and process optimization that generates charge generation. In this paper, we apply ZnO / PEDOT:PSS / ZnO to the charge generation layer, so that charge generation could be smoothly performed, and the surface characteristics of ZnO were improved through toluene treatment, and PEDOT:PSS was coated stably. As shown in Figure 1b, the color reproducibility characteristics were improved by minimizing the intensity of the sub-peak when driving red and green colors and the luminance of red is 157nit and the luminance of green is 2000nit, which is about 500% or more compared to before optimization.

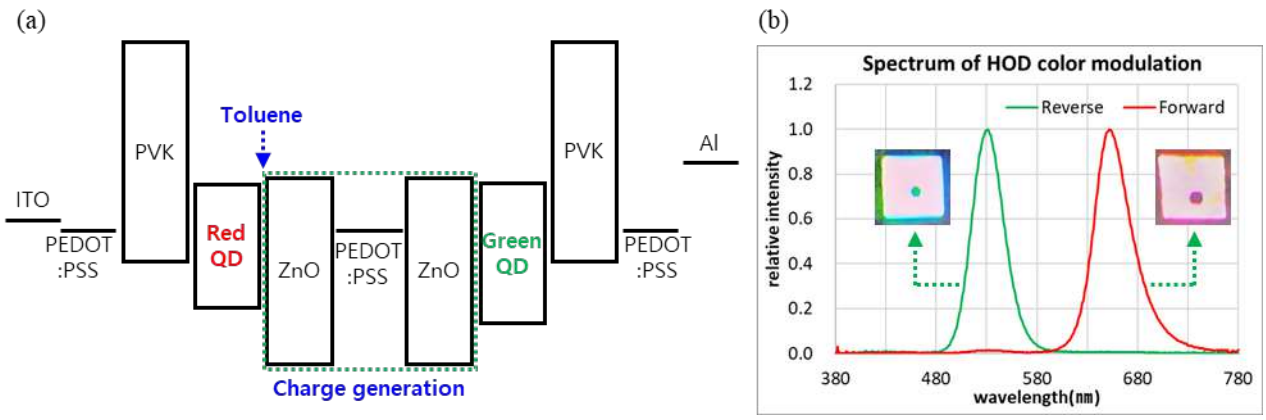

Fig. 1. (a) Schematic of the HOD color modulation QD-LED device structure. (b) Normalized electroluminescence spectrum according to direction of bias.

Acknowledgment

This work was supported by the National Research Foundation of Korea(NRF) grant funded by the Korea government(MSIP)(NRF-018R1D1A1B07048166).

References

1. Fei Guo, Andre Karl, Qi-Fan Xue, Kai Cheong Tam, Karen Forberich, Christoph J Brabec, *Light-Science & applications,* p. 68 (2017).
2. Run Wang, Yige Qi, Dianli Zhou, Junsheng Yu, *Synthetic Metals 231,* p. 58-64 (2017).
3. Hyun-koo Lee, Hyun-su Cho, Chun-Won Byun, Jun-Han Han, Byoung-Hwa Kwon, Su-kyung Choi, Jong-hee Lee, Nam-Sung Cho, *Optics Express Vol, 26, Issue 14,* p. 18351-18361 (2018).
4. Shengqiang Liu, Ruofan Wu, Jiang Huang, Junsheng Yu, *Organic Electronics and Photonics 6(9),* 181_1 (2013).

High Luminance Top-emitting White Organic Light-emitting Diodes for Microdisplay Applications

Seong Ji Lee[1,2], Jin-Wook Shin[1], Dae Hyun Ahn[1], Chul Woong Joo[1], Hyunsu Cho[1], Nam Sung Cho[1], Jonghee Lee[2], Hyoc Min Youn[3], Young Jae An[3], Hyunkoo Lee[4], and Chan-mo Kang[1]

[1]Reality Display Research Section, Electronics and Telecommunications Research Institute (ETRI), Daejeon 34129, Republic of Korea

Tel.:82-42-860-5229, E-mail: nkcm@etri.re.kr

[2]Department of Creative Convergence Engineering, Hanbat National University, Daejeon 34158, Republic of Korea

[3]DONGJIN SEMICHEM CO.,LTD, Hwaseong 18635, Republic of Korea

[4]Department of Electronics Engineering, Sookmyung Women's University, Seoul 04310, Republic of Korea

Tel.:82-2-710-9182, E-mail: lhk108@sookmyung.ac.kr

As augmented reality and virtual reality (AR/VR) technologies have been rapidly growing, organic light-emitting diode (OLED) microdisplays have been studied intensively due to their merits such as high contrast ratio, fast response time, and self-emissive properties.[1–3] To fabricate OLED microdisplays, top-emitting white OLED (WOLED) should be developed due to use of opaque silicon substrates. In this study, we developed the high luminance top-emitting WOLEDs for microdisplay applications.

The complementary metal–oxide–semiconductor (CMOS) compatible TiN/Al anode was used to adopt microdisplay applications. Seperated three emissive layers with red, green phosphorescent and blue fluorescent materials were used for white emission. The interlayer was inserted between blue and red/green emitting layers to avoid Förster energy transfer. Figure 1 shows the current density–voltage–luminance (*J–V–L*) characteristics of the demonstrated top-emitting WOLED. The device exhibited the luminance of ~16,000 cd/m^2 and the color coordinates of (0.297, 0.329) at a driving voltage of 4.2 V. Additionally, the maximum luminance of the device reached up to approximately 170,000 cd/m^2. Finally, we measured the color gamut for the microdisplay applications by fabricating the color filters onto the developed WOLEDs. The color gamut was 136% compared to sRGB. Therefore, the developed WOLED can be utilized for full-color OLED microdisplays of AR/VR devices.

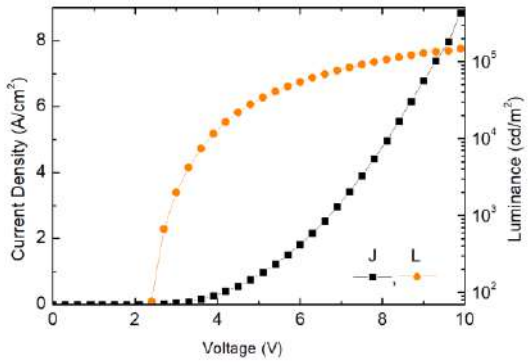

Fig. 1. *J–V–L* characteristics of the top-emitting WOLED.

Acknowledgment

This work was supported by Electronics and Telecommunications Research Institute (ETRI) grant funded by the Korea government (21ZB1200).

References

1. C. Kang, J. Shin, S. Choi, B. Kwon, H. Cho, N. Cho, J. Lee, H. Lee, J. Lee, H. Kim, A. Cho, S. Park, M. Kim, J. Lee, S. Lee and Y. Im and C. Byun, *J. Inf. Disp.*, published online (DOI: 10.1080/15980316.2021.1902405) (2021).
2. H. Jang, J. Lee, J. Kim, J. Kwak and J. Park, *J. Inf. Disp.*, 21(1), 1 (2020).
3. G. Haas, *SID Symp. Dig. Tech. Pap.*, 50(1), 713 (2019).

Study of vertical thin-film transistor applied pn-heterojunction channel layer

Gyeonghyeon Choi[1], Goeun Pyo[2], and Jaeeun Jang[1]
[1]Information and Communication Engineering, Daegu Gyeongbuk Institute of Science and Technology (DGIST), Daegu, 42988, South Korea
Tel.:+82-(53)-785-6309, E-mail: jang1@dgist.ac.kr

Smaller thin film transistor (TFT) with high current is required for ultra-high resolution display or various applications such as VR/AR system. The lateral type TFT, which is commonly used, is reducing the channel length to solve these issues. However, to reduce channel length, it requires the use of expensive equipment, which increases the cost and has limitations. This can be solved by a vertical type TFT(V-TFT) structure design. The short channel length of V-TFT is achieved easily by controlling a thickness of channel layer, so that it is possible to get a low cost and easy fabrication.

However, important issues of V-TFT are how to penetrate a gate-field to channel structure and how to minimize off-state current, mainly due to the structural originality. To solve these problems, in here, we embeded micro hole array into source metal structure, and then, the gate field can pass through the source metal layer. However the on/off current ratio is not high because the gate field does not still penetrate to the front of remaining source metal. To decrease off-state current, p-type material was deposited on the source to make pn-heterojunction. The pn-heterojunction can block off-state current flow. By applying this, the on/off ratio was enhanced and it leads to high probability to apply this V-TFT structure for various high performance devices.

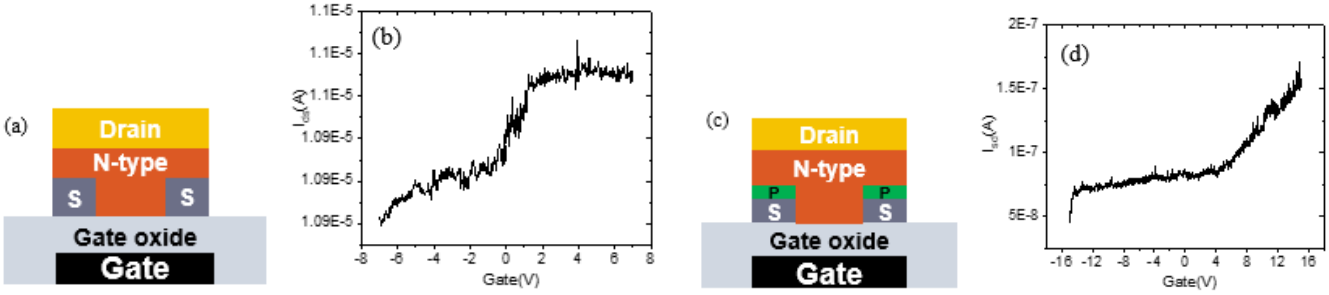

Fig.1 (a) Schematic diagram of VTFT in a basic metal hole structure. (b) The transfer curve of the device having metal hole array (c) Schematic diagram of VTFT with pn junction. (d) Transfer curve of VTFT with pn-heterojunction

Acknowledgment

This research was supported by the Basic Science Research program through the National Research Foundation of Korea (NRF) Funded by the MSIT (no. 2020R1A2C1006295)

References

1. Y. Uchida, Y. Nara and M. Matsumura, *IEEE Electron Device Letters* (Volume: 5, Issue: 4, Apr 1984)
2. Liping Ma and Yang Yang, *Appl. Phys. Lett. 85*, 5084 (2004).

Investigation of Hydrogen diffusion mechanism and Electrical properties in In-Ga-Zn-O Thin Film through PECVD SiN:H and Post-annealing

*Hee Yeon Noh, Joonwoo Kim, June-Seo Kim, Myoung-Jae Lee and Hyeon Jun Lee**
Division of Nanotechnology, DGIST, Daegu 42988, Korea
Tel.:82-53-785-3503, E-mail: dear.hjlee@dgist.ac.kr

Recent research has shown that hydrogen plays an important role improving many electronic devices such as solar cells, MOS devices, and thin film transistors (TFTs) through passivation of impurities and defects. Especially, hydrogenation of a-IGZO material is carried out to improve the electrical characteristics of TFTs as hydrogen is known to be a donor for n-type oxide semiconductors and is as an effective passivator for defects. To date, there have been reports various methods to hydrogenate IGZO materials such as H_2 plasma treatment, addition of H_2 gas during the IGZO film deposition, and post annealing [1-3]. However, the detailed knowledge of the hydrogen transport mechanisms is still lacking and one of the issues that need to be investigated is how hydrogen is diffused and/or passivated into the a-IGZO. As the association of hydrogen diffusion and/or passivation can change their electric character, leading to unwanted changes in material properties such as resistivity, it is important part of the process conditions.

In this study, the introduction of hydrogen in oxide semiconductors and their electrical characteristics were analyzed. Hydrogen in the oxide semiconductor is sometimes injected unintentionally during the process, but a large amount of hydrogen is frequently injected due to the influence of the SiNx process. However, it was confirmed that a large amount of hydrogen was not introduced only through the junction of SiNx and the oxide semiconductor, and that hydrogen was introduced only through a specific process step. The amount of hydrogen inflow was analyzed through SIMS evaluation, and the presence or absence of donor was confirmed through electrical characteristic evaluation.

Acknowledgment

This research was supported in part by the DGIST R&D Program of the Ministry of Science, ICT, and Future planning (21-IT-01, 21-CoE-NT-02).

References

1. J. Kim, S. Bang, S. Lee, S. Shin, J. Park, H. Seo, and H. Jeon, *J. Mater. Res.,* vol. 27, no. 17, p. 2318-2325 (2012).
2. W. K. Kim, S. H. Lee, Y. C. Cho, H. Koinuma, S. Y. Jeong, J. M. Shin, C. R. Cho, J. S. Bae, T. Y. Kim, and S. K. Park, *App. Phys. Lett.*, vol. 93, no 20, p. 203506-1-203506-3 (2008).
3. D. H. Son, D. H. Kim, S. J. Sung, E. A. Jung, and J. K. Kang, *Current Appl. Phys.*, Vol. 10, no. 4, p. e157-e160 (2010).

Influence of Post-Annealing Temperature on the Electrical Characteristics and Bias Stability of c-Axis Aligned Crystalline IGZO TFTs

Hyun-Woo Kim[1], Young-Jin Kang[2], Tae-Kyu Kim[2] and Yong-Hoon Kim[2]*
[1]Department of Semiconductor and Display Engineering, Sungkyunkwan University, Suwon, 16419, Korea
[2]School of Advanced Materials Science and Engineering, Sungkyunkwan University, Suwon 16419, Korea
*Tel.:82-31-290-7407, *E-mail: yhkim76@skku.edu*

Metal oxide semiconductors have been used as active channel layers in thin film transistors (TFTs) due to their high mobility, excellent uniformity and low off-current operating characteristics compared to amorphous silicon TFTs. Among several metal oxide semiconductors, indium-gallium-zinc oxide (IGZO) is known as one of the most suitable materials due to its excellent electrical properties. When the c-axis-aligned-crystalline-IGZO (CAAC-IGZO) film, which is known to be more reliable than the amorphous IGZO, is produced by sputtering, high power should be applied because high energy is required to form the crystal structure. However, during mass production, the deposition condition may be unstable, especially the pressure condition, due to equipment problems or substrate replacement. In this study, the electrical properties and stability on bias stress of CAAC-IGZO film according to the interface condition between the gate insulator and IGZO were analyzed and compared. Also, the electrical performance variation due to the post annealing was studied.

As shown in Figure 1, there was a large difference in the transfer characteristics between porous and dense interface conditions for CAAC-IGZO fabricated at a low post annealing temperature. However, as the post-annealing temperature increased, the difference in the transfer characteristics was reduced. Also, the device reliability of CAAC-IGZO TFT tends to vary depending on the interface conditions by the type of applied bias stress.

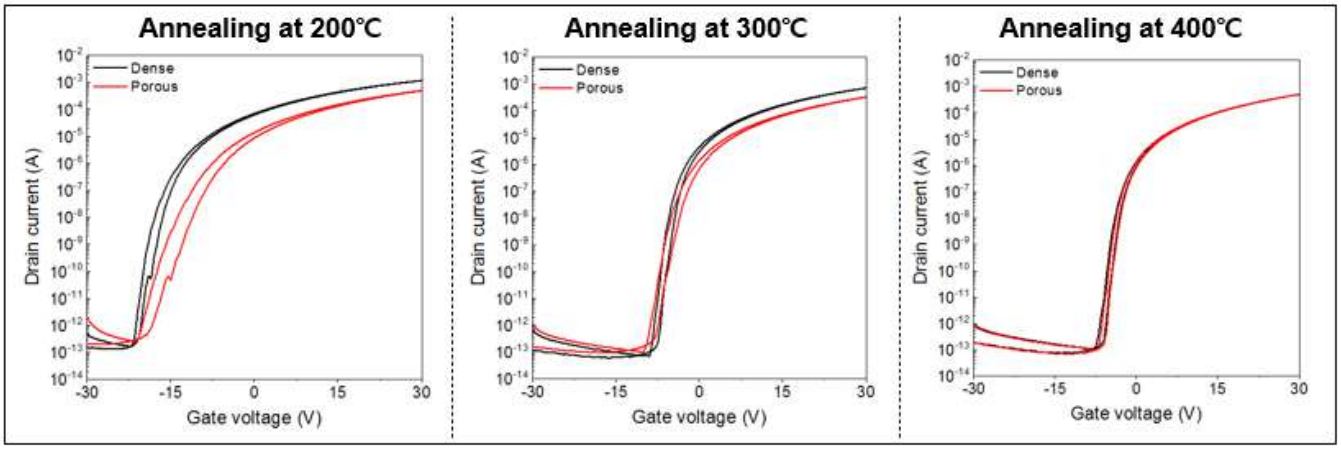

Fig. 1. Transfer characteristics of CAAC-IGZO TFTs with dense and porous interfaces according to post-annealing temperature.

References

1. K. Nomura et al, *Jpn. J. Appl. Phys.* 45 4303(2006).
2. J. F. Conley, *IEEE Trans. on Device and Mater. reliability* 10 460-475 (2010).
3. J. Robertson and Y. Guo, *Appl. Phys. Lett.* 104, 162102 (2014).
4. S. Yamazaki et al, *Jpn. J. Appl. Phys.* **53** 04ED18 (2014).

Positive Bias Stress and Negative Bias Illumination Stress Stability of amorphous InSnZnO (a-ITZO) Dual Layer Thin Film Transistor

Jeongho Lee[1], Seohyun Maeng[1], Hayoung Kim[1], Sohee Kim[1] and Jaekyun Kim[1]
[1]Dept. of Photonics and Nanoelectronics, Hanyang University, Ansan, Gyenggi 15588, Korea
Tel.:82-31-400-4679, E-mail: jaekyunkim@hanyang.ac.kr

We investigated amorphous-Indium-Tin-Zinc-Oxide Thin Film Transistors (a-ITZO TFTs) RF sputtering (target; In_2O_3 : SnO_2 : ZnO = 4:1:4 mol %) process that oxygen partial pressure ([O_2] / [Ar + O_2]) were set to deposit dual layer (O_2 10 %/ O_2 0 %), DL10/0, as a back channel oxygen-rich layer 10 % on a front channel oxygen-poor layer (0 %) to improve instability under positive bias stability (PBS), negative bias illumination stability (NBIS), and negative bias thermal illumination stability (NBTIS) for 3600s with AC bias stress mode, Compared with Single layer (O_2 0 %), SL0, and Single layer (O_2 10 %), SL10. As the results, ΔV_{th} and electron trapping time (τ) of dual layer were improved from 4.1 to 2.07 V, and from 2.27×10^5 to 2.759×10^5, respectively, compared with conventional single layer (0 %) TFT under PBS [1]. In additional, ΔV_{th} shift of each device under all kinds of illumination negative bias stress for 3600 s were -16.89 V (SL0), -13.16 V (DL10/0), and -15.45 V (SL10) of green, -28.58 V (SL0) illumination as shown in Figure 1. These enhanced results were induced by self-passivation effect, and decreased oxygen vacancy (Vo) relevant trap sites of the active layer [2].

Moreover, with the value of V_{th} shift in each device were observed in temperature-dependent NBIS, we investigated the following results that k_BT is associated with large distribution of energy barriers and increases the value of V_{th} shift faster within the early stress time as shown in Figure 2. The self-passivation layer of high oxygen ratio suppresses the O_2 adsorption/desorption in the back channel of a-ITZO film and decrease the overall oxygen vacancy of the dual layer TFTs [3]. As a result, we confirmed that the dual layer film by controlling oxygen partial pressure during film deposition is an effective process to improve PBS, and NBIS stabilities without degradation mobility and additional processes. In addition, under NBTIS, SL0 is highest activation energy (E_a) of insulator interface, although DL10/0 is E_a lower than SL0 because of oxygen diffusion. Large $d(\Delta V_{th})/dT$ can be caused by high E_a and trap energy distribution.

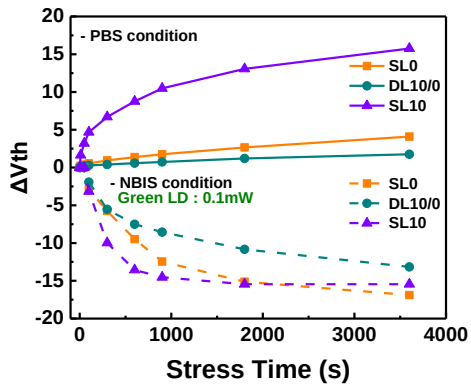

Fig. 1. Characteristics of PBS and NBIS of each device

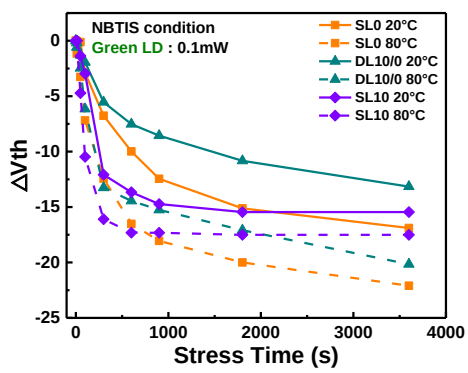

Fig. 2. Characteristics of NBTIS of each device

Acknowledgment

References

1. T. Miuadera, S. D. Wang, T. Minari, K. Tsukagoshi, and Y. Aoyagi, *Applied Physics Letters*, 93, 033304 (2008)
2. J. H. Park, Y.G. Kim, S. H. Yoon, S. H. Hong, and H. J. Kim. *ACS Appl. Mater. Interface.*, 6, 21363-21368 (2014).
3. G. Kin. Jeon, S. H. Lee, S. H. Lee, J. B. Shim, J. H. Ra, K. W. Park, H. I. Yeoom, O. K. Kwon, and S. H. K. Park, *Nature*, 9:3216 (2019)

High Performance Metal-Oxide TFTs Using ITZO/IGZO Double-Layer Channel Structure

Youngjin Kang[1], Boyeon Park[1], Jeehoon Kim[1] and Yong-Hoon Kim[1]*

[1]School of Advanced Materials Science and Engineering, Sungkyunkwan University, Suwon 16419, Korea
*Tel.:82-31-290-7407, *E-mail: yhkim76@skku.edu*

Recently, metal-oxide thin-film transistors (TFTs) have attracted great attention in active-matrix displays and memory devices for their unique characteristics such as low off-state current, good uniformity, decent mobility, and large-area scalability. Among various metal-oxide TFTs, *a*-IGZO TFTs have shown good electrical stability and high uniformity. However, compared to conventional low-temperature polysilicon TFTs, the *a*-IGZO TFTs have limitation increasing the field-effect mobility. In order to improve the mobility, we utilized a heterojunction structure ITZO/IGZO channel for the metal-oxide TFTs. When two different oxide semiconductors are made in contact which have different work functions and conduction band minimum, it is reported that a 2-dimensional electron gas could be formed at the interface between the channel materials, increasing the carrier concentration and field-effect mobility. Therefore, by adopting the heterojunction channel structure, the TFTs having field-effect mobility higher than individual channel materials can be obtained.

In this study, we used ITZO/IGZO double-layer as the channel for TFTs, and particularly, we varied the concentrations and thicknesses of ITZO and IGZO to obtain high mobility devices. Figure 1 compares the transfer curves of IGZO and ITZO/IGZO TFTs. As displayed, the ITZO/IGZO TFTs exhibited relatively high field-effect mobility compared to IGZO TFTs. Here, the thickness of ITZO and IGZO films were around 7 nm and 10 nm, respectively. We further analyzed the effects of ITZO concentration and thickness of IGZO film on the electrical properties of ITZO/IGZO TFTs.

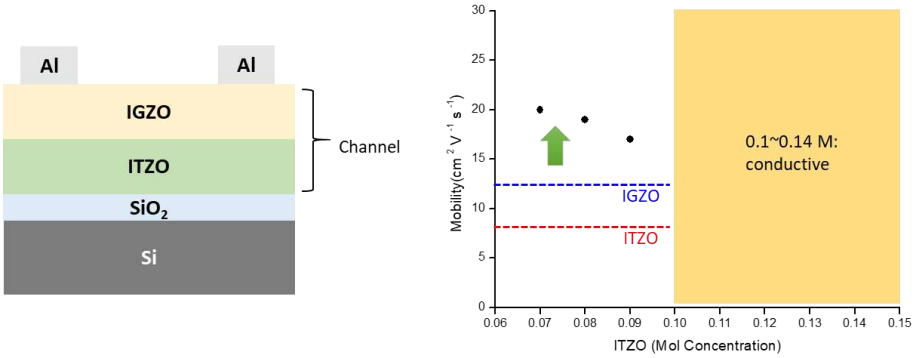

Fig. 1. Device structure of ITZO/IGZO TFT and the effect of ITZO mol concentration on the field-effect mobility.

High performance Thin-Film Transistor Using IGO by Low Temperature Crystallization

HyeongJin Park and Jaekyeong Jeong
Dept. of Electronic Engineering, Hanyang University, Seoul 04763, Korea
Tel.:82-2-2220-2327, E-mail: jkjeong1@hanyang.ac.kr

Thin-film transistors (TFTs) fabricated on flexible plastic substrates play an important role in flexible applications, such as flexible displays and electronic skins. Oxide-Semiconductor TFTs were regarded as the promising candidates for high-performance flexible TFTs. Recently, great attention has been focused on the flexible active matrix organic light-emitting diodes (AMOLEDs) because of its superior properties such as lightweight, flexibility, bendable, unbreakable and wearable. Flexible thin film transistors (TFTs) as the key part have attracted increasing attention and there are some reports on the flexible TFTs. But the mobility for most of these flexible devices are about 5-15 cm^2/Vs which is not enough for future flexible high-resolution, high-frame rate, or 3D displays. To realize flexible displays, some of key features such as the choice of plastic substrate. Oxide TFTs such as In-Ga-Zn-O(IGZO) have received much attention because of their high mobility and stability characteristics than a-Si:H TFTs better uniformity characteristics than LTPS TFTs, and lower process temperature than other conventional Si based TFTs. In this study, a simple process to obtain high-quality polycrystalline oxide channel layers is suggested with a low temperature of 200°C that does not involve catalytic elements. The InGaO(IGO) system as a semiconducting channel layer for TFTs is chosen. Compared to commercially available a-IGZO channels, the elements Zn is excluded since Zn forms a network of atoms and leads to an amorphous structure, it plays a role in increasing the crystallization temperature. In addition, higher mobility than a-$In_{0.40}Ga_{0.40}Zn_{0.20}O$ can be expected by increasing the ratio of In, which improves mobility, and using c-$I_{0.90}G_{0.10}O$ from which Zn has been removed. In have a small effective electron mass due to 5s orbital overlapping structure, leading to an effective percolation pathway and exceptionally high mobility. IGO TFTs were manufactured by controlling the oxygen partial pressure among the deposition conditions under a common 200°C annealing condition, and the device characteristics were checked after depositing the passivation layer. As a result, excellent characteristics of mobility 55 cm^2/Vs, threshold voltage of 0.47 V, low subthreshold gate swing of 110 mV/decade, and $I_{ON/OFF}$ ratio of $>1 \times 10^8$ were output under optimal conditions

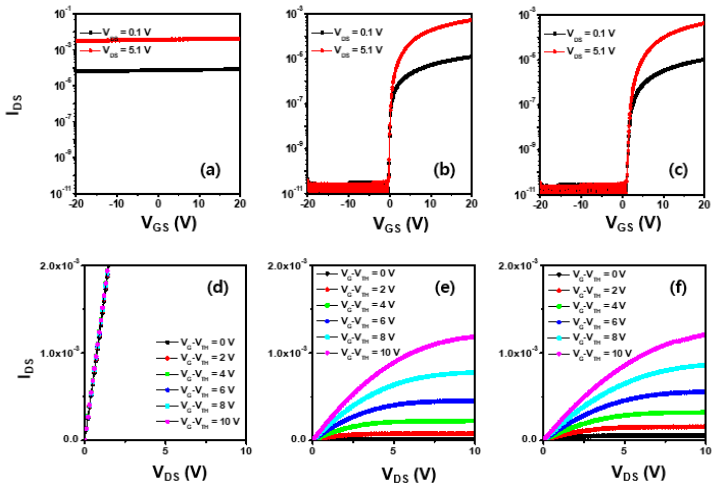

Fig. 1. (a), (b), (c) Transfer Characteristics, (d), (e), (f) Output Characteristics

References

1. R. L. Hoffman, "ZnO-channel thin-film transistors: Channel mobility," *J. Appl. Phys.*, vol. 95, no. 10, pp. 5813–5819, 2004.

Rapid Fabrication of Amorphous IGZO TFTs by Using Solution Combustion Synthesis

Tae-gyu Kim[1], Jaeyoung Kim[1], Kyobin Keum[1], and Yong-Hoon Kim[1]*
[1]School of Advanced Materials Science and Engineering, Sungkyunkwan University, Suwon 16419, Korea
*Tel.:82-31-290-7407, *E-mail: yhkim76@skku.edu*

Indium-gallium-zinc oxide (IGZO) is a renowned material among other metal oxide semiconductors for its high mobility, low off-current, high on/off ratio, and low-temperature process availability. Recently, solution process is considered as an alternative fabrication process due to its low manufacturing costs and applicability to flexible electronic devices. Solution-processed IGZO thin-film transistors (TFTs) exhibit advances in lowering film-processing temperature as the investigation continues. Previously, a combustive fuel is introduced for further reduction of the processing temperature of metal oxide TFTs. Typically, acetylacetone (AcAc) is used for metal precursor solution with oxidizers, enabling combustion process as the coated film is annealed. However, reduction of processing time is not concerned as a favorable topic. In this study, 1,1,1-trifluoroacetylacetone (FAcAc), which is an addtional fluorinated fuel, was applied to the conventional combustive solution to shorten the annealing time [1-2]. In this study, the composition of AcAc and FAcAc was varied to find out the most effective fuel mixture for the combustion synthesis and rapid fabrication of IGZO films.

As shown in Figure 1, the annealing time required for solution-processed IGZO film could be decrease down to 5-20 min which is relatively shorter than previous studies (~1 hr). Particularly, reliable transfer characteristics of IGZO TFT were obtained when the IGZO film was annealed at least for 10 min. Also, in the case of the composition of AcAc and FAcAc, the IGZO TFTs exhibited comparably low hysteresis behavior.

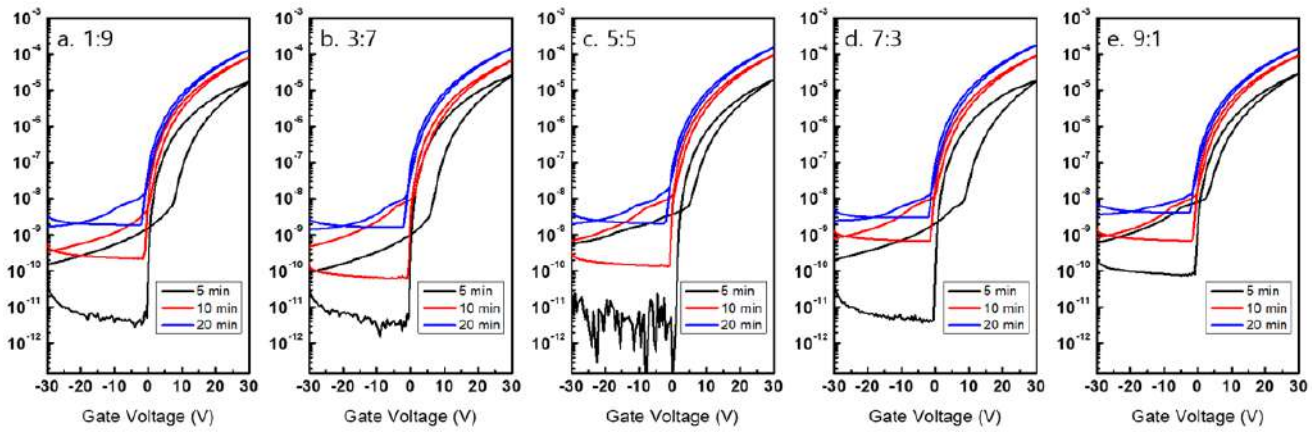

Fig. 1. Transfer characteristics of solution-processed IGZO TFTs as a function of AcAc:FAcAc ratio

References

1. Wang, Binghao, et al., *Proc. Natl. Acad. Sci. U.S.A.* 116 9230-9238 (2019).
2. Chen, Yao, et al., *Chem. Mater.* 30, 3323-3329 (2018).

Key Roles of Trace Oxygen Treatment for High-Performance Zn-Doped CuI p-Channel Transistors

*Ao Liu, Huihui Zhu, and Yong-Young Noh**
Department of Chemical Engineering, Pohang University of Science and Technology (POSTECH), Pohang, Gyeongbuk, 37673, Republic of Korea
Tel.:82-10-5044-9649, E-mail: yynoh@postech.ac.kr

The development of transparent and high-performance p-type semiconductors as a counterpart of n-type metal oxide semiconductors has attracted significant interest for the integration of complementary circuits and p–n junction devices.[1-5] In this study, we investigate the effect of trace O_2 for high-performance and solution-processed inorganic p-channel Zn-doped CuI thin-film transistors (TFTs) via a combined computation–experiment approach. The absorbed O_2 molecules in the CuI film can occupy iodine vacancies, acting as trap passivator. Meanwhile, the strong electronegativity of O_2 enables electron capture from the CuI matrix, leading to p-doping. Trace O_2-treated Zn-doped CuI TFTs exhibit significantly improved electrical performance compared to untreated devices. Optimised TFTs exhibited a high field-effect hole mobility of 4.4 $cm^2 V^{-1} s^{-1}$, high on/off current ratio of ~10^7, and small hysteresis. These findings provide a clear basis for realising reproducible and high-performance metal-halide (e.g., CuI and perovskite) optoelectronic devices using low cost solution process.

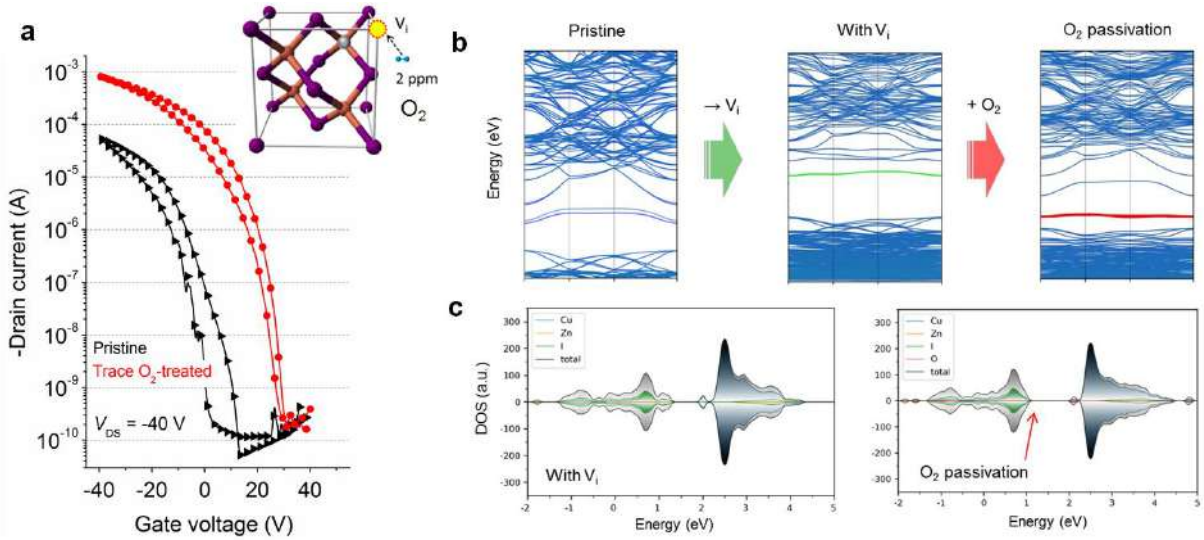

Fig. 1. (a) Transfer curves of Zn-doped CuI TFTs before and after trace O_2 treatment; (b) band structure of neat CuZnI, with V_i and O_2 occupation on V_i; and (c) PDOS of CuZnI with V_i and after O_2 occupation.

Acknowledgment

This study was supported by Ministry of Science and ICT through the National Research Foundation, funded by the Korean government (2017R1E1A1A01075360, 2020R1A2C4001617, 2020R1A4A1019455). This research was supported by National R&D Program through the National Research Foundation of Korea (NRF) funded by Ministry of Science and ICT (2020M3F3A2A01085792). This research was also supported by the Samsung Display Corporation.

References

1. A. Liu, H. H. Zhu, Y.-Y. Noh, *Mat. Sci. Eng. R* 135, 85 (2019).
2. A. Liu, H. H. Zhu, W.-T. Park, S.-J. Kang, M.-G. Kim, Y.-Y. Noh, *Adv. Mater.* 30, 1802379 (2018).
3. A. Liu, H. Zhu, Y.-Y. Noh, *ACS Appl. Mater. Interfaces* 11, 33157 (2019).
4. A. Liu, H. Zhu, K.-I. Shim, J. Hong, H. Jung, J-W. Han, Y.-Y. Noh, *Adv. Electron. Mater.* 7, 2000933 (2021).
5. A. Liu, H. Zhu, Y.-Y. Noh, *Adv. Sci.* 2100546 (2021) 10.1002/advs.202100546

Sodium Incorporation for Enhanced Performance of Two-Dimensional Tin-Based Perovskites Transistors

Ji-Young Go[1], Huihui Zhu[1], Youjin Reo[1], Ao Liu[1], and Yong-Young Noh[1]
[1]Department of Chemical Engineering, Pohang University of Science and Technology, 77 Cheongam-Ro, Nam-Gu, Pohang 37673, Korea
Tel.:82-54-279-8265, E-mail: yynoh@postech.ac.kr

Two-dimensional metal halide perovskites (MHPs) are promising for transistor channel materials due to their low effective mass and good air stability owing to hydrophobic large organic based cation.[1-2] However, the intrinsic defects and high ion migration of MHPs cause great hysteresis in transistor characteristics. To overcome this issue, we incorporate NaI to passivate defects and improve the electrical performance of devices.

Here, we report high-performance and low hysteresis 2D MHPs transistors based on phenethylammonium tin iodide ($(PEA)_2SnI_4$) by incorporation of NaI to passivate defects and improve the electrical performance of devices. The $(PEA)_2SnI_4$ transistors with NaI additive exhibited high hole mobility of 2.24 $cm^2V^{-1}s^{-1}$ with small dual-sweep hysteresis and robust bias stability (Fig. 1). The highly increased grain sizes and crystallinity were observed in Na^+-incorporated $(PEA)_2SnI_4$ films by atomic force microscopy and grazing wide-angle X-ray diffraction result. The p-doping effect of NaI to $(PEA)_2SnI_4$ was also observed by photoelectron spectroscopy.

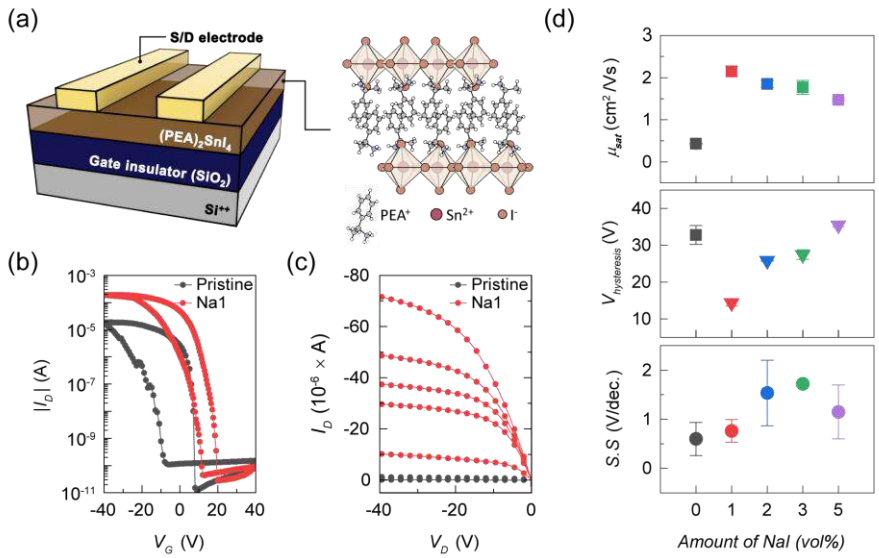

Fig. 1. (a) The bottom-gate/top-contact structure of perovskite TFTs and chemical structure of $(PEA)_2SnI_4$. (b) Transfer and (c) output characteristics of pristine (black) and Na1 (red) devices (V_D=-40). (d) Summary of fundamental TFT parameters with the incorporation of 0, 1, 2, 3, and 5% Na^+.

Acknowledgment

This research was supported by the Samsung Display Corporation and National R&D Program and Basic Research Program through the National Research Foundation of Korea (NRF) funded by Ministry of Science and ICT(2020M3F3A2A01085792, 2020R1A4A1019455).

References

1. Y. Liang, F. Li, and R. Zheng, *Adv. Electron. Mater.*, 6(9), 2000137 (2020).
2. S. Zhou *et al.*, *ACS Energy Lett.*, 5(8), 2614–2623 (2020).

Metal-oxide thin-film transistors operating at low-voltages for display backplanes

Sang-Joon Park, Jun-Young Jeon and Tae-Jun Ha*
Department of Electronic Materials Engineering, Kwangwoon University, Seoul 01897, Korea
Tel.: 82-2-940-8678, E-mail: taejunha0604@gmail.com

Low-voltage operating backplanes have attracted much attention for low power-consumption in the next-generation active-matrix displays [1]. Significantly, the development of low-voltage operating thin-film transistors (TFTs) based on advanced materials are highly demanded in pixel circuits [2]. Among them, metal-oxide semiconductor (MOS) based TFTs consisting of metal-oxide dielectric films with a high dielectric constant (high-k) have been intensively investigated due to their electrical characteristics, low-voltage operation, optical transparency, and solution processability [3]. In this presentation, we will demonstrate low-voltage operating MOS-based TFTs with high-k dielectrics fabricated by solution-process. The optimized metal-ion doping enhanced the film-quality of metal-oxide dielectrics by suppressing the formation of oxygen vacancies, which was verified by analyzing various characterizations. We will also discuss the comparative analysis of charge transport in MOS based TFTs with low-k and high-k dielectrics by investigating the activation energy and density of states.

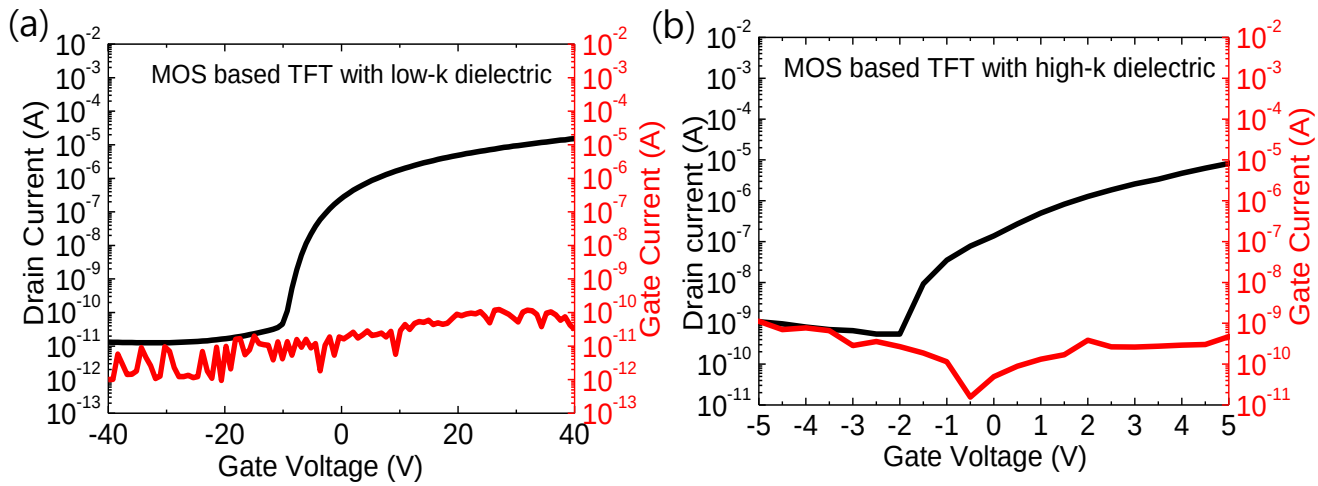

Fig. 1. Representative transfer curve and gate current of MOS based TFTs with (a) low-k and (b) high-k dielectrics as a function of the applied gate voltage

Acknowledgment

This work was supported by the National Research Foundation of Korea (NRF) grant funded by the Korea government (MSIT) (NRF-2021R1A2C2012855)

References

1. K. Paxinos, G. Antoniou, D. Afouxenidis, A. Mohamed, U. Dikko, I. Tsitsimpelis, W. I. Milne, A. Nathan and G. Adamopoulos, *Appl. Phys. Lett.* 116(16), 163505 (2020).
2. M. A. McCarthy, B. Liu, E. P. Donoghue, I. Kravchenko, D. Y. Kim, F. So and A. G. Rinzler, *Science*, 332(6029), 570-573 (2011).
3. A. Liu, H. Zhu, H. Sun, Y. Xu and Y. Y. Noh, *Adv. Mater.*, 30(33), 1706364 (2018).

The restorative effect of fluorocarbon encapsulation on the device performance of molybdenum disulphide thin-film transistors operating at low-voltages for active-matrix displays

Jun-Young Jeon, Byeong-Cheol Kang, Sang-Joon Park and Tae-Jun Ha*
Department of Electronic Materials Engineering, Kwangwoon University Seoul 01897, Republic of Korea
Tel.: 82-2-940-8678, E-mail: taejunha0604@gmail.com

The potential of transition metal dichalcogenides (TMDs) on electronic applications has been widely explored to provide new routes for realizing high performance [1]. Among them, molybdenum disulfide (MoS_2) based thin-film transistors (TFTs) for active-matrix devices have been of scientific and technological interests in display technologies owing to their outstanding performance of high field-effect mobility, large on-off current ratio, and low sub-threshold swing [2]. However, unexpected impurity doping during the fabrication processes including patterning may affect the intrinsic electrical characteristics of MoS_2 TFTs, which limits the potential on the display backplanes [3]. Although many studies for improving the performances of MoS_2 TFTs have been demonstrated, very few have focused on a practical and reliable method using fluorocarbon encapsulation to suppress the effect of impurity doping on charge transport. In this presentation, we will demonstrate an optimized encapsulation technique for restoring the intrinsic performances of MoS_2 TFTs operating at low-voltages by employing solution-processed carbon-fluorine copolymers. In addition, the origin of improved performance of MoS_2 TFTs will be discussed by investigating the effect of carbon-fluorine dipole interactions with impurities on charge transport underlying device physics. The statistical results of improved device performance of MoS_2 TFTs conclusively proved the fluorocarbon encapsulation can be promising for stimulating the potential of TMDs on active-matrix displays.

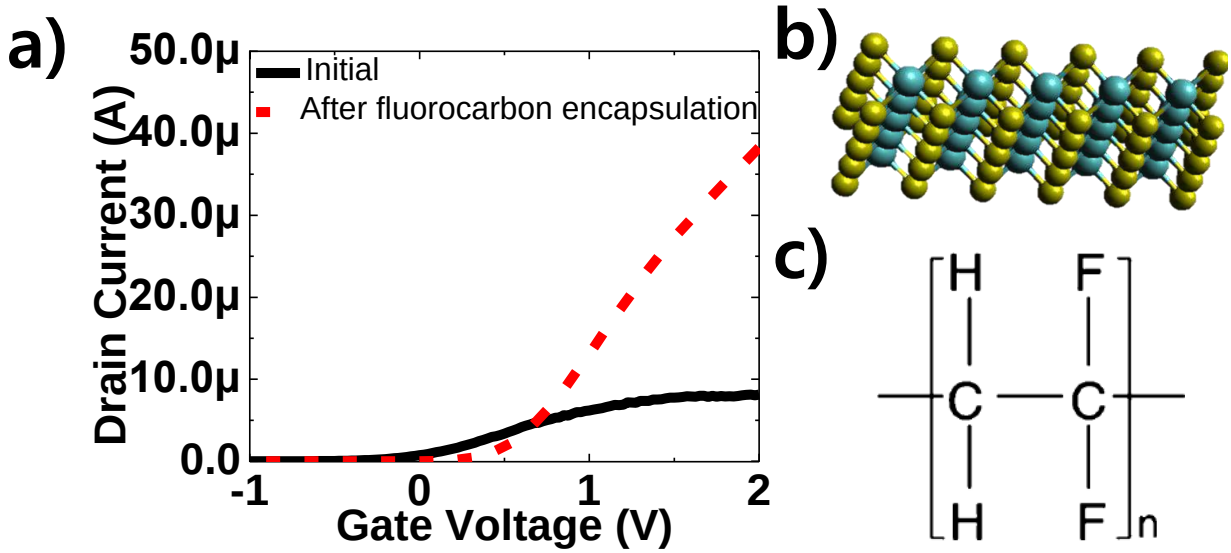

Fig. 1. (a) Transfer curves of MoS_2 TFTs before and after fluorocarbon encapsulation and the chemical structures of (b) MoS_2 and (c) carbon-fluorine copolymers

Acknowledgment

This work was supported by the National Research Foundation of Korea (NRF) grant funded by the Korea government (MSIT) (NRF-2021R1A2C2012855)

References

1. G. W. Shim, W. Hong, J. H. Cha, J. H. Park, K. J. Lee and S. Y. Choi, *Adv. Mater.*, 32(35), 1907166 (2020)
2. K. Cho, W. Park, J. Park, H. Jeong, J. Jang, T. Y. Kim, W. K. Hong, S. Hong and T. Lee, *ACS Nano*, 7(9), 7751-7758 (2013)
3. T. Jin, J. Kang, E. S. Kim, S. Lee and C. Lee, *J. Appl. Phys.*, 114(16), 164509 (2013)

Abnormal Thermal Instability of Al-doped InSnZnO Thin-Film Transistor with SiN_x/SiO_x double passivation layer

Junghoon Yang[1] and Sang-Hee Ko Park[1]
[1]Dept. of Materials Science, KAIST, Guseong-dong/Daejeon 34141, Korea
Tel.:82-42-350-3356, E-mail: shkp@kaist.ac.kr

Amorphous oxide semiconductors (AOS) have attracted much attention due to their many advantages such as high mobility, uniformity, stability, and application to the diverse electronic devices [1]. Among them, the high-mobility of oxide thin-film transistors (TFTs) is very essential for achieving high-resolution of active matrix-type electronic devices, not only for displays but for diverse sensors [2]. Despite their demands, realizing high-mobility oxide TFTs with superior environmental stability is still challenging. In the case of a high-mobility oxide TFT, the device performances can be considerably affected by the passivation process [3]. Typically, SiO_x and SiN_x deposited by plasma-enhanced chemical vapor deposition (PECVD) are widely used for passivation layers of oxide TFTs. For both excellent barrier capability and electrically stable device performance, a double-stacked layer, such as SiN_x/SiO_x, has been studied for the passivation of IGZO TFTs [4]. Despite these findings, there were no related reports about the effects of external heat and/or water on the electrical stability of Al-doped InSnZnO (Al-ITZO) TFTs with SiN_x/SiO_x double passivation layer (PL).

In this study, we observed a dramatic negative shift of turn-on voltage (V_{on}) of Al-ITZO TFT with SiN_x/SiO_x PL under high temperature and humidity. We fabricated BCE-structured high mobility Al-ITZO with SiN_x/SiO_x layers. To evaluate the environmental stability of TFTs with SiN_x/SiO_x PL, all TFTs were stored in a chamber under a temperature of 85 °C and a relative humidity of 85 % for 30 days. Interestingly, the initial V_{on} of TFTs was shifted more negatively due to the increased doping of H during the SiN_x deposition (as shown in Fig. 1(a)). The BCE TFT was not recovered to its initial state even after post-annealing at 200 °C in a vacuum. SiN_x film is known to be an excellent barrier to water and/or hydrogen, so it is difficult to conclude that this abrupt shift in BCE TFT occurred by the permeation of water. However, to our surprise, the TFT with SiN_x/SiO_x PL showed huge a negative V_{on} shift under the thermal effect (Fig. 1(b)). The Al-ITZO TFT passivated by SiN_x/SiO_x contains relatively high portion of hydroxyl group in active layer. At an elevated temperature, it seems to be vulnerable to generate V_o from the reaction of M-OH and H^+ to yield water and V_o.

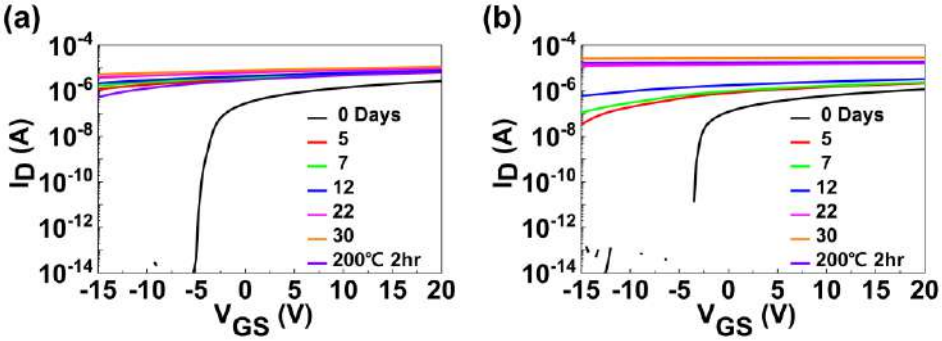

Fig. 1. Stability of Al-ITZO TFTs with SiN_x/SiO_x PLs at (a) temperature of 85 °C and a relative humidity of 85 % and (b) a temperature of 85 °C in an air-drying oven.

Acknowledgment

This work was supported by the National Research Foundation of Korea (NRF) Grant funded by the Korean Government under Grant 2018R1A2A3075518 and Grant 2020R1A6A3A13061266.

References

1. K. Nomura, H. Ohta, A. Takagi, T. Kamiya, M. Hirano, and H. Hosono, *Nature*, 432(7016), 488 (2004).
2. T. Kamiya, K. Nomura, and H. Hosono, Sci. Technol. Adv. Mater., 11(4), Art. no. 44305 (2010).
3. S-H. K. Park, M.-K. Ryu, H. Oh, C.-S. Hwang, J.-H. Jeon, and S.-M. Yoon, J. Vac. Sci. Tech-nol. B, 31(2), Art. no. 020601 (2013).
4. M. D. H. Chowdhury, M. Mativenga, J. G. Um, R. K. Mruthyunjaya, G. N. Heiler, T. J. Tredwell, and J. Jang, IEEE Trans. Electron Devices, 62(3), 869 (2015).

Effect of Ti Interlayer on the Contact Resistance of In-Ga-Sn-O Thin Film Transistors

Ho jae Lee[1], Min jae Kim[1], Jae seok Hur[1], Seong hun Yoon[1], Hee sung Han[1], and Jae kyeong Jeong[1]
Dept. of Electronic Engineering, Hanyang University, Seoul 04763, Korea
Tel.:82-2-2220-4180, E-mail: jkjeong1@hanyang.ac.kr

Power consumption of dynamic random access memory (DRAM) devices has increased by the significant improvement in the integration density. As the unit device is scaled down, several hindrances such as increasing contact resistance and leakage current *etc.* have been occured. In recent years, amorphous oxide semiconductors (AOSs) such as indium-gallium-zinc-oxide (IGZO) and indium-gallium-tin-oxide *etc.* are widely studied as one of the most promising materials which can replace conventional silicon-based semiconductors because of their high-performances including a low leakage current, moderate mobility, and complementary metal oxide semiconductor (CMOS)-compatible fabrication method *etc*. However, a contact resistance (R_C) of the oxide field-effect transistors (FETs) is higher than that of Si FETs, which results in the higher power consumption during the operation. Up to date, many approaches have been reported to improve their high R_C, one of which is to increase a carrier density (n_D) of oxide layer under source/drain contact electrode like a Ar plasma treatment.

In this study, we report a novel method using a thin titanium (Ti) interlayer to improve the R_C of the IGTO FETs because the IGTO semiconductor has the higher n_D than the IGZO semiconductor. Note that standard enthalpy of fomation(ΔH^O) of TiO_2 (-936.5 kJ·mol^{-1}O_2) is much lower than that of In_2O_3 (-616.03 kJ·mol^{-1}O_2), Ga_2O_3 (-729.08kJ·mol^{-1}O_2), and SnO_2 (-580.7kJ·mol^{-1}O_2). The Ti interlayer was deposited to absorb the oxygen from the IGTO channel layer underneath. In detail, we obtained a low specific contact resistivity (ρ_C) of 4.79E-6Ω·cm^2 using the 3-nm-thick Ti interlayer with a post deposition annealing at 300°C under vacuum condition for 1 hour, which is extracted by the transmission line measurement (TLM). This enhancement in the ρ_C might be attributed to the electron doping effect on the IGTO contact region from the oxygen absorbtion by the 3-nm-thick Ti interlayer. This work can suggest the way to apply oxide semiconductor to memory devices demanding extremely low contact resistance.

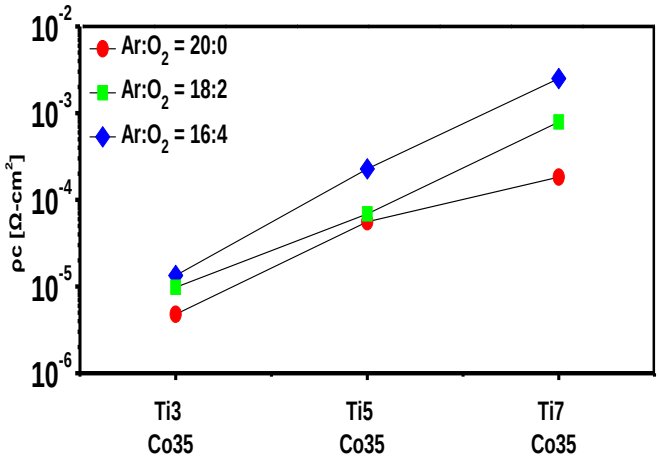

Fig. 1. Specific contact resistivity(ρ_C) of the IGTO TFTs with Interlayer Ti

References

1. P. S. Yun and J. Koike 2011 *J. Electrochem. Soc*. 158 H1034 (2011).
2. K. H. Choi and H. K. Kim Appl.Phys.Lett 102, 052103 (2013)

Improved Field-Effect Mobility of In-Zn-Sn-O Thin Film Transistor by Oxidized Metal Layer

Gwang Bok Kim, Jeong A Lee, Min Hoe Cho, Sang Won Chung, Jae Hoon Cho and Jae Kyeong Jeong
[1]Dept. of Electronic Engineering, Hanyang University, Seoul 04763, Korea
Tel.:82-2-2220-4182, E-mail: jkjeong1@hanyang.ac.kr

Currently, oxide thin-film transistors (TFTs) based on amorphous indium gallium zinc oxide (a -IGZO) have become industrial standard backplane electronics for advanced liquid crystals and organic light-emitting display devices due to their high mobility (~10 cm^2/Vs), low leakage current, low temperature process and good uniformity. However, As the demand for large size, high frame rate and ultra-high resolution display increases, the necessity for the high mobility(≥50 cm^2/Vs) TFTs is increased. To increase the electron mobility of TFTs, researchers have studied various oxide semiconductor materials such as InZnO and InGaO. In addition, they have studied various cation combinatorial approach and device structure to enhance the electron mobility.

In this work, we study electrical characteristics of InZnSnO (IZTO) TFTs which represents higher mobility (~30 cm^2/Vs) than a-IGZO. Also we suggest low temperature(≤ 300 °C) crystallization of IZTO by metal catalytic method and subsequent annealing process. Tantalum (Ta) is deposited as metal catalytic layer on a-IZTO channel layer and annealed at different temperatures of 200, 250, 300 and 400 °C under O_2 ambient. The effects of Ta catalytic layer and post annealing temperature on IZTO films were assessed by X-ray diffraction (XRD). During annealing, the Ta layer is oxidized amorphous TaO_x while expediting partial crystallization of the IZTO layer at temperatures as low as 300 °C. Amorphous IZTO TFTs exhibited the field-effect mobility (μ_{FE}) of 42.44 cm^2/Vs, subthreshold swing (SS) of 0.13 V/decade, threshold voltage (V_{TH}) of -3.06 V and $I_{ON/OFF}$ ratio of ~10^8. Interestingly, the devices with the crystallized IZTO channel at 300 °C had the improved μ_{FE} of 91.73 cm^2/Vs, SS of 0.13 V/decade, V_{TH} of -0.6 V and $I_{ON/OFF}$ ratio of ~10^8. The superior performance can be attributed to the high-quality crystallization effect. These results suggest that the crystallized IZTO TFTs are expected to be an alternative to LTPS and a-IGZO TFTs for high-pixel- density, large sized AM-OLED.

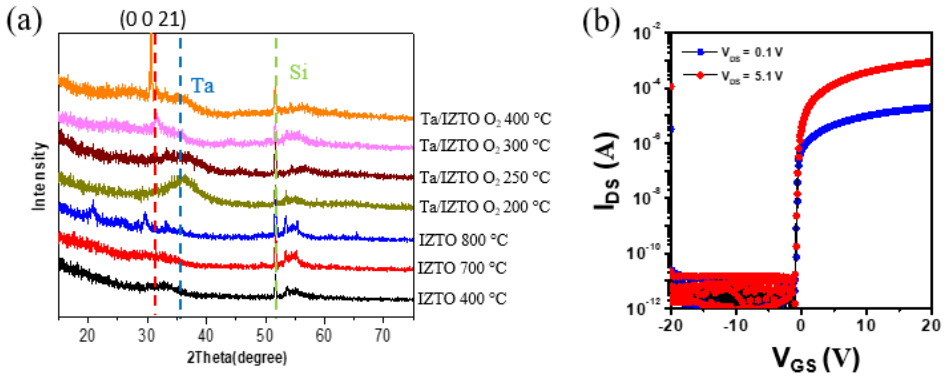

Fig. 1. (a) XRD spectra of the IZTO stacked with and without Ta catalytic layer on SiO_2/p++ Si. (b) Transfer characteristics of the Ta capped IZTO TFTs PDA 300 °C under O_2 ambient

References

1. K. Nomura et al., *Nature,* 432, 488 (2014).
2. Y. W. Shin et al., *SCI. Reports,* 7, 10885 (2017).

High-Performance Solution-processed WSe_2 Transistors

*Taoyu Zou, Hyunjun Kim, and Yong-Young Noh**
Department of Chemical Engineering, Pohang University of Science and Technology, 77 Cheongam-Ro, Nam-Gu, Pohang 37673, Republic of Korea
*Corresponding author: Y. Y. Noh (yynoh@postech.ac.kr)

Two-dimensional (2D) transition-metal dichalcogenides (TMDC) is considered as one of the promising candidates for next-generation optoelectronics.[1] Among chemical vapor deposition (CVD), mechanical exfoliation, solution-phase chemical synthesis, liquid-phase exfoliation (LPE), and intercalation-based exfoliation methods, the solution-processable method for synthesizing 2D nanosheets offers significant potential in thin-film electronics for large-area flexible and wearable devices. Solution-processed n-type transistors (MoS_2) have reached high mobility of over 10 $cm^2\ V^{-1}\ s^{-1}$.[2] However, the performance for the solution-processed p-type 2D transistor is still inferior. Here, we demonstrate high-performance solution-processed WSe_2 transistors. The optimized WSe_2 transistor exhibits increased mobility up to 0.2 $cm^2\ V^{-1}\ s^{-1}$ from bare devices with relatively low mobility of 10^{-4} $cm^2\ V^{-1}\ s^{-1}$, as shown in Figure 1. Especially, the high on/off ratio of the solvent-treated WSe_2 transistor increased to over 10^6 from 10^4, which is over 4 orders of magnitude greater than that of the reported solution-processed WSe_2 transistor (~10^2).[3] We will present details on how we achieve high performance at the conference.

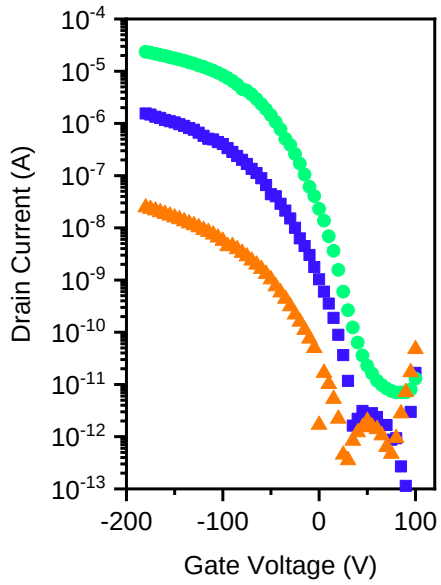

Fig. 1. I_{sd}-V_g transfer characteristics of bare WSe_2 (solid triangle) and optimized (solid square and circles) at V_{ds} of 1 V solvent treatment.

Acknowledgment

This study was supported by Ministry of Science and ICT through the National Research Foundation, funded by the Korean government (2020R1A2C4001617, 2020R1A4A1019455, 2020M3F3A2A01085792).

References

1. Y. Liu, X. Duan, H.-J. Shin, S. Park, Y. Huang and X. Duan, *Nature*, 591(7848), 43 (2021).
2. Z. Lin, Y. Liu, U. Halim, M. Ding, Y. Liu, Y. Wang, C. Jia, P. Chen, X. Duan, C. Wang, F. Song, M. Li, C. Wan, Y. Huang and X. Duan, *Nature*, 562(7726), 254 (2018).
3. A.G. Kelly, T. Hallam, C. Backes, A. Harvey, A.S. Esmaeily, I. Godwin, J. Coelho, V. Nicolosi, J. Lauth, A. Kulkarni, S. Kinge, L.D. Siebbeles, G.S. Duesberg and J.N. Coleman, *Science*, 356(6333), 69 (2017).

Current modulation in conducting polymer composites with overcoating of a dedoping layer in organic field-effect transistors

Chaeseon Jeong[1], Donguk Kim[1], and Felix Sunjoo Kim[1]*
[1]School of Chemical Engineering and Materials Science, Chung-Ang University, Seoul, 06974, Korea
Tel.:82-2-820-5200, E-mail: fskim@cau.ac.kr

Poly(3,4-ethylenedioxythiophene) (PEDOT) and its composites have been widely used as an electrode in organic electronic devices because of their high electrical conductivity and water-/alcohol-based processing methods. As their high electrical conductivity originates from the chemical doping, the conductance can be reversibly controlled by doping and dedoping procedures. Previous studies with the dedoped PEDOT films showed a couductor-like behavior with a small current modulation in organic field-effect transistors (OFETs)[1,2]. In this work, we have investigated control of doping levels of PEDOT composites by using an overcoating of dedoping agents. Device structures and overcoating components were varied to induce changes in the current modulation characteristics. Fig. 1 shows representative current (I)–voltage (V) curves of the OFETs. While the pristine PEDOT composites show high drain current (I_D) without any modulation when gate voltage (V_G) is applied, the overcoating-dedoped films showed semiconducting behaviors with the current on/off ratios in the range of 10^2–10^3. The dedoped PEDOT has a field-effect mobility of ~10^{-3} $cm^2 V^{-1} s^{-1}$ in saturation regime.

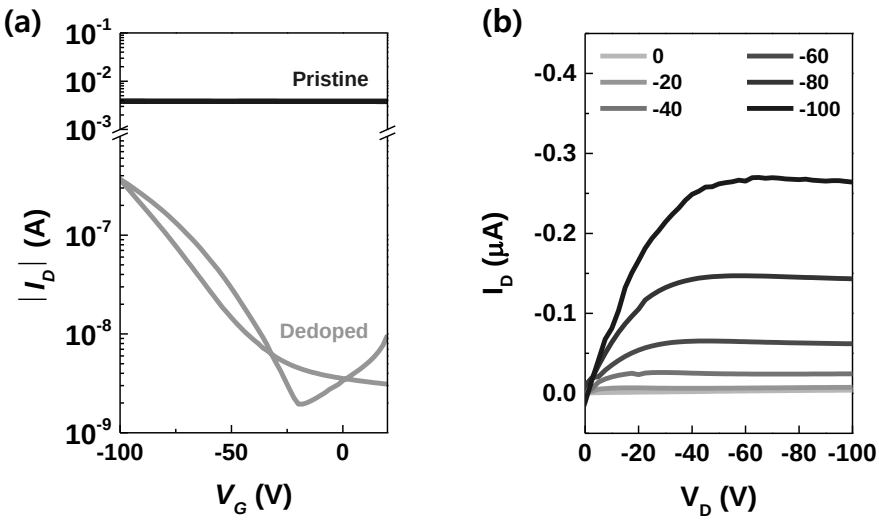

Fig. 1. I– V characteristics of OFETs based on a pristine conducting polymer and a dedoped polymer: (a) Drain current (I_D)–gate voltage (V_G) curves. (b) Drain current (I_D)–drain voltage (V_D) curves of the OFETs.

Acknowledgment

This research was funded and conducted under "the Competency Development Program for Industry Specialists" of the Korean Ministry of Trade, Industry and Energy (MOTIE), operated by Korea Institute for Advancement of Technology (KIAT), with the project No. P0012453, Next-generation Display Expert Training Project for Innovation Process and Equipment, Materials Engineers. This work was also supported by the research programs (2019M3F3A1A03079821 and 2019R1A2C1087234) through the National Research Foundation of Korea (NRF) funded by the Ministry of Science and ICT.

References

1. Q. Wei, M. Mukaida, K. Kirihara, Y. Naitoh, and T. Ishida, *ACS Appl. Mater. Interfaces*, 8(3), 2054 (2016).
2. D. Kim, H. Jang, S. Lee, B. J. Kim, and F. S. Kim, *ACS Appl. Mater. Interfaces*, 13(1), 1065 (2021).

High Performance Indium Gallium Oxide Transistors at a Low Temperature Using a Tantalum Catalytic Layer for Flexible Applications

Yoonji Choi[1,2], Seong Jip Kim[1], Gwangbok Kim[2], Jae Kyeong Jeong[2] and Byungwook Yoo[1]
[1]Display Research Center, Korea Electronics Technology Institute, Seongnam 13509, Republic of Korea
Tel.:82-31-789-7420, E-mail: bwyoo@keti.re.kr
[2]Dept. of Electronic Engineering, Hanyang University, Seoul 04763, Republic of Korea
Tel.:82-2-2220-2327, E-mail: jkjeong1@hanyang.ac.kr

Oxide thin film transistors (TFTs) have been the focus of intense worldwide research during the past decade because of their superior performance compared with conventional amorphous Si TFTs such as high mobility, low off current, optical transparency and low cost fabrication process [1]. Display manufacturing companies have already used oxide TFTs for TV applications, but there are some issues remained for oxide TFTs to be used for flexible displays. One of the issues is the high-temperature annealing process (> 300°C). Most flexible substrates cannot be processed in this high temperatures due to their low thermal durability. Therefore, high performance oxide TFTs that can be processed at low temperature are required to expand the field of application [2]. There have been several reports of high mobility oxide TFTs using low temperature by metal catalytic layer [3-4]. However, the annealing temperature of oxide semiconductor should be further reduced under 200℃ to use low cost flexible substrates such as polyethylene naphthalate or polyestersulfone. In this study, we investigated high performance indium gallium oxide (IGO) TFTs via tantalum catalytic layer at low temperature for low cost flexible display.

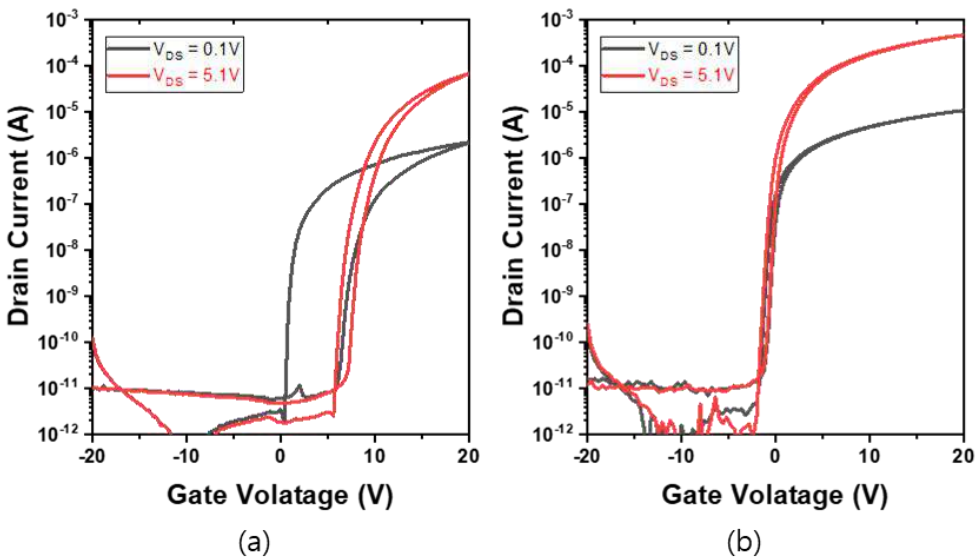

Fig. 1. Transfer characteristic of IGO TFTs (a) without catalytic layer and (b) with catalytic layer.

Acknowledgment

This work was supported by the Future Growth Engine R&D Program (20010082 and 20010442) funded by the Ministry of Trade, Industry & Energy(MOTIE) in Republic of Korea.

References

1. T. Kamiya, K. Nomura, and H. Hosono, J. Disp. Technol. 5, 273 (2009).
2. S. Hong, S. P. Park, Y. Kim, B. H. Kang, J. W. Na, and H. J. Kim, Sci. Rep., 7(1),16265 (2017).
3. Y. W. Shin, S. T. Kim, K. Kim, M. Y. Kim, S. Oh, and J. K. Jeong, *Sci Rep 7*, 10885 (2017).
4. A. Y. Hwang, S. T. Kim, H. Ji, Y. Shin, and J. K. Jeong, *Applied Physics Letters 108*, 152111 (2016).

Low-Temperature Processable Polyimide Gate Dielectrics for Flexible Pentacene Thin Film Transistors

Taek Ahn*
Dept. of Chemistry, Kyungsung University, 309, Suyeong-ro, Nam-gu, Busan 48434, Korea
Tel.:82-51-663-4632, E-mail: taekahn@ks.ac.kr

Polyimides (PIs) are currently considered as promising gate dielectrics because of their good chemical resistance, excellent thermal stability, and mechanical properties. The major problem in the use of PI materials is their high processing temperature. A polyamic acid (PAA)-based PI gate dielectric must be treated at a minimum of 230 ^{o}C to fabricate a thin film. To apply a polymeric gate insulator on a plastic substrate, the processing temperature must be below 200 ^{o}C. Another important property of a gate insulator is its ability to interface with an organic semiconductor. To form a well-defined interface between the organic semiconductor and the gate insulator during semiconductor deposition or solution processing, the gate insulator should not be damaged. Therefore, a photo-crosslinking process is required to produce a well-packed gate insulator layer. In addition, the photo-crosslinkable PIs could be patterned by a facile and cost-effective method.

In this paper, first we have synthesized hydroxyl group containing polyimide through one-step condensation polymerization. The polyimides (DOCDA-6FHAB and DOCDA-HAB) were polymerized from 5-(2,5-dioxotetrahydrofuryl)-3-methyl-3-cyclohexene-1,2-dicarboxylic anhydride [DOCDA] as dianhydride monomer and 3,3'-dihydroxybenzidine [HAB] or 2,2-bis(3-amino-4-hydroxyphenyl) hexafluoropropane [6FHAB] as diamine monomer. And then, photo-sensitive and photo-patternable cinamoyl functional group was attached into the side chain of polyimide through the post-functionalization method. Post-functionalized polymer (D6FC) showed good solubility in common organic solvent such as cyclohexanone and thin film could be fabricated at maximum 160 ^{o}C. Pentacene TFT with D6FC as gate insulator on flexible PES substrate showed field effect mobility as 0.10 cm^2/Vs with excellent current on/off ratio as 5.5×10^7 as shown in Fig.1. A detailed synthetic route, device fabrication condition and electrical properties of the pentacene TFT with photosensitive soluble polyimide gate insulator will be presented.

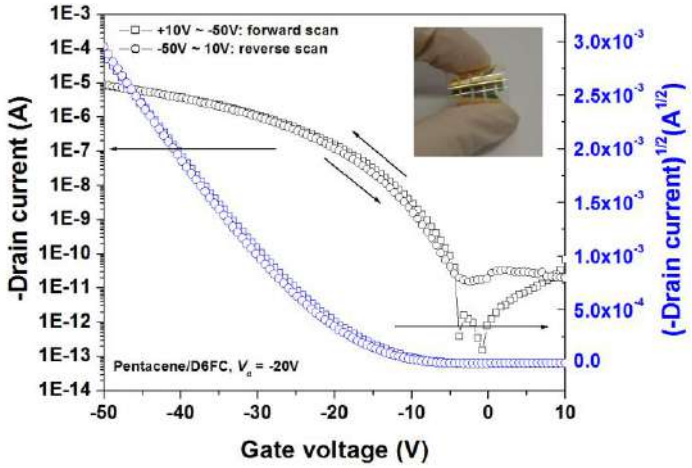

Fig. 1. Transfer characteristic curves ($I_{ds}^{1/2}$ vs. V_{gs}) of flexible pentacene TFTs. Inset: a flexible TFT image.

Acknowledgment

This research was supported by the National Research Foundation of Korea (NRF) grant funded by the Korea government (MSIT) (2019R1F1A1060813).

References

1. G. Horowitz, *J. Mater. Res.*, 19, 1946 (2004).
2. T. Ahn, Y. Choi, and M. H. Yi, *Appl. Surf. Sci.*,255, 2185 (2008).
3. T. Ahn, Y. Choi, H. M. Jung, and M. H. Yi, *Org. Electron.*,10, 12 (2009).

Transfer Characteristics of InGaZnO Thin Film Transistors with Different Oxygen Partial Pressures

Jongyoon Lee, and Byoungdeog Choi
Department of Electrical and Computer Engineering, Sungkyunkwan University, Suwon, Gyeonggi 16419, Republic of Korea
Tel.:+82-31-299-4966, E-mail: bdchoi@skku.edu

Transfer characteristics and degradation analysis of indium-gallium-zinc-oxide thin film transistors (IGZO TFTs) with different oxygen partial pressures (OPP) were investigated. IGZO TFTs were fabricated on the oxidated p-type silicon substrate by sputtering method. 20 nm thick IGZO was deposited on the SiO_2 film under various OPP ($Ar : O_2$ = 30 : 0, 30 : 3 and 30 : 6) conditions with sputtering target of $In_2O_3 : Ga_2O_3 : ZnO$ = 1 : 1 : 1.

Electrical parameters of the devices were obtained from the transfer curves as shown in figure 1. As OPP increased, saturation mobility slightly decreases from 3.61 cm^2/Vs to 3.49 cm^2/Vs while threshold voltage (V_{th}) drastically increased from -2.85 V to 2.06 V. This is because that more oxygen vacancies (V_O) that act as donors are compensated by oxygens as OPP increases, so the carrier concentration decreases and the conductivity of IGZO is lowered. Off current was reduced when OPP increased due to the reduction of carrier concentration. Subthreshold swing reduced from 0.61 V/decade to 0.37 V/decade with increased OPP. This is due to the compensation of V_O which act as not only donors but also trap site near the interface between gate insulator and IGZO [1]. Figure 2 shows V_{th} shift (ΔV_{th}) after positive bias stress (PBS) at room temperature. Voltage was applied to the gate electrode for 1000 secs. The value of ΔV_{th} is larger in oxygen poor condition than oxygen rich under PBS. This is because V_O are reduced under high OPP sputtering conditions. Therefore, the less carriers are trapped and consequently ΔV_{th} decreases in oxygen rich condition.

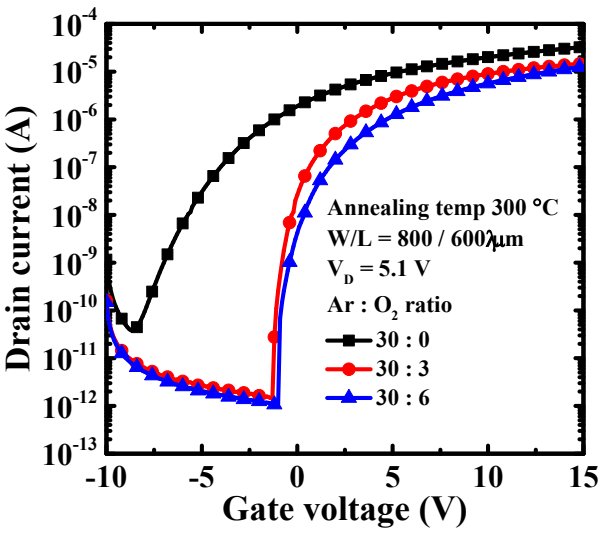

Fig. 1. Transfer characteristics of IGZO TFTs fabricated under various OPP

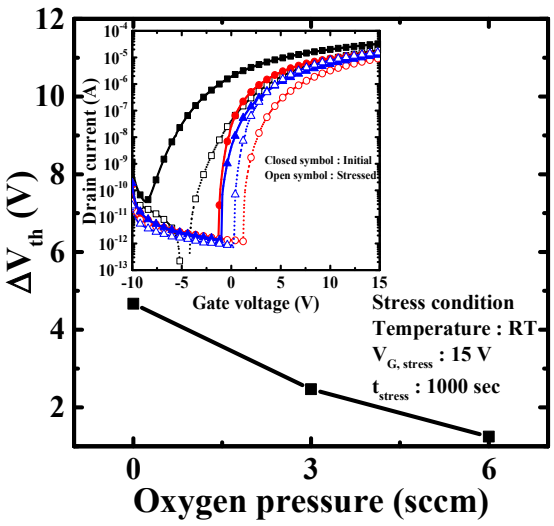

Fig. 2. ΔV_{th} under PBS

References

1. Chong, E. G., Chun, Y. S., Kim, S. H., & Lee, S. Y. *Journal of Electrical Engineering and Technology*, *6*(4), 539-542. (2011).

Mechanism of Low Frequency Noise and Trap Density Profile in Dual Gate Metal Oxide Thin Film Transistor

Kanghyun Kim[1], Min Jung Kim[2], Younggil Park[1], Seung Hee Jin[2], and Jae Woo Lee[2]
[1]Samsung Display, Asan 31454, Republic of Korea
[2]Interdisciplinary Graduate Program for Artificial Intelligence Smart Convergence Technology, Korea University, Sejong 30019, Republic of Korea
Tel.:82-44-860-1421, E-mail: orion627@korea.ac.kr

Indium gallium zinc oxide(IGZO) channel thin film transistor(TFT) has great electrical characteristics, transparancy, and simple fabrication process in low temeprature as same as amorphous silicon TFT. TFT with IGZO channel is a major point of realizing high resolution, huge, and flexible display in these days. But, there are still problems to be solved, such as enhancement of device performance and reliability. Low frequency noise(LFN) analysis will be a method to figure out these problems.

In this study, we measured dual gate IGZO TFT structure (top and bottom gate separately). Each case shows different transfer characteristics, and we prove this result through LFN analysis. We extract mobility coefficient(α), and trap density(N_t) to analysis. Figure 1-(a) and (b) show that trap density(N_t) distribution is different. Top gate structure has high trap density level in all overdrive voltages(V_{ov}) which is formed in the range of 10^{18}~10^{19} $cm^{-3}eV^{-1}$. But in bottom gate structure, trap density formed in the range of 10^{17}~10^{18} $cm^{-3}eV^{-1}$. In both cases, trap density on the oxide and channel interface side are lower than bulk side. This result shows that trap distribution varies depending on the gate type and trap density affects the device performance.

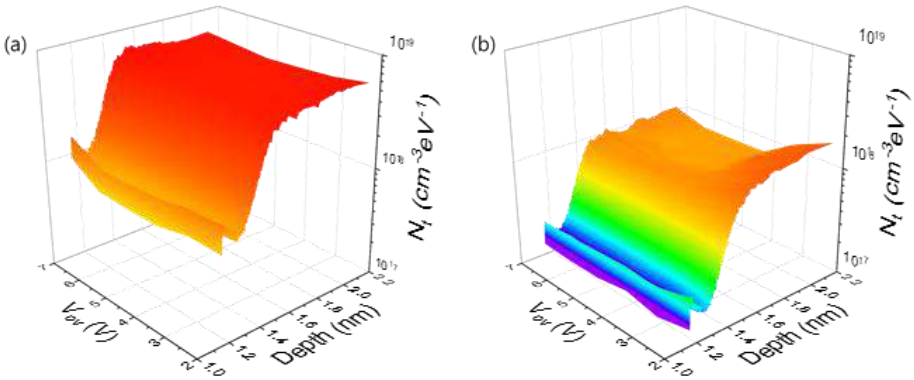

Fig. 1. Trap Density plot. (a) Top gate contact (b) Bottom gate contact

Acknowledgment

This work is supported by Samsung Display, NRF-2019R1F1A1060687 and the MOTIE (Ministry of Trade, Industry & Energy (10067808) and KSRC (Korea Semiconductor Research Consortium) support program for the development of the future semiconductor device.

Kanghyun Kim and Min Jung Kim are contributed equally to this work.

References

1. Kim, Donghyun, et al. "Influence of flexible substrate in low temperature polycrystalline silicon thin-film transistors: temperature dependent characteristics and low frequency noise analysis." *Nanotechnology* 31.43 (2020): 435201.
2 Chun, Yoon Soo, Seongpil Chang, and Sang Yeol Lee. "Effects of gate insulators on the performance of a-IGZO TFT fabricated at room-temperature." *Microelectronic Engineering* 88.7 (2011): 1590-1593.

The effect of silicon incorporation on threshold voltage shift of solution-processed indium-zinc oxide thin film transistor

Hyuntaek Woo[1], and Byoungdeog Choi[1]
Department of Electrical and Computer Engineering, Sungkyunkwan University, Suwon, Gyeonggi 16419, Republic of Korea
Tel.:+82-31-299-4966, E-mail: bdchoi@skku.edu

The effect of silicon incorporation of indium-zinc oxide (IZO) thin film transistor (TFT) on threshold voltage shift were identified. 0.1 and 0.2 mol silicon doped IZO active layers were formed on the p-Si substrates that SiO2 was dry oxidized. The transfer characteristics of TFTs under positive bias stress (PBS) for 1,000 sec were measured while source and drain terminals were grounded when a gate bias stress (VG, stress = 10 V) was applied. For TFTs with 0.1 mol silicon doped active layer, threshold voltage shift (ΔVth) was 7.78 V, while ΔVth was reduced to 5.01 V for the case of 0.2 mol silicon doped. During the PBS test, electrons accumulated in the channel are trapped in the gate oxide or oxide/activation layer interface trap. The trapped electrons cause the Vth to move to the positive direction. Comparing two different types of TFTs with silicon doping concentration, because silicon which have stronger oxygen binding energy than indium or zinc reduces the interfacial trap density, ΔVth of 0.2 mol silicon doped TFT was relatively smaller than the case of 0.1 mol silicon doped TFT. This means that the reliability of the TFT can be improved by increasing the doping concentration of silicon in the active layer.

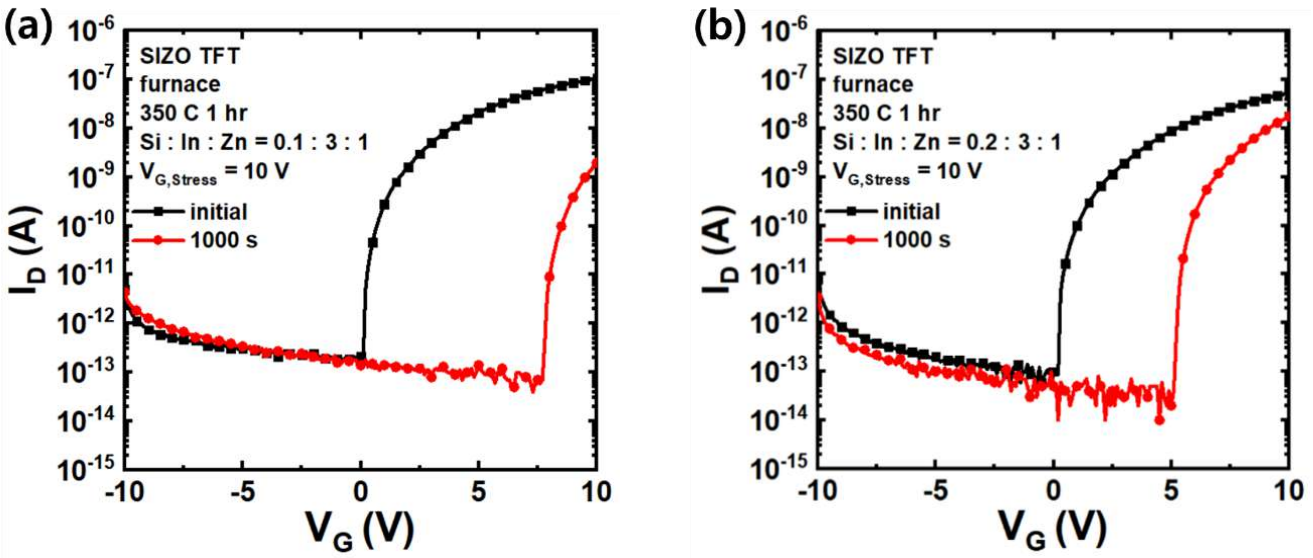

Fig 1. Transfer curve of Si-doped IZO TFT under PBS (a) 0.1 mol of silicon (b) 0.2 mol of silicon

References

1. Hyung Do Kim, et al. "Origin of instability by positive bias stress in amorphous Si-In-Zn-O thin film transistor." Applied Physics Letters 99.17 (2011): 172106.

Performance Improvement in p-Channel Tin Monoxide Thin-Film Transistors via Bilayer Gate Dielectric Stack using Hafnium Zirconium Oxide and Aluminum Oxide

Hochang Lee[1], Taikyu Kim[1], Hongwei Xu[1], Seungwan Seo[1], Cheol Hee Choi[1], and Jae Kyeong Jeong[1]
[1]Department of Electronic Engineering, Hanyang University, Seoul 04763, South Korea
Tel.:82-2-2220-4180, E-mail: jkjeong1@hanyang.ac.kr

Amorphous oxide semiconductors (AOSs) have received remarkable attention as advanced display materials for flat panel display application such as ultrahigh-pixel-density liquid crystal screens and large-sized organic light-emitting diodes, due to their low-temperature processability and high carrier mobility. However, the current status of the development of p-type oxide semiconductors remains poor compared with the great progress and success of n-type oxide semiconductors. Among the possible candidates for p-type oxide semiconductors such as copper oxide (Cu_XO), nickel oxide (NiO_X), and tin monoxide (SnO), the SnO is considered as the most promising material because it has a low hole effective mass (m_h^*) of ~1.25 m_e compared with the other p-type oxide semiconductors [1].

Gate dielectric films play an important role in determining the device performance because the transporting properties of hole carriers along the channel layer are strongly affected by scattering and trapping of charge carriers at the channel/gate dielectric interface. Recently, hafnium zirconium oxide (HZO) have been explored widely for its high potential in various applications such as ferroelectric random-access memory (FeRAM), and dynamic random-access memory (DRAM) but its characterization for an employment as a high-k dielectric is still insufficient.

This study examines a performance improvement in the p-channel SnO TFTs using the HZO gate dielectric layer. We show that inserting thin aluminum oxide (Al_2O_3) layer between the SnO and HZO greatly enhances its thin-film transistor (TFT) performance. This bilayer gate dielectric stack takes full advantage of its high *k* value and low interfacial trap density, accompanying the significant improvement in the range of driving voltage and subthreshold gate swing (SS). In conclusion, we demonstrate the strong potential of the Al_2O_3/HZO stack as efficient gate dielectric layer for the p-channel SnO TFTs. At the same time, this study shows its high device performance including a field-effect mobility of ~1 cm^2/Vs, SS of 0.6 V/decade and on/off current modulation ratio of ~4×10^5.

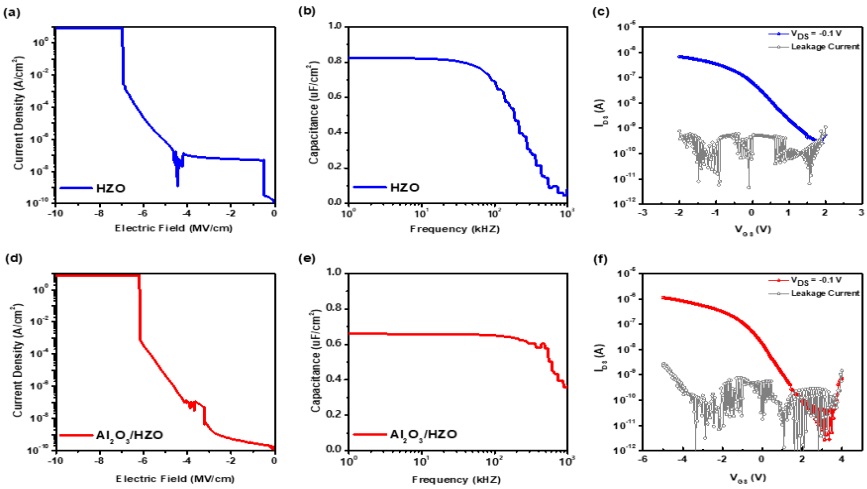

Fig. 1. Electrical properties of high-k dielectrics for MIM capacitors: (a,d) Leakage current and breakdown field. (b,e) Variations in frequency-dependent capacitances. (c,f) Transfer characteristic of bottom gate top contact p-channel SnO TFTs with HZO and Al_2O_3/HZO gate dielectric layer.

References

1. Y. Ogo, H. Hiramatsu, K. Nomura, H. Yanagi, T. Kamiya, M. Kimura, M. Hirano, and H. Hosono, *Phys. Status Solidi* 206, 2187-2191 (2009)

Perfluorocyclobutane Containing Crosslinked Polyimide Gate Dielectric for Thin Film Transistors

*Jae Kyung Lee and Taek Ahn**
Dept. of Chemistry, Kyungsung University, 309, Suyeong-ro, Nam-gu, Busan 48434, Korea
Tel.:82-51-663-4632, E-mail: taekahn@ks.ac.kr

There is increasing interests in using polymeric materials as gate dielectrics. Several polymeric gate dielectrics, such as poly(4-vinylphenol) (PVP), poly(methyl methacrylate) (PMMA), poly(vinyl alcohol) (PVA), and polyimide (PI) have been investigated. Among them, PI currently considered promising gate dielectrics because of their good chemical resistance, excellent thermal stability, and mechanical properties. And also, perfluorocyclobutane (PFCB) containing polymers possess many advantages over other fluorinated polymers such as their low surface energy, optical transparency, ease of processing, and excellent thermal and mechanical properties. Therefore, PFCB polymers would be expected to serve as good candidates for organic gate dielectrics because the solution processing of semiconducting polymers or patterning of top electrodes is possible onto cross-linked PFCB polymers. To increase the packing density and chemical resistance of gate insulator layers, the cross-linking process of each polymer backbone is essential. In this paper, we firstly synthesized hydroxyl group-containing soluble PI (SPI) polymer. And then, SPI polymer was chemically modified by thermally curable 4-(1,2,2-trifluorovinyloxy)benzoyl (TFVOB) moiety. A thermal cross-linking of the TFVOB substituted SPI (TFVOB-SPI) was conducted and produced the cross-linked TFVOB-SPI containing perfluorocyclobutane (PFCB) structure. The PFCB was formed by the radical mediated thermal cycloaddition of trifluorovinyl ether of TFVOB. Thin film properties of a thermally cross-linked TFVOB-SPI such as thermal property, surface roughness, and surface energy were systematically investigated. The insulating property and the pentacene TFT device with the cross-linked TFVOB-SPI as a gate insulator were also investigated.

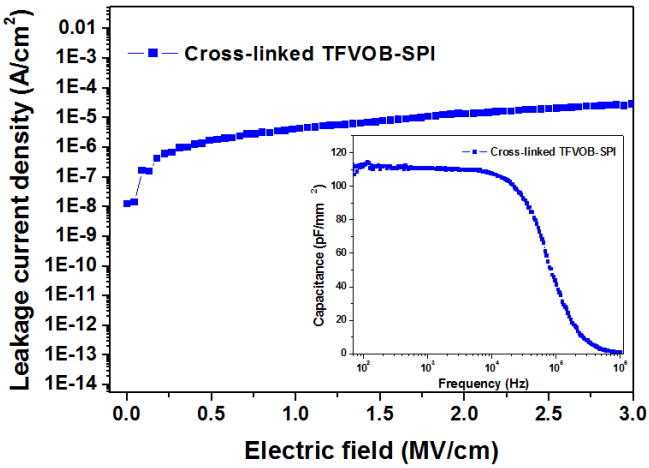

Fig. 1. Leakage current density as a function of the applied electric field for the MIM structure (ITO/C-TFVOB-SPI/Au). Inset: capacitance as a function of the frequency.

Acknowledgment

This research was supported by the National Research Foundation of Korea (NRF) grant funded by the Korea government (MSIT) (2019R1F1A1060813).

References

1. H. Sirringhaus, *Adv. Mater.*,17, 2411 (2000).
2. T. Ahn, J. W. Kim, Y. Choi, and M. H. Yi, *Org. Electron.*, 9, 711 (2008).
3. J. W. Kim, M. H. Yi and T. Ahn, *Thin Solid Films*, 546, 147 (2013).

Bay-Substitution Effect of Peryelene Diimides Nanowires on Supramolecular Chirality and Phototransistors

Jaeyong Ahn[1], Xiaobo Shang[1], Jeong Hyeon Lee[2], Jin Chul Kim[2], Hiroyoshi Ohtsu[3], Wanuk Choi[4], Inho song[1], Sang Kyu Kwak[2], and Joon Hak Oh[1]

[1]School of Chemical and Biological Engineering, Seoul National University, Seoul 08826, Republic of Korea

Tel.:82-2-880-7421, E-mail: jaeyongahn@snu.ac.kr

[2]Dept. of Energy Engineering, Ulsan National Institute of Science and Technology (UNIST), Ulsan 44919, Republic of Korea

[3]Dept. of Chemistry, Tokyo Institute of Technology, Tokyo 152-8550, Japan

[4]Energy Materials Laboratory, Korea Institute of Energy Research (KIER), Daejeon 34129, Republic of Korea

Supramolecular chirlaity has attracted a great deal of attention in the field of optoelectronics. Introducing chirality into nanostructures can potentially lead to more advanced applications such as 3D displays and optical communications. Single-crystalline nanowires (NWs), despite their superior performance, have not been frequently used in organic devices based on *n*-channel materials. Perylene diimides (PDIs) have been extensively studided for use in *n*-channel organic devices due to their high stability and tunability. However, previous research of chiral PDIs in organic devices is rare and most chiral PDIs mainly focus on *N*-substituted groups at the imide position. Only few reports describe the effect of bay substitution on self-assembled chiral PDIs.

Here, we synthesized various bay-substituted chiral PDIs and self-assembled them into 1D nanomaterials. Each of the nanomaterials exhibited unique circular dichroism spectra due to the bay-subsitution effect, indicating that modification of bay substitution plays an important role on supramolecular chirality. Structural modification through the bay position also affect the electronic and optical properties. Among them, mono-cyanated (*R*)-CPDI-CN-Ph NW-based organic phototransistors (OPTs) exhibited the highest electron mobility up to 0.17 $cm^2 V^{-1}s^{-1}$ and a low threshold voltage of −1 V. In addition, they showed outstanding optoelectronic performance with maximum photoresponsivity of 209 A W^{-1}. Our results paved the way to utilize the bay substitution effect to tune the optoelectronic performance and supramolecular chirality effectively.

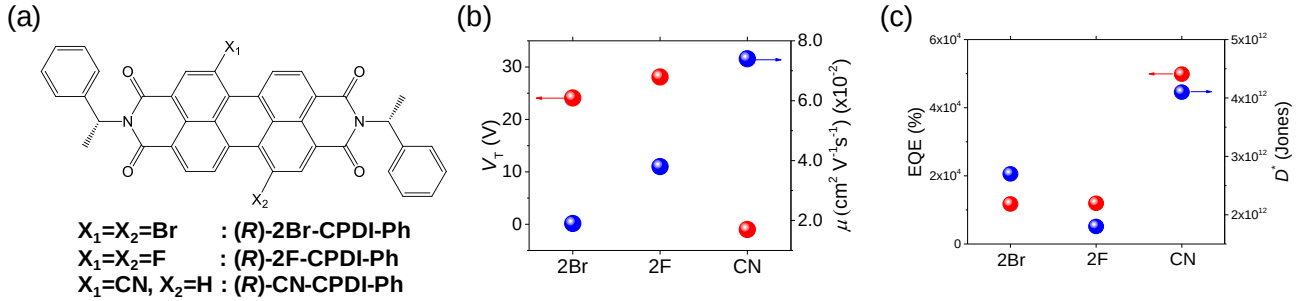

Fig. 1. (a) Chemical structures of bay-substituted PDIs. (b) Mobility, threshold voltage, (c) EQE and specific detectivity comparison graph of bay-substituted PDI NW-based OPTs.

Acknowledgment

This work was supported by the Samsung Research Funding Center of Samsung Electronics (SRFC-MA1602-51), the Nano Material Techonology Dvelopment Program (2017M3A7B8063825), and the National Research Foundation of Korea (NRF) grant (2020R1A2B5B03094499).

References

1. X. Shang, J. Ahn, J. H. Lee, J. C. Kim, H. Ohtsu, W. Choi, I. Song, S. K. Kwak and J. H. Oh, *ACS Appl. Mater. Interfaces*, *13*, 12278 (2021).

Low-Dimensional Semiconductor-Based Complementary Inverters with Tunable Switching Threshold

Seoyeon Jung[1], Jihyun Lee[1], Sangyeon Pak[2], Jungmoon Lim[2], SeungNam Cha[2], and Bongjun Kim[1]
[1]Dept. of Electronics Engineering, Sookmyung Women's University, Yongsan-gu, Seoul 04312, Korea
Tel.:82-2-710-9007, E-mail: bongjun.kim@sookmyung.ac.kr
[2]Dept. of Physics, Sungkyunkwan University, Suwon, Gyeonggi-do 16419, Korea

Complementary circuits have been widely utilized in most integrated circuits for several decades due to their low static power consumption and high noise immunity. Among various complementary logic gates, a complementary inverter, which is composed of a n-type and a p-type field-effect transistors (FETs), is the most basic builiding block in digital electronics. In order to implement such inverter circuits with large noise margins, it is necessary to employ n- and p-type semiconductors that exhibit comparable performances. In the case that n- and p-type semiconductors with imbalanced performaces are chosen to construct complementary inverters, different channel widths are typically employed in n- and p-FETs to compensate their device performances.[1] Balanced noise margins are attained when switching threshold voltages are located at $V_{DD}/2$ by matching n- and p-FET currents. However, it is not ideal to design circuits with significantly different channel dimensions for device integration since larger channel widths result in larger device area. In this presentation, we will show a facile and efficient method to control swithcing threshold of complementary inverters by varying numbers of printed semiconductor layers. N-type monolayer MoS_2 is deposited by chemical vapor deposition (CVD), and p-type random network single-walled carbon nanotubes (SWCNTs) are deposited by inkjet printing to form semiconducting channels. Fig. 1(a) and (b) illustrate a structure and a circuit diagram of the inverter based on low-dimensional semiconductors, respectively. Fig. 1(c) shows p-FET characteristic changes as the number of printed SWCNT layers increases. Adjusted p-FET characteristics lead to large shift of switching threshold of the complementary inverter without changing channel dimensions as shown in Fig. 1(d). The resultant inverter exhibits improved noise margins.

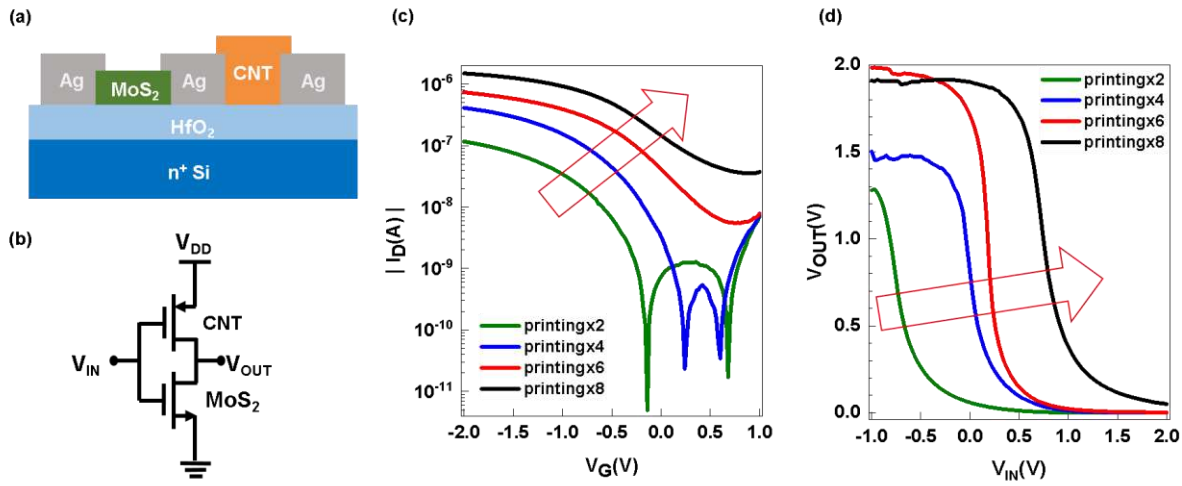

Fig. 1. (a) Schematic cross-section and (b) circuit diagram of the complementary inverter. (c) Transfer characteristics (I_D-V_g) of p-FET with different numbers of printed SWCNT layers at V_D = -0.1 V. (d) Voltage transfer characteristics with different numbers of printed SWCNT layers at V_{DD} = 2 V.

Acknowledgment

This work was financially supported by the Ministry of Trade, Industry and Energy (MOTIE) and Korea Institute for Advancement of Technology (KIAT) through the International Cooperative R&D program (Project No. P0016035).

References

1. B. Kim, S. Pak, H. W. Choi, Y. Choi, A. R. Jang, J. Lee, Y. T. Chun, S. Cha, and J. I. Sohn, *2D Mater.*, *6*, 025017 (2019).

Plasma Treatment of Amorphous IGZO with O_2 and Ar Reactive Gases

Jae Geun Woo, Chan Min Jeong, Eun Seong Yu, Hyuck Su Lee, Seo Jin Kang and Byung Seong Bae
Division of Electronics and Display Engineering, Hoseo University, Asan City, Chungnam, 336-795, Korea
Tel.:82-41-540-5221, E-mail: bsbae3@hoseo.edu

Amorphous IGZO (indium gallium zinc oxide) is the most common oxide semiconductor used in thin film transistors (TFTs) which have been applied to commercial flat panel displays and studied actively for various applications such as sensors, memories, and circuits. A self-aligned coplanar top gate structure has advantage that prevent the diffusion of oxygen and H_2O because the electrodes and insulator cover the active layer like passivation layer. In addition, it has the advantage of the small parasitic capacitance. However, additional process of doping is required to reduce the contact resistance at source and drain regions. The plasma process under a certain gas is one of the representative methods. The doping effect of IGZO through plasma treatment by various gases such as O_2 and Ar were investigated in this study. Figure 1 shows the sheet resistances for various doping gases. The doping time and doping gases affect the sheet resistance of the IGZO layer. After doping, sheet resistance was decreased. However, it increased again after thermal anneal. The recovery of the sheet resistance by thermal anneal was investigated in terms of temperature and doping gases.

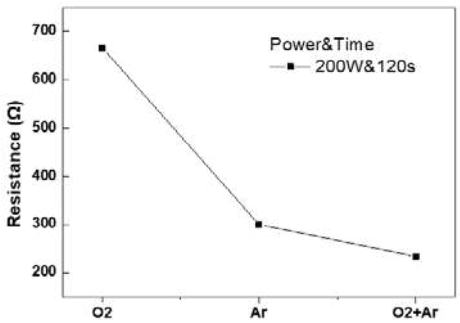

Fig. 1. Sheet resistance according to plasma treatment

This template is for IMID 2021 Technical Digest. Your file should be submitted via our home page below. (http: //www.imid.or.kr/2021/online_paper_submission.asp). If you follow the foregoing, your paper will conform to the requirements of the publisher and facilitate a problem-free publication process.

Acknowledgment

This work was supported by the Technology Innovation Program (20012556, Development of blue emitter and eco friendly quantum dot color conversion ink material for flexible QD OLED) funded By the Ministry of Trade, I ndustry & Energy(MOTIE, Korea)

Energy band offset induced threshold voltage shift of a-InGaZnO TFTs under bias light illumination

Hyojung Kim[1,2], Jangkun Song[3], and Byoungdeog Choi[3,]*
[1]OLED Business Samsung Display Co., Ltd, Korea
[2]Dept. of Semiconductor and Display Engineering, Sungkyunkwan University, Korea
[3]Dept. of Electrical and Computer Engineering, Sungkyunkwan University, Korea
Tel.:82-31-299-4589, E-mail: bdchoi@skku.edu

In this paper, the dependence of threshold voltage (V_{th}) changes to amorphous-indium gallium zinc oxide (a-IGZO) TFTs under PBIS and NBIS on the height of the energy bnad offset was studied. Using SiO_2, HfO_2 and Al_2O_3 as gate dielectrics, three different types of a-IGZO TFTs were used in the experiment. Electrical parameters, density of state (DOS) of each TFT were measured. The interface characteristics between a-IGZO and gate dielectric were excellent in the order of SiO_2, HfO_2, and Al_2O_3. To determine the E_g of the gate dielectrics used in this experiment, we extrapolated from the UV/Vis data using the Tauc method. The band gaps extracted were HfO_2 (5.8 eV), Al_2O_3 (6.5 eV), and SiO_2 (8.9 eV). [1] Additionally, conduction band offset (CBO) and VBO were extracted by core-level XPS based method to confirm band alignment between the gate dielectric and a-IGZO.
Single layer (a-IGZO, gate dielectric) was deposited on the Si wafer to measure the core level binding energies, and then the binding energy difference between the two reference core levels in heterojunction (a-IGZO/gate dielectric) was measured. The value of VBO is obtained by combining these three quantities. The extracted VBOs were 0.38 eV (device A), 0.96 eV (device B) and 1.43 eV (device C). In addition, the CBOs were 4.27 eV (device A), 2.34 eV (device B), and 2.26 eV (device C). After PBIS, the V_{th} shifts in device A, device B, and device C were 0.24 V, 2.1 V, and 2.32 V, respectively. The smaller the CBO, the larger the generated V_{th} shift. And after NBIS, the V_{th} shift was largest for device A at -1.01 V, followed by device B at -2.58 V and device C at -3.82 V. The interfacial characteristics of IGZO and gate dielectric did not change before/after PBIS and NBIS, and only Q_{ot} increased.
We confirmed that the main cause of PBIS and NBIS deterioration is that photoinduced electrons or holes generated are injected into the gate dielectric beyond the CBO or VBO through tunneling. Therefore, if a material having a large CBO and VBO is used as the gate dielectric when fabricating an a-IGZO TFT, the V_{th} shift in PBIS and NBIS can be reduced.

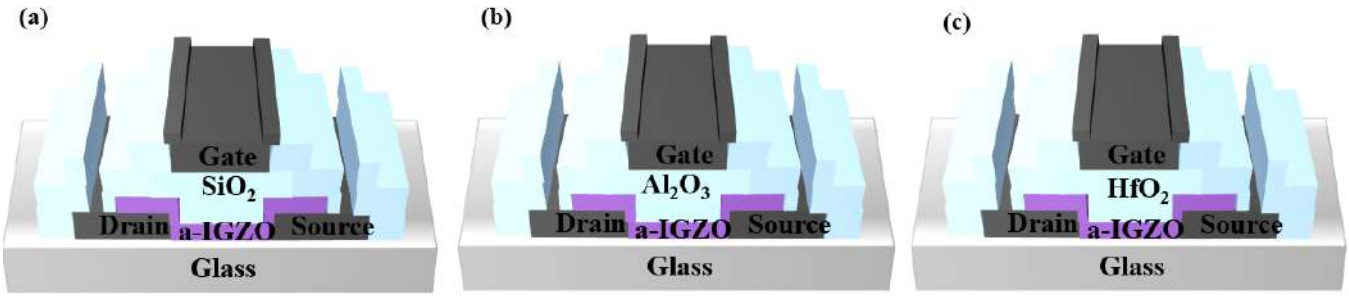

Fig. 1. Schematic cross-sectional view of an a-IGZO TFTs; (a) Device A (GI=SiO_2), (b) device B (GI=Al_2O_3), and (c) device C (GI=HfO_2)

References

1. H. J. Kim K. J. Im, T. Y. Khim, H.C. Hwang, S.K. Kim, S. M. Lee, M. J. Song, P. H. Choi, J. K. Song, and B. D. Choi, *IEEE electron device letter*, 41(5), 737-740. (2020).

Polyimide-Doped Indium-Gallium-Zinc-Oxide Based Flexible Phototransistor for Visible Light Detection

Ki Seok Kim, Min Seong Kim, Jusung Chung, Dongwoo Kim, I Sak Lee and Hyun Jae Kim
School of Electrical and Electronic Engineering, Yonsei University, 50 Yonsei-ro, Seodaemun-gu, Seoul 03722, Republic of Korea
Tel.:82-2-2123-5865, E-mail: hjk3@yonsei.ac.kr

Recently, online meetings are actively taking place, and personal time spent at home is increasing. Accordingly, the era of internet of things is growing, and the sensor technology of various devices is becoming more important. Indium-gallium-zinc-oxide (IGZO), which it could be used in the display industry and studied in various applications such as gas sensors and photo sensors, has advantages such as low off-current and uniformity. In addition, using IGZO as a phototransistor has the advantage of using the manufacturing process of the display industry.[1] However, due to the wide bandgap (>3 eV) [2], it is used for ultraviolet and blue light detection. If visible light can be detected, the scope of application can be widened such as image sensor. Until now, several improved methods for detecting visible light have been studied. One of the most widely used methods is to add absorption layers such as chalcogenides, organics, perovskites, and nanodots. However, the manufacturing process for these methods may become complicated as new manufacturing methods may be required.

In this study, an IGZO phototransistor that detects visible light with a simple manufacturing process is introduced. The IGZO and the polyimide (PI) can be deposited simultaneously in the same process. PI is well known in the display industry as a flexible substrate and can be made into a sputter target, so it can be used in sputter equipment.

Fig. 1a shows a schematic diagram of a phototransistor structure in which IGZO and PI are deposited simultaneously. Fig. 1b shows an actual bending image of a phototransistor on a PI substrate. Fig. 1c and d show the transfer curve of IGZO phototransistor without and with PI under red light, respectively. As can be seen in the figures, IGZO phototransistor with PI clearly shows improved optoelectronic characteristics to the visible light. Specifically, the photoresponsivity was improved from 14.43 to 623.79 A/W, photosensitivity was improved from 2.30×10^{0} to 9.89×10^{6}, and detectivity improved from 8.92×10^{6} to 5.83×10^{11} Jones under red light (i.e., wavelength: 635 nm, intensity: 1 mW/mm^2). Furthermore, as the bending test was conducted 10,000 times, the flexible phototransistors exhibited stable optoelectronic characteristics.

As the phototransistors can be fabricated with an organic material, this manufacturing method will show mechanical flexibility and reliability, which enables its usage in the wearable electronics in the future.

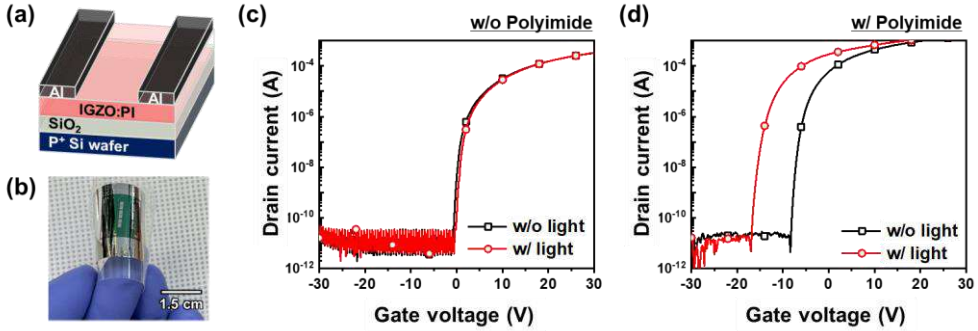

Fig. 1. (a) Schematic diagram of phototransistor. (b) The actual bending image of the phototransistor on the PI substrate. (c) and (d) Transfer curve of IGZO phototransistor without and with PI under red light.

Acknowledgment

This work was supported by the Technology Innovation Program (20010371, development of 4K level flexible display device and panel technology by inkjet pixel printing method) funded by the Ministry of Trade, Industry & Energy (MOTIE, Korea).

References

1. S. E. Ahn, I. Song, S. Jeon, Y. W. Jeon, Y. Kim, C. Kim, B. Ryu, J. H. Lee, A. Nathan, S. Lee, G. T. Kim, and U. I. Chung, *Adv. Mater.*, 24, 2631 (2012).
2. J. Chung, Y. J. Tak, W. G. Kim, B. H. Kang, and H. J. Kim, *ACS Appl. Mater. Interfaces*, 11, 38964 (2019).

Inorganic Sn-rich Perovskite/Metal-Oxide Phototransistors fabricated through Partial UV irradiation for Optoelectronic Applications

Chanho Jo[1], Seojun Lee[2], Dong-Won Kang[2] and Sung Kyu Park[1]
[1]Department of Electrical and Electronics Engineering, Chung-Ang University, Seoul 06974, Korea
E-mail: skpark@cau.ac.kr
[2]School of Energy Systems Engineering, Chung-Ang University, Seoul 06974, Korea

Until now, organic-inorganic halide perovskites have attracted a lot of attention due to their low temperature solution processes and excellent photodetection characteristics for optoelectronics.[1,2] However, the lead halide-based perovskites have been challenged with limited absorption range from ultraviolet (UV) to visible light and the toxicity of lead (Pb) to be obstacle for commercialization.[3] Furthermore, organic composition in perovskites triggers instability to moisture and heat.[4]

Here, we suggest an inorganic tin (Sn)-rich perovskite as a light harvester that allows for a wide range of sensing from the visible to near-infrared light regions and improved device stability. For efficient photo-excited carrier transport, the heterojunction phototransistor was introduced with an amorphous indium-gallium-zinc oxide (a-IGZO) semiconducting channel fabricated by low temperature solution process. However, since the Sn-rich perovskite film has unintended high conductivity due to Sn vacancies, it caused a high off-current and a deterioration in the gate modulation of the devices.[5] To solve this problem, the partial UV irradiation is applied to increase the resistance of perovskites near source and drain, leading to an electrical isolation of unirradiated perovskite region. Based on these, we demonstrated the inorganic perovskite/a-IGZO heterojunction phototransistor with a broaden photoresponse range to near-infrared (860 nm), decent electrical switching characteristics, and improved photosensitivity.

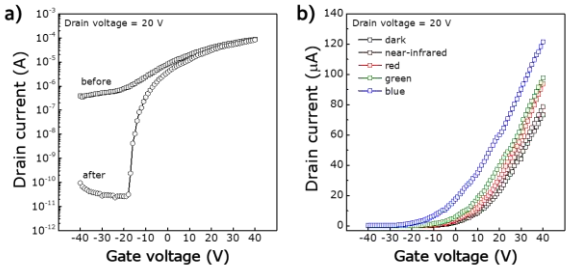

Fig. 1. Transfer curves of (a) the heterogeneous phototransistor before and after UV process and (b) the UV processed heterogeneous phototransistor measured in dark and light conditions.

Acknowledgment

This research was funded and conducted under 「the Competency Development Program for Industry Specialists」 of the Korean Ministry of Trade, Industry and Energy (MOTIE), operated by Korea Institute for Advancement of Technology (KIAT). (No. P0002397, HRD program for Industrial Convergence of Wearable Smart Devices)

References

1. F. Li, C. Ma, H. Wang, W. Hu, W. Yu, A. D. Sheikh, T. Wu, Nat. Commun., 6, 8238 (2015).
2. M. Ahmadi, T. Wu, B. Hu, Adv. Mater., 29, 1605242 (2017).
3. N. K. Noel, S. D. Stranks, A. Abate, C. Wehrenfennig, S. Guarnera, A.-A. Haghighirad, A. Sadhanala, G. E. Eperon, S. K. Pathak, M. B. Johnston, A. Petrozza, L. M. Herz, H. J. Snaith, Energy Environ. Sci., 7, 3061 (2014).
4. M. Grätzel, Nat. Mater., 13, 838 (2014).
5. I. Chung, J.-H. Song, J. Im, J. Androulakis, C. D. Malliakas, H. Li, A. J. Freeman, J. T. Kenney, M. G. Kanatzidis, J. Am. Chem. Soc., 134, 8579 (2012).

Low-voltage operating metal-oxide thin-film transistors with high-k crystalline metal-oxide dielectrics for active-matrix displays

Sang-Joon Park, Jun-Young Jeon and Tae-Jun Ha*
Department of Electronic Materials Engineering, Kwangwoon University, Seoul 01897, Korea
Tel.: 82-2-940-8678, E-mail: taejunha0604@gmail.com

Metal-oxide dielectrics with high dielectric constant (high-k) have been intensively investigated to realize low-voltage operating thin-film transistors (TFTs) for active-matrix devices (AMDs) in terms of low power consumption with equivalent oxide thickness [1]. Recently, solution-process technologies to fabricate sol-gel based metal-oxide dielectric films have been extensively utilized due to their advantageous properties, including practical mass-production, low fabrication cost, and large-area deposition [2]. However, solution-processed metal-oxide dielectrics exhibit the challenging issue of relatively poor film quality compared to the vacuum-processed ones, which can mainly affect the performances of AMDs [3]. For this reason, big efforts to improve the dielectric performance of solution-processed high-k metal-oxide films have been reported by optimizing the crystallinity and metal-oxide bonding. In this presentation, we will demonstrate low-voltage operating metal-oxide TFTs with high-k crystalline metal-oxide dielectrics fabricated by solution-process. The effect of structural characteristic in metal-oxide dielectrics on the device performance will be discussed by analyzing various characterizations. We believe that this study can provide important information about high-k metal-oxide dielectrics toward the low-voltage operating AMD technologies.

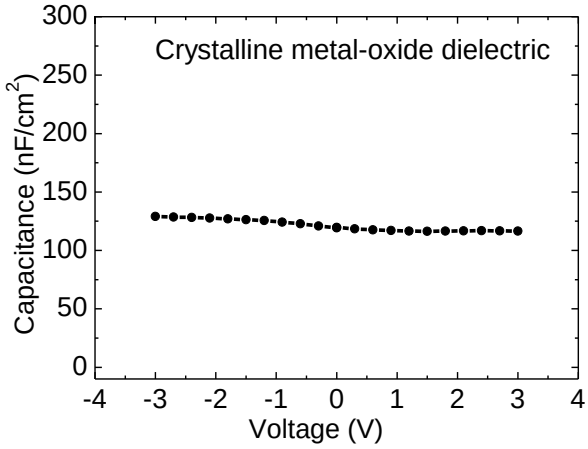

Fig. 1. C-V characteristics of solution-processed high-k crystalline metal-oxide dielectrics for low-voltage operating AMDs

Acknowledgment

This work was supported by the National Research Foundation of Korea (NRF) grant funded by the Korea government (MSIT) (NRF-2021R1A2C2012855)

References

1. M. Salmani-Jelodar, H. Ilatikhameneh, S. Kim, K. Ng, P. Sarangapani and G. Klimeck, *IEEE T. Nanotechnol.*, 15(6), 904-910 (2016).
2. M. H. Boratto, L. V. A. Scalvi, L. V. Goncharova and G. Fanchini, *J. Am. Ceram. Soc.*, 99(12), 4000-4006 (2016).
3. Y. B. Yoo, J. H. Park, K. H. Lee, H. W. Lee, K. M. Song, S. J. Lee and H. K. Baik, *J. Mater. Chem. C*, 1(8), 1651-1658 (2013).

Effect of O_2 Flow Rate on the IGZO thin films properties for transistor performance

Gi-Young Hong[1], Chur-Hyun Shin[1], Jong-Hoon Kim[1] , Ho-Chang Yang[1] , Il-Gu Kim[1] and Seung-Hyun-Lee[1]
[1]Smart Electronics Technology Research Center, Korea Electronics Technology Institute,
Jeonju, Jeollabuk-do 54853, South Korea
Tel.:82-63-219-0049, E-mail: leesh0512@keti.re.kr

An oxide TFT based on IGZO semiconductor has attracted a great deal of attention due to good optical and electrical properties such as a high transmittance, a high electron mobility, a ratio of On-to-Off current and a good uniformity in large-area applications. It is well known that the O_2 flow rate is an important factor in determining the characteristics of TFTs when IGZO thin film is deposited by sputtering process. Therefore, in this study, we evaluated the characteristics of the TFTs according to the O_2 flow rate, and tried to find the optimized experimental conditions.

We have fabricated IGZO TFT backplanes by DC sputtering and PECVD process and the TFT manufacturing process is as follows: (1) Mo gate was patterned by sputtering and photolithography process. (2) Gate dielectric (SiO_2) layer was formed by PECVD and Dry etch process. (3) the IGZO semiconductor was formed by sputtering and photolithography process and then the films were treated Excimer UV for 1hour and thermal treatment for 3hour at 350 ℃, respectively. (4) Mo source/drain electrodes were formed by sputtering and wet process as same the gate electrode.

The IGZO TFTs were evaluated under the conditions of -30V ~ 30V for Vgs and 30V for Vds to investigate the characteristics of three TFTs according to O_2 flow rate of 15sccm, 20sccm and 25sccm. As shown in Fig. 1, the TFT by formed IGZO at the O_2 flow rate of 15sccm had the highest mobility as 20.4 cm^2/Vs.

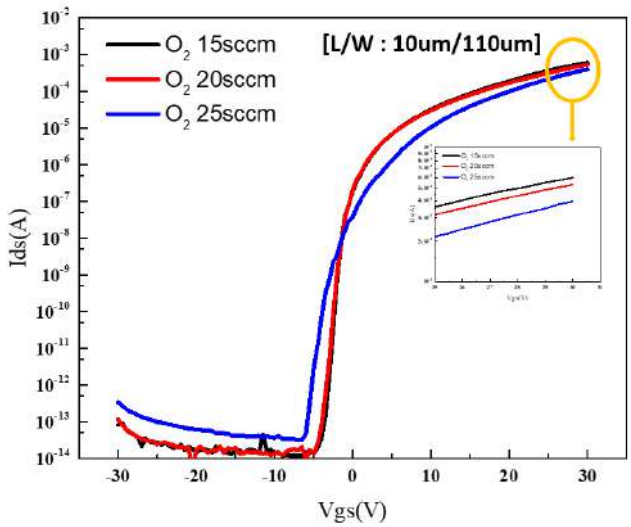

Fig. 1. Transfer characteristics of IGZO TFTs according to O_2 flow rate

Acknowledgment

This work was supported by NRF (National Research Foundation of Korea) Grant funded by the Korean Government. (2019M3F5A1A02092660)

References

1. S. J. Park and T. J. Ha, *Thin Solid Films.*,708 (2020).
2. M. H. Cho, M. J. Kim, H. Seul, P. S. Yun, J. U. Bae, K. S. Park and J. K. Jeong , *J, Inf. Disp. 20* (2019).
3. W. G. Kim, Y. J. Tak and H. J. Kim, *J, Inf. Disp. 19* (2018).

Super Stable Self-Aligned Oxide TFT with High Mobility via Optimizing Oxygen Plasma Time during SiO_2 Deposition by PEALD

Seong-In Cho[1], Jong Beom Ko[1], and Sang-Hee Ko Park[1]
[1]Dept. of Materials Science and Engineering, KAIST, Yuseong-gu, Daejeon 34141, Korea
Tel.:042-350-3316, E-mail: shkp@kaist.ac.kr

Oxide semiconductor based thin-film transistors (TFTs), also known as oxide TFTs are evaluated as great candidates for driving components of the next-generation high-end display. Especially, self-aligned (SA) structured oxide TFTs which can minimize RC delay are getting great attention [1]. Including SA strucutre, most of the novel structures are based on top-gate structures. In case of top-gate, fabricating oxide TFT with proper characteristics can be difficult, due to exposed oxide semiconductor during gate insulator (GI) deposition process [2]. So, each parameter of GI deposition process should be carefully considered.

Here, we found out the effect of oxygen plasma time during one cycle of GI deposition which is one of the variables of plasma enhanced atomic layer deposition (PEALD) process. A simple change of oxygen plasma time during PEALD induced dramatic change in electric properties and stability of oxide TFTs. An optimized oxygen plasma time was found in the top-gate staggered structure, and the SA structured oxide TFT was fabricated by applying it. Manufactured SA oxide TFT showed high mobility over 30 $cm^2/V\cdot s$ and super stable characteristic under positive bias temperature stress (PBTS), as shown in Fig 1.

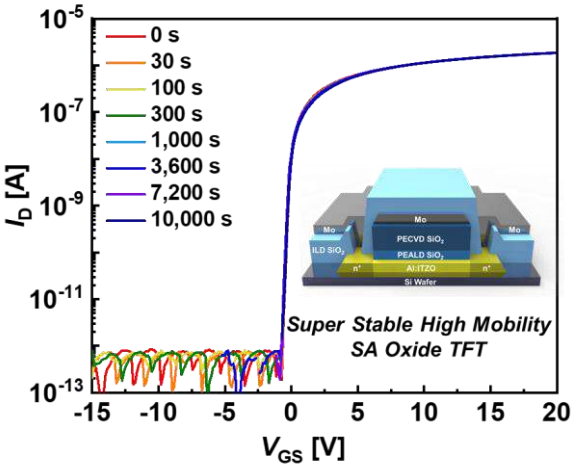

Fig. 1. Transfer curves of fabricated SA oxide TFT under PBTS condition during 10,000 s.

Acknowledgment

This work was supported by Samsung Display Corporation through KAIST Samsung Display Research Center Program.

References

1. W. Jeong, J. Winkler, H. Schmidt, K.-H Lee, S.-H. K. Park, J. Alloys Compd., vol. 859, 5 (2021)
2. J. B. Ko, S.-H. Lee, K. W. Park, S.-H. K. Park, RSC Adv., 9, 36293 (2019)

How to Boost the Ion Mobility in the Enhancement-mode Organic Electrochemical Transistors

Seongmin Heo[1] , Jimin Kwon[1,], Insang You[1] , Mingyu Jung[2], Junghoon Lee[3], Changduk Yang[2,*] and Yong-Young Noh[1,*]*

[1]Department of Chemical Engineering, Pohang University of Science and Technology (POSTECH), 77 Cheongam-Ro, Nam-Gu, Pohang 37673, Republic of Korea.

Tel.:82-54-279-8265, E-mail: nalge@postech.ac.kr yang@unist.ac.kr yynoh@postech.ac.kr

[2]Department of Energy Engineering, School of Energy and Chemical Engineering, Perovtronics Research Center, Low Dimensional Carbon Materials Center, Ulsan National Institute of Science and Technology (UNIST), 50 UNIST-gil, Ulju-gun, Ulsan 44919, Republic of Korea.

[3]Division of Chemical Engineering, Dongseo University, 47, Jurye-ro, Sasang-gu, Busan, Republic of Korea.

The Organic electrochemical transistors (OECTs) have been received a lot of attentions in bioelectronic devices. Poly(3,4-ethylenedioxythiophene) and poly(styrene sulfonate) (PEDOT:PSS) is the most typical material in OECTs due to its high transconductance and processability. One of the its main drawbacks is that operates in depletion-mode which is normally on state, so it is inefficient in terms of power consumption and can induce device degradation. Therefore, there are various approach to develop enhancement-mode OECT. However, the limitation of those approach is that ions can not easily penetrate because of poor ion mobility of general conjugated polymer. we have utilized fluorinated benzothiadiazole (BT) groups polymer to demonstrate enhancement-mode OECTs with intrinsic semiconductors by using printing process. We uncover the mechanism that cause the difference in volumetric capacitance due to fluorinated functional group. Then, we investigate how to enhance the ion mobility in the organic semiconductor films.

Air-Stable Ambipolarity of Organic Semiconductors in Embedded Nanofibril Structure for Complementary-like Electronic Circuits

Byeong-Chan Park[1], Young-Jae Lee[1] and Kang-Jun Baeg[1]
[1]**Dept. of Smart Green Technology Engineering, Pukyong National University, Nam-gu, Busan 48513, Korea**
Tel.:82-51-629-6397, E-mail: kangjun100@pknu.ac.kr

For organic microprocessors based on the complementary metal-oxide-semiconductor (CMOS) architecture, integrated circuits (ICs) have to be constructed by combining the equivalently high-performance p-type and n-type organic field-effect transistors (OFETs). Although the CMOS circuits are ideal configuration in terms of high noise margins and negligible power consumption at the static states, CMOS-like circuitry using the ambipolar organic semiconductors are attractive to fabricate the low-cost electronic applications by removing the additional fabrication step. Thus, simply blanket coated layer can operate both p- and n-channel regimes of the same transistors without the development of different types of organic semiconductors as well as without the sophisticated patterning process.

Herein we report air-stable ambipolar OFETs based on the nanofibril composite polymer semiconductors. As a representative donor-acceptor copolymer semiconductor, PDBT-co-TT was blended with an elastomer and introduced the spinodal decomposition to optimize the morphological feature of active layers. At the optimized blending ratio, we can obtain well-balanced and high mobility p-type and n-type characteristics of PDBT-co-TT OFETs. The anisotropic one-dimensional nanofibril structure is enabled by direction printing methods to induce the arrangement of polymer chains in the parallel direction to the semiconductor channel. Moreover, the embedded nanofibril polymer semiconductor exhibited significantly improved air-stability, especially for the n-channel region owing to the encapsulation effect by the surrounded polymer matrix. Moreover, the n-type properties showed excellent air-stability compared to reference devices without nanofibril structures. It is expected that the nanofibril polymeric active layers can be widely used for building blocks of complementary-like electronic circuits for applications in stretchable opto-/electronics.

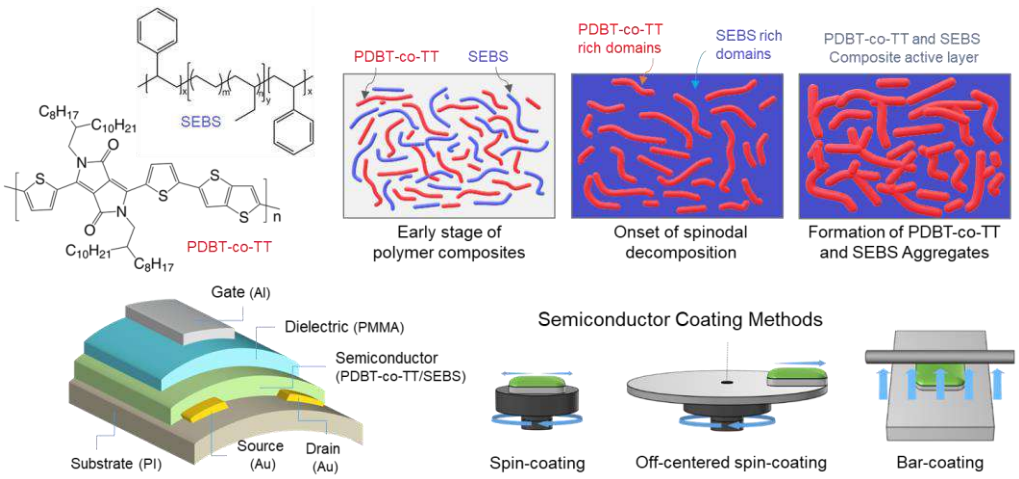

Fig. 1. OFET device configuration and molecular structures of ambipolar polymer semiconductor and elastomer, which induced spinodal decomposition for achieving nanofibrillar composite semiconductor.

Acknowledgment

This study was supported by grants from the National Research Foundation of Korea (NRF) funded by the Korean government (No. 2020R1F1A1071718 and No. 2020R1A4A1019463).

References

1. Kang-Jun Baeg, Mario Caironi, Yong-Young Noh, *Adv. Mater.*, 25(31), 4210-4244 (2013).

Low-voltage operation of solid-state electrolyte gate insulator CNT transistors with high transconductance

Haksoon Jung[a#], Jimin Kwon [a#,] Seongmin Heo[a#] and Yong-Young Noh[a*]
[a] Department of Chemical Engineering, Pohang University of Science and Technology (POSTECH), 77 Cheongam-Ro, Nam-Gu, Pohang 37673, Republic of Korea.
Corresponding author. Email: yynoh@postech.ac.kr

Keywords: single-walled carbon nanotubes, field-effect transistor, solid-state electrolyte gate insulator

Semiconducting single-walled carbon nanotubes (SWNTs) are promising for active material in modern thin film transistors(TFTs) for their intrinsically superior carrier transport characteristic, low operating voltage and processability. Though these clear advantages, TFTs with SWNTs suffer from high off-state current due to strong ambipolarity by small band-gap. Thus, controlling electrostatics of charge carrier in active channel is one of the most important issues these days.

Here, we report successfully fabricated CNTs transistors with solid-state gate insulator with high normalized transconductance over 0.1mS at 0.5V of drain voltage. Their active channel is modulated not by dipole of molecular-scale dipole but atomic-scale EDL which has much higher capacitance. Details of electrical properties of sorted large-diameter semiconducting SWNTs and characteristics of FETs will be discussed in our presentation.

[References]

(1) CHEN, Zhihong, et al. The role of metal− nanotube contact in the performance of carbon nanotube field-effect transistors. Nano letters, **2005**, 5.7: 1497-1502.

Effect of Thermally Induced Phase Transition on the Carrier-Transport of $CH_3NH_3PbI_3$ Thin Film Transistor

Farjana Haque, and Mallory Mativenga
Dept. of Information Display, Kyung Hee University, Seoul, 02447, Republic of Korea
Tel.:82-2-961-9642, E-mail: mallory@khu.ac.kr

The hybrid perovskites are promising candidates for solution processed devices.[1,2] Despite being emerging materials for the display technology, the well-known problem of hysteresis in perovskite-based devices is hindering their progress.[3] Here we comprehensively investigate the temperature-dependent carrier transport and phase transition properties in $MAPbI_3$ to understand the mechanisms leading to hysteresis in halide perovskite-based devices. We show that the hysteresis window is large at low temperature and decreases with increasing temperature. Such distinct behaviors are related to the polarization effect at low temperature in contrast to trapping and ion migration at higher temperatures.[3,4] These findings provide fundamental insight into the key electrical properties of halide perovskites and guidelines for advancing their application in a wider temperature range.

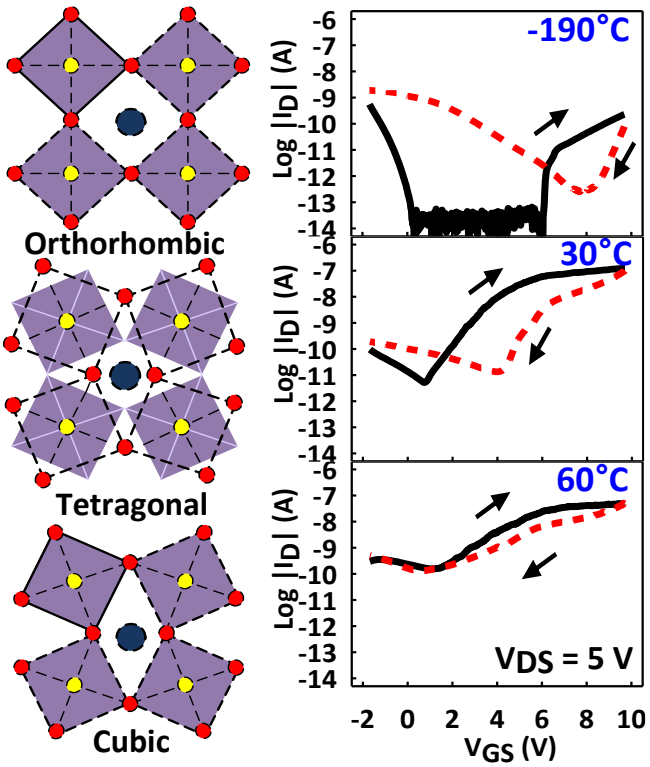

Fig. 1. Schematic crystal structures of $MAPbI_3$ in the orthorhombic, tetragonal, and cubic phases and the corresponding transfer characteristics.

Acknowledgment

We acknowledge the final support from the National Research Foundation of South Korea (NRF) through the Korean Government (Ministry of Science, ICP and Future Planning) under grant NRF-2019R1F1A1059601.

References

1. X. Y. Chin, D. Cortecchia, J. Yin, A. Bruno, C. Soci, Nat. Commun., 6, 7383 (2015).
2. S. D. Stranks, H. J. Snaith, *Nat. Nanotechnol.*, 10, 391 (2015).
3. F. Haque, N. T. T. Hoang, J. Ji, M. Mativenga, *IEEE Electron Device Lett.*, 40 (11), 1756 (2019).
4. C. Wehrenfennig, M. Liu, H. J. Snaith, M. B. Johnston, L. M. Herz, *APL Mater.*, 2 (8), 081513 (2014).

Real-time healthcare monitoring platform with solution based high-sensitivity metal oxide electrochemical transistors

Joon Hui Park, You Seung Rim*
[1]School of Intelligent Mechatronics Engineering, Sejong University
209 Neungdong-ro, Gwangjin-gu, Seoul 05006, Republic of Korea
**Corresponding E-mail: youseung@sejong.ac.kr*

Recently, the necessity of real-time and non-invasive detection-based biosensors has been increasing by using electrical device platforms. Metal oxide semiconductors-based electrochemical transistors (MOECTs) have been attracting attentions in biosensor applications due to their high sensitivity, selectivity, and strong chemical resistance for biomolecule detections under physiological environment. Therefore, research that can be directly connected to a real-time monitoring platform was required along with the fabrication of the high-sensitive biosensor.

So we developed an In_2O_3 channel layer-based FET biosensor based on solution process. In this study, we examined the effect of surface passivation effects of In2O3-based ECTs by doping Ga. As gallium contents increased (0-5%), the oxygen deficient of IGO films was gradually reduced and the sensitivity of the device was improved. Experiments were conducted within different pH buffer solutions to confirm changes in electrical characteristics of devices in the pH environment, resulting in high stability in a wide range of pH environments and linear characteristics for each pH value.

Electrical signals received from the biosensor was converted and connected to signals readable by the MCU board. Finally, the self-monitoring system was visualized with self-programmed software programs based on signals transmitted from MCU board. As a result, we established a total solution platform that enables real-time monitoring based on high sensitive and stable biosensor.

Acknowledgment

This work has supported by the National Research Foundation of Korea(NRF) grant funded by the Korea government(MSIT)(2020R1A2C1013693) and Korea Institute for Advancement of Technology(KIAT) grant funded by the Korea Government(MOTIE)(P0012451, The Competency Development Program for Industry Specialist)

References

1. High-Performance Amorphous Indium Oxide Thin-Film Transistors Fabricated by an Aqueous Solution Process at Low Temperature, Kook hyun Choi, Min seok Kim, JJAP
2. Hexaaqua Metal Complexes for Low-Temperature Formation of Fully Metal Oxide Thin-Film Transistors", You Seung Rim, Huajun Chen, Yang Yang, Chemistry of Materials

Carbon chain length and annealing temperature dependency of Self-Assembled Monolayer-doped IGZO Thin-Film Transistors

*Juhyung Seo, Hocheon Yoo**
Dept. of Electronic Engineering, Gachon University, Seongnam 13120, Republic of Korea
Tel.:82-31-750-5802, E-mail: hyoo@gachon.ac.kr

Owing to excellent properties high carrier mobility[1] and easy-to-fabricate processes in oxide thin-film transistors (TFTs), they have received a lot of attention. However, an efficient doping technique that can control the electrical characteristics of the oxide TFTs is needed to implement practical electronic applications. In this context, the effects of silane-based self-assembled monolayers (SAMs) doping on IGZO TFTs are investigated in depth in this paper. Instead of a complicated doping method, the charge transport characteristics of the indium–gallium–zinc oxide (IGZO) TFTs can be improved by simply anchoring the silane-based SAMs on it[2]. Furthermore, differences in doping effect depending on SAMs' carbon chain length and annealing temperature were also investigated; the results provide a systemic guideline for efficient doping technique in IGZO TFTs[3].

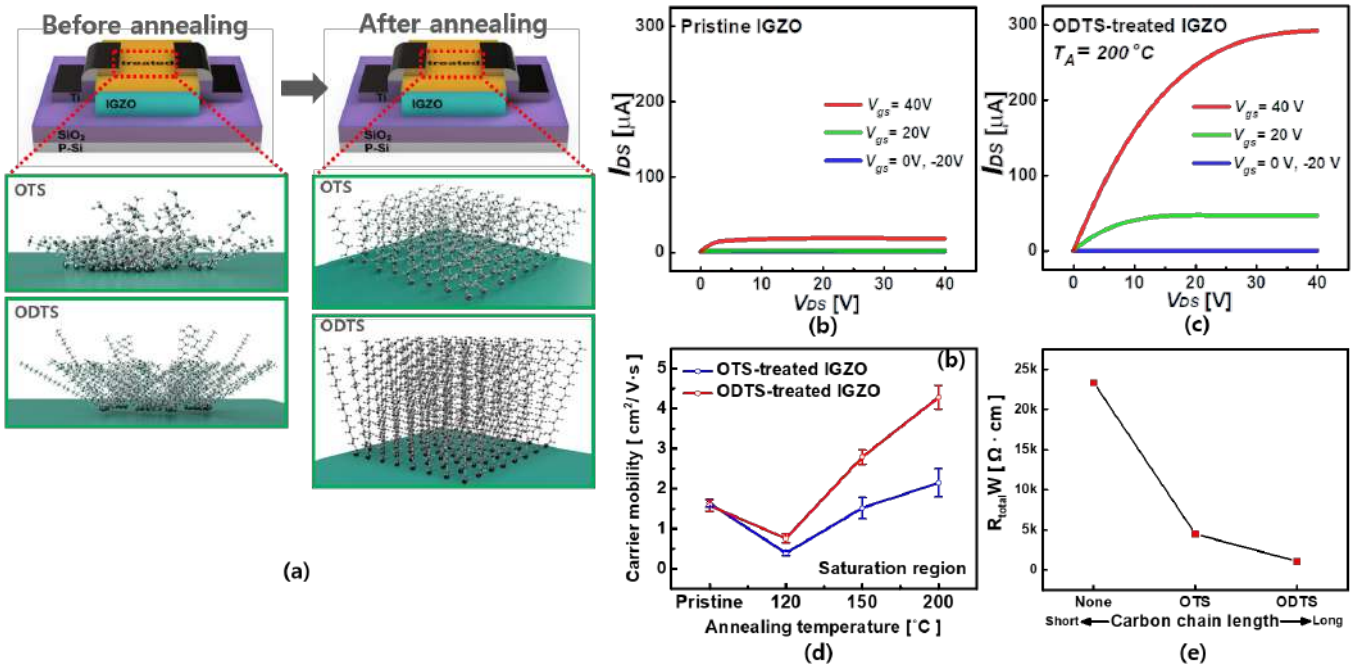

Fig. 1. (a) Heat treatment (annealing) causes structural modifications in the carbon chain; configurations are aligned during heat treatment. Pristine output curve (b) and ODTS-treated IGZO (c). (d) effective carrier mobility of SAMs treated transistors. (e) The connection between carbon chain length and contact resistance.

Acknowledgment

This research was supported by a National Research Foundation of Korea (NRF) grant funded by the Korean Government (MSIT) (NRF-2020R1A2C1101647). This work was supported in part by the Gachon University research fund of 2020 (GCU-2019-0764).

References

1. Yabuta, H.; Sano, M.; Abe, K.; Aiba, T.; Den, T.; Kumomi, H.; Nomura, K.; Kamiya, T.; Hosono, H. High-mobility thin-film transistor with amorphous In Ga Zn O 4 channel fabricated by room temperature rf-magnetron sputtering. Appl. Phys. Lett. 2006, 89, 112123.
2. Cai, W.; Wilson, J.; Zhang, J.; Brownless, J.; Zhang, X.; Majewski, L.A.; Song, A. Significant performance enhancement of very thin InGaZnO thin-film transistors by a self-assembled monolayer treatment. ACS Applied Electronic Materials 2020, 2, 301-308.
3. Seo, J.; Yoo, H. Remote Doping Effects of Indium–Gallium–Zinc Oxide Thin-Film Transistors by Silane-Based Self-Assembled Monolayers. Micromachines 2021, 12, 481.

Organic-Inorganic Hybrid Gate Dielectrics Synthesized using Plasma Polymerization for Flexible Electronics

*Gwan In Kim, Dong Hyun Choi, Min Seong Kim, Won Kyung Min, Jin Hyeok Lee, and Hyun Jae Kim**
School of Electrical and Electronic Engineering, Yonsei University, Korea
Tel.:82-2-2123-5865, E-mail: hjk3@yonsei.ac.kr

Flexible electronics have attracted tremendous interest in a variety of applications such as wearable electronics, health care and smart sensors, since they can be bent, twisted and conform to complicated non-planar surfaces. To achieve high performance flexible electronics, such as switching and memory devices, gate dielectrics should have flexible and remarkable dielectric properties with low leakage current. Accordingly, organic-inorganic hybrid dielectrics have recently been proposed to realize these properties, where the organic components provides outstanding mechanical flexibility and the inorganic component contributes satisfactory insulating and dielectric properties. Recently, many researches have been investigated on solution-based hybrid dielectrics. However, solution-based process suffered from contaminant issues, which made it difficult to form pure, uniform and dense hybrid dielectrics.

To overcome the limitations of solution process, a facile fabrication of organic-inorganic hybrid gate dielectric is introduced using plasma polymerization of poly-tetrafluoroethylene (PTFE). PTFE is a synthetic fluoropolymer of tetrafluoroethylene (C_2F_4) which is known as a hydrophobic and flexible polymer.[1] By utilizing plasma polymerization of PTFE, we fabricated HfO_x:PTFE dielectric film using radio frequency magnetron co-sputtering, thus implementing the flexibility of PTFE into hafnia based gate dielectric. The schematic diagram of the HfO_x:PTFE gate dielectric TFTs is shown in **Figure 1a** with the chemical structure of PTFE. **Figure 1b and 1c** shows leakage current density-electric field (J-E) curves of HfO_x:PTFE dielectric film and transfer characteristics of HfO_x:PTFE gate dielectric TFTs, respectively. As a result, the HfO_x:PTFE (100W:30W) hybrid film fabricated via plasma polymerization has dielectric characteristics: a breakdown electric field of 7.02 MV/cm, a leakage current density of ~10^{-7} A/cm^2, and a dielectric constant of 16.82. Furthermore, the HfO_x:PTFE (100W:30W) hybrid film was implemented as a gate dielectric for flexible TFTs with indium-gallium-zinc oxide (IGZO) as a channel layer. As a result, HfO_x:PTFE (100W:30W) gate dielectric TFT exhibits the field-effect mobility of 5.34 cm^2 V^{-1} s^{-1}, an on/off current ratio of 3.27 × 10^9, and a subthreshold swing of 0.53 V dec^{-1}. We believe that the results will open up a new area for the flexible dielectrics to satisfy future needs of flexible electronics.

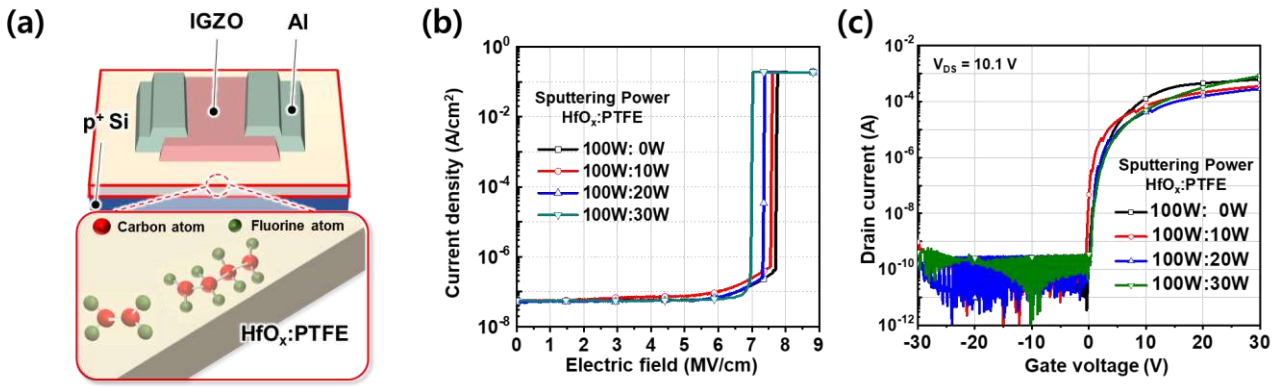

Figure 1. (a) Schematic diagram of the HfO_x:PTFE gate dielectric TFT, (b) Leakage current density-electric field (J-E) curves of HfO_x:PTFE dielectric film, (c) Transfer characteristics of HfO_x:PTFE gate dielectric TFTs.

Acknowledgment

This work was supported by the National Research Foundation of Korea (NRF) Grant funded by the Korea Government (MSIT) (no. 2020M3H4A1A02084896).

References

1. J. W. Na, H. J. Kim, S. H. Hong, H. J. Kim, *ACS Applied Materials & Interfaces* 10, 37208 (2018).

Crystallization of SiN Capped InSb Films on Glass by Rapid Thermal Annealing

Otokichi Shimoda[1], Yuki Sawama[1], C. J. Koswaththage[1], Takashi Noguchi[1], Takashi Kajiwara[2], Taizoh Sadoh[2], and Tatsuya Okada[1]
[1]Faculty of Engineering, University of the Ryukyus, 1 Senbaru Nishihara Okinawa, Japan
Tel.:+81-98-895-8674, E-mail: k208534@eve.u-ryukyu.ac.jp, tokada@tec.u-ryukyu.ac.jp
[2]Department of Electronics, Kyushu University, 744 Motooka, Fukuoka, Japan

InSb is a semiconductor material which has very high mobility, and it is widely used as hall sensors. In our previous work, we have reported that hall mobility of InSb films deposited by RF sputtering was increased by Rapid Thermal Annealing (RTA), and SiO_2 capping film on the InSb film played an important role in the increase of Hall mobility [1-3]. In this work, we evaluated effects of SiN capping on InSb films against RTA.

300 nm-thick InSb thin films were deposited on the glass by RF sputtering, followed by 50 nm-thick SiN film deposited by reactive sputtering using N_2 gas and Si target. After that, RTA was performed at 500°C in N_2 ambient, and Hall mobility was evaluated using van der Pauw method.

Fig. 1 shows Hall mobility after RTA. The conduction type was n-type. At the condition of 500°C for 60 s, the samples with SiN capping had higher mobility than that with SiO_2 capping. It seems that gas barrier effect of SiN capping films was effective to RTA InSb compared to SiO_2 capping films. By increasing a duration of RTA to 60 s, Hall mobility of InSb with SiN capping was increased, and 2020 cm^2/Vs was obtained. As capping films on InSb, not only SiO_2 but also SiN films had a potential to increase Hall mobility using RTA.

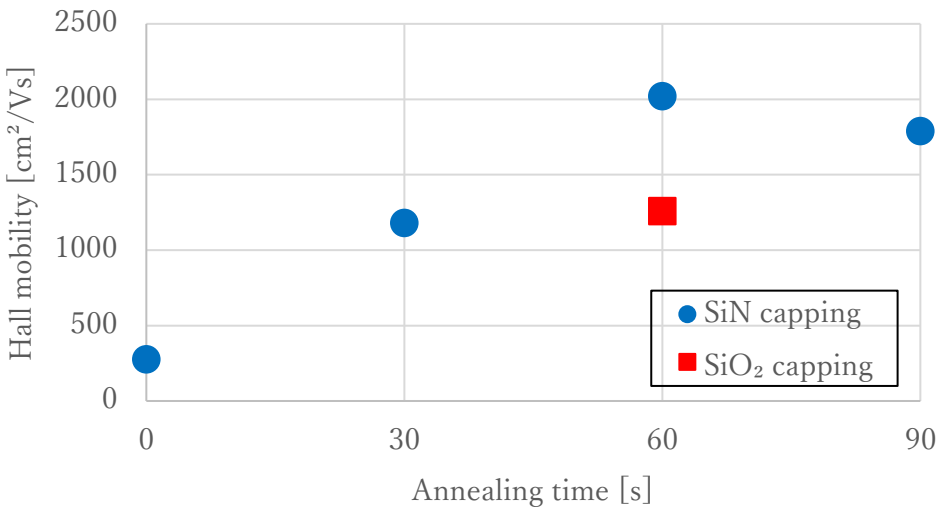

Fig. 1. Effect of annealing time on mobility

Acknowledgment

This research is supported by Adaptable and Seamless Technology transfer Program through Target-driven R&D (A-STEP) from Japan Science and Technology Agency (JST) Grant Number JPMJTM20GV.

References

1. C. J. Koswaththage, T. Okada, T. Noguchi, S. Taniguchi, and S. Yoshitome, AIP Advances, Volume 6, Issue 11 (2016) 115303.
2. G. Sakamoto, A. Shimabukuro, T. Noguchi, and T. Okada, Jpn. Soc. Appl. Phys. Spring Meeting (Mar. 2021), [18p-Z24-8]. (in Japanese)
3. T. Kajiwara, O. Shimoda, T. Okada, C. J. Koswaththage, T. Noguchi, and T. Sadoh, Jpn. Soc. Appl. Phys. Fall Meeting (Sep. 2021) to be presented. (in Japanese)

Measuring Channel Potential in Solution-processed, Dual-Gate Amorphous InGaZnO Thin-Film Transistors Using Gated Multiprobe Method

Soyoung Choi and Jaewook Jeong*

School of Information and Communication Engineering, Chungbuk National University,

Cheongju, Chungbuk 28644, Korea

*Tel.:82-43-261-3598, *E-mail: jjeong@cbnu.ac.kr*

Understanding channel potential distribution along to source/drain electrodes is important to characterize electrical paramters of the active region such as parasitic resistance, channel electron distribution, and defect density of states for amorphous-based thin-film transistors (TFTs)[1]. There are various methods for measuring the channel potential distribution in the active region. In example, scaning kelvin probe microscopy (SKPM) and gated four-probe and multiprobe methods (GFP and GMP methods) have been used for accurate characterization of the channel potential[2-4]. In this paper, solution-processed, dual-gate amorphous indium-gallium-zinc-oxide thin-film transistors (a-IGZO TFTs) with bottom and top gate insulators of silicon oxide and PMMA, respectively, were fabricated implementing multiple probe patterns in the active region shown in Fig. 1 and their channel potential distributions were analyzed applying top, bottom, and dual gate biasing by using GMP methods. It was found that the channel potential distribution was dominantly dependent on the quality of PMMA top gate insulator and the dual-gate a-IGZO TFTs shows conventional linear increase of channel potential from source to drain electrodes when the process condition of top gate insulator (PMMA) is optimized. From the channel potential distribution, the parasitic resistance, intrinsic field-effect mobility, and threshold voltage values were extracted and compared for each operation mode of top, bottom, and dual gate biasing conditions.

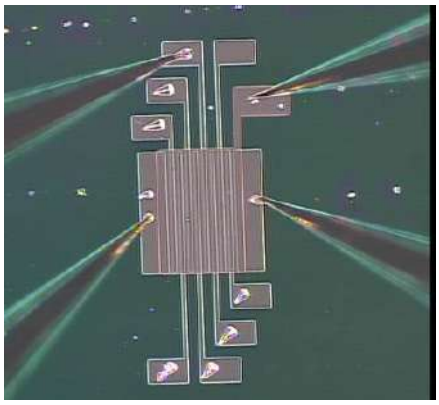

Fig. 1. Top view of dual-gate a-IGZO TFTs implementing gated multiprobe patterns

Acknowledgment

This work was supported by the National Research Foundation of Korea funded by the Korean Government under Grant NRF-2021R1A2C1013759

References

1. C.-S. Chiang, C.-Y. Chen, J. Kanicki and K. Takechi, Appl. Phys. Lett. 72(22), p. 2874 (1998).
2. G. Koley and M. G. Spencer, J. Appl. Phys. 90(1), p. 337 (2001).
3. M. Mativenga, S. An, S. Lee, J. Um, D. Geng, R. K. Mruthyunjaya, G. N. Heiler, T. J. Tredwell, and J. Jang, IEEE Trans. Electron Devices, 61(6), p. 2106 (2014).
4. J. Jeong, J. Kim, and S. M. Jeong, IEEE Trans. Electron Devices, 61(11), p. 3757 (2014).

Extension of a 10 mm long {100}-Oriented Grain Boundary Free Silicon Domain Crystallized by Continuous Wave Green Laser.

Muhammad Arif[1], Nobuo Sasaki[1,2,3], Satoshi Takayama[1] and Yukiharu Uraoka[1]
[1]Nara Inst. of Sci. and Tech. 8916-5 Takayama-cho, Ikoma, Nara, 630-0192, Japan
Tel.: +81-7-4372-6064, E-mail: sassasaki@yahoo.co.jp
[2]Sasaki Consulting, 3-16-4-2007 Nakasaiwaicho, Saiwaiku, Kawasaki 212-0012, Japan

The research on polycrystalline silicon (poly-Si) thin film transistors (TFTs) for display applications are actively progressing amidst the mass production in the industry; owing to the use of fast processing time and high throughput excimer laser annealing (ELA) for the crystallization of a-Si film precursor. However, furher improvement in the fabrication are necessary especially for large area displays to overcome the point-to-point TFT performance uniformity. This uniformity issue emerged from the random crystallization of poly-Si which induce the formation of grain boundaries (GBs) and mixed crystal orientations. The use of continuous wave (CW) lasers are prominent in controlling the growth of lateral poly-Si domains during the crystallization.[1]

In this experiment, a CW beam (532 nm) sourced from Nd :YVO_4 diode pumped solid state (DPSS) laser was used for the crystallization of 60 nm a-Si film on quartz substrate. A rectangular beam having a flat-top profile in the long axis and Gaussian profile in the short axis scanned on the capped (85 – 130 nm SiO_2) a-Si film with varying laser power at laser scan speed of 12 – 15 mm/s.

Fig. 1 shows the grain boundaries with rotation angle 15°-65°. {100}-oriented growh also confirmed by Inverse pole figure (IPF) mapping from EBSD in surface normal, rolling (laser scan direction), and transverse directions at the same region. A clear region without any GBs extended to more than 10 mm long is clearly seen which indicates that a stable growth of silicon film was achieved during the crystallization by CW laser.

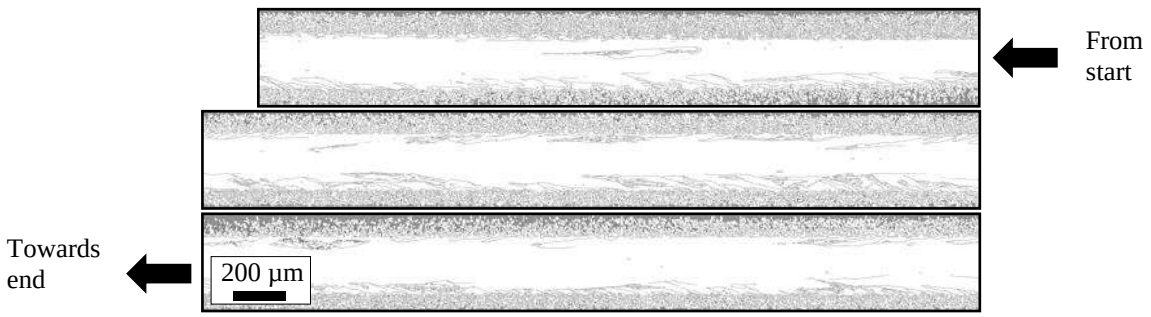

Fig. 1. Grain misorientation angle within 15°-65° for silicon film crystallized at 3.55 W under 92 nm C/L.

The solidification process is assumed to complete by trailing a sinusoidally perturbed solid/liquid interface which usually induced whenever growth conditions produced an adjacent layer of constitutionally supercooled liquid.[2] This was evidenced by the formation of columnar structure on the surface of the crytallized silicon film where the direction of the columnar structure directly represent the.silicon domain's growth direction. Deviation from an optimum parameters for long columnar structure will cause a chaotic structure on the surfae which again indicates the nonunidirectional in-plane growth of the silicon domain.[3]

The formation the long, GB-free silicon domain is expected to enhance the performance of TFTs and eliminate the uniformity issue.

References

1. M. Arif, N. Sasaki, Y. Ishikawa, and Y. Uraoka, *Thin Solid Films* 708, 138127 (2020).
2. W. W. Mullins, and R. F. Sekerka, *Journal of Applied Physics* 35, 444 (1964).
3. C. Grigoropoulos, M. Rogers, S. H. Ko, A. A. Golovin, and B. J. Matkowsky, *Phys. Rev. B* 73, 184125 (2006).

Optimization of the OLED Charging Delay for Improving Low Gray Scale Picture Quality in the AMOLED Displays

Se-Hwan Na[1,2], Won-Kyung Min[1], Do-Hyung Kim[2], Han-Wook Hwang[2], Hyun-Chul Choi[2], and Hyun-Jae Kim[1]*
[1]School of Electrical and Electronic Engineering, Yonsei University, 50 Yonsei-ro, Seodaemun-gu, Seoul 03722, Republic of Korea
[2]LG Display Co., Ltd. 245, Wollong-myon, Paju-si, Gyeonggi-do 10845, Republic of Korea
Tel.:82-2-2123-5865, E-mail: hjk3@yonsei.ac.kr

According to improvements of camera performance in smart devices with AMOLED display panel, display panel has required the performance for expression of low gray scale more precisely. However, the enhancement of corresponding performance by optimization of pixel compensation circuits or process was limited. Therefore, the fundamental cause analysis and study for improvement have been required.

For light emission of low gray scale, a low amount of current is needed. Furthermore, turning on the OLED requires charging to the parasitic capacitance of the OLED. As a result, charge delay is caused by a small amount of current. In case of low gray scale, the current is extremely low, and the anode voltage did not reach to saturation voltage. So, charging delay difference in the panel induced the deterioration display quality such as luminance uniformity in low gray scale.

To reduce the charging delay, the electrical potential applied to both the anode and cathode of the OLED should be minimized [1]. However, modifying the electric potential induced the constraints to performance enhancement of the pixel compensation circuits. Consequently, the study on the additional method for minimizing the charging delay was needed.

Figure 1 shows the effect of improving the charging delay when reducing C_{OLED}. The method of reducing the C_{OLED} can be acquired through reduced aperture ratio of OLED, increased OLED thickness, and reduced the permittivity of organic layers between the anode and cathode. Therefore, it is possible to improve the charging delay and the picture quality enhancement on low gray scale was achieved.

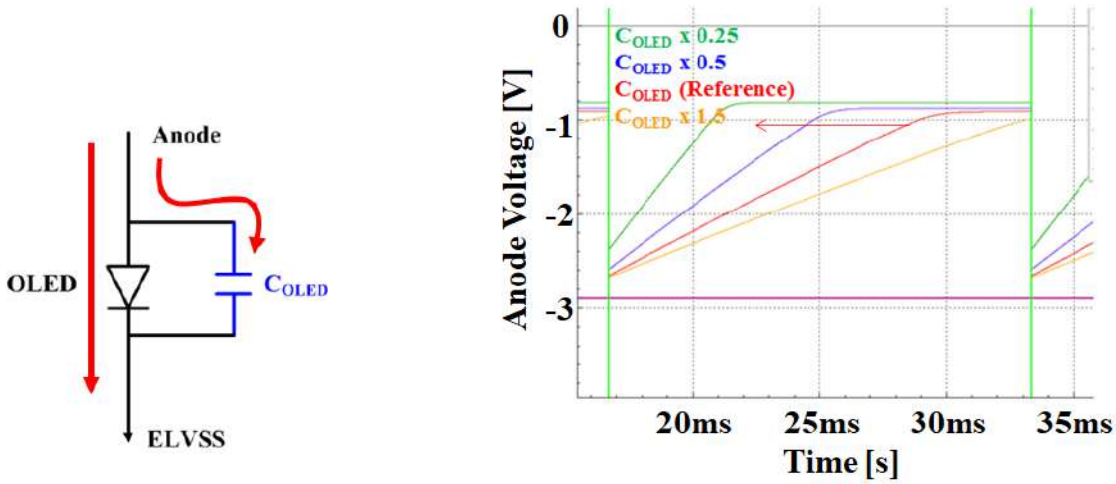

(a) (b)

Fig.1. (a) Modelling for charging delay simulation and (b) simulation result by changing C_{OLED}.

Acknowledgment

This research was supported by LG Display and the National Research Foundation of Korea (NRF) Grant funded by the Korea Government (MSIT). (no. 2020M3H4A1A02084896).

References

1. H. J. Kim and S. H. Na, "Enhancement of picture quality on ultra-low brightness by optimizing the electrical potential required for OLED charging in the AMOLED displays." *Journal of Information Display* (2021): 1-10.

Solution-Processed Calcium Titanate Perovskite Film and Its Thickness-Dependent Hysteresis Behaviors

Subin Lee[1] and Hocheon Yoo[1]
[1]Dept. of Electronic Engineering, Gachon University, Seongnam, Korea
Tel.:82-31-750-8802, E-mail: bini0211@gachon.ac.kr

Perovskite, which is used in electronic devices, is often used with efficient hybrid lead-halide perovskites[1]. However, these lead-based perovskites have unstable chemical structure and are vulnerable to ambients such as moisture and oxygen. It is also very harmful to the human body[2]. To solve this problem, it was processed in electronic devices by synthesizing lead-free halide perovskite, which has orthorhombic crystal structure. Here, we present a solution processed calcium titanate perovskite and its applications to memristive switching devices. Low-voltage switching behaviors of a few hundred millivolts level are observed in a metal-calcium titanate-metal structure.

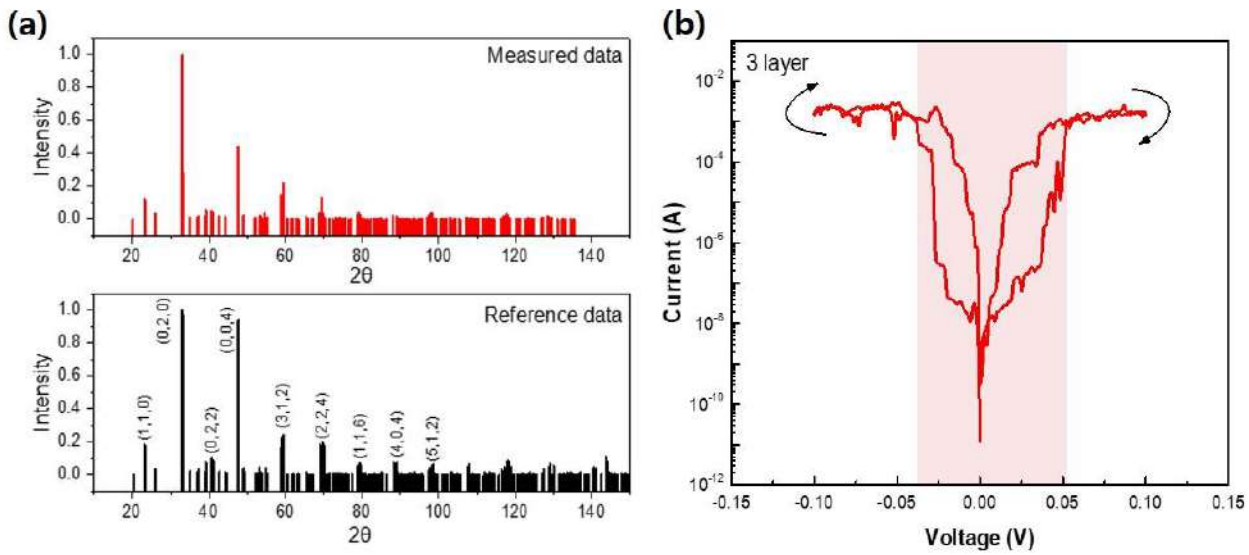

Fig. 1. (a) Measured XRD data of the $CaTiO_3$ perovskite film with reference data (ICSD). (b) Electrical hysteresis behavior of the $CaTiO_3$ perovskite film

Acknowledgment

This work was supported by a National Research Foundation of Korea (NRF) grant funded by the Korean government (MSIT) (NRF-2020R1A2C1101647).

References

1. Jeong, J., Kim, M., Seo, J. *et al. Nature* **592,** 381–385 (2021)
2. Li, J., Cao, HL., Jiao, WB. *et al. Nat Commun* **11,** 310 (2020)

Negative differential resistance performance in 0D/3D mixed dimensional heterostructure using ZnO quantum dots

Somi Kim [1], Taehyun Park [1,2], and Hocheon Yoo [1]
[1] Department of Electronic Engineering, Gachon University, Korea
[2] Department of Chemical & Biological Engineering, Gachon University, Korea
Tel.:8210-9243-6279, E-mail: soomee123@gachon.ac.kr

Due to unusual properties of negative differential resistance (NDR) which the current does not monolithically increase as a function of the applied voltage bias, NDR switching device is receiving considerable attentions in the development of next generation[1]. These NDR devices have been applied to various devices such as tunneling diodes, Gunn diode oscillators, and reflection amplifiers. Also, NDR devices that respond to external stimuli are presented[2,3]. However, in the manufacturing process of the existing NDR device, issues still remain, such as complex manufacturing process, operation stability and NDR characteristics only when irradiating light of a specific wavelength[4,5]. Herein, we present 0D/3D heterostructure NDR devices with low process temperature and high performance using solution process which is 0D QDs ZnO. We synthesized ZnO QDs and finely controlled the bandgap. As a result, we present a high-performance NDR device with a PVCR= 4.13, and NDR characteristics come out without irradiating light.

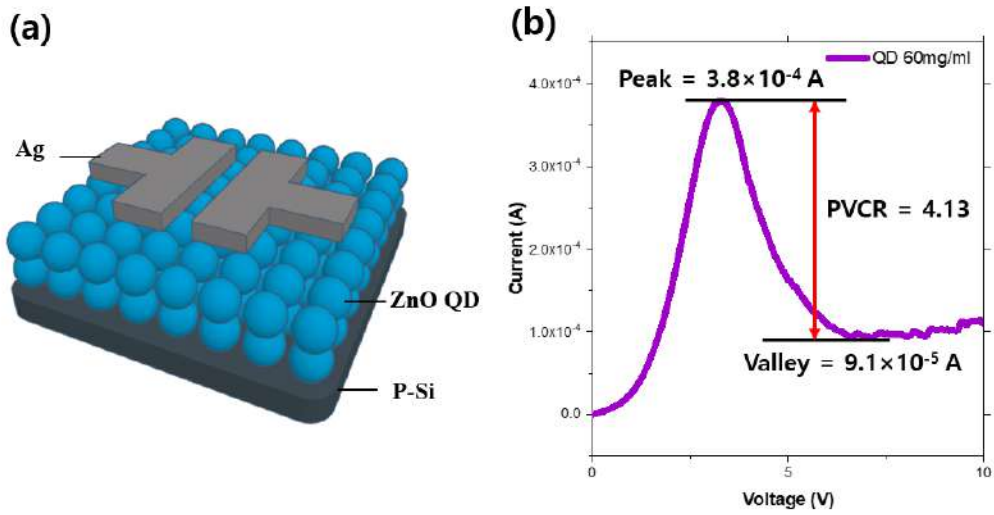

Fig. 1. (a) Structure of ZnO quantum dots heterostructure diodes. (b) NDR performance with a peak-to-valley current ratio = 4.13

Acknowledgment
This work was supported by the National Research Foundation of Korea (NRF) grant funded by the Korea government (MSIT) (No.NRF-2020M3A9E4104385 and 2020R1A2C1101647)

References

1. Gan, K.-J., Tsai, C.-S., Chen, Y.-W., & Yeh, W.-K., *Solid-State Electronics* 54(12), 1637 (2010).
2. Woo, G., Lee, E.K., Yoo, H., & Kim, T., *ACS Applied Materials & Interfaces* (2021).
3. Wang, S., Pan, A., Chui, C.O., & Gupta, P., *IEEE Transactions on Electron Devices* 64(1), 121 (2017).
4. Shim, J., Oh, S., Kang, D.H., et al., *Nat Commun 7*, 13413 (2016).
5. Salomon, A., Arad-Yellin, R., Shanzer, A., Karton, A., & Cahen, D., *Journal of the American Chemical Society* 126(37), 11648 (2004).

Investigation of performance improvement through boron implantation in the source/drain area of self-aligned coplanar a-IGZO TFTs

*Seung Hee Kang[1,2], I Sak Lee[1], Kyungmoon Kwak[1], Nack Bong Choi[2], Han Wook Hwang[2], Hyun Chul Choi[2] and Hyun Jae Kim[*1]*

[1]School of Electrical and Electronic Engineering, Yonsei University, 50 Yonsei-ro, Seodaemun-gu, Seoul 03722, Republic of Korea

Tel.:82-2-2123-5865, E-mail: hjk3@yonsei.ac.kr

[2]LG Display Co., Ltd. 245, LG-ro, Wollong-myeon, Paju-si, Gyeonggi-do 10845, Republic of Korea

Recently, low-temperature poly-crystalline silicon and oxide (LTPO) thin film transistor (TFT) technology on flexible substrate has attracted a lot of attention in the display field because of its advantages such as versatile design, high resolution, and low power consumption. Amorphous Indium Gallium Zinc Oxide (a-IGZO) is a representative material among oxide TFTs for LTPO owing to possibility to fabricate on flexible substrates and extremely low off-state leakage current [1]. However, a-IGZO TFT require continuous improvement of electrical properties to be applied to all-oxide TFT technology which is the next-generation backplane technology of display. Here, we fabricated self-aligned coplanar a-IGZO TFTs with improved electrical properties and thermal stability by boron implantation into the source/drain regions. Boron, known as the n-type dopant of a-IGZO films, reduces the series resistance of source/drain (n^+ region) with implantation, improving the electrical properties of TFT [2]. Since the distribution of boron ions in a-IGZO films directly affects the resistance of the n^+ region, we measured the resistivity of a-IGZO films doped with various implantation energies. At the implantation energy of 30 keV, the resistivity of a-IGZO was 48.6 x 10^{-3} Ω·cm, and when the implantation energy was increased to 40 keV, the resistance decreased more than 20 times to 2.1 x 10^{-3} Ω·cm. Based on these results, the field-effect mobility (μ_{FE}) of self-aligned coplanar a-IGZO TFTs can be improved from 6.56 cm^2/V·s to 16.92 cm^2/V·s. Furthermore, boron doped a-IGZO TFTs showed a potential to enhance thermal stability.

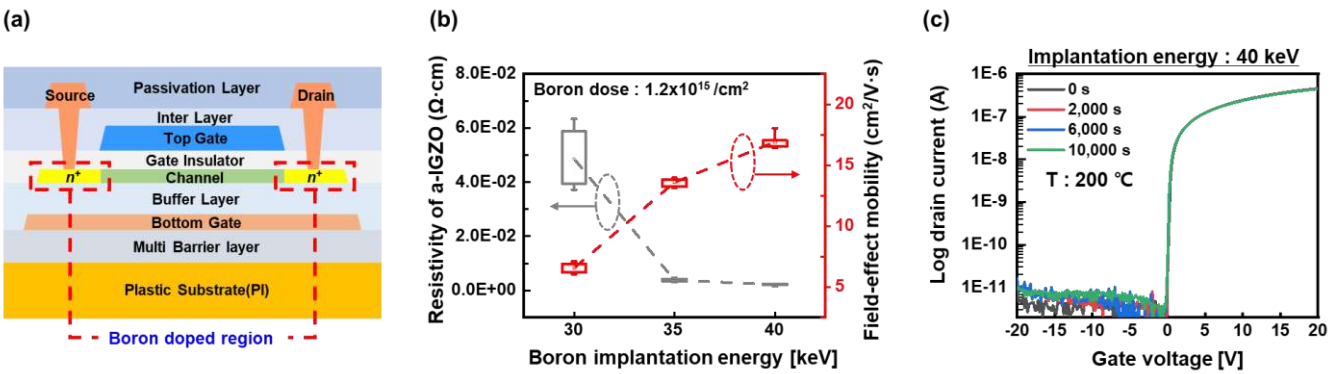

Fig. 1. (a) Schematic cross-sectional structure of the coplanar a-IGZO TFT, (b) Dependence of resistivity of boron doped a-IGZO films and field effect mobility of coplanar a-IGZO TFTs on implantation energy, (c) TFT characteristics of coplanar a-IGZO TFT (W/L = 3 ㎛/5 ㎛) with implantation energy 40 keV for 10,000 s at 200 ℃

Acknowledgment

This work was supported by the National Research Foundation of Korea (NRF) grant funded by the Korea government (MSIT) (No. NRF-2018M3A7B4071517).

References

1. T. K. Chang, C.W. Lin, and S. Chang, *in SID 2019 Digest*, pp. 545-548 (2019)
2. R. R. Chowdhurya , M. S. Kabirb , R. G. Manleyc , and K. D. Hirschman, *J. Electrochem. Soc*, 92 (4) 135-142 (2019)

Effect of N_2O Plasma treatment on the IGZO TFTs and its V_{th} distribution

Namsik Kim, Jee Ho Park, Jonghun Lim, Hyeongjung Kim Sangbin Suh, Jintae Kim*

Dept of Oxide Device Development, LG Display, Paju, Gyeonggi-do 413-811, Korea

Tel.:82-31-933-0036, E-mail: kknamsik@lgdisplay.co.kr

The electrical properties of the IGZO TFT were great affected by passivation layer and, recently, there are many studies about reliability of the IGZO TFT device with various oxide passivation materials. On the other hand, there are rarely studied about N_2O plasma treatment power and time before depositing passivation layer and its V_{th} distribution. In this study, we investigated the electrical properties of the IGZO TFT by varying N_2O plasma treatment power and time.

Figure 1 shows the ratio of metal-oxygen bonds and oxygen vacancies in the IGZO thin film with various N_2O plasma treatment time and power. As plasma treatment time and power increase, the ratio of M-O bonds increase. From the result of the XPS analysis, N_2O plasma treatment supplied oxygen to the IGZO thin film and it diminished oxygen vacancy.

We fabricated back-channel-etched structures IGZO TFT and the electrical characteristics were summarized in the table 1. As the time and power of N_2O plasma treatment increase, the V_{th} increases and the mobility decreases. By applying N_2O plasma treatment, oxygen vacancies were filled by oxygen originated from N_2O gas and it reduced effectively. As the oxygen vacancy decreases, the carrier concentration decreases and it results in the increment of V_{th} and decrement of mobility. When the strong N_2O plasma treatment is applied, the excess oxygen is supplied to the IGZO layer and it results in deterioration of V_{th} shift under positive gate bias temperature stress (PBTS), because excess oxygen is origin of electron trap sites. In addition, As the N_2O plasma treatment increases interface trap site (N_{it}) also increases and it related with PBTS deterioration.

From the result of above experiments, the lowest N_2O plasma treatment is needed in the view of mobility and PBTS. However, weak N_2O plasma treatment degrades the V_{th} distribution and it is shown in the figure 2. The N_2O plasma condition of Middle shows the best V_{th} distribution and high powered N_2O plasma condition worsen V_{th} dispersion. The weakest N_2O plasma condition shows negative V_{th} value and it means that the device normally-On.

In conclusion, we investigated the influence of the N_2O plasma treatment on the IGZO TFT. As the N_2O plasma treatment increases, the defect sites of the IGZO layer are increased. On the contrary, when As the N_2O plasma treatment decreases, the V_{th} dispersion is degraded. Therefore, optimal N_2O Plasma treatment conditions are required.

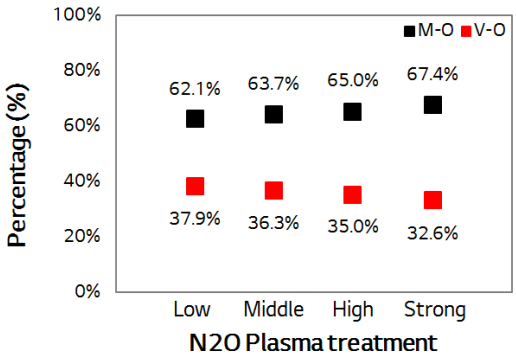

Fig. 1. Metal-Oxide and OxygenVacancy Ratio of IGZO TFT with various PAS N2O Plasma treatment via XPS analysis

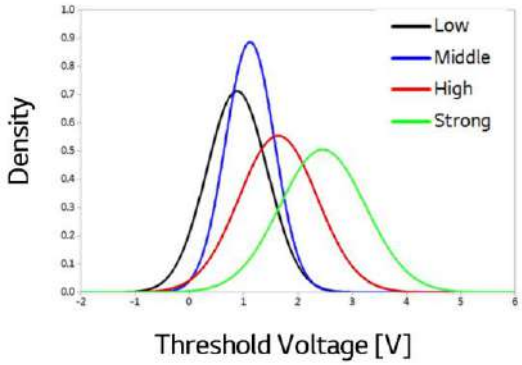

Fig. 2. Normal Distribution of IGZO TFT with various PAS N2O Plasma Treatment

	Mobility (cm^2/Vs)	V_{th} (V)	S-factor (mV/dec)	PBTS ΔV_{th} (V)	Nit ($/cm^3$)
Low	8.3	1.48	1512	2.1	1.85×10^{12}
Middle	9.3	1.67	1620	2.2	1.98×10^{12}
High	7.5	2.23	2509	2.4	3.06×10^{12}
Strong	3.0	4.01	3053	3.1	3.73×10^{12}

Table 1. Summarized electrical properties of TFTs with various PAS N2O Plasma treatment

References

1.J.S. Kim, M.K.Joo, *J. Appl. Phys.*, 115, 114503 (2014).

Improve electrical properties of IGZO TFTs by adopting Zn, Ga Rich Layer

HyungTae Kim, Jeeho Park*, JeongWoong Baek, SungHan Lim, YongJo Kim and Jintae Kim
Dept. of Oxide Device Development, LG Display Co., Ltd, Paju-si, Gyeonggi-Do 10845, Korea
Tel.:82-31-933-2798, E-mail: maestro_park@lgdisplay.com

In the oxide semiconductor fabrication process, the most important thing is maintaining the performance of oxide thin-film Transistor (TFT). Various methods have been studied and are applied to minimize the damage to the active layer from source/drain metal etchant and plasma. Therefore, subsequent processes such as heat and surface treatment are added to restore appropriate electrical properties.

In this work, we developed multi-layer active structured IGZO TFT and it could minimize the damage of IGZO thin film from plasma, which is a weakness of the back-channel-etched structure. In multi-layer active structure, the IGZO thin film acted as a main channel, which is lied at lower layer, and Gallium, Zinc-rich(GZ) IGZO thin film placed at upper layer. The role of GZ-IGZO thin film is preventing damage of main channel layer from etchant and reduces defect sites in the channel layer from metal contamination, which is originated from source/drain metal.

The IGZO thin film showed amorphous phase and the GZ-IGZO thin film exhibited crystallne phase (Fig.1). It means that GZ-IGZO thin film is denser than IGZO thin film and it can protect IGZO thin film from etchant or plama damage. The electrical properties are summarized in table 1. The Multi-layer TFT showed higher mobility and stability under positive gate bias temperature stress (PBTS) and negative gate bias illumination temperature stress (NBTIS) than IGZO TFT because GZ-IGZO layer sufficient protects main channel and suppresses trap sites.

In conclusion, we fabricated multi-layer structured IGZO TFT by using GZ-IGZO thin film. The role of upper thin film is protecting main channel layer from etchant and plasma damage generated during the fabrication process and it is possible to fabricate a robust IGZO TFT with an excellent V_{th}, mobility and V_{th} reliability.

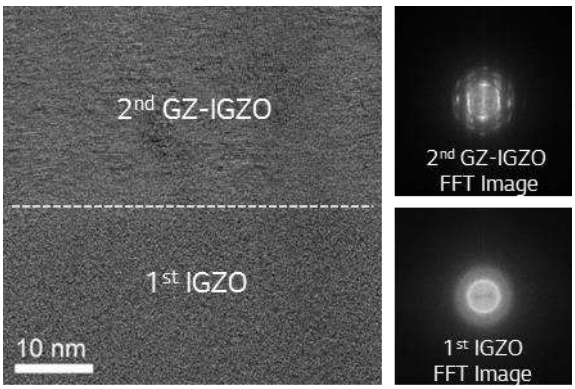

Fig. 1. The TEM(crystallization) results of IGZO, GZ-IGZO

	Mobility [cm^2/Vs]	Vth [V]	S-factor [mV/dec]	PBTS $\triangle V_{th}$[V]	NBTIS $\triangle V_{th}$[V]
Single Layer (IGZO)	8.25	-1.5	381	6.1	-3.4
Single Layer (GZ-IGZO)	0.05	3.8	1294	2.9	-1.6
Multi-Layer (IGZO / GZ-IGZO)	10.35	0.6	768	2.5	-1.5

Table. 1. Summarized electrical properties of TFTs with various Active Layer Structures.

Effect of Multi-Layer Thickness on the Reliability of the IGZO TFTs

Sangbin Suh, Jeeho Park*, Jonghoon Lim, Hyeongjung Kim, Namsik Kim and Jintae Kim
Dept. of Oxide Device Development, LG Display Co., Ltd, Paju-si, Gyeonggi-Do 10845, Korea
Tel.:82-31-933-2798, E-mail: maestro_park@lgdisplay.com

Multi-layer active structure enable realizing high-performance IGZO TFTs. There are two adventages by using multi-Layer active structure to realize high-performance device ; the first is to achieve high mobility and another is to satisfy high-realiability. Most of studies focus on the advantages of high mobility realization of multi-layer ative structures. Effect of multi-layer active structure on reliability of IGZO TFTs is rearly researched.

In this work, we fabricated back-channel-etched structured IGZO TFT and controlled the thickness of bottom/top IGZO layer and summarized electrical properties in Table 1. The bottom active layer thickness significant affects V_{th} value. This is because the bottom active layer is the area where the main channel is formed and it has a direct causal relationship to the V_{th}. On the other hand, the increase of top active layer thickness is less variable in V_{th} than bottom one. The top active layer thickness also affects V_{th} shift, but the variation of V_{th} per thickness is lower than the bottom layer's. It means that the bottom active layer plays a role in controlling V_{th} value. In case of top active layer, it enhances Beta (β) properties of the IGZO TFT, because top active layer protects channel damage from post-manufacturing process.

In conclusion, we investigated the role of bottom/top active layer in the multi-layer active structured IGZO TFT. The top active layer protected the main channel from manufacturing-damage. The bottom active layer, acted as main channel, controlled V_{th} value. Therfore the optimal top and bottom layer thickness selection is necessary for device development that satisfies both High mobility and High Reliability.

Table. 1. Summarized electrical properties of TFTs with various Active Layer Thickness

Thickness Ratio	Mobility [cm²/Vs]	V_{th} [V]	S-factor [mV/dec]	PBS ΔV_{th} [V]	β
1.0 : 2.0	5.12	0.3	734.8	2.9	0.4661
1.5 : 1.0	5.43	0.1	786.0	2.4	0.4956
1.5 : 2.0	6.07	-0.8	815.8	2.0	0.4663
1.5 : 3.0	6.25	-1.4	1059.1	1.9	0.4668
2.0 : 2.0	6.68	-1.0	924.6	1.8	0.4398

Effect of Passivation Oxygen Contents on the Performance of IGZO TFTs

Eunji Jang, Jeeho Park*, Wonil Han, Yeonhoo Jung and Jintae Kim
Dept. of Oxide Device Development, LG Display Co., Ltd, Paju-si, Gyeonggi-Do 10845, Korea
Tel.:82-31-933-2798, E-mail: maestro_park@lgdisplay.com

To protect main channel from ambient conditions, the passivation layer is essentially needed. There are many reports about organic and inorganic passivation layers such as PMMA, HfO_x, ZrO_x and SiO_x. Among them SiO_2 thin film is mainly used for passivation layer, however, effect of oxygen contents on the electrical properties of thin-film transistor (TFT) is rearly researched.

In this work, we fabricated back-channel-etched structured TFTs and controlled oxygen contents of SiO_x passivation layer by varying SiH_4:N_2O gas ratio. Therefore, oxygen contents were expressed in the order of O1<O2<O3<O4 according to the amount of oxygen. The oxygen contents were verified by electron spin resonance (ESR) and fourier transform infrared spectroscopy (FT-IR) measurement. As the SiH_4:N_2O gas ratio enlarges, the spin density increases. It means that the SiOx thin film desposited with high gas ratio has large amount of defect site with excess oxygens (Fig. 1). Moreover, as the SiH_4:N_2O gas ratio increases, the Si-O symmetric peak shifts toward upper wavenumer (Fig. 2). It means that as the high SiH_4:N_2O gas ratio of SiO_x thin film have large amounts of oxygens. From the results of ESR and FT-IR evaluation, the higher the SiH_4:N_2O gas ratio, the more oxygen-rich characteristics were formed.

We fabricated IGZO TFT with SiO_x passivation layer as a function of SiH_4:N_2O gas ratio and summarized electrical properties in Table 1. As a result, the more oxygen-rich SiO_x passivation layer is formed, the more oxygen diffuses from passivation layer into active layer. Since it captures free electrons, the initial V_{th} shifts positively and positive bias temperature stress (PBTS) ΔV_{th} is deteriorated. However, negative bias temperature illumination stress (NBTiS) ΔV_{th} is improved. In case of IGZO TFT with oxygen-poor SiO_x passivation layer, the oxygen diffuses from active into passivation layer and it makes oxygen vacancies in the active layer. Therefore, the IGZO TFT with O-poor SiO_x passivation layer shows opposite performances compared with O-rich one; negative shift of initial V_{th}, improved PBTS ΔV_{th} and degraded NBTiS ΔV_{th}. Consequently, we controlled oxygen contents by simply adjusting SiH_4:N_2O gas ratio and it affects initial V_{th} and stability. Therefore, to implement the suitable performance of IGZO TFTs, adjusting proper oxygen contents of SiO_x passivation layer is required.

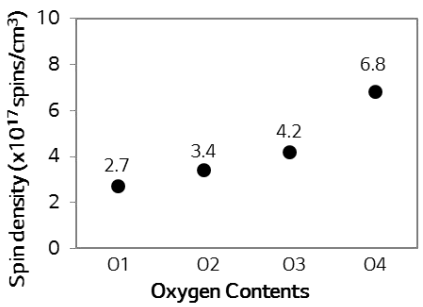

Fig. 1. The spin density of SiO_2 thin films as a function of gas ratio.

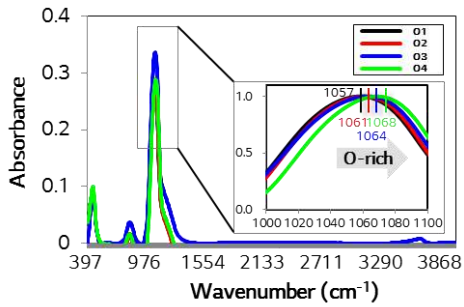

Fig. 2. The FT-IR values of the SiO_2 thin films as a function of gas ratio.

Table. 1. Summarized electrical properties of TFTs with various Passivation gas ratio.

	Mobility (cm^2/Vs)	V_{th} (V)	S-factor (V/dec)	Nit (/cm^3)	PBTS ΔV_{th}(V)	NBTiS ΔV_{th}(V)
O1	-	-20	-	-	-	-
O2	18.19	0.06	628	7.67×10^{11}	1.9	-4.7
O3	15.51	1.11	807	9.86×10^{11}	3.2	-1.8
O4	11.65	3.90	811	9.91×10^{11}	5.3	-0.6

References

1. J. H. Park and S. Y. Yoon, *Currnet Appl. Physics*, vol. 18, p. 1447-1450 (2018).

One-way Observable Edge-lit Window Signage Display Using Dye-doped Thin Resin Layer Which Enables to Make Images Invisible from Back Side

Kunio Sakamoto and Yusuke Fujie
Dept. of Intelligence and Informatics, Konan University, 8-9-1 Okamoto, Higashinada, Kobe 658-8501, Japan
Tel.:81-78-431-4341, E-mail: kunio@konan-u.ac.jp

An LED acrylic sign is transparent signage which has floating and light-emitting graphics and catches customers' eye. But this eye-catching sign has one defect that is mirrored imaging problem. It stands to reason that someone observes mirrored image according to the direction of viewing if you draw something on the transparent material. This paper shows a one-way observable edge-illuminated window signage display using dye-doped thin resin layers for unidirectional color generating by light controls. You know that water is generally clear and transparent but the water in a bath tub is little blue. The color changes depending on the depth of water. The deeper, the darker water becomes blue. Fig. (a) shows the principle of color generating. A dye-doped resin block has different thickness and makes color changing from transparent to blue gradually.

A single layer of dye-doped resin is transparent, but the double-piled resin layers generate some color. If you used a mirror, you could make the single resin layer generating some color like double-piled resin layers. As shown in fig. (b), it is the important technical point that all transmission light waves pass through all optical materials and observed signage is formed by the reflection light waves of the half mirror. At transmission light path from the back, all transmission light waves are still original because light waves pass single resin layer or not in addition to the half mirror. As the result, observers can watch the sights behind these optical materials. At reflection light path by the half mirror, there are also two cases whether the waves pass through the resin layers or not. The case of passing the resin layers makes the same phenomenon that light waves pass through the double-piled resin layers. After this twice same layer passing, the transparent resin layers generate some color. At the observing from back side, all transmission light wave from front side can pass through all optical materials without generating colors although some light wave passes through the resin layer once. This is the reason why the observer can watch the sights behind these optical materials without watching the mirrored image of signage.

The acrylic lighting guide transmits lights through only an optical material so that no light is transmitted into air using the total internal reflection phenomenon as shown in fig. (a). This principle is utilized in an optical fiber cable for long-distance communications. Therefore light beams of the guide illuminate the signage graphics.

Fig. (c) shows observed images of our edge-lit unidirectional imaging display. The authors paint the letterings "LUCUA" made by hand drawings using a resin ink on a light guide. You can confirm that the color generating mechanism using a transparent material realizes the one-way imaging which enables to make invisible from back.

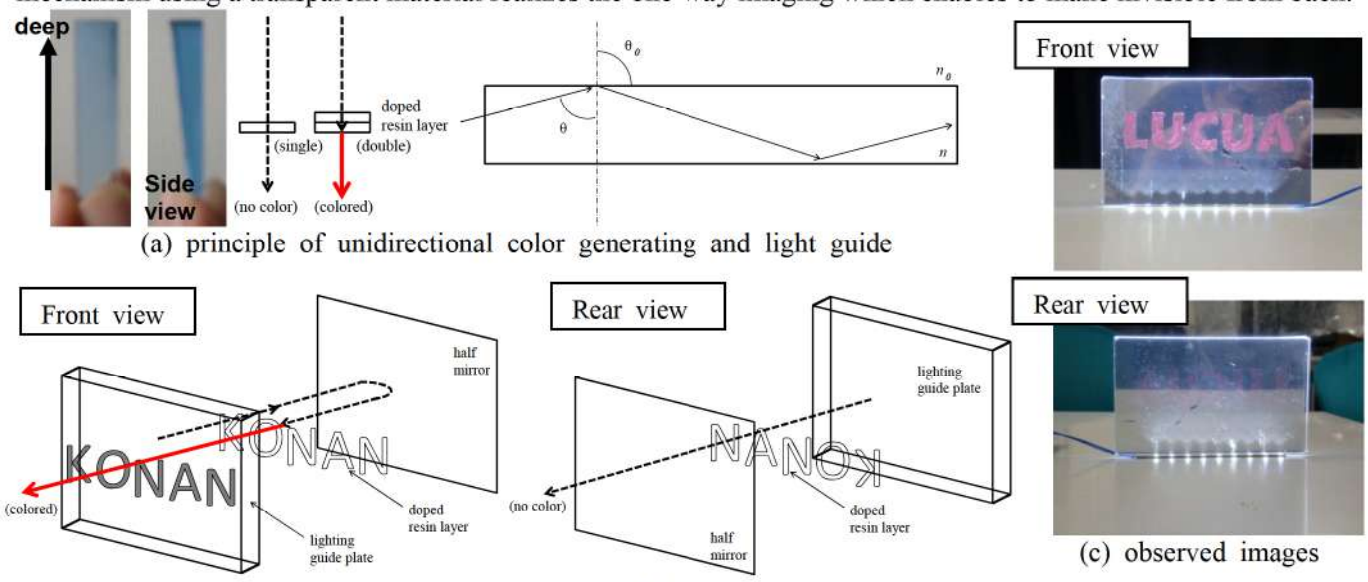

(a) principle of unidirectional color generating and light guide

(b) principle of one-way observable imaging

(c) observed images

Fig. 1. One-way observable window signage using dye-doped thin layer by resin printing ink

Unidirectional Projection Screen for Window Signage Which Enables to Make Images Invisible from Back Side Using Polarized Light Control Technology

Kunio Sakamoto and Hikaru Tanouchi
Dept. of Intelligence and Informatics, Konan University, 8-9-1 Okamoto, Higashinada, Kobe 658-8501, Japan
Tel.:81-78-431-4341, E-mail: kunio@konan-u.ac.jp

This paper shows the one-way observable projection display screen using polarized light control technology.

Fig. (a) shows the principle of polarized light control in 2019 model of a one-way observable display. It is the important technical point that all transmission light waves pass through all optical materials and observed signage is formed by the reflection light waves of the half mirror. At reflection light path by the half mirror, there are two cases whether the waves pass through the 1/4 wave plate or not. In case of not passing the wave plate, the light wave can again pass through the same polarizer. In case of passing the wave plate, the polarized light wave passed a polarizer passes through the 1/4 wave plate twice by mirror reflection. After this twice wave plate passing, the direction of polarization rotates 90 degrees. Therefore this polarization-axis-rotated light wave is blocked by the polarizer at the second time. As the result, the brightness of light waves is made a difference. You can utilize this different brightness for drawing and also projecting the text and graphics of signage.

In image projection screens, the important thing is the same that all transmitting light waves pass through all optical materials and reflection lights are blocked by the polarizer, or vice versa as shown in fig. (b).

In rear projection, the polarizer blocks the reflected light waves by the diffusion screen because the twice passing of the 1/4 wave plate(or film) rotates polarizing orientations, too. Then the mirroring image is invisible. Meanwhile the observer can perceive the directly projected image on the diffusion screen. Moreover, all transmission light waves can pass through the polarizer because natural light waves have all directions of polarization. Consequently, observers can watch the sights behind these optical materials.

As above mentioned, the polarized light control mechanism for projection display is simpler than the case of the 2019 signage model. The reason is that the projecting light beams of a projector have polarizing orientation because of a polarizer attached on an LCD panel and that screen images are generated by the brightness modulation of the LCD (It is no need to generate the letterings and graphics on the screen by optical film materials such as the 2019 signage model). Ultimately, the observer can watch the sights behind these optical materials without watching the mirrored image of signage. This is why the mirrored image is made invisible.

At front projection, the mechanism is very simple that the polarizer blocks transmitting light wave directly. You can confirm that the light control technique realizes one-way observable projection as shown in fig. (c).

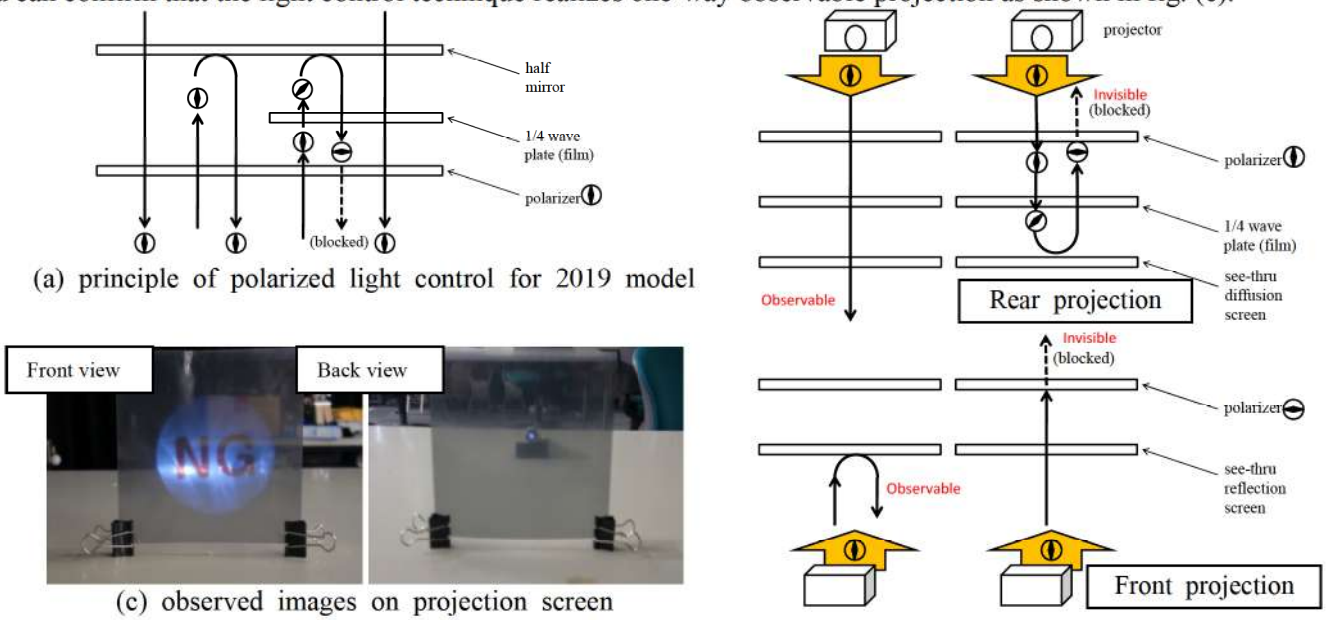

(a) principle of polarized light control for 2019 model

(c) observed images on projection screen

(b) principle of unidirectional projection screen

Fig. 1. One-way observable window signage using unidirectional projection screen

Optimally Modulated Luminance for Suppressing Flicker in Displays

Eunjung Lee, Hyungsuk Hwang, Jaejoong Kwon, Sungchan Jo
Display Research Center, Samsung Display, Yongin-si, Gyunggi-do, 17113, Korea
Tel.:82-31-5181-6446, E-mail: ej45.lee@samsung.com

Reducing power consumption and retaining performance at once would be one of the common challenges to electronics engineers. Therefore many researches for lowering power consumption are ongoing in display industry as well. One thing is low frequency driving technology. Most of 60Hz displays we are recently watching refresh their contents per every 16.67msec. The faster the refresh rate is, the more power is needed. But lower driving frequency could save power, there might occur image qulaity degradation. Main symptom is flicker which is defined as an unsteady movement of a flame or light that causes rapid variations in brightness.

In general, human can only detect particular range of variation of light, variation out of range of that is scarecely sensed. It is explained by spatio-temporal contrast sensitiviy model of human eye. Spatial contrast sensitivity represents sensitivity of human eye depending on target's spatial variation, temporal contrast sensitivity is for target's temporal variation. It is plotted as sensitivity versus varying frequency of target. A person who has normal vision can hardly perceive faster changing stimuli than 60Hz, on the other hand, display varying at 10~30Hz speed is vulnerable to generating flicker.

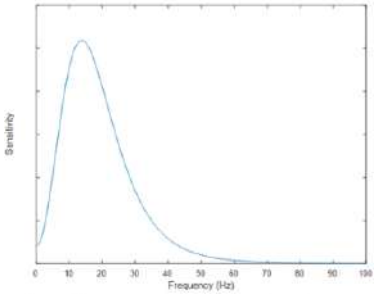

Fig. 1. Temporal contrast sensitivity of human eye

Display's flicker level is mostly caculated by applying these sensitivity function as weighting factors. Here, JEITA flicker index is used as comparing perceiving flicker level. JEITA flicker amount is the ratio of AC and DC signal power, P_0 is DC signal power, and P_x is AC signal power. The amount is expressed as decibel(dB).

$$\text{JETIA Flicker (dB)} = 10\log\frac{P_x}{P_0}$$

We simulated varying luminance that changing shape is sawtooth-falling signal in one frame assuming various refresh rate 10~144Hz display. When unperceivable flicker level set to -55dB, under 1% luminance variation is allowed in 10~20Hz display, about 1.5% in 30Hz display, about 2.5% in 40Hz display, 5% in 50Hz display. In case of display refreshed at over 60Hz speed, there would be rarely flicker problem in the range of even 30% luminance variation a frame. But if the luminance range get increased than 30%, or off period get longer, flicker might appear even though display refresh rate is over 60Hz.

Plus, there would be concerns about inconsistency with calculated flicker metrics, JEITA and perceptual amout of flicker in low frequency display under 20Hz. For evaluating diverse case of display, new metric for flicker would be necessary.

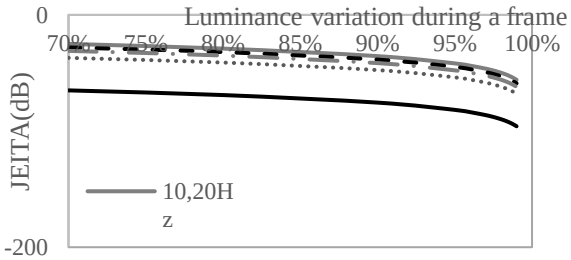

Fig. 2. JEITA flicker level depending on displays' refresh rate and luminance variation

References

1. P. G. J. Barten, Contrast sensitivity of the human eye and its effects on image quality, HV press (1999)
2. EIAJ ED-2522, Measuring methods for Matrix Liquid Crystal Display modules, JEITA (Standard of Electronic Industries Association of Japan)

Attitude toward Use(ATU) of New Screen Form Factor Considering Contents

Daeun Park and YungKyung Park
College of Art & Design, Color Design, Ewha Womans University, Seoul 03760, South Korea
E-mail: yungkyung.park@ewha.ac.kr

As the advent of modular screens, screen forms have been diversifying. This study conducted a survey using the Technology Acceptance Model (TAM) on 208 men and women in their 20s and 30s to confirm the general consumer's acceptance of the new screen form. There were a total of six Screen Form Factors used in the survey, consisting of small, medium, and large sizes for 1:1 Square and 32:9 Extra Wide ratios. Since content characteristics could affect acceptance of screen form, four types of content were used: 'Movie', 'Exercise', 'Game' and 'Smart Home' ('Smart Home' includes Internet search, weather and IOT information utilization). As a stimulus for the survey, images including human scale, space and screen were produced, and images using each content in six screen formats were shown to subjects. The questionnaire consisted of a 7-point Likert scale utilizing TAM's Perceived Usefulness (PU), Perceived Ease of Use (PEOU), and Attitude toward Use (ATU) questions.

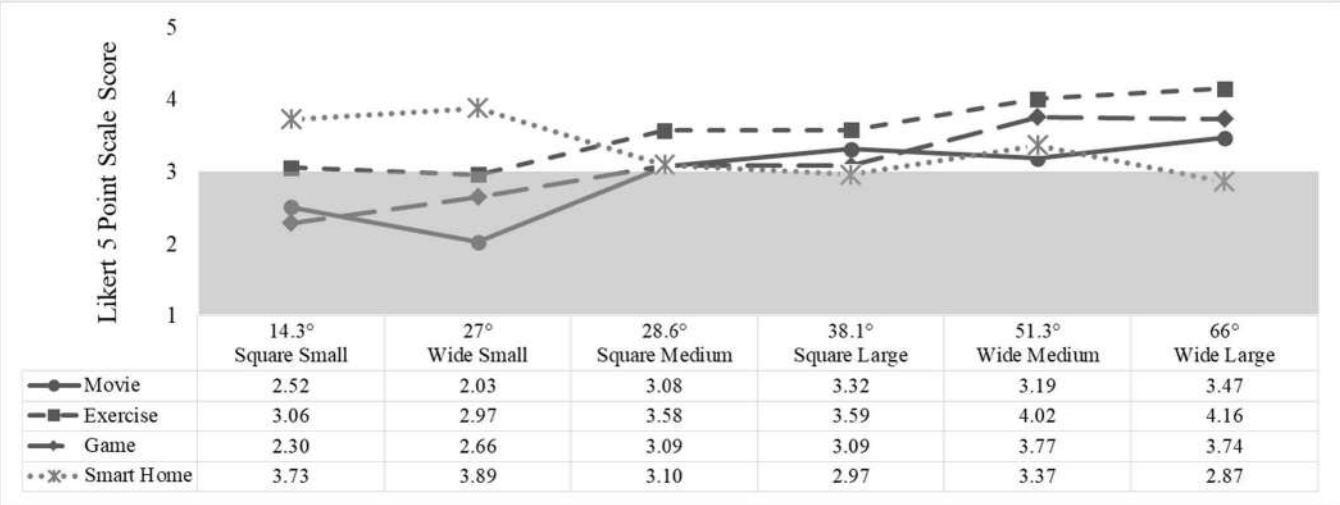

Fig. 1. ATU Score Fitted to Horizontal FOV of Screen(viewing distance : 3m)

Horizontal FOV 28° point was identified as a critical point by fitting the ATU (Attitude Toward Use) score to the horizontal FOV (FOV) of the screen<Fig. 1>. In the case of Entertainment contents (Movie, Exercise, Game), the ATU increased as the FOV increased from above 28°, but in the case of Smart home, the Information Contents, the ATU was evaluated positively (more than 3 points) under 28°. Central Visual Field is 60°, peripheral vision is 60°~180°(Wandell, 1995). The character identification limit of the Central visual field is 10 to 20° and the sign identification limit is within 30° (Panero & Zelnik, 1979). This confirms that the appropriate screen size threshold regarding the utilization of information is around 30°, including Zanden (2014)'s research that the appropriate screen size of the classroom utilizing various infotainment is FOV 35°. The results of this study suggest that for new types of screens, such as Square(1:1) and Extra Wide(32:9), the optimal size exists depending on the type of contents. In order to utilize Entertainment contents, both Square and Extra Wide forms need to meet at least horizontal FOV 28°(which is similar to 65-inch for 16:9 ratio) on viewing distance 3m.

.

References

1. Wandell, B. A. (1995). Useful quantities in vision science. Inner cover pages in "Foundation of vision." Sunderland, MA: Sinauer Associates.
2. Panero, J., & Zelnik, M. (1979). Human dimension & interior space: a source book of design reference standards. Watson-Guptill.
3. Van der Zanden, A. H. W. (2014). Readability in classrooms. University of Technology, Netherlands.

Color gamut volume inconsistency over chromatic adaptation transforms

Youn Jin Kim[1], Kyung Jin Kang[1] and Myoung Young Lee[1]
[1]LG Electronics Inc., Pyeongtaek-si, Gyeonggi-do 17709, Korea
Tel.:82-10–7188-1834, E-mail: younjin01.kim@lge.com

Chromatic adaptation is one of the substantial components for modelling of color appearance mechanism of the human visual system. There are several chromatic adaptation transform (CAT) methods[1] originally designed to predict corresponding colors more accurately in color appearance and difference studies. Performance and merits of those CAT methods may rely upon the training data sets used. Measuring of color gamut volume of a given color space or device was not considered well whilst determining the coefficients of matrix within CAT. The CIE 168 technical report[2] proposed a color gamut metric which can be defined as the total CIELAB gamut volume encompassed by the color encoding. A given color encoding space is represented by a tetrahedral complex in the ICC PCS space and the gamut volume is computed by summing the volumes of each tetrahedron. During conversion of the tristimulus values into CIELAB, a chromatic adaptation transformation from the reference CIEXYZ colorimetry to D50 was recommended by using von Kries chromatic adaptation with the Hunt-Pointer-Estevez cone primaries matrix. This chromatic adaptation transformation step is supposed to convert the encoding color space into corresponding output-referred colors under D50 illuminant; thus the conversion accuracy of CAT is of a great importance to preserve the original color gamut properties. There is an underlying hypothesis set, in our current research, that color gamut volume should be consistent across the change in adaptive white point, if complete discount of the illuminant is assumed.

Measuring of the CIE color gamut volumes for the three standard color spaces – such as Rec.2020, DCI-P3, and Rec.709 – takes place in three steps.[1] Since the reference white of those color spaces is D65 illuminant, a D65-to-D50 chromatic adaptation transformation should be carried out for each computation firstly. Then this procedure was repeated with three more CAT methods including Bradford matrix, CMC2000, and CAT02. Finally, their legacy color gamut volume values under D65 (w/o CAT) were also calculated for normalization purpose. The normalized discrepancy of color gamut volumes occurred through chromatic adaptation transformation from the reference D65 to its corresponding D50 is shown in Fig. 1. CAT02 shows a relatively better consistency (~1/discrepancy) and Bradford matrix, von Kries, and CMC2000 followed. CAT02 shows the highest consistency for Rec.2020 (3.79%) while the results from other methods reach more than 7.97%. Performance of CAT02 appears reasonably consistent for DCI-P3 (1.57%) and Rec.709 (1.94%) but Bradford matrix outperformed as 0.92% and 0.91%, respectively.

Comprehensive analysis and suggestions to the selection of CAT for color gamut volume have been analyzed in this paper. Consequently, CAT02 is found to be more optimal so tends to preserve color gamut consistency across chromatic adaptation. The findings could have been confirmed through more practical measurement data sets according to the variation in display white point and driving schemes.

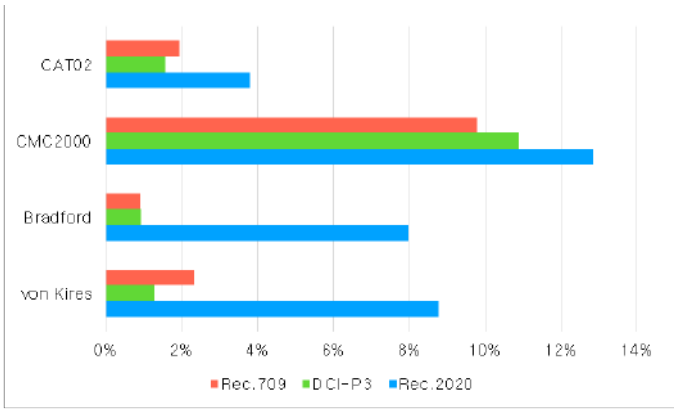

Fig. 1. Normalized discrepancy of color gamut volumes from D65 to D50 by using various CATs

References

1. M. Wei S. Chen, *Optics Express*, 27(6), 9276 (2019).
2. de L'eclaraige, Commision Internationale. *Technical Report 168*. (2005).

Donut-Shaped Fourier Peplography

Jiheon Lee[1], Jaehoon Lee[2], Hyun-Woo Kim[2], Min-Chul Lee[2], and Myungjin Cho[1,]*
[1]School of ICT, Robotics, and Mechanical Engineering, IITC, Hankyong University, Anseong, Kyonggi-do, Republic of Korea
E-mail: mjcho@hknu.ac.kr
[2]Dept. of Computer Science and Networks, Kyushu Institute of Technology, Iizuka City, Fukuoka, Japan

Recently, scatter noise removal techniques have been a great issue for autonomous vehicle applications. To remedy the scatter noise, Fourier Peplography can be used [1]. In Fourier domain of the image, DC term has the scatter noise information. Considering this phenomenon, DC term in Fourier domain of the image is remedied by Fourier Peplography. However, reducing this DC term may cause the saturation of high spatial frequency component. Therefore, to solve this problem, we modify the Fourier mask which reduce the DC term and avoid the saturation of high spatial frequency component as donut-shaped mask with low-pass filtering mask. Figure 1 shows the mask in donut-shaped Fourier Peplography which combines both masks in conventional Fourier Peplography and our proposed Fourier Peplography. Finally, the processed image can be obtained by inverse Fourier transform as shown in Fig. 2. It is noticed that the result by our method as shown in Fig. 2 (b) has better visual quality than the result by conventional Fourier Peplography as shown in Fig. 2 (a).

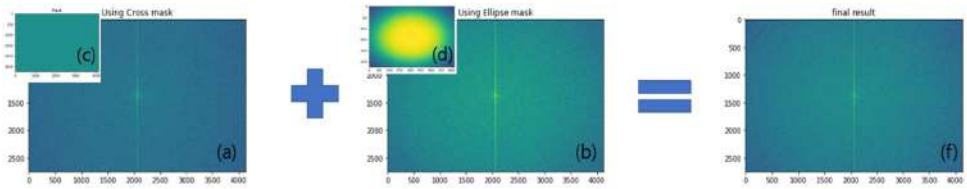

Fig. 1. (a)Fourier spectrum by conventional Fourier Peplography, (b) Fourier spectrum by donut-shaped mask only, (c) mask for conventional Fourier Peplography, (d) donut-shaped mask, and (f) Fourier spectrum by our proposed method.

Fig. 2. Results. (a) original image and (b) processed image by our proposed method.

Acknowledgment

This work was supported by the National Research Foundation of Korea(NRF) grant funded by the Korea government(MSIT) (NRF-2020R1F1A1068637).

Reference

1. M. Cho, "Fourier Peplography – real-time passive 3D imaging through scattering media by optical signal processing," IMID (2018).

Enhanced depth estimation using histogram matching

Jiheon Lee[1], Jaehoon Lee[2], Hyun-Woo Kim[2], Min-Chul Lee[2], and Myungjin Cho[1,]*
[1]School of ICT, Robotics, and Mechanical Engineering, IITC, Hankyong University, Anseong, Kyonggi-do, Republic of Korea
E-mail: mjcho@hknu.ac.kr
[2]Dept. of Computer Science and Electronics, Kyushu Institute of Technology, Iizuka City, Fukuoka, Japan

Recently, the depth estimation of objects under low light conditions has been a challenge issue for many applications. To estimate the depth of the scene, Volumetric Computational Reconstruction (VCR) can be used [1]. In addition, to visualize the object in a dark environment, the photon counting method can be used with VCR [1]. However, it is difficult to estimate the depth accurately because the object with out-of-focus may be slightly focused. Thus, it is not easy to find the best focused part for accurate depth estimation. Therefore, to solve this problem, we propose a new depth estimation using histogram matching.

Figure 1 illustrates the conventional and our proposed depth estimation methods. Conventional and our proposed methods use the original image and histogram matched image of the original image, respectively. Figure 2 shows our experiment setup with 3 objects with different depth. Figure 3 shows the reconstruction result at 405mm. The best focused object is right car. However, in conventional method, other objects are not out-of-focus. On the other hand, in our proposed method, they are more out-of-focus. Therefore, our method can estimate the depth more accurately than conventional method.

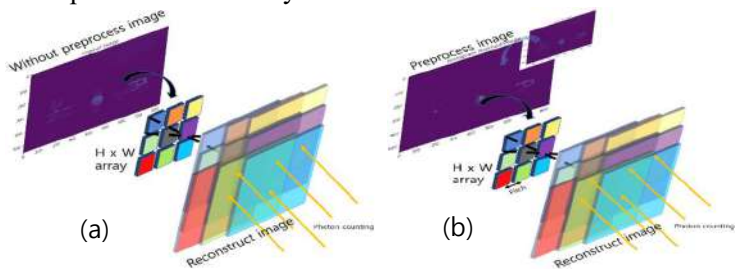

Fig. 1. Depth estimation by (a) conventional method and (b) our proposed method.

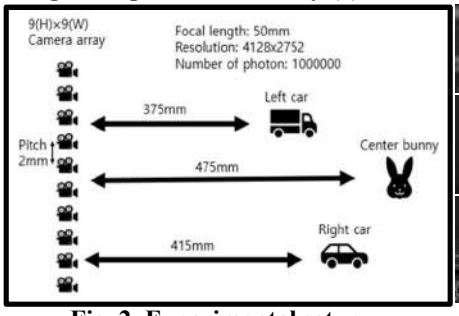

Fig. 2. Experimental setup.

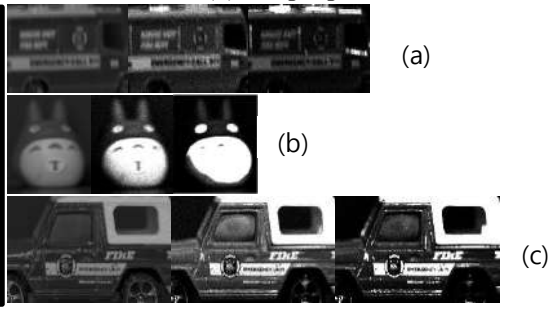

Fig. 3. Reconstruction result at 405mm (left: original, center: conventional, right: proposed).
(a) left car, (b)center bunny, (c) right car.

Acknowledgment

This work was supported by the National Research Foundation of Korea(NRF) grant funded by the Korea government(MSIT) (NRF-2020R1F1A1068637).

Reference

1. M. Cho, "Three-dimensional color photon counting microscopy using Bayesian estimation with adaptive priori information," Chinese Optics Letters, Vol. 13, No. 7, pp. 070301 (2015).

Computational photon counting visual quality enhancement by using wavelet denoising

Jaehoon Lee[1], Kazuaki Honda[1], Jiheon Lee[2], Myungjin Cho[2], and Min-Chul Lee[1,]*
[1]Dept. of Computer Science and Networks, Kyushu Institute of Technology, Iizuka City, Fukuoka, Japan
Tel.:+81-0948-29-7699, E-mail: lee@cse.kyutech.ac.jp
[2]Dept. of ICT, Robotics, and Mechanical Engineering, IITC, Hankyong National University, Anseong, Kyonggi-do, Republic of Korea

Recently, the visualization under the dark situation has been essential through the development of the autonomous drive system industries. To visualize the scene under the photon-starved conditions, the photon counting technique can be used. Since photons occur randomly in unit time and space, we can estimate the photons using statistical methods such as Poisson random process, maximum likelihood estimation (MLE), and Bayesian approaches [1]. To generate the photon-limited image, the normalized scene is used. Through the Poisson random process, photons can be generated. However, the background noise can degrade the image visual quality. To reduce the background noise and enhance the visual quality, our proposed method uses the wavelet denoising technique.

Figure 1 shows the computational photon counting model process. Since the background noise occurs using the Poisson random process, it is not easy to distinguish the object well. To reduce this noise, an average filter may be used. However, it may remove the noise without considering the presence of the object. To solve this problem, we use the 2D wavelet multilevel decomposition. One-level decomposition can generate the high frequencies in the image. Additional level decomposition can extract from the low-frequency detail to high-frequency detail coefficients discretely. To reduce the noise, the threshold value can be used to the coefficients. To show visual quality of our method, we show the photon-limited image, median filtered photon-limited image, and wavelet denoised photon-limited image in Fig. 2 and we use various analysis metrics as shown in Fig. 3.

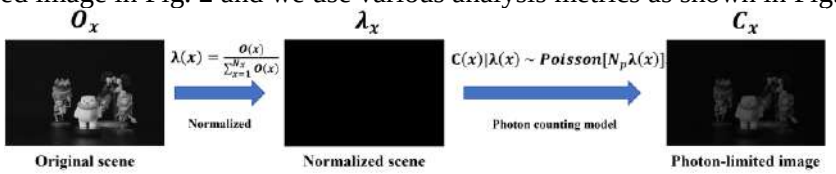

Fig. 1. Computational Photon Counting model.

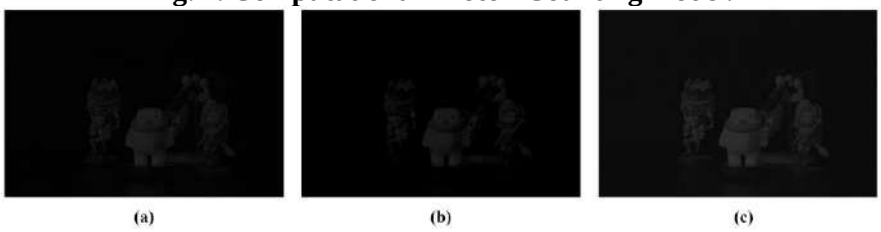

Fig. 2. Images, (a) original photon-limited image, (b) median filtered image, (c) wavelet denoised image.

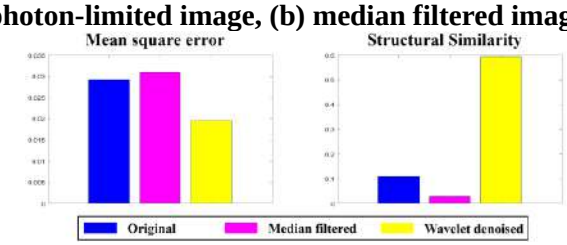

Fig. 3. Image quality analysis.

Acknowledgment

This work was supported by the National Research Foundation of Korea(NRF) grant funded by the Korea government(MSIT) (NRF-2020R1F1A1068637)

References

1. M. Cho, "Three-dimensional color photon counting microscopy using Bayesian estimation with adaptive priori information," *Chinese Opt.Letters*, 13(7), 010301 (2015).

Car A-pillar blind spot visualization and object recognition system using car dash cam

Jaehoon Lee[1], Hyun-Woo Kim[1], Jiheon Lee[2], Myungjin Cho[2], and Min-Chul Lee[1,]*
[1]Dept. of Computer Science and Networks, Kyushu Institute of Technology, Iizuka City, Fukuoka, Japan
Tel.:+81-0948-29-7699, E-mail: lee@cse.kyutech.ac.jp
[2]Dept. of ICT, Robotics, and Mechanical Engineering, IITC, Hankyong National University, Anseong, Kyonggi-do, Republic of Korea

Recently, the prevalence of automobiles has been common and it can increase the quality of life. Therefore, automobile manufacturers try to make safe cars for attracting customers. To make safe cars, there are four main pillars in the vehicle which can prevent and absorb the accident's impact. However, these pillars can interfere with the driver's vision [1]. Especially, a pillar located next to the driver, referred to as the A-pillar, can cause many accidents because they interfere with the driver's vision when the vehicles turn around. To visualize the blind spot from the A-pilar, we present the autonomous system that can visualize and recognize the object in the blind spot.

Figure 1 shows our optical experimental setup. To calculate the blind spot area, we have to input some parameters (i.e., the camera sensor size, distance between car windows and drivers) in our system as shown in Fig. 2. When we input the parameters, the blind spot can be visualized. To prevent the accident with cars in the blind spot area, we use the YOLOv3 which can recognize the object automatically. Figure 3 shows the system result image. It shows the blind spot area and detected car with the monitor by using YOLOv3. In addition, when the car detected in the blind spot area, the warning alert sound comes out from the speaker. To verify our system, the accuracy analysis data of the system is shown in Table 1. To measure the recognition accuracy, we calculate the accuracy according to the car shape and color respectively by using recall method. Finally, our system can recognize the car in the blind spot effectively and it can be utilized to reduce the accident rate in the blind spot.

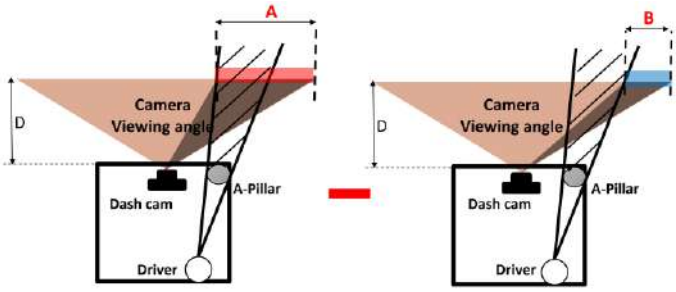

Fig. 1. Optical experiment setup.

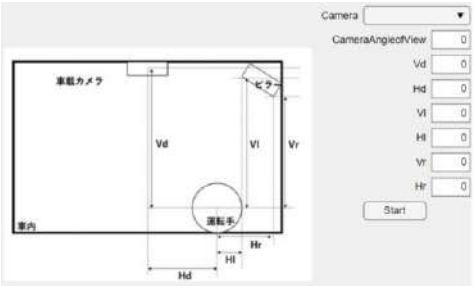

Fig. 2. System software.

Fig. 3. Blind spot visualization

Car	Accuracy (%)
Compact car	78.6
Sedan	85.3
Truck	50.6
Bus	70.8

Table. 1. Recognition accuracy

Acknowledgment

This work was supported by the National Research Foundation of Korea(NRF) grant funded by the Korea government(MSIT) (NRF-2020R1F1A1068637)

References

1. M. Yang, "Study on A-pillar Display Algorithm through Image Registration," *International Conference on Computer and Communications*, 18882693, (2018).

Accurate depth map reconstruction method by using optimum distance calculation

Kazuaki Honda[1], Jaehoon Lee[1], Hyun-Woo Kim [1], Jiheon Lee[2], Myungjin Cho [2], and Min-Chul Lee[1,]*
[1]Dept. of Computer Science and Networks, Kyushu Institute of Technology, Iizuka City, Fukuoka, Japan
Tel.:+81-0948-29-7699, E-mail: lee@cse.kyutech.ac.jp
[2]Dept. of ICT, Robotics, and Mechanical Engineering, IITC, Hankyong National University, Anseong, Kyonggi-do, Republic of Korea

Recently, the three-dimensional (3D) reconstruction technique has been significant. To generate the 3D scene computationally in integral imaging, volumetric computational reconstruction (VCR) has been proposed [1]. To obtain the 3D image in integral imaging, elemental images and their shifting pixel values are used. Elemental images are back-projected through the virtual pinholes and overlapped each other according to the shifting pixel values. Then the 3D image can be obtained. Through the 3D image, the depth map can be generated using the variance calculation of overlapped elemental images. Since the shifting pixel values cannot express the float number, it may provide wrong depth information in the reconstruction. In addition, to generate the depth map, the conventional method calculate the variances of all 3D images. Therefore, it takes lots of time to generate the depth map. To solve these problems, we propose the optimum distance calculation that calculates the integer shifting pixel value only. To verify our proposed method, we carried out the simulation experiment to compare the depth map accuracy of both the conventional method and our proposed method.

Figure 1 illustrates the simulation setup. Two cars are located in front of the camera with different depths. We use 5(H) × 5(V) camera array to pick up the elemental images and the pitch between the cameras is 2mm. Difference between the conventional method and our proposed method is that the optimum shifting pixel values are used (i.e., integer values). Therefore, our proposed method can generate 3D images accurately. We calculate each pixel variance and find out the depth with the threshold value. Figure 2 shows the total processing time to generate the depth map. It is noticed that our proposed method can generate the depth map about 4 times faster than conventional method. Figure 3 shows depth map results. The conventional method may generate wrong depth information through the reconstruction process as shown in Fig. 3 (a). However, our proposed method can generate depth map accurately as shown in Fig. 3 (b). As a result, our proposed method can enhance the processing speed and depth map accuracy.

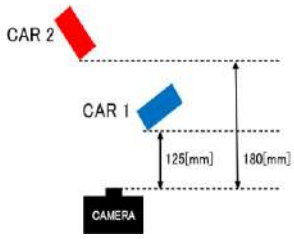

Fig. 1. Simulation setup.

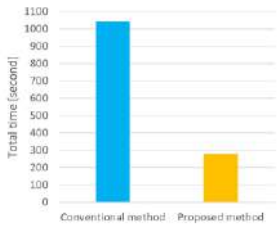

Fig. 2. Reconstruction process time.

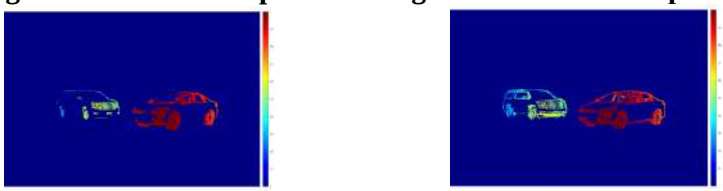

(a) **(b)**

Fig. 3. Depth map result. (a) conventional method and (b) proposed method.

Acknowledgment

This work was supported by the National Research Foundation of Korea(NRF) grant funded by the Korea government(MSIT) (NRF-2020R1F1A1068637)

References

1. S.-H. Hong, J.-S. Jang, and B. Javidi, Three-dimensional volumetric object reconstruction using computational integral imaging, Optics Express, Vol12, No.3, pp.483-491 (2004).

Research on noise reduction techniques for the 3D visualization under the scattered media conditions

Ryo Shinohara[1], Hyun-Woo Kim [1], Jaehoon Lee[1], Jiheon Lee[2], Myungjin Cho [2], and Min-Chul Lee[1,]*
[1]Dept. of Computer Science and Networks Institute of Technology, Fukuoka, Japan
Tel.:81-948-29-7699, E-mail:lee@cse.kyutech.ac.jp
[2] School of ICT, Robotics, and Mechanical Engineering, IITC, Hankyong National University, Anseong, Kyonggi-do, Republic of Korea

Recently, many researchers have been studied to remove the noise under scattered media conditions such as fog and turbid water circumstances. Several researchers have applied integral imaging (InI) and spatial frequency filtering to remove scatter noise [1]. Spatial frequency filtering is one of the techniques which can remove specific spatial frequency components in the image [1]. However, previous scatter removal method cannot remove scatter media effectively. Besides, the color of the result image may be distorted through the histogram equalization. To solve these problems, we propose a new method for improved scatter denoising. The proposed method can remove the scatter media clearly and it can enhance the visual quality. Figure 1 shows the algorithm of the proposed method. As shown in Fig. 1, we reconstruct the 3D image using band-pass filtered elemental images. Then, we apply the low pass filter to the reconstructed image. Finally, we can generate scatter-removed image by subtracting the low pass filtered image from the reconstructed image.

Figure 2 shows the result of the proposed method. As shown in Fig. 2 (c), conventional method result image still contains scatter media. Also, it shows the color distortion. On the other hand, the proposed method can remove scatter media without color distortion compared with the previous algorithm. To verify our method, we use peak signal to noise ratio (PSNR) and cross-correlation as performance metric. The comparison result shows that the proposed method is 20% and 35% higher than the previous method in PSNR and cross-correlation, respectively.

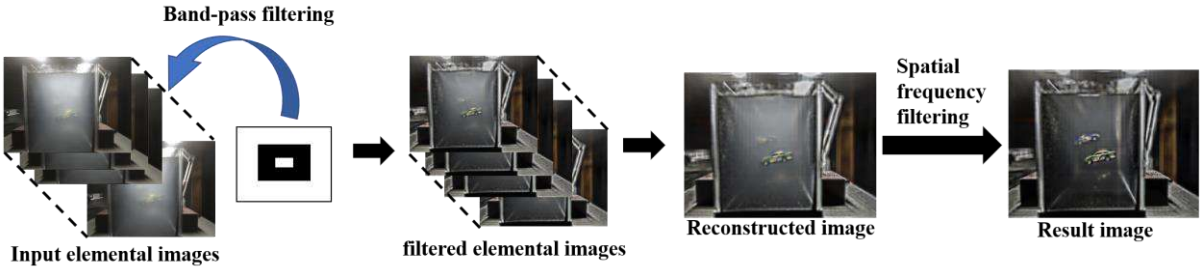

Fig. 1. Algorithm of the proposed method

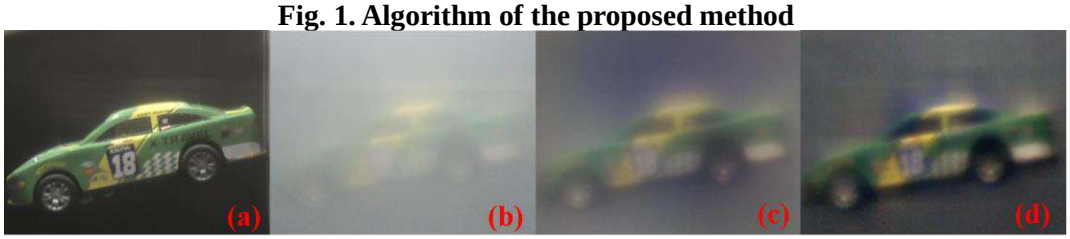

Fig. 2. (a)Original image and(b)image with noise, and result of (c) the previous method and (d) the proposed method

Acknowledgment

This work was supported by the National Research Foundation of Korea(NRF) grant funded by the Korea government(MSIT) (NRF-2020R1F1A1068637).

References

1. J. Lee, K. Inoue, M. Cho and M. -C. Lee, "3D Visualization of Objects under scattering media conditions using Integral Imaging," 2019 International Conference on Information and Communication Technology Convergence (ICTC), Jeju, Korea (South), 2019, pp. 1091-1095

A study on statistical analysis using segmentation and numbering in digital holographic microscopy (DHM) technology

Hyun-Woo Kim[1], Jaehoon Lee[1], Jiheon Lee[2], Myungjin Cho[2], and Min-Chul Lee[1,]*
[1] Dept. of Computer Science and Networks, Kyushu Institute of Technology, Iizuka City, Fukuoka, Japan
Tel.:81-948-29-7699, E-mail: lee@cse.kyutech.ac.jp
[2] School of ICT, Robotics, and Mechanical Engineering, IITC, Hankyong National University, Anseong, Kyonggi-do, Republic of Korea

Red blood cells (RBCs) in patients infected with blood diseases such as malaria and sickle cell disease change the ratio of the cell surface to volume. Therefore, to diagnose the disease, the acquisition of a 3D profile of RBCs using digital holographic microscopy (DHM) has been studied by many researchers [1]. When we acquire a 3D profile of the RBC with DHM, there are several RBCs in the image. Thus, single cell extraction is required to analyze the details of individual RBC in the image and to identify the disease. For this reason, we propose a marker-controlled watershed segmentation to classify each RBC. Figure 1 illustrates the image processing of the proposed method. Using the calculated phase difference image, each RBC is segmented and numbered, and the volume and surface area of the separated RBCs are recorded. Besides, when we select one of the RBCs, it shows a 3D profile after phase unwrapping. Figure 2 shows the segmentation and numbering process of the proposed method. Using the proposed method, it is possible not only to obtain the volume and surface area of all the RBCs to be analyzed but also to visualize the 3D profile of the selected RBC at the same time.

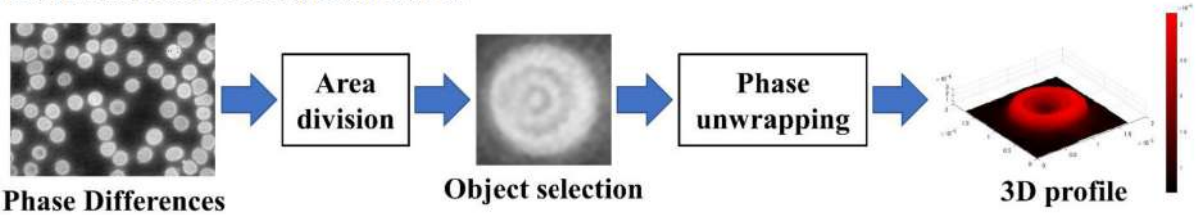

Fig. 1. Image processing of the proposed algorithm.

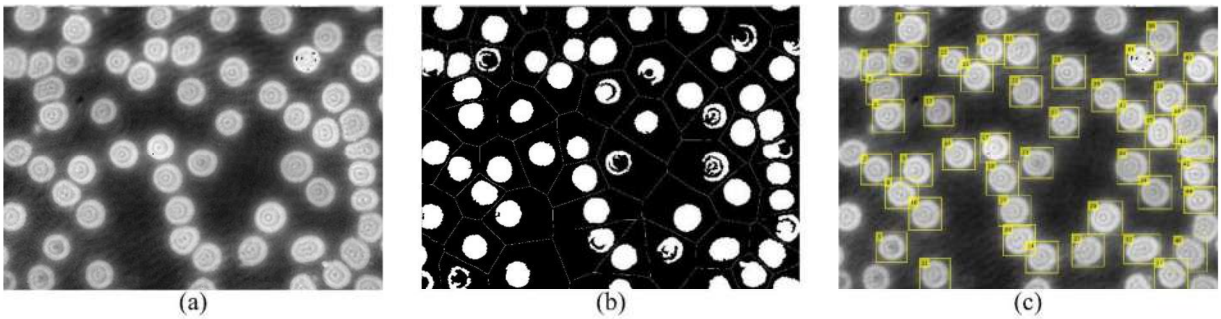

Fig. 2. (a) Phase differences (b) Area division using marker-controlled watershed segmentation (c) Result of the segmentation and numbering each specimen

Acknowledgment

This work was supported by the National Research Foundation of Korea(NRF) grant funded by the Korea government(MSIT) (NRF-2020R1F1A1068637).

Reference

1. B. Javidi, I. Moon and A. Anand, "Automated disease identification with 3D optical imaging," *2017 16th Workshop on Information Optics (WIO)*, Interlaken, 2017, pp. 1-2.

A study of digital holographic microscopy (DHM) using a Gaussian weighted sideband in the Fourier domain

Hyun-Woo Kim [1], Jiheon Lee[2], Myungjin Cho [2], Naoki Konishi [1], and Min-Chul Lee [1,]*
[1] Dept. of Computer Science and Networks, Kyushu Institute of Technology, Iizuka City, Fukuoka, Japan
Tel.:81-978-29-7699, E-mail: lee@cse.kyutech.ac.jp
[2] School of ICT, Robotics, and Mechanical Engineering, IITC, Hankyong National University, Anseong, Kyonggi-do, Republic of Korea

In image processing of the depth reconstruction in digital holographic microscopy (DHM), it is difficult to classify between the DC component and sideband by phase information [1]. In addition, the window size of the sideband depends on the high spatial frequency information of the specimen, since the wider window size is used the more specific object shape information can be obtained. However, as the window size increases, the noise is also heavy because of DC term in Fourier domain. To solve this problem, we use a Gaussian weighted sideband in Fourier domain. The proposed method windows the sideband as wide as possible and multiplies with the normalized Gaussian distribution to reduce the noise by DC term. Figure 1 (a) and (c) show the result by conventional method. On the other hand, Fig. 1 (b) and (d) show the result by proposed method. The result by proposed method shows that our method can reduce the noise by DC term more effectively than the conventional method. As a result, the proposed method can enhance the denoising effect in DHM.

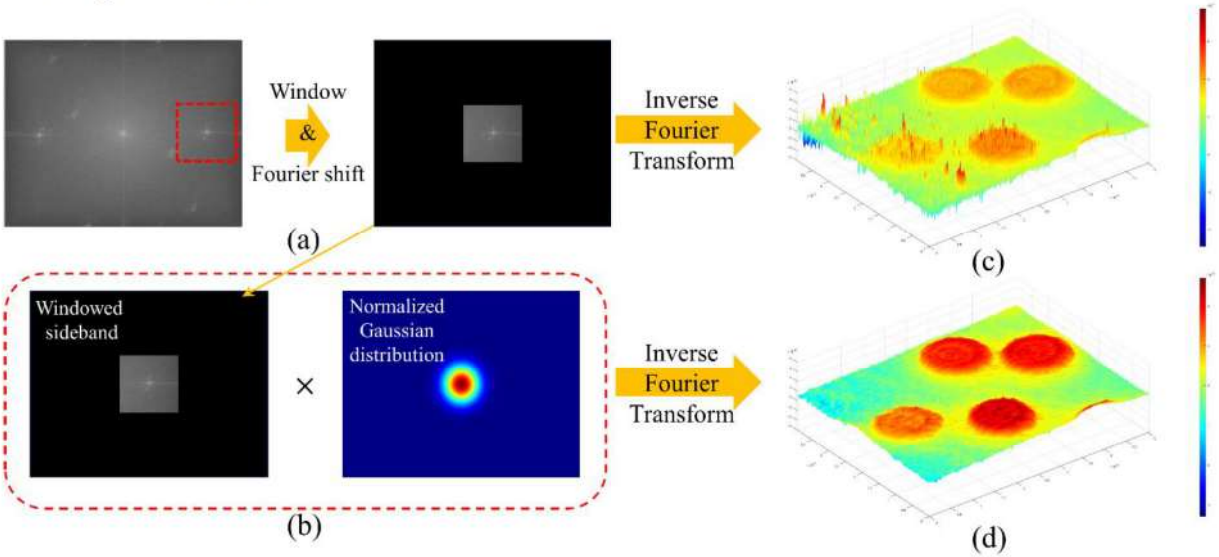

Fig. 1. Depth reconstruction process by (a) the conventional method and (b) the proposed method. (c) and (d) show the depth reconstruction result of (a) and (b), respectively.

Acknowledgment

This work was supported by the National Research Foundation of Korea(NRF) grant funded by the Korea government(MSIT) (NRF-2020R1F1A1068637).

Reference

1. K. Inoue, A. Anand, and M. Cho, "Angular spectrum matching for digital holographic microscopy under extremely low light conditions," Optics Letter Vol. 46, pp. 1470-1473 (2021)

VR Synchronization Using Muscle Activity Strain Textile Sensors

SangUn Kim[1], SeongMo Gu[2], EunJi Yeun[3] and JooYong Kim[1]
[1]Dept. of Smart Wearables Engineering, Soongsil Unviersity, Sangdo-dong, Seoul 156-743, Korea
Tel.:82-2-828-0631, E-mail:tkddnsl0723@naver.com
[2]Dept. of Organic Materials and Fiber Engineering, Soongsil Unviersity, Sangdo-dong, Seoul 156-743, Korea

In this research, we make textile sensors using the Piezo-resistive principle by impregnating, where SWCNTs-based conductive particles are positioned between textile matrix through entanglement, and when the matrix changes by strain, changes in resistance. To measure the resistance of the textile sensors to the strain, the strain-resistance graph was analyzed through the Universal Testing Machine (UTM). First, of VR synchronization, the muscle activity strain textile sensors are to measure the movement of human thigh muscle activity in standing, walking, running, sitting, and jumping for recognizing human behaviors. The trends of sensor values which were each behavior in real-time were analyzed through Arduino's Micro Controller Unit (MCU). Finally, for VR synchronization, VR production and Arduino-connected software Unity3D were used to get real human behaviors that were recognized sensor data trends through the serial communication with USB and synchronized the behaviors of characters.

Fig. 1. VR synchronization using Muscle activity strain textile sensors

Acknowledgment

This research was funded and conducted under 「the Competency Development Program for Industry Specialists」 of the Korean Ministry of Trade, Industry and Energy(MOTIE), operated by Korea Institute for Advancement of Technology (KIAT). (No. P0002397, HRD program for Industrial Convergence of Wearable Smart Devices)

References

1. C. C. Vu and J. Y. Kim, *Sensors and Actuators A: Physical*, vol. 283, p. 263 (2018).
2. C. C. Vu and J. Y. Kim, *Sensors*, 18(9), p.3109 (2018).
3. Z. H. Ma, W. Wang and D. Yu, *Energy Technology,* vol. 8(6), (2020).
4. J. l. Wang, C. H. Lu, K. Zhang, *Energy&Environmental Materials*, vol. 3(1), (2019).

One-way Observable Light-emitting Aero Signage Display Using Light Transmission Tube Which Enables to Make Transparent View from Back Side

Kunio Sakamoto and Suguru Monzen
Dept. of Intelligence and Informatics, Konan University, 8-9-1 Okamoto, Higashinada, Kobe 658-8501, Japan
Tel.:81-78-431-4341, E-mail: kunio@konan-u.ac.jp

You end up observing mirrored images of graphic signs when you watch light-emitting glass tubes from back. So our research group proposed passive light-emitting aero signage display which is floating in the air and enables to make transparent view from back side to avoid observing mirrored images in 2020. But this signage display has a defect that it emits no light itself and you cannot observe its signage in the dark night without another light source for illuminating surfaces of the signage display. This paper shows a one-way observable display for aero signage which enables to make transparent from back side and emits light itself using a lighting guide tube.

Fig. (a) shows the principle illustration of the light transmission guide using total internal reflection in optics. Here let consider a light ray passing from glass into air and assume that all light beams are in the material. An angle θ of this case is smaller than the critical angle. Then it is at this point no light is transmitted into air. And all beams pass only in a material because the beams are completely reflected. This is called the total internal reflection. The acrylic optical guide can pass through in only a material so that no light is transmitted into air using the total internal reflection phenomenon. Therefore light beams of the lighting guide tube illuminate the surfaces of signage attached with the guide tube. Fig. (b) shows the principle of our proposed one-way observable signage display using light transmission guide tube for self light emitting. The optical lens expands a slender colored line into the width $2r$ of lens' diameter for displaying images of the signage when the colored line is settled apart from the lens with the distance f of focal length (set at focal point). In expanding by a plano-convex lens, the relation of focal length f and curvature radius r is the approximate expression as follows; $f = r / (n - 1)$, where n is the refractive index of a lens material. If we could use a biconvex lens, it would be a convenient optical material for making a self light-emitting signage with a glass-like light tube.

In expanding by the biconvex lens, the relation of focal length f and curvature radius r is shown as follows; $f = r / 2(n - 1)$. If you assume that the light guide material is an acrylic tube, then the relation between focal length f and curvature radius r is approximately calculated as follows; $f = r$, because the refractive index of an acrylic is approximately $n = 1.5$. Then we can utilize the acrylic tube as a lighting guide tube on which a slender colored line is directly attached at the focal point of the biconvex lens. Therefore the authors can realize the one-way observable light tube signage which enables to make transparent from back side because the width of colored line is narrow than the diameter of transparent guide tube and you cannot perceive the narrow line apart long distance. Fig. (c) shows observed images of our trial unidirectional imaging display. You can confirm that '7' is the light-emitting signage and the color generating mechanism using a lighting guide material realizes the one-way observable imaging which enables to make invisible from back side.

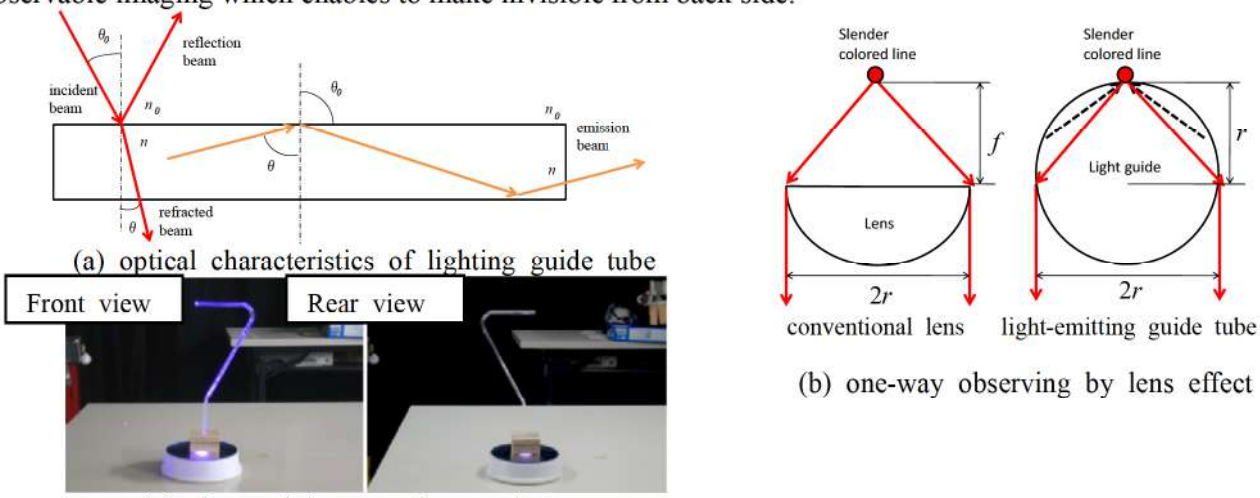

(a) optical characteristics of lighting guide tube

(b) one-way observing by lens effect

(c) observed images of aero signage

Fig. 1. One-way observable light-emitting aero signage using light transmission guide tube

SMA's power efficiency improvement plan using silver paste layer in lighter tactile realization VR device

Sang Jin Kim[1], Sang Un Kim[1], and JooYong Kim[1]
[1]**Department of Smart Wearable Engineering, SoongSil University, Sangdo-dong, Seoul 156-743, Korea**
Tel.:82-10-5114-7082, E-mail: dnu02075@naver.com

In last presentation, we suggested a method about lighter tactile VR device by using shape memory alloy. However, the longer the length and thickness of the feature memory alloys are, the greater the power consumption increases. This increase in power consumption will be a major problem in VR devices where wireless and lightweight are important. In this presentation, we decided to construct another heating layer to overcome these shortcomings of SMA. Sliver paste can be used at heating source and can be heated quickly at low voltages. So we would like to use silver paste to make heating layer for shape memory alloys. The material used to make the heating layer is DM-SIP2001 of Dycotec Materials, they are flexible, so they are better than other paste when making gloves that require stretchable flexibility.

We made a sample printed with silver paste where shape memory alloy will be located as shown in Fig. 1. And we prepared a shape memory alloy with a diameter of 0.5mm about 800mm, which is similar to the length of the heating layer. The prepared heating layer and shape memory alloy were supplied using a power supply to reach temperatures of 50 degrees Celsius, and the magnitude of the voltage and current applied was determined.

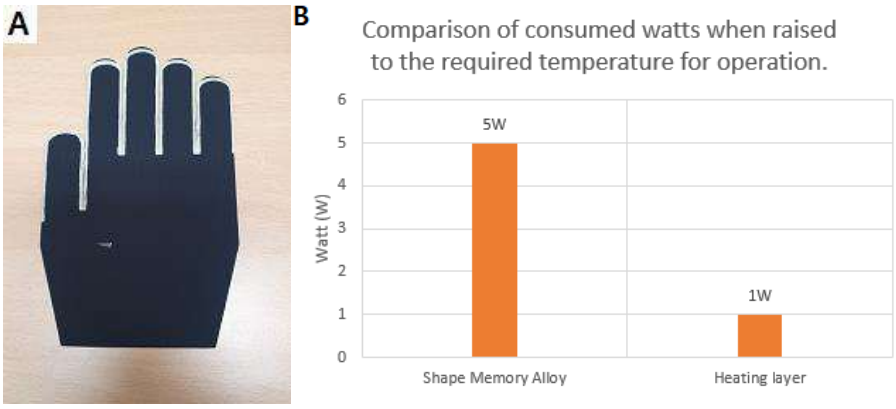

Fig. 1. A. Heating layer sample(printed with silver paste) and B. Graph of Comparison of consumed watts when raised to the required temperature for operation

As you can see at fig.1. B, the shape memory alloys were found to have a surface temperature of 35 with a current of 1A when 5v was applied, while the sample confirmed that a current of 0.2A when 5v was applied and a temperature of 40 degrees.

Using of heating layer, we will be free to deploy the configuration memory alloys and will be able to develop more efficient products.

Acknowledgment

This Presentation was supported by Korea Institute for Advancement of Technology(KIAT) grant funded by the Korea Government(MOTIE) (P0012770)

References

1. Ming H. Wu and L. McD. Schetky, Industrial applications for shape memory alloys, Proceedings of the International Conference on Shape Memory and Superelastic Technolgies, P.171-182 (2000).
2. Jaronie Mohd Jani, Martin Leary, Aleksandar Subic, Mark A. Gibson, A review of shape memory alloy research, applications and opportunities, Materials & Design Volume 56, April 2014 (1078-1113)
3. Jing-Han Guan, Yong-Chen Pei, and Shun Wang, Jilin University, CrossMark (2020)
4. Siqi Zhao, Bowen Li, Tengfei Li, Chenghao Deng, Guangxi University, Springer (2020)

Real-time 3D Rendering and Eye-tracking for High Resolution Light Field 3D Display

Rang Kyun Mok[1], Hyun Jin Cho, Su Bin Jung and Beom Shik Kim
[1]Display Research Center, Samsung Display Co., LTD., Giheung-Gu, Yongin-Si, Gyeonggi-Do, Korea
Tel.:82-31-5181-6594, E-mail: rk.mok@samsung.com

We have been studying Light Field (LF) 3D display for several years, starting from the question 'why do we need 3D Display'. The real life we see is 3-dimensional environment which can't be seen with the 2D technology. It is a human instinct to want to see a stereoscopic environment like reality on Display. Recently, various technologies that can greatly improve 3D performance have been developed rapidly. CPU / GPU performances have been greatly improved, and the number of cameras that can be obtained in various 3D object sources, and a large amount of image sources are sufficiently transportable by 5G. JPEG and MPEG are developing 3D and Hologram standards in 2022.

In this paper, a high-resolution and wide-viewing angle Volumetric LF display is proposed to confirm the limit of 3D technology. In order to implement realistic 3D, the 3D resolution was greatly improved (2.5 times ↑) more than 202.4PPI (existing < 80PPI) and the narrowed viewing angle was expanded to 60 ° or higher using Eye-tracking. In order to implement a volumetric environment, the 3D depth was maximized using high refractive index Half-Mirror Cube. Eye-tracking and 3D rendering system were processed using Unity 3D tools. The driving rate is more than 20fps that has greatly improved (2.5 times ↑) compared to the existing 8fps. The display panel used was Galaxy S10, 6.11 ", 550PPI (3040x1440) OLED. The lens design used a technique of placing in both eyes in the side-lobe to implement high resolution LF. The designed LF optical characteristics were 440mm viewing distance, 6 ° viewing angle, 16 viewpoints, 9.46 ° Slanted Angle Lens and 2.7mm viewpoint interval.

For the first time in the world, we have combined LF technology with volumetric augmented reality technology to create a high-resolution 3D stereoscopic image. We confirmed the possibility of LF display by high resolution LF in real-time rendering.

In the future, LF technology will be applied to various fields such as large stereoscopic displays and automotive 3D displays as well as high resolution and wide viewing angle.

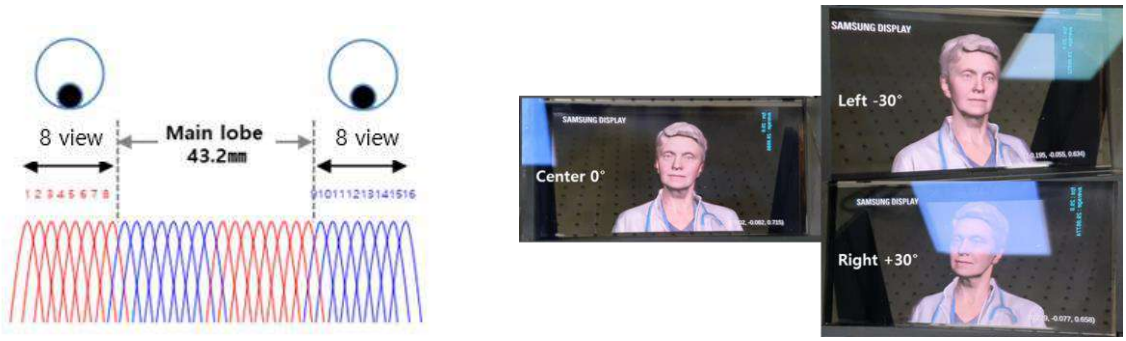

Fig. 1. Lens desing using Side-lobe and 3D rendering LF display in real time

References

1. Kajiki,Y. ,Yosikawa,H., Honda,T. Ocular Accommodation by Super Multi-View Stereogram and 45-View Stereoscopic Display, *in Proceedings of The Third International Display Workshops (IDW'96),* Vol.2, p. 489-492 (1996)
2. Min-Sung Uk, Light Field 3D Display, *Telecommunications Technology Association,* Special Report 6
3. JS Hong, Computational Methods for Light Field Displays, *KETI (2017)*
4. C Van Berkel et al, Design and Applications of Multiview 3D-LCD, *Proc SID Euro-Display96, pp 109~112*
5. BH Lee et al, Design and Implementation of Autostereoscopic Displays, *SPIE Press Book*

A Study on 3D Pixel for High-definition 3D Display

Young-Sang Ha, Beom-shik Kim, Jae-Joong Kwon and Young-Chan Kim
Advanced Research Team, Samsung Display, Yongin-si, Gyeonggi-do 17113, Korea
Tel.:82-31-5181-6667, E-mail: y.ha@samsung.com

Among the methods for implementing a glassless 3D display, light field display (LFD) is one of the methods that combines a panel and a lenticular lens array (LLA) to produce three-dimensional images. In order to improve the quality of 3D images in LFD, the LLA designed to tilt at a specific angle for minimizes the moiré visibility to the display panel. But the image quality level of 3D images displayed in 3D is significantly lower than that of 2D because of the asymmetric form of 3D pixel (Fig. 1). As this is one of the problems that must be overcome for commercialization of LFD, new 3D pixel design is needed to improve 3D image quality. Therefore, the present paper proposes an optimal 3D pixel design for implementing a high-definition 3D display and a pixel design of a panel dedicated to LFD. Through the test, the current level of LFD developed using the existing 2D dedicated panel was analyzed and the virtual 3D Pixel was implemented to study the optimal pixel design of the 3D dedicated panel (Fig. 2). In summary, the present paper analyzes the asymmetric 3D pixel, which is the cause of the degradation of the stereoscopic image quality of the existing LFD through cognitive evaluation, and derives the optimum 3D pixel shape through the analysis results, and propose RGB and diamond pixel structure for implementing optimum 3D pixel.

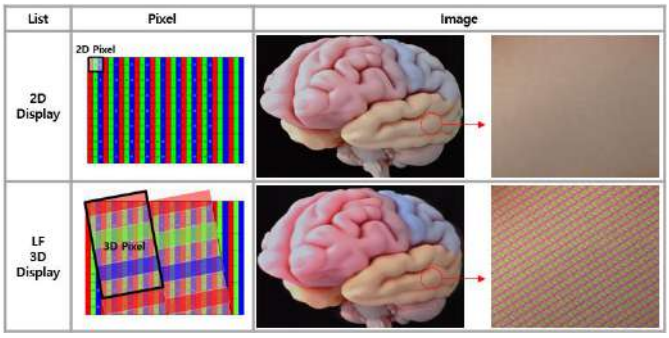

Fig. 1. 2D, 3D pixel structure and moiré pattern.

Pixel Form	Asymmetry	Symmetry
Pixel Angle	0°, 9.46°, 90°	
Font Image		

Fig. 2. Parameters for virtual 3D pixel evaluation.

References

1. G. Wu, B. Masia, A. Jarabo, Y. Zhang, L. Wang, Q. Dai, T. Chai, Y. Liu, *IEEE J. Sel. Topics Signal Process*, 11(7), 926 (2017).
2. M. Kim, S. Lee, C. Choi, G. M. Um, N. Hur, J. Kim, *IEEE 3DTV-CON'08The True Vision –Capture, Transmission and Display of 3D video*, p. 181(2008).

Development of rewritable hologram with high efficiency azobenzene polymer optimized for green-laser

Kyung-Il Joo[1], Hye Ju Kang[2], Seon Kyu Yoon[1], Kwang-Hoon Lee[1], Jae-Won Ka[2], and Hak-Rin Kim[3,]*
[1]Spatial Optical Information Research Center, Korea Photonics Technology Institute, Gwangju 61007, Korea
[2]Advanced Functional Polymers Research Center, Korea Research Institute of Chemical Technology, Daejeon 34114, Korea
[3]School of Electronic and Electrical Engineering, Kyungpook National University, Daegu 41566, Korea.
*Tel.:82-53-940-8622, E-mail: rineey@knu.ac.kr

Holographic display is an ultimate three-dimensional(3D) display capable of resolving the vergence-accommodation conflict(VAC) problem pointed out in an auto-stereoscopic 3D display [1]. Holographic display can be divided into analog-hologram and digital-holographic display depending on the operating principles. Digital-holographic display can implement the real-time holographic video, but in order to be applied to various applications, the viewing angle characteristics caused by the technical limitation of the spatial light modulator(SLM) must be improved. The analog-hologram display can reproduce the almost same quality of holographic images compared with the real 3D objects based on the high resolution and full color recording capabilities of the holographic recording material. However, analog-hologram recording material has a weak point about the image updating capability due to the analog-hologram recording materials can not rewritable. Rewritable holographic display is a promising research topic that is recognized as an ideal holographic display technology because it has the high resolution characteristics of an analog-hologram and can optically or electrically update the holographic images [2,3]. In this study, the rewritable hologram recording material optimized for green wavelength laser (λ=532 nm) was synthesized based on photo-isomerizable azobenzene polymer, and holographic updating characteristics were confirmed for rewritable hologram display application. Finally, a rewritable holographic display system was developed by using polarization interference scheme.

Fig. 1(a) shows the chemical structure of the rewritable hologram recording material synthesized in this paper. In order to obtain high diffraction efficiency under low optical power illumination condition, an acetylene group was added for inducing high birefringence. Fig. 1(b) shows the measurement result of diffraction efficiency characteristics by using the obtained azobenzene polymer. It was confirmed that the diffraction efficiency was improved by about 160 % under the 10% optical energy illumination condition compared to the previously reported rewritable hologram recording materials [4].

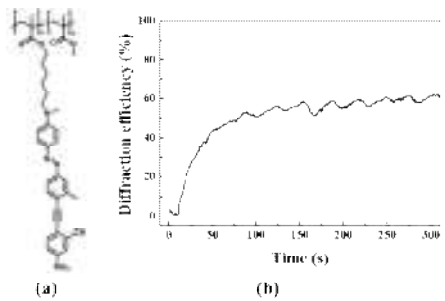

Fig. 1. (a) Chemical structure of the synthesized azobenzene polymer, (b) The measured diffraction efficiency result with azobenzene polymer

Acknowledgment

This work was supported by Institute of Information & communications Technology Planning & Evaluation (IITP) grant funded by the Korea government(MSIT) (No.2020-0-00997, Development of hologram reconstruction and measurement inspection authoring module technology)

References

1. H. Yu, K. Lee, J. Park, and Y. Park, *Nat. Photon.,* 11, 186-198 (2017).
2. N. Peyghambarian, et al., *Nature,* 451, 694-698 (2008).
3. N. Peyghambarian, et al., *Nature,* 468, 80-83 (2010).
4. R. Kirby, R. G. Sabat, J. M. Nunzi, O. Lebel, *J. Mater. Chem. C,* 2, 841-847 (2014).

Impact of Partial Masking Black Matrix on Lenticular Lens Array Film for High Quality Multiview 3D Display Image

Jeong Woo Park, Hyun Jin Cho, Beom-Shik Kim, Su-bin Jeong, Young-chan Kim, and Seong-Chan Cho
Display Research Center, Samsung Display Co.,Ltd., Giheung-gu,Yongin-city, Gyeonggi-do, Korea
Tel.:82-31-5181-6597, E-mail: jwjohn.park@samsung.com

One of the main hurdle for developing high-quality multiview three-dimensional (3D) displays, crosstalk [1-3], which is caused by the partial interference of each viewing point image channel was significantly reduced by partial masking at the valley line on lenticular lens array film surface. It has been known that the 3D display image's crosstalk was reduced by the hardware based technology [4-5] and or software based technology [6-7]. Especially, calibration algorithm that compensates for misalignment between two-dimensional (2D) display panel and lenticular lens array film layer based on software technology was a good candidate for minimizing the physical alignment error of 2D display panel and lenticular lens array film layer [8]. Even though the software based image processing technologies are powerful and physical alignment of 2D display panel and lenticular lens array film layer is perfect, the inherent crosstalk problem caused by the spherical aberration from the lenticular lens films' shape still exists.

In this study, we proposed a partial masking of lenticular lens surface design and attempted the masking process at the valley line within the structure of lenticular lens surface. Direct jetting process with Black Matrix (BM) ink was done and regular BM pattern line was realized at the valley line within the structure of lenticular lens film. Improved image quality was shown in fig. 1 (b) and especially positive/negative depth image blurring (dot circles) were almost disappeared by the partial masking of BM ink, suggesting that the partial masking of lenticular lens surface design is the promising method for minimizing the crosstalk of 3D displays.

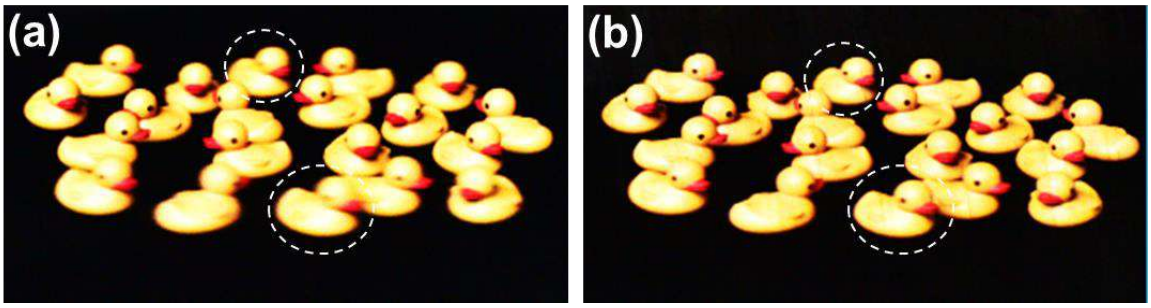

Fig. 1. (a) Reference 3D image. (b) Partial masking BM applied 3D image. Top area and bottom area within 3D image display negative depth expression and positive depth expression, respectively. (A flock of duck image was provided by E.B.S)

References

1. L. Xing, J. You, T. Ebrahimi, and A. Perkis, "Assessment of stereoscopic crosstalk perception," *IEEE Transactions on Multimedia*, vol. 14, no. 2, pp. 326–337, 2012.
2. A. J. Woods, "Crosstalk in stereoscopic displays: a review," J. Electron. Imaging 21(4), 040902 (2012).
3. P. J. H. Seuntiëns, L. M. J. Meesters, and W. A. IJsselsteijn, "Perceptual attributes of crosstalk in 3D images," Displays 26(4–5), 177–183 (2005).
4. M. Zhou, H. Wang, W. Li, S. Jiao, T. Hong, S. Wang, X, Sun, X. Wang, J. Y. Kim, and D. Nam, "A unified method for crosstalk reduction in Multiview displays," Journal of Display Technology, vol. 10, no. 6, pp. 500-507, 2014.
5. J. Park, D. Nam, G. Sung, Y. Kim, D. Park, and C. Kim, "Active crosstalk reduction on multi-view displays using eye detection," SID Symposium Digest of Technical Papers, vol. 42, pp.920-923, 2011.
6. Y. C. Chang, C. Y. Ma, and Y. P. Huang, "Crosstalk suppression by image processing in 3D display," SID Symposium Digest of Technical Papers, vol. 41, pp.124-127, 2010.
7. J. S. Lipscomb and W. L. Wooten, "Reducing crosstalk between stereoscopic views," IS&T/SPIE 1994 International Symposium on Electronic Imaging: Science and Technology, pp. 92-96, 1994.
8. Kim J., Lee G., Eum H., Shin H.C., Park Y., Seo J. "Iterative calibration of a multiview 3D display with linear extrinsic crosstalk using camera feedback" Appl. Opt., 57 (2018), pp. 4576-4582.

Distortion Correction in Tomographic Near-Eye Displays with Light Field Optimization

Siwoo Lee, Seungjae Lee, Dongyeon Kim, and Byoungho Lee
School of Electrical and Computer Engineering, Seoul National University
Gwanak-Gu Gwanakro 1, Seoul, 08826, Korea
Tel.:82-2-880-7245, E-mail: byoungho@snu.ac.kr

Recently, the tomographic near-eye display, the system which alleviates vergence accommodation conflict (VAC) by providing a quasi-continuous depth cue, has been introduced [1]. However, the magnification varies relative to the depth of virtual planes in near-eye display systems if eye relief exists. This change in magnification causes defects, which appear when the image is not depicted in the areas where the depth of the image is discontinuous. Since a specific range of eye relief needs to be guaranteed due to the user's face structure or the additional placement of eyeglasses, these defects should be mitigated.

This paper suggests a novel optimization algorithm that considers magnification variations in near-eye display systems, alleviating defects due to magnification variations. The system expresses 80 depth planes from 5.5 diopters (D) to 0D with 0.07D separations using a display panel, a digital micromirror device (DMD), and a focus-tunable lens. The backlight sequences and a display image are optimized according to the magnification of each depth to reproduce the original light field.

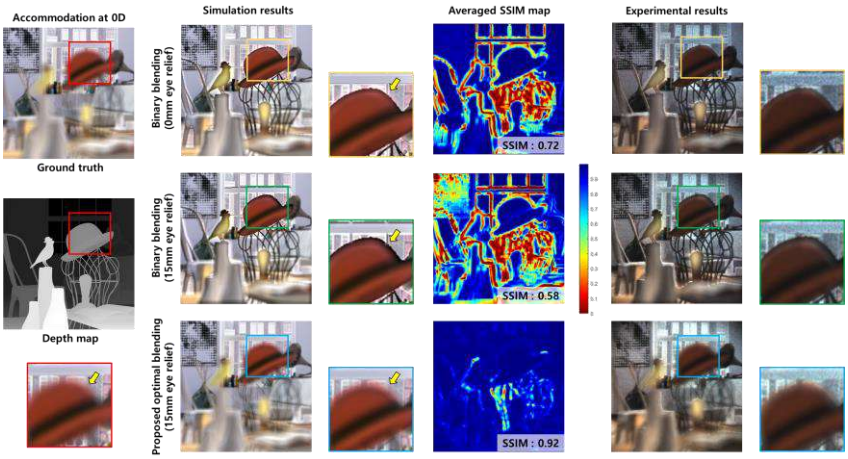

Fig. 1. The simulation and experimental results with room scenes focused on 0D

Fig. 1 illustrates the simulation results and experimental results focused on 0D with an eye relief of 0mm and 15mm. Distortion due to magnification differences between virtual image planes is observed where the depth changes significantly (green box). The averaged structure similarity index metrics (SSIMs) of the simulation results compared to the ground truth demonstrate that the distortion corrected image is reproduced with the proposed optimization.

We confirm that the proposed optimization compensates the magnification variations, which induce defects. We expect this optimization to be applied to other tomographic display systems [2] and near-eye display systems.

Acknowledgment

This work was supported by the Institute for Information and Communications Technology Promotion Grant funded by the Korea Government (MSIT) (Development of vision assistant HMD and contents for the legally blind and low visions) under Grant 2017-0-00787.

References

1. S. Lee, Y. Jo, D. Yoo, J. Cho, D. Lee, and B. Lee, *Nature Comm.*, 10(1), 2497 (2019).
2. D. Yoo, S. Lee, Y. Jo, J. Cho, S. Choi, and B. Lee, *IEEE Transactions on Visualization and Computer Graphics*, (2020). Doi: 10.1109/TVCG.2020.3011468

Analysis on underestimation of eye-box measurements in near-to-eye displays with considering rotation center of eye

Sehwan Lim, Kwang-Soon Choi, and Jiwoon Yeom
Korea Electronics Technology Institute, World cup buk-ro 54-gil, Mapo-gu, Seoul 03924, Korea
Tel.:82-2-6388-6680, E-mail: jiwoon.yeom@keti.re.kr

The near-to-eye dispays (NEDs) are promising for the applications of augmented and virtual reality. Most of measurement methods for NEDs have been investigated with the light measuring devices (LMDs), where the rotation center of LMDs were assumed as the entrance pupil [1]. However, considering the practical movement of the eye-ball, the rotation center for measuring the optical properties of NEDs should identical to the eye center. The rotation center for the LMDs recommended by the international electrotechnical commission (IEC) is two points : the entrance pupil corresponding to the iris of human eye, and the eye center which is 10 mm from the iris to the inside [2]. However, when one measures the eye-box of NEDs at aformentioned two standard points, the results show a significant difference. In Fig.1, case 1 is the entrance pupil rotation and case 2 is the eye center rotation. Unlike the rotation of the entrance pupil, the rotation of the eye center leads the entrance pupil of LMD to move Δy , Δz from the center of the eye-box. In this case, the evaluated eye-box in case 2 is underestimated compared to the case 1. In order to correct the underestimated eye-box measured according to case 2, with rotating the LMD by the field of view(FOV) as proposed in Ref. [2], the position of LMD should be corrected by Eq. (1).

$$\Delta y = \alpha \times sin\left(\frac{FOV}{2}\right), \Delta z = \alpha \times \left[1 - cos\left(\frac{FOV}{2}\right)\right], \quad (1)$$

where α is the distance between the eye center and the iris in the human eye, and assumed to be 10 mm [2].

Figure 2 presents the different evaluation values for the eye-box measurements accoridng to the FOV of NEDs. In square point in Fig. 2, is the previously measured data of Galaxy Gear VR[3]. The dashed line is case 1 representing the relationship between the eye-box and FOV. From the solid line in Fig. 2, when the LMDs was rotated considering the eye center, the evaluated eye-box size is found to be underestimated due to the pupil shift of LMD during the rotation like case 2. The difference between the dashed line and solid line indicates the size of the error, ε, as expresses in Eq. (2). By adding an ε according to the FOV, measurement error can be corrected, even though the LMD measuring by eye center.

$$\varepsilon = 2 \times \alpha \times tan\left(\frac{FOV}{2}\right) \quad (2)$$

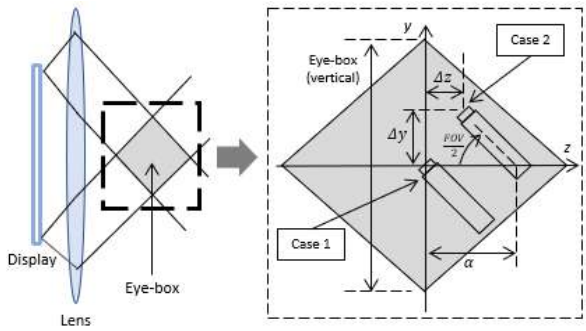

Fig. 1. Entrance pupil position by rotation center

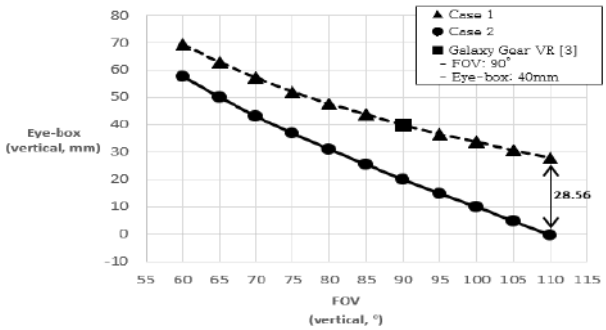

Fig. 2. Eye-box graph by FOV

Acknowledgment

This work was supported by Korea Institute for Advancement of Technology (KIAT) grant funded by the Korea government (the Ministry of Trade, Industry and Energy(MOTIE)) (No.P0014183, Establishment on the Empirical Grounding for AR/VR Device And Service)

References

1. X. Mou, C. Xu and T. Mou, SID. SID Symp. Dig. 48, 1579-1580 (2017).
2. IEC, 63145-20-10, (2019).
3. K. Tsurutani, K. Naruse, K. Oshima, S. Uehara, Y. Sato, K. Inoguchi, K. Otsuka, H. Wakemoto, M. Kurashige, O. Sato, M. Cho, S. Ouchi and H. Oka, SID Symp. Dig. 48, 954-957 (2017).

Hologram synthesis method based on ray-tracing rendering for holographic stereogram printing

Erkhembaatar Dashdavaa[1], Chang-Won Shin[1], Hui-Ying Wu[1], Seong Gyoon Park[2], Jung-Jae Ko[3] and Nam Kim[1]*
[1]School of Information and Communication Engineering, Chungbuk National University, Cheongju-si, Chungbuk 361-763, South Korea
[2]Department of Information and Communication Engineering, Kongju National University, 1223-24 Cheonandae-ro, Seobuk-gu, Cheonan, Chungnam 31080, South Korea
[3]Department of Industrial Artificial Intelligence, Chungbuk National University, Cheongju-si, Chungbuk 361-763, South Korea

[*]Tel.:+82-43-267-8490, E-mail: namkim@chungbuk.ac.kr

Holography is a two-step technique that is used to record and reconstruct the intensity and phase information of a wavefront scattered from a three-dimensional (3D) object [1]. In the recent years, the holographic printers have attracted researcher's attention as a technique to visualize 3D holographic content. The 3D virtual models can be easily printed by holographic printer system [2, 3]. Of the various holographic representations, the holographic stereogram (HS) is the most common incoherent reconstruction technique. The HS printer records a set of two-dimensional (2D) parallax-related images created from an array of perspective projections of a 3D scene [4]. In this paper, we report on two main tasks in the development of hologram synthesis method for 3D rendering of computer-generated HSs acquired from light field data. One task is to adopt ray-tracing technique for the rendering of perspective images to improve the depth illusion afforded by holographic stereogram. Another task is an improvement on angular resolution without increasing hogel size, overcoming the spatial-angular resolution tradeoff that existing HS algorithms face. Figure 1 presents the schematic configuration of the hologram synthesis technique for holographic stereogram printing.

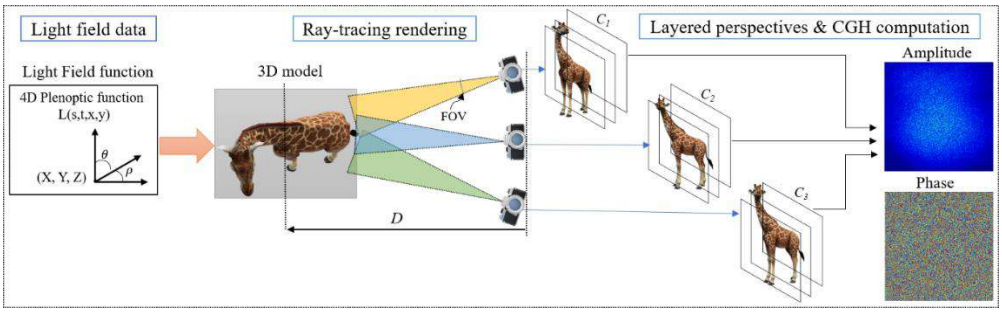

Fig. 1. Schematic configuration of the HS synthetization process.

Acknowledgment

This work was supported by Institute of Information & Communications Technology Planning & Evaluation (IITP) grant funded by the Korea government (No. 2020-0-00929, (General) Development of Digital Hologram Window Reconstruction, (Sub1) Development of Authoring Tool for Digital HOE Hologram Generation Using Optical Simulation) and the MSIT (Ministry of Science and ICT), Korea, under the ITRC (Information Technology Research Center) support program (IITP-2020-0-01846) supervised by the IITP (Institute of Information & Communications Technology Planning & Evaluation).

References

1. N. Kim, Md. A. Alam, L. T. Bang, A. -H. Phan, M. -L. Piao and M. -U. Erdenebat, *Chin. Opt. Lett,* 12, 060005 (2014).
2. K. Hong, S. -G. Park, J. Yeom, J. Kim, N. Chen, K. Pyun, C. Choi, S. Kim, J. An, H. -S. Lee, U. -I Chung and B. Lee, *Opt. Exp*, 21, 14047-14055 (2013).
3. E. Dashdavaa, A. Khuderchuluun, H. -Y. Wu, Y. -T. Lim, C. -W. Shin, H. Kang, S. -H. Jeon and N. Kim, *Appl. Sci*, 10, 8088 (2020).

Design Method of Freeform Holographic Mirror for Near-Eye Display

Songhyun Lee, Chanhyung Yoo, Kiseung Bang, and Byoungho Lee
School of Electrical and Computer Engineering, Seoul National University, Gwak-Gu, Seoul 08826, Korea
Tel.:82-2-880-9570, E-mail: byoungho@snu.ac.kr

For augmented reality (AR) near-eye display, holographic mirrors have been widely studied [1]. When using a photopolymer film as a holographic mirror for a near-eye display, it has the advantage of a compact form factor due to the photopolymer film's thinness and transparency. However, astigmatism and other optical aberrations become a problem.

In order to correct the aberration due to the horizontal off-axis, a previous study presented a method of using a cylindrical lens in the signal beam path during the recording process [2]. In this study, to correct more aberrations and provide a wider eyebox, we place a phase plate in the signal beam path to design the recording optical system for holographic mirror.

We performed the phase optimization of the plate using Zemax, a commercial ray-tracing-based simulation tool. To express the phase, the Zernike coefficient was used. The Zernike coefficients up to the 15th order were set as a variable. The size of the used holographic mirror is 20 mm diameter circle, the eye relief is 25 mm, and the eyebox is set to a 10 mm diameter circle. In the recording process, a reference beam diverges from the point, which is at a distance of 152.403 mm and 30° from the HOE plane. A signal beam passes through the phase plate and is incident perpendicularly on a HOE plane. As a floating lens, a convex lens with a diameter of 0.5 inches and a focal length of 19 mm is used.

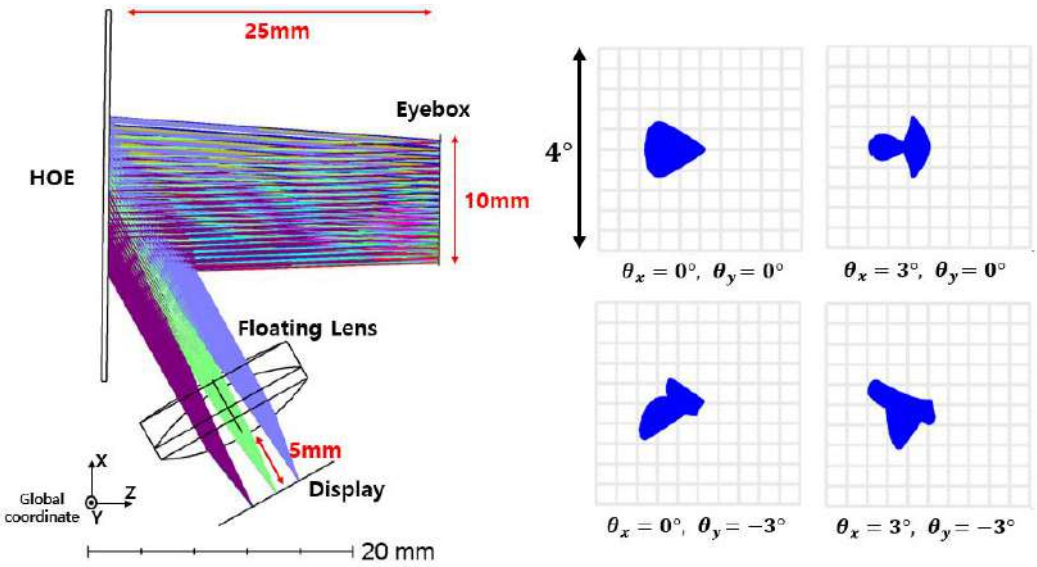

Fig. 1. (Left) Simulation layout. (Right) Spot diagram of rays' angles of incidence on the eyebox.

As a result of optimization, RMS radius of point spread function was 0.459° when the horizontal vewing angle (H) was 0°, and the vertical vewing angle (V) was 0°. In another condition, RMS radius was 0.431° (H:3°, V:0°), 0.472° (H:0°, V:-3°), 0.460° (H:3°, V:-3°), as shown in Fig. 1.

Acknowledgment

This work was supported by Institute of Information & Communications Technology Planning & Evaluation(IITP) grant funded by the Korean government(MSIT) (No.2020-0-00970, (Sub2) Development of hologram HUD display technology for high efficiency commercial vehicles).

References

1. C. Yoo, K. Bang, M. Chae, and B. Lee, *Opt. Lett.* 45(10), 2870-2873 (2020).
2. S. Lee, B. Lee, J. Cho, C. Jang, J. Kim, and B. Lee, *IEEE Photon. Technol. Lett.* 29(1), 82-85 (2017).

Deep learning and hologram compression

Juhyun Lee[1] and Byoungho Lee[1]
[1]Dept. of Electrical and Computer Engineering, Seoul National University, Seoul 08826, Korea
Tel.:82-2-880-9570, E-mail: byoungho@snu.ac.kr

A holographic display is in the spotlight as a next-generation display since it can reconstruct a 3D object by modulating the wavefront of light. A computer-generated hologram is the interference pattern uploaded on the holographic display and reproduces object light. Conventionally it is calculated by numerical propagation model accompanied by large computational load, so a high-performance computer is required. However, holographic displays are evolving in the form of a head-mounted display (HMD) currently, and there is an issue of hardware's weight. Therefore, it is not easy to install hardware capable of high-performance computing, such as graphics processing units. While many studies are conducted to reduce hologram generation computation using deep learning technology [1-3], it has not been confirmed enough whether these networks work effectively in low computing environments such as HMD systems. In this paper, we propose an idea of a holographic compression using deep neural network of encoder-deconder architecture We predict it may replace holographic generation tasks with decompression tasks which has lighter computations. The performance of the proposed network is demonstrated through numerical simulation.

The encoder has two convolution layers for down-sampling, and eight more for residual calculation. The decoder has two convolution layers for up-sampling, and the last output layer consists of one convolution layer. Every convolution layer except the last layer has a batch normalization layer and a rectified linear unit. The last convolution layer has a hyperbolic tangent as the nonlinear function limiting the pixel value between -1 and 1. Dataset is composed of two holograms consisting of real and imaginary parts, and the input and target are the same. We created the artificial intensity maps by referring to our previous study's dataset, the multi-depth hologram generation network [3]. Complex holograms are generated using the angular spectrum method (ASM). The target holographic display's pixel pitch and the resolution are set to 8 μm and 512 pixels, and the light source has wavelength of 532 nm. Five depth planes are assumed to be equally spaced, the plane closest to the observer is 15 mm away from the holographic display, and the farthest plane is 5 mm away. Figure 1 is a reconstructed image of ASM-based CGH and hologram compressed and decompressed by the proposed network. In the reconstruction simulation, we used ASM as a numerical propagation model.

In conclusion, we proposed a deep neural network for hologram compression. The proposed network is in the form of an encoder-decoder, and by using it, the high-performance computers and HMD system can quickly transmit and receive high-quality holograms.

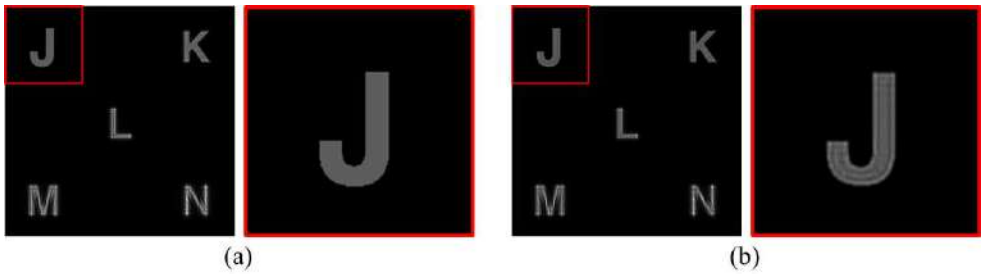

Fig. 1. Reconstruction result of (a) ASM-based CGH and (b) hologram decompressed by the proposed network

Acknowledgment

This work was supported by Institute of Information & Communications Technology Planning & Evaluation (IITP) grant funded by the Korean government (MSIT) (No.2020-0-00548, (Sub3) Development of technology for deep learning-based real-time acquisition and pre-processing of hologram for 5G service).

References

1. R. Horisaki, R. Takagi, and J. Tanida, *Appl. Opt.*, 57(14), 3859-3863 (2018).
2. Y. Peng, S. Choi, N. Padmanaban, J. Kim, and G. Wetzstein, *SIGGRAPH '20*, 8, (2020).
3. J. Lee, J. Jeong, J. Cho, D. Yoo, B. Lee, and B. Lee, *Opt. Express*, 28(18), 27137-27154 (2020).

Occlusion-Capable Augmented Reality Display with Reduced Size and Expanded Field of View

*Minseok Chae, Kiseung Bang, Youngjin Jo, Dongheon Yoo and Byoungho Lee**
Dept. of Electrical and Computer Engineering, Seoul National University, Seoul 08826, Korea
Tel.:82-2-880-9570, E-mail: byoungho@snu.ac.kr

Occlusion-capable augmented reality displays (OCARDs) can improve the contrast and the depth perception of the virtual scene by blocking the light from the real scene with an occlusion mask [1]. To realize a sharp occlusion, most studies on OCARD use a 4-f system which forms the image of the real scene, and place an occlusion mask on the imaging plane. Since a 4-f system rotates the real scene by 180°, an additional 4-f system is required to restore the real scene. Hence, the overall size of such OCARDs are too bulky up to tens of centimeters. Although the bulky size can be reduced by using lens arrays for imaging the real scene, the field of view (FoV) gets limited to few degrees by the low numerical aperture of the lenslets [2].

In this paper, we introduce an OCARD with a reduced size and expanded FoV. We simulate and build the system using two lens arrays for imaging the real scene. We install a concave-convex lens pair on the front and rear focal plane of the lens arrays to expand the FoV. Without the concave-convex lens pair, the ray with a high incident angle cannot be transferred by the lens arrays. The concave lens in front of the system lowers the high incident angle of the ray. After propagating through lens arrays, the ray meets the convex lens and its initial incident angle is restored. Therefore, the high incident angle can be transferred and the FoV is expanded. Also, we apply the optical folding structure to further reduce the system size. This structure is composed of the right circular polarizer, a half mirror, a quarter-wave plate, and a polarizing beam splitter [3]. This structure reduces the physical size of the system while maintaining the optical path length. Since the light propagates the same lens array three times, fewer lens arrays and space are required. The schematic diagram and the experimental result of the proposed system are as follows.

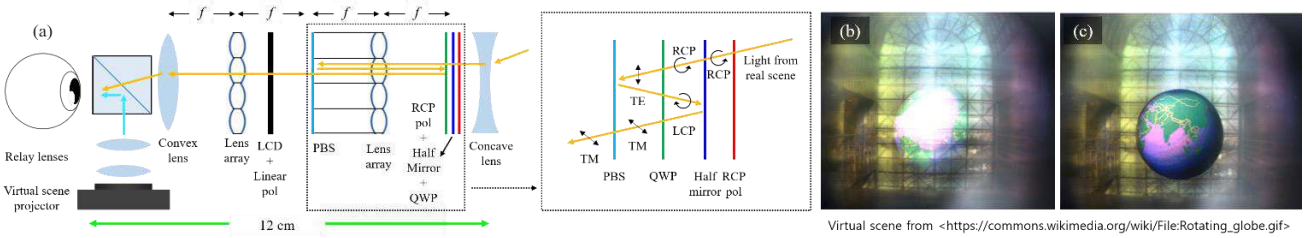

Fig. 1. Schematic diagram of the proposed system (a) and the experimental result without the occlusion (b) and with the occlusion (c).

The lens arrays have a focal length of 16.9 mm and 4 mm horizontal pitch. The focal length of the concave-convex lens pair is ± 40 mm. The OCARD with lens arrays only has a system length of 20 cm and a limited FoV of 11.5°, while the proposed system with the same lens arrays has a reduced size of 12 cm and the observable maximum FoV is expanded up to 40.4°. The contrast of the virtual scene is highly improved and the depth information became prominent by the occlusion of the proposed system, as shown in Fig. 1(c). Throughout the study, we confirmed the feasibility of the proposed system to be applied to more compact and wide-FoV AR displays.

Acknowledgment

This work was supported by Institute of Information & Communications Technology Planning & Evaluation(IITP) grant funded by the Korean government(MSIT) (No. 2017-0-00787, Development of vision assistant HMD and contents for legally blind and low visions)

References

1. B. Lee, C. Yoo, J. Jeong, B. Lee, and K. Bang, *Proc. SPIE Advances in Display Technologies X*, vol. 11304, 1130402 (2020).
2. Y. Yamaguchi, and Y. Takaki, *Appl. Opt*, 55(3), A144-A149 (2016).
3. K. Bang, Y. Jo, M. Chae, and B. Lee, *IEEE Trans. Vis. Comput. Graph.*, doi:10.1109/TVCG.2021.3067758 (2021).

Horizontal field of view enhancement of a waveguide-type near-eye-display by re-structuring input image

*Woongseob Han, Jae-Min Jeon, Myeong-Ho Choi and Jae-Hyeung Park**
Dept. of Electrical and Computer Engineering, Inha University, Michuhol-gu, Incheon 22211, Korea
*Tel.:82-32-860-7114, *E-mail: jh.park@inha.ac.kr*

A lot of attention is now on near-eye displays (NEDs) due to their advantages in connecting physical reality with virtual reality. Small form factor makes waveguide-type NEDs one of the most promising device configurations.[1] Waveguide-type NEDs, however, have a small field of view (FOV) which disturbs the user's immersive experience. Most of the previous research on the waveguide-type NEDs are targeting eyebox expansion without enhancing the FOV.[2] In this paper, we propose a novel method to increase the FOV while keeping a small form factor. The key idea is to give different propagation paths to the upper and lower parts of the projected image at the input coupler, achieving side-by-side arrangement at the output coupler with enhanced horizontal FOV.

Fig. 1(a) shows a schematic diagram of the proposed NED. We use a laser projector as a display and collimate the projected image using a convex lens. An in-coupler, composed of two holographic optical elements (HOEs), couples the collimated image to a waveguide and the coupled-image propagates with total internal reflections (TIRs). As illustrated in Fig. 1(a), the upper HOE diffracts the upper image part such that the diffracted image propagates inside the waveguide with a slightly downward direction. The lower HOE diffracts the lower image part with a slightly upward direction. The diffracted upper and lower image parts propagate with different numbers of TIRs, reaching the out-coupler at different horizontal positions. The out-coupler, composed of two HOEs corresponding to the in-coupler, functions as a convex lens which makes the out-coupled beam focus to user's eye after passing through Pancharatnam-Berry deflector (PBD). The PBD corrects the vertical beam angle of the out-coupled images so that user can see the restructured image shown in Fig. 1(a). The real-scene separation created by the PBDs is compensated by another PBDs with a circular polarizer between the real-scene and the waveguide. One of the requirements of the proposed approach is that the out-coupler should have a vertical angular tolerance larger than the PBD diffraction angle which is around 10° in our setup. To test vertical angular tolerance, we fabricated the waveguide-type Maxwellian NED with thickness of 6mm. Then, vertically tilted beam is delivered to the in-coupler with specific angle, which is gradually increased up to 10°. From this preliminary experiment, we confirmed that the HOE in our experimental setup maintains sufficient diffraction efficiency up to 10° vertical tilt as shown in Fig. 1(b). In presentation, we will show further experimental results, demonstrating the vertical angle compensation by the PBD and the image display with increased horizontal FOV.

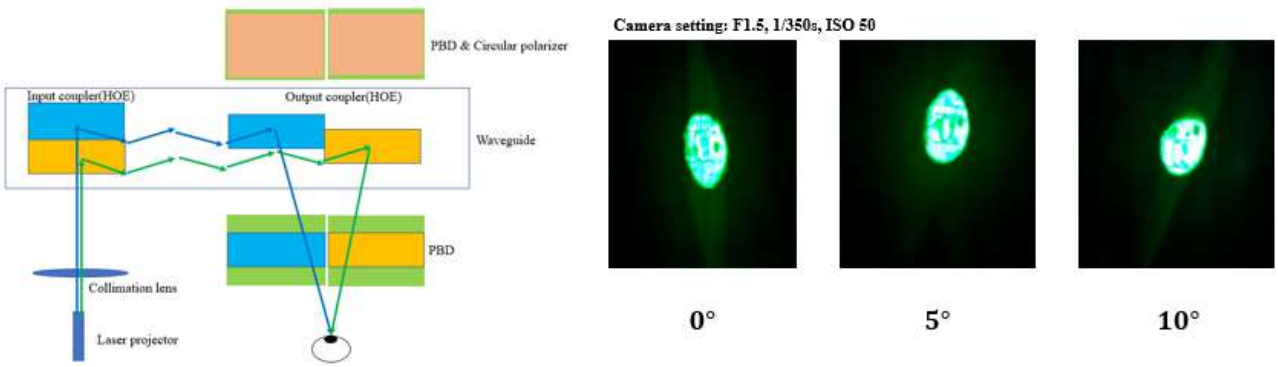

Fig. 1.(a) Schematic diagram of the proposed NED (b) Experiment results

Acknowledgment
This work was supported by National Research Foundation of Korea (2017R1A2B2011084).

References

1. H. J. Jang, J. Y. Lee, J. Kwak, D. Lee, J.-H. Park, B. Lee and Y. Y. Noh, J. Inf. Disp., 20(1), p. 1–8 (2019).
2. M.-H. Choi, Y.-G. Ju, and J.-H. Park, Opt. Express., 28(1), p. 533–547 (2020).

Analysis of Multiplexed Holographic Optical Element with Rigorous Coupled Wave Theory

Junyoung Jang, and Jae-Hyeung Park*
Electrical and Computer Engineering, Inha University, Michuhol-gu, Incheon 22211, Korea
*Tel.:82-32-860-7114, *E-mail: jh.park@inha.ac.kr*

Holographic optical element (HOE) is used for diffracting lights in limited space with its thin structure and high diffraction efficiency by modulating refractive index volumetrically. Diffraction efficiency of HOEs is a major factor to assess whether the HOE recorded at specific beam angles is suitable for experiment. For analyzing HOE, coupled wave theory (CWT) method is majorly used; however, its result implies assumptions to simplify the behaviors of diffracted lights [1]. The difference between actual diffracted light and calculated diffraction efficiency is minor enough to neglect for thick HOEs recorded with uniform gratings, but it could become considerably large for thin HOEs with multiple gratings. Accordingly, analyzing multiplexed HOEs, recorded with various beams of different angles or wavelengths, of arbitrary thickness with CWT method may have disregarded factors of the diffracted lights. Hence, in order to analyze general multiplexed HOEs properly, rigorous analysis method must be adopted.

In this presentation, we propose the analysis of multiplexed HOEs with rigorous coupled wave analysis (RCWA) including comparisons of CWT analysis. RCWA is a rigorous method of analyzing multi-layered device in Fourier Space [2]. While CWT is focused on analyzing diffraction efficiency of the strongest diffracted wave, RCWA includes analysis of reflectance and transmittance by different modes of plane waves. HOE is designed to have multiple thin layers to properly demonstrate gratings inside the HOE. Using RCWA, reflectance and transmittance of a uniform grating HOE is analyzed by 25 modes and changing thicknesses from 16 um to 160 nm, as shown in the Fig. 1. In Fig. 2, power of a multiplexed HOE with two different gratings is analyzed by 9 modes and different incident angles of beams.

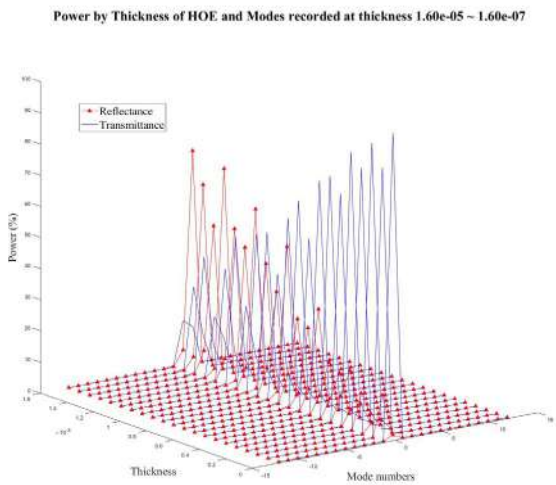

Fig. 1. Analysis of uniform grating HOE

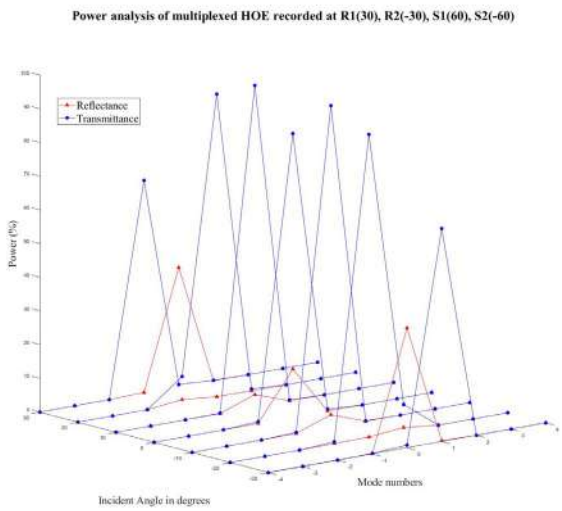

Fig. 2. Analysis of multiplexed HOE

In this presentation, we propose comparisons of RCWA and CWT methods for analyzing multiplexed HOEs. We expect to apply suitable analysis method for analyzing HOEs for experiments.

Acknowledgment

This work was supported by Institute for Information and Communications Technology Promotion (IITP-2020-0-00929);

References

1. H. Kogelnik, *Bell System Technical Journal*, 48(9), 2909 (1969).
2. N. Chateau and J.-P. Hugonin, *J. Opt. Soc. Am.*, 11(4), 1321 (1994).

Depth Perception Improvement of Distant 3D Image from Sticking Depth on Real Object by Moving Head or 3D Image in Arc 3D Display

Takeshi Yasui, Kisa Nakano, Haruki Mizushina, Kenji Yamamoto and Shiro Suyama
Dept. of Optical Engineering, Faculty of Science and Technology, Tokushima univ.,
2-1 Minamijyousanjima, Tokushima 770-8506 Japan
Tel.: +81 88 656 9427, E-mail: c612136002@tokushima-u.ac.jp

For safe driving, Head-Up Display has been studied to provide useful visual informations using signs, characters and arrows at any depth in the world. However, there is a serious problem that the floating 3D image is not perceived at designed depths and tends to be stuck to real object surface when displayed behind real object. In order to solve this problem, Nakano[1] utilized arc 3D display with moving head or 3D image.

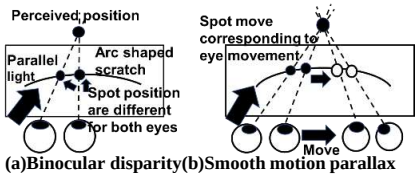

(a)Binocular disparity(b)Smooth motion parallax

Fig. 1. Principle of arc 3D display

Arc 3D display (Fig. 1) is composed of many arc-shaped scratches, where a bright spot is moved corresponding to an eye position, resulting in binocular disparity and continuous motion parallax. Nakano reported that 3D image can be perceived behind of a real object at short distance of 10 cm to 20 cm by using arc 3D display with moving head or 3D image. In this paper, we evaluate whether the distant 3D image can be perceived behind the real object or not, even at several meters away from observer located between the 3D image and the observer.

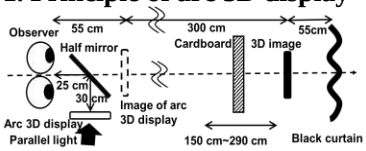

Fig. 2. Experimental system for evaluating depth perception of distant 3D image designed behind a real object

Figure 2 shows the experimental system for evaluating depth perception of distant 3D image designed behind a real object. Without real object and with the black curtain at 355 cm away from arc 3D display, 3D image depth was perceived at 300 cm depth. Perceived depth was estimated under the three conditions of (a) fixing head and arc 3D display, (b) moving head, and (c) moving arc 3D display. Real object of cardboard was randomly placed. Subjects were let memorize 3D image depth, and after turning off stimulus, move the reference to memorized perceived position of 3D image for three times. Moving head width was 8.5 cm, and width of moving arc 3D display was 6 cm and the both periods were 1 second.

Figure 3 shows the perceived depth dependences. When perceived depth are on the dashed line, the 3D image is perceived on the real object of cardboard surface. In Fig. 3(a), the almost constant depths of 3D images were perceived at about 250 cm. These depths are behind real object and 50 cm in front of the designed depth without real object. In Figs. 3(b) and (c), the almost constant depths of 3D images were perceived around 270 cm. These depths are behind real object and 30 cm in front of the designed depth without real object. This indicates that the constant perceived depth is improved by moving head or 3D image. Next, at real object position from 250 cm to 290 cm in Fig. 3(a), perceived depths are on dashed line of real object positions and stuck on real object surface. On the other hand, by moving head or 3D image in Figs. 3(b) and (c), stuck positions to real object are reduced only at the real object position of 290 cm. These results mean perceived depths of distant arc 3D images with continuous motion parallax can be improved to behind real object by moving head or 3D image.

Thus, arc 3D display can successfully provide distant 3D image around 300 cm even behind the real object.

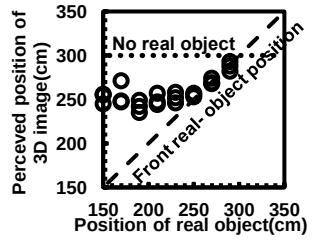

(a)Fixing head and arc 3D display

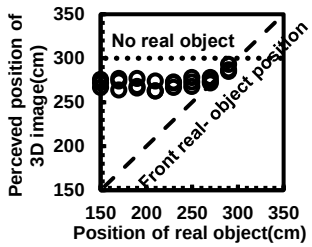

(b)Moving head

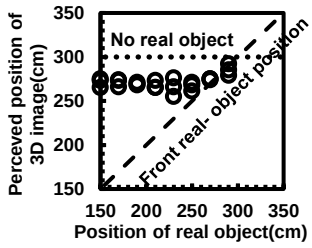

(c)Moving arc 3D display

Fig. 3. Depth perception of distant 3D image behind a real object

Acknowledgment

This study was supported by JSPS KAKENHI JP19H04155, JP20K11919, JP20K21817, JP20H05702 Grant

References

1. K. Nakano, T. Yoshida, H. Mizushina, and S. Suyama, "Perceived Depth in Arc 3D Display Can Penetrate into Behind Real Object by Moving Arc 3D Image in Contrast to Non-Penetrated Perceived Depth in Stereoscopic Display," IDW'19, Vol.26, pp. 179-182 (2019).

Advanced secure display using DFD display with fuzzy perceived depth images by combining random dot configuration and fuzzy luminance distribution

Kazuya Fujikawa, Haruki Mizushina, Kenji Yamamoto and Shiro Suyama
Dept. of Science and Engineering, Tokushima University, Tokushima, 770-8506, Japan
Tel:+81 88 656 9427, E-mail:c611701121@tokushima-u.ac.jp

As many displays are usually used in various situations, the protection of personal information on displays becomes more and more important issue. In particular, the security against peeping or voyeurism is important such as at the bank, etc. For such security, it is promising if only humans at a restricted position can recognize hidden information on the display. In this paper, we have proposed a new secure display to prevent peeping or voyeurism by using DFD (Depth-fused 3D) display[1], in which overlap of the front and rear images is an essential for perceiving 3D depth.

Principle of our proposed secure display is shown in Fig. 1. When the front-rear image is viewed from the designed angle (Fig. 1(a)), dots of hidden information are overlapped and their fuzzy depths can be perceived, resulting in recognizing hidden information, such as desired figure or character. Since the distribution and colors of random dot randomized in the front and rear images, hidden information cannot be recognized outside the overlapped position of designed angle (Fig. 1(b)). Furthermore, by fuzzy arranging the color and luminance ratio in the front and rear dots of hidden information, it is difficult to derive hidden information only from front and rear image photographs (Figs. 1(a) and 2).

Experimental system (Fig. 2) consisted of two displays and a half mirror, and random dots were used so that dots of hidden information "4" overlapped only from frontal direction (0 degrees). Luminance ratios of hidden information between front and rear images were fuzzy changed from 4:6 to 6:4. Another dot positions and luminance were arranged randomly. Recognizabilities by two subjects were estimated at viewing angles of −15, 0, 15 degrees and the photograph at viewing angle of 0 degrees.

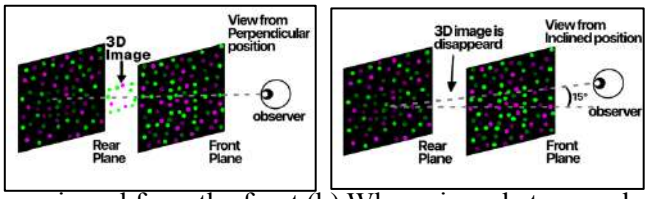

(a) When viewed from the front (b) When viewed at an angle

Fig. 1 Principle of our proposed secure display

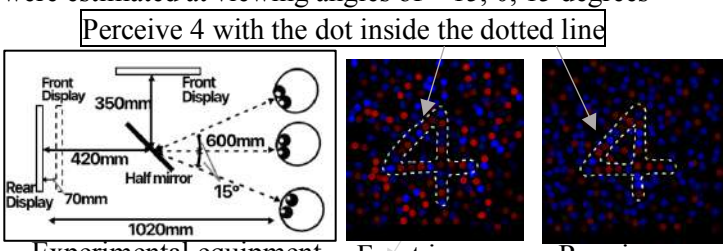

Experimental equipment Front image Rear image

Fig. 2 Experimental system of half mirror DFD

Table. 1 Evaluation results of Our Proposed Secure Display

	Observer's viewing angle			Image taken with camera(0°)
	-15°	0°	15°	
Observer A	×	○	×	×
Observer B	×	○	×	×
	Can be perceived (○)		Cannot be perceived (×)	

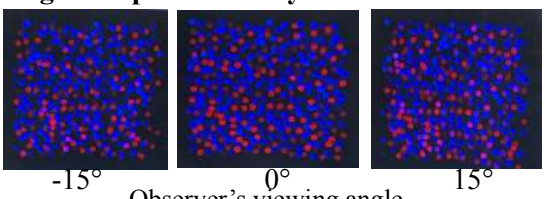

-15° 0° 15°
Observer's viewing angle

Fig. 3 Observation image

Table 1 shows the recognizabilities at viewing angles of −15, 0, 15 degrees and the photograph at viewing angle of 0 degrees. When viewed from angle 0° (Table 1), hidden information "4" in the random dots can be recognized by fuzzy depth perception. However, when observed from 15° and -15°, hidden information cannot be obtained both by two subjects. In addition, photographs at viewing angles of −15, 0, 15 degrees in Fig. 3 shows that the hidden information "4" images cannot be recognized.

Thus, we proposed a new secure display using DFD display with fuzzy depths, and clarify to improve the security against peeping or voyeurism.

Acknowledgment

This research was supported by JSPS Grant-in-Aid for Scientific Research.
19H04155, 20K11919, 20K21817, 20H05702

References

1) S. Suyama, S. Ohtsuka, H. Takada, K. Uehira and S. Sakai, Vision Research, 44, 785-793 (2004).

Reduction of Perceived Depth Instability in Aerial Image by Reaching Hand for Aerial Image Position

Naoki Kiyose, Haruki Mizushina, Kenji Yamamoto,and Shiro Suyama
Dept. of Opt. Sci. & Tech., Tokushima Univ, 2-1 Minamijosanjima, Tokushima 770-8506, Japan
Tel.: +81 88 656 9427, E-mail:{c612036027, suyama.shiro}@tokushima-u.ac.jp

In recent years, aerial images are expected as a promising approach for non-contact interfaces. However, perceived depth position of the aerial image is sometimes unstable using only visual information. If this depth instability can be removed, aerial images can be utilized for various applications such as touchless buttons. Previous study reported that the optical illusion of perceived object size does not affect the grasping behaviour because the visual informations for visual and action trials are processed by different visual pathways in the brain [1]. This is an advantageous property for accurate touch even when the visual trial process for aerial image has instability. In this study, we evaluated whether the aerial image is perceived at wrong position in visual trial, and whether reaching-hand action can correct the perceived this wrong position.

Fig. 1 shows the principle to reduce the instability of aerial image position by hand-reaching action to the aerial image. Fig. 1(a) shows usual depth perception using only visual information in which the subject is let move the reference to the memorized position (Visual trial). Fig. 1(b) shows our proposed method in which the subject is let move his hand to trying position to reach the hand for aerial image (Action trial).

As shown in Fig. 2, LCD and Fresnel lens were used for forming an optical image as an aerial image. The distance between subject and lens was 50 cm, and aerial real image distances from lens were 15, 20, and 25 cm. The subjects observed the aerial image with both eyes.

In the Visual trial, after the aerial image was displayed for one second, the subject was let move arrow-style indicator to memorized perceived depth position. In the Action trial, the aerial image was disappeared before the subject's hand reaches it. The depth position of the aerial image was randomly changed at three trials. Black board with a rectangular opening was set in front of the Fresnel lens so that the only aerial image and black board position can be seen.

Fig. 3 shows perceived depth difference between visual trial and action trial. In the Visual trial, the perceived depth positions have large deviations of 10 cm to 16 cm in the direction to the lens apart from aerial image positions. On the other hand, in the Action trial, the hand-reaching depth positions almost coincide with depth positions of aerial image, indicating that hand-reaching can improve the depth perception of aerial image.

Thus, our proposed hand-reaching method can successfully reduce instability of perceived depth in aerial images using only visual information and will be promising for many applications using aerial images.

Acknowledgement This work was supported by JSPS KAKENHI Grant Numbers JP19H04155, JP20K11919, JP20K21817, JP20H05702.

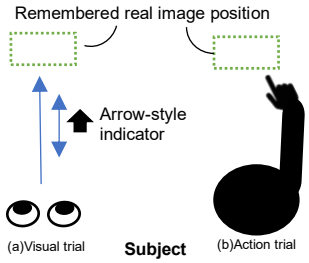

Fig. 1. Our proposed method for reducing aerial-image instability
(a) The subject is let move reference to the remembered perceived position.
(b) The subject is let move his hand to the trying position to reach his hand for aerial image.

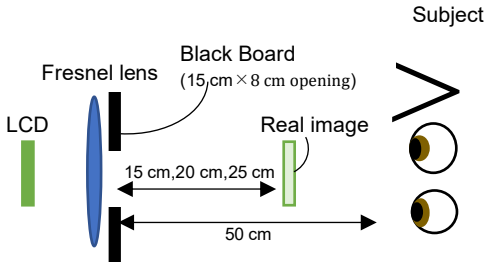

Fig. 2. Experimental system for evaluating perceived and hand-reaching positions of the aerial image

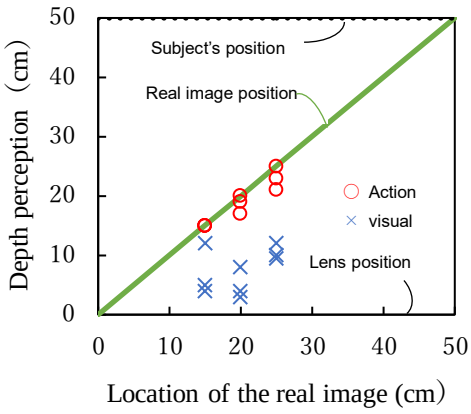

Fig. 3. Perceived and hand-reaching position of the aerial image

References [1]. M. A. Goodale, A .D. Mikner, L. S. Jakobson & D. P. Carey, Nature, Vol.349(1991).

Deep learning to Improve the performance of Fingerprint Sensor under display

Soongyu Lee, Jinwoo Kim
Mobile Display Business, Samsung Display Co., Ltd., Giheung-gu, Yongin-si, Gyenggi-do, 17113, Korea
Tel.:82-31-5181-4507, E-mail: sg27.lee@samsung.com

A.I (Artificial Intelligence) can be used to upgrade the performance of fingerprint sensor in smartphones. Fingerprint authentication is a process of determining whether the fingerprint sensed in real time matches the fingerprints registered by the user [1]. In this process, fingerprint images registered by the user were basically saved in the template. However, fingerprint sensors do not work properly in certain environments such as in cold weather or after washing hands. It makes fingers dry, and dry fingers could lose some important features of fingerprints. Extending the template with fingerprint images that have many features of the user is one of the most expeditious ways to enhance matching performance in various environments as shown in Fig. 1.

Deep learning algorithm is used to create pseudo dry fingerprint images which are uploaded to the template as shown in Fig. 1(b). Cycle GAN [2] is the most appropriate algorithm for managing sensitive fingerprint images. Cycle GAN operates under the condition with minimal consistency loss [2], so that output image maintains features of an input image. And, the model is designed to create a dry style according to the input image based on the learning information. After that, the model combines the input image and dry style in two steps as shown in Fig. 2. These two methods help the model not only create more precise pseudo dry fingerprint images but also act as a security measure.

(1line spacing)

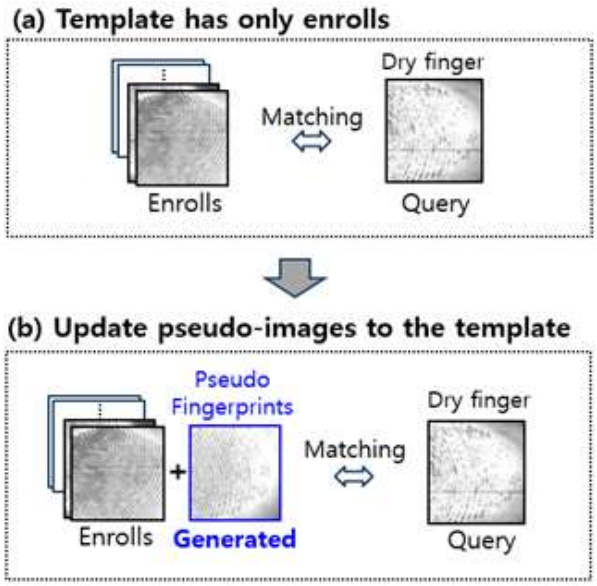

Fig. 1. Template extension concept

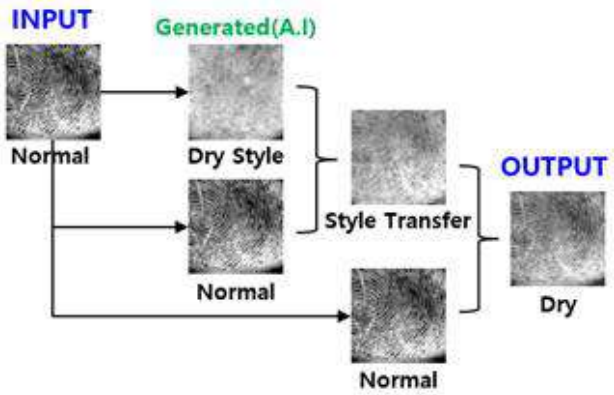

Fig. 2. Image composition diagram

(1line spacing)

Dry fingerprints downgrade fingerprint authentication. By extending template using the novel deep learning alghrithm, the performance of fingerprint sensors can be upgrade for low-quality fingerprint images including dry fingerprints. The model is under 10MB so there is no hesitation to apply it to the product. Several security measures are also applied to the model. Therefore, when adding the Cycle GAN to fingerprint sensors, dry fingerprint recognition improved by 28.6%.

(1line spacing)

Acknowledgment

References

1. A. P. Russo, Method and system for fingerprint template matching, US Patent 6,681,034, issued Jan 20, 2004.
2. J. Y. Zhu et al, IEEE International conference on computer vision, p. 2242-2251 (2017).

Tearing effect free Single Buffering for a Field Sequential Color Display

Wook Hong, Hokwon Kim, and Joon Goo Lee
Research & Development Group of RAONTECH, Seongnam-si, Korea
Tel.:82-31-786-4621, E-mail: Joon.Lee@raon.io

Image tearing occurs when a display device shows multiple frames in a single screen since it is not in sync between the frame rendering of video feed and the display's refresh rate. It should be avoided for user experience. However, in general, it requires multiple buffering which consumes lots of frame buffer memory. In this paper, we propose a vertical blank interval (VBI) method to remove the tearing effect with single buffering.

The proposed method utilizes extreme VBI as shown in Fig. 1. If a video renderer can reduce T_{FSin} to be less than the summation of T_{Fout} + T_S, the display system can guarantee the torn free image by adjusting frame buffer read timing with respect to the vertical sync signal, where T_{FSin} is the time for pixel data transferring from the renderer to a display driver IC except vertical blank time, T_{Fout} is the total time for each color field including both data read time and vertical blank time for the interfacing field sequential color (FSC) display panel, and T_S is the data read time consumed per color field for the panel. The critical regions shown in Fig 1 is timing control margin to ensure torn free images. When T_{FSin} is larger than the summation, but still less than the summation of $2T_{Fout}$ + T_S, the system can make only the last color field to be torn with similar manner. The display driver IC may mask the last field image not to show by turning off the backlight.

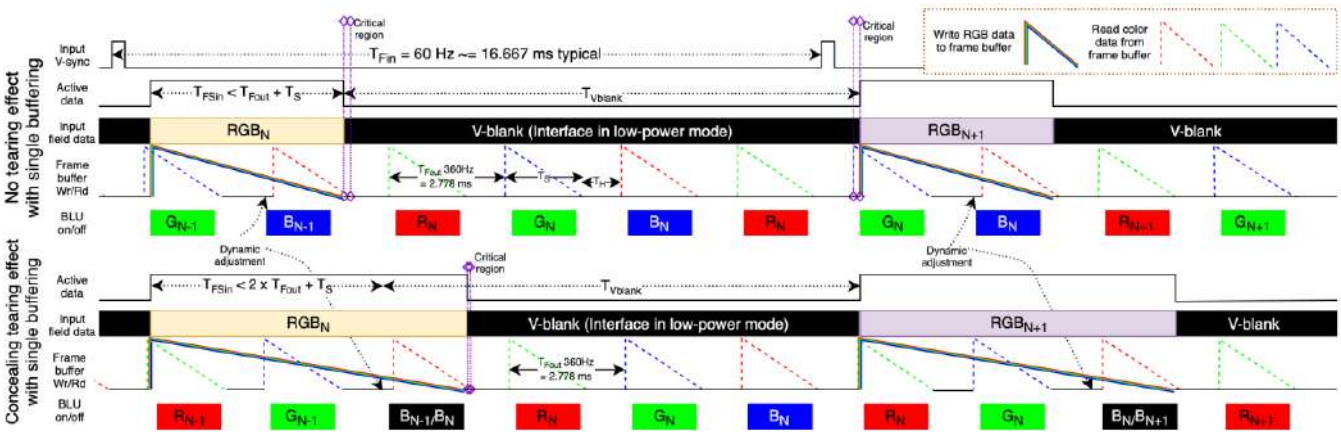

Fig. 1. Synchronization timing for tearing free display with the vertical blank interval method

The proposal can reduce the size of frame buffer memory when compare to multiple buffering. Since the frame buffer memory tends to consume huge area of the display driver IC, the area reduction directly affects IC and system size, cost, and power consumption positively. The downside of this method is that it requires around 2 ~ 3 times higher data transmission rate between the renderer and the display driver IC than the conventional one. The increased data transmission rate can be managed with a video data compression algorithm widely accepted in the display industry [2-3]. We verified the feasibility of the proposal with our in-house display driver IC and FSC-type liquid crystal on silicon (LCoS) panels supporting HD (1280x720) or FHD (1920x1080) resolution.

Acknowledgment

This material is based upon work supported by the Ministry of Science & ICT (MSIT, Korea) under Industrial Technology Innovation Program. No.2020-0-00083, Development of Low MTP Latency Microdisplay and SoC technology for VR·AR devices.

References

1. Achintya K. Bhowmik, Zili Li, and Philip J. Bos, Mobile Displays: Technology and Applications, John Wiley & Sons, 2008.
2. VESA, VESA Display Stream Compression (DSC) Standard, 2014.
3. VESA, VESA Display Compression-M (VDC-M) Standard, 2019.

Evaluation of Adverse Health Effects from OLED Display Flicker of Smartphone

Minhyuk Kim, Young-mook Choi, and Sangkok Kim
Electronics Development Team, Samsung Display Co., Ltd.,
1 Samsung-ro, Giheung-gu, Yongin-si, Gyeonggi-do, 17113, Korea
Tel.:82-31-5181-0991, E-mail: minhyuk0214.kim@samsung.com

As artificial lighting is widely used and the eyes are exposed for a long time, symptoms such as eye fatigue and headache, which are side effects of artificial lighting, have been reported. These adverse effects on human health are caused by the flicker produced by the pulse-width method (PWM) dimming technique. IEEE standard lighting working group, IEEE standard PAR1789, was established in 2008 to report the impact on the human body of the flicker and flicker reduction driving technology of LEDs. The standard flicker assessment method established here is currently being used to research the adverse health effects of flicker in various light sources.

OLED (Organic Light-Emitting Diode) displays are being used as new artificial lighting in more and more fields based on the advantages of thinness, flexibility, low power consumption and high contrast ratio. Health side effects from OLED displays flicker are becoming an issue in some internet user communities, but detailed research is lacking. However, as the market's influence grows, so does the interest in health issues.

Therefore, in this paper, the IEEE standard PAR1789 were reviewed to assess the adverse health effect caused by OLED display flicker. The human impact of the PWM driving was evaluated through measurements according to standards. In addition, the cognitive characteristics of OLED display were evaluated by varying the distance. Finally, the effect of the OLED display flicker on the human body was explained.

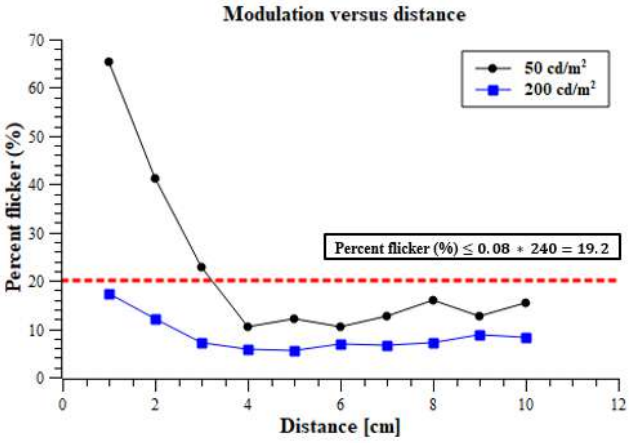

Fig. 1. Percent flicker calculation of OLED display by distance

The evaluation result of this paper is expected to be used for study in related fields as interest in human health effect is increasing as the expansion of OLED displays.

AMOLED Pixel Circuit for VDD Compensation

Hyuck Su Lee[1], Seo Jin Kang[1], Eun Seong Yu[1], Jae Geun Woo[1], Jong Mo Lee[1], Chan Min Jeong[1], and Byung Seong Bae[1]

[1]School of Electronics and Display Engineering, Hoseo University, Asan, South Korea

Tel.:82-41-540-5221, E-mail: bsbae@hoseo.edu

AMOLED is a next-generation flat-panel display technology in terms of self-light-emission, thin thickness, contrast, and power efficiency. The resolution and screen size of the display are getting larger. As the resolution and screen size of the display increase, the length of the bus line increases. Consequently, the voltage drops by the resistance of the bus lines occur, which is called I-R drop. For the uniform brightness of the OLED display, IR drop should be compensated [1]. Until now, various compensation methods have been proposed to compensate I-R Drop, and the circuit which compensate IR drop with reduction of the VDD line was proposed [2]. The internal compensation method has the advantages that it can be applied to various TFT models and has lower cost compared to external compensation methods. This study proposes an internal compensation pixel circuit which compensation IR drop for high resolution AMOLED using TFT (thin film-transistor) based on Indium-Gallium-Zinc-Oxide (IGZO). The proposed circuit consists of four TFTs and two capacitors. The proposed pixel circuit uses bootstrapping phenomena generated by pulse signals. Despite the difference in VDD caused by IR drop, the OLED current by the proposed circuit showed invariant constant currents. Figure 1 shows the comparison of the OLED currents between the proposed pixel circuit and 2T1C pixel circuit. Compared to the 2T1C pixel circuit, proposed circuit shows the invariant currents down to under 2 V.

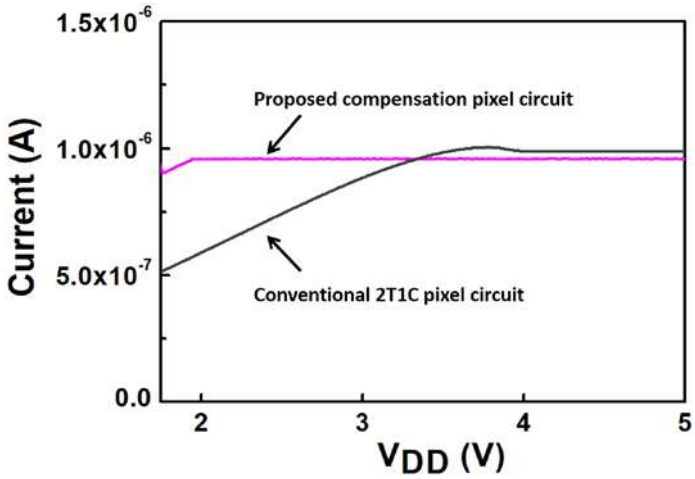

Fig. 1. OLED currents in 2T1C and the proposed pixel circuits as function of VDD.

Acknowledgment

This research was funded and conducted under 「the Competency Development Program for Industry Specialists」 of the Korean Ministry of Trade, Industry and Energy (MOTIE), operated by Korea Institute for Advancement of Technology (KIAT).

(No. P0012453, Next-generation Display Expert Training Project for Innovation Process and Equipment, Materials Engineers)

References.

1. J. Yum, Y. Yu, H. Park, H. Lim, and J. Lee, "A Novel Method to Reduce Luminance Variation Due to IR-drop in Active Matrix OLED Displays," 2020 IEEE International Conference on Consumer Electronics (ICCE), Las Vegas, NV, USA, 2020, pp. 1-4.
2. J. Lee, H. Jeon, D. Moon and B. S. Bae, "Threshold Voltage and IR Drop Compensation of an AMOLED Pixel Circuit Without a VDD Line," in IEEE Electron Device Lett. vol. 35, no. 1, pp. 72-74, 2014.

Stretching Compensation Pixel Circuit Using a-IGZO TFTs

Seo Jin Kang[1], Hyuck Su Lee[1], Eun Seong Yu[1], Jae Geun Woo[1], Chan Min Jeong[1], Jong Mo Lee[1] and Byung Seong Bae[1]

[1]School of Electronics and Display Engineering, Hoseo University, Asan, Chungnam 31499. Korea

Tel.:82-2-563-7992, E-mail: bsbae3@hoseo.edu

A flexible display is a light, flexible and deformable display that uses plastic substrates instead of conventional rigid glass.[1] Recently, foldable displays that can be folded are commercialized and rollable displays that can be rolled like paper were developed. Stretchable displays, the last step of flexible displays, can be freely changed in size and can be applied to many applications such as body attachment bio and healthcare.[2] Active-matrix organic light-emitting diode (AMOLED) display is a next-generation display because of its vivid color, high contrast ratio, thin/light module, and low energy consumption.[3] In addition, OLED does not need a BLU (Back Light Unit) that supplies light because OLED emits light by itself when the current flows. Therefore, AMOLED is suitable for stretchable displays. Since the screen luminance is inversely proportional to pixel area ratio, stretchable displays have a problem of decreasing luminance as the size of the panel increases. Therefore, we proposed a pixel circuit that compensates the OLED currents so that the brightness can be maintained even if the size of the panel increase. The proposed compensation pixel circuit consists of 4 thin-film-transistors (TFTs) and Cst (Storage Capacitor) on the rigid region and Cs (Sensing Capacitor) on the soft region. As the panel stretches, Cs increases proportionally to the strain, which is used for the stretching compensation. In this study, we verified the AMOLED stretching compensation pixel circuits with a-IGZO (Amorphous Indium-Gallium-Zinc-Oxide) TFTs. Figure 1 shows the OLED currents for the comparison between different strains. The proposed circuit shows higher currents than the conventional 2T1C pixel circuits, which compensate the stretching effect on the brightness.

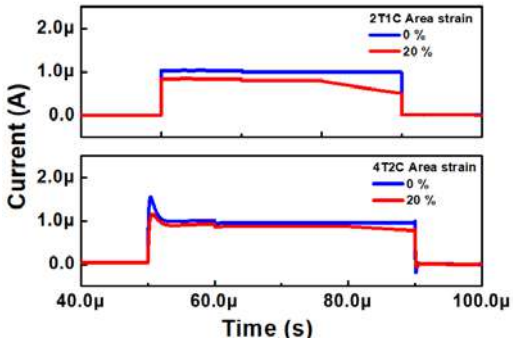

Fig. 1. OLED currents of conventional 2T1C pixel circuit and proposed 4T2C pixel circuit for the 0% and 20 % strains.

Acknowledgment

This research was funded and conducted under 「the Competency Development Program for Industry Specialists」 of the Korean Ministry of Trade, Industry and Energy (MOTIE), operated by Korea Institute for Advancement of Technology (KIAT). (No. P0012453, Next-generation Display Expert Training Project for Innovation Process and Equipment, Materials Engineers)

References

1. H. Zhu et al, *Adv. Funct. Materia*, 1904588, 1-36 (2019).
2. T. Wu, J.-M. Redouté, and M. Yuce, *Advances in Body Area Networks* I 49(1), 165–173 (2019).
3. C. Chen et al, *Journal of the SID* 17/6, 525-534 (2009)

An Quantification Method of Horizontal Line defects caused by the Interference between Flexible OLED and Touch Sensor

Junyoung Ko[1], Hyung-Bae Kim, Jaewoo Choi[1], Eunsol Seo[1], and Yujin Shin[1]
[1]Mobile Display Business, Samsung Display Co., Ltd., Giheung-gu, Yongin-si, Gyeonggi-do, 17113, Korea
Tel.:82-31-5181-2439, E-mail: joonyoung.ko@samsung.com

The absence of standardized methods of the visible defects quantification has induced inconsistent results in quality assurance of OLED displays. Herein, an effective quantification method for evaluating visible defect arisen from mutual interference of flexible OLED and touch sensor were proposed, and a specific contrast sensitivity (CS) level below 1.0 was established as meaning "invisible defect". The degree of the distortion was evaluated by the level from V0 to V3 under *blind test* condition. A visibility level of V0 was defined as "invisible" and a visibility level of V3 indicates "clearly observable". Considering that the visible defect arising from non-uniform of display transistor has been to be necessarily eliminated, the average luminance difference between activation and deactivation of touch driving was measured by the 2D measuring system for few seconds. Then luminance difference curves were treated by the modified algorithm of *Contrast Sensitivity Function* (CSF). Various filtering tools were also employed for attenuating noise peaks and for amplifying defective peaks more distinguishably. The treated luminance difference is designated as contrast sensitivity (CS) levels. When the CS levels is about 1.0, the visual defect has been theoretically, known to be perceived with a probability of 50%. Figure 1. shows one period waveform of a transmitter electrode (Tx) in touch driving, CS level distributions, and a schematic 2D image. The same 120Hz of display frame rate and TSP report rate shows that there are consistent position between TSP driving waveform, CS levels, and the visible defect. Visible defects could have been fluctuated in case that a touch sensor works in asynchronous processing time zone. Although the fluctuated visible defects is probable to look like waterfall lines along the direction of display scanning, 2D measurement system can capture the defects on average (Figure 1b-c). Figure 2 shows that the CS levels has increased proportionally to the visibility levels. Considering that the visibility levels of V0 has been exclusively observed at the CS level below 1.0, the specific CS level below 1.0 could be considered to be crucial criterion for the determination of the invisible defects.

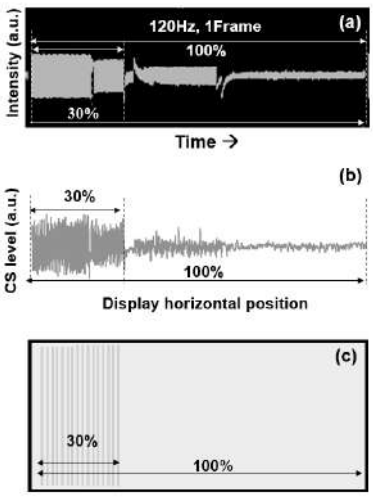

Fig. 1 Wave transmission phenomena

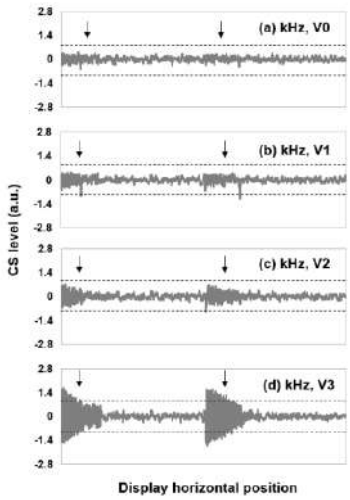

Fig. 2 Measured Display Noise Level by driving frequency

References

1. Cho, H.W., Lee, I., Lee, H.J., Kim, M.H., Park, J.H. The Mechanism and Solution of Horizontal Line Defects by Mutual Interference of Flexible OLED and Touch Sensor : *SID Symposium Digest of Technical Papers*, **2020**, 35-1, 489-492.
2. Vladimir S. Minimum detectable change in the light intensity incremental threshold △I over visual range
3. Jerry H, Todd O. Capacitive touch system using both self and mutual capacitance[Patents], [Worldwide applications 2011US],

An a-IGZO TFTs based Scan Driver Circuit for Depletion Mode with Triple Pull-Down Units

Yong-Hoo Hong, Eun Kyo Jung, Sung-Hyuck Ahn, and Yong-Sang Kim
Department of Electrical and Computer Engineering, Sungkyunkwan University, Suwon, 16419, Korea
Tel.:82-31-299-4640, E-mail: yongsang@skku.edu

Thin film transistors (TFTs) using metal oxides including amorphous In-Ga-Zn-O (a-IGZO) as semiconductor materials have attracted a lot of attention due to their higher mobility and smaller threshold voltage shifts than conventional hydrogenated amorphous silicon (a-Si:H) TFTs [1]. However, oxide TFTs often have a negative threshold voltage, even if the gate-source voltage is 0 V, there is a problem that a leakage current flows [2]. Such leakage current lowers the reliability of circuit operation and causes high power consumption. Therefore, it is essential to develop a scan driver that can ensure stable output even if it is composed of oxide TFTs operating in depletion mode.

Thus, we propose the scan driver circuit for depletion mode which is composed of a-IGZO TFTs using triple pull-down units as shown in Fig. 1, (a). It can reduce the electrical bias stress for pull-down units (T12, T13, and T14) due to AC-driving by CLK signals. Using the three-phase CLK signals, the bias stress time applied to each pull-down unit is reduced by a duty ratio of 33.3%. Moreover, for application to the depletion mode a-IGZO TFTs, we designed an A [n] node for preventing leakage current paths that could flow from the Q [n] node.

Fig. 1, (b) shows the waveforms of A [n], Q [n], and VOUT [n] of the proposed scan driver circuit. A pre-charging and bootstrapping voltage of the Q [n] node can be respectively maintained by VGH-V_{TH_T1} and VGH-V_{TH_T1}+ΔV for depletion mode a-IGZO TFTs. Assuming a 120-Hz Ultra-High Definition (UHD) graphics (3840×2160) display panel, we set the 1H time (1 line time) as 3.8 μs. Also, we simulated the last 10 stages in 2160 stages scan driver circuit, and the preceding 2150 stages were emulated using an equivalent circuit of a resistor and a capacitor.

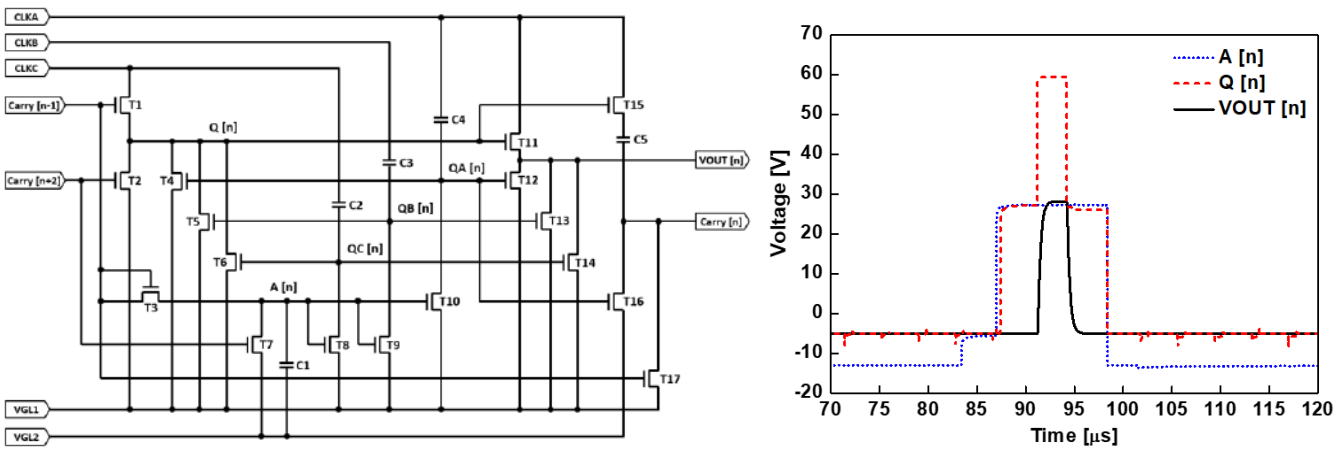

(a) **(b)**

Fig. 1. Proposed scan driver (a) circuit schematic and (b) voltage waveforms of A [n], Q [n], and VOUT [n]

Consequently, the proposed circuit can be normally operated in not only enhancement mode but also depletion mode a-IGZO TFTs. The result shows that the proposed circuit can be normally operated under the V_{TH} shift conditions from -4 V to +12 V.

References

1. H. H. Hsieh, H. H. Lu, H. C. Ting, C. S. Chuang, C. Y. Chen, and Y. Lin, "Development of IGZO TFTs and their applications to next-generation flat-panel displays," Journal of Information Display, vol. 11, no. 4, pp. 160–164 (2010).
2. J. Oh, K.-M. Jung, S.-Y. Lee, K. C. Park, J.-H. Jeon, and Y.-S. Kim, "Novel Driving Methods of Gate Driver Circuit for Depletion Mode Oxide TFTs," Proceedings of the International Display Workshops, p. 1524 (2019).

Scan Driver Circuit for Leakage Current Suppression in Enhancement-mode and Depletion-mode

Sung-Hyuck Ahn, Eun Kyo Jung, Yong-Hoo Hong, Hwarim Im, and Yong-Sang Kim
Department of Electrical and Computer Engineering, Sungkyunkwan University, Suwon, 16419, Korea
Tel.:82-31-299-4640, E-mail: yongsang@skku.edu

The amorphous-indium gallium zinc oxide (a-IGZO) thin-film transistors (TFTs) have higher mobility than a-Si TFTs. Due to this feature, the size of the circuit can be reduced. Compared to low-temperature poly silicon (LTPS) TFTs, a-IGZO TFT has better uniformity, so it can be applied to various displays. The a-IGZO TFTs are also used for the backplane technology of active-matrix organic light-emitting diode (AMOLED) display panels. However, a problem occurs in the circuit when the threshold voltage of a-IGZO TFTs has a negative value [1]. When the TFT has a negative threshold voltage, circuit malfunction may occur due to leakage current. In order to reduce the leakage current that can cause problems during circuit operation, the research is ongoing such as the structure of series-connected two transistors (STT) and the use of two or more VSS supply voltages [2].

In this paper, we propose a new scan driver circuit that can operate in both enhancement-mode (V_{TH}>0) and depletion-mode (V_{TH}<0). The proposed a-IGZO TFTs-based circuit consists of 12 TFTs and 3 capacitors (12T3C). The leakage current can be improved using the two methods in the proposed circuit. The two methods are as follows. The first method is to apply a negative gate-source voltage (V_{GS}<0) to the pull-down TFT to control leakage current. The second method used a STT structure to prevent the Q [n] node from producing unstable output by leakage current. Therefore, the proposed circuit can be operated in depletion-mode. The higher voltage was applied to the Q [n] node using the coupling effect through the C1 capacitor and CLK signal. For this reason, the proposed circuit can lead to stable output due to the above two methods and bootstrapping of the Q [n] node. We confirmed that SOUT [3], SOUT [5], and SOUT [7] waveforms are kept close to +28 V under V_{TH} shift conditions from -4 V to +9 V as shown in Fig 1. (a).

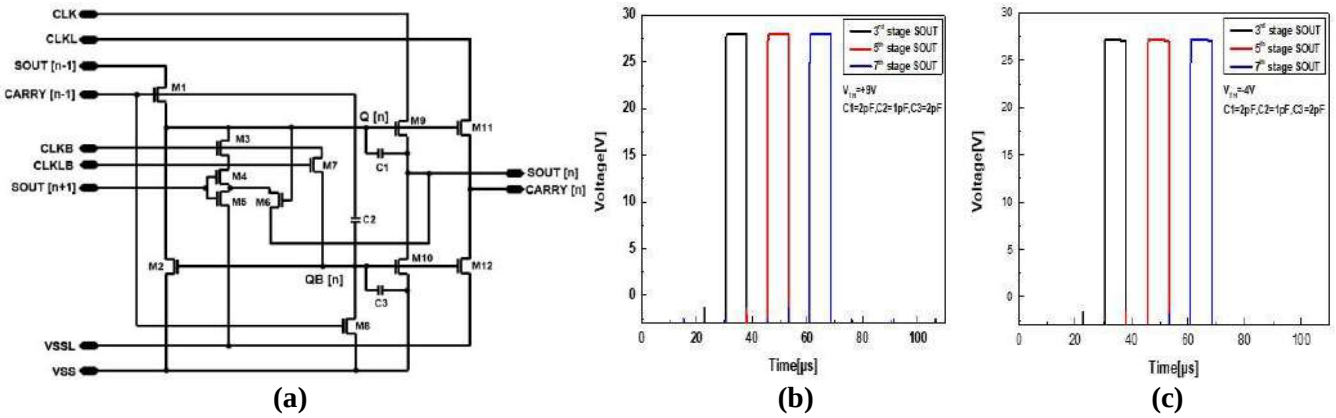

Fig 1. The proposed scan driver circuit for enhancement-mode and depletion-mode a-IGZO TFTs: (a) proposed circuit schematic; (b) 3rd, 5th, and 7th stage SOUT in enhancement-mode (V_{TH} = +9 V); (c) 3rd, 5th, and 7th stage SOUT in depletion-mode (V_{TH} = -4 V)

The output waveforms of the scan driver in enhancement-mode (V_{TH} = +9 V) and depletion-mode (V_{TH} = -4 V) are shown in Fig 1. (b) and Fig 1. (c), respectively. These results show that the proposed circuit can operate in both in both enhancement-mode and depletion-mode.

References

1. J.-H. Kim, J. S. Oh, K. C. Park, and Y.-S. Kim, *Displays*, vol. 53, pp. 1–7 (2018).
2. B. Kim, S.C. Choi, S.-Y. Lee, S.-H. Kuk, Y.-H. Jang, C.-D. Kim, M.-K. Han, *IEEE Electron Device Lett.* vol 32, no. 8, pp. 1092-1094 (2011).

The low power architecture for display driver IC

Seokhwan Roh[1] and Geunyoung Jeong[1]
[1] **OLED Drive Development Team, Samsung Display Company, Yongin-City 446-711, Korea**
Tel.:82-31-5181-2915, E-mail: seokhwannoh@gmail.com

The display system such as a smartphone or tablet has capabilities to support variable refresh rates (VRR)[1][2]. The latest display driver IC (DDI) support higher frame-rate than 90Hz for mobile application. The system power increase because high frame rate requires high bandwidth interface as well as high frequency driving. In order to reduce the chip power, this paper proposes the low power architecture with variable refresh rates.

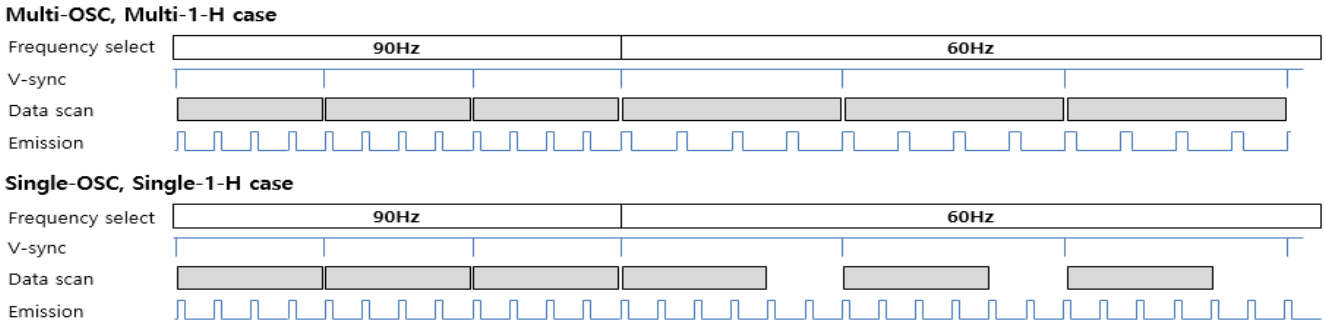

Fig. 1. Variable refresh rates in display system

The main idea of the power reduction is stronger clock gating and a parallelization of logic structure. In order to gate clocks, special clock gates are inserted to disable the clock signal when possible. In logic parallelization, a logic block or a data path can be parallelized into a number of similar parallel slower low-power units that together produce the same result with the same performance as the original single logic block.

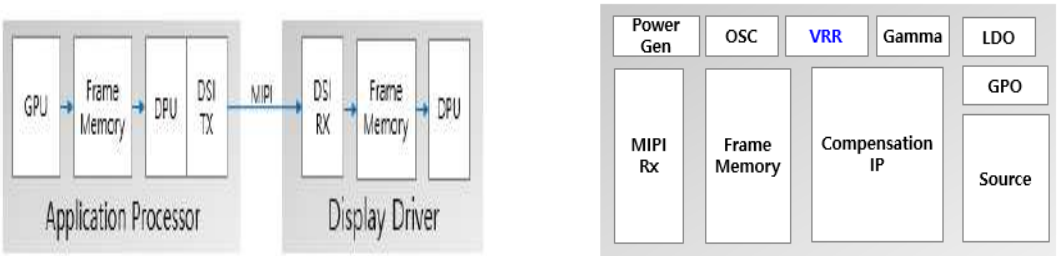

(a) Display system (b) Block Diagram of DDI

Fig. 2. Architecture in display system

WQHD DDI with power optimization was developed for validation. The DDI was fabricated in 28 nm CMOS process with high-voltage device. Compared to the previous WQHD DDI using same process, The DDI power saving ratio is about 19%. The power consumption is about 122mW.

WQHD DDI	2019 IC	2020 IC
Display Resolution	1440 x 3360 (WQHD)	
Frame rate	1~144Hz	
Color Depth	30 bit	
CMOS Technology	28nm	
Logic Power Measurement	150mW	122mW
Power Saving ratio	-	19%

Table 1. Power measurement with power optimization

References

1. G. A. Slavenburg, Variable Refresh Rate Displays, SID (2020)
2. Choi, Won Jae, "Display screens with variable refresh rate", Technical Disclosure Commons, (2019)

High Dynamic Range Gamma Correction in Organic Light Emitting Diode Displays

Kevin Kam[1], Wei Fan[1], and Ioannis Kymissis[1]
[1]Dept. of Electrical Engineering, Columbia University, New York, NY, USA
E-mail: kevin.kam@columbia.edu

As an extension of the OLED panel aging experiments shown in [1], the gamma correction curves were measured for displays operating in High Dynamic Range (HDR) mode. The test setup for this experiment involved an LG SONY XBR55A8F (named 2W) and LG OLED55B8 (named 3W) that was aged using the image seen in Figure 1(a). This image was displayed on a constant cycle with four hours on and one hour off for a total of 2000 hours. After the long-term aging experiment, the image shown in Figure 1(b) was used to find the gamma correction curve. This was done by creating multiple HDR versions of Figure 1(b) and cycling between 10% - 100% of the total display luminance. The luminance (in nits) was measured for each of these points and was collected using a Konica Minolta CA210 colormeter. The plotted HDR gamma correction curves for 2W and 3W are found in Figure 1(c) and 1(d) respectively. Our results show that in the middle brightness areas, the aged displays in HDR viewing mode show a wildly different correction curve than expected for their standard dynamic range (SDR) measured counterparts.

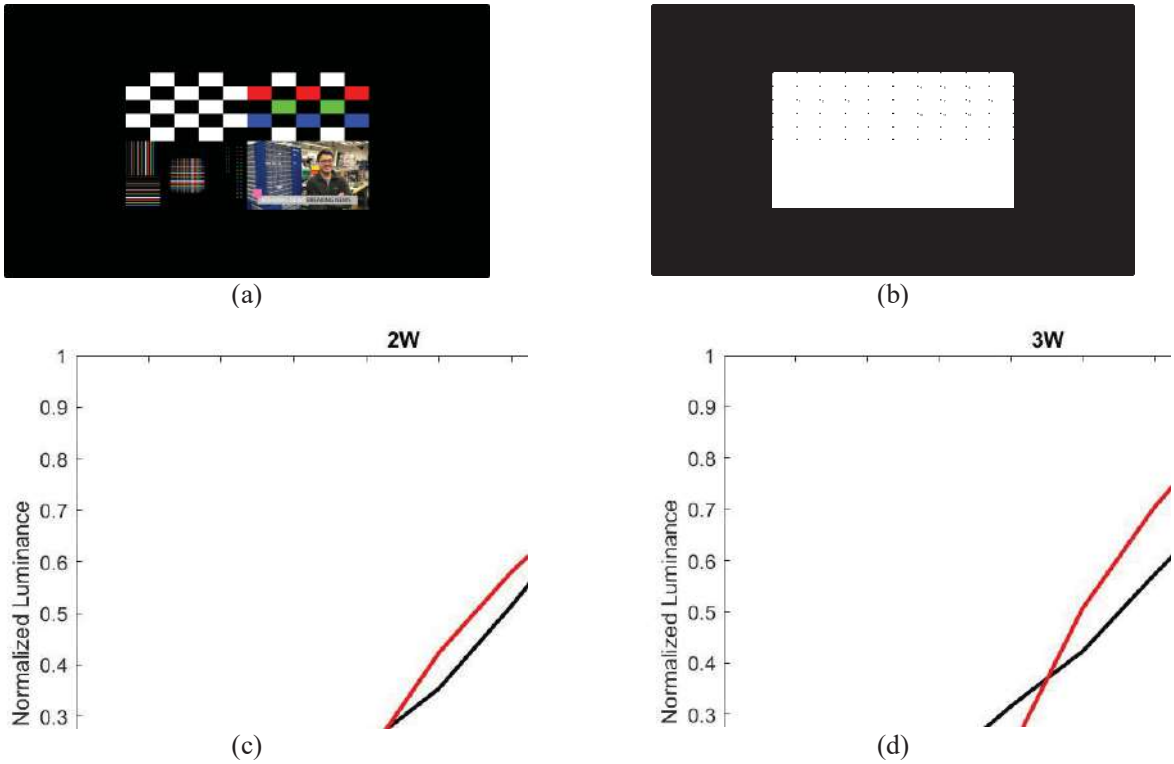

Fig. 1. (a) Static aging pattern (b) HDR Measurement pattern (c) HDR Gamma Correction for TV 2W (d) HDR Gamma Correction for TV 3W

Acknowledgment

The authors would like to acknowledge Samsung Electronics for their support.

References

1. Kam, K., Yu, T., Behrman, K., Yu, C. and Kymissis, I. (2020), SID Symposium Digest of Technical Papers

Color Shifting in High Dynamic Range Organic Light Emitting Diode Displays

Kevin Kam[1], Wei Fan[1], Vikrant Kumar[1], and Ioannis Kymissis[1]
[1]**Dept. of Electrical Engineering, Columbia University, New York, NY, USA**
E-mail: kevin.kam@columbia.edu

This work builds upon previous OLED panel aging and characterization found in [1]. Measurements were taken to see if the average luminance difference between aged panels viewed in both the HDR mode and SDR modes were significant. Two TVs, a SONY XBR55A8F (2W) and LG OLED55B8 (3W) were shown HDR targets ranging from 10% to 100% of the displays peak luminance through an amazon firestick illustrated in Figures 1(a) and 1(b). These images were measured in both SDR mode and HDR mode using a Konica Minolta CA210 Colormeter. Both the luminance values and x and y color coordinates were measured for both 2W and 3W. The results show an overall shift in the average overall color for the SDR and HDR viewing modes of two displays aged for 2000 hours. TV 2W saw a more pronounced shift in HDR mode towards the deeper blues while TV3W saw a shift in HDR mode toward the green part of the CIE 1931 xy diagram.

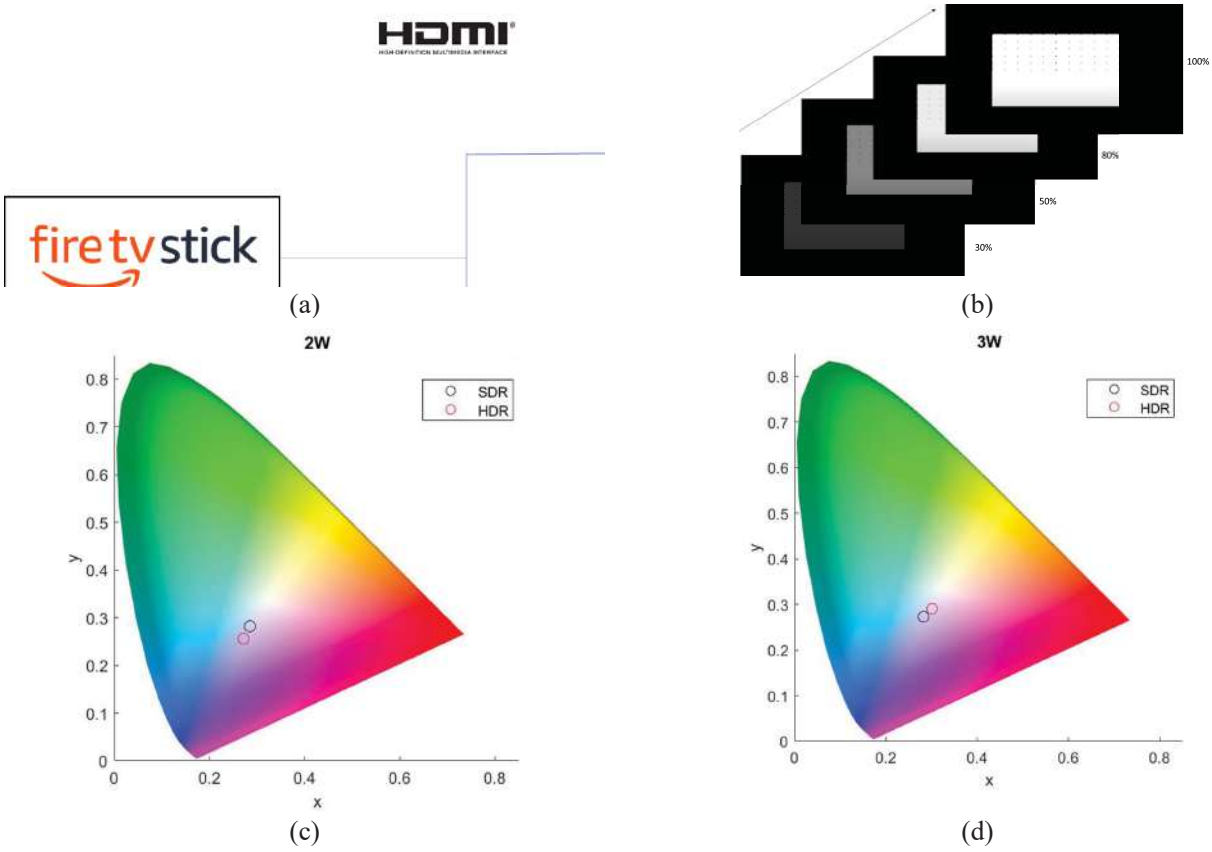

Fig. 1. (a) Experimental setup (b) HDR Measurement pattern at different brightness levels (c) HDR Gamma Correction for TV 2W (d) HDR Gamma Correction for TV 3W

Acknowledgment

The authors would like to acknowledge Samsung Electronics for their support.

References

1. Kam, K., Yu, T., Behrman, K., Yu, C. and Kymissis, I. (2020), SID Symposium Digest of Technical Papers

Low-Voltage Driving Shift Register based on Coplanar a-InGaZnO TFTs Using Photo-patternable Ionic Elastomer

Changhyeon Cho[1], Yongchan Kim[2], Eseudeo Yun[2], Hanbin Choi[3], Do Hwan Kim[3], and Hojin Lee[1,2]*
[1]Dept. of IC Convergence Technology, Soongsil University, Seoul 156-743, Korea
Tel.:82-2-820-0634, E-mail: hojinl@ssu.ac.kr*
[2]School of Electronic Engineering, Soongsil University, Seoul 156-743, Korea
[3]Department of Chemical Engineering, Hanyang University, Seoul 04763, Korea

Recently, due to the increasing attention on wearable and portable electronics as a future key technology, high-performance devices and their integrated circuits with the solution-processible a-InGaZnO thin-film transistors (TFTs) have been highly researched. At the same time, lowering the operation voltage is an important factor because a high operating voltage results in high energy usage, which can be a big obstacle to battery-powered portable electronics. Currently, the gate dielectric for TFTs using the ionic polymer comprising ionic liquids (IL) in a polymer matrix to form the electric double layer (EDL) has been extensively studied thanks to its advantages of induced ultra-high-density carrier attainability in the channel, improved capacitive coupling, low-voltage operation. However, to be used as a gate dielectric for the integrated circuits, the ionic polymer needs to be patterned so that there have been many different approaches [1-2], but most of the methods have limitation on realizing micron-sized fine patterns.

In this talk, we developed a low-voltage driving shift register circuit that adopted photo-patternable ionic polymer as a gate dielectric in the coplanar TFT structure where the gate, source, and drain electrodes were deposited simultaneously. Solution-processed a-InGaZnO layer was adopted to add advantages such as low temperature, simple process, high electrical characteristics. Fig. 1 shows the transfer characteristics of the ionic polyurethane acrylate (i-PUA) based TFT measured by sweeping the gate voltage from -2 to 4 V, while the drain voltage was fixed at 1 V. According to measurement results, we could extract outstanding electrical characteristics of the fabricated TFTs with a high on-off ratio of ~10^6, high field-effect mobility of 8.1 $cm^2 V^{-1} s^{-1}$. Fig. 2(a) shows single-stage shift register comprising six coplanar a-InGaZnO TFTs and one storage capacitor. The bank structure using i-PUA was applied to solve overlap problem of the signal lines that usually occurs in the coplanar structure. As shown in Fig. 2(c), we simulated the output signal ($Out_{[n]}$) and three input signals ($Out_{[n-1]}$, V_{DD}, and CLK) of the proposed single-stage shift register driving at 1 Hz. From the simulated results, we confirmed the bootstrap using a storage capacitor through the $Q_{[n]}$ node signal, and the output signal was perfectly generated sequentially.

Through this study, we confirmed that the proposed shift register circuit based on photo-patterned ionic polymer gate dielectric was successfully operated without any distortion on the output signal with low-voltage driving. We believe that the proposed shift register circuit can be applicable to future electronics with low-power consumption.

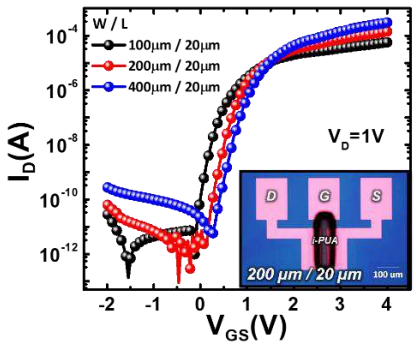

Figure 1. Measured transfer characteristics of the fabricated coplanar a-InGaZnO TFTs and its optical microscopy.

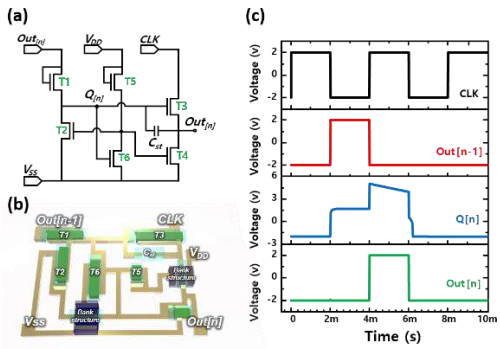

Figure 2. (a) Circuit diagram of the proposed shift register. (b) Schematic of the single-stage shift register. (c) The simulated result of the output signal for input signal.

Acknowledgment

This research was supported by the National Research Foundation of Korea (NRF) grant funded by the Korean government(MSIP)(NRF-2017R1A5A1015596)

References

1. K. H. Kee, *Adv. Mater.*, 24, 4457 (2012).
2. Mami N. Fulii, *Sci. Rep.*, 5, 18168, (2015).

Low-power Capacitive Pressure Sensor Circuit Based on Coplanar a-IGZO TFTs Using Photo-Patternable Ionic Polymer Gate Dielectric

Heejoo Park[1], Yongchan Kim[2], Changhyeon Cho[1], Jinho Moon[1], and Hojin Lee[1,2]
[1]Dept. of Information Communication Convergence Technology, Soongsil University, Seoul 06978, Korea
Tel.:82-2-820-0634, E-mail: hojinl@ssu.ac.kr
[2]School of Electronic Engineering, Soongsil University, Seoul 06978, Korea

Pressure sensor circuits based on thin-film transistors (TFTs) have emerged as promising candidates for future technologies such as human-machine interfaces, wearable health monitoring, and electronic skins. To be utilized in the future sensing system, high performance and low-operating voltage are essential factors, and, in this regard, ionic polymer electrolyte have attracted considerable attention as gate dielectric of TFT to give superior advantages including exhibit high capacitance, excellent mechanical flexibility, and optical transparency. [1-3] However, most approaches for patterning ionic polymer electrolyte such as transfer or nozzle-based printing methods often suffer from low spatial resolution and inaccurate fine pattern control. In this paper, we developed a novel low-power capacitive pressure sensor circuit based on coplanar amorphous indium gallium zinc oxide (a-InGaZnO) TFTs with ionic polyurethane acrylate (i-PUA) fabricated by conventional photolithography.

Fig.1 shows transfer characteristics for coplanar a-IGZO TFTs measured at a fixed V_D of 1 V, while sweeping V_G from -2 to 4 V. The device represents excellent electrical properties with the field-effect mobility (μ) and threshold voltage (V_{TH}) calculated to be 6.45 $cm^2 V^{-1}s^{-1}$ and 0.65 V, respectively, and high ionic capacitance of 2.2 $\mu F/cm^2$ for 80 wt% i-PUA. Fig. 2(a) shows the schematic of the proposed capacitive pressure sensor circuit consisted with three TFTs and two capacitors, and optical image of the fabricated circuit is displayed in Fig. 2(b). T1 is a driving TFT that converts the pressure sensing voltage on C_{Sen} during sensing period, and T2 is a pull-down TFT which prevents the floating state. T3 is a reset TFT that pulls the output voltage of circuit back to V_{SS} after sensing period. To analysis the sensing performance of circuit, the output waveforms of the pressure sensor circuit were measured as shown in Fig. 2(c). As the pressure applied to sensor (C_{sen}), the output voltage decreased according to pressure intensity, and the diverse output voltages were observed with soft and hard pressures of 20 mV and 50 mV, respectively. From the experimental results, we expect that our proposed pressure sensor circuit could contribute to future wearable sensor systems with low power consumption.

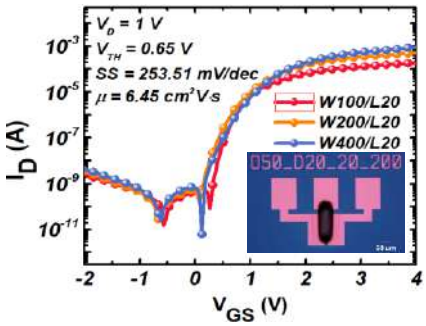

Fig. 1. Transfer characteristics of coplanar a-IGZO TFTs

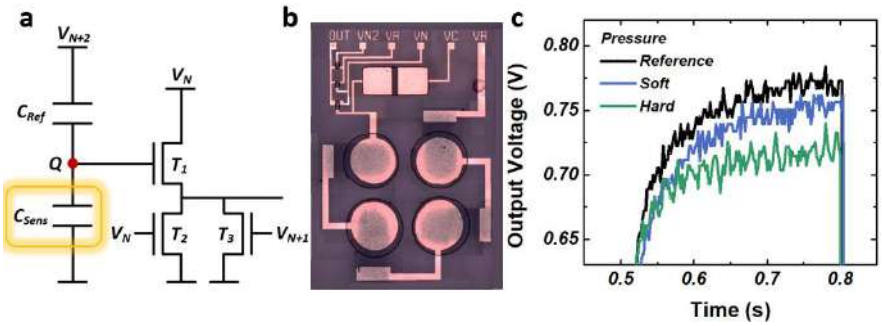

Fig. 2. (a) Circuit diagram and (b) optical image of the pressure sensor circuit, (c) measured output waveform for the various pressure

Acknowledgment

This work was supported by the National Research Foundation of Korea (NRF) grant funded by the Korean government(MSIP)(NRF-2017R1A5A1015596).

References

1. Y. Joo, *Adv. Electron. Mater.*, 3(4), 1600455, 2017
2. Q. Sun, *Adv. Mater.*, 26(27), 4735, 2014.
3. S. W. Lee, *Sci. Technol. Adv. Mater.*, 7(5), 874, 2015

Pseudo face-orientation change for 2D communications by spatial blending of 2D face images with different face orientations

Yurie Nakagawa, Haruki Mizushina, Kenji Yamamoto, and Shiro Suyama
Dept. of Optical Science and Technology, Faculty of Engineering, Tokushima Univ.
2-1 Minamijyosanjima, Tokushima 770-8506 Japan
Tel.:+81 88 656 9427, E-mail: c612136014@tokushima-u.ac.jp

In meetings over a few people, such as web conferencing tools that have become mainstream in today's COVID-19 situation, it is a problem that the listeners are difficult to know whom the speaker is talking to [1]. In order to solve this problem practically, we propose a pseudo face-orientation change method by spatial blending of 2D face images that can easily express the orientation of the face using only a 2D display and two cameras. In this paper, we evaluated the possibility of expressing a pseudo face-orientation change by spatial blending of 2D face images with different face orientations.

(a)Front face ratio:50.0% **(b)Front face ratio:40.3%**

Fig. 1. Examples of composite face images by spatial blending of 2D face images

Fig. 1 shows the principle and example of composite face image for a line-of-sight expression method that combines 2D face images taken by two cameras with different camera angles in Fig. 2. When face images taken from the front and left or right are combined using a thick line at the joint, it looks like it is facing slightly to the right from the front as shown in Fig. 1(a). In Fig. 1(b), by increasing the size ratio of right directed face image in the combined two face images, the perceived line of sight of the composite face image can be changed to right direction.

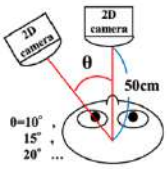

Fig.2. Camera angles for taking face photographs at the same time

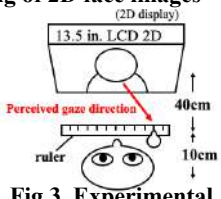

Fig.3. Experimental system for evaluation of perceived line of sight in the composite face image

In this experiment, subject's photographs taken simultaneously by two cameras as shown in Fig. 2 were combined as shown in Fig. 1 and the size ratio between front and left or right directed face images were changed. Perceived line of sight was evaluated by pointing a ruler in front of the subject as shown in Fig. 3. The line-of-sight direction of the composite face image was evaluated using the combination of the left directed face images:-10°, -15°, -20°, or right directed face images:10°, 15°, 20° and the frontal face image:0°.

Figs. 4 and 5 show perceived line-of-sight by changing front-face ratio in the composite face image. Figs. 4 (Fig. 5) shows combination of front and right (left) directed faces. Perceived line-of-sight direction of the composite face image can be successfully changed smoothly only by changing size ratio. Figs. 4 and 5 show that the lines of sight are changed to the same absolute extent of face orientations in both composite photographs even using right or left directed face images. Thus, it was clarified that simple pseudo method for line-of-sight changing display by spatial blending of the face image can be successfully achieved.

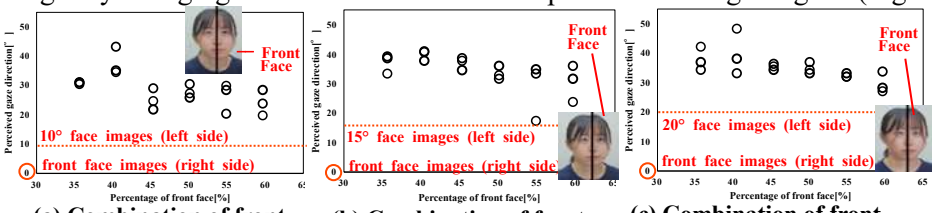

(a) Combination of front and 10 ° face images to right **(b) Combination of front and 15 ° face images to right** **(c) Combination of front and20 ° face images to right**

Fig. 4. Perceived direction of the line-of-sight of the composite face images between front and right directed faces

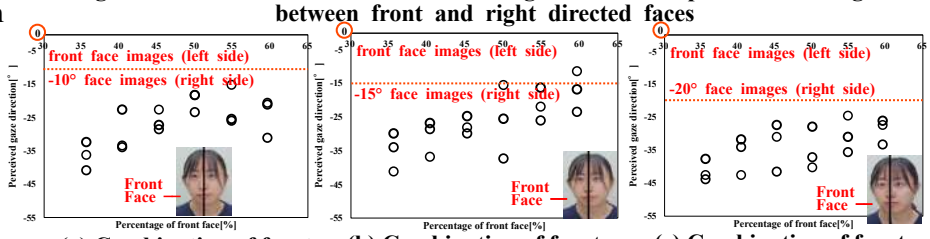

(a) Combination of front and -10 ° face images to **(b) Combination of front and -15 ° face images to left** **(c) Combination of front and -20 ° face images to left**

Fig. 5. Perceived direction of the line-of-sight of the composite face images between front and left directed faces

Acknowledgment

This study was supported by JSPS KAKENHI Grant Numbers JP19H04155, JP20K11919, JP20K21817, JP20H05702

References

1. Y.Takemae, The Journal of Image Information and Television Engineers, vol.12, No.59, pp. 1822–1829 (2005)

Image Quality Enhancement in Variable-Refresh-Rate AMOLED Displays Using an Initial Voltage Compensation Method

Li Jin Kim[1,2], Sujin Jung[1], Hee Jun Kim[1], Chang Hoon Jeon[2], Kyung Joon Kwon[2] and Hyun Jae Kim [1]
[1] The School of Electrical and Electronic Engineering, Yonsei University, Seoul 03722, Republic of Korea
[2] The LG Display Co., Ltd. Gyeonggi-do 10845, Republic of Korea
Tel.:82-2-2123-5865, E-mail: hjk3@yonsei.ac.kr

In active matrix organic light emitting diode (AMOLED) displays, when a variable refresh rate is applied, the image quality deteriorates, especially in color and luminance. This phenomenon is caused by the dependence in the emission time of OLED and the data programming time. In this study, we characterized the image degradation by measuring the color and luminance deviations at various frequencies, and the frequency-dependent cognitive differences were experimentally demonstrated using 6.76'' AMOLED display. Then, a new driving method to prevent this image quality degradation during the frequency change was proposed.

In Fig. 1(a), the right axis shows the absolute difference in luminance, and the left axis shows the difference rate expressed in percentage. While the absolute difference is large for high luminance, the difference rate increased as the luminance decreased. As human vision concerning luminance has non-linear characteristics, the cognition of luminance is more sensitive to the difference rate of luminance rather than to the absolute difference [1]. From Fig. 1(a) inset, it was confirmed that the value of just noticeable color difference (JNCD)-measurements for evaluating the color accuracy of a display-exceeded 1 under a luminance of 20 nit, and increased further as the luminance decreased. On the other hand, when the variable initial voltage (V_{INI}) was applied to the OLED anode individually for each frequency, the image quality degradation during the frequency change was prevented as shown in Fig. 1(b). After applying the voltage compensations, the color fluctuations decreased from 7.5 to less than 1 JNCD.

As our approach could prevent image quality distortion by utilizing an existing compensation pixel structure without additional compensation steps or modification of the pixel structure, it would be a promising technique for improving the picture qualities in AMOLED displays.

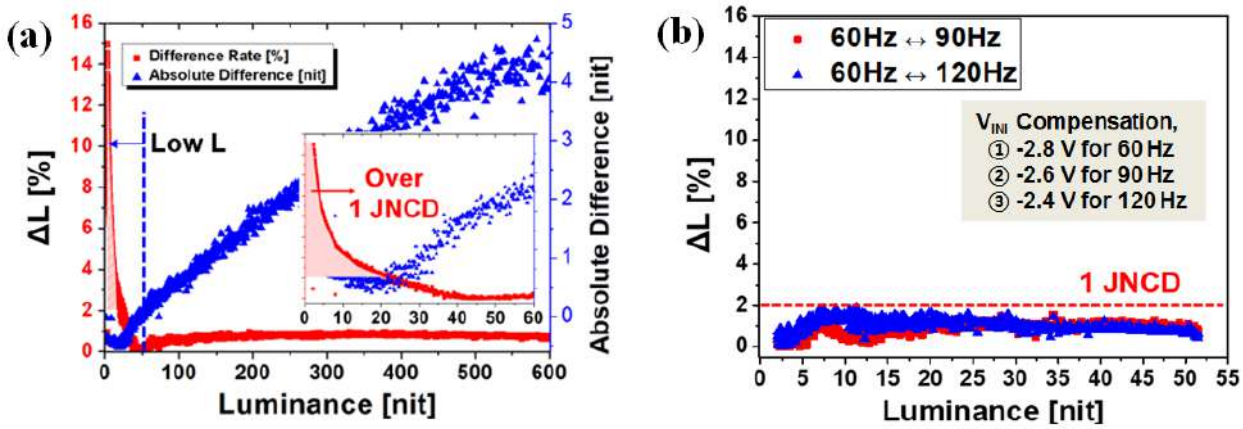

Fig. 1. (a) The differences in luminance between frequencies of 60 Hz and 120 Hz without compensation. (b) The differences in luminance under frequency changes. The V_{INI} were: -2.8 V for 60 Hz, -2.6 V for 90 Hz, and -2.4 V for 120 Hz.

Acknowledgment

This work was supported by the LG Display Co., Ltd. and the Nano Material Technology Development Program through the National Research Foundation of Korea (NRF) funded by Ministry of Science and ICT under Grant 2018M3A7B4071521.

References

1. T. Acharya and A. K. Ray. "Image Processing: Principles and Applications," John Wiley & Sons, Inc., pp. 37–39, 2005

A New Evaluation System for Metal Oxide Compound Semiconductor Film

Kook Chul Moon[1], JungUn Na[2], Hyoungsik Kim[2], GyoHyuk Yoon[2], JongPill Choi[2], Wonyoung Kim[3], Yong-Sang Kim[3]
[1]School of Electrical Engineering. KonKuk University, Seoul, Seoul 05029, Korea
Tel.:82-10-3507-7040, E-mail: gairgear@konkuk.ac.kr
[2]Engion Co.Ltd, Hwasung, Hwasung 18487, Korea.
[3]Department of Electrical and Computer Engineering, Sungkyunkwan University, Suwon, Suwon16419, Korea

Metal-Oxide compound semiconductor (MOx) such as IGZO(Indium-Gallium-Zinc-Oxide) has been widely used for TFT(Thin Film Transistor) on various applications [1][2]. However, it is difficult to realize in-situ monitoring of MOx film [3]. Several optical measurement methods such as micro PCD (Photo-conductive Decay) and optical absorption have been suggested but the extracted data are too indirect to well represent TFT characteristics. To overcome this problem, the new method is suggested for in-situ monitring without complex processes.

Fig.1(a) shows the concept of new method, which is to imitate 3-terminal measurement for a bottom-gate TFT. The method requires only common electrode deposition. The electrode of the backside takes the role of the common gate electrode in TFT and two probe terminals correspond to the source and drain electrode in TFT. Fig.1(b) is the scheme of specially designed probe unit to generate sufficient carriers.

Fig.2 shows measurement data of 3 kind samples using the new method. The different samples having different property show different measured data, which means that the new method can detect the process difference.

This new method would be very useful for mass production line.

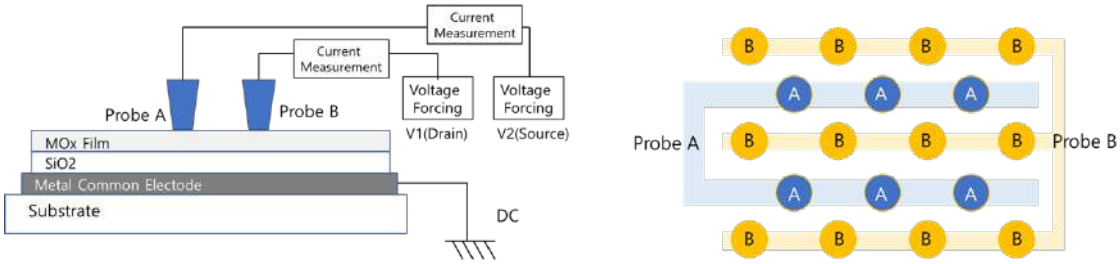

(a) Measurement Scheme (b) Probe Unit Scheme

Figure.1 The concept of measurement

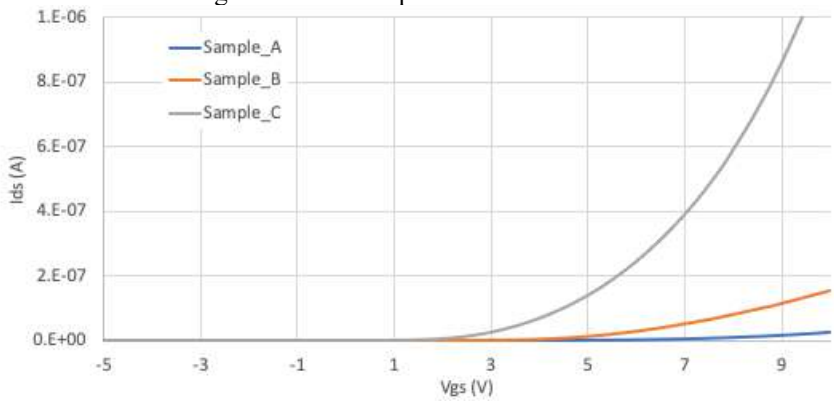

Figure.2 Measurement Data

References

1. Byung Du Ahn, et al., "Effect of Excimer Laser Annealing on the Performanceof Amorphous Indium Gallium Zinc OxideThin-Film Transistors" Electrochemical and Solid-State Letters, 12, ppH430-H432, (2009)
2. Narihiro Morosawa, et al, "Self-Aligned Top-Gate Oxide Thin-Film Transistor Formed by Aluminum Reaction Method" Japanese Journal of Applied Physics, 50, pp. 096502-1-096502-4, (2011)
3. Satoshi YASUNO, et al, "Application of Microwave Photoconductivity Decay Method to Characterization of Amorphous In-Ga-Zn-O Films" IEICE TRANS. ELECTRON, E95-C, No11, pp1724-1729(2012)

Direct Photolithography of Quantum Dot Films by Diethylzinc Treatment for High-Resolution Emissive Display Applications

Joon Yup Lee,[1] Gi-Hwan Kim,[1] Jisu Han,[2] Jaehoon Lim,[2] and Seong-Yong Cho[1,]*
[1]Department of Materials Science and Engineering, Myongji University, 17058, Korea

Tel: 031-330-6485 e-mail: goras26@mju.ac.kr

[2]Department of Energy Science, Sungkyunkwan University, 16419, Korea

Quantum dot light-emitting diodes (QD-LEDs) are one of the future emissive displays, but it is hard to fabricate high resolution multicolored pixel displays. In this study, diethylzinc treatment is introduced by atomic layer deposition (ALD) technique to pixelated QD display. Due to effects of the high reactivity of ALD precursors, it allows them to react with existing QDs' ligands on the surface. The QD film becomes insoluble and photoresist can be directly coated on top of the QD film. Ultraviolet exposure and development process enable patterned red/green/blue QD display pixels at resolution of higher than 800 ppi (pixels per inch). According to our previous work, ALD interlayer was proved to enhanced QD-LED luminance significantly.[1] This vacuum phase crosslinking mechanism of the QD surface can provide nondestructive high-resolution patterning platform for QD display.

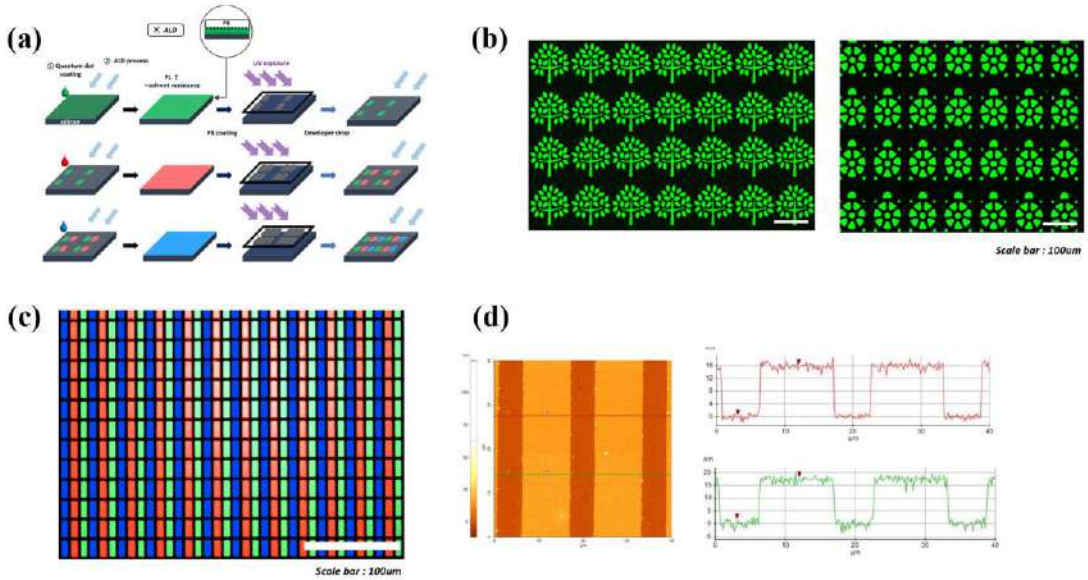

Fig. (a) Schematic illustration showing patterning process using photolithography, (b) various shapes of QD film obtained via photolithography, (c) red/green/blue tricolor pixel image obatained through sequencial processes, and (d) AFM data showing surface roughness of QD film after patterning process

Reference

1. Gi-Hwan Kim *et al.*, *Adv. Mater. Inter. 7, 2000343 (2020)*

One-way Observable Aero Signage Display Using Micro Optical Prism by Intaglio Printing Which Enables to Make Transparent View from Back Side

Kunio Sakamoto and Ryo Sakata
Dept. of Intelligence and Informatics, Konan University, 8-9-1 Okamoto, Higashinada, Kobe 658-8501, Japan
Tel.:81-78-431-4341, E-mail: kunio@konan-u.ac.jp

Suppose that you look Arabic numerals on transparent glass windows or in the air. Which does it mean '85' or '28'? You end up watching the mirrored images when you view from back side. This paper shows a one-way observable display for aero signage which means images are floating in the air. To solve mirrored image problems of an aero signage, the authors utilized prisms and total internal reflection in optics. You know that water is generally clear and transparent but the water in a bath tub is little blue. The color changes depending on the depth of water. The deeper, the darker water becomes blue. This is the reason why some color is generated in the dye-doped material. So we prototyped an optical resin block whose shape is a wedge. This dye-doped resin block has different thickness and makes color changing from transparent to blue gradually as shown in fig. (a). The authors utilize this color changing mechanism to make pixel dots transparent from back side.

In fig. (a), assume that a light ray is passing from the air into a glass. The light emanating from the interface is bent towards the normal of the boundary in the glass; $n_0 \sin \theta_0 = n \sin \theta$, where each θ is the angle measured from the normal of the boundary and each n is the refractive index of a material. This formula is called the Snell's law which calculates the relation of angles between incident and refracted beams. Here let consider a light ray passing from glass into air and assume that all light beams are in the material. An angle θ of this case is smaller than the critical angle. Then it is at this point no light is transmitted into air. And all beams pass only in a material because the beams are completely reflected. This is called the total internal reflection. Therefore light beams of signage are reflected by the edge of a slope on the prism like a mirror as shown in fig. (b).

No reflection light path generates no color. But multi-reflected light path generates some color because the length of light path in the dye-doped material is proportionate to the frequency of reflection and then the longer, the thicker material becomes dark. So we have devised that we utilize the total internal reflection phenomenon in order to realize one-way observable optical tiny blocks shown in fig. (b). When you watch the optical block from back side, you cannot perceive any color because the light path in the block is short. At your observation from front side, you can observe some color by the doped dye in the block because of long light path. The total internal reflection makes long light path because the beams are completely reflected in the material. That is why you can perceive color-dyed resin blocks from only front side. Fig. (c) shows observed images of one-way observable aero signage display whose unidirectional mechanism is realized by dye-doped tiny resin prisms. The authors put the letterings "HOPE" made by intaglio printings for arranging dye-doped tiny resin prisms on a glass window. You can watch colored letterforms of "HOPE" from front and transparent pixels from back side.

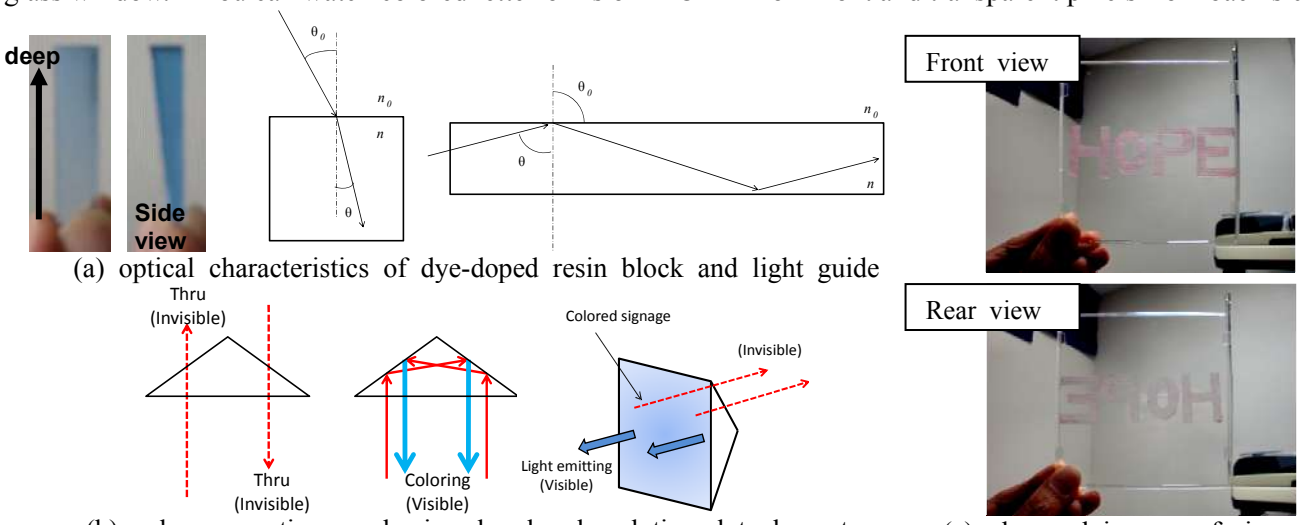

(a) optical characteristics of dye-doped resin block and light guide

(b) color generating mechanism by dye-doped tiny dot element

(c) observed images of signage

Fig. 1. One-way observable window signage using dye-doped tiny optical prisms by resin printing ink

High Performance, Ultra-flexible Metal Oxide Thin-Film-Transistor(TFT) Enabled by Polyimide Film for Wearable Application

Jeonghyoung Lee[1], Jiyun Tak[1], Soobin Lee[1], Jaekyun Kim[1]
[1]Dept. of Photonics and Nanoelectronics, Hanyang University, Ansan-si, 15588, Korea
Tel : 82-31-400-5521, E-mail : jaekyunkim@hanyang.ac.kr

Due to the uprising demands of wearable devices, transparency and flexibility are becoming the mainstream in fabrication of the TFT. The electrical properties of TFTs such as high mobility should be also guaranteed to meet the demands of future wearable application.

In this study, we fabricated indium tin zinc oxide (ITZO) TFTs with chromium (Cr) bottom gate and aluminum(Al) top contact metal on dual layer polyimide film/glass. In addition, low-temperature deposition of 50-nm-thick Al_2O_3 by plasma enhanced atomic layer deposition (PEALD) was employed to give rise to the accumulation of carriers at the interface between ITZO and Al_2O_3 [1]. Finally, the electrical characterization of ITZO TFTs on a dual layer PI film revealed that the field-effect mobility is as high as 18.96$cm^2 / V \cdot s$ while the current on/off ratio and sub-threshold swing are estimated as high as 10^{-7} and 0.5V/dec, respectively. After the delamination of PI film from the carrier substrate and bending, the ultra-flexible ITZO TFTs still exhibited the switching characteristics of TFTs with minimal degradation. Therefore, we believe that our ultra-flexible ITZO TFT platform can be used in the various application of wearable electronics including the display, sensors and internet of thing (IOT) devices.

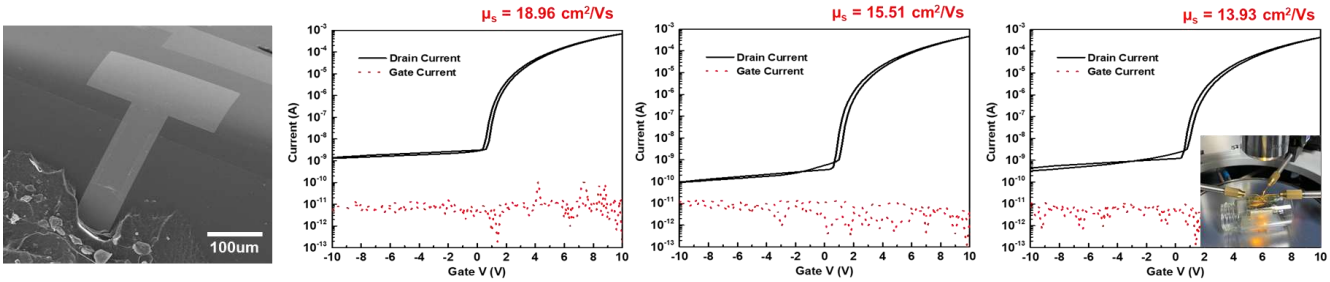

Fig. 1. SEM image of PI film(left), electrical properties of ITZO TFTs on a dual layer PI film after fabrication / delamination / bending (graphs in a row from left)

Development of Bilayer Inorganic Thin Film to Prevent Oxidation of Metal Layer

W.Y. Kim, H.Y. Lee, H.J. Kang, O.J. Kwon, S.J. Kim, D.J. Suh, and S.H. Kim[1]
[1]Display R&D Center, Materials Research Team, Samsung Display Co. Ltd.,
Giheung-gu, Yongin-City, Gyeonggi-Do, 17113, Republic of Korea
Tel.:82-70-0111-6085, E-mail: wooyoung17.kim@samsung.com

Deposition technologies for OLED (Organic Light-Emitted Diode) have been developed to various applications such as automotive, mobile and fiexible displays[1, 2]. In the condition of severe environment such as atmospheric exposure, typical OLED display shows decrease in life time and luminance due to degradation of EL (Electro Luminance) diode. Also, it shows change in transmittance of a metal layer due to oxidation of the layer. In order to prevent the oxidation, complete isolation from oxygen during deposition processes is demanded. In this work, bilayer inorganic thin film to prevent oxidation of metal layers is developed. Change in tansmittance of layer was evaluated in the condition of atmospheric exposure for 336 hours.

To prevent oxidation of a metal layer, a capping layer which is deposited by PECVD[3] (Plasma Enhanced Chemical Vapor Deposition) was applied. Despite of the capping layer (SiON), the oxidation was occurred by oxygen from ionized and dissociated reactant gas ($N_2O \rightarrow 2N + O$) during the PECVD process. Before the deposition of the capping layer (SiON), an inorganic thin film which is SiNx thin layer was deposited for complete isolation from oxygen. Fig. 1 shows transmittance change of metal layer in the condition of atmospheric exposure as a function of wavelength. According to Fig. 1, the transmittance sharply increased (from 59.2 to 68.8% @ 460 nm) after 408 hours. Fig. 2 shows transmittance of the metal layer with (a) single capping layer of SiON and (b) bilayer of SiON / SiNx as a function of wavelength. Despite of the single capping layer, the change in transmittance (from 70.6 to 67.2% @ 460 nm after 336 hours) and shift of the curve was occurred by the oxidation. On the other hand, the metal layer under bilayer showed little change in transmittance (from 66.7 to 65.0% @ 460 nm) after 336 hours. It means that the change in properties of the layer was not occurred by the complete isolation of oxygen from the metal layer with the application of strengthened bilayer.

In summary, the authors proposed the bilayer of SiON / SiNx to prevent oxidation of a metal layer. Compare with capping effect of the single layer, the oxidation was completely prevented by the bilayer. It opens the possibility of application range for OLED devices in severe environment conditions.

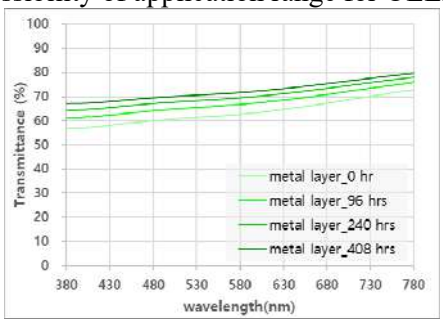

Fig. 1. Transmittance change of metal layer in the condition of atmospheric exposure as a function of wavelength.

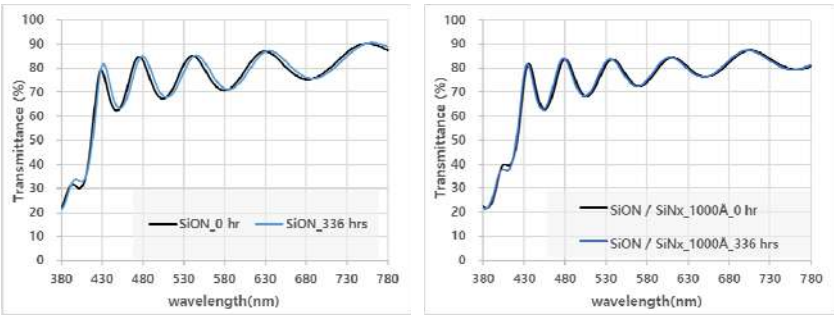

(a) **(b)**

Fig. 2. Transmittance of metal layer with (a) single capping layer of SiON and (b) bilayer of SiON / SiNx as a function of wavelength.

References

1. J.H. Park and T.S. Sudarshan, Chemical Vapor Deposition (1st ed.), ASM international, 481 (2001).
2. P.F. Carcia, R.S. McLean, M.D. Groner, A.A. Dameron and M. George, J. Applied Physics, 106, 023533 (2009).
3. H. Lin, L.Q. Xu, X. Chen, X.H. Wang, M. Sheng, F. Stubhan, K.H. Merkel and J. Wilde, Thin Solid Films, 333, 71 (1998).

Solution-Processed Aluminum-Titanium Oxide as Gate Insulator for a-IGZO Thin Film Transistors

Sung-Won Kim, Won-Young Kim, Hwarim Im and Yong-Sang Kim

Dept. of Electrical and Computer Engineering, Sungkyunkwan University, Suwon, 16419, Korea

Tel.:82-31-299-4640, E-mail: yongsang@skku.edu

We investigated solution-processed Aluminum-Titanium Oxide ($AlTiO_x$) gate insulator for amorphous Indium-Gallium-Zinc Oxide Thin Film Transistors (a-IGZO TFTs). The solution-process is promising technique because it has many advantages such as a large-area deposition, high uniformity and low fabrication cost. Many groups have investigated solution-processed high-k dielectrics, such as Al_2O_3, ZrO_2, and TiO_2 by using spin coating method [1]. High-k materials are an important requirement for minimizing leakage currents affecting TFT's transmission performance, stability and lifetime. However, the high leakage current of solution-processed inorganic high-k insulators is one of critical problems to be solved.

Among high-k materials, TiO_2 has a high dielectric constant (ε_r = ~85), but TiO_2 tends to exhibit low breakdown voltage and higher leakage current density. In contrast, Al_2O_3 is an attractive material in terms of a high breakdown voltage but has a relatively low dielectric constant (ε_r = ~9) [2]. We report a high-performance solution processed $AlTiO_x$ gate insulator by combining titanium compounds with aluminum oxide.

We demonstrate $AlTiO_x$ gate insulator using multi-stacking to obtain sufficient thickness to prevent leakage current. $AlTiO_x$ solution 0.5 M was prepared by dissolving aluminum oxide with titanium oxide in 2-methoxyethanol and 1 mL, 2 mL, 3 mL and 4 mL of HCl(35 %) were respectively added. This is because HCl is used as a catalyst to reduce the annealing temperature required to have an anatase phase of TiO_2 [3]. To evaporate the organic solvent, the spin-coated $AlTiO_x$ film was pre-annealed at 200 ℃ for 10 min. This process was repeated 3 times. Then the $AlTiO_x$ film was annealed using RTA at 450 ℃ for 1 hour under oxygen condition.

Fig. 1. (a) shows the plots of leakage current density versus bias voltage of MIM devices. $AlTiO_x$ insulator exhibited the leakage current densities of 1.15×10^{-2} A/cm^2, 2.60×10^{-3} A/cm^2, 5.83×10^{-9} A/cm^2, 1.33×10^{-8} A/cm^2, and 5.26×10^{-7} A/cm^2, at 5 V for 0 mL, 1 mL, 2 mL, 3 mL, and 4 mL of HCl(35 %), respectively. The leakage current density decreases as the HCl increases and the lowest at 2 mL of HCl, and then it increased. Therefore $AlTiO_x$ film with 2 mL of HCl was selected as a gate insulator for TFTs. Fig. 1. (b) show the transfer curve of solution-processed a-IGZO TFTs on the $AlTiO_x$. The a-IGZO TFTs on the $AlTiO_x$ mobility of 0.43 cm^2/V·s, on-off current ratio (I_{on}/I_{off}) of 4.96×10^5, and threshold voltage (V_{th}) of 0.28 V at V_D 1 V.

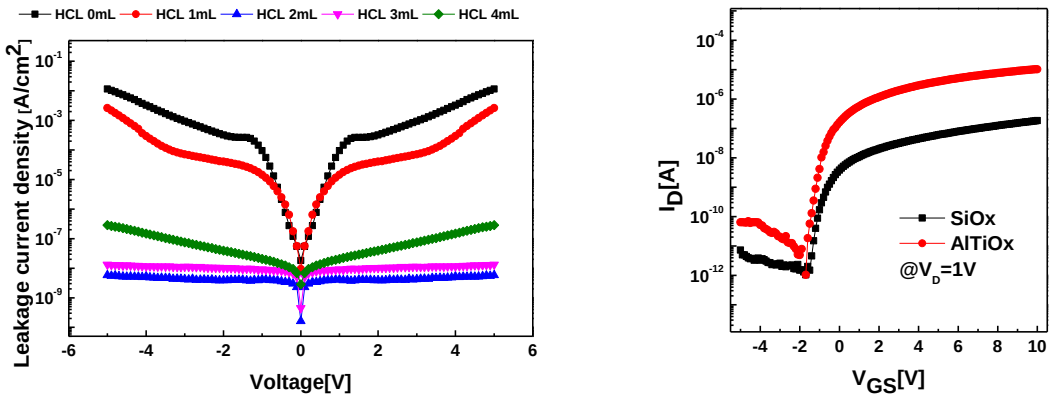

(a) (b)

Fig. 1. (a) Leakage current density characteristics of the $AlTiO_x$ according to the amount of HCl and (b) I−V transfer curves of IGZO TFTs with $AlTiO_x$ and SiO_x gate dielectrics at V_D 1V

References

1. W. Xu, H. Wang, L. Ye and J. Xu, J. Mater. Chem. C, vol 2, p. 5389–5396 (2014)
2. M. Kadoshima, et al, Thin Solid Films, 424, p. 224-228 (2003)
3. B.Morales, O.Novaro, T.López, E.Sánchez and R.Gómez, Journal of Materials Research, vol 10, p. 2788 (1995)

Eco-Friendly All Water-Based Solution Process for Robust Ag Nano-Mesh Transparent Electrodes

Sung Min Lee, In Hyeok Oh, Yeon Woo Kim, and Suk Tai Chang
School of Chemical Engineering and Materials Science, Chung-Ang University,
84 Heukseok-ro/Dongiak-gu, Seoul 06974, Korea
Tel.:82 10-6674-5591, E-mail: stchang@cau.ac.kr

Transparent conducting electrodes have attracted substantial attentions as an essential component o various optoelectronic devices. Recently, the grid-structured metal mesh electrodes are considered as highly efficient transparent electrodes that possess high optical transmittance while maintaining sufficient electrica conductivity and are suitable for flexible conductors with isotropic electrical conductivity. Here, we report a simple and effective approach for the fabrication of highly transparent Ag nano-mesh prepared by all water-based solution process. The Ag mesh electrodes were formed by combination of colloidal gold nanoparticles deposition and silver enhancement. The optical and electrical properties of the Ag mesh can be finely tunec by varying condition of gold nanoparticle deposition and silver enhancement. The smallest feature size o the obtained metal mesh patterns is about 700 nm with a thickness of 30-60 nm. The transparent electrodes with the Ag nano-mesh structure exhibit not only excellent electrical conductivity with a sheet resistance o 70 Ω/sq at a transmittance of 96.2% but also strong adhesion strength to substrate which is confirmed by peeling off test. Our all water-based solution processed metal mesh electrodes is applied to transparent heater which is able to heat up to 250 °C at 7 V. Through this study, Not only fabrication of high performance meta mesh but also low cost fabrication without any hazardous wastes is succeeded.

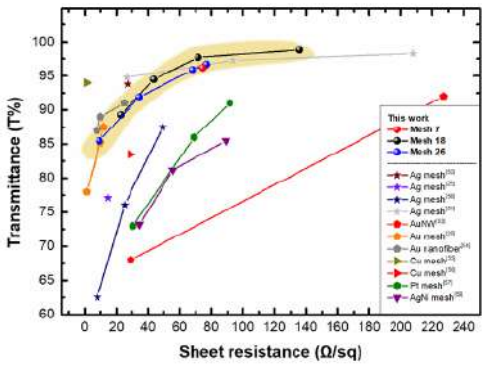

Fig. 1. Transmittance at 500 nm versus sheet resistance for recently reported transparent conducting electrodes, including our samples

Acknowledgment

This research was funded and conducted under [the Competency Development Program for Industry Specialists] of the Korean Ministry of Trade, Industry and Energy(MOTIE), operated by korea Insstitute fo Advancement of Technology (KIAT). (No. P0012453, Next-generation Display Expert Training project fo Innovation Process and Equipment, Materials Engineers)

References

1. Ballif, C. *Adv. Electron. Mater.* 2017, *3*, 1600529.
2. Crawford, G. P. *Appl. Phys. Lett.* 2000, *76*, 1425−1427
3. Irvin, G.*Adv. Mater.* 2011, *23*, 1482−1513.
4. Liu, Z. *ACS Nano* 2016, *10*, 11136− 11144

Study on the Solution Processed Organic Light Emitting Diode Using a Polyetherimide Adhesion Layer

Tae-Jin Lee[1], Jun-Yeong Lee[1], and Cheol-Hee Moon[1]
[1]Dept. of Electronics and Display Eng., Hoseo University, Asan, Chungnam 336-795, Korea
Tel.:82-41-540-5923, E-mail: chmoon@hoseo.edu

For the realization of all solution processed OLED(Organic Light-Emitting Diode), which is a whole solution process including the cathode, there have been reports using Al ink[1], and Ag paste[2]. However, due to the intermixing problem between the adjacent organic layers and thermal unstability of the organic emitting layer under the process condition, still remarkable progress of the study has not been reported yet. The biggest difficulty of the solution process of the OLED relates to the manufacturing of the cathode electrode by printing technology[3].

In this study, we developed a bonding OLED manufacturing technology by bonding two substrates for the anode and the cathode respectively using a PEI(Polyetherimide) as an adhesion layer, as is shown in Fig. 1(a). In order to confirm the applicability of this technology, experimental elements such as concentration of the solution, thickness of the layer, spinning conditions, thermal treatment conditions, pressure load, type of the substrates and addition of the other solution were checked. The adhesion strength was investigated using a spring scale and sufficient data was obtained in the case of the PDMS substrate. We also manufactured an EOD device to check the current density and observed a good characteristics in this bonded structure. Finally, we manufactured the OLED device which has an electrode structure shown in Fig. 1(b), and results show the possibility of the all solution processed OLED using cathode electrode by printing in the next step.

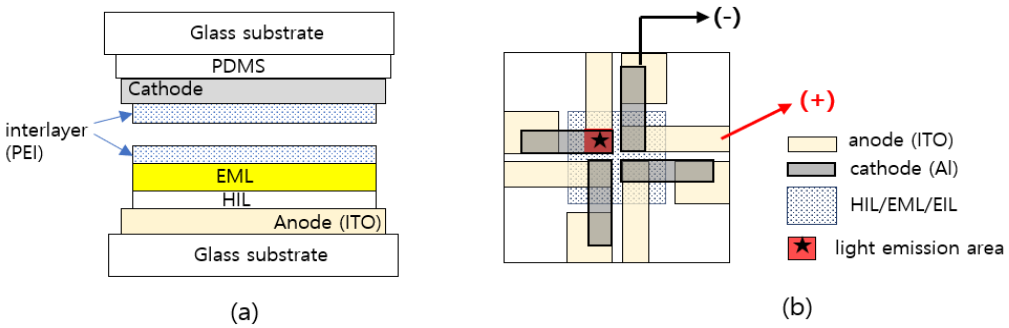

Fig. 1. Layer structure and electrode design of the OLED for the light emitting experiment. (a) Crosssectional view. (b) Electrode design of the device.

Acknowledgment

This research was funded and conducted under 「the Competency Development Program for Industry Specialists」 of the Korean Ministry of Trade, Industry and Energy (MOTIE), operated by Korea Institute for Advancement of Technology (KIAT). (No. P0012453, Next-generation Display Expert Training Project for Innovation Process and Equipment, Materials Engineers)

References

1. Hua Zheng, Yina Zheng, Nanliu Liu, Na Ai, Qing Wang, Sha Wu, Junhong Zhou, Diangang Hu, Shufu Yu, Shaohu Han, Wei Xu, Chan Luo, Yanhong Meng, Zhixiong Jiang, Yawen Chen, Dongyun Li, Fei Huang, Jian Wang, Junbiao Peng and Yong Cao, *Nature Communications,* 4(1), pp. 1-7, (2013).
2. W. J. Zeng, H. B. Wu, C. Zhang, F. Huang, J. B. Peng, W. Yang and Y. Cao, *Advanced Materials,* Vol. 19, no. 6, pp. 810-814, (2007).
3. P. S. Ko, N. D. Thuan, S. Kwon, K. H. Woo, T. M. Lee, Zhaoyang Zhong and H. S. Youn, *Journal of the Korean Society of Manufacturing Technology Engineers,* 27(5), pp. 446-447, (2018).

Crystalline Boundary Reduction of 6,13-Bis(triisopropylsilylethynyl)pentacene Thin Films on a Surface-Hydrophobicity-Modified Polymeric Insulator

Jin-Hyuk Kwon[1], Min-Hoi Kim[1,2*], Jin-Hyuk Bae[3,4*], and Jaehoon Park[5*]

[1]Research Institute of Printed Electronics & 3D Printing, Industry University Cooperation Foundation, Hanbat National University, Daejeon 305-719, South Korea

[2]Department of Creative Convergence Engineering, Hanbat National University, Daejeon 305-719, South Korea

[3]School of Electronic and Electrical Engineering, Kyungpook National University, Daegu 41566, South Korea

[4]School of Electronics Engineering, Kyungpook National University, Daegu 41566, South Korea

[5]Department of Electronic Engineering, Hallym University, Chuncheon 24252, South Korea

Tel.: 82-42-821-1973, E-mail: mhkim8@hanbat.ac.kr (M.-H. Kim); Tel.: 82-53-950-7222, E-mail: jhbae@ee.knu.ac.kr (J.-H. Bae); Tel.: 82-33-248-2357, E-mail: jaypark@hallym.ac.kr (J. Park) (Corresponding Authors)

Over the past decade, organic semiconductors have been in the spotlight as a promising candidate for next-generation electronics owing to their mechanical flexibility, solution processability, and applicability to various electronic devices [1-3]. Crystalline boundaries in organic semiconductors are often considered to provide charge-trapping sites or potential energy barriers. Accordingly, reducing the density of crystalline boundaries can be a critical consideration for more extensive and practical applications of organic semiconductors. It is worth noting that the physicochemical properties of underlying supporting surfaces significantly affect the growth of organic semiconductor thin films. Diverse viable methods for modifying such properties of supporting surfaces should be developed to realize a better state in organic semiconductor thin films. In this work, a liquid etchant was treated onto a supporting polymeric gate insulator to grow 6,13-bis(triisopropylsilylethynyl)pentacene (TIPS-pentacene) thin films with reduced boundary density. The etchant treatment effectively modified the surface hydrophobicity of the insulator without discernible morphological deterioration, such as an increase in surface roughness. Subsequently, TIPS-pentacene thin films were formed on the insulators. Figs. 1(a) and 1(b) show the optical microscopy images of the surface morphologies of the TIPS-pentacene thin films formed on a normal and the treated insulators, respectively. The TIPS-pentacene thin film on the treated insulator clearly exhibited a lower density of crystalline boundaries than that on the normal one. These results will offer useful knowledge for improving the electrical characteristics of solution-processed organic semiconductor devices.

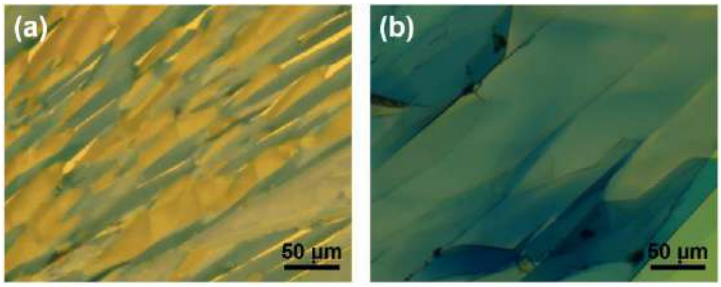

Fig. 1. Optical microscopy images of the TIPS-pentacene thin films formed on (a) the normal and (b) the surface-engineered polymeric insulators.

References

1. H. F. Haneef, A. M. Zeidell, and O. D. Jurchescu, *J. Mater. Chem. C*, 8(3), 759 (2020).
2. J. Chen, Y. Chen, L.-W. Feng, C. Gu, G. Li, N. Su, G. Wang, S. M. Swick, W. Huang, X. Guo, A. Facchetti, and T. J. Marks, *Energy Chem.*, 2(5), 100042 (2020).
3. Q. Liu, S. E. Bottle, and P. Sonar, *Adv. Mater.*, 32(4), 1903882 (2020).

Research on luminance inspection of Mini-LED using Light Control Film

Byeong-Chan Choi, Byung-Chul Lee, Kwan-Young Han*
Department of Display Engineering, Dankook University, 119, Dandae-ro, Cheonan-si, Chungnam, 31116, Korea
Tel.: 82-41-550-3590, E-mail: kyhan@dankook.ac.kr

Mini-LED was presented as a next generation display instead of LCD's Back Light Unit(BLU) because it improves low contrast ratio and brightness and does not have the degardation that is a disadvantage of OLED. However, there is a problem that the uniformity of luminance between individual Mini-LEDs mounted on the Display pannel is low. Therefore, it is necessary to perform an image inspection to identify the Mini-LED in which such a luminance difference occurs. Therefore, in this study, we present a luminance inspection method using a Light Control Film(LCF) without adjusting the ISO and Exposure Time of the image sensor for the blur phenomenon due to the high brightness of the Mini-LED, which acts as a difficulty in image inspection.

The LCF should reduce the blur and minimize the mutual influence of individual Mini-LEDs during luminance inspection. For that purpose, it is necessary to reduce the intensity of the ambient light generated by the Mini-LED and transmit the light having straightness in the Z-axis direction. In this study, we conducted an experiment to adjust the Quater Wave Plate(QWP) angle by consisting of two Polarizer Films and QWP whose polarization axes cross each other a LCF.

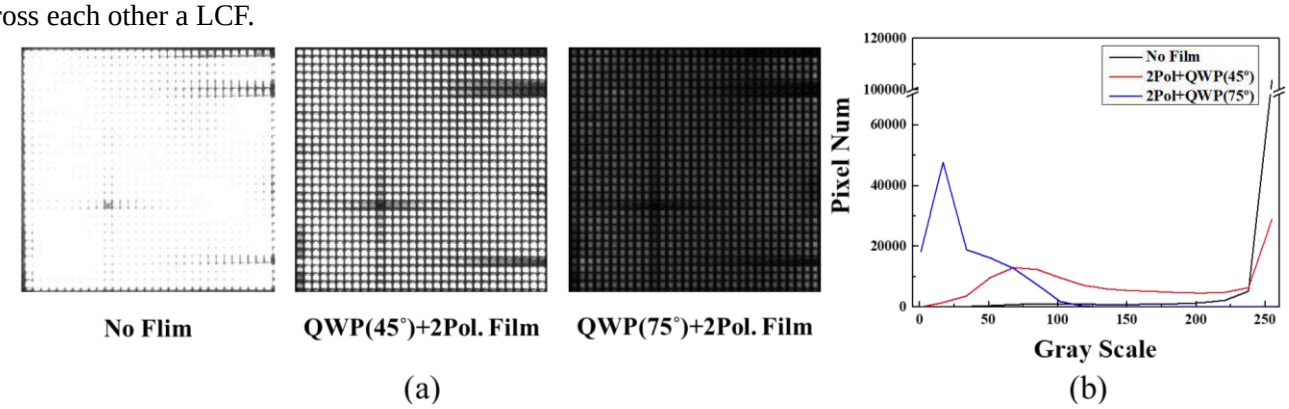

Fig. 1. (a) Mini-LED image using light control film, (b) Distribution of pixels according to gray scale

Figure 1 (a) shows a Mono image of a Blue Mini LED with a pixel size of 150 μm × 150 μm, indicating that the blur is reduced when the LCF is used, enabling the distinguishing between individual Mini LEDs. This is caused by the phase delay that occurs when the linearly polarized light passes through the QWP.

Fig. 1(b) shows the number of pixels according to the gray scale of the image of Fig. 1(a) as a graph. The distribution graph is used as an indicator to set the standard for dividing the lighting part and the non-lighting part of the Mini-LED during the luminance inspection through the change in slope. In the absence of film, 86% of all pixels were 255, the maximum Gray Scale that can be expressed in 8bit images, making it impossible to distinguish the non-lighting part of Mini-LEDs, which is unsuitable for luminance inspection. When the rotation angle of the QWP is 75°, the slope changes rapidly at the point where the gray scale of the pixel is 17, which is the standard for distinguishing the lighting part of the Mini-LED. gray scale However, since pixels with a gray scale of less than 100 are 90% of the total pixels, sufficient resolution cannot be ensured during luminance inspection. When the rotation angle of the QWP is 45°, the point at the gray scale of 51 is the luminance inspection standard. Further, if the section after that (gray scale 52 to 255) is set in the luminance inspection range, sufficient resolution can be secured, and as a result, the case where the rotation angle of the QWP is 45 ° is suitable for the luminance inspection.

Acknowledgment

This work was supported by the Technology Innovation Program (20011140) funded By the Ministry of Trade, Industry & Energy(MOTIE, Korea)“

References

1. Avner Safrani and I. Abdulhalim, Optics Letters, Vol.34, p. 1801, 243 (2009).
2. R Manish, Adigopula Venkatesh and S Denis Ashokc , International Conference on Materials Manufacturing and Modelling, Vol. 5, p.12791 (2018).

OCR spreading characteristics on the curved substrate for lamination of the flexible display

Young-Gyun Kim[1] and Kwan-Young Han[1]*
[1]**Dept. of Display Engineering, Dankook University, 119, Dandae-ro, Cheonan-si, Chungnam, 31116, Korea**
Tel.: 82-41-550-3590, E-mail: kyhan@dankook.ac.kr

Recent years have seen the development of display technology with the transformation from flat to flexible displays. In addition to bended and foldable, recently, it has been expanded to a curved display with constant curvature and is widely used as a display for automobiles. Accordingly, the technology of the lamination process for joining window cover glass with a panel substrate also increases, and continuous research and development is required. In this paper, a study on the characteristics of resin spreading on curved substrates was conducted using optical clear resin (OCR), which has the advantage of cheaper than the film-type optically clear adhesive (OCA) and does not involve microbubble generation at the edge during bonding. The spread of the OCR between two parallel glasses with a thin cell gap was extended to the spread of the OCR in a certain pattern using vectors, and further, the spread of the OCR pattern on the substrate having a certain curvature (400R or more) Consistency was confirmed by comparing the calculated value obtained in this way with the value obtained through an actual experiment.

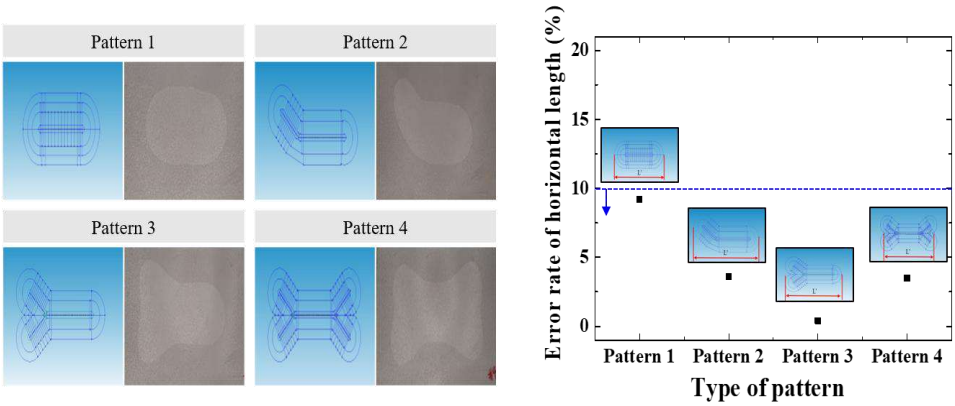

Fig. 1. Error rate between theoretical and experimental values of horizontal length for each pattern shape

As shown in Fig. 1, it was confirmed that the error rates of the theoretical and experimental values in various patterns were within 10%, with the minimum error rate of 0.4% and the maximum error rate of 9.2%. Through this, we find that this theory can be applied to curved substrates with a curvature of more than 400R. It was not suitable for curvature below 400R, It was not suitable for curvature below 400R, because the imbalance in thickness due to the fluidity of OCR is a problem for substrates with extremely low curvature However, since the actually the substrates used for automobile applications usually have curvatures exceeding 400R, this theoretical equation is expected to be highly useful in application and practical use These results are expected to be widely used in the lamination and manufacturing technologies for next-generation displays that will evolve in the future.

Acknowledgment

The authors gratefully acknowledge the financial support from ZEUS CO., LTD. in Korea.

References

1. Y. G. Kim and B. M. Park and K. Y. Han, *Japanese Journal of Applied Physics*, vol. 59, 080901 (2020).
2. 2. Y. G. Kim and B. M. Park and K. Y. Han, *SID'19 Technical Digest*, vol. 50, p. 1617-1619 (2019).
3. 3. K. D. Ha and K. Y. Han, *J. Mech. Eng. Sci. Technol.* 29 (8), p.3257-3265 (2015).
4. 4. I. D. G. A. Subagia and Y. J Kim, *J. Mech. Eng. Sci. Technol.* 27 (4), p.987-992 (2013).
5. 5. S. Han, N. Choi and M. Lee, *J. Mech. Eng. Sci. Technol.*, 26 (5), p.1477-1482 (2012).

Fabrication of Organic Light Emitting Diode Micropixels using Plasma Etching without Photolithography

Hyungki Park[1], Chanho Kim[1], Sangmin Lee[1], Hangil Lee[1], Jiho Jeon[1], and Sung Min Cho[1]
[1]School of Chemical Engineering, Sungkyunkwan University (SKKU), Jangan-gu/Suwon, Seobu-ro 2066, Korea
Tel.:82-31-290-7262, E-mail: gudrl1761@g.skku.edu

A micron-sized organic light-emitting diode (OLED) pixel array was fabricated without the use of photolithography. The OLED pixels were patterned down to a size of 40μm using imprint lithography and plasma etching. The imprinted mold has a three-dimensional four-layer structure and the OLED pixels were fabricated by removing each layer in order. In order to separately drive the patterned OLED pixels, a through-hole was drilled in the pixel and filled with an anode metal so that the anode electrode was located in the same plane as the cathode electrode. The anode and cathode electrodes for the operation of the OLED were separatd using a simple lift-off process. The feasibility of the fabrication process was verified by operating a larger OLED pattern fabricated by the same process. In this study, it was shown that a high-resolution OLED pixel array can be fabricated using the proposed simple process without using a photolithography process.

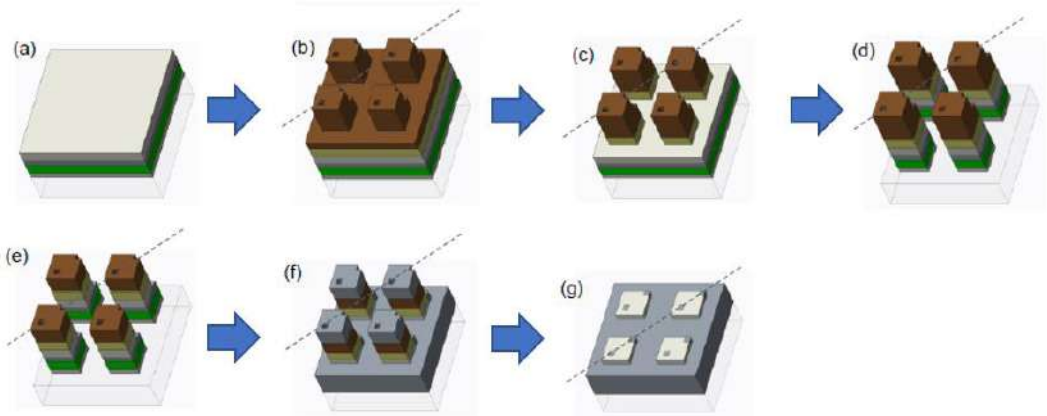

Fig. 1. Step-by-step images of the OLED pixel fabrication process

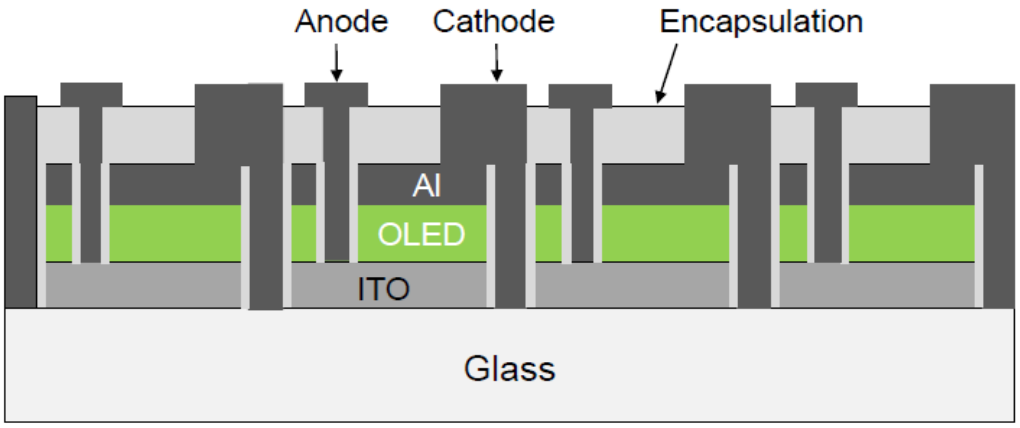

Fig. 1. Step-by-step images of the OLED pixel fabrication process

References

1. C. Kim, K. Kim, O. Kwon, J. Jung, J. K. Park, D. H. Kim, K. Jung, Fine metal mask material and manufacturing process for high-resolution active-matrix organic light-emitting diode displays, J. Soc. Inf. Display 1-12 (2020).
2. C.-W. Han, Y.-H. Tak, B.-C. Ahn, 15-in. RGBW panel using two-stacked white OLED and color filters for large-sized display applications, J. SID 19 (2) 190-195 (2011).

Effects of Al Capping Layer Thickness on Electrical Performance and Stability of IGTO TFTs

Seong-Hyun Hwang, Hyun-Seok Cha, Hwan-Seok Jeong, Dong-Ho Lee and Hyuck-In Kwon
Department of Electrical and Electronics Engineering, Chung-Ang University,
221, Huesuk-Dong, Dongjak-Gu, Seoul, 156-756, Korea
Tel.:+82-02-820-5293, E-mail: hyuckin@cau.ac.kr

We examined the aluminum (Al) capping layer thickness effects on the electrical performance and stability of high-mobility indium-gallium-tine oxide (IGTO) thin-film transistors (TFTs). The Al capping layer with thicknesses (t_{Al}s) of 0, 3, 5, and 8 nm were deposited on top of the IGTO thin film using electron beam evaporation technique, and the fabricated IGTO TFTs were subjected to low thermal annealing at 200 °C for 1 h in air ambient.

Among the Al-capped IGTO TFTs with different values of t_{Al}, the TFT with a 3-nm thick Al capping layer exhibits the excellent electrical performance (field-effect mobility: 26.4 cm^2/Vs, subthreshold swing: 0.20 V/dec, and threshold voltage: -1.7 V) and better electrical stability under positive bias and negative bias illumination stresses than other TFTs.

The observed phenomenon was attributed to the thickness dependent oxidation power of the Al capping layer. The oxidation power of the Al capping layer increased with an increase in the t_{Al} and the 3 nm is found as the optimum thickness of the Al capping layer which can selectively remove the weakly bonded oxygen species from the IGTO channel layer without significantly generating oxygen vacancies (V_O) within the IGTO. The results of this study thus demonstrate that the formation of the Al capping layer having the optimal thickness is the practical and useful method to enhance the electrical performance and stability of high-mobility IGTO TFTs.

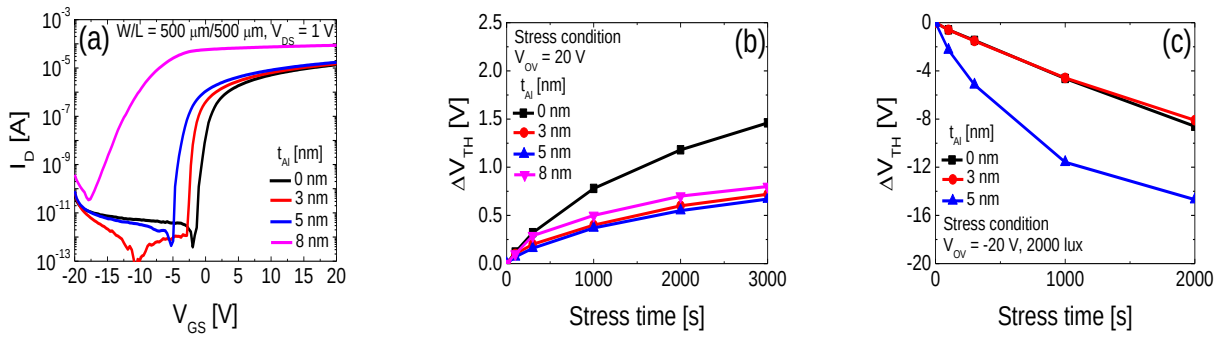

Fig. 1. Representative transfer curves of the IGTO TFTs with t_{Al} values of 0, 3, 5, and 8 nm on a (a). Time dependence of ΔV_{TH} obtained from IGTO TFTs with different values of t_{Al} after each (b) PBS time and (c) NBIS time.

In this work, we studied the effect of Al capping layer thickness on the electrical performance and stability of high-mobility IGTO TFTs. Our experimental results show that the electrical performance and stability of IGTO TFTs can be effectively improved by forming an Al capping layer with the optimal thickness.

Acknowledgment

This research was funded and conducted under 'the Competency Development Program for Industry Specialists' of the Korean Ministry of Trade, Industry and Energy (MOTIE), operated by Korea Institute for Advancement of Technology (KIAT) (No. P0012453, Next-generation Display Expert Training Project for Innovation Process and Equipment, Materials Engineers) and in part by a National Research Foundation of Korea (NRF) grant funded by the Korea government (MSIT) (No. 2020R1A2B5B01001765).

References

1. E. Fortunato, P. Barquinha, R. Martins, *Adv. Mater.*, *24*, 2945–2986, (2012).
2. H.-S. Jeong, H.S. Cha, S.H. Hwang, H.-I. Kwon, *Electronics.*, 9, 1875 (2020).
3. T. Kamiya, K. Nomura, M. Hirano, H. Hosono, *Phys. Stat. Sol.*,5, 3098-3100 (2008).
4. B.-H. Lee, A. Sohn, S.-S. Kim, S.-Y. Lee, *Sci. Rep.*, 9, 886 (2019).

Fabrication of Auxiliary Electrodes using Layer-by-Layer Inkjet Printing Process for OLED Lighting

Sung-min[1], Jun Ho You[1], and Sang-Ho Lee[1]
[1]Korea Institute of Industrial Technology, Sangnok-gu, Ansan-si 15588, Korea
Tel.:82-31-8040-6427, E-mail: sholee7@kitech.re.kr

An anode of OLED lighting mainly uses indium tin oxide (ITO) to emit light generated from an emitting layer. A specific resistance of ITO is low but higher than that of metals. If ITO is used as the anode of a large OLED lighting, a voltage drop across the anode becomes an issue. Due to the voltage drop, different voltages are applied depending on the location in an OLED lighting and the luminance is not uniform [1]. The voltage drop across the anode can be mitigated by placing auxiliary electrodes on ITO [2]. Semiconductor fabrication processes such as a photo lithography process, a deposition process, and an etching process are generally required to fabricate auxiliary electrodes. Unlike conventional semiconductor fabrication processes, inkjet printing process is more suitable for manufacturing auxiliary electrodes because it can quickly and economically fabricate structures only in a desired area without a photo mask [3].

Fig. 1 shows an OLED lighting without the auxiliary electrodes when 4.5 V is applied between the cathode and anode. The fabricated OLED lighting with a red-light emitting area of 7x7 cm^2 is composed of a glass substrate, 150 nm-thick-ITO layers, 60 nm-thick-OLED layers (HIL, HTL, EML and ETL layers), and 1 μm-thick-Al layers. The OLED and Al layers were fabricated through thermal evaporation process. Fig. 2 shows the fabricated OLED lighting with the auxiliary electrodes. Hydrophobic banks were fabricated by printing a FC solution to increase the thickness of the auxiliary electrodes while maintaining the width of the auxiliary electrodes. Ag nanoparticle ink is printed inside the hydrophobic bank, which prevents the ink from spreading out of the bank. The auxiliary electrodes were fabricated by overlapping three Ag layers using a layer-by-layer inkjet printing method. The height and width of the Ag auxiliary electrode were 1.2 μm and 43 μm, respectively. The auxiliary electrodes were printed at 2 mm intervals. A photosensitive resist was used as an insulator for covering the auxiliary electrode. The height and width of the insulator were 3.0 μm and 225 μm, respectively. Table 1 shows the luminance of OLED lights with and without the auxiliary electrodes. By the auxiliary electrode, the average luminance was improved by 21.0% and the standard deviation was decreased by 21.7%. In this paper, the OLED lighting panels were fabricated using an inkjet printing process. The measurement results show that the luminance and uniformity of the OLED lighting were improved by the auxiliary electrodes.

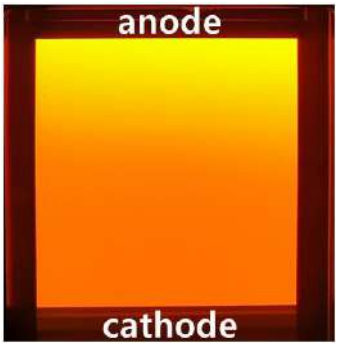

Fig. 1. OLED lighting without auxiliary electrode

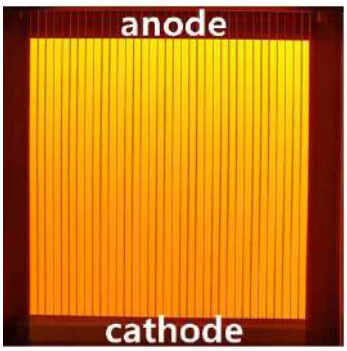

Fig. 2. OLED lighting with auxiliary electrode

Table 1. Luminance of the fabricated OLED lightings

OLED lighting	Luminance (cd/m^2)	
	Average	Standard Deviation
without auxiliary electrode	347	±193 (±55.7%)
with auxiliary electrode	420	±101 (±24.0%)

Acknowledgment

This study has been conducted with the support of the Korea Institute of Industrial Technology as " Development of Core Technologies for a Working Parter Robot in the Manufacturing Field(kitech EO-20-0018)"

References

1. K. Neyts, M. Marescaux, A. U. Nieto, A. Elschner, W. Lovenich, K. Fehse, Q. Huang, K. Walzer and K. Leo, *Journal of Applied Physics*, vol. 100, p.114513 (2006)
2. S. K. Choi, S. J. Kim, C. Fuentes-Hernandez and B. Kippelen, *Optics Express*, vol. 19, S4, p. A793 (2011)
3. J. H. You and K. H. Cho, K. T. Kang, Y. I. Cho, C. S. Lee and S. H. Lee, *SID 2018 Digest*, vol. 49, 1, p. 843 (2018).

Stabilization Effect of S or Se Incorporation with Indium Oxide

Paul Lee[1], and Myung-gil Kim[1]

[1]Dept. of advanced material science and engineering, Sungkyunkwan university, Suwon-si, Gyeonggi-do, 16419, Korea

Tel.:82-10-7247-7589, E-mail: impaullee91@gmail.com

Over past decades, metal oxide semiconductors (MOS) have attracted significant interests as next generation channel materials of thin-film transistors (TFTs). In particular, amorphous indium-gallium-oxide (a-IGZO) is the most representative material of various candidates due to its excellent electrical and optical properties compared to the conventional hydrated amorphous Si (Si:H). Despite these advantages, most MOSs have a chronic drawback that MOS-based TFTs are unintentionally very conductive since oxygen defects in metal-oxygen bonds create extra excess charge carriers. Therefore, a number of studies have recently been reported on the suppression of oxygen vacancy generations such as changing metal cations, building superlattice structure, and using organic-inorganic hybrid bilayers. However, a problem remains that most of the effort is focused on metal cation engineering, and furthermore, this approach is reaching technical limits. So, here we report a whole new idea of radically reducing the occurrence of oxygen vacancies through anion incorporation by adding S or Se to indium-based oxide-semiconductors. This study shows that S or Se atoms substituted at oxygen vacancy sites bring about an inductive effect and this effect reduces the oxygen vacancies generation. We demonstrated this concept by calculating the oxygen vacancies formation energy within the In_2O_3, $In_2(OS)_3$, $In_2(OSe)_3$ structures, and analyzing the components of the thin-films via XPS. As a result of measuring the electrical properties, it was confirmed that mobility of more than 6 cm^2/Vs can be obtained in the thin-films with less than 3% S or Se.

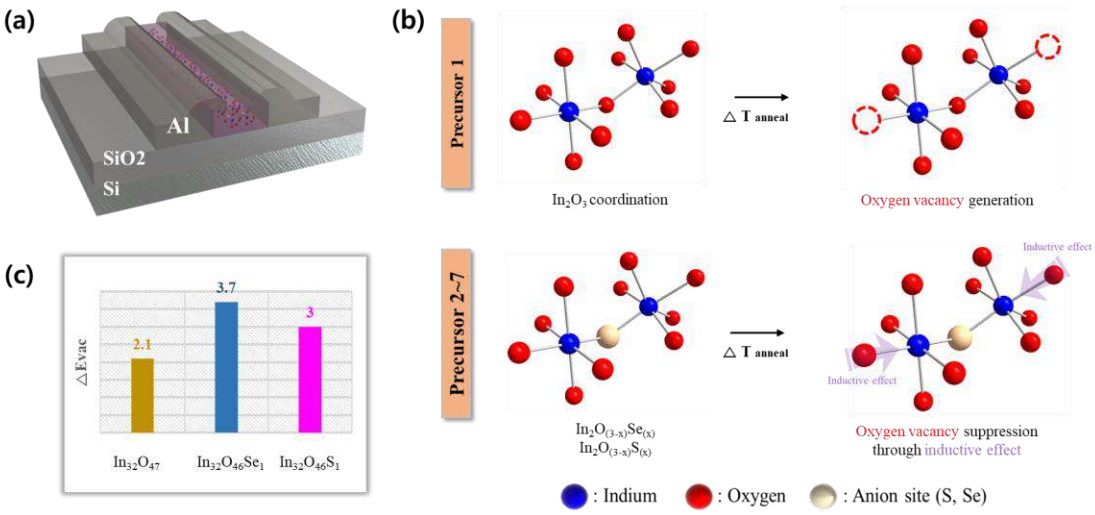

Fig. 1. schematic illustration of (a) the TFT structure and (b) the concept of stabilization effect induced by partially substituting S or Se for oxygen in indium oxide structure, (c) a graph comparing oxygen vacancies formation energy of $In_{24}O_{47}$, $In_{24}O_{46}Se_1$, and $In_{24}O_{46}S_1$

References

1. Fortunato, E.; Barquinha, P.; Martins, R., Oxide semiconductor thin-film transistors: a review of recent advances. Adv Mater 2012, 24 (22), 2945-86.
2. Yao, J. K.; Xu, N. S.; Deng, S. Z.; Chen, J.; She, J. C.; Shieh, H. P. D.; Liu, P. T.; Huang, Y. P., Electrical and Photosensitive Characteristics of a-IGZO TFTs Related to Oxygen Vacancy. Ieee T Electron Dev 2011, 58 (4), 1121-1126.
3. Banger, K. K.; Yamashita, Y.; Mori, K.; Peterson, R. L.; Leedham, T.; Rickard, J.; Sirringhaus, H., Low-temperature, high-performance solution-processed metal oxide thin-film transistors formed by a 'sol-gel on chip' process. Nat Mater 2011, 10 (1), 45-50.

a-IGZO TFTs with CYTOP Gate Dielectric

Won-Young Kim, Sung-Won Kim, Hwarim Im, and Yong-Sang Kim
Dept. of Electrical and Computer Engineering, Sungkyunkwan University, Suwon, 16419, Korea
Tel.:82-31-299-4640, E-mail: yongsang@skku.edu

We investigated amorphous indium gallium zinc oxide (a-IGZO) thin-film transistors (TFTs) with CYTOP gate dielectric. a-IGZO thin-film transistors (TFTs) have been widely used because of its high field-effect mobility, good uniformity for wide area and low processing temperature [1]. a-IGZO semiconductor have advantages for large areas and low-cost production. However, a-IGZO TFTs has bad reliability due to oxygen vacancies which acts as a trap center and operating in the depletion mode [2]. To overcome these problem, Kim *et al* reported that CYTOP passivation layer can passivate oxygen vacancies by fluorine diffusion from CYTOP layer to IGZO layer and Yoo *et al* reported that CYTOP gate dielectric modification layer can modulating charge carrier which induce enhancement-mode operation [3, 4]. However, these studies only explains how to reduce the influence of external environmental effects from ambient atmosphere through CYTOP passivation or modulating the charge carrier density by introducing surface dipoles onto dielectric surfaces, respectively.

In this study, we investigated CYTOP gate dielectric layer by fabricate a-IGZO TFT with CYTOP gate dielectric layer. Fig 1(b) show the optical band gap energy of a-IGZO layer according to fluorine diffusion from CYTOP layer to IGZO layer. The diffusion of fluorine at an annealing temperature of 350 ℃ for 2 hours led an increase of bandgap energy which evidence of improve realiability under illumination stress.

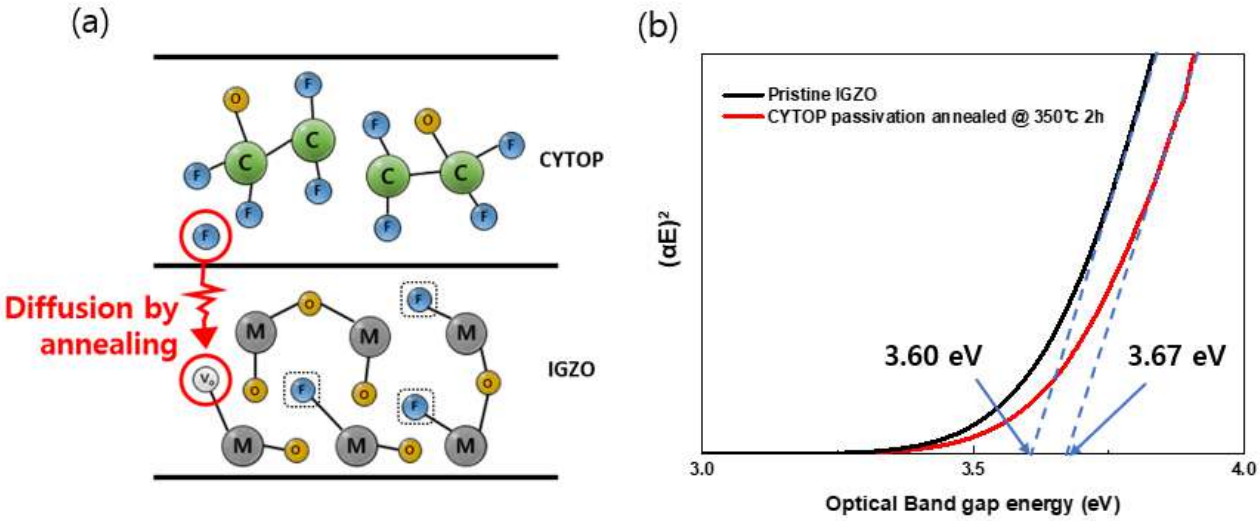

Fig. 1. (a) Mechanism for diffusion of fluorine and passivation of V_o in IGZO layer and (b) optical band gap energy of IGZO according to F diffusion

References

1. T. Kamiya, K. Nomura and H. Hosono, *Science and Technology of Advanced Materials*, vol. 11, no. 4, p. 044305 (2010)
2. A. Meux, A. Bhoolokam, G. Pourtois, J. Genoe and P. Heremans, *applications and materials science*, vol. 214, no. 6, p. 1600889 (2017)
3. K-M Jung, J. Oh, H. E. Kim, A. Schuck, K. Kim, K. Park, J-H. Jeon, S-Y. Lee and Y-S. Kim, *Journal of Physics D: Applied Physics*, vol. 53, no. 35, p. 355107 (2020)
4. G. Yoo, S. L. Choi, S. Lee, B. Yoo, S. Kim and M. S. Oh, *Applied Physics Letters*, vol. 108, p. 263106 (2016)

Flexible inorganic-organic nanolaminate encapsulation for next generation display

Heeyong Lee[1], Myung soo Huh[1], Jung Eun[1], Jung gon Kim[1], Dong pyo Jeon[1], Choel min Jang[1]
[1]Samsung Display, 1, Samsung-ro, Giheung-gu, Youngin-si, Gyeonggi-do, Korea
Tel.:82-31-5181-0552, E-mail: heeyong7.lee@samsung.com

Recently, commercialized foldable organic light emitting diodes (OLED) displays are attracting great interest and the displays such as stretchable and rollable are also extensively studied owing to their technical importance. But these flexible displays require considerable stress on the front of panel, so it is requisite to research a technique to keep the outermost encapsulation layer flexible. The currently used inorganic layer for the encapsulation which is brittle and contains high strain is located far from neutral plane, it can easily tend to fail during bending. Inserting the organic layers between inorganic layers leads to enhance the overall flexibility of multilayers. In order to increase the mechanical flexibility of the encapsulation layer, not only combining organic film with inorganic layer but also the thinner inorganic layer is necessary. The thickness of commercial inorganic films using plasma enhanced chemical vapor deposition (PECVD) is usually over 0.5μm to prevent water and oxygen permeation. In order to reduce the thickness of the inorganic film, it is known that the denser and pin-hole free film is required and normally can be deposited using atomic layer deposition (ALD) [1]. However, its low growth rate impedes to apply mass production and in addition, depositing organic layers needs additional fabrication processes. For commercial production, the encapsulation process which consists of inorganic-organic nanolaminate films should be deposited by high deposition rate in the same reaction chamber.

We deposited Si based inorganic and organic nanolaminate films using plasma enhanced ALD and CVD process in the same equipment to replace the outermost inorganic layer in the encapsulation process. To evaluate the reliability, the panels applied nanolaminate films and reference encapsulation films was tested in the evaluation chamber for 240 hours under 85℃ and 85% humidity conditions as shown Fig. 1. Although the thickness of nanolaminate films was thin (35%) compared with that of the reference CVD outermost layer, none of both samples are detected any dark spots and device shrinkages, which shows no induced deterioration of water and oxygen permeation. The flexible characteristic of the device was observed at the condition of various radius curvatures using a bending jig tester (repeated 200,000 cycles of out-bending). In the case of encapsulation applying nanolaminate films, any cracks were not occurred even at 62.5% of radius 'D' while the reference device solely endured the bending test at the radius 'D'. Inserting the organic layers between the inorganic films is demonstrated as an effective way to reduce the modulus of elasticity and stresses of the films, which indicates that nanolaminate encapsulation layer can be applied to flexible displays which required a low radius of curvature.

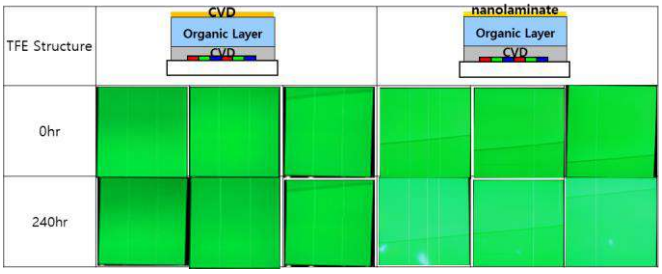

Fig. 1. The panel reliability results of the Ref. CVD and nanolaminate encapsulation for 240 hours under 85℃ and 85% humidity conditions at the curvature radius 'D'

References

1. Meng X. et al. A review of recent progress, challenges and outlooks Materials 9(12), 1007 (2016)

Area Selective Atomic Layer Deposition of Al_2O_3 using Self-Assembled Monolayers

Wung Sun Eo[1], Hye Jin Cho[1], Chan Ho Kim[1], Se Jin Ahn[1], Seung Woo Lee[1], and Sung Min Cho[1]
[1]School of Chemical Engineering, Sungkyunkwan University, 2066, Seobu-ro, Jangan-gu, Suwon-si, Gyeonggi-do, Republic of Korea
Tel.:82-10-9280-0654, E-mail: djdndtjs96@naver.com

The ultra-thin film deposition and fine patterning processes have been investigated for next generation technologies of semiconductor industry. Area selective atomic layer deposition (AS-ALD) is one of the future technologies. It is a kind of ALD where thin layer is deposited selectively on substrate with reactive functional group only by chemical adsorption. In this study, we carried out investigation of AS-ALD of Al2O3 using SAMs. Trimethylaluminium (TMA) and ozone were used as precursor and oxidant, respectively. Octadecyltrichlorosilane (OTS) and 1H, 1H, 2H, 2H-Perfluorooctyltrichlorosilane(FOTS) were used as SAMs for blocking deposition of Al2O3. However, SAMs cannot block deposition permanently. After several cycles, SAM chains get damages and TMA is physically adsorbed. They become nucleation site on passivation layers for deposition of Al2O3. For blocking deposition of Al2O3, materials and methods of SAMs for passivation were selected and process conditions were found. The functional group of SAMs are evaluated by FT-IR. Wetting property of SAMs and damage and physical adsorption on SAMs were evaluated by water contact angle (WCA).

Acknowledgment

This work was supported by Samsung Display

References

1. Seo, S.; Yeo, B.C.; Han, S.S.; Yoon, C.M.; Yang, J.Y.; Yoon, J.; Yoo, C.; Kim, H.-J.; Lee, Y.-B.; Lee, S.J.; et al. Reaction Mechanism of Area-Selective Atomic Layer Deposition for Al2O3 Nanopatterns. ACS Appl. Mater. Interfaces 2017, 9, 41607–41617. https://doi.org/10.1021/acsami.7b13365.
2. Xu, Y.; Musgrave, C. B. A DFT Study of the Al2O3 Atomic Layer Deposition on SAMs: Effect of SAM Termination Chem. Mater. 2004, 16, 646– 653 DOI: 10.1021/cm035009p

Characterization and of UV LED cured acrylic pressure-sensitive adhesives for flexible displays.

*Ji-Soo Kim[1], Youngdo Kim[2], and Hyun-Joong Kim[1,] **
[1]Laboratory of Adhesion and Bio-Composites, Department of Agriculture, Forestry and Bioresources, College of Agriculture & Life Sciences, Seoul National University, Seoul 08826, Republic of Korea
**Tel.:82-2-880-4784, E-mail: hjokim@snu.ac.kr*
[2]Samsung Display Co., Ltd., Cheonan 31086, Republic of Korea

PSAs used in flexible displays should have sufficient flexibility tolerance under stress during repeated folding to prevent fracture or delamination of the display products. The flexibility characteristics of PSAs include both elongation and recovery.

For display applications, UV curability and the excellent clarity properties of acrylic PSAs favorably support their use and suitability for UV curing systems [1, 2]. Our research group has consistently studied UV-curable adhesives using conveyor-type UV curing devices equipped with conventional UV mercury lamps and more recently as UV metal halide lamps. However, this type of UV curing device has several shortcomings including heat emission causing thermal deformation or unwanted thermal reactions and difficulty in constant precise control of UV exposure by the conveyor. Therefore, a UV light-emitting diode (LED) curing device was newly introduced for UV-curable PSAs; it has advantages such as a more compact device, selective UV wavelength, almost constant temperature due to the lack of heat emission, accurate and uniform curing due to the densely arranged lamps, and easily controllable UV exposure by exposure level and time [3]. These differences in curing methods are expected to lead to improved properties and better curing reactions.

Acrylic PSA films were prepared under several curing conditions using the UV LED curing device. The UV curing behaviors, optical properties, adhesion performance, and flexibility of the acrylic PSAs were investigated through gel fraction and Fourier transform infrared spectroscopy (FTIR) conversion, UV-vis transmittance, 180° peel strength, and shear strain and strain recovery. The purpose of study is to develop an acrylic PSA with both excellent shear deformation and high recovery properties and to provide data for application in flexible displays.

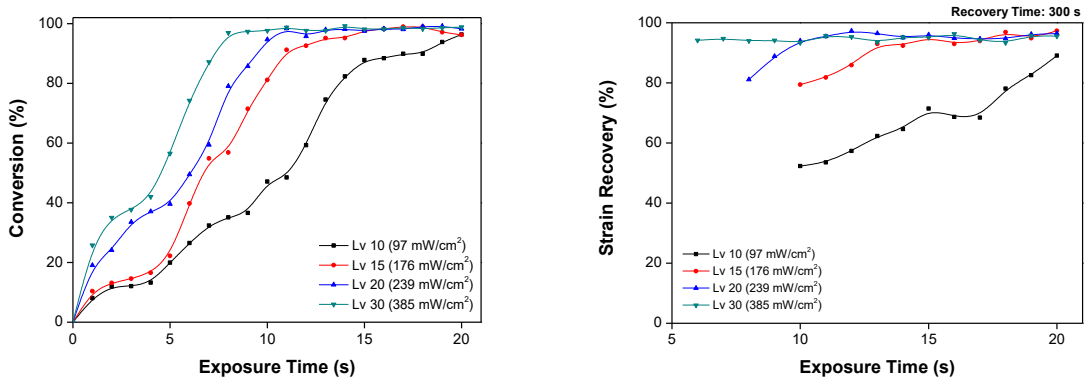

Fig. 1. Effects of UV exposure time on the monomer conversion(left) and strain recovery(right) of acrylic PSA samples for UV exposure intensity of Level 10, 15, 20, and 30. The lines are drawn for easier figure reading.

Acknowledgment

This work was financially supported by the Samsung Display Co., Ltd.

References

1. C. H. Park, et al. *React. Funct. Polym*, 100, 130-141. (2016).
2. J. G. Lee, et al. *Int. J. Adhes. Adhes*, 70, 249-259. (2016).
3. T. S. Natarajan, et al. *Ind. Eng. Chem. Res*, 50 (2011) 7753-62.

Organic-Inorganic Hybrid Transparent Conductive Electrode for Flexible Electronics

Minh Nhut Le[1], Byung Doo Choi[2], and Myung Gil Kim[1]
[1]School of Advanced Materials Science and Engineering, Sung Kyun Kwan University, Suwon, 16419, Korea
Tel.:010-3200-1812, E-mail: myunggil@skku.edu
[2] Department of Chemistry, Chung-Ang University, Seoul, 06974, Korea

The crystalline transparent conductive oxide (TCO) films, such as ITO, ZnO:Al, and FTO, have been widely used in various optoelectronic devices due to high optoelectronic performance derived from wide optical band and high electrical conductivity. However, the highly crystalline TCO films are vulnerable to the mechanical stress, which hinders the implementation of crystalline TCO in emerging flexible electronic applications. In contrast to the inherent brittleness of the inorganic materials, the organic material possesses the flexibility while having tunable optical and electrical properties. In this study, we have demonstrated the attempt to integrate the organic-inorganic hybrid materials to overcome the mechanical limitation of crystalline TCOs.

By utilizing low-cost, large area solution process to facilitate implementation of industrial metal oxide material into flexible electronic application. The hybrid transparent electrode shows good mechanical resistance at 1 mm bending radius up to 300 cycles (resistance difference is only 107%) and moderate electrical conductivity (538 S/cm).

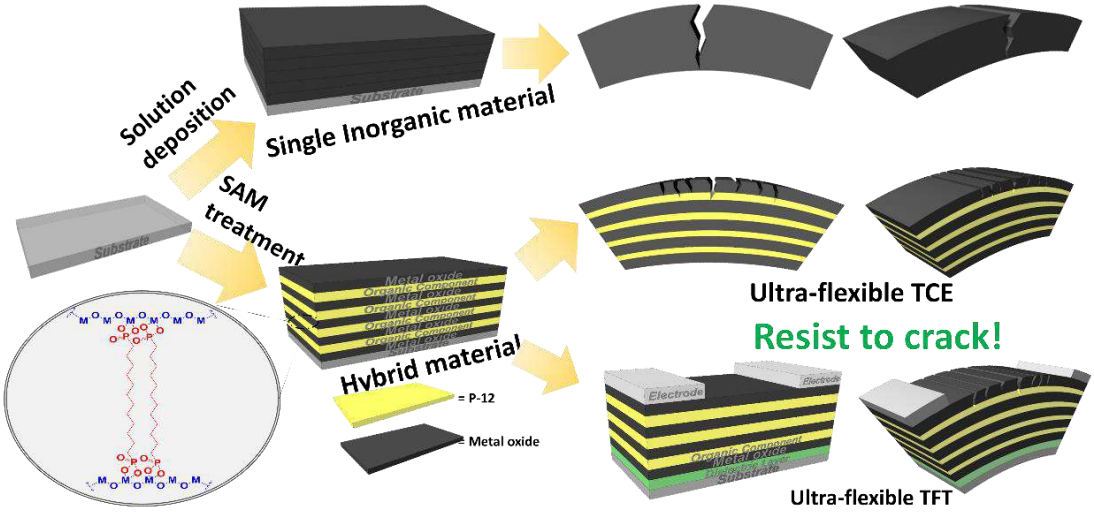

Fig. 1. Main scheme

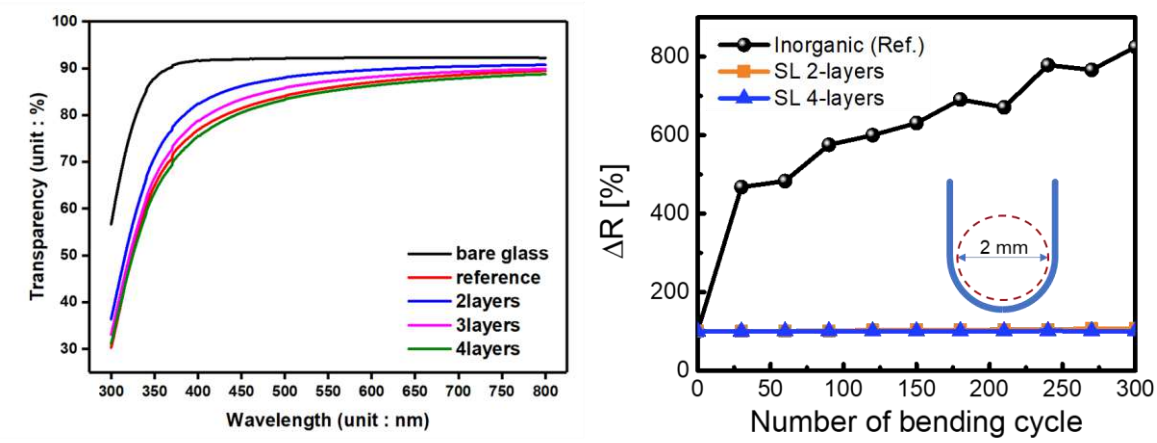

Fig. 2. Optical characteristic (left) and electrical performance of flexible TCO

References

1. Kwon, G.; Kim, K.; Choi, B. D.; Roh, J.; Lee, C.; Noh, Y. Y.; Seo, S.; Kim, M. G.; Kim, C., Multifunctional Organic-Semiconductor Interfacial Layers for Solution-Processed Oxide-Semiconductor Thin-Film Transistor. *Adv Mater* **2017,** *29* (21).

The effect of pump configuration in an ink circulation system on jetting quality in inkjet printer

Wooree Ko, Giwoon Sung, Futoshi Yoshida, Euna Ko and Younggeun Cho
Dept. of Equipment Core Technology Development, Samsung Display, Yongin city, Samsung-ro 1, Korea
Tel.:82-31-5181-0698, E-mail: wr.ko@samsung.com

Inkjet process is drawing attention in the display industry especially due to high degree of freedom in customizing patterns and low ink consumption compared to photolithography(1-4). When using an ink containing pigment, the inkjet printer usually includes an ink circulation system which continuously circulates the ink through a printhead to an ink tank in order to prevent the pigment aggregation and sedimentation. The ink circulation system plays a significant role in stabilizing the meniscus pressure at nozzles of printhead and affects the quality of jetting. This study analyzes how the performance of the circulation system can be optimized by the pump configuration in the system. A pump was adopted in the system and the effect of pump location within the system on the maximum flow rate the system can reach was investigated by circulating the ink through bypass line to disregard the resistance and pressure drop at the printhead. A lower maximum flow rate was achieved when the pump was located at the outlet of the printhead than locating at the inlet of the printhead due to the flow moving against the gravitational force and, thus, the easier generation of cavitation which decreases the performance of the pump. When circulating through the printhead, it was found that the pump at inlet requires a higher range of vacuum control while the pump at outlet requires the higher range of positive pressure control. Such requirements need to be taken into consideration when designing a circulation system to the best of performance. Also the effect of damper along with a pump was investigated by measuring the drop placement and the pressure at each inlet and outlet. When using a damper with the pump, the variation of pressure was approximately 25~45% smaller than the variation without the damper. Also, the straightness of the drop placement increased when not using a damper, implying that the meniscus pressure at nozzles was unstable.

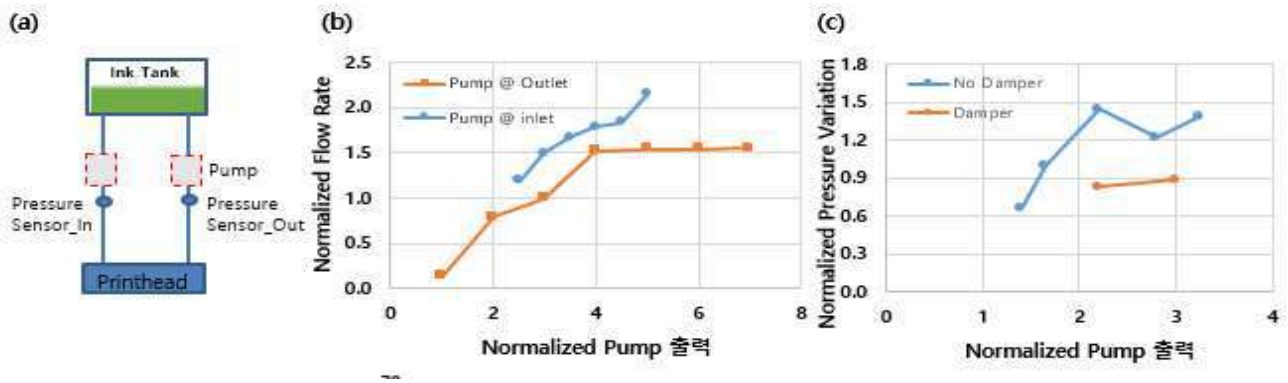

Fig. 1. (a) a schematic of an ink circulation system (b) the flow rate through bypass line with increasing pump output for each pump at inlet and outlet (c) the pressure variations with and without a damper

References

1. ROMANO JR, Charles E.; TRAUERNICHT, David P.; VANHANEHEM, Richard C. *Ink recirculation system for ink jet printers*. U.S. Patent No 6,631,983, 2003.
2. LANGFORD, Jeffrey D.; HARRIS, Carrie E. *Ink recirculation system*. U.S. Patent No 8,002,395, 2011.
3. HUDSON, Kevin R.; COWAN, Philip B.; GONDEK, Jay S. *Ink drop volume variance compensation for inkjet printing*. U.S. Patent No 6,042,211, 2000.
4. NALLAN, Himamshu C., et al. Systematic design of jettable nanoparticle-based inkjet inks: Rheology, acoustics, and jettability. *Langmuir*, 2014, 30.44: 13470-13477.

Laser micro patterning of carbon complex materials for lightweight and robust display

Junghwa You[1], Hyungsik Kim[1], Jeongho Kim[1], Joongsung Lee[1], Kyunghan Yoo[1], Alexander Voronov[1], Emil Aslanov[1], Jekil Ryu[1], SeongHo Jeong[1], and Cheol Lae Roh[1]*

[1]Samsung Display, 1 Samsung-ro, Giheung-gu, Yongin-si, Gyeonggi-do, 17113, Republic of Korea

[*]Tel.: +82-31-5181-5709, E-mail:hsnix.kim@samsung.com

While carbon complex materials have shown better mechanical properties than others have, the applications of them have limited due to fabrication difficulty [1]. Likewise, the needs which reduce weight and strengthen robustness of products have been growing faster and faster for lightweight and robust display. Laser fabrication of carbon complex materials requires high power laser over a few kW but the thermal degradation of polymers covering carbon materials have been imperative [2,3]. To adapt these for display, micro patterns having least damage on the edge of carbon complex materials should be available [4]. Productivity as well as fabrication quality are required to be enormously improved. Here, ultrafast laser fabrication of carbon complex materials for micro patterns is studied to form multiple micro patterns without destruction of the material structures. The heat affected zone on the materials could significantly been reduced by adjusting net fluence. Comparing with nanosecond lasers, mesh structures of carbon complex materials are reserved well by reducing heat damage of polymers up to 20μm. Such fine laser fabrication paves the way for enlargement of carbon material applications in display products.

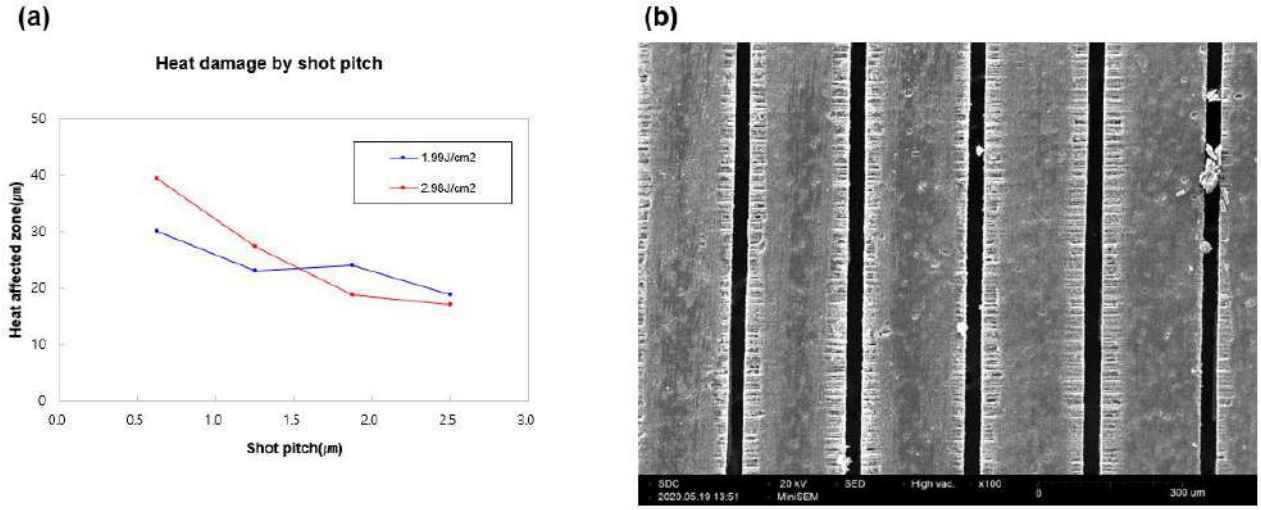

Fig. 1. a. Heat affected zone of carbon complex materials when laser shot pitch increase from 0.5μm to 2.5 μm. b. A SEM image in the laser fabrication of 1.99J/cm^2 and 1.25 ㎛ shot pitch.

References

1. A. Yakovlev, E. Trunova, D. Grevey, M. Pilloz, I. Smurov, *Surf. Coat. Technol.*, 190(1), 15-24 (2005)
2. D. Herzog, M. Schmidt-Lehr, M. Oberlander, M. Canisius, M. Radek, C. Emmelmann, *Mater. Des.*, 92, 742-749 (2016)
3. H. Xu, J. Hu, *Polymers*, 8(8) (2016)
4. A. Wolynski, T. Herrmann, P. Mucha, H. Haloui, J. L'huilliera, *Phys. Procedia*, 12, 292-301 (2011)

Jetting Reliability Improvement for Pixel Printing of QD Display

Katsuyuki Hirato[1], Wooree Ko[1], and JaiHyuk Choi[1]
[1] Mechatronics Technology Center Samsung Display Inc., Giheung-gu, Yongin-si, Gyeonggi-do 17113, Korea
Tel.:82-31-5181-0558, E-mail: katsu.hirato@samsung.com

Nowadays, displays are indispensable components of electronic devices. Recently there is growing demand of displays using quantum dot, so-called Quantum Dot Display(QD-Display).

QD-Display is very promising and outstanding in the next-generation display, because of high color purity, wide color gamut, flexible and thin form factors, and high brightness with low turn-on voltage etc.

Normally organic and inorganic QD materials are used to make red/green/blue colors in every pixel, and the prices are relatively expensive. Therefore, cost-effective method for pixel printing is needed in QD-Display [1].

Inkjet printing is a widely available, comparatively straightforward technique that is material- effective and can form individual pixels and is very flexible in the design of the printed device [2]. The inkjet printing equipment accurately drops a small drop of several pl into a sub pixel of several tens of um while moving a large 8.5G size substrate at high speed.

However, inkjet sometimes shows jetting failure and it causes defect of electrical devices, such as Mura, Luminescence failure. To prevent jetting failure, head care method and detection of jetting failure are being studied [4], but it is still the one of biggest issue of inkjet printing process.

In this study, we develop waveforms to detect potential defective nozzles before starting printing not to use these nozzles as shown in Figure 1.

Besides, we developed new maintenance waveform which can prevent production from stopping printing for head care process..

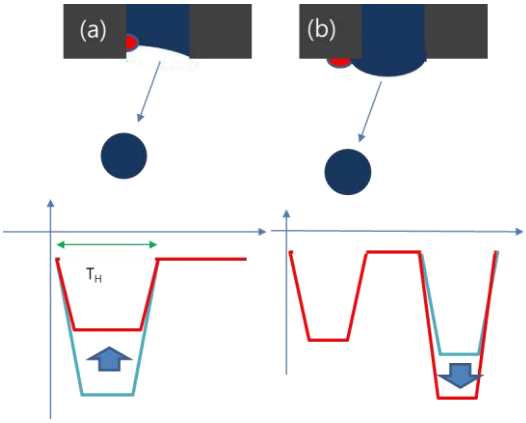

Fig. 1. A concept of detection waveforms

References

1 Yang, P. et al. High- Resolution Inkjet Printing of Quantum Dot Light- Emitting Microdiode Arrays. Advance Optical Materials 8, 1–7 (2020)
2 Cui, Z. Printed Electronics: Materials, Technologies and Applications, (Higher Education Press, 2016)
3 Mackey, R. 8K and 5G lead the TV industry to hit bottom and rebound? Let's watch 2019 TV. https://www.gearbest.com/blog/tech-news/8k-and-5g-lead-the-tv-industry-to-hit-bottom-and-rebound-lets-watch-2019-tv-11923 (2020)
4 Kwon, K. et al. Inkjet failures and their detection using piezo self-sensing. Sensors and Actuators A 201, 335–341 (2013)

Fine Organic Stripe Coating Using a Hydrophobic Needle for OLEDs

Jinyoung Lee, Gieun Kim, Songeun Hong, Jiho Choi, and Jongwoon Park
[1]School of Electrical, Electronics & Communication Engineering, Korea University of Technology and Education, Cheonan 330-708, Korea
Tel.:82-41-560-1467, E-mail: pjwup@koreatech.ac.kr

Solution process has attracted much attention in various fields such as organic light-emitting diode (OLED) displays, organic solar cells, sensors, and metal electrodes due to advantages such as low fabricaton cost, simple process, low material loss, and high scalability [1]. For OLEDs, various printing and coating technologies have been proposed to fabricate multilayer organic thin films [2]. Of them, needle coating is a facile method, which can facilitate pre-metered solution discharge. To apply needle coating to the fabrication of organic thin films with tens of nanometer thickness using very low viscosity solutions for OLEDs, a highly stable meniscus formed between the flat end of the needle and the substrate is required to ensure the inter-stripe thickness and width uniformities. Due to the hydrophilicity of needle shaft, moreover, lateral and vertical capillary flows may occur, swaying the downstream meniscus and the stripe profile. To investigate the feasibility of coating of fine organic thin-film stripes using the needle, we have performed a fine stripe coating of an aqueous poly(3,4-ethylenedioxythiophene):poly (4-styrenesulfonate) (PEDOT:PSS) by varying the outer surface of the needle from hydrophilic to hydrophobic. It is found that the lateral capillary force is suppressed by the hydrophobic needle, resulting in a decrease in the PEDOT:PSS stripe (Fig. 1(a)). It is also observed that the smaller the diameter of the needle, the smaller the stripe width. Using the hydrophobic needle (inner diameter = 51 μm), we have achieved the 54-μm-wide PEDOT:PSS stripe at a maximum coating speed of 30 mm/s. To demonstrate the potential applicability of needle coating in OLEDs, we coated 110 conductive PEDOT:PSS stripes for anodes on PET film using the hydrophilc needle with an inner diameter of 108 μm (Fig. 1(b)). The coated PEDOT :PSS stripes showed the average width and thickness of 74.3 μm and 87.7 nm, respectively. The intra-stripe width non-uniformity was as low as 16.2% and intra-stripe thickness non-uniformity was 14.8%. Finally, we have fabricated the 110 OLED stripes with the emission area of 12.7 mm × 12.7 mm and achieved light emission from all OLED stripes with the luminance of 254 cd/m^2 at 5V (Fig. 1(c)).

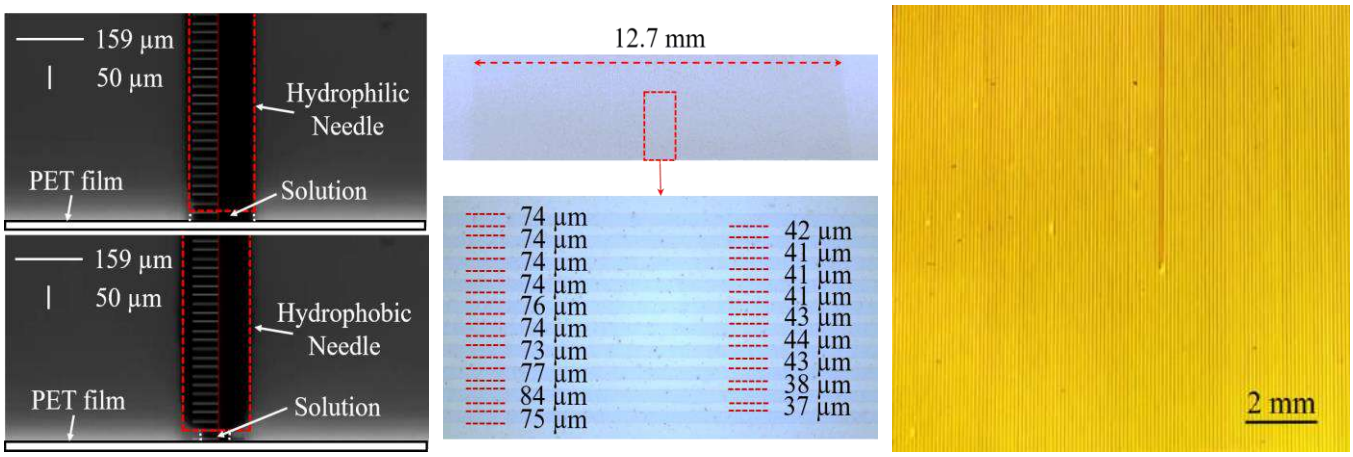

(a) (b) (c)

Fig. 1. (a) Fluid distribution from the hydrophilic and hydrophobic needles with an inner diameter of 51 μm, (b) photography of 110 PEDOT:PSS stripes with the coating area of 12.7 mm × 12.7 mm, and (c) an image of light emission from 110 OLED stripes at 5V.

References

1. R. Chesterfield, A. Johnson, C. Lang, M. Stainer, J. Ziebarth, *Information Display*, vol. 27, p. 24 (2011).
2. A. Sandström, H. F. Dam, F. C. Krebs, L. Edman, *Nat. Commun.*, vol. 3, p. 1 (2012).

Mechanism Study of Wide Color-gamut TFT-LCD's Light-caused Mura

Dong Wang[1], Dan Wang[2], Hongming Zhan[2], Xi Chen[2], and Xibin Shao[2]
[1, 2]Beijing BOE Display Technology Co., Ltd., Beijing, 100176, China
Tel.:86-10-57676797, E-mail: wangdong_dt@boe.com.cn

The wide color-gamut TFT-LCD need to use RGB resin with high pigment concentration, which is easy to appear green mura after illuminated by various lights. Microscopic analysis shows that the green sub-pixel of TFT-LCD show local brightness, while the red and blue sub-pixels are no such phenomenon.

The green mura results of TFT-LCD fabricated by four green resin and illuminated by different light sources and time, as shown in Table 1. High sensitivity photo-initiator in green resin can enhance the film compactness and improve mura, but the improvement degree is very small. Lower proportion of pigment G to Y in green resin can effectively improve mura. Base on the same Chroma specification of TFT-LCD, the novel pigment G can reduce the proportion of G to Y in green resin by 40%, and show the best mura result. On the other hand, photoelectric properties of the above resins are also evaluated, such as Chroma, volume resistance, voltage holding ratio and dielectric loss factor. Except for dielectric loss factor, the other photoelectric properties are basically the same, as shown in Table 1. All resins' dielectric loss factor in LED light on state is higher than that in LED light off state. By comparing and analyzing the mura of the TFT-LCD and the photoelectric properties of the green resins, it is inferred that the dielectric loss factor of the green resin is the cause of the green mura of TFT-LCD. The higher dielectric loss factor of the resin, the more serious mura of the TFT-LCD.

The pigment of green resin consists of a phthalocyanine metal complex. The central metal of the complex's molecular framework is copper or zinc, and the outermost part is connected with halogen atoms. Aromatic rings around the molecule have the characteristics of both electron donors and acceptors. Such pigment has conjugated structure and certain semiconductor property, which reduces the insulation and increases the dielectric loss factor of the resin. The liquid crystal in TFT-LCD will deflect under the applied voltage. After the TFT-LCD is turned on for a period time, the polarization of liquid crystal will induce the coupling electric field in the opposite direction of the current electric field, then gradually weaken the deflection of liquid crystal and the light passing through the liquid crystal, red, green and blue layers. If the green resin has high dielectric loss factor, it is equivalent to the parallel circuit of the resistor R and the capacitor C in TFT-LCD, then the liquid crystal of green sub-pixel will deflect abnormally, and result in the darkening speed of green sub-pixel slower than red and blue sub-pixels, finally showing the green mura of TFT-LCD. With the extended turn on time of TFT-LCD, the coupling electric field strengthens gradually, then the green sub-pixel darkens gradually, and the green mura of TFT-LCD disappears eventually.

Table 1. The mura of TFT-LCD and dielectric loss factor of green resin with different light sources and time
(√：No Mura, ×：Have Mura)

Test Item	Sample	Light	Time	A	B	C	D
Green Mura	TFT-LCD	LED	30sec	√	×	√	√
			60sec	√	×	√	√
			120sec	√	×	√	√
			600sec	√	×	×	√
		Fluorescent	1hr	√	√	√	√
			5hr	√	×	√	√
			9hr	√	×	√	√
			36hr	√	×	×	√
Dielectric Loss Factor	Green Resin	LED	LED On	0.6	0.7	0.6	0.4
			LED off	1.0	1.3	1.2	0.6

References

1. L. Y. Xu and J. Yu, *Chinese Journal of Liquid Crystals and Displays*, 31(5), 454 (2016).
2. Y. Luo, *14th National electrochemical Conference*, vol. 1, p. 969 (2007).
3. H. X. Dong, *Journal of Shangqiu Vocational and Technical College*, 8(5), 75 (2009).

A Study on Improvement and Diagnosis Method of Manufacturing in EtherCAT communication

Tae Min Kim [1 2], Jae Wook Jeon [1]
[1] **Semiconductor and Display Engineering Dept., Sungkyunkwan University, Korea**
E-mail: nazirekim@g.skku.edu
[2] **Memory Technology Innovation Team, Samsung Electronics, Hwaseong, Korea**

New processes are constantly being developed as the demand for the production of new products increases.

Because process development is directly related to the performance of equipment and equipment parts, manufacturing equipment requires three points.

The first is to improve the performance of the equipment that can be produced per unit in terms of mass production. The second is the stability of equipment with solidly identical performance against internal/external problems. The last is maintenance that guides the user when problems are found and prevents expansion.

While utilizing the EterCAT communication method, the speed improvement of 200 times to as much as 10000 times is achieved compared to the speed of the existing communication method used in production facilities. Above all, the synchronization control method does not cause communication delay between components, so that the stabilization time for synchronization between each component is not required or minimized.

Also, in the case of parts using analog communication or serial communication method, communication distortion or errors may occur due to external electromagnetic fields caused by the rotation of the motor or parts using high voltage.[Fig. 1.] However, the problem can be solved through the cable shielding design and error correction communication adopted in EtherCAT communication.[Fig 2.]

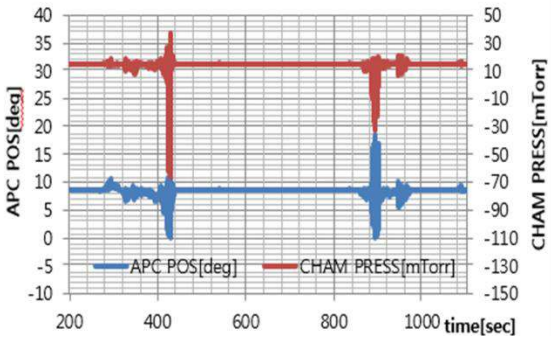

Fig. 1. Analog Communication

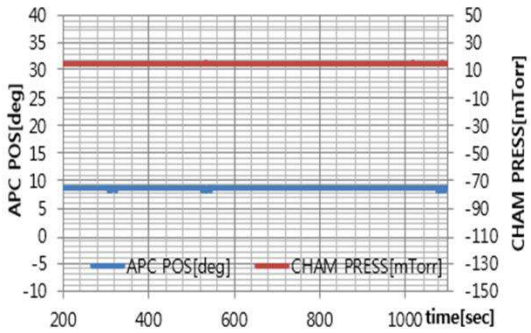

Fig. 2. EtherCAT Communication

Finally, through the EtherCAT communication standard, the service life and history management are easy by putting the usage time, specification, and version of each part in a common address. In the case of part usage time, the total usage time and the usage time after power-on are separately managed in the specifications, so it is possible to proceed according to the usage time rather than replacing all parts for preventive maintenance.

References

1. M. Rostan, J. E. Stubbs, p. 39-44, ASMC, San Francisco, USA(2010).
2. X. Chen, D Li, Microprocessors and Microsystems, Vol 46, Part B, p. 211-218(2016).
3. P. D. Burlacu, L. Mathe, p. 3064-3071 ICIT(2015).
4. G. Prytz, p. 408-415, ICETFA, Hamburg, Germany(2008).

Relation of the Intense Pulsed Light Energy to characteristic of the Fabricated OLEDs Device by Sublimation Transfer Process

Jun Yeub Lee[1,2], Byung Kwon Ju[2], and Kwan Hyun Cho[1]
[1]Manfacturing process platform R&D Dept., Korea Institute of Industrial Technology, Ansan-si, Gyeonggi-do, 15588, Korea
Tel.:82-31-8040-6256, E-mail: khcho@kitech.re.kr
[2]Dept. of Micro/Nano Systems, College of Engineering, Korea University, 145, Anam-ro, Seoungbuk-gu, Seoul, 02841, Korea
Tel.:82-2-3290-3210, E-mail: bkju@korea.ac.kr

Previously, in our research, the sublimation transfer process with the co-solvented solutions has been researched which has sucessfully induced into the micro channel and transferred to the device substrate. [1,2] However, the influence of the intense pulse light (IPL) energy on the transferred films and device performances have been not investigated in detail. In this paper, we investigated the relation of the IPL energy to the sublimation trasnfer process and interfacial phenomenon through the ToF-SIMS depth profile analysis. As shown in Fig.1(a), the cases with the inssufficient IPL energy as 10.8J/cm^2 or excessive IPL energy as 18.8J/cm^2 arise the unexpected emission on the range of 400 – 500nm wavelength. Fig.1(b) shows the reduced thickness of transferred emitting layer (EML), which induced the shift of the recombination zone to anode side due to the incomplete sublimation transfer process. Fig.1(c) shows no reduced thickness or intermixed layers with the proper IPL energy as 13.1J/cm^2. Fig.1(d) shows the intermixed state of the deposited layers altogether on the device substrate during sublimation transfer process due to the excessive IPL energy. The mixed layer arises the exciplex emissions due to the easy transport of electrons to the hole transport layer and hole injection layer. [3] In conclusion, the proper IPL energy for the sublimation transfer process has necessary to the fabrication of OLEDs device.

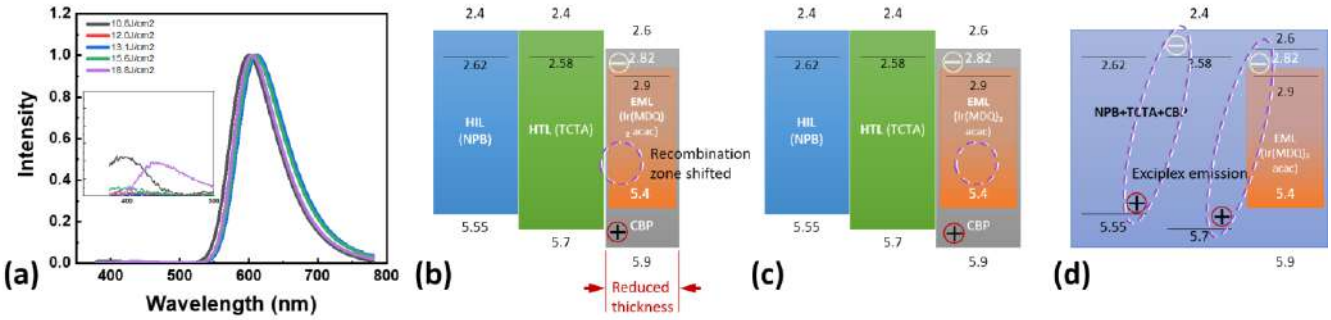

Fig. 1. (a) Electroluminescence spectra of fabricated OLEDs with the variation of IPL energy. Inset indicates the spectra of unexpected emission. The schematic of energy diagram of fabricated OLEDs devices with (b) insufficient, (c) proper, and (d) excessive IPL energy for sublimation transfer process, respectively.

Acknowledgment
This study was conducted with supported by Ministry of Trade, Industry & Energy (MOTIE, No. 20010459).

References

1. K.H. Cho, Y.C. Jeong, H.N. Lee, H.C. Cho, Y.M. Park, S.H. Lee, and K.T. Kang, SID Symposium Digest of Technical Papers, 50: 1507-1510 (2019).
2. H.C. Cho, H.N. Lee, Y.C. Jeong, Y.M. Park, K.T. Kang, and K.H. Cho, ACS Appl. Mater. Interfaces 2020, 12, 40, 45064–45072 (2020).
3. Y.S. Park, W.I. Jeong, and J.J. Kim , Journal of Applied Physics 110, 124519 (2011)

Particle Removal Prediction on Thin-Film Transistor Through Mist-based Cleaning Simulation

Yujin Seong, Hyojoon Gong, Changrok Choi, Ilho Kim, Seokwoo Lee, and Sooyoung Yoon
LG Display Co., LTD., Gangseo-gu, Seoul, 07796, Korea
E-mail: yjsseong@lgdisplay.com

In this study, prediction of particle removal efficiency on thin-film transistor(TFT) is presented through mist-based cleaning simulation and applied to the cleaning process of display panel. The efficiency is predicted based on balance between adhesion and removal torque applied to contaminant particle on the TFT substrate. Adhesion occurs between a particle and the substrate due to van der Waals and chemical interactions [1].

Removal torque is induced by drag force acting on the particle [2]. The drag is generated by the fluid dynamics during the collision of a mist on a substrate. It was calculated through computational fluid dynamics(CFD) conjugated with volume of fluid(VOF) method. Diameter of the mist was measured via Spraytec(Malvern Panalytical LTD) for various pump pressures and velocity of the mist was estmiated based on specification of the nozzle. Contaminant particle was set to be an aluminum powder with diameter of 0.1 μm, which is located on an IGZO layer of the substrate. Because the particle size is small enough compared to the mist size, it can be assumed that the adhesion torque is constant.

Fig. 1 presents the adhesion and the removal torque for various pump pressure of high pressure micro jet (HPMJ). It is observed that particles can be removed in the region where the removal torque is higher than adhesion torque. The higher the pump pressure, the higher the removal torque and the particle removal efficiency. Through this work, the cleaning process parameter could be linked with the particle removal efficiency so it could give us insight of the cleaning process.

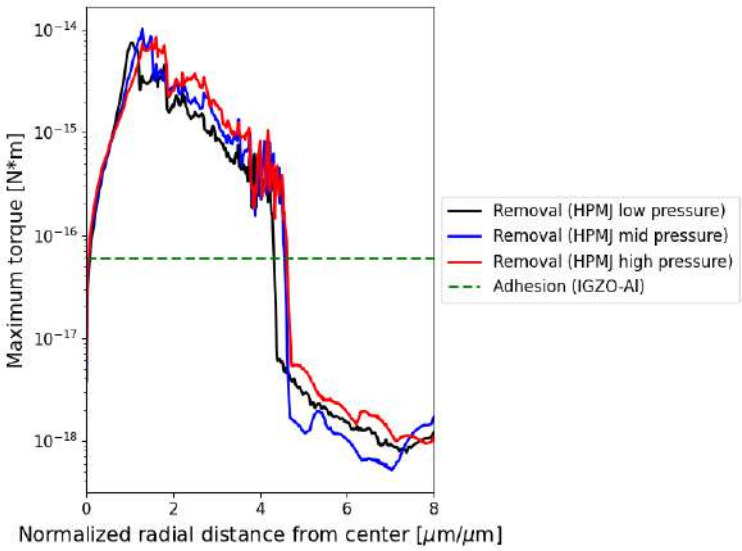

Fig. 1. Maximum adhesion and removal torque depending on the pump pressure of nozzle

References

1. F. L. Leito *et al.*, *Int. J. Mol. Sci.*, 13, 12773 (2012).
2. M. E. O'Neill, *Chem. Engrg. Sci.*, 23, 1293 (1968).

Effect of Ar Atmospheric Plasma Treatment time on Al-doped Zinc Oxide Thin Films Sputtered on Flexible Substrates

Haechang Lee† Younggon Choi†, Kirak Kim, Yuanrui Qi, Minseok Song,
Van Tuan Nguyen, DongWoon Lee, Sang Jik Kwon, and Eou-Sik Cho
Dept. of Electronic Engineering, Gachon University, Seongnam, Gyeonggi-do 13120, Korea
Tel.:82-31-750-5297, E-mail: es.cho@gachon.ac.kr.
† These authors contributed equally to this work.

As a new doping process or conductivity improvement method in the fabrication of thin film transistor(TFT) or electronic device, plasma treatment has been widely used on the semiconductor or electrode materials. As a new transparent conductive electrode(TCE) materials, aluminum-doped zinc oxide(AZO) has been used as a replacement of indium tin oxide (ITO). Some research results also showed the possibility of AZO as a semiconductor TFT channel material. However, AZO has a much higher resistivity than ITO and its resistance should be controlled by annealing or surface treatment.

Our recent reseach results show the enhanced conductivity of AZO films sputtered on flexible substrate such as polyimide(PI) and polyethylene terephthalate(PET). Ar atmospheric plasma jet was used for the surface treatment and the sheet resistance was reduced after plasma treatment as shown in Fig. 1. The Ar plasma treated AZO films were structually characterized using X-ray diffraction(XRD), atomic force microscopy (AFM), and X-ray photoelectron spectroscopy(XPS) and the enhancement mechanism and its dependency on treatment time was also clearly investigated.

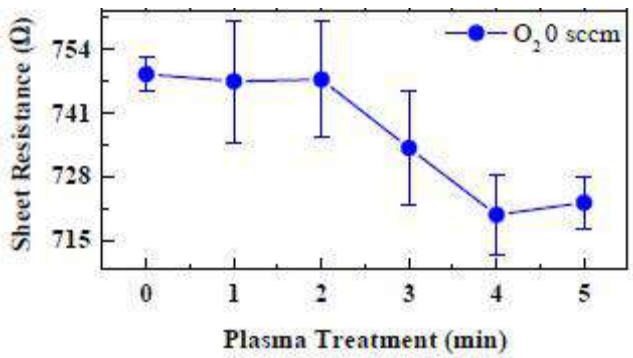

Fig. 1. Sheet resistance of AZO films on PI substates with a different Ar atmospheric plasma treatment time

Acknowledgment

This research was supported by the Femto Science Co. Ltd in the uasge of atmospheric plasma jet (plasma pipette). This research was also funded and conducted under 「the Competency Development Program for Industry Specialists」 of the Korean Ministry of Trade, Industry and Energy (MOTIE) operated by Korea Institute for Advancement of Technology (KIAT) (No. P0012453, Next-generation Dispay Expert Traning Project for Innovation Process and Equipment, Materials Engineers).

References

1. T. Abuzairi, M. Okada, S. Bhattacharjee, and M. Nagatsu, *Appl. Surf. Scim.,* 390, 289 (2016).
2. M. C. Kim, S. H. Yang, J. H. Boo, and J. G. Han, *Surf. Coat. Technol.* 174, 839 (2003).
3. D. H. Lee, H. Ryu, S. J. Kwon, and E.-S. Cho, *Sci. Adv. Mater.* 12, 1607 (2020).
4. D.-K. Hwang, M. Misra, Y.-E. Lee, S.-D. Baek, J.-M. Myoung, and T. I. Lee, *Appl. Surf. Scim.,* 405, 344 (2017).

Effect of Thermal Induced Degradation on the 8-Hydroxyquinolato - Lithium (Liq) Organic Material by Evaporation Process

Mi-Young Ha [1,2], Byeong-Doo Kang [3], Ye-Bin Eun [4] and Dae-Gyu Moon [1]

[1]Dept. of Materials Engineering, Soonchunhyang University, Asan, Chungnam 31538, Republic of Korea
Tel.:82-41-530-1312, E-mail: dgmoon@sch.ac.kr
[2]Display New Technology Institute, Soonchunhyang University, Asan, Chungnam 31538, Republic of Korea
[3]Dept. of R&D Center, SFA Engineering, Hwasung, Kyoungki 18472, Republic of Korea
[4]Dept. of Electronic Materials and device engineering, Soonchunhyang University, Asan, Chungnam 31538, Republic of Korea

Recently, extensive studies have been reported to improve the performance of OLEDs with the aim of achieving high brightness, high efficiency, low cost and long lifetime [1]. Particularly, the electrical, chemical and thermal stability of the material for OLED greatly influences the performance of the device [2]. Thermal instability of the material causes degradation of the device. Currently, the vacuum evaporation method has been used for the deposition of organic layers for the OLEDs with small molecular materials using evaporation cells. In this method, organic materials are possibly degraded by the high temperature during heating inside the cell for the vaporization of the organic materials. We have investigated the effect of the thermal degradation of organic material that occur during the vacuum evaporation process using 8-Hydroxyquinolato-Lithium (Liq) organic material. We heated Liq to temperature of 480 °C and induced thermal degradation in a vacuum evaporation system. We fabricated organic light-emitting devices (OLEDs) using degraded Liq and fresh Liq as the organic electron transport layer (ETL). Our research exhibited similar current density characteristics for both degraded Liq and fresh Liq devices in the OLED. The required voltages for achieving a current density of 100 mA/cm^2 were 17.6 and 17.8 V, respectively, in the degraded Liq and Fresh Liq ETL devices. However, the device with fresh Liq layer exhibited better luminance and higher current efficiency than the degraded Liq device. The maximum current efficiencies of the degraded Liq devices and fresh Liq devices are 35 cd/A and 55 cd/A, respectively.

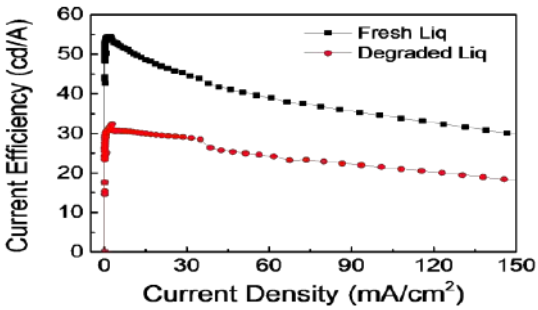

Fig. 1. Current efficiency of OLEDs with fresh Liq and degraded Liq layers

Acknowledgment

This This research was supported by the Soonchunhyang University Research Fund, and also funded and conducted under 「the Competency Development Program for Industry Specialists」 of the Korean Ministry of Trade, Industry and Energy (MOTIE), operated by Korea Institute for Advancement of Technology (KIAT). (No. P0012453, Next-generation Display Expert Training Project for Innovation Process and Equipment, Materials Engineers).

References

1. A. B. Chwang, M. Hack and J. J. Brown. J. Soc. Info. Display, 13(6), 481 (2012).
2. H. Funimoto, T. Suekane, K. Imanishi, S. Yukiwaki, H. Wei, K. Nagayoshi, M. Yahiro and C. Adachi. Sci. Rep. 6. 38482 (2016).

Reinforcement learning for one-armed transfer robots in display manufacturing

Hwa-Jong Lee[1], Sihyeon[2] Jo, and Seong-Woo Kim[3]
[1]Graduate School of Engineering Practice, Seoul National University
[2]Dept. of Electrical and Computer Engineering, Seoul National University
[3]Graduate School of Engineering Practice, Seoul National University
E-mail:ewioty@snu.ac.kr

Productivity is one of the desired aspects when designing the display manufacturing process. A flow control system is a critical part of the display manufacturing system in increasing production capacity. Tackling the scheduling optimization problem related to flow control for improving productivity requires experts in the domain to design the flow control system, otherwise leading to a cost-inefficient production setting. As an alternative approach to the heuristic design of the flow control system, reinforcement learning has been considered to deal with the scheduling optimization problem with the emergence of deep neural networks. The reinforcement learning framework using DQN achieved considerable performance in simulation settings [1], which can be applied to scheduling problems. However, previous research in reinforcement learning was faced with challenges in applying to a new environment [2], which is strenuous to utilize in display manufacturing. We propose a novel method of finding feasible flow control system designs in display manufacturing by implementing transfer robots and simulation environments for reinforcement learning.

We use Unity software to develop the agent and the simulation environment for flow control system design. An overview of the simulation configuration is shown in Fig. 1(a). The environment consists of a loader chamber where glass is loaded and an unloader chamber where the glass finally arrives by the one-armed transfer robot. The transfer robot is equipped with one arm which can move back and forth, up and down (pitch axis), to load/unload the glass while the robotic body rotates (yaw axis) to convey the glass. Five actions (pause, rotate to loader chamber, rotate to unloader chamber, glass loading, and glass unloading) are defined for the action set. The Proximal Policy Optimization [3] algorithm is used to find an optimal behavior of the transfer robot for the flow control system. The agent gets a reward when the glass is delivered to the unloader chamber successfully and receives a penalty as time passes or the glass is broken. As a result of training, the number of successes increases while the number of breaks decreases after 80,000 steps, achieving 40:1 as the maximum success ratio. We present the possibility of reinforcement learning in the flow control system for display production leveraging a simulator. In the future, we also plan to test the method in diverse display manufacturing settings.

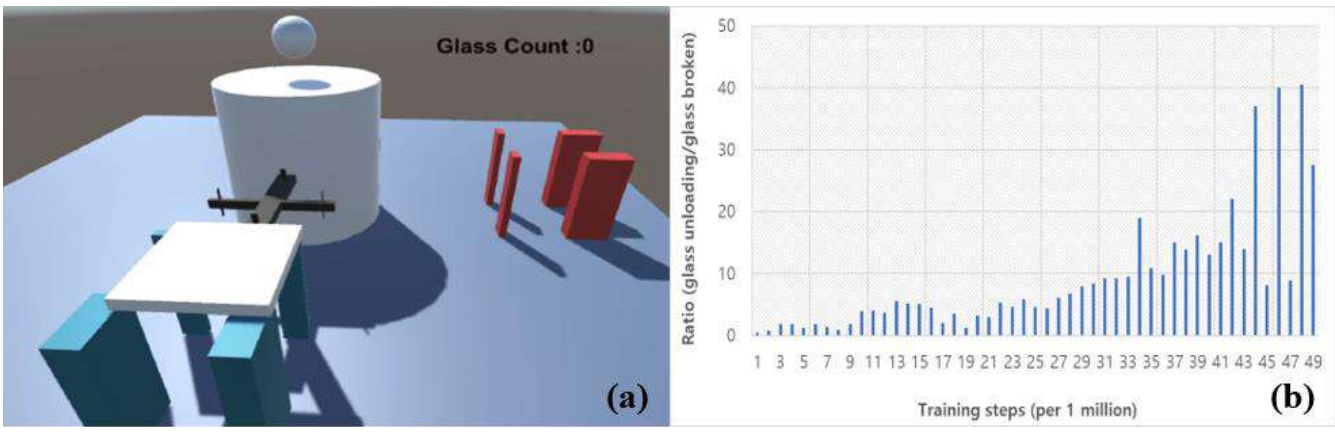

Fig. 1. Overview of the system: (a) Configuration of simulation environment, and (b) Result of training.

References

1. V. Mnih et al., Human-level control through deep reinforcement learning, Nature, vol. 518, no. 7540, p. 529, (2015).
2. C. Zhang, et al., A study on overfitting in deep reinforcement learning. arXiv preprint arXiv:1804.06893 (2018).
3. Schulman, John, et al. "Proximal policy optimization algorithms." arXiv preprint arXiv:1707.06347 (2017).

Mechanism Study of Wide Color-gamut TFT-LCD's Light-caused Mura

Dong Wang[1], Dan Wang[2], Hongming Zhan[2], Xi Chen[2], and Xibin Shao[2]
[1, 2]Beijing BOE Display Technology Co., Ltd., Beijing, 100176, China
Tel.:86-10-57676797, E-mail: wangdong_dt@boe.com.cn

The wide color-gamut TFT-LCD need to use RGB resin with high pigment concentration, which is easy to appear green mura after illuminated by various lights. Microscopic analysis shows that the green sub-pixel of TFT-LCD show local brightness, while the red and blue sub-pixels are no such phenomenon.

The green mura results of TFT-LCD fabricated by four green resin and illuminated by different light sources and time, as shown in Table 1. High sensitivity photo-initiator in green resin can enhance the film compactness and improve mura, but the improvement degree is very small. Lower proportion of pigment G to Y in green resin can effectively improve mura. Base on the same Chroma specification of TFT-LCD, the novel pigment G can reduce the proportion of G to Y in green resin by 40%, and show the best mura result. On the other hand, photoelectric properties of the above resins are also evaluated, such as Chroma, volume resistance, voltage holding ratio and dielectric loss factor. Except for dielectric loss factor, the other photoelectric properties are basically the same, as shown in Table 1. All resins' dielectric loss factor in LED light on state is higher than that in LED light off state. By comparing and analyzing the mura of the TFT-LCD and the photoelectric properties of the green resins, it is inferred that the dielectric loss factor of the green resin is the cause of the green mura of TFT-LCD. The higher dielectric loss factor of the resin, the more serious mura of the TFT-LCD.

The pigment of green resin consists of a phthalocyanine metal complex. The central metal of the complex's molecular framework is copper or zinc, and the outermost part is connected with halogen atoms. Aromatic rings around the molecule have the characteristics of both electron donors and acceptors. Such pigment has conjugated structure and certain semiconductor property, which reduces the insulation and increases the dielectric loss factor of the resin. The liquid crystal in TFT-LCD will deflect under the applied voltage. After the TFT-LCD is turned on for a period time, the polarization of liquid crystal will induce the coupling electric field in the opposite direction of the current electric field, then gradually weaken the deflection of liquid crystal and the light passing through the liquid crystal, red, green and blue layers. If the green resin has high dielectric loss factor, it is equivalent to the parallel circuit of the resistor R and the capacitor C in TFT-LCD, then the liquid crystal of green sub-pixel will deflect abnormally, and result in the darkening speed of green sub-pixel slower than red and blue sub-pixels, finally showing the green mura of TFT-LCD. With the extended turn on time of TFT-LCD, the coupling electric field strengthens gradually, then the green sub-pixel darkens gradually, and the green mura of TFT-LCD disappears eventually.

Table 1. The mura of TFT-LCD and dielectric loss factor of green resin with different light sources and time
(√：No Mura, ×：Have Mura)

Test Item	Sample	Light	Time	A	B	C	D
Green Mura	TFT-LCD	LED	30sec	√	×	√	√
			60sec	√	×	√	√
			120sec	√	×	√	√
			600sec	√	×	×	√
		Fluorescent	1hr	√	√	√	√
			5hr	√	×	√	√
			9hr	√	×	√	√
			36hr	√	×	×	√
Dielectric Loss Factor	Green Resin	LED	LED On	0.6	0.7	0.6	0.4
			LED off	1.0	1.3	1.2	0.6

References

1. L. Y. Xu and J. Yu, *Chinese Journal of Liquid Crystals and Displays*, 31(5), 454 (2016).
2. Y. Luo, *14th National electrochemical Conference*, vol. 1, p. 969 (2007).
3. H. X. Dong, *Journal of Shangqiu Vocational and Technical College*, 8(5), 75 (2009).

Synthesis of Organolead Halide Perovskite Nanoparticles Without Quantum Confinement Effects and Their Applications to LEDs

Bong-Jun CHOI[1], and Jung-Yong LEE[1]
[1] School of Electrical Engineering (EE), Korea Advanced Institute of Science and Technology (KAIST), Daejeon 34141, Republic of Korea

E-mail: jungyong.lee@kaist.ac.kr

Organolead halide perovskite quantum dots (OHP-QDs) emerged as promising next generation light emitter due to their easy color tunability, high color purity and high photoluminescence quantum yield (PLQY). However, size-dependent bandgap difference of QDs cause the change of emission wavelength and relatively low color purity.[1] Here, we report the synthesis method of tens of nanometers sized perovskite nanoparticles (NPs), which characteristics are not affected by quantum confinement effect by using an ultrasonic spray. To control the size of perovskite NPs, we controlled temperature, ligand materials and concentration of precursor solution. With this synthesize method, we fabricated perovskite NPs which emit the red, green, and blue photoluminescence (PL) with narrow full width at half maximum (FWHM) around 20nm. With

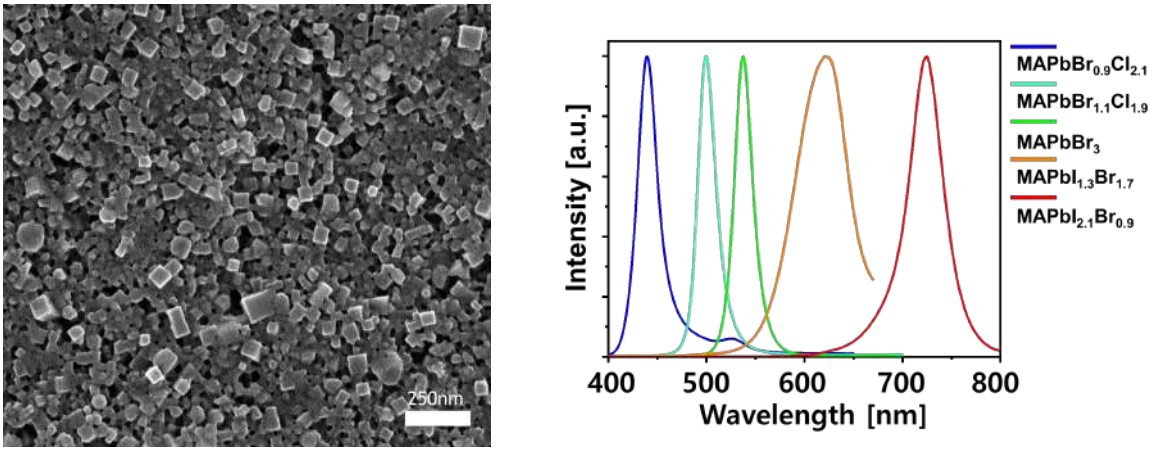

Fig. 1. Scanning electron microscope (SEM) image of synthesized perovskite nanoparticles and their PL spectrum

Acknowledgment

References

1 Kim, Young-Hoon, Himchan Cho, and Tae-Woo Lee. "Metal halide perovskite light emitters." *Proceedings of the National Academy of Sciences* 113.42 (2016): 11694-11702.
2. Kim, Young-Hoon, et al. "Highly efficient light-emitting diodes of colloidal metal–halide perovskite nanocrystals beyond quantum size." ACS nano 11.7 (2017): 6586-6593.s

Effect of single structure on the performance of Light-emitting Electrochemical Cells

Woo Jin JEONG[1], Jong Ik LEE[2], Hee Jung KWAK[1], Jae Min JEON[1], Moon Sung Kang[2,3] and Jun Young KIM[1]
[1]Department of Semiconductor Engineering. Display, Gyeongsang National University, Jinju 52828, Republic of Korea
Tel.:82-55-772-1732, E-mail: kimjy86@gnu.ac.kr
[2]Department of Chemical and Biomolecular Engineering, Sogang University, Seoul 04107, Republic of Korea
[3]Institute of Emergent Materials, Sogang University, Seoul 04107, Republic of Korea

Organic Light-Emitting Diode(OLED) manufacturing system is currently being commercialized and it is attracting a lot of as an electroluminescent display. Researchers currently be made a lot of efforts to find high efficient and low-priced manufacturing technology such as structural changes or use new organic materials. Recently, many researchers have been conducting research on various light-emitting displays based on solution process such as quantum-dot light emitting diode(QLED) and light-emitting electrochemical cells(LEC), and have published many research results to improve the device performance.[1,2] In this research, we studied on the performance of LEC devices according to the various thickness and heat treatment for a simple single structure that is consist of electrode/emittion-layer/electrode. The characteristic of our LEC device is that there is no charge injection and transfer layer, in which used compound with a mixture of luminophore (Tris(2,2'-bipyridine)ruthenium(II)hexauo rophosphate)[$Ru(bpy)_3(PF_6)_2$], electrolyte (1-ethyl3-methylimonium bis(trifloromethomethylophyllum)imide)[EM IM][TFSI] and (poly methyl methacrylate)[PMMA] at 9:1:1 wt% as a emission-layer. As a result of structural optimization through spin coating process, the emittion-layer was formed with a thickness of 150nm and heat treatment at 100℃, in which the luminance increased up to 3505 cd/m^2 at 4.4V and also shows compliant performance about current efficiency of 1.35 cd/A, EQE of 1.36 % at the luminance of 1503 cd/m^2

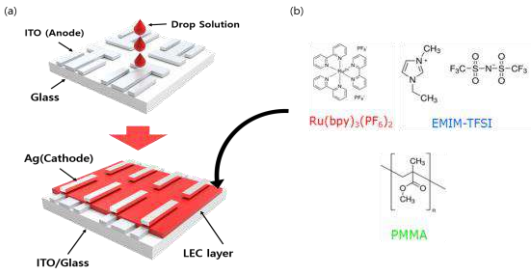

Fig 1. (a) Device structure of LECs (b) materials of the compound used in the emission layer

Table 1. Device performance of LECs with different thickness of emission layer

	J (mA/cm^2)	Turn-on Voltage (V)	Luminance (cd/m^2)	EQE (%)	Roughness, Rs (nm)	RMS, Rq (nm)
260nm	1800	3.0	1147	1.47	3.61	4.52
150nm	2250	3.0	3505	1.36	1.09	1.36
120nm	1782	3.0	2755	1.2	1.04	1.35
100nm	1955	3.0	2223	0.31	0.79	1.03

Acknowledgment
The research was conducted by the Undergraduate Research Program(URP) supported by Korea Foundation for the advancement of science&creativity and GNU-Samsung Display Center

References

1. Y. Liu, F. Li, Z. Xu, C. Zheng, T. Guo, X. Xie, L. Qian, D. Fu and X. Yan, *ACS Appl. Mater. Interfaces*. 9, 25506 (2017)
2. Y.-H. Won, O. Cho, T. Kim, D.-Y. Chung, T. Kim, H. Chung, H. Jang, J. Lee, D. Kim, E. Jang, *Nature*. 575, 634 (2019)

Electroluminescence of Inverted Perovskite Quantum Dot Light Emitting Diode Based on $CsPbBr_3$

Hee Jung kwak[1], Min-Sik Gong[2], Woo Jin Jeong[1], Jeong Ha Hwang[1], Donggu Lee[1], Gi-Hwan Kim[2] and Jun Young Kim[1]

[1]Department of Semiconductor Engineering, Gyeongsang National University, Jinju 52828, Republic of Korea

Tel.:82-55-772-1732, E-mail: kimjy86@gnu.ac.kr

[2] Department of Material Science and Engineering, Gyeongsang National University, Jinju 52828, Republic of Korea

Perovskite quantum dot light-emitting diode (Pe-QLED), which has a narrow and finely tunable emission spectrum that shows high color purity, was selected as a promising candidate for emerging display. Halide perovskites quantum dots have high photoluminescence quantum yields (PLQY) reached over 95% and 20nm of narrow full width at half maximum (FWHM) make them applicate in the high-quality display. Inorganic perovskite cesium halide perovskite ($CsPbX_3$, X=Cl, Br, and I) have higher thermal and chemical stability and less moisture affinity than other quantum dots materials and can synthesize at room temperature [1]. Recently, In standard structure, 21.6% of external quantum efficiency (EQE) was reported in green $CsPbX_3$-based perovskite QLEDs [2], suggesting that they can compete with other Cd, Zn-based QLEDs, or OLED. However, in the inverted structure, only about 6% lower EQE has been reported [3], indicating that it needed to be optimized. In this study, we fabricated with optimization of the inverted Pe-QLED based on CsPbBr3 quantum dots [4]. The device structure is consists of ITO/ETL/perovskite quantum dot/HTL/MoO_3/Ag and it measured with IVL measurement to analyze electroluminescence characteristics. In addition, the performance of the device proved by measuring a morphological and structural analysis of each thin film using an Atomic Force Microscope (AFM), Scanning Electron Microscope (SEM), and X-ray Photoelectron Spectroscopy (XPS). As a result, the performance of the inverted Pe-QLED device could enormously improve through optimization.

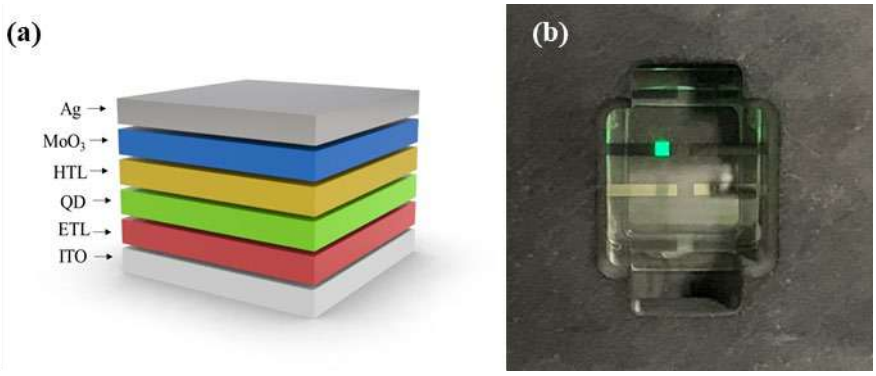

Fig. 1. (a) Device structure of Pe-QLED and (b) Image of electroluminescence

Acknowledgment

This work was supported by GNU-Samsung Display Center.

References

1. QA. Akkerman, G. Rainò, MV. Kovalenko and L. Manna, *Nat. Mater*. **17**, 394 (2018).
2. T. Fang, T. Wang, X. Li, Y. Dong, S. Bai, J. Song, *Sci. Bull.* **66**, 36 (2021).
3. J. Pan, C. Wei, L. Wang, J. Zhuang, Q. Huang, W. Su, Z. Cui, A. Nathan, W. Lei and J. Chen, *Nanoscale.* **10**, 592 (2018).
4. J. Song, J. Li, L. Xu, J. Li, F. Zhang, B. Han, Q. Shan, H. Zeng, *Adv. Mater*. **30**, 1800764 (2018).

Unidirectional Window Signage Display Using Resin Printing Ink for Making Dye-doped Thin Layer Which Enables to Make Images Invisible from Back Side

Kunio Sakamoto and Takeru Hasegawa
Dept. of Intelligence and Informatics, Konan University, 8-9-1 Okamoto, Higashinada, Kobe 658-8501, Japan
Tel.:81-78-431-4341, E-mail: kunio@konan-u.ac.jp

It stands to reason that someone observes mirrored imaging according to the direction of viewing if you draw something on the transparent material. Our research group proposed one-way observable window signage using transparent optical films such as a 1/4 wave plate in 2019. But this window display had a defect that transparency was less than the original glass window because of a polarizer for light controls. To solve this weak point, we needed to find new technology for generating color using a transparent material. This paper shows a one-way observable imaging display on the glass window using dye-doped thin resin layers for unidirectional color generating by light controls and material development. You know that water is generally clear and transparent but the water in a bath tub is little blue. The color changes depending on the depth of water. A dye-doped resin block has different thickness and makes color changing from transparent to blue gradually as shown in fig. (a). The authors utilize this color changing mechanism to make one-way observable window signage.

Fig. (a) shows the principle of color generating. A single layer of dye-doped resin is transparent, but the double-piled resin layers generate some color. As shown in fig. (b), it is the important technical point that all transmission light waves pass through all optical materials and observed signage is formed by the reflection light waves of the half mirror. At transmission light path from the back, all transmission light waves are still original because light waves pass single resin layer or not in addition to the half mirror. Consequently, observers can watch the sights behind these optical materials. At reflection light path by the half mirror, there are also two cases whether the waves pass through the resin layers or not. The case of passing the resin layers makes the same phenomenon that light waves pass through the double-piled resin layers. After this twice same layer passing, the transparent resin layers generate some color. In other words, the frequency of passing through thin layers makes a color difference. You can use this color generating for drawing the text and graphics of signage.

At the observing from back side(far side of the half mirror), all transmission light wave from front(resin layer) side can pass through all optical materials without generating colors although some parts of the light wave pass through the resin layers once. As the result, the observer can watch the sights behind these optical materials without watching the mirrored image of signage. This is why the mirrored image is made invisible.

Fig. (c) shows observed images of our trial unidirectional imaging display. The authors paint the lettering "2" made by hand drawings using a dye-doped resin ink on a half mirror. You can confirm that the color generating mechanism using a transparent material realizes the one-way imaging which enables to make invisible from back.

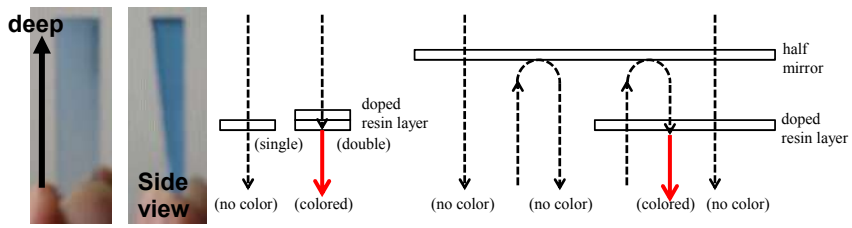

(a) principle of unidirectional color generating

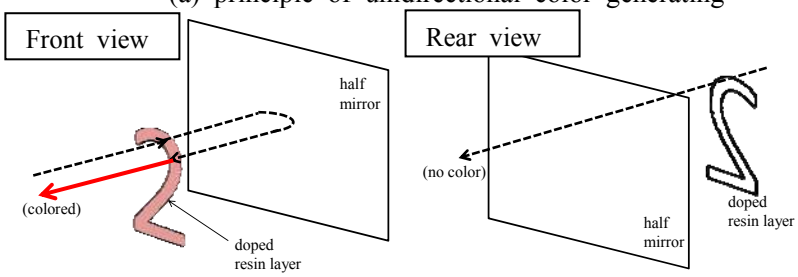

(b) principle of one-way observable imaging

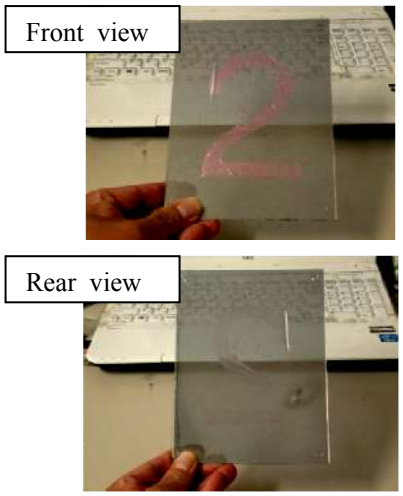

(c) observed images of signage

Fig. 1. One-way observable window signage using dye-doped thin layer by resin printing ink

Highly efficient double gate light emitting transistor based on van der Waals hetero structure

June-Chul Shin[1], Junyoung Kwon [2], Yeon Ho Kim[3], Chul-Ho Lee[3] and Gwan-Hyoung Lee[1]
[1]Department of Materials Science And Engineering, Seoul National University, Seoul, Korea
E-mail: gwanh.lee@gmail.com
[2]Department of Materials Science and Enginnering, Yonsei University, Seoul, Korea
[3]KU-KIST Graduate School of Converging Science and Technology, Korea University

Two-dimensional (2D) semiconductors, such as transition metal dichalcogenides (TMDs), are promising candidates for various optoelectronic applications since TMDs in the monolayer limitation havea large exciton binding energy and strong light-matter interactions due to broken inversion symmetry. [1-2] Therefore, TMDs have been used in the exotic optoelectronic quantum devices with functions of chiral light emitting, transport of excitonic complexes, and high-temperature exciton condensation, that have not been realized in bulk materials. [3-4] Despite great potential of TMDs, low external quantum efficiency (EQE) of TMD-based light emitting devices is the obstacle to be overcome for their practical applications. The main reason for the low efficiency is high Schottky barrier for injection of electrons and holes into the TMD channel due to the Fermi level pinning and unintentional doping of the active channel layer. Here, we demonstrate a light emitting transistor based on van der Waals (vdWs) heterostructure with double gates. Monolayer WSe_2, graphene, and hBN are used as the light emitting layer, electrode (or gate), and dielectric, respectively. By using double gates, the WSe_2 light emitting layer was electrostatically doped into p- and n-type regions, leading to a sharp p-n junction. The work functions of monolayer graphene source-drain electrodes were modulated to lower the Schottky barriers for injection of electrons and holes. The injected charges are efficiently recombined in the p-n junction region, leading to a strong light emission with high EQE of ~40 % at room temperature. Our work shows a great potential of 2D light emitting devices for novel optoelectronic applications.

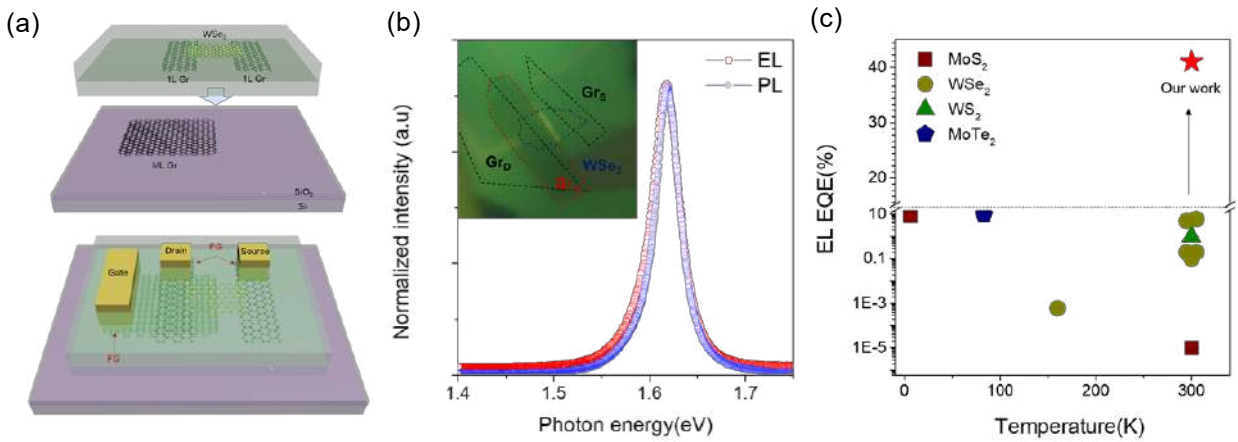

Fig. 1. (a) Device geometry of double gate WSe_2 light emitting transistor (b) Nomalized EL and PL spectrum of the device. Optical microscope image of the inset shows EL operation in PN junction of the device (c) Comparsion of EL EQE(external quantum yield) to different 2D emitters.

References

1. D. Xiao. et al. Phys. Rev. Lett. 108, 196802 (2012).
2. L. Britnell. et al. Science 340, 1311-1314 (2013).
3. Y. J. Zhang. et al. Science 344, 725-728 (2014).
4. D. Unuchek. et al. Nature 560, 340-344 (2018).

Elucidating chemical origin of photoluminescence of Cesium-Bismuth-Bromide perovskite nanocrystals and improved emissive properties via metal chloride additives

Joonyun Kim[1], Jinu Park[1], and Byungha Shin[1]
[1]Dept. of Materials Science and Engineering, KAIST, Daejeon, Daehakro 291, Korea
Tel.:82-42-350-3355, E-mail: wnsdus@kaist.ac.kr

Lead halide perovskites are considered as a potential candidate for the next generation lighting application due to their extremely narrow of photo/electroluminescence spectrum, i.e., high color purity. However, inclusion of lead is a concern, which is toxic element, motivates active research efforts on lead-free perovskite light emitters.

Here, we synthesized lead-free perovskite nanocrystals with are composed to Cs, Bi and Br, using ligand assisted re-precipitation (LARP) method. Contrary to the common acceptance in the previous researches, the photoluminescence (PL) spectrum of the Cs-Bi-Br nanocrystals was identical to a reference nanocrystal synthesized without Cs, strongly suggests that the origin of the PL from the Cs-Bi-Br nanocrystals is $BiBr_3$, which is also revealed by detailed chemical analysis. We further improved luminescence of Cs-Bi-Br nanocrystals by adding transition metal-chloride salts in the synthesis step, achiving PL quantum yield as high as 15%. Detailed experiments and analysis will be presented.

Highly Conductive Ionic Gel Polymer Electrolyte Based on In-planar Microsupercapacitors for Display Applications

Gaeun Park[1], Dawoon Lee[1], Jaekyun Kim[1]
[1] **Dept. of Photonics and Nanoelectronics, Hanyang University, Ansan 15588, Republic of Korea**
Tel.:82-31-400-5521, E-mail: jaekyunkim@hanyang.ac.kr

Recently, solid state polymer electrolyte (SSPE) has been attracted for next-generation energy storage devices from the benefit of the both rigid mechanical modulus of polymer matrix and highly conductive ionic liquid while possessing non-flammable, chemically stable, and wide potential window properties.

However, compared to conventional liquid state electrolyte, the relatively lower ionic conductivity (~10-3 S/cm) of solid state electrolyte can be a critical limitation to apply on actual energy storage devices.

Arising from these demands, 1-Ethyl-3-methylimidazolium bis(fluorosulfonyl)imide (EMIM-FSI) is the effective solution to enhance the ionic conductivity due to the higher ion carrier concentration per mass compared with other ionic liquids. To further render the advantages of EMIM-FSI ionic liquid, mechanical, electrical, and electrochemical investigations were performed.

In conclusion, this EMIM-FSI based electrolyte has been successfully demonstrated the high ionic conductivity (~4 mS/cm) (Figure 1) and exhibited high-performance electrochemical characteristics where the capacitance retention value is extremely stable after severe 20,000th cycle test (Figure 2).

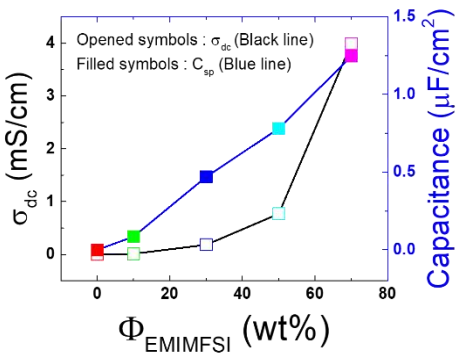

Figure 1. electrical characteristics of concentration dependence as a function of EMIMFSI ionic liquid (opened symbols : ionic conductivity, filled symbols : capacitance).

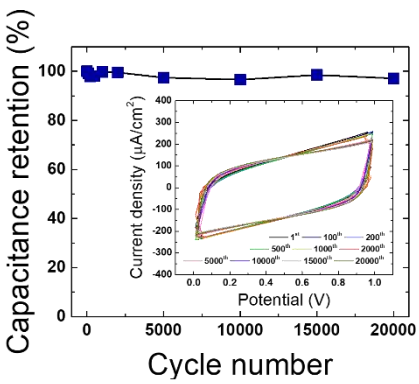

Figure 2. Electrochemical life-cycle characteristics using Cyclic voltammograms for PEGDA 30 wt% + EMIMFSI 70 wt% IGPE with 20,000 cycles

High Performance Micro-supercapacitor Array using Hybrid Ion-gel Polymer Electrolyte (IGPE) as Next-generation Energy Storage Device for Display Applications

Dawoon Lee[1], U Hyeok Choi[2] and Jaekyun Kim[1*]*
[1]Dept. of Photonics and Nanoelectronics, Hanyang University, Ansan 15588, Republic of Korea
Tel.:82-31-400-5521, E-mail: jaekyunkim@hanyang.ac.kr
[2]Dept. of Polymer Science and Engineering, Inha University, Incheon 22212, Republic of Korea
Tel.:82-32-860-7485, E-mail: uhyeok@inha.ac.kr

Gel polymer electrolyte (GPE), composing of polymer framework and ionic phase, has been spotlighted as next-generation energy storing device due to its high ionic conductivity and reasonable mechanical strength. This GPE can dramatically reduce the size of devices compared to conventional liquid electrolyte-based devices. It is also possible to enable large-area and flexible energy storage such as the wearable battery and supercapacitor for display device. In particular, an incorporation of hybrid polymer with ionic composites allows to combine benefits of each component as well as achieve both excellent electrochemical performance and structural stabilities.

We prepared multifunctional ion-gel polymer electrolyte (IGPE) using acrylate monomer (PEGDA), bisphenol-A epoxy resin (DGEBA) and coordinated ionic complexes based on ionic liquid (EMIM-TFSI), via dual-curing process Firstly, electrical characteristics of IGPEs show the Arrhenius temperature dependence of ionic conductivity for thermoset IGPE, UV-curable IGPE, and hybrid IGPE for 0.2, 2.6, and 6 mS/cm, respectively (Fig. 1). These results suggest that the hybrid process can dramatically enhance the electrical performance beyond conventional solid-state electrolytes. In conclusion, we fabricated an all-solid-state microsupercapacitor array, consisting of IGPE film and laser scribed interdigitated structure of graphene electrodes. IGPE-based on-chip MSC array exhibits superior electrochemical performance with further improved structural stability. Therefore, our method provides valuable insights to design IGPE having both high electric properties and rigid structural integrities for the development of micro-scale energy storage devices which is suitable to next-generation flexible display application.

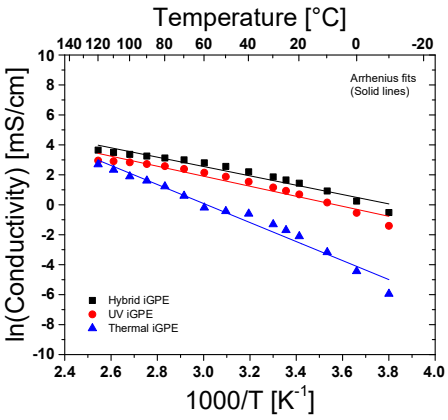

Fig. 1. Arrhenius plot from conductivity-temperature graph as a function of different types of IGPE.

Acknowledgment

References

Highly Deformable Transparent Au Film Electrodes and Their Uses in Deformable Displays

Dong Wook Kim[1], Chae-Eun Shim[2], and Unyong Jeong[1]
[1] Department of Materials Science and Engineering, Pohang University of Science and Technology (POSTECH), 77 Cheongam-Ro, Nam-Gu, Pohang, Gyeongbuk 37673, Republic of Korea
Tel.:82-10-7317-7040, E-mail: chaeeunhello11@gmail.com

With emerging interest in foldable and stretchable displays, the need to develop transparent deformable electrode and interconnection is increasing. Even though metal films have been standard electrodes in conventional electronic devices due to their high conductivity and well-established process, they have never been used for transparent deformable electrodes. We present highly conductive transparent deformable Au film electrodes and use them to fabricate a foldable perovskite light-emitting diode (PeLED) and a biaxially-stretchable alternating current electroluminescence (ACEL) display. We exhibit the formation of an ultrathin (6 nm) continuous Au film on an anisotropic conductive ultrathin film (ACUF) of amorphous carbon. The ultrathin Au film was first formed on an ACUF-coated Si wafer (4 inch scale) through metal evaporation and transferred to the polymer substrates by a simple and effective water-assisted delamination process. Then a hybrid electrode (ACUF/ACUF/Au) was produced as the transparent deformable electrode. Complicated interconnections could be created by metal deposition through a mask. The electrical conductance of the hybrid electrode was not affected by the crack formation in the Au film during electrode folding, crumpling, and stretching. We reveal the reason why the hybrid electrode can maintain such excellent electrical stability under deformation.

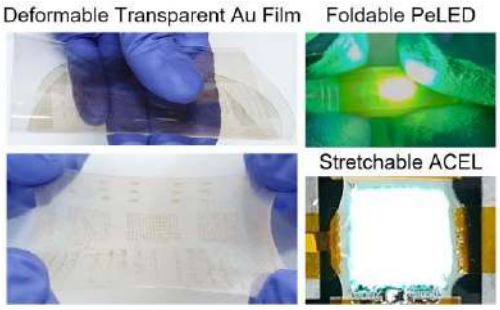

Fig. 1. A foldable PeLED and a stretchable ACEL display with the ACUF/ACUF/Au electrodes and interconnections

References

1. D. W. Kim et al, *ACS Appl. Mater. Interfaces* 12(37), 41969 (2020).

High Performance Piezoelectric Nanoparticle-embedded Micro-structure Triboelectric Nanogenerator(TENG) for Wearable and Human-interactive Applications

Junsu Seong[1], Dakyung Yu[2], Minwoo Kim[2], and Jaekyun Kim[1]
[1]Dept. of photonics and Nanoelectronics, Hanyang University, Ansan 15588, Republic of Korea
Tel.:+82-31-400-5521, E-mail: jaekyunkim@hanyang.ac.kr

Various studies have been focused to improve the power generation ability by developing new materials and micro-structures for wearable displays and sensor. Remarkable improvement has been achieved upon the several issues on the traditional battery-based operation of wearable systems. Recently, triboelectric nanogenerator (TENG) is rising as one of the most promising strategies for energy harvesting due to a outstanding design that converts mechanical power into electrical power.

In this study, we introduce the piezoelectric barium titanate ($BaTiO_3$) nanoparticle-embedded TENG device. $BaTiO_3$ nanoparticles, which have the high permittivity of ~6,000, can potentially result in the formation of strong internal polarization induced by the electric field from triboelectric charges. A high-k composite material based on the polydimethylsiloxane (PDMS) and $BaTiO_3$ nanoparticles as a triboelectric boosting layer intended to enhance the output performance of TENG. Furthermore, the TENG used in this study has patterned pyramidal micro-structure which promotes the surface friction, consequently increasing the amount of triboelectric induced surface charge, compared to that of flat surface.

As a result, it was found that the $BaTiO_3$-embedded pyramidal TENG devices show significant improvement of output performance such as open-circuit voltage (143 V to 360 V), short-circuit current (31 μA to 71 μA), and charge density (37 $\mu C/m^2$ to 93 $\mu C/m^2$), compared to flat PDMS TENG counterpart. Therefore, this result demonstrates that our piezoelectric nanoparticle-embedded surface modified TENG device can be used for next-generation energy harvesting devices for portable wearable and sensor devices.

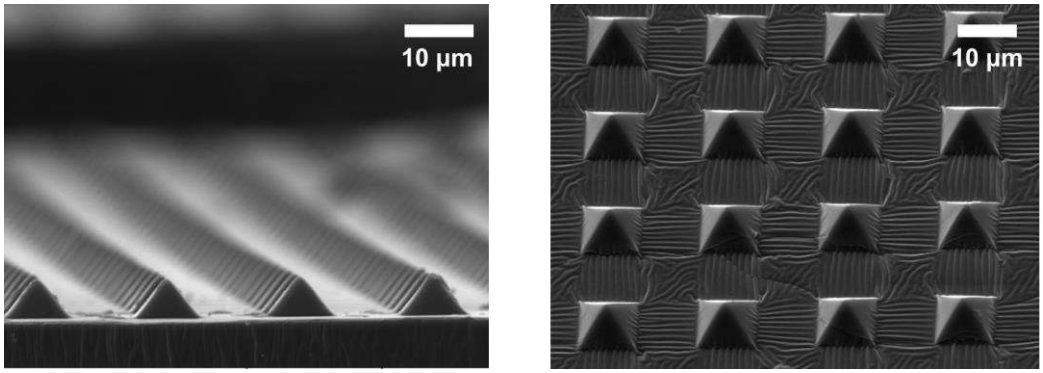

Fig. 1. SEM image of micro-structure BT/PDMS surface.

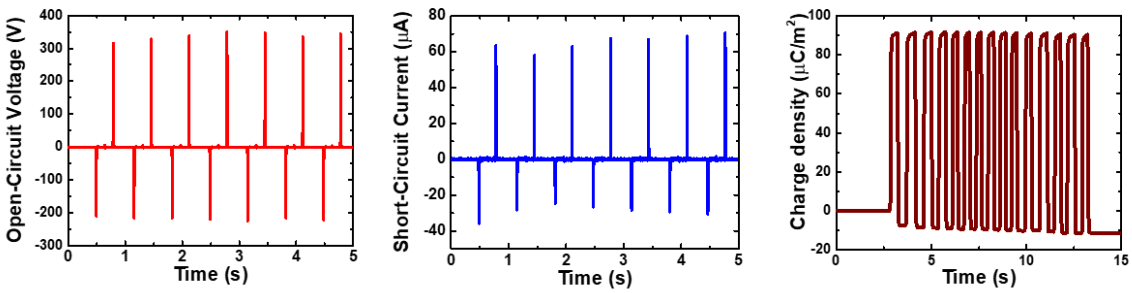

Fig. 2. V_{0C}, I_{SC}, and charge density of our device.

Large-Scale Ultrathin IGZO/MoS_2 Heterostructure Device for Highly Sensitive Visible Photodetectors

Kumin Kang[1], Sunkyung Kang[2], Dongyun Lee[1], Hyunseok Lee[2], Jaekyun Kim[1]
[1]Dept. of Photonics and Nanoelectronics, Hanyang University, Ansan 15588, Korea
Tel.:82-31-400-5521, E-mail: jaekyunkim@hanyang.ac.kr
[2]Dept. of Physics, Chungbuk National University, Cheongju 28644, Korea
Tel.:82-43-261-2276, E-mail: hsl@chungbuk.ac.kr

Two-dimensional transition metal dichalcogenides (2D-TMDs) and its heterostructures extensively have been intensively investigated for various application such as optoelectronics, ultrathin field effect transistors (FETs) for beyond the silicon. Molybdenum disulfide (MoS_2) has also been extensively studied in recent years because of the highly sensitive photodetection by its tunable bandgap and thickness. However, MoS_2 grown by chemical vapor deposition suffered in performance due to wet process. Here, we propose an inverted heterostructure of an amorphous indium gallium zinc oxide (a-IGZO) stacked on top of molybdenum disulfide (MoS_2) material for visible range detecting. For this heterostructure, a-IGZO thin films were sequentially deposited by low-damage sputtering on large-area of MoS_2 to serve as encapsulation and carrier supplier of hybrid device. Due to passivation and optical transparency of a-IGZO thin film with low-temperature annealing, it can prevent water and solvent from penetrating into the water-soluble MoS_2 layer. The photodetectors exhibit responsivities of approximately 3.1, 4.5, 48 A/W at a wavelength of 633, 532, 405 nm (an optical power of 10 μW) demonstrating that these phototransistors can be achieved by using photodetectivity of MoS_2 and high electrical properties based on IGZO.

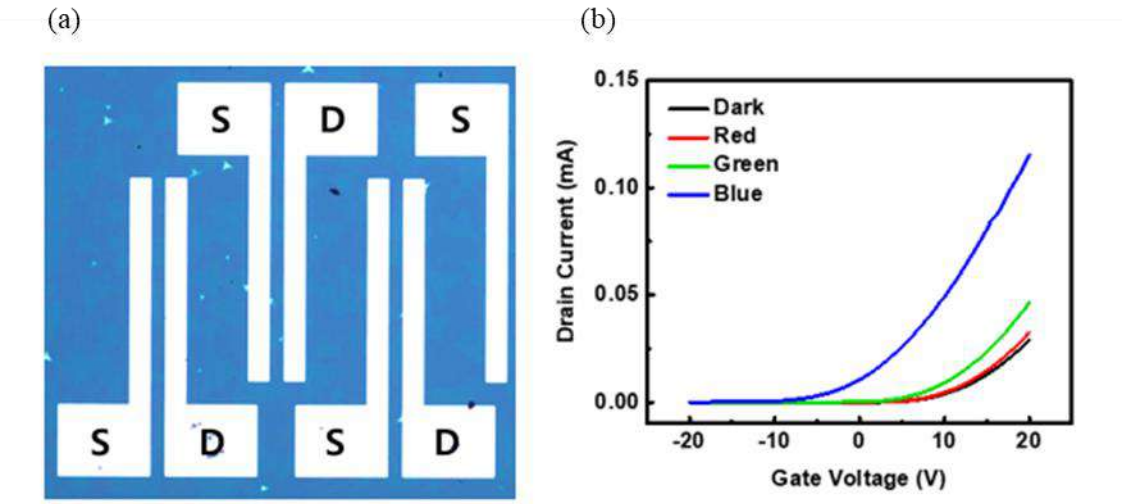

Fig. 1. (a) Optical image of heterostructure photodetectors, (b) I-V characteristic of them

Acknowledgment

References

1. Wang, Q., Kalantar-Zadeh, K., Kis, A. et al., *Nature Nanotech*, 7, 699–712 (2012).
2. Huo, N., Kang, J., Wei, Z., Li, S.-S., Li, J. and Wei, S.-H., *Adv. Funct. Mater.*, 24, 7025-7031 (2014).
3. Sang Woo Pak et al., *Nanotechnology*, 28, 475206 (2017)

Highly controllable segregation in the mixed-halide peovskite with electrical in-situ observations.

*SeungJae Lee[1], **JungYong Lee[1]
[1] Department of Electrical Engineering, KAIST, Daejeon, Korea
Tel.:82-42-350-7628, E-mail : tmdwo1103@kaist.ac.kr

Perovskite materials have been used as various optoelectronic devices such as solar cell, light emitting diode, laser, etc. Beyond using the pure perovskite materials, there have been lots of works to try to make complex perovskite materials with various organic ligands. However, the fundamental understanding the effect of the ligands on the perovskite materials are still unclear. Especially, there have been stability problems for perovskite applications under operating conditions, such as photo-decomposition of solar cells, color-changing during operations of light emitting devices. Therefore, the straightforward and distinct experiments were conducted to verify the effect of the electrical bias on the ionic path which may cause the phase segregation or degradation of the crystal structure. For controlling how much the segregation effects occur, the ligand materials (ammonium salts) can be used, which can affect the degree of the ionic movement.

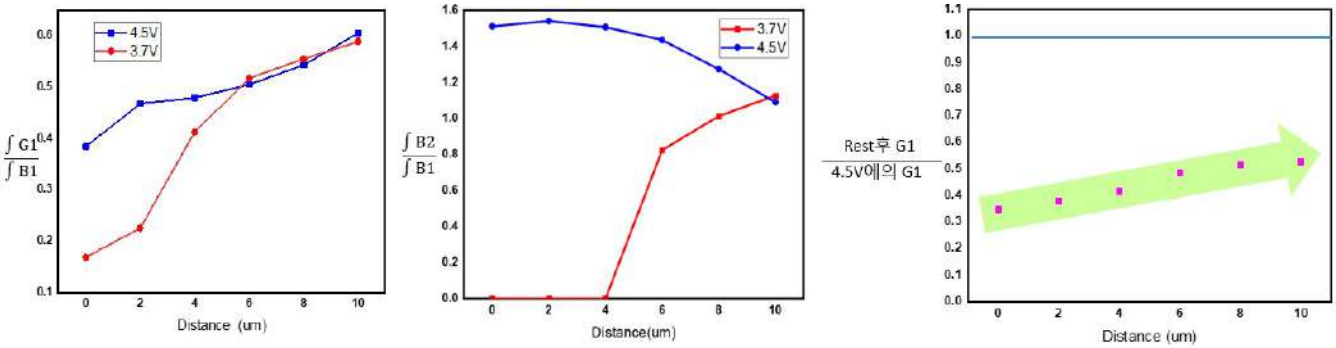

Fig. 1. In-situ PL line mapping

Above figures show the halide ions' movement under the operating conditions, which show the chlorine ions dominantly move under electrical bias.

Acknowledgment

The authors thank Bongjun for his input on perovskite film preparation and discussion of experimental outcomes. The authors thank Junho for interpretation of experimental results.

References

1. Tanaka, K. et al. Comparative study on the excitons in lead-halide-based perovskite-type crystals CH3NH3PbBr3 CH3NH3PbI3. Solid State Commun.127, 619–623 (2003)

2. Sun, S. et al. The origin of high efficiency in low-temperature solution processable bilayer organometal halide hybrid solar cells. Energy Environ. Sci. 7, 399–407 (2014).

The Design of Circular Polarization Dependent Dual Focusing Metalens

Yeseul Kim[1], and Junsuk Rho,[1,2]
[1]Dept. of Mechanical Engineering, Pohang University of Science and Technology (POSTECH), Pohang 37673, Korea
[2] Dept. of Chemical Engineering, Pohang University of Science and Technology (POSTECH), Pohang 37673, Korea
E-mail: jsrho@postech.ac.kr

Metalenses are the practical application of metasurfaces which are ultrathin and contain arrays of subwavelength optical antennas. Compared with conventional bulk lenses, the metalenses have a few micrometer-scale thicknesses and achieve the demand for the continuous miniaturization of optical components.

In this presentation, we introduce how to design the metalens which has dual focus depending on circular polarization of incident light (LCP or RCP) by utilizing geometric and propagation phases. We confirmed wave propagation by MATLAB simulation from the phase map and observed dual focal points from experimental measurment. This dual focusing metalens could be applied to sensing, imaging, and security platform.

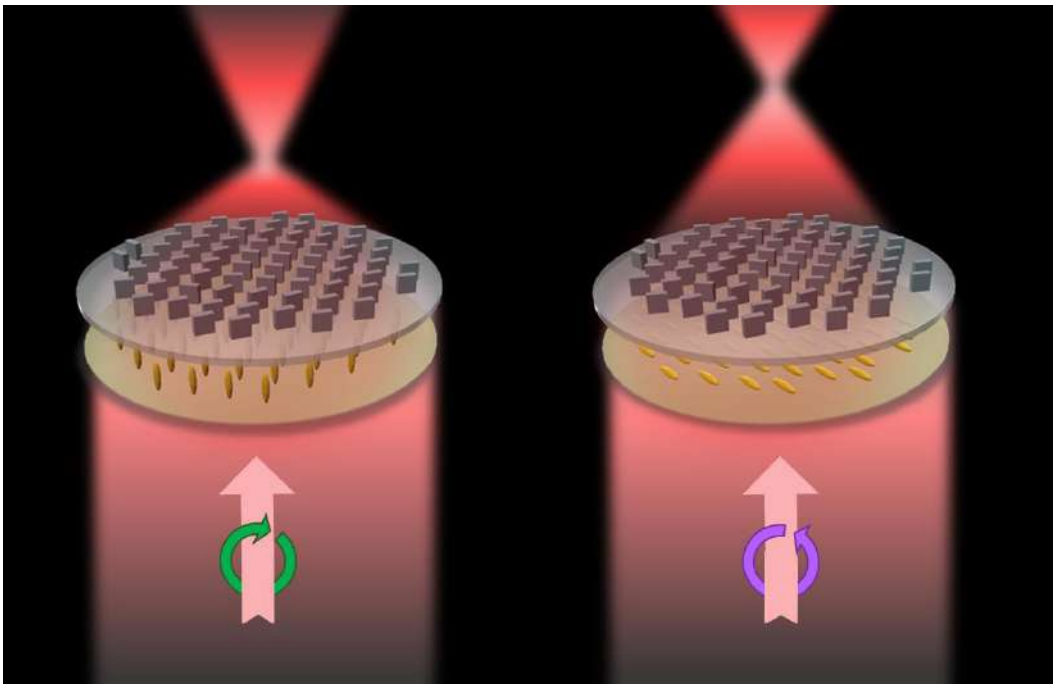

Fig. 1. Schematics of optical chirality dependent dual focusing metalens

Enhancement of Luminous Intensity from LED source at Detection Angle of 10° by Using Metalens

Hanlyun Cho[1], Heonyeong Jeong[1], and Junsuk Rho[1, 2]
[1]Dept. of Mechanical Engineering, Pohang University of Science and Technology, Pohang 37673, Korea.
[2]Dept. of Chemical Engineering, Pohang University of Science and Technology, Pohang 37673, Korea.
Tel.:82-54-279-2187, E-mail: jsrho@postech.ac.kr

Metalenses have been widely studied because of their superior performance and compact size, but the metalenses are usually designed with coherent light sources. In this study, the metalens using incoherent white light from LED as a light source is designed. In addition, polarization-insensitive and achromatic design is required if the metalens can use the LED source.

The phase profile φ of typical metalens is expressed as

$$\varphi(r,\lambda) = -\frac{2\pi}{\lambda}\left(\sqrt{r^2+f^2}-f\right), \tag{1}$$

where r, λ, and f is the radial coordinate, wavelength and a focal length, respectively. Spherical waves from the LED source are transmitted through the metalens and collimated. A modified metalens is proposed to enhance the luminous intensity at the detection angle of 10°. The phase profile of the modified metalens is express as

$$\varphi(r,\lambda) = -\frac{2\pi}{\lambda}\left[\left(\sqrt{r^2+f^2}-f\right)-\left(\sqrt{r^2+\left(\frac{D}{2\tan\alpha}\right)^2}-\frac{D}{2\tan\alpha}\right)\right], \tag{2}$$

where D is the diameter of the metalens and α is the target detection angle. α is 10° in this study. The first term of equation (2) is originated from equation (1). The second term of equation (2) allows the transmitted light to spread out to the detection angle region.

The simulation results after 25 m propagation are shown in Fig. 1. Both metalenses enhance the luminous intensity near the angle of 0°. The luminous intensity at the detection angle of 10° is enhanced by 206% and 233% when the typical and the modified metalens are used, respectively. The result with the modified metalens shows relatively lower maximum intensity. However, the width of the peak becomes wide when the modified metalens is used, so the luminous intensity at the detection angle of 10° is enhanced.

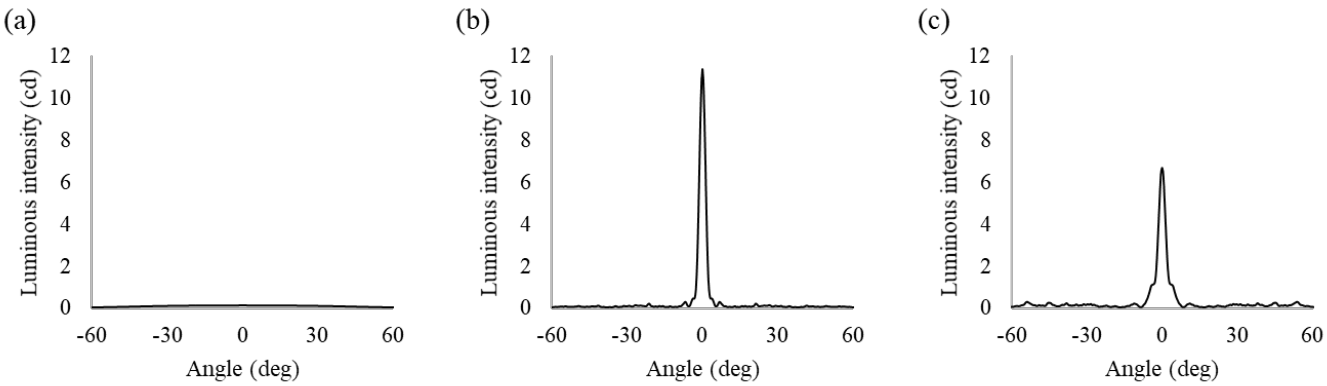

Fig. 1. Simulated angular distribution of the luminous intensity after 25 m propagation without metalens (a), with typical metalens (b), and with modified metalens (c).

References

1. N. Yu and F. Capasso, *Nat. Mater.*, 2(13), 139 (2014).

Fabrication and Electrochromic Performance of Textile Electrochromic Devices

Yu Seon Eom, Raksha Pal, and Jong Seung Park
Department of Organic Material Science and Engineering, Pusan National University, Busan 46241, Korea
Tel.:051-510-2154, E-mail: jongpark@pusan.ac.kr

An electrochromic device (ECD) exhibits reversible color change on applying voltage due to electrochemical redox reactions. Most ECDs have been fabricated using indium tin oxide (ITO)-coated glass as an electrode, which finds applications in smart windows, displays, and camouflage. Due to the growing interest in wearable devices, the demand for textile ECDs has been increased rapidly. From this perspective, the ITO surface has a critical disadvantage in terms of mechanical flexibility. Moreover, the ITO electrode requires a heat annealing process at a high temperature, which creates difficulty in constructing a flexible substrate.

In this study, two types of textile ECDs are fabricated in fabric and fiber forms. Various techniques like spray-coating, doctor-blading, and electrospinning techniques have been used to manufacture textile ECDs. Viologen functionalized polyhedral oligomeric silsesquioxane (POSS) derivatives and dihexyl viologen (DHV) are used in the electrochromic layer which are known for their outstanding electrochromic performances. The electrochemical, mechanical, and morphological properties of the prepared fabric-type ECDs are investigated using cyclic voltammetry (CV), universal testing machine (UTM), and scanning electric microscopy (SEM) measurements. Besides, we have demonstrated the practical applicability by stitching fiber-type electrochromic devices into plain textured structures.

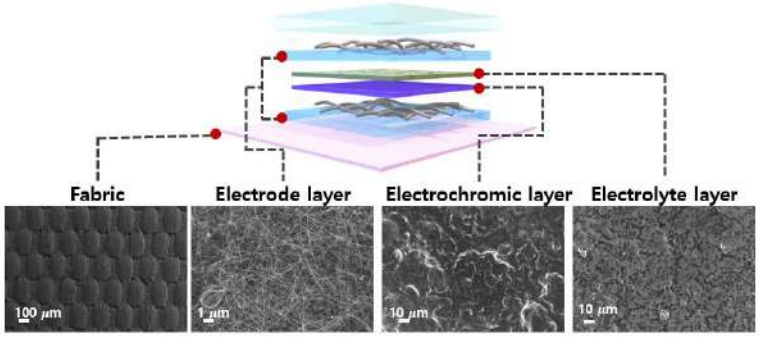

Fig. 1. Schematic illustration of the fabric-type electrochromic devices

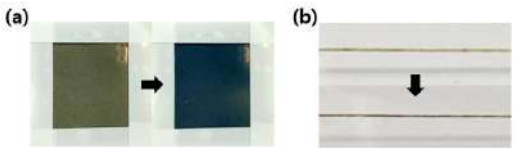

Fig. 2. Photo images of electrochromic devices (a) fabric (b) fiber

Acknowledgment

This work was support by the Technology Innovation Program and Industrial Strategic Technology Development Program (10062383) funded by the Ministry of Trade, Industry, and Energy (MOTIE, Korea).

References

1. G. K. Pande, J. H. Choi, J. E. Lee, Y. E. Kim, J. H. Choi, H. W. Choi, H. G. Chae*, J. S. Park*, Chem. Eng. J., 2020, **393**, 124690.
2. Hongwei Fan, Kerui Li*, Xuelong Liu, Kaixuan Xu, Yun Su, Chengyi Hou, Qinghong Zhang, Yaogang Li, and Hongzhi Wang*, ACS Appl. Mater. Interfaces 2020, 12, 25, 28451–28460.

Tunable structural color for encryption enhancement

***Byoungsu Ko*[1], *Trevon Badloe*[1], *Younghwan Yang, and Junsuk Rho*[1, 2*]**
[1]Dept. of Mechanical Engineering, POSTECH, Pohang 37673, Korea
Tel.:82-(054)-279-2187, E-mail: jsrho@postech.ac.kr
[2]Dept. of Chemical Engineering, POSTECH, Pohang 37673, Korea

Structural color [1] exploits the interaction between nanostructures and visible light to implement color. It represents colors through the light-nanostructure interactions, making it more Ultraviolet resistive than conventional dyes and organic paints, hard to duplicate, and suitable for encryption image. However, the structural color is difficult to commercialize as the structure needs to modify geometry parameters to change color. To overcome these limitations, many studies have been conducted that utilize phase change material's tunable optical properties to change the color. However, phase change materials (e.g. VO_2, GST) have a high fabrication temperature and a high phase-transition temperature is not suitable for real-life applications [2]. In this study, we present an encryption image based on the structural color that can be tuned at room temperature using Polyvinylalcohol (PVA). The PVA thin films can absorb humidity, increase up to 3 times the thickness depending on the relative humidity [3]. The changeable thickness can indicate a color change, thereby, it is suitable for structural color. Besides, PVA solution can be patterned as nanoimprint lithography. Therefore, it is expected that they can be actively applied in large-area tunable encryption images.

References

1. M. A. Kats, R. Blanchard, P. Genevet, and F. Capasso, *Nat Mater*, 12(1), 20–24 (2013).
2. B. Ko, T. Badloe, S.-J. Kim, S.-H. Hong, and J. Rho, *J. Opt.*, 22(11) (2020).
3. K. Lazarova, D. Christova, R. Georgiev, B. Georgieva, and T. Babeva, *Nanomaterials*, 9(6) (2019).

One-step fabrication of high efficiency hologram using particle embedded resin

Joohoon Kim[1], Dong-Kyo Oh[1], and Junsuk Rho[1,2]
[1]Dept. of Mechanical Engineering, Pohang University of Science and Technology, Pohang 37673, Korea
[2]Dept. of Chemical Engineering, Pohang University of Science and Technology, Pohang 37673, Korea
E-mail: jsrho@postech.ac.kr

Metasurfaces that consist of subwavelength periodic structures have shown great potential in controlling the propagation of light. By using the ability to modulate the amplitude and phase of EM wave, metasurfaces have been researched to realize high-resolution holography, metahologram. Especially, dielectric metahologram have been researched to achieve high efficiency. However, the fabrication of dielectric metaholograms using e-beam lithography have limitation in high cost and low throughput. Single-step manufacturing of hierarchical dielectric metalens has been demonstrated using nanoimprinting with particle embedded rein (PER) [1,2].

Here, we demonstrate a one-step fabrication of metahologram reaching 95% efficiency. We use an ultraviolet (UV)-curable resin as a final structure of meta-atoms. Since typical UV-curable resin has a low refractive index *n* in the visible regime, we use particle embedded resin consisting of titanium dioxide nanoparticle inclusion in a matrix of UV-curable resin. The refractive index of PER film are measured using ellipsometry and fitted using the Cauchy dispersion model.

Rigorous coupled-wave analysis (RCWA) is used to simulate the optical property of meta-atoms with measured refractive index. We use the geometric phase to modulate propagating light, due to its broadband property. **Figure 1a** represents simulated conversion efficiency of meta-atoms. Meta-atom with a length of 410 nm and a width of 120 nm has a conversion efficiency of 95.52%. The period and height of meta-atoms are 450nm and 900nm.

Figure 1b shows an SEM image of the master mold which is fabricated by e-beam lithography. Hard polydimethylsiloxane (h-PDMS) and vinyl polydimethylsiloxane are used to fabricate the soft mold. The PER is dropped on the glass substrate, then covered with the soft mold. UV illumination is used to harden the PER. After demolding the soft mold, the final structure is created on the substrate, as shown in **Figure 1c**.

We demonstrate that the TiO2 PER has sufficient optical properties to reach high efficiency. In addition, this research will contribute to the commercialization metahologram by creating high-efficiency metahologram at low cost for large-scale and high-throughput production.

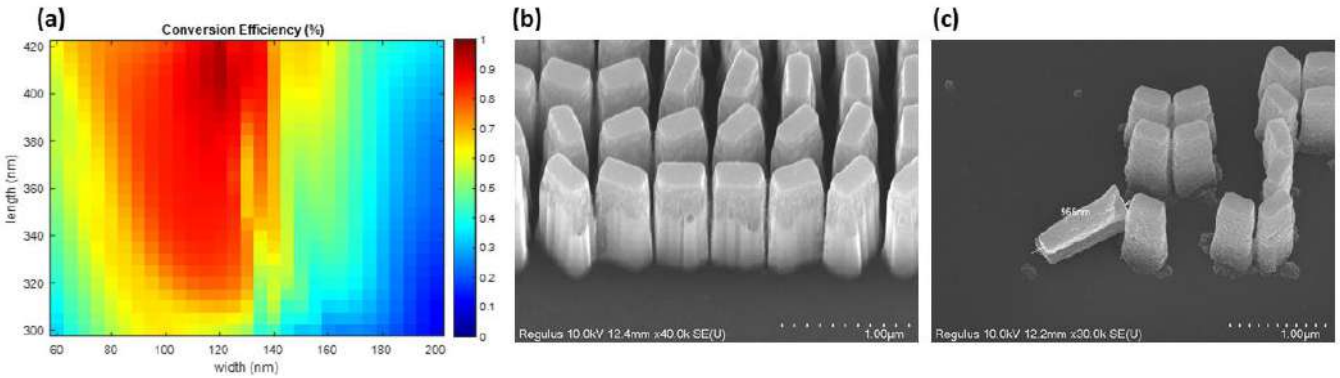

Fig. 1. One-step fabrication of metahologram reaching 95% efficiency
(a) Simulated conversion efficiency of meta-atoms, (b) Fabricated PER mold for high efficiency hologram, (c) Fabricated PER structure with TiO2 nanoparticle

References

1. G. Yoon, K. Kim, D. Huh, H. Lee, J. Rho, *Nat. Commun*. 11, 2268 (2020).
2. G. Yoon, K. Kim, S.-U. Kim, S. Han, H. Lee, J. Rho, *ACS Nano*, 15, 698-706 (2021).

Near-infrared Detectors Using Semiconducting Carbon Nanotubes with Narrow Band-gap.

Dongseob Ji[1], Haksoon Jung[1], and Yong-Young Noh[1]
[1]Dept. of of Chemical Engineering, Pohang University of Science and Technology (POSTECH), Pohang 37673, Republic of Korea
Tel.: 82-54-279-8265, E-mail: yynoh@postech.ac.kr

Single-walled carbon nanotube (SWNT) is a promising candicate for infrared (IR) detectors due to its strong optical absorption in IR wavelength region, excellent charge carrier mobility, light weight and solution processability. Because large-diameter semiconducting SWNT (sc-SWNT) shows narrow band gap and weak exciton binding energy, high performance-IR detector can be developed by utilizing large-diameter sc-SWNTs. For the use of sc-SWNTs, it is necessary to sort tubes with certain kinds of electrical properties from as-synthesized SWNTs bundles.

Here, we report the sorting technique of large-diameter sc-SWNTs by conjugated polymers and high performances of sc-SWNT IR detectors.

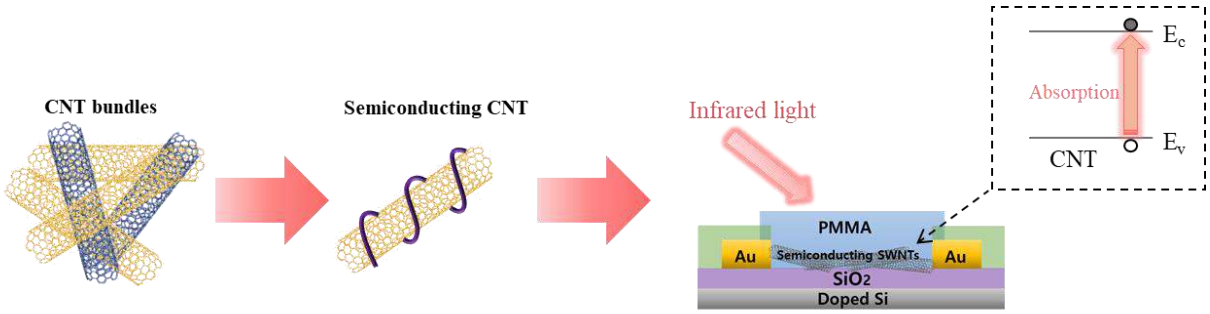

Fig. 1. Scheme illustrations of developing process for carbon nanotube based IR detector.

Acknowledgment

This work was supported by National Research Foundation of Korea (NRF) grant funded by the Korea government (2017R1E1A1A01075360).

References

1. S. Park, S. J. Kim, J. H. Nam, G. Pitner, T. H. Lee, A. L. Ayzner, H. Wang, S. W. Fong, M. Vosgueritchian, Y. J. Park, M. L. Brongersma, Z. Bao, *Adv. Mater.*, 27, 759–765 (2015).
2. R. Lu, C. Christianson, A. Kirkeminde, S. Ren, J. Wu, *Nano Lett.*, 12, 6244−6249 (2012).

Stretchable strain sensor for wearable device by UV curing patterning method

Yongjun Song[1], Dawoon Lee[1], and Jaekyun Kim[1]*
[1]**Dept. of Photonics and Nanoelectronics, Hanyang University, Ansan 15588, Republic of Korea**
Tel.:82-31-400-5521, E-mail: jaekyunkim@hanyang.ac.kr

A number of studies have been conducted to develop the high conductive and stretchable electrolyte in which possess high potential for various applications such as high-power and mechanically stable energy storage devices, generator, sensor, and self-light-emitting devices. However, intrinsic limitations of those stretchable electrolyte from trade-off relationship between electrical performance and mechanical stability restrict the actual applications on wearable devices. As a strategy to overcome this trade-off relationship, hydrogel, a hydrophilic polymer material in which including dispersed water molecular in network chain, shows reasonable electrical conductivity and modulus, but its relatively low ionic conductivity and short life-time in air due to fast water evaporation from the surface of gel cannot be a complete solution. From this reason, introduction of ionic-liquid based polymer electrolyte is another strategy to compensate both electrical and mechanical properties and it has been attracted significantly because of the presence of rigid polymer chain and high mobile ionic liquid phase which can attribute to synergistic effect of robust polymer chain and ionic channel path.

In this research, we synthesized a stretchable ion-gel polymer electrolyte by composing an acrylic acid monomer and a PEGDA cross-linker as a mechanical backbone phase and an 1-ethyl-3-methylimidazolium bis(trifluoromethylsulfonyl)imide (EMIM-TFSI) ionic liquid, a tetraethylene glycol dimethyl ether (TEGDME) plasticizer, in order to achieve both high ion conductivity and flexible mechanical properties. Furthermore, we fabricated patterned capacitive and resistive sensor arrays by selective UV curing method with deformable ion gel polymer substrate and demonstrated its electrochemical performance and flexibility under the strain deformation which can be attribute to next-generation ultra-flexible wearable devices.

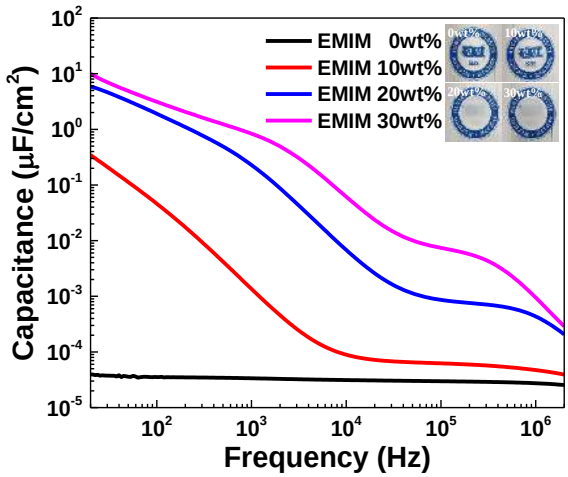

Fig. 1. Frequency-Capacitance of EMIM 0~30wt%

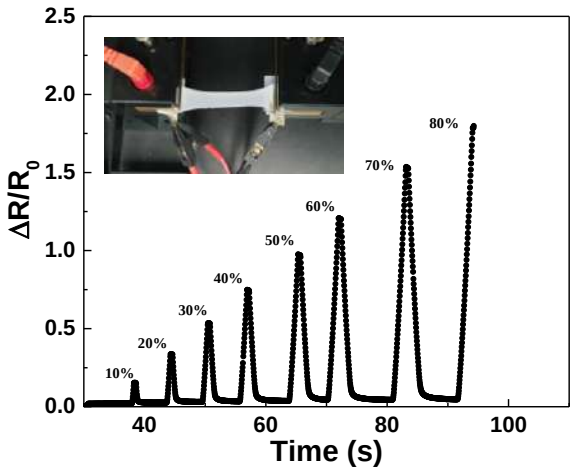

Fig.2 Resistance change of EMIM 30wt% film

Acknowledgment

References

Enhancement of Blue-light emitter CsPbBr3 Nanoplatelets through Post-treatment Surface Passivation

Jinu Park[1], Joonyun Kim[1], and Byungha Shin[1]
[1]Dept. of Material Science and Engineering, KAIST, Daejeon, Korea
Tel.:82-42-350-3355, E-mail: Jinu.p@kaist.ac.kr

Lead halide perovskite has emerged as a good candidate for the next-generation light-emitting diodes (LEDs) due to its extremely narrow photoluminescence (PL) spectrum with a typical full width half maximum (FWHM) < 20 nm. Especially, all-inorganic $CsPbX_3$ (X=Br, I) has indicated the photoluminescence quantum yield (PLQY) of ~100% for green and red light emission. A more challenging, yet technologically important, work is developing a high performance for emitting material of blue light. By moderately replacing Br with Cl in $CsPbBr_3$, the light emission spectrum can be fitted to the blue to UV emission; nonetheless, the mixed halide component, $CsPbBr_{3-x}Cl_x$, suffers from phase segregation with ion migration which introduces low PLQY and poor spectral stability.

Here, we show a production method of low-dimensional $CsPbBr_3$ in the morphology of nanoplatelets (NPLs) that is efficient at emitting blue light without the need for anion-substitution. $CsPbBr_3$ NPLs with 2 monolayer (ML) and 3 ML of thickness yielded PL peak at 435nm with extremely narrow FWHM of 14.2 nm and PL peak at 456nm with FWHM of 19.6nm, respectively. The optical properties of these nanoplatelets were further enhanced by post-synthesis treatment with tetrafluoroborate salts—almost 1150% increase in PL intensity was observed with spectral stability. Details of the results and discussion of a possible mechanism behind the improvement with the post-synthesis treatment will be described.

Full-colored Polarization Colorfilter by Near-zero Reflection with Triple-nanofin Metasurfaces

Chunghwan Jung[1] and Junsuk Rho[1, 2]*
[1] Dept. of Chemical Engineering, Pohang University of Science and Technology (POSTECH), Korea
[2] Dept. of Mechanical Engineering, Pohang University of Science and Technology (POSTECH), Korea
E-mail: jsrho@postech.ac.kr

Structural color with metasurface is studied to overcome the drawbacks of traditional color printing such as low resolution, environmental toxicity, and time durability. Many metasurfaces have been developed for dynamic structural coloring to transform images in the visible spectrum. Here, we suggest a fully switchable display using polarization-sensitive metasurfaces displaying full-color images with polarization of incident light. The proposed triple-nanofin structures show polarization-dependent magnetic field distributions, and we get that near-zero scattering under the incident polarization is perpendicular to the long axis of the nanofins. The lengths of each nanofin structue affect the resonant peak position, providing a full-color spectral range. With these advantages, QR code images, two-color object images, and an overlapped double-person images are acquired with the proposed structures. These demonstrations offer potential applications in the fields of high-security information encryption, security tags, multi-channel imaging, and dynamic displays.

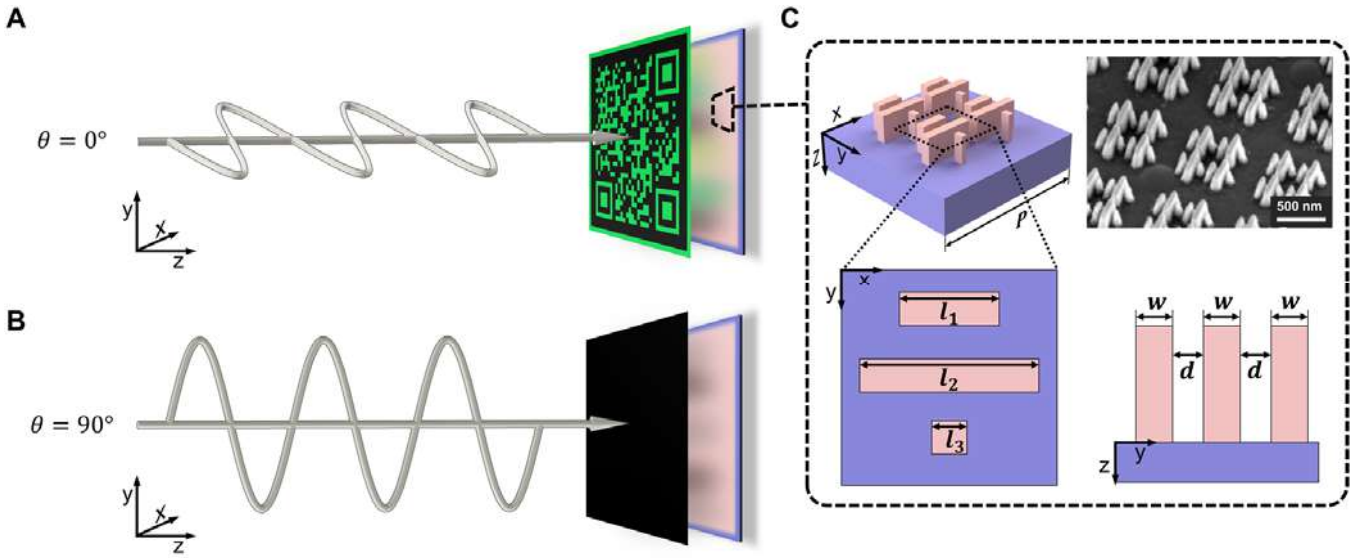

Fig. 1. Schematic of switchable display using metasurface coloration.

Highly Flexible, Large-area MoS_2/Ion-gel Composite Film for Photodetection

Soobin Lee[1], Seohyun Maeng[1], Dawoon Lee[1], and Hyunseok Lee[2], Jaekyun Kim[1]

[1]Dept. of Photonics and Nanoelectronics, Hanyang University, Ansan-si, 15588, Korea

Tel.:82-31-400-5521, E-mail: jaekyunkim@hanyang.ac.kr

[2]Dept. of Physics, Chungbuk National University, Cheongju-si, 28644, Korea

Tel.:82-43-261-2276, E-mail: hsl@chungbuk.ac.kr

Molybdenum disulfide (MoS_2) is attracting great interest for the application of photodetector because of the ease of large synthesis, and the tunable direct bandgap of 1.3~1.9eV, in which depends on the number of stacked layer. Also, MoS_2 represents high responsivity for visible light.

However, the performance of the MoS_2-based devices continuously needs to be improved for the low power consumption and reliability of fabrication process. In order to lower operating voltage of phototransistor, high-capacitance electrochemical ion-gel dielectric layer in which forms an electrical double layer (EDL) under the applied electric field is proposed to offer high specific capacitance value (~10 μF/cm^2). Moreover, its transparency in the visible range is promising for wearable devices.

To address the large-area and transparent ion-gel/MoS_2 heterostrucure, we propose the adhesive ion-gel stamping method in which the large-area MoS_2 were released from the growth substrate by the adhesion force of ion-gel. In terms of flexible device, the PI(Polyimide) film was used as substrate and high-performance indium-tin-zinc-oxide (ITZO) thin film was deposited by RF sputtering followed with metal electrode deposition using thermal evaporator. After the fabrication of ITZO TFTs, the devices were separated from the rigid glass. This ultrathin ITZO devices were attached to the MoS_2/ion-gel film for the transparent and free-standing photodetectors. The raman spectrum of MoS_2/Ion-gel freestanding film indicates that two characteristic wavelength peaks. The offset between the two peaks is 17.55cm^{-1} and 22.32cm^{-1}, which indicated the formation of monolayer and bilayer. Transfer curve exhibits the electron mobility of ~1.1 cm^2/Vs and on/off ratio of ~ 10^4 while showing low voltage operation. As a result, our results suggest that ion gel stamping method can be used to fabricate the transparent MoS_2/ion-gel films for the flexible oxide semiconductor-based photodetector devices.

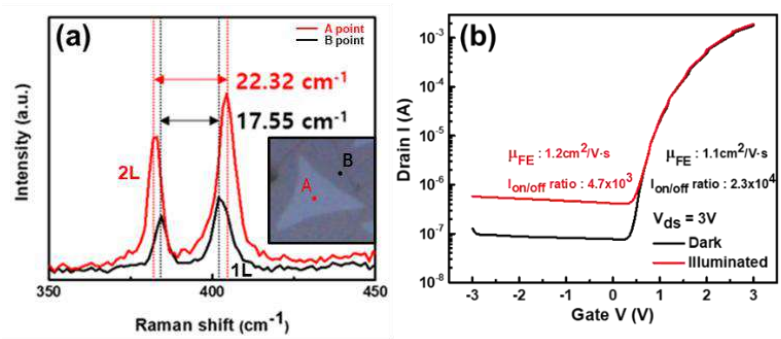

Fig. 1. (a) Raman spectra of MoS_2/ion-gel freestanding film. The inset shows optical Image of MoS_2/ion-gel freestanding film. 1L,2L indicate monolayer, bilayer, respectively.
(b) Transfer curve of ITZO TFTs with MoS_2/ion-gel film photodetector

References

1. ACS Appl. Mater. Interfaces 2016, 8, 8576−858

2. Appl. Phys. Lett. 103, 023505 (2013)

Enhanced Photoluminescence of Two-Dimensional van der Waals Heterostructures Fabricated by Layer-by-Layer Oxidation of MoS_2

Sojung Kang[1], Yoon Seok Kim[2], Jae Hwan Jeong[1], Junyoung Kwon[1], Jong Hun Kim[1,3], Yeonjoon Jung[3], Jong Chan Kim[4], Bumho Kim[5], Sang Hyun Bae[6], Pinshane Y. Huang[6], James C. Hone[5], Hu Young Jeong[4], Jin-Woo Park[1], Chul-Ho Lee[2] and Gwan-Hyoung Lee[3]

[1]Department of Materials Science and Engineering, Yonsei University, Seoul 03722, Korea
[2]KU-KIST Graduate School of Converging Science and Technology, Seoul 02841, Korea
[3]Department of Materials Science and Engineering, Seoul National University, Seoul 08826, Korea
[4]Department of Materials Science and Engineering, Ulsan National Institute of Science and Technology, Ulsan 44919, Korea
[5]Department of Mechanical Engineering, Columbia University, New York, New York 10027, United States
[6]Department of Materials Science and Engineering, University of Illinois at Urbana-Champaign, Urbana, Illinois 61801, United States

Tel.:82-2-880-8366, E-mail: gwanlee@snu.ac.kr

Since monolayer transition metal dichalcogenides (TMDs) are promising for optical and optoelectronic application because of strong photoluminescence, the thickness control of two-dimensional TMDs is one of the most important issues. Many efforts have been made to fabricate monolayer TMDs. However, because of damage-prone characteristics of TMDs, it is difficult to achieve monolayer TMDs with high optical properties preserved. Here we utilized customized plasma system for layer oxidation of MoS_2. We directly oxidized multilayer MoS_2 into MoO_x/1L-MoS_2, which showed enhanced photoluminescence intensity by 3-times higher than as-exfoliated 1L-MoS_2 by suppression of defect-induced and charged exciton-related light emission. We demonstrate two-dimensional van der Waals heterostructures of $MoO_x/MoS_2/MoO_x/MoS_2$. We first oxidized bilayer MoS_2 into MoO_x/1L-MoS_2. Another bilayer MoS_2 was transferred, followed by subsequent oxidation. The final structure shows high photoluminescence from two decoupled MoS_2 monolayers. Our work shows a facile technique for fabrication of MoO_x/MoS_2, which is beneficial for high performance two-dimensional optoelectronics.

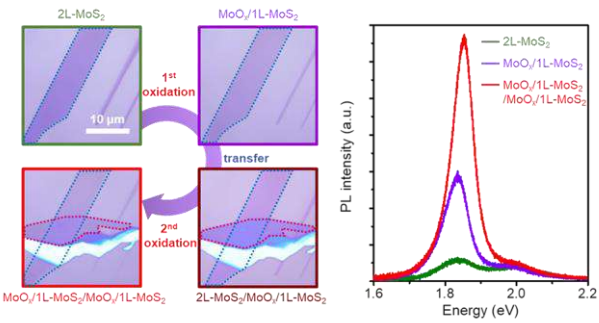

Fig. 1. $MoO_x/MoS_2/MoO_x/MoS_2$ van der Waals heterostructure

Reference

1. S. Kang et al, *ACS Appl. Mater. Interfaces*, 13(1), 1245-1252 (2021).

High Conductivity Sodium Ionic Gel Polymer Electrolyte and its application on Excellent All-solid-state Micro-supercapacitor for Display

Nguyen Thi Huyen[1], Dawoon Lee[1], U Hyeok Choi[2], and Jaekyun Kim[1]
[1]Dept. of Photonics and Nanoelectronics, Hanyang University, Ansan 15588, Korea
Tel.:82-31-400-5521, E-mail: jaekyunkim@hanyang.ac.kr
[2]Dept. of Polymer Science and Engineering, Inha University, Incheon 22212, Korea.
Tel.:82-32-860-7485, E-mail: uhyeok@inha.ac.kr

High conductive micro-supercapacitors (MSCs) have received enlarged attention due to the outstanding advantages and application for the next-generation storage devices with the combination of ionic gel-type electrolyte. Recently, sodium ion (Na+) has been attracting much attention as the most promising alternative to the existence of lithium ion (Li+) for several advantages such as natural abundance, cost-effectiveness, and low-toxicity. Moreover, electrochemical performance of Na+-based electrolyte is similar characteristics to Li+-based electrolyte. Arising from these needs, there are many efforts which have been devoted to achieving sodium-based ionic gel polymer electrolyte to construct high performance and large-scale-eco-energy storage.

In terms of fabricating the electrode for MSCs, directly scribable laser irradiation method has been chosen to achieve microscale interdigitated pattern, assuring that the good productivity and reliability for graphene-based micro-supercapacitor. Converting graphene oxide aqueous solution into reduced graphene oxide by laser-scribed have been presented under a role like the planar graphene MSCs to obtain the desired size, structure, and ability to overcome these mentioned issues. For the electrolyte phase systems, we used the gel polymer system by associating poly(ethylene glycol) diacrylate (PEGDA) as UV curing polymer, 2-hydroxy-2-methylpropiophenone (HOMPP) as UV initiator, and an ionic phase which contents sodium salt as the material in the supply of conductive ions to build sodium ionic gel polymer electrolyte (SIGPE) to satisfy the expected intention of electrical performance. The combination of substances by thermal method brings many great advantages, as well as attaining the excellent electrochemical performance, and stability devices at ambient temperature within a short time. In conclusion, electric double-layer (EDL) MSCs based on sodium gel polymer electrolyte can offer a great density, reaching hight power density, fast charge/discharge rate, safety, long durability, and relatively simple design, and also contribution to further improved eco-friendly next-generation energy storage devices.

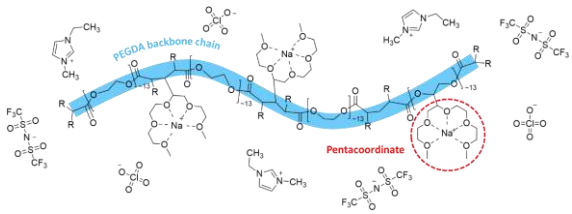

Fig. 1. Schematic structure of cross-linking of ionic gel polymer electrolyte

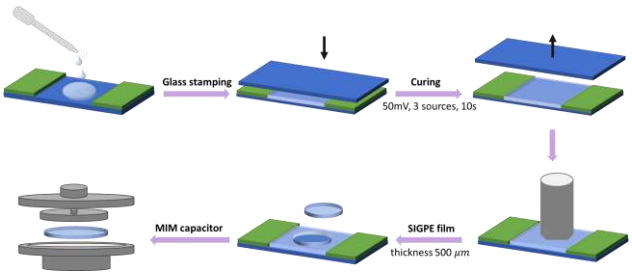

Fig. 2. Device investigation properties of MIM structure and MSC device based on SIGPE film

Acknowledgment

References

Highly Efficient Thermally-Deposited Perovskite Light-Emitting Diodes with a Polymer Passivation Layer

Nakyung Kim[1], Mingue Shin[1], Joonyun Kim[1], Jinu Park[1], Seongmoon Jun[2], Yong-Hoon Cho[2], and Byungha Shin[1]
[1]Dept. of Materials Science and Engineering, Korea Advanced Institute of Science and Technology (KAIST), Daejeon 34141, Korea
Tel.: 82-42-350-3315, E-mail: byungha@kaist.ac.kr
[2]Dept. of Physics, Korea Advanced Institute of Science and Technology (KAIST), Daejeon 34141, Korea

Halide perovskite has been reported as the next-generation materials for light-emitting diodes (LEDs) due to its high color purity and tunable bandgaps by adjusting halide components. Although most of the perovskite LEDs are fabricated via a solution process, the vacuum deposition process is suitable for large-scale mass production. Here, we demonstrate highly efficient vacuum-deposited perovskite LEDs by introducing a separate passivation layer. The x-ray diffraction (XRD) patterns in **Fig 1 a,b** show that under the same flux ratio, a larger quantity of the Cs_4PbBr_6 phase is formed in the films on the polyethylene oxide (PEO) layer. A perovskite film deposited on the PEO layer shows remarkable improvement in photoluminescence (PL) intensity compared to a reference sample without the PEO layer. A PL intensity reached maximum at $CsBr/PbBr_2$=1.1. This great enhancement in PL intensity is attributed to the passivation of interfacial defects of the perovskite, which is proven by temperature-dependent photoluminescence measurements as shown in **Fig 1 d,e**. However, a direct application of the polymer layer to a LED device was challenging because of the electrically insulating nature of the PEO. We solved this charge transport issue by doping PEO with alkali salts. This strategy resulted in an enhanced luminance and EQE up to 7486 cd/m^2 and 6.6 %, respectively. Details of the materials characterization and device analysis will be discussed.

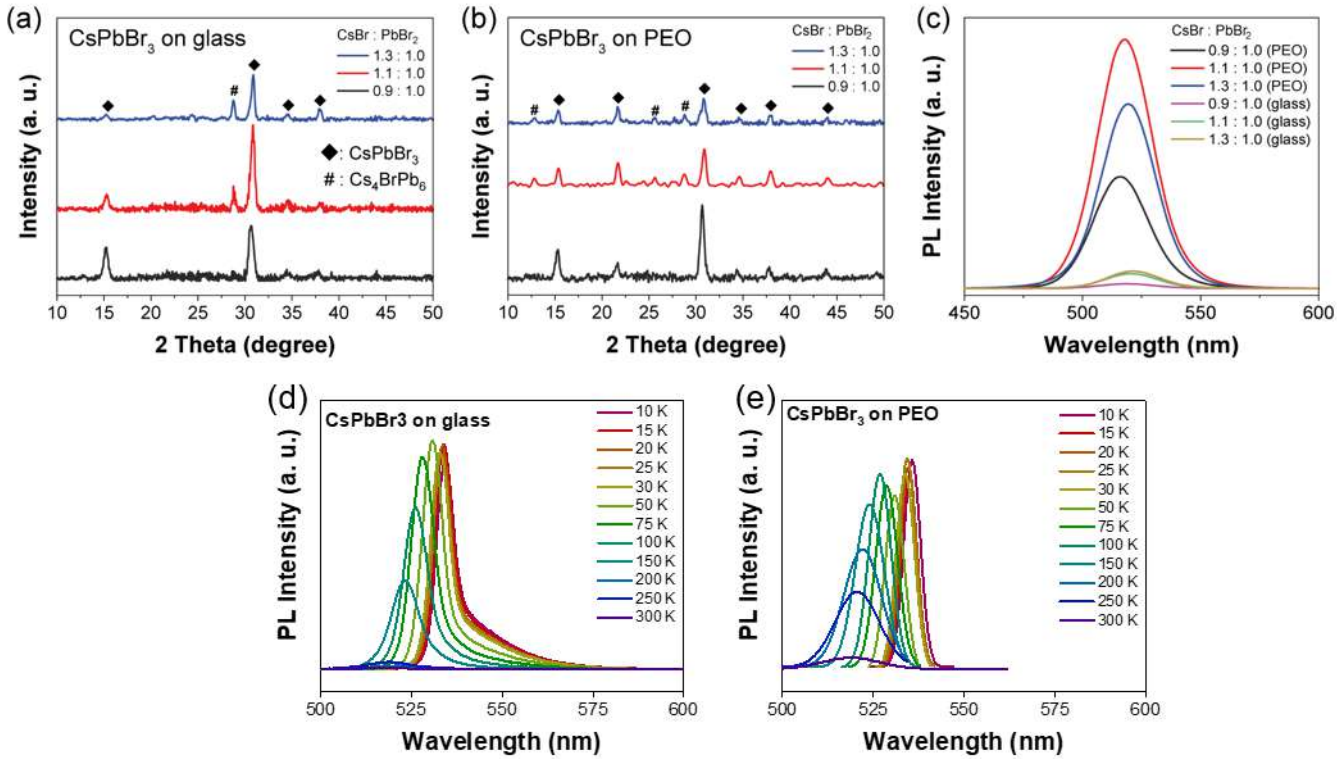

Fig. 1. XRD patterns of a) $CsPbBr_3$ on glass substrate and b) $CsPbBr_3$ on PEO passivation layer with various ratio of CsBr to $PbBr_2$. c) steady-state PL spectra of various perovskite films. Temperature-dependent PL intensity spectra of c) $CsPbBr_3$ on glass substrate and d) $CsPbBr_3$ on PEO passivation layer.

Acknowledgment

This work was supported by the National Research Foundation of Korea (NRF) grant funded by the Korea government (MSIT) (No. 2020R1A2C3008111). There was financial support from the Korea Institute of Energy Technology Evaluation and Planning (KETEP) and the Ministry of Trade Industry & Energy (MOTIE) of the Republic of Korea (No. 20183010014470).

Polarization-Insensitive Metasurface Hologram with Low-Noise Optimization

Changhyun Kim, Jangwoon Sung, and Byoungho Lee
Inter-University Semiconductor Research Center and School of Electrical and Computer Engineering
Seoul National University, Gwanak-Gu Gwanakro 1, Seoul 08826, Korea
Tel.:82-2-880-9564, E-mail: byoungho@snu.ac.kr

Metasurface is two-dimensional array composed of artificially fabricated subwavelength antennas. The image quality and field of view of holography can be improved when metasurface platform is adopted due to subwavelength resolution [1,2]. Moreover, noise of hologram can be further reduced by using nanostructures that can control amplitude and phase simultaneously [3,4]. However, these works are limited to specific polarization. In this paper, we propose low-noise metasurface hologram with polarization-insensitive operation utilizing phase-only modulation. The designed device is further optimized for low noise to operate at 660 nm.

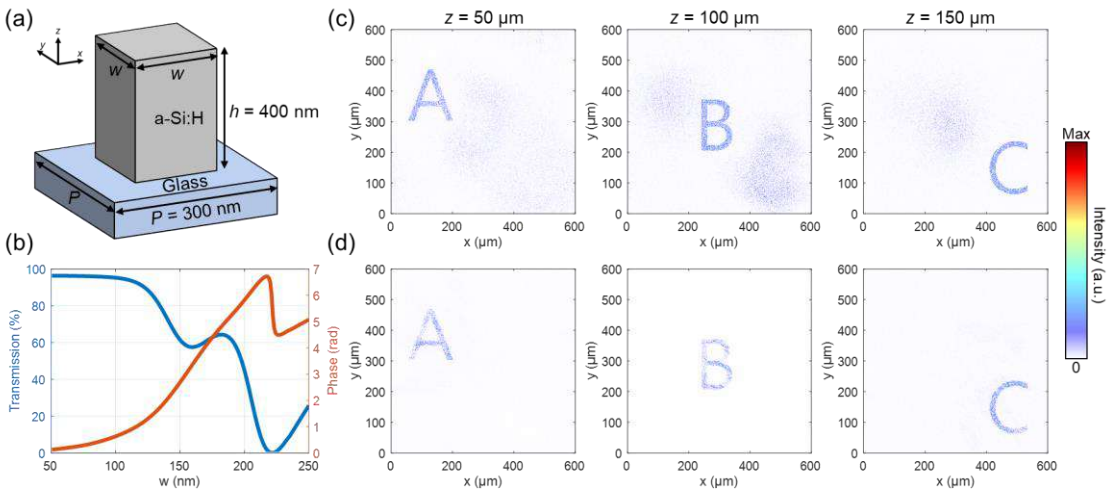

Fig. 1. (a) A schematic of the isotropic square nanopillar (b) Line plot graph showing simulated transmittivity according to the width of nanopillar (c) Simulation results of initial metasurface (d) Simulation results of optimized metasurface

The isotropic unit cell structure and its modulation profiles are shown in Fig. 1a,b. Phase maps are made using the result at Fig. 1b and we only use structures having only 50 % or higher transmittance. We perform phase map optimization to reduce the noise with phase-only modulation. To do this, we first define a merit function which reflects the average intensity of image and the standard deviation of background noise. Next, we apply gradient ascent algorithm where initial condition is summation of the back propagated profiles from images. As compared in Fig. 1c,d, the background noise of the generated image is significantly reduced. The simulations of nanopillar and hologram are performed with rigorous coupled wave analysis and angular spectrum method, respectively.

In conclusion, we demonstrated the phase-only metasurface hologram operating with low-noise and arbitrary polarization. Our research can sufficiently improve performance even under limited conditions, and we expect that this optimization technology has potential for various optical applications and display technologies.

Acknowledgment

This work was supported by the National Research Foundation of Korea (NRF) grant funded by the Korea government (MSIT). (No. 2020R1A2B5B02002730)

References

1. G.-Y. Lee, J. Sung, and B. Lee, *ETRI Journal*, 41(1), 10-22 (2019).
2. J. Sung, G.-Y. Lee, and B. Lee, *Nanophotonics*, 8(10), 1701-1718 (2019).
3. G.-Y. Lee et al., *Nanoscale*, 10(9), 4237-4245 (2018).
4. X. Ni, A. V. Kildishev, and V. M. Shalaev, *Nat. Commun.*, 4(1), 2807 (2015).

High Performance Blue Hyperfluorescence System by Prohibiting Dexter Energy Transfer of Triplet Exciton

*Hyuna Lee, Ki joon Yang, Soon Jae Hwang, Kenkera Rayappa Naveen and Jang Hyuk Kwon**
Department of Information Display, Kyung Hee University, 26, Kyungheedae-ro, Dongdaemun-gu, Seoul, 02447, Republic of Korea.
Tel.:82-2-961-9147, E-mail: jhkwon@khu.ac.kr

In 2019, a new di-boron multi-resonance (MR) type blue thermally activated delayed fluorescence (TADF) material, ν-DABNA, was reported.[1] Unlike other single boron DABNA materials, ν-DABNA exhibits small ΔEst value of 0.03 eV and narrower full width at half maximum (FWHM) of 14 nm. Despite of small ΔEst value, the low reverse intersystem crossing rate constant (k_{RISC}, 2.0 x10^5 s^{-1}) triggers high triplet exciton density in emissive layer (EML), resulting in severe roll-off efficiency and short device lifetime in TADF devices. However, high photoluminescence quantum yield (PLQY) and extremely narrow FWHM satisfies almost all requirements as an ideal blue emitter in the hyperfluorescence (HF) system. In this system, TADF materials act as assistant host and transfer recycled singlet exciton to final fluorescent emitter. Normal fluorescence DABNA type materials exhibit the final emission with 1.0% of low doping concentration with higher efficiency by harvesting large amount of singlet excitons from TADF assistant host. However, even small doping percentage, it is hard to prohibit the triplet-triplet energy transfer (Dexter energy transfer, DET) completely to fluorescent emitter.

In this study, in order to prohibit the unwanted DET process in HF system and to maximize the merit of ν-DABNA, we attached ancillary groups on the terminal site of the ν-DABNA[2] and synthesized KHU-034 and KHU-036. Compared with ν-DABNA, KHU-034 and KHU-036 showed similar photophysical properties, with increased PLQY due to reduced aggregation effect. Especially, KHU-036 exhibited the 2~3 nm of blue shifted emission wavelength. For efficient Forster resonance energy transfer (FRET), large spectrum overlap between TADF assistant material and fluorescent emitter is crucial. Thus, we selected the highly efficient TADF material showing deep blue emission around 475 nm, KHU-TADF. With 30 wt% of KHU-TADF and 1wt% of KHU-034 or KHU-036, HF device performances were optimized. As a result, KHU-034 and KHU-036 exhibited higher efficiency with alleviated roll-off efficiency than ν-DABNA. It is believed that blocking groups on ν-DABNA reduced DET process in HF system and decreased the activation of triplet exciton on ν-DABNA. Detailed device performance and analysis will be discussed on the presentation.

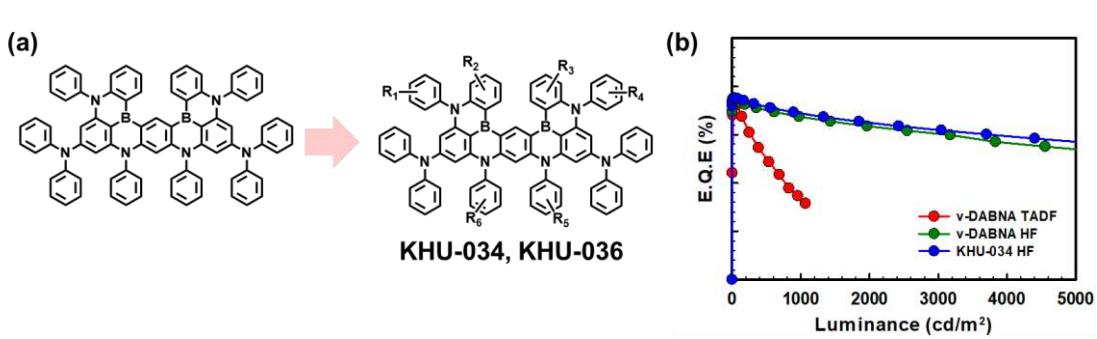

Fig. 1. (a) Design strategy of KHU-034, and KHU-036 (b) Comparison of device performance.

Acknowledgment

This work was supported by the National Research Foundation of Korea (Grant No. NRF-2019M3D1A2104019) and by BK21 FOUR Program (Department of Information Display, Kyung Hee University) funded by Ministry of Education (MOE, Korea).

References

1. Yasuhiro Kondo et al. Nature photonics, 13, 678-682 (2019).
2. Hyocheol Jung et al. ACS Appl. Mater. Interfaces, 10, 36, 30022-30028 (2018)

Organic thin-film transistors with a water-processable solid electrolyte as a gating element

Solin Lee[1] and Felix Sunjoo Kim[1]
[1]Dept. of Chemical Engineering and Materials Science, Chung-Ang University, Seoul 06974, Korea
Tel.:82-2-820-5200, E-mail: fskim@cau.ac.kr

Organic thin-film transistors (OTFTs) have been of interest for their unique properties and advantages applicable to the display component.[1] OTFTs can utilize various insulating layers and electrolytes for the gating elements.[2] In this study, we have fabricated and characterized water-processable solid electrolyte layers composed of water-soluble polymers and ionic liquids. We selected two different ionic liquids, 1-ethyl-3-methylimidazolium bis(trifluoromethylsulfonyl)imide ([EMIM][TFSI]) and 1-ethyl-3-methylimidazolium tetrafluoroborate ([EMIM][BF4]), and conducted the miscibility test of the ionic liquids in water (Fig. 1). [EMIM][BF4] is miscible in water while [EMIM][TFSI] is immiscible. We fabricated thin films of ionic liquid/polymer composites to form solid electrolyte layers and investigated their electrolytic characteristics using electrochemical impedance spectroscopy. These layers of the water-processable solid electrolytes were applied as a gating element in OTFTs and both static and transient behaviors of the transistors were analyzed to see the feasibility and effectiveness of the electrolytes in device applications. These solid electrolytes can be industrially advantageous because of their eco-friendly processability in mild conditions without use of toxic organic solvents and easy removal with aqueous solvents on demand.

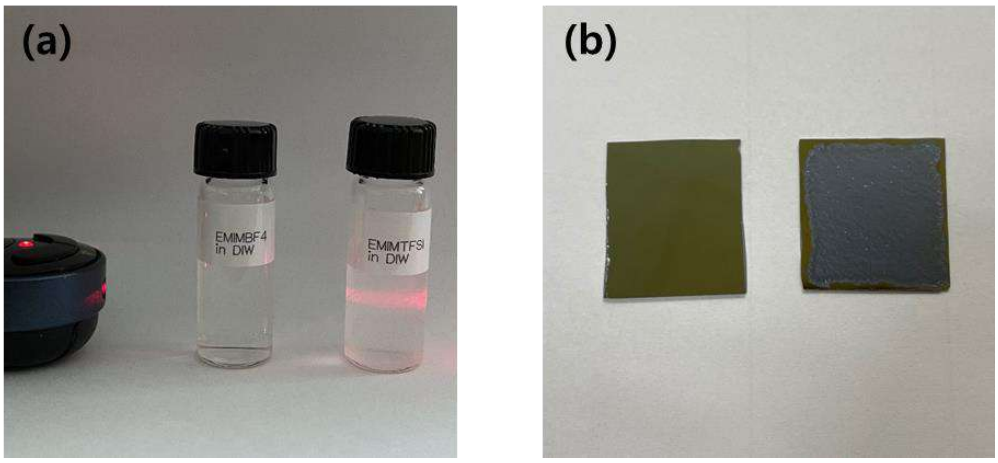

Fig. 1. (a) Digital photography of two different ionic liquids dispersed in water. (b) Digital photography of water-processable solid electrolytes.

Acknowledgment

This research was funded and conducted under "the Competency Development Program for Industry Specialists" of the Korean Ministry of Trade, Industry and Energy (MOTIE), operated by Korea Institute for Advancement of Technology (KIAT), with the project No. P0012453, Next-generation Display Expert Training Project for Innovation Process and Equipment, Materials Engineers. This work was also supported by the research programs (2019M3F3A1A03079821 and 2019R1A2C1087234) through the National Research Foundation of Korea (NRF) funded by the Ministry of Science and ICT.

References

1. M. Mizukami, S. Oku, S.I. Cho, M. Tatetsu, M. Abiko, M. Mamada, T. Sakanoue, Y. Suzuri, J. Kido, and S. Tokito, *IEEE Electron Device Lett.*, 36(8), 841 (2015).
2. R. P. Ortiz, A. Facchetti, and T. J. Marks, *Chem. Rev.*, 110(1), 205 (2010).

Understanding the Origin of Sub-Bandgap Emission from Zero-Dimensional Perovskite Cs_4PbBr_6

Mingue Shin[1], Sung-Wook Nam[2], Aditya Sadhanala[3], Ravichandran Shivanna[4], Miguel Anaya[4], Alberto Jiménez-Solano[5], Hyewon Yoon[1], Seokwoo Jeon[1], Samuel D. Stranks[4], Robert L. Z. Hoye[4, 6], Byungha Shin[1*]*

[1]Department of Materials Science and Engineering, Korea Advanced Institute of Science and Technology (KAIST), Daejeon 34141, Republic of Korea

Tel.:82-42-350-3315, E-mail: byungha@kaist.ac.kr

[2]School of Medicine, Kyungpook National University, Daegu 41405, South Korea

[3]Cavendish Laboratory, JJ Thomson Ave, University of Cambridge, Cambridge, CB3 0HE UK

[4]Department of Materials Science and Metallurgy, 27 Charles Babbage Road, University of Cambridge, Cambridge, CB3 0FS, UK

[5]Max Plank Institute for Solid State Research, Heisenbergstrasse 1, Stuttgart, 70569, Germany

[6]Department of Materials, Imperial College London, South Kensington, London SW7 2AZ, UK

Due to exceptional color purity and good thermal stability, all-inorganic halide perovskite ($CsPbBr_3$) has been attracting interest as the next-generation materials for light-emitting diodes (LEDs). However, its low exciton binding energy is one of the factors limiting luminescence efficiency and spatial confinement of excitons is a promising way to resolve this issue. Here, we present strategy of confining excitons in vacuum-deposited low-dimensional Cs-Pb-Br light emitters. We have controlled dimensionality of by adjusting the deposition ratio of the two source materials, CsPb and $PbBr_2$, to deposit Cs-Pb-Br films. Under the excess deposition ratio of CsBr the so-called zero-dimensional Cs_4PbBr_6 formed, producing strong green emission with high photoluminescence quantum yield close to 90%. The green emission from Cs_4PbBr_6 is unusual considering its large bandgap of 3.9 eV. Diverging opinions, which are still under debate, have been proposed for the origin of the green luminescence from Cs_4PbBr_6: (i) the presence of $CsPbBr_3$ nanoparticles (approximately 2.4 eV band gap) embedded in the Cs_4PbBr_6 matrix that down-convert the emission;[1-3] or (ii) defect states, originating from halogen (Br) vacancy, formed within the gap of the Cs_4PbBr_6.[4-5] Through in-depth transmission electron microscopy study and optical measurement such as photothermal deflection spectroscopy and photoluminescence contour map, we identified the inclusion of trace amount of $CsPbBr_3$ "impurities" as the source of the green emission.

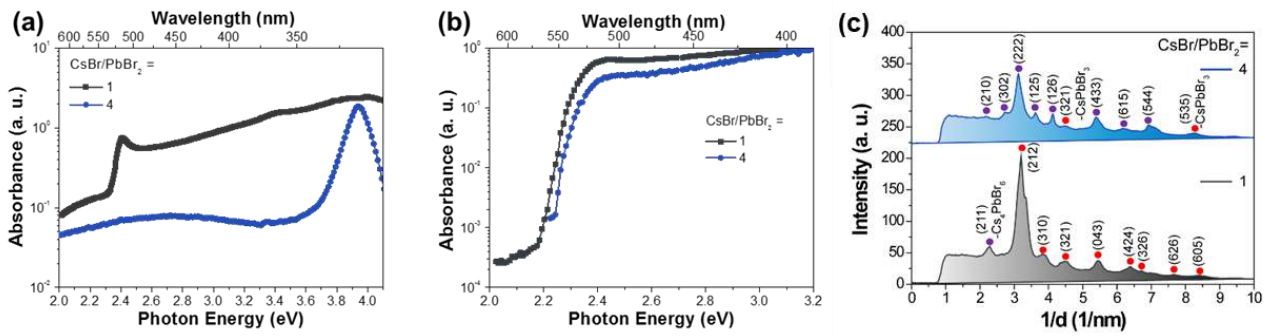

Fig. 1. Absorption spectra measured by (a) UV-vis spectroscopy and (b) PDS measurement. (c) A graph plotting the rotational average intensity at the 1/d value from the center of the selected area electron diffraction (SAED) patterns of samples with ratio of $CsBr/PbBr_2$ = 1 and 4. The red and purple spots correspond to $CsPbBr_3$ and Cs_4PbBr_6, respectively.

Encouraged by the high PLQY, we proceeded with fabricating perovskite LEDs (PeLEDs) based on the films with $CsBr/PbBr_2$ = 4 as an emitting layer. We have achieved a 60-fold improvement in external quantum efficiency from an LED with a $CsPbBr_3$-embedded Cs_4PbBr_6 light emitter compared to the control device with $CsPbBr_3$. Details of the materials characterization and device analysis will be discussed.

Acknowledgment

The work at KAIST was supported from the Korea Institute of Energy Technology Evaluation and Planning (KETEP) and the Ministry of Trade Industry & Energy (MOTIE) of the Republic of Korea (No. 20183010014470), supported by development of smart chemical materials for IoT devices (KRICT SI 1921-20) and funded by Saudi Aramco-KAIST CO2 Management Center. RLZH acknowledges support from the Royal Academy of Engineering under the Research Fellowship scheme (No.: RF\201718\17101), as well as support from Magdalene College, Cambridge. A.S. acknowledges support from the EPSRC (Grant no.: EP/M005143/1), Indo-UK APEX project, and UKIERI. The work at Kyungpook National University was supported by the Bio & Medical Technology Development Program of the National Research Foundation (NRF) funded by the Ministry of Science & ICT (2017M3A9G8083382). A.J.-S. gratefully acknowledges a postdoctoral scholarship from the Max Planck Society. M.A. acknowledges funding from the European Union's Horizon 2020 research and innovation programme under the Marie Skłodowska-Curie grant agreement No 841386.

References

1. Chen, X.; Zhang, F.; Ge, Y.; Shi, L.; Huang, S.; Tang, J.; Lv, Z.; Zhang, L.; Zou, B.; Zhong, H., *Advanced Functional Materials* 28, 1706567 (2018)
2. Chen, Y. M.; Zhou, Y.; Zhao, Q.; Zhang, J. Y.; Ma, J. P.; Xuan, T. T.; Guo, S. Q.; Yong, Z. J.; Wang, J.; Kuroiwa, Y.; Moriyoshi, C.; Sun, H. T., *ACS Appl. Mater. Interfaces* 10, 15905-15912 (2018)
3. Zhai, W.; Lin, J.; Li, Q.; Zheng, K.; Huang, Y.; Yao, Y.; He, X.; Li, L.; Yu, C.; Liu, C.; Fang, Y.; Liu, Z.; Tang, C., *Chemistry of Materials* 30, 3714-3721 (2018)
4. De Bastiani, M.; Dursun, I.; Zhang, Y.; Alshankiti, B. A.; Miao, X.-H.; Yin, J.; Yengel, E.; Alarousu, E.; Turedi, B.; Almutlaq, J. M.; Saidaminov, M. I.; Mitra, S.; Gereige, I.; AlSaggaf, A.; Zhu, Y.; Han, Y.; Roqan, I. S.; Bredas, J.-L.; Mohammed, O. F.; Bakr, O. M., *Chemistry of Materials* 29, 7108-7113 (2017)
5. Yin, J.; Yang, H.; Song, K.; El-Zohry, A. M.; Han, Y.; Bakr, O. M.; Bredas, J. L.; Mohammed, O. F., *J. Phys. Chem. Lett.* 9, 5490-5495 (2018)

Facile Synthesis of $CsPbBr_3$ Nanorods Using Stripping Method for High Performance Light-Emitting Diodes

Myeonggeun Han [1] and Yong-Young Noh [1]
[1] **Department of Chemical Engineering, Pohang University of Science and Technology (POSTECH), Pohang, Korea**
Tel.:82-54-279-2265, E-mail: yynoh@postech.ac.kr

All-inorganic lead halide perovskite nanocrystals (NCs) are promising by light-emitting diodes (LEDs) due to their high light absorption coefficient, high photoluminescence and wide color gamut properties. Despite the great performance of photoluminescence quantum yields and external quantum efficiency achieved, there research is still lacking in performance and stability. To improve the efficiency of metal halide perovskite NCs-based LEDs, excellent charge transport and outcoupling efficiency should be taken through matching refractive index between each layer and removing an insulating ligand.

In this paper, we report cesium lead halide ($CsPbBr_3$) nanorods (NRs) as emission layer for high performance LEDs. The performance of $CsPbBr_3$ NRs-based LEDs with ligand post-treatment can be enhanced due to passivation effect. Interestingly, the $CsPbBr_3$ NRs-based LEDs show different performance depending on the various aspect ratio that can be controlled by reaction time. Detail results will be discussed in our presentation.

Acknowledgment

This research was supported by the Basic Research Program through the National Research Foundation of Korea(NRF) funded by the MSIT(2020R1A4A1019455)

References

1. J. Shamsi, *Chem. Rev.,* 119, 3296−3348 (2019).
2. D. Chen and X. Chen, *J. Mater. Chem. C.*, 7, 1413 (2019).
3. L. Wu and H. Hu, *Nano Lett.*, 17, 5799−5804 (2017).
4. D. Yang and P. Li, *Chem. Mater.*, 31, 5, 1575–1583 (2019).

Electrical modulation of exciton complexes in light emitting tunnel transistors of van der Waals heterostructure

Huije Ryu[1], Junyoung Kwon[2], Seunghoon Yang[3], Young Duck Kim[4], Chul-Ho Lee[3], Gwan-Hyoung Lee[1]*
[1] Department of Materials Science and Engineering, Seoul National University, Seoul 08826, Korea
[2] Department of Materials Science and Engineering, Yonsei University, Seoul 03722, Korea
[3] KU-KIST Graduate School of Converging Science and Technology, Korea University, Seoul 136-701, Korea
[4] Department of Physics, Kyung Hee University, Seoul 02447, Korea
Tel.:82-2-880-7191, E-mail: gwanlee@snu.ac.kr

Here we demonstrate electrical modulation of exciton complexes in light emitting tunnel transistors (LETTs) of van der Waals heterostructure with tunnel junction of monolayer WSe_2 sandwiched by tunnel barriers of hexagonal boron nitride (hBN) and graphene electrodes. Electrons and holes are electrically driven into the monolayer WSe_2 by tunneling through hBN, leading to strong electroluminescence (EL) *via* recombination. To control a ratio of electrons and holes and electrically control the exciton complexes, we constructed an additional electrode (control electrode) in direct contact with WSe_2. We modulated Fermi energy of WSe_2 by gate bias, allowing for strong EL of exciton complexes at room temperature. We also switched gate dependent EL spectra by reversing the control electrode bias. Our work shows a novel way to electrically stabilize exciton complexes in light emitting devices of van der Waals heterostructure, beneficial for electrically driven excitonic devices.

Large-scale synthesis of two-dimensional rhenium disulfide for high-performance photodetectors

Bo Hyeon Kim[1,2], Da Som Song[1], Sunyoung Shin[1], Wooseok Song[1], Sang Don Bu[,2], and Jongsun Lim[*,1]*

[1]Thin Film Materials Research Center, Korea Research Institute of Chemical Technology (KRICT), 141 Gajeong-ro, Yuseong-gu, Daejeon 34114, Republic of Korea

[2]Department of Physics and Research Institute of Physics and Chemistry, Jeonbuk National University, Jeonju, 54896, Republic of Korea

E-mail: sbu@jbnu.ac.kr and jslim@krict.re.kr

Despite may encouraging properties of two-dimensional (2D) layered semiconductors, a central challenge in the realms of optoelectronic applications based on 2D materials is to connect (i) the reliable synthesis of large-scale 2D materials with a spatial homogeneity and (ii) the development of emerging 2D materials for high-performance photodetectors. Previous attempts accomplished a facile synthesis of large-scale and homogeneous molybdenum disulfide, through a solution-based synthetic strategy using single source precursors [1-3]. However, this approach is technically hindered for high-performance optoelectronic applications due to their inability to synthesize monolayer with direct bandgap. Rhenium disulfide (ReS_2) is one of 2D layered semiconductors and possesses distorted octahedral phase. Notably, weak interlayer coupling of ReS_2 enables to preserve a direct bandgap of 1.5 eV from bulk to monolayer, corroborating exciting opportunities for achieving high-performance photodetectors.

In this presentation, we primarily aim to resolve the two crucial issues through the solution-based large-area compatible synthetic strategy using a simple coating and subsequent thermal decomposition of tetraethylammonium-tetrasulfidorhenate ($(TEA)ReS_4$) single source precursor. The resulting ReS_2 multilayers synthesized on SiO_2/Si possessed excellent uniformity and optimum stoichiometry. Structural and chemical characterizations of ReS_2 layers were implemented by X-ray photoelectron spectroscopy combined with Raman spectroscopy. Their photoelectrical properties were also studied. Our synthetic approaches will become the predominant choice of modern nanophotonic applications in the simultaneous pursuit of high photoresponsivity and the realization of photodetector arrays with identical response from all devices.

References

[1] Yi Rang Lim, Wooseok Song, Jin Kyu Han, Young Bum Lee, Sung Jun Kim, Sung Myung, Sun Sook Lee, Ki-Seok An, Chel-Jong Choi, and Jongsun Lim, *Adv. Mater.*, **28**, 5025-5030 (2016)

[2] Yi Rang Lim, Jin Kyu Han, Seong Ku Kim, Young Bum Lee, Yeoheung Yoon, Seong Jun Kim, Bok Ki Min, Yooseok Kim, Cheolho Jeon, Sejeong Won, Jae-Hyun Kim, Wooseok Song, Sung Myung, Sun Sook Lee, Ki-Seok An, and Jongsun Lim, *Adv. Mater.*, **30**, 1705270 (2018)

[3] Yi Rang Lim, Jin Kyu Han, Yeoheung Yoon, Jae-Bok Lee, Cheolho Jeon, Min Choi, Hyunju Chang, Noejung Park, Jung Hwa Kim, Zonghoon Lee, Wooseok Song, Sung Myung, Sun Sook Lee, Ki-Seok An, Jong-Hyun Ahn, and Jongsun Lim, *Adv. Mater.*, **31**, 1901405 (2019)

The Effect of Thermal Annealing to Radiatively Recombination of Interlayer Exciton in $MoSe_2/WSe_2$ heterobilayer

Ji-Hwan Baek [1], Huije Ryu[1], Soo Yeon Lim[2], Jung Cheol Kim[2], Hyeonsik Cheong[2], and Gwan-Hyoung Lee[1]

[1]Department of material science and engineering, Seoul National University, Seoul, KOREA

Tel.: 82-2-880-8316, E-mail: gwanlee@snu.ac.kr

[2]Department of Physics, Sogang University, Seoul, KOREA

A twist angle of stacked two-dimensional (2D) van der Waals heterostructures with transition metal dichalcogenides (TMDs) can determine physical dynamics and optical properties of excitons. For instance, spatially indirect excitons, interlayer excitons (IXs), in TMD heterobilayer can radiatively recombine when the twist angle of constituent TMDs is close to 0° or 60°, since +K and -K points are well aligned in momentum space. [1] In other words, the probability of non-radiative recombination of IXs increases as the twist angle deviates from 0° or 60°.

Here we investigated the effect of annealing on radiative recombination of IXs in $WSe_2/MoSe_2$ heterobilayer, encapsulated by hexagonal boron nitride (h-BN), with various twist angle. The IX photoluminescence (PL) peak was observed near 1.33 eV in small twist angle regions (<1.6 °) while not observed in large twist angle region (12.3 °) as expected. However, after annealing at 800 °C, the IX peak was emerged in large twist angle region as well. Thus, our experimental results indicate the possibility of controlling the radiative recombination of IXs regardless of the twist angle of TMD heterobilayer.

1. Pasqual Rivera *et al.* Nat. Nanotechnol. 13, pp.1004-1015 (2018)

Self-Controlled Electroactive Tunable Liquid Lens for Stabilized Focal Length Change

Jong hyeon Ka[1], Im bo Gong[1], and Wook sung Kim[1]
[1]Dept. of Electrical Engineering, POSTECH, Pohang, Gyeongbuk 37673, Korea
Tel.:82-54-279-2363, E-mail: wsungkim@postech.ac.kr

Focus tunable lenses have played a crucial role in an optical system such as photography, microscopy, and extended reality [1]. There are two ways to change the lens's focal length, changing the refractive index or the lens's curvature. A varifocal lens using a dielectric elastomer actuators (DEA), which is one of the latter methods, has the advantage of having a simple structure and operation mechanism. The principle of changing the focal length of the lens is as follows. When voltage is applied to the electrode, the DEA on one side expands in the radial direction, and the DEA on the other side relatively contracts. At this time, the liquid between the membranes moves fluidly and induces deformation in the curvature of the lens, which then causes a focal length change according to the lens manufacturer's equation. The overall lens structure refers to the concept of Samuel Shian's paper [2], and we attempt to apply the configuration to this paper. The proposed tunable lens consists of DEA membranes, transparent electrodes, an acryl frame, and clear liquid. The lens structure is as given in Fig. 1, and Fig. 2 shows the operating principle of the varifocal lens.

However, there is a problem that the shape of DEA changes continuously when a constant voltage is applied because the conventional DEA has non-linear response characteristics [3]. This means that the lens system is unstable and may lead to a device error. We tried to solve the issue by operating them with a circuit-based control system. Since the DEA has the form of parallel capacitance, it is possible to estimate the DEA's shape from the capacitance as an electrical parameter in real-time. Therefore, we can control the shape of the DEA by adjusting the voltage with the information of the capacitance variance. We experimentally confirmed the change of the focal length when voltage is applied. Additionally, we showed the stable control of the DEA's shape change through the control circuit system.

The proposed liquid lens can adjust the focal length through a simple structure and be applied to various optical systems. Moreover, it can ensure the stability of the system by preventing device deformation.

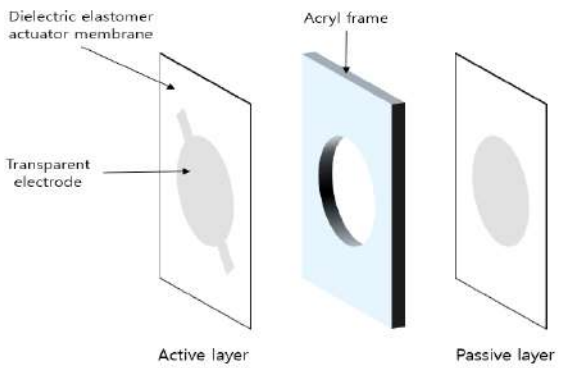

Fig. 1. Structure of the tunable liquid lens

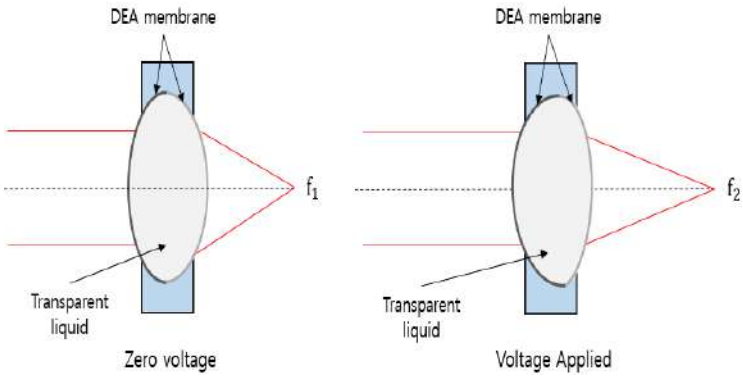

Fig. 2. Principle of the focal length change

Acknowledgment
Authors were supported by the National Research Foundation of Korea.

References

1. Shane Colburn, et al., *Optics express.*, 5(7), 825 (2018).
2. Samuel Shian, et al., *Optics express.*, 21(7), 8669-8676 (2013).
3. Guo-Ying Gu, et al., *IEEE Transactions on Robotics.*, 33(5), 1269 (2017).

High Efficiency, High NA, Large-Area Metalens in Near-Infrared for LiDAR

Seong-Won Moon[1], Younghwan Yang[1], and Junsuk Rho[1]
[1]Dept. of Mechanical Engineering, Pohang University of Science and Technology,
Pohang 37673, Korea
Tel.:82-54-563-7992, E-mail: jsrho@postech.ac.kr
[2]Dept. of Chemical Engineering, Pohang University of Science and Technology,
Pohang 37673, Korea

Light detection and ranging (LiDAR) is the object detection method by illuminating laser pulse and measuring time of flight of reflected light [1]. LiDAR can detect objects with ultrafast and high resolution, it is widely used in various applications such as satellite, aircraft, and autonomous vehicles. Further, compact LiDAR system with high performance should be developed to use artificially intelligent (AI) robots and drones. Therefore, ultrathin lens with high numerical aperture (NA) is required to receive reflected pulse signal in wide ranging.

In this study, we proposed high efficiency, high NA metalens to detect near-infrared for LiDAR. Metalens is ultrathin flat optical components that focusing light by well designed subwavelength unit-structures array [2]. We designed a metalens with diameter D = 500 μm, focal length f = 400 μm at the wavelength λ = 940 nm. We used nanopost to modulate the polarization-independent local phase. To find candidates that can control phase from zero to 2π with high transmission, complex transmission coefficients of nanoposts with varying radius are calculated by using Fourier modal method. The focusing characteristics of the proposed metalens are calculated by using Rayleigh-Sommerfeld diffraction theory [3].

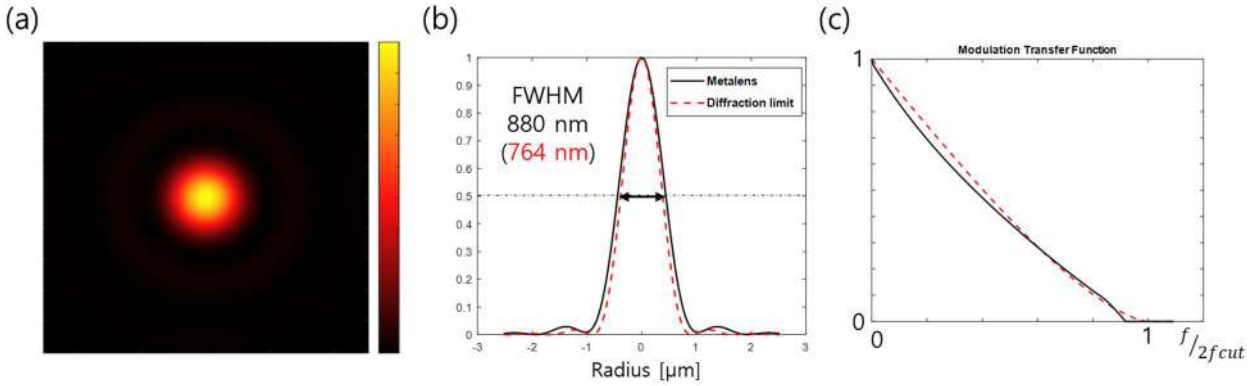

Fig. 1. Focusing properties of large-scale metalens: (a) 2D and (b) 1D intensity profile at the focal plane, and (c) MTF graph

Figure 1 shows focusing characteristics of metalens at the focal plane. The proposed metalens can focus close to diffraction limit with full width half maximum (FWHM) of 880 nm, as shown in Fig. 1(b) and 1(c). Further, we will increase the diameter and field of view of metalens to 1 cm and 90° respectively while maintaining high NA and high efficiency. We believe that the proposed metalens will contribute to overall optical sensing including night-vision camera and LiDAR for autonomous vehicles, AI robots and drones.

Acknowledgment

References

1. L. D. Smullin and G. Fiocco, *Nature* 194, 1267 (1962).
2. N. Yu and F. Capasso, *Nat. Mater.* 13, 139–150 (2014).
3. J. W. Goodman, Introduction to Fourier Optics, Roberts & Company (2005).

Electrical and Optical Characterization of Visible Parylene C Films

Ye-Seul Lee[1], Ji-Hyeon Yoon[1], Akpeko Gasonoo[2], Yoonseuk Choi[3], Jonghee Lee[1], and Jae-Hyun Lee[1,]*
[1]Department of Creative Convergence Engineering, Hanbat National University, Daejeon, 34158, South Korea
Tel.: +82-2-821-1970, E-mail: jhyunlee@hanbat.ac.kr
[2]Research Institute of Printed Electronics & 3D Printing, Industry University Cooperation Foundation, Hanbat National University, Daejeon, 34158, South Korea
[3]Department of Electronic Engineering, Hanbat National University, Daejeon, 34158, South Korea

Parylene C film is made from a chemical vapor deposition process where monomeric gases are polymerized on the target surface at room temperature and is used as a transparent insulating coating film [1]. Parylene C forms high-quality and conformal thin films with uniform thickness even in fine cracks, structures, and bumps [2]. However, due to its high transparency, the insulation film is not visually identified, making it difficult to inspect the coating process and check for any defect.

In this study, the characteristics of visible parylene C thin films produced by tuning the ratio of dimer gases to monomer gases via adjustments of the pyrolyzing temperature, are analyzed by electrical and optical methods. The deposition flow, process temperatures and molecular structures of parylene C dimer (di-para-xylylene), monomer (para-xylylene) and polymer C (poly-chloro-para-xylylene) are shown in Fig. 1. The optical transmittance and haze of the parylene films were analyzed by ultraviolet–visible–near infrared spectrophotometry (UV–Vis–NIR), and Fourier transform infrared (FT-IR) spectrophotometry, respectively. Structural and thermal characteristics of the parylene films were analyzed by X-ray diffractometry (XRD) and differential scanning calorimetry (DSC), respectively. The haze within the ranges of 10-90% is achieved for parylene C films deposited in the temperature range of 400-700 °C. The resistivity of parylene C films measured by the transmission line measurement (TLM) method is 10^{10} Ωcm. The visible parylene C films can be applicable as insulation coatings for various electronic devices.

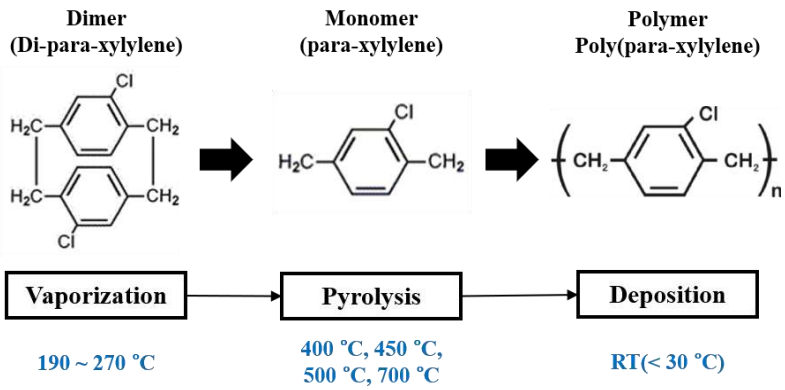

Fig. 1. Schematic mechanism for chemical vapor deposition process of visible parylene C.

Acknowledgment

This research was supported by Basic Science Research Program through the National Research Foundation of Korea (NRF) funded by the Ministry of Education (2020R1I1A3073634 and 2018R1A6A1A03026005) and by the Collabo R&D between Industry, Academy, and Research Institute funded Korea Ministry of SMEs and Startups in 2020 (S2902545).

References

1. W. F. Gotham, *J. Polym. Sci. Pol. Chem.*, 4, 3027 (1996).
2. J.-H. Lee and A. Kim, *Organic Electronics*, 47, 147 (2017).

Application of Multi-layer Visible Parylene Films in Advance Optical Systems

Seung-Yo Baek[1], Ye-Seul Lee[1], Akpeko Gasonoo[2], Jonghee Lee[1], and Jae-Hyun Lee[1,*]
[1]Department of Creative Convergence Engineering, Hanbat National University, Daejeon, 34158, South Korea
Tel.: +82-42-821-1970, E-mail: jhyunlee@hanbat.ac.kr
[2]Research Institute of Printed Electronics & 3D Printing, Industry University Cooperation Foundation, Hanbat National University, Daejeon, 34158, South Korea

Poly-para-xylylene (parylene) and substituted parylene have been used in the conformal coating industry to protect electrical devices and mechanical parts from outer stresses, such as chemical reactions or physical stress [1]. Parylene films are deposited uniformly and transparently without restrictions on the shape of the object to be coated [2]. However, to be able to visually identify the coated area, visible parylene films are required. It has been investigated that pyrolyzing sublimed polychloro-para-xylylene (parylene C) dimers below 600 °C yields visible parylene films with high light scattering properties due to the formation of uniformly distributed dimer crystals [3,4]. However, weak surface adhesion and tensile strength have become a concern in achieving stable visible parylene films.

In this study, we propose visible multi-layer parylene C films. The schematic structure of a single layer, bi-layer and multi-layer parylene C films are shown in Fig. 1, respectively. The multi-layer films are deposited by a chemical vapor deposition process in a single chamber at room temperature. Adjustment of the pyrolyzing temperature and structural optimization of the layers are key factors considered to achieve visible films with the desired optical properties. Tuning the pyrolysis temperature controls the distribution and ratio of dimer crystals in the parylene film; a technique that forms the basic mechanism of the deposition of the visible parylene films. The haze, transmittance and reflectance of the films were analyzed by ultraviolet visible near-infrared spectrophotometry. It is investigated that a haze of 80% or more could be achieved for the multi-layer visible parylene C films while maintaining good surface adhesion and tensile strength. It is further confirmed that the haze is significantly affected by surface roughness of the films. The single-chamber fabrication process of this conformal multi-layer visible parylene C films at room temperature paves the way to achieve stable commercial insulation coatings and substrates for high-performance electronic devices.

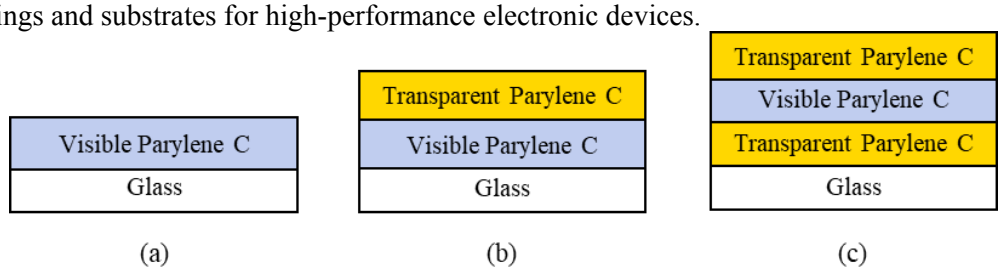

Fig. 1. Schematic structure of (a) single layer (b) bi-layer and (c) multi-layer visible parylene C films.

Acknowledgment

This research was supported by Basic Science Research Program through the National Research Foundation of Korea (NRF) funded by the Ministry of Education (2020R1I1A3073634 and 2018R1A6A1A03026005) and by the Collabo R&D between Industry, Academy, and Research Institute funded Korea Ministry of SMEs and Startups in 2020 (S2902545).

References

1. A. Hogg, T. Aellen, S. Uhl, B. Graf, H. Keppner, Y. Tardy and J. Burger, J. Micromech. Microeng. 23, 075001 (2013).
2. W. F. Gotham, J. Polym. Sci. Pol. Chem., 4, 3027 (1996).
3. J.-H. Lee and A. Kim, Organic Electronics, 47, 147 (2017).
4. A. Gasonoo, Y.-S. Lee, J.-H. Yoon, B.-S. Sung, Y. Choi, J. Lee and J.-H. Lee, Optics Express, 28, 26725 (2020).

Wavelength dependent light induced degradation of inverted perovskite solar cells

BeomHee Yoon[1], Jeonghun Kwak[2], and Hyunho Lee[1]
[1] Department of Electronic Engineering, Kwangwoon University, Seoul 01897, Korea
Tel.:82-2-940-8126, E-mail: hyunho@kw.ac.kr
[2] Department of Electrical and Computer Engineering, ISRC, Seoul National University, Seoul, 08826, Korea

The stability of methylammonium (MA)-based perovskite solar cells remains one of the most urgent issues to be discussed. Inherent weak binding forces between MAs and halides lead the perovskite structure to be unstable under the exposure of environmental factors such as air and light. In particular, the degradation of perovskite films under light exposure causes and accelerates deterioration of the device mainly due to ion-migration of iodine ions. In this work, we investigated the effect of wavelength dependent light induced degradation of an inverted perovskite solar cells. Solar cells were tested under the different wavelength of lights using the band-pass lens. The blue (450 nm to 496nm), green (495 nm to 570 nm) and red (620 nm to 780 nm) filters are used to verify the correlation between the energy of light and the device stability under light exposure. The analysis on the device performance and degraded perovskite films is performed to investigate which wavelength of light mostly causes degradation of inverted perovskite solar cells. Finally, degradation mechanism regarding different wavelength of light will be given.

Acknowledgement
This work was supported by the Basic Science Research Program (NRF-2020R1F1A1074263) through the National Research Foundation of the Ministry of Education, Republic of Korea. This research (for Hyunho Lee) was partially supported by Basic Science Research Program through the National Research Foundation of Korea (NRF) funded by the Ministry of Education (No. 2018R1A6A1A03025242). This research was funded and conducted under 「the Competency Development Program for Industry Specialists」 of the Korean Ministry of Trade, Industry and Energy (MOTIE), operated by Korea Institute for Advancement of Technology (KIAT). (No. P0002397, HRD program for Industrial Convergence of Wearable Smart Devices)

Polarization-selective Metasurface Structural Color Display via Deep Neural Network

Hyunwoo Son, Jangwoon Sung, and Byoungho Lee
Inter-University Semiconductor Research Center and School of Electrical and Computer Engineering, Seoul National University, Gwanak-Gu Gwanakro 1, Seoul 08826, Korea
Tel.:82-2-880-7245, E-mail: byoungho@snu.ac.kr

Deep learning technology has led to many advances in various fields of engineering. Among them, in optics, inverse design method through deep learning has received much attention due to their magnificent efficiency in terms of design speed and accuracy [1]. Unlike conventional methods of finding desired spectral response through repeated parametric sweeps, the deep learning inverse design methodology with delicately trained network can intelligently detect the geometric parameters of optical elements for the target spectral response in an instant.

Metasurface means an array of scattering elements with sub-wavelength dimensions, which enables anomalous optical phenomena. As an example, metasurface designed with anisotropic nanostructure shows distinct optical properties according to the polarization of incident light [2]. Furthermore, metasurface structural color display with high resolution transcending that of colors by pigments and dye is one of the fields that attract much attention [3]. Because the color shown by the structure of the materials is caused by scattering phenomenon from materials, rather than by absorbing light at particular wavelengths, much broader gamut than dye-color can be obtained as well as higher resolution due to the sub-wavelength scale of metasurface's unit-cell.

In this paper, using abovementioned properties of metasurface, we designed polarization-selective structural color display. To obtain desired structural color for each polarization, we used deep learning inverse design techniques. Fig. 1(a) represents a schematic diagram of designed neural network. The right-side inset shows the unit-cell of metasurface which consists of four rods. The input of network is set to CIE La*b* coordinate value of the target structural color for the two incident lights which are linearly polarized and orthogonal to each other, and this network predicts corresponding geometric parameters (L_1, W_1, L_2, W_2) of nanostructure for target colors. From Fig. 1(b), we could observe accurate color prediction performance of designed network. Finally, by utilizing polarization selectivity of designed display, we made a switchable display for three colors of red, green, and blue, which produces vivid colors for *x*-polarized light, and dark when *y*-polarized. Fig. 1(c) represents the structural colors calculated from electromagnetic simulation results for the geometric parameters network predicted. Corresponding values are (L_1, W_1, L_2, W_2)=(83 nm, 87 nm, 248 nm, 140 nm) for red, (236 nm, 78 nm, 184 nm, 130 nm) for green, and (173 nm, 55 nm, 71 nm, 151 nm) for blue.

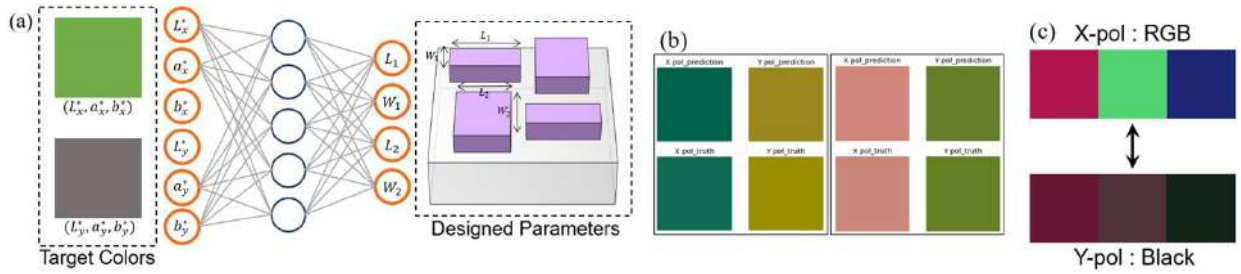

Fig. 1. (a) Schematic diagram of deep neural network for inverse design of polarization-selective metasurface structural color display, (b) Structural color for each polarization. Upper-side shows color predicted by network, and bottom is the target color. (c) polarization-switchable display for RGB

Acknowledgment

This work was supported by the National Research Foundation of Korea (NRF) grant funded by the Korea government (MSIT) (No. 2020R1A2B5B02002730).

References

1. So, S., Badloe, T., Noh, J., Rho, J., and Bravo-Abad, J., *Nanophotonics*, 9(5), 1041-1057 (2020).
2. Arbabi, A., Horie, Y., Bagheri, M., and Faraon, A., *Nature Nanotechnology*, 10(11), 937-943 (2015).
3. Yang, W., Xiao, S., Song, Q., and Tsai, D. P., *Nature Communications*, 11(1), 1864 (2020).

Inverse Design for Multi-Wavelength Meta-Holograms

Junhyeok Jang, Hyunwoo Son, Chulsoo Choi and Byoungho Lee
School of Electrical and Computer Engineering, Seoul National University, Gwanak-Gu, Seoul, 08826, Korea
Tel.:82-2-880-7245, E-mail: byoungho@snu.ac.kr

Metasurfaces are planar diffractive optical devices consisting of meta-atoms which can locally control electromagnetic properties of light [1]. Meta-holograms, which mean metasurface devices applied to holography, have attracted attentions thanks to the outstanding performances unachievable in conventional holograms [2]. However, multiplexing methods for multi-wavelength meta-holograms have suffered from color-crosstalk effects and low diffraction efficiencies [3]. We propose an algorithm to optimize phase profiles for multi-wavelength meta-holograms with improved image quality and efficiencies.

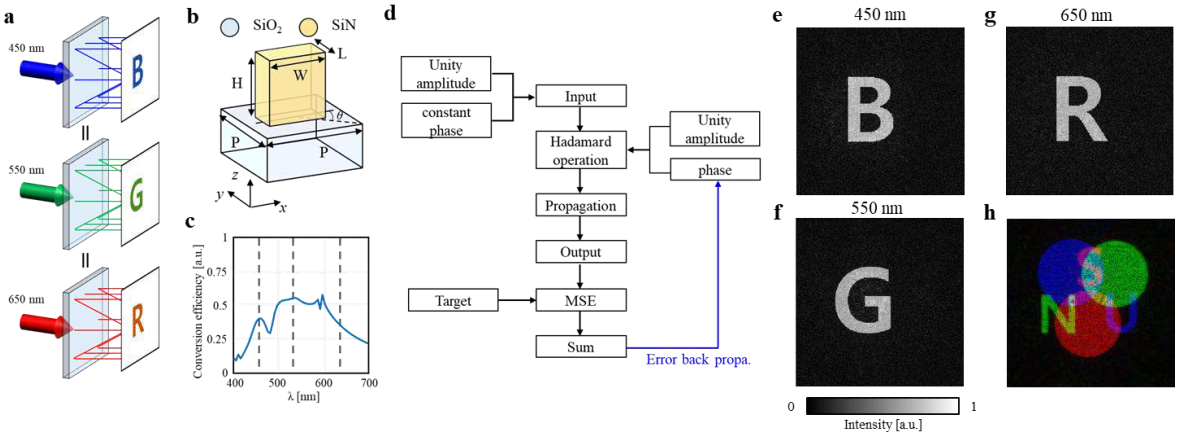

Fig. 1 Simulation results for multi-wavelength meta-holograms. (a) A schematic illustration of multi-wavelength meta-holograms with identical spatial phase profiles which generate different images according to the wavelengths. (b) A schematic illustration of the designed meta-atom. P = 400 nm, H = 500 nm, W = 350 nm, L = 110 nm. (c) Polarization conversion efficiency of the meta-atom. (d) A flow chart of the optimization algorithm for multi-wavelength meta-holograms. (e) Calculated binary images for wavelengths 450 nm, 550 nm and 650 nm. (f,g) Calculated full-color images by using (f) one layer and (g) two layers of metasurfaces.

The phase profile of meta-holograms is optimized to impose the independent optical scattering for RGB target wavelength (Fig. 1a). As a meta-atom, the SiN nanorod is exploited and the phase is modulated through the Pancharatnam-Berry phase (Fig. 1b). The dimension of SiN nanorod is determined to exhibit high polarization conversion efficiencies for RGB target wavelengths (Fig 1c). We optimize spatial phase profiles of meta-holograms based on the scalar diffraction model for Fresnel holograms by using Wirtinger derivatives [4]. Fig. 1d shows the flow chart of the optimization algorithm. Based on our proposed optimization process, the two types of meta-hologram are numerically designed; one is multi-wavelength binary hologram and the other is full-color hologram. As shown in Fig. 1e-g, three different binary images are reconstructed without crosstalk effects. And the full-color holographic image is reconstructed with high fidelity (Fig. 1h).

In conclusion, we presented an optimization algorithm for multi-wavelength meta-holograms without crosstalk effects and with high diffraction efficiency. In addition, with multilayer design which provides higher degree of freedom, the image quality can be more improved. The algorithm is applicable to not only meta-holograms but also holographic display for full-color implementation, which can overcome the limitation in frame rates.

Acknowledgment
This work was supported by Samsung Science and Technology Foundation under Project Number SRFC-IT2001-05.

References

1. N. Yu and F. Capasso, *Nat. Mater*. 13, 139 (2014).
2. J. Sung, G.-Y. Lee and B. Lee, *Nanophotonics* 8, 1701 (2019).
3. B. Wang *et al*., *Nano Lett.* 16, 5235 (2016).
4. P. Chakravarthula *et al*., *ACM Trans. Graph.* 38, 213 (2019).

3D printed highly conductive stretchable electrodes for deformable display applications

Hyunjoo Cho[1], Youngpyo Ko[1], Heesuk Kim[1], Jaewook Jeong[2], Byeongmoon Lee[1], and Seungjun Chung[1]
[1]Soft Hybird Materials Research Center, Korea Institute of Science and Technology, Seoul 02792, Republic Korea
[2]School of Information and Communication Engineering, Chungbuk National University, Cheongju, Chungbuk 28644, Korea
Tel.:82-2-958-5305, E-mail: seungjun@kist.re. kr

Soft electrical components capable of conforming to complex three-dimensional (3D) geometries have gained attention as an essential building block for the Internet of Things (IoT) devices[1]. Unlike traditional rigid electronics, soft electronics need to be tailored to form a seamless interface with target geometries that have the different types of form factors. In this manner, for integrating tremendous devices onto stretchable platforms, a promising approach is direct writing of stretchable interconnects in that it can effectively customize the system layouts. Printable elastic conductors based on composites of conductive fillers and elastomers have been widely reported due to their outstanding stretchability and printability that promises the realization of further reliable display applications under mechanical deformation. Among these promising candidates, silver (Ag) particles/polydimethylsiloxane (PDMS) composites used as a conductive filler and elastomeric matrix, respectively, have been investigated owing to their attractive advantages, such as low viscoelasticity, controllable modulus, and low-cost processability[2]. However, their low electrical conductivity and stability have to be addressed to be employed in high-performance deformable display applications.

In this presentation, we report 3D printable and highly conductive stretchable electrodes using an auxiliary filler and a co-solvent system. Multi-walled carbon nanotubes were used as auxiliary fillers that facilitate the dispersion of Ag particles in the PDMS matrix maintaining the conductive percolation paths under tensile strain. Furthermore, the co-solvent system consists of two functional solvents facilitates that the 3D printable ink can maintain the engineered viscosity without the nozzle clogging issues during the whole printing process. As a result, the sophisticated fine patterns can be stably printed with a minimum width of ~160 μm, highlighting a high degree of design freedom. The 3D printed conductors show a high electrical conductivity over 3000 S cm^{-1} and stretchability of > 150%. Our approach opens a new route to large-area and high-resolution soft electronics such as stretchable displays.

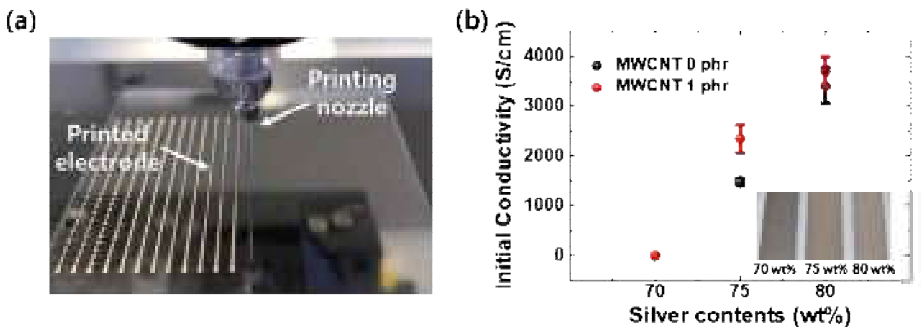

Fig. 1. a) 3D-printing of Ag/PDMS composites b) Conductivity of stretchable conductors depending on silver and MWCNT contents.

Acknowledgment

This research was supported by National R&D Program through the National Research Foundation of Korea(NRF) funded by Ministry of Science and ICT(2020M3D1A2101799).

References

1. B. Lee, H. Cho, K. T. Park, J.-S. Kim, M. Park, H. Kim, Y. Hong, S. Chung , Nat. Commun 11, 5948 (2020)
2. Y.Hwang, J.Ldd, Y.Kim, S.Jeong, S.Lee, J.Jung, J.Kim, Y.Choi, S.Jung, ACS Appl. Mater. Interfaces, 11, 48459 (2019).

Active metafilm for enhanced amplitude modulation of visible light

Kyuho Kim[1], Sun-Je Kim[2], and Byoungho Lee[1]
[1]Inter-University Semiconductor Research Center and School of Electrical and Computer Engineering, Seoul National University, Gwanak-Gu Gwanakro 1, Seoul 08826, Korea
[2]Department of Physics, Myongji University, Myongjiro 116, Namdong, Cheoin-gu, Yongin, Gyeonggi-Do 17058, Korea
Tel.:82-2-880-9564, E-mail: byoungho@snu.ac.kr

In this study, we analyze the complex resonance modes that occur in the nanograting made of aluminum and a phase transition material, vanadium dioxide (VO_2). The goal of this study is to analyze the active resonances in reflected light in a simple grating structure made of aluminum and VO_2 when TM or TE polarized light is incident normally. Active resonance analysis in the visible region has the potential to be used in many applications, such as image sensors and display components.

The optical resonance characteristics and the electromagnetic energy density near the nanograings in the visible and near-infrared region are analyzed using a commercial software based on the finite element method. As shown in Fig. 1(a), the device is composed of an Al reflector and a VO_2-Al grating with VO_2 thickness t_{VO2} = 40 nm, and the grating has an aluminum beam of width w_{Al} at each period p. The fill factor of aluminum is defined as $f_{Al} = w_{Al}/p$. At p = 200 nm, and the modulation depth η_m according to f_{Al} can be seen in Fig. 1 for TM and TE polarized incidence. Here, η_m is defined as $\eta_m = |I_i - I_m|/\max(I_i, I_m)$ and I_i and I_m correspond to reflection intensities at the insulationg and metallic phases, respectively. When the incident light is TM polarized, it can be observed that the modulation depth of the metafilm increases compared to bare VO_2 at a wavelength of 450 to 550 nm. Also, as f_{Al} increases, the peaks of η_m are redshift in the visible region. On the other hand, when the incident light is TE polarized, modulation depth of metafilm in the same wavelength region decreases compared to bare VO_2. Also, as f_{Al} increases, the peaks of η_m are blueshift in the visible region.

In conclusion, we propose metal-dielectric nanograting resonances that can modulate the amplitude of reflectance according to the phase transition of VO_2. Also, this device is expected to be an important platform for electrically tunable optical devices working at visible wavelengths.

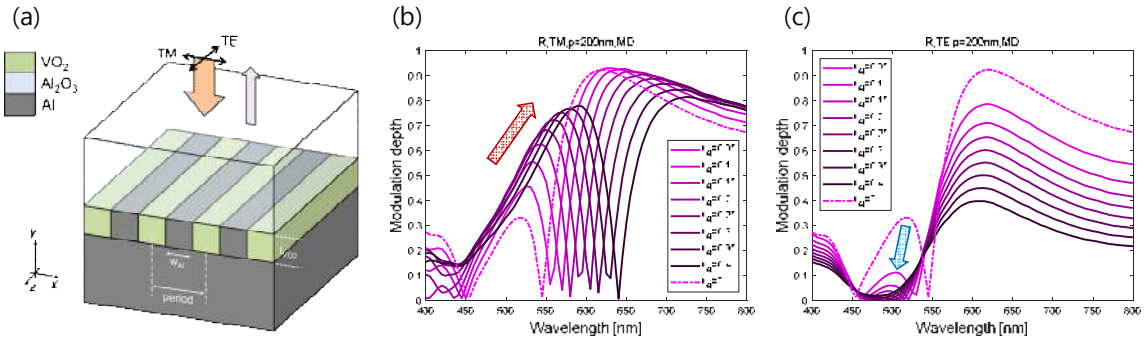

Fig. 1. (a) Schematic diagram of Al-VO_2 nanograting structure. Modulation depth spectra of reflection intensity from the Al-VO2 nanograting obtained from (b) TM polarized and (c) TE polarized incident light.

Acknowledgment

This work was supported by the National Research Foundation of Korea(NRF) grant funded by the Korea government(MSIT).(No. 2020R1A2B5B02002730)

References

1. J. E. Harvey and R. N. Pfisterer, *Opt. Engin*. 58(8), 087105 (2019).
2. A. Cordaro et al., *ACS Photon*. 6(2), 453-459 (2019).
3. S.-J. Kim et al., *Opt. Express* 26(26), 34641-34654 (2018).
4. S.-J. Kim et al, *Nanophotonics*, 10(1), 713-725 (2021).

Analysis of the oxygen assisted defect control effect at metal-MoS_2 junction

Woonggi Hong, Cheol Min Park, Gi Woong Shim, Sang Yoon Yang, and Sung-Yool Choi
Graphene/2D Materials Research Center, Center for Advanced Materials Discovery towards 3D Display, School of Electrical Engineering, Korea Advanced Institute of Science and Technology (KAIST), Daejeon 34141, Republic of Korea
Tel.:82-042-350-7427, E-mail: sungyool.choi@kaist.ac.kr

Compared to mechanically exfoliated TMDs with a perfect crystalline structure, CVD-grown TMDs has various kinds of intrinsic defects such as chalcogen vacancy or grain boundary. These intrinsic defects are inevitably generated during the synthesis process, resulting in the degradation of electrical performance. In this study, we investigated the defect control of MoS_2 thin film using O_2/N_2 gas mixture to improve the electrical performance of MoS_2 transistors. As a result of the defect control process, the stoichiometry of MoS_2 was changed from 1:1.85 (Mo:S) to 1:1.71:0.35 (Mo:S:O). In other words, oxygen not only made a sulfur vacancy but also covalently bonded with Mo. More specifically, we confirmed that oxygen was dominantly reacted at the grain boundary because it is the most active site in polycrystalline MoS_2 thin film. By passivating the dangling bonds at grain boundaries through oxygen, the mid-gap states in bandgap was effectively reduced. As a result of the reduced mid-gap states, we found that the charge neutrality level (CNL) was re-arranged at metal-MoS_2 junction, which induced the reduction of Schottky barrier height from 210 to 113 meV in the case of Cr contact metal used transistor.

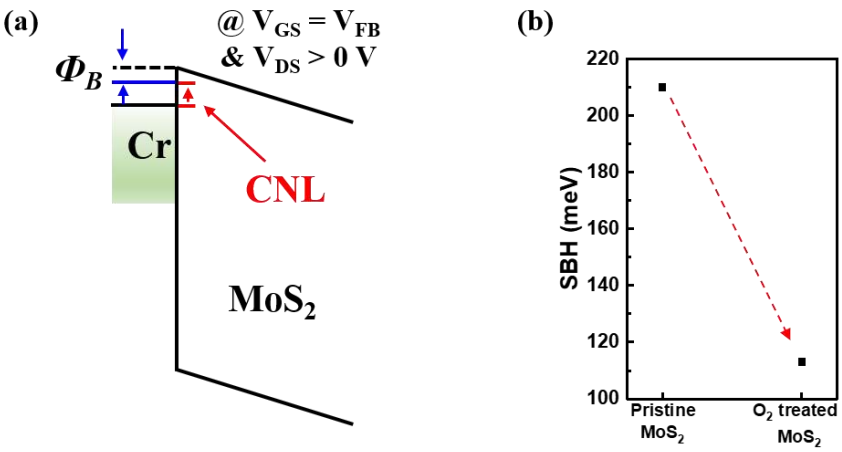

Fig. 1. (a) Schematic illustration of CNL change and (b) Schottky barrier height reduction after oxygen assisted defect control

Acknowledgment

This research was supported by the Creative Materials Discovery Program through the National Research Foundation of Korea (NRF) funded by Ministry of Science and ICT (2016M3D1A1900035).

References

1. K. Kang et al., *Nature*, 520, 656 (2015).
2. Y. Rong et al., ACS Nano, 9, 3695 (2015).
3. L. Li ea al., J. Am. Chem. Soc. 141, 10451 (2019).

Performance Enhancement of Nonvolatile Organic Floating-Gate Phototransistor Memory for Image Sensor Applications

Reitaro Hattori[1], Takashi Nagase[1,2], Naoyuki Nishida[1], Takashi Kobayashi[1,2], and Hiroyoshi Naito[1,2]
[1]Dept. of Physics and Electronics, Osaka Prefecture University, Naka-ku, Sakai 599-8531, Japan
Tel.:81-72-254-9490, E-mail: reitaro.hattori.oe@pe.osakafu-u.ac.jp
[2]Res. Inst. Molecular Electronic Devices, Osaka Prefecture University, Naka-ku, Sakai 599-8531, Japan

There has been considerable interest in the development of organic field-effect transistors (OFETs) with high photosensitivity because they enable to fabricate image sensor arrays in a simple pixel configuration, thereby enabling the low-cost production of large-area sensor arrays through solution processes. An approach to enhance the photosensitivity is to integrate a memory element in the OFET device, which can facilitate large-area imaging by enabling the simultaneous capture of the photogenerated signals on all the image pixels across the array. In a previous study, we developed a nonvolatile OFET memory with good solution processability by using a polymer-based OFET with a top-gate configuration and an organic floating-gate layer formed through vertical phase separation of a polymer insulator and a soluble pentacene derivative (TIPS-pentacene) [1-3]. Here, we report the effect of the addtion of soluble fullerene derivatives to the organic floating-gate layer on the optical memory characterisitics of solution-processed top-gate OFET memories based on poly[2,5-bis(3-tetradecylthiophen-2-yl)thieno[3,2-b] thienophene] (PBTTT) [Fig. 1(a)] for their appicaltions to organic image sensors.

We found that PBTTT FET memories with PMMA:TIPS-pentacene (80 :20) floating-gate layers do not exhibit large threshold voltage shifts when programmed with blue LED light (1 mW/cm^2), which can be improved by the addtion of small amount of [6,6]-diphenyl-C_{62}-bis(butyric acid methyl ester) (Bis-PCBM) to the PMMA:TIPS-pentacene floating-gate layer [Figs. 1(b) and (c)]. Further, the PBTTT FET memories with 140 nm-thick polymer gate insulators (parylene C) allows programming with a low gate voltage of 20 V and achieving a on/off current ratio of 10^4 after programming and erasing processes [Fig. 1(d)].

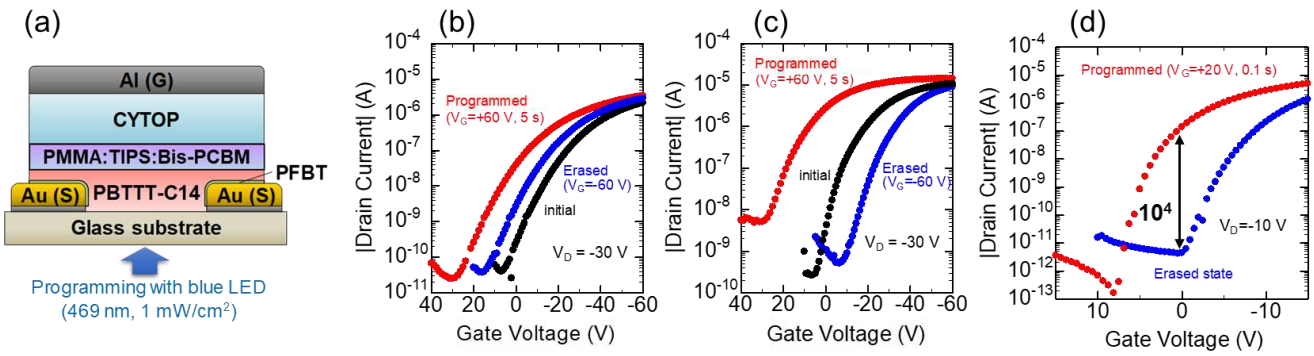

Fig. 1. (a) Structure of solution-processed top-gate floating-gate OFET memory. Transfer curves of the memory devices with (b) PMMA:TIPS-pentacene (80:20) and (c) PMMA:TIPS-pentacene:Bis-PCBM (80:17:3) floating-gate layers after programming under blue LED light illumination and erasing in the dark. (d) Transfer curves of the memory device with 140 nm-thick parylene C gate insulator.

Acknowledgment

This work was supported by Iketani Science and Technology Foundation, the Murata Science Foundation, the Mitsubishi Foundation, and JSPS KAKENHI (Grant Nos. JP19H02599, JP20H02716, JP21H04564, and JP20K21007).

References

1. F. Shiono, H. Abe, T. Nagase, T. Kobayashi, and H. Naito, *Org. Electron.* 67, 109 (2019).
2. M. Higashinakaya, T. Nagase, H. Abe, R. Hattori, S. Tazuhara, T. Kobayashi, and H. Naito, *Appl. Phys. Lett.* 118(10), 103301 (2021).
3. H. Abe, R. Hattori, T. Nagase, M. Higashinakaya, S. Tazuhara, F. Shiono, T. Kobayashi, and H. Naito, *Appl. Phys. Express* 14(4), 041007 (2021).

Control of Domain Structure in Catalyst-assisted Growth of Single-layer MoS_2

Min-Yeong Choi1,, Chang-Won Choi2,, Seong-Jun Yang1, Hojeong Lee2, Jinho Lee1, Shinyoung Choi1, Jun-Ho Park1, Jong Heo2, Si-Young Choi2,* and Cheol-Joo Kim1,*

[1]Department of Chemical Engineering, Pohang University of Science and Technology, Pohang, Gyeongbuk 37673, South Korea

Tel.:82-54-279-2335, E-mail: kimcj@postech.ac.kr

[2]Department of Material Science & Engineering, Pohang University of Science and Technology, Pohang, Gyeongbuk 37673, South Korea

(2 line spacing)

Catalysts play crucial roles for determination of the growth kinetics of two-dimensional transition metal dichalcogenides by chemical vapor deposition. However, the roles of various catalytic intermediates on each growth step are largely unknown yet. Here, we carried out catalyst-assisted growth of single-layer MoS_2 by metal-organic chemical vapor deposition with different atomic/molecular components, supplied by growth substrates. Na components embedded in the surface similarly improve the growth rates, regardless of the surrounding mediums. Surprisingly, the domain sizes can vary by an order of magnitude, depending on the chemical composition of seed. Na-Mo-O eutectic alloys reduced the density of nucleation seed by Ostwald ripening, resulting in large MoS_2 domains by growth via liquid-intermediate state. Growths promoted by different catalysts resulted in films with high crystalline structure as electrical channel of field-effect transistor, and nano-crystalline structure for improved hydrogen evolution reaction.

Graphene Multi-Via Contacts for 3D Integration of 2D Devices

Yongjun Shin[1], Junyoung Kwon[2], and Gwan-Hyoung Lee[1]
[1]Dept. of Materials Science and Engineering, Seoul National University, Seoul, 08826, Korea
Tel.:82-2-880-8316, E-mail: syj04140@gmail.com
[2]Dept. of Materials Science and Engineering, Yonsei University, Seoul, 03722, Korea

Three-dimensional (3D) integration technique of 2D devices in van der Waals heterostructures is critical to miniaturize the whole circuits and maximize the advantages of 2D devices. Even though various 2D devices, such as transistors, memory, and sensors, have been demonstrated recently, high density integration of those 2D devices is still challenging. In this study, we demonstrate a graphene multi-via contacts that can electrically connects graphene electrodes (or leads) embedded in van der Waals heterostructure of graphene, transition metal dichalcogenides (TMDs) and hexagonal boron nitride (hBN). We combined the fluorinated graphene (FG) contact[1], our former technique, and the edge contact[2] to form multiple contact paths with single via electrode. Graphene multi-via contacts enable high degree of integration of 2D devices in vertical direction without any additional space while keeping the system below the device intact thanks to the etch-stop property of bottom graphene electrode layer. As a proof of concept, we also fabricated vertically integrated inverter circuit with our new technique. Our work opens up a novel way to integrate 2D devices, which is essential for the next step of nanoelectronics based on 2D materials.

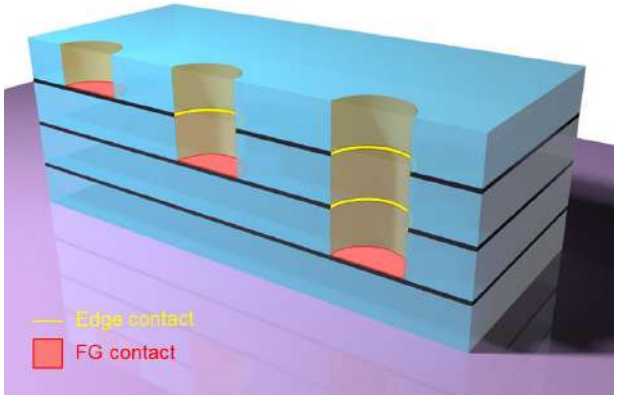

Fig. 1. The schematic illustration of the multi-via contacts.

Acknowledgment

References

1. J. Son, J. Kwon, Nat. Comunn., 9, 3988 (2018).
2. L. Wang, *Science*, vol. 342, issue 6158, p. 614-617 (2013).

Photocatalytic layer on IGZO for nonvolatile visible light photomemory

Jong Bin An, Byung Ha Kang, Kunho Moon, Sujin Jung, I Sak Lee, Jong Hyuk Ahn and Hyun Jae Kim*
School of Electrical and Electronic Engineering, Yonsei University, 50 Yonsei-ro, Seodaemun-gu, Seoul 03722, Korea
Tel.:82-2-2123-5865, E-mail: hjk3@yonsei.ac.kr

With the advent of the 4th industrial revolution, the era of display of things (DoT) has arrived. In the era of DoT, display not only visually transmits but also effectively stores and processes information as a key communication channel between things and humans. Therefore, integration of memory devices into display came to be essential. Among various memory devices, photomemory using light as a signal is receiving significant attention due to its ultra-high sensitivity and multi-level function. A wide range of materials including organic materials [1] and 2D materials [2] have been used to realize photomemory, but their integration into a display has not been achieved due to high operating voltage and low applicability into the existing process. Indium-gallium-zinc-oxide (IGZO) is considered one of the most promising candidates to overcome such shortcomings, owing to its properties including low leakage current and high compatibility with the display industry. However, the IGZO film has a limitation to be used in optoelectronic applications in that it cannot absorb visible light due to its wide bandgap.

In this paper, a 3-terminal IGZO-based photomemory with a photocatalytic layer for operation in the visible light region was fabricated using electrohydrodynamic (EHD) jet printing. As shown in Figure 1 (a), after depositing tungsten (W) on IGZO with the same channel mask, 30 vol% H_2O_2 oxidizing agent was selectively printed by EHD jet printing to form a WO_3 photocatalytic layer. When the WO_3 layer is exposed to visible light, ambient O_2 transforms into O_2^- through a photocatalytic reaction, leading the photocatalytic layer to be negatively charged. This induces the electrons within the channel layer to move toward the front channel, thereby enabling visible light detection. The fabricated 3-terminal photomemory with WO_3 layer exhibits photosensitivity of 3.87×10^4 under 5 mW/mm^2 green light (532 nm, Figure 1 (b)). Moreover, the device showed nonvolatile photomemory property under visible light of various wavelengths (405, 532, and 635 nm, Figure 1 (c)).

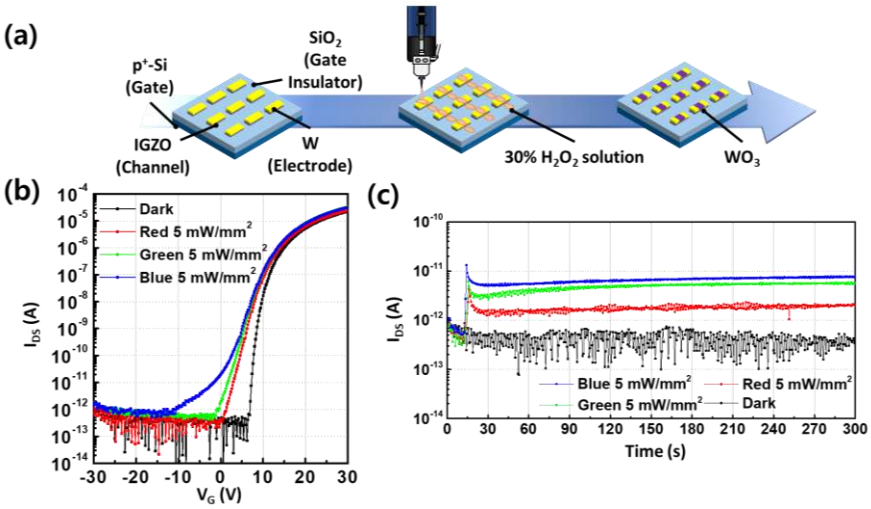

Fig. 1. (a) Fabrication process of 3-terminal IGZO-based photomemory. (b) Transfer characteristics of 3-terminal IGZO-based photomemory under visible light. (c) Temporal I_{DS} curves at V_{DS} = 5.8 V.

Acknowledgment

This work was supported by Samsung Display.

References

1. S. Lan, J. Zhong, E. Li, X. Wu, Q. Chen, W. Lin, T. Guo, and H. Chen, *ACS Appl. Mater. Interfaces*, 12(28), 31716-31724 (2020).
2. D. Xiang, T. Liu, J. Y. Tan, Z. Hu, B. Lei, Y. Zheng, J. Wu, A. H. C. Neto, L. Liu, W. Chen, *Nature Communication*, 9, 2996 (2018).

$MoSe_2$ Transistor with Improved P-type Characteristics through Low-Temperature Annealing

Seongjae Kim[1], Seongin Hong[2], and Hocheon Yoo[1]
[1]Dept. of Electronic Engineering, Gachon University, Seongnam 13120, Republic of Korea
Tel.:82-31-750-5802, E-mail: hyoo@gachon.ac.kr
[2]Dept. of Electrical and Computer Engineering, The University of Texas at Austin, Austin, Texas 78758, USA
E-mail: mindbrain@skku.edu

Transition metal dichalcogenides (TMDs) attract attention as a next-generation semiconductor material due to their mechanical flexibility[1] and high transparency[2]. A large part of the research using TMDs is to modulate the characteristics of transistors through doping. In the case of most TMDs-based transistor doping, chemical doping[3] or substitution of some elements is applied[4]. Here, we demonstrate that $MoSe_2$ transistors can be improved having p-type properties through only annealing without additional doping process. To verify the characteristics of the $MoSe_2$ transistor according to the annealing temperature, we performed the annealing temperature at various temperature. The electrical characteristics of the $MoSe_2$ transistor for each annealing temperature are shown in Fig. 1. While the n-type characteristic was dominant before the annealing treatment, as the annealing temperature increased, the p-type characteristic was improved as an increase of the temperature. Finally, at the annealing at 250 °C, the p-type has a predominant characteristic.

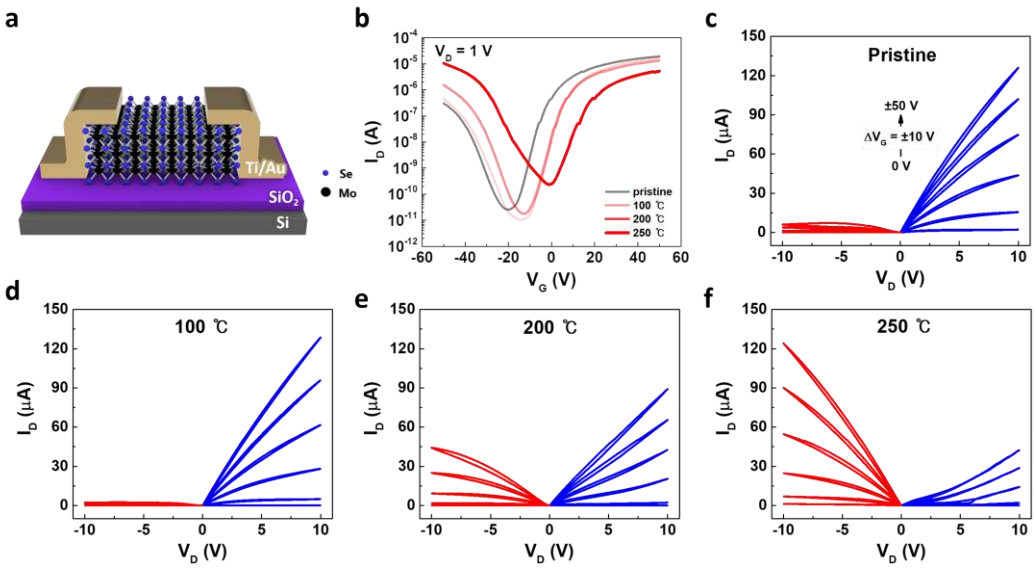

Fig. 1. (a) Illustration of $MoSe_2$ Transistor. (b) Transfer characteristics of $MoSe_2$ Transistor according to each annealing temperature. (c) Output characteristics of the pristine $MoSe_2$ transistor and output curve at each annealing temperature of (d) 100 °C, (e) 200 °C, and (f) 250 °C.

Acknowledgment

This research was supported by a National Research Foundation of Korea (NRF) grant funded by the Korean Government (MSIT) (NRF-2020R1A2C1101647).

References

1. Gao, Li. "Flexible device applications of 2D semiconductors." *Small* 13.35 (2017): 1603994.
2. Das, Saptarshi, et al. "All two-dimensional, flexible, transparent, and thinnest thin film transistor." *Nano letters* 14.5 (2014): 2861-2866.
3. Yoo, Hocheon, et al. "Chemical doping effects in multilayer MoS2 and its application in complementary inverter." *ACS applied materials & interfaces* 10.27 (2018): 23270-23276.
4. Xia, Yin, et al. "Tuning electrical and optical properties of MoSe2 transistors via elemental doping." *Advanced Materials Technologies* 5.7 (2020): 2000307.

Development of low-temperature sintered silver paste for flexible displays

Sun Hong Yoon
Dept. of IT Application Research Center, KETI, Jeonju 54853, Korea
Tel.:82-63-219-0051, E-mail: yoonsh@keti.re.kr

Printed electronics technology which is capable of mass production and microelectrode pattern formation is widely used for flexible displays. Printing technology is well known as a reliable and low cost process for mass production. With an increasing demand for flexible displays, the technologies for low-temperature sintered electrodes have been investigated and attracted a lot of attention. In this work, we developed low-temperature sintered silver paste for screen printing. Flexible electrodes by screen printing showed excellent resistance of 6.5 x 10^{-5} Ω·cm and 0 class adhesion when dried at 80℃ for 30 minutes as shown in Fig 1. We developed low-temperature sintered silver paste with high electrical conductivity and excellent adhesion which can be used for flexible displays.

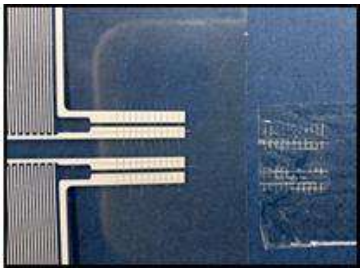

Fig. 1. Screen printed silver paste electrode dried at 80℃ and its adhesion test

Acknowledgment
This work was supported by the research program funded by the Ministry of SMEs and Startups (MSS) of Korea (S3004467, Development of traffic safety lighting fence for school zone using pedestrian recognition technology).

References
1. S. Lee, H. Park, E. Choi, S. Y, I. Hong, *J. KICS*, 42, 716 (2017).

a-IGZO TFTs with transparent ultrathin metal source and drain electrodes fabricated on flexible glass substrates for transparent and flexible electronics application

Yujin Hwang, Sujin Heo, and Hongki Kang
Dept. of Information and Communication Engineering, Daegu Gyeongbuk Institute of Science and Technology (DGIST), Dalseong-gun, Daegu, 42988, Korea
Tel.:82-53-785-6328, E-mail: hkang@dgist.ac.kr

In-Ga-Zn-O (a-IGZO) have been developed for flexible and transparent electronics applications owing to high mobility, large-area uniformity, and optical transparency. We demonstrated high performance IGZO TFTs with transparent source and drain (S/D) electrodes on ultra-thin flexible glass substrates. We applied transparent ultrathin metal S/D electrodes to a-IGZO TFTs for improved transparency. The S/D electrodes were fabricated with 2 nm of aluminum (Al) as seed layer which helps forming ohmic contact with a-IGZO followed by 10 nm of silver (Ag) to enhance the electrode conductivity. The Fig. 1 shows representative transfer characteristics of the a-IGZO TFTs with two types of electrodes: typical 50nm-thick Al, and ultrathin Al/Ag (2nm/10nm), respectively.

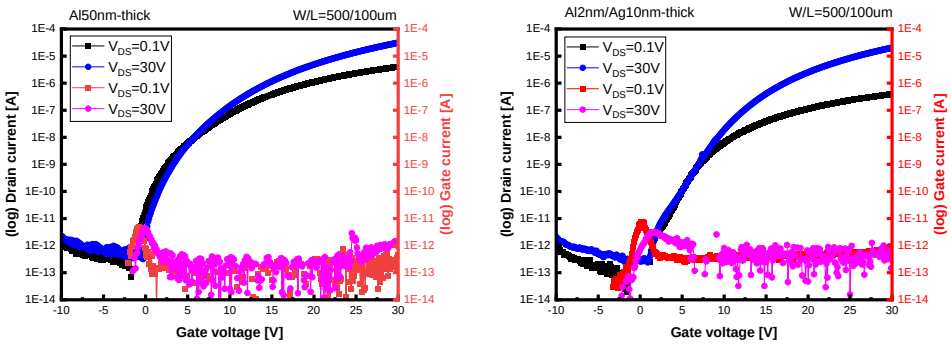

Fig. 1. I-V curve of IGZO TFTs with Al (50 nm) (left) and Al/Ag (2 nm/10 nm) (right) S/D electrodes

Table1 summarizes the electrical characteristics from the transfer curve. The IGZO TFTs with transparent ultrathin S/D electrodes showed no significant degradation in the electrical characteristics while providing better transparency (40~60%) in the visible range (400-700 nm). With previously reported mechanical robustness of the ultrathin metal electrodes, we expect that our IGZO TFTs would be a great candidate for flexible and transparent electronics applications.

Table1. Electrical characteristics (V_{GS}: -10~+30V, V_{DS}:0.1V, 30V)

	W/L=500μm/100 μm	
	50nm-thick Al	Al/Ag (2nm/10nm)
Linear Mobility [cm^2/Vs]	4.42	4.17
Saturation Mobility [cm^2/Vs]	3.8	2.9
Threshold Voltage [V]	-0.8	1.2
Subthreshold Swing [V/dec]	0.37	0.48

Acknowledgment
This work has supported by the DGIST R&D Programs of the Ministry of Science and ICT(19-CoE-BT-03, 21-IJRP-01)

References

1. K. Alzoubi et al., *Journal of Display Technology*, 7(11), 593-600 (2011).
2. Y. Yun, *Adv. Func. Mater.* 27(18), 1606641 (2017).

Pressure effects on structural and electrical properties of spray coated, stretchable silver nanowire electrode on PDMS substrate

*Jonghyun Jeong and Jaewook Jeong**

School of Information and Communication Engineering, Chungbuk National University,

Cheongju, Chungbuk 28644, Korea

*Tel.:82-43-261-3598, *E-mail: jjeong@cbnu.ac.kr*

Stretchable silver nanowire (AgNW) electrodes have been studied for the applications of stretchable display, wearable devices, and bio-compatible devices[1-3]. In this paper, pressure effects on the AgNW electrodes were investigated. The AgNWs were spray coated on the pre-strained poly-dimethylsiloxane (PDMS) substrates, and the pressure of 0.8 to 5.6 Mpa were applied on the AgNWs electrodes during top PDMS substrates were mechanically bonded to the bottom PDMS substrate using hydraulic press shown in Fig. 1. It was found that applying pressure can greatly reduce the sheet resistance of the AgNWs electrodes from 1.3 to 0.6 Ω/square as the pressure increases from 0.8 to 5.6 Mpa. However, muti-cycling strain test (1000-cycle) shows that the AgNWs electrode is electrically stable with small variations of sheet resistance only when the pressure is sufficiently low (~0.8 Mpa). The atomic force microscopy (AFM) and scanning electron microscopy (SEM) images reveal that applying pressure can increase the density of AgNWs networks leading to increase of percolation path between AgNWs, while, it induces additional micro-size cracks with formation of AgNWs peeling region under the high pressure conditions.

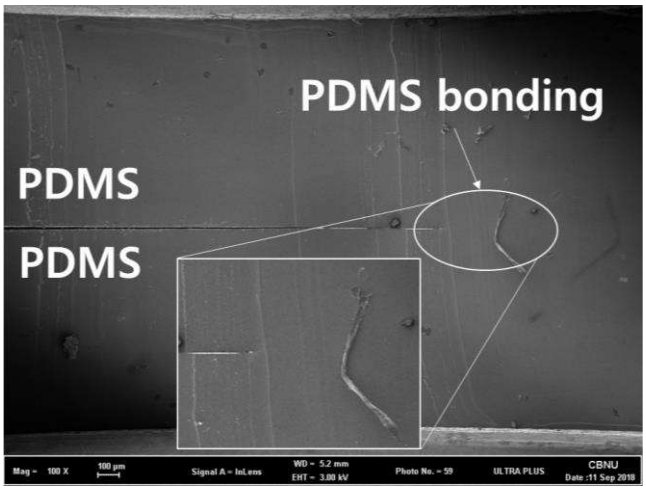

Fig. 1. SEM image of cross-sectional view of PDMS-PDMS bonding. The AgNWs are spray coated on the bottom PDMS substrates. The top PDMS was mechanically bonded using hydraulic press by applying constant pressure.

Acknowledgment

This work was supported by the AURI(Korea Association of University, Research institute and Industry) grant funded by the Korea Government(MSS : Ministry of SMEs and Startups). (No. S3047889, HRD program for 2021)

References

1. F. Xu and Y. Zhu, Adv. Matter. 24, p. 5117 (2012).
2. S. Lee, S. Shin, S. Lee, J. Seo, J. Lee, S. Son, H. J. Cho, H. Algadi, S. Sayari, D. E. Kim, and T. Lee, Adv. Funct. Matter. 25, p.3114 (2015).
3. H. –S. Liu, B. –C. Pan, and G. –S. Liou, Nanoscale, 9 p.2633 (2017).

Highly Transparent and Wide Viewing Optical Films Using Hierarchical Double-Shell Layered Nanoparticle with Gradient Refractive Index Surface

Jin-Wook Choi, Seung-Rak Son, Jongil An, Soyern Kim, Jisung Park, Chan Beom Park, and Jun Hyup Lee*
Department of Chemical Engineering, Soongsil University, Seoul 06978, Republic of Korea
Tel.:82-2-829-8329, E-mail: junhyuplee@ssu.ac.kr

The essential improvements in the performance of light-diffusing materials for wide viewing angles in potential optoelectronic applications have attracted considerable attention. Light scattering materials have been used in various industrial applications including deoxyribonucleic acid probes for biological detection, diffuser films for liquid crystal displays, scattering layers for organic light emitting diodes, and dye-sensitized solar cells [1–4]

In this study, a simple and unprecedented strategy is proposed to simultaneously provide exceptional light scattering performance and high optical transparency for transparent optical thin films using hierarchical double-shell nanoparticles possessing refractive index gradient on the nanoparticle surface. The hierarchical SiO_2/TiO_2/poly(methyl methacrylate) (PMMA) double-shell layered nanoparticles induce enhanced light scattering properties by their nanolayered gradient refractive index structure. The spectroscopic analyses show the successful formation of the multiple nanolayered structure of the double-shell nanoparticles. The synthesized nanoparticles with a diameter of 40 nm and TiO_2 layer thickness of 4.5 nm exhibit the highest diffuse reflectance of 87% in the visible region. An ultraviolet-light-cured optical film with an extremely low content of double-shell nanoparticles exhibits efficient light scattering characteristics while maintaining a high optical transparency. This study provides a facile yet effective, scalable approach to improve the viewing angle performances of optoelectronic devices and paves the new way for further studies on the wide applications of light scattering phenomenon using optically active hierarchical nanoparticles with multiple refractive indices.

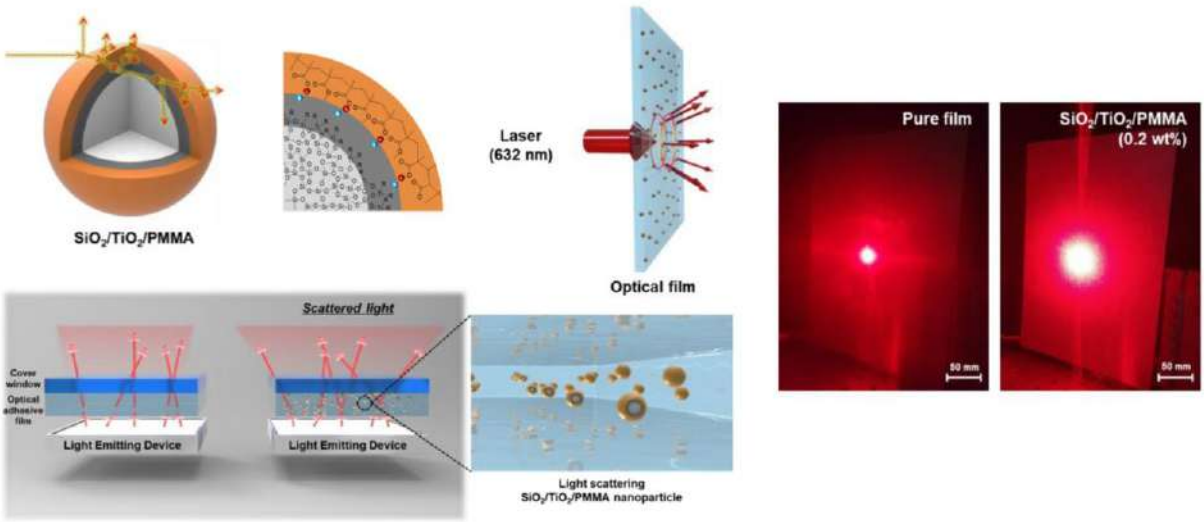

Fig. 1. Schematics of generation of wide viewing characteristics in the functional optical adhesive film

Acknowledgment

This work was supported by a National Research Foundation of Korea (NRF) grant funded by the Korea government (MSIT) (No. NRF-2018R1A5A1024127). This work was also supported by Korea Institute for Advancement of Technology (KIAT) grant funded by the Korea Government (MOTIE) (P0012770).

References

1. X. Xu, D. G. Georganopoulou, H. D. Hill, C. A. Mirkin, *Anal. Chem.*, 79, 6650 (2007).
2. T. W. Koh, J. A. Spechler, K. M. Lee, C. B. Arnold, B. P. Rand, *ACS Photonics*, 2, 1366 (2015).
3. M. I. Tribelsky, *Phys. Rev. A*, 93, 053837 (2016).
4. H. Pang, H. Yang, C. X. Guo, J. Lu, C. M. Li, *Chem. Commun.*, 48, 8832 (2012).

Effect of anode-interface adhesion on stress stability of organic light-emitting diodes

Byung Min Jeon[1] and Sung Min Cho[1]
[1]School of Chemical Engineering, Sungkyunkwan Univ., Suwon, 16419, Korea
Tel.:82-31-290-7251, E-mail: sungmcho@skku.edu

Foldable OLED displays have already been commercialized, but for displays requiring more severe deformation. There is a need to solve the delamination problem between the metal electrode and the organic material used in the OLED. Since the semi-transparent cathode metal for the top emission OLEDs must be very thin, the delamination problem is less important, but the adhesion between the bottom anode metal and the substrate or organic thin film needs to be further improved.

Due to brittle problem of oxide-based electrode, utilizing metal-based electrodes which have ductility is desirable way for stable from more harsh compressive stress. When Ag is used as the bottom electrode, the work of adhesion at the top and bottom interfaces of the Ag electrode was measured by the contact angle measurements to confirm the adhesive force between each layer. The theoretically predicted work of adhesion was experimentally verified by a film scratch method using a nano-indenter.

Through this study, it was confirmed that the adhesive strength of the Ag interfaces can be improved by using a 'adhesive layer' composed of dopamine and SBMA without affecting the operation characteristics of the OLEDs. In principle, dopamine's good anchoring property to the substrate contributes to the immobilization and SBMA helps to induce electrostatic bonding with Ag atoms due to its abundant functional groups such as amine and sulfur trioxide. After the modification, it showed improved interfacial adhesion force at the top and bottom interfaces of the Ag electrode by 115% and 110%, respectively.

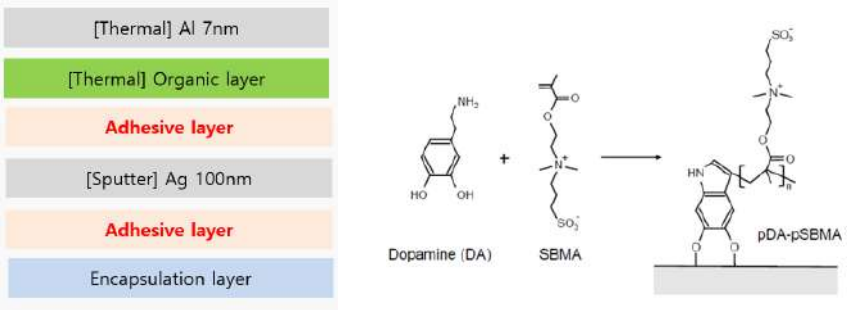

(a) **(b)**

Fig. 1. (a) Structure of both lower and upper adhesive layer OLED device and (b) Adhesive material

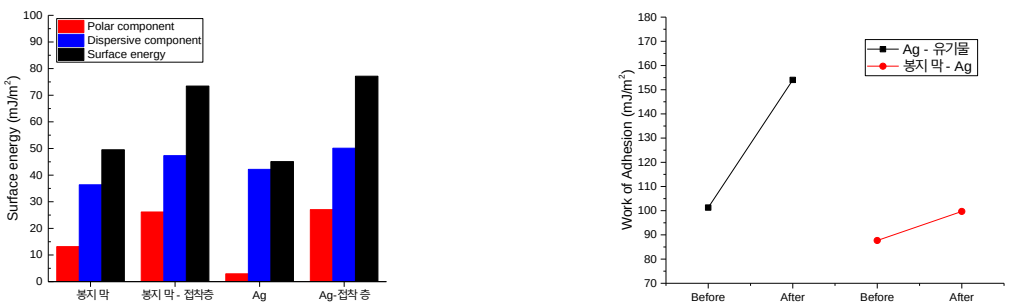

(a) **(b)**

Fig. 2. Change in (a) Surface energy (b) Adhesion force of Ag-organic layer and Ag-encapsulation

Photoalignment Properties of Photopolymer based on Chalcone Groups for Optical Retarder film

Yeong Rang Kim, Jeong Ju Baek, Youn-Jung Heo, Ki cheol Chang, Sung Man Park, Young Hun Kim, Geun Yeol Bae, Hyo sun Lee, Kyung Ho Choi, and Gyo Jic Shin*

Green and Sustainable Material R&D Department, Korea Institute of Industrial Technology, Cheonan-si 31056, South Korea

Tel.:82-010-4127-7307, E-mail: liwa1209@kitech.re.kr

During the last two decades, organic light-emitting diodes (OLEDs) have attracted considerable interest owing to their promising applications in flat-panel displays by replacing cathode ray tubes (CRTs) or liquid crystal displays (LCDs)[1].

OLED panels, one of the parts of OLED, have very high reflectivity. Therefore, the retarder film is necessary part because of the high reflectivity of OLED panels.The retarder film blocks external light reflected by OLED panels and makes true black for OLED product.

The retarder film consists of a liquid crystal layer and alignment layer for arranging these layer of liquid crystal. There are methods of arranging liquid crystals such as rubbing processs and photoalignment process. The rubbing process of conventional technique has many problems for LCD such as generation of electrostatic charge and light leakage. On the other hand, the chemical method, photoalignment process, is a non-contact method that not only solves the problem of rubbing process, but also can has the effect of increasing yield and contrast ratio. Therefore, many kind of research have been conducted on photoalignment process[2].

In this study, we have synthesized the photopolymer based on chalcone moiety-containing side chain in the backbone of polymaleimide. Originally, toluene and methyl ethyl ketone (MEK) were used for film casting solution. However, Tri-Acetyl Cellulose(TAC) film is damaged by MEK solution. Therefore, we replaced the solvents MEK of film casting solution with PGMEA and observed the photoalignment properties on TAC film. As a result, we successfully demonstrate a retardation film exhibiting distinct black/white image at 50mj/cm^2.

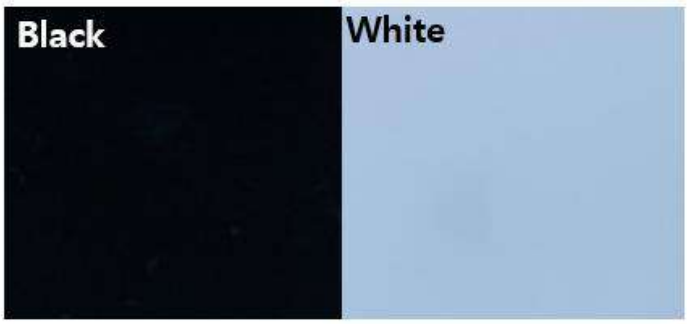

Fig 1. Image of retardation film

References

1. Bernard Geffroy, Philippe le Roy, and Christophe Prat, *Polymer International*, vol. **55**, Issue 6 (2006)
2. Ju Hui Kang, Si Yeol Yang, Seung Yong Jeong, Sangkug Lee, Kyung Ho Choi, and Gyo jic Shin, *IACSIT International Journal of Engineering and Technology*, vol. 4, no.4 (2021).

Effectice conversion of perhydropolysilazne to silicon oxide by UV processes with addition of photobase generator.

Sung-Man Park[1], Jeong-Ju Baek, youn-Jung Heo, Ki-Cheol chang, Young-Hum Kim
*Yeong-Rang Kim, Geun-Yeol Bae, Hyo-Sun Lee, Kyung-Ho Choi, and Gyo-Jic Shin**
Green and Sustainable Materials R&D Department. Korea Institute of Industrial Technology, Chenan-Si 31056, South Korea
Tel.:82-10-6660-9305, E-mail: sungman@kitech.re.kr

PHPS (Perhydropolysilazane) is an inorganic compound with Si-N bonds that can be treated in solution and has properties similar to glass after curing. In general, for curing of PHPS, there are several methods including ammonia vapor exposure, thermal, and VUV irradiation. Among the various curing methods, the UV irradiation curing method can be processed at a low temperature, so there is almost no deformation or damage to the substrate when it is cured by coating it on a polymer substrate.

In this study, PHPS was cured using Hg lamp UV and pulsed UV after adding a photobase generator. The photobase generator is irradiated with UV to form an amine. The formed amines hydrolyze the Si-H groups of PHPS and promote the formation of Si-O-Si groups. Therefore, we can successfully obatine a densly cured silica film by irradiating low energy UV.

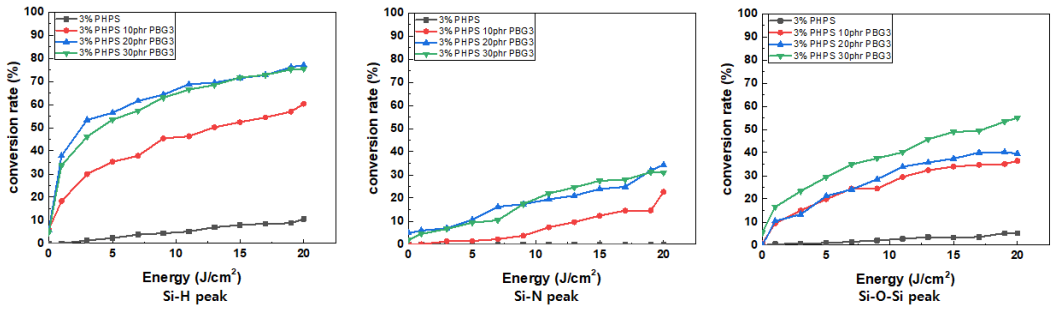

Fig. 1. Conversion rate of PHPS according to exposure energy with and without PBG.

References

1. Harkness, Brian R., Takeuchi, Kasumi, Tachikawa, Mamoru, Macromolecules, 31, 4798-4805 (1998)

Preparation of fluorinated silica-zirconia thin layers derived from perhydropolysilazane and their properties

Jeong Ju Baek[1], Sung Man Park[2], Yeong Rang Kim[2], Young Hun Kim[2], Ki Cheol Chang[2], Youn-Jung Heo[2], Geun Yeol Bae[2], Hyo sun Lee[2], Kyung Ho Choi[2], and Gyo Jic Shin[1]
[1,2]Green and Sustainable Materials R&D Department, Korea Institute of Industrial Technology, Cheonan-si, 31056, Korea
Tel.:82-41-589-8415, E-mail: gyshin@kitech.re.kr

As flexible displays based on transparent plastics such as PC (polycarbonate), PMMA (polymethylmethacrylate), CPI (colorless polyimide), etc. have received attention, recently, it has been getting increasement demands of functional film having anti-fingerprint, antifouling, anti-reflection, anti-scratch properties, simultaneously. These plastic films have some drawbacks that it is easily scratched by friction and has major disadvantages against solvents, due to its low surface hardness. Therfore, there has been various studies to enhance suface properties of plastic films for applied to functional film industries.

In this study, our group developed fluorinated silica-zirconia coating solution derived from perhydropolysilazane. Zirconia is well known for its strong covalent character, excellent mechanical strength with a very high bond dissociation energy, thermal stability as well as strong alkali and acid resistant property compared to other ceramic materials. Particular interest exists for the SiO_2–ZrO_2 system due to its properties such as hardness, chemical resistance in alkaline environment, wear resistance, etc. In order to study the surface properties due to zirconia in the silica coatings, in the first step, the fluorinated silica-zirconia precursors were synthesized by the simple sol–gel route. In the second step, functional coating materials were synthesized using synthesized fluorinated silica-zirconia precursor and perhydropolysilazane by hydrolysis reaction. The coating solutions were coated on the glass substrate and exposed to vapor from aqueous ammonia to form cured fluorinated silica-zirconia thin layers. And then, the wettability, pencil hardness, suface roughness, optical properties, wear resistance, and chemical resistance of the layers were evaluated.

References

1. G. Yi, M. Sayer, J. Sol-Gel Sicence and Technology, 6(1), 65 (1996)
2. R. Figueira, C. Silva, E. Pereia, J. Coatings Technology and Research, 12(1), 1 (2015)
3. S. Dhere, Current Science, 108(9), 1647 (2015)
4. I. Das, G. De, Scientific Reports, 5, 1 (2015)

Ambipolar Charge Transport Behavior of Poly(9,9-di-n-octylfluorenyl-2,7-diyl)-Molybdenum Disulfide Heterojunction Phototransistors

Dong Hyun Lee[1], Hyung Joong Yun[2], Seongin Hong[3], and Hocheon Yoo[1]
[1]Dept. of Electronic Engineering, Gachon University, 1342 Seongnam-daero, Seongnam 13120, Korea
Tel.:82-31-750-5802, E-mail: hyoo@gachon.ac.kr
[2]Advance Nano Research Group, Korea Basic Science Institute (KBSI), Daejeon 34126, Korea
E-mail: hjyun@kbsi.re.kr
[2]Dept. of Electrical and Computer Engineering, The University of Texas at Austin, Austin, Texas 78758, USA
E-mail: mindbrain@skku.edu

Molybdenum disulfide (MoS_2) that representative materials of two-dimensional transition metal dichalcogenide [1-3], is an attractive semiconductor material with excellent electrical, optical, and mechanical properties that can be applied to a wide range of next-generation semiconductor devices, such as flexible thin-film transistor, photodetectors, and neuromorphic devices. However, MoS_2 field-effect transistors (FETs) with dominant n-type semiconductor characteristics have rarely been reported on the increase in p-type conductivity characteristics. In this study, we demonstrate p-doping effect by simply coating poly(9,9-di-n-octylfuorenyl-2,7-diyl) (PFO) on the top of the MoS_2FET which fabricated by mechanical exfoliation. In Fig. 1, the proposed PFO-MoS_2 heterostructure FETs were observed positive shift in threshold voltage and decrease in the on-current, which operated to n- and p-type charge carriers coexisted ambipolar transistor. In particular, p-type conductivity becomes higher at the optimized annealing temperature 350 ^{o}C. Moreover, PFO doping effect enhanced photosensitivity of the ambipolar PFO MoS_2 device and exhibit reliable photoswitching operation.

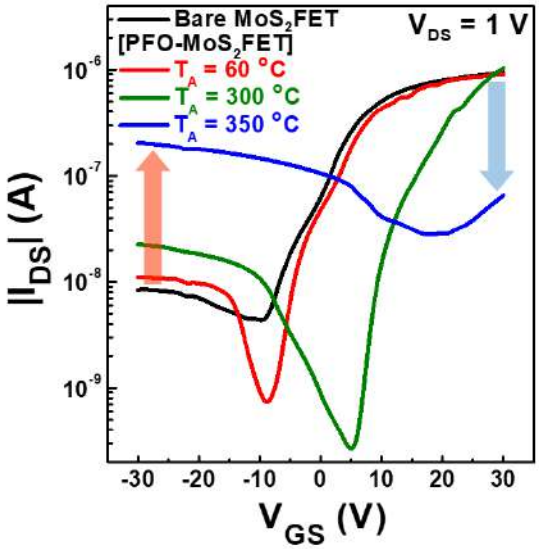

Fig. 1. Electrical characteristics of the bare MoS_2FET and PFO-MoS_2FET. (T_A = 60, 300, 350 ^{o}C).

Acknowledgment

This research was supported in part by a National Research Foundation of Korea (NRF) grant funded by the Korean Government (MSIT) (NRF-2020R1A2C1101647 and NRF-2020M3A9E4104385). This research was supported in part by the Basic Science Research Program through the National Research Foundation of Korea (NRF), which is funded by the ministry of Education (2020R1I1A1A01070907)

References

1. Y. Yoon and K. Ganapathi (eds.), *Nano Letters*, vol. 11, p. 3768-3773 (2011)
2. W. Zhou and X. Zou (eds.), *Nano letters*, vol. 13, p. 2615-2622 (2013).
3. B. Radisavljevic and A. Radenovic (eds.), *Nature nanotechnology*, vol. 6, p. 147-150 (2011).

Gold-welded silver nanowire network-based stretchable electrodes for wearable applications

Dongju Jang[1,2], Hyeon Cho[1,2], Byeongmoon Lee[1,2,3] and Yongtaek Hong[1,2]*
[1]Department of Electrical and Computer Engineering, Seoul National University, Seoul 08826, Korea
[2]Inter-University Semiconductor Research Center, Seoul National University, Seoul 08826, Korea
[3]Soft Hybrid Materials Research Center, Korea Institute of Science and Technology, Seoul 02792, Korea
**Tel.:82-2-880-9567, E-mail: yongtaek@snu.ac.kr*

As the field of stretchable electronics has expanded towards various applications including health monitoring, soft robotics and implantable devices, the development of new stretchable components and platforms has become significant. Especially, stretchable conductors are in need for the integration of individual components and realization of stretchable systems and devices. Silver nanowires (AgNWs) are one commonly used conductor in stretchable electronics. AgNWs are highly conductive, robust, flexible and stretchable when used together with elastomeric materials such as polydimethylsiloxane (PDMS) in the form of a nanocomposite[1]. However, despite these advantages, AgNWs have chronic problems with being used in stretchable applications. It is difficult for AgNW networks to maintain their conductivity when stretched because most of its resistance comes from the contact resistance at inter-nanowire junctions, which widen under deformation resulting in an increase in this value[2]. In order to solve these issues, many researchers have reported AgNW welding methods, both chemical and mechanical, but most have not addressed its stretchability or cyclic properties which are necessary features for applications in stretchable electronics.

In this work, we report stretchable electrodes based on gold-welded AgNW networks. AgNWs were welded by a simple galvanic reaction in a gold chloride aqueous solution, $HAuCl_4$ (Fig. 1a). Gold-based welding was chosen because it provides a facile fabrication process and results in a highly conductive network compared with organic material-based welding mechanisms[3]. Experimental conditions such as the solution concentration and reaction time were carefully controlled in order to find the optimal condition of welding that results in a highly conductive nanowire network (Fig. 1b). Also, the effect of welding on the stretchability and cyclic properties of AgNW networks was explored, resulting in a stretchable conductor capable of stable and reliable cyclic operations and therefore adequate for stretchable applications (Fig. 1c). The results here demonstrate the potential of AgNW welding in stretchable, wearable applications by enhancing its electrical stability under deformation. Detailed experimental methods and results will be presented at the conference.

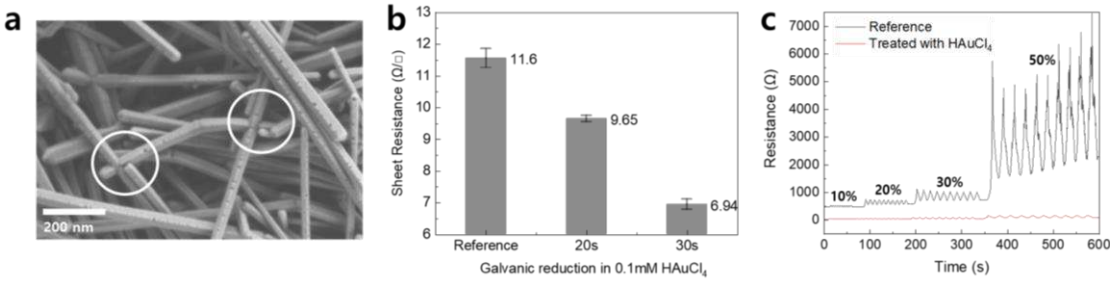

Fig. 1. (a) An SEM image of the welded AgNW network, (b) The effect of reaction time on electrode sheet resistance, (c) The effect of welding on the stretchability of AgNW networks

Acknowledgment

This work was supported by Institute for Information & communications Technology Promotion(IITP) grant funded by the Korea government(MSIP) (No.2017-0-00048, Development of Core Technologies for Tactile Input/Output Panels in Skintronics(Skin Electronics)).

References

1. F. Xu, Y. Zhu, *Adv. Mater.*, 24, 37, 5117-5122 (2012)
2. Q. Huang, *et al.*, *ACS Appl. Nano. Mater.*, 1, 4528-4536 (2018)
3. Liang, *et al.*, *ACS Nano*, 8, 2, 1590-1600 (2014)

Charge Trapping and Hysteresis Behavior in Carbon Nanotube Thin-Film Transistor with Ferroelectric Dielectric Layer

Hyunjun Yoo[1,2], Jiseok Seo[1,2], and Yongtaek Hong[1,2]*
[1] Department of Electrical and Computer Engineering, Seoul National University, Seoul 08826, Korea
[2] Inter-university Semiconductor Research Center (ISRC), Seoul National University, Seoul 08826, Korea
*Tel.:82-2-880-9567, E-mail: yongtaek@snu.ac.kr

Carbon nanotube thin-film transistors (CNT TFTs) have excellent electrical and mechanical properties, which is suitable for future soft electronics [1]. However, their practical application is limited by high off-current and large hysteresis behavior, due to the charge trapping through water molecule absorption [2]. In addition to the charge trapping at the active channel layer, the dielectric layer also can be a site of the charge trapping. In the case of silicon dioxide, oxidation process conditions can change the charge trapping behavior by controlling the film quality of dielectric layers [3]. Ferroelectric dielectric material also can change the charge trapping behavior, but few studies have been reported for solution-processed CNT TFTs.

In this paper, solution-processed CNT TFTs with different dielectric layers were fabricated. We used silicon dioxide, poly(4-vinylphenol) (PVP), and poly(vinylidene fluoride-co-hexafluoropropylene) (PVDF-HFP) for dielectric layer. Silicon oxide wafers were used for the bottom gate and dielectric layer. PVP was inkjet-printed, and PVDF-HFP was spin-coated on the inkjet-printed silver gate electrode. Hysteresis behavior was measured as shown in Figure 1. In the case of the SiO_2 dielectric layer, counter-clockwise hysteresis was measured from the charge trapping behavior of the CNT active channel. However, hysteresis was reduced with the porous PVP dielectric layer. Moreover, hysteresis was almost eliminated with PVDF-HFP, because of the opposite charge trapping at the ferroelectric PVDF-HFP layer. To verify the opposite charge trapping of ferroelectric dielectric, hysteresis was measured after annealing which reduces the charge trapping from the water molecule absorption at the CNT layer. After annealing, the direction of hysteresis was reversed, which means that the charge trapping at the ferroelectric dielectric layer induced clockwise hysteresis. The details will be discussed at the conference.

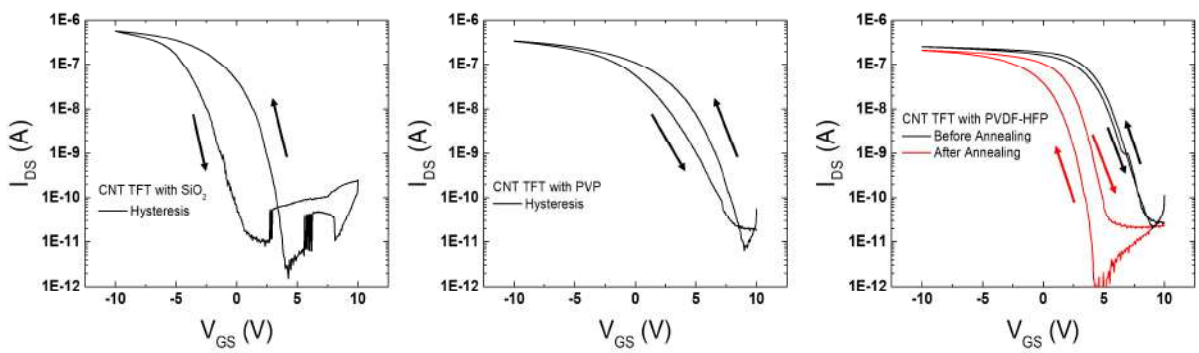

Fig. 1. (a) Hysteresis of CNT TFT with SiO_2 dielectric layer (b) PVP dielectric layer (c) PVDF-HFP dielectric layer before and after annealing

Acknowledgment

This research was supported by National R&D Program through the National Research Foundation of Korea(NRF) funded by Ministry of Science and ICT(2020M3D1A2101801)

References

1. D. Sun, M. Y. Timmermans, Y. Tian, A. G. Nasibulin, E. I. Kauppinen, S. Kishimoto, T. Mizutani, and Y. Ohno, *Nat. Nanotechnol.,* 6(3), 156 (2011).
2. S. H. Jin, A. E. Islam, T-I. Kim, J-H. Kim, M. A. Alam, and J. A. Rogers, *Adv. Funct. Mater.,* 22(11), 2276-2284 (2012).
3. Y. Zhao, Y. Huo, X. Xiao, Y. Wang, T. Zhang, K. Jiang, J. Wang, S. Fan, and Q. Li, *Adv. Electron. Mater.,* 3(3), 1600483 (2017).

Augmented Phase Correction for Improving the Sensing Image Quality of the Ultrasonic Fingerprint Sensor Integrated OLED System

Hyundo Shin[1], Hyun Sung Park[1], Yudeok Seo[1], Dongjin Seo[1] and Yongjo Kim[1]
[1]CAE team, Display Research Center, Samsung Display Co., ltd, Yongin-si, Gyeonggi 17113, Korea
Tel.:82-31-5181-6906, E-mail: hyundo83.shin@samsung.com

In this work, we proposed the augmented phase correction method to improve the sensing image quality o f the ultrasonic fingerprint sensor on display (FoD). The propagated wave is diffracted by difference imped ance of the ridge and the valley on the finger so that the interference patterns are captured by the sensor [1]. In general, the diffracted image can be usually corrected by convolving the specific point spread functi on (PSF) in previous studies [2]. However, the mentioned method has a problem that specific function mus t be applied depending on the sensing image. In addition, the method has not yet been proven to be applic able for wave propagation problems with the sensor integrated OLED system.

Different from the previous method, our method intends to overcome the diffraction by using the modified phase correction method without the specific PSF based convolution and it provides the improved image for the sensor performance. In Fig. 1, the analyzed pressure distributions for the samples are represented with the checkerboard-like patterns as shown in the inset of the Fig. 1 (A). The magnitude spectrum is derived from the analyzed pressure distribution using the two-dimensional Fast Fourier Transformation (FFT) [3]. The proposed phase correction function is applied to correct the diffracted phase based on the sample configuration. The modified pressure distribution is finally built by using the magnitude and the modified spectrum. In the inset of the Fig. 1 (B), the diffracted pattern is stabilized by attenuating the diffraction and the corrected pattern is similar to the sample configuration.

We verified the simulation results by testing the five different types of flagship models. The experimental measurements were recorded using an ultrasonic sensor mounted on smartphone models. The measured SNR values represent good agreement between numerical simulations and experimental measurements with an error rate of 5%. The proposed approach is available for the multi-physical structure such as acoustic, elastic and viscoelastic mediums in the multi-layered structure. All of the methods in this study are performed using P ython programing associated with the commercial package ABAQUS [4].

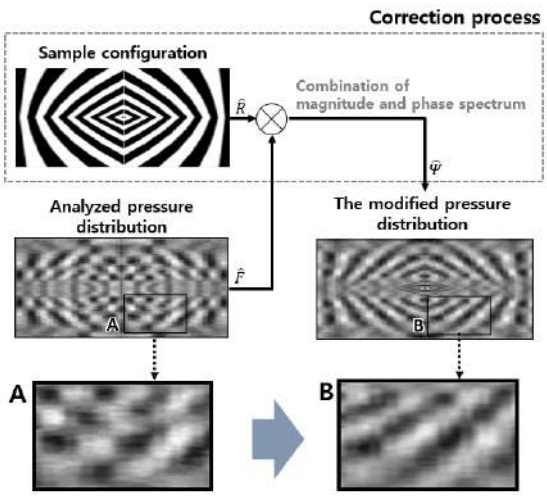

Fig. 1. The phase correction procedure for improving the diffraction image quality

References

1. H. S.Park, H. Shin, Y. Seo, D. Seo and Y. Kim. *SID'20 Technical Digest*, 51(1), p. 1851 (2020).
2. B. Poduval, C. E. Deforest, J.T. Schmelz and S. Pathak, *.Astrophys J.,* 765(2), 144 (2013).
3. A. Palvanov and Y. i. Cho, *Sensors (Basel)*, 19(6), 1343 (2019).
4. ABAQUS Inc, ABAQUS 6.14 Theory Manual, RI: Dassault Systèmes Simulia Corp (2014)

Touchless User Interactive High-Resolution Light Field Display System Using a Three-Dimensional Tracking Camera

*Md. Shahinur Alam[1], Joon Hyun Kim[1], Jin Kyu Jung[1], Young-Tae Lim[1], Md. Biddut Hossain[1], Kwon-Yeon Lee[2], Yong-Joo Yoo[3], and Nam Kim[1, *]*

[1]Department of Computer and Communication Engineering, Chungbuk National University, Cheongju, Chungbuk 28644, South Korea

**Tel.:82-43-267-8490, E-mail: namkim@chungbuk.ac.kr*

[2]Department of Electronics Engineering, Sunchon National University, 255 Jungang-ro, Suncheon, Jeonnam 57922, South Korea

[3]Department of Industrial Artificial Intelligence, Chungbuk National University, Cheongju, Chungbuk 28644, South Korea

Three-dimensional (3D) displays are the emerging research area nowadays. Normal two-dimensional (2D) display devices are unable to perceive 3D information. Visualizing full 3D information requires a 3D display device. Light field (LF) display is one of the methods to deliver 3D images by generating the distribution of the light in the space. However, 3D displays are still under development because of the narrow viewing angle, lack of motion parallax, and low resolution. To enhance the above parameters of an LF display, several researchers have proposed different techniques such as a temporal multiplexed LF display [1,2]. However, a higher frame rate is required. In this work, a head tracking camera-based light field display system has been presented.

Fig. 1 shows the detail of the proposed LF display. The whole process is divided into two principal parts: LF capturing and the display system. The process diagram is shown in Fig. 1(a). An electrically controllable camera slider is used to capture 71 horizontal views of a 3D object. Moreover, the slider rig is mounted with three cameras that provide 3 vertical views. The slice is taken in a 30° span where the minimum motor rotation is 0.04°. The captured LF images are displayed in the 3D display according to the user's gaze direction. An Intel Realsense SR300 camera is used to track the observer's head position. The vertical and horizontal views can be perceived by moving head up-down and left-right, respectively.

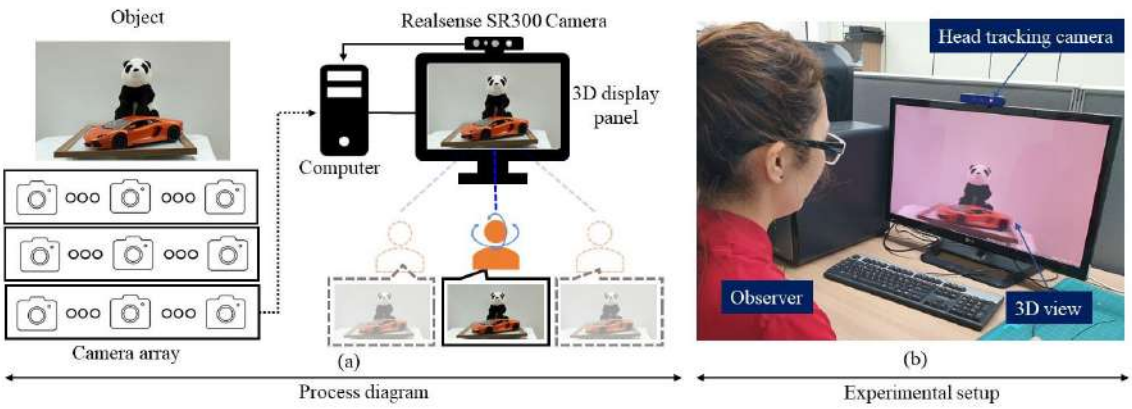

Fig. 1. Head tracking based LF display system: (a) schematic diagram, (b) experimental setup.

The original experimental setup for the LF display system is shown in Fig. 1(b). The observer's head position is tracked using the tracking camera and the view slices are displayed according to the viewing direction. The observer can sense real-time 3D views in high resolution. In this system, we mitigate the flicker and low-resolution problems by enhancing the frame rate and capturing the high-resolution images, respectively.

Acknowledgment

This research was supported by the National Research Foundation of Korea (NRF) grant funded by the Korea government (No. NRF-2018R1D1A3B07044041 and No. NRF-2020R1A2C1101258).

References

1. Y. Oh, D. Shin, B.-G. Lee, S.-I. Jeong, and H.-J. Choi, *Opt. Express*, 22(15), 17620-17629 (2014).
2. Y. Watanabe, and H. Kakeya, *Appl. Opt.* 60, 2517-2517 (2021).

Stretchable Capacitance Sensor against Strain Deformation

Sang Gyeong Nam[1], Jun Hyuk Shin[1], Su An Lee[1], and Su Seok Choi[1]*
[1]Dept. of Electrical Engineering, POSTECH, Pohang, Gyeongbuk 37673, Korea
Tel.:82-54-279-2228, E-mail: choiss@postech.ac.kr

Recently, stretchable electronics and sensor attracts increasing research interest with wearable and deformable electronics. For well combination with display applications capacitive based stretchable sensor is highly desired. However, the electrical stability of capacitance sensitivity between selection and non-selection states stretchable and the mechanical stability of capacitance are still challengeable. Poly(dimethylsiloxane)(PDMS) is widely used as the substrate material for stretchable electronics based on the beneficial merits of stable chemical properties, good thermal stability, transparency, and biological compatibility and its capability of attaining designer functionalities via surface modification and bulk property tailoring.[1] Metals that are liquid at or near room temperature are the only materials that have both metallic and fluidic properties.[2] Because they are liquid, they offer promising opportunities for electronics that are soft, flexible, stretchable, and even reconfigurable.[3] In this study, we approached to build stretchable capacitance sensor by multi-stacking combining of PDMS and liquid metals in specific laminated structure, which can preserve similar capacitance and stable capacitance selection sensitibity against of strain stress.

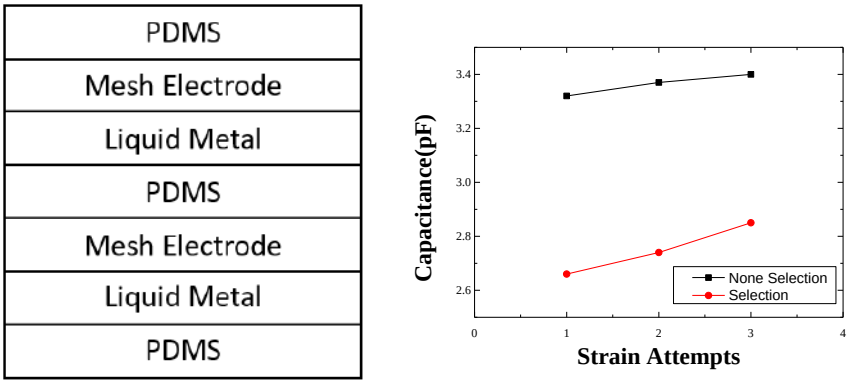

Fig. 1. (A) Structure of Stretchable Touch Sensor using Liquid Metal (B) Capacitance Change Sensing while Stretching.

In order to obtain stability of capacitance sensing against addressing stretching stress, multi-layered capacitance sensing electrodes structure of PDMS/Liquid Metal was designed, Fig 1(A). Also the sensor device was fabricated under low temperature curing condition of 80℃ where thermal stability condition of OLED Display is comparable. As a result, it was found that good stability of capacitance sensibility against addressing stress up to 20% strain stretching deformation. In this report, results of this study will be discussed in detail.

Acknowledgment

This research was supported by the Technology Innovation Programs (20010442, Development of 28GHz and over 5G mm Wave Antenna Technology Integrated on Mobile Display and 20010690, Development of 12inch panel (20% stretch) and module process technology for mass production of stretchable display) funded by the Ministry of Trade, Industry & Energy(MOTIE, Korea) and Next Generation Engineering Research Program of National Research Foundation of Korea (NRF) funded by the Ministry of Science, ICT (No.2019H1D8A2106519).

References

1. Dianpeng, Qi., et al., Advanced Materials 2003155 (2020)
2. Michael D., Dickey, Advanced Materials 1606425 (2017)
3. Michael D., Dickey, ACS Appl. Mater. Interfaces, 6, 18369 (2014)

Polarization Induced Deformation Sensing in Thin Film Transistor

Jae Wook Lee[1], Jun Hyuk Shin[1] and Su Seok Choi[1]*
[1]**Dept. of Electrical Engineering, POSTECH, Pohang, Gyeongbuk 37673, Korea**
Tel.:82-54-279-2228, E-mail: choiss@postech.ac.kr

Recently, as rapidly growing research interest in shape deformable electronics including display technical demands for shape deformation sensing devices are also increased. Including various sensing methods using resistivity, capacitance, and also optical system deformation sensing systems integrated with display systems is highly desired. Obviously, active deformation sensing using a thin film transistor (TFT) is most desirable due to the good compatibility with a pixelated array but this is still in challengable. Shortly, converting mechanical deformation energy into the electrical signal and further integrated signal in TFT is ideally desired. Electroactive material based on polarized materials such as ferroelectric polymers or dielectric elastomers can convert energies between mechanical deformation stress and electrical polarization change which results in charge volume density and also current change [1]. In particular, the resulting charge density amount is reversibly switchable by the polarization rotation induced by mechanical deformation. This is caused by a change in the direction of molecular arrangement due to the influence of external stress, resulting in a change in the direction of the dipole moment [2,3]. Using these polarization switching material properties, various sensor devices can be implemented.

In this work, we investigated a feasibility study of strain deformation sensing in the TFT device structure by exploiting the polarization rotation switching of electroactive materials. As result, we could found a good reversible current changing selectivity from I_D of field-effect transistor sensor which has an embedded rotational polarity change of polarization layer (Fig 1). We will report details of shape deformation stress sensing mechanism in TFT structure from the investigation of modified depletion property by strain-induced polarization change.

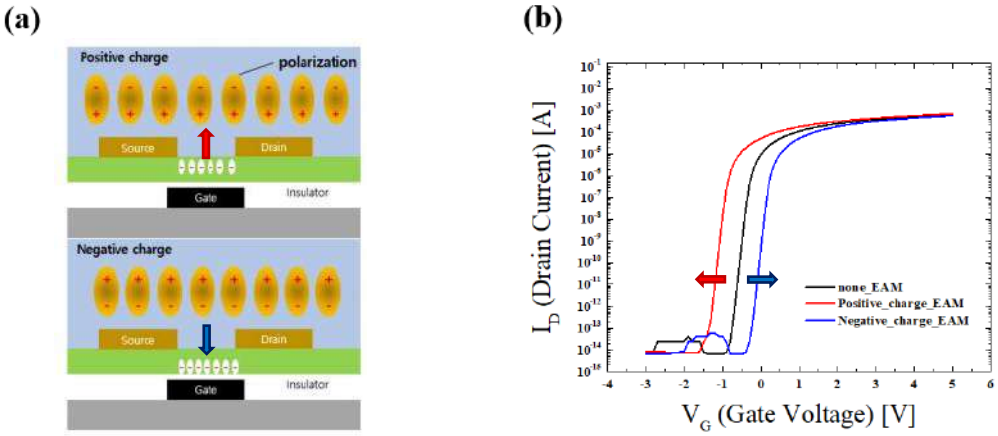

Fig 1. (a) Schematic diagram of TFT which controlling current by changing polarization. (b) Drain current - Gate voltage (I-V) characteristics due to polarization change.

Acknowledgment

This research was supported by *LG Display-POSTECH incubation research program*, the Technology Innovation Program (20010690, Development of 12inch panel (20% stretch) and module process technology for massproduction of stretchable display) funded By the Ministry of Trade, Industry & Energy (MOTIE, Korea)

References

1. H. Lu, C.-W. Bark, D. Esque de los Ojos, J. Alcala, C. B. Eom, G. Catalan, A. Gruverman1, Science 336, 6077 (2012)
2. Xin Chen, Xu Han, and Qun-Dong Shen, Adv. Electron. Mater. 3, 1600460 (2017)
3. Liqun Xiong, YunChen, JingYu, WeimingXiong, XiaoyueZhang, and YueZheng, Appl. Phys. Lett. 115, 153107 (2019)

Low Cost, Highly Efficient Silicon Microwires Based FET Gas Sensor

Quang Trung Le, Kumin Kang, and Jaekyun Kim
Dept. of Photonics and Nanoelectronics, Hanyang University, Ansan, Gyeonggi 15888, Korea
Tel.:82-31-400-4679, E-mail: jaekyunkim@hanyang.ac.kr

Rapid development of industries and the continuous increase of social demand, the exhausted gases significantly influence to environment and human health, that put an importance in monitoring air quality, particularly the pollutants. The innovation and improvement of gas sensors is always essential.

Silicon nanowires (SiNWs) is the most potential candidate for room temperature gas sensing. Most of SiNWs gas sensors based on resistor are fabricated according to the vertical SiNW arrays, which is typically etched by metal assisted chemical etching (MaCE) or VLS growth, then two electrodes are deposited on the surface [1]. This structure may have low reproducibility due to the collapse of vertical SiNWs during drying. Field-effect transistor (FET) type gas sensor shows a greater performance of gas sensing even though at low concentration. Nanofabrication of SiNWs require highly precise technique and process, consequently resulted in high cost. Due to the outstanding and significantly fast development of nanotechnology, the potential of micro-sized structure is still not fully exploited. Notly, the fabrication of micro-sized structure is more facile and economic compared to nanofabrication. The improvement of silicon microwires (SiMWs) based FET is also a good path to fabricate a low cost and highly effective gas sensor.

Desired SiMW arrays with different wire diameters, lengths, orientations, are easily fabricated by controlling the metal catalyst layer, initial silicon wafer, etching conditions (concentration, temperature, time) with MaCE technique [2]. The as-fabricated vertical SiMWs (Fig. 1) can be broken by sonication in ethanol solution. The resulted SiMWs then can be horizontally aligned on the plana substrate [3], which is more compatible with the process of FET devices fabrication. The surface of SiMWs would be functionalized with different metals, chemicals, which can help improving the selectivity of the sensor, especially in the ambient humidity, the parameter strongly affects the performance of sensor devices [4].

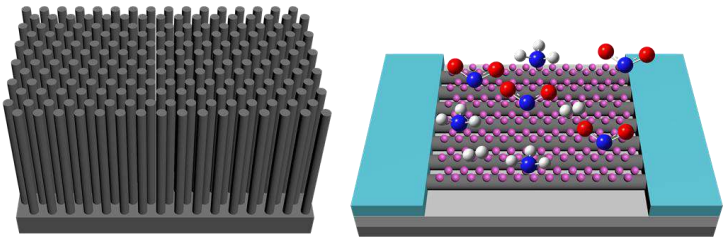

Fig. 1. As-fabricated vertical SiMWs (left) and SiMWs based FET gas sensor (right)
(1line spacing)

SiMWs based FET gas sensor will efficiently work at room temperature, adapt the requirement of gas sensors. The precisely functionalized metal on the surface of SiMWs will improve the selectivity of the device, as well as the working performance at any humidity. This work promises a low cost, high efficient gas sensor. Additionally, this widen the potential of micro-sized structures in research and practical applications.

Acknowledgment

Quang Trung Le and Kumin Kang have contributed equally in this research.

References

1. H. Han, Z. Huang, W. Lee, Nano Today., 9, 271–304 (2014)
2. Z. Huang, H. Fang, J. Zhu, Adv. Mater., 19, 744–748, (2007)
3. U.H. Choi, J.H. Park, J. Kim, Nanomaterials., 8 (2018)
4. Y. Qin, J. Zang, Z. Wen, Phys. E Low-Dimensional Syst. Nanostructures., 118, 113957 (2020)

Ion-gel Gated Organic Synaptic Tactile Transistor Based on Piezo-modulated Ion Dynamics

Chi Hoon In, Yunah Kim, Joo Sung Kim, Hyukmin Kweon, Hanbin Choi and Do Hwan Kim
Dept. of Chemical Engineering, Hanyang University, Seoul 04763, Korea
Tel.:82-2-2220-2671, E-mail: dhkim76@hanyang.ac.kr

Neuromorphic tactile interface has attracted attention as a next-generation electronic skin that enables low energy consumption, high processing efficiency. In recent studies, integrated tactile sensors connected in parallel with synaptic transistors to detect external stimuli and modulate synaptic plasticity sequentially. However, their circuit complexity is a major drawback that causes power consumption and processing efficiency. Herein, we describe a novel design of an ion-gel gated synaptic tactile transistor (IGSTT) that enables stimulation detection and synaptic plasticity modulation in a monolithic device based on a hydrogen-triggered mechanosensitive ion channel layer that selectively responds to pressure stimulus. The IGSTT has high sensitivity due to the electrochemically doped multi-level channel conductance originated from the change in ion concentration by pressure stimuli. Consequently, we believe that novel material design will provide new insight into developing synaptic electronics for neural prosthetics and soft robotics.

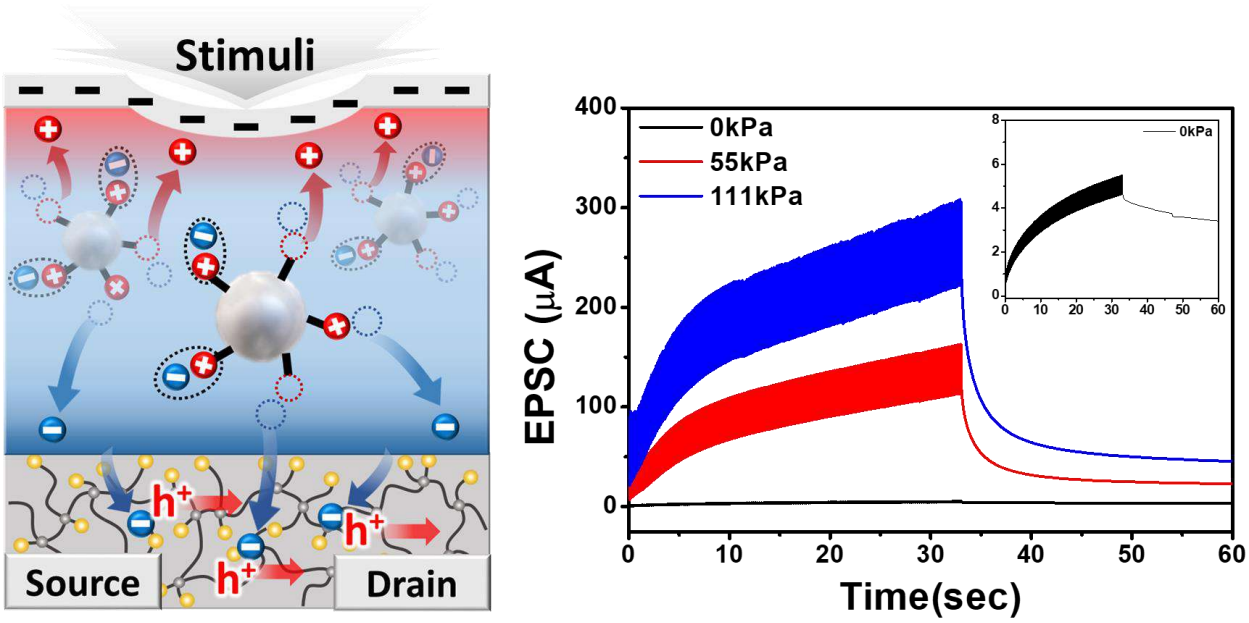

Fig. 1. Schematic diagram of the synaptic tactile transistors under pressure stimuli.

Acknowledgment

This work was supported by the Basic Science Research Program (2020R1A2C3014237) of the National Research Foundation of Korea (NRF) funded by the Ministry of Science, ICT.

References

1. Amoli, V., Kim, J.S., Jee, E. et al., *Nat Commun*, 10, 4019 (2019)
2. Rivnay, J., Inal, S., Salleo, A. et al., *Nat Rev Mater*, 3, 17086 (2018)
3. Ji, T. et al., *J. Appl. Polym. Sci.*, 135, 46089 (2017)

Effects of Edge Passivation and Intense Pulsed Light (IPL) Treatment on Organic Photodiode for Image Sensor Array

Yoon-Su Kim[1,2], Soryeong Jeong[1], Byungwook Yoo[1], Chul Jong Han[1], Byeong-Kwon Ju[2], and Min Suk Oh[1,*]
[1] Display Research Center, Korea Electronics Technology Institute (KETI), Seongnam, Gyeonggi-do 13509, Korea
Tel.:82-31-789-7417, E-mail: ohms@keti.re.kr
[2]Department of Electrical Engineering, Korea University, Seongbuk-gu, Seoul, 02841
(2 line spacing)

Recently, there have been many researches and attentions to flexible photonic devices. However, it is not easy to use conventional p-i-n Si photodiode technology for large flexible system due to its rigid components. Therefore, flexible photodiodes using organic semiconductor materials have become a promising device technology for large-area flexible applications. However, when the size of each pixel decreases, dark current of OPD increase due to the leakage current from edge of bottom electrode. And, in the previous results, researchers introduced hole blocking layer (HBL) to reduce dark current. However, there were several drawbacks such as low stability to oxygen or humidity [1], impossibility of solution process, and long thermal treatment process [2].

In this report, we fabricated top-illuminated organic photodiode (OPD) devices with transparent oxide top electrode, bulk-hetero-junction (BHJ) materials and solution oxide semiconductor as HBL. We used the edge passivation technologies of each pixel for low dark current and the intense pulsed light (IPL) treatment in air ambient for low-temperature solution oxide semiconductor as HBL. To overcome the drawbacks of organic hole blocking layers, we chose solution-based inorganic IGZO as HBL which show higher stability to oxygen and humidity, higher transparency with wide bandgap (~3.2 eV), and good matching with the energy level of P3HT:PCBM. And, since the edge passivation technology was introduced by using ALD-grown Al_2O_3, we could reduce dark current by suppressing leakage current caused from sidewall surface by 1/1,000. Therefore, we could reduce power consumption and improve Signal-to-Noise-ratio (SNR). Based on these results, we can expect that our OPD devices can be used for flexible image sensor array in the near future.

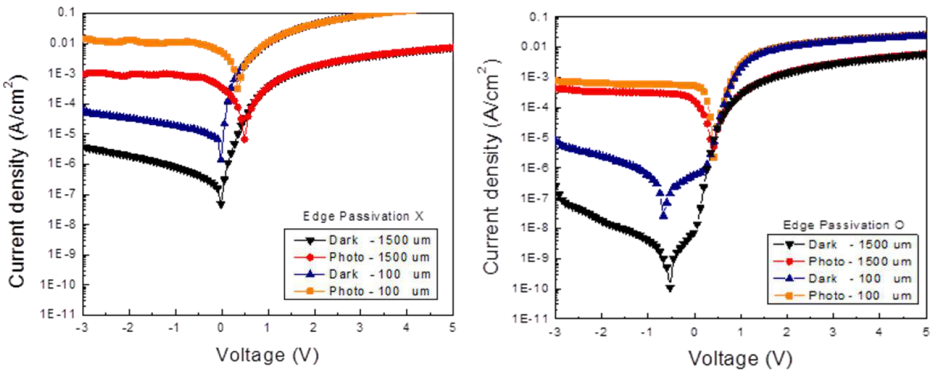

(a) (b)

Fig. 1. Current density vs. voltage characteristics (a) without edge passivation, (b) with edge passivation.

Acknowledgment

This work was supported by the Ministry of Trade, Industry and Energy (MOTIE) through the R&D program (20007145).

References

1. K. K. Banger, Y. Yamashita, K. Mori, et al. Nature Mater, vol 10, p. 45–50 (2011).
2. Y. H. Kim, J. S. Heo, TH. Kim, et al. Nature, vol. 489, p. 128–132 (2012).

Flexible pressure sensors based on heterogeneous graphene oxide

Sung Chan Jo[2] and Tae Hoon Lee[1]
[1,2] **Department of Electrical Engineering, Kwangwoon University, Seoul 01897, Republic of Korea**
Tel.:82-2-940-5140, E-mail: lthoon@kw.ac.kr

Graphene has been widely investigated for a variety of flexible electronic devices including pressure sensors owing to its outstanding electrical and mechanical characteristics.[1-2] However, since the resistivity of graphene itself does not change significantly with pressure, most graphene-based pressure sensors exploit the change in contact resistance between two graphene-based electrodes under applied pressure, which tends to cause unstable initial resistance right after the contact is made. Here, we demonstrate the use of large-area heterogeneous graphene oxide for flexible pressure sensors of high stability. Large-area chemical vapor deposited graphene is oxidized into graphene oxide in ozone and the resistance of the graphene oxide gradually increases with oxidation time. We observed the resistance change of graphene oxide by four orders of magnitude. By varying oxidation conditions including time, some parts of graphene are oxidized and some other parts remain as highly conductive graphene, which generates heterogeneous graphene oxide. Two heterogeneous graphene oxide layers are synthesized and placed face-to-face for the fabrication of resistive pressure sensors. As pressure is applied, the two heterogeneous graphene oxide layers in the pressure sensors contact each other and the conducting graphene regions in one layer can bridge conductive regions separated by insulating regions in the other layer, which significantly modulates the resistance of graphene oxide layers. We obtained flexible pressure sensors with a sensitivity of 1.4 kPa^{-1} using the heterogeneous graphene oxide layers. Also, we found that the sensor performances such as sensitivity and detection range are tunable by varying the degree of oxidation for graphene oxide. We believe that the flexible pressure sensors based on heterogeneous graphene oxide have high tunability for various applications and large room for further improvement.

Acknowledgment

This research was supported by the 「Nano Convergence Foundation」 funded by the Ministry of Trade, Industry and Energy (MOTIE) of Korea (no. 20000272). This work was also supported by the National Research Foundation of Korea (NRF) grant funded by the Korea government (MSIT) (No. 2019R1F1A1063572).

References

1. Chun S et al, *Nanoscale*, 7, 11652-11659 (2015)
2. Tian. H et al, *Sci. Rep*, 5, 8603 (2015)

Inkjet Printed Cellulose Nanofiber/Carbon Nanotube-based Flexible Pressure Sensor

Dong Keon Lee[1], Daesik Kim[1], and Yongtaek Hong[1*]
[1]Dept. of Electrical and Computer Engineering, ISRC, Seoul National University, Seoul, Korea
Tel.:82-2-880-9577, E-mail: yongtaek@snu.ac.kr

Flexible pressure sensors have been widely researched for new functionalities such as human-machine interaction, health monitoring, and electronic skins. Among various structures of flexible pressure sensors, porous structures have been widely implemented to improve sensor sensitivity for their high deformability. In this regard, cellulose has drawn attention for its intrinsic porous structure in pressure sensors. The porous cellulose structures were utilized as pressure sensor by applying conductive materials onto cellulose templates by soaking[1] or carbonizing[2] to form porous conductive structure sensitive to pressure. However, while fabrication of multiple pressure sensors in array form is essential for advanced applications like electronic skins, the conventional fabrication methods of conductive cellulose structure were not efficient in building pressure sensor arrays since each pixel needs to be fabricated individually due to incapability of patterning.

In this work, we report facile fabrication of a piezoresistive flexible pressure sensor by inkjet printing of cellulose nanofiber (CNF)/carbon nanotube (CNT) composite. The CNF/CNT aqueous dispersion was developed and optimized for inkjet printing by addition of polyvinyl alcohol (PVA) and ethylene glycol (EG). As shown in Figure 1(a), a top flexible electrode was perpendicularly laminated onto CNF/CNT film printed on a bottom electrode, forming vertical sandwich structure. The fabricated sensor transduced pressure applied to the CNF/CNT film to resistance change with sensitivity of 0.267 kPa^{-1}, as the fibroin structure (Fig. 1(b)) in CNF/CNT film was compressed. With inkjet printing of CNF/CNT composites, the facile patterning of sensor layers for high-resolution pressure sensor array is expected to be realized in future.

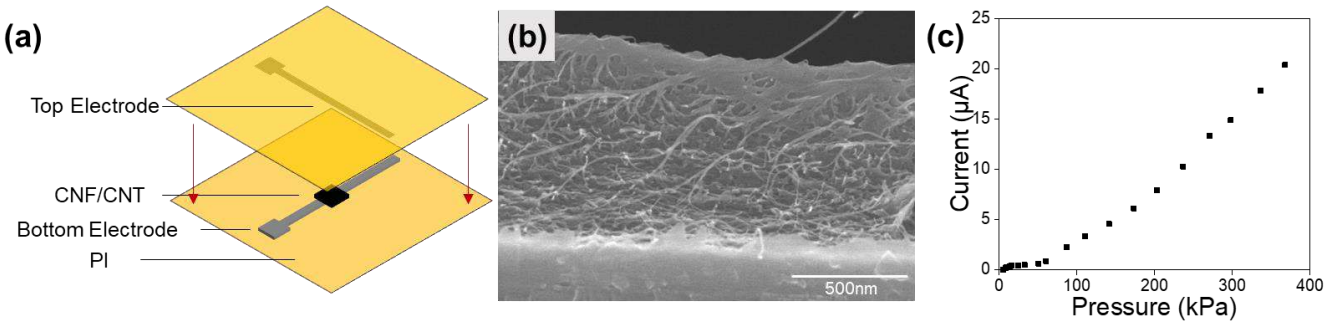

Fig. 1. (a) A schematic of the pressure sensor, (b) a cross-sectional scanning emission microscope (SEM) image of a fibroin structure in CNF/CNT film, and (c) sensor characteristics.

Acknowledgment

This research was supported by Samsung Electronics.

References

1. Z. Zhan, R. Lin, V. -T. Tran, J. An, Y. Fei, H. Du, T. Tran, and W. Lu, *ACS Appl. Mater. Interfaces*, 9, 37921 (2017).
2. S. Chen, Y. Song, F. Xu, *ACS Appl. Mater. Interfaces*, 10, 34646 (2018).

Facile Adhesive Patterning of 3-D Curved PDMS for Various Human-interactive Sensors

Jinsu Yoon[1,2], Geonhee Kim[1,2], Jongho Park[2], Hayun Kim[1,2], and Yongtaek Hong[1,2]
[1]Department of Electrical and Computer Engineering, Seoul National University, Seoul 08826, Korea
[2]Inter-University Semiconductor Research Center (ISRC), Seoul National University, Seoul 08826, Korea
Tel.:82-2-880-9567, E-mail: yongtaek@snu.ac.kr

The adhesion between human-interactive sensors and the skin is essential to increase the data fidelity of human vital signals. Numerous commercialized products as well as various researches have implemented soft and elastic materials such as acrylates[1], hydrogels[2], and silicons[3] to achieve the aforementioned goal. However, adhesives used in most epidermal sensors have an inevitable gap on arbitrary three-dimensional (3-D) curved surfaces, which lowers the fidelity of the signal received by the sensor. In this study, we introduce a simple method for patterning the adhesive that follows the curvature of an arbitrary 3-D curved surface conformably. After making an intaglio mold of a 3-D curved surface, ultraviolet (UV)-curable resin is printed on regions where adhesive patterns are required. Subsequently, thermosetting resin is poured on the mold and cured, thereby embedding the printed resin to form the final mold with the original curved shape. Finally, polydimethylsiloxane (PDMS) is thinly coated onto the manufactured final mold. Since UV-curable resin interferes the curing of PDMS, the uncured PDMS formed along the shape of the resin patterned in the desired shape acquires high stickyness (Fig. 1), and the produced PDMS substrate perfectly matches the original 3-D curved shape. Not only ultraconformity but also peel-off strength of 2.8 [N/m] is similar to or higher than that of a commercialized dermal tape as shown in Figure 2. Moreover, the substrate is bio-compatible, being made from PDMS and also it shows enough stretchability which exceeds that of human skin (≈ 30%). Due to these characteristics, when used as a substrate of a human-interactive sensor, high synchronization with a human vital signal is expected.

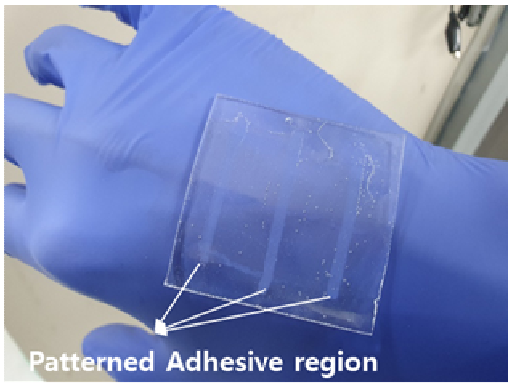

Fig. 1. Adhesive patterned PDMS

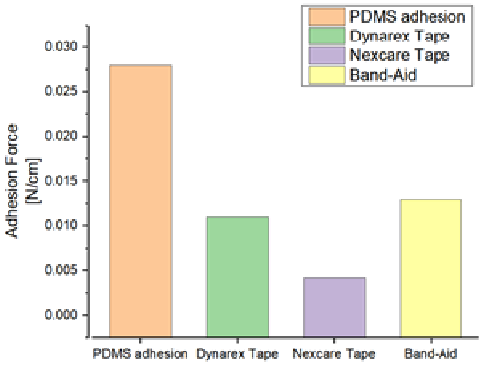

Fig. 2. Peel-off strength of various adhesives[4]

Acknowledgement

This work was supported by the Technology Innovation Program (No.20008801, Development of muscular function management solution based on electronic skin with EMG IMU and Strain sensor) funded By the Ministry of Trade, Industry & Energy(MOTIE, Korea).

References

1. R. Jovanovic, and M. A. Dube, *Can. J. Chem. Eng.*, 85(3), 341-349 (2007).
2. C. E. Brubaker, and P. B. Messersmith, Biomacromolecules, 12(12), 4326-4334 (2011).
3. Z. Gu, X. Wan, Z. Lou, F. Zhang, L. Shi, S. Li, B. Dai, G. Shen, and S. Wang, *ACS Appl. Mater. Interfaces*, 11(1), 1496-1502 (2018).
4. L. Liu, K. Kuffel, D. K. Scott, G. Constantinescu, H.-J. Chung, and J. Rieger, *Biomed. Phys. Express*, 4(1), 015004 (2018).

Stretchable Pressure Sensor Using Conductive Silicone Elastomer Composite with Rigid Island Structure

Jiseok Seo[1,2], Seongdae Choi[1,2], Hanul Kim[1,2], Daesik Kim[1,2], Hyungsoo Yoon[1,2], and Yongtaek Hong[1,2]*
[1] Department of Electrical and Computer Engineering, Seoul National University, Seoul 08826, Korea
[2] Inter-university Semiconductor Research Center (ISRC), Seoul National University, Seoul 08826, Korea
**Tel.:82-2-880-9567, E-mail: yongtaek@snu.ac.kr*

Among various sensors integrated with electronic skin (e-skin), pressure sensors enable e-skin to mimic the human tactile sense detecting the human body motion or applied mechanical stimuli. To enhance the comfort of wearing and the ability to collect signals, the stretchability of e-skin is needed to achieve conformability. In general, composites of elastomer and conductive particles are widely used for forming electrical connections in stretchable systems. Especially, ferromagnetic particles in elastomer composites are aligned along the applied magnetic field and lower the percolation threshold, thereby showing high electrical conductivity when the low Young's modulus of elastomer is retained.[1] These kinds of composites are applied to various stretchable components including electrodes, vertical interconnect access, and heat conductors due to their easy patterning process with magnetic fields.[2,3,4] In addition to an approach to stretchable electronics with elastomer composites, rigid island structures can be applied to disperse the mechanical stress in a stretched state. Combining these two strategies for stretchable systems, minimizing the change of device performances in a stretched state and enhancing stretchability can be achieved.

In this work, we demonstrated a stretchable pressure sensor using nickel/silicone elastomer composite with rigid island structures. Epoxy with Young's modulus of 1000 times higher than that of PDMS is employed as a rigid island to maximize the effect of redistribution of the mechanical stress. To verify the effectiveness of the rigid island, a strain simulation was conducted with the structure depicted in Fig. 1(a) and 1(b). When the entire device with the rigid island was stretched 30% in the x-axis, the mechanical stress was dispersed to the rest of the substrate and the maximum strain applied to the active area of pressure sensors was only about 4% in Fig. 1(c). Fabricated devices can be stretched up to 30% without any cracks or damage to the active area, consistent with the simulation result. As shown in Fig. 1(d), the sensitivity of the pressure sensor (*S*) changed only 2.6% when the strain of 30% was applied to the device.

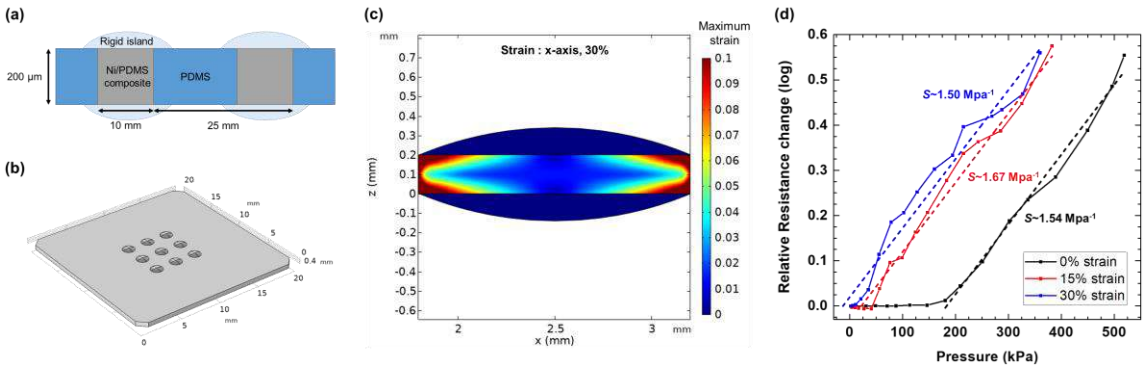

Fig. 1. Schematic images of the stretchable pressure sensor for stretching simulation presented at (a) side view and (b) quarter view. (c) Simulation results of maximum strain applied to the device under 30% strain of x-axis. (d) Log plot of relative resistance change according to the applied pressure under various strain.

Acknowledgment

This work was supported by the Industry technology R&D program (20006467) funded By the Ministry of Trade, Industry & Energy (MOTIE, Korea).

References

1. S.-H. Jang, Y.-L. Park, and H. Yin, *Mater.*, 9(4), 239 (2016).
2. S. Kim, J. Byun, S. Choi, D. Kim, T. Kim, S. Chung, and Y. Hong, *Adv. Mater.*, 26(19), 3094 (2014).
3. E. Oh, J. Byun, B. Lee, S. Kim, D. Kim, J. Yoon, and Y. Hong, *Adv. Electron. Mater.*, 3(3), 1600517 (2017).
4. B. Lee, H. Cho, K. T. Park, J.-S. Kim, M. Park, H. Kim, Y. Hong, and S. Chung, *Nat. Commun.*, 11, 5948 (2020).

Edge-illuminated Connectable Modular-pixel Aero Signage Display Whose Pixel Elements Enable to Joint Light Guides and Change Colors for Spatial Imaging

Kunio Sakamoto and Daiki Honda
Dept. of Intelligence and Informatics, Konan University, 8-9-1 Okamoto, Higashinada, Kobe 658-8501, Japan
Tel.:81-78-431-4341, E-mail: kunio@konan-u.ac.jp

Our research group presented one-way observable monocrome signage display in 2019 and the color signage in 2020. But the proposed signnage display has a defect that it emits no light itself and you cannot observe its signage in the dark night without another light source for illuminating surfaces of the signage display. This paper shows a one-way observable display for aero signage which enables to joint pixel modules having optical lighting guide block and emit light itself using this lighting guide.

Fig. (a) shows the principle of the light transmission guide using total internal reflection in optics. Let consider a light ray passing from glass into air and assume that all light beams are in the material. An angle θ of this case is smaller than the critical angle. Then it is at this point no light is transmitted into air because the beams are completely reflected. This is called the total internal reflection. The acrylic optical guide can pass through in only a material so that no light is transmitted into air using the total internal reflection phenomenon.

Fig. (b) shows the principle of generating colors by optical films sandwiched between a polarizer and a half mirror. It is the important technical point that all transmission light waves pass through all optical materials and observed signage is formed by the reflection light waves of the half mirror. At reflection light path by the half mirror, there are two cases whether the waves pass through the 1/4 wave plate or not. In case of not passing the wave plate, the light wave can again pass through the same polarizer. In case of passing the wave plate, the polarized light wave passed the polarizer passes through the 1/4 wave plate twice by mirror reflection. After this twice wave plate passing, the direction of polarization rotates 90 degrees, then the light wave whose polarization axis was rotated is blocked by the polarizer at the second time. As the result, the brightness of light waves is made a difference. To emit light itself, the authors attached the light transmitting guide block in front of the optical film components as shown in fig. (c). This is one element which emits light itself and shows a pixel dot.

You can also utilize cellophane(*or* OPP) films instead of 1/4 wave plate. The cellophane has birefringence characteristics. This birefringence of the cellophane can reconstruct color imaging. Moreover rotate the polarizer on dual OPP layers and each color shifts to some colors; blue, green and red. All you have to do is that you only choose the direction of polarizer or cellophanes as shown in fig. (d). Therefore you can change colors one by one after you rotate the dual OPP film layers between the polarizer and the half mirror shown in fig. (c).

This birefringence of the cellophane reconstructs color imaging as shown in fig. (e). The connectable lighting guide blocks reconstruct the unidirectional imaging which enables to emit lights and make invisible from back.

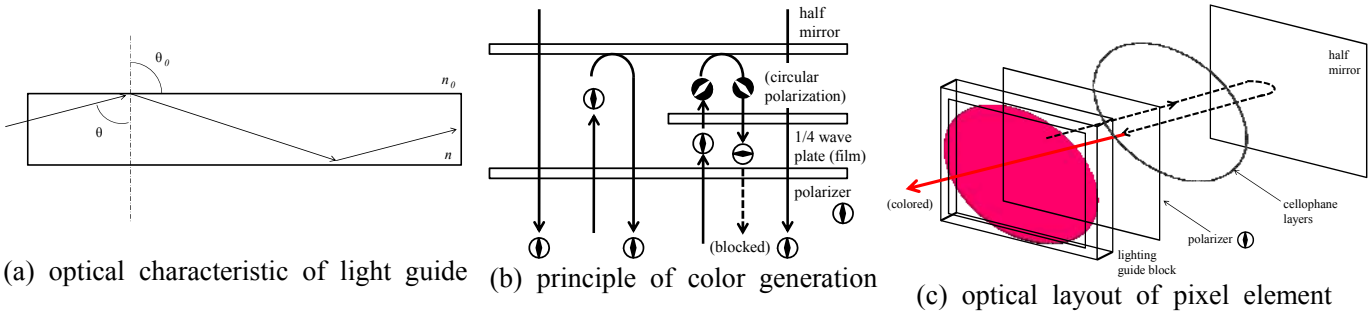

(a) optical characteristic of light guide (b) principle of color generation (c) optical layout of pixel element

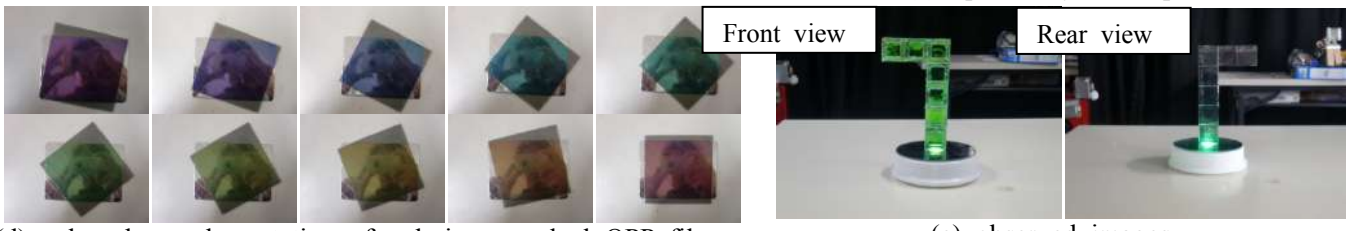

(d) color change by rotating of polarizer on dual OPP films (e) observed images

Fig. 1. Edge-lit one-way observable signage display using color change & pixel joint mechanism

A Study on the Performance Improvement of High-Power White LED Lightings Depending on the Arrangement of the Red Quantum Dot Caps

Gi Jung Lee[1], Jung Gyun Lee[1], Seung Chan Hong[1], Taehee Park[2], Young Wook Ko[2] and Jae-Hyeon Ko[1]
[1]School of Nano Convergence Technology, Nano Convergence Technology Center, Hallym University, Chuncheon, Gangwon-do, 24252, Korea
Tel.:82-33-248-2056, E-mail: hwangko@hallym.ac.kr
[2]GLVISION Co, Ltd., Geumgang-ro, Seo-myeon, Cheorwon-gun, Gangwon-do, 24062, Korea

In the case of WLED (White Light Emitting Diode) lightings, applying a yellow phosphor coating on a blue LED chip is the most conventional, but the wavelength component in the deep red region is insufficient, which reduces the color rendering index (CRI), which is one of the evaluation indicators for the performance of lighting.

In order to solve this problem, research has been conducted to apply quantum dots having high color purity and a narrow peak width to conventional WLEDs [1-2]. In this study, we tried to improve the CRI of commercial white LED lightings by fabricating a red quantum dot with a core-shell structure of CdSe/ZnS as a cap-shaped structure that could be attached on each WLED.

In order to accurately evaluate the improvement of the WLED lighting performance by applying the quantum dot cap, we have studied an optimized arrangement pattern of QD caps with sufficient chromaticity and luminance uniformities. Three types of quantum dot caps having different emitting spectra and QD concentrations were arranged in an optimized pattern to compare the optical performance.

Figures 1(a) and (b) are the emission spectra of the WLED lighting without and with QD caps and the color rendering properties of the R1~15 color samples. It can be seen that the intensity of the short wavelength region decreases while the intensity of the red region increases as blue and green light is converted partly into red light, thereby improving color rendering. This study clearly shows that the adoption of QD caps is an effective way to enhance CRI of conventional white LED lightings.

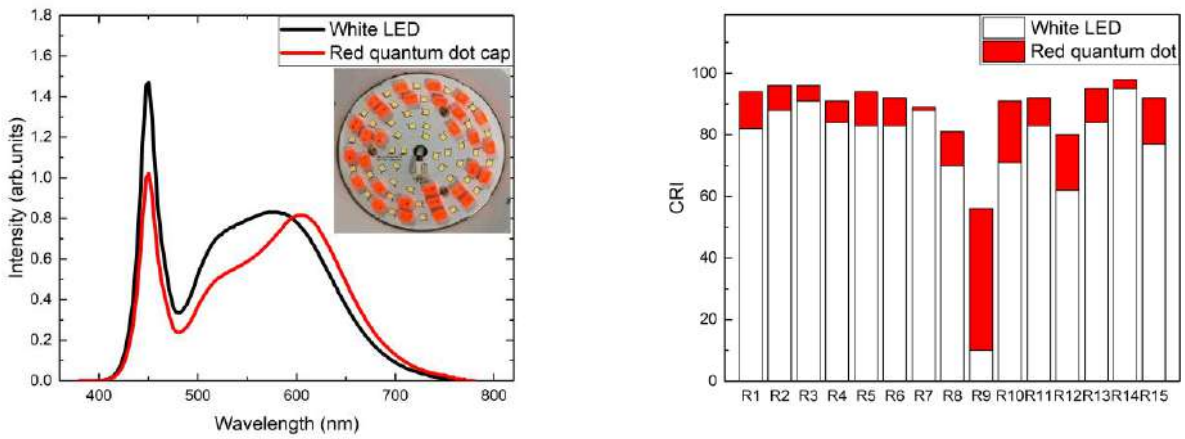

(a) (b)

Fig. 1. (a) The appearance of the lighting with the red quantum dot cap used in the actual measurement, and the front spectrum of the light with the red quantum dot cap and the Wihte LED. (b) Color rendering index of white LED lighting with white LED and red quantum dot cap attached.

References

1. Jong-Oh Kim, Hyeong-Seob Jo, and Uh-Chan Ryu, " Improving CRI and Scotopic-to-Photopic Ratio Simultaneously by Spectral Combinations of CCT-tunable LED Lighting Composed of Multi-chip LEDs", Current Optics and Photonics Vol. 4, No. 3, June 2020, pp. 247-252 (2020)
2. J. Y. Lien, C. J. Chen, R. K. Chiang, and S. L. Wang, “High color-rendering warm-white lamps using quantum-dot color conversion films,” Opt. Express 24, A1021–A1032 (2016)

Realization of High Color Rendering Index of Conventional White Lighting by Using Red Quantum Dot Films

Seung Chan HONG[1], Gi Jung LEE[1], Se Ri PARK[1], Sung Tae GWAK[1], Young Wook KO[2], Young Duk KIM[3] and Jae Hyeon KO[1]

[1]School of Nano Convergence Technology, Hallym University, Chuncheon 24252, Korea

E-mail: hwangko@hallym.ac.kr

[2]Cheorwon Plasma Research Institute, Cheorwon-gun, Gangwon-do, 24062, Korea

[3]GLVISION Co, Ltd., 7400 Geumgang-ro, Seo-myeon, Cheorwon-gun, Gangwon-do, 24062, Korea

Many white LEDs used in the lighting market consist of YAG ($Y_3Al_5O_{12}$), which is a yellow phosphor, and an InGaN blue LED chip. In this case, CRI (Color Rendering Index) is not sufficient because of the lack of deep red component [1]. One of the methods for improving CRI is to apply red-green phosphors to blue LED. However, there are side effects, such as thermal stability or cost. Another way is to use red quantum dots to enhance long-wavelength components in the emitting spectrum [2].

To verify this, we applied red QD films to a conventional 15W white LED lighting having CRI~80 and CCT (Color Correlated Temperature) of ~5700K. Red QD film and QD wall were synthesized by using QDs of a CdSe/ZnS core/shell structure. The QD wall was attached on a highly reflecting film. We tested six different configurations using a diffuser plate of thickness 2mm. The "none" case is the one without any QDs; the "wall" case uses only QD wall; the "top" and the "bottom" case denotes the case where the QD film is attached on or below the diffuser plate, respectively. Especially, when comparing the top and the bottom cases, the CRI of the bottom case was higher. Figure 1 shows that the CRI increases more substantially when QD wall is combined with QD film. Interestingly, in the case of bottom+wall, the CRI increases to 95.7. In the case of bottom configuration, the light passes through the diffuser plate after red excitation via the QD film, which makes it more favorable to additionally utilize the unconverted blue light in the optical cavity. In this study, we clearly showed that the CRI can be increased by more than 90 through proper placement of the QD film in the conventional white LED lighting. Further improvement can be expected by applying the QD wall.

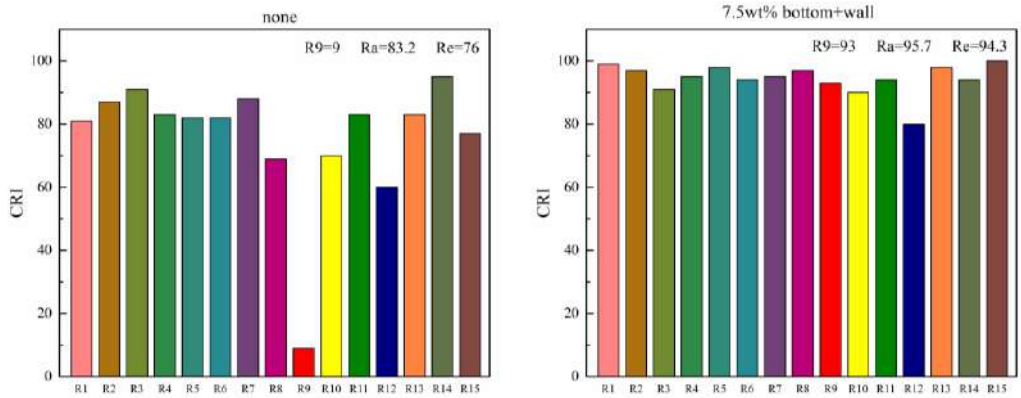

[Figure1] CRI of case of "none" and "bottom+wall" using QD film and QD wall

Acknowledgment

This research was supported by the Ministry of Trade, Industry & Energy (MOTIE), Korea Institute for Advancement of Technology (KIAT) through the program of Smart Specialized Infrastructure Construction (No. P0013743).

References

[1] Y. N. Ahn, K. D. Kim, G. Anoop, G. S. Kim, and J. S. Yoo, "Design of highly efficient phosphor-converted white light-emitting diodes with color rendering indices (R1 - R15) >/ = 95 for artificial lighting," Sci. Rep. 9(1), 16848 (2019).

[2] J. Y. Lien, C. J. Chen, R. K. Chiang, and S. L. Wang, "High color-rendering warm-white lamps using quantum-dot color conversion films," Opt. Express 24, A1021− A1032 (2016)

Methacrylate-Functionalized Perovskite Nanocrystals Encapsulated by Siloxane Hybrid for Stable Color-Converting Materials in Display

Yongmin Shin[1], Junho Jang[1], Hyungshin Kweon[1] and Byeong-Soo Bae[1]
[1]**Wearable Platform Materials Technology Center, Dept. of Mater. Sci. & Engineering, Korea Advanced Institute of Science and Technology, Daejeon 34141, Korea**
Tel.:82-42-350-5119, E-mail: bsbae@kaist.ac.kr

Perovskite nanocrystals (PNCs) have attracted significant interest in display industry due to facile wavelength tunability, high photoluminescence quantum yield (PLQY), very narrow emission bandwidth that induces the wide color gamut, compared to inorganic quantum dots. However, PNCs are vulnerable to oxygen, moisture and light. Especially, they are easily decomposed in moisture-contained environments. To overcome these instability issues, several strategies have been suggested such as fabrication of inorganic shell structure and dispersion into polymeric matrix. However, those methods encountered limited stabilities due to the physical protection of PNCs from oxygen and moisture.

Previously, our group reported stable cross-linked PNCs (passivated by oleic acid (OA) and oleylamine) chemically encapsulated in siloxane matrix at molecular scale. However, it featured low PLQY of as-cured film, and it is necessary to improve photostability under light illumination with high flux.

Herein, we report methacrylate-functionalized PNC (M-PNC), passivated by OA and amine-methacrylate-siloxane ligand that is synthesized via in situ sol-gel reaction during PNC fabrications. Amine-methacrylate-siloxane ligand passivates the A-site defect of PNC, and improve the compatibility to siloxane matrix. M-PNC/siloxane resin is synthesized via in situ sol-gel reaction in the presence of M-PNCs. Subsequently, synthesized resin is solidified by UV-induced curing method. During curing process, unsaturated carbon bond in siloxane ligand and OA is chemically cross-linked to the siloxane matrix, which induces enhancing stability of PNCs. As a result, M-PNC/siloxane composite exhibits high initial PLQY of ~70%. With chemical cross-linking between M-PNC and siloxane matrix, the composite maintains its high PLQY in ambient condition, water, and various polar solvents. In particular, M-PNC/siloxane composite film shows highly stable luminescence even in high temperature with high humidity (85 ℃/ 85% relative humidity, RH), and continuous blue light illumination.

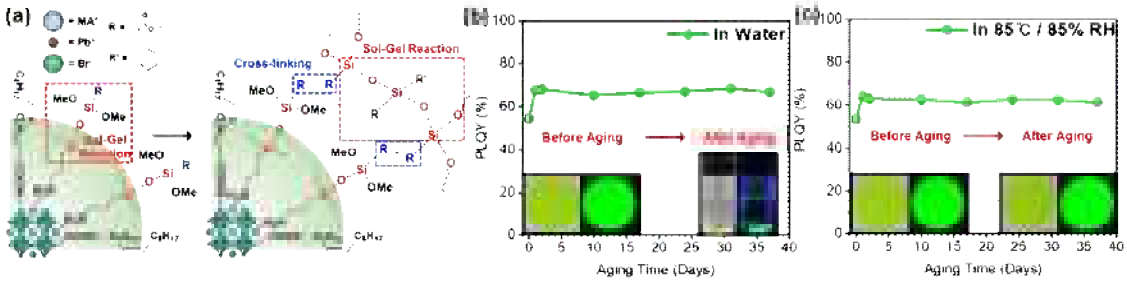

Fig. 1. (a) Schematic diagram of M-PNC/siloxane Hybrid. PLQY traces of highly stable M-PNC/siloxane composite film in (b) water and (c) 85 ℃/ 85% RH

Acknowledgment

This work was supported by the Wearable Platform Materials Technology Center (WMC) (NRF-2016R1A5A1009926) funded by National Research Foundation of Korea (NRF) Grant of the Korean Government (MSIT)

References

1. J. Jang, Y.-H. Kim, S. Park, D. Yoo, H. Cho, J. Jang, H. B. Jeong, H. Lee, J. M. Yuk, C. B. Park, D. Y. Jeon, Y. -H. Kim, B. -S. Bae, and T. -W. Lee, *Adv. Mater.,* 33(3), 2005255 (2021).
2. H. Y. Kim, D.-E. Yoon, J. Jang, D. Lee, G.-M. Choi, J. H. Chang, J. Y. Lee, Doh. C. Lee, and B.-S. Bae, *J. Am. Chem. Soc.,* 138(50), 16478 (2016)

Microfluidic strain sensor using electroluminescent ZnS:Cu particles

Hong-Sik Eom[1] and Suk Tai Chang[1]
[1]School of Chemical Engineering and Materials Science, Chung-Ang University,
84 Heukseok-ro, Dongjak-gu, Seoul 06974, Korea
Tel.:82-2-820-5889, E-mail: stchang@cau.ac.kr

Wearable devices should be wireless in order to be used on the human body in real life. Nowadays, sensors are biocompatible, skin-mountable, stickable on skin, possible to express stimuli applied to the skin as some type of signal. However, almost sensors are not completely wireless. Wireless means no physical connect with multimeter and battery. Proposed concept in this paper is the free from multimeter through changes in the type of signal that expressing stimuli. Herein, the sensor expresses strain by using the ZnS:Cu electroluminescence particles that emitting light in the electric field which is formed from LiCl electrolyte electrode as an light signal. The pattern of sensor that fabricated with PDMS refer to a strain gauge. Strain in two direction of this sensor can be expressed and signals in each direction can be clearly distinguished. And there is application that express the color signal with light signal by overlapping the two sheets.

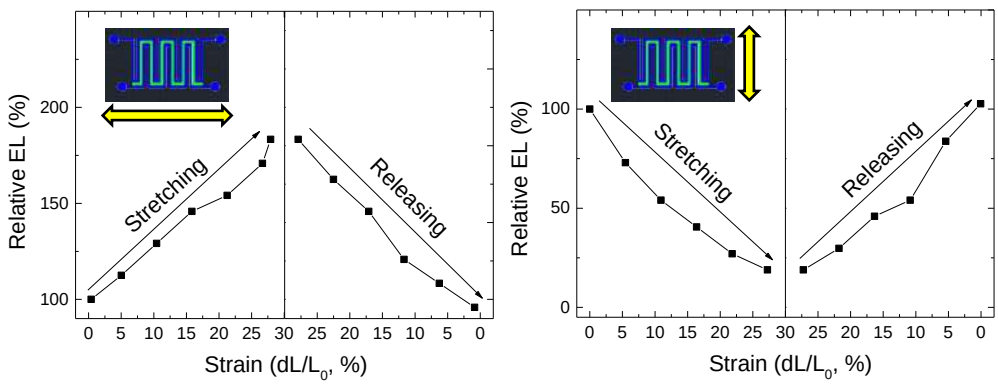

Fig. 1. Relative electroluminescent as a function of strain

Acknowledgment

This work was supported by the National Research Foundation of Korea (NRF) grant funded by the Korean government (MSIT) (No. 2019R1A2C1006413) and the Competency Development Program for Industry Specialists of the Koran Ministry of Trade, Industry and Energy (MOTIE) operated by Korea Institute for Advancement of Technology (KIAT) (No. P0012453, Next-generation Display Expert Training Project for Innovation Process and Equipment, Materials Engineers).

References

1. H.M. Souri, et al, *Advanced intelligent systems.*, 2, 20000039 (2020).
2. S.B. Cheng, et al, *Advanced materials interfaces.*, 6, 1900985 (2019).
3. A.D. Leber, et al, *Advanced functional materials.*, 29, 1802629 (2019).
4. B. Nie, et al, *Advanced functional materials.*, 29, 1808786 (2019).

Efficiency Variation Analysis Depending on Hosts in ν-DABNA TADF Devices

*Kijoon Yang[1#], Hyuna Lee[1], Soon Jae Hwang[1], Kenkera Rayappa Naveen[1] and Jang Hyuk Kwon[1]**
[1]Department of Information Display, Kyung Hee University, 26, kyungheedae-ro, Dongdaemun-gu, Seoul, 02447, Republic of Korea
Tel.:82-2-961-9147, E-mail: jhkwon@khu.ac.kr

Recently, ν-DABNA has been actively researched as a highly efficient blue thermally activated delayed fluorescence (TADF) material in organic light emitting diodes (OLED) due to its high photoluminescence quantum yield (PLQY), narrow full width at half maximum (FWHM), small ΔE_{ST} of 0.03eV, and short delayed exciton lifetime. [1] Interestingly, ν-DABNA TADF device exhibits large variation of external quantum efficiency (EQE) values depending on the host materials. We selected several types of hosts and compared the efficiency of devices utilizing several host materials. The selected hosts were hole type non-polar 3,3'-di(9H-carbazol-9-yl)-1,1'-biphenyl (mCBP), bipolar 2,6-bis(3-(carbazol-9-yl)pyridine (DCzpy), electron type polar host dibenzo[b,d] furan-2,8-diylbis (diphenyl- phosphine oxide) (DBFPO), and electron type pyridine based host material (E-TH). We fabricated four TADF devices with these hosts and optimized the device efficiencies. The $EQEs_{max}$ of devices using mCBP, DCzpy, DBFPO and E-TH host were 19.0, 20.1, 28.7 and 25.2% respectively (Fig. 1. (a)). These devices show large efficiency variation.

Therefore, in order to investigate the reason of such variation, we check device efficiency values based on this equation [$EQE = \Phi_{PL} \times \beta \times \gamma \times \eta_{out}$]. Here Φ_{PL} is the PLQY, β is the exciton generation factor, γ is the carrier balance ratio, and η_{out} is the light extraction efficiency. Assuming η_{out} is constant and γ is optimized, we firstly measured and compared the PLQY. It is noticed that the PLQYs of mCBP, DCzpy, DBFPO and E-TH hosts based film were 90.2, 88.9, 96.7 and 84.1% respectively. However, the PLQY values solely cannot explain the reason completely. Hence, we analyzed the amount of β depending on light-emitting method. Since DBFPO and E-TH have deeper HOMO energy level than mCBP and DCzpy, trap-assisted emission (TAE) is more dominant in DBFPO and E-TH based devices, whereas energy transfer emission (ETE) is more dominant in mCBP and DCzpy based devices relatively. Since ν-DABNA has small delayed portion (Φ_{Delay}) and the triplet spin density distribution is surrounded by phenyl moieties (Fig. 1. (b)), it is supposed that utilization of triplet excitons may be inferior in ETE than TAE (Fig. 1. (c)). [2] Thus, it has some differences in β value. Accordingly, so as to prove the assumption, we analyzed and compared Dexter energy transfer (DET) rate tendency by equation and experiments. [3] The detailed analysis about DET will be discussed at the presentation.

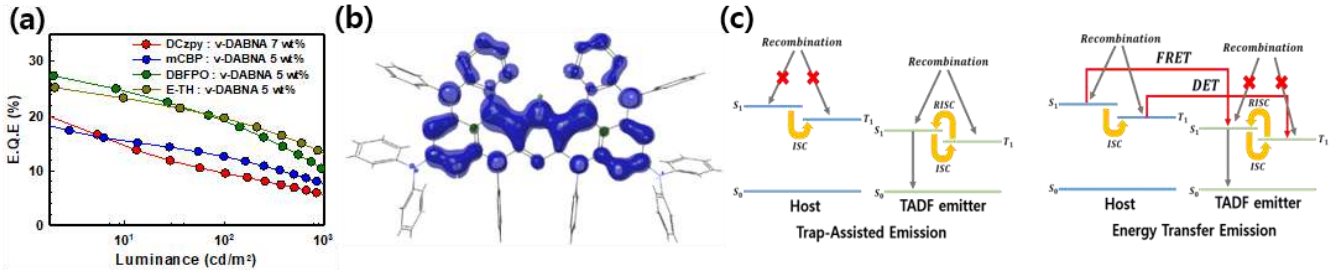

Fig. 1. (a) EQE vs Luminance curve, (b) Triplet spin density distribution of ν-DABNA, (c) Trap-assisted emission vs Energy transfer emission

Acknowledgment

This work was supported by the National Research Foundation of Korea (Grant No. NRF-2019M3D1A2104019) and by BK21 FOUR Program (Department of Information Display, Kyung Hee University) funded by Ministry of Education (MOE, Korea).

References

1. Yasuhiro Kondo, Yasuyuki Sasada, and Takuji Hatakeyama, Nature photonics, 13, 678-682 (2019).
2. Minghan Cai, Dongdong Zhang and Lian Duan, ACS Appl Mater & Interfaces, 11, 1096-1108 (2019).
3. Akitaka Ito, David J. Stewart, and Thomas J. Meyer, J. Phys. Chem. B, 117, 3428-3438 (2013).

Analysis of recombination zones using sensing layer method with aging in phosphorescent organic light emitting diodes

Hojung Shin[1], Yoonkyoo Lee [1], Jin Won Sun[1] and Changwoong Chu[1]
[1]Display Research Center, Samsung Display Co., Yongin, Korea
Tel.:82-31-5181-5010, E-mail: changwoong.@samsung.com

In this paper, the change of recombination zones as different aging times are demonstrated. In a variety of hole transporting (HT): electron transporting (ET) host ratios, emitting zone are formed in different distributions. The study of the emission zone in the emitting layer (EML) is vital factor to optimize the perfomance device structure. The spatial of exciton recombination is an important factor because it is profoundly relative to exciton quenching and OLED high efficiency with excitation. There is a wide variety of techniques to used to provide the knowlege of the emission zone, nemely, the use of sensing layers(1-2), messuring and modeling of the angle-dependent electroluminescence(3), electro-optical simualtion. (4-5). We are used to sensing layer, which is direct analysis method for recombination zone. Different HOMO level dopants shows different spatial distributions of exciton density. Initial distribution of exciton profile is mainly affected by host ratios and degradation of exciton density is correlated with dopant characteristics. It is not easy to conclude that the change of recombination spatial distribution as degradation with sensing layer method because it is mixed with both pure change of emitting intensity and lifetime degradation, which decreases quantum efficiency. As inital exciton distribution centered, the lifetime(T95) is long.

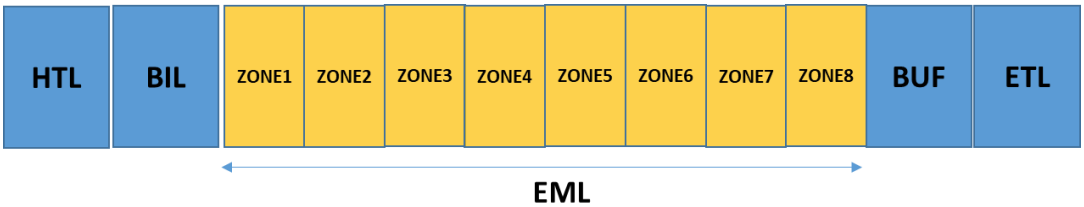

Fig. 1. Schematic of Sensing layer structure for study of spatial exciton recombination zone.

Acknowledgment

References

1. Erickson N. C., Holmes R. J., Investigating the Role of Emissive Layer Architecture on the Exciton Recombination Zone in Organic Light-Emitting Devices. *Adv. Funct. Mater.*, 23, 5190−5198 (2013).
2. Coburn C., Lee, J., Forrest S. R., Charge Balance and Exciton Confinement in Phosphorescent Organic Light Emitting Diodes. *Adv. Opt. Mater.,* 4, 889−895 (2016).
3. van Eersel H., Bobbert P. A., Janssen R. A. J., Coehoorn, R. Monte Carlo Study of Efficiency Roll-off of Phosphorescent Organic Light-Emitting Diodes: Evidence for Dominant Role of Triplet-Polaron Quenching. *Appl. Phys. Lett.*, 105, No. 143303 (2014).
4. van Mensfoort S. L. M., Carvelli M., Megens M., Wehenkel D., Bartyzel M., Greiner, H., Janssen, R. A. J., Coehoorn, R., Measuring the Light Emission Profile in Organic Light-Emitting Diodes with Nanometre Spatial Resolution. *Nat. Photonics*, 4, 329−335 (2010)
5. M. Regnat, K. P. Pernstich, S. Zufle, and B. Ruhstaller, Analysis of the Bias-Dependent Split Emission Zone in Phosphorescent OLEDs, *ACS Appl. Mater. Interfaces*, 10, 31552-31559 (2018)

Metal-Free and Pure Organic Phosphorescent Green Emitters for Non-Doped OLEDs by Using Secondary Interaction Effect

*Taehyun Kim, Hae Un Kim and Taiho Park**
Dept. of Chemical Engineering, Pohang University of Science and Technology (POSTECH), Pohang, Gyeongbuk 37673, Korea
Tel.:82-54-279-5295, E-mail: kth1792@postech.ac.kr

There are aggregation-caused quenching issues and environmental problems of conventional fluorescent OLEDs and transition metal based phosphorescent OLEDs (PhOLEDs). Therefore, achieving the 100% internal quantum efficiency of pure organic emitters with aggregation-induced emission (AIE) characteristics for non-doped OLEDs can solve the conventional host-guest system issues of conventional OLEDs. Herein, we synthesize two metal-free green emitters, adopting A-π-D structure consisting of electron acceptor, π linker, and electron donor moieties. As shown in Fig. 1., introducing phenyl (Ph) and pyridine (Py) linkers, we can achieve triplet harvesting ability and AIE features. Moreover, secondary interactions are observed in N atom of Py emitter, which can suppress the non-radiative decay pathway and increase high photoluminescence quantum yield. Also, we figure out that the intramolecular secondary interaction triggers room temperature phosphorescence (RTP) whose lifetime is about milliseconds. Therefore, according to the enhanced PLQY and AIE effect, we fabricate non-doped devices via vacuum deposition. The devices perform high external quantum efficiency (EQE) of 11.06% which is high efficiency among the AIE featured pure organic PhOLEDs.

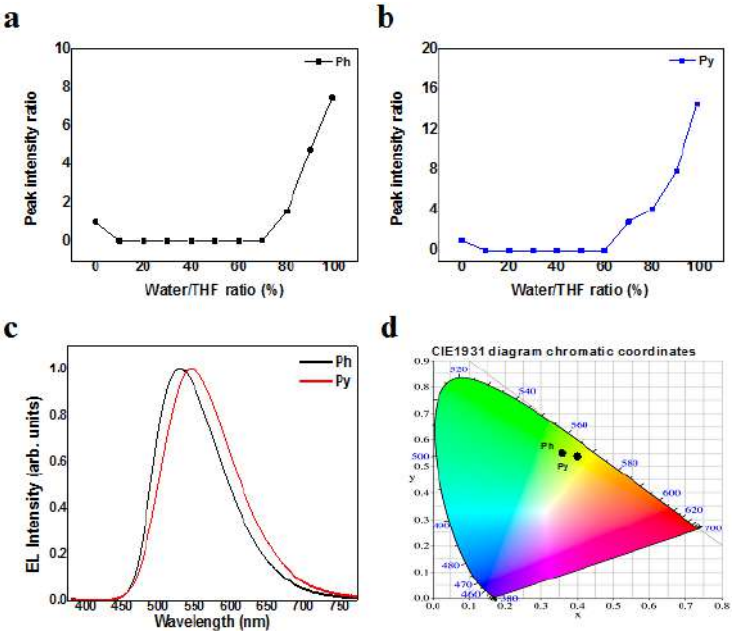

Fig. 1. Emission peak intensity ratio of (a) Ph and (b) Py, (c) Electroluminescence intensity profile, (d) CIE 1931 coordinates of non-doped OLEDs.

Investigation of substituent effects on cyclometalating ligand Ir(III) complexes for solution-processable red-NIR organic light-emitting diodes

Chanhyeok Kim, Hae Un Kim, and Taiho Park*
Dept. of Chemical Engineering, Pohang University of Science and Technology (POSTECH), Pohang, Gyeongbuk 37673, Korea
Tel.:82-54-279-5295, E-mail:chanhkkim@postech.ac.kr

For the next-generation devices such as information-secure devices and night vision displays, the fundamental and practical understanding of the near-infrared(NIR)-emitting materials have been studied. However, the small emissive bandgap toward several nonradiative decay pathways is still vulnerable, which approaches highly efficient, stable, inexpensive NIR-emitting luminophores an enormous challenge. Appropriate structural designs are essential for producing an intense NIR-emission. We developed a series of deep-red to NIR-emissive iridium(III) complexes(Ir1-Ir4) to research the effects of electron-donating and accepting substituents from the quinoline moiety of (benzo[*b*]thiophen-2-yl)quinoline ligands, and also performed an in-depth and comparative photophysical study in the solution, neat powder, doped polymer film, and freeze matrix to inquire about the effects of substitution on the excited state properties. Ir1, Ir2, and Ir4 were prospective novel materials with bright phosphorescence quantum efficiency in doped polymer films. Using these molecules, deep-red to NIR emissive organic light-emitting diodes(OLEDs) were developed using a solution-processable method.

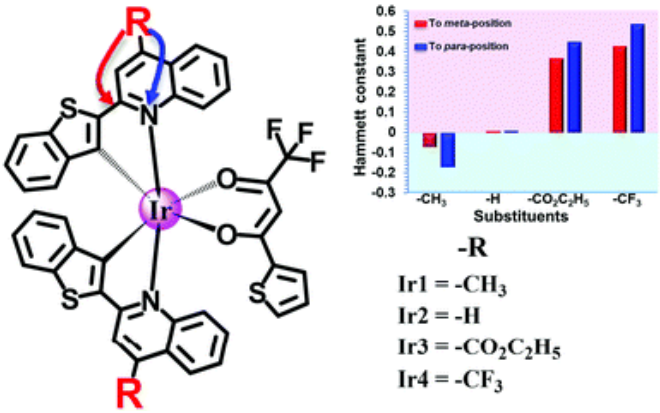

Fig. 1. Structure of Ir1-Ir4 and relative electronic effects of the substituents represented as Hammett constants toward the *ortho* and *para* positions.

Acknowledgment

This work was supported by grants from the Center for Advanced Soft Electronics under the Global Frontier Research Program (2012M3A6A5055225), and the Technology Development Program to Solve Climate Changes of the National Research Foundation (NRF) of Korea (2015M1A2A2056216 and 2016M1A2A2940912).

References

1. Adachi, C.; Baldo, M. A.; Thompson, M. E.; Forrest, S. R., Nearly 100% internal phosphorescence efficiency in an organic light-emitting device. *J Appl Phys* **2001,** *90* (10), 5048-5051.
2. Williams, E. L.; Li, J.; Jabbour, G. E., Organic light-emitting diodes having exclusive near-infrared electrophosphorescence. *Appl. Phys. Lett.* **2006,** *89*, 083506.
3. Qiao, J.; Duan, L.; Tang, L.; He, L.; Wang, L.; Qiu, Y., High-efficiency orange to near-infrared emissions from bis-cyclometalated iridium complexes with phenyl-benzoquinoline isomers as ligands. *J. Mater. Chem.* **2009,** *19*, 6573.

Introducing Rigid Ancillary Ligand for Structural Robustness towards Highly Efficient Red to NIR Emissive OLEDs

*Jeongsu Kim, Chanhyeok Kim, and Taiho Park**
Dept. of Chemical Engineering, Pohang University of Science and Technology,
77 Cheongam-Ro, Nam-Gu, Pohang, Gyeongbuk 37673, Korea
Tel.:82-54-279-5295, E-mail: integerkim@postech.ac.kr

The need for the development of flexible, highly efficient and inexpensive deep-red emitting luminophores has increased for the potential application such as medical nosology, dark-vision displays and photobiomodulation therapy. In this work, two deep-red emissive iridium(III) complexes, **Ir1-pic** and **Ir2-pic**, have been synthesised, having electron-donating group (-CH_3) substituted and unsubstituted cyclometalating (benzo[b]thiophen-2-yl)quinoline and picolinate auxiliary ligands. The structure and coordination design were certified by single-crystal X-ray diffraction (Fig. 1). The picolinate ligand enabled a deep-red emission due to rigid structure and high levels of triplet. Whereas, the b-diketonate ligand caused an excited-state geometrical distortion because of the triplet spin density population and flexibility. Therefore, both complexes achieved outstanding emission efficiencies (FPL = 0.48 and 0.37, respectively) and were applicable to deep-red dopants in OLEDs solution-processing. The unoptimized devices with varied dopant concentrations were observed to have the highest external quantum efficiencies of 5.03% and 3.41%, respectively.

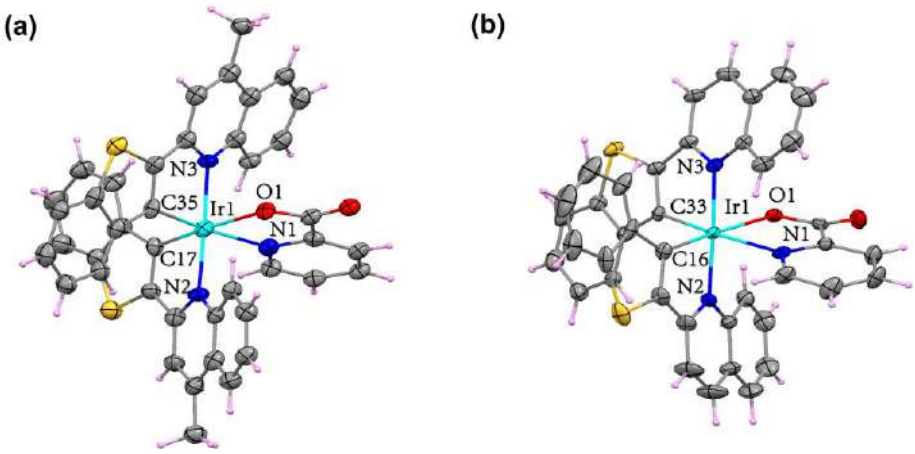

Fig. 1. Crystal structure of the (a) Ir1-pic complex, (b) Ir2-pic complex

Acknowledgment

Synchrotron single crystal X-ray diffraction (XRD) were performed on the 2D beamline of the Pohang Acceleration Laboratory (PAL; Pohang, Korea). This work was supported by grants from the Center for Advanced Soft Electronics under the Global Frontier Research Program (2012M3A6A5055225), and the Technology Development Program to Solve Climate Changes of the National Research Foundation (NRF) of Korea (2015M1A2A2056216 and 2016M1A2A2940912). This research was also partially supported by the Samsung Display Corporation.

References

1. C. Adachi, M. A. Baldo, M. E. Thompson and S. R. Forrest, *J Appl Phys*, 2001, **90**, 5048-5051.
2. A. F. Rausch, M. E. Thompson and H. Yersin, J. Phys. Chem. A, 2009, 113, 5927‑ 5932.
3. W. Cho, G. Sarada, A. Maheshwaran, Y.-S. Gal, Y.Nam, J. Yong Lee and S.-H. Jin, J. Mater. Chem. C, 2017, 5, 10029–10038.
4. V. G. Sree, W. Cho, S. Shin, T. Lee, Y.-S. Gal, M. Song and S.H. Jin, Dyes Pigm., 2017, 139, 779–787.

Laser desorption/ionization time of flight mass spectrometry for OLED materials and devices

Yoonseok Oh[1], Min Gee Kim[1], Jooyeon Oh[1], Dongjin Shin[1]
KyoungHee Sung[2], SeokRyoul Lee[2]
[1]ASTA Inc., 660, Daewangpangyo-ro, Bundang-gu, Seongnam-si, Gyeonggi-do, Korea
Tel.:82-31-606-1847, E-mail: ysoh@astams.com
[2]LG Display, 245, LG-ro, Wollong-myeon, Paju-si, Gyeonggi-do, Korea

Mass spectrometry is the precise analytical method for measuring the mass-to-charge ratio of molecules in the sample. It is useful for monitoring the change of the chemical composition such as the degradation of raw materials. Many mass spectrometry instruments are being used for OLED analysis such as liquid chromatography mass spectrometry (LC-MS) [1], time of flight secondary ion mass spectrometry (TOF-SIMS) [2], and laser desorption/ionization time of flight mass spectrometry (LDI-TOF MS) [3].

In this study, we introduce the LDI-TOF MS system with built-in optical microscope and tightly focused laser with beam size less than 5 μm diameter that is suitable for analyzing both OLED materials and devices. Mass spectra of raw powder materials were obtained directly by LDI-TOF MS with simple preparation step without any solvent. Therefore, it can give information of unsolubable materials that can't be analyzed by LC-MS. Also, built-in optical microscope and tightly focused laser system make it possible to analyze the narrow space like the single pixel of OLED panel. The mass imaging of OLED panel (Fig. 1) with high spatial resolution of 5 μm was obtained. Each pixel of OLEDs were clearly distinguished with mass images.

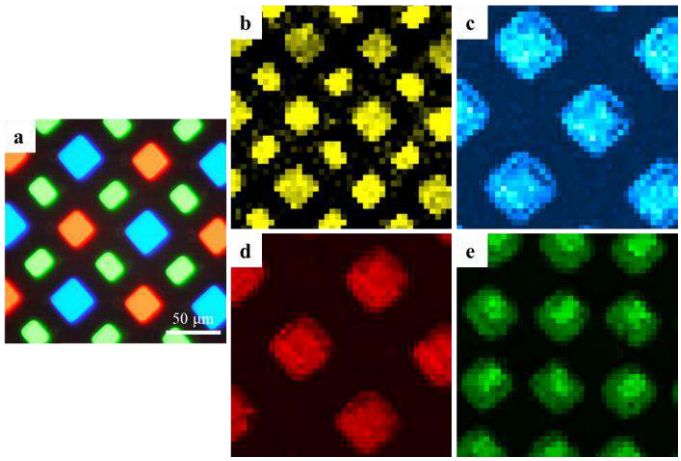

Fig. 1. (a) Optical microscopic image of OLED panel and (b-e) LDI-MSI images at different mass-to-charge ratio. All images have the same magnification.

Acknowledgment

This work was supported by the Technology Innovation Program (or Industrial Strategic Technology Development Program, 20010443, Development of mass spectrometry for OLED structure and stability analysis) funded By the Ministry of Trade, Industry & Energy (MOTIE, Korea).

References

1. V. Sivasubramaniam, *et al.*, *Cent. Eur. J. Chem.*, 7, 836 (2009).
2. W.-Y. Chen, *et al.*, *App. Surf. Sci.*, 252(19), 6594-6596 (2006).
3. A. E. Paulson, *et al.*, *J. Am. Soc. Mass Spectrom.* 31(12), 2443–2451 (2020).

Ideality Factor of InGaN-Based Light-Emitting Diodes Investigated by Photovoltaic Parameters

SangJin Min[1], Gyeong Won Lee [1], Jong-In Shim[1] and Dong-Soo Shin[1]
[1]**Dept. of Photonics and Nanoelectronics, Hanyang University ERICA, Ansan, Gyeonggi-do 15588, Korea**
Tel.:82-031-400-5488, E-mail: dshin@hanyang.ac.kr

Nowadays, InGaN-based light-emitting diodes (LEDs) are commonly found in various commercial lighting products. Applications such as displays and visible-light communications are the areas where the InGaN LEDs can also be utilized. In InGaN LEDs, however, there still exist some unsolved issues such as sidewall leakage, efficiency droop and thermal dissipation due to nonradiative recombinations. For solving these problems, it is sometimes beneficial to exclude an additional potential drop outside the active junction in order to have a better understanding of the carrier consumption in the active region.

In this work, we focus on the ideality factor of the InGaN-based blue LEDs, which reflects the recombination mechanisms of the device [1]. We utilize the photovoltaic paramters such as short-circuit current (I_{SC}), open-circuit volatage (V_{OC}) and photoluminecsence spectrum to deepen the understanding of recombination mechanisms in InGaN LEDs. The photovoltaic information utilized in this work can provide an ideal behavior of a pn diode, eliminating the effect of the series resistance [2]. We thereby aim to elucidate the dominant carrier recombination process that contributes to the nonradiatve recombination from the discrpency bewteen electrical and optical pumpings.

For experiments, a 405-nm continuous-wave laser (Coherent CUBE 405-100C) was adopted as a light source for quasi-resonant optical excitation. We controlled the spot size of the incident light with a focusing lens to accomodate the sample size. For comparison between optical and electrical pumpings, I_{SC}-V_{OC} and current-voltage (I-V) characterisitcs depending on each excitation power were measured using a Keithley 2602 sourcemeter.

The discrepency between I-V and I_{SC}-V_{OC} curves are depicted in Fig. 1. Fig. 2 shows the ideality factors varied by various excitaion powers. ΔV reflects an additional potential drop under electrical excitation. More details on the experiments and analysis given in the presentation will shed more light on the nature of the dominant recombination process in the InGaN LEDs.

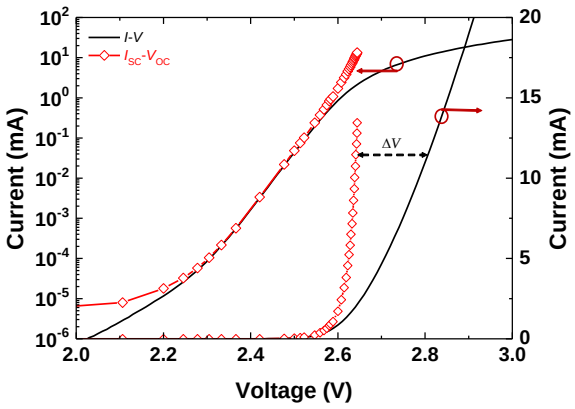

Fig .1. Comparison between *I-V* and I_{SC}-V_{OC} curve

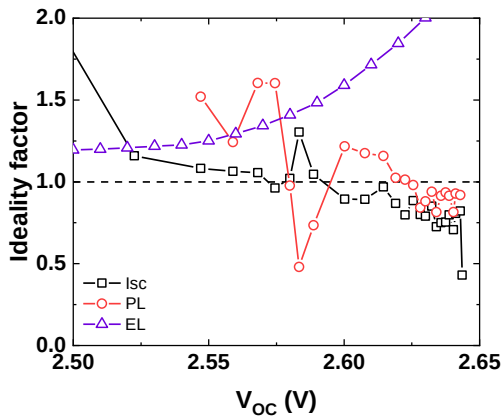

Fig. 2. Ideality factors depending on electrical and optical excitation

Acknowledgment

This works was supported by the Technology Innovation Program funded by the Ministry of Trade, Industry and Energy, Republic of Korea, under Grant 20006908.

References

1. G. W. Lee, J.-I. Shim, and D.-S. Shin, Appl. phys. Lett. 109, 031104 (2016).
2. C.-H. Oh, J.-I. Shim, and D.-S. Shin, Jpn. J. Appl. Phys. 58, SCCC08 (2019).

Lifetime Improvement in DABNA Type Blue Emitter Devices

*Sang Min Cho, Hye In Yang, Seung Hyun Lee and Jang Hyuk Kwon**
Department of Information Display, Kyung Hee University, Dongdaemun-gu, Seoul 02447, Korea
Tel.: 82-2-961-9147, E-mail: jhkwon@khu.ac.kr

High efficiency and good lifetime deep blue dopant development is very important for organic light emitting diodes (OLEDs) display applications. Over the years, there have been many efforts to develop good blue dopants, but phosphorescence and thermally activated delay fluorescent blue OLED still show insufficient performances of color purity and operational lifetime. On the other hand, the fluorescent blue material is doing continuously evolution to provide new characteristics. Many papers have been reported deep blue fluorescent emitter using pyrene and anthracene derivatives, but they have disadvantages such as broad full width at half maximum (FWHM), and poor color purity. Recently, a new DABNA type blue emitter with multiple-resonance effects is reported with narrow FWHM and very good color purity. The lifetime performance of this DABNA type blue emitter is not fully investigated to date.

In this study, we report long operational stability of this DABNA type blue OLED with analysis of degradation origins compared with pyrene type device. We fabricated two fluorescent OLED devices with deep-blue DABNA-NP-TB [1] or pyrene type emitter in KHU-BH01 anthracene host system. We have confirmed that this DABNA fluorescent device has a very short lifetime at 60 hours at LT_{95} (10mA/cm^2). Although both color and efficiency are good, operational stability is very poor compared with a pyrene device. We analyzed the reason of unstability by making electron-only (EOD) and hole-only devices (HOD) with the following structure: ITO/ HTL & ETL/ KHU-BH01 : 5% DABNA-NP-TB/ HTL & ETL/ Al. Voltage increase in the EOD observed about 0.17 V in 15 hours, but HOD almost remained unchanged from 0.07 V in 15 hours (Fig. 1(a)). From these results, we understood that DABNA-NP-TB emitter is vulnerable to anion state. For the lifetime improvement, we designed a mixed-host device. We mixed triazine type electron transporting KHU-BH02 host in KHU-BH01. As a result, the device lifetime increased 10 times from 60 hours to about 600 hours (Fig. 1(b)). We will report more details at the conference.

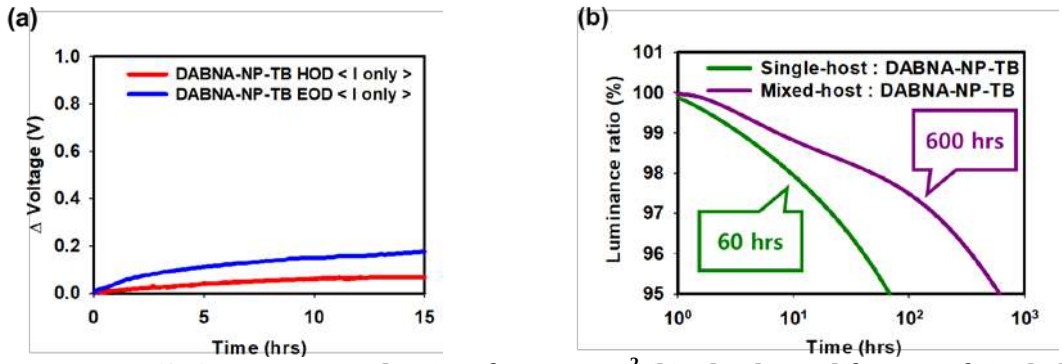

Fig. 1. (a) Voltage increse (ΔV) at a current density of 10 mA/cm^2 (b) The device lifetimes of single-host and mixed-host devices.

Acknowledgment

This work was supported by BK21 FOUR Program (Department of Information Display, Kyung Hee University) funded by Ministry of Education (MOE, Korea).

References

1. S. Oda, T. Hatakeyama, W. Kumano, T. Hama, R. Kawasumi and K. Yoshiura, *Angew. Chem.*, 133, 2918-2922 (2021)
2. Q. Wang, H. Aziz, *ACS Applied Materials & Interfaces*, 5, 8733-8739 (2013)

Ortho-terphenyl Core Based High Triplet Energy Bipolar Host Materials for Stable and Efficient Blue TADF Device

Seung Hyun Lee, Hyuna Lee[1], Jun Hyuk Park[2], Chil Won Lee[2*], and Jang Hyuk Kwon[1*]
[1]Department of Information Display, Kyung Hee University, 26, Kyungheedae-ro, Dongdaemun-gu, Seoul, 02447, Republic of Korea.
[2]Department of Chemistry, College of Science and Technology, Dankook University, Cheonan, 31116, Republic of Korea
Tel.:82-2-961-9147, E-mail: chili@dankook.ac.kr, jhkwon@khu.ac.kr

The importance of thermally activated delayed fluorescence (TADF) materials in blue organic light emitting diodes (OLEDs) has been increased due to its good progress of lifetime and efficiency improvement. However, the device lifetime is still not sufficient, thereby, simultaneous accomplishment of both high efficiency and good stability in blue TADF device has been required. For long device lifetime, assistance from host material is essential, thus, the development of stable and high triplet energy host materials draw attention from both research and commercial communities. To the pursuit of good TADF blue host materials, they should have high triplet energy level (>2.9 eV) and bipolar characteristics for balanced carrier transporting ability with proper energy level.

Among many high T_1 structures, o*rtho*-terphenyl structure with carbazoles (DCz-OTP) [1] achieves high T_1 energy value and higher thermal stability. Thus, we designed two novel bipolar host materials by substituting the *ortho*- or *meta*- position of CN moiety on DCz-OTP structure, and synthesized *o*CN-OTP and *m*CN-OTP, respectively. In order to evaluate the device performances of newly synthesized host materials, TADF-OLEDs were fabricated with 30 wt% of DBA-DI TADF material[2]. The maximum external quantum efficiencies of DCz-OTP, *o*CN-OTP, *m*CN-OTP based TADF device were 24.6%, 29.5%, and 21.9%, respectively. Among them, *o*CN-OTP based blue TADF device exhibited excellent efficiencies, and such efficiency enhancement substantiates with the characteristics of well-balanced carrier transportation and high triplet energy of *o*CN-OTP. Subsequently, the device lifetime at 1,000 cd/m^2 of initial luminance were conducted to support our design strategy of introducing CN moiety in the DCz-OTP structure. The devices with *o*CN-OTP and *m*CN-OTP host materials exhibited extended device lifetime (LT_{90}) of 28.8 and 9.0 hrs compared to 5.6 hrs of DCz-OTP. The detailed photophysical properties, device performances and deeper analysis of device lifetime will be discussed in the presentation.

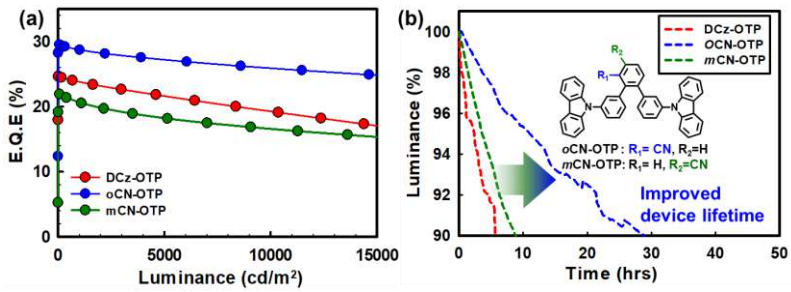

Figure 1. (a) EQE versus luminance, and (b) device lifetime of DCz-OTP, *o*CN-OTP, and *m*CN-OTP based devices,

Acknowledgment

This work was supported by the National Research Foundation of Korea (Grant No. NRF-2019M3D1A2104019) and by the Technology Innovation Program (20006464) funded by the Ministry of Trade, Industry & Energy (MOTIE, Korea).

References

1. C. W. Lee, and J. Y. Lee, *Organic Electronics*, 14, 1602-1607 (2013).
2. D. H. Ahn, J. H. Maeng, H. Lee, H. Yoo, R. Lampande, J. Y. Lee and J. H. Kwon, *Adv. Optical Mater.*, 8, 2000102 (2020).

InGaN based Core-shell Nanowire Photonic Crystals for Display Applications

Sung-Un Kim[1,2], Hye-Young Kwon[1], Dong-Wook Shin[2,*], and Yong-Ho Ra[1,*]
[1]Optic & Electronic Component Material Center, Korea Institute of Ceramic Engineering & Technology, Jinju 52851
E-mail: sungunkim26@gmail.com
[2]Division of Materials Science and Engineering, Hanyang University, 222, Wangsimni-ro, Seongdong-gu, Seoul 04763, Korea.
[*]Correspondence: yhra@kicet.re.kr

One-dimensional nanowires based on group III-nitride materials are the most promising structures for light-emitting diodes (LEDs), laser diodes due to their excellent structural, optical and electrical properties. There are still various difficulties to be solved. GaN-based LEDs exhibit efficient operation in the blue wavelength range, however, their efficiency and stability degrade considerably with increasing wavelengths, leading to the "green gap" in LED and laser technology. The nanowire structures were fabricated on a Si (111) substrate using a molecular beam epitaxy (MBE) system. We investigated various crystal growth and optical/structural properties of high-aspect-ratio GaN-based nanowires operating in the entire visible spectral range. From SEM and TEM results, it is shown that the developed nanowires have high-quality crystalline compared to conventional nanowire structures. A high-quality multi-band nanowire, which can emit the entire visible spectral range, was successfully grown with a core–shell structure that can protect the InGaN surface from surface recombination. Emission properties of a semiconductor light emitter are determined not only by the properties of the device active medium but also by the optical density of states surrounding the active region. Additionally, strong light confinement can be expected near the center region of the nanowire by covering with aluminum core-shell reflector. The fabricated InGaN based core-shell nanowire photonic crystals are ideally suited for high-efficiency LED, and laser operation.

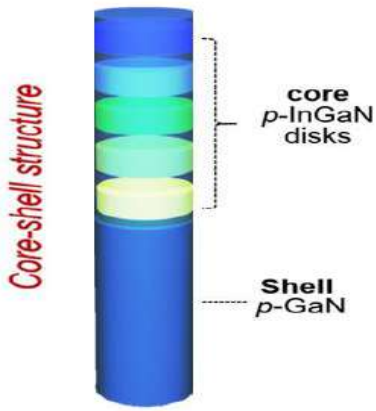

Fig. 1. Schematic of multi-band InGaN/GaN core–shell nanowire heterostructure.

Acknowledgment

This research was supported by the National Research Foundation of Korea (NRF) grant funded by the Korea government (No. 2020M3F3A2A03082762)

References

1. Y. H. Ra, C. R. Lee, Nano lett. 20, 4162-4168 (2020)
2. Y. H. Ra, R. T. Rashid, X. Liu, S. M. Sadaf, K. Mashooq, Z. Mi, Sci. Adv. 6, eaav7523 (2020)
3. Y. H. Ra, R. Wang, S. M. Sadaf, Z. Mi, Nano Lett. 16, 4608 (2016)

Fabrication of highly efficient and flexibility NIR $LaMgGa_{11-x}O_{19}:xCr^{3+}$ phosphor film for wearable PBM bio-OLED

Thi My Linh Dang [a,b,1], Thien Tri Tran [a,b,1], Ho Kyoon Chung[a,b], Sung Min Cho[c], Deok Su Jo [a,b,*]

[a] Sungkyunkwan Advanced Institute of Nanotechnology (SAINT), Sungkyunkwan University, Suwon 16419, Republic of Korea
[b] *DSLAB, Inc.* Suwon 16419, Republic of Korea
[c] School of Chemical Engineering, Sungkyunkwan University (SKKU), Suwon 16419, Republic of Korea
Tel: 82-31-299-6845, *corresponding author: jods@skku.edu

[1] Co-first authors with equal contribution.

Abstract

Near-infrared organic light-emitting diodes (NIR-OLEDs) are potential light-sources for wearable photobiomodulation (PBM) as OLEDs have unique characteristics such as the non-heating, surface light source, ultra-flexibility and low-cost fabrication. This study presents highly efficient and flexibility NIR $LaMgGa_{11-x}O_{19}:xCr^{3+}$ phosphor films as color conversion layer (CCL) to fabricate a down-conversion NIR-OLEDs from a red-emitting source of the OLED. The NIR $LaMgGa_{11-x}O_{19}:xCr^{3+}$ phosphor was synthesized via simple solid-state reaction (SSR), showing broad-band emission at centered at 725 nm. The synthesis temperature, holding time and x values of Cr^{3+} were investigated. The easily adhesive transfer (AT) method was used for fabrication of highly efficient and flexibility NIR $LaMgGa_{11-x}O_{19}:xCr^{3+}$ phosphor CCLs to improve the NIR light extraction efficiency and uniformity. The highest red to NIR photoconversion rate reaches at 30.59%.

Siloxane Encapsulated Upconversion Nanoparticle and Flexible Near Infrared Detectable MoS_2 Phototransistors

Injun Lee[1], Minsoo Kang[2], Tae Soo Kim[2], Kibum Kang[2], Wonryung Lee[3] and Byeong-Soo Bae[1]
[1]Wearable Platform Materials Technology Center (WMC),
Dept. of Mater. Sci. & Eng., KAIST, Daejeon 34141, Republic of Korea
Tel.:82-42-350-5119, E-mail: bsbae@kaist.ac.kr
[2]Dept. of Mater. Sci. & Eng., KAIST, Daejeon 34141, Republic of Korea
[3]Center for Theragnosis, Biomedical Research Institute, Korea Institute of Science and Technology (KIST), Seoul 136-791, Republic of Korea

There is a tremendous attention in flexible and soft electronic devices for the personalized health monitoring applications. Among the most commonly used non-invasive technologies for healthcare monitoring are optoelectronic devices. In particular, near infrared (NIR) is non-toxic and have long penetration within tissues, thus NIR are widely used in healthcare engineering devices for diagnosis and physiological data capture.

Here, we investigated flexible NIR detectable phototransistor, utilizing high visible photoresponse of Molybdenum disulfide (MoS_2) phototransistors and highly stable and biocompatible siloxane encapsulated upconversion nanoparticle to convert the NIR to visible light. Fig 1a showed the schematic of ultrathin(~5μm) flexible MoS_2 phototransistors with siloxane encapsulated upconversion nanoparticle, which is conformable on the skin. Lanthanide doped upconversion nanoparticles (β-$NaYF_4$:Yb,Er) were synthesized by thermal decomposition method, which exhibit stable upconversion luminescence properties under 980nm irradiation within sol-gel synthesized siloxane polymer. (Fig 1b) By integrating the UCNP-Siloxane polymer with flexible MoS_2 phototransistors, our devices are highly NIR sensitive with a 0.78 A/W, which is two times of value compared to bare MoS_2 phototransistors. (Fig 1c)

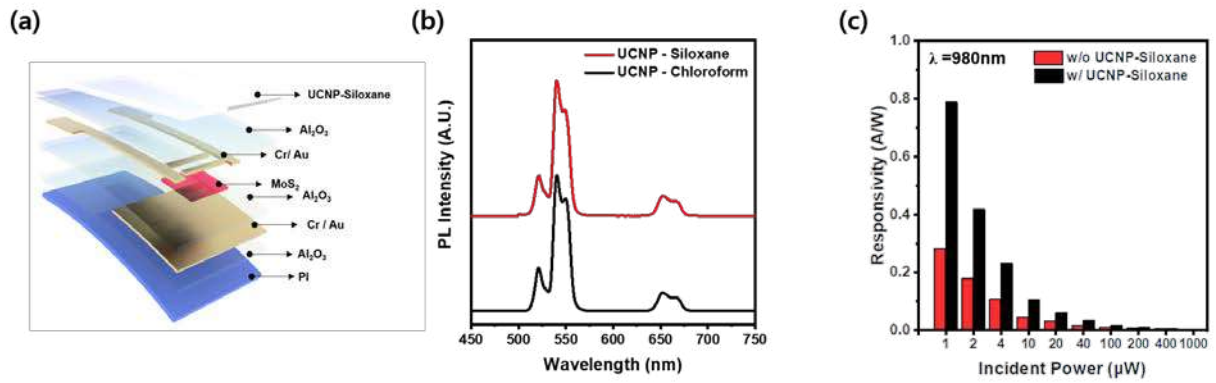

Fig. 1. (a) Schematic of flexible MoS_2 phototransistor with UCNP-Siloxane polymer.
(b) Photoluminescence(PL) intensity of UCNP dispersed in chloroform and UNCP-Siloxane polymer.
(c) Photoresponsivity of device under 980nm as a function of the incident laser power from 1μW to 1mW, for V_{GS} = 10V, V_{DS}= 5V

Acknowledgment

This work was supported by the Wearble Platform Materials Technology Center (WMC) (NRF-2016R1A5A1009926) funded by National Research Foundation of Korea (NRF) Grant of the Korean Government(MSIT)

References

1. K. Kang, S. Xie, L. Huang, Y. Han, P. Y.Huang, K. F. Mak, C.-J. Kim, D. Mullar, and J. Park., *Nature*. **520**, 656–660 (2015).
2. S. K. Kuk, J. Jang, H.J. Han, E. Lee, H. Oh, H. Y. Kim, J. Jang, K. T. Lee, H. Lee, Y. S. Jung, C. B. Park and B.-S. Bae., *ACS Appl. Mater. Interfaces*. **11**. 17 (2019)

Optogenetic brain stimulation by self-powered flexible micro light-emitting diodes

Han Eol Lee[1]
[1] Division of Advanced Materials Engineering, Jeonbuk National University,
Jeonju, Jeollabuk-do 54896, South Korea
Tel.:82-63-270-2379, E-mail: haneol@jbnu.ac.kr

Optogenetic brain modulation has been attacted as a key technology of therapeutic treatment medthod for various neurological diseases.[1,2] Optogenetic stimulating systems have been developed by several research teams. However, they still have some issues about flexible light sources and power sources with long lifetime. Among conventional light sources (e.g., bulk LED, OLED, etc), μLEDs have been spotlighted for the emerging light sources because of their excellent properties, including great efficiency, strong light output, extremly long lifetime and theraml/humid/chemical stability. We realized vertically-structured flexible μLEDs (f-VLED).[1,3] Especially, the thermal stability issue of flexible μLED could be resolved by heatdissipating layer of f-VLED. Herein we report an optogenetic neuromodulation system, which is operated by the wasted magnetic field of household appliances. f-VLEDs were operated by a flash light-enhanced magneto-mechanical triboelectric nanogenerator (MMTENG). The electrical power of MMTENG could be improved by making nano/microstructure on the nylon film surface, which was induced by high-power flash light treatment. Flash-enhanced MMTENG showed high output power over 8 mW in a gentle alternating current (AC) magnetic field of 7 Oe, and successfully operated f-VLEDs by the magnetic field of the home appliance. Optogenetic stimulating system with MMTENG and f-VLEDs was implanted under the living mouse skull without mechanical brain damage.[4]

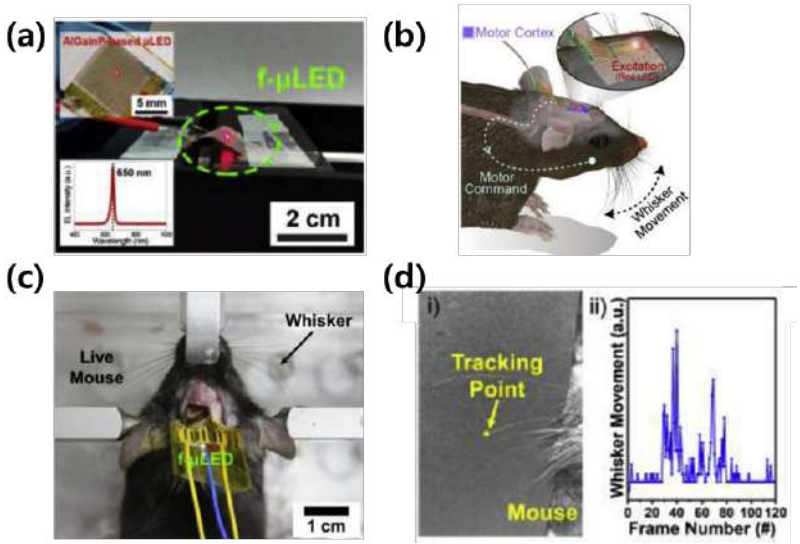

Fig. 1. (a) Image of f-VLED array. (b) Concept illustration of self-powered optogenetic brain neuromodulation. (c) Optical image of the implanted f-VLEDs on the living mouse brain. (d) Tracking image and graph of the mouse whisker tracking, which is induced by optogenetic stimulations.

Acknowledgment

References

1. S. H. Lee et al. *Nano Energy* 44, 447 (2018).
2. A. H. Park et al. *ACS nano* 10, 2797 (2016).
3. H. E. Lee et al. *Advanced Materials* 30, 1800649 (2018).
4. H. E. Lee et al. *Nano Energy* 75, 104951 (2020).

Highly Mechanosensitive, Biocompatible Ionogel with Trap and Release Ion Dynamics for Implantable Bioelectronics

Junjae Park, Joo Sung Kim, Yunah Kim, and Do Hwan Kim
Dept. of Chemical Engineering, Hanyang University, Seoul 04763, Korea
Tel.:82-2-2220-2671, E-mail: dhkim76@hanyang.ac.kr

According to increased concerns over the health management, tactile sensors for implantable medical devices have been widely demonstrated for monitoring physiological signals in real-time. In particular, ionogel is promising candidate for tactile sensors due to the nature of its flexibility and ionic conductivity. However, their toxicity and low sensitivity caused by limited structural deformation are highly debatable for the applicability of bioelectronics in human body. To overcome these drawbacks, we developed biocompatible ionogel composed of biopolymer and choline-derived ionic liquids, which exhibit low cytotoxicity without affecting the viability of tissue. In addition, the mechanotransduction mechanism, in which the hydrogen-bond triggered ion trap and release behavior, enables higher sensitivity compared with the geometric deformation mechanism. Successful integration of the biocompatible ionogel composite into implantable device that is capable of perceiving subtle signals from human body which will likely attract the scope of applications our material to next generation health monitoring system.

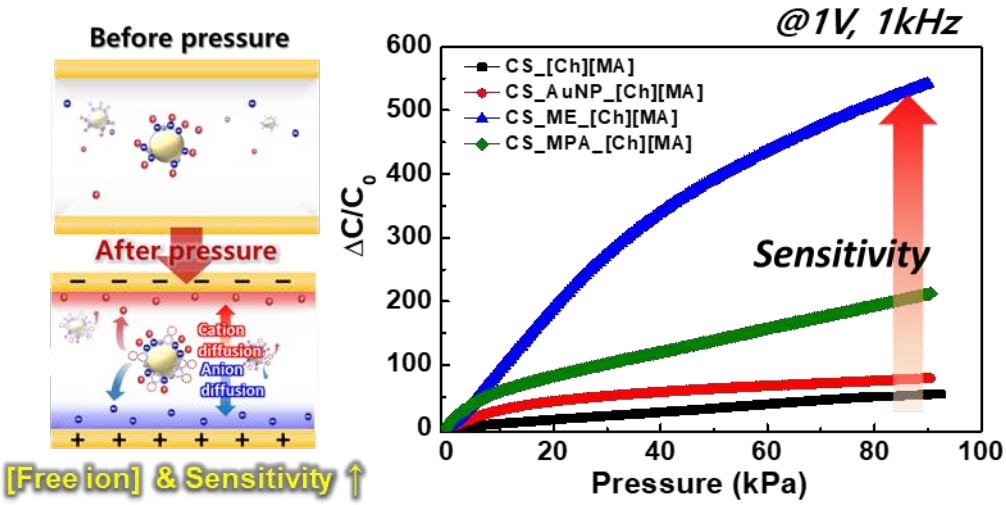

Fig. 1 Sensing mechanism and performance of the biocompatible artificial ionogel based pressure sensor

Acknowledgment

This work was supported by the Basic Science Research Program (2017R1A5A1015596 ,2020R1A2C3014237) of the National Research Foundation of Korea (NRF) funded by the Ministry of Science, ICT

References

1. Amoli, V., Kim, J.S., Jee, E. et al., Nat Commun 10, 4019 (2019)
2. X. Wu et al., International Journal of Pharmaceutics 558 (2019) 380–387

Design of Ethylene Oxide based Interpenetrating Conducting Polymer Network for Highly Efficient Bio-signal Transduction

Sangjun Park, Hyukmin Kweon, Chaeyoung Lee, Junjae Park, and Do Hwan Kim
Dept. of Chemical Engineering, Hanyang University, Seoul 04763, Korea
Tel.:82-2-2220-2671, E-mail: dhkim76@hanyang.ac.kr

PEDOT:PSS is a promising conducting polymer in bioelectronics, because of its mixed ionic-electronic transporting property. Since biological environment is dominated by ions, the coupled ion-electron conducting system of PEDOT:PSS is an outstanding capability for high efficient bio-signal transducer. However, PEDOT:PSS is vulnerable to aqueous media, so that it is hard to secure long-term stability in biological environment. Alternatively, crosslinking method can be adopted for improvement of the stability, however, the crosslinker would hinder ion transporting capability of PEDOT:PSS. Herein, we demonstrate an ethylene oxide based interpenetrating conducting polymer network (EO-ICPN) in which PEDOT:PSS and EO based ladder-like network are entangled physically. The EO-ICPN can obtain superior physical and chemical resistance, resulting in long-term stability in an aqueous state. Furthermore, ion transport and water contents of PEDOT:PSS were enhanced by ion compatibility of EO groups of EO-ICPN. Consequently, we believe that our approach will provide guidance for next-generation bioelectronics.

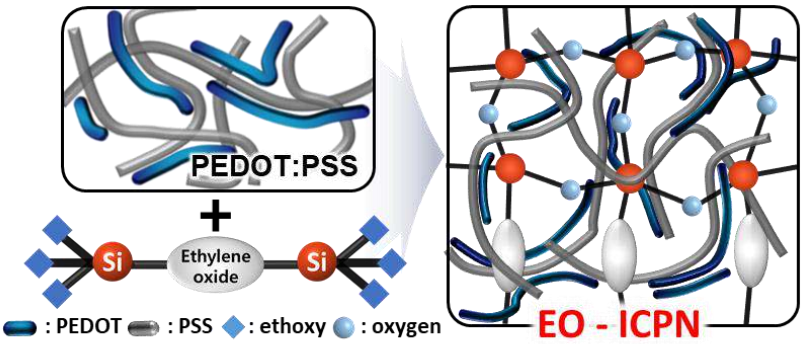

Fig. 1. Ethylene oxide based interpenetrating conducting polymer network (EO-ICPN)

Acknowledgment

This project is supported by the Basic Science Research Program (2017R1A5A105596 and 2020R1A2C3014237) of the National Research Foundation of Korea (NRF) funded by the Ministry of Science and ICT

References

1. Park, H. W., *Adv. Mater.*, 1901400 (2019)
2. Feig, Vivian R., *Nat Commun.*, 9, 2740 (2018)

Medifoam-based Biocompatible Resistive Random-Access Memory for Skin-wearable Healthcare Devices

Min Seong Kim, Sujin Jung, Dong Hyun Choi, Hyung Tae Kim, Jusung Chung, and Hyun Jae Kim*
School of Electrical and Electronic Engineering, Yonsei University, Seodaemun-gu, Seoul 03722, Korea
Tel.:82-2-2123-5865, E-mail: hjk3@yonsei.ac.kr

Recently, various nonvolatile memory devices have been applied to real-time data storage in skin-wearable healthcare devices.[1] There are a number of candidates for potential non-volatile memory, such as phase-change random-access memory (PCRAM), magnetoresistive random-access memory (MRAM), and resistive random-access memory (ReRAM).[2] Among these, ReRAM has been intensively studied owing to its distinct advantages, such as low manufacturing cost, low power consumption, faster switching time compared to PCRAM, and simpler cell structure compared to MRAM. These merits are beneficial in applying ReRAM to skin-wearable healthcare devices as they can be manufactured in a simple method and operate in low-power settings (i.e. longer active time).[3] In this study, we introduced the use of biocompatible and water-resistant organic materials, medifoam, as the switching layer of ReRAM. Medifoam in liquid form is already used in everyday pharmaceutical it ems that are applied to human skin to create a protective, water-resistant layer in order to cover up vari ous wounds. Therefore, their biocompatibility and flexibility are highly proven, meeting the qualifications as a powerful contender in organic ReRAM production applicable in skin-wearable healthcare devices. Th e structural diagram of the medifoam-based ReRAM devices is shown in **Figure 1a** along with the chem ical structure of medifoam. As shown in **Figure 1b,** medifoam-based ReRAM featured bipolar switching operation. The "set" voltage denotes a conversion from a high resistance state (HRS) to a low resistance state (LRS), and the "reset" voltage indicates a conversion from LRS to HRS. In its first cycle, medifoa m-based ReRAM showed a set voltage value of 3.00 V and a reset voltage value of –1.75 V. Moreover, medifoam-based ReRAMs demonstrated stable switching operations as their performances remained more or less similar even at their 100th consecutive cycles. At a read voltage of 0.5 V, in medifoam-based Re RAM, HRS to LRS ratio revealed a resistance switching characteristic of ~ 10^3. Based on these switching results, medifoam-based ReRAM reliability as a memory device was confirmed.

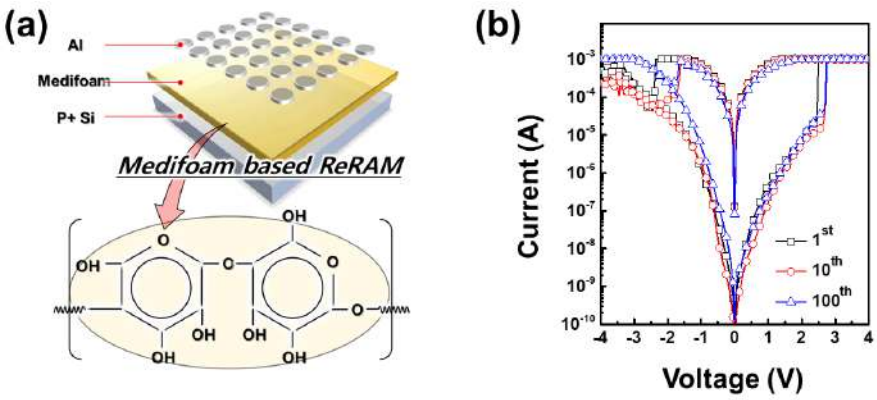

Figure 1. (a) Device schematics of fabricated medifoam-based ReRAM and chemical structures of medifoam, (b) I-V resistive switching characteristic of medifoam-based ReRAM.

Acknowledgment

This work was supported by the Technology Innovation Program (20010371, development of 4K level flexible display device and panel technology by inkjet pixel printing method) funded by the Ministry of Trade, Industry & Energy (MOTIE, Korea).

References

1. S. P. Park, Y. J. Tak, H. J. Kim, J. H. Lee, H. Yoo, H. J. Kim, *Adv. Mater.*, 30, 1800722 (2018).
2. H. Wang, X. Yan, *Phys. Status Solidi RRL*, 13, 1900073 (2019).
3. H. Ling, M. Yi, M. Nagai, L. Xie, L. Wang, B. Hu, W. Huang, *Adv. Mater.*, 29, 1701333 (2017).

Mussel Protein-Based Flexible Resistive Random Access Memory for Wearable Electronic Applications

Sung Min Rho, Kunho Moon, Min Seong Kim and Hyun Jae Kim*
School of Electrical and Electronic Engineering, Yonsei University, Korea
Tel.:82-2-2123-5865, E-mail: hjk3@yonsei.ac.kr

There has been a growing interest in flexible memory devices for wearable applications. For use as wearable applications, flexible memory devices should meet the requirements such as flexibility, reliability, and bio-compatibility. Organic material-based ReRAM (resistive random access memory) is one of the solutions of flexible memory for wearable applications owing to the high flexibility, but it is difficult to find specific organic materials satisfying all three characteristics (i.e. flexibility, reliability, and bio-compatibility).

Herein, we introduce a promising biomaterial, the mussel protein, as the switching layer of ReRAM. Representative mussel protein, L-DOPA (3,4-Dihydroxy-L-phenylalanine) is mainly used for a natural suture in vascular surgery because it does not react with surrounding tissues and cells.[1] Besides, L-DOPA is used as an additive to improve the stretchability of Carbon Nanotube fibers.[2] Therefore, its bio-compatibility and flexibility are proved, meeting the requirements as definitive candidates in organic ReRAM based wearable applications. **Figure 1a** shows the structure schematic of the L-DOPA based ReRAM devices. L-DOPA solution was prepared by synthesizing the L-DOPA powder and 2-Methoxyethanol with a 5% mass ratio. After aging 24 hr, L-DOPA thin film was deposited by spin-coating (3000 rpm, 30 sec) on p^+ Si substrate. Next, the samples were annealed at 85°C for 1 hr on a hot plate in air condition. Finally, L-DOPA based ReRAM was fabricated with deposition of Mg (Magnesium) top electrode using an e-beam evaporator. **Figure 1b** shows the chemical structure of L-DOPA protein from mussels. Generally, in ReRAM devices, it is known that resistive switching characteristics are attributed to the oxygen ion migration at the interface oxide.[3] We can infer that hydroxyl functional groups in L-DOPA react with the Mg top electrode through redox reactions and the formation of conducting filaments due to oxygen ion migration occurs at the Mg/L-DOPA interface. **Figure 1c** demonstrates the bipolar switching operation of L-DOPA based ReRAM. At a read voltage of 0.2 V in L-DOPA based ReRAM, the ratio of high resistance state and low resistance state is about 10^3. Moreover, L-DOPA ReRAM demonstrated highly reliable switching operations as the I-V characteristics are similar even after 100th repetitive cycles. The following advantages such as biocompatibility, flexibility, and reliability demonstrated the considerable potential of L-DOPA based ReRAM for wearable applications.

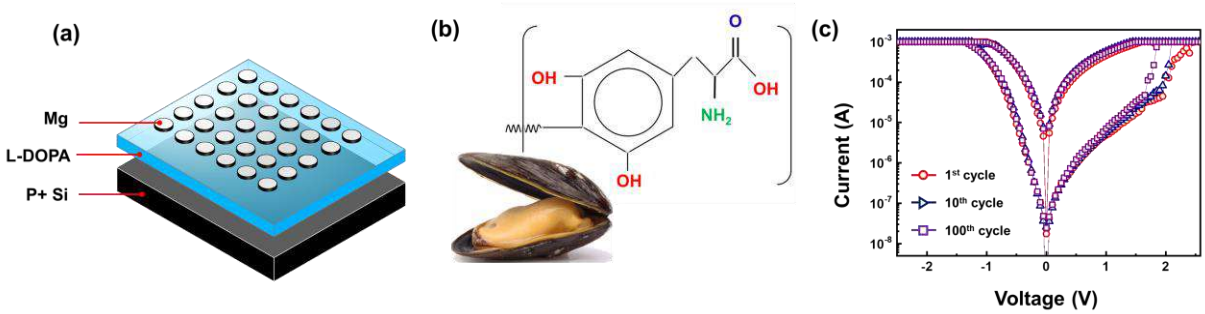

Figure 1. (a) Device schematics diagram of L-DOPA-based ReRAM
(b) Chemical structures of L-DOPA, (c) I-V characteristics of L-DOPA-based ReRAM.

Acknowledgment
This work was supported in part by Samsung Display and in part by the Nano Material Technology Development Program through the National Research Foundation of Korea (NRF) funded by the Ministry of Science and ICT under grant 2018M3A7B4071521.

References

1. M. Rahimnejad, and W. Zhong, *RSC Advances*, 7, 47380 (2017)
2. S. Ryu, Y. Lee, J-W Hwang, S. Hong, C. Kim, T. G. Park, H. Lee, S. H. Hong, *Advanced Materia ls* 13, 1971-1975 (2011)
3. Y. Zhang, H. Wu, Y. Bai, A. Chen, Z. Yu, J. Zhang, and H. Qian, *Applied Physics Letters* 102, 233502 (2013)

Fucoidan-based Resistive Random-Access Memory for Edible Electronics

Kyungmoon Kwak, Hyung Tae Kim, Kyungho Park, I Sak Lee and Hyun Jae Kim*
School of Electrical and Electronic Engineering, Yonsei University, Korea
Tel.:82-2-2123-5865, E-mail: hjk3@yonsei.ac.kr

In recent years, the edible material-based device is drawing attention as an essential device for implementing an implantable healthcare platform because there is no severe immune response at the implant site.[1] Among the devices, resistive random-access memory (RRAM) based on edible bio-organic materials has been attracted much attention as a nonvolatile memory for the data storage device of the implantable healthcare platform due to fast switching speed, low-power consumption, and low cost.[2] In this research, fucoidan is proposed as a novel edible biomaterial for the active layer of RRAM. Fucoidan is a representative material to treat gastric ulcers. In particular, since fucoidan is known to have a gastrointestinal cancer treatment effect, an additional effect can be expected as a healthcare device used for monitoring gastrointestinal diseases. We fabricated fucoidan-based RRAM through a simple solution process at the low temperature of 90°C and then measured their switching characteristics. The fabricated device structure of fucoidan-based RRAM is shown in **Figure 1a**. The fucoidan solution was synthesized by dissolving fucoidan powder in deionized (DI) water and filtered through 0.2 μm PVDF syringe filter. The obtained solution was deposited onto a p^+-Si substrate by spin coating method. Following the active layer deposition, Mg electrodes were patterned using the electron-beam evaporation with a shadow mask. The figure below the device structure shows the molecular structure of fucoidan. In general, it is known that resistive switching characteristics in RRAM devices are due to the oxygen ion migration at the interface oxide.[3] We can assume that hydroxyl functional groups in fucoidan react with the Mg top electrode through redox reactions and the formation of conducting filaments due to oxygen ion migration occurring at the interface between Mg/fucoidan. As shown in **Figure 1b**, the fucoidan-based RRAM showed bipolar switching operation. And, the set and reset processes are performed at 2.95 V and –1.65 V, respectively. At a read voltage of 0.3 V, it showed the switching resistance ratio from HRS to LRS with a value of about 10^3. Based on these switching characteristics, we confirmed that the fucoidan-based RRAM can be used for the nonvolatile memory device for the implantable healthcare platform.

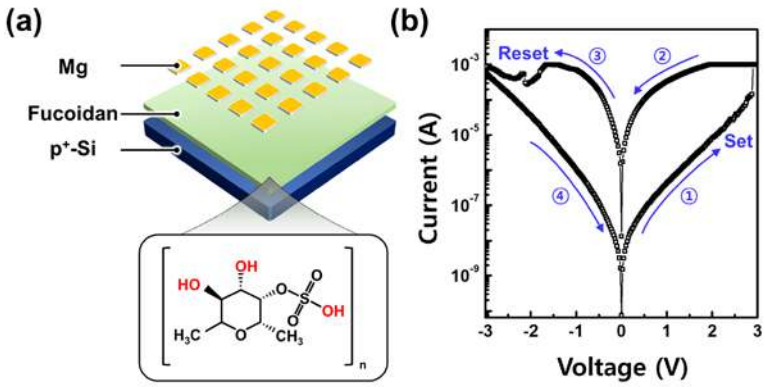

Figure 1. (a) Fabricated device structure of fucoidan-based RRAM, (b) I-V switching characteristic of fucoidan-based RRAM.

Acknowledgment
This work was supported by the Nano Material Technology Development Program through the National Research Foundation of Korea (NRF) funded by Ministry of Science and ICT (no. 2018M3A7B4071521).

References

1. A. S. Sharova, F. Melloni, G. Lanzani, C. J. Bettinger, M. Caironi, *Adv. Mater. Technol*., 6(2), 2000757 (2020)
2. S. P. Park, Y. J. Tak, H. J. Kim, J. H. Lee, H. Yoo, H. J. Kim, *Adv. Mater*., 30(26), 1800722 (2018)
3. Y. Zhang, H. Wu, Y. Bai, A. Chen, Z. Yu, J. Zhang, and H. Qian, *Applied Physics Letters*., 102, 233502 (2013)

Optical Design Considerations for Safe Ultraviolet Wearable Light Therapeutic Devices

Jaehyeok Park[1], Hyuk Joo Lee[2], Sunhyoung Koo[1], In-Young Yoon[2], and Seunghyup Yoo[1]*
[1]School of Electrical Engineering, KAIST, Daejeon 34141, Korea
Tel.:82-42-350-8083, E-mail: syoo@ee.kaist.ac.kr
[2]Dept. of Psychiatry, Seoul National University Bundang Hospital, Seoul National University College of Medicine, Seongman, Gyeonggi-do 13620, Korea

Ultraviolet (UV) radiation is known to have treatment effects on the human body at specific wavelengths but, at the same time, has the potential to yield hazardous results if not controlled well. While a moderate dose of visible and near-infrared light does not cause acute or chronic damage to the skin, UV light may induce erythema on human skin due to the high-energy photons. Conventional UV-based light therapy devices are installed at large distances, and thus light energy is spread out to produce nearly uniform radiation on the body surface. In this configuration, a large portion of light energy is lost into the ambient or reaches unwanted body parts. For the sake of efficient use of light energy, safety, and portability, an array of UV light-emitting diodes (LEDs) may be integrated into wearable devices. However, in a wearable form factor, there is less space for light to be spread, which increases the risk by the concentrated irradiation of UV light.

Here we attempt to provide a set of optical design considerations for the safety in the development of wearable UV light therapeutic devices. The optical design is done carefully to consider an LED array as a whole for uniform irradiance on the skin under its specific operating conditions such as bending. In particular, we pay attention to the area where illumination from adjacent LEDs overlaps at such site can cause unwanted high brightness, risky for erythema formation. It is also noted that the erythema spectral weighting function has a sharp transition in the UV-B range and that the optimization of emission wavelength can therefore be significant due to the narrow-band nature of UV LEDs. We also discuss the subject dependence of minimal erythemal dose and skin phototype to prevent skin burns on individual subjects, identifying statistically meaningful conditions for UV light therapy protocols.

Acknowledgment

This work was supported by the Engineering Research Center of Excellence (ERC) Program funded by the National Research Foundation (NRF), Korean Ministry of Science, ICT & Future Planning (MSIP)(Grant No. NRF-2017R1A5A1014708)

References

1. Leiner, C. et al. OSA Contin. 1, 1144 (2018).
2. International Organization for Standardization/Comission Inernationale de l'Eclairage (ISO/CIE) 17166:2019 (2019)
3. Welti, M. et al. Photodermatol. Photoimmunol. Photomed. 36, 200 (2020).
4. Baquié, M. & Kasraee, B. Ski. Res. Technol. 20, 218 (2014).

A Comprehensive Strategy for Reducing the Dark Current in Organic Photodiodes

SangIn Hahn[1], Ramakant Sharma[1], and Seunghyup Yoo[1]
[1]School of Electrical Engineering, KAIST, Daejeon, 34141, Korea
Tel.:82-42-350-7287, E-mail: syoo.ee@kaist.ac.kr

Organic photodiodes have been widely studied and utilized for numerous applications such as photovoltaic solar cells and healthcare monitoring [1,2], but can also be useful for imaging that prefer low-cost, large-area compatibility and versatile form factor advantages of organic technologies such as under display image sensors for biometric identification. Although their efficiency and stability were lower than inorganic photodiodes, continuous research done worldwide has led to significant improvements in their overall performance. Additional advantages such as tunable absorption spectra, mechanical flexibility, and scalability of polymer-based photodiodes have also attracted academic interests and illustrated their versatile functionality. Especially in view of the photovoltaic (PV) application, organic solar cells already achieved high power conversion efficiencies higher than 16% by combining polymer donors and non-fullerene acceptors [3].

Given such progress in PVs, however, only a few works have been reported for organic image sensors. One possible reason can be found in their larger dark current compared to that of inorganic photodiodes. Large dark current density would degrade the overall detectivity and eventually increase the power consumption. Several methods for suppressing the dark current, such as introducing blocking layers and increasing active layer thickness, have been suggested, but they can often accompany an unwanted drop in the sensitivity [4,5].

This work suggests the comprehensive, systematic design strategy for suppressing the dark current and achieving high sensitivity without degrading efficiency. Relationships between the dark current and the equivalent circuit model with series and shunt resistance have been explored, and previously suggested methods for dark current suppression have also been analyzed for comparison.

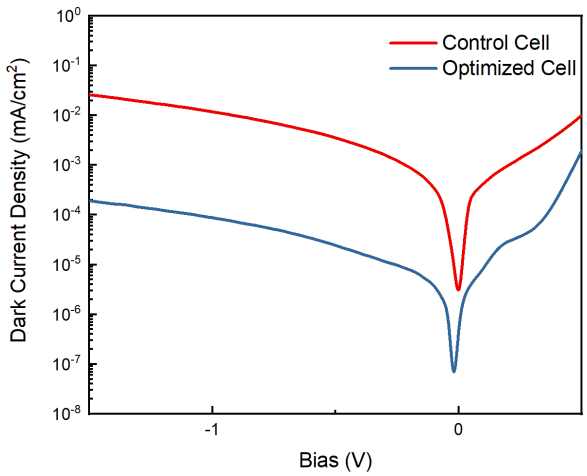

Fig. 1. Dark current comparison between the optimized cell and the un-optimized control cell

Acknowledgment

This work was supported by the Industry technology R&D program (20006476) funded By the Ministry of Trade, Industry & Energy (MOTIE, Korea)

References

1. Lee, H., et al. *Science Advances* 4, 11 (2018).
2. van Breemen, A. J. J. M., Et al. *npj Flexible Electronics* 4, 22 (2020)
3. Fan, B., et al. *Science China Chemistry* 62, 746-752 (2019)
4. Gong, X., et al. *Sensors* 10, 6488-6496 (2010)
5. Fuentes-Hernandez, C., et al. *Science* 370, 698-701 (2020)

High-Efficiency Solution-Processed Near-Infrared Organic Photodiodes

Jeoungmin Ji[1], Hyung Suk Kim[1], Ramakant Sharma[1], Woochan Lee[1], Carmela Michelle Esteban[1], and Seunghyup Yoo[1]
[1]School of Electrical Engineering, KAIST, Daejeon, 34141, Korea
Tel.:82-42-350-3483, E-mail: syoo.ee@kaist.edu

Organic photodiodes (OPDs) have recently been studied for various applications such as organic image sensors, bio-inspired artificial eyes, and wearable bio sensors. By taking advantage of tunable optical properties, large-area scalability, and mechanical flexibility of organic electronic materials [1-4], OPD-based image sensors may be beneficial in large-sized or bendable image sensors that can be coupled with displays in various form factors. In particular, the need of near-infrared (NIR) organic photodiodes is growing as it can be useful for detection of clear images under low-light conditions (e.g. face recognition in dark) or for detection of various biosignals (e.g. vein-imaging based identification, or pulse oximetry data). To fully utilize the potential of NIR organic photodiodes, however, the external quantum efficiency (EQE) and simplicity in fabrication need to be improved further to match the requirements for many of the applications.

The aim of this study is to fabricate NIR organic photodiodes and improve EQE in a simple manner compatible with the existing infrastructure and common process. In this regard, we adopt common solution-processed organic donor-acceptor blendsand try to exploit their charge-transfer (CT) absorption band in the NIR region. On top of that, the microcavity effect is applied to compensate a relatively low CT absorption in the NIR region to improve EQE. Upon optimization, we demonstrate approximately ten-fold increase in EQE from 1.16% to 10.60% in the wavelength of 985 nm, illustrating that the proposed approach holds a great promise in detecting NIR photons with relatively long wavelength at high efficiency.

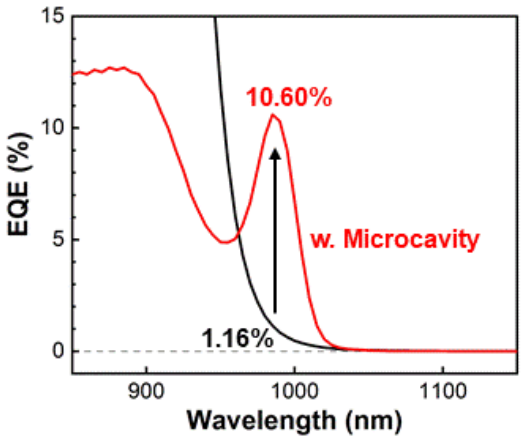

Fig. 1. EQE of the fabricated NIR organic photodiode with and without microcavity effect

Acknowledgment

This work was supported by the Industry technology R&D program(20006476) funded By the Ministry o f Trade, Industry & Energy(MOTIE, Korea)

References

1. X. Xu, M. Davanco, X. Qi, S. R. Forrest, *Organic Electronics*, 9(6), 1122-1127 (2008).
2. C. Choi, J. Leem, M. S. Kim, A. Taqieddin, C. Cho, K. W. Cho, G. J. Lee, H. Seung, H. J. Bae, Y. M. Song, T. Hyeon, N. R. Aluru, S. W. Nam, D. H. Kim, *Nature communications*, 11(1), 1-9 (2020).
3. T. Yokota, T. Nakamura, H. Kato, M. Mochizuki, M. Tada, M. Uchida, S. Lee, M. Koizumi, W. Yukita, A. Takimoto, T. Someya, 3(2), 113-121 (2020).
4. B. Siegmund, A. Mischok, J. Benduhn, O. Zeika, S. Ullbrich, F. Nehm, M. Böhm, D. Spoltore, H. Fröb, C. Körner, K. Leo, K. Vandewal, *Nature communications*, 8(1), 1-6 (2017).

Application of UV-filtering Down-conversion Layer on Flexible Organic Solar Cells

Carmela Michelle Esteban[1], Ramakant Sharma[1], Woochan Lee,[1]and Seunghyup Yoo[1]
[1]School of Electrical Engineering, KAIST, Daejeon, 34141, Korea
Tel.:82-42-350-3483, E-mail: syoo.ee@kaist.edu

Solar cells made up of organic materials such as polymers and small molecules have been established as a cheaper alternative to conventional silicon solar cells. Although the performance had significantly improved through the years, organic solar cells (OSCs) still exhibit low efficiency and high device instability preventing their commercialization [1,2].

The theoretical energy conversion efficiency limit of any single-junction solar cell is a function of the band-gap energy of the semiconductor, referred to as Shockley-Queisser (SQ) limit [3]. Down-conversion (DC) is one of the suggested approaches to overcome the SQ limit wherein high-energy photons are converted into low-energy photons of which the energy is just enough to overcome the band-gap energy to minimize the thermalization of the charge carriers [4].

In this work, we discuss the effect of luminescent organic material as an ultra-violet (UV)-filtering down-conversion (UVDC) layer on the efficiency of a flexible organic solar cell. With the help of the UVDC layer, high-energy photons in the UV spectrum can be converted into photons which fall on the absorption spectra of the active layer. Absorption of these down-converted photons within the cell leads to an increase in the photocurrent in the device and eventually improve the power conversion efficiency. In addition, the DC layer should be able to filter out UV light to slow down the degradation in the active layer caused by UV radiation. Furthermore, the proposed approach can be beneficial for UV-enhanced photodetection as well.

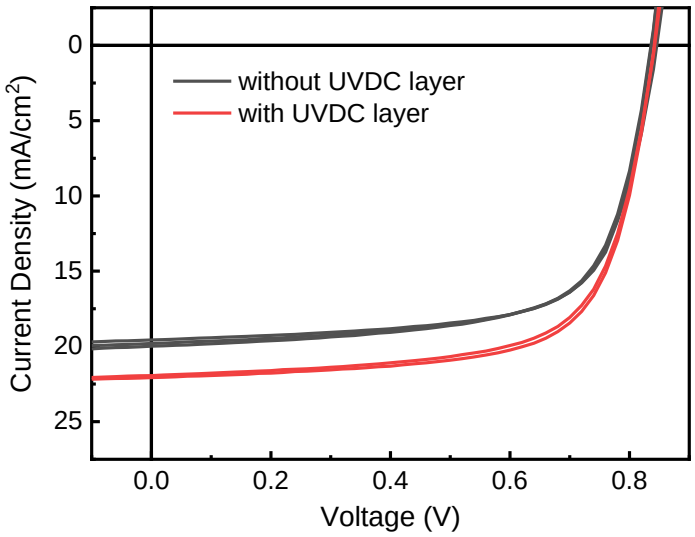

Fig. 1. J-V curve of the fabricated devices

Acknowledgment

This work was supported by the Industry technology R&D program(20006476) funded By the Ministry of Trade, Industry & Energy(MOTIE, Korea)

References

1. G. Cook, L. Billman, R. Adcock, "Photovoltaic Fundamentals", *Solar Energy Research Institute*, (1991).
2. X. Li, R. Xia, K. Yan, H. L. Yip, H. Chen, C. Z. Li, *Chinese Chemical Letters*, 31(6), 1608-1611 (2019).
3. W. Shockley, H. J. Queisser, *Journal of Applied Physics*, 32(3), 510-519 (1961).
4. B. S. Richards, A. Ivaturi, S. K. W. MacDougall, J. Marques-Hueso, *Proc. SPIE 8438, Photonics for Solar Energy Systems IV*, 8438, 11-18 (2012).

Study on tuning Red emission spectra for biological OLED application

Thien Tri Tran[a,b], Thi My Linh Dang[a,b], Ho Kyoon Chung[a,b], , Deok Su Jo[a,b,*] , Sung Min Cho[c,*]

[a] Sungkyunkwan Advanced Institute of Nanotechnology (SAINT), Sungkyunkwan University, Suwon 16419, Korea.

[b] DSLAB, Inc. Sungkyunkwan University, Suwon 16419, Korea.

[c] School of Chemical Engineering, Sungkyunkwan University, Suwon 16419, Korea.

*Corresponding author: sungmcho@skku.edu

*Co-corresponding author: jods@skku.edu

Abstract

Photo-biomodulation (PBM) therapy activates the enzyme of cytochrome C oxidase under a broad red emission or near-infrared light to produce a beneficial effect on cells or tissues. In this study, we introduce a simulation method based on the Fabry-Perot theory to broad the red OLED emission spectra for activating the enzyme in PBM bio-OLED. The different thickness of H-series (consist of hole injection layer and hole transport layer), E-series (consist of hole blocking layer, electron transport layer and electron injection layer) and emissive layer were studied. At H-series of 100nm, E-series and emissive layer at 70nm on anode which is Indium Tin Oxide (ITO) 50nm, the emission spectra have highest value of full width at half maximum (FWHM). Ultimately, this simulation method is highly nominated as a tool to tune thickness of each red OLED layers, which aim to effectively activate cytochrome C oxidase by a broad red emission for PBM application.

Optoelectrical Determination of Blood Components by Tin Oxide Quantum Dots-Fluorene Copolymer Heterojunction Self-powered Photodetectors

Taehyun Park[1] and Hocheon Yoo[2]
[1]Dept. of Chemical and Biological Engineering, Gachon University, Seongnam, Gyeonggi 13120 Korea
[2] Dept. of Electronic Engineering, Gachon University, Seongnam, Gyeonggi 13120 Korea
Tel.:82-031-750-5802, E-mail: hyoo@gachon.ac.kr

A rapid and efficient optoelectrical method for determination of blood components has demonstrated through Tin oxide quantum dots-fluorene copolymer heterojunction photodetector (SnO_2 QDs/FP-PD). The photo-active materials, device structure and sensing system were carefully designed to enable low cost and miniaturization. SnO_2 QDs were synthesized via one step solvothermal reaction and photodetector were fabricated by simple sequential spin coating process. With the optimal condition, SnO_2 QDs/FP-PD showed the remarkable responsivity, detectivity, fast response and stability under self-powered operation. In this research, optical characteristic of blood components and interaction between photodetector and blood components by illuminating two different wavelengths of ultraviolet light were systemically investigated. Furthermore, the successful determination of three different blood components mixtures by SnO_2 QDs/FP-PD based on specific absorption phenomena, which provides a simple and efficient technique for urgent medical field and health monitoring system.

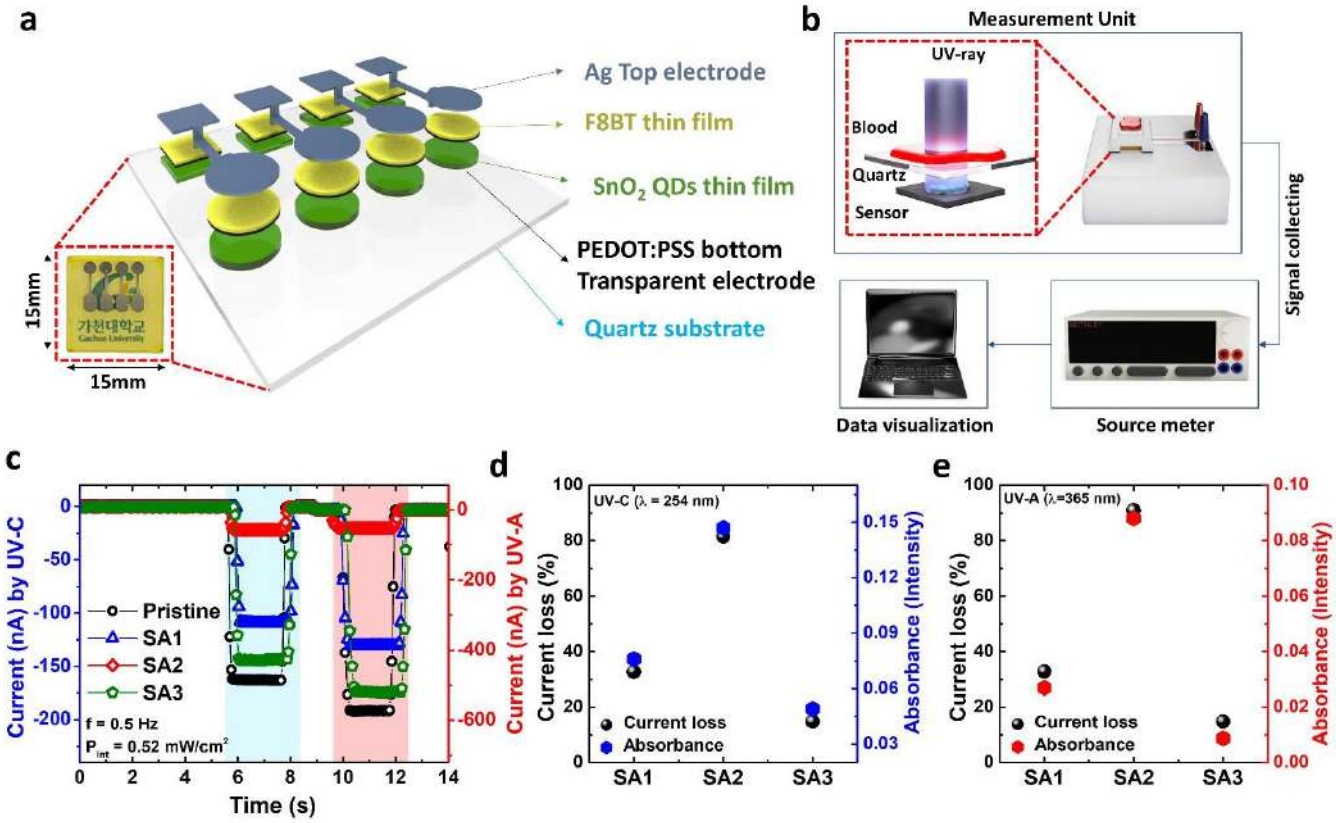

Fig. 1. Schematic description of a) SnO_2 QDs/FP-PD and b) optoelectrical sensing system. c) current-time characteristic of different component blood samples. photo current–absorbance correlation results under d) UV-C and UV-A illumination.

Dependency of Current Compliance Level on Electrical Characteristics of a Peptide-Based Memristor

Jeong Hyun Yoon[1], Min-Kyu Song[1], and Jang-Yeon Kwon[1]
[1]School of Integrated Technology, Yonsei University, Incheon 21983, South Korea
Tel.:82-032-749-5916, E-mail: jangyeon@yonsei.ac.kr

Recently, biomaterial memristors are considered as next generation memory devices due to its non-volatile resistive switching and biocompatibilites. Among them, YYACAYY (Y7C) have controllability in resistive switching characteristics by external humidity. Previous reports described that this is originated from proton mediated redox reactions between tyrosine and silver followed by silver filament formation between electrodes [1-2].

In this research, Pt/Y7C/Ag structure was fabricated. 100 nm Pt and 200 nm Ag layers were deposited by evaporation, and the peptide layer was spin-coated with trifluoroacetic acid (TFA) solution. I-V characteristics (Fig.1) , endurance (Fig.2) and stability tests of the device were measured in various humidities. However, reset failures were observed, which may originated from unstable filament. Therefore, compliance level variation from 1E-7 to 1E-3 and voltage sweep range reduction were applied. In consequence, stable cycle endurance was obtained in 90 % RH, +2V~-2V sweep range, and around 1E-4 compliance level of the device.

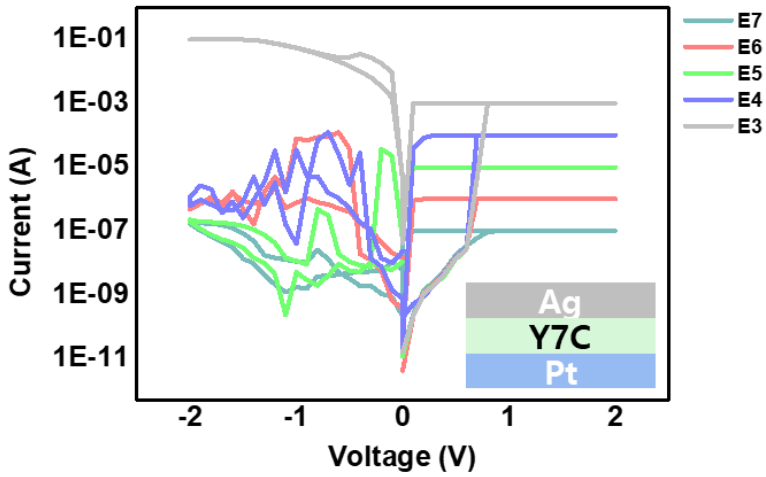

Fig.1. I-V curve of a Y7C memristor with various current compliance level

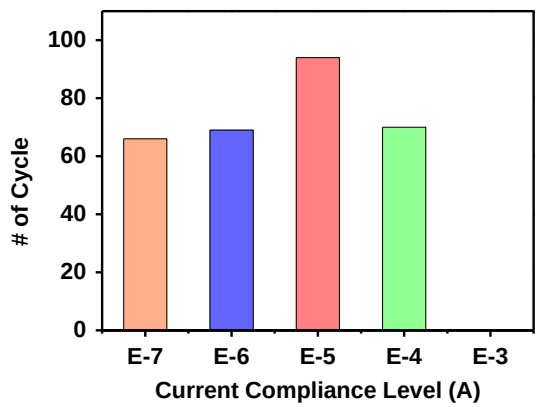

Fig.2. Endurance test results of a Y7C memristor as a function of current compliance level

Acknowledgment

This work was supported by the National Research Foundation of Korea (NRF) grant funded by the Korea government (MSIT) (No. 2020R1A2C2004864).

References

1. Lee, Jaehun, et al. "Proton conduction in a tyrosine-rich peptide/manganese oxide hybrid nanofilm." Advanced Functional Materials 27.35 (2017): 1702185.
2. Song, Min-Kyu, et al. "Proton-enabled activation of peptide materials for biological bimodal memory." Nature Communications 11.1 (2020): 1-8.

Identifying the Role of the Sidewall Defects for GaN-based Micro Light-Emitting Diodes by Comparative Analysis

Jinwoo Park[1], Gyeong Won Lee[1], Jun-Seok Hwang[1] and Jaekyun Kim[1]
[1]**Dept. of Photonics and Nanoelectronics, Hanyang University, Ansan 15588, Republic of Korea**
Tel.:82-31-400-5521, E-mail: jaekyunkim@hanyang.ac.kr

Next-generation displays, which will be applied on augmented reality and virtual display and so on, require high pixel per inch[1]. Micro light-emitting diodes (Micro-LEDs) based on GaN is one of the potential candidates to meet the demand. However, Micro-LEDs suffer from the sidewall defect due to the high surface to volume ratio compared with conventional device[2]. One of the device performances affected by sidewall defects is its efficiency. Mainly, it would have an effect on their internal quantum efficiencies (IQE, η_{IQE}). However, it is not clear what degrades IQE dominantly since IQE is the product of injection efficiency (IE, η_{IE}) and radiative efficiency (RE, η_{RE}). In this paper, the electrical and optical characteristics of Micro-LEDs and conventional one are measured to separate what leads to the degradation of IQE for Micro-LEDs from comparative analysis.

Current-voltage (*I-V*) curves of conventional LED are measured with the resistance connected in parallel (R_p) as shown in Fig. 1. (a). After connecting R_p with conventional one, most of current flow through R_p at low bias region. Except the *I-V* curve for device (black line), the shape of other curves is similar to that of Micro-LEDs[3,4]. Thus, *I-V* curve of Micro-LEDs can be expressed as Fig. 1. (b). From the comparison between *I-V* curves, R_p acts as the leakage current, which reduces IE.

Also, photoluminescence (PL) spectroscopy is measured to investigate the effect of sidewall defect on RE. In order to excite the active region selectively, 405 nm continuous-wave laser diode is used. After measuring PL of conventional and Micro-LEDs depending on excitation power and temperature, it is expected that the dominant factor affecting the IQE of Micro-LEDs can be distinguished.

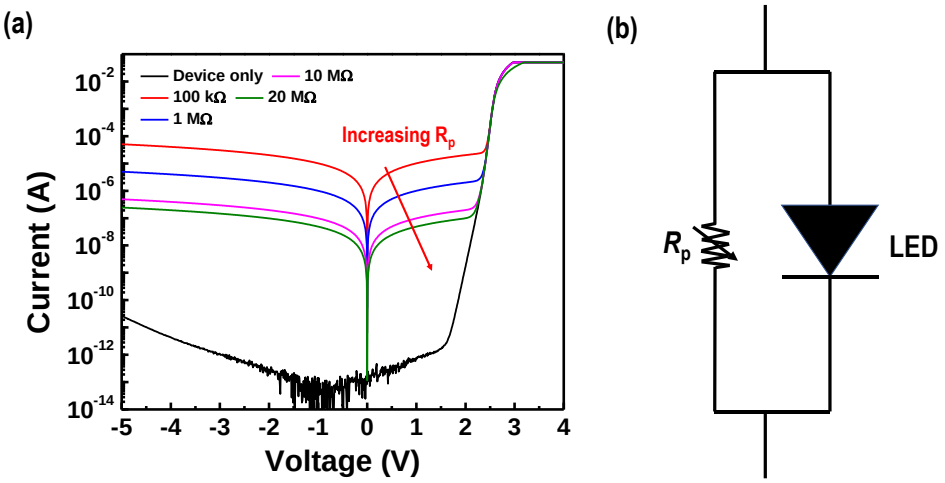

Fig. 1. (a) *I-V* curves of conventional LED connecting with increasing R_p (b) Equivalent circuit of *I-V* curve for Micro-LEDs

References

1. MicroLED Displays 2018 Report, Yole Development (2018).
2. M. S. Wong, D. Hwang, A. I. Alhassan, C. Lee, R. Ley, S. Nakamura and S. P. Denbaars, *Opt. Express*, vol. 26, p. 21324 (2018).
3. E. F. Schubert (2nd), Light-Emitting Diodes, Cambridge Univ. Press, Cambridge (2006).
4. D. H. Lee, J. H. Lee, J. S. Park, T. Y. Seong, and H. Amano, ECS J. Solid State Sci. Technol., vol. 9, p. 055001 (2020).

Effect of Size-dependent Leakage Current from Sidewall Defects of InGaN-based Green Micro Light-Emitting Diodes

Youngwook Shin[1], Jun-Beom Park[2], Sangjin Min[2], Dong-Soo Shin[1], Jong-In Shim[1], Tak Jeong[2], and Jaekyun Kim[1]

[1]Dept. of Photonics and Nanoelectronics, Hanyang University, Ansan 15588, Republic of Korea

Tel.:82-31-400-5521, E-mail: jaekyunkim@hanyang.ac.kr

[2]Micro-LED Research Center, Korea Photonics Technology Institute, Gwangju 61007, Republic of Korea

Tel.:82-62-605-9312, E-mail: tjeong@kopti.re.kr

The growing interest in wearable electronic devices and their numerous potential applications have spotlighted the need for high-performance displays with micro-scale pixels. Recently, GaN-based micro-sized light-emitting diodes (micro-LEDs) have become promising candidates for such display applications.[1,2] Several advantages of the micro-LEDs such as long lifetime, high brightness, and chemical robustness[3–5] make potential candidate for next-generation display. Even though micro-LEDs show outstanding performance, leakage current through the sidewall of the LEDs is regarded as one of the dominant reasons for degrading device performance. However, the effect of the sidewall leakage current has not been clarified in case of micro-LEDs. In this work, the mechanism of the size-dependent leakage current at the sidewall is suggested.

In this work, the electrical and optical characteristics of the LEDs with decreasing active areas, ranging from 90 × 90 μm^2 to 37 × 37 μm^2, were measured to investigate the effect of leakage current. From current density-voltage (*J-V*) curve shown as Fig. 1. (a), the resistive component at low bias is pronounced at the smallest LEDs, which reflects the leakage current via surface defect.[6] And, the reverse bias luminescence via defect is measured to observe the leakage path optically, as depicted in Fig. 1. (b).[7] Combining all of results, the mechanism of leakage current conduction is proposed. From these analyses, low-power consuming and micro-pixelated LED-based displays are available if the sidewall defects of micro-LEDs are suppressed.

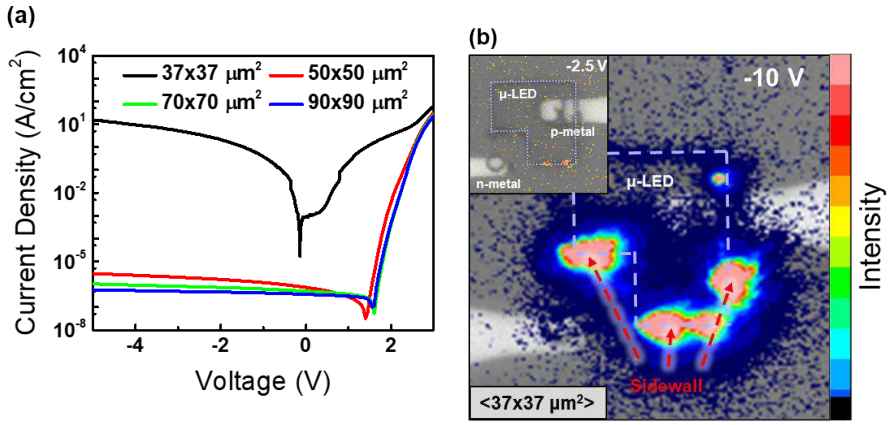

Fig. 1. (a) *J-V* curves for LEDs with different size. (b) Emission image of the smallest LED under reverse bias -10 V.

References

1. F. Olivier, S. Tirano, L. Dupré, B. Aventurier, C. Largeron, and F. Templier, J. Lumin., **191**, 112 (2017).
2. H. X. Jiang, S. X. Jin, J. Li, J. Shakya, and J. Y. Lin, Appl. Phys. Lett., **78**, 1303 (2001).
3. D. Hwang, A. Mughal, C.D. Pynn, S. Nakamura, and S.P. DenBaars, Appl. Phys. Express, **10**, (2017).
4. J. Day, J. Li, D. Y. C. Lie, C. Bradford, J. Y. Lin, and H. X. Jiang, Appl. Phys. Lett., **99**, 1 (2011).
5. Z. Gong, E. Gu, S. R. Jin, D. Massoubre, B. Guilhabert, H. X. Zhang, M. D. Dawson, V. Poher, G. T. Kennedy, P. M. W. French, and M. A. A. Neil, J. Phys. D. Appl. Phys., **41**, (2008).
6. S. W. Lee, D. C. Oh, H. Goto, J. S. Ha, H. J. Lee, T. Hanada, M. W. Cho, T. Yao, S. K. Hong, H. Y. Lee, S. R. Cho, J. W. Choi, J. H. Choi, J. H. Jang, J. E. Shin, and J. S. Lee, Appl. Phys. Lett., **89**, 132117 (2006).
7. D.-P. Han, C.-H. Oh, H. Kim, J.-I. Shim, K.-S. Kim, and D.-S. Shin, IEEE Trans. Electron Dev., **62**, 587 (2015).

Optimization of Dielectrophoretic Assembly of Micro Light-Emitting Diodes by Numerical Analysis

Byeong-u Bak[1] and Jaekyun Kim[1]
[1]Dept. of Photonics and Nanoelectronics, Hanyang University, Ansan 15588, Korea
Tel.:+82-10-3442-7566, E-mail: jaekyunkim@hanyang.ac.kr

Micro-light emitting diodes (Micro-LEDs) have been envisioned a promising approach for low-cost fabrication of next-generation display with superior performance. Micro-LEDs have been demonstrated to fulfill the anticipated future demands on the light-emitting devices and displays.

Various assembly methods have been used to create these devices. However, Micro-LED assembly are less ideal for targeted applications with relatively lower productivity. To address the issue of Micro-LED assembly, electric field assisted assembly methods have demonstrated a great potential to integrate Micro-LEDs array into various forms. Alternating current (AC) dielectrophoretic (DEP) assembly is an efficient method for capturing the Micro-LEDs and assembling them at the predefined locations with precise control.

We have investigated the DEP force for controlling and assembling GaN-based nanorods (NR) at the electrode gap of substrate by COMSOL Multiphysics using finite element analytic simulation. It was found the DEP force depends on the strength of electric field, AC frequency, dielectric constant between NR and surrounding medium, etc. In order to maximize the DEP assembly for Micro-LED fabrication, the magnitude of the DEP force should be large enough to dominate other forces such as the drag force, electrothermal force, buoyancy force, AC electro-osmotic force and the Brownian motion. By simulating DEP assembly experiment using COMSOL, we can visualize the electrohydrodynamic behavior of Micro-LEDs in the solvent and eventually assembly at desired locations and orientation as shown in Figure 1.

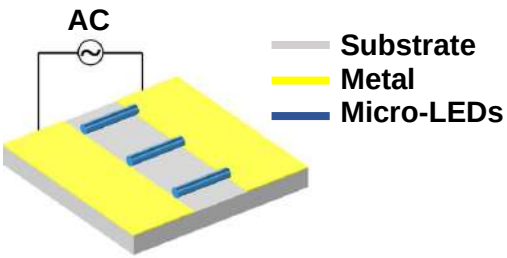

Fig. 1. Schematic of assembled Micro-LEDs after DEP assembly

Acknowledgment

References

1. Devon A. Brown, Jong-Hoon Kim, Hyun-Boo Lee, Gareth Fotouhi, Kyong-Hoon Lee, Wing K am Liu and Kae-Hyun Chung, Sensor, **12**, 5725-5751 (2012).
2. Brian C. Gierhart, David G. Gowitt, Shiahn J. Chen, Rosemary L. Smith and Scoot D. Collin s, Langmiur. **23**, 12450-12456 (2007).
3. Babaros Cetin and Dongqing Li, Electrophoresis, **32**, 2410-2427 (2011).

Change in optoelectronic performances of InGaN-based flip-chip blue micro light-emitting diodes under continuous current stress

Abu Bashar Mohammad Hamidul Islam[1], Tae Kyoung Kim[2], Yu-Jung Cha[2], Dong-Soo Shin[3], Jong-In Shim[3], and Joon Seop Kwak[1]

[1]Dept. of Energy Technology, Korea Institute of Energy Technology, 72, Ujeong-ro, Naju-si, Jeollanam-do, South Korea

Tel.:+82-10-8393-3537, E-mail: jskwak9023@gmail.com

[2]Dept. of Printed Electronics Engineering, Sunchon National University, Jeonnam 540-742, South Korea

[3]Dept. of Photonics and Nanoelectronics, Hanyang University ERICA, Ansan, Gyeonggi 15588, South Korea

Recently, micro light-emitting diodes (μ-LEDs) are getting much more attention due to fast response time, low power consumption, high brightness, and long lifetime. The development of advanced semiconductor technologies helps the μ-LEDs be used in small/large-size displays as well as in other new applications such as biomedical devices, vehicle headlights, and visible light communications. For these applications, it is essential to investigate the performance and reliability issues of μ-LEDs under external stresses. Under high/low-current stress, many processes have been specified as being responsible for the degradation of performances in large-size LEDs by various research groups [1]. However, there are not many researches reported on the reliability issues of μ-LEDs.

In this wok, we investigate the effect of current stress on InGaN/GaN blue μ-LEDs which are bonded on flip-chip packages for measuring various kinds of optoelectronic performances. At constant room temperature, an enclosed chamber is used to apply a continuous current stress (75 A/cm^2) for providing external stress across the μ-LEDs. The current-voltage, the light output power (LOP), the external quantum efficiency (EQE), the electroluminescence (EL) spectra, and the capacitance-voltage characteristics have been measured at a fixed interval of aging time for the stressed μ-LEDs. The forward and reverse leakage currents, the EQE, the EL spectra, and the EL distribution at low currents are systematically studied for understanding the change in performances of μ-LEDs with increasing aging time. It is observed that both the forward and reverse leakages slightly increase with the aging time [Fig. 1(a)] as expected. On the other hand, the EQE [Fig. 1(b)] and the LOP also increase with the aging time up to 200 hours. The improvement of optoelectronic performances is due to gathering of in-plane point defects, which is understood by calculating ideality factor [Fig. 1(c)], and the S values [2].

The measured experimental results show that the optoelectronic properties of μ-LED are enhanced due to current stress. During the presentation, we will describe the detailed theory about the increase in efficiency with aging time.

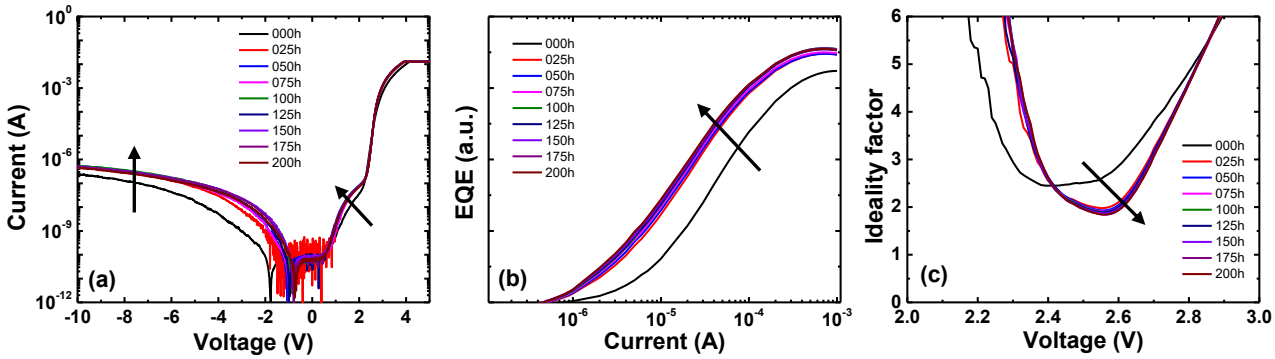

Fig. 1. Changes of (a) current-voltage, (b) EQE, and (c) ideality factor characteristics of μ–LED under continuous current stress.

References

1. P. Tian, J. J. D. McKendry, Z. Gong, B. Guilhabert, I. M. Watson, E. Gu, Z. Chen, G. Zhang, and M. D. Dawson, Appl. Phys. Lett. 101, 231110 (2012).
2. A. B. M. H. Islam, D.-S. Shin, and J.-I. Shim, Appl. Sci. 9, 871 (2019).

Thermal stability and adhesion improvement of InGaN-based flip-chip blue micro light-emitting diodes with sputtered silver alloy reflective contacts

Yu-Jung Cha[1], Xuan Zhang [1], Tae Kyoung Kim[1], Abu Bashar Mohammad Hamidul Isla[2] and Joon Seop Kwak[2]
[1]Dept. of Printed Electronics Engineering, Sunchon National University, Jeonnam 540-742, South Korea
[2]Dept. of Energy Technology, Korea Institute of Energy Technology, 72, Ujeong-ro, Naju-si, Jeollanam-do, South Korea
Tel.:+82-10-8393-3537, E-mail: jskwak9023@gmail.com

The micro light-emitting diodes (μ-LEDs) have attracted great attention due to their wide application to self-emissive micro-displays, biomedical device, vehicle headlights and visible light communication. In addition, the μ-LEDs show fast response time, low power consumption and long-lift time. However, as the chip size reduced, the μ-LEDs has other properties and issue compare with large-size LEDs such as performance, reliability, sidewall effect, thermal stability, chip transfer and adhesion with ohmic contact on metal to semiconductor.

In this work, we investigate the ohmic contact of a silver reflective electrode on p-GaN with the thermal stability on μ-LEDs. In the previous work, the directly deposited silver on p-GaN had bad electrical contact with adhesion. Thus, we examined the formation of ITO nanoparticle on p-GaN for ohmic contact [1]. Then, the Ag reflective electrode was deposited on p-GaN with the ITO nanoparticle for 1024 pixelated micro-LED arrays by radio-frequency magnetron sputter and electron-beam evaporator. The electrical properties of the Ag electrode were evaluated by the transmission line method. Sputtered Ag showed low contact resistance with better ohmic contact than E-beam evaporated Ag (sputter Ag: $1.407e^6$ Ωcm^2, E-beam Ag: $1.874e^6$ Ωcm^2). Both films have high reflectance over the 91 % at 450 nm. These films applied on the 1024 pixelated μ-LEDs arrays to the reflective electrodes. After μ-LEDs arrays fabrication, the E-beam Ag applied device shows an adhesion problem. In addition, the sputtered Ag applied device showed a lower voltage to 3.26 V than the E-beam Ag applied device to 4.21 at 11 mA. The light output power showed that sputtered Ag applied μ-LEDs arrays higher than E-beam evaporated Ag applied μ-LEDs arrays even after thermal aging at 200 ºC. It means that sputtered Ag applied μ-LEDs arrays has high thermal stability than E-beam evaporated Ag applied μ-LEDs arrays.

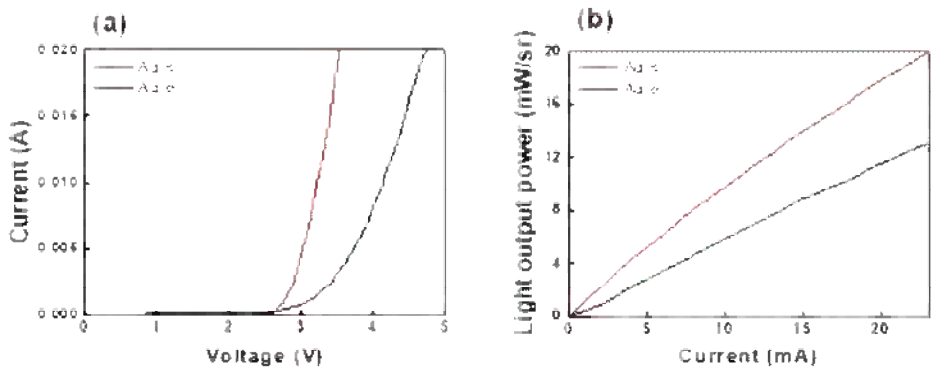

Fig. 1. (a) I-V and (b) L-I curve on sputtered and E-beam evaporated Ag applied μ-LEDs arrays

References

1. J. H. Lee, A. B. M. H. Islam, T. K. Kim, Y. -J. Cha, and J. S. Kwak, *Photonics Res.,* 8(6), p. 060001 (2020).

Realization of RGB Full-color LED Array by Selective Area Growth and Adhesive Bonding

Soo-Young Choi, Hoe-Min Kwak, Seung-Hyun Mun, Je-Sung Lee and Dong-Seon Lee*
School of Electrical Engineering and Computer Science, Gwangju Institute of Science and Technology, 123 Cheomdan-gwagiro, Buk-gu, Gwangju 61005, Korea
Tel.:82-62-715-2248, E-mail: dslee66@gist.ac.kr

In recent years, micro-LEDs are receiving a lot of attention in the development of high-resolution displays. Many researchers have attempted monolithic methods, which have advantages in realizing high-resolution displays over other methods. However, since the inorganic LED structure emits only one color on a single substrate, implementing full-color LEDs with monolithic methods is still challenging without color conversion layers. In this study, a method of manufacturing full-color LEDs by integrating red, green, and blue LEDs on one substrate was realized through selective area growth and adhesive bonding.

First, green and blue LEDs were integrated through the selective area growth method. In the InGaN/GaN green LED structure grown with MOCVD on the sapphire substrate, the part where the blue LED structure will be grown was etched with inductive coupled plasma (ICP), and then the blue LED structure was selectively grown through the SiO_2 insulating layer with MOCVD. After that, each of the green and blue LED pixels (100 μm x 250 μm) was manufactured and green/blue two-color LED arrays could be implemented on one substrate.

Second, wafer bonding of a red LED having an AlGaInP/GaInP structure on GaAs substrate was performed on green/blue two-color LED arrays.[1,2] After bonding the red LED wafer on the green and blue LED substrates using the SU-8, the GaAs substrate was removed and the red LED pixels were fabricated to implement red, green, and blue full-color LED arrays (16 x 16) on one substrate. In this study, the optical and structural characteristics of these full-color LEDs were analyzed.

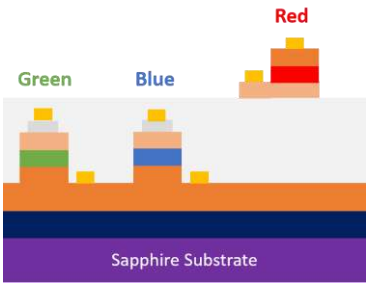

Fig. 1. Cross-sectional views of full-color LEDs structure.

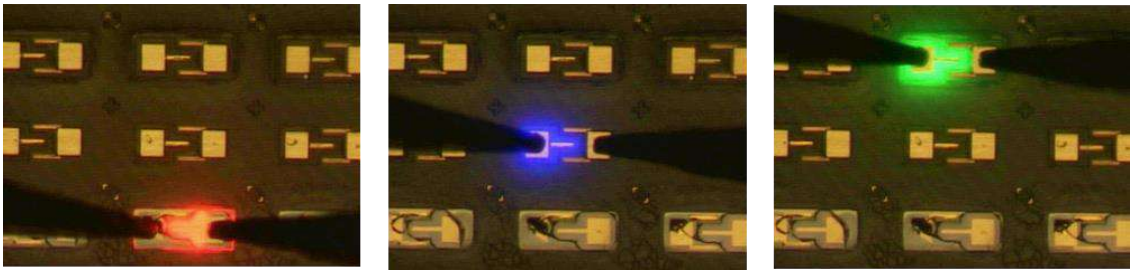

Fig. 2. Microscopic images of full-color LEDs with 0.1 mA injection current.

Acknowledgment
This research was supported by Samsung Electronics.

References

1. C.-M. Kang, *ACS photonics*, vol. 5, p. 4413-4422 (2018)
2. C.-M. Kang, *Scientific Reports*, vol. 7, p. 10333 (2017)

Acoustic Manipulation of LED Chips on the Fine Metal Mask for LED Display Application

S. H. Noh[1], J. J. Ryu[1], C. W. Park[1], Y. Sung[2] and J. S. Yoo[1]
[1]Dept. of Chemical Engineering, Chung-Ang University, Seoul 06974, Korea
Tel.:010-7277-5274, E-mail: jsyoo@cau.ac.kr
[2]APS Holdings 23-12, Dongtansandan 9-gil, Hwaseong-si, Gyeonggi-do 18487, Korea

As the human activities are getting limited due to the COVID-19, they spend more time looking at displays and optical qualities become requiring aesthetic needs in Maslow's hierarchy. When purchasing devices, the performance of the display has become one of the essential check items. The color gamut, refresh rate, contrast ratio, dynamic characteristics of image, and resolution of the display are continuously improving. Among other points, the contrast ratio, which allows us to real experience HDR technology, has been difficult to improve. To solve this problem, the method of using mini-LED backlight and the method of using micro-LED on the front panel draws big attention. However, the difficulty in transporting LED chips to substrates is a big challenge to overcome. To address this, acoustic manipulation of LED chips on the fine metal mask is considered for placing the LEDs on the right position of the substrate. This method has the advantage of being able to transport chips that exist within the area at once compared to other mass transfer technique, which results in less time variation in transportation compared to an increase in area. For understanding the correlation between wave and particle moving, numerical simulation as well as experiments were carried out. Figure 1 shows the fluidic pattern with LED chips on the FMM and the resultant LED chip array. we also want to further understand the movement of LED chips using wave by simulating the action between the vibrating plate and the chips and looking at the chip behavior according to the independent variables. Figure 2 shows the chips pattern to be obtained by numerical simulation. We hope that we can discuss the process feasibility for micro-LED display application in presentation.

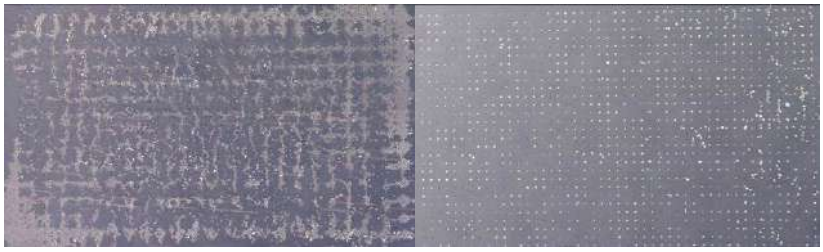

Fig. 1. Pattern of LED Chips on the FMM and the resultant LED chips array

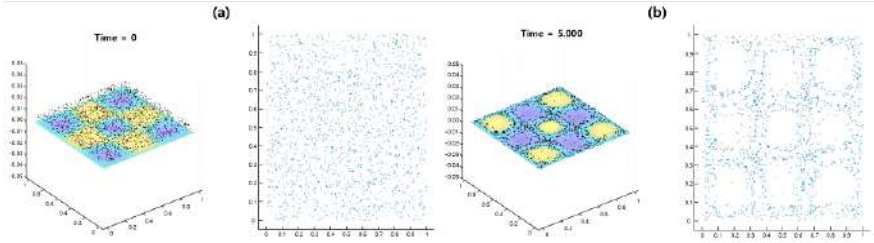

Fig. 2. Particles Moving Simulation on FMM (a) at 0 sec. and (b) at 5 sec.

Acknowledgment

This research was financially supported by the Ministry of Trade, Industry and Energy(MOTIE) and Korea Institute for Advancement of Technology(KIAT) through the International Cooperative R&D program. (Project No. 20201498)

References

1. Zhou, Q., Sariola, V. Latifi, K. et al., *Nat. Commun.*, 7, 12764 (2016).
2. Tuan, P. H. and Wen, C. P. and Yu, Y. T. and Liang, H. C. and Huang, K. F. and Chen, Y. F., *Phys. Rev. E*, 89, 022911 (2014).
3. C. Vella, "Gravitas: An extensible physics engine framework using object-oriented and design pattern-driven software architecture principles," Master in Information Technology Thesis, University of Malta, Msida (2008).

PWM controlled Micro LED Display with double-gate thin-film transistors

Taesoo Kim and Jaehong Jeon
Korea Aerospace University, Gyeonggi-do, Goyang-city 10540, Republic of Korea
E-mail: ktsrlaxotn@gmail.com

Micro LED displays have recently attracted much attention for their application to the next generation display panel. In the case of organic light emission diode (OLED), the gray scale is controlled by modulating the driving current level. However, the wavelength of emitted light from micro LED is shifted according to the drivin g current level. Therefore, it is not proper to adopt the driving method used in OLED to Micro LED displays. In our study, we propose a gray scale control method based on the modulation of duration time of light emission, which is similar to pulse width modulation (PWM) method. In PWM method, if the slope of falling edge of the pulse is not steep enough, it becomes difficult to control the the gray scale precisely. Furthermore, the slow change of the LED driving current from high level to zero level may cause the color distortion due to the wavelength shift, especially at low gray scale. In order to solve this problem, we propose the PWM-controlled micro LED pixel circuit based on CMOS thin-film transistors (TFTs). By using CMOS inverter structure, we can reduce the number of storage capacitors from the circuit and make the operating speed faster. Most of all, our circuit is designed to make operating speed of PWM circuit faster by adopting feedback effect through double-gate TFT structure as well as Schmitt trigger circuit. As a result, it takes about 0.45 μs to turn on the LED and about 2 μs to turn off it. This time is short enough to avoid the color distortion and help the precise control of the gray scale.

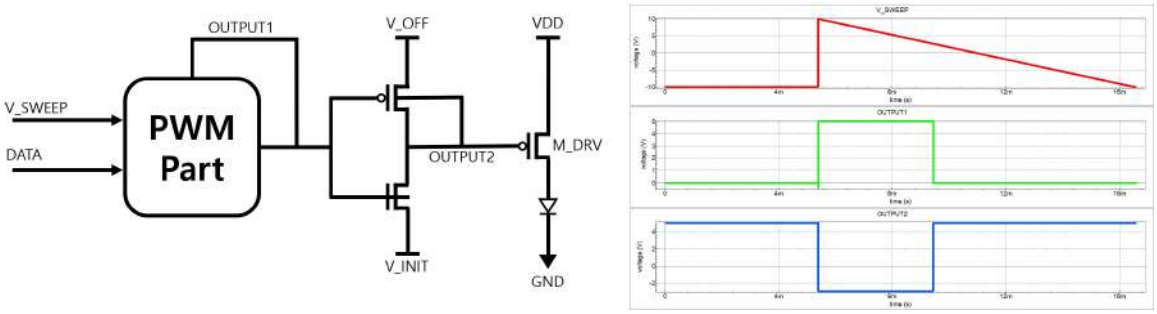

(a) (b)

Fig. 1. (a) Proposed circuit and (b) timing diagram

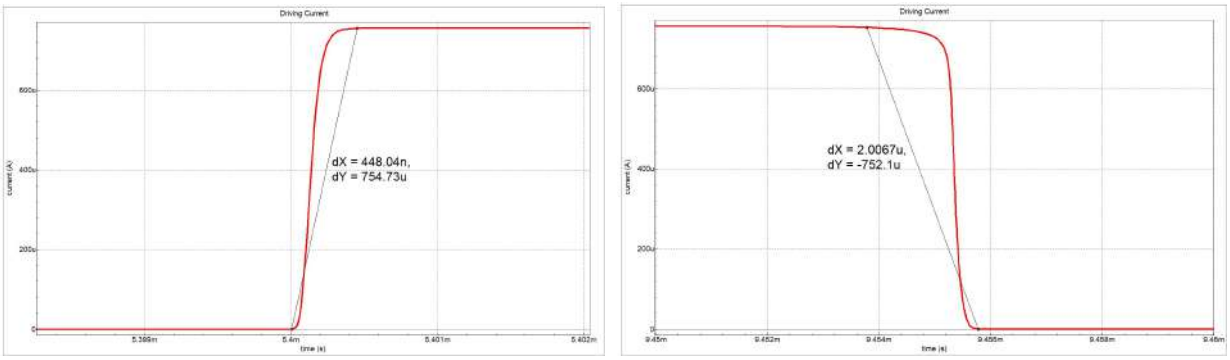

(a) (b)

Fig. 2. Plots of driving current near (a) rising edge and (b) falling edge

Acknowledgment

References

1. C. Zhang, A. Srivastava and P.K. Ajmera, *ELECTRONICS LETTERS,* Vol. 39, No. 24 (2003).
2. Minkyu Chun, Md Delwar Hossain Chowdhury, and Jin Jang, *AIP Advances* 5, 057165 (2015).

Reduced Power Consumption in Blue micro-LED Display with P-type LTPS TFT Using Short-Emission-Time Pulse Amplitude Modulation(PAM)

Sara Hong, Eun Kyo Jung, Yong-Hoo Hong, Eunho Kim, Hwarim Im, and Yong-Sang Kim
Dept. of Electrical and Computer Engineering, Sungkyunkwan University, Suwon, Gyeonggi 16419, Korea
Tel.:82-31-299-4323, E-mail: yongsang@skku.edu

The conventional Pulse Amplitude Modulation (PAM) 3T1C driving scheme of a P-type LTPS TFT OLED [1] commonly has long emission time with low driving current, as organic materials are vulnerable to heat. However, unlike the OLED, a micro-LED display consists of inorganic materials which are free from a burn-in issue. Thus, the driving current for micro-LEDs could be higher than those of OLEDs. In addition, since the luminance (L) is derived from the integral of current over time, adopting higher current signifies shortening time.

Experimentally, the External Quantum Efficiency (EQE) is proportional to a certain level of current [2]. This indicates that high current enables us to apply high EQE up to specific points of current which are varied by colors. Therefore, if we apply current with efficient EQE levels to micro-LED displays, the micro-LED display could achieve better performance in terms of light emission. Therefore, cutting down emission times as a result of high current inputs having high EQE levels could contribute to reducing the total power consumption (P_{total}) based on the same amount of L.

We conducted a power consumption evaluation on the typical 3T1C P-type LTPS TFT with a PAM driving scheme as shown in Figure 1. We assumed the basic specification for a progressive-emission type blue micro-LED display as follows: V_{dd}=8 V, V_F =3 V, scan rate=60 Hz, resolution=320 × 180, and PPI=82. Using $L \propto EQE \times \int Idt$, we estimated emission time and driving current considering the same amount of L. Then, the number of gate lines emitting light simultaneously can be determined. Finally, because the P is the product of current (I) and voltage (V), i.e. P = I × V, the P_{total} can be acquired according to Table 1, where driving current, emission time, and EQE factors are experimentally measured from the micro-LED display.

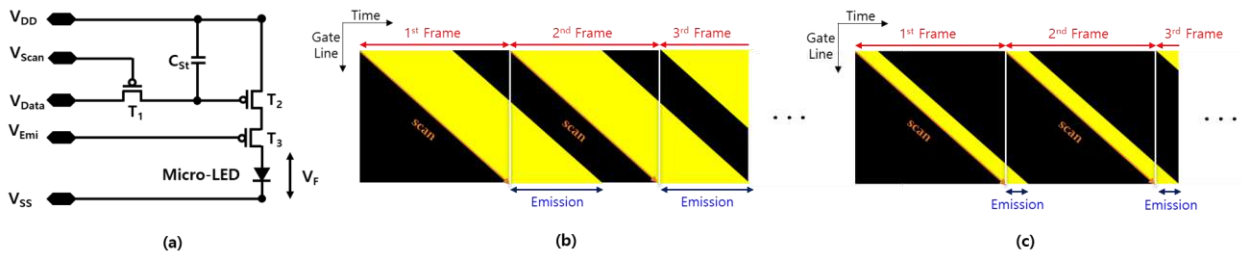

Fig. 1. (a) 3T1C Driving scheme, (b) Long-emission-time progressive emission scheme, and (c) Short-emission-time progressive emission scheme

Table 1. Power consumption comparison between long and short emission times in a micro-LED display

Division	Driving Current(μA)	Emission Time(ms)	# of gate lines emitting light simultaneously	EQE(%)	Power Consumption(W)
Long emission time	2.00	15.50	171	23.40	0.88
Short emission time	80.00	0.25	3	36.20	0.61

Consequently, we found that the overall power consumption of the short-emission-time PAM driving micro-LED display decreased to approximately 70.1% of the long-emission-time case due to the EQE, current, and emission time variance.

References

1. S. Hong, H. W. Hwang, S. S. Hwang, K.W. Kim, Y. M. Ha, and H. J. Kim, *SID Symp. Dig. Tech. Papers*, vol. 50, no. 1, pp. 105-108 (2019).
2. A. Daami, F. Olivier, L. Dupré, F. Henry, and F. Templier, *SID Symp. Dig. Tech. Papers*, vol. 49, no. 1, pp. 790-793 (2018).

The effect of dry etching condition on the micro-LED

Jeong-Hwan Park[*1], *Heajeong Cheong*[2], *Yasuhisa Ushida*[2], *Wentao Cai*[1], *Yuta Furusawa*[2], *and Hiroshi Amano*[2]
[1]**Department of Electronics, Nagoya University, Nagoya, 464-8603, Japan**
*Tel.:81-52-789-5275, *E-mail: park.jeong.hwan@a.mbox.nagoya-u.ac.jp*
[2]**Institute of Materials and Systems for Sustainability (IMaSS), Nagoya University, Nagoya, 464-8601, Japan**

Relatively large light-emitting diodes (LED) based on III–Nitride material have been demonstrated their high levels of performance, and they are being used to backlight units in LCD. Regarding the next-generation display such as AR and VR, the pixel size should be decreased for ultra-high resolution display. Although III–Nitride material based LEDs have good physical and material properties, it is difficult to retain high performance as LED chip size decreases (e. g., <100 μm).[1] Because the dry etching damage at sidewall seriously becomes dominant as chip size decreases, which leads the efficiency droop. Therefore, it is necessary to control and suppress the sidewall damage caused by plasma based ICP-RIE.[2,3]

Here, we report the influence of dry etching condition on the micro-LED. We designed 40 × 40, 20 × 20, and 10 × 10 μm^2 size micro-LED structure that has a p-contact metal pad (Ni/Au =20/300 nm) of 20 × 20, 10 × 10, and 5 × 5 μm^2. All samples had 20 × 20 μm^2 n-contact metal pad (Ti/Al/Ti/Au = 20/100/30/200 nm). To investigate the effect of dry etching condition, we controlled the etching bias power from 30 to 2.5 W, where ICP power was fixed to 150 W. Interestingly, we observed that the sidewall and etched surface become rough as etching bias decreases. Over 15W, the surface looked like smooth; however, under 5 W was very rough. We speculate the low bias process is closed to chemical etching rather than physical etching.[4,5] Figure 1a shows the improved output power with low etching bias. Because low bias mechanism is based on chemical etching, it created rough sidewall morphology, thus, improved output power.[6] Moreover, it was observed that the low bias can suppress sidewall damage, which leads to the reduced leakage current as shown in Figure 1b.

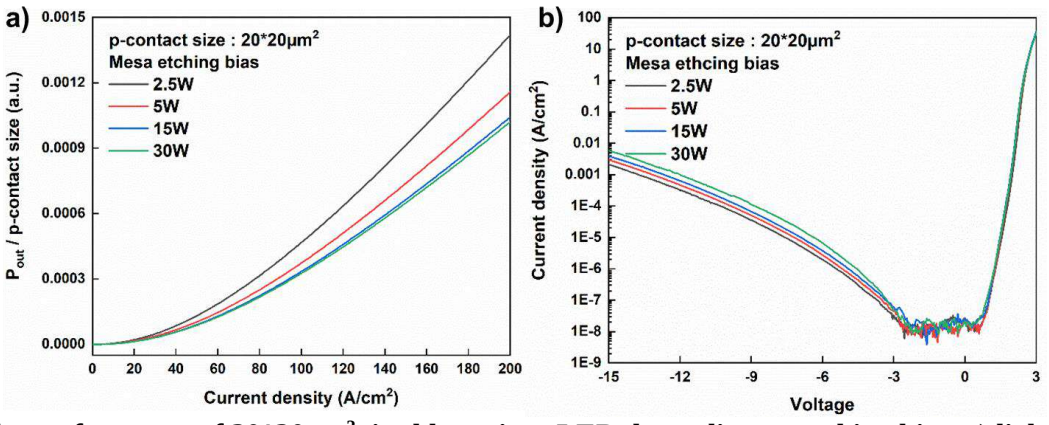

Fig. 1. The performance of 20*20μm^2 size blue micro-LED depending on etching bias. a) light output power-current density and b) current density-voltage characteristics.

Acknowledgment

This work was supported by the Global Research Laboratory (GRL) program through the National Research Foundation of Korea (NRF) funded by the Ministry of Science, ICT, and Future Planning (NRF-2017K1A1A2013160) and a collaborative research contract between Gwangju Institute of Science and Technology and Nagoya University.

References

1. M. S. Wong, S. Nakamura, S. P. DenBaars, ECS J. Solid State Sci. Technol. **9**, 015012 (2020).
2. F. Olivier, A. Daami, C. Licitra, F. Templier, Appl. Phys. Lett. **111**, 022104 (2017).
3. T.-Y. Seong, H. Amano, Surf. Interfaces **21**, 100765 (2020).
4. T. Hino, S. Tomiya, T. Miyajima, K. Yanashima, S. Hashimoto, M. ikeda, Appl. Phys. Lett. **76**, 3421 (2000).
5. Z. Liu, M. Imamura, A. Asano, K. Ishikawa, K. Takeda, H. Kondo, O. Oda, M. Sekine, M. Hori, Appl. Phys. Express **10**, 086502 (2017).
6. M. S. Wong, C. Lee, D. J. Myers, D. Hwang, J. A. Kearns, T. Li, J. S. Speck, S. Nakamura, S. P. DenBaars, Appl. Phys. Express **12**, 097004 (2019).

Anticounterfeiting using mosaics of pixelated wrinkles of liquid crystalline polymer

Kitae Kim[1], Subi Choi[2], Suk-kyun Ahn[2], and Jun-Hee Na[1]
[1]Convergence System Engineering, Chungnam National University, Daejeon 34134, Republic of Korea
Tel.:82-2-821-7978, E-mail: junhee.na@cnu.ac.kr
[2]Dep. of Polymer Science and Engineering, Pusan National University, Busan 46241, Republic of Korea

We demonstrate the anti-counterfeiting concept based on pixelated wrinkling technology[1]. A quick response (QR) code was constructed using pixelated wrinkles of $\theta = 0°$ and 45° (Figure 1) and implemented on a banknote. Under the usual circumstance without the polarization, this QR code is not observed because there are no effective phase differences across the pixels. This image is retrieved only when appropriate optical filters (i.e., the crossed polarizers) are used. The principle of using optical phase retardation can apply to ultraviolet or infrared light sources, which are currently used to discriminate against counterfeits. This image is also readable when placed on the opaque surface by the reflection mode with one polarizer. We note that other configurations of the optical filter can be employed. The capability of producing pixelated wrinkles with a high pixel resolution and density affords their use in informative labels and security tags to prevent the forgery of products.

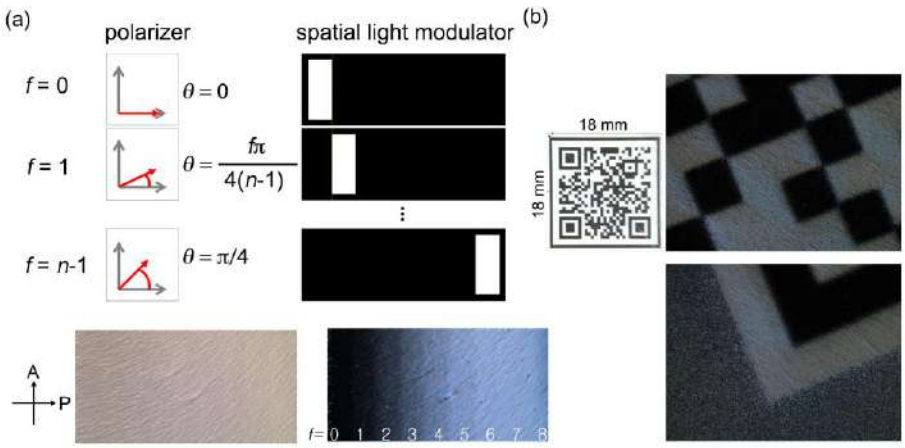

Fig. 1. (a) Procedure of pixelated wrinkles and (a) QR code havaing different wrinkling direction of θ = 0 and 45°

Acknowledgment

This work was supported by the National Research Foundation of Korea (NRF) grant funded by the Korean government (MSIT) (no. NRF-2017R1D1A1B03029573 and NRF-2020R1C1C1012757).

References

1. K. Kim, S.-U. Kim, S. Choi, S.-k. Ahn, and J.-H. Na, *Adv. Sci.* 7(24), 2002134 (2020).

Comparison of Figure-of-Merit Efficiency in Liquid Crystal Phase Shifter Operating Modes: Electrically Controlled Birefringence vs. In-Plane Switching

Jinyoung Choi[1], and Wooksung Kim[1]
[1]**Dept. of Electrical Engineering, POSTECH, Pohang, Gyeongbuk, 37673, Korea**
Tel.:82-54-279-8097, E-mail: jychoi0227@postech.ac.kr

Liquid crystals (LCs) have received attention in the display industries as switching materials. By applying various LCs' operating modes, liquid crystal display (LCD) panels can attain unique characteristics. Recently, the characteristics of LCs' anisotropic dielectric permittivity have been attracted interest from the radio-frequency (RF) industries. Unlike conventional phase shift switches which has discrete operating frequencies, LCs can induce continuously-tunable phase delay, and they have unique characteristics that the loss tangent decreases as frequency increases. Therefore, LCs have been evaluated for many uses in RF applications such as filters, phase shifters, and meta-surfaces.

Twisted nematic (TN) mode and in-plane switching (IPS) mode have been widely stood for the LCDs' operating mode. Likewise, microstrip lines (MSLs) and coplanar waveguides (CPWs) have been extensively used as transmission lines in the RF fields. Both transmission lines are, in addition to a low profile, easy to fabricate, and compatible with monolithic microwave integrated circuit (MMIC) designs. Unlike metallic waveguides, both transmission lines operate as quasi-transverse electromagnetic (TEM) modes. Therefore, they have advantages that DC bias can be applied, which controls LCs' alignment. The more use of LCs makes the higher figure-of-merit (FoM), however, it is needed to research how to get the maximum FoM with the smallest LCs usage.

This paper devised the algorithm to get the maximum FoM per LCs volume for MSLs and CPWs liquid crystal phase shifter (LCPS) at 28 and 60 GHz. We set the differential phase shift angle as -180 degrees and extracted the optimized design parameters by changing LCs thickness from 10 to 200 micrometers. Based on the design parameters, we verified the calculation results through ANSYS HFSS simulation. By comparing the maximum FoM efficiency results for each configuration, we could decide an appropriate LC alignment condition (i.e., LC modes such as EBC or IPS), and optimum LCs for the design purpose.

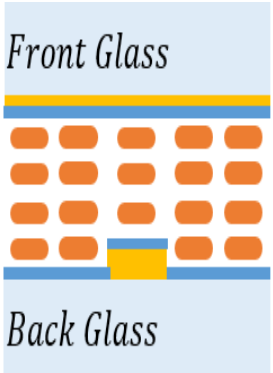

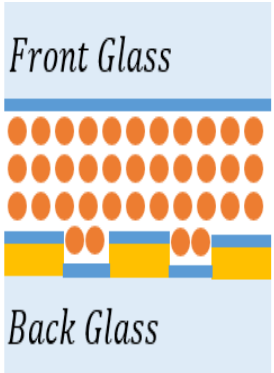

Fig. 1. (a) ECB mode (MSLs) vs. IPS mode (CPWs)

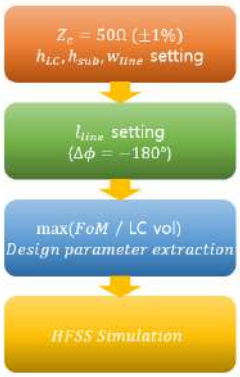

(b) Optimization algorithm for the maximum FoM efficiency (MATLAB + HFSS)

Acknowledgment

Authors appreciate the kind support of the company Nepes in Korea and JNC Corporation in Japan for this study.

References

1. J. Svacina, IEEE *Microw. Guid. Wave Lett.*, **2(10)**, 385(1992).
2. R. Garg, I.J. Bahl, M. Bozzi, Microstrip lines and slotlines, *Artech House, Boston*, 1(2013).
3. A.K. Verma, P. Singh, R. Bansal, *Prog. Electromagn. Res.* **48**, 395(2013).
4. A.K. Verma, G.H. Sadr, IEEE Trans. *Microw. Theory Techn.* **49(7)**, 1587(1992).
5. O.H. Karabey, Electronic beam steering and polarization agile planar antennas in liquid crystal technology, *Springer Science & Business Media*, (2013).

Analytical Study of Bi-Layered Chiral Liquid Crystal Photonic Band Filter

Dahee Wang[1], Seungmin Nam[1], and Su Seok Choi[1]*
[1]Dept. of Electrical Engineering, POSTECH, Pohang, Gyeongbuk 37673, Korea
Tel.:82-54-279-2228, E-mail: choiss@postech.ac.kr

Owing to their peculiar helical structure, Chiral Liquid Crystals (CLCs) are well known for the selective spectral photonic band. This unique photonic band property is resulted from the optical rotation effect of electromagnetic wave propagation depending on the material birefringence (Δn) and rotational repeating pitch (p) following the elegant equation $\Delta\lambda=\Delta n \cdot p$. Hitherto, a number of researchers have investigated the photonic bandgaps (PBGs) control of this fascinating chiral liquid crystal materials for various applications [1,2]. In particular, over visible wavelength range, the concept of the selective color filter exploiting the optical characteristics of CLCs can be suggested beyond the Bayer color filter which is based on chemical dye absorption. Especially, from the well design of chiral liquid crystal parameter, controllable tuning of the wavelength position is possible in CLC band filter. In addition to the single CLC structure, bi-layered CLCs can be approached for further elaborate photonic band filters [3].

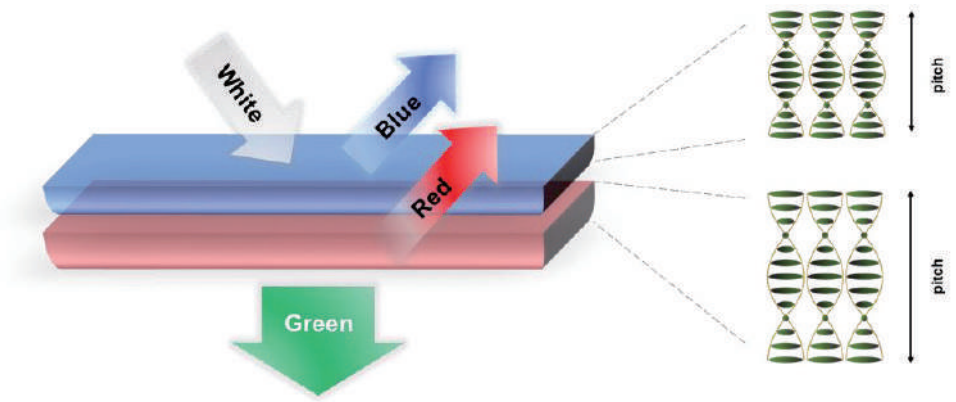

Fig. 1 Schematic representation of the bi-layered Chiral Liquid Crystal photonic color band filter.

Herein, we studied a mathematical analysis of the reflection and transmission spectra of the bilayer CLC photonic color filter modeling. Through this analytical modeling, it was possible to achieve an in-depth understanding of the optical properties of the bilayer CLC color filter. In addition, this study will contribute to exploring a variety of further promising CLC applications including selective band filters and other various photonics sensing applications.

Acknowledgement

This research was supported by Nano Material Technology Development Program through the National Research Foundation of Korea(NRF) funded by Ministry of Science and ICT (NRF-2018M3A7B4089670) and Samsung Electronics Co., Ltd (IO201211-08048-01).

References

1. Balamurugan, R., & Liu, J. H. (2016). A review of the fabrication of photonic band gap materials based on cholesteric liquid crystals. *Reactive and Functional Polymers*, *105*, 9-34.
2. Wang, L., Urbas, A. M., & Li, Q. (2020). Nature-Inspired Emerging Chiral Liquid Crystal Nanostructures: From Molecular Self-Assembly to DNA Mesophase and Nanocolloids. *Advanced Materials*, *32*(41), 1801335.
3. Huang, Y., & Zhang, S. (2011). Optical filter with tunable wavelength and bandwidth based on cholesteric liquid crystals. *Optics letters*, *36*(23), 4563-4565.

Optical Characteristics of Stretchable Chiral Photonic Film based on Chiral Liquid Crystals via *in situ* Photopolymerization

Seungmin Nam[1], Dahee Wang[1] and Su Seok Choi[1*]
[1]Dept. of Electrical Engineering, POSTECH, Pohang, Gyeongbuk 37673, Korea
Tel.:82-54-279-2228, E-mail: choiss@postech.ac.kr

Chiral liquid crystals (CLCs) spontaneously form a supramolecular helical structure due to the helicoidal molecular rotations. This helical structure of CLC provides a periodic variation of dielectric tensor and results in electromagnetic light propagation forbidden band so-called photonic band gaps (PBGs) [1]. Similar to other LC phase materials, CLC shows stimulus responsive behaviours against various external stress including light, temperature, electric field, and mechanical strain. Thanks to the self-organizing feature of photonic band structures as well as, the band tunability by various external stimuli, CLCs have attracted considerable interest in diverse applications, such as sensors [2], laser devices [3], and reflective displays [4]. Especially, the PBG tuning by mechanical deformation is of interest for sensing or micro-actuating applications with great potential. Among several fabrication methods for mechanochromic CLC gels, including anisotropic deswelling or inducing biaxial stress method, *in situ* photopolymerization grants us highly aligned samples with a qualitative optical performance and a simple fabrication process. In this study, we demonstrate the fabrication procedure and optical characteristics by a mechanical strain of free-standing CLC film via *in situ* photopolymerization (Fig. 1).

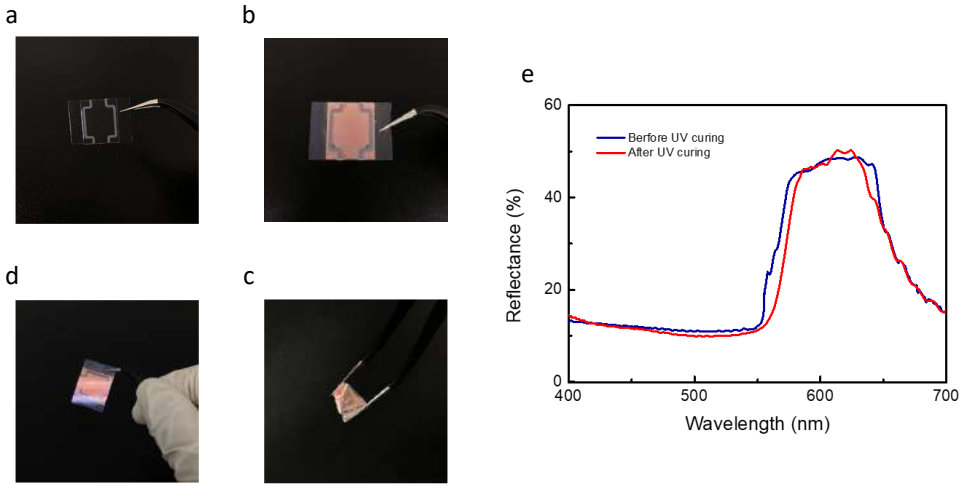

Fig. 1. The fabrication process of chiral photonic films. (a) Glass cell with surface alignment (20 μm cell gap), (b) LC mixture injection, (c) *in-situ* photopolymerization, (d) delamination of free-standing CLC film and (e) optical characteristics of CLC film

Acknowledgment

This research was supported by the Technology Innovation Program (20010690, Development of 12inch panel (20% stretch) and module process technology for massproduction of stretchable display) funded By the Ministry of Trade, Industry & Energy(MOTIE, Korea) and Next Generation Engineering Research Program of National Research Foundation of Korea (NRF) funded by the Ministry of Science, ICT (No.2019H1D8A2106519).

References

1. P. G. de Gennes et al., *The Physics of Liquid Crystals*, Oxford, Clarendon, 1995
2. S. S. Lee et al., Structural Color Paletees of Core-Shell Photonic Ink Capsules Containing Chole steric Liquid Crystals, Adv. Mater. 29, 1606894 (2017).
3. S. M. Wood et al., Wavelength-tuneable laser emission from stretchable chiral nemtic liquid cryst al gels via in situ photopolymerization, *RSC Adv.*, 6, 31919-31924 (2016).
4. S. S. Choi et al., Simultaneous red-green-blue reflection and wavelength tuning from an achiral liquid crystal and a polymer template, *Adv. Mater.* 22, 53-56, (2010).

Programmable liquid crystal defect arrays via electric field modulation for mechanically functional liquid crystal networks

*Ra You [1], Changjae Lee [1], and Dong Ki Yoon [1]**
[1] Department of Chemistry, KAIST, Daejeon, 34141, Republic of Korea

Tel.:82-10-4124-5348, E-mail: zzajae2@kaist.ac.kr

As an approach for developing organic materials with new functionalities, controlling defects of liquid crystal (LC) materials is simple in process since the LC defects have peculiar physical and chemical properties.[1-4] Previously, we reported development of defect arrays by applying AC electric field to nematic LC in a sandwich cell consisting of two glass substrates where patterned indium–tin–oxide electrode is interdigitated. [1]

In this study, it is demonstrated that the defect array in ref [1] can be used to fabricate a functional polymer film. The LC monomeric mixtures with periodic defect structures in nematic phase are photopolymerized to form a liquid crystal polymer network (LCN). As can be seen in **Fig. 1a**, the film produced in this way maintains the defect array even at room temperature. We compared the tensile properties of films with defect arrays consisting of units of different shapes and sizes. It is shown that as the size of the unit is smaller, the crack propagation is hindered by the heterogeneity of the mesogenic unit orientation, which makes the toughness enhanced. Also, the film shows the deformation accompanied by indentations at the defects when heated to high temperature (**Fig. 1b**). In this regard, the friction change according to magnitude of the deformation was also investigated. As the deformation of the film intensifies, the contact area with the flat glass is reduced, so the corresponding friction decreases.

In conclusion, we fabricated a polymer film that can control the functionality on-demand using the LC defect structure array. These results are expected to be helpful in increasing the mechanical reliability of the polymer film and widening its applicability in the future.

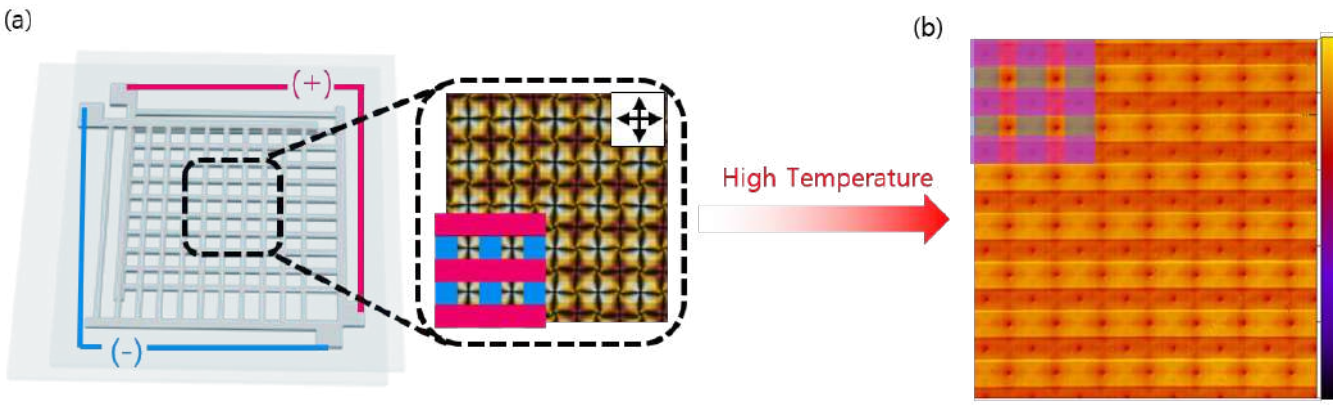

Fig. 1. Representative structure of the fabricated liquid crystal polymer network film. (a) Polarized optical microscope image of defect array. (b) Deformed structure in high temperature.

References

1. You, R.; Choi, Y.-S.; Shin, M. J.; Seo, M.-K.; Yoon, D. K. *Adv. Mater. Technol.* 4, 1900454 (2019).
2. Suh, A.; Ahn, H.; Shin, T. J.; Yoon, D. K. *J. Mater. Chem. C,* 7(6), 1713–1719 (2019).
3. Kim, M.; Serra, F. Tunable Dynamic Topological Defect Pattern Formation in Nematic Liquid Crystals. Adv. Optical Mater., 8 (1), 1900991 (2020)
4. Yoon, D. K.; Choi, M. C.; Kim, Y. H.; Kim, M. W.; Lavrentovich, O. D.; Jung, H.-T. Nat. Mater., 6 (11), 866–870 (2007).

Liquid Crystal Elastomers with Slide-Ring Cross-links: Mechanical Properties, Actuation, and Self-Healing

Subi Choi [1], Bit Ga Ram Kim [2], Ji-hun Seo [2], Suk-kyun Ahn[1,]*

[1]Dept. of Polymer Science and Engineering, Pusan National University, Busan, Korea

Tel.:82-51-510-2405, E-mail: skahn@pusan.ac.kr

[2] Dept. of Materials Science and Engineering, Korea University, Seoul, Korea

Herein, we present a new series of liquid crystal elastomers (LCEs) incorporating various amount of polyrotaxane cross-linkers (LCE-PRX), and investigate their structure-property relationship. Toughness and damping property of the LCE-PRX can be maximized at optimum PRX content (0.5 wt%), while preserving the thermally-driven reversible actuation of the LCE. Specifically, the LCE-PRX can represent high work capacity corresponding with high mechanical properties and good actuation ability. Interestingly, in Figure 1, dynamic nature of PRX crosslinker along with shape memory property of LCE enables thermally-induced self-healing, which is ineffective for the pristine LCE under the same condition.

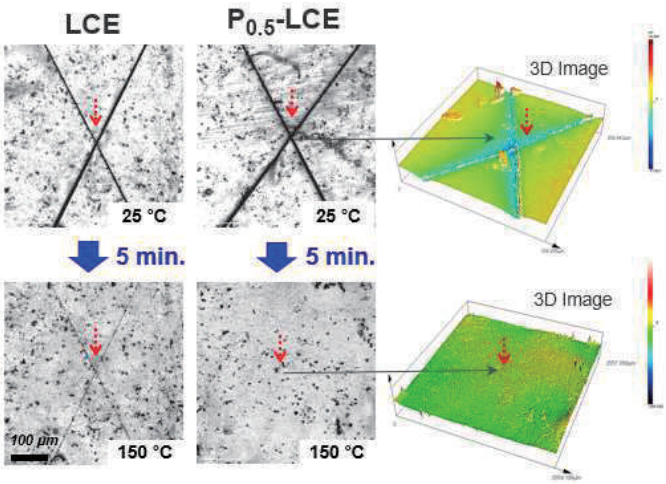

Fig. 1. Self-healing on scratched surface of LCE incorporating PRX cross-linker

Acknowledgment

This work was supported by Basic Science Research Program and the by BK21 plus program through the National Research Foundation of Korea (NRF) funded by the Ministry of Education.

References

1. D.R. Merkel, *Polymer*, 166, 148 (2019).
2. Mohand O. Saed, *Soft Matter,* 13, 7537 (2017).

Shape Reprogrammble and Reprocessable Liquid Crystal Elastomers with Poly(ether-thiourea) Dynamic Crosslinker

Jin-Hyeong Lee[1], Dong-Gyun Kim[2], Yong Seok Kim[2], Suk-kyun Ahn[1,]*
[1]Dept. of Polymer Science and Engineering, Pusan National University, Busan, Korea
[2]Advanced Materials Division, Korea Research Institute of Chemical Technology, Daejeon, Korea

Tel.:82-51-510-2405, E-mail: skahn@pusan.ac.kr

The incorporation of dynamic covalent bonds within liquid crystal elastomers (LCEs) can bring great benefits including reprocessability, shape reprogrammability and self-healing which are not allowed in the conventional LCEs. In this study, we present a new class of reprogrammable and reprocessable LCEs using poly(ether-thiourea) crosslinkers. Interestingly, the thiourea linkages undergo a dissociation above 140 °C evidenced by FT-IR investigation. By exploiting the dynamic nature of poly(ether-thiourea) crosslinker, we successfully demonstrate that the reprocessability of the LCE by compression molding, solution reprocessing, and the reprogrammability of the permanent shape by mechanical manipulation at elevated temperature, while preserving the capability of reversible actuation.

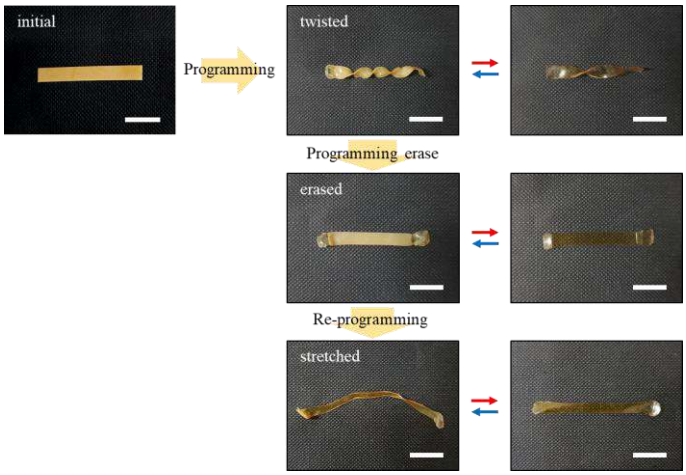

Fig. 1. Reversible actuation and reprogramming of LCEs with poly(ether-thiourea) bonds

Acknowledgment

This work was supported by Basic Science Research Program and the by BK Four program through the National Research Foundation funded by the Ministry of Education.

References

1. E. J. Cha, D. S. Lee, H. Kim, B. G. Kim, Y. Yoo, Y. S. Kim and D. G. Kim, *RSC Adv.*, 9, 15780 (2019).
2. X. Qian, Q. Chen, Y. Yang, Y. Xu, Z. Li, Z. Wang, Y. Wu, Y. Wei and Y. Ji, *Adv. Mater.*, 30, 1801103 (2018).

Resolution-improved autostereoscopic 3D display by using virtual-moving lenticular lens array

Min-Kyu Park[1,2], Tae-Hyun Lee[2], Seon Kyu Yoon[1], Kwang-Hoon Lee[1], and Hak-Rin Kim[2,]*
[1]Spatial Optical Information Research Center, Korea Photonics Technology Institute, Gwanju 61007, Korea
[2]School of Electronic and Electrical Engineering, Kyungpook National University, Daegu 41566, Korea
[*]Tel.:82-53-950-7211, E-mail: rineey@knu.ac.kr

Autostereoscopic 3D display can provide 3D information to viewers using stereo-channel separation technology based on conventional 2D display panels. However, the resolution of 3D image is inevitably degraded compared to conventional 2D display, and there is a concern of vergence-accommodation conflict (VAC) in the autostereoscopic 3D displays because of the mismatch between a vergence depth location and an accommodation layer [1]. In order to resolve the VAC problem, increasing the angular resolution of the 3D views like the super-multi-view 3D displays have been proposed [2]. Nevertheless, these approaches inevitably induce the reduced 3D image resolution since the autostereoscopic 3D displays are in under a trade-off relationship between the angular-resolution and spatial-resolution in 3D images.

In this paper, we analyzed the laterally shifting effect of a lenticular lens array (LLA) relative to a pixel array of flat panel display in time-sequential autostereoscopic 3D display. By using the laterally shifting of LLA in units of half size of the sub-pixel, we confirmed that not only the spatial resolution but also the angular resolution can be improved by time-multiplexed superposition effect analytically. For the shifting condition of half pitch of sub-pixel, the angular-resolution and view-points are doubled without degradation of the initial spatial-resolution. In order to verify the angular-resolution improvement, we demonstrated a time-multiplexing autostereoscopic 3D display with 30 frames per second by using the fast-switching virtual-moving LLA. As the angular resolution and the number of 3D viewpoints were doubled without degradation of the spatial resolution, a 20-view autostereoscopic 3D display could be demonstrated, which is shown in Fig. 1.

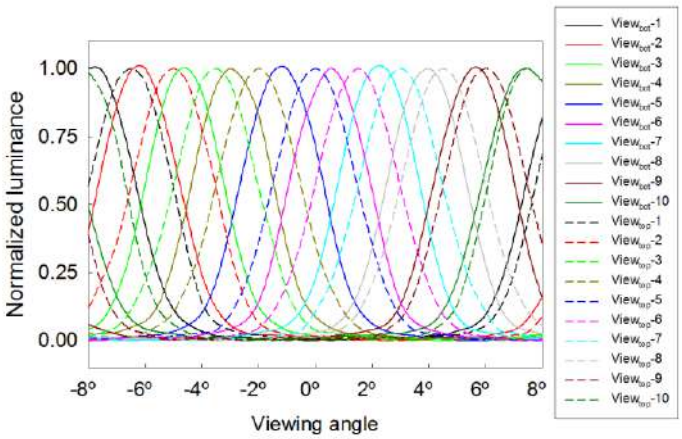

Fig. 1. Normalized luminance distribution of the time-sequential autostereoscopic 3D display using the virtual-moving LLA.

Acknowledgment

This work was supported by Institute of Information & communications Technology Planning & Evaluation (IITP) grant funded by the Korea government(MSIT) (No. 2020-0-00083, Development of Low MTP Latency Microdisplay and SoC technology for VR·AR devices)

References

1. Y. Takaki and Nichiyo Nago, *Opt. Express*, 18(9), 8824 (2010).
2. O. H. Willemsen, S. T. Zwart, M. G. Hiddink, D. K. Boer and M. P. Krijn, *SID'07 Technical Digest*, p. 1154 (2007).

High-responsivity phototransistor based on large-grain boundary Perovskite/IGZO hybrid structures

Gi-Sang Choi[1], Seohyun Maeng[1], Hansol Kim, Ki-Ha Hong[2] and Jaekyun Kim[1]*
[1]Department of Photonics and Nanoelectronics, Hanyang University, Ansan 15588, Republic of Korea
Tel.:82-31-400-5521, E-mail: jaekyunkim@hanyang.ac.kr
[2]Department of Materials Science and Engineering, , Hanbat National University, Daejeon 34158, Republic of Korea

Thin-film transistors (TFT) based on indium gallium zinc oxide (IGZO) have excellent electrical properties such as high carrier mobility, high on/off ratio and low subthreshold swing. However, thin-film device based on IGZO makes it difficult to realize an efficient visible photosensor because IGZO thin films respond only to the light with short wavelength range (< 400 nm). To overcome these problems, we developed a hybrid phototransistor based on IGZO thin films with overgrown perovskite ($RbCsFAPbI_3$) thin film. Solution-processed perovskite have attracted extensive attention in the research area of optoelectronic devices. It is because the perovskite film features excellent advantages such as a direct bandgap, ease of low-cost synthesis, long charge carrier diffusion length, low recombination rate and high absorption coefficient in the visible light range. Therefore, we propose the hybrid structure of high-sensitivity perovskite thin film on a IGZO device for synergistic performance of photosensor. First, a metal oxide IGZO thin film is formed on the SiO_2/Si substrate by sputtering, and Al metal electrodes is deposited by thermal evaporator and shadow mask. And then, perovskite (RbCsFAPbI3) is deposited on Al/IGZO film by using a shear coating method. The rapid-shear-deposited perovskite thin films possess a large-grained, densely-packed and highly-crystalline phase. These large-grained perovskite thin films with less grain boundaries can attribute to the enhanced carrier recombination characteristics. To confirm the possibility of phototransistor based on IGZO/perovskite heterostructure, we measured its performance by an exposure of visible light. The perovskite/IGZO devices exhibited that the photocurrent increased under visible range illumination and observed high photoresponsivity and detectivity.

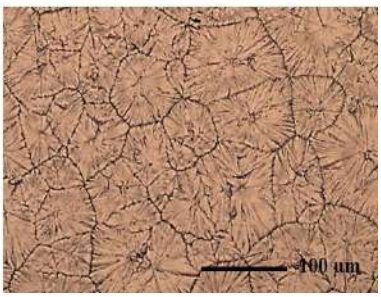

Figure 1. Optical image of large-grained perovskite film

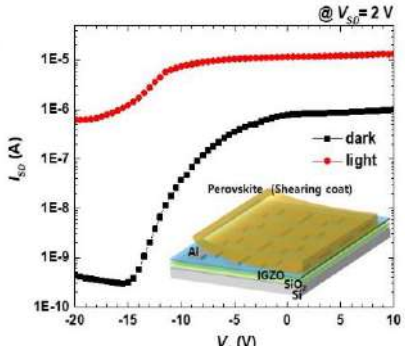

Figure 2. Transfer curves of phototransistor based on IGZO/perovskite heterostructure without and with visible light illumination.

This template is for IMID 2021 Technical Digest. Your file should be submitted via our home page below. (http://www.imid.or.kr/2021/online_paper_submission.asp). If you follow the foregoing, your paper will conform to the requirements of the publisher and facilitate a problem-free publication process.

Acknowledgment

References

Multi-directional Orientation Control of Lyotropic Chromonic Liquid Crystals via Capillary Bridge

Hee Seong Yun[1], Geonhyeong Park[1], and Dong Ki Yoon[1,2*]
[1]Department of Chemistry, KAIST, Daejeon, 34141, Republic of Korea
Tel.:82-42-350-2848, E-mail: nandk@kaist.ac.kr
[2]Graduate School of Nanoscience and Technology, KAIST, Daejeon, 34141, Republic of Korea

Well-ordered lyotropic chromonic liquid crystals (LCLCs) composed of 1D aggregates of disc-shaped molecules in water are widely used for sensor[1], display[2], and biotechnology[3]. Commonly, LCLCs can be controlled by surface modification[4-6]. However, It is difficult to create complex 3D structures in this ways.

Here, we suggested a new approach to controlling the spontaneous alignment of the LCLCs in the capillary bridge assembly. When LCLC solution is injected into the sandwich cell fabricated with intaglio line patterned Si microchannel, capillary bridge is formed due to inhomogeneous capillary action. Various dimensional assembled structures from 1-dimension to 3-dimensions are spontaneously generated by controlling the effect of interface between the capillary bridge and air. We figure out the mechanism of self-assembly with polarized microscope analysis and liquid crystal elastic theory. This approach can homogeneously and fast control the LCLCs in large area and be applied on broad fields, such as organic semiconductor, display, and scaffold for living matters.

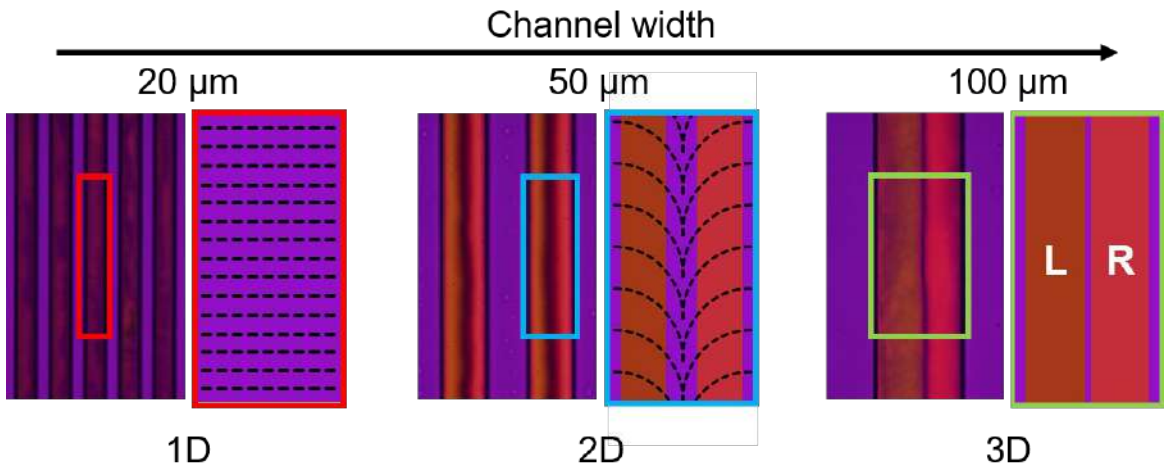

Fig. 1. Various dimensional assembled LCLC structures controlled by length of microchannel

References

1. S. V. Shiyanovskii, T. Schneider, I. I. Smalyukh, T. Ishikawa, G. D. Niehaus, K. J. Doane, C. J. Woolverton, and O. D. Lavrentovich*, *Phys. Rev. E.,* 71, 020702(R) (2005).
2. Hyuk Jun Kim, Woo-Bin Jung, Hyeon Su Jeong and Hee-Tae Jung*, *J. Mater. Chem. C.,* 5, 12241 (2017).
3. Chenhui Peng, Taras Turiv, Yubing Guo, Qi-Huo Wei, Oleg D. Lavrentovich*, *Science* 354, 882–885 (2016).
4. Joonwoo Jeong, Ganghee Han, A. T. Charlie Johnson, Peter J. Collings, Tom C. Lubensky, and Arjun G. Yodh, *Langmuir,* 30, 2914−2920 (2014).
5. Netra Prasad Dhakal, Jinghua Jiang, Yubing Guo, and Chenhui Peng*, *ACS Appl. Mater. Interfaces,* 12, 13680−13685 (2020).
6. Yubing Guo, Hamed Shahsavan, Zoey S. Davidson, and Metin Sitti*, *ACS Appl. Mater. Interfaces,* 11, 36110−36117 (2019).

Engineering Optical Rotation in Chiral Photonic Film for Configurable Color Filter

*Wongi Park[1], Yun-Seok Choi[2], Hyewon Park[2], and Dong Ki Yoon[1,2]**
[1]Graduate School of Nanoscience and Technology, KAIST, Daejeon 34141, Republic of Korea
[2]Department of Chemistry, KAIST, Daejeon 34141, Republic of Korea
Tel.: 042-350-2848, E-mail: nandk@kaist.ac.kr

Photonic crystals (PC) are periodic optical micro- or nanostructure, and they have structural colors by reflecting a specific wavelength of light, also known as photonic bandgap (PBG)[1]. Since the structural colors originate from the interference of light, they are more stable than chemical dyes and widely used in everyday life. In chiral PC, there is optical rotation (β), in which the incident linearly polarized light rotates as it passes through the chiral medium[2]. Optical rotation tends to diverge at around PBG due to the resonance effect and dramatically varies depending on the wavelength of light. When the chiral PC film is observed under transmission mode microscope between two rotatable linear polarizers, polarization-dependent transmission color change can be observed depending on the rotation angle of polarizer[3].

Herein, we demonstrate the relationship between optical rotation and PBG using cholesteric liquid crystals (CLC), which can act like 1D chiral PC by forming spontaneous helical superstructure[4]. Because the helical pitch of CLC can be controlled by the concentration of chiral dopant, we can also easily control the wavelength of PBG. As a result, we can engineer optical rotation and PBG precisely by controlling the helical pitch of CLC, which in turn changes the transmission colors. We can realize various colors within one PC film by simply rotating the polarizer due to the optical rotatory dispersion. Moreover, this PC film can reflect certain wavelength while remaining transparent. We expect to use this film in advanced optical applications, such as smart windows and protective goggles.

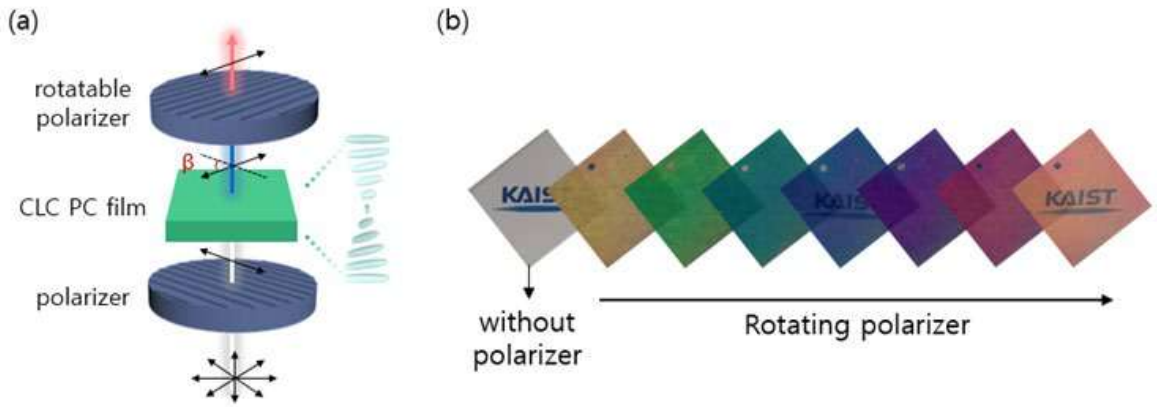

Fig. 1. (a) Experimental set-up of transmission mode with two rotatable linear polarizers. (b) Polarization-dependent color change in chiral PC film.

References

1. S. Y. Lin, J. G. Fleming, D. L. Hetherington, B. K. Smith, R. Biswas, K. M. Ho, M. M. Sigalas, W. Zubrzycki, S. R. Kurtz and J. Bur, *Nature*, 394, 251 (1998)
2. W. Park, J. M. Wolska, D. Pociecha, E. Gorecka and D. K. Yoon, *Adv. Opt. Mater.*, 7, 1901399 (2019)
3. W. Park, T. Ha, T. S. Jung, K. I. Sim, J. H. Kim, J. M. Wolska, D. Pociecha, E. Gorecka, T.-T. Kim and D. K. Yoon, *Nanoscale*, 12, 21629 (2020)
4. M. Mitov, *Adv. Mater.*, 24, 6260 (2012)

4D Printing of Hygroscopic Liquid Crystal Elastomers

Keumbee Kim, Yuanhang Guo, Jaehee Bae, Subi Choi, Suk-kyun Ahn*

Dept. of Polymer Science and Engineering, Pusan National University, Busan, Korea

Tel.:82-51-510-2405, E-mail: skahn@pusan.ac.kr

Herein, we present a new class of humidity-responsive liquid crystal elastomer (LCE)[1] incorporating dimethylamino moities that can be prepared by versatile processing, including surface alignment as well as 4D printing. The humidity-responsive properties are introduced by activating one of the LCE surfaces with an acidic solution, which generates cations on the surface, and provides asymmetric hydrophilicity to the LCE. The resulting humidity-responsive LCE undergoes programmed and reversible hygroscopic actuation, and its shape transformation can be directed by the cut angle with respect to a nematic director or by localizing activation regions in the LCE. Most importantly, various humidity-responsive LCE actuators, including a flower, a concentric square array, and a soft gripper, are successfully fabricated by employing LC inks in UV-assisted direct-ink-writing (DIW)-based 3D printing[2].

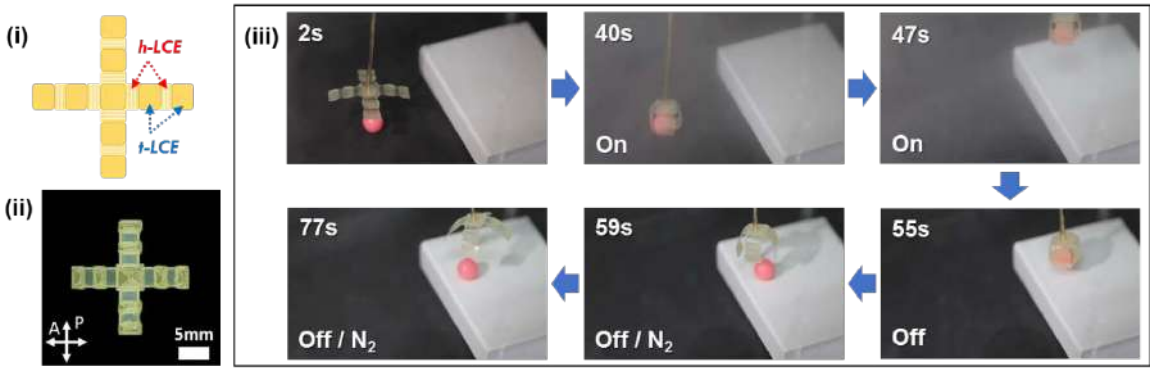

Fig. 1. Humidity-responsive Soft gripper

Acknowledgment

This work was supported by Basic Science Research Program and the by BK Four program through the National Research Foundation funded by the Ministry of Education.

References

1. Kularatne, R. S., *J. Polym. Sci. Part B. Polym. Phys.*, 55, 395 (2017).
2. Zhang, C., *ACS Appl. Mater. Inter.* 11,47,44774 (2019).

Advanced Bistable Cholesteric Light Shutter

Gwan Yong Lee[1], Eun Ji Kim[2], Young Jin Lim[1], MinSu Kim[1] and Seung Hee Lee[1]
Applied Materials Institute for Department of Nano Convergence Engineering and Department of Polymer Nano-Science and Technology, Jeonbuk National University, Jeonju, Jeonbuk, 54896, Korea
Tel.:063-270-2343, E-mail: lsh1@jbnu.ac.kr

Smart window technology is an active control technology that can actively adjust transmittance, reduce energy loss, and provide a pleasant environment to consumers. It is possible to pursue high efficiency in energy use and is a base technology that can be applied in common to various industrial fields.

Our previous light shutter glass made of dual frequency cholesteric liquid crystals (DFCLC) has weakness such as structure deformation of LC alignment from external stress and glass-based substrate. [1,2] In order to overcome it with use of plastic substrate, polymer network to prevent structure deformation is challenged with use of reactive mesogen (RM). The initial DFCLC cell shows randomly oriented state of LC not a pure planar state. And this multi-domain decreases transmittance in both transparent state (Planar state) and opaque state (Focal conic state) after polymerization, as shown Fig. 1(a). To minimize transmittance decrease, we applied high voltage and high frequency (60KHz,100V) and then the cell became mono domain state. Then we try photo polymerization while high voltage and frequency is applied. After polymerization, the mono-domain shows stable state in both planar and focal conic state after removing voltage and frequency and transmittance decrease was minimized, as shown in Fig. 1(b).

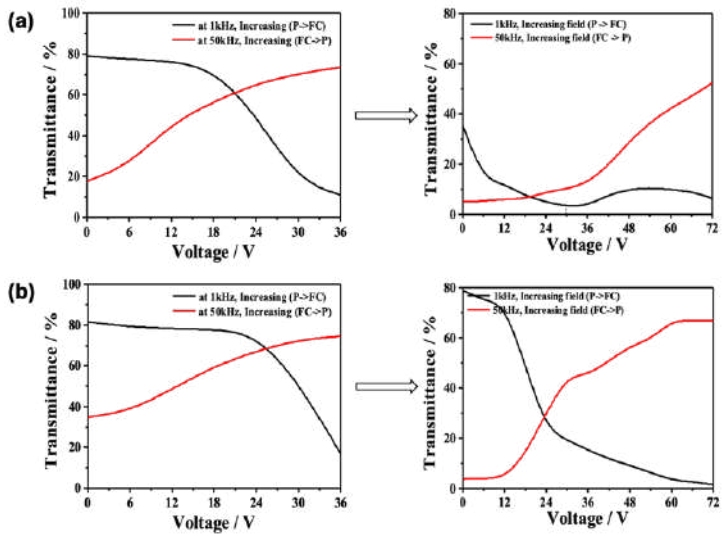

Fig. 1. Transmittances changes of the (a) multi domain state (initial state) and (b) mono domain state (applying 60V 100KHz) before/after polymerization.

Acknowledgment

This work was supported by the Innovation Lab support program for material, parts, equipments (20012555, Commercialization of nanocarbon composites materials in electric and electronic display and energy industries) funded by the Ministry of Trade, Industry & Energy (MOTIE, Korea)

References

[1] M. Xu and D.-K. Yang, "Dual frequency cholesteric light shutters," Appl. Phys. Lett. 70(6), 720–722 (1997).
[2] Lee SH, et al., Optical Materials Express, 2,8,1121(2012)

Tunable optic axis of optically isotropic liquid crystals between negative C and positive C

Hyoung Soo Park[1], Da Yeon Lee[1], MinSu Kim[1], Young Jin Lim[1] and Seung Hee Lee[1*]
[1]Applied Material institute for Department of Nano Convergence Engineering and Department of Polymer Nano-Science and Technology, Jeonbuk National University, Jeonju, Jeonbuk 54896, Korea
E-mail: lsh1@jbnu.ac.kr

To protect the information displayed on the screen, we usually use a light control film, called "louver film", in which light propagation is blocked in an oblique viewing directions. However, this method has the disadvantage of not only sacrificing transmittance of the display at normal direction, but also making it difficult to share information with others.

In this study, optically isotropic liquid crystals (OILC) cell using dual frequency liquid crystal (DFLC) was fabricated to reveal either wide or narrow the viewing angle according to the driving frequency. The effectiveness of negative C plates in these VA mode displays was demonstrated [1,2]. The fabricated OILC cell works as a positive ($\Delta\varepsilon = +3$ at 1kHz) and negative ($\Delta\varepsilon = -2.8$ at 50kHz) C-plate by vertical electric field. Figuer 1 shows the simulatiom results of the normal VA-mode and viewing angle controllable VA-mode with proposed OILC cell. As shown in Figure 1(a) shows light leakage of 30.8% at a polar angle of 60°, resulting in poor viewing angle. Figure 1(b) shows only the light leakage of 7.2% at an polar angle of 60° in a cell driven by a negative C-plate. This shows that a wide viewing angle characteristic can be obtained. Figure 1(c) shows the light leakage increased to 33.1% at polar angle of 60° when the OILC cell operated to a positive C plate. The viewing angle is narrower than that of a normal VA cell. We believe that the cell proposed by us will be useful in various displays

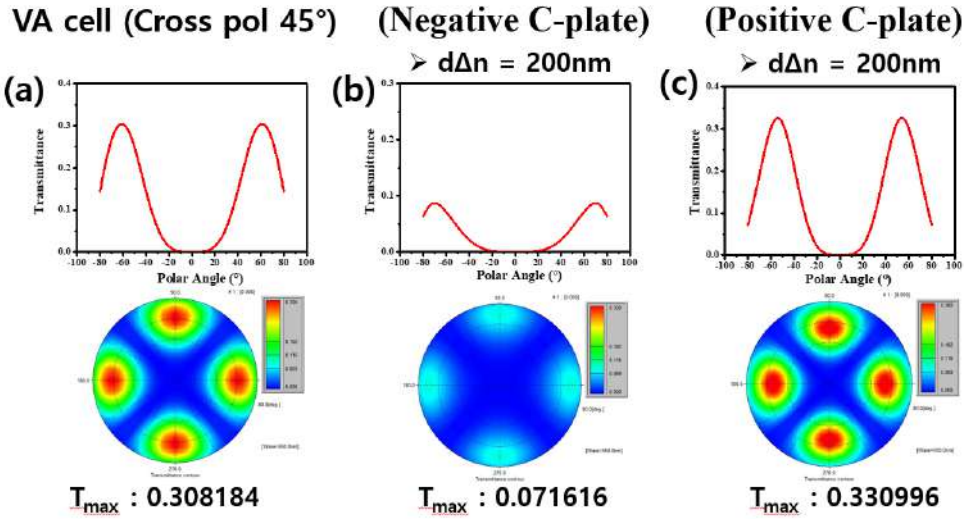

Fig. 1. Calculated viewing angle properties of (a) a vertical alignment (VA) cell and the VA cells in which a tunable cell is added as (b) negative C and (c) positive C plates.

Acknowledgment

This research was supported by the Basic Science Research Program through the National Research Foundation of Korea (NRF) funded by the Ministry of Education (2016R1D1A1B01007189) and by the NRF grant funded the Korea government (MSIT) (2019R1A5A8080326).

References

1. J. Chen, K.-H. Kim, J.-J. Jyu, J. H. Souk, J. R. Kelly, P. J. Bos. Optimum Film Compensation Modes for TN and VA LCDS.SID pp 315-318(1998)
2. Seung-Hoon Ji, Jung-Min Choi, Gi-Dong Lee. An Optical Configuration of VA LC Cell for Improvement of the Viewing Angle. IDW pp 395-398(2008)

Polymer Stabilized Optical Vortex Generation of the Standing Wave Mediated Defects in the Nematic Liquid Crystals

*Vijay Kumar Baliyan[1], Doyeon Lee[1], and Jang-Kun Song[1]**
[1]Dept. of Electrical and Computer Engineering, Sungkyunkwan University 2066 Seobu-ro, Suwon, Gyeonggi-do 16419, Republic of Korea.
E-mail: jk.song@skku.edu

Optical vortex beams hold promises for their ability to significantly increase the transmission capacity of data communication defined by different topological charges associated with the optical angular momentum. Here in this presentation, we proposed a simple method to create an electrically switchable and permanent topological defect in nematic liquid crystals that can be used for optical vortex arrays at fixed positions without using a specific patterned electrode. For that purpose, we have applied pulse waves to the vertically aligned LC to create standing wave mediated topological defect arrays (1-3). The low concentration (~1 wt%) of RM is polymerized by UV light in the deformed state of LC to control the pretilt angle. The positions of topological defects in nematic liquid crystals are decided before photo-polymerization of reactive mesogen (RM). After polymer network formation in the LC film, it behaves as a simple electro-optic switching device that can be used for switchable optical vortex generation. Figure 1. Shows the POM and macropicture of topological defects with optical vortices at applied electric field. The density of polymer networks is varied by changing the RM concentration to study the internal morphology of the defect formation in the LC. We have optimized the density of polymer networks in the deformed state of LC for permanent stabilization of the topological defect arrays film. The topological defect LC film is studied for optical vortex generations which can use for different applications.

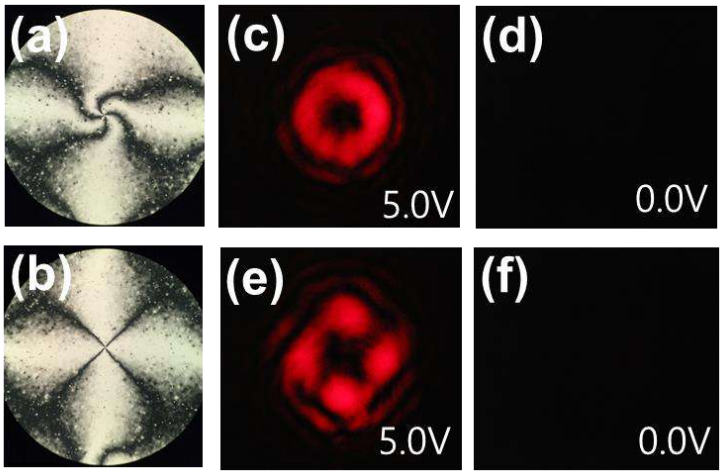

Fig. 1. (a), (b) POM texture +1 and -1 defects in the cell, (c), (d) and (e), (f) switchable +2ħ and -2ħ optical vortex under electric, respectively

Acknowledgment

This work was supported by the National Research Foundation of Korea (NRF) funded by the Ministry of Science and ICT (NRF-2019R1I1A1A01062248).

References

1. L K Migara and J.-K. Song, *NPG Asia Materials* 10, e459 (2018).
2. L.K. Migara, C.-M. Lee, K. Kwak, H. Lee, J.-K. Song, *Current Applied Physics* 18 819‐823(2018).
3. L. K. Migara, H. Lee, C.-M. Lee, K. Kwak, D. Lee, J.-K. Songa, *AIP ADVANCES* **8**, 065219 (2018).

Electro-optical Properties of Hockey-Stick-Shaped and Nematic Liquid Crystals Mixture for Fast Response Time

Phuc Toan Dang[1], Anoop Kumar Srivastava[2], E-Joon Choi[3], and Ji-Hoon Lee[1,]*
[1]Division of Electronics Engineering, Jeonbuk National University, Jeonju, Jeonbuk 54896, Korea
[2]Department of Applied Science and Humanities, Institute of Engineering and Technology, Dr. Rammanohar Lohia Avadh University, Ayodhya, 224001, India
[3]Department of Polymer Science and Engineering, Kumoh National Institute of Technology, Gumi, 39177, South Korea
*Tel.: 82-63-270-2476, E-mail: *jihoonlee@jbnu.ac.kr*

The hockey stick-shaped liquid crystal (HLC) has drawn considerable attention in recent years owing to its interesting physicochemical properties. The HLC molecules possess an intermediate structure between the cylindrical and the bent-core LC materials generated the expected properties such as high thermal and chemical stability and photoluminescent properties [1]. We synthesized an HLC molecule called as 4-{[4-({4-[(4-{[4-dodecyloxy) phenoxy] carbonyl} phenoxy) carbonyl] phenoxy} carbonyl) phenoxy] carbonyl} phenyl 2,4,6trifluoro benzoate in our previous work [2]. For convenience, we called the HLC as 4PTF hereinafter.

In this work, we investigated the dielectric properties of the 4PTF molecule. Accordingly, we found the two dielectric relaxation modes of the 4PTF liquid crystal in isotropic, smectic, and nematic phases. Also, we measured the dielectric relaxation strength and the relaxation frequency versus temperature. Furthermore, we investigated a commercial nematic liquid crystal (ZSM-7270XX) mixture's electro-optical property by doping the 4PTF molecule and obtaining the fastened response time due to the decrease of the rotational viscosity, as shown in Fig. 1 [3].

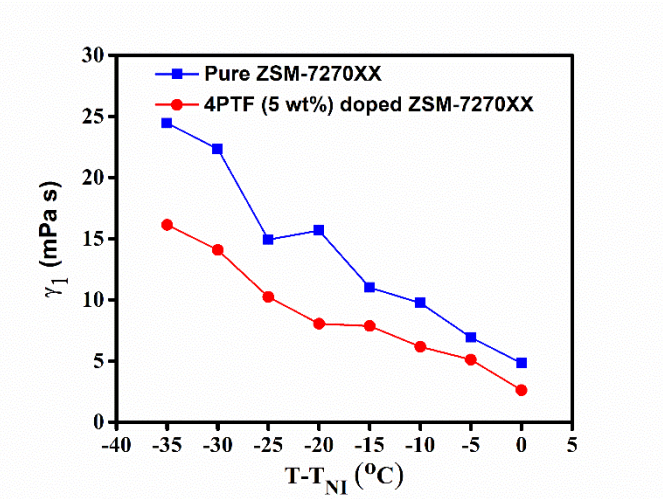

Fig. 1. Rotational viscosities γ_1 of the pure and the 4PTF-doped ZSM-7270XX samples vs. T - T_{NI}.

Acknowledgment

This study was supported by a grant from the National Research Foundation (NRF, 2019R1A2B5B01069580, 2019R1A6A1A09031717), Ministry of Trade, Industry, and Energy (20011031).

References

1. S.K. Saha, J. Deb, U. Sarkar, M.K. Paul, Liq. Cryst. 44, 2203–2221 (2017).
2. E.-J. Choi, K.-M. Park, D.-Y. Kim, K.-U. Jeong, J.-H. Lee, *Liq. Cryst*., 43,1597–1605 (2016).
3. P.T. Dang, A.K. Srivastava, E.J. Choi and, J.-H. Lee, *Curr. Appl. Phys.,* 23, 8-14 (2021).

Color Glass by Layered Nitride Films for Building Integrated Photovoltaic System

Akpeko Gasonoo[1], Hyeon-Sik Ahn[2], Seongmin Lim[2], Jae-Hyun Lee[3], and Yoonseuk Choi[2,]*
[1]Research Institute of Printed Electronics & 3D Printing, Industry University Cooperation Foundation, Hanbat National University, Daejeon 34158, South Korea
[2]Department of Electronic Engineering, Hanbat National University, Daejeon 34158, South Korea
Tel.: +82-42-821-1134, E-mail: ychoi@hanbat.ac.kr
[2]Department of Creative Convergence Engineering, Hanbat National University, Daejeon 34158, South Korea

The building integrated photovoltaic (BIPV) system provides a novel and an efficient technique for solar energy to be harvested from the envelope of buildings and to generate renewable energy mainly for the constructed environment [1]. Conventional solar systems installed on large areas of buildings (roofs and facades) come in standard black or grey solar modules, mostly due to the antireflective coating layers within the photovoltaic cell [2]. This is generally not well accepted by most users, especially where aesthetic considerations are required. An approach to solving this problem is adopting front color glasses that can hide the active components of the photovoltaic cell but transmits the non-reflected radiation entirely to the absorber with little or no absorption and can withstand degradation over time. Some conventional approaches adopt pigment-based coloring, which, however, absorbs radiation and does not withstand degradation over time [3].

We investigated layered titanium nitride (TiN) and aluminum nitride (AlN) for color glasses in BIPV systems. AlN and TiN are among suitable and cost-effective optical materials to be used as thin multilayer films, owing to the significant difference in their refractive index. The schematic structures of the multilayers used are shown in Fig. 1. To fabricate the structure, we used radio frequency magnetron deposition method to achieve the target thickness uniformly. A simple, fast, and cheap fabrication method is achieved by depositing the multilayer films in a single sputtering chamber. It is demonstrated that a multilayer stack that allows light to be transmitted from a low refractive index layer to a high refractive index layer or vice-versa can effectively create various distinct color reflections for different film thicknesses and multilayer structures. It is investigated from simulation based on wave optics that TiN/AlN multilayer offers better color design freedom and a cheaper fabrication process as compared to AlN/TiN multilayer films. Blue, green, and yellow color glasses with optical transmittance of more than 80% was achieved by indium tin oxide (ITO)-coated glass/TiN/AlN multilayer films. This technology exhibits good potential in commercial BIPV system applications.

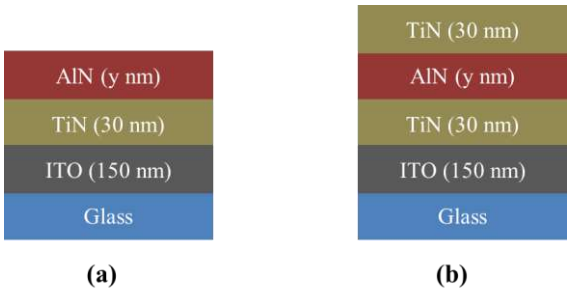

Fig. 1. Schematic structure of (a) three-layered and (b) four-layered color glasses

Acknowledgment

This work was supported by basic science research program through the NRF funded by the ministry of Education (NRF-2018R1A6A1A03026005) and by the research fund of Hanbat National University in 2017.

References

1. I. Cerón, E. Caamaño-Martín, F.J. Neila, *Renew. Energy*, 58, 27 (2013).
2. L.L. Kazmerski, *Renew. Sustain. Energy Rev.*, 1, 71 (1997).
3. Y. Guo, K. Shoyama, W. Sato, E. Nakamura, *Adv. Energy Mater.*, 6, 1502317 (2016).

Analysis of Hole-Transporting Organic Molecules by Time-Drive Electrochemical and Optical Spectroscopic Methods

Hye-Ri Joe[1], Seo-Yoon Lee[1], Akpeko Gasonoo[2], Jonghee Lee[1], and Jae- Hyun Lee[1,]*
[1] Department of Electronics, Hanbat National University, Daejeon, 34158, Korea
Tel.: +82-42-821-1970, E-mail: jhyunlee@hanbat.ac.kr
[2]Research Institute of Printed Electronics & 3D Printing, Industry University Cooperation Foundation, Hanbat National University, Daejeon 34158, South Korea

Hole transporting small molecules in organic electronics are chemically or electrically stressed at the radical state when they are oxidized to transfer charges through the layer in the devices or when they are mixed with dopant molecules for electrical doping to form charge tranfer complexes [1,2]. Several studies have been conducted in organic semiconductor devices with multi-layers to determine the effect of the electrical and optical properties of small molecule radicals on the overall device stability and performance [3]. However, most of these approaches are complex and expensive as they involve the use of several experimental setups and steps that are required to generate the radicals. Moreover, few studies have adequately investigated the stability in organic hole-transport materials.

In this study, the radicals in 4'-Tris [2-naphthyl (phenyl) amino] triphenylamine (2TNATA) molecules are analyzed by a time-drive cyclic voltammetry and ultraviolet-visible-near infrared (UV-Vis-NIR) spectroscopy at specific wavelengths and voltages. The molecular structure of 2TNATA and schematic figure of electrochemical spectroscopic analysis setup are shown in Fig. 1. It is demonstrated that the time-drive of voltage causes absorption by radicals in the 2TNATA films at 445 nm and 1125 nm, respectively. This investigation is crucial in precisely understanding the radical state of small molecules, and the stability and operation mechanism of organic electronic device.

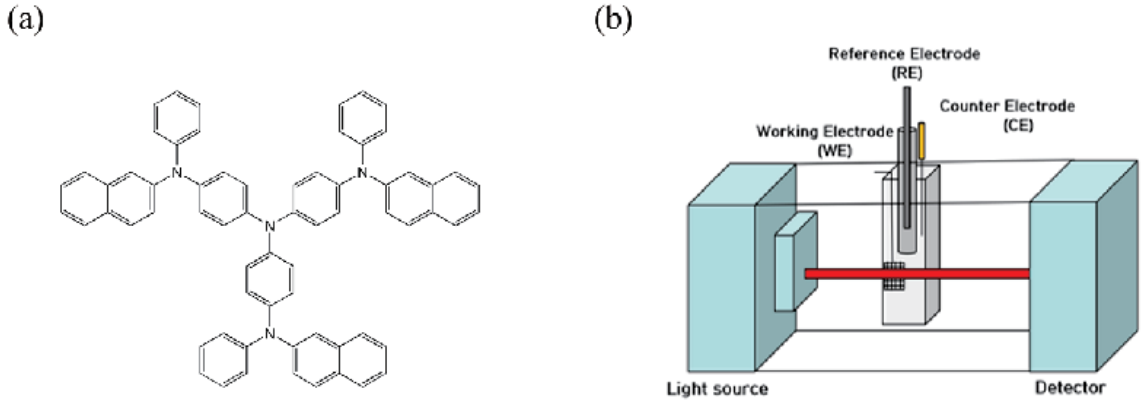

Fig. 1. Molecular structure of 2TNATA and schematic figure of measurement setup

Acknowledgment

This research was supported by Basic Science Research Program through the National Research Foundation of Korea (NRF) funded by the Ministry of Education (2020R1I1A3073634 and 2018R1A6A1A03026005) and by the Collabo R&D between Industry, Academy, and Research Institute funded Korea Ministry of SMEs and Startups in 2020 (S2902545).

References

1. J.-H. Lee, D.-S. Leem, H.-J. Kim and J.-J. Kim, *Appl. Phys. Lett*., 94, 123306 (2009).
2. J. F. Rusling and S. L. Suib, *Adv. Mater*., 6, 922 (1994).
3. T. T. Dao, T. Matsushima, R. Friedlein and H. Murata, *Organic Electronics* 14, 2007 (2013).

PI-less Normally Transparent Polymer Networked Liquid Crystal Light Shutter with Two-Step Exposure Method

Mira Jo[1], Minji Kang[1], Young Jin Lim[1] and Seung Hee Lee[1]*
[1]Applied Material institute for Department of Nano Convergence Engineering and Department of Polymer Nano-Science and Technology, Jeonbuk National University, Jeonju, Jeonbuk 54896, Korea *
Tel.:82-63-270-2343, E-mail: lsh1@jbnu.ac.kr

For controlling the incident daylight, liquid crystal (LC) based smart windows that are switched between scattering and transparent states can be used. Normally scattering polymer network liquid crystal (PNLC) or polymer dispersed LC (PDLC) mode has disadvantage of high-power consumption because it has to apply voltage to use it in a transparent state like normal glass. For application fields that require transparent state in a voltage-off state, normally transparent PNLC (NT-PNLC) mode is more suitable for switchable windows. In general, NT-PNLC uses polyimide (PI) for initial vertical alignment. In case, without PI, transmittance is not well achieved and operation consistency is not guaranteed.

We fabricate a PI-less NT-PNLC mode by using negative dielectric anisotropy of LC containing homeotropic alignment material and UV curable monomer by polymerization induced phase separation (PIPS). Two-step UV exposure method is used to make stable vertical orientation and polymer network. First exposure on the top side makes vertical orientation be reinforced and second exposure on the bottom side makes robust polymer network in the cell. This method improves resiliency of LC by strengthening the vertical orientation force. In addition, initial LC alignment is kept well because the polymer network is maintained by applying voltage. As shown in Fig. 1(a), one side exposure NT PNLC cell has initial transmittance drop during repeated operation, causing hysteresis. However, Fig. 1(b) shows that two-side exposure cell maintains same transmittance during repeated operation. PI less NT-PNLC using two-step UV exposure method reduces the cost by processes for PI coating and can be applied for film type substrate.

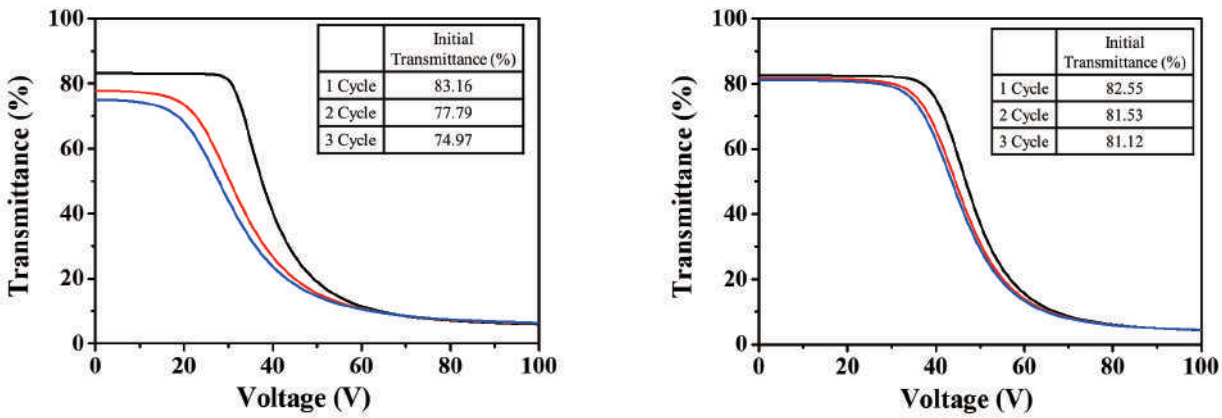

(a) **(b)**

Fig. 1. VT curves at each exposure conditions from 1 Cycle to 3 Cycle (a) 1 side exposure at 50 mW, 60min, (b) Two-side exposure at 50mW, 10min on the top side and 50mW, 50min on the bottom side.

Acknowledgment

This work was supported by the Innovation Lab support program for material, parts, equipments (20012555, Commercialization of nanocarbon composites materials in electric and electronic display and energy industries) funded by the Ministry of Trade, Industry & Energy (MOTIE, Korea)

References

1. Wang, Jiaqi, et al. *ACS nano*, 14(3), 3630-3639 (2020).
2. Wang, Dong, et al. *Liquid Crystals,* 42(12), 1689-1697 (2015).

Chiral Detection by Mesogenic Luminophore with Orthogonally Polarized Emission

*Myoung-Jin Han, Jae-Hoon Kim, and Chang-Jae Yu**
Dept. of Electronic Engineering, Hanyang University, Seoul 04763, Korea
Tel.:82-2-2220-2314, E-mail: cjyu@hanyang.ac.kr

Chiral detection has attracted great interest in bio-applications such diabetes diagnosis. Fructose is known as a monosaccharide closely related to diabetes, which is an isomer with the same molecular formula as glucose but with a different structure. Optically, glucose and fructose exhibit different optical activities by their circular birefringence due to different chirality [1]. Glucose rotates linearly polarized (LP) light clockwise (dextrorotatory) but fructose rotates it counterclockwise (levorotatory). In this work, we demonstrate chiral detection in a single substrate with orthogonally polarized emission from aligned mesogenic luminophore. The mesogenic conjugate polymer, poly(9,9-di-n-octylfluorenyl-2,7-diyl) (PFO), was used as emission material on an orthogonally rubbed surface. As shown in Figure 1(a), the aligned PFO on the ±45° rubbed alignment layer emitted the LP light with high ratio of linear polarization about 72 at 432 nm. The orthogonally polarized light is indistinguishable passing through water as a solvent of both glucose and fructose under 0° linear polarizer as shown in Figure 1(b). On the other hand, levorotatory fructose rotates both LP lights counterclockwise about 45° and thus right region changes brighter than left region. However, dextrorotatory glucose rotates them clockwise and thus left region is brighter than right region.

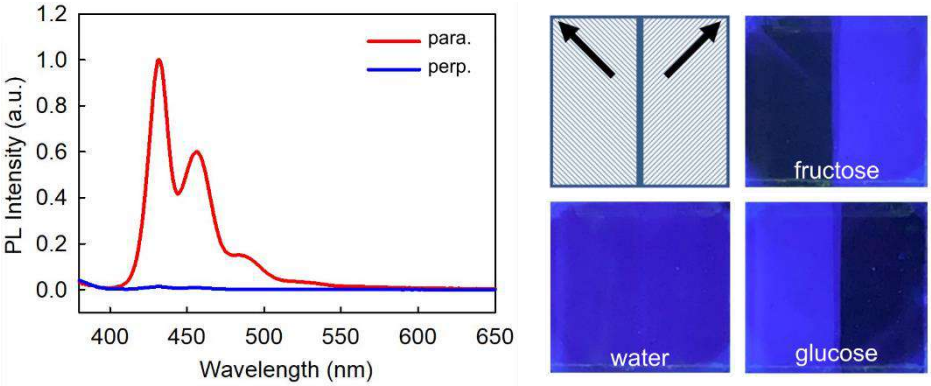

(a) (b)

Fig. 1. (a) PL spectrum of the orthogonally patterned polarized emission and (b) PL textures passing through water, fructose, and glucose under 0° linear polarizer.

In general, the rotating angle (ϕ) by optical activity is linearly proportional to a concentration (c) of glucose or fructose following as [2],

$$\phi = \alpha \times c \times L, \quad (1)$$

where α and L are specific rotation and path length of solution. Therefore, both isomers can be identified by brighter region and their concentration can be estimated by measuring the rotating angle.

Acknowledgment

This study was supported by the National Research Foundation(NRF) of Korea for funding(No. NRF-2018R1A2A3075276) and the ITECH R&D program of MOTIE/KEIT (No. 20012560, Development of material component equipment for inkjet printing in flexible QD-OLED).

References

1. McNichols, R. J. and G. L. Cote. *J. Biomed. Opt.* **5**, 8 (2000).
2. W. G. Park, J. M. Wolska, D. Pociecha, E. Gorecka, and D. K. Yoon. *Adv. Opt. Mater*, **7**, 1901399 (2019).

Time-Dependent Degradation of Circular Polarization Ratio in Chiral Mesogenic Luminophore

Cheong-Min Shin[1], Yanqiu Chen[1], E-Joon Choi[2], Chang-Jae Yu[1], and Jae-Hoon Kim[1*]*
[1]Dept. of Electronic Engineering, Hanyang University, Seoul 04763, Korea
[2]Dept. of Polymer Science and Engineering, Kumoh National Institute of Technology, Gumi 39177, Korea
Tel.:82-2-2220-2314, E-mail: jhoon@hanyang.ac.kr

Emission of circularly polarized (CP) light has attracted great attention for improving device performance. The degree of CP emission is defined by the dissymmetric factor, $g = 2(I_L - I_R)/(I_L + I_R)$, where I_L and I_R denote the intensities of left-handed and right-handed CP light, respectively. Especially, high degree of CP emission was achieved in a helical configuration of mesogenic luminophore by doping a chiral agent [1] or by rubbing two different surfaces [2]. In this work, we investigate the dissymmetric factor of the intrinsic chiral luminophore as a function of elapsed time after sample fabrication. The fluorene moiety containing chirality was used for an emitting layer (EML) and annealed thermally above its mesogenic temperature after coating on the rubbed alignment layer. The EML constructed the twisted structure without any treatment after cooling down at room temperature. The twisted EML generates the CP light, whose dissymmetric factor is governed by helical twisting power (HTP) and thickness of the EML. Interestingly, the dissymmetric factor (g_{PL}) of the photoluminescence (PL) was gradually degraded according to time elapsed after sample preparation as shown in Figure 1. These degradation behaviors were observed in both rapidly and slowly cooling processes. Such phenomenon is expected to be originated from weaker HTP of the intrinsic chirality than the specific chiral dopant such as S(R)05011 [1]. Restoring process of the dissymmetric factor was also investigated.

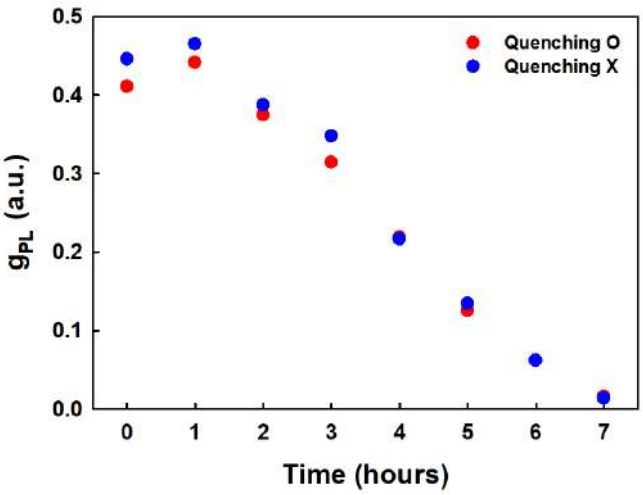

Fig. 1. The dissymmetric factor of the PL process according to elapsed time after sample preparation.

Acknowledgment

This study was supported by the National Research Foundation(NRF) of Korea for funding(No. NRF-2018R1A2A3075276) and the ITECH R&D program of MOTIE/KEIT (No. 20012560, Development of material component equipment for inkjet printing in flexible QD-OLED).

References

1. D. M. Lee, J. W. Song, Y. J. Lee, C. J. Yu, and J. H. Kim, *Adv. Mater.* **29**, 1700907 (2017).
2. K. Baek, et al., *Light: Sci. Appl.* **8**, 120 (2019).

Bidirectional orientation control of elongated particle using symmetry breaking in nematic liquid crystals

Jun-Yong Lee[1], Jeong-Seon Yu[2], and Jong-Hyun Kim[1]
[1]**Department of Physics, Chungnam National University, 99 Daehak-ro, Yuseong-gu, Daejeon, 34134, Korea**
E-mail: jxk97@cnu.ac.kr
[2]**Institute of Quantum Systems, Chungnam National University, 99 Daehak-ro, Yuseong-gu, Daejeon, 34134, Korea**

Colloidal particles suspended in nematic liquid crystals tend to be aligned along the orientation minimizing the elastic free energy[1]. If an electric field is applied to a nematic colloidal system, the director around the particles rotates; in result, the particles realign via rotation to reduce the total free energy that is the sum of the elastic and electric free energies. Herein, if the preferred rotation directions contributed by elastic and electric free energies are different, the rotation direction can be decided by the way to apply electric field[2]. When applying a weak electric field and increasing the strength gradually, the particles rotate with the same direction that the director rotates. On the other hand, when suddenly applying a sufficiently strong electric field, the particles rotate with the opposite direction to the former case. We analysed this bidirectional behaviour of elongated particles with a theoretical model.

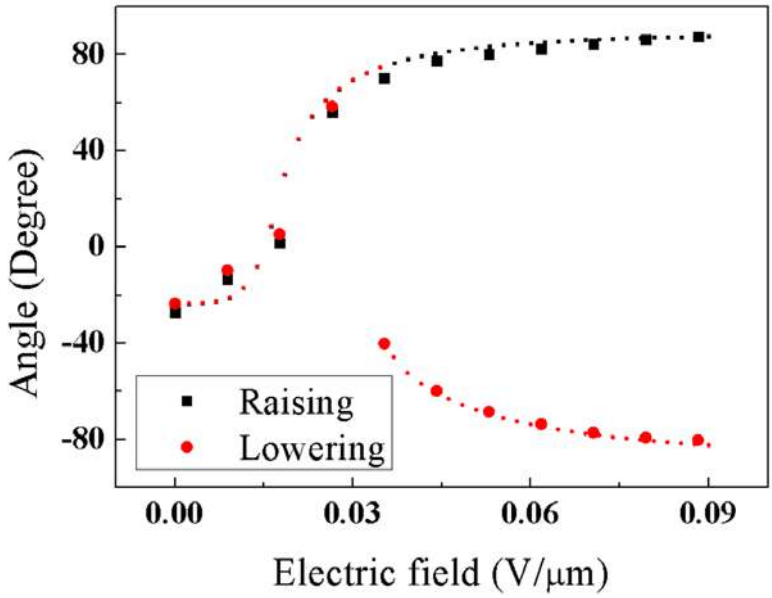

Fig. 1. The graph of angle by the strength of an electric field. We measured the angle with two different ways. One is applying a weak electric field and increasing the strength gradually. The other is applying a sufficiently strong electric field and decreasing the strength. The large marks mean experimental results and the small marks indicate calculation results.

Acknowledgment

This research was supported by Basic Science Research Program through the National Research Foundation of Korea (NRF) funded by the Ministry of Education (NRF-2017R1A2B4011758, NRF-2018R1D1A1B07047808, NRF-2020R1A6A1A03047771)

References

1. P. Poulin, H. Stark, T. C. Lubensky. & D. A. Weitz, *Science* **275**, 1770-1773 (1997)
2. JY Lee, JS Yu & JH Kim, *Sci. Rep.* **10**, 18650 (2020)

Control of Surface Anchoring Energy of Nematic Liquid Crystals via Nano-spikes of Reactive Mesogen

Eunsu Cho[1], Jun-Hyung Im[1], and Young-Ki Kim[1]*

[1]Dept. of Chemical Engineering, Pohang University of Science and Technology (POSTECH), Pohang, Gyeongbuk 37673, Korea

Tel.:82-54-279-2267, E-mail: ykkim@postech.ac.kr

Liquid crystals (LCs) possess both long-range molecular ordering and fluidity, leading to anisotropic properties (e.g. elasticity, birefringence). Because the material characteristics are controllable via reorientation of LCs in response to a variety of stimuli, LCs have been widely used to design stimuli-responsive materials, including triggered release system, sensor, and actuators [1-3]. In this context, precise control on the interfacial properties (e.g., surface anchoring energy, initial orientation of molecules) is significantly important because it determines sensitivity and response time of LCs.

Herein, we propose a simple and versatile approach to manipulate the surface anchoring energy (W) of LCs by doping reactive mesogens (RMs) into a vertical alignment layer of polyimide (PI). When the sandwich cells assembled with two substrates coated with RM-PI is irradiated by UV light and then LC is injected (Fig. 1a), we observe the polar anchoring energy (W_p) to increase with irradiation time (Fig. 1b). We demonstrate the result to be associated with the formation of RM nano-spikes on RM-PI. Specifically, first, we found RM monomers grew perpendicular to the substrates and form nano-spikes. The nano structures cause the interdigitation of LCs, thus enhancing W_p [4]. Second, based on surface retardation measurements, we showed a director of RMs in the spikes is aligned parallel to the normal direction of substrates. The internal orientation of RM in our nano-spike also contributes to the increase of W_p, because previous studies demonstrated the surface orientation of RMs determine the orientation of contacting LCs [5].

Overall, our findings provide additional options for programming the properties of stimuli-responsive LC materials. Furthermore, it offers access to the wide range of LC molecules for responsive materials because the proposed method can induce the vertical orientation of LCs with nontrivial shape (e.g., bent-core molecules), which are challenging to assume vertical alignment with previous alignment techniques [6].

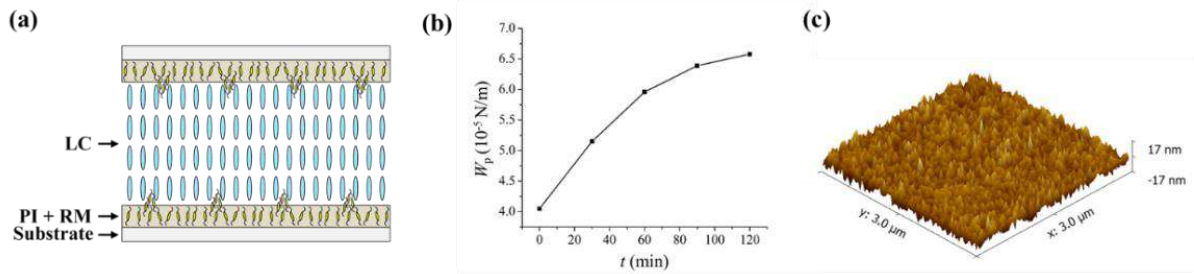

Fig. 1. (a) Schematic illustration of the sandwich cell coated with RM–PI alignment layer. (b) Measured polar anchoring strength W_p with respect to UV irradiation time t. (c) AFM image at t = 30 min to LC injection

References

1. Y. -K. Kim, X. Wang. P. Mondkar, E. Bukusoglu, and N. L. Abbott. *Nature,* 557, 539 (2018).
2. I. Kim, W.-S. Kim, K. Kim, M. A. Ansari, M. Q. Mehmood, T. Badloe, Y. Kim, J. Gwak, H. Lee, Y.-K. Kim, and J. Rho, *Sci. Adv*. 7, eabe9943 (2021).
3. J. Hu, W. Wang, and H. Yu, *Adv. Intell. Syst.,* 1, 1900050 (2019)
4. Y.-K. Kim, J. Noh, K. Nayani, and N.L. Abbott, *Soft Matter*, 5, 6913 (2019).
5. H.-G. Park, H. M. Lee, H. -C. Jeong, and D. -S. Seo, *RSC Adv*., 4, 34610 (2014).
6. Y. -K. Kim, G. Cukrov, F. Vita, E. Scharrer, E. T. Samulski, O. Francescangeli, O. D. Lavrentovich, *Phys. Rev. E*, 93, 062701 (2016)

Design of Liquid Crystalline Sensor for Carbon Nanotube Agglomerations

Jin-Kang Choi[1], Won-Sik Kim[1], and Young-Ki Kim[1]*
[1]Dept. of Chemical Engineering, Pohang University of Science and Technology (POSTECH), Pohang 37673, Korea
Tel.:82-54-279-2267, E-mail:ykkim@postech.ac.kr

Carbon nanotube (CNT)-based transistor has been considered as a promising substitute for silicon-based transistor due to low power consumption and propagation delay time.[1] In the preparation of CNT thin film, it has been shown that CNTs naturally bundle together forming agglomerations. Because the CNT agglomerations play as defect sites impeding electron flow,[2] the detection of CNT agglomerations is required for the design of CNT-based devices. Due to their nanoscale size, however, they were detected by Scanning Electron Microscope (SEM) that is time consuming and can only be applied to nano-to-micro scale area.

In this work, we propose a facile and generalized method to instantaneously detect the surface defects in large area by leveraging anisotropic properties (elasticity and birefringence) and long range molecular ordering of liquid crystals (LCs). We prepared LC injected non-agglomeration and agglomeration-rich samples and compared them by POM image. (Fig 1)

While the non-agglomeration sample shows a black texture, the agglomeration-rich sample shows a distinct bright dot texture in POM image. The dark texture is caused by vertical ordering of LCs. The bright texture is caused by tilted long range ordering of LCs against the substrate magnifying the nanoscale defect to the visible scale texture. The proposed method enables fast and whole-area detection of CNT agglomerations possible. Furthermore, this method can be used to detect general surface defect.

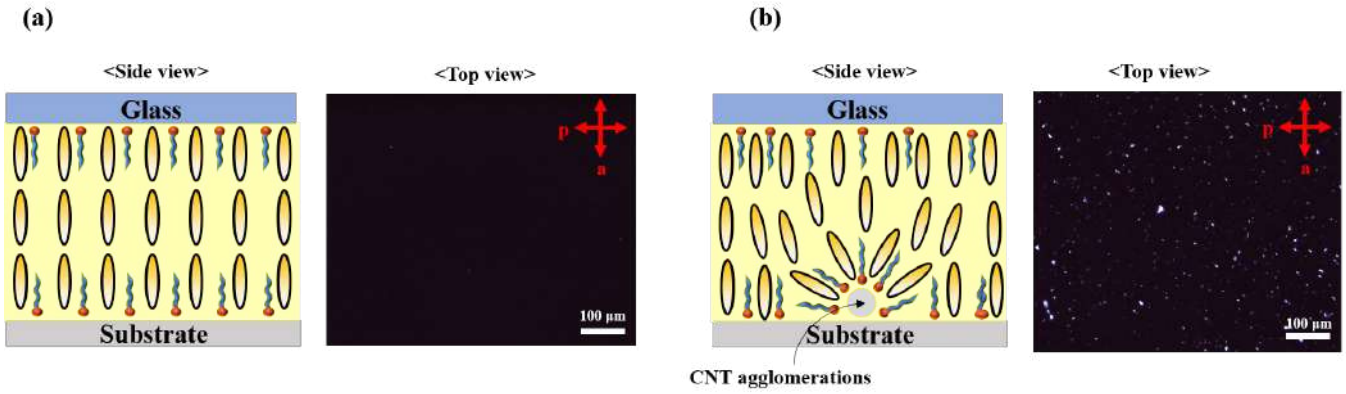

Fig. 1. Schematics and POM images of non-agglomeration sample (a) and agglomeration-rich sample (b)

References

1. Shulaker, M. M., Hills, G., Patil, N., Wei, H., Chen, H. Y., Wong, H. S. P., & Mitra, S. *Nature*, *501*(7468), 526-530 (2013).
2. Hills, G., Bardon, M. G., Doornbos, G., Yakimets, D., Schuddinck, P., Baert, R., ... & Ritzenthaler, R. *IEEE Transactions on Nanotechnology*, *17*(6), 1259-1269. (2018).

Molecular Reorientation of Nematic Liquid Crystals by Diarylethene-based Molecular Switch

Hyein Kim[1], Kwang-Suk Oh[1], and Young-Ki Kim[1]*
[1] **Department of Chemical Engineering, Pohang University of Science and Technology (POSTECH), Pohang, Gyeongbuk 37673, Republic of Korea**
Tel.:82-54-279-2267, E-mail: ykkim@postech.ac.kr

Previous studies showed that the trans-cis isomerization of azobenzene (azo) molecules can be used to manipulate molecular ordering of LCs. These properties have been widely exploited for responsive materials such as sensor, self-propelled colloids and soft actuators [2-5]. However, there are critical issues for the azo molecules that trans-to-cis transition occur only via UV light below 400 nm and return to the trans even in the absence of stimulus due to the metastable cis-isomer [3], which limits diverse applications. To overcome the inherent limitations, in this work, we propose diarylethene (DAE) as promising molecular switches for the design of responsive LC materials. As compared to azo molecules, DAE offers the access to (1) larger volumetric change between ring-opening and ring-closing isomers, (2) superior thermal stability of each state, (3) wide range of response wavelength (from visible to IR), and (4) high fatigue resistance after alternating cycles of light irradiation [1]. We demonstrate that the configuration of LCs can be controlled by the reversible photoisomerization of newly synthesized DAE-molecular switch. We found that DAE-open form induces planar anchoring of the LCs. Subsequently, when visible 1 is irradiated to a DAE-open form, DAE molecules change to a closed form which leads to vertical anchoring of the LCs (Figure 1). These findings allow one to enrich the set of control parameter. For instance, the use of various type of DAEs-molecular switches enable the design of wavelength-selective actuation in soft LC actuators, leading to the expansion of their application fields.

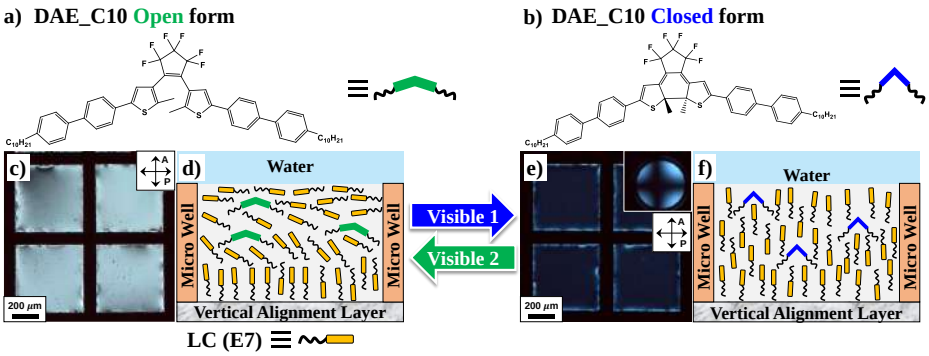

Fig. 1. a), b) DAE molecular structures with reversible photoisomers. c), e) Optical micrographs (top view, crossed polars) and d), f) corresponding schematic illustrations (side view) of LC film containing DAE molecules according to the irradiation of UV light. e) The inset is the corresponding to a conoscopic texture.

Acknowledgment

References

1. M. Lahikainen, K. Kuntze, H. Zeng, S. Helantera, S. Hecht and A. Priimagi, ACS Appl. Mater. Interfaces 12, 47939 (2020)
2. Y. Yuan, G. N. Abuhaimed, Q. Liu and I. I. Smalyukh, Nat. Commun. 9, 5040 (2018)
3. M. L. Baczkowski, D. H. Wang, D. H. Lee, K. M. Lee, M. L. Smith, T. J. White and L.-S. Tan, ACS Macro Lett. 6, 1432 (2017)
4. A. H. Gelebart, D. J. Mulder, M. Varga, A. Konya, G. Vantomme, E. W. Meijer, R. L. B. Selinger and D. J. Broer, Nature 546, 632 (2017)
5. C. Ohm, M. Brehmer and R. Zentel, Adv. Mater., 22, 3366 (2010)

Optical Conditions of α-ZrP Colloid for Electro-Optical Reflectance

Ju-Young Park[1], PANS. Priyadharshana[1], Asela Perera[1], Seung-Ho Hong[1] and Jang-Kun Song[1,]*
[1]Department of Electrical and Computer Engineering, Sungkyunkwan University, Suwon, Gyeonggi-do 16419, South Korea
Tel.:82-31-299-4631, E-mail: jk.song@skku.edu

α-Zirconium Phosphate(ZrP) nanoplates have reported that colloidal phase can be shift as nematic phase when applied low frequency electric fields have horizontally aligned layered structures.[1] By using this phenomenon and reflective light known as Bragg diffraction, the colloid can have the electro-optical property of a specific color spectrum depending on the distance between layers.[2] Especially the color spectrum can be observed roughly when the concentration of colloid is less then 1wt% and the percentage of nematic phase is high enough.[3]

In this work, we analyzed the optical conditions for electro-optical reflectance depending on α-ZrP particle size, concentration and nematic phase ratio of ZrP dispersed in a dimethylformamide solvent. We synthesized ZrPs with hydrothermal method using the oven at 200°C for 24h, and controlled the particle size by the different mole concentrations of phosphoric acid. The synthesized particle sizes of 14M, 10M, 8M and 4M are 1.3 μm, 0.9 μm, 0.78 μm and 0.45 μm, respectively. As shown in Fig. 1a, ZrP(14M, 1.02wt%) at 0 V shows a blue color (420 nm). When 5 V with a low frequency is applied vertically to the cell, ZrP particles are aligned parallel to the electric field. Then, the reflected blue color disappears. When the frequency change from 50 Hz to 10 kHz, ZrP particles start aligning vertical to the electric field, and the color recovers showing the blue (420 nm). However, ZrP(4M, 1.04wt%) has no color at 0 V. Even in the high and low frequency, there is no electro-optical reflectance because of tiny ratio of nematic phase less than 1 wt% [3]. Fig. 1b shows electro-optical reflectance of different concentrations of 14M and 4M ZrP colloids. As the concentration of 14M ZrP colloid decreases from 1.23 wt% to 0.8 wt%, the peak wavelength shifts from 390 nm to 520 nm, and the reflectance also decreases from 23.8 % to 8.7 % (Peak-14M, red line). However, there is no wavelength shift for 4M ZrP colloid and only decrement of the reflectance when the concentration decreases from 1.26 wt% to 0.77 wt% (Peak-4M). As shown in Fig. 1c, only 14M ZrP colloid has the blue color reflectance. 10M, 8M and 4M ZrP colloids have no color property and showing only low reflectance at 370 nm. As a result, the electro-optical reflectance is strongly depending on ZrP nanoparticle size, concentration, and the nematic phase ratio. In order to apply the ZrP colloids for next generation display, the concentration and nematic phase ratio should be considered as showing the color in visible range, and the particle size should be larger than 1μm for the Bragg diffraction.

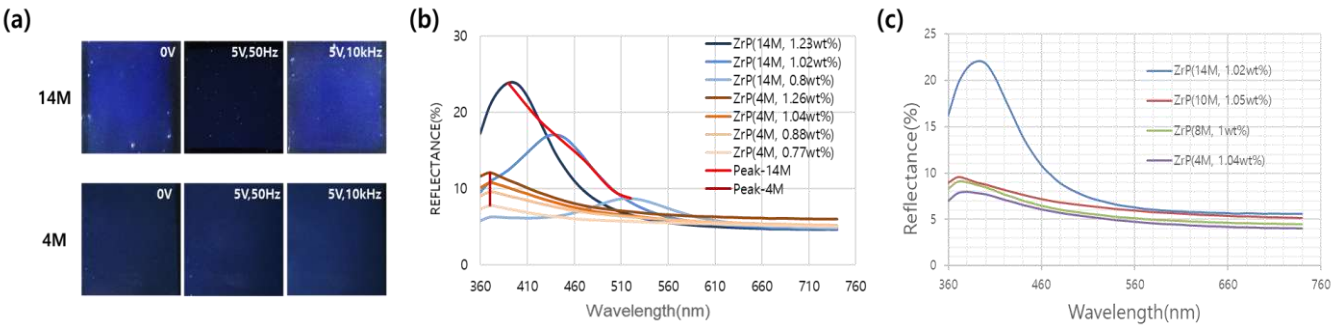

Fig. 1. (a) Electro-optical reflectance for 14M and 4M ZrP colloids. (b) Color reflectance variations of 14M and 4M ZrP colloids in different concentrations. (c) Color reflectance of ZrP colloids depending on nanoparticle sizes.

Acknowledgment

"This research was supported by the MSIT(Ministry of Science and ICT), Korea, under the ICT Creative Consilience Program(IITP-2021-2020-0-01821) supervised by the IITP(Institute for Information & communications Technology Planning & Evaluation)"

References

1. A. R. Masud, S. H. Hong, T. Z. Shen, C. H. Ahn, and J. K. Song, *Opt. Express*, 26(1), 173-178 (2018).
2. A. R. Masud, S. H. Hong, T. Z. Shen, A. Shahzad, and J. K. Song, *RSC Adv.*, 8(30), 16549-16556 (2018).
3. C. H. Ahn, A. R. Masud, S. H. Hong, T. Z. Shen, and J. K. Song, *Liq. Cryst.*, 46(2), 159-165 (2019).

Window shutter with low driving voltage

Jeong Won Ryu[1], Hui Su Shin[2], Hyeon Jong Choi[3], Gyu Jin Choi[4], and Jin Seog Gwag[1]
Department of Physics, Yeungnam University, Gyeongsan, Gyeongsangbuk-do, 712-749, Republic of Korea
e-mail: sweat3000@ynu.ac.kr

A window shutters have the ability to selectively transmits or blocks light using optical characteristics such as light absorption, scattering, and transmission. Among them, window shutters using liquid crystals (LCs) are being studied in various ways such as polymer dispersed liquid crystal (PDLC) and polymer stabilized liquid crystal (PSLC). In the case of PDLC, the initial state is opaque while the initial state of the PSLC is transparent.

Advantages of PDLC include easy manufacturing of large-area films and low cost. It has excellent impact resistance with high stability, good scattering and transparent properties. PSLC is a representative method for implementing reverse PDLC, and has the advantage that the initial state is transparent. However, they have a drawback requiring very high voltage to transit completely state, which needs a high energy consumption and exposes users to the risk of electrocution. Thus, a liquid crystal type smart window operating at lower voltages is desperately required.

To reduce operation voltage of smart window with LCs, we propose a window shutter with low voltage characterized by electro-hydrodynamics of LCs that drives strong dynamic light scattering (DLS) and a method to lower the operating voltage of the electroconvection with DLS. It is achieved by strong UV irradiation into LC cell. In the ultraviolet irradiation, the radicals weakly bonded to the liquid crystals separate from the liquid crystal. The radicals serve as some ion impurities within LCs Cell, which activates electroconvection. Consequently, the driving voltage to opaque state can be reduce by under 20 V by the activation of convection.

References

1. B.-G. Jeon, T.-H. Choi, S.-M. Do, J.-H. Woo, and T.-H. Yoon, *IEEE TRANSACTIONS ON ELECTRON DEVICES,* 65(10), 4387 (2018).
2. C. G. Jhun, G. J. Choi, D. G. Ryu, J.-H. Huh, and J. S. Gwag, *Phys. Rev. E*, 98, 052704 (2018).

Hybrid-aligned polymer network liquid crystal for window shutter

Huisu Shin[1], Hyeon Jong Choi[1], Jeong Won Ryu[1] and Jin Seog Gwag[1]*
[1]Department of Physics, Yeungnam University, 280 Daehak-Ro, Gyeongsan, Gyeongbuk 38541, Republic of Korea
E-mail: sweat3000@ynu.ac.kr

Window shutters have function to block and transmit light from the outside using optical features such as absorption, scattering, and transmission, and they are studied in a variety of ways including polymer dispersed liquid crystal (PDLC) and polymer stabilized liquid crystal (PSLC). In window shutters, initial state in which power is not applied to the window is important in terms of power consumption and transparent or opaque states will be determined by the user's preference. Those who want to see the outdoor landscape for a long time will prefer the initially transparent window state, while those who do not want to show the indoor environments will prefer the initially opaque state[1, 2].

In this paper, in order to meet the above two requirements, we proposes a new type of smart window using a dual frequency liquid crystal. It is initially translucent and becomes a transparent under a voltage of low frequency and opaque under a voltage of higher frequency. The initial translucent state is that while inside people is near the window can see the external environment well, outside people who are somewhat remote from the window cannot see the internal environment well. The other hand, only if we want to completely block and fully open the internal and external images, we can generate an opaque or transparent state by applying the voltage with the appropriate frequency to the window.

As a result, the proposed window shutter, which can adjust haze according to frequency, is expected to be used as an alternative window shutter in the future because we believe that there will be a high preference for the window condition that will allow indoor people to see external images and prevent outsiders from seeing indoor images, in initial state with no power consumption.

References

1. P. J. Collings, Princeton University Press (1995).
2. P.G. de Gennes and J. Prost, Oxford University Press (1995).

Optically Tunable PEDOT:PSS Coated Liquid Crystal Elastomer Optical Devices

Sung-Min Jang[1], Young-Woo Park[1], Sung-Chum Kang[1], Doyeon Lee[1] and Jang-Kun Song[1,]*
[1]Department of Electrical and Computer Engineering, Sungkyunkwan University, Suwon, Gyeonggi-do 16419, South Korea
Tel.:82-31-299-4631, E-mail: jk.song@skku.edu

A liquid crystal elastomer (LCE) film is a flexible polymer film that responds to light or heat. When the LCE film has a planar alignment (PA) structure on the top and a vertical alignment (VA) structure on the bottom, the liquid crystal molecules aligned by the PA expand relatively a little compared to the liquid crystal molecules aligned by the VA. Because of this, the LCE film has the property of being bent in the PA direction. Due to the optically controllable property, research is being conducted in the field of soft robots and sensors.

In this work, the top plate was coated in the order of PA, VA, and PA, and the bottom plate was coated with an alignment layer opposite to this to make a structure that bends into a wave shape (Fig.1(a)) when light is absorbed. In addition, the conductive material PEDOT:PSS was coated on the LCE film, which is an insulator, to make it conductive. The LCE films of this structure were made in thicknesses of 15 μm, 30 μm, 60 μm and 120 μm, and the performance of the conductive LCE film controlled by light as a switching device was compared by using the setup shown in Fig.1(b). The bottom electrode is made of aluminum tape, the top electrode is made of ITO glass to allow UV light to pass through and the distance between the upper and lower electrodes was set to 4 [mm]. And by applying 60 [V] as a voltage source and irradiating a UV lamp, the middle part of the conductive LCE film touched the upper electrode, and the experimental setup circuit was turned on. At this time, the current was measured with an ammeter. When the LCE film was irradiated with 365nm ultraviolet lamp at the same intensity and for the same time, the bending angle decreased as the thickness increased as shown in the graph in Fig. 1(c). This means that the thicker the LCE film, the longer the UV lamp is irradiated. As shown in Fig.1(d), because the 120μm LCE film does not contact the ITO electrode, no current flows. The largest current of 2A flowed in the 60m LCE film because the thicker the LCE film, the stronger the bending force. Therefore, the LCE film with the designed alignment layer pattern can be adjusted to a wave shape by UV light, and PEDOT:PSS is spin-coated on the insulator LCE film to make it conductive. And it was confirmed that the bending angle and bending force can be controlled by adjusting the thickness. In other words, it showed the possibility of being used as an optical device that can optically control the flow of electric current using the conductive LCE film.

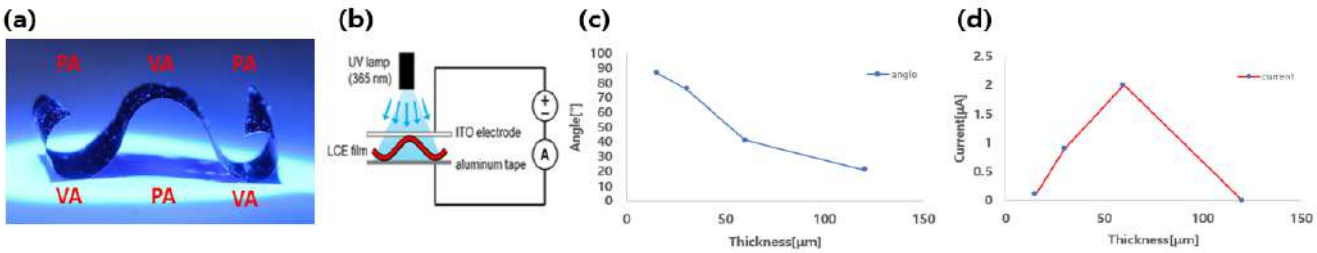

Fig. 1. (a) The designed alignment layer pattern and the arrangement of liquid crystal molecules in the LCE film. (b) Experimental setup curcuit for Current Measurement of Conductive LCE Films (c) Current of Conductive LCE Film by Thickness (d) The bending angle of the middle part of the LCE film by thickness

Acknowledgment

This work was supported by the National Research Foundation of Korea(NRF) grant funded by the Korea government(MSIP) (NRF-2019R1A2C2008359) and the Competency Development Program for Industry Specialists of the Korean Ministry of Trade, Industry and Energy(MOTIE) operated by Korea Institute for Advancement of Technology(KIAT). (No. P0012453)

References

1. Zeng, H., Wani, O. M., Wasylczyk, P., & Priimagi, A., " Light-driven, caterpillar-inspired miniature inching robot ", Macromolecular rapid communications 39(1), 1700224 (2018).

Light Driven Artificial Joint for Soft Robotics using Azo Dye Doped Liquid Crystal Elastomers

Sung-Cheon Kang[1], Doyeon Lee[1], Seong-Min Jang[1], Yong-Woo Park[1], Jang-Kun Song[1,*]
[1]Department of Electrical and Computer Engineering, Sungkyunkwan University, Suwon, Gyeonggi-do 16419, South Korea
Tel.:82-31-299-4631, E-mail: jk.song@skku.edu

Liquid crystal elastomers (LCEs) are unique materials that combine the molecular orientation order of liquid crystals (LCs) and rubber elasticity. LCEs have deformation property by the external stimulus such as heat and light[1,3]. Because of these properties, it can be applied to various fields such as soft actuators, sensors[4] and soft robotics[2]. Recently, LCE studies in soft robotics have attracted many researchers. Especially, artificial muscle and artificial skin are being actively studied.

In this work, we propose a light driven artificial joint using azo dye doped LCE for controlling targeted areas. This artificial joint can operate using light without electronic circuit and deform along the certain direction. When the UV light expose on azo dye doped LCE, the azo dye absorbs light, and it causes deformations. The bending direction is determined by molecular orientation of LC. When the LCE has a horizontal orientation at bottom and a vertical orientation at top, the LCE has bending motion from vertical to horizontal direction. And this motion appeared perpendicular to rubbing direction of the horizontal alignment layer. As shown in Fig. 1a, we fabricated a soft robot having artificial joints linked between transparent LCE (without azo dye). As shown in Fig. 1b, if 365 nm UV is exposed on the soft robot, the transparent LCE does not move, and artificial joint areas start bending. From the result, it shows that the azo dye causes light driven reactions. Fig. 1c shows that the artificial joints recovered to the initial state after the UV light was turned off. Consequently, the azo dye doped artificial joint has the light driven functionality for controlling the soft robots, and it can be utilized in soft robotics applications.

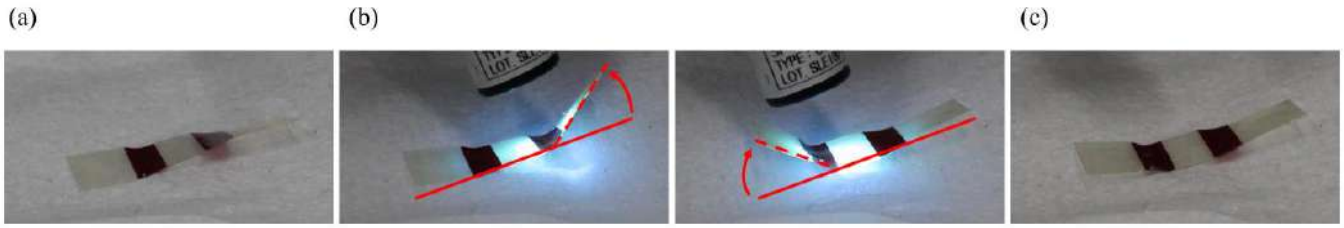

Fig. 1. (a) Initial state of the soft robot. (b) Artificial joints motion when the 365nm UV light is exposed. (c) The soft robot recovery after the UV light is turned off.

Acknowledgment

This research was funded and conducted under 'the Competency Development Program for Industry Specialists' of the Korean Ministry of Trade, Industry and Energy (MOTIE), operated by Korea Institute for Advancement of Technology (KIAT). (No. P0012453, Next-generation Display Expert Training Project for Innovation Process and Equipment, Materials Engineers)

References

1. O. M. Wani, H. Zeng & A. Priimagi, *Nat. Commun.*, 8, 15546 (2017).
2. Q. He, Z. Wang, Y. Wang, A. Minori, M. T. Tolley & S. Cai, *Sci. Adv.*, *5*, *eaax5746* (2019).
3. H. Zeng, H. Zhang, O. Ikkala & A. Priimagi, *Matter.*, 2, 194 (2020).
4. C. Ohm, M. Brehmer & R. Zentel, *Adv. Matter*., 22, 3366 (2010).

Colorful Perovskite Solar Cells with Cholesteric-based Reflective Filters

Sangwok Bae, and Suk-Won Choi
[1]Dept. of Advanced Materials Engineering for Information & Electronics, and Integrated Education Institute for Frontier Science & Technology (BK21 Four), Kyung Hee University, Yongin, Gyeonggi 17104, Korea
Tel.:82-31-201-2256, E-mail:schoi@khu.ac.kr

Application of perovskite solar cells (PSCs) in building-integrated photovoltaics (BIPVs) has been proposed owing to their superior device performance and processability. Applications of colored PSCs in BIPV have been demonstrated using liquid crystalline cholesteric-base reflective filters (ChRFs). These PSCs with ChRFs utilize the surface area in buildings, such as rooftops, facades, and exteriors, to realize ultimate energy harvesting, thereby achieving net-zero energy consumption. In this study, we propose two different types of colored PSCs: colored PSCs containing a Ch monolayer (ChRF1) and colored PSCs containing a Ch bilayer (ChRF2). The colored PSCs with ChRF1 exhibit minimal power conversion efficiency (PCE) loss; however, they show a narrow color gamut because of the limitation of the reflective layer. On the other hand, colored PSCs with ChRF2 enhance the color gamut; however, they increased the PCE loss because of their increased reflective feature. Therefore, the colored PSCs with ChRF1 are favorable when we pursue minimal PCE loss rather than esthetic features, while the colored PSCs with ChRF2 are favorable when we pursue esthetic features rather than PCEs. Our colored PSCs with ChRFs originating from the formation of well-organized nanosized superstructures inspired by a living system have a huge potential for application in BIPVs.

Circularly Polarized Luminescence from Nano-segregated Phases

Jae-Jin Lee, and Suk-Won Choi
[1]Dept. of Advanced Materials Engineering for Information & Electronics, and Integrated Education Institute for Frontier Science & Technology (BK21 Four), Kyung Hee University, Yongin, Gyeonggi 17104, Korea
Tel.:82-31-201-2256, E-mail:schoi@khu.ac.kr

A mixed system constituted of achiral bent-core (BC) molecule and rod-like nematogen has been reported as one of promising chiroptic material. In this system, nano-sized phase seperation between helical nanofilaments (HNF) originated from BC molecule and calamitic liquid crystalline nematic (N) phase originated from rod-like nematogen shows giant chiroptic phenomena such as optical rotatory power or circular dichroism. Recently, intriguing approach was presented to fabricate CPL material using this nano-segregated phase. CPL was successfully observed from the nano-segregated phase blended with fluorescent molecule (guest dye). This is because the helix of HNF affected the structure of the embedded N phase doped with guest dye, forming self-assembled chiral aggregates associated with the helix of the HNF phase in spite of a mixed system consisting of only chemically achiral molecules. The calamitic guest dyes are well known to obey the rod-like mesogen's orientational ordering when they are mixed with rod-like mesogenic molecules, a N phase that is blended with the guest dye molecule and segregated from the HNFs forms a chiral aggregate; hence, CPL attributed to dye molecules in the chiral aggregates can be observed. Because both the host and guest in this system are chemically achiral, we can regard this method as "achiral host–achiral luminescent guest method". The merit of this approach is to eliminate complicated chiral molecular design to fabricate CPL materials. However, this approach has vulnerable point; insufficient luminescence dissymmetry factor (g_{lum}) value for the actual applications. Although the observed g_{lum} value was comparable with the values reported for low molecular weight chiral organic compounds in the solution phase, further enhancement of the value of g_{lum} in this system should be desirable to utilize this system for the actual potential applications. Herein, we observed enhanced CPL in an intriguing nano-segregated phase system, <HNF/HNF>, from the HNFs from different two BC molecules. The observed g_{lum} value in this nano-segregated phase <HNF/HNF> was larger than that in nano-segregated phases reported before.

Highly efficient blue fluorescent OLED using localized surface plasmonic resonance by Ag-Au nanoparticles

Hakjun Lee[1], Hye Won Nam[3], Ki Ju Kim[1], Sun-kyo Kim[4], Heesun Yang[5], Young Kwan Kim[1], and Taekyung Kim[1,2]
[1]Dept. of Information Display Engineering, Hongik University, Seoul 04066, Korea
Tel.:82-2-3142-3750, E-mail: kimyk@hongik.ac.kr
[2]Dept. of Materials Science and Engineering, Hongik University, Sejong, 3006, Korea.
Tel.:82-44-860-2506, E-mail: taekyung.kim@hongik.ac.kr

When metals such as gold (Au) and silver (Ag) are small in nanometre sizes, they have unique optical properties in visible light range [1]. Coated in the of 2D array, these metal particles are called plasmonic arrays, and each metal has its own resonant wavelength. When the resonance wavelength of light and metal overlaps, the metal resonates and interacts with each other to strengthen the emission characteristics of a particular light [2,3]. We achieve an external quantum efficiency of up to 16.49% at blue-fluorescent organic light-emitting diode (OLED) using these properties by Ag-Au NPs. This property is called localized surface plasmonic resonance (LSPR) [4], and the efficiency improvement of blue fluorescence using this structure is a new concept approach that can satisfy high efficiency and operational lifespan at the same time. This increase in efficiency is a dominant factor in the distance between the plasmonic array and the exciton, which can be expected to improve the higher efficiency by regulating the distance between those. So far, the development of blue-fluorescent materials has been the main trend. However, the improvement of efficiency of blue fluorescence using these device structure and plasmonic array will be significant and a new method of research and development.

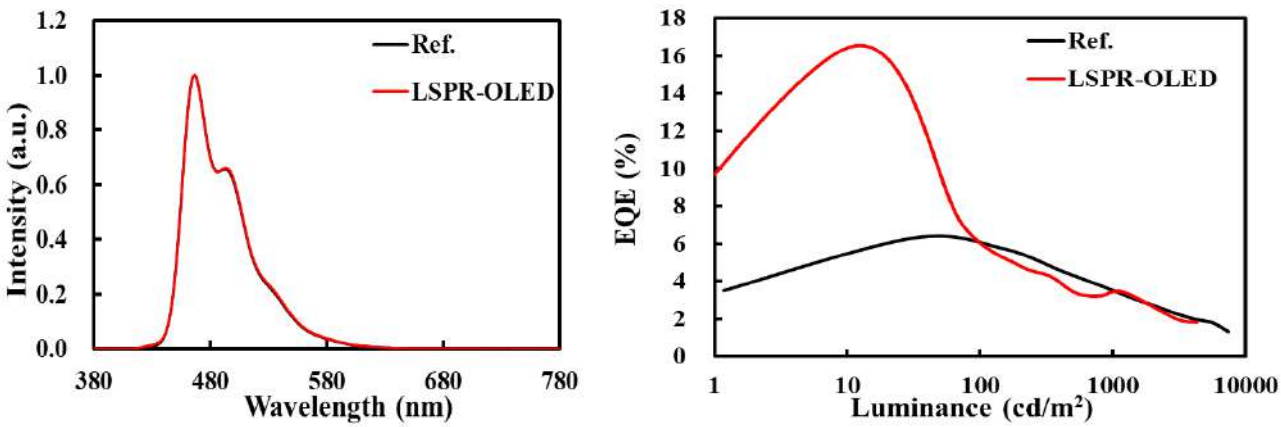

Fig. 1. (left) EL spectra of Ref. and LSPR-OLED, indicating no effects of microcavity caused by Ag-Au NPs (right) The external quantum efficiency (EQE) of devices.

The left side of Figure 1 shows the EL spectra of the two devices, with no microcavity effect caused by Ag-Au NPs, showing only the spectra of dopants. This disproves that improvements in efficiency have not resulted in out-coupling or other variations of optical paths.

Acknowledgment

This research was supported by Basic Science Research Program through the National Research Foundation of Korea (NRF) funded by the Ministry of Education (No. 2015R1A6A1A0303183323)

References

1. E.Cao, W. Lin, M. Sun, W. Liang, and Y. Song, *Nanophotonics*, 7(1), 145-167 (2018).
2. Y. Xu, H. Zhou, R. Zhang, Y. Liu, and W. Huang, *AIP Advances*, vol. 5, 067121 (2015).
3. M. Shabaninezhad, and G. Ramakrishna, *J. Chem. Phys*, 150, 144116 (2019).
4. K. Okamoto, M. Funato, Y. Kawakami, and K. Tamada, *Journal of photochemistry and Photobiology C: Photochemistry Reviews*, 32, 58-77 (2017).

Electro-Optical Characteristics and Lifetime Study of Green Phosphorescent Organic Light-Emitting Diode Using Mixed Host

Nuri Oh[1], Ho-jin Jang[2], and Jun-Yeob Lee[2]
[1]Department of Semiconductor and Display Engineering, Sungkyunkwan University, Suwon, Gyeonggi-do 16419, South Korea
Tel.:82-41-599-0833, E-mail: nr.oh@samsung.com
[2]Department of Chemical Engineering, Sungkyunkwan University, Suwon, Gyeonggi-do 16419, South Korea

For the high efficiency and long lifetime of phosphorescent organic light-emitting diodes (PhOLEDs), the host-dopant systems have been used in the emitting layer. In particular, studies have been actively conducted to improve the lifetime of the PhOLEDs by using a mixed host. In this paper, we analyzed the causes of lifetime improvement for green organic light emitting devices using bis(4-(9´ -phenyl-9H,9´ H-[3,3´ -bicarbazol]-9-yl)phenyl)methanone (BPBCz) which is a strong hole transport type host.

As shown in Figure 1a, the device structure was ITO (50nm)/DNTPD (60nm)/BCFN (20nm)/PCZAC (10nm)/BPBCZ:PBICTl:Ir(ppy)$_3$(1:1, 5% doped, 30nm)/DBFTrz (5nm)/ZADN (30nm)/LiF (1nm)/Al (200nm).

An organic light-emitting diode (OLED) in which mCBP was used instead of BPBCz and an OLED using only PBICT as a host were used as control devices. As shown in Figure 1b and 1c, the current density and luminance of the BPBCz:PBICT device were high, and the lifetime was 1.7 times longer than that of the mCBP:PBICT device. Figure 1d shows that the positive polaron stability of BPBCz:PBICT is better than that of other devices, which was the main reason for the extended device lifetime.

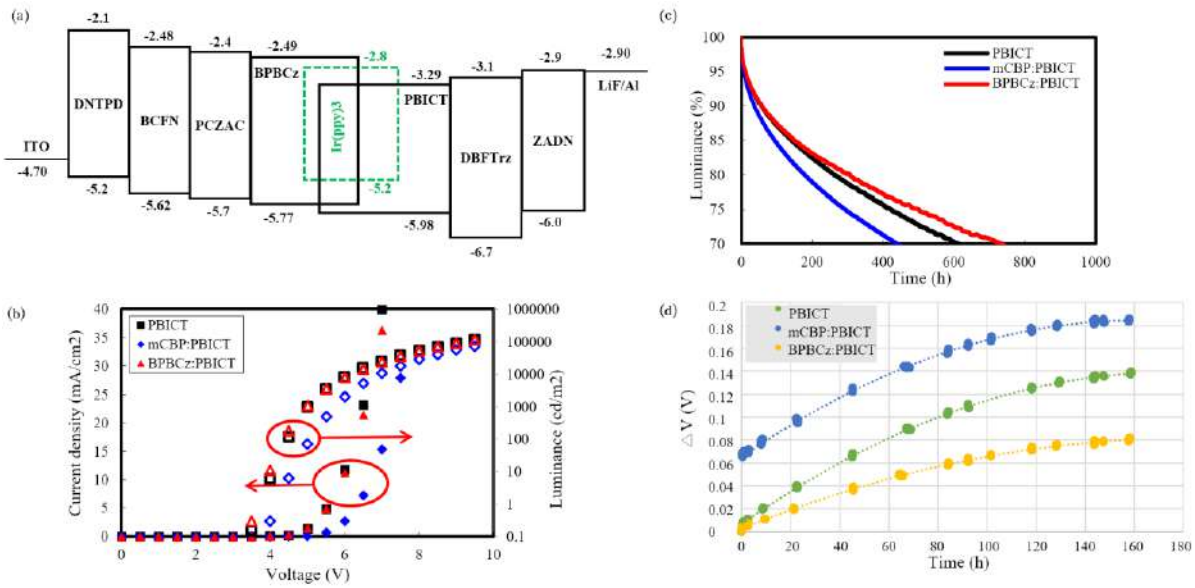

Fig. 1. (a) Energy levels of materials in the device. (b) Current density-voltage-luminance, (c) Devices lifetime at 3000 cdm-2. (d) Change of voltages of hole only devices.

References

1. C. W. Tang, S. A. VanSlyke and C. H. Chen, *Journal of Applied Physics*, 65, 3610 (1989).
2. M. A. Baldo, D. F. O'Brien, Y. You, A. Shoustikov, S. Sibley, M. E. Thompson and S. R. Forrest, *Nature 395*, 151-154 (1998).
3. H. Uoyama, K. Goushi, K. Shizu, H. Nomura and C. Adachi, *Nature 492*, 234-238 (2012).
4. S. K. Jeon, H. L. Lee, K. S. Yook and J. Y. Lee, *Advanced Materials*, Vol. 31, Issue 34, 1803524 (2019).

Doping effect of the polymer hole injection layer on the performance of solution processed organic light-emitting diodes

Seung Wan Woo[1], Gunel Huseynova[1], Jae-Min Yoo[1], Baeksang Sung[1], Jangwon Lee[1], Seung-Hoon Lee[1], Jinhwa Kim[1], Yong Hyun Kim[2], Jae-Hyun Lee[1], and Jonghee Lee[1]**

[1]Department of Creative Convergence Engineering, Hanbat National University, Daejeon, 34158, Republic of Korea
[2]Department of Smart Green Technology Engineering, Pukyong National University, Busan 48513, Republic of Korea
Tel.: +82-42-828-8802, E-mail: jonghee.lee@hanbat.ac.kr

A doped polymer hole injection layer (HIL) consisting of (3,4-ethylenedioxythiophene):poly(styrenesulfonate) PEDOT:PSS (AI4083), was employed to enhance the performance of solution processed organic light-emitting diodes (OLEDs). Highly conductive PEDOT:PSS (AI4083) was achieved using an organic small molecule, methyl red (MR) as a solution-processed dopant. The electrical conductivity of the polymer films was enhanced by more than an order of magnitude after doping compared to the pristine films. The fabricated polymer OLEDs with the doped PEDOT:PSS HILs displayed yellow emission at 550 nm with increased current density and external quantum efficiencies as well as twice the luminance of the PLED with an undoped HIL. This improved light-emitting characteristics originate from the increased conductivity of PEDOT:PSS HIL that boosted its hole injection properties. Thus, our results show that the performance of PLEDs can be significantly enhanced by simple modification of the conductivity of polymer HILs using low-cost and solution-processed organic dopant molecules.

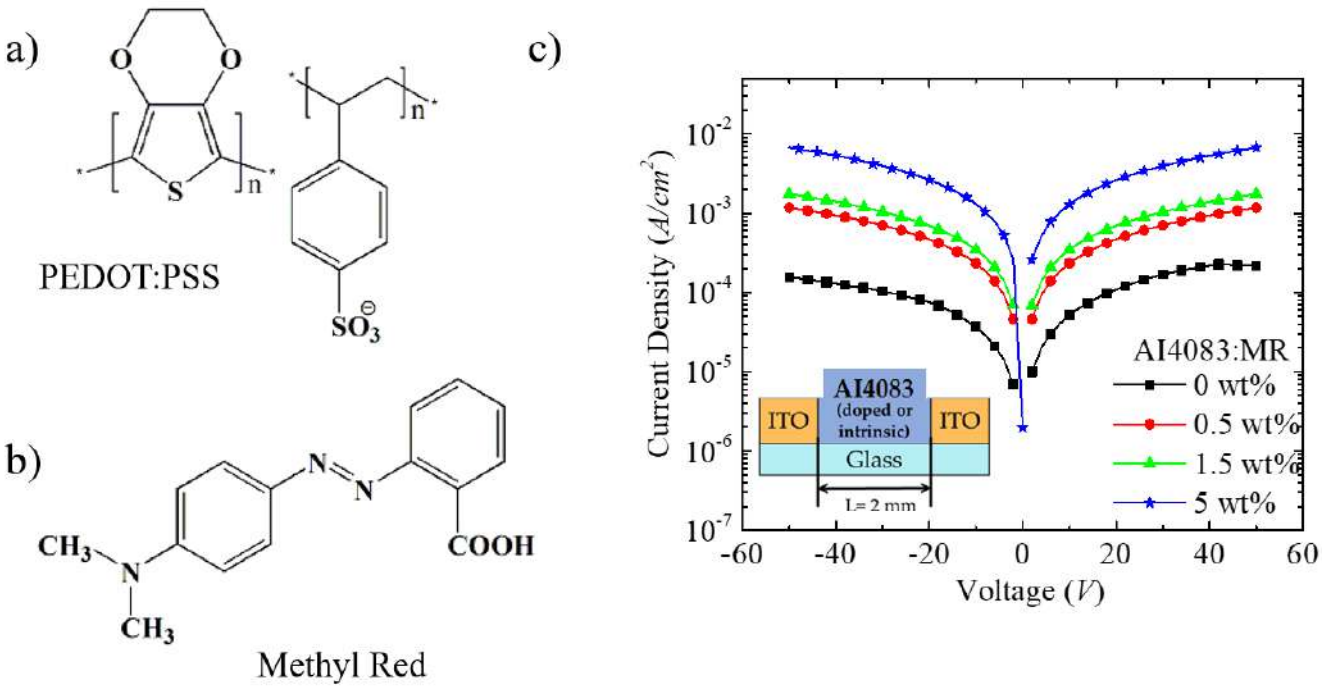

Figure (a) Chemical structures of the host (PEDOT:PSS (AI4083)) and (b) dopant (Methyl Red (MR)), and (c) conductivity of the pristine and doped AI4083 films.

A New Approach Using High-Transmission Polarizers in OLED

Young Wook Kim, Min-Hyung Kim, Tae-Woon Ko, Hyun-Jong Noh, Joun-Ho Lee[1]

[1]**LG Display, LG Science Park, Seoul 07796, Korea**

Tel.:82-2-6987-0604, E-mail: kkyyww@lgdisplay.com

The polarizer is an essential component of a display and a representative optical film. In particular, in organic light-emitting diodes (OLEDs), as a circularly polarizer along with quarter-wave plate (QWP), it has played a role of anti-reflection, thereby realizing a clearly differentiated picture quality from LCD with perfect black [1]. However, even if it is an ideal polarizer, it has a disadvantage of lowering the luminance of the OLED because the single transmission (Ts) is 50%. To improve this problem, a technique for increasing Ts while maintaining polarization efficiency (PE) has also been proposed [2]. This study reported that by improving the Ts-PE property, the luminance increase effect of about 4% was achieved with the effect of increasing the transmission without changing the reflectance.

In this study, we propose a new approach based on simulation that applies polarizers with higher Ts than previous studies. OLEDs reflection design factors are divided into surface reflection, substrate reflection, and circularly polarizer. Among them, we designed the complementary method to further increase the Ts of the polarizer by lowering the substrate reflection and simulated. As shown in Fig. 1, we calculated the OLED reflectance according to the change of the substrate reflection and the polarizer DR using the Berreman 4x4 matrix method [3]. Here, the anti-reflection film and QWP layer were fixed and calculated. Based on a reflectance of 2% or less, the polarizers with Ts 48% or more has a DR 40 or more for a 40% reflective panel, a DR 30 or more for a 20% reflective panel, and a DR 20 or more for a 10% reflective panel. Interestingly, it has shown that even if higher Ts polarizers having low DR, with a complementary design, the calculated reflectance reveal that the higher Ts polarizers achieve sufficiently the anti-reflection function. In particular, the polarizers with Ts 48% and 50% can increase luminance of about 9% and 14%, respectively, which has increased much more than previous studies, and the same time achieves low-reflective properties.

Actually, it is very hard to increase the Ts of the polarizers because it is directly related to durability. In the high-Ts polarizer, the DR decreases due to relatively low absorbance, because when a slight change in absorbance occurs under certain environmental conditions, the PE changes even more. Dye-based polarizer, a candidate material that can achieve both high transmission and durability, is expected to be a promising candidate material that can achieve the durability of high transmission polarizer because it is relatively robust under certain environmental conditions [4].

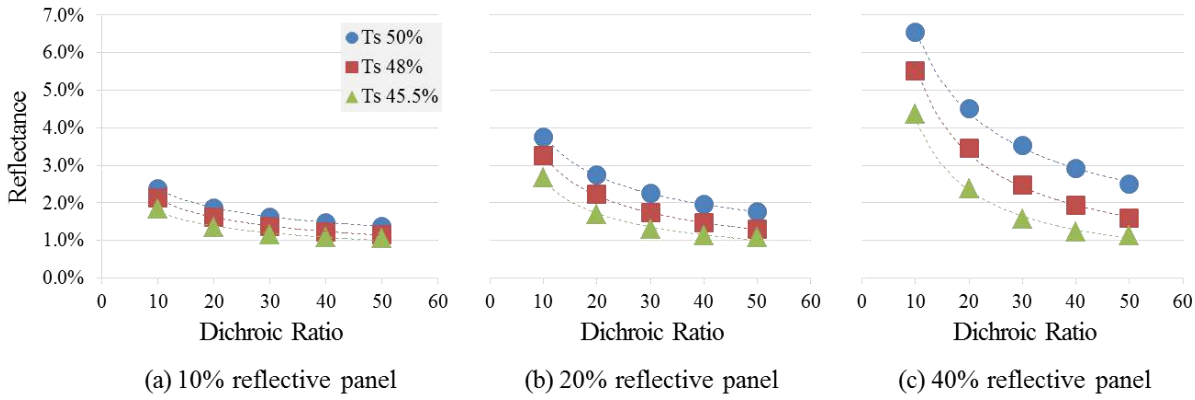

Fig. 1. The calculated reflectance results by Ts and DR at each panel

References

1. H. S. Kim, et. al., SID Digest, P-139L (2013).
2. S. H. Hwang, *et, al., SID Digest*, 60-3, 850 (2019).
3. S. Stallinga, *J. Appl. Phys.*, 85, 6, 3023 (1999).
4. S. Pan, *et. al., SID Digest*, 44-2, 596 (2016).

Impedance analysis of Thermally Activated Delayed Fluorescence OLED based on Debye model

Dongyoun yoo[1], Hyosup shin[1], Eungdo kim[1], and Changwoong chu[1]
[1]Giheung Research Center, Samsung Display, Samsung-Ro 1, Giheung-Gu, Yongin-City, Gyeonggi-Do Korea
Tel.:82-10-3505-9865, E-mail: dongyoun.yoo@samsung.com

To analyze OLEDs in terms of charge transport and electrical properties in a non-destructive way, impedance spectroscopy is widely used[1,2]. In the case of OLED, each organic layer usually has several orders of different zero-field mobility. There is a significant difference in zero-field mobility between electron and hole transport layers, so it is possible to assign the imaginary part of modulus (Im-M) peaks for each layer especially in the low voltage region. First, we performed layer assignment experiemnt for TADF device by changing the thickness of each layers. The signal around 10^5Hz and 10^4Hz at 2.8V was assigned to the hole transport layer (HTL) and the electron transport layer (ETL) respectively. The modulus signal appeared around 10^2~10^3Hz at 2.8V represent the conductive properties caused by every layers including EML. We can see the change of conductivity of each layer by analyzing the Im-M.[3]. Meanwhile, it is usaully accepted that height of Im-M peak reflect the inverse of the capacitance of the layers acoording to the RC parallel circuit model. However, in this article, we confirmed that the HTL peak is increased as the increase of hole concentraition within HTL by comparing capacitance-volage and Im-M plot. (Fig.1 (a)) This cannot be explained by the conventional RC parallel circuit model. To explain this result, we derive the equation based on Debye model and successfully reproduce the experiment results. (Fig.1 (b)) The Debye model assume an ideal relaxation due to a collection of noninteracting, fixed dipoles with the relaxation time constant τ without the conductive current pathway[4]. We concluded the layer with higher mobility in multi-layered device would follow Debye model, while the lower mobility layer follow the simple RC parallel equivalent circuit.
Finally, we compared the Im-M of the initial and degraded devices. We present the experimental results are well explained by Debye model. As hole transport is decreased, the peak height of hole transport side decreased, while the electron transport side of Im-M shifted to lower frequency according to the Debye and the simple RC parallel circuit model respectively.

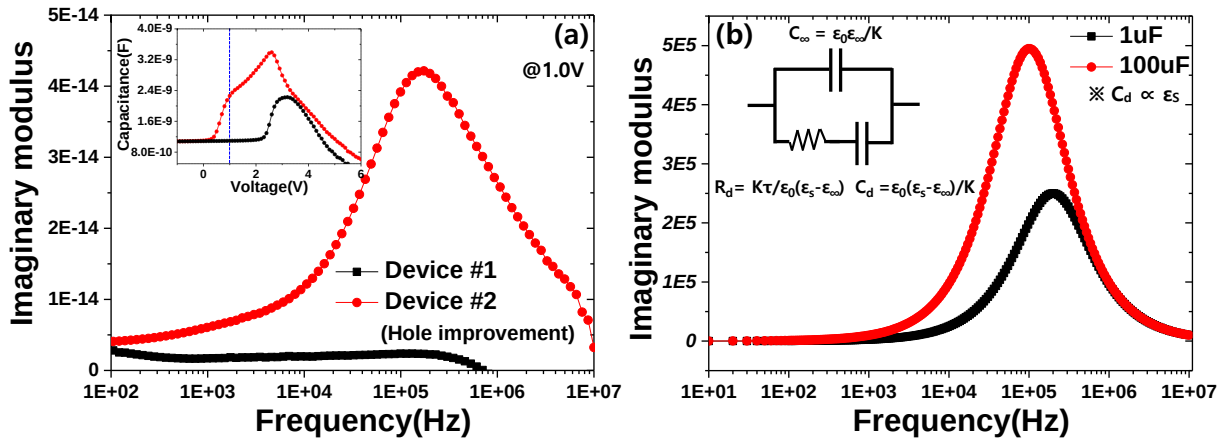

Fig. 1 (a) Comparison of devices with different hole transport properties. (b) Imaginary part of modulus bode plot based on Debye model.

References
1. S. Nowy. Et.al. *Proc. SPIE* 7415. (2009)
2. R. Maeda. Et. al. *AD. Mat. Phy. Chem* 5, 1-9 (2005)
3. T. OGIWARA. Et. al. *IEICE TRANS. ELECTRON.*, VOL. E92-C (2009)
4. Elizabeth von Hauff. *J. Phys. Chem. C* 123, 11329-11346 (2019)

A Study On The Different Properties Of Triplet-Triplet Fusion (TTF) And External Quantum Efficiency (EQE) Curves Of ADN- And MADN- Based Blue Organic Light-Emitting Diodes (OLEDs)

You Na Song[1], Kyo Min Hwang[1], Bu Bae Park[1], Seonghwan Hong[3], Young Kwan Kim[1], and Taekyung Kim[1,2]
[1]Dept. of Inform. Display Engineering, Hongik University, Seoul 121-791, Korea
Tel.:82-2-320-1646, E-mail: kimyk@hongik.ac.kr
[2]Dept. of Materials Science and Engineering, Hongik University, Sejong, Chungnam 30016, Korea
*Tel.:82-44-860-2506 *E-mail: taekyung.kim@hongik.ac.kr*

We analyzed the differences in EQE curve trend due to different TTF properties in blue fluorescent OLEDs using anthracene-based ADN (9,10-bis (2-naphthyl) anthracene) and MADN (2-methyl-9,10-bis (2-naphthyl) anthracene) hosts. Although the only structural difference between the two materials is methyl substituent attached at 2-position of the anthracene core, it caused a significant difference in the delayed electroluminescence (EL) characteristics of TTF obtained with transient EL, especially in the low luminance and/or current density region. For a deeper understanding of the interrelationship between film morphology and TTF characteristics, we proceeded with the analysis of TTF properties in conjunction with charge dynamics in the devices. According to the previous report and recent experimental results [1,2], it was revealed that the charge imbalance and the exciton formation in electron blocking layer caused by dominant electron current over hole current give rise to an unusual EQE behavior in low luminance region. The Bode plot of modulus obtained with impedance spectroscopy clearly showed that in the low luminance or voltage region, electron current in ADN-based OLED was much more dominant over hole current. In other words, the charge imbalance in the ADN-based OLED was worse than that of MADN-based OLED. Thus, the lower TTF rate or portion of delayed EL in the low luminance region was attributed to the charge imbalance in ADN host. For further investigation of film morphology and the electrical properties of ADN and MADN, density functional theory (DFT) analysis is undergoing.

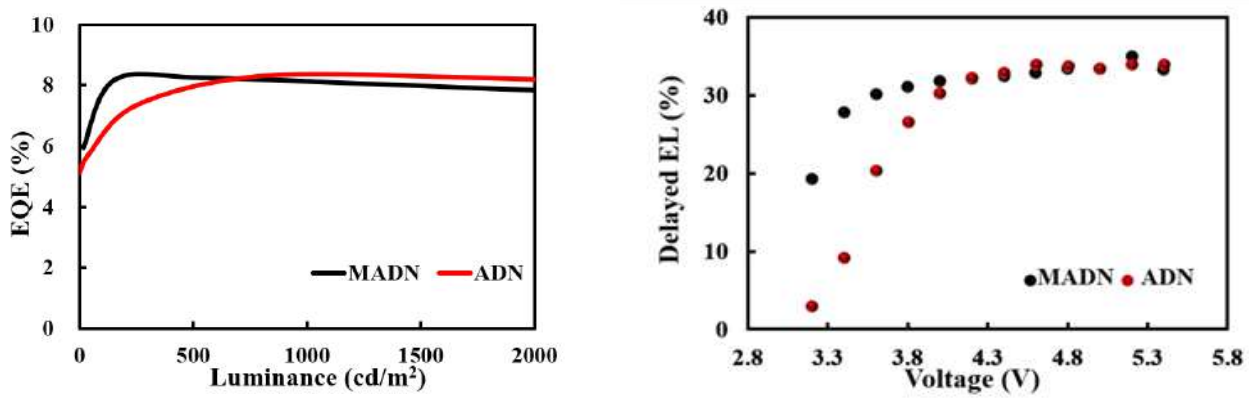

Fig. 1. (left) Luminance-dependent EQE curves of MADN- and ADN-based devices, (right) voltage-dependent delayed EL component of MADN- and ADN-based devices.

Acknowledgment

This research was supported by Basic Science Research Program through the National Research Foundation of Korea (NRF) funded by the Ministry of Education (No. 2015R1A6A1A03031833).

References

1. S. Kang, J. Y. Lee, and T. Kim, *Electronic Materials Letters* 16, 1 (2020).
2. K.M. Hwang, et al. *in preparation.*

Improved out-coupling efficiency of organic light-emitting diodes using micro-sized perovskite crystalline template

*Jangwon Lee, Seung Wan Woo, Baeksang Sung, Jae-Hyeok Cho, Jinhwa Kim, Jae-Hyun Lee, Min-Hoi Kim, and Jonghee Lee**

Department of Creative Convergence Engineering, Hanbat National University, Daejeon, 34158, South Korea
Tel.: +82-42-828-8802, E-mail: jonghee.lee@hanbat.ac.kr

In this study, we demonstrated that the out-coupling efficiency of organic light-emitting didoes (OLEDs) is enhanced using external light extraction film obtained from the $CH_3NH_3PbBr_3$ perovskite template. We found that the perovskite crystalline is very suitable for making as a template because its crystal growth is in micro-size by changing process conditions such as solvent types. In addition, the perovskite template can be used repeatably, allowing multiple films can be imprinted from one sample. By attaching an imprinted polydimethylsiloxane (PDMS) film produced from a perovskite crystalline template, we found that the light-emitting performances of bottom-emitting OLEDs is improved. The characteristics of the perovskite template as well as imprinted external out-coupling PDMS film were investigated with an optical microscope and a scanning electron microscope (SEM). The electrical and optical characteristics of OLEDs with the film will be reported in this presentation.

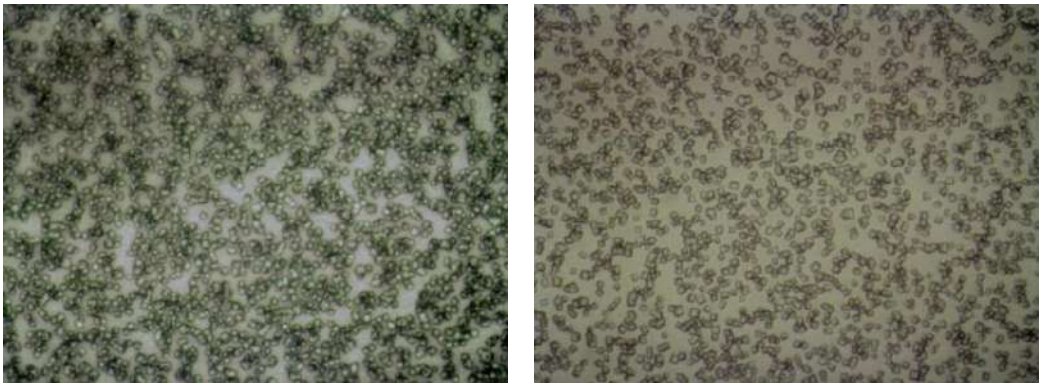

Fig. 1. Optical microscope images of perovskite template (left) and PDMS film (right)

Acknowledgment

References

Fabrication of outcoupling enhancement film with bumped surface through polymer blending and selective etching

Baeksang Sung, Jae-Hyeok Cho, Jangwon Lee, Seungwan Woo, Jinhwa Kim, Jae-Hyun Lee, Min-Hoi Kim, and Jonghee Lee*

Department of Creative Convergence Engineering, Hanbat National University, Daejeon, 34158, South Korea
Tel.: +82-42-828-8802, E-mail: jonghee.lee@hanbat.ac.kr

Even though the internal quantum efficiency in organic light-emitting diodes (OLEDs) have reached nearly 100%, the external quantum efficiency of those is poor around 25 % because of the limited light out-coupling efficiency. The reasons of low out-coupling efficiency is known as the difference in refractive index of each consisting layers. Therefore, many researches are being conducted to extract the trapped light. Among the various out-coupling enhancement methods, the external light extraction method is very simple because it is directly attached to the substrate. In this study, an outcoupling layer with a bumped surface structure was fabricated from simple and inexpensive method. The blending of poly(VDF-TrFE) and polymethyl methacrylate(PMMA), and then selective PMMA etching provide a template with a bumpy surface. The external light-extraction film of imprinted polydimethylsiloxane (PDMS) with this bumpy template was prepared, and the light emitting performance of OLEDs was enhanced due to improved out-coupling efficiency.

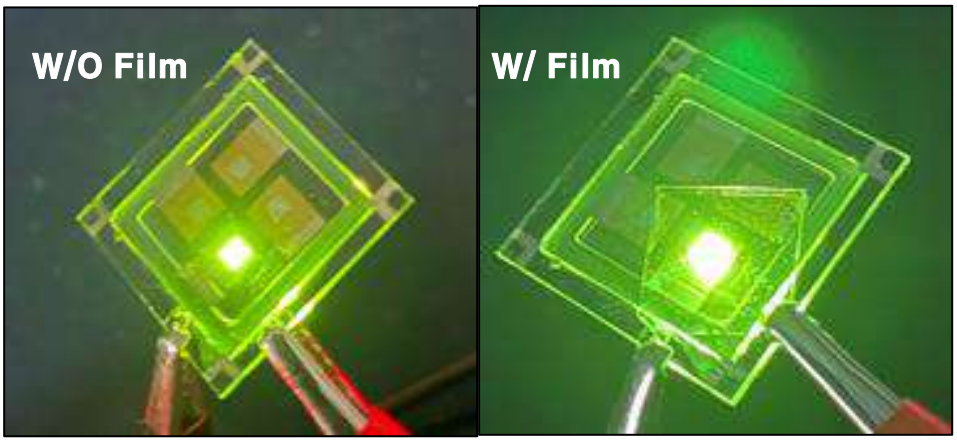

Fig. 1. Actual photos of light emitting image without film (left), and with film (right)

Analysis of Hole Injection Characteristics Solution-processed CuSCN

Eun-Jeong Jang[1], Akpeko Gasonoo[2], Yoonseuk Choi[1], Jonghee Lee[3], and Jae-Hyun Lee[3,]*
[1]Department of Electronic Engineering, Hanbat National University, Daejeon, 34158, Korea
[2]Research Institute of Printed Electronics & 3D Printing, Industry University Cooperation Foundation, Hanbat National University, Daejeon, 34158, South Korea
[3]Department of Creative Convergence Engineering, Hanbat National University, Daejeon, 34158, Korea
Tel.: +82-42-821-1970, E-mail: jhyunlee@hanbat.ac.kr

CuSCN has the advantage of wide band gap (> 3.4eV), favorable energy level to facilitate hole injection, high hole mobility, good chemical stability, high optical transparency, and easy processing at low temperature with solution process. Due to these excellent material properties, CuSCN has become a promising material for application in the emerging large area optoelectronics [1]. Therefore, it is important to understand the material properties of CuSCN from several aspects.

In this study, we investigated the hole injection characteristics of CuSCN by spin coating and depositing an NPB layer thereon. CuSCN was analyzed at various thicknesses by varying the concentration of the solution. The schematic structure of the bi-layer and absorbance spectra of CuSCN at various thicknesses are shown in Fig. 1. The optical and electrical properties of CuSCN films were analyzed by ultraviolet-visible-near infrared (UV-Vis-NIR) spectroscoopy and transmission line measurement (TLM), respectively. It was confirmed that the absorbance peak near 240 nm increased linearly as the concentration increased. The investigation is crucial in understanding the hole injection characteristics of CuSCN in hole transporting layers of organic electronic devices.

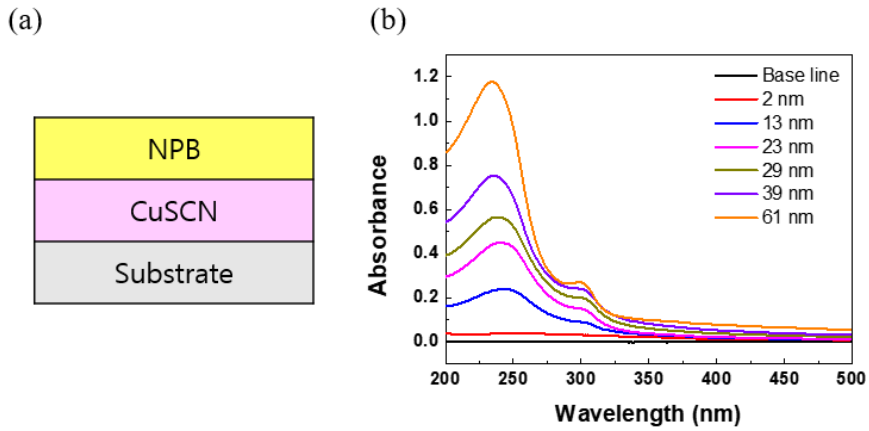

Fig. 1. (a) Schematic structures of NPB/CuSCN. (b) Absorbance of solution-processed CuSCN

Acknowledgment

This research was supported by Basic Science Research Program through the National Research Foundation of Korea (NRF) funded by the Ministry of Education (2020R1I1A3073634 and 2018R1A6A1A03026005) and by the Collabo R&D between Industry, Academy, and Research Institute funded Korea Ministry of SMEs and Startups in 2020 (S2902545).

References

1. N. Wijeyasinghe, T.D. Anthopoulos, *Semicond. Sci. Technol*, 30, 104002 (2015).

Organic Radicals for Efficient Near-infrared Organic Light-emitting Diodes

Hwan-Hee Cho[1], Shun Kimura[2], Neil C. Greenham[1], Richard H. Friend[1], Tetsuro Kusamoto[2], and Emrys W. Evans[3]

[1] Cavendish Laboratory, Department of Physics, University of Cambridge, J J Thomson avenue, CB3 0HE, UK

Tel.: +44 1223 337200, E-mail: recept@phy.cam.ac.uk

[2] Department of Life and Coordination-Complex Molecular Science, Institute for Molecular Science, 5-1 Higashiyama, Myodaiji, Okazaki, Aichi 444-8787, Japan

[3] Department of Chemistry, Swansea University, Singleton Park, Swansea, SA2 8PP

Despite extensive research on near-infrared organic light-emitting diodes, the external quantum efficiency (EQE) of these devices is far lower than devices with visible light emission: typically under 5% EQE for 800 nm and longer wavelengths. Recently, doublet fluorescent emission from organic radicals has emerged as a new route to more efficient light-emitting devices than those using established non-radical organic emitters. Charge recombination in radical devices results in doublet excitons with nanosecond emission and avoids the efficiency limit usually associated with singlets and triplets. In 2018, our group demonstrated almost 100% internal quantum efficiency in optoelectronic devices by exploiting the radical emitters. However, the trap-assisted emission resulting from the host's much wider energy gap than the dopant detrimentally affects efficiency characteristics and operational lifetime due to the narrow emission zone and poor charge balance in the emitting layer. For more efficient and stable near-infrared devices, we have designed a novel near-infrared radical emitter based on (3,5-dichloro-4-pyridyl)bis(2,4,6-trichlorophenyl)methyl (PyBTM) radical showing around 800 nm emission. Using the radical, not only higher than 5% EQE was attained, but also the efficiency roll-off and operational lifetime were substantially improved in addition to decreasing turn-on and driving voltage significantly. This shows the disruptive potential of efficient and stable near-infrared electroluminescence based on doublet emission.

References

1. X. Ai1, E. W. Evans, S. Dong, A. J. Gillett, H. Guo, Y. Chen, T. J. H. Hele, R. H. Friend, F. Li, Nature 563, 536-540 (2018).
2. Y. Hattori, T. Kusamoto, H. Nishihara, Angew. Chem. Int. Ed. 126, 12039-12042 (2014).

Enhanced barrier property and stability of H:SiN_x encapsulation film.

Jingyu Kim [1] and Sang-Hee Ko Park[1]
[1]Dept. of Materials Science and Engineering, KAIST, 291, Daehak-ro Yuseong-gu, Daejeon, Korea
Tel.:82-42-350-3316, E-mail: shkp@kaist.ac.kr

In recent years, as the necessity of flexible electronic devices and solar cell devices emerged in the market, research on improving the performance of organic light emitting diodes and perovskite solar cell devices has been actively carried out. However, deterioration of characteristics by moisture makes device require high performance encapsulation to improve reliability. Thin film encapsulation compatible with flexible devices has become a major trend instead of rigid encapsulation such as glass lid of metal lid encapsulation. The thin film deposited at low temperature, however, could not provide sufficient barrier property. Therefore, securing thin film encapsulation with excellent water barrier property at a low temperature has become one of the most important activity.
The architecture of thin film encapsulation is mainly multi-dyad structure made by alternating inorganic and organic layers. Multi-dyad structure can minimize the propagation of pin-hole in the inorganic layer and maximize the effective path of water vapor by means of lag time effect [1]. Various inorganic materials such as Al_2O_3, TiO_2, and SiN_X have been investigated in a multi-dyad structure and they showed excellent water barrier properties [2]. In a multi-dyad structure, as the number of stacks increases, WVTR becomes smaller. The increased number of stacks induced increased film thickness, yielding limitation of flexiblity. Therefore, it is essential to reduce the number of stacks, while maximizing the barrier property of inorganic layer.
In this work, we improved the water vapor barrier property and long-term stability of H:SiN_X film deposited by PECVD at 100 °C through H_2 gas addition. The water vapor permeability of H:SiN_X film was extremely reduced to control the flow rate of H_2 gas in PECVD, shown in Fig. 1. Then, we identified the effects of H_2 gas introduction on the chemical properties of the H:SiN_X films and the relationship between chemical properties and water vapor permeability. In order to find out the environmental stability of H:SiN_X film, the water vapor permeability and chemical property of H:SiN_X samples after 85°C/85% relative humidity test were investigated.

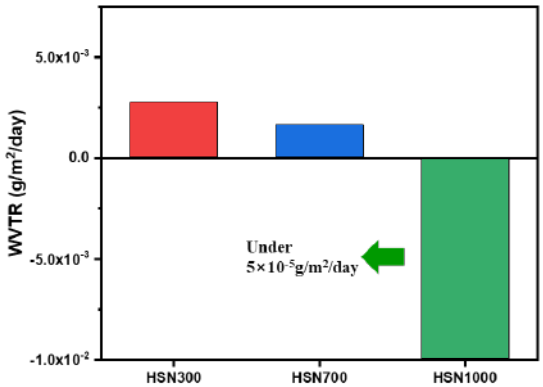

Fig. 1. WVTR values of HSN300, HSN700, and HSN1000.

Acknowledgment

This work was supported by the Wearable Platform Materials Technology Center (WMC) funded by the National Research Foundation of Korea (NRF) Grant by the Korean Government (MSIP) (No. 2016R1A5A1009926)

References

1. G. L. Graff, *J. Appl. Phys.*, 96(4), 1840 (2004).
2. N. Kim, *Thin Solid Films,* 547, 57 (2013).

Understanding diffusion behaviors of light element in OLEDs

Moonsung Kim, Jaebum Han, Myeongkyu Park and Nari Ahn
Samsung Display Co., Ltd., 1, Samsung-ro, Giheung-gu, Yongin-si, Gyeonnggi-Do, 17113, Rep. of Korea
Tel.:82-41-623-4450, E-mail: moon12.kim@samsung.net

To understand diffusion behaviors of light element in the display panel was approached and verified from various points of view. We have developed and applied nanoscale SIMS evaluation methods and preprocessing techniques to find the root cause of defective samples. Using this developed analysis method, the diffusion of light elements in the failure panel was investigated. The evaluation results showed that the Hydrogen diffused through the insulating film increased in the channel edge area of the defective sample. This result strongly suggests that H in the insulator diffuses into the a-IGZO layer, diffused hydrogen from insulators during deposition and annealing process to a-IGZO layer can be able to increase the carrier concentration in a-IGZO layers. Here, excessively hydrogen leads to interstitial defects (Hi) rather than acting as a passivator. The mechanism was established based on the examined in greater depth.

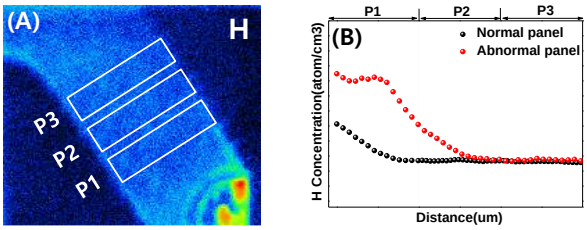

Figure 2. Hydrogen Ion Mapping Image in channel area (A), Hydrogen Line Profile N+ area to channel area, P stands for position (B)

Also, we developed a cross-sectional ion mapping evaluation method and investigated the diffusion of outgassing from the PI. It was analyzed with Nano-Scale SIMS to confirm source of the outgassing. As above, the identification of moisture diffusion in OLED panels through the Cross-Sectional Ion Mapping analysis method suggests many possibilities in the future. This is because it is possible to evaluate the thick film and observe the three-dimensional diffusion behavior in a complex structure.

The diffusion of light element in the display panel is a risk factor that can occur at any time, so, development and verification of the evaluation method will be necessary continuously.

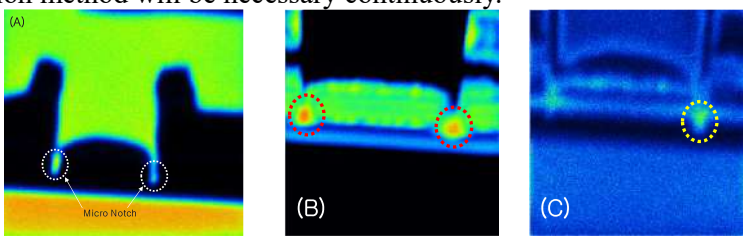

Figure 5. Carbon Ion Mapping Image in cross-sectional area (A), Oxygen Ion Mapping Image (B), hydroxide Ion Mapping Image (C)

References

1. Kamiya, T. et al. Origins of High Mobility and Low Operation Voltage of Amorphous Oxide TFTs: Electronic Structure, Electron Transport, Defects and Doping, J. Disp. Technol. 5, 273-288 (2009)
2. Nam, Y. et al. Royal Society of Chemistry. 8, 5622-5628 (2018)
3. Van deWalle, Hydrogen as a Cause of Doping in Zinc Oxide. C.G. Phys. Rev. Lett. 85, 1012 (2000)
4. Tang, H.; Kishida, Y.; Ide, K.; Toda, Y.; Hiramatsu, H.; Matsuishi, S.; Ueda, S.; Ohashi, N.; Kumomi, H.; Hosono, H.; et al. Multiple Roles of Hydrogen Treatments in Amorphous In–Ga–Zn–O Films. ECS J. Solid State Sci. Technol. 2017, 6, P365–P372.
5. Nomura, K. et al. Effects of Diffusion of Hydrogen and Oxygen on Electrical Properties of Amorphous Oxide Semiconductor, In-Ga-Zn-O ESC J. Solid State Sci.Technol., 2, 5-8 (2012)

Synthesis and Evaluation of Bipolar Host Using *Ortho*-terphenyl Derivatives for Balanced Recombination

Min I Han[1], Tae Hoon Ha[1], Byung Doo Chin[2], and Chil Won Lee[1]
[1]Dept. of Chemistry, College of Science and Technology, Dankook University, Cheonan, 31116, Korea
[2]Dept. of Polymer Science and Engineering, Dankook University, Suji-gu/Yongin-si, Gyeonggi-do, 16890, Korea
Tel.:82-41-529-6112, E-mail: chili@dankook.ac.kr

Typically, the emissive layer (EML) within the multi-layered organic light-emitting diodes (OLEDs) is composed of host and dopant. [1] In years of research for appropriate dopants for the EML in OLEDs, thermally activated delayed fluorescence (TADF) emitters have recently been considered to be the key dopant materials leading to highly efficient devices.[2] However, despite the high external quantum efficiency obtained from TADF OLED devices, the operating lifespan of the devices is known to be less than that of conventional fluorescent and phosphorescent devices.[3] The main causes of this short lifespan are known to be due to trplet-triplet annihilation(TTA) and triplet-polaron annihilation(TPA),which produce enough energy to decompose organic materials, due to the long triplet-state lifetime of the TADF material. In particular, TPA, which has a relatively large impact on device lifetime, can increase significantly as a result of unbalanced carrier injection or transport when using a unipolar host or for various other reasons. [4-6] So, it is necessary to develop a bipolar host for balanced recombination of electrons and holes. However, the design for stable bipolar hosts is very challenging as the molecular structure of the host must be consisted of bonds such as C-N, which are weak towards injected electrons.[7] One of the ways to strengthen C-N bonds with relatively weak bond dissociation energy is to introduce an electron-withdrawing group near the C-N bond.[8]

In this study, 9,9'-(pyridine-2,3-diylbis(3,1-phenylene))bis(9*H*-carbazole) and 3,3''-di(9*H*-carbazol-9-yl)-[1,1':2',1''-terphenyl]-3'-carbonitrile, which introduced pyridine and -CN unit into the *ortho*-terphenyl structure of the 3,3''-di(9*H*-carbazol-9-yl)-1,1':2',1''-terphenyl, were synthesized and evaluated. A schematic diagram of the basic skeletal structure of the host material synthesized in this study and the concept of strengthening the bond dissociation energy is shown in Figure 1.

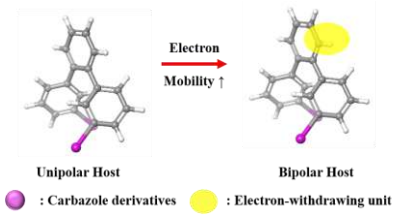

Fig. 1. Molecular structure of *ortho*-terphenyl and increased BDE by substituted electron-withdrawing unit.

The structure with the benzonitrile and pyridine strengthened the C-N bond compared to that of 3,3''-di(9*H*-carbazol-9-yl)-1,1':2',1''-terphenyl. A material having a more stable C-N bond, that is, a material having a greater C-N bond dissociation energy, obtained a device with a better lifespan.

Acknowledgment

This work was supported by the National Research Foundation of Korea (Grant No. NRF-2019M3D1A2104018) and the Technology Innovation Program (20006464) funded by the Ministry of Trade, Industry & Energy (MOTIE, Korea).

References

1. I. Manoj, D. Barah, S. Sahoo, J. Bhattacharyya and D. Ray, Synthetic Metals. 270, 116599 (2020).
2. H. Uoyama, K. Goushi, K. Shizu, H. Nomura and C. Adachi, *Nature*. 492, 234 (2012).
3. Y. Xiang, Z. Zhu, D. Xie, S. Gong, K. Wu, G. Xie, C. Lee and C. Yang, J. *Mater. Chem*. 6, 7111 (2018).
4. J. Moon, D. Ahn, S. Kim, S. Lee, J. Lee and J. Kwon, *RSC Adv*, 8, 17025 (2018).
5. D. Liu, K. Sun, G. Zhao, J. Wei, J. Duan, M. Xia, W. Jiang and Y. Sun, J. Mater. Chem. C, 7, 11005 (2019).
6. M. Regnat, K. P. Pernstich, B. Ruhstaller, Organic Electronic. 70, 219 (2019)
7. M. Hong, M. Ravva, P. Winglet and J. Brédas, Chem. Mater. 28, 5791 (2016).
8. R. Wang, Y. Wang, N. Lin, R. Zhang, L. Duan and J. Qiao, Chem. Mater. 30, 8771 (2018).

Novel n-type host materials based on 2,6-disubstituted dibenzofuran and dithiophene segments for high-efficiency and long-lived blue TADF OLEDs

Hyeonwoo Jung[1], Seokhoon Jang, and Youngu Lee[1]
[1]Department of Energy Science & Engineering, DGIST, Daegu, Korea
Tel.:82-53-785-6422, E-mail: youngulee@dgist.ac.kr

Thermally activated delayed fluorescence (TADF) organic light-emitting diodes (OLEDs) have 4 times higher quantum efficiency than fluorescent OLEDs in that they can use both singlet and triplet excitons. Although many researchers have been studied to enhance the performance of TADF-OLEDs, we have not obtained satisfactory performance and lifetime for blue emitters. Most organic semiconductors tend to have higher hole mobility than their electron mobility, and charge imbalance occurs in the EML, resulting in poor color purity, device efficiency and short device lifetime. In addition, TADF emitters generally tend to have deep HOMO and LUMO energy level. Therefore, bicomponent host system consisting of p- and n-type organic semiconductors is required to effectively transfer the charge and energies of holes and electrons from the host material to the TADF emitter. However, only a few numbers of n-type host materials with low-lying LUMO energy levels, high E_T, excellent electron transport property, and superior thermal stability is reported. In this work, novel tricyclic aromatic compound based n-type host materils 2(4,6-dipheyl-1,3,5-triazin-1-yl)dibenzo[b,d]furan-6-carbonitrile (2Trz6CNDBF) and 2(4,6-dipheyl-1,3,5-triazin-1-yl) dibenzo[b,d]thiophene-6-carbonitrile (2Trz6CNDBT) are rationally designed and synthesized for high-efficiency blue TADF OLEDs for the first time. computational simulation is employed to investigate optimal structure, orbital distribution, and physicochemical property of both molecules. Thermal, optical, and electrochemical analysis show that 2Trz6CNDBF and 2Trz6CNDBT possess high thermal stability, deep LUMO energy level (-3.43 and -3.16 eV), and E_T (2.95 and 2.88 eV). Blue TADF OLEDs with 2Trz6CNDBF or 2Trz6CNDBT as a n-type host material exhibit low turn-on voltage (3.34 and 3.26 V, respectively) than a TADF OLED with only a p-type host material, mCBP(3.83 V). In addtion, the blue TADF OLEDs with 2Trz6CNDBF or 2Trz6CNDBT show superior external quantum efficiency (η_{ext} 15.6 and 14.7 %), current efficiency (η_{ce} 33.8 and 32.7 cd A^{-1}) and power efficiency (η_{pe} 25.6 and 25.7 lm W^{-2}), respectively. In addition, the device lifetimes of blue TADF OLEDs with 2Trz6CNDBF and 2Trz6CNDBT increased by more than 1000 %.

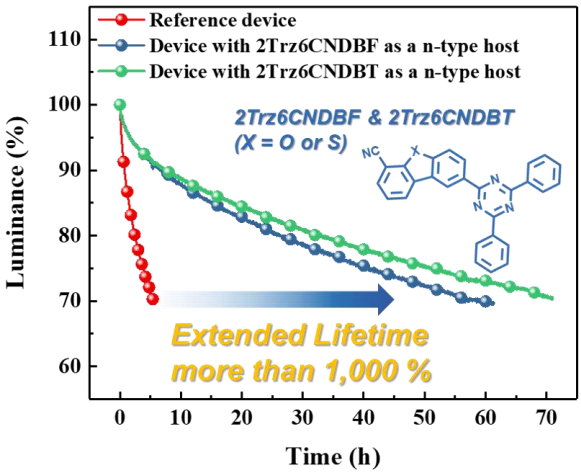

Fig. 1. lifetime test of devices

High color purity of a blue dual microcavity OLED with an absorption layer

Jun Yong Kim[1], and Yun Seon Do[1]*
[1]School of Electronic and Electrical Engineering, Kyungpook National University, 80, Daehak-ro, Buk-gu, Daegu 41566, Republic of Korea
E-mail: yuns.do@knu.ac.kr

The microcavity structure has been utilized to manipulate the optical characteristics of light-emitting devices. In the organic light-emitting diodes (OLEDs), it has been studied to improve the light intensity and purity of red, green, and blue (RGB) colors, respectively [1]. However, micropatterning work such as an e-beam lithography is required due to the different cavity thickness of the microcavity RGB subpixels, respectively [2]. It requires additional process cost and time. By optically designing a vertically dual microcavity OLED (DMOLED) structure, the microcavity RGB OLEDs can be realized with the same thickness. This structure consists of an active cavity, which is a microcavity OLED, and an external cavity. An external cavity was designed perpendicular to an active cavity. Three peaks at the RGB wavelengths can be simultaneously generated through the resonant mode of the external cavity. However, two peaks at the blue and green wavelengths were created in the blue DMOLED. It can reduce the purity of a blue color. In this paper, we verified that a lower-order resonant mode can be suppressed by placing an absorption layer within the external cavity. This was analyzed by the three-dimensional (3D) finite difference time domain (FDTD) method (FDTD Solution, Lumerical Inc., Canada). A chromium (Cr) thin film as an absorption layer was used to suppress a peak value at a green wavelength. Fig. 1 shows the electrical field intensity profile at 540 nm and spectral changes according to the thickness of the Cr thin film. When the Cr thin film was located in a place with high electric field intensity at 540 nm, the electric field intensity decreased as its thickness increased, as shown in Fig. 1 (a). This location was determined by taking into account the resonance condition of the blue wavelength. Fig. 1 (b) shows that as the thickness of Cr thin film increases, the light intensity in a green wavelength decreases. Therefore, it indicates that the resonant mode at a specific wavelength can be suppressed by the position and thickness of an absorption layer in an external cavity.

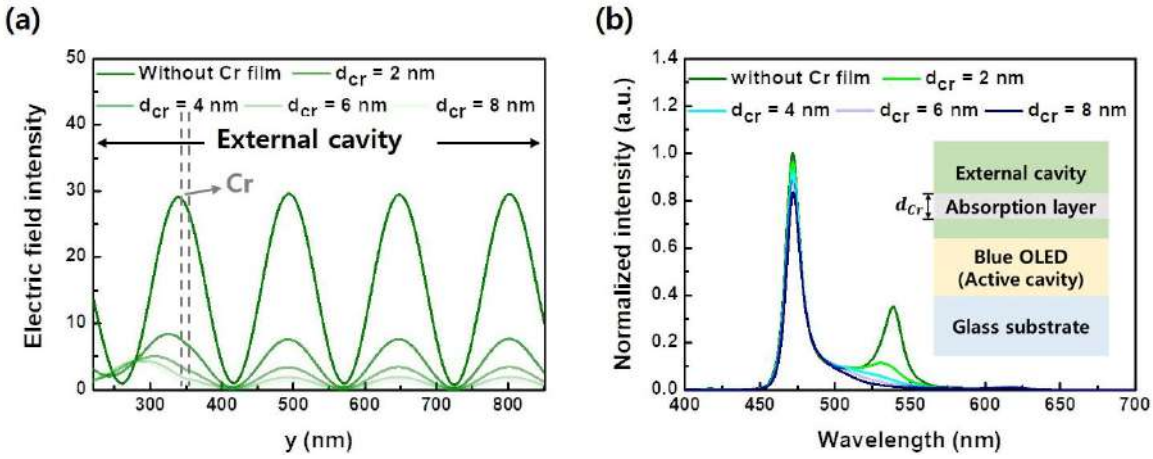

Fig. 1. Calculated results of a blue DMOLED. (a) Profile of electric field intensity at 540 nm and (b) spectral changes according to change in the thickness of a Cr thin film, which is an absorption layer.

Acknowledgment

This work was supported by the Basic Science Research Programs through the National Research Foundation of Korea (NRF), Ministry of Education, under Grant NRF-2018R1D1A1B107045853.

References

1. C. Xiang, W. Koo, F. So, H. Sasabe, and J. Kido, *Light Sci. Appl.*, vol. 2, no. e74, p. 1-7 (2013).
2. E. Bodenstein, M. Schober, M. Hoffmann, C. Metzner, and U. Vogel, *J. Soc. Inf. Disp.*, vol. 26, no. 9, p. 555-560 (2018).

Study of Blue TADF OLED Using Co-Host System for Increasing Lifetime

Hyuk Woo Jang[1], Tae Hoon Ha[1], Byung Doo Chin[2] and Chil Won Lee[1]
[1]Dept. of Chemistry, College of Science and Technology, Dankook University, Cheonan, 31116, Korea
[2]Dept. of Polymer Science and Engineering, Dankook University, Suji-gu/Yongin-si, Gyeonggi-do, 16890, Korea
Tel.:82-41-529-6112, E-mail: chili@dankook.ac.kr

Among RGB OLED devices, it is known that blue OLED devices are difficult to achieve high external quantum efficiency and long life characteristics at the same time. In order to secure high efficiency/long life characteristics in such a blue OLED device, it is most important to improve the durability of the host and dopant material constituting the light emitting layer.[1-2] Recently, studies on Themally Activated Delayed Fluorescence (TADF) emitters have been steadily progressed in order to secure high-efficiency characteristics, but relatively much research has not been conducted on the development of a host for a blue TADF dopant. Therefore, it is necessary to develop a host material optimized for blue TADF dopants. [3-4] The host role in OLED devices is to transport electrons and holes, generate excitons through their recombination, and then transfer the generated excitons to a dopant. [4] The ratio of electrons and holes injected into the emission layer, their balanced recombination, and the range of the recombination region directly affect the efficiency and lifetime of the device. [5-7] For this reason, a common host composed of a combination of an n-type host and a p-type host is used in commercially available green OLED devices. These co-hosts optimized the recombination and recombination regions of electrons and holes by controlling the deposition ratio of n-type and p-type to secure high efficiency and long lifespan characteristics of the device. [8-9]

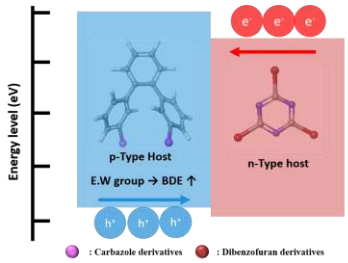

Fig. 1. Diagram of co-host device using *ortho*-terphenyl and triazine derivatives

In this study, we designed a co-host system optimized for blue TADF devices. As an n-type host, a Host in which a dibenzofuran unit is bound to triazine was used, and as a p-type host, a host composed of *ortho*-terphenyl and carbazole was used. The co-host of this combination showed high EQE and relatively long lifespan in the blue TADF device.

Acknowledgment

This work was supported by the National Research Foundation of Korea (Grant No. NRF-2019M3D1A2104018) and the Technology Innovation Program (20006464) funded by the Ministry of Trade, Industry & Energy (MOTIE, Korea).

References

1. S. K. Jeon, H. L. Lee, K. S. Yook and J. Y. Lee, *Adv. Mater.* 31, 1803524 (2019).
2. P. L. d. Santos, J. S. Ward, M. R. Bryce and A. P. Monkman, *J. Phys. Chem. Lett.* 7, 3341 (2016)
3. T. B. Nguyen, H. Nakanotani, T. Hatakeyama and C. Adachi, *Adv. Mater.* 32, 1906614 (2020)
4. M. Hong, M. Ravva, P. Winglet and J. Brédas, Chem. Mater. 28, 5791 (2016)
5. R. Wang, Y. Wang, N. Lin, R. Zhang, L. Duan and J. Qiao, Chem. Mater. 30, 8771 (2018)
6. Y. Tao, Q. Wang, C. Yang, Q. Wang, Z. Zhang, T. Zou, J. Qin, D. Ma, *Angew. Chem. Int. Ed.* 47, 8104 (2008)
7. M. Regnat, K. Pernstich and B. Ruhstaller, organic Electronics. 70, 219 (2019)
8. S-G. Ihn, N. Lee, S. O. Jeon, M. Sim, H. Kang, Y. Jung, D. H. Huh, Y. M. Son, S. Y. Lee, M. Numata, H. Miyazaki, R. Gómez-Bombarlli, J. Aguilera-Iparraguirre, T. Hirzel, A. Aspuru-Guzik, S. Kim and S. Lee, Adv. Sci. 1600502 (2017)
9. D. H. Ahn, J. H. Maeng, H. Lee, H. Yoo, R. Lampande, J. Y. Lee and J. H. Kwon, *Adv. Optical Mater*. 2000102 (2020)

Synthesis and Evaluation of TADF Material of Triazine Core for Roll-off Mitigation and Lifetime Increase

Kyeoung Wan Kim[1], Tae Hoon Ha[1], Byung Doo Chin[2], and Chil won Lee[1]
[1]Dept. of Chemistry, College of Science and Technology, Dankook University, Cheonan, 31116, Korea
[2]Dept. of Polymer Science and Engineering, Dankook University, Suji-gu/Yongin-si, Gyeonggi-do, 16890, Korea
Tel.:82-41-529-6112, E-mail: chili@dankook.ac.kr

The OLED devices with high efficiency and long lifetime are very important in commercialization. Devices using a thermally activated delayed fluorescent (TADF) material show inferior characteristics compared to phosphorescent devices in terms of lifespan despite high efficiency characteristics. [1-2] Most TADF materials are a combination of donor and acceptor units, and the donor is primarily an amine derivative, forming a single bond with the sp2 carbon of aromatic backbone units. Since such a C-N single bond is weaker than other bonds (sp2C-sp2C bonds, etc.) in the TADF molecule, it exhibits weaker properties compared to other bonds for the injected carriers or various excitation energy states. [3] Therefore, in order to increase the durability of the TADF molecule, a method of first strengthening the C-N bond is effective, and this can be achieved by introducing an electron withdrawing group near the C-N bond. The strengthened C-N bonds can improve molecular stability and, consequently, increase device lifetime. [4] Thus, we synthesized 3-(9*H*-carbazol-9-yl)-4-(4,6-diphenyl-1,3,5-triazin-2-yl)benzonitrile[Cz-pCNTrz] and 4-(9*H*-carbazol-9-yl)-3-(4,6-diphenyl-1,3,5-triazin-2-yl)benzonitrile[Cz-mCNTrz] by introducing cyano group by position into 9-(2-(4,6-diphenyl-1,3,5-triazin-2-yl)phenyl)-9*H*-carbazole[Cz-Trz], a well-known TADF dopant[5], and investigated the increase in lifespan due to the introduction of cyano group. The device evaluation results of the three materials are shown in Fig. 1, and the maximum quantum efficiency, current efficiency, and power efficiency of the device using Cz-mCNTrz were measured as 23.4%, 49.6cd/A, and 38.9lm/W, respectively, and these results were superior to the device characteristics using Cz-Trz. In the case of Cz-pCNTrz, the maximum quantum efficiency decreased than that of Cz-Trz, but the driving voltage decreased, current efficiency and power efficiency increased, and efficiency roll-off was improved.

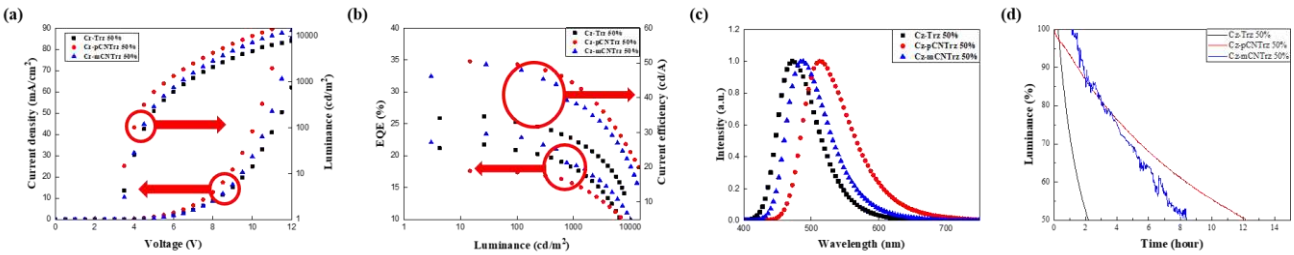

Fig. 1. Device performance of fabricated devices a) Current density-Voltage-Luminance b) EQE-Luminance-Current efficiency c) EL spectra d) Device lifetime

As a result of lifespan evaluation at LT50@200nit, Compared to Cz-Trz, Cz-pCNTrz and Cz-mCNTrz were observed to be increased by 6 and 4 times, respectively. These results suggest that the electron-withdrawing group, such as the cyano group, strengthened the C-N bond and increased the stability of the molecule.

Acknowledgment

This work was supported by the National Research Foundation of Korea (Grant No. NRF-2019M3D1A2104018) and the Technology Innovation Program (20006464) funded by the Ministry of Trade, Industry & Energy (MOTIE, Korea).

References

1. H. Uoyama, K. Goushi, K. Shizu, H. Nomura and C. Adachi, *Nature*, 492, 234 (2012).
2. T. Higuchi, H. Nakanotani and C. Adachi, *Adv. Mater*, 27 (2019).
3. M. Hong, M. K. Ravva, P. Winget and J.-L. Bredas, *Chem. Mater*, 28, 5791 (2016).
4. J. V. sundar, V. Subramanian and B. Rajakumar, Phys. Chem. Chem. Phys., 21, 438 (2019).
5. J. R. Cha, C. W. Lee, J. Y and Lee and M. S. Gong, Dyes and Pigments., 134, 562 (2016).

Improvement of pattern uniformity for inkjet-printed OLED by the surface energy control of pixel confinement layer

Min Young Kim, Hyun Jun Kim*, Eun Young Lee*, Chil Won Lee**, Byung Doo Chin*†*
***Dept. of Polymer Science and Engineering, Dankook University, Yongin-si, Gyeonggi-do, 16890, Korea**
**** Dept. of Chemistry, Dankook University, Dongnam-gu/Cheonan-si, Chungcheongnam-do, 31116, Korea**
†Tel.:82-31-8005-3587, E-mail: bdchin@dankook.ac.kr

Inkjet printing has been attractive for efficient large area OLED fabrication process, whereas a deposition of uniform, sub-50 nm organic thin film still remains challenging, requiring an ink that complies with certain specifications in terms of viscosity, surface tension, and vapor pressure [1]. The supply of good soluble light-emitting materials as well as stable solution system is prerequisite for the excellence of inkjet printing fabrication of OLED. However, more attention should be drawn for the surface properties of receptor materials [2] (usually hole-transporting layer; HTL) and pixels in the substrate which are defined by additionally photo-patterned insulator; pixel confinement layer (PCL). In this work, we have fabricated inkjet OLED test coupons with different PCL materials, processed with etching, resist coating, exposure, and developing/baking steps. The surface energies of PCLs fabricated with polyimide, SU-8, and surface-repellent resin (ATX6602SPf-02 from AGC Inc.) were found to be 47.7, 48.5, and 22.6 mN/m, respectively. Using the solvent system with methyl benzoate as primary solvent and other high-boiling solvent additives as Marangoni flow modifier (surface tension value of ink with representative composition : 39.1 mN/m), PCL with ATX6602SPf-02 showed better image of ink-filling at pixel-inside area. Fig. 1 represents the concept and image of pixel printing (with Fujifilm sapphire QS-256 -10AAA inkjet printhead) on the substrate test coupons inside of the different PCL areas. It was found that some mismatch between ink-surface-tension and substrate-surface-energy is beneficial for the confinement of printed emitter line patterns. We have conducted a systematic study on the surface material property vs. the homogeneity of printed line pattern relationship. Position of the printed edge that is being pinned and corresponding evaporation phenomena at the printed edge were important for a control of the linewidth/thickness uniformity in the PCL-defined area (pixel inner-wall). Using the optimized selection of ink formulation and HTL at surface-repellent PCL cells, smooth and uniform (less than 10% thickness variation) emitter deposition of emitters at inkjet test coupon with 80μm×240μm scale pixels were obtained.

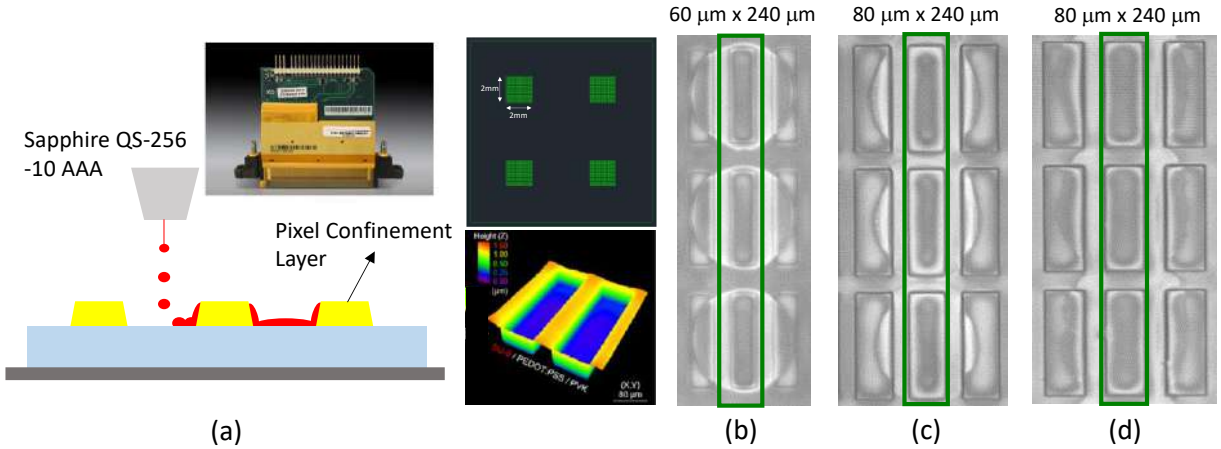

Fig. 1. (a) Inkjet printing of OLED emitter ink in the substrate with pixel confinement layer (PCL) (b) SU-8 PCL with rounded pixels (c) polyimide PCL with squared pixels (d) AGC ATX6602SPf-02 PCL with squared pixels

References

[1] B. He, S. Yang, Z. Qin, B. Wen, C. Zhang, Sci. Report 7, 11841 (2017)
[2] Y. J. Kang, R. Bail, C. W. Lee, B. D. Chin, ACS Appl. Mater. Interfaces 11, 21784 (2019)

Near-Infrared Phosphorescent Organic Light-Emitting Diodes using Perfect Square Planar type *cis*-Pt(II) Complex

Woochan Lee[1], Palanisamy Rajakannu[1], Hyungsuk Kim,[1]and Seunghyup Yoo[1]
[1]School of Electrical Engineering, KAIST, Daejeon, 34141, Korea
Tel.:82-42-350-3483, E-mail: syoo.ee@kaist.edu

Healthcare and wearable devices have taken a great interest in the field of near-infrared (NIR) light sources since they can provide various functionalities that visible light sources cannot do. With the various benefits of organic materials, such as flexibility and the possibility to make them in a large area, research on NIR organic light-emitting diodes (OLEDs) is regarded more and more important in the fields of OLEDs. Hence great attention has recently been paid to the field of NIR OLED to enhance their efficiencies as well as to increase the emission wavelength towards longer wavelengths beyond 700 nm [1-2]. However, the device performance still lags behind when compared to OLEDs in the visible spectral range.

To overcome the low performance of the NIR OLEDs, we have designed a new type of Pt(II)-based phosphorescent molecule that emits light in the NIR region over 800 nm. These Pt(II) complexes are designed to have a perfect square planar (PSP) structure that can stack parallel to each other in the solid-state through Pt···Pt interactions and subsequently enhance the metal-metal-to-ligand charge transfer (MMLCT) character. These PSP type Pt(II) emitters are utilized for the fabrication of NIR OLEDs and display a maximum external quantum efficiency of 2.5 % with an emission centered at 841 nm. These results in the study give solid support for the development of Pt(II) based near-IR emitters for various applications.

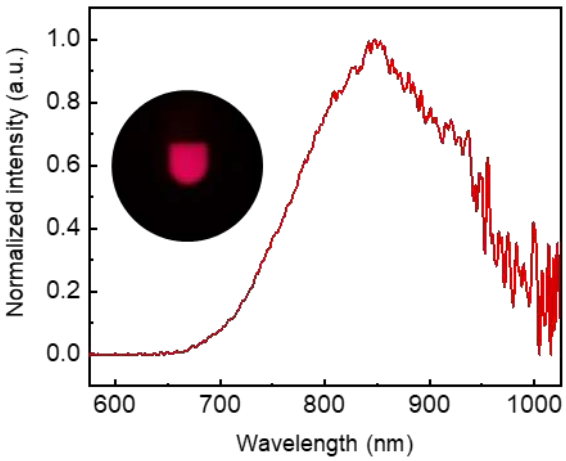

Fig. 1. EL spectrum and the photograph of the fabricated NIR PHOLED.

Acknowledgment

This work was supported by the Engineering Research Center of Excellence (ERC) Program funded by National Research Foundation (NRF), Korean Ministry of Science & ICT (Grant No. NRF-2017R1A5A1014708).

References

1. Tuong Ly, K., Chen-Cheng, RW., Lin, HW. et al. Near-infrared organic light-emitting diodes with very high external quantum efficiency and radiance. *Nat Photonics* 11, 63–68 (2017).
2. Wei, YC., Wang, S.F., Hu, Y. et al. Overcoming the energy gap law in near-infrared OLEDs by exciton–vibration decoupling. *Nat. Photonics* 14, 570–577 (2020).

Layered interfaces and pattern quality of inkjet-printed organic light emitting diodes on thermally crosslinked small molecular thin film

Eun Young Lee, Min Young Kim*, Hyun Jun Kim*, Robert Bail*, Chil Won Lee**, Byung Doo Chin*†*
***Dept. of Polymer Science and Engineering, Dankook University, Yongin-si, Gyeonggi-do, 16890, Korea**
**** Dept. of Chemistry, Dankook University, Dongnam-gu/Cheonan-si, Chungcheongnam-do, 31116, Korea**
†Tel.:82-31-8005-3587, E-mail: bdchin@dankook.ac.kr

Fabrication of a highly efficient and stable solution-processed organic light emitting diode (OLED), especially by the inkjet process, is difficult due to severe interfacial mixing [1] since the receptor organic layers are persistently exposured to ink with relatively low-vapor-pressure solvent system. Employment of a crosslinked hole transport layer (x-HTL), as a receptor at a printing of OLED light emitter, is typical approach to overcome this problem. However, many x-HTLs often suffer from non-uniformity of surface induced by the uneven shrinkage and poor homogeniety of their reactant solution during the crosslinking [2]. In this work, we have fabricated inkjet OLEDs with thermally crosslinkable small molecular thin films made of N4,N4'-di(naphthalen-1-yl)-N4,N4'-bis(4-vinylphenyl)biphenyl-4,4'-diamine (VNPB). This x-HTL was dissolved in a binary solvent mixture of chlorobenzene/cyclohexanone, showing that VNPB solution with 20% cyclohexanone additive yielded fairly improved surface morphology. For the desired set of VNPB in binary solvents, we have compared the macroscopic flatness, rms roughness, shrinkage after drying process, and solvent resistivity upon rinsing of solvent used for emitter ink. On the optimized crosslinked VNPB film with homogeniety inside of micrometer-scale pixel pockets (pre-patterned by photolithography), line patterning of ink (phosphorescent green emitter solution in methyl benzoate-based mixture with low-vapor-pressure solvents) was performed using a piezoelectric multi-nozzle printhead, Fujifilm sapphire QS-256-10AAA. Fig. 1 shows x-HTL material/solvent composition as well as printed emitter/x-HTL in stripe-pixel test coupon). Precise tuning of the ink spreading/repelling behavior at the x-HTL surface and pixel confinement layer wall could be possible through the control of mismatch at the ink-surface-tension and substrate-surface-energies, suggesting the process window for 60-to-80μm-scale pattern printing. Properties of the crosslinked x-HTL film/printed emitter stack interface, which can be explained by solvent resistivity (remaining layer thinkness upon solvent washing and exposure) and layer-by-layer spreading/adhesion, were analyzed in detail.

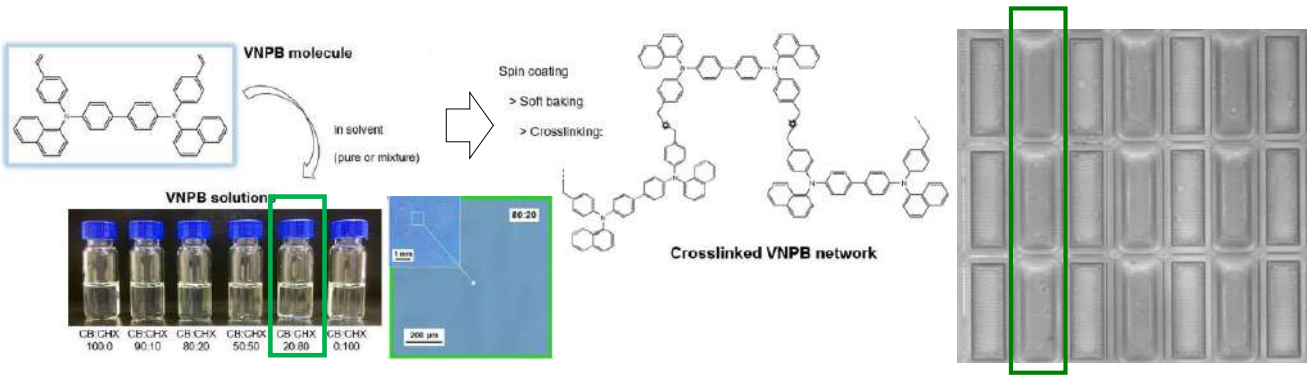

Fig. 1. Inkjet printing of OLED emitter on the VNPB processed with various composition of chlorobenzene /cyclo-hexanone, with an image of printed green emitter on x-HTL/PEOT:PSS (80 μm × 240 μm stripe-pixel test coupon)

References

[1] S. Ho, S. Liu, Y. Chen, F. So J. of Photonics for Energy, 5(1), 057611 (2015)
[2] R. Bail, J. W. Kang, Y. J. Kang, B. D. Chin, Elect. Mater. Lett. 17(1), 74 (2021)

The SiO_2 and SiN_x Multilayer Thin Film Deposition for Encapsulation of OLED Using a NSi-01 Single Precursor by PEALD

Sang Yong Jeon, Sang Chan Lee, Yong Hee Kwon, Tae Seok Byun, Sang Ick Lee and Myoung Woon Kim
DNF Co. LTD., 142, Daehwa-ro 132 beon-gil, Daedeok-gu, Daejeon, Korea
Tel.:82-42-932-7939, E-mail: silee@dnfsolution.com

OLEDs are already being used in many mobile devices and TVs, and the next generation of OLED displays will be flexible and foldable. These foldable and flexible OLED displays tend to reduce the radius of curvature under 2.5R and require excellent encapsulation characteristics at thin thicknesses. To satisfy these requirements, multilayer barrier films are considered to be indispensable for the OLEDs. Unlike a single thin film such as SiO_2 and SiN_x, which is currently applied, the multi-layer itself can produce an antireflection film effect due to a difference in refractive index of each thin film in laminated thin films, thereby reducing diffuse reflection. Also It is effective for blocking ultraviolet rays and loss stress.[1], [2]. Recently, The ALD method is used for developing thin film encapsulation technology, due to advantages of self limiting surface reaction and controlling the fraction of reaction.

In this paper, SiO_2, SiN_x and multi-layer thin films were deposited on PEN (polyethylene naphthalate) films by using the NSi-01 single precursor by PEALD technique at low temperature (90℃), and thin film thickness and refractive index were measured using a M2000D Spectroscopic Ellipsometer from Woollam. Also, the WVTR characteristics of the deposited films were confirmed using a MOCON Aquatran 2. The refractive index of the SiO_2 and SiN_x film was 1.47 and 1.85 respectively, which confirmed the possibility of antireflection effect through the multi-layer thin film. The WVTR characteristics were measured according to the thickness of SiO_2 and SiN_x film over 100hrs. The both deposited SiO_2 and SiN_x thin film below 150Å showed poor or breakdown encapsulation property. In order to overcome this, the SiO_2 film and SiN_x film were stacked in order(Fig. 1). The deposited multi-layer film showed excellent WVTR characteristics with a breakdown prevention of encapsulation property at thin thickness. Also, 2 to 3% of the carbon in the deposited SiNx film is expected to lower film stress and maintain the flexibility of the entire film. [3] From this research, we confirmed the possibility of deposit multi-layer thin film consist of silicon oxide film and nitride film in one chamber using a one precursor by PEALD. Especially, multilayer type thin film deposition suggested the possibility of preventing reflection and water vapor simultaneously.

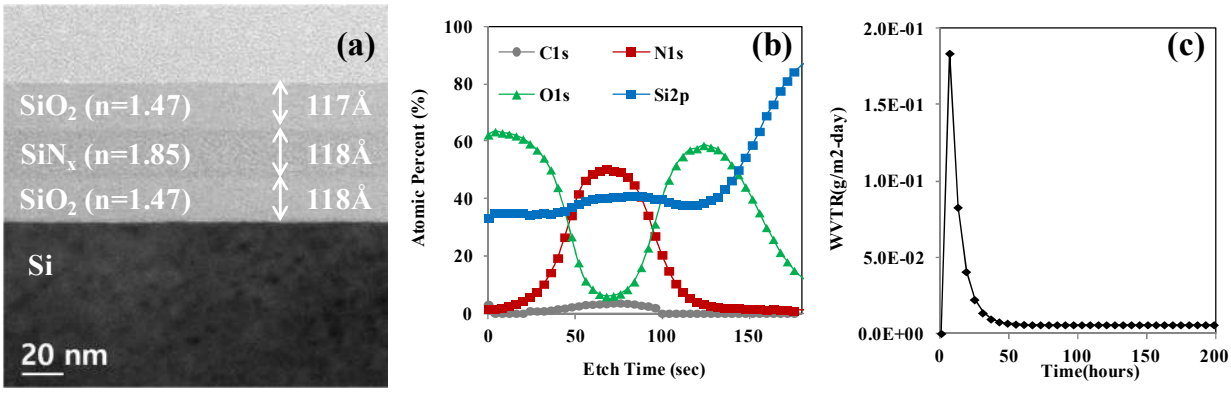

Fig. 1. The deposited multilayer was stacked the $SiO_2/SiN_x/SiO_2$ film in order. The multilayer film was analyzed by (a)TEM, Ellipsometer and (b)XPS depth profile. (c)WVTR conformed 5.59E-03g/m^2-day.

References

1. Hemant Kumar Raut, V. Anand Ganesh, A. Sreekumaran Nair and Seeram Ramakrishna, *Energy Environ. Sci.*, 3784, 2011
2. S. Chhajed, M. F. Schubert, J. K. Kim, and E. F. Schubert, *Applied Physics Letters*, vol. 93, p. 251108, 2008
3. K. D. Kim, S. H. Jang, J. M. Kim and S. M. Chang, *Korean Chem.* 575, 2012

The Perovskite and Organic Hybrid White Light Emitting Diode

*Min Woo Hyeon and Min Chul Suh**
Dept. of Information Display, Kyung Hee University, Seoul 02447, Korea
Tel.:82-2-961-0694, E-mail: mcsuh@khu.ac.kr

Recently, perovskite light emitting diodes (PeLEDs) have attracted attention as next-generation display materials and a successor to organic light emitting diodes (OLEDs) due to their advantages such as low cost, narrow bandwidth, color purity, high photoluminescence quantum yield, and tunable light emission [1]. The PeLED has the structure of ABX_3, where the material of the anion X site is changed to Br, Cl, I, etc. to control the color. The device structure is normally similar to that of OLEDs except that emitting layer (EML) is replaced by perovskite. Because of this similarity, many researches have been conducted on PeLEDs prepared with red, green, and blue perovskite to apply to display application.

However, research on white PeLEDs has not been conducted compared to independent RGB PeLEDs. So, we proposed the white PeLED using RGB perovskite quantum dot (PeQD) materials in this study. On the other hand, it is really difficult to obtain reproducibility for the white spectrum when all red, green, and blue materials are mixed together in a single layer [2]. Hence, we used a crosslinkable solution processed blue organic material (X-KHU-B) instead of a blue PeQD to fabricate a white device. To obtain clear interface between this EML (X-KHU-B) and its underlayer, we also introduced a new cross-linkable hole transport layer material (X-HTL). Also, we introduced a bipolar interlayer between X-KHU-B and the yellow PeQDs layer to suppress the color mixing, which yielded a good white color coordinate. As a result, we successfully realized a hybrid white LED composed of organic and perovskite EML as shown in **Fig. 1**. We expect this approach could be very useful for display applications.

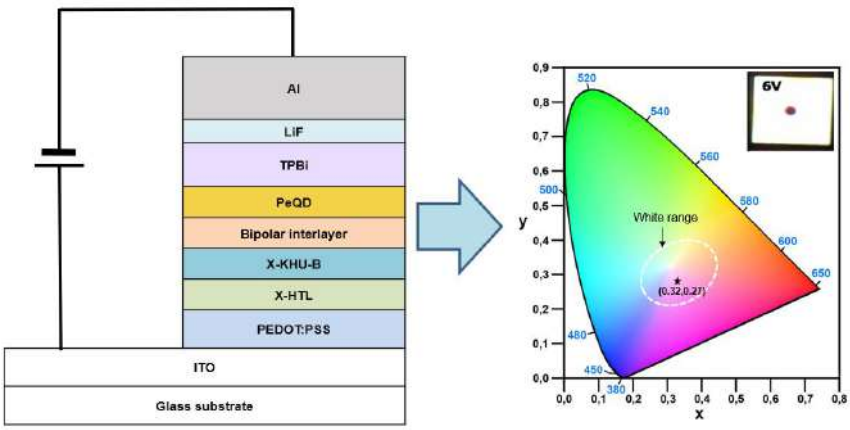

Fig. 1. The schematic of white LED.

Acknowledgment

This research was supported by National R&D Program through the National Research Foundation of Korea (NRF) funded by the Ministry of Science & ICT (No. 2020M3A7B4002030). This work was also supported by the National Research Foundation of Korea (NRF) funded by the Korea government (MSIP) (NRF-2021R1A2C1008725).

Reference

1. L. N. Quan, B. P. Rand, R. H. Friend, S. G. Mhaisalkar, T.-W. Lee and E H. Sargent Chem. Rev. 119, 7444−7477 (2019)
2. J. Mao, H. Lin, F. Ye, M. Qin, J. M. Burkhartsmeyer, H. Zhang, X. Lu, K. S. Wong, and W. C. H. Choy ACS Nano 12, 10486-10492 (2018)

Inorganic Polysilazane-based Solution-processable Thin-film Encapsulation for Flexible Polymer Light-emitting Diodes

Dahyun Kim[1,2], Sujin Jeong[1,2], Hyungsoo Yoon[1,2], and Yongtaek Hong[1,2]
[1]Department of Electrical and Computer Engineering, Seoul National University, Seoul 08826, Korea
[2]Inter-University Semiconductor Research Center (ISRC), Seoul National University, Seoul 08826, Korea
Tel.:82-2-880-9567, E-mail: yongtaek@snu.ac.kr

Recent developments in organic electronics enable commercially available devices of ultrathin, light and flexible applications via innovative low-cost manufacturing processes. While most of organic materials are vulnerable to oxygen and moisture, various encapsulation methods have been widely investigated for enhancing device lifetime. Among them, thin film encapsulation (TFE) is one of the representative approaches for a transparent and flexible encapsulation. Using multilayers with alternating inorganic and organic layers, TFEs can achieve high barrier performance with moderate strain tolerance[1]. However, since most of the TFEs are currently achieved with complex time-consuming vacuum processes such as atomic layer deposition (ALD) or molecular layer deposition (MLD), the solution-processed TFEs can be developed as an alternative way of encapsulation. Solution-processing method in organic electronics has shown various merits of large area scalability, simple fabrication process or low cost compared to conventional vacuum-based techniques. Few studies suggested solution-processed TFEs using spray coating[2] or spin-coating[3], however, encapsulation performance in flexible applications has not yet been reported. In this work, we report solution-processable inorganic polysilazane, perhydropolysilazane (PHPS) for bendable encapsulation with PEN substrate film. After simple spin-coating of PHPS precursor solution, the coated layer sufficiently converted into silicon oxide by low temperature heat treatment as shown in peak decrease of Fourier Transform Infrared Spectroscopy (FTIR) absorbance results (Fig. 1 (a)). Here, PHPS solution was further diluted to make film much thinner for better flexibility. Furthermore, water vapor transmission rate (WVTR) was measured under accelerated condition (85 ℃, 85%RH) by lab-made electrical calcium test equipment. As shown in Fig. 1 (b), PHPS coated film exhibited improved WVTR compared to pristine PEN substrate. No crack was appeared after bending test with bending radius of 7 mm, and the bended film maintained lower WVTR compared to pristine PEN substrate. The data was accomplished with single PHPS coating, so our fabrication method can be developed into high performance encapsulation via multilayer integration. Moreover, our fabrication method has the potential to be developed for all-solution processable fabrication of devices, realizing an in-situ fabrication of reliable all-solution PLEDs by direct coating method.

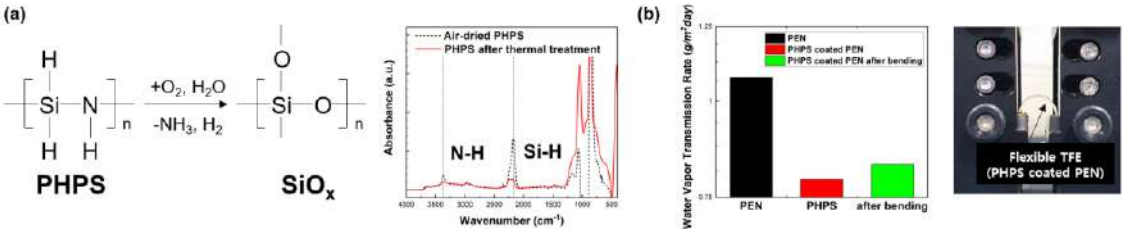

Fig. 1. (a) Conversion mechanism of PHPS to silicon oxide (left) and FTIR absorbance results of PHPS coating before & after thermal treatment (right), (b) WVTR measured by electrical Calcium test results of PEN film & PHPS coating on PEN film (left), bending test set-up with bending radius of 7 mm (right).

Acknowledgment

This work was supported by the Industry technology R&D program(20010427) funded By the Ministry of Trade, Industry & Energy(MOTIE, Korea).

References

1. J. H. Kwon, E. G. Jeong, Y. Jeon, D.-G. Kim, S. Lee, and K. C. Choi, *ACS Appl. Mater. Interfaces*, 11, 3251-3261 (2019).
2. J. Han, J. Bong, T. Lim, K.-H. Lee, and H. Yang, *Appl. Surf. Sci*., 353, 338-341 (2015).
3. L. Sun, K. Uemura, T. Takahashi, T. Yoshida, and Y. Suzuri, *ACS Appl. Mater. Interfaces*, 11, 43425-43432 (2019).

Unraveling Chemisorption of Organometallic Precursors on Semiconductor Nanocrystals

Yeong-Ho Choi[1], Donghyo Hahm[2], Jun Hyuk Chang[2], Wan Ki Bae[2] and Jaehoon Lim[1]*

[1]Department of Energy Science and Center for Artificial Atoms, Sungkyunkwan University, Suwon 16419, Republic of Korea

Tel.:82-31-299-6273, E-mail: j.lim@skku.edu

[2]SKKU Advanced Institute of Nanotechnology, Sungkyunkwan University, Suwon 16419, Republic of Korea

Chemistry of semiconductor nanocrystals have been interpreted from the viewpoint of classical colloid theory in which precursors or monomers are consumed on the surface of nanocrystals. While the progress of reaction can be translated into the minimization overall Gibbs free energy, detailed chemistry behind this phenomenon is still vague, for example, all possible reaction pathways between reaction precursors and nanocrystals, intermediate steps leaving metal ions on surface and surface ligand formation. Here, we study the reaction pathways occurring between semiconductor nanocrystals and organometallic precursors. XPS and NMR analysis revealed that cation (anion) precursors first adsorb on the surface and react with anion (cation) precursors. The nanocrystal growth can be understood as the sequential chemisorption and reaction of cationic and anionic precursors. We believe that our study helps broaden our understanding on the growth mechanism of semiconductor nanocrystals.

Acknowledgment

J. L and Y.-H. C. acknowledge the support from the National Research Foundation of Korea funded by Ministry of Science and ICT (NRF-2019R1C1C1006481 and NRF-2019M3D1A1078299). This work was also supported by Samsung Display Co., Ltd.

Alumina Infilled PbS Quantum Dot Hybrid InGaZnO Red-NIR Phototransistor via Atomic Layer Deposition

Hye-Jin Oh [1], Yoon-Seo Kim [1], Hyun-Jun Jeong[1], Seungki Shin[1], Hyun-Mo Lee[1], Nuri Oh[1,] and Jin-Seong Park[1,*]*

[1]Division of Materials Science and Engineering, Hanyang University, 222, Wangsimni-ro, Seongdong-gu, Seoul 04763, Republic of Korea

Tel.:82-2-2220-0401, E-mail: jsparklime@hanyang.ac.kr

The visible-near infrared photosensors are expected to be used in applications where various devices and sensors are combined, such as smart homes, mobile devices, automobiles, and medical components due to the influence of the Internet of Things(IoT).

Oxide semiconductors are an attractive candidate because they have advantages such as high mobility, low off current, and low power consumption, and can be applied to next-generation devices that require large-area processing, ultra-small size, flexible, and wearable. Recently, the most commonly studied InGaZnO has a high optical band gap (> 3.0eV), so it is limited to use as a visible-NIR phototransistor. Therefore, various studies on hybrid phototransistors using light absorption layers such as quantum dots[1], perovskite, and nanoparticles have been reported. In this case, for high photoresponsivity, it is important that a large number of electron-hole pairs are generated and seperated from the photo absorption layer so that the electrons are transported to IGZO active layer. For this, it is required that the interface trap site between the two layers and the trap density of photo absorption layer should be reduced, and enhancing stability of absorption layer is also important. Thus, studies such as ligand exchange process[2], core-shell structure[3], and application of the passivation layer[4] are being conducted.

In this study, we fabricated hybrid phototransistors by applying PbS QD as a photo absorption layer and IGZO as a photo-generated charge transport layer, and infiltration of Al_2O_3 through the ALD process. As a result, Al_2O_3 infilled PbS QD/IGZO hybrid phototransistor exhibited excellent photoresponsivity of 1.65×10^2 A/W, detectivity of 1.11×10^{13} Jones when illuminated by NIR light (880nm).

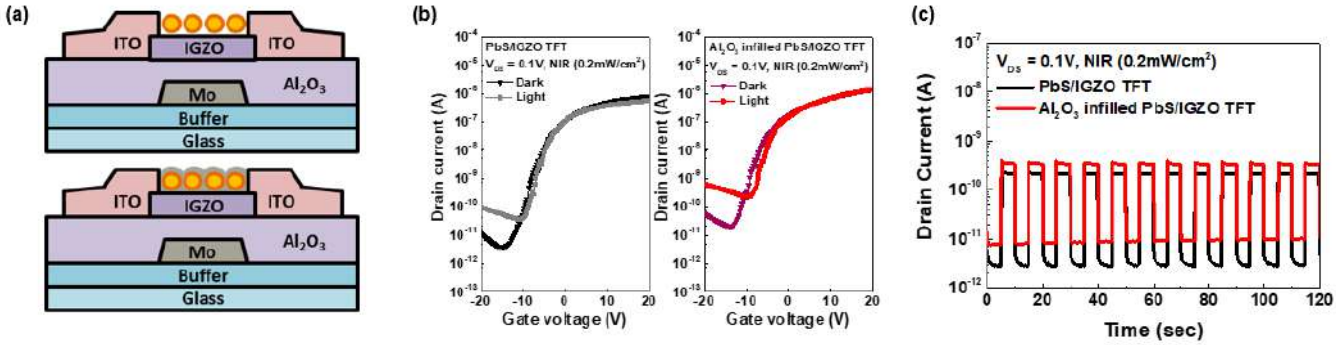

Fig. 1. (a) Schematic diagram of the PbS QD/IGZO TFT and Al_2O_3 infilled PbS QD/IGZO TFT
(b) Electrical characteristics of PbS QD/IGZO phototransistors according to Al_2O_3 infiltration under NIR light illumination
(c) Transient response to NIR light of the PbS QD/IGZO phototransistors according to Al_2O_3 infiltration

Acknowledgment

References

1. Konstantatos, Gerasimos, et al. *Nature nanotechnology* 7.6 (2012).
2. Hwang, Do Kyung, et al. *NPG Asia Materials* 8.1 (2016).
3. Kim, Jaehyun, et al. *Science advances* 5.11 (2019).
4. Valdesueiro, David, et al. *The Journal of Physical Chemistry C* 120.8 (2016).

Facilitated Hole Injection of Quantum Dot Light-Emitting Diodes adopting Multilayered Hole Transport Layer

Jeong Ha Hwang[1], Junmo Kim[2,6], Byong Jae Kim[3], Jun Young Kim[1], Wonho Lee[2,6], Jaehoon Lim[3] and Donggu Lee[1]

[1]Department of Semiconductor Engineering, Gyeongsang National University, Jinju, Gyeongnam-do 52828, Republic of Korea
Tel.:82-055-722-1735, E-mail: dglee@gnu.ac.kr
[2]Department of Polymer Science and Engineering, Kumoh National Institute of Technology, Gumi, Gyeonsangbuk-do 39111, Republic of Korea
[3]Department of Energy Science, Center for Artificial Atoms, Sungkyunkwan University (SKKU), Suwon, Gyeonggi-do 16419, Republic of Korea
[6]Department of Energy Engineering Convergence, Kumoh National Institute of Technology, Gumi, Gyeonsangbuk-do 39111, Republic of Korea

We suggest a multilayer hole transport layer (HTL) structure to improve the efficiency and operating lifetime of quantum dot light-emitting diode (QD-LED). The HTL structure was constructed by inserting a thin molybdenum trioxide (MoO_3) layer into an organic HTL layer. This multilayer HTL structure improves the hole conductivity similar to the doping effect. The QD-LED with optimal HTL exhibited improved efficiencies such as themaximum power efficiency of 10.19lm/W, and the maximum external quantum efficiency of 9.66%. Furthermore, T_{80} lifetime had 336 hours at 1000 cd/m^2, which is 15 times longer than monolayer HTL.

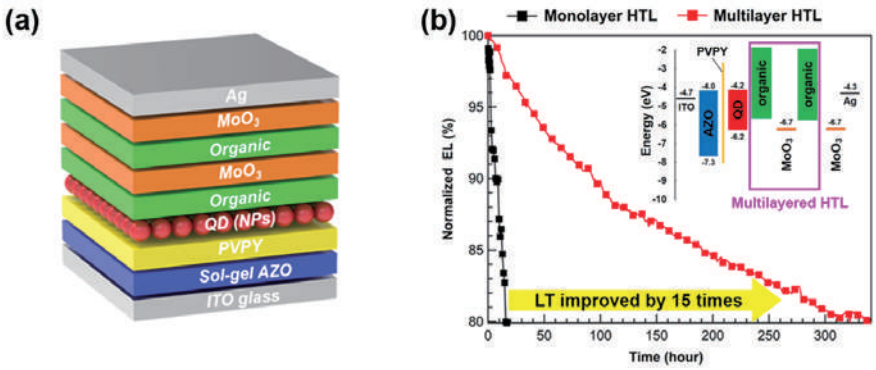

Fig. 1. (a) Schematic of the QD-LED and (b) Relative ELs for different HTL structure (insertion figure is energy band diagram with multilayered HTL)

Acknowledgment

This work was supported by the National Research Foundation of Korea (NRF) grant funded by the Korea government (Ministry of Science and ICT) (NRF-2019R1C1C1005258).

References

1. V. L. Colvin, M. C. Schlamp, A. P. Allvlsatos, *Nature*, 370(6488), 354 (1994).
2. Z. Gao, Z. Feng, W. Chen, W. Qu, W. Ao, T. Yang, J. Li, F. Gao, *RSC Adv.*, 9(9), 4957 (2019).
3. T. Glaser, S. Beck, B. Lunkenheimer, D. Donhauser, A. Köhn, M. Kröger, A. Pucci, *Org. Electron.*, 14(2) 575 (2013).
4. J. Lim, Y. -S. Park, K. Wu, H. J. Yun, V. I. Klimov, *Nano lett.*, 18(10), 6645 (2018).
5. J. Yun, J. Kim, H.-K. Jang, K. J. Lee, J. H. Seo, B. J. Jung, G. Kim, J. Kwak, *Org. Electron.*, 50, 82 (2017)

Near-Unity Quantum Yield and Narrow Emissivity of Aminophosphine-Derived, Ga-Incorporated InP Quantum Dots

Jung-Ho Jo, Dae-Yeon Jo, Hyun-Min Kim, Seung-Wan Choi, Seong-Min Park, and Heesun Yang*
Dept. of Materials Science and Engineering, Hongik University, Seoul 121-791, Korea
Tel.:82-2-320-3039, E-mail: hyang@hongik.ac.kr

Indium phosphide (InP) quantum dots (QDs) are in an unrivaled position in photoluminescence (PL) performances particularly for green and red color over other heavy metal-free QD visible emitters. Recently reported InP QDs have shown excellent optical properties (which are close to those of Cd-based QDs) with narrow full-width-at-half-maximum (FWHM) of ~35 nm and high PL quantum yield (QY) of ~95% in green and red emission regions [1,2]. Synthesis of state-of-the-art InP QDs aforementioned has been relied on use of a highly reactive, pyrophoric, and costly phosphorus (P) reagent of tris(trimethylsilyl)phosphine ($(TMS)_3P$). On that account, some alternative P precursors to $P(TMS)_3$ including PCl_3, P_4, and aminophosphines (i.e., tris(dialkylamino)phosphines) have been attempted for synthesis of InP QDs. Among them, aminophosphine shows the greatest promise in obtaining highly efficient, color-pure InP QDs among alternative P precursors above. In this work, we synthesize the high-quality fluorescent aminophosphine-based InP QDs through optimization of double shelling scheme and Ga treatment. Two InP QD heterostructures with dissimilar double shells of $ZnSe_{0.5}S_{0.5}$/ZnS versus ZnSe/ZnS are first compared. As an inner shell, ZnSe is found to be more advantageous over $ZnSe_{0.5}S_{0.5}$, specifically resulting in PL QY and FWHM for final InP/ZnSe/ZnS and InP/$ZnSe_{0.5}S_{0.5}$/ZnS QDs, respectively. To further enhance the emissivity of InP/ZnSe/ZnS QDs, a novel Ga treatment is implemented by introducing varied amounts (0−0.5 mmol) of GaI_3 simultaneously with ZnSe inner shelling. Fig. 1(a-b) shows the change of PL spectra and optical properties according to the amounts of GaI_3. Properly Ga-treated InP/ZnSe/ZnS QDs, where Ga is presumed to play a beneficial role in removing surface P dangling bond of InP core, produce a near-unity PL QY (97%) and narrow FWHM of 37 nm.

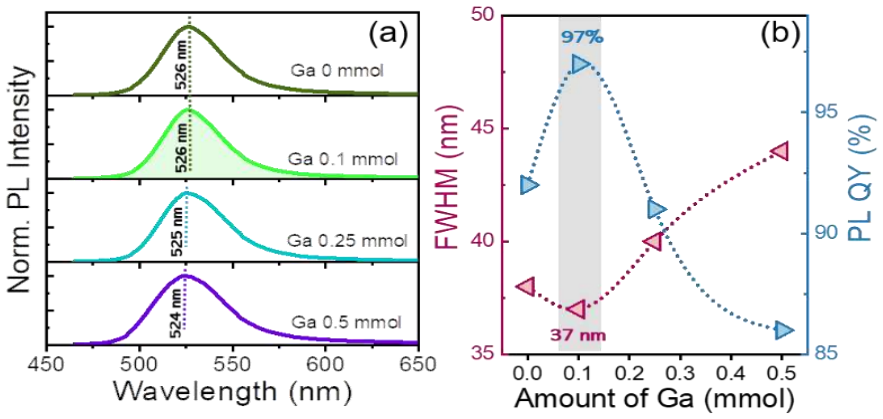

Fig. 1. Comparisons of (a) normalized PL spectra and (b) FWHM and PL QY of untreated and Ga-treated InP/ZnSe/ZnS QDs with varied Ga amounts.

Acknowledgment

This work was supported by NRF grant funded by Ministry of Science, ICT & Future Planning (MSIP) (No. 2017R1A2B3008628, 2020M3H4A3082656), and the Technology Innovation Program (20005011) funded by the Ministry of Trade, Industry & Energy (MOTIE, Korea).

References

1. Y. Kim, S. Ham, H. Jang, J. H. Min, H. Chung, J. Lee, D. Kim, and E. Jang, *ACS Appl. Nano Mater.* **2**, 1496 (2019).
2. Y. H. Won, O. Cho, T. Kim, D. Y. Chung, T. Kim, H. Chung, H. Jang, J. Lee, D. Kim, and E. Jang, *Nature* **575**, 634 (2019).

Effects of Heterostructural Modulation of Blue ZnSeTe Quantum Dots on Photo- and Electroluminescence

Sun-Hyoung Lee, Hyun-Min Kim, Suk-Young Yoon, Seung-Won Song, Seong-Min Park, Young-Ju Lee, and Heesun Yang*

Dept. of Materials Science and Engineering, Hongik University, Seoul 121-791, Korea

Tel.:82-2-320-3039, E-mail: hyang@hongik.ac.kr

A well-designed multi-shell structure in order to prevent the generation of lattice mismatch-derived interfacial defects [1] and proper shell thickness that suppress energy transfer and Auger recombination [2] is essential for the superior optical properties of core/shell quantum dots (QDs). Moreover, the thickness of formed shell is related to device performance of the quantum dot light-emitting diodes (QLEDs) [3]. In this work, we explore both the synthesis of ZnSeTe/ZnSe/ZnS QDs possessing pure blue emission and near-unity photoluminescence quantum yield (PL QY) and the correlation between shell thickness of QDs and device characteristics of QLEDs. Firstly, a change in optical properties is observed as the increasing thickness of the ZnSe inner shell formed on the ZnSeTe core surface. Through the ZnSe shell growth, a peak wavelength of 440 nm of the core shifts to 458 nm, and a full-width-at-half-maximum significantly decreases from 52 nm to 24 nm, as shown in Fig. 1(a). Then, ZnSeTe QDs with *medium*-ZnSe shell are coated by *thin*-, *medium*-, and *thick*-ZnS shell, respectively. Among above three kinds of QDs, the highest PL QY of 95% results from *thick*-ZnS shell coated one. Furthermore, a QLED fabricated by utilizing the *thick*-ZnS shelled QD exhibits a luminance of 10398 cd/m^2 and a maximum external quantum efficiency (EQE) of 18.6%. Finally, electron-only-device (EOD) and hole-only-device (HOD) are analyzed to justify such excellent electroluminescence characteristics as above. We figure out that the appropriate thickness of ZnS shell play a crucial role in enhancing the charge balance by suppressing charge injection (especially electron) to QD emissive layer, which contribute to the improved device performance.

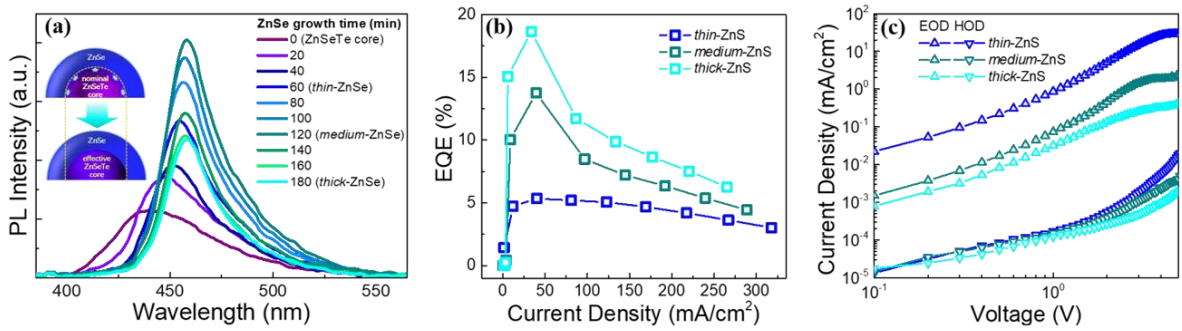

Fig. 1. (a) PL spectral evolution of ZnSeTe/ZnSe QDs. (b) Current density dependence of EQE and (c) comparison of current density-voltage traces of EOD and HOD based on ZnSeTe/ZnSe/ZnS QDs with different ZnS shell thickness.

Acknowledgment

This work was supported by NRF grant funded by Ministry of Science, ICT & Future Planning (MSIP) (No. 2017R1A2B3008628), Basic Science Research Program through the NRF funded by Ministry of Education (No. 2015R1A6A1A03031833), and the Technology Innovation Program (20010737) funded by the Ministry of Trade, Industry & Energy (MOTIE, Korea).

References

1. S.-H. Lee, C.-Y. Han, S.-W. Song, D.-Y. Jo, J.-H. Jo, S.-Y. Yoon, H.-M. Kim, S. Hong, J. Y. Hwang, and H. Yang, *Chem. Mater.* **32**, 5768 (2020).
2. Y. H. Won, O. Cho, T. Kim, D. Y. Chung, H. Chung, H. Jang, J. Lee, D. Kim, and E. Jang, *Nature* **575**, 634 (2019).
3. J. Lim, B. G. Jeong, M. Park, J. K. Kim, J. M. Pietryga, Y. S. Park, V. I. Klimov, C. Lee, D. C. Lee, and W. K. Bae, *Adv. Mater.* **26**, 8034 (2014).

Efficiency Enhancement of Blue Quantum Dot-Light-Emitting Diode Enabled by Localized Surface Plasmon Resonance of Au-Ag Alloy Nanoparticles

Sun-Kyo Kim, Jee-Na Han, Sun-Hyoung Lee, Dae-Yeon Jo, Suk-Young Yoon, Seung-Wan Choi, Yuri Kim, and Heesun Yang*

Dept. of Materials Science and Engineering, Hongik University, Seoul 121-791, Korea

Tel.:82-2-320-3039, E-mail: hyang@hongik.ac.kr

Over the past years, numerous studies have been conducted to replace the Cd-based quantum dot (QD) due to the environmental issues. Among the three primary color sources, the performance of Cd-free blue quantum dot light emitting diodes (QLEDs) relatively lags behind to that of Cd-free red and green QLEDs [1]. By inserting metal nanoparticles into QLED devices, the performance of QLEDs can be enhanced by localized surface plasmon resonance (LSPR) effect. However, the attempts applying LSPR effect into QLEDs are mainly implemented in green QLEDs. LSPR enhanced performance of blue QLEDs is rarely found in literature with the reported external quantum efficiencies (EQE) only around 5% or less [2]. In this paper, Au-Ag alloy nanoparticles with matched resonance frequency to the emission wavelength of blue QD are inserted into blue QLED devices. Fig. 1(a) shows a schematic of blue QLED integrated with Au-Ag alloy nanoparticles. Synthesized 10 nm-sized Au-Ag alloy nanoparticles are embedded in PVK hole transport layer by mixing metal nanoparticle solution and PVK polymer solution. The concentrations of PVK and Au-Ag nanoparticle solutions are varied to control the distance between QDs and metal nanoparticles. Fig. 1(b) shows the PL intensity with and without applying Au-Ag nanoparticles. It is verified that the PL intensity is increased by 10% depending on the concentrations of metal nanoparticle solution and PVK polymer solution. Fig. 1(c) shows electrical performance of blue QLEDs with and without Au-Ag nanoparticles. At a specific condition, the blending ratio of PVK polymer solution (5 mg/ml) and Ag-Au nanoparticle solution at a ratio of 20:1, we observe that the luminance and efficiency are increased by above 10%, which is well matched with the result in with Fig. 1(b), indicating that the enhanced performance is originated form LSPR effect.

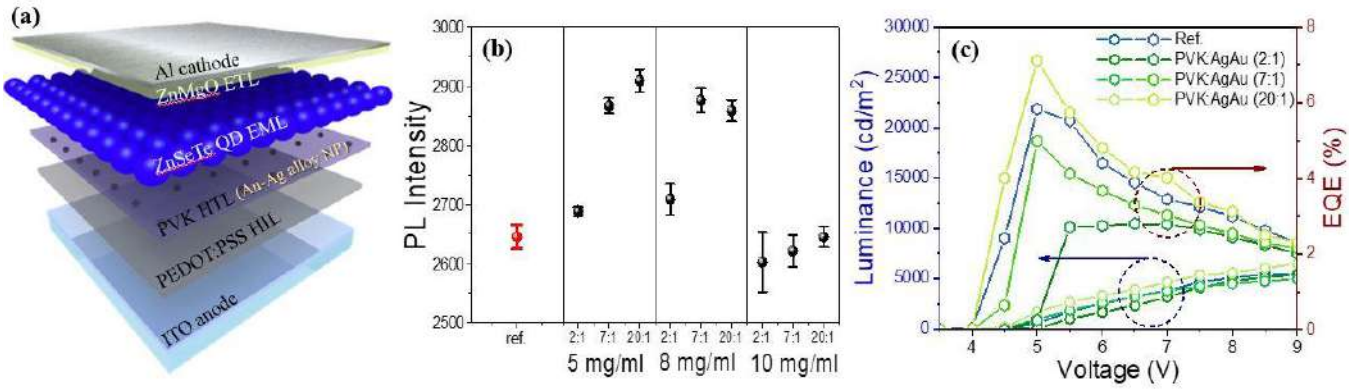

Fig. 1. (a) Schematic of blue QLED with Au-Ag alloy nanoparticles. (b) PL data with and without Au-Ag alloy nanoparticles. (c) electrical performance of blue QLEDs with and without Au-Ag nanoparticles.

Acknowledgment

This work was supported by NRF grant funded by Ministry of Science, ICT & Future Planning (MSIP) (No. 2017R1A2B3008628), Basic Science Research Program through the NRF funded by Ministry of Education (No. 2015R1A6A1A03031833), and the Technology Innovation Program (20010737) funded by the Ministry of Trade, Industry & Energy (MOTIE, Korea).

References

1. C.-Y. Han, S.-H. Lee, S.-W. Song, S.-Y. Yoon, J.-H. Jo, D.-Y. Jo, H.-M. Kim, B.-J. Lee, H.-S. Kim, and H. Yang, *ACS Energy Lett.* **5**, 1568 (2020).
2. X. Gu, T. Qiu, W. Zhang, and P. K. Chu, *Nanoscale Res. Lett.* **6**, 1 (2011).

Mn and/or Cu Doping in II−VI ZnSeTe Quantum Dots: Photoluminescence and Electroluminescence

Seung-Won Song, Sun-Hyoung Lee, Yuri Kim, Jee-Na Han, Young-Ju Lee, and Heesun Yang*
Dept. of Materials Science and Engineering, Hongik University, Seoul 121-791, Korea
Tel.:82-2-320-3039, E-mail: hyang@hongik.ac.kr

Among various compositions of quantum dots (QDs), II−VI ZnSeTe QD has been considered one of the most promising Cd-free blue emitters. It has fascinating merits for optoelectronic applications with its excellent optical properties such as high photoluminescence (PL) quantum yield and narrow full-width-at-half-maximum [1]. The emission wavelength of the QDs can be controlled by simply adjusting the particle size or impurity doping into QDs. Commonly used dopants are transition-metal ions involving Ag^{+}, Mn^{2+} and Cu^{+}, but only a few studies using them have been explored [2,3]. In this study, to demonstrate the emission wavelength modulation with the dopant species and concentration, Mn and/or Cu doped ZnSeTe QDs are synthesized and further adapted for the QD-light-emitting diode (QLED) application. Initially, single-doped ZnSeTe QDs are synthesized with Mn ions or Cu ions, respectively. For the synthesis of single-doped ZnSeTe QDs, each dopant ion is mixed with Zn, Se and Te precursors in the nucleation stage. In the case of dual Mn and Cu doping, unfortunately, Mn ions are difficult to react properly due to the difference in reactivity between two ions. Therefore, Mn is doped first during core nucleation prior to Cu doping and subsequently Cu is doped via diffusion into the nucleus. Depending on doping concentration, single-doped QDs show one or two peaks (i.e., excitonic and/or dopant PL) (Fig. 1a,b), and dual-doped QDs exhibit well resolved three peaks (i.e., excitonic and two dopant PLs) (Fig. 1c). These single and dual doped QDs are then employed as emitting layers for the solution-processed QLEDs and their electroluminescence (EL) characteristics are discussed in detail.

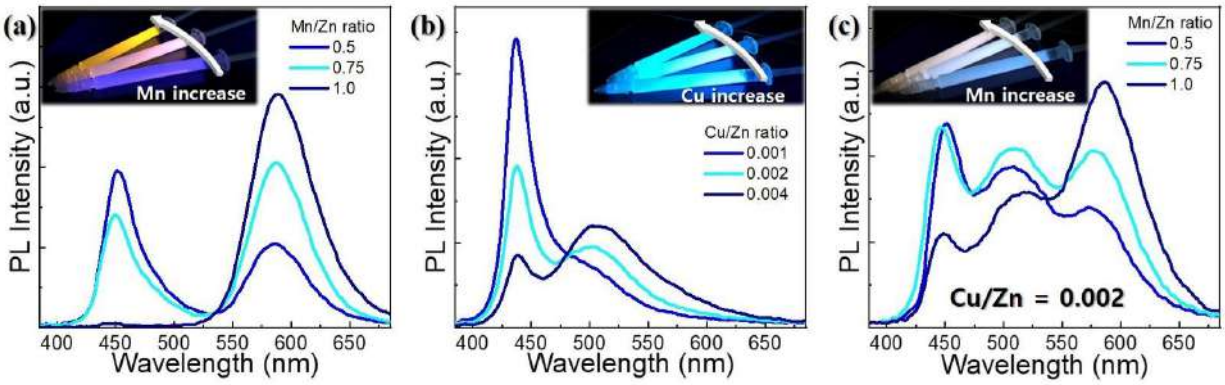

Fig. 1. PL spectra of (a) Mn single-doped ZnSeTe QDs, (b) Cu single-doped ZnSeTe QDs and (c) Mn and Cu co-doped ZnSeTe QDs.

Acknowledgment

This work was supported by NRF grant funded by Ministry of Science, ICT & Future Planning (MSIP) (No. 2017R1A2B3008628, 2015M3D1A1069755) and the Technology Innovation Program (20010737) funded by the Ministry of Trade, Industry & Energy (MOTIE, Korea).

References

1. C.-Y. Han, S.-H. Lee, S.-W. Song, S.-Y. Yoon, J.-H. Jo, D.-Y. Jo, H.-M. Kim, B.-J. Lee, H.-S. Kim, and H. Yang, *ACS Energy Lett.* **5**, 1568 (2020).
2. N. Pradhan, and X. Peng, *J. Am. Chem. Soc.* **129**, 3339 (2007).
3. X. Wei, S. Mei, G. Zhang, D. Su, F. Xie, W. Zhang, and R. Guo, *Appl. Surface Science* **605**, 493 (2019).

Suppression of the Dark Current in Colloidal Quantum Dot Photodiode with Selective Post-treatment

Byung Ku Jung[1], and Soong Ju Oh[1]*
[1]Department of Materials and Engineering, Korea University, 145, Anam-ro Seongbuk-gu Seoul, 02841, Republic of Korea
Tel.:82-2-3290-4587, E-mail: sjoh1982@korea.ac.kr

PbS quantum dot photodiode (PbS QDPD) has been extensively studied because it shows direct bandgap, low exciton binding energy, and widely tunable bandgap[1]. To date, most research efforts have focused on improving junction between layers and surface passivation to maximizing photo-induced current and EQE[2]. While dark current is a major concern in other PD fields to minimize noise sources and achieve high detectivity, PbS QDPD has rarely been investigated to understand dark current mechanism in the device. High dark current density can also limit the compatibility of PbS CQD with other applications. Herein, we illuminate the origin of the dark current in PbS QDPD using a trap-assistance charge injection model and band engineering in p-n junction. We introduce the post-treatment fabrication process, which successfully reduces minority carrier in PbS-Ink and reduce trap site in the PbS-EDT layer. We successfully suppress dark current under -3.8*10^{-5} mA/cm^{-2} at -3 V (Fig 1B).

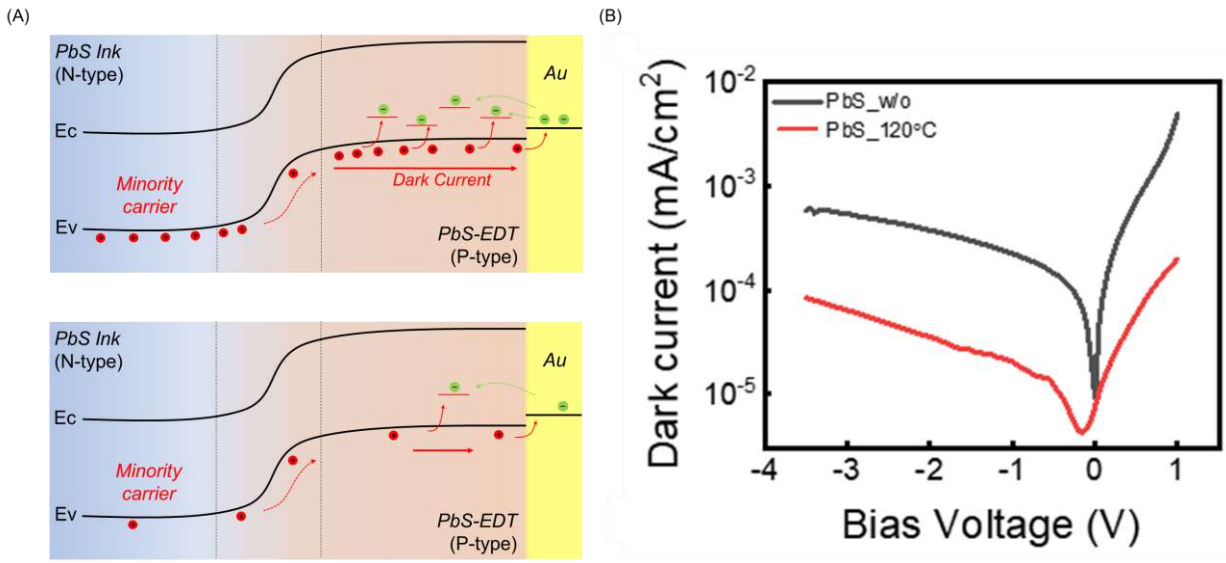

Fig. 1. (A) Schematic of the transport mechanism of dark current. (B) Voltage vs dark current density. (C) detectivity of pristine (black) and selective-temperature fabricated PbS QDPD.

Acknowledgment

This research was supported by the Basic Science Research Program through the National Research Foundation of Korea (NRF) funded by the Ministry of Science, ICT and Future Planning (2019R1C1C1003319).

References

1. Choi, M. J., García de Arquer, Sargent, E. H. (2020), *Nature Communications*, *11*(1), 1–9.
2. Zheng, S., Chen, J., Johansson, E. M. J., & Zhang, X. (2020). PbS Colloidal Quantum Dot Inks for Infrared Solar Cells. *IScience*, *23*(11), 101753

Hybrid Emission Layer for The Enhancing Carrier Injection Balance of All-Inorganic Inverted Quantum-Dot Light-Emitting Diodes

Dong-Jin Kim, and Ho-Nyeon Lee*

Dept. of Electronic Materials and Device engineering, Soonchunhyang University, Asan 31538, Korea

* *E-mail: hnlee@sch.ac.kr*

The Colloidal quantum dots (QDs) have attracted significant attention in recent years for use in next-generation display applications due to their benefits such as high quantum yield, superior color gamut, and fast response.[1-5] However, quantum-dot light-emitting diodes (QLEDs) have faced with device performance degradation due to carrier injection imbalance arising from the excess of electrons.[2-5] In addition, the organic charge transport materials of QLED are expected to be replaced with inorganic materials for higher device stability and lower cost. However QD/Inorganic interfaces have poor junction properties and a low energy transfer efficiency.[2-4] In this work, we fabricate inverted QLED with indium a tin oxide (ITO) cathode, a zinc oxide nanoparticles (ZnO NPs) electron transport layer (ETL), a tungsten oxide (WO_x) hole injection layer, and a silver (Ag) anode. Inorganic materials such as molybdenum oxide (MoO_x), nickel oxide (NiO), and copper iodide (CuI) are tested as HTL materials, and the QD/Inorganic interface properties and carrier injection balance are investigated. We use Hybrid QD emission layer fabricated by mixing Di-[4-(N, N-di-p-tolyl-amino)-phenyl]cyclohexane (TAPC) and CdSe/ZnS green QD, and the hole injection properties according to the mixing ratio are exmained. Figure 1(a) shows the characteristics of devices that have ITO/ ZnO NPs/ QD/ TAPC (10nm)/ inorganic HTL (50nm)/ WO_x/ Ag structures. The TAPC between QD and inorganic HTL greatly improved interface characteristics and carrier injection balance resulting the maximum luminance of 60,000 cd/m2 and the maximum current efficiency of 10.5cd/A. Figure 1(b) shows the performance of the device that used hybrid QD as an emission layer, and MoO_x as an HTL according to TAPC weight ratio.

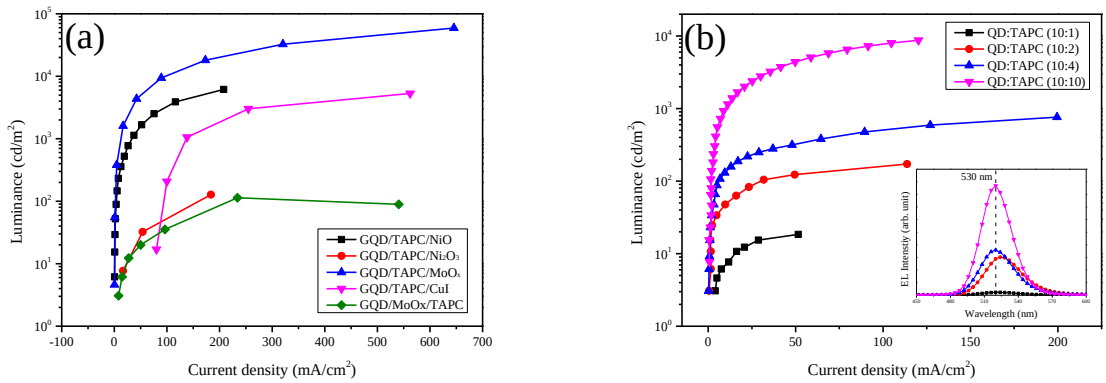

Fig. 1. The luminance-current density curves of QLED (a) using QD/TAPC/inorganic HTL structure and **(b) Hydrid QD emission layer/inorganic HTL structure**

Acknowledgment

This work was supported by the National Research Foundation of Korea (NRF) grant funded by the Korea government (MSIP) (No. NRF-2018R1D1A1B07045476) and by the Soonchunhyang University Research Fund.

References

1. Y. Shirasaki, G. J. Supran, M. G. Bawendi, and V. Bulović, *Nat. Photonics*, 7, pp. 13-23 (2013).
2. H. R. Jia, F. Z. Wang, and Z. A. Tan, *Nanoscale, 25(12)*, pp. 13186-13224 (2020).
3. W. Y. Ji, H. B. Shen, H. Zhang, Z. H. Kang, and H. Z. Zhang, *Nanoscale*, 23(10), pp. 11103-11109 (2018).
4. J. Pan, J. Chen, Q. Huang, L. Wang, and W. Lei, *RSC adv.*, 7(69), pp. 43366-43372 (2017).
5. H. J. Cho, S. J. Park, H. J. Shin, M. H. Kim, H. H. Jang, J. H. Park, J. H. Yang, C. W. Han, J. H. Baek, Y. S. Jung, and D. Y. Jeon, *small*, 16(40), p. 2002109 (2020).

High-Performance Inorganic Charge Generation Layers for Tandem Quantum-dot Light-Emitting Diodes

*O-Hun Kwon, and Ho-Nyeon Lee**

Dept. of Electronic Materials and Device engineering, Soonchunhyang University, Asan 31538, Korea

* *E-mail: hnlee@sch.ac.kr*

Quantum-dot Light-Emitting Diodes(QLEDs)[1, 3] can have higher efficiency and better color reproducibility than the Organic Light-Emitting Diodes(OLEDs). Therefore, QLEDs are considered as a promising next-generation display technology. To achieve a high performance and stability tandem[2,3] QLED technology with simple structure, we examine simple structured inorganic charge generation layers (CGLs) for tandem QLEDs composed of molybdenum trioxide(MoO3), tungsten trioxide(WO3) and copper iodide(CuI). We compared three devices having a MoO3/WO3, WO3, or CuI with CGL. The luminance and efficiency curves in Figures 1 and 2 show that the device with a WO3 CGL had higher luminance and efficiency than the single stack reference device. Based on these results, we are improving the device performance and stability, and studying the mechanism dominating the CGL functions.

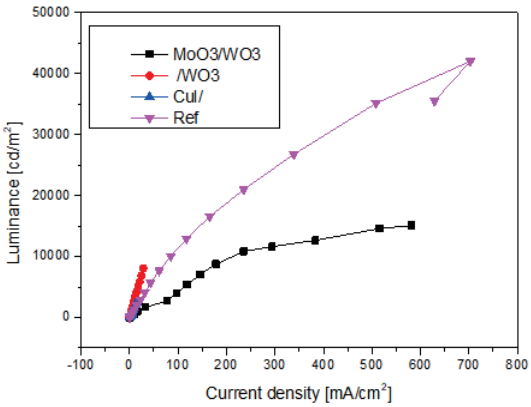

Fig. 1. Plots of luminance versus current density for the tandem QLEDs

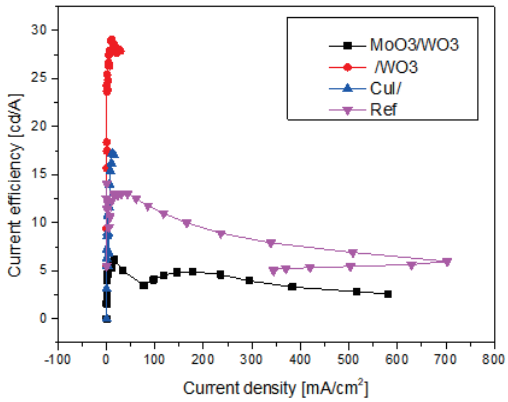

Fig. 2. Plots of current efficiency versus current density for the tandem QLEDs

Acknowledgment

This work was supported by the National Research Foundation of Korea (NRF) grant funded by the Korea government (MSIP) (No. NRF-2018R1D1A1B07045476) and by the Soonchunhyang University Research Fund.

References:

1. Debasis Bera and Lei Qian, Materials, 3, 2260-2345. (2010)
2. Linsen Li and Min Guan, Solid State Communications 150 1683-1685. (2010)
3. Dong-Jin Kim and Ho-Nyeon Lee, Japaness Journal of Applied Physics 58, 106502. (2019)
4. Yonghua Chen and Dongge Ma, J. Mater. Chem. 22, 18718. (2012)

Fabrication of cesium lead halide perovskite light emitting diodes by single source vacuum evaporation

Sa-Rang Bae[1], and Soo Young Kim[1]
[1]Dept. of Materials Science and Engineering, Korea University, Seoul 02841, Korea
Tel.:82-2-3290-3279, E-mail: sooyoungkim@korea.ac.kr

Recently, organic-inorganic hybrid perovskite materials have the most research in the field of thin film semiconductors. This material has properties such as high photoluminescence quantum yields (PLQYs), wavelength tunability across the visible spectrum, and narrow emission bandwidth. Most studies of perovskite light emitting diodes(LEDs) today focus on techniques using spin-coating and dual-source vacuum deposition. However, cesium halide salts have low solubility, which hinders crystal growth and reduces the efficiency of the device. One of the alternatives to this drawback is vacuum-based deposition, and vacuum deposition is effective in manufacturing optoelectronic devices such as OLEDs. The single-source vacuum deposition method will solve the most problematic deposition rate and vacuum maintenance problems in dual-sources. In the present study, we synthesized $CsPbBr_3$ perovskite by slow evaporation method and solid-state reaction method. The synthesized perovskite was characterized by UV-vis spectrophotometer, X-ray diffraction, etc., and device properties were confirmed through the OLED IVL Test System.

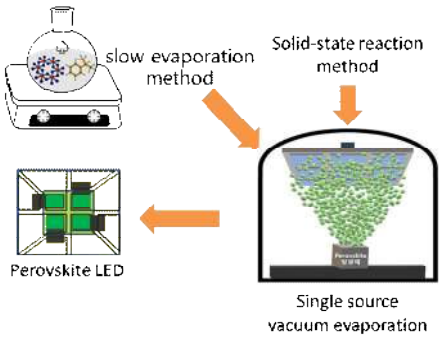

Fig. 1. Fabrication of single source perovskite LED

Acknowledgment

This research was supported by the National Research Foundation of Korea (NRF) (NRF-2020R1A2C2100670).

References

1. X. Du, *RSC. Adv.,* 7, 10391 (2017)
2. H. B. Kim, *Energy Environ. Sci.,* 10, 1950 (2017)
3. S. Xie, *APL Mater.,* 8, 051113 (2020)

InP based Quantum Dots Light-Emitting Diodes with Double ZnO Layers by RF Sputtering Method

Myoungsuk Kang[1], Heesun Yang[2] and Jiwan Kim [1,*]
[1]Dept. of Advanced Materials Engineering, Kyonggi University, Suwon, 16227, Korea
Tel.:82-31-249-1308, E-mail: jiwank@kyonggi.ac.kr
[2]Department of Materials Science and Engineering, Hongik University, Seoul, Korea
Tel.:82-2-320-3039, E-mail: hyang@hongik.ac.kr

Colloidal quantum dots (QDs) have been applied to various fields, especially quantum dots light-emitting diodes (QLEDs) for the next generation display.[1] ZnO nanoparticles (NPs) are the most widely used materials for the electron transport layer (ETL) of QLEDs, but the charge imbalance in the emission layer (EML) is occurred by due to their high electron mobility.[2]

In this study, we fabricated the QLEDs with double ZnO layers by rf sputtering. After deposition the first ZnO layer (ZnO1) to perform the role of general ETL by rf sputtering process, the second ZnO layer (ZnO2) was deposited to limit electron transport under different condition using the same ZnO target. The deposition condition of ZnO2 was controlled by different partial pressure of O_2 for the optimized EL performance. As a result, the performance of QLEDs with the inverted structure was improved dramatically by the balanced charge transport.

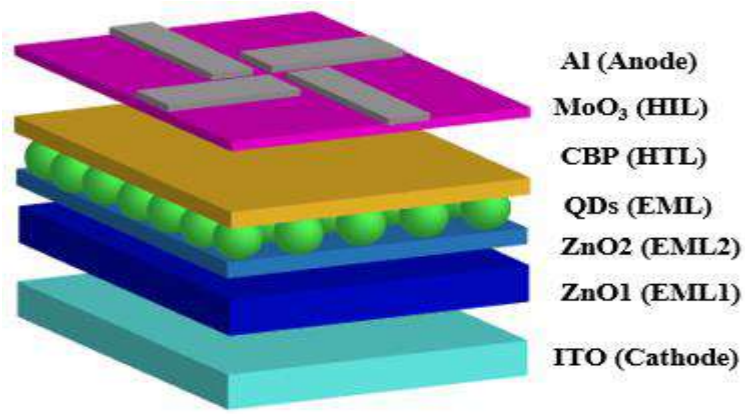

Fig. 1. A schematic of QLEDs with double ZnO layer

Acknowledgment

This research was financially supported by MOTIE and KIAT through the International Cooperative R&D program (P0011268).

References

1. Sun, Q, *Nat. Photonics*, 1, 717−722 (2007).
2. Eric Moyen and Jin Jang, *ACS Applied Nano Materials*, 3(6), 5203-5211 (2020).

Unique Quantum Dots Light-Emitting Diodes Using a Mixed Layer of Emitting Layer and Electron Transport Materials

*Changgi Yoon, Aram Moon and Jiwan Kim**
Dept. of Advanced Materials Engineering, Kyonggi University, Suwon, 16227, Korea
E-mail:jiwank@kyonggi.ac.kr

Quantum dots light-emitting diodes (QLEDs) have been spotlighted as next generation devices in the display industry because colloidal quantum dots (QDs) have the advantages over organic light-emitting diodes due to color purity and solution processability. Recently, various studies for QLEDs using inkjet printing has been actively conducted. [1] Multilayers in QLEDs need an orthogonal process inevitably using different solvents and it makes the inkjet printing process more difficult and expensive. Therefore, coating two layers in a single process can reduce the fabrication step, resulting in the process time.

In this study, we fabricated QLEDs using a mixture of emission layer and electron transport layer. The mixed layer was fabricated by dissolving SnO_2 and QDs in chlorobenzene. Device optimization was achieved by applying various film formation conditions. The device showed a maximum luminance of 130,401 cd/m^2 and it shows the bright future for the inkjet printing process of large area electroluminescence devices.

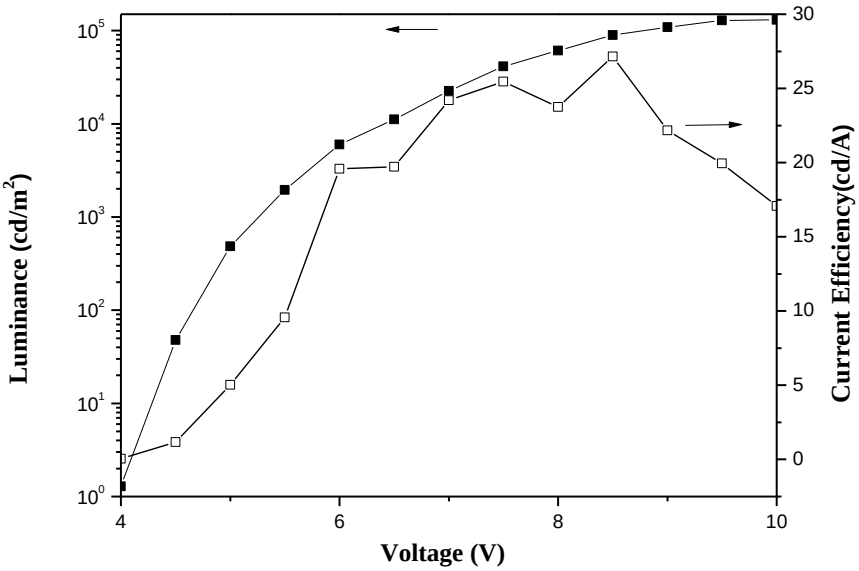

Fig. 1. Characteristics in luminance-current efficiency with applied voltage.

Acknowledgment

This research was financially supported by MOTIE and KIAT through the International Cooperative R&D program (P0011268).

References

1. Z. Xing *et. al*, ACS Appl. Mater. Interfaces, 9, 16351-16359 (2017).

Macroscopic and Microscopic Analysis of Energy Level in Quantum Dot Light-Emitting Diodes

Hyeonjun Lee[1*], Byeong Guk Jeong[2], Wan Ki Bae[2], Doh C. Lee[1], and Jaehoon Lim[3**]**

[1]Department of Chemical and Biomolecular Engineering,
Korea Advanced Institute of Science and Technology (KAIST), Daejeon 34141, Republic of Korea
[2]SKKU Advanced Institute of Nanotechnology (SAINT),
Sungkyunkwan University (SKKU), Suwon, Gyeonggi-do 16419, Republic of Korea
[3]Department of Energy Science, Center for Artificial Atoms, Sungkyunkwan University (SKKU), Suwon, Gyeonggi-do 16419, Republic of Korea

** Presenting author (hjlee161@kaist.ac.kr)*
*** Corresponding author (j.lim@skku.edu)*

Balancing electron and hole injection rates is a long lasting issue in colloidal quantum dot light-emitting diodes (QLEDs). Hybrid QLEDs employing ZnO electron transport layers (ETLs) and organic hole transport layers successfully resolved the retarded hole injection problem and resulting high device performance. However, there is no clear interpretation how the ZnO ETL can mitigate the hole injection issue and realize barrierless carrier injection of hybrid QLEDs. Here, we unveil the barrierless carrier injection phenomenon in hybrid QLEDs from the viewpoint of macroscopic and microscopic energetics of carriers at interfaces. We elucidate the Fermi level alignment derived by surface states of QDs builds up strong electrostatic potential gain allowing for barrierless hole injection. Under the modified energy landscape, individual dots containing carriers regulate the injection rate of opposite charges. Our finding would paves the way to generalized operation mechanism for QD-based optoelectronic devices.

Acknowledgment

D. C. L. and H.L. gratefully acknowledges support from the National Research Foundation (NRF) grants funded by the Korean Government (NRF-2016M3A7B4910618, NRF-2021M3H4A1A01004332, NRF-2020M3D1A2101310) and the Ministry of Trade, Industry & Energy (MOTIE, Korea) under Industrial Strategic Technology Development Program (No. 10077471). J. L. and H. L. acknowledge the support from the National Research Foundation of Korea funded by Ministry of Science and ICT (NRF-2019R1C1C1006481 and NRF-2019M3D1A1078299) and the Samsung Research Funding & Incubation Centre of Samsung Electronics under Project Number SRFC-TB1903-02.

Enhanced performance of inkjet-printed quantum dot light-emitting diodes by atomic layer deposited ZnO

Seyoung Oh[1], Ju-Hwan Han[2], Hae Lin Yang[2], Jin-Seong Park[2] and Jeonghun Kwak[3]*

[1]Dept. of Engineering Practice, Graduate School of Engineering Practice, Seoul National University, Seoul 08826, Korea

[2]Division of Materials Science and Engineering, Hanyang University, Seoul 04763, Korea

[3]Dept. of Electrical and Computer Engineering, Inter-university Semiconductor Research Center, Seoul National University, Seoul 08826, Korea

Tel.:82-2-880-1781, E-mail: jkwak@snu.ac.kr

Colloidal quantum dot (QD) light-emitting diodes (QLEDs) are attracting great attention in both academia and industry, due to the various advantages, such as narrow emission bandwidth, high photoluminescence quantum yield, superb photo-stability, and size-dependent emission wavelength owing to the quantum confinement effect [1]. Fabrication of the full-color-display panel with QLEDs requires a technology that can pattern individual pixels with a red, green, and blue emissive layer, respectively. Among the various patterning methods, inkjet printing is the most promising technology because of its quick processability and fewer material usage. To achieve an inkjet-printed high-performance full-color display, it is necessary to form a uniform QD layer by tailoring the ink conditions and designing the pixel-defining layer (i.e., a bank structure). In particular, a recent report demonstrated that the surface energy of the pixel-defining area highly affects the drying process of the inks [2].

In this work, we modified the surface energy of the pixel banks by depositing a thin ZnO layer via atomic layer deposition (ALD) to form a uniform QD layer by inkjet printing. Due to the conformal deposition of ZnO onto the sidewall of the bank structure, the external quantum efficiency (EQE) and maximum luminance of the inkjet-printed QLEDs were improved by 27% and 17%, respectively, compared to those of the control device. We investigated the effect of the thickness of the ALD layer on the performance of inkjet-printed QLEDs and analyzed the morphology using microscopic techniques. We believe that our results will provide useful insights into developing mass-productive, highly efficient inkjet-printed QLEDs.

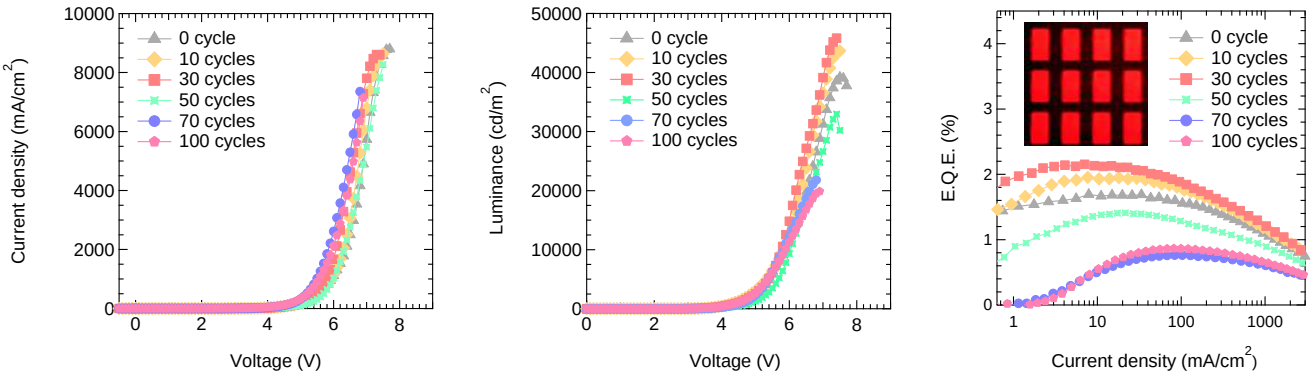

Fig. 1. Performance of QLEDs with an ALD ZnO layer: (a) Current density–voltage, (b) luminance–current density, and (c) the EQE–current density characteristics with an EL image of inkjet-printed pixels.

Acknowledgment

This work was supported by the Technology Innovation Program (Grant No. 20010737) funded by the Ministry of Trade, Industry & Energy (MOTIE, Korea).

References

1. A. P. Alivisatos, *Science*, 271, 933 (1996).
2. H. Roh et al., *Adv. Opt. Mater.*, 2002129, (2021) https://doi.org/10.1002/adom.202002129.

Synthesis a Cd-free ZnSexTe1-x/ZnSe/ZnS blue-light-emitted quantum dots

Haewoon Seo[1], Hyogeun Gwon[1], Jinsu Ha[1], Jehyeon Ryu[1], and Sang-Wook Kim[1]
[1]Department of Molecular Science and Technology , Ajou University, 206, World cup-ro, Yeongtong-gu, Suwon-si, Gyeonggi-do, Republic of Korea
Tel.:82-31-219-2611, E-mail: swkim@ajou.ac.kr

Quanntum Dots (QDs) have been attracted much attention due to their unique optical properties originating from the quantum confinement effect and also studied extensively over the past two decades for their potential application such as light-emitting diodes, lasers, and biological labels. Especially, Blue-emitting quantum dots have a great attention for light-emitting devices. For realizing QLED that is a perfectly self-luminous format, so essential that blue QDs develop. There were many Cd-based blue-emitting QDs, but the use of Cd is increasingly restricted due to environmental issues. Then the development of the QDs of the Cd-free is necessary. The diphenylphosphine reagent method has been reported to be highly reactive and capable of producing uniform particles, but with a limit of 420 nm, they are not suitable for display use. We got emissions of 440-460nm SILAR method, which controls the ratio of Zn to Se to a small amount of Te alloy. We also performed spectral analysis according to the ratio of Te. Finally, we used halide surface passivation and get a very efficient blue QDs and a maximum quantum yield of 80.6%. This is the highest of the PLQY reported so far in 440-460nm.

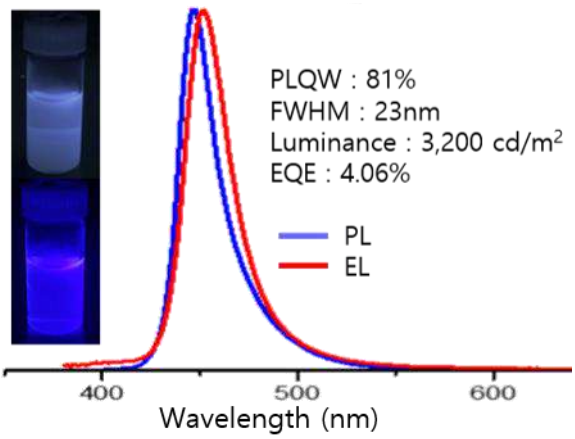

Fig. 1. Picture of ZnSeTe QDs(Left), PL(blue line), EL(red line) spectrum, optical property info(Right)

Acknowledgment

This work was supported by the Basic Science Research Program through the National Research Foundation of Korea (NRF) funded by the Ministry of Science, ICT & Future Planning (no. 2014R1A5A1009799), Republic of Korea.H. B. J. thanks the research grant of Kwangwoon University in 2016.

References

1. Murray, C. B.; Norris, D. J.; Bawendi, M. G. J. Am. Chem. Soc. 1993, 115, 8706−8715.
2. M. Bawendi, Annu. Rev. Phys. Chem., 1990, 41, 477–496.
3. S. Kim, S. H. Im and S. W. Kim, Nanoscale, 2013, 5, 5205–5214.
4. K. Lim, H. S. Jang and K. Woo, Nanotechnology, 2012, 23, 485609.

Predicting ligand-dependent nanocrystal shapes of InP quantum dots and their electronic structures

Hyeri Yoo[1,2], Sahn Nahm[2], Sangtae Kim[3], and Gyu Weon Hwang[1]
[1]Center for Neuromorphic Engineering, Korea Institute of Science and Technology, Seoul 02792, Republic of Korea
Tel.:82-2-958-4865, E-mail: gwhang@kist.re.kr
[2]Department of Material Science and Engineering, Korea University, Seoul 02841, Republic of Korea
[3]Department of Nuclear Engineering, Hanyang University, Seoul 04763, Republic of Korea

Despite the non-toxicity, InP quantum dots (QDs) suffer from limited conversion efficiency compared to other QD systems such as CdSe. The limited efficiency is expected to arise from the surface trap states distributed at the surfaces, yet, our understanding of the chemical species or physical origin behind the surface trap states has been severely limited due to the complex chemistry in the length-scales of QDs. Here, we use ab initio computations to study the thermodynamic characteristics of InP surfaces in contact with three different ligand chemistries, namely the amines, halides and carboxylic acids. We first compute the surface energies of bare InP surfaces of {100} and {111}, and study the binding energies and coverage-dependent surface energies for the three ligand chemistries. Our results show that ligand chemistry significantly affects the dominant surfaces and equilibrium crystal shapes, the Wulff shape, of InP nanocrystals. The stable Wulff shape of amine-bound InP crystals forms an octahedron with mostly (111)In surfaces exposed, while that of fluorine-bound InP crystals is a cube with (100)In surfaces exposed. We further reveal the quantitative maps of surface energies and Wulff shapes according to the chemical nature and the surface coverage of the working ligands. The fundamental understanding of the surface energies of InP provides the foundation for the electronic structure analysis. The surface-dependent electronic structure of InP quantum dots will also be discussed briefly.

Ligand	None	Halide ion, Acetate ion	Methylamine	Halide ion
Wulff construction	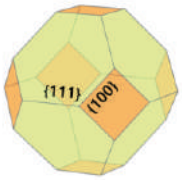	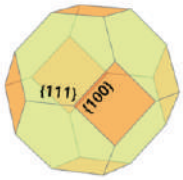	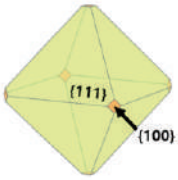	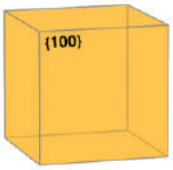
Chemical potential (eV/atom)	-	All conditions	All conditions	In-rich conditions
Coverage (ligand/nm^2)	-	2.24 > (30% >)	4.53 < (75% <)	4.78 < (80% <)

Table 1. The brief summary of Wulff shapes according to the binding group of ligands

Acknowledgment
This work was supported in part by Samsung Research Funding & Incubation Center of Samsung Electronics under Project Number SRFC-TB1903-02, and by KIST Institution Program under Project Number 2E31041.

Fabrication of Flexible Quantum dot-Light-Emitting Diodes using an Epoxy Planarization Layer and an Oxide/Metal/Oxide cathode

Mi-Jin Kim, and Ho-Nyeon Lee*

Dept. of Electronic Materials and Device engineering, Soonchunhyang University, Asan 31538, Korea

**E-mail: hnlee@sch.ac.kr*

Flexible quantum-dot light-emitting diodes (QD-LEDs) are receiving much attention because of their high bending and folding ability, and high purity color generation ability. However, the rough surface morphology of flexible substrates and the difficulty in the encapsulation process are the points to be solved before their commercialization.[1-5] In addition, it should be avoided to use brittle indium tin oxide (ITO) for ensuring the stability of flexible QD-LEDs. In this work, we fabricate inverted green flexible QD-LEDs on PET films. The rough surface the PET films was planarized using an epoxy resin.[3] Oxide/Metal/Oxide (OMO) multilayer was adopted as a cathode instead of brittle indium tin oxide (ITO)[4,5]. A zinc oxide nanoparticle (ZnO NP) layer was used as a high performance electron transport layer (ETL).[1-2] In addition, Di-[4-(N, N-di-p-tolyl-amino)-phenyl]cyclohexane (TAPC) hole transport layer(HTL), tungsten oxide (WO_x) hole injection layer and silver (Ag) anode were used. Figure 1. shows of optical transmittance curves of OMO multilayers. We used tungsten oxide (WO_x) and molybdenum oxide (MoO_x) for the oxide layer and silver (Ag) 12nm for the metal layer. It was found that the 30-nm thick oxide layer resulted in the highest transmittance value. Figure 2 shows of luminance-current density and current efficiency-current density curves of the fabricated QD-LED. The results from the flexible devices are compared with those from the rigid devices fabricated on the glass substrates. From the flexible device, the maximum luminance of 22,000 cd/m^2 and the maximum current efficiency of 26 cd/A were obtained.

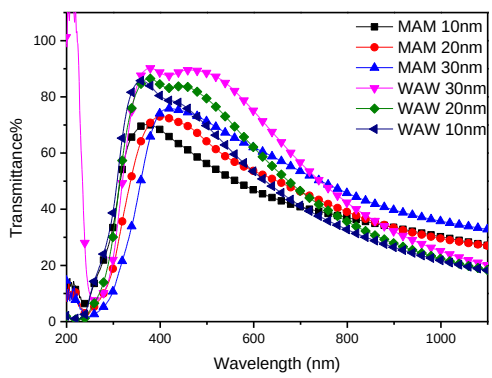

Fig. 1. Optical Transmittance of OMO multi-layer

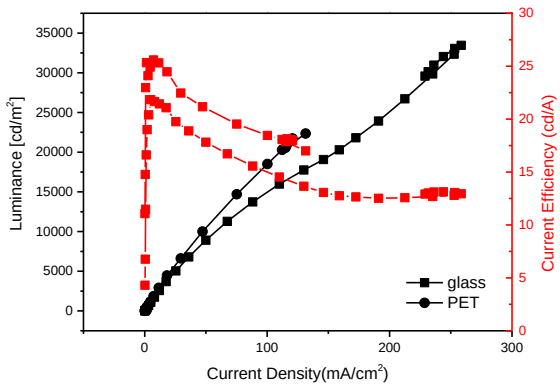

Fig. 2. luminance-current density and current efficiency-current density curves of a flexible QD-LED and a rigid QD-LED

Acknowledgment

This work was supported by the National Research Foundation of Korea (NRF) grant funded by the Korea government (MSIP) (No. NRF-2018R1D1A1B07045476) and by the Soonchunhyang University Research Fund.

References

1. Y. Shirasaki, G. J. Supran, M. G. Bawendi, and V. Bulović, *Nat. Photonics*, 7, pp. 13-23 (2013).
2. L. Qian, Y. Zheng, J. G. Xue and P. H. Holloway, *Nat. Photonics*, 5, pp 543-548 (2011).
3. M. K. Choi, J. Yang, K. Kang, D. C. Kim, C. Choi, C. Park, S. J. Kim, S. I. Chae, T. H. Kim, J. H. Kim, T. Hyeon and D. H. Kim, *Nat. Commum*, 6, 7149 (2015).
4. S. H. Lim and H. K. Kim, *Scientific Reports*, 10, 8357 (2020).
5. T. Abachi, L. Cattin, G. Louarn, Y. Lare, A. Bou, M. Makha, P. Torchio, M. Fleury, M. Morsli, M. Addou and J.C. Bernède, *Thin Solid Films*, 545, pp. 438–444 (2013).

ZnO and QD layer with Inkjet printing process for high-resolution pixel pattern of inverted QLED devices

Youngwoo Lee[1,2] and Yong-Cheol Jeong[1]
[1]Process Platform R&D Department, KITECH, Ansan, 426-910, Korea
Tel.:82-31-8040-6197, E-mail: ycjeong@kitech.re.kr
[2]Department of Materials Science and Chemical Engineering, Hanyang University ERICA Campus, Ansan, 426-791, Korea

Quantum dots (QD) have very interesting properties in the field of optoelectronic devices such as low driving voltage, high color purity, and high luminance. When forming pixels using the printing process, it is very important to form a flat and uniform QD solution because the quantum dot light emitting diode (QLED) device is composed of multi-layered nano-layers. Since the surface flatness of the nano-thick QD layer is determined by the effected of the surface flatness of the ZnO layer, which is the underlying layer, it is important to form a layer with low flatness for uniform light emission of the QLED device. Also, in order to form pixels with high resolution, droplets with low size are important. ZnO and QD layers were printed using a 1 pL nozzle to form low-sized droplets. In this study, we studied the printing of ZnO nanoparticles (NPs) electron transport layer (ETL), and QD layer using inkjet printing process for inverted QLED devices.

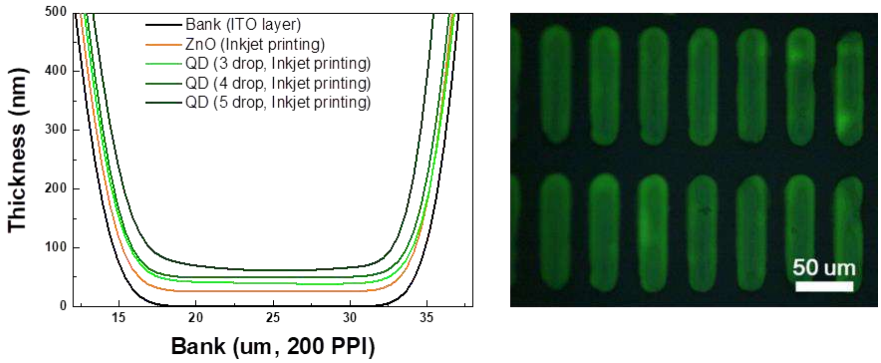

Figure 1. (a) ZnO NPs and QD layer surface profile in pixel (b) PL microscope image of inkjet printed QD in bank structure

Acknowledgment

This research was supported by the MOTIE (Ministry of Trade, Industry & Energy (10077471)) support program for the development of future devices technology for display industry.

References

1. Y. Liu et al, “Efficient All-Solution Processed Quantum Dot Light Emitting Diodes Based on Inkjet Printing Technique”, ACS Applied Materials & Interfaces, 2017, 9, 25506– 25512
2. P.Yang et al,“High-Resolution Inkjet Printing of Quantum Dot Light-Emitting Microdiode Arrays”, Adv. Optical Mater. 8 (2020) 1901429

The steady-state mid-IR intraband transition from Ag2Se colloidal nanocrystal

HaeMin Song[1], Mihyeon Park[1], Dongsun Choi[1], and Kwang Seob Jeong[1]
[1]Dept. of Chemistry, Korea University, Seoul, 02841, Republic of Korea
Tel.:82-02-3290-3792, E-mail: kwangsjeong@korea.ac.kr

Steady-state intraband has been a promising electronic transition in IR applications because it enables smaller energy than the bandgap transition. However, it has been challenging due to the immediate oxidation of the electrons in 1Se state. Here, we present the mid-IR absorption and photoluminescence arising from the steady-state intraband transition in Ag2Se nanocrystals. By spectroelectrochemistry, it was observed that one of the two absorption peaks increases with applying reduction potential while it decreases by oxidation potential, which identified the peak to be the intraband transition. Also, it was shown that Ag2Se CQDs with tunable mid-IR intraband transitions can be used for thin film transistors, which manifested the photoresponse of the transfer characteristics under mid-IR irradiation. The steady-state intraband transition presented here was revealed to have the potential for nontoxic mid-IR application.

Acknowledgment

This work is supported by the Basic Science Research Program and Creative Materials Discovery Program through the National Research Foundation of Korea (NRF) funded by the Ministry of Science, ICT, & Future Planning (NRF-2016R1C1B2013416 and 2019M3D1A1078299), Ministry of Education (NRF-20100020209). The authors gratefully acknowledge use of the facilities of the Korea Basic Science Institute (KBSI).

References

1. M. Park, D. Choi, Y. Choi, H-b. Shin, K. S. Jeong, ACS Photonics, 5, 1907-1911 (2018)

Tailored growth control of InP nanocrystals

Youngsik Kim[1], Eunhye Cho[1], Taewan Kim,[1] and Sohee Jeong[1]*

[1]Department of Energy Science and Center for Artificial Atoms, Sungkyunkwan University (SKKU), Suwon 16419, Republic of Korea

Tel.:82-031-299-4058, E-mail: s.jeong@skku.edu

InP quantum dots (QDs) have been actively explored due to their promising optoelectronic properties.[1] Although dramatic development of InP QD researches such as size uniformity control and high quantum yield, tailored growth control still lags behind.[2] In this research, we demonstrate the tailored growth control of InP nanocrystals that can realize anisotropic shaped InP nanocrystals based on thermodynamic and kinetic control.[3] Interestingly, anisotropic grown InP nanocrystals show unique optoelectronic properties speculating originated from the shape. We believe our nanoparticle growth direction control could be a useful example for other nanocrystal growth control.

Acknowledgment

This research was supported by the Creative Materials Discovery Program through the National Research Foundation (NRF) of Korea funded by the Ministry of Science and ICT (NRF-2019M3D1A1078299, 2019M3D1A1078302)

References

1. Tamang, S., Lincheneau, C., Hermans, Y., Jeong, S. & Reiss, P. Chemistry of InP Nanocrystal Syntheses. *Chem. Mater.* **28**, 2491–2506 (2016).
2. Won, Y.-H. *et al.* Highly efficient and stable InP/ZnSe/ZnS quantum dot light-emitting diodes. *Nature* **575**, 634–638 (2019).
3. Wang, Y., He, J., Liu, C., Chong, W. H. & Chen, H. Thermodynamics versus kinetics in Nanosynthesis. *Angew. Chemie - Int. Ed.* **54**, 2022–2051 (2015).

Heating-up Synthesis of Lead-free Cesium Metal Halide Nanocrystals with Tailored Composition, Morphology, and Optical Properties

Minji Lee[1], Donguk Lee[2], and Taejong Paik[1]
Dept. of Integrative Engineering, Chung-Ang University, Seoul, 06974, Republic of Korea
Tel.:+82-2-820-5435, E-mail: paiktae@cau.ac.kr

This study represents the heating-up synthesis of lead-free metal halide nanocrystals (NCs). CsX and MX3 (M = metal , X = halide) precursors are used to synthesize uniform and phase-pure cesium metal halide NCs, and the reaction is performed via an injection-free, heating-up method in the presence of a solvent mixture with a high boiling point. Nearly monodisperse cesium metal halide NCs are synthesized via heating-up method with high shape purity. The size and composition of cesium metal halide NCs are readily controlled by changing the reaction time, temperature, and amount of surfactant added to the reaction mixture. Furthermore, the absorption and photoluminescence properties of lead-free cesium metal halide NCs are characterized to investigate their composition-dependent optical properties. This work provides the potential to synthesize various types of lead-free cesium metal halide NCs by tailoring the size and compositions.

Tailoring Photoluminescence Properties of Aluminum Hydroxide Nanostructures with Carbazole Derivatives

Ji-Yeon Chae[1], Ho-Young Woo[1], MinHye Kim[1], Donguk Lee[1], Da-Won Lee[1], and Taejong Paik[1]
[1]Dept. of Integrative Engineering, Chung-Ang University, Seoul, 06974, Republic of Korea
Tel.:82-2-820-5435, E-mail: paiktae@cau.ac.kr

Here, we synthesize greenish-blue- and yellow-emitting aluminum oxide nanostructures with tailored absorption and PL properties by adding 1,2,3,4-tetrahydrocarbazol-4-one. The luminescent nanostructures are synthesized *via* a single-step high-temperature thermal-decomposition reaction using aluminum acetate precursors in a 1-octadecene solution. We observed that the addition of 1,2,3,4-tetrahydrocarbazol-4-one to the reaction mixture significantly affects the PL properties of the aluminum hydroxide nanostructure. Characteristic PL peaks are observed at 406 and 483 nm, which are attributed to the emission from O- and C-related defect centers, respectively. When the reaction is conducted with 1,2,3,4-tetrahydrocarbazol-4-one, a red-shift of the emission spectra of aluminum hydroxide is observed, with greenish-blue PL under ultraviolet excitation. Additionally, when the reaction temperature increases, the PL is further red-shifted, resulting in a yellow-emitting aluminum hydroxide nanostructure. Structural characterization is conducted to investigate the optical properties of the aluminum hydroxide nanostructures synthesized under different reaction conditions. Our method allows the PL properties of aluminum hydroxide nanostructures to be tailored.

Efficiency Improvement of Full-Solution-Processed Inverted Quantum Dot Light-Emitting Diodes via Modified Surface Ligands

Yonghyeok Choi[1], Woosuk Lee[1], and Heeyeop Chae[1,2]
[1]School of Chemical Engineering, Sungkyunkwan Univerisity (SKKU),
Suwon, 16419, Republic of Korea
[2]Sungkyunkwan Advanced Institute of Nanotechnology (SAINT), Sungkyunkwan University (SKKU),
Suwon, 16419, Republic of Korea
Tel.:82-31-290-7263, E-mail: hchae@skku.edu

The conventional Quantum Dot(QD) with oleic acid ligand is impacted by hydrophobic HTL solvent such as Toluene, Chlorobenzene and Chloroform.[1,2] Therefore, the surface hydrophilicity of the QD was modified via ligand exchange to prevent damage to the QD layer. The hydrophobic ligand was partially substituted by hydrophilic ligand through one-pot synthesis, without any losing optical properties. Due to this replacement, the contact angle of a water droplet on the hydroxyl QD (OH-QD) films was reduced to 71.7° from 89.5° on the oleic acid QD (OA-QD) films, indicating the conversion to hydrophilic hydroxyl ligands. The QD emitting layer (EML) maintained its integrity with the ligand exchange even after exposure to chlorobenzene, a typical HTL solvent, resulting in the efficiency enhancement of the all-solution-processed inverted QD light-emitting diodes (QLEDs). Inverted QLEDs with OH-QDs performance was compared with that of inverted QLEDs with OA-QDs; As illustrated in Fig. 1, the maximum current efficiency (CE) of the device with the OH-QDs considerably increased to 39.0 cd A^{-1} from 5.3 cd A^{-1}, and simultaneously the peak external quantum efficiency (EQE) increased to 9.3% from 1.2%. This work is expected to provide effective solutions for producing efficient all-solution-processed inverted QLEDs.

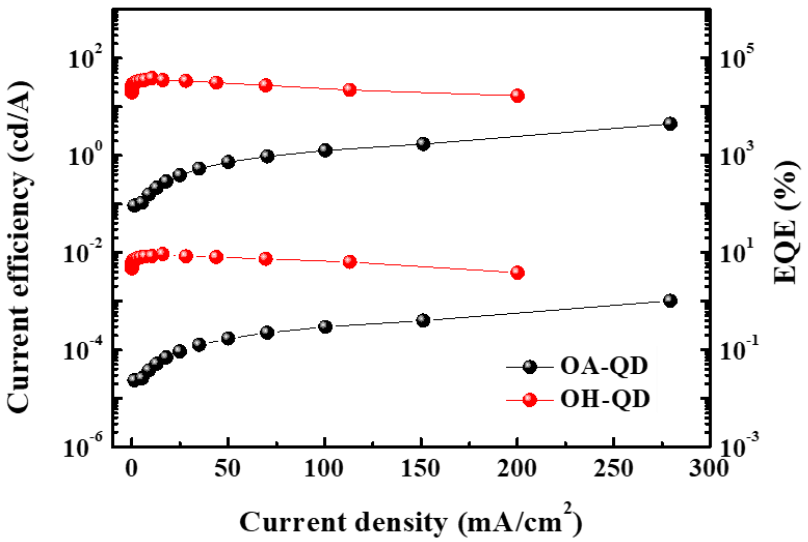

Fig. 1. CE-current density-EQE characteristics of QLED with native OA-QDs and OH-QDs.

References

1. Y. Fu, D. K. Kim, H. S. Moon, H. S. Yang and H. Y. Chae, *J. Mater. Chem. C.*, 5, 522 (2017)
2. K. H. Lee, C. Y. Han, E. P. Jang, J. H. Jo, S. Hong, J. Y. Hwang, E. S. Choi, J. H. Hwang and H. S. Yang, *Nanoscale*, 10, 6300 (2018).

PbSe Quantum Dots/ITZO Hybrid Thin-film Based Devices for Infrared Detection

Ali Sehpar Shikoh[1], Gi Sang Choi[1], Sungmin Hong[2], Jaekyun Kim[1], and Kwang Seob Jeong[2]
[1]Department of Photonics and Nanoelectronics, BK21 FOUR ERICA-ACE Center, Hanyang University, Ansan 15588, Republic of Korea
Tel.: 031-400-5521, E-mail: jaekyunkim@hanyang.ac.kr
[2]Department of Chemistry and Center for Molecular Spectroscopy and Dynamics, Korea University, Seoul 02841, Republic of South Korea

Colloidal quantum dots (CQDs) have attached a great deal of attention owing to the numerous advantages offered by them i.e., solution-based synthesis, low-temperature fabrication, and size-dependent tunable bandgap transition. Thus, they have found applications in various fields like optoelectronics, photovoltaics, and bioimaging. The recent emergence of self-doped QDs that are already filled with one or two electrons per state in the conduction band has broadened the QD scope further as they offer increased surface charge sensitivity. The current work deals with the incorporation of self-doped PbSe QDs into ITZO based thin-film transistors (TFTs) for infrared (IR) detection. Initially, the PbSe QDs having an absorption peak occurring in the IR range were synthesized using a solution-based process [1]. In the second phase, ITZO based TFT devices having a "bottom gate, top contact" configuration were fabricated with subsequent deposition of multiple PbSe QD layers via spin-coating process. Capping ligands like Tetra-n-butylammonium iodide (TBAI) and 3-Mercaptopropionic acid (3-MPA) were tried to replace long amphiphilic OA ligands. In the end, the fabricated samples were characterized for their morphology and I-V characteristics using various sets of equipment including Probe Station, Scanning Electron Microscope (SEM), Atomic Force Microscope (AFM), Fourier-transform infrared spectroscopy (FTIR), etc.

Based on the morphological analysis, the deposited PbSe QDs were found to have a uniform coverage with the thickness of a single QD layer ranging from 10 nm to 25 nm, Figure 1 (a). When establishing a comparison between TBAI and 3-MPA ligand capped PbSe devices in terms of I-V characteristics, TBAI ligand exchange process based TFT showed enhanced source-drain current (I_{ds}) and superior time series related parameters, i.e. response time, reset time, responsivity, etc., Figure 1(b) and (c). This opens doors for the implementation of complex TFT configurations needed to fully exploit quantum confined states and make use of possible inter as well as intraband transitions for low-cost IR detection applications.

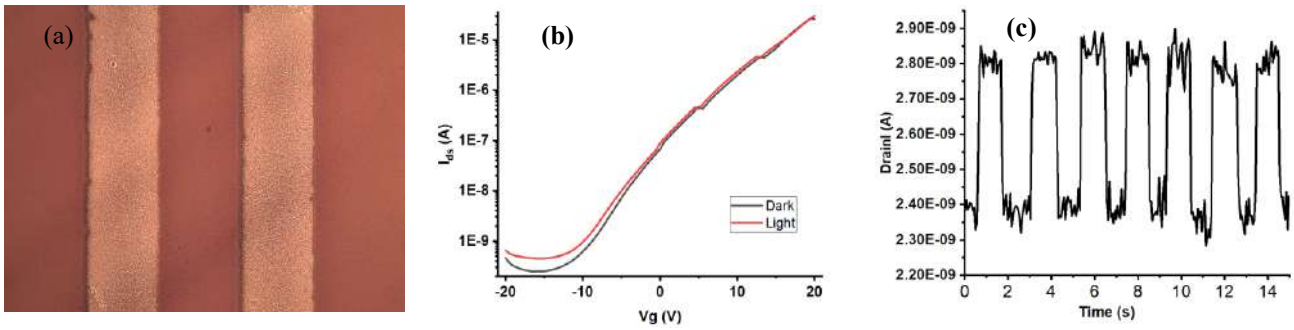

Figure 1: (a) Optical microscope image of 2-layered PbSe TFT, (b) transfer curves for TBAI capped PbSe in dark and light (IR) conditions, (c) Time series for TBAI capped PbSe TFTs.

Acknowledgment

This work was supported by the research fund of Hanyang University.

References

1. J. Kim, D. Choi, K.S. Jeong, ChemComm., 54(61), pp.8435-8445 (2018).

Stability and Dispersion Improvement of Acrylate-Terminated Indium Phosphide Quantum Dots/Siloxane Composite via Ligand Exchange

Eunhwa Jeon[1], Yonghyeok Choi[1], and Heeyeop Chae[1,2]
[1]School of Chemical Engineering, Sungkyunkwan University(SKKU), Suwon 16419, Korea
[2]Sungkyunkwan Advanced Institute of Nanotechnology (SAINT), Sungkyunkwan University(SKKU), Suwon 16419, Korea
E-mail: hchae@skku.edu

Colloidal quantum dots (QDs) have unique optical property that make them promising light emitting materials due to their excellent efficiency and narrow emission bandwidth, and solution processability.[1] In particular, a lot of research studies have been done as non-toxic Cd-free QDs.[2] The representative example is indium phosphide (InP) QDs. The application of QDs in photoluminescence is often limited due to incompatibility between QDs and polymer.[3,4] Normally conventional QDs capped with oleic acid are insoluble in eco-friendly solvents such as propylene glycol methyl ether acetate (PGMEA), which are commonly used in industry. We functionalized ligands into acrylate group to disperse QDs in eco-friendly solvents. The conventional ligands were partially substituted by acrylate ligand through the ligand exchange process. The molecular structure during the ligand modification process was confirmed by FT-IR and ^{1}H-NMR. The QDs with acrylate ligand were then reacted with polymer to form QDs/siloxane composite by UV curing. The QDs/siloxane composite showed improved stability against moisture at 85℃ and 85% relative humidity (RH) by 22% compared to the conventional QDs/poly(methylmethacrylate) (PMMA) blended films. This work is expected to provide effective solutions for producing efficient all-solution-processed QDs/siloxane composite.

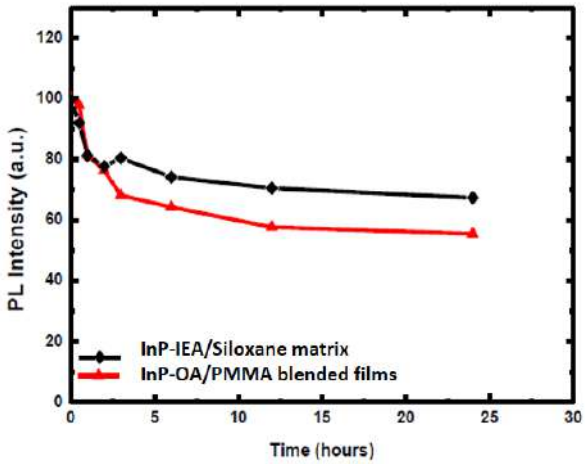

Fig. 1. The time-dependent relative PL intensity of InP-IEA/Siloxane matrix and InP-OA/PMMA blended films under 85℃/85% RH conditions.

References

1. L. Wang, J. Lin, Y. Hu, X. Guo, Y. Lv, Z. Tang, J. Zhao, Y. Fan, N. Zhang, Y. Wang, and X. Liu, *ACS Appl. Mater. Interfaces*, **9**, 38755 (2017).
2. D. Hahm, D. Ko, B. Jeong, S. Jeong, J. Lim, W. Bae, *J. Inf, Disp.*, **20**, 61 (2019).
3. S. Lee, *Polymer*, **182**, 121839 (2019).
4. C. Lee, E. Nam, W. Lee, and H. Chae, *Polymers*, **11**, 905 (2019).

Polarized Emission of Uniaxially Oriented Semiconductor Nanorods in Light-Emitting Applications

*Do Joong Shin and Doh C. Lee**
Department of Chemical and Biomolecular Engineering, KAIST Institute for the Nanocentury, Korea Advanced Institute of Science and Technology (KAIST), Daejeon 34141, Republic of Korea
Tel.:82-42-350-3937, E-mail: dclee@kaist.edu

The transmittance through the display polarizer used for outdoor visibility is the limit of the highly luminescent device. The unidirectional orientation of nanorod not only improves the optical extraction efficiency of the device immediately, but also reduces light loss through linear polarizers [1]. Despite the tremendous existing efforts [2, 3] on assembled structures of nanorods (NRs), approaches based on solvent evaporation with external forces often causes unwilling thick NR stacks, hindering thin-film applications. Here, we report the photo- and electroluminescent polarization of CdSe/CdS core/shell semiconductor nanorod emissive films by flow-induced orientation (Fig. 1). In particular, a conductive polymer with massive molecular weight such as poly(9-vinylcarbazole) (PVK) suppresses the out-of-plane orientation of NRs and provides conductivity to suppress leakage currents in the emitting layers of electroluminescent devices. The orientation of blend film with NRs and PVK molecules directly observed with SEM and contrast ratio defined as $I_{\parallel}/I_{\perp}$. EL polarization leads to 70% transmittance of linear polarizers, which in turn contributes to overcoming the inherent optical extraction of EL devices. This study on flow-induced alignment of anisotropic nanocrystals provides quantitative understandings in the solution processible film formation, which expands to prerequisites that can be directly used for next-generation film forming techniques

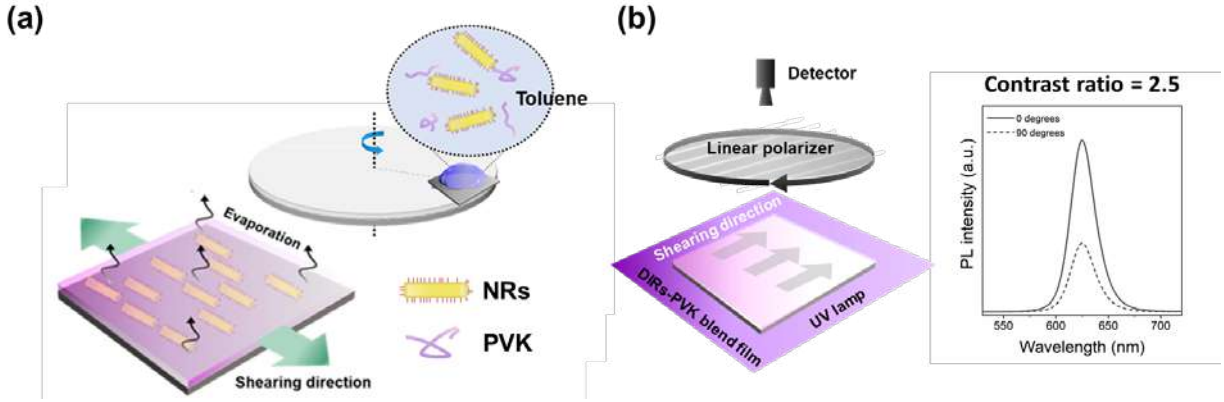

Fig. 1. (a) The schematic images of off-centered spin coating with nanorods and PVK blend ink, (b) The measurements of contrast ratio of NRs and PVK blend film

References

1. W. D. Kim, *Chem. Mater.*, 31(9), 3066-3082 (2019)
2. P. D. Cunningham, *ACS Nano* 10(6), 5769–5781 (2016)
3. B. T. Diroll, *Chem. Mater.* 27(8), 2998–3008 (2015)

Electrohydrodynamic jet Printed Quantum Dot Micro/nanopatterns for Applications of Light-Emitting Diodes

Min Kyu Jung[1], Simon Kim[2], Young Taek Oh[1], Seung Hee Kim[2], Se Gi Lee[2], Han Sang Sung[2], Jeong Heun Ko[2], Jung Woo Lee [2], Ho Jun Jin[2], and Bong Hoon Kim[1,2]

[1] Dept. of Smart Wearable Engineering, SoongSil University, Seoul 06978, South Korea.

[2] Dept. of Organic Materials and Fiber Engineering, Soongsil University, Seoul 06978, South Korea.

Tel.: 82-2-820-0620, E-mail: bonghoonkim@ssu.ac.kr

Quantum dot light-emitting diodes (QD LEDs) are of interest due to their wide-range color tunability, high brightness, and narrow emission bandwidth. Challenges remain, however, in achieving optimized control of light emission and in forming the necessary multilayer device structures. Electrohydrodynamic jet (e-jet) printing is a printing technology where the printed liquid is driven by an electric field. When it exceeds a critical limit, the stress from the surface charge repulsion at the cone apex exceeds the surface tension and a droplet of fluid is emitted towards the grounded substrate.

Here we demonstrate materials and operating conditions that allow for high-resolution printing of layers of quantum dots (QDs) with precise control over thickness and submicron lateral resolution and capabilities for use as active layers of QD light-emitting diodes (LEDs). The shapes and thicknesses of the QD patterns exhibit systematic dependence on the dimensions of the printing nozzle and the ink composition in ways that allow nearly arbitrary, systematic control when exploited in a fully automated printing tool. Fig. 1 demonstrates the ability of e-jet printing to form diverse patterns of multiple types of QDs with good registration. Here, solutions of QDs in organic solvents (dichlorobenzene) serve as the inks.

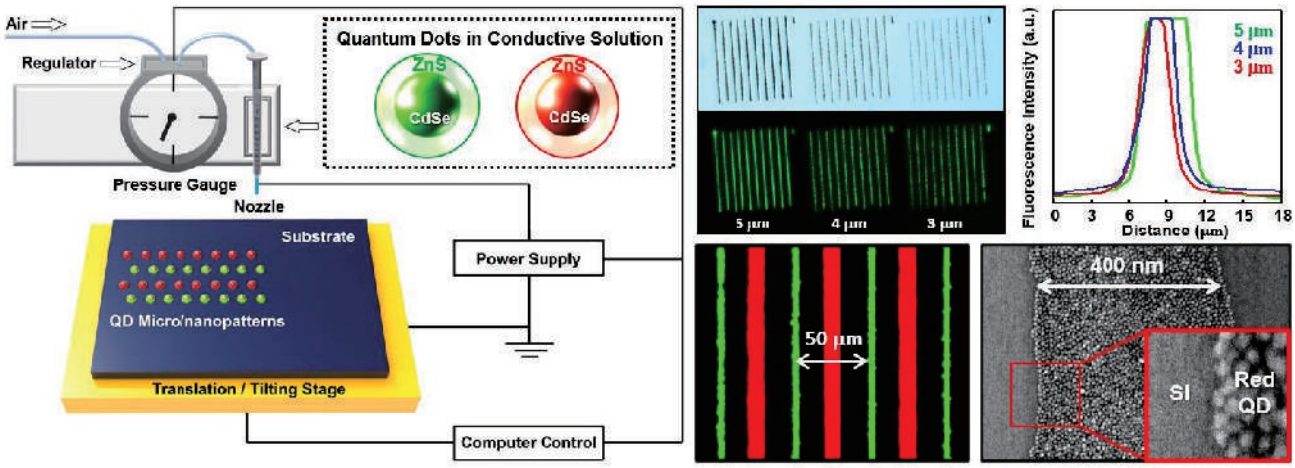

Fig. 1. The schematic illustration of electrohydrodynamic jet (e-jet) printer and e-jet printed heterogeneous QDs array for quantum dot light-emitting diodes (QD LEDs).

Acknowledgment

This research was supported by (1) the National Research Foundation of Korea (NRF) grant funded by the Korea government (MSIT) (No.2020R1C1C1014980) and (2) Korea Institute for Advancement of Technology (KIAT) grant funded by the Korea Government (MOTIE) (P0012770).

References

1. J. U. Park and J. A. Rogers, *nature materials*, vol. 6, p. 782 (2007).
2. J. U. Park, *Nano Lett*, vol. 10, p. 584 (2010).
3. B. H. Kim, *Nano Lett*, vol. 15, p. 969 (2015).

The effect of Mg-doped ZnO on the InP quantum dot light-emitting diodes

Dongbeom Heo[1], Junhyuk Chang[2], Jeonghun Kwak[3], Wanki Bae[2], Hyunho Lee[1*]
[1] Department of Electronic Engineering, Kwangwoon University, Seoul 01897, Korea
Tel.:82-2-940-8126, E-mail: hyunho@kw.ac.kr
[2] Department of Nano Engineering, Sungkyunkwan University, Gyeonggi-do 03063, Korea
[3] Department of Electrical and Computer Engineering, ISRC, Seoul National University, Seoul, 08826, Korea

InP based quantum dots (QDs) have been widely studied for the light-emitting diodes (LEDs) because of their non-toxic nature and decent optoelectric effects. The reported external quantum efficiency (EQE) of InP based QLEDs has reached over 20% which seems to be ready for the commercialization. However, QLEDs suffers severe degradation under constant current bias. The efficient charge injection to the QD layer or transportation through the entire device governs the device performance, as well as the operational lifetime. Here, we investigated the effect of the Mg-doped ZnO to control the electron injection properties to the QD layer. The doping ratio of Mg to ZnO nanoparticles were precisely controlled. The following device performance and operational lifetime were measured and analyzed. The single carrier devices would be presented to verify the effect of changing electron transport characteristics. The steady-state and time-resolved photoluminescence (PL) of doped ZnO films will be given to investigate excitonic behavior in the QD and QD/doped ZnO interfaces.

Acknowledgement
This work was supported by the Basic Science Research Program (NRF-2020R1F1A1074263) through the National Research Foundation of the Ministry of Education, Republic of Korea. This research (for Hyunho Lee) was partially supported by Basic Science Research Program through the National Research Foundation of Korea (NRF) funded by the Ministry of Education (No. 2018R1A6A1A03025242). This research was funded and conducted under 「the Competency Development Program for Industry Specialists」 of the Korean Ministry of Trade, Industry and Energy (MOTIE), operated by Korea Institute for Advancement of Technology (KIAT). (No. P0002397, HRD program for Industrial Convergence of Wearable Smart Devices)

Efficient Interlayer for High Efficiency Inverted Green Indium Phosphide-Quantum Dot Light-Emitting Diodes

Su Jeong Kim, Chae Yeon Jeon, and Raju Lampande, Jang Hyuk Kwon**
Department of Information Display, Kyung Hee University, Dongdaemoon-gu, Seoul, Republic of Korea
Tel.:82-2-961-9147, E-mail: jhkwon@khu.ac.kr

Quantum Dot (QD) is being spotlighted as a material for the development of next-generation displays. QD has the advantages of narrow full width at a half maximum (FWHM), good color purity, and high photoluminescence quantum yield (PLQY). Although Cd-based QDs have been commonly studied, these QDs have limited practical applications because of the toxic nature of Cd. Therefore, as an alternative, indium phosphide (InP)-based QDs are actively studied. However, InP-QLEDs show relatively low device performance, hence more research is still needed. In general, inverted QLED structure has the advantage of easy fabrication process, good efficiency, and high stability, so it has been widely used in QLED research. ZnO is commonly used as an electron transport layer (ETL) in QLED due to its fast electron mobility. Also, inverted QLED used small molecule hole transport materials, which has low hole mobility compared to the inorganic ZnO, causing charge unbalance in the device. To solve this problem, recently, ZnMgO was used as efficient ETL in the QLED, which shows high efficiency by improving the charge balance.[1] However, ZnMgO is very unstable ETL material.

In this study, we introduced an efficient interlayer between the ZnO ETL and green InP-QDs to improve charge balance and performance of the device. We fabricated an inverted green InP-QLED with the following structure. QLED: ITO/ZnO/KHU-ETL/InP-GQD/DBTA/PCBBiF/HATCN/Al. Our optimized inverted green InP-QLED exhibited a maximum current efficiency of 48.4 cd/A and maximum external quantum efficiency (EQE) of 13.6% (Fig. 1a). However, reference device with ZnMgO ETL exhibited lower current efficiency and EQE. To check the reason behind improvements of device performance, the exciton quenching at the interface of ETL and green InP-QDs were measured by transient photoluminescence (PL) measurement. As shown in Fig. 1b, the ZnMgO sample showed exciton decay lifetime of 24.3ns. However, sample with KHU-ETL showed longer lifetime of 39.8ns due to reduction of interfacial exciton quenching. These results show that the introduction of interlayer is an effective way to develop high-efficiency QLEDs.

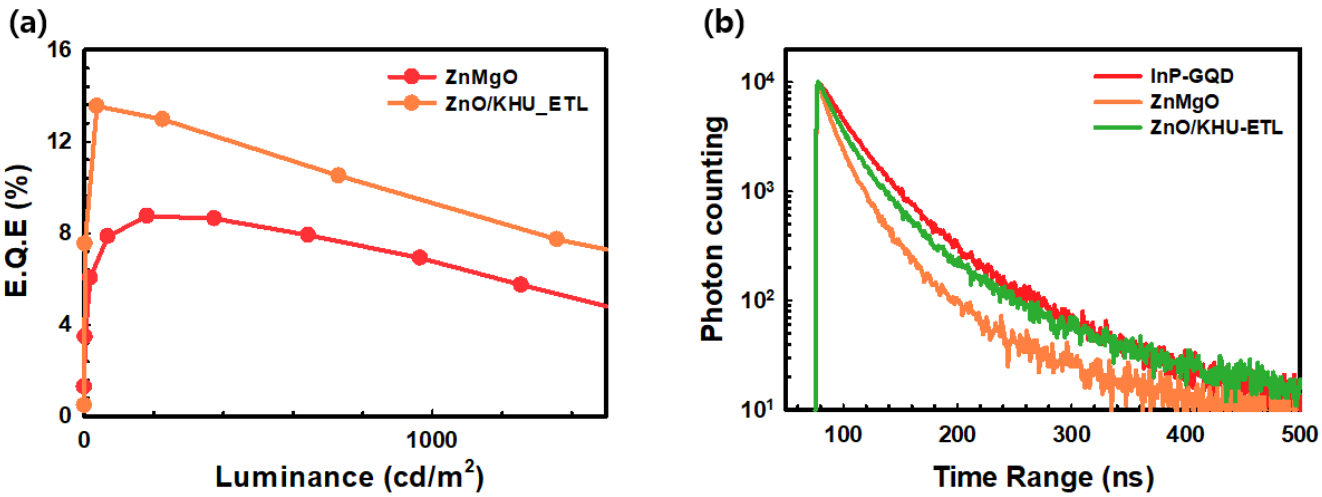

Fig. 1. (a) External quantum yield (EQE) versus Luminance characteristics of QLED introducing interlayer (b) transient photoluminescence (PL) of InP-GQD (red line), ZnMgO (orange line), and the ETL introducing interlayer (green line).

Acknowledgment

This work was supported by the Technology Innovation Program (20010737) funded by the Ministry of Trade, Industry and Energy (MOTTE, Korea).

References

1. J. E. Yeom, D. H. Shin, R. Lampande, Y. H. Jung, N. N. Mude, J. H. Park, J. H. Kwon, Good Charge Balanced Inverted Red InP/ZnSe/ZnS-Quantum Dot Light-Emitting Diode with New High Mobility and Deep HOMO Level Hole Transport Layer, ACS Energy Lett. 2020, 5, 3868-3875

High-resolution Inkjet Printed Quantum Dot films by Optimizing Ink Formulation

Seongkwon Hwang[1,2], Inho Jeong[1,3], Donghyo Hahm[4], Wan Ki Bae[4], Seungjun Chung[1]
[1]Soft Hybird Materials Research Center, Korea Institute of Science and Technology, Seoul 02792, Republic Korea
[2] Dept. of Electrical and Computer Engineering, Seoul National University, Seoul 08826, Republic of Korea
[3]School of Electrical Engineering, Korea University, Seoul 02841, Republic of Korea
[4]SKKU Advanced Institute of Nanotechnology (SAINT), Sungkyunkwan University, Suwon-si, Gyeonggi-do 16419, Republic of Korea
Tel.:82-2-958-5305, E-mail: seungjun@kist.re.kr

Quantum dot light-emitting-diodes (QLEDs) have regarded as a promising candidate for realizing next-generation applications in low-cost large-area full-color pixelated displays due to their great color purity and compatibility with the inkjet printing process[1]. One of the key requirements of high-performance inkjet-printed QLEDs is the formation of high-resolution uniform quantum dot (QD) films by creating a well-defined ink droplet and optimizing the morphology of the QD layers. Therefore, in-depth studies from the ink formulation to inkjetting conditions are highly desirable with considering the fluid characteristics of QD inks[2].

In this presentation, we report the optimization of the fluid characteristics (*e.g.* viscosity, surface tension, density, and inertia force) of the prepared QD inks to deposit high-quality QD films. The three independent non-dimensional parameters, Weber number (*We*), Reynolds number (*Re*), and Capillary number (*Ca*), which are critical to determine inkjettability are carefully optimized and systematically designed the solvent system that their inverse Ohnesorge number ($Z = Oh^{-1} = R_e/\sqrt{W_e} = \sqrt{\sigma\rho d}/\eta$) ranging from 1 to 10 resulting in a well-defined ink droplet having a volume of ~2 pL in flight.

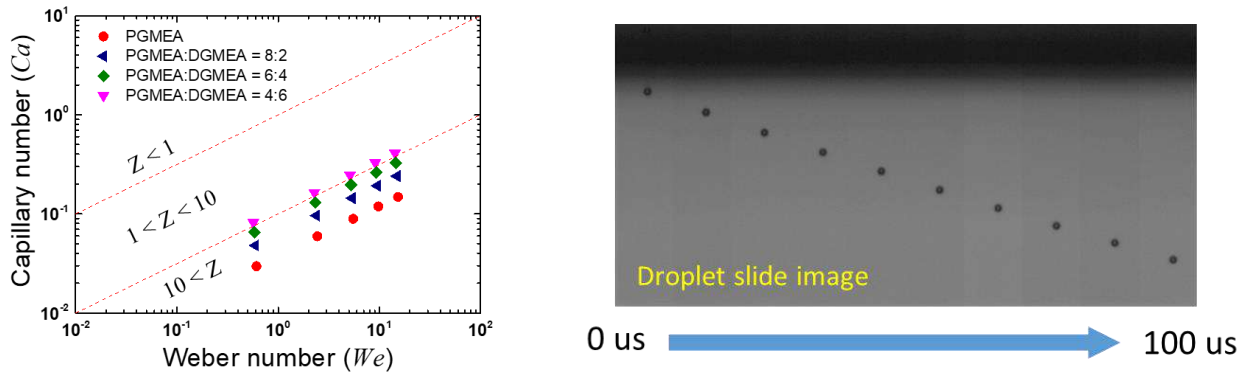

Fig. 1. Inverse Ohnesorge number values of QD inks with different ratio of PGMEA and DGMEA and sequentially captured images of an ink droplet having a volume of ~ 2 pL.

Acknowledgment

The authors appreciate the support from the National Research Foundation of Korea (NRF) grant funded by the Korea government (the Ministry of Science and ICT) (No.NRF- 2020R1A2C4001948) and and the Korea Institute of Science and Technology (KIST) Young Fellow Program (Grant No. 2E31163).

References

1.W. K. Bae, J. Lim, D. Lee, M. Park, H. Lee, J. Kwak, K. Char, C. Lee, S. Lee, *Adv. Mater.,* 26, 6387 (2014).
2. D. Hahm, J. Park, I. Jeong, S. Rhee, T. Lee, C. Lee, S. Chung, W. K. Bae, and S. Lee, *ACS Appl. Mater. interfaces*, 12, 10563 (2020).

Room Temperature Amplified Spontaneous Emission in colloidal Quantum dots under nanosecond pumping

Suhyeon Kim[1], Hyekyeong Kwon[1], and Jiwon Bang[1]
[1] Department of Chemistry, Wonkwang Institute of Materials Science and Technology, Wonkwang University, 460 Iksandae-ro, Iksan, Jeonbuk 54538, Republic of Korea

Quantum confinement semiconductors attract new gain media for laser. In particular, colloidal quantum dots (QDs) have received considerable attention for versatile gain material due to their solution processability and size-tunable optical transitions.[1, 2] The requirement for light amplification of QDs is population inversion, and therefore, biexciton is required in band edge state of the QDs. However, the presence of strong Coulomb interactions in the three-dimensional quantum confinement colloidal QDs using as gain media has been impeded by greatly increase the rate of multi-exciton Auger decay. To enable practical implementation of colloidal QD lasers, operation with nanosecond or longer pulse duration is necessary, but laser demonstrations of QDs have been mostly used ultrafast (sub-ps) optical pulse excitation to preserve population inversion state.
Herein, we demonstrated amplified spontaneous emission (ASE), a prerequisite for the lasing action, of the colloidal CdSe/CdS/ZnS (core/shell/shell) QDs under nanosecond optical pumping. When the QDs in close-packed structure is optically pumped by a frequency tripled Nd:YAG laser emitting 4 ns pulses with a 355 nm at a 10 Hz repetition rate, emission from the QD film edge is abrupt increase with increasing pump power in output intensity and narrowing the band-width on the higher-energy side of the photoluminescence band. This result represents a clear transition from photoluminescence to ASE. The blue shifting ASE peak of the QDs indicated that repulsive charge carriers interaction in biexcton state QDs, which implies that our CdSe/CdS/ZnS QDs represent the quasi-type II band structures.[3, 4] The spatially separated carrier distribution in quasi-type-II CdSe/CdS/ZnS QDs expected to reduce the unwanted Auger process, and promote the radiative recombination of biexciton.

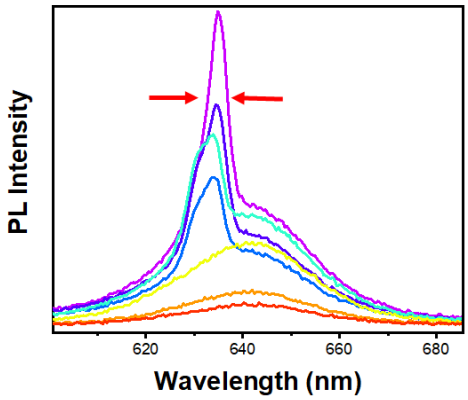

Fig. 1. PL spectra of QD film under Nd:YAG pulsed excitation (355nm, 4ns) at various pump intensities

References

1. J. M. Pietryga, Y.-S. Park, J. Lim, A. F. Fidler, W. K. Bae, S. Brovelli and V. I. Klimov, *Chem. Rev.*, 2016, **116**, 10513-10622.
2. V. I. Klimov, A. A. Mikhailovsky, S. Xu, A. Malko, J. A. Hollingsworth, C. A. Leatherdale, H.-J. Eisler and M. G. Bawendi, *Science*, 2000, **290**, 314-317.
3. P. Klenovský, P. Steindl and D. Geffroy, *Scientific Reports*, 2017, **7**, 45568.
4. V. I. Klimov, S. A. Ivanov, J. Nanda, M. Achermann, I. Bezel, J. A. McGuire and A. Piryatinski, *Nature*, 2007, **447**, 441-446.

Ligand Exchange Strategies toward Bright and Stable Ag_2S Nanocrystals with Ag-rich, S-rich and Stoichiometric Surface Stoichiometry

Yunmo Sung[1], Wonseok Lee[1], Eunjae Lee[1], Young Ho Ko[3], and Sungjee Kim[1,2]*

[1]Department of Chemistry and [2]School of Interdisciplinary Bioscience and Bioengineering, Pohang University of Science and Technology (POSTECH), 77 Cheongam-ro, Nam-gu, Pohang 37673, Korea

[3]Center for Self-assembly and Complexity, Institute for Basic Science, Pohang 37673, Korea

Tel.:82-54-279-1495, E-mail: sungym@postech.ac.kr

Ag_2S NCs have the heavy metal free composition and a narrow band gap which make them advantageous for applications in biomedical imaging and near-infrared devices. However, low chemical stability originating from the low lattice energy and unexplored characterizations on the surface chemistry limit their practical applications. Here, we report a simple method for the synthesis of Ag_2S NCs with Ag-rich surface (Ag-Ag_2S) and Ag_2S NCs with S-rich surface (S-Ag_2S) by controlling the mixing ratio of $AgNO_3^-$ and S powder with octylamine. Then, we investigated their ligand exchange reactions by ion-pair ligands: cetyltrimethylammonium bromide (CTAB) and cetyltrimethylammonium sulfide (CTA_2S). Following the designed protocol, we synthesized Ag-Ag_2S NCs, S-Ag_2S NCs and stoichiometric surface Ag_2S NCs with cetyltrimethylammonium ligands on their surface. Through the systematic characterizations of surface stoichiometry and ligand coverages of Ag_2S NCs, We verified that cetyltrimethylammonium ligands very statically bind to Ag_2S NC surface. Moreover, the PL intensity of the stoichiometric Ag_2S NCs increased to more than 10 times after the ligand treatment and reached PL QY of ~10%.

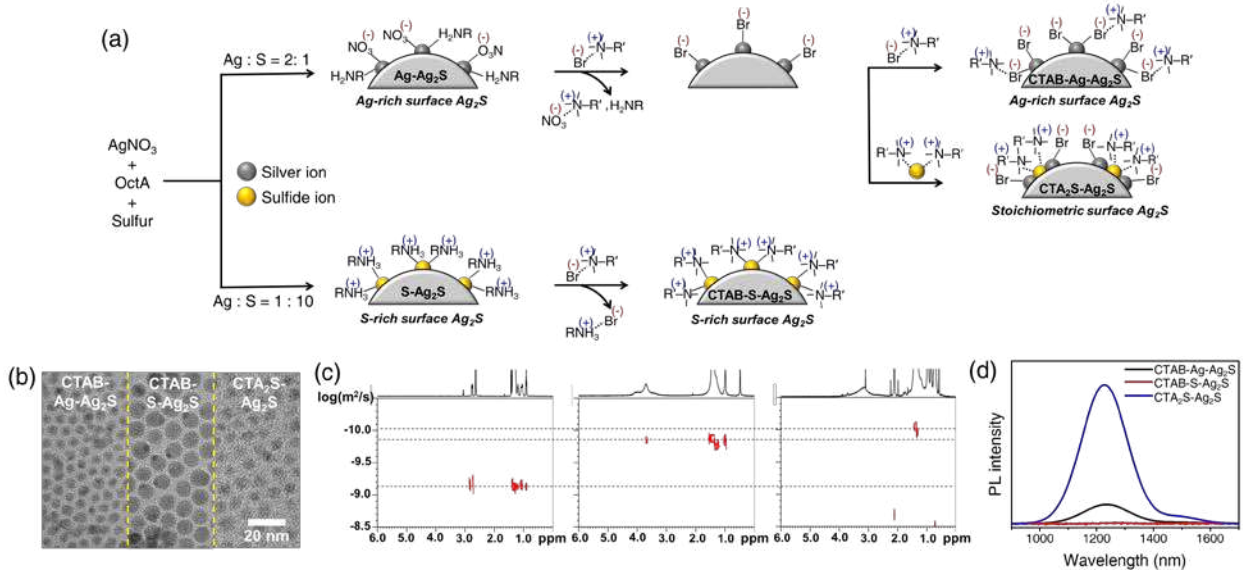

Fig. 1. (a) Schematic of surface reactions in ligand exchanges of Ag-Ag_2S (top row) and S-Ag_2S (bottom row) by CTAB and CTA_2S. (b) TEM images of Ag-rich, S-rich, and stoichiometric Ag_2S NCs with CTA^+. (c) diffusion-ordered NMR spectroscopy (DOSY) spectra of free CTAB, Ag-rich and S-rich Ag_2S with CTA^+. (d) PL spectra of Ag-rich, S-rich, and stoichiometric Ag_2S NCs with CTA^+.

Acknowledgment

This research was supported by Creative Materials Discovery Program through the National Research Foundation of Korea(NRF) funded by Ministry of Science and ICT(NRF-2019M3D1A1078302).

References

1. H. Doh, S. Hwang, S. Kim, *Chem. Mater.*, 28, 8123 (2016).
2. Y. Du, B. Xu, T. Fu, M. Cai, F. Li, Y, Zhang, Q. Wang, *J. Am. Chem. Soc.*, 132, 1470 (2010).
3. J. W. Thomson, K. Nagashima, P. M. Macdonald, G. A. Ozin, *J. Am. Chem. Soc.*, 133, 5036 (2011).

Colloidal Synthesis of Shape-Controlled Cs_2NaBiX_6 (X = Cl, Br) Double Perovskite Nanocrystals

Doowon Choi[1], Wonseok Lee[2], and Sungjee Kim,[1,2]
[1]School of Interdisciplinary Bioscience and Bioengineering, Pohang University of Science and Technology (POSTECH), Pohang 37673, South Korea
[2]Dept. of Chemistry, Pohang University of Science and Technology (POSTECH), Pohang 37673, South Korea
Tel.:82-54-279-1495, E-mail: doowon@postech.ac.kr

As an alternative to lead halide perovskites, various types of lead-free perovskites have been recently studied for optoelectronic materials. This research reports the synthesis of highly phase-pure Cs_2NaBiX_6 (X = Cl, Br) double perovskite (DP) nanocrystals (NCs). They show characteristic absorption features of sharp and discrete peaks mostly originating from the Bi^{3+} s−p transition ($6s^2 \rightarrow 6s^1p^1$) in $[BiX_6]^{3-}$ units within the crystal lattice of the elpasolite structure. Such discrete optical transition characteristics have not been observed for Ag/M^{3+} DP or for $Cs_3Bi_2X_9$ materials. This unique optical properties are attributed to the non-bonding character of electropositive sodium and electronically isolated $[BiX_6]^{3-}$ units in crystals. The shape of Cs_2NaBiX_6 NCs could be quantitatively controlled by adjusting the reaction temperature. Reaction temperatures above 180 °C favor development of a cuboctahedral (CO) shape, whereas development of a cuboidal (CB) shape is favored below 170 °C. CB NCs can be subsequently converted to CO NCs by heating to 200 °C. The CO NCs promote the growth of heterostructure adducts on the (111) facets; these adducts could be post-eliminated by etching. Mn-doped $Cs_2NaBiCl_6$ NCs are synthesized; they show efficient energy transfer from the NC host to the dopants because of the spatial confinement of excitons. The synthesis and shape control of Cs_2NaBiX_6 NCs and Mn-doped $Cs_2NaBiCl_6$ NCs may expand a new class of lead-free DP NCs applicable to optoelectronic applications.

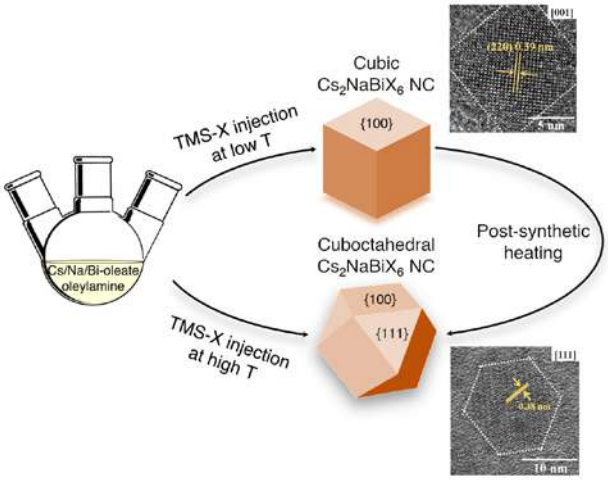

Fig. 1. Synthesis protocol of Cs_2NaBiX_6 nanocrystals and high resolution TEM images

Acknowledgment

This research was supported by Creative Materials Discovery Program through the National Research Foundation of Korea(NRF) funded by Ministry of Science and ICT(NRF-2019M3D1A1078302).

References

1. Protesescu, L., Yakunin, S., Bodnarchuk, M. I., Krieg, F., Caputo, R., Hendon, C. H., Yang, R. X., Walsh, A. and Kovalenko, M. V., *Nano Lett*, 15, 3692−3696 (2015).
2. Shi, H. and Du, M.-H., *Appl. Phys. Rev.*, 3, 054005 (2015).
3. Creutz, S. E., Crites, E. N., De Siena, M. C. and Gamelin, D. R., *Nano Lett*, 18, 1118−1123 (2018).
4. Lee, W., Hong, S. and Kim, S., *J. Phys. Chem. C*, 123, 2665−2672 (2019).
5. Majher, J. D., Gray, M. B., Strom, T. A. and Woodward, P. M., *Chem. Mater.*, 31, 1738−1744 (2019).

Achieving high efficiency by improving mobility of oxide nanoparticles in quantum dot light-emitting devices

Da-Young Park[1], Ji-Ho Kang[1], Hee-Jin Park[1], Hyun-A Hwang[1] and Dae-Gyu Moon[1]
[1]Dept. of Materials Engineering, Soonchunhyang University, Asan, Chungnam 31538, Korea
Tel.:82-41-530-1312, E-mail: dgmoon@sch.ac.kr

Quantum dot light-emitting diodes (QLEDs) have attracted a surge of interest because of promising properties such as high quantum yield, size-dependent emission wavelength, the narrow emission spectra and wide color gamut [1-3]. In QLEDs, oxide nanoparticles have been widely used as an electron transport layer (ETL) due to their substantial electrical characteristics [4-5]. The annealing temperature of the oxide nanoparticle is important on the electrical features of devices [6]. In this study, magnesium zinc oxide (MgZnO) nanoparticles were annealed to improve the efficiency of the QLEDs.

The QLEDs were constructed using sol-gel synthesized MgZnO nanoparticles with an average particle size of 3 nm as ETL materials. CdSe/ZnS quantum dots and poly-TPD were used emitting layer and hole transport layer, respectively. The MgZnO was coated on devices and thereafter the devices were annealed according to following conditions; 50 ℃ for 20 min, 100 ℃ for 20 min. The annealed devices were compared with device at room temperature. The annealed QLED at 50 ℃ exhibited maximum luminance of 32,670 cd/m^2 and 1.5 times higher current efficiency to the room temperature QLED device. Meanwhile, the annealed QLED at 100 ℃ was obtained maximum luminance of 61,410 cd/m^2 and intermediate value of 22.85 cd/A. Such a outstanding improvement of current efficiency is attributed to advancement of mobility result from MgZnO nanoparticles annealing.

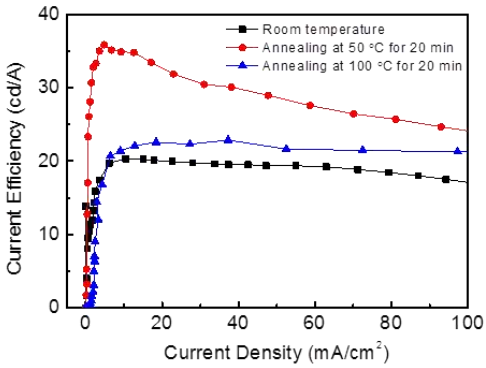

Fig. 1. Current efficiency versus current density characteristics of the annealed QLEDs based on MgZnO nanoparticles.

Acknowledgment

This work was supported by the Industry Technology R&D program (20006511) funded by Ministry of Trade, Industry & Energy (MOTIE, Korea).

References

1. C.B.Murray, D. J. Norris and M. G. Bawendi, *J. Am. Chem. Soc.*, 115 (19), p. 8706 (1993).
2. S. Coe, W. K. Woo and M.G. Bawendi, *Nature*. 420, p. 800 (2002).
3. X. Dai, Z. Zhang and Y. Jin, *Nature*, 515, p. 96 (2014).
4. K. Harun, F. Hussain, A. Purwanto, B. Sahraoui, A. Zawadzka and A. A. Mohamad, *Mater. Res. Express*, 4(12), p. 122001 (2017).
5. J.A. Anta, E. Guillen and R. Tena-Zaera, *J. Phys. Chem. C.*, 116, p. 11413 (2012).
6. H. Hongping, C. Jianglin, F. Xunchang and D. Ning, *Environ. Int.*, 130, p. 104930 (2019).

Ligand-Assisted Sulfide Surface Treating Method of $CsPbI_3$ Perovskite Quantum Dots to Increase Photoluminescence and Recovery

Jeong Woo Han[1], Sa-Rang Bae[1], Soo Young Kim[1]
[1] **Department of Materials Science and Engineering, Korea University, 145 Anam-ro, Seongbuk-gu, Seoul 02841, Korea**
Tel.:+82 010-8284-4977, E-mail: cloudy2014@korea.ac.kr

Recent researches of perovskite-based light emitting diode (PeLED) are increasingly important for quantum dot (QDs) light emitting diodes. Cesium lead halide perovskite ($CsPbX_3$: (X = I^-, Br^-, Cl^-)), one of all-inorganic halide perovskite, is a rising star in PeLED research field. Their great contribution to progressed PeLED research is truly respectful, but there is still a long way to achieve a goal. Low Properties like short lifetime and moisture weakness make $CsPbX_3$ more difficult to apply to PeLED. The strong red emission from fresh $CsPbI_3$ QDs gradually declines to a weak emission from aged QDs at room temperature, so $CsPbI_3$ needs a more advanced method for increasing stability. Herein, we introduce the facile surface treating method of $CsPbI_3$ to enhance phase stability and increase photoluminescence. Sulfur-oleylamine (S-OLA) complex was utilized to etch the defect-rich surface of the $CsPbI_3$ QDs and then self-assembly to form a matrix outside the $CsPbI_3$ QDs protected the QDs from environmental moisture and solar irradiation. As a result, the photoluminescence intensity of $CsPbI_3$ increased by 21% of its initial value and aged $CsPbI_3$ QDs that changed into nonluminous phase was recovered its intensity 95% of that of the fresh QDs. Therefore, this work paves the way for increasing the performance of perovskite-based devices in the near future.

References

1. Feng Liu, Yaohong Zhang, Chao Ding, Syuusuke Kobayashi, Takuya Izuishi, Naoki Nakazawa, Taro Toyoda, Tsuyoshi Ohta, Shuzi Hayase, Takashi Minemoto, Kenji Yoshino, Songyuan Dai and Qing Shen, *ACS Nano*., **11**, 10373-10383 (2017).
2. L. Protesescu, S. Yakunin, M. I. Bodnarchuk, F. Krieg, R. Caputo, C. H. Hendon, R. X. Yang, A. Walsh, M. V. Kovalenko, *Nano Lett.,* 15(6), 3692-3696 (2015).

Surface Halide Treatment of ZnSeTe Blue Emitting Quantum Dots and Their Device Performance of Quantum Dot Light-Emitting Diode

Yoon-Jeong Choi[2], Jeong-Yeol Yoo[2], Jong-Gyu Kim[2], Chil Won Lee[2], Byung Doo Chin[3], and Jang Sub Kim[1]
[1]I-Dasan Link+ Educational Development Institute, Dankook University, Yongin 16890, Korea
Tel.:82-(0)10-8831-1994, E-mail: goodnews316@dankook.ac.kr
[2]Dept. of Chemistry, Dankook University, Cheonan 31116, Korea
[3]Dept. of Polymer Science and Engineering, Dankook University, Yongin 16890, Korea

Colloidal Quantum dots (QDs), due to their unique size dependent optical properties, have been received much attention as an ideal material in the next generation display industries [1]. Herein, we synthesized ZnSeTe based QDs to obtain blue emitting photoluminescence (PL) by alloying ZnTe with a relatively small bandgap (2.25 eV) and ZnSe (2.7eV) with a large bandgap [2] and treated the resulting QD surface with zinc halide (ZnX_2, X=Cl, Br, I) to enhance luminescence efficiency. Using TGA and FT-IR, it was confirmed that halide treatment was successfully performed. PL spectra and TEM images show that the emission wavelength (453 nm), FWHM (27 nm), and the size (5.1 nm) of the QDs were not changed after treatment, but the PL quantum yield (PL QY) was significantly increased from 53 % to 75-80 %. Also, we fabricated quantum dot light emitting diode (QLED) devices using these halide treated blue ZnSeTe QDs (ZnSeTe-X_2) as emitting materials in emissive layer (EML). Resulting devices showed an efficient improvement in device performance. As incated in Fig. 1, the $ZnCl_2$ treated QLED device shows the best performance with an emission peak of 456 nm, a maximum current density of 1,142 mA/cm^2, a luminance of 4,515 cd/m^2 at 7 V, and an external quantum efficiency of 3.26 %.

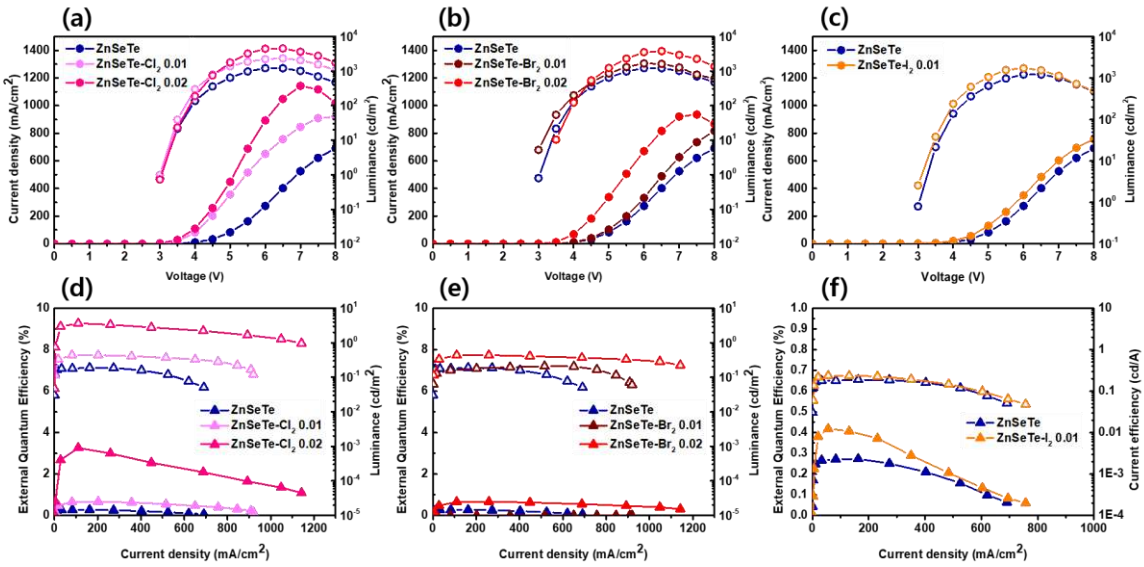

Fig. 1. Electronic performance (a, b, c) current density-voltage-luminance, (d, e, f) external quantum efficiency-current efficiency as a function of current density of ZnSeTe-X_2 (X=Cl, Br, I) in QLED devices.

Acknowledgment

This work was supported by the Soft Chemical Materials Research Center for Organic-Inorganic Multi-Dimensional Structures, funded by Gyeonggi Regional Research Center Program (GRRC Dankook 2016-B01) and funded by the National Research Foundation of Korea (NRF) grant funded by the Korea government (MSIT: Ministry of Science and ICT) (No. 2019R1A2C1005784)

References

1. H. C. Wang, H. Zhang, H. Y. Chen, H. C. Yeh, M. R. Tseng, R.J. Chung, S. Chen, R. S. Liu, *small*, 13, 1603962, (2017).
2. C. -Y. Han, S. -H. Lee, S. -W. Song, S. -K. Yoon, J. -H. Jo, D. -Y. Jo, H. -M. Kim, B. -J. Lee, H. -S. Kim, H. Yang, *ACS Energy Lett*, 5, 1568-1576, (2020).

Improvement of Hole Injection Efficiency in Quantum Dot Light-Emitting Diode via Quantum dot Surface Modification using Dipyridyl group

Jeong-Yeol Yoo[1], Yoon-Jeong Choi[1], Jang Sub Kim[2], Byung Doo Chin[3], Jong-Gyu Kim[1], and Chil Won Lee[1]
[1]Dept. of Chemistry, Dankook University, Cheonan 31116, Korea
Tel.:82-41-550-3430, E-mail: chili@dankook.ac.kr
[2]I-Dasan Link+ Educational Development Institute, Dankook University, Yongin 16890, Korea
[3]Dept. of Polymer Science and Engineering, Dankook University, Yongin 16890, Korea

Colloidal quantum dots (QD) are semiconductor materials with a several nanometers size, exhibiting significantly different unique electronical and optical properties from bulk materials [1]. Recently, considerable efforts have been made for research of Cd-free such as indium phosphide (InP) based QD, because of their relatively low toxicity, emission wavelength covering most visible region wavelengths, high PLQY, and stability [2]. Quantum dot light-emitting diodes (QD-LED) devices have similar structures and materials used for organic light-emitting diode devices, except for the light-emitting layer. In QD-LED devices, hole and electron are injected and transported from the anode and cathode, respectively, to form excitons at the QD emitting layer and emitted via their radiative recombination. However, due to the difference in charge injection and mobility of the QD emitting layer, the imbalance between holes and electrons is unavoidable, and consequently reduces the efficiency of device performance.

In this study, we modified the surface of InP/ZnSeS/ZnS QD (RQD-OLA) to improve the charge injection and transport properties of the light emitting layer. In addition, the modified QD was applied to the QD-LED device to study the device's charge balance characteristics.

In order to increase the charge injection/transport properties, the surface modification was performed by replacing the commonly used ligand, oleylamine, with two types of bipyridyl derivatives (TBPY and NBPY). The performance of QD-LED devices used the surface-modified QD is shown in Figure 1.

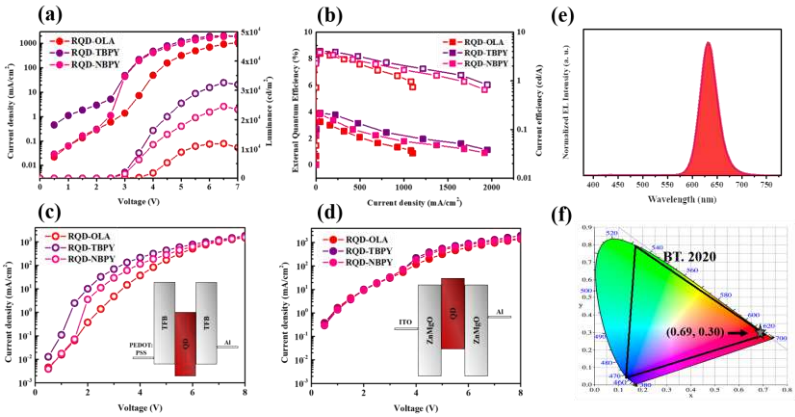

Fig. 1. The device performance of (a) Current density-voltage-luminance, (b) external quantum efficiency and current efficiency as function of the current density of RQD-based QLED, and current density as a function of voltage of (c) hole only device, (d) electron only device, (e) EL spectrum, and (f) CIE color coordinates of the QLED device compared to BT.2020

As a result, in the device using the modified QD, the current density was improved by 2 times and the luminance was improved by 3 times, and this property can be considered to be due to the efficient charge injection property.

Acknowledgment

This work was supported by the Soft Chemical Materials Research Center for Organic-Inorganic Multi-Dimensional Structures, funded by Gyeonggi Regional Research Center Program (GRRC Dankook 2016-B01) and funded by the National Research Foundation of Korea (NRF) grant funded by the Korea government (MSIT: Ministry of Science and ICT) (No. 2019R1A2C1005784)

References

1. J. Lim, W. K. Bae, J. Kwak, S. Lee, C. Lee, K. Char, Opt. Mater. Express, 2, 594-628 (2012).
2. E. Jang, Y. -H. Won, H. Jang, S. -M. Choi, *ACS Energy Lett.*, 5, 1316-1327 (2020).

Strain-Induced Deactivation of Nonradiative Pathway Enabling High Efficient Quantum Dots with Near-Unity Quantum Yield

Byong Jae Kim[1], Hyeonjun Lee[2] and Jaehoon Lim[1]*

[1]Department of Energy Science and Center for Artificial Atoms, Sungkyunkwan University, Suwon 16419, Republic of Korea

Tel.:82-31-299-6273, E-mail: j.lim@skku.edu

[2]Department of Chemical and Biomolecular Engineering, KAIST Institute for the Nanocentury, Korea Advanced Institute of Science and Technology (KAIST), Daejeon 34141

Type-I quantum dots (QDs) with thick shell have been actively studied as active materials in light-emitting diodes due to enhanced photophysical stability and suppressed energy transfer between dots in densely packed QD films. However, misfit dislocation derived from compressive strain of overgrown shell is likely to provide nonradiative decay center and lower quantum yield of QDs. Most synthesis strategies have aimed to mitigate the compressive strain applied to the core, such as introduction of lattice adaptor at interface or alloyed core and shell materials. Contrary to the previous approaches, here, we demonstrate the band gap engineering based on the lattice strain to promote high efficiency QDs. Elaborate tuning of compressive strain allows us to modify energy level of the core to exclude involvement of trap states incorporated during the shell growth, which realizes near-unity photoluminescence (PL) QY QDs. We believe that our study suggests the bright side of lattice strain as one of tools for band gap engineering, not merely harmful side effect in core/shell heterostructures.

Acknowledgment

J. L and Y.-H. C. acknowledge the support from the National Research Foundation of Korea funded by Ministry of Science and ICT (NRF-2019M3D1A1078296 and NRF-2019R1C1C1006481).

Quantum Dot Color Conversion Layers with Mixed Scattering Particles for Improved Color Conversion Efficiency

Hyunji Park[1,2], Donghyo Hahm[3], Byeong Guk Jeong[3], Hyunsu Cho[1], Byoung-Hwa Kwon[1], Nam Sung Cho[1], Wan Ki Bae[3], Jonghee Lee[2] and Sukyung Choi[1]

[1]Reality Display Research Section, Electronics and Telecommunications Research Institute (ETRI), Daejeon 34129, Republic of Korea

Tel.:82-42-860-1010, E-mail: skchoi915@etri.re.kr

[2]Department of Creative Convergence Engineering, Hanbat National University, Daejeon 34158, Republic of Korea

[3]SKKU Advanced Institute of Nanotechnology (SAINT), Sungkyunkwan University, Suwon 16419, Republic of Korea

Colloidal quantum dots (QDs) have received considerable interest as a next-generation display material due to their fascinating optical properties such as a wide absorption range, narrow full width half maximum, and high photoluminescence quantum yield. Through these advantages, QDs can replace commercial color filters for liquid crystal displays, organic light-emitting diodes (OLEDs) and LEDs. Especially combining QD color conversion layers (CCLs) with blue OLED is a promising approach to develop full-color displays. We develop an efficient non-toxic QD CCL and combine it with a blue OLED. We investigate the effect of scattering particle concentration and shape on the performance of QD CCL. The QD CCL with mixed scattering particles shows high color conversion efficiency and low blue leakage. This allowed us to obtain high performance QD CCL by controlling scattering particles even at low concentration of them.

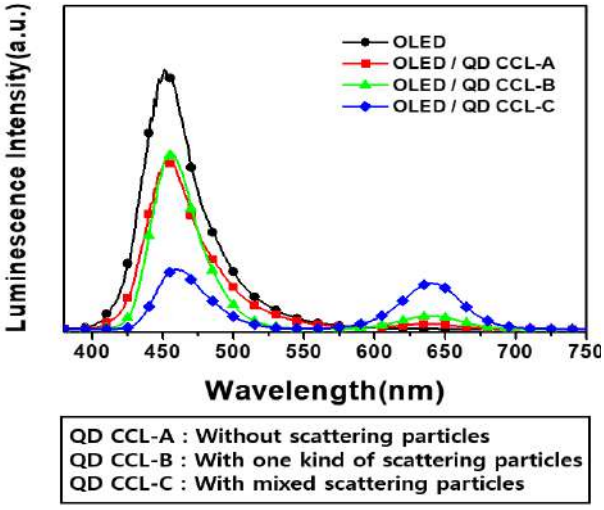

Fig. 1. Luminescence spectra of blue OLED with QD CCL

Acknowledgment

This work was supported by Electronics and Telecommunications Research Institute (ETRI) grant funded by the Korea government (21ZB1200).

References

1. H. Yang, M. Zhou, H. Tang, M. Sun, P. Liu, Y. Liu, L. Chen, D. Li, D. Wu, J. Hao, B. Xu, Z. Zhao, Z. Ren, S. Jia, K. Wang and X. Sun, *RSC Adv.*, *10*(53), 31705-31710 (2020)
2. R. Tangirala, E. Lee, C. Hotz, Y. Kunai, Y. Komatsu, Y. Harada, M. Komada, M. Tokuda, T. Fukuura, *SID Symp. Dig. of Tech. Papers*, 51(1), 1299-1302 (2020)

Improvement of Charge Balance in Quantum Dot Light Emitting Diode with Multi-Component Amorphous Oxide Electron Transport Layer

Hyun Jae Kim[1,2], Jiwon Kim[1], Hyeon-ji Baek[1], Kyoung Won Park[1], Chul Jong Han[1], Kimoon Lee[3], Kyu Hyoung Lee[2], and Min Suk Oh[1,]*

[1]Display Research Center, Korea Electronics Technology Institute (KETI), Seongnam, Gyeonggi-do 13509, Korea

Tel.:82-31-789-7417, E-mail: ohms@keti.re.kr

[2]Department of Materials Science and Engineering, Yonsei University, Seoul 03722, Korea

[3]Department of Physics, Kunsan National University, Gunsan, Jeollabuk-do 54150, Korea

(2 line spacing)

In this study, we report on the method of improving charge balance in order to enhance the electrical properties of quantum dot light emitting diode (QD-LEDs). In general, it is not easy to coat zinc oxide nanoparticles, which have been widely studied as material for the electron transport layers (ETL), on the electrode uniformly when we fabricate QD-LEDs devices. In addition, there might be a problem such as stability issue of dispersion in solvent and ZnO-based oxide semiconductor shows higher electron mobility compared to the hole mobility of hole transport layer (HTL) due to high electron concentration caused by oxygen vacancies. In this case, since the charge balance between electrons from cathode and holes from anode can deteriorate, these problem can cause the decrease of current efficiency and the roll-off phenomenon. Therefore we fabricated charge transport layers by sol-gel process to improve the uniformity of ETL thin film layer. And, in order to improve the charge balance further, gallium (Ga) was added to the ZnO-based semiconductor and ETL was fabricated according to the mole ratio of gallium and zinc. Then the electrical and optical characteristics of the QD-LEDs were analyzed. When Ga was added to ZnO-baed ETL layers, the electron concentration coule be controlled by high binding energy of Ga with oxygen. When ZnO was used as ETL, the maximum values of the luminance and current efficiency of QD-LED were 19,240 cd/m^2 and 7.743 cd/A, respectively. When GaZnO, which was properly mixed with gallium and zinc in a molar ratio of 6 : 4, was used as ETL, the electrical properties of QD-LED were improved and the max luminance and max currrent efficiency were 20,800 cd/m^2, 10.503 cd/A, respectively. These results means that QD-LEDs with improved electrical and optical properties can be realized when multi-component amorphous oxide semiconductors are used as ETL.

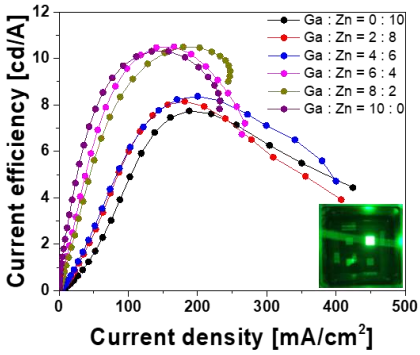

Fig. 1. Current efficiency *vs.* current density of QD-LEDs with various Ga-Zn-O ETLs

Acknowledgment

This work was supported by the Ministry of Trade, Industry and Energy (MOTIE) and Korea Institute for Advancement of Technology (KIAT) through the International Cooperative R&D program (P0011268).

References

1. S. Parthiban and J. -Y. Kwon, J. Mater. Res., 29(15), 1585 (2014)
2 Y. Lee, B. G. Jeong, H. Roh, J. Roh, J. Han, D. C. Lee, W. K. Bae, J. -Yup. Kim and C. Lee, Adv. Quantum Technol. 1(1), 1700006 (2018)
3. M. -C. Jun, S. -U. Park and J. -H. Koh, Nanoscale Res. Lett, 7(1), 1 (2012)

The Fixation of Ligand-Functionalized Quantum Dot to the Siloxane Film via Hydrosylation

Boram Kim[1], Changmin Lee[1], Heeyeop Chae[1,2]*

[1] *School of Chemical Engineering, Sungkyunkwan University (SKKU), Suwon 16419 Korea*

[2] *Sungkyunkwan Advanced Institute of Nanotechnology (SAINT), Sungkyunkwan University (SKKU), Suwon, 16419, Republic of Korea*

**E-mail address:* hchae@skku.edu

Abstract

The Acrylate-terminated Quantum Dots (QDs) were prepared by effective Ligand Exchange to bond with siloxane matrix via Hydrosilylation.

The Acrylate-terminated QDs is fixed to the matrix, the aggregation is controlled and a constant distance between the QDs is maintained, improving the quantum efficiency and stability of the QDs films. In addition, the fixed QDs in the matrix through hydrosilyation became uniform dispersion

Acrylate-terminated QDs go further react with hydride-terminated polydimethylsiloane to form a QD-Siloxane matrix by thermal curing. The improved covalent bonding between the QDs and the Siloxane matrix improve the stability against oxygen and moisture.

Stability at 85℃ relative humidity (RH) were both improved by 22% for the QD-connected siloxane QD film compared with the corresponding values for conventional QD-embedded poly(methylmethacrylate) Films.

We also confirmed excellent photo-stability under Blue light-emitting diode (LED) and the Siloxane film shows 45% higher photo-stability after 26 hour under blue (LED).

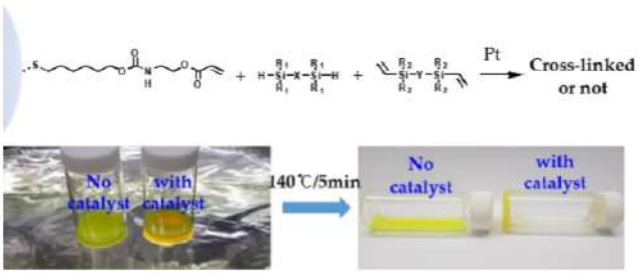

Figure 1. Results of the functionalized QDs were reactive toward the siloxane hydrides.

Keywords: Quantum Dots, Ligand exchange, Suspension polymerization, Color conversion films

References

1. C. Lee, E. Nam, W. Lee and H. Chae, Polymer, 905, 11 (2019)
2. C. Lee, E. Nam and H. Chae, Polymer, 177, 19-24 (2019)
3. E. Nam, C. Lee, S. J. Kim, H. K. Choung and H. Chae, Opt. Express, 27, 14 (2019)

Versatile Colloidal Synthesis of Zn-based Chalcogenide Alloy Nanocrystals from Elemental Chalcogen Precursors

Sooyeon Yeon[1], Seongchan Kim[1], and Nuri Oh[1]
[1]Dept. of Material Science and Engineering, Hanyang University, Seoul 04763, Korea
Tel.:82-2-2220-0403, E-mail: irunho@hanyang.ac.kr

With increasing demands for high color purity in display applications, colloidal quantum dots (QDs) have been considered as a promising light-emitting material due to their high luminescent efficiency and narrow emission spectrum. As the development of QDs has been focused on the structural formation for enhancing the optical properties, the state-of-the-art core/shell QDs have been comprised of a desired band-gap core and multiple wide band-gap shell layers. In particular, Zn-based chalcogenide materials including ZnS, ZnSe, and ZnTe play a major part in those multi-component luminescent QDs. For example, the wide band-gap ZnS, ZnSe, and their alloy can passivate the surface of most core materials and impose a barrier to confine both charge carriers in the core. In addition to the excellent role as shells, recent studies suggest that the Zn-based chalcogenide can be a suitable core material for blue or green emission. Especially, ZnTeSe QDs with ternary compositions are presented for their color tunability from violet to green by control of the Te/Se ratio. However, the exquisite control in reactivity and compositional distribution of chalcogen elements remains an issue and a challenge for stable and color-pure emission properties. Common synthesis of Zn-based chalcogenide QDs includes phosphine such as diphenylphosphine, trioctylphosphine, since they easily form a complex with elemental chalcogens. Along with toxicity, high cost, and air sensitivity of phosphine themselves, phosphine affect the deformation of QD shape, and increment of trap emission. Here we introduce the novel synthesis of Zn-based chalcogenide alloy nanocrystals with elemental chalcogen precursors, without using phosphine. The elemental chalcogen precursors can be prepared by a stoichiometrically mixing and alloying of chalcogen elements, tuning the reactivity of chalcogens, and enabling the QD nucleation at relatively low temperatures. We also demonstrate blue ZnTeSe/ZnSe/ZnS QDs synthesized by the elemental chalcogen precursors with high color purity of FWHM < 25nm. This phosphine-free synthesis from the core to the shell of QDs opens the possibility of numerous chalcogenide QD syntheses, further leading to efficient, economical mass production in commercial applications.

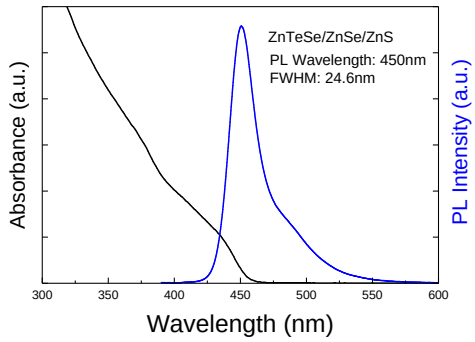

Fig. 1. UV Absorbance and Photoluminescence Spectra

References

1. Jang, E.-P.; Han, C.-Y. *ACS applied materials & interfaces*, *11* (49), 46062–46069. (2019)
2. Sameer S.; Rogach A. L.; Feldmann J. *Journal of Materials Chemistry* 16.33, 3391-3395 (2006)

Effect of Zwitterionic Ligands on Organic-Inorganic Hybrid Perovskite Nanocrystals

Inyoung Jeong[1], Namyoung Gwak[1], Kyeongwan Kang[1], Minwoo Lee[1] and Nuri Oh[1]
[1]Division of Material Science and Engineering, Hanyang University, Seoul, Wangsimni-ro 222, Korea
Tel.:82-2-2220-0403, E-mail: irunho@hanyang.ac.kr

Perovskite nanocrystals (PNCs) have been attracting attention in light emitting devices due to their unique optical properties which are tunable band gap, pure color emission, and high photoluminescence (PL). PNCs are synthesized with various routes such as hot-injection, ball milling and ligand-assisted reprecipitation (LARP). Especially, LARP is a versatile method, because the formation of PNCs takes only a few seconds in the air without heating. During the synthesis step, the ligands play an important role in determining size and shapes and also contribute to maintain colloidal stability. Several studies recently reported improved stability of PNCs through synthesis using zwitterionic ligands, which have hydrophobic chains and the hydrophilic head group containing both positive and negative ions[1]. Others demonstrated electroluminescence external quantum efficiency by 20.3 percent through exchanging with the zwitterionic ligands[2]. However, it still remains challenges to understand how different types of zwitterionic ligands are associated with the optical properties and stability of PNCs. Herein, we study the effect of various zwitterionic ligands such as phosphatidylcholine (PC), phosphatidylethanolamine (PE) on the organic-inorganic hybrid PNCs. Based on the type of zwitterions in the ligands, the emission properties of colloidal PNCs can either be enhanced or be diminished. By the appropriate selection of the head group and combination with multiple zwitterionic molecules, we can achieve high stability of PNC colloids and PL intensity improvement of up to 75% (Fig.1). This ligand exchange process allows us to demonstrate the proof-of-concept electroluminescence devices in which the zwitterionic ligand-coated PNCs are embedded as an emissive layer.

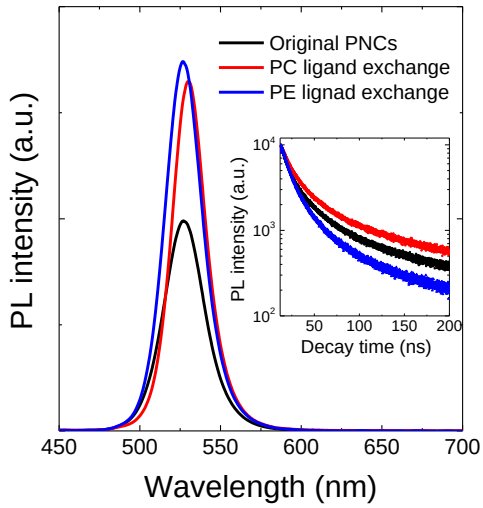

Figure 1. PL spectra of PNCs before and after exchanging with zwitterionic ligands

reference

1. Krieg, F. *et al.* Colloidal CsPbX3 (X = Cl, Br, I) Nanocrystals 2.0: Zwitterionic Capping Ligands for Improved Durability and Stability. *ACS Energy Lett.* **3**, 641–646 (2018).
2. Hassan, Y. *et al.* Ligand-engineered bandgap stability in mixed-halide perovskite LEDs. *Nature* **591**, (2021).

Effective Surface Engineering via Metal Halide Complexes for Green InP Quantum Dots

Seungki Shin[1], Namyoung Gwak[1], and Nuri Oh[1]
[1]**Division of Material Science and Engineering, Hanyang University, Seoul, Wangsimni-ro 222, Korea**
Tel.:82-2-2220-0403, E-mail: irunho@hanyang.ac.kr

Colloidal quantum dots (QDs) have shown excellent optical properties such as tunable band gap, narrow emission spectra, and high photoluminescence (PL). Indium phosphide QDs are one of the most successful visible light emitting materials for commercial use. However, the strong covalent character of the InP core seems to decrease the efficiency of surface ligand passivation compared with II-VI QDs. Consequently, the InP core has very low (<1%) photoluminescence quantum yields (PLQYs) that originate from surface defects such as uncoordinated dangling bonds. To remove the surface defects, the most common method is the growth of inorganic shells such as zinc sulfide on the InP core. Epitaxially grown inorganic shell with wide band gap materials passivates the surface and makes type-I heterostructure, which helps to improve luminescence properties. Unfortunately, unwanted surface oxides are inevitably formed during or after synthesis. The surface oxides are retained even after shell coating on the InP core, which affects the optical properties of final products.

Post-synthetic surface treatment is one of the most effective methods to remove the surface defects and/or oxides on the InP. Recent study suggests that addition of hydrofluoric acid (HF) can etch the surface oxides, allowing to increase luminescence efficiency. It has been also reported that incorporation of metal halide salts to InP core solution can also increase PLQY. However, the effect of these additives on the shell growth on InP core still remains unclear.

In this study, we have engineered the surface of the InP core via post-synthesis treatment using metal halide complexes (MHCs). The metal halide complexes can remove the oxides but also prevent additional oxidation to the InP core, resulting in luminescence improvement of the InP core. The MHC treated InP cores exhibit high PLQY up to 40% without shell growth. X-ray photoelectron spectroscopy (XPS) study reveals that oxides on the InP QDs are removed after MHC treatment. The clean surface of InP cores by removal of surface oxides are retained during the shell coating process. As a result of effective surface treatment with MHC, InP/ZnSeS core/shell QDs were achieved high PLQY (~95%).

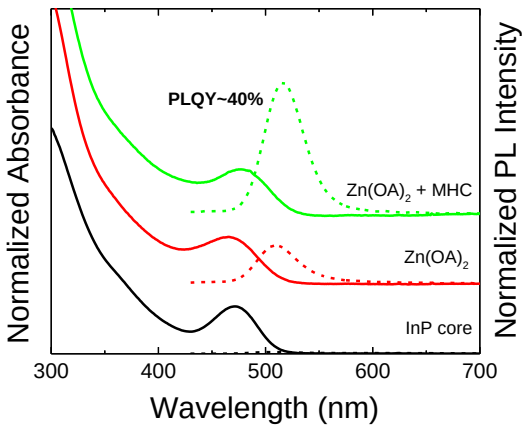

Fig. 1. Changes in PLQY of InP/ZnSeS (Gray) and InP/ZnSeS-MHC (Green) during synthesis

References

1. Micic, O. I.; Sprague, J.; Li, Z.; Nozik, A. *J. Appl. Phys. Lett.*, 68, 3150 (1997).
2. Calvin, J. J.; Swabeck, J. K.; Sedlak, A. B.; Kim, Y.; Jang, E.; Alivisatos, A. P. *J. Am. Chem. Soc.*, 142(44), 18897 (2020).

Analysis of Tandem Structure Quantum Dot Light-emitting Diodes modulating Electron Transport Layer

Jae-In Yoo[1], Suk-Ho Song[1], Hyo-Bin Kim[1], Sung-Cheon Kang[1] and Jang-Kun Song[1,]*
[1]Department of Electrical and Computer Engineering, Sungkyunkwan University, Suwon, Gyeonggi-do 16419, South Korea
Tel.:82-31-299-4631, E-mail: jk.song@skku.edu

Quantum-dot light-emitting diode (QD-LED) showed high luminance, high color purity, high efficiency, and low operating voltage, leading to a potential candidate for future display applications. To achieve high resolution using solution processed QD-LED, conventional RGB sub-pixel has limitation because of TFT array. In other words, low fill factor disturb high resolution in RGB sub-pixel application. New approach to achieve high solution was suggested using AC driving color-tunable tandem structure.

In this work, we suggest novel tandem structure emitting different colors depending on the bias. This device is combined of conventional structure and inverted structure. PEDOT:PSS used as hole injection layer (HIL), Poly(9-vinylcarbazole) (PVK) used as hole transport layer (HTL). ZnO nanoparticles (ZnO NPs) used as electron transport layer (ETL). Configuration of device is in order ITO/ PEDOT:PSS/ PVK/ Red QD/ ZnO NPs/Green QD/ PVK/ PEDOT:PSS/ Al. This device is fabricated by all-solution process.

This tandem QD-LED device emitted red on forward bias and green on reverse bias. In forward bias, red peak is dominant and little green peak is observed. however, reverse bias showed mixed color. Green peak is still majority, red peak has half portion of green peak intensity. When we modulating thickness of ETL, more think ETL showed low turn-on voltage and high luminance on reverse bias.

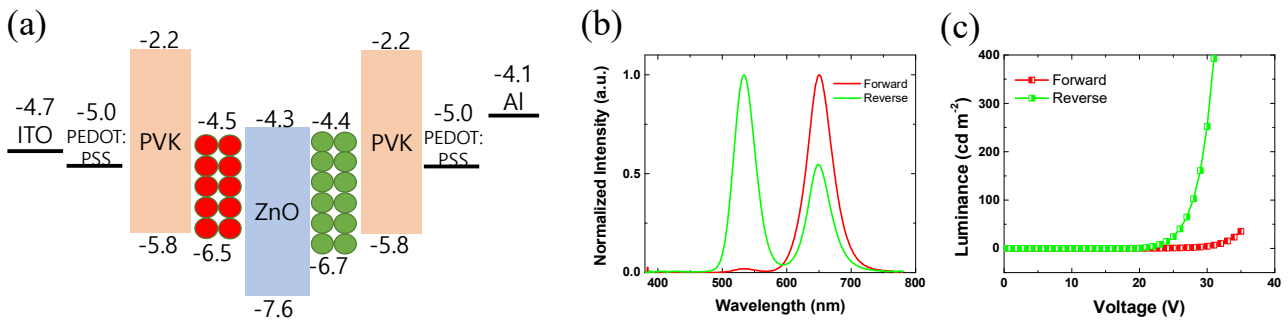

Fig. 1. (a) Energy level diagram of Tandem Structure QD-LED device (b) Electroluminescent characteristics of Tandem Structure QD-LED (c) L-V characteristics of Tandem Structure QD-LED

Acknowledgment

This research was funded and conducted under 'the Competency Development Program fro Industry Specialists' of the Korean Ministry of Trade, Industry and Energy(MOTIE), operated by Korea Institute for Advancement of Technology(KIAT).
(No. P0012453, Next-generation Display Expert Training Project for Innovation Process and Equipment, Materials Engineers)

References

1. H. Moon., C. Lee., W. Lee., J. Kim., H. Chae., Adv Mater, 31(34), 1804294 (2019).
2. S.H. Song., S.J. Park., T.J. Bae., K.M. Jung., W.H. Park., Y.S. Kim., Q. F. Yan., S. S. Kim., J.K. Song., Nanoscale, 12(32), 17020 (2020).

Narrow Bandgap Approach for All-day Operation Solar Cell

Yongju Lee[1,2], Hyeon-Won Lee[1], Swarup Biswas [1], Hyeok Kim[1]*

[1]School of Electrical and Computer Engineering, Institute of Information Technology, University of Seoul, 163 Seoulsiripdaero, Seoul 02504, Korea

[2]Applied Robot R&D Department, Korea Institute of Industrial Technology (KITECH), Ansan 15588, Korea

Fax: 82-2-6490-2354; E-mail: hyeok.kim@uos.ac.kr

The demand for low dimensional, micro powered and wireless indoor electronic devices has been increasing. To power-up those devices, organic photovoltaic (OPV) cells are being employed. The OPV cells exhibit good spectral matching and mechanical flexibility, and can harvest artificial indoor light energy efficiently [1]. Hole transport layer (HTL) is an important component of an OPV cell. Hole transport layer (HTL) is an important component of an OPV cell. Water stable, low temperature processable poly (3, 4-ethylene dioxythiophene): poly (4-styrenesulfonic acid) (PEDOT:PSS) based HTL is commonly used in the indoor OPV cells. However, strongly acidic, highly hydrophilic and expensive PEDOT:PSS resulted in the development of cheaper, mildly acidic and less humidity sensitive alternative hole transport material (HTM) for the indoor OPV cells [2]. Here, we utilized an economic and low acidic, water-stable PSS doped Polypyrrole (PPY) as HTM for PTB7-th:PC70BM active material-based indoor OPV cell. The device was also optimized by adjusting the concentrations of PPY and PSS, and the OPV device exhibited higher shunt resistance and greater power conversion efficiency (PCE) while operating in an indoor environment. For 1000 lux white LED light, the device showed around 14.15% PCE

Acknowledgment

This work was supported by the Technology development Program (S2987793) funded by the Ministry of SMEs and Startups(MSS, Korea). This work was supported by the Korea Institute of Industrial Technology as Research Source Technique Project [KITECH EO180026]. This work was supported by the Basic Study and Interdisciplinary R&D Foundation Fund of the University of Seoul (2020).

References

1. Swarup Biswas, Young-Jun You, Yongju Lee, Jae Won Shim, Hyeok Kim, Dyes and Pigment, 183, 108719 (2020)
2. Swarup Biswas, Hyeok Kim, Polymers, 12, 1338 (2020)
3. Ian Mathews, Sai Nithin Kantareddy, Tonio Buonassisi, Ian Marius Peters, Joule, 3, 1315 (2019)
4. Sang-Chul Shin, Premkumar Vincent, Jin-Hyuk Bae, Jae Joon Lee, Minwoo Nam, Doo-Hyun Ko, Hyeok Kim, Jae Won Shim, Dyes and Pigment, 163, 48 (2019)
5. Martin A. Green, Progress in Photovoltaics, 17, 183 (2009)
6. Swarup Biswas, Young-Jun You, Jae Won Shim, Hyeok Kim, Thin Solid Films, 700, 137921 (2020)

Stability Study on Inverted Organic Photovoltaics under Various Light Conditions Towards Stable Operation of Portable Display

Hyeong-Won Lee[1], Hyojeong Choi[1], Yongju Lee[1], Biswas Swarup[1], Hyeok Kim[1**]
[1]School of Electrical and Computer Engineering, University of Seoul, 163 Seoulsiripdaero, Dongdaemun-gu, Seoul 02504, Republic of Korea
Fax: 82-2-6490-2314; E-mail: hyeok.kim@uos.ac.kr

As organic photovoltaics (OPVs) have advantages such as diversity of synthesis method, ease of manufacturing method, light weight, low production cost, and high productivity, many new materials have been developed and applied research using them has been actively conducted. With the recent development of wireless communication and microelectromechanical system technology, the demand for wireless sensor nodes and low-power consumption electronic devices is rapidly increasing, and the development of OPVs indoor light harvester is an area to be interested in terms of utilizing indoor light absorption. However, OPVs is in the early stages of stability research and the stability of the device for commercialization is an important task. In this study, we would like to test light stability in various light sources using Poly [[4,8-bis[(2-ethylhexyl)oxy] benzo [1,2-b:4,5-b'] dithiophene-2,6-diyl] [3-fluoro-2-[(2-ethylhexyl)carbonyl]thieno[3,4-b]thiophenediyl]](PTB7) and phenyl-C_{70}-butyric acid methyl ester ($PC_{70}BM$) fullerene material as an active layer and using reverse structure OPV which is more stable than conventional structure OPV.

Acknowledgment

This work was supported by the Technology development Program (S2987793) funded by the Ministry of SMEs and Startups(MSS, Korea). This work was supported by the Korea Institute of Industrial Technology as Research Source Technique Project [KITECH EO180026]. This work was supported by the Basic Study and Interdisciplinary R&D Foundation Fund of the University of Seoul (2020).

References

1. G. Yu, J. Gao, J. C. Hummelen, F. Wudl and A. J. Heeger, *Science*, **270**, 1789 **(1995)**
2. Z. He, C. Zhong, S. Su, M. Xu, H. Wu and Y. Cao, *Nat.Photonics*, **6**, 591, **(2012)**
3. B. C. Thompson and J. M. J. Fréchet, *Angew. Chem., Int. Ed.*, **47**, 58, **(2007)**
4. Y. Zhou, C. Fuentes-Hernandez, J. Shim, J. Meyer, A. J. Giordano, H. Li, P. Winget, T. Papadopoulos, H. Cheun, J. Kim, M. Fenoll, A. Dindar, W. Haske, E. Najafabadi, T. M. Khan, H. Sojoudi, S. Barlow, S. Graham, J.-L. Bre´das, S. R. Marder, A. Kahn and B. Kippelen, *Nat.Photonics*, **6**, 591, **(2012)**
5. J. Tong, S. Xiong, Y. Zhou, L. Mao, X. Min, Z. Li, F. Jiang,W. Meng, F. Qin, T. Liu, R. Ge, C. Fuentes-Hernandez,B. Kippelen and Y. Zhou, *Mater. Horiz*, **3**, 452, **(2016)**

Stabilization of the injection and line-edge pattern uniformity of the QD inks printed with low-surface-tension octane-cyclohexane mixture

Sun Ho Choo*, Ji Hye Kim*, Min Young Kim*, Chil Won Lee**, Byung Doo Chin*†
****Dept. of Polymer Science and Engineering, Dankook University, Suji-gu/Yongin-si, Gyenggi-do 16890, Korea***
***** Dept. of Chemistry, Dankook University, Dongnam-gu/Cheonan-si, Chungcheongnam-do, 31116, Korea***
†Tel.:82-31-8005-3587, E-mail: bdchin@dankook.ac.kr

Quantum dot light emitting diode (QLED) can be directly patterned for pixel array by solution processing [1-2], while the limitation of resolution and device stability exist unless proper solvent system and multilayer design are established. With a small-sized nozzle inkjet printing process, solvent formulation effects on the morphology and precision of printing for quantum dot layer was investigated. To achieve a solvent orthogonality as well as smooth surface characteristics of dried QD film on typical high-mobility hole transporting layer such as poly(9,9-dioctylfluorene-alt-N-(4-sec-butylphenyl)-diphenylamine); TFB, alkanes can be commonly applied. However, pure alkanes are not easy to be tuned as inkjet printing due to their relatively low surface tension, which makes unstable droplet formation and ink streaming out of the nozzle. In this work, mixtures of octane with various surface tension modifying sub-solvents were designed for a control of stable drop formation, ink spreading, and wetting on the non-crosslinked TFB as a non-erosive solvent formulation [3]. While the ink composition (octane-cyclohexane) formed low-contact angle droplet on surface (hence tends to widely spread) and was not completely ideal for defect-less high-resolution pixelating process of inkjet QLED, its controllability of wetting, uniform drying, and orthogonal characteristics with an effective hole transport layer resulted in a high-performance green inkjet QLED more than 6 cd/A at > 19,000 nit highly bright region. This amounted to about 50% of efficiency performance compared to an identical device prepared with spin coating, but one of the best green inkjet QLED properties reported with less than 120μm sub-pixel pitch.

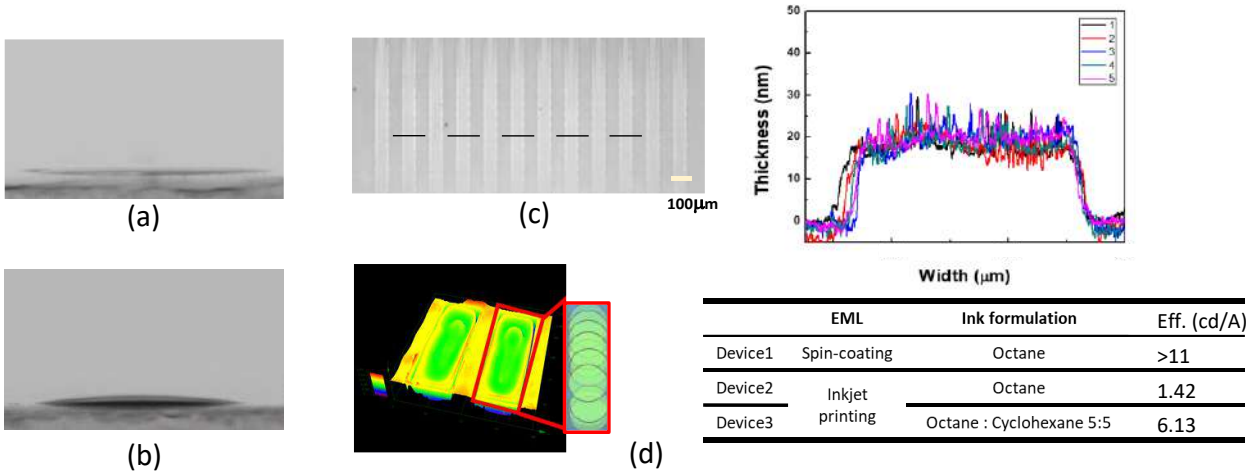

	EML	Ink formulation	Eff. (cd/A)
Device1	Spin-coating	Octane	>11
Device2	Inkjet printing	Octane	1.42
Device3		Octane : Cyclohexane 5:5	6.13

Fig. 1 (a) Octane 100% on TFB (b) Octane-cyclohexane 5:5 on TFB (c) Multiple printed line patterns for a comparison of line-width and their morphology; each line 1-5 with 20nm-target printing on flat TFB (average 19.5nm) without noticeable coffee-ring (d) QLEDs on 80μm × 240 μm test coupon with cd/A efficiency properties

References

1. C. Jiang, Lan Mu, J. Zou, Z. He, Z. Zhong, L. Wang, M. Xu, J. Wang, J. Peng, Y. Cao, Science China Chemistry, 60, 1349 (2017)
2. J. Han, D. Ko, M. Park, J. Roh, H. Jung, Y. Lee, Y. Kwon, J. Sohn, W. K. Bae, B. D. Chin, and C. Lee, Journal of the SID 24(9), p545 (2016)
3. J. A. Lim, W. H. Lee, H. S. Lee, J. H. Lee, Y. D. Park, K. Cho, Adv. Funct. Mater. 18, 229 (2008)

Photoluminescent Surface-Confined Graphene Quantum Dots for Spontaneous Interfacial Molecular Alignment

Seung-Rak Son, Jin-Wook Choi, Jongil An, Soyern Kim, Jisung Park, Chan Beom Park, and Jun Hyup Lee*
Department of Chemical Engineering, Soongsil University, Seoul 06978, Republic of Korea
Tel.:82-2-829-8329, E-mail: junhyuplee@ssu.ac.kr

Quantum dots (QDs) are attracting considerable attention as next-generation semiconductor materials because of their narrow emission spectra, tunable colors, and high stability [1,2]. Owing to these attractive properties, they have been utilized and studied in various devices such as displays, batteries, solar cells, and biosensors [3,4].

Herein, we propose an elegant method that can efficiently control the initial configuration of liquid crystal (LC) molecules and simultaneously provide strong photoluminescence (PL) emission based on the facile self-assembly of octadecylamine-functionalized graphene quantum dots (O-GQDs) inside the LCs (Fig. 1). Owing to the presence of hydrophilic functional groups in the O-GQDs, they can spontaneously self-assemble on the hydrophilic surface of an indium tin oxide (ITO) substrate in the confined LC cell through polar intermolecular interactions. In addition, the use of octadecylamine groups during O-GQD preparation results in the presence of a hydrophobic long alkyl chain structure, which is expected to lead to a stable, uniform homeotropic orientation of LC molecules. Furthermore, the novel nanostructured O-GQD layer can be constructed over a large area at a low cost through a simple doping method without an additional coating or a high-temperature process. Moreover, this layer can successfully afford the adaptive control of LC alignment and remarkable electro-optical properties comparable to those of commercial alignment materials. Our proposed method is expected to be applicable in the preparation of functional flexible displays and self-emitting optoelectronic devices.

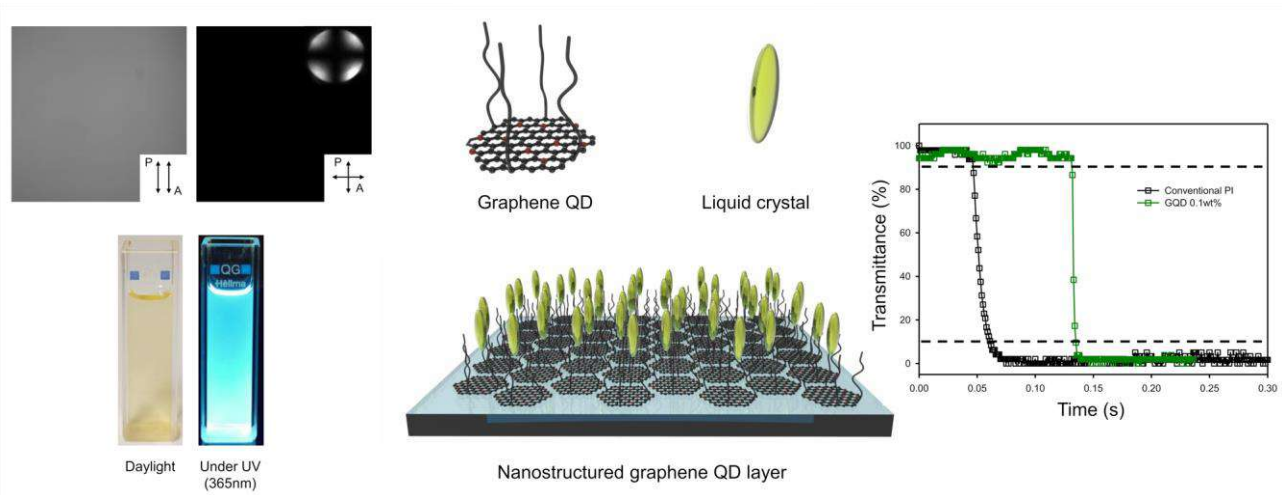

Fig. 1. Schematic illustration of construction of the nanostructured O-GQD layer for LC orientation

Acknowledgment

This work was supported by a National Research Foundation of Korea (NRF) grant funded by the Korea government (MSIT) (No. NRF-2018R1A5A1024127). This work was also supported by Korea Institute for Advancement of Technology (KIAT) grant funded by the Korea Government (MOTIE) (P0012770).

References

1. M. Arita, F. L. Roux, M. J. Holmes, S. Kako, Y. Arakawa, *Nano Lett.*, 17, 2902 (2017).
2. H. Moon, C. Lee, W. Lee, J. Kim, H. Chae, *Adv. Mater.*, 31, 1804294 (2019).
3. Y. Ji, J. Hu, J. Biskupek, U. Kaiser, Y. F. Song, C. Streb, *Chem. Eur. J.*, 23, 16637 (2017).
4. F. Ma, C. C. Li, C. Y. Zhang, *J. Mater. Chem. B*, 6, 6173 (2018).

Efficiency Improvement of Quantum-Dot Light-Emitting Diode Using PVK and TFB Mixture for Hole Transport Layer

Hyo-Bin Kim[1], Jae-In Yoo[1], Suk-Ho Song[1], and Jang-Kun Song[1,*]
[1]Department of Electrical and Computer Engineering, Sungkyunkwan University, Suwon, Gyeonggi-do 16419, South Korea
Tel.:82-31-299-4631, E-mail: jk.song@skku.edu

Quantum-dot light-emitting diode (QD-LED) is a promising light source for future displays because of several advantages, such as high color purity and cost-effective fabrication using the solution process. However, the low power efficiency (PE) feature in QD-LEDs is a bottleneck for actual display applications. One of the main causes for the low device efficiency is the charge imbalance in the QD layer. This is because QDs have a deep highest occupied molecular orbital (HOMO) level, resulting the hole injection relatively more difficult than the electron injection. The charge imbalance in the QD layer leads to the non-radiative Auger recombination, which degrade the device performances. Therefore, efficient hole transport to the QD layer is essential to improve the device efficiency.

In this paper, the mixture of PVK and TFB is used for hole transport layer (HTL) to improve the hole transport ability. PVK is a widely used HTL material, which exhibit a deep HOMO level of 5.8 eV, resulting high current efficiency.[1] However, the deep HOMO level increases the turn-on voltage (voltage @ 1 cd/m^2) of the QD-LED, which decreases the PE characteristic. Hence, we mixed TFB, which has a shallow HOMO level of 5.2 eV, with PVK to improve the PE characteristic by decreasing the turn-on voltage of the QD-LED. QD-LEDs are fabricated in the following structure: ITO/PEDOT:PSS/HTL/QDs/ZnO/Al. For HTL, we prepared PVK and TFB mixtures, dissolved in chlorobenzene in a total concentration of 0.3 wt%, in the weight ratio of 1:0, 1:2, 1:1, 2:1, 3:1, 4:1, and 0:1. QD-LEDs with mixed HTL showed lower turn-on voltages than PVK only and TFB only devices, as shown in Fig. 1a. As a result, the PE of the QD-LED, especially the device using PVK and TFB mixture with the weight ratio of 2:1, showed the highest maximum PE (0.94 lm/W), which is a significantly improved characteristic than PVK only (0.55 lm/W) and TFB only (0.21 lm/W) devices, as shown in Fig. 1b. Moreover, devices with mixed HTL showed higher current densities than PVK only and TFB only devices, resulting improved maximum luminance characteristics, as shown in Fig. 1c. Therefore, PVK and TFB mixture can role as an efficient HTL and improve the charge balance in QD-LEDs.

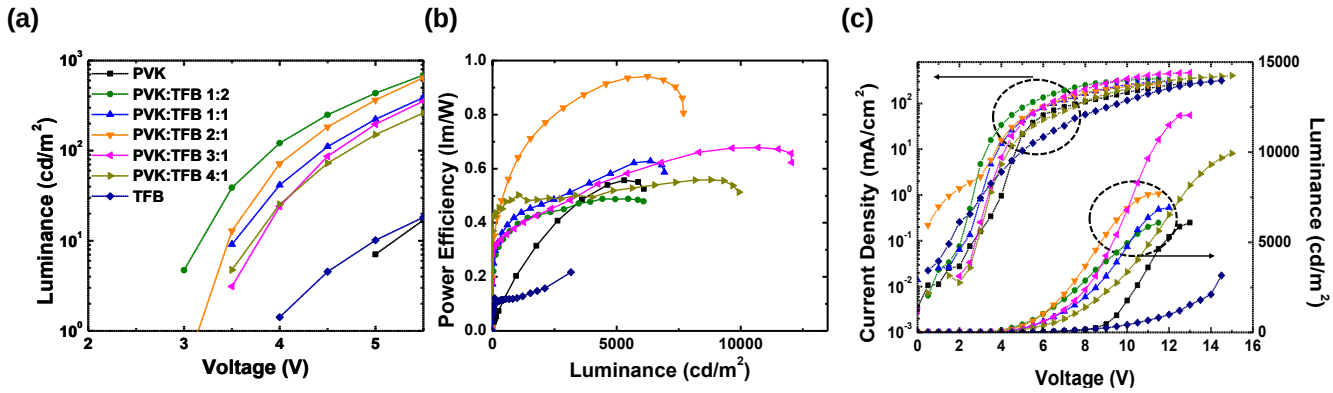

Fig. 1. (a) Luminance versus voltage, (b) power efficiency, and (c) current density-voltage-luminance characteristics of QD-LEDs with various HTLs.

Acknowledgment

This research was funded and conducted under 'the Competency Development Program for Industry Specialists' of the Korean Ministry of Trade, Industry and Energy(MOTIE), operated by Korea Institute for Advancement of Technology(KIAT).
(No. P0012453, Next-generation Display Expert Training Project for Innovation Process and Equipment, Materials Engineers)

References

1. M. D. Ho, D. Kim, N. Kim, S. M. Cho, and H. Chae, *ACS Appl. Mater. Interfaces*, 5(23), 12369-12374 (2013).

Improvement of Efficiency Roll-off in Red Quantum-dot Light Emitting Diodes by Controlling Electron Injection

Yiseul Kim[1,2], Hyungsoo Yoon[1,2], Geonhee Kim[1,2], Sujin Jeong[1,2], Jinsu Yoon[1,2], Dahyun Kim[1,2] and Yongtaek Hong[1,2]*

[1]Department of Electrical and Computer Engineering, Seoul National University, Seoul 08826, Korea

[2]Inter-University Semiconductor Research Center(ISRC), Seoul National University, Seoul 08826, Korea

Tel.:82-2-880-9567, E-mail: yongtaek@snu.ac.kr

Quantum dot light-emitting diodes(QLEDs) is one of the next-generation displays thanks to many advantages such as high efficiency, high color purity, color tunability and low energy consumption. Moreover, QLEDs have process benefits like solution processability and comparability with flexible substrates. Despite many advantages, QLEDs have a critical problem of efficiency drop at high current levels, as known as efficiency roll-off. [1] Among the various causes of roll-off effect, charge imbalance is considered one of the biggest reasons. In general, hole injection barrier in QLEDs is much larger than that of electron injection barrier because of Cd-based QD's deep HOMO(Highest Occupied Molecular Orbital). As a result, excess electrons are injected into the device and the device becomes electron-rich state which increases the possibility of non-radiative recombination like Auger-recombination.[2] To solve this problem, various studies have been conducted by boosting hole injection. To improve charge balance by boosting hole injection, Inverted QLEDs have been developed which are fabricated by deposition of monomer with appropriate energy level on solution processed quantum dots. Its advantage is that it can utilize various materials that are difficult to process in solution.[3]

In this work, we show that controlling electron injection into the device significantly affects the efficiency roll-off phenomena. To suppress electron injection, we adopt high LUMO(Lowest Unoccupied Molecular Orbital) buffer and m-ETL(mixed-ETL) with monomer which has low electron mobility. As shown in fig. 1(a), the current density with buffer/m-ETL is decreased than that of reference. As can be seen from Fig. 1(b), the normalized current efficiency of QLEDs with reference or buffer/m-ETL have improved from 0.72 to 0.91 at 10,000 cd due to suppressed electron injection.

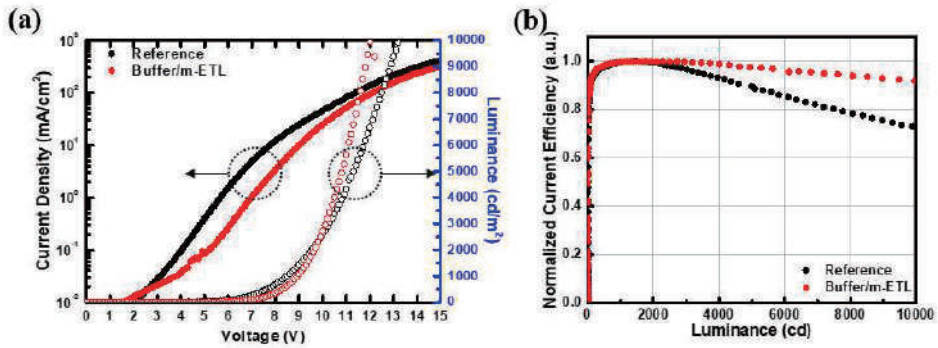

Fig. 1. (a) The IVL characteristics of QLEDs. (b) The normalized current efficiency of QLEDs.

Acknowledgment

This work was supported by the Industry technology R&D program (20010427) funded by the Ministry of Trade, Industry & Energy (MOTIE, Korea).

References

1. Yizhe Sun, QiangSu, Heng Zhang, Fei Wang, Shengdong Zhang and Shuming Chen, *ACS NANO,* 13, 11433-11442 (2019).
2. Benchang Liu, Luhua Lan, Yaoyao Liu, Hong Tao, Hongmeng Li, Hua Xu, Jianhua Zou, Miao Xu, Lei Wang, Junbiao Peng and Yong Cao, Organic Electronics, 74, 144-151 (2019).
3. Jeong Ha Hwang, Junmo Kim, Byong Jae Kim, Myeongjin Park, Yong Woo Kwon, Myungchan An, Dong Yeol Shin, Jae Min Jeon, Jun Young Kim, Wonho Lee, Jaehoon Lim and Donggu Lee, Applied Surface Science, 558, 149944 (2021)

Realizing High Coverage Ratio for BT.2020 Using Cadmium-free Red, Green, and Blue Quantum Dot Light-emitting Diodes with Emitting Layer Combined with Organic Electron-transporting Materials

Yukiko Iwasaki, Genichi Motomura, and Toshimitsu Tsuzuki
NHK Science & Technology Research Laboratories, 1-10-11 Kinuta, Setagaya-ku, Tokyo 157-8510, Japan
Tel.:81-3-5494-3257, E-mail: iwasaki.y-iq@nhk.or.jp

Quantum dot light-emitting diodes (QD-LEDs) are expected to be applied to various types of wide-color-gamut display because the emission colors of quantum dots (QDs) are highly saturated and tunable. To realize displays compliant with Recommendation ITU-R BT.2020 (BT.2020) [1], the development of red, green, and blue (RGB) light-emitting devices with high color purity is essential. Although high color purity and high efficiency have been reported in QD-LEDs using Cd-based QDs [2], the use of Cd is restricted owing to its toxicity. We have reported green InP-based QD-LEDs with emitting layers (EMLs) composed of QDs and organic electron-transporting materials (ETMs) [3,4]. These mixed EMLs enable QD-LEDs with electroluminescence (EL) spectra that coincide with the photoluminescence spectra of QD films. The defect emission derived from QDs, which deteriorate the chromaticity coordinates, and the change in the EL spectra with different luminances were suppressed by using the mixed EMLs. Although some combinations of the organic ETM and the hole-transporting material induce exciplex formation, it can be suppressed by optimizing the device configuration. In this study, we developed RGB QD-LEDs using Cd-free QDs with mixed EMLs of QDs and organic ETMs, and achieved the high area-coverage ratio (~80%) for BT.2020 in the CIE 1931 *xy* color space by suppressing the defect and exciplex emissions.

The structure of the fabricated bottom-emitting QD-LEDs is shown in Fig. 1. InP-based QDs (QDA-RH001 and QDA-GO001 (Merck)) and ZnSeTe QDs were used as RGB QDs. Triazine or trimesitylborane derivatives were used as organic ETMs. The developed RGB QD-LEDs exhibited narrow full-widths at half-maximum of 40, 34, and 23 nm. The chromaticity coordinates of the RGB QD-LEDs with and without organic ETMs are shown in Fig. 2. The BT.2020 area-coverage ratio of the developed RGB QD-LEDs with organic ETMs was 80%, which is higher than that of the RGB QD-LEDs without organic ETMs (~73%). The improvement of the area-coverage ratio was caused by the suppression of both the defect emission from QDs and the exciplex emission from peripheral materials.

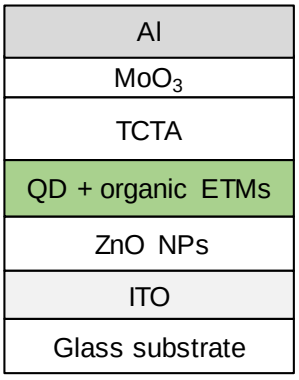

Fig. 1. Device structure of QD-LEDs.

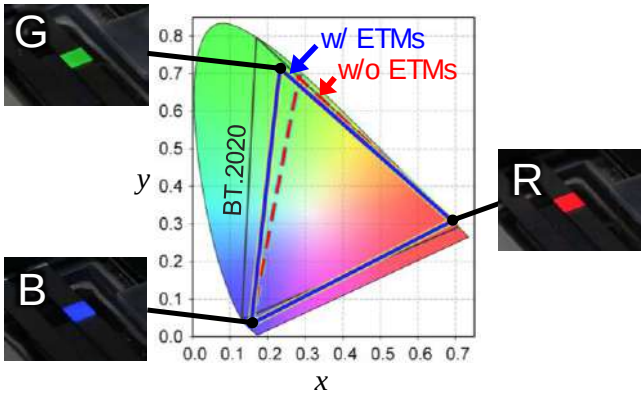

Fig. 2. Chromaticity coordinates of developed RGB QD-LEDs and photographs of EL from QD-LEDs.

References

1. Recommendation ITU-R BT.2020-2 (2015).
2. X. Dai, Z. Zhang, Y. Jin, Y. Niu, H. Cao, X. Liang, L. Chen, J. Wang and X. Peng, *Nature*, 515, 96 (2014).
3. G. Motomura, K. Ogura, Y. Iwasaki, J. Nagakubo, M. Hirakawa, T. Nishihashi and T. Tsuzuki, *AIP Adv.*, 10, 065228 (2020).
4. Y. Iwasaki, G. Motomura, K. Ogura and T. Tsuzuki, *Appl. Phys. Lett.*, 117, 111104 (2020).

Improved Stabilities and Production Yields of $MAPbBr_3$ Perovskite Quantum Dots and Their Applications as Stretchable and Self-Healable Color Filters

Han Sol Yang, Sung Hoon Noh, Eui Hyun Suh, Jaemin Jung, Jong Gyu Oh, Kyeong Ho Lee, and Jaeyoung Jang*
Department of Energy Engineering, Hanyang University, Seoul 04763, Republic of Korea.
Tel.:82-2-2220-4118, E-mail: jyjang84@gmail.com

Organic–inorganic hybrid $CH_3NH_3PbBr_3$ ($MAPbBr_3$) perovskite quantum dots (PQDs) are considered promising materials for optoelectronic devices. However, during purification step, polar protic and aprotic non-solvents can destroy the nanocrystal structure of $MAPbBr_3$ perovskites, which will significantly reduce the production yields and degrade the optical properties of the PQDs. This study demonstrates the use of methyl acetate (MeOAc) as an effective non-solvent for purifying $MAPbBr_3$ with high production yields. The MeOAc-washed $MAPbBr_3$ PQDs maintain their photoluminescence quantum yields and crystalline structures for long periods. MeOAc undergoes a hydrolysis reaction in the presence of the PQDs, and the resulting acetate anions partially replace the original surface ligands without damaging the PQD cores. Time-resolved photoluminescence analysis reveals that the MeOAc-washed PQDs show suppressed nonradiative recombination. Finally, it is demonstrated that a composite of $MAPbBr_3$ PQDs and a thermoplastic elastomer is feasible as a stretchable and self-healable color filter for a white LED device.

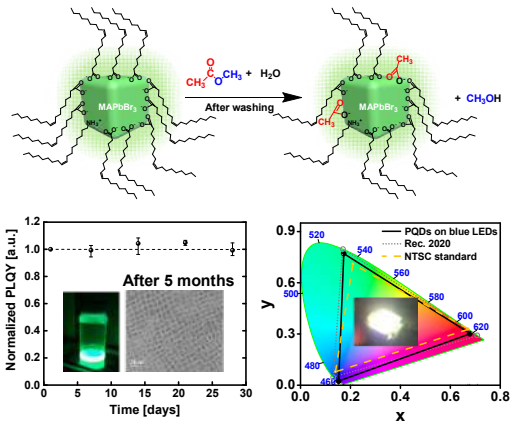

Fig. 1. (a) Schematic illustration of proposed mechanism of ligand exchange on surface of $MAPbBr_3$ PQDs during washing with MeOAc. (b) Time-dependent normalized PLQY values of $MAPbBr_3$ PQDs washed with MeOAc. (c) CIE chromaticity coordinates of the fabricated white LED device.

Acknowledgment

This work was supported by the Korea Institute of Energy Technology Evaluation and Planning (KETEP) and the Ministry of Trade, Industry & Energy (MOTIE) of the Republic of Korea. (No. 2018201010636A). This work was also supported by National R&D Program through the National Research Foundation of Korea (NRF) funded by Ministry of Science and ICT (2020M3F3A2A01085792).

References

1. H. Huang, A. S. Susha, S. V. Kershaw, T. F. Hung, A. L. Rogach, *Adv. Sci. (Weinheim Ger.)*, 2, 1500194 (2015).